VOLUME 27 / NUMBER 19
OCTOBER 8, 1989
ACC. NOS. N89-25113 TO N89-25947

STAR
AN ABSTRACT JOURNAL

Scientific and Technical Aerospace Reports

PRODUCED BY THE
SCIENTIFIC AND TECHNICAL
INFORMATION
DIVISION

NASA

NATIONAL AERONAUTICS AND SPACE ADMINISTRATION

WHAT YOU CAN DO FOR *STAR*

All users of this abstract service are urged to forward reports to be considered for announcement in *STAR*. This will aid NASA in its efforts to provide the fullest possible coverage of all scientific and technical publications that might support aeronautics and space research and development. If you have prepared relevant reports (other than those that you will transmit to NASA, DoD, or DOE through the usual contract- or grant-reporting channels), please send them for consideration to the NASA Scientific and Technical Information Facility, P.O. Box 8757, BWI Airport, Maryland 21240.

Reprints of journal articles, book chapters, and conference papers are also welcome. These will be considered for announcement in *STAR's* companion journal, *International Aerospace Abstracts*.

You may specify a particular source to be included in a report announcement if you wish; otherwise the report will be placed on public sale at the National Technical Information Service. Copyrighted publications will be announced but not distributed or sold.

PURCHASE OF *STAR*

The semimonthly issues are available to registered users on annual subscription for $99.00 from the NASA Scientific and Technical Information Facility, ATTN: Registration Services, P.O. Box 8757, BWI Airport, MD 21240. *STAR* is publically available on annual subscription for $99.00 from the Superintendent of Documents, U.S. Government Printing Office, Washington, DC 20402.

PUBLISHED BY:

UNITED STATES GOVERNMENT
NATIONAL AERONAUTICS AND SPACE ADMINISTRATION
SCIENTIFIC AND TECHNICAL INFORMATION DIVISION
Scientific and Technical Aerospace Reports, Volume 27, is prepared by the NASA Scientific and Technical Information Facility operated for the National Aeronautics and Space Administration by RMS Associates.

The Administrator of the National Aeronautics and Space Administration has determined that the publication of this periodical is necessary in the transaction of the public business required by law of this Agency. Use of funds for printing this periodical has been approved by the Director of the Office of Management and Budget through March 22, 1989.

US ISSN 0036-8741

INTRODUCTION

Scientific and Technical Aerospace Reports (STAR) is a major component of a comprehensive National Aeronautics and Space Administration information system covering aeronautics, space, and supporting disciplines. *STAR* is issued on the 8th and 23rd of each month and announces current publications of the following types:

- NASA, NASA contractor, and NASA grantee reports
- Reports issued by other U.S. Government Agencies, domestic and foreign institutions, universities, and private firms
- Translations in report form
- NASA-owned patents and patent applications
- Other U.S. Government Agency and foreign patents and patent applications
- Domestic and foreign dissertations and theses

Journal, book, and conference literature, cover-to-cover journal translations, and certain foreign dissertations are announced in a companion journal, *International Aerospace Abstracts (IAA),* available on subscription from the American Institute of Aeronautics and Astronautics, Technical Information Service, 555 West 57th Street, 12th Floor, New York, New York 10019.

SUBJECT SCOPE

Subject scope of *STAR,* and *IAA* includes all aspects of aeronautics and space research and development, supporting basic and applied research, and applications. Aerospace aspects of earth resources, energy development, conservation, oceanography, environmental protection, urban transportation, and other topics of high national priority are also covered.

OTHER NASA PUBLICATIONS

Other NASA publications and information services are described in the publication, *The NASA Scientific and Technical Information System ... and How to Use It,* available without charge from the NASA Scientific and Technical Information Facility, P.O. Box 8757, BWI Airport, Maryland 21240.

HOW TO USE *STAR* SUBJECT CATEGORIES

STAR is categorized by 10 major subject divisions divided into 76 specific subject categories and one general category/division. The major subject divisions are listed in the Table of Contents, together with a note for each that defines its scope and provides any cross-references. For example:

AERONAUTICS

Includes aeronautics (general); aerodynamics; air transportation and safety; aircraft communications and navigation; aircraft design, testing and performance; aircraft instrumentation; aircraft propulsion and power; aircraft stability and control; and research and support facilities (air).

For related information see also *Astronautics.*

Each major division is further divided into as many as nine specific categories, which are identified by category numbers.

Abstracts in *STAR* are grouped by specific category, the categories appearing in sequential order. Category breaks in the abstract section are identified by the category number and title, and a scope note. Cross-references to other categories are provided as appropriate. For example:

02 AERODYNAMICS

Includes aerodynamics of bodies, combinations, wings, rotors, and control surfaces; and internal flow in ducts and turbomachinery.

For related information see also *34 Fluid Mechanics and Heat Transfer.*

CROSS-REFERENCES

Individual *STAR* abstracts are not ordinarily cross-referenced, except for certain conference reports or book translations that have had separate abstracts written for their component papers or chapters. Citations and abstracts of the components follow immediately after those of the parent document. When the subject content of a component differs sufficiently from the general content of the parent, a cross-reference citation also is printed at the end of the category to which it normally would have been assigned if it were independent.

DOCUMENTS ON MICROFICHE

Documents on microfiche(1) are designated by a pound sign (#) following the accession number. The pound sign is used without regard to the source or quality of the microfiche.

AVAILABILITIES

One or more sources from which a document announced in *STAR* is available to the public is given in each citation. The most commonly indicated sources and their acronyms or abbreviations are listed below. If the publication is available from a source other than those listed, the publisher and his address will be displayed on the availability line or in combination with the corporate source line.

Avail: NTIS. Sold by the National Technical Information Service. Prices for hard copy (HC) and microfiche (MF) are indicated by a price code following the letters HC or MF in the *STAR* citation. Current values for the price codes are given in the tables on page vii.

Initially distributed microfiche under the NTIS SRIM (Selected Research in Microfiche) is available at greatly reduced unit prices. For this service and for information concerning subscription to NASA printed reports, consult the NTIS Subscription Section, Springfield, Va. 22161.

NOTE ON ORDERING DOCUMENTS: When ordering NASA publications (those followed by the * symbol), use the N accession number. NASA patent applications (only the specifications are offered) should be ordered by the US-Patent-Appl-SN number. Non-NASA publications (no asterisk) should be ordered by the AD, PB, or other *report number* shown on the last line of the citation, not by the N accession number. It is also advisable to cite the title and other bibliographic identification.

Avail: SOD (or GPO). Sold by the Superintendent of Documents, U.S. Government Printing Office, in hard copy. The current price and order number are given following the availability line. (NTIS will fill microfiche requests, as indicated above, for those documents identified by a # symbol.)

(1) A microfiche is a transparent sheet of film, 105 by 148 mm in size, containing as many as 60 to 98 pages of information reduced to micro images (not to exceed 26:1 reduction).

Avail: BLL (formerly NLL): British Library Lending Division, Boston Spa, Wetherby, Yorkshire, England. Photocopies available from this organization at the price shown. (If none is given, inquiry should be addressed to the BLL.)

Avail: DOE Depository Libraries. Organizations in U.S. cities and abroad that maintain collections of Department of Energy reports, usually in microfiche form, are listed in *Energy Research Abstracts*. Services available from the DOE and its depositories are described in a booklet, *DOE Technical Information Center - Its Functions and Services* (TID-4660), which may be obtained without charge from the DOE Technical Information Center.

Avail: ESDU. Pricing information on specific data, computer programs, and details on ESDU topic categories can be obtained from ESDU International Ltd. Requesters in North America should use the Virginia address while all other requesters should use the London address, both of which are on page vi.

Avail: Fachinformationszentrum, Karlsruhe. Sold by the Fachinformationszentrum Energie, Physik, Mathematik GMBH, Eggenstein Leopoldshafen, Federal Republic of Germany, at the price shown in deutschmarks (DM).

Avail: HMSO. Publications of Her Majesty's Stationery Office are sold in the U.S. by Pendragon House, Inc. (PHI), Redwood City, California. The U.S. price (including a service and mailing charge) is given, or a conversion table may be obtained from PHI.

Avail: NASA Public Document Rooms. Documents so indicated may be examined at or purchased from the National Aeronautics and Space Administration, Public Documents Room (Room 126), 600 Independence Ave., S.W., Washington, D.C. 20546, or public document rooms located at each of the NASA research centers, the NASA Space Technology Laboratories, and the NASA Pasadena Office at the Jet Propulsion Laboratory.

Avail: Univ. Microfilms. Documents so indicated are dissertations selected from *Dissertation Abstracts* and are sold by University Microfilms as xerographic copy (HC) and microfilm. All requests should cite the author and the Order Number as they appear in the citation.

Avail: US Patent and Trademark Office. Sold by Commissioner of Patents and Trademarks, U.S. Patent and Trademark Office, at the standard price of $1.50 each, postage free. (See discussion of NASA patents and patent applications below.)

Avail: (US Sales Only). These foreign documents are available to users within the United States from the National Technical Information Service (NTIS). They are available to users outside the United States through the International Nuclear Information Service (INIS) representative in their country, or by applying directly to the issuing organization.

Avail: USGS. Originals of many reports from the U.S. Geological Survey, which may contain color illustrations, or otherwise may not have the quality of illustrations preserved in the microfiche or facsimile reproduction, may be examined by the public at the libraries of the USGS field offices whose addresses are listed in this Introduction. The libraries may be queried concerning the availability of specific documents and the possible utilization of local copying services, such as color reproduction.

Avail: Issuing Activity, or Corporate Author, or no indication of availability. Inquiries as to the availability of these documents should be addressed to the organization shown in the citation as the corporate author of the document.

NASA PATENTS AND PATENT APPLICATIONS

Patents and patent applications owned by NASA are announced in *STAR* under appropriate subject categories and are referenced in the *STAR* indexes. In the Report/Accession Number Index, patents are indexed by the NASA Case Number (which appears in lieu of the report number in other indexes), the U.S. Patent Number, the U.S. Patent Application Serial Number, and the U.S. Patent Class. Patent applications for which patents have not yet been issued are indexed by the NASA Case Number and the U.S. Patent Application Serial Number.

NASA *patent application specifications* are sold in paper copy by the National Technical Information Service at price code A02. Microfiche are sold at price code A01. The US-Patent-Appl-SN- number should be used in ordering either paper copy or microfiche from NTIS. Printed copies of *patents* (which are not microfiched) are available for purchase at $1.50 per copy from:

Commissioner of Patents and Trademarks
U.S. Patent and Trademark Office
Washington, D.C. 20231

When ordering patents, the U.S. Patent Number should be used, and payment must be remitted in advance, preferably by money order or check payable to the Commissioner of Patents and Trademarks. Prepaid purchase coupons for ordering are also available from the Patent and Trademark Office. The patents and patent applications announced in *STAR* are owned by NASA and are available for royalty-free licensing. Requests for licensing terms and further information should be addressed to:

Associate General Counsel for Intellectual Property/Code GP
National Aeronautics and Space Administration
Washington, D.C. 20546

ELIGIBILITY AND REGISTRATION FOR NASA INFORMATION PRODUCTS AND SERVICES

A variety of services is available to organizations of the following types that have registered with NASA to receive specific services or products:

1. NASA offices, research centers, contractors, subcontractors, grantees, and consultants;
2. Other U.S. Government agencies and their contractors;
3. Libraries in the United States that have arrangements with NASA to maintain collections of NASA documents for public reference;
4. Other organizations in the United States having a need for NASA documents in work related to aeronautics and space research;
5. Organizations abroad that have established reciprocal document exchange arrangements with NASA.

Only the central service points or central points of document acquisition and control within qualified organizations are eligible to register for NASA products and services. Domestic organizations that may be eligible to receive various classes of NASA publications and services should address their requests for registration or for further information to:

NASA Scientific and Technical Information Facility
ATTN: Registration Services
Post Office Box 8757
BWI Airport, Maryland 21240

Organizations abroad should direct requests to Manager, International STI Activities, NTT, NASA Headquarters, Washington, D.C. 20546.

AVAILABILITY OF *STAR* ABSTRACTS ON MICROFICHE

Microfiche of the abstract sections of this issue and other issues of *STAR* are available on annual subscription from NTIS as PB89-911300, Attn: Subscriptions, 5285 Port Royal Road, Springfield, Virginia 22161. Annual subscription rates are $70.00 North America; $140.00 foreign. Abstract sections for previous years retroactive to 1964 are available at the current rates. Microfiche for individual *STAR* issue abstract sections are not available.

PUBLIC COLLECTIONS OF NASA DOCUMENTS

DOMESTIC: NASA and NASA-sponsored documents and a large number of aerospace publications are available to the public for reference purposes at the library maintained by the American Institute of Aeronautics and Astronautics, Technical Information Service, 555 West 57th Street, 12th Floor, New York, New York 10019

EUROPEAN: An extensive collection of NASA and NASA-sponsored publications is maintained by the British Library Lending Division, Boston Spa, Wetherby, Yorkshire, England for public access. The British Library Lending Division also has available many of the non-NASA publications cited in *STAR*. European requesters may purchase facsimile copy or microfiche of NASA and NASA-sponsored documents, those identified by both the symbols # and * from ESA - Information Retrieval Service European Space Agency, 8-10 rue Mario-Nikis, 75738 Paris CEDEX 15, France.

FEDERAL DEPOSITORY LIBRARY PROGRAM

In order to provide the general public with greater access to U.S. Government publications, Congress established the Federal Depository Library Program under the Government Printing Office (GPO), with 50 regional depositories responsible for permanent retention of material, inter-library loan, and reference services. At least one copy of nearly every NASA and NASA-sponsored publication, either in printed or microfiche format, is received and retained by the 50 regional depositories. A list of the regional GPO libraries, arranged alphabetically by state, appears on the inside back cover. These libraries are *not* sales outlets. A local library can contact a Regional Depository to help locate specific reports, or direct contact may be made by an individual.

ADDRESSES OF ORGANIZATIONS

American Institute of Aeronautics and Astronautics
Technical Information Service
555 West 57th Street, 12th Floor
New York, New York 10019

British Library Lending Division,
Boston Spa, Wetherby, Yorkshire,
England

Commissioner of Patents and Trademarks
U.S. Patent and Trademark Office
Washington, D.C. 20231

Department of Energy
Technical Information Center
P.O. Box 62
Oak Ridge, Tennessee 37830

ESA-Information Retrieval Service
ESRIN
Via Galileo Galilei
00044 Frascati (Rome) Italy

ESDU International
P.O. Box 1633
Manassas, Virginia 22110

ESDU International, Ltd.
251-259 Regent Street
London, W1R 7AD, England

Fachinformationszentrum Energie, Physik, Mathematik GMBH
7514 Eggenstein Leopoldshafen
Federal Republic of Germany

Her Majesty's Stationery Office
P.O. Box 569, S.E. 1
London, England

NASA Scientific and Technical Information Facility
P.O. Box 8757
B.W.I. Airport, Maryland 21240

National Aeronautics and Space Administration
Scientific and Technical Information Division (NTT)
Washington, D.C. 20546

National Technical Information Service
5285 Port Royal Road
Springfield, Virginia 22161

Pendragon House, Inc.
899 Broadway Avenue
Redwood City, California 94063

Superintendent of Documents
U.S. Government Printing Office
Washington, D.C. 20402

University Microfilms
A Xerox Company
300 North Zeeb Road
Ann Arbor, Michigan 48106

University Microfilms, Ltd.
Tylers Green
London, England

U.S. Geological Survey Library
National Center - MS 950
12201 Sunrise Valley Drive
Reston, Virginia 22092

U.S. Geological Survey Library
2255 North Gemini Drive
Flagstaff, Arizona 86001

U.S. Geological Survey
345 Middlefield Road
Menlo Park, California 94025

U.S. Geological Survey Library
Box 25046
Denver Federal Center, MS914
Denver, Colorado 80225

NTIS PRICE SCHEDULES

(Effective January 1, 1989)

Schedule A
STANDARD PRICE DOCUMENTS AND MICROFICHE

PRICE CODE	NORTH AMERICAN PRICE	FOREIGN PRICE
A01	$ 6.95	$13.90
A02	10.95	21.90
A03	13.95	27.90
A04-A05	15.95	31.90
A06-A09	21.95	43.90
A10-A13	28.95	57.90
A14-A17	36.95	73.90
A18-A21	42.95	85.90
A22-A25	49.95	99.90
A99	*	*
NO1	55.00	70.00
NO2	55.00	80.00

Schedule E
EXCEPTION PRICE DOCUMENTS AND MICROFICHE

PRICE CODE	NORTH AMERICAN PRICE	FOREIGN PRICE
E01	$ 9.00	18.00
E02	11.50	23.00
E03	13.00	26.00
E04	15.50	31.00
E05	17.50	35.00
E06	20.50	41.00
E07	23.00	46.00
E08	25.50	51.00
E09	28.00	56.00
E10	31.00	62.00
E11	33.50	67.00
E12	36.50	73.00
E13	39.00	78.00
E14	42.50	85.00
E15	46.00	92.00
E16	50.50	101.00
E17	54.50	109.00
E18	59.00	118.00
E19	65.50	131.00
E20	76.00	152.00
E99	*	*

*Contact NTIS for price quote.

IMPORTANT NOTICE

NTIS Shipping and Handling Charges

U.S., Canada, Mexico — ADD $3.00 per TOTAL ORDER

All Other Countries — ADD $4.00 per TOTAL ORDER

Exceptions — Does NOT apply to:

ORDERS REQUESTING NTIS RUSH HANDLING
ORDERS FOR SUBSCRIPTION OR STANDING ORDER PRODUCTS *ONLY*

NOTE: Each additional delivery address on an order requires a separate shipping and handling charge.

VOLUME 27 NUMBER 19 / OCTOBER 8, 1989

TABLE OF CONTENTS

AERONAUTICS

Includes aeronautics (general); aerodynamics; air transportation and safety; aircraft communications and navigation; aircraft design, testing and performance; aircraft instrumentation; aircraft propulsion and power; aircraft stability and control; and research and support facilities (air).

For related information see also *Astronautics.*

01 AERONAUTICS (GENERAL) 2659

02 AERODYNAMICS 2659

Includes aerodynamics of bodies, combinations, wings, rotors, and control surfaces; and internal flow in ducts and turbomachinery.

For related information see also *34 Fluid Mechanics and Heat Transfer*

03 AIR TRANSPORTATION AND SAFETY 2663

Includes passenger and cargo air transport operations; and aircraft accidents.

For related information see also *16 Space Transportation* and *85 Urban Technology and Transportation.*

04 AIRCRAFT COMMUNICATIONS AND NAVIGATION 2664

Includes digital and voice communication with aircraft; air navigation systems (satellite and ground based); and air traffic control.

For related information see also *17 Space Communications, Spacecraft Communications, Command and Tracking* and *32 Communications and Radar.*

05 AIRCRAFT DESIGN, TESTING AND PERFORMANCE 2664

Includes aircraft simulation technology.

For related information see also *18 Spacecraft Design, Testing and Performance* and *39 Structural Mechanics.* For land transportation vehicles see *85 Urban Technology and Transportation.*

06 AIRCRAFT INSTRUMENTATION N.A.

Includes cockpit and cabin display devices; and flight instruments.

For related information see also *19 Spacecraft Instrumentation* and *35 Instrumentation and Photography.*

07 AIRCRAFT PROPULSION AND POWER 2680

Includes prime propulsion systems and systems components, e.g., gas turbine engines and compressors; and onboard auxiliary power plants for aircraft.

For related information see also *20 Spacecraft Propulsion and Power, 28 Propellants and Fuels,* and *44 Energy Production and Conversion.*

08 AIRCRAFT STABILITY AND CONTROL 2680

Includes aircraft handling qualities; piloting; flight controls; and autopilots.

For related information see also *05 Aircraft Design, Testing and Performance.*

09 RESEARCH AND SUPPORT FACILITIES (AIR) 2681

Includes airports, hangars and runways; aircraft repair and overhaul facilities; wind tunnels; shock tubes; and aircraft engine test stands.

For related information see also *14 Ground Support Systems and Facilities (Space).*

ASTRONAUTICS

Includes astronautics (general); astrodynamics; ground support systems and facilities (space); launch vehicles and space vehicles; space transportation; space communications, spacecraft communications, command and tracking; spacecraft design, testing and performance; spacecraft instrumentation; and spacecraft propulsion and power.

For related information see also *Aeronautics*

12 ASTRONAUTICS (GENERAL) 2682

For extraterrestrial exploration see *91 Lunar and Planetary Exploration.*

13 ASTRODYNAMICS 2682

Includes powered and free-flight trajectories; and orbital and launching dynamics.

14 GROUND SUPPORT SYSTEMS AND FACILITIES (SPACE) 2683

Includes launch complexes, research and production facilities; ground support equipment, e.g., mobile transporters; and simulators.

For related information see also *09 Research and Support Facilities (Air).*

15 LAUNCH VEHICLES AND SPACE VEHICLES 2683

Includes boosters; operating problems of launch/space vehicle systems; and reusable vehicles.

For related information see also *20 Spacecraft Propulsion and Power.*

16 SPACE TRANSPORTATION 2684

Includes passenger and cargo space transportation, e.g., shuttle operations; and space rescue techniques.

For related information see also *03 Air Transportation and Safety* and *18 Spacecraft Design, Testing and Performance.* For space suits see *54 Man/System Technology and Life Support.*

17 SPACE COMMUNICATIONS, SPACECRAFT COMMUNICATIONS, COMMAND AND TRACKING N.A.

Includes telemetry; space communications networks; astronavigation and guidance; and radio blackout.

For related information see also *04 Aircraft Communications and Navigation* and *32 Communications and Radar.*

18 SPACECRAFT DESIGN, TESTING AND PERFORMANCE 2685

Includes satellites; space platforms; space stations; spacecraft systems and components such as thermal and environmental controls; and attitude controls.

For life support systems see *54 Man/System Technology and Life Support.* For related information see also *05 Aircraft Design, Testing and Performance, 39 Structural Mechanics,* and *16 Space Transportation.*

19 SPACECRAFT INSTRUMENTATION N.A.

For related information see also *06 Aircraft Instrumentation* and *35 Instrumentation and Photography.*

20 SPACECRAFT PROPULSION AND POWER 2687

Includes main propulsion systems and components, e.g. rocket engines; and spacecraft auxiliary power sources.

For related information see also *07 Aircraft Propulsion and Power, 28 Propellants and Fuels, 44 Energy Production and Conversion,* and *15 Launch Vehicles and Space Vehicles.*

CHEMISTRY AND MATERIALS

Includes chemistry and materials (general); composite materials; inorganic and physical chemistry; metallic materials; nonmetallic materials; propellants and fuels; and materials processing.

23 CHEMISTRY AND MATERIALS (GENERAL) 2690

24 COMPOSITE MATERIALS 2690

Includes physical, chemical, and mechanical properties of laminates and other composite materials.

For ceramic materials see *27 Nonmetallic Materials.*

25 INORGANIC AND PHYSICAL CHEMISTRY 2693

Includes chemical analysis, e.g., chromatography; combustion theory; electrochemistry; and photochemistry.

For related information see also *77 Thermodynamics and Statistical Physics.*

26 METALLIC MATERIALS 2694

Includes physical, chemical, and mechanical properties of metals, e.g., corrosion; and metallurgy.

27 NONMETALLIC MATERIALS 2698

Includes physical, chemical, and mechanical properties of plastics, elastomers, lubricants, polymers, textiles, adhesives, and ceramic materials.

For composite materials see *24 Composite Materials.*

28 PROPELLANTS AND FUELS 2701

Includes rocket propellants, igniters and oxidizers; their storage and handling procedures; and aircraft fuels.

For related information see also *07 Aircraft Propulsion and Power, 20 Spacecraft Propulsion and Power,* and *44 Energy Production and Conversion.*

29 MATERIALS PROCESSING 2701

Includes space-based development of products and processes for commercial application.

For biological materials see *55 Space Biology.*

ENGINEERING

Includes engineering (general); communications and radar; electronics and electrical engineering; fluid mechanics and heat transfer; instrumentation and photography; lasers and masers; mechanical engineering; quality assurance and reliability; and structural mechanics.

For related information see also *Physics.*

31 ENGINEERING (GENERAL) 2702

Includes vacuum technology; control engineering; display engineering; cryogenics; and fire prevention.

32 COMMUNICATIONS AND RADAR 2703

Includes radar; land and global communications; communications theory; and optical communications.

For related information see also *04 Aircraft Communications and Navigation* and *17 Space Communications, Spacecraft Communications, Command and Tracking.* For search and rescue see *03 Air Transportation and Safety,* and *16 Space Transportation.*

33 ELECTRONICS AND ELECTRICAL ENGINEERING 2707

Includes test equipment and maintainability; components, e.g., tunnel diodes and transistors; microminiaturization; and integrated circuitry.

For related information see also *60 Computer Operations and Hardware* and *76 Solid-State Physics.*

34 FLUID MECHANICS AND HEAT TRANSFER 2710

Includes boundary layers; hydrodynamics; fluidics; mass transfer and ablation cooling.

For related information see also *02 Aerodynamics* and *77 Thermodynamics and Statistical Physics.*

35 INSTRUMENTATION AND PHOTOGRAPHY 2715

includes remote sensors; measuring instruments and gages; detectors; cameras and photographic supplies; and holography.

For aerial photography see *43 Earth Resources and Remote Sensing.* For related information see also *06 Aircraft Instrumentation* and *19 Spacecraft Instrumentation.*

36 LASERS AND MASERS 2718

Includes parametric amplifiers.

For related information see also *76 Solid-State Physics.*

37 MECHANICAL ENGINEERING 2719

Includes auxiliary systems (nonpower); machine elements and processes; and mechanical equipment.

38 QUALITY ASSURANCE AND RELIABILITY 2722

Includes product sampling procedures and techniques; and quality control.

39 STRUCTURAL MECHANICS 2723

Includes structural element design and weight analysis; fatigue; and thermal stress.

For applications see *05 Aircraft Design, Testing and Performance* and *18 Spacecraft Design, Testing and Performance.*

GEOSCIENCES

Includes geosciences (general); earth resources and remote sensing; energy production and conversion; environment pollution; geophysics; meteorology and climatology; and oceanography.

For related information see also *Space Sciences.*

42 GEOSCIENCES (GENERAL) **N.A.**

43 EARTH RESOURCES AND REMOTE SENSING **2727**

Includes remote sensing of earth resources by aircraft and spacecraft; photogrammetry; and aerial photography.

For instrumentation see *35 Instrumentation and Photography.*

44 ENERGY PRODUCTION AND CONVERSION **2729**

Includes specific energy conversion systems, e.g., fuel cells; global sources of energy; geophysical conversion; and windpower.

For related information see also *07 Aircraft Propulsion and Power, 20 Spacecraft Propulsion and Power,* and *28 Propellants and Fuels.*

45 ENVIRONMENT POLLUTION **2732**

Includes atmospheric, noise, thermal, and water pollution.

46 GEOPHYSICS **2734**

Includes aeronomy; upper and lower atmosphere studies; ionospheric and magnetospheric physics; and geomagnetism.

For space radiation see *93 Space Radiation.*

47 METEOROLOGY AND CLIMATOLOGY **2737**

Includes weather forecasting and modification.

48 OCEANOGRAPHY **2739**

Includes biological, dynamic, and physical oceanography; and marine resources.

For related information see also *43 Earth Resources and Remote Sensing.*

LIFE SCIENCES

Includes life sciences (general); aerospace medicine; behavioral sciences; man/system technology and life support; and space biology.

51 LIFE SCIENCES (GENERAL) **2739**

52 AEROSPACE MEDICINE **2740**

Includes physiological factors; biological effects of radiation; and effects of weightlessness on man and animals.

53 BEHAVIORAL SCIENCES **2741**

Includes psychological factors; individual and group behavior; crew training and evaluation; and psychiatric research.

54 MAN/SYSTEM TECHNOLOGY AND LIFE SUPPORT **2741**

Includes human engineering; biotechnology; and space suits and protective clothing.

For related information see also *16 Space Transportation.*

55 SPACE BIOLOGY **N.A.**

Includes exobiology; planetary biology; and extraterrestrial life.

MATHEMATICAL AND COMPUTER SCIENCES

Includes mathematical and computer sciences (general); computer operations and hardware; computer programming and software; computer systems; cybernetics; numerical analysis; statistics and probability; systems analysis; and theoretical mathematics.

59 MATHEMATICAL AND COMPUTER SCIENCES (GENERAL) **N.A.**

60 COMPUTER OPERATIONS AND HARDWARE **2742**

Includes hardware for computer graphics, firmware, and data processing.

For components see *33 Electronics and Electrical Engineering.*

61 COMPUTER PROGRAMMING AND SOFTWARE **2743**

Includes computer programs, routines, algorithms, and specific applications, e.g., CAD/CAM.

62 COMPUTER SYSTEMS **2749**

Includes computer networks and special application computer systems.

63 CYBERNETICS **2752**

Includes feedback and control theory, artificial intelligence, robotics and expert systems.

For related information see also *54 Man/System Technology and Life Support.*

64 NUMERICAL ANALYSIS **2754**

Includes iteration, difference equations, and numerical approximation.

65 STATISTICS AND PROBABILITY **2757**

Includes data sampling and smoothing; Monte Carlo method; and stochastic processes.

66 SYSTEMS ANALYSIS **N.A.**

Includes mathematical modeling; network analysis; and operations research.

67 THEORETICAL MATHEMATICS **2757**

Includes topology and number theory.

PHYSICS

Includes physics (general); acoustics; atomic and molecular physics; nuclear and high-energy physics; optics; plasma physics; solid-state physics; and thermodynamics and statistical physics.

For related information see also *Engineering.*

70 PHYSICS (GENERAL) **2757**

For precision time and time interval (PTTI) see *35 Instrumentation and Photography;* for geophysics, astrophysics or solar physics see *46 Geophysics, 90 Astrophysics,* or *92 Solar Physics.*

71 ACOUSTICS 2758
Includes sound generation, transmission, and attenuation.
For noise pollution see *45 Environment Pollution.*

72 ATOMIC AND MOLECULAR PHYSICS 2760
Includes atomic structure, electron properties, and molecular spectra.

73 NUCLEAR AND HIGH-ENERGY PHYSICS 2761
Includes elementary and nuclear particles; and reactor theory.
For space radiation see *93 Space Radiation.*

74 OPTICS 2761
Includes light phenomena and optical devices.
For lasers see *36 Lasers and Masers.*

75 PLASMA PHYSICS 2763
Includes magnetohydrodynamics and plasma fusion.
For ionospheric plasmas see *46 Geophysics.* For space plasmas see *90 Astrophysics.*

76 SOLID-STATE PHYSICS 2768
Includes superconductivity.
For related information see also *33 Electronics and Electrical Engineering* and *36 Lasers and Masers.*

77 THERMODYNAMICS AND STATISTICAL PHYSICS 2772
Includes quantum mechanics; theoretical physics; and Bose and Fermi statistics.
For related information see also *25 Inorganic and Physical Chemistry* and *34 Fluid Mechanics and Heat Transfer.*

SOCIAL SCIENCES

Includes social sciences (general); administration and management; documentation and information science; economics and cost analysis; law, political science, and space policy; and urban technology and transportation.

80 SOCIAL SCIENCES (GENERAL) N.A.
Includes educational matters.

81 ADMINISTRATION AND MANAGEMENT 2773
Includes management planning and research.

82 DOCUMENTATION AND INFORMATION SCIENCE 2774
Includes information management; information storage and retrieval technology; technical writing; graphic arts; and micrography.
For computer documentation see *61 Computer Programming and Software.*

83 ECONOMICS AND COST ANALYSIS N.A.
Includes cost effectiveness studies.

84 LAW, POLITICAL SCIENCE AND SPACE POLICY 2775
Includes NASA appropriation hearings; aviation law; space law and policy; international law; international cooperation; and patent policy.

85 URBAN TECHNOLOGY AND TRANSPORTATION N.A.
Includes applications of space technology to urban problems; technology transfer; technology assessment; and surface and mass transportation.
For related information see *03 Air Transportation and Safety, 16 Space Transportation,* and *44 Energy Production and Conversion.*

SPACE SCIENCES

Includes space sciences (general); astronomy; astrophysics; lunar and planetary exploration; solar physics; and space radiation.
For related information see also *Geosciences.*

88 SPACE SCIENCES (GENERAL) N.A.

89 ASTRONOMY N.A.
Includes radio, gamma-ray, and infrared astronomy; and astrometry.

90 ASTROPHYSICS 2777
Includes cosmology; celestial mechanics; space plasmas; and interstellar and interplanetary gases and dust.
For related information see also *75 Plasma Physics.*

91 LUNAR AND PLANETARY EXPLORATION 2779
Includes planetology; and manned and unmanned flights.
For spacecraft design or space stations see *18 Spacecraft Design, Testing and Performance.*

92 SOLAR PHYSICS 2783
Includes solar activity, solar flares, solar radiation and sunspots.
For related information see *93 Space Radiation.*

93 SPACE RADIATION N.A.
Includes cosmic radiation; and inner and outer earth's radiation belts.
For biological effects of radiation see *52 Aerospace Medicine.* For theory see *73 Nuclear and High-Energy Physics.*

GENERAL

Includes aeronautical, astronautical, and space science related histories, biographies, and pertinent reports too broad for categorization; histories or broad overviews of NASA programs.

99 GENERAL 2802

Note: N.A. means that no abstracts were assigned to this category for this issue.

SUBJECT INDEX I-1
PERSONAL AUTHOR INDEX I-49
CORPORATE SOURCE INDEX I-57
CONTRACT NUMBER INDEX I-67
REPORT/ACCESSION NUMBER INDEX I-69

TYPICAL CITATION AND ABSTRACT

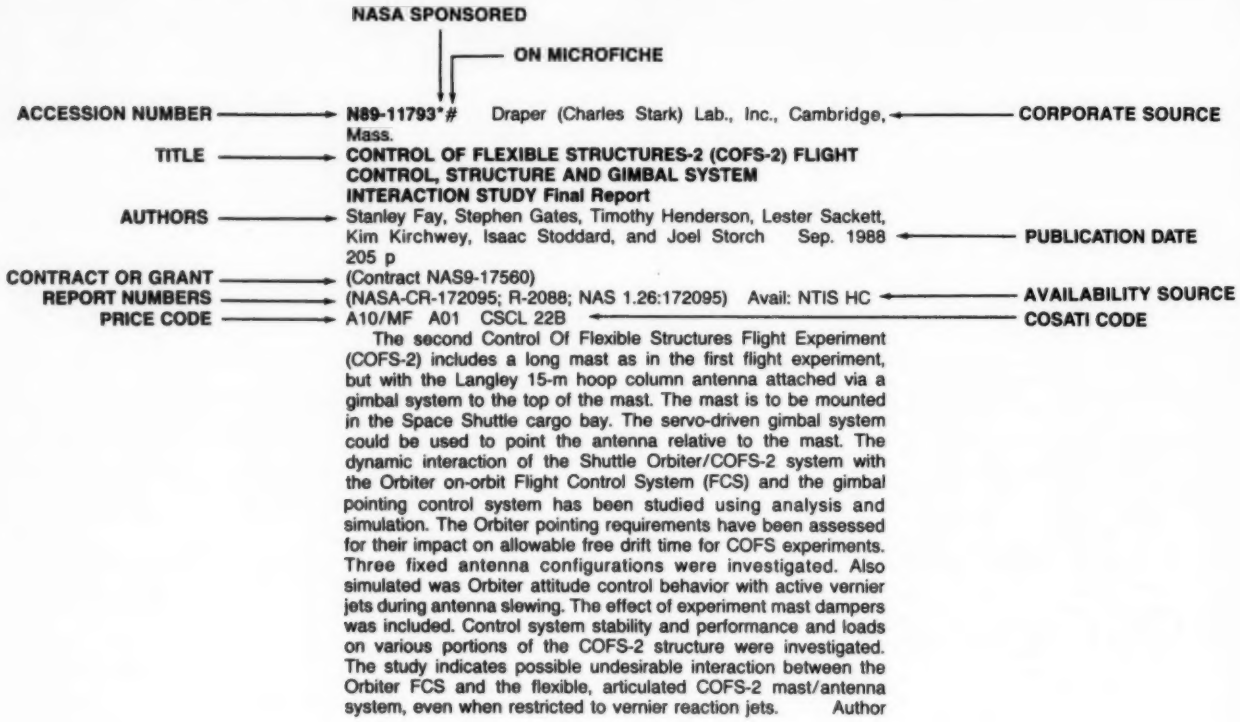
NASA SPONSORED
ON MICROFICHE
ACCESSION NUMBER
N89-11793*# Draper (Charles Stark) Lab., Inc., Cambridge, Mass.
CORPORATE SOURCE
TITLE
CONTROL OF FLEXIBLE STRUCTURES-2 (COFS-2) FLIGHT CONTROL, STRUCTURE AND GIMBAL SYSTEM INTERACTION STUDY Final Report
AUTHORS
Stanley Fay, Stephen Gates, Timothy Henderson, Lester Sackett, Kim Kirchwey, Isaac Stoddard, and Joel Storch Sep. 1988
PUBLICATION DATE
205 p
CONTRACT OR GRANT
(Contract NAS9-17560)
REPORT NUMBERS
(NASA-CR-172095; R-2088; NAS 1.26:172095) Avail: NTIS HC
AVAILABILITY SOURCE
PRICE CODE
A10/MF A01 CSCL 22B
COSATI CODE
The second Control Of Flexible Structures Flight Experiment (COFS-2) includes a long mast as in the first flight experiment, but with the Langley 15-m hoop column antenna attached via a gimbal system to the top of the mast. The mast is to be mounted in the Space Shuttle cargo bay. The servo-driven gimbal system could be used to point the antenna relative to the mast. The dynamic interaction of the Shuttle Orbiter/COFS-2 system with the Orbiter on-orbit Flight Control System (FCS) and the gimbal pointing control system has been studied using analysis and simulation. The Orbiter pointing requirements have been assessed for their impact on allowable free drift time for COFS experiments. Three fixed antenna configurations were investigated. Also simulated was Orbiter attitude control behavior with active vernier jets during antenna slewing. The effect of experiment mast dampers was included. Control system stability and performance and loads on various portions of the COFS-2 structure were investigated. The study indicates possible undesirable interaction between the Orbiter FCS and the flexible, articulated COFS-2 mast/antenna system, even when restricted to vernier reaction jets. Author

VOLUME 27 NUMBER 19 / OCTOBER 8, 1989

Scientific and Technical Aerospace Reports

A Semimonthly Publication of the National Aeronautics and Space Administration

01 AERONAUTICS (GENERAL)

N89-25113# Federal Aviation Administration, Washington, DC. Office of Management Systems.
FAA STATISTICAL HANDBOOK OF AVIATION: CALENDAR YEAR 1987
1987 212 p
(AD-A200917) Avail: NTIS HC A10/MF A01 CSCL 01/3

Statistical information is presented pertaining to the Federal Aviation Administration, the National Airspace System, Airports, Airport Activity, U.S. Civil Air Carrier Fleet, U.S. Civil Air Carrier Operating Data, Airmen, General Aviation Aircraft, Aircraft Accidents, Aeronautical Production and Imports/Exports. A Glossary of the terms used in this publication is contained. GRA

N89-25114* National Aeronautics and Space Administration, Washington, DC.
AERONAUTICAL ENGINEERING: A CONTINUING BIBLIOGRAPHY WITH INDEXES (SUPPLEMENT 239)
Dec. 1988 124 p
(NASA-SP-7037(239); NAS 1.21:7037(239)) Avail: NTIS HC A08; NTIS standing order as PB89-914100, $10.50 domestic, $21.00 foreign CSCL 01A

This bibliography lists 454 reports, articles, and other documents introduced into the NASA scientific and technical information system in April, 1989. Subject coverage includes: design, construction and testing of aircraft and aircraft engines; aircraft components, equipment and systems; ground support systems; and theoretical and applied aspects of aerodynamics and general fluid dynamics. Author

N89-25115* National Aeronautics and Space Administration, Washington, DC.
AERONAUTICAL ENGINEERING: A CONTINUING BIBLIOGRAPHY WITH INDEXES (SUPPLEMENT 240)
Jun. 1989 167 p
(NASA-SP-7037(240); NAS 1.21:7037(240)) Avail: NTIS HC A08; NTIS standing order as PB89-914100, $10.50 domestic, $21.00 foreign CSCL 01A

This bibliography lists 629 reports, articles, and other documents introduced into the NASA scientific and technical information system in May, 1989. Subject coverage includes: design, construction and testing of aircraft and aircraft engines; aircraft components, equipment and systems; ground support systems; and theoretical and applied aspects of aerodynamics and general fluid dynamics. Author

N89-25116*# National Aeronautics and Space Administration. Ames Research Center, Moffett Field, CA.
THE 3DGRAPE BOOK: THEORY, USERS' MANUAL, EXAMPLES
Reese L. Sorenson Jul. 1989 122 p
(NASA-TM-102224; A-89176; NAS 1.15:102224) Avail: NTIS HC A06/MF A01 CSCL 01B

A users' manual for a new three-dimensional grid generator called 3DGRAPE is presented. The program, written in FORTRAN, is capable of making zonal (blocked) computational grids in or about almost any shape. Grids are generated by the solution of Poisson's differential equations in three dimensions. The program automatically finds its own values for inhomogeneous terms which give near-orthogonality and controlled grid cell height at boundaries. Grids generated by 3DGRAPE have been applied to both viscous and inviscid aerodynamic problems, and to problems in other fluid-dynamic areas. The smoothness for which elliptic methods are known is seen here, including smoothness across zonal boundaries. An introduction giving the history, motivation, capabilities, and philosophy of 3DGRAPE is presented first. Then follows a chapter on the program itself. The input is then described in detail. A chapter on reading the output and debugging follows. Three examples are then described, including sample input data and plots of output. Last is a chapter on the theoretical development of the method. Author

02 AERODYNAMICS

Includes aerodynamics of bodies, combinations, wings, rotors, and control surfaces; and internal flow in ducts and turbomachinery.

For related information see also *34 Fluid Mechanics and Heat Transfer.*

N89-25117*# National Aeronautics and Space Administration. Langley Research Center, Hampton, VA.
EFFECT OF MILLING MACHINE ROUGHNESS AND WING DIHEDRAL ON THE SUPERSONIC AERODYNAMIC CHARACTERISTICS OF A HIGHLY SWEPT WING
Christine M. Darden Washington Aug. 1989 88 p
(NASA-TP-2918; L-16546; NAS 1.60:2918) Avail: NTIS HC A05/MF A01 CSCL 01A

An experimental investigation was conducted to assess the effect of surface finish on the longitudinal and lateral aerodynamic characteristics of a highly-swept wing at supersonic speeds. A study of the effects of wing dihedral was also made. Included in the tests were four wing models: three models having 22.5 degrees of outboard dihedral, identical except for surface finish, and a zero-dihedral, smooth model of the same planform for reference. Of the three dihedral models, two were taken directly from the milling machine without smoothing: one having a maximum scallop height of 0.002 inches and the other a maximum scallop height of 0.005 inches. The third dihedral model was handfinished to a smooth surface. Tests were conducted in Test Section 1 of the Unitary Plan Wind Tunnel at NASA-Langley over a range of Mach numbers from 1.8 to 2.8, a range of angle of attack from -5 to 8 degrees, and at a Reynolds numbers per foot of 2 x 10(6). Selected data were also taken at a Reynolds number per foot of 6 x 10(6). Drag coefficient increases, with corresponding lift-drag ratio decreases were the primary aerodynamic effects attributed to increased surface roughness due to milling machine grooves. These drag and lift-drag ratio increments due to roughness increased as Reynolds number increased. Author

N89-25118*# National Aeronautics and Space Administration. Langley Research Center, Hampton, VA.
INTERACTIONS OF TOLLMIEN-SCHLICHTING WAVES AND DEAN VORTICES. COMPARISON OF DIRECT NUMERICAL SIMULATION AND A WEAKLY NONLINEAR THEORY
Bart A. Singer (High Technology Corp., Hampton, VA.) and Thomas

A. Zang Washington Aug. 1989 21 p
(NASA-TP-2919; L-16559; NAS 1.60:2919) Avail: NTIS HC A03/MF A01 CSCL 01A

Direct numerical simulation is used to evaluate a weakly nonlinear theory describing the interaction of Tollmien-Schlichting waves with Dean vortices in curved channel flow. The theory and the simulation agree for certain combinations of parameters, but the two approaches give conflicting results for other combinations. Some possibilities for these discrepancies are discussed. Author

N89-25119*# National Aeronautics and Space Administration. Lewis Research Center, Cleveland, OH.

NUMERICAL ANALYSIS OF SUPERSONIC FLOW THROUGH OSCILLATING CASCADE SECTIONS BY USING A DEFORMING GRID

Dennis L. Huff and T. S. R. Reddy (Toledo Univ., OH.) 1989 18 p Presented at the 25th Joint Propulsion Conference, Monterey, CA, 10-12 Jul. 1989; cosponsored by the AIAA, ASME, SAE and ASEE
(NASA-TM-102053; E-4805; NAS 1.15:102053; AIAA-89-2805)
Avail: NTIS HC A03/MF A01 CSCL 01A

A finite difference code was developed for modeling inviscid, unsteady supersonic flow by solution of the compressible Euler equations. The code uses a deforming grid technique to capture the motion of the airfoils and can model oscillating cascades with any arbitrary interblade phase angle. A flat plate cascade is analyzed, and results are compared with results from a small-perturbation theory. The results show very good agreement for both the unsteady pressure distributions and the integrated force predictions. The reason for using the numerical Euler code over a small-perturbation theory is the ability to model real airfoils that have thickness and camber. Sample predictions are presented for a section of the rotor on a supersonic throughflow compressor designed at NASA Lewis Research Center. Preliminary results indicate that two-dimensional, flat plate analysis predicts conservative flutter boundaries. Author

N89-25120 Virginia Polytechnic Inst. and State Univ., Blacksburg.

TECHNIQUES FOR COMPRESSIBLE FLOW CALCULATIONS ON MULTIZONE GRIDS Ph.D. Thesis

Taekyu Reu 1988 132 p
Avail: Univ. Microfilms Order No. DA8904994

In order to simulate inviscid/viscous compressible flowfields about 3-D realistic aerodynamic bodies, the combined use of an implicit, upwind biased real gas scheme with 3-D fully conservative patched grid techniques is discussed. An equivalent gamma formulation is implemented in order to model real gas effects in Van Leer's flux vector splitting (FVS) and Roe's flux difference splitting (FDS) scheme. A hybrid approximate-factorization (AF)/relaxation algorithm is used as an efficient solver of the Euler, parabolized Navier-Stokes, and thin-layer Navier-Stokes equations. Two different approaches, clipping and Ramshaw's rezoning algorithms, for performing a conservative flux calculation are described and compared in terms of numerical efficiency. In order to show the real gas effects in the upwind schemes, two test problems are solved. Also to demonstrate the capability of the patched grid approach, the turbulent flowfield about 3-D analytic forebody is calculated as another test problem. Due to the poor results of the Baldwin-Lomax turbulent model for separated flows, only the attached flowfield is considered in the analytic forebody calculation. Finally, as applications of this approach, the inviscid/viscous flowfields about several aerodynamic bodies are calculated including a generic hypersonic aircraft, a model of the SR-71 aircraft, and F-18 forebody with strakes. Dissert. Abstr.

N89-25121*# National Aeronautics and Space Administration. Lewis Research Center, Cleveland, OH.

LOW-SPEED WIND TUNNEL PERFORMANCE OF HIGH-SPEED COUNTERROTATION PROPELLERS AT ANGLE-OF-ATTACK

Christopher E. Hughes and John A. Gazzaniga (Sverdrup Technology, Inc., Cleveland, OH.) 1989 47 p Presented at the 25th Joint Propulsion Conference, Monterey, CA, 10-12 Jul. 1989; cosponsored in part by AIAA, ASME, SAE, and ASEE
(NASA-TM-102292; E-4883; NAS 1.15:102292; AIAA-89-2583)
Avail: NTIS HC A03/MF A01 CSCL 01A

The low-speed aerodynamic performance characteristics of two advanced counterrotation pusher-propeller configurations with cruise design Mach numbers of 0.72 were investigated in the NASA Lewis 9- by 15-Foot Low-Speed Wind Tunnel. The tests were conducted at Mach number 0.20, which is representative of the aircraft take-off/landing flight regime. The investigation determined the effect of nonuniform inflow on the propeller performance characteristics for several blade angle settings and a range of rotational speeds. The inflow was varied by yawing the propeller model to angle-of-attack by as much as plus or minus 16 degrees and by installing on the counterrotation propeller test rig near the propeller rotors a model simulator of an aircraft engine support pylon and fuselage. The results of the investigation indicated that the low-speed performance of the counterrotation propeller configurations near the take-off target operating points were reasonable and were fairly insensitive to changes in model angle-of-attack without the aircraft pylon/fuselage simulators installed on the propeller test rig. When the aircraft pylon/fuselage simulators were installed, small changes in propeller performance were seen at zero angle-of-attack, but fairly large changes in total power coefficient and very large changes of aft-to-forward-rotor torque ratio were produced when the propeller model was taken to angle-of-attack. The propeller net efficiency, though, was fairly insensitive to any changes in the propeller flowfield conditions near the take-off target operating points. Author

N89-25122*# Kansas Univ. Center for Research, Inc., Lawrence.

SPANWISE LIFT DISTRIBUTIONS AND WAKE VELOCITY SURVEYS OF A SEMI-SPAN WING WITH A DISCONTINUOUS TWIST

Hiroyuki Kumagai May 1989 208 p
(Contract NCC2-175)
(NASA-CR-177532; NAS 1.26:177532) Avail: NTIS HC A10/MF A01 CSCL 01A

A wind tunnel test was conducted in the NASA-Ames 7 x 10 ft wind tunnel to investigate the lift distribution on a semispan wing with a discontinuous change in spanwise twist. The semispan wing had a tip with an adjustable pitch angle independent on the inboard section pitch angle simulating the free tip rotor blade when its free tip is at a deflected position. The spanwise lift distribution over the wing and the tip were measured and three component velocity surveys behind the wing were obtained with a 3-D laser Doppler velocimeter (LV) with the wing at one angle of attack and the tip deflected at different pitch angles. A six-component internal strain gage balance was also used to measure total forces and moments on the tip. The 3-D lift was computed from the 2-D lift distributions obtained from the LV and from the strain gage balance. The results from both experimental methods are shown to be in agreement with predictions made by a steady, 3-D panel code, VSAERO. Author

N89-25123*# Institute for Computer Applications in Science and Engineering, Hampton, VA.

ON THE GORTLER VORTEX INSTABILITY MECHANISM AT HYPERSONIC SPEEDS Final Report

Philip Hall and Yibin Fu (Exeter Univ., England) May 1989 28 p Prepared in cooperation with NASA. Langley Research Center, Hampton, VA Submitted for publication
(Contract NAS1-18605)
(NASA-CR-181844; ICASE-89-23; NAS 1.26:181844) Avail: NTIS HC A03/MF A01 CSCL 01A

The linear instability of the hypersonic boundary layer on a curved wall is considered. As a starting point the viscosity of the fluid is taken to be a linear function of temperature and real-gas effects are ignored. It is shown that the flow is susceptible to Gortler vortices and that they are trapped in the logarithmically thin adjustment layer in which the temperature of the basic flow changes rapidly to its free stream value. The vortices decay exponentially in both directions away from this layer and are most

unstable when their wavelength is comparable with the depth of the adjustment layer. The non-uniqueness of the neutral stability curve associated with incompressible Gortler vortices is shown to disappear at high Mach numbers if the appropriate fast streamwise dependence of the instability is built into the disturbance flow structure. It is shown that in the hypersonic limit wall-cooling has a negligible effect on the stability of a fluid with a given value of the Chapman constant. Author

N89-25124*# National Aeronautics and Space Administration. Langley Research Center, Hampton, VA.
FREE-MOLECULE-FLOW FORCE AND MOMENT COEFFICIENTS OF THE AEROASSIST FLIGHT EXPERIMENT VEHICLE
Robert C. Blanchard and Edwin W. Hinson (ST Systems Corp., Hampton, VA.) Jul. 1989 25 p
(NASA-TM-101600; NAS 1.15:101600) Avail: NTIS HC A03/MF A01 CSCL 01A

Calculated results for the aerodynamic coefficients over the range of + or - 90 deg in both pitch and yaw attitude angles for the Aeroassist Flight Experiment (AFE) vehicle in free molecule flow are presented. The AFE body is described by a large number of small flat plate surface elements whose orientations are established in a wind axes coordinate system through the pitch and yaw attitude angles. Lift force, drag force, and three components of aerodynamic moment about a specified point are computed for each element. The elemental forces and moments are integrated over the entire body, and total force and moment coefficients are computed. The coefficients are calculated for the two limiting gas-surface molecular collision conditions, namely, specular and diffuse, which assume zero and full thermal accommodation of the incoming gas molecules with the surface, respectively. The individual contribution of the shear stress and pressure terms are calculated and also presented. Author

N89-25125# Deutsche Forschungs- und Versuchsanstalt fuer Luft- und Raumfahrt, Goettingen (Germany, F.R.). Abteilung Instationaere Aerodynamik.
TWO-DIMENSIONAL ELLIPTIC GRID GENERATION FOR AIRFOILS AND CASCADES
Volker Carstens Dec. 1988 77 p
(DFVLR-FB-88-52; ISSN-0171-1342; ETN-89-94638) Avail: NTIS HC A05/MF A01; DFVLR, VB-PL-DO, Postfach 90 60 58, 5000 Cologne, Fed. Republic of Germany, DM 28.50

Based on the solution of two coupled transformed Poisson equations, a method to generate two-dimensional grids for airfoils and cascades is presented. With the method it is possible to control line spacing and intersection angle of the grid lines at the physical boundaries by a particular choice of inhomogeneous terms in the Poisson equations. The numerical solution of the grid generating equations is performed by a Newton relaxation algorithm which significantly improves stability and convergence of the numerical solution compared to the classical SLOR method. Examples of airfoil and cascade grids demonstrate the efficiency of the existing procedure. ESA

N89-25126# Technische Hochschule, Aachen (Germany, F.R.). Sonderforschungsbereich 25.
VORTEX FLOWS IN FLYING TECHNIQUE [WIRBELSTROEMUNGEN IN DER FLUGTECHNIK]
1988 378 p In GERMAN IUTAM Symposium: On Fundamental Aspects of Vortex Motion held in 1987
(ETN-89-94428) Avail: NTIS HC A17/MF A01

Flows with free vortices were investigated by the integration of the conservation equations. The mechanisms leading to vortex breakdown were clarified. Velocity fields in vortex structures were measured. Strongly unsteady vortex fields at elastic helicopter rotor blades were studied. The interaction between compression shocks and vertical flows, the dissipation of vortex power in longitudinal flow on wings, and vortex structures in the wake of transonic flow about profiles were investigated. Flow field changes of wing profiles in unsteady flow and unsteady flow on profiles in a liquid tunnel are treated. The effect of winglets on the loading mechanics and wing assembly reactions and the reduction of the adverse effects of wing tip vortices by modifying the wing tips were studied. For individual titles, see N89-25127 through N89-25141.

N89-25127# Technische Hochschule, Aachen (Germany, F.R.).
INTEGRATION METHOD FOR THE CALCULATION OF FLOW WITH FREE VORTICES [INTEGRATIONSVERFAHREN ZUR BERECHNUNG VON STROEMUNGEN MIT FREIEN WIRBELN]
S. Menne and M. Breuer *In its* Vortex Flows in Flying Technique 1988 p 5-16 In GERMAN (For primary document see N89-25126 19-02)
Avail: NTIS HC A17/MF A01

Flows with free vortices were investigated by the investigation of the conservation equations. The approximation of stender vortices is especially suited for predictions concerning the amplitude of the flow parameters responsible for a vortex breakdown and concerning the breakdown length. The solution of the complete Navier-Stokes equations allows predictions concerning the global flow field of a broken-down vortex and hence concerning the internal structure of the breakdown bubble. The essential assumption for both numerical simulations is axisymmetry. To give up this assumption requires the solution of the three-dimensional time-dependent Navier-Stokes equations and hence a very large numerical effort. ESA

N89-25128# Technische Hochschule, Aachen (Germany, F.R.).
INVESTIGATIONS OF VORTEX BREAKDOWN [UNTERSUCHUNGEN ZUM AUFPLATZEN VON WIRBELN]
Th. Helming *In its* Vortex Flows in Flying Technique 1988 p 17-40 In GERMAN (For primary document see N89-25126 19-02)
Avail: NTIS HC A17/MF A01

Contributions to clarify the mechanisms leading to vortex breakdown were made. Based on Leibovich criterion for vortex flow instability, a general sufficient condition for vortex instability was deduced. In order to assess if vortex instability is a sufficient condition for breakdown, the stability limit was determined and confirmed by laser Doppler anemometry and optical observations. Instability is found not to be sufficient for breakdown. A simulation model shows how far the observed, small, almost helical perturbations of the vortex orbit in the instability domain lead to self-destruction by self-induction. The experimentally observed increasing liability to interference for enhanced vortex circulation was simulated. ESA

N89-25129# Technische Hochschule, Aachen (Germany, F.R.).
UNSTEADY PHENOMENA ON DELTA WINGS WITH PARTIALLY BROKEN-DOWN VORTEX REGIONS [INSTATIONAERE VORGAENGE AN DELTAFLUEGELN MIT TEILWEISE AUFGEPLATZTEN WIRBELBEREICHEN]
Bernd Steckemetz *In its* Vortex Flows in Flying Technique 1988 p 41-68 In GERMAN (For primary document see N89-25126 19-02)
Avail: NTIS HC A17/MF A01

Delta wings were investigated in water and wind tunnels to clarify unsteady flow phenomena in the vortex system of the delta wing occurring during wing maneuvers and in gust fields. The investigations in the water tunnel concentrated on the visualization of the leading vortex; the pictures show the temporal shift of the vortex and breakdown positions for the different test parameters. The pressure distribution measurements in the subsonic wind tunnel can be directly compared with the water tunnel test data, while the force and moment measurements in steady flow provide data on the total wing. Assuming quasi-stationarity, the effects of breakdown and heading phenomena on the force and moment balance of the wing were assessed using the coupled water and wind tunnel data, and verified by unsteady force and moment measurements. ESA

N89-25130# Technische Hochschule, Aachen (Germany, F.R.).
MEASUREMENT OF VELOCITY FIELDS IN VORTEX STRUCTURES [MESSUNG VON GESCHWINDIGKEITSFELDERN BEI WIRBELSTRUKTUREN]
R. M. Oebels and H. St. Buchkremer *In its* Vortex Flows in Flying Technique 1988 p 69-87 In GERMAN (For primary document see N89-25126 19-02)
Avail: NTIS HC A17/MF A01

The quantitative determination of velocity structures in a decaying vortex was studied. The measurements were performed as a clean flow experiment, i.e., in an apparatus producing a reproducable model vortex. Using holographically produced optical elements, the spatial correlation between velocities was determined by laser Doppler anemometry (LDA). It is observed that vortex breakdown is not spatially stationary, but is subject to random changes in location in axial direction. Therefore, the short-time measuring methods, laser speckle and double-pulse holography, are more suitable for the determination of the velocity field; however, the data processing problems are not fully solved. The time-averaging LDA method is redesigned as a short-time method to allow the measurement of cross sections in the vortex in a shorter time than any temporal drift of the vortex breakdown. ESA

N89-25131# Technische Hochschule, Aachen (Germany, F.R.).
STRONGLY UNSTEADY VORTEX FIELDS AT ELASTIC HELICOPTER ROTOR BLADES [STARK INSTATIONAERE WIRBELFELDER AN ELASTISCHEN HUBSCHRAUBERROTORBLAETTERN]
K. Gruenspahn *In its* Vortex Flows in Flying Technique 1988 p 89-113 In GERMAN (For primary document see N89-25126 19-02)
Avail: NTIS HC A17/MF A01

Unsteady flow phenomena at helicopter rotor blades during forward flight were studied in the framework of two-dimensional profile theory. The flow medium was assumed to be compressible, inviscid, and heat-conduction free. Starting from the Euler equations, a numerical bicharacteristic method of a second order for the calculation of two-dimensional, unsteady, compressible flow was developed, allowing the simulation of flow about accelerating profiles. Fast angle-of-attack oscillations of a profile and profile motions with translatory acceleration were analyzed; the results are in good agreement with the Jameson stationary transonic potential method. ESA

N89-25132# Technische Hochschule, Aachen (Germany, F.R.).
INTERACTION BETWEEN COMPRESSION SHOCKS AND VERTICAL FLOWS [WECHSELWIRKUNG ZWISCHEN VERDICHTUNGSSTOESSEN UND WIRBELHAFTEN STROEMUNGEN]
W. Althaus *In its* Vortex Flows in Flying Technique 1988 p 115-131 In GERMAN (For primary document see N89-25126 19-02)
Avail: NTIS HC A17/MF A01

The interaction between compression shocks and vertical supersonic flows was investigated to determine the origin of the formation of Karman vortex streets. Wind tunnel tests were performed in a model flow consisting of a flow along a flat plate whose surface is smooth or roughened under different conditions. Boundary layers and waves were measured in two dimensions using laser Doppler anemometry; the density distribution was measured using holographic interferometry. For the roughened plate a Karman vortex street was observed in the subsonic as well as the supersonic range. The origin of the vortex street has to lie in the formation of the boundary along the flat plate. ESA

N89-25133# Technische Hochschule, Aachen (Germany, F.R.).
DISSIPATION OF VORTEX POWER IN LONGITUDINAL FLOW ON WINGS [DISSIPATION VON WIRBELSTAERKE IN LAENGSWIRBELN AN TRAGFLAECHEN]
W. Stuettgen *In its* Vortex Flows in Flying Technique 1988 p 133-142 In GERMAN (For primary document see N89-25126 19-02)
Avail: NTIS HC A17/MF A01

The growth of a vortex sheet separating from a wing to a wing tip vortex was investigated as a function of turbulent diffusion and circulation distribution, using a stochastic calculation method. The flow field behind the wing was treated in two dimensions, assuming a high flow velocity. The velocity field induced in the region subject to rotation leads to a motion of the wing tip vortex, which can cause a curvature of the vortex lines. This curvature is affected by convection, diffusion, and induced motion. The acceleration or deceleration of vortex particles in axial direction can lead to dissipation of vortex power by friction or to local breakdown. ESA

N89-25134# Technische Hochschule, Aachen (Germany, F.R.).
VORTEX STRUCTURES IN THE WAKE OF TRANSONIC FLOW ABOUT PROFILES [WIRBELNSTRUKTUREN IM NACHLAUF SCHALLNAH ANGESTROEMTER PROFILE]
H.-J. Romberg *In its* Vortex Flows in Flying Technique 1988 p 143-157 In GERMAN (For primary document see N89-25126 19-02)
Avail: NTIS HC A17/MF A01

Measurements were performed on wing profiles in transonic and supersonic wind tunnels with a view to the investigation of the mechanisms responsible for the formation of vortex structures. The measuring chambers of the wind tunnels are equipped with adaptive walls to minimize wall interferences. The pressure distributions with and without adaptive walls were measured and compared with Navier-Stokes calculations. Pressure distribution and pressure variations in the wake were also measured. The measurements were correlated with the numerical evaluation of Mach-Zehnder recordings, which clarifies the mechanisms and the quantities affecting the formation of vortex structures. ESA

N89-25135# Technische Hochschule, Aachen (Germany, F.R.).
FLOW ABOUT TRAILING EDGES IN UNSTEADY FLOW [HINTERKANTENUMSTROEMUNG IN INSTATIONAERER ANSTROEMUNG]
B. Schweitzer and K. Dortmann *In its* Vortex Flows in Flying Technique 1988 p 159-182 In GERMAN (For primary document see N89-25126 19-02)
Avail: NTIS HC A17/MF A01

The flow field changes at wing profiles in an unsteady flow and constant angle of attack were investigated experimentally as well as numerically. Water tunnel experiments show clearly that the profile flow and especially the separation domain are affected by flow velocity changes. Unsteady pressure distributions and boundary layer profiles were measured in a wind tunnel. Despite the different test conditions, the fundamental similarity between the flow in the wind and the water tunnel was demonstrated. The measurement of the unsteady pressure distributions allows the determination of the unsteady lift coefficient. A force and moment measurement was performed to determine the aerodynamic forces on the profile. ESA

N89-25136# Technische Hochschule, Aachen (Germany, F.R.).
UNSTEADY FLOW ON PROFILES IN A LIQUID LUDWIG TUNNEL [INSTATIONAERE UMSTROEMUNG VON PROFILEN IN EINEM FLUESSIGKEITS-LUDWIEG-KANAL]
W. Kerres *In its* Vortex Flows in Flying Technique 1988 p 183-222 In GERMAN (For primary document see N89-25126 19-02)
Avail: NTIS HC A17/MF A01

Experiments were performed to determine the flow structure on several models in unsteady flow. Flow visualization as well as force and moment measurements were made. The comparison of the temporal evolution of force and moment with the flow pictures clarifies the effect of the starting vortex and the flow state at the profile. It is shown that this tunnel is very well suited for the study of starting flows. The results show that the flow structure is very reproducible, and that the profile contour, especially the trailing edge, has a large effect on the flow structure. Comparison with

potential flow calculations shows that inertial forces do not play an essential role in the starting flow phenomena. ESA

N89-25137# Technische Hochschule, Aachen (Germany, F.R.).
EFFECT OF WINGLETS ON LOADING MECHANICS AND WING ASSEMBLY REACTIONS [EINFLUSS VON WINGLETS AUF DIE BELASTUNGS MECHANIK UND TRAGWERKSREAKTIONEN]
Graham Butt and Athanassios Dafnis *In its* Vortex Flows in Flying Technique 1988 p 223-260 In GERMAN (For primary document see N89-25126 19-02)
Avail: NTIS HC A17/MF A01

The structural mechanical effects of winglets on the lifting structure of wings were investigated on the laboratory aircraft Morane Rallye. The pressure distribution on the Morane wing was calculated. A six-component force measurement was performed on the Morane model with and without winglets. The structural data of the Morane wings were obtained. Flutter calculations with three degrees of freedom were made. The unsteady aerodynamic forces were measured on the vibration test stand in the wind tunnel. ESA

N89-25138# Technische Hochschule, Aachen (Germany, F.R.).
DAMPING OF WING TIP VORTEX SYSTEMS BY THE MODIFICATION OF THE WING TIPS [ABSCHWAECHUNG VON RANDWIRBELSYSTEMEN DURCH MODIFIKATION DER FLUEGELSPITZEN]
T. Scherer and T. Vitting *In its* Vortex Flows in Flying Technique 1988 p 261-287 In GERMAN (For primary document see N89-25126 19-02)
Avail: NTIS HC A17/MF A01

The reduction of the adverse effects of wing tip vortices by the design of wing tips and by active and passive control of the evolution of the vortex orbit, was investigated. The aim was to prevent the formation of single vortices or the perturbation of ordered wortex structures by self-induction. The vortex behavior was described using water tunnel experiments and simulation calculations. The results show that the highest circumferential velocity in the wing tip vortex can be reduced by more than 60 percent if the vortex formation process can be hindered or if the ordered vortex structures can be perturbed by self-induction. Experiments and simulations show that behind semi-delta winglets with small angle of attack, double vortices are built which lead to strongly reduced circumferential velocities. Winglets were developed for the Dromedar aircraft, providing a clearly improved spray distribution. ESA

N89-25139# Technische Hochschule, Aachen (Germany, F.R.).
MECHANICAL REACTION OF WINGS MOVING THROUGH A VORTEX REGION [MECHANISCHE REAKTIONEN VON FLUEGELN, DIE DURCH EIN WIRBELGEBIET BEWEGT WERDEN]
Dieter Holzdeppe and Hans-Werner Lindert *In its* Vortex Flows in Flying Technique 1988 p 289-312 In GERMAN (For primary document see N89-25126 19-02)
Avail: NTIS HC A17/MF A01

The dynamic reactions of rotor blades on loading by vortex perturbations were investigated. The principal item in the structural dynamic calculations is the reconstruction of the exciting functions from a few measured structural responses such as cutting moments, displacements, and accelerations. By modelling the rotor blade as a beam structure, the distribution of the resulting aerodynamic forces over the rotor blade length can be reconstructed. The reconstruction of the aerodynamic moments from simultaneously measured torsion torques also provide the position of the resulting aerodynamic forces with respect to the profile depth. The results can also be used to improve the analytical unsteady aerodynamic force models. ESA

N89-25140# Technische Hochschule, Aachen (Germany, F.R.).
STRUCTURAL LOADING AND NOISE DISTURBANCE OF HELICOPTERS [STRUKTURBEANSPRUCHUNG UND LAERMBELAESTIGUNG BEIN HUBSCHRAUBER] **c71**
R. Mueller *In its* Vortex Flows in Flying Technique 1988 p 313-337 In GERMAN (For primary document see N89-25126 19-02)
Avail: NTIS HC A17/MF A01

Test experiments were performed and calculation methods were developed to study the structural loading of helicopter rotor blades and the resulting noise emission which can strongly reduce operational conditions of a helicopter. An optimized winglet was constructed which reduced rotor blade loading and rotor noise emission by changing position and structure of the wing tip vortices. The use of such winglets is especially advantageous in case of fast descent. In fast forward flight the flow at the winglet can become a problem due to the high angles of attack at the winglet; however, no separation phenomena at the winglet were observed. ESA

N89-25141# Technische Hochschule, Aachen (Germany, F.R.).
FLIGHT-MECHANICAL INVESTIGATIONS OF THE LATERAL MOTION OF CONFIGURATIONS WITH WINGLETS [FLUGMECHANISCHE UNTERSUCHUNGEN ZUR SEITENBEWEGUNG VON KONFIGURATIONEN MIT WINGLETS] **c08**
A. Diekmann and A. Josten *In its* Vortex Flows in Flying Technique 1988 p 339-371 In GERMAN (For primary document see N89-25126 19-02)
Avail: NTIS HC A17/MF A01

The effect of an aerodynamically optimized winglet with trailing edge flap, on the flight characteristics was investigated, using the Rallye Morane aircraft. The static forces and moments, as well as the effect of the winglet on roll damping were determined in wind tunnel tests. The dynamic behavior and winglet action during spinning were determined during flight tests. The calculation of the dynamic behavior of the aircraft with tip strips or winglets is based on the measured static force and moment coefficients as well as on the estimated dynamic derivatives. The effect of the winglet on the coupling between longitudinal and lateral motion was calculated. Nonlinear effects for large angles of attack and sideslip angles were taken into account. ESA

N89-25198*# National Aeronautics and Space Administration. Langley Research Center, Hampton, VA.
FINITE ELEMENT FLOW-THERMAL-STRUCTURAL ANALYSIS OF AERODYNAMICALLY HEATED LEADING EDGES
Pramote Dechaumphai, Allan R. Wieting, and Ajay K. Pandey (Planning Research Corp., Hampton, VA.) *In its* Recent Advances in Multidisciplinary Analysis and Optimization, Part 2 Apr. 1989 p 971-990 (For primary document see N89-25173 19-05)
Avail: NTIS HC A22/MF A01 CSCL 01A

03 AIR TRANSPORTATION AND SAFETY

Includes passenger and cargo air transport operations; and aircraft accidents.

For related information see also *16 Space Transportation* and *85 Urban Technology and Transportation.*

N89-25142# Federal Aviation Administration, Atlantic City, NJ.
NOTICE TO AIRMEN (NOTAM) SYSTEM OPERATIONAL CONCEPT Final Report
Betty K. Falato Dec. 1988 56 p
(DOT/FAA/CT-TN89/10; DOT/FAA/DS-89/05) Avail: NTIS HC A04/MF A01

A requirement for the National Airspace System (NAS) to provide timely knowledge to users of information which is essential to safety of flight is identified in the NAS System Requirement Specification, NAS-SR-1000. The primary method of providing timely aeronautical information is via the Notice to Airmen (NOTAM) system. A concept of operations is presented for the NOTAM system. It describes NOTAM system capabilities and shows the relationships between subsystems, facilities, information, and operators/users. It is intended to provide a common perspective

for personnel involved in NOTAM-related activities, assist in determining whether the NOTAM system meets formal requirements, and support coordination among the organizations involved with the NOTAM system. Author

N89-25143 Civil Aviation Authority, London (England).
UK AIRMISSES INVOLVING COMMERCIAL AIR TRANSPORT
Dec. 1988 73 p
(CAA-3/88; ISSN-0951-6301; ETN-89-94326) Copyright Avail: Civil Aviation Authority, Greville House, 37 Gratton Road, Cheltenham, England, 5 sterling pounds

Statistics on commercial air transport airmisses in United Kingdom airspace from 1978 to Apr. 1988 are presented. Numbers of incidents; aircraft involved; and airmisses related to flying hours are shown. Incident reports for the period Jan. to Apr. 1988 are reproduced. During this period, there were 21 incidents, involving a total of 31 aircraft, giving an average 3.8 commercial air transport aircraft in risk-bearing airmisses per 100,000 hr flown. ESA

N89-25144# Deutsche Forschungs- und Versuchsanstalt fuer Luft- und Raumfahrt, Brunswick (Germany, F.R.). Abteilung Glaechenflugzeuge.
CONTRIBUTIONS TO THE IMPROVEMENT OF FLIGHT SAFETY IN WIND SHEAR Ph.D. Thesis - Technische Univ., Brunswick
Reinhard Koenig Dec. 1988 186 p In GERMAN; ENGLISH summary Report will also be announced as translation (ESA-TT-1141)
(DFVLR-FB-88-49; ISSN-0171-1342; ETN-89-94635) Avail: NTIS HC A09/MF A01; DFVLR, VB-PL-DO, Postfach 90 60 58, 5000 Cologne, Fed. Republic of Germany, DM 65.50

From the description of the wind shear effects on the energy state of the aircraft, measures are derived in order to define a controller that improves flight safety. In comparison to a conventional flight control system, this approach presents advantages for reducing windshear effects. The actual windshear problem stems from neither the controlled flight nor the limited aircraft performance, but rather from manual flight. The pilot is unable to perform with conventional instrumentation the necessary measures, such as setting the thrust at the right time and level. Indicating the energy and power loss via signals sent into modified instruments leads to an improvement in flight performance during windshear. It is therefore shown that through suitable instrumentation modifications the effects of wind shear can be reduced. ESA

04 AIRCRAFT COMMUNICATIONS AND NAVIGATION

Includes digital and voice communication with aircraft; air navigation systems (satellite and ground based); and air traffic control.

For related information see also *17 Space Communications, Spacecraft Communications, Command and Tracking* and *Communications and Radar.*

N89-25145# Deutsche Forschungs- und Versuchsanstalt fuer Luft- und Raumfahrt, Brunswick (Germany, F.R.). Abteilung Systemtechnik und Navigation.
TESTING OF A GPS RECEIVER
Karlheinz Hurass Oct. 1988 43 p In GERMAN; ENGLISH summary Report will also be announced as translation (ESA-TT-1146)
(DFVLR-Mitt-88-30; ISSN-0176-7739; ESA-TT-1146; ETN-89-94644) Avail: NTIS HC A03/MF A01; DFVLR, VB-PL-DO, Postfach 90 60 58, 5000 Cologne, Federal Republic of Germany, 18 deutsche marks

In order to test the accuracy of GPS flight tests were carried out. A Litton GPS navigation set (LTN-700) for the C/A Code was used. The reference trajectories were determined by the Avionics Flight Evaluation System of DFVLR (Deutsche Forschungs- und Versuchsanstalt fuer Luft- und Raumfahrt). The measured position errors consist of a high frequency and low frequency noise. The standard deviation of the latter is 30 m. ESA

05 AIRCRAFT DESIGN, TESTING AND PERFORMANCE

Includes aircraft simulation technology.

For related information see also *18 Spacecraft Design, Testing and Performance* and *39 Structural Mechanics.* For land transportation vehicles see *85 Urban Technology and Transportation.*

N89-25146*# National Aeronautics and Space Administration. Langley Research Center, Hampton, VA.
RECENT ADVANCES IN MULTIDISCIPLINARY ANALYSIS AND OPTIMIZATION, PART 1
Jean-Francois M. Barthelemy, ed. Washington Apr. 1989 527 p Symposium held in Hampton, VA, 28-30 Sep. 1988; sponsored by NASA, Langley Research Center, NASA, LeResear Center, and Wright Research Development Center
(NASA-CP-3031-Pt-1; L-16568-Pt-1; NAS 1.55:3031-Pt-1) Avail: NTIS HC A23/MF A01 CSCL 01C

This three-part document contains a collection of technical papers presented at the Second NASA/Air Force Symposium on Recent Advances in Multidisciplinary Analysis and Optimization, held September 28-30, 1988 in Hampton, Virginia. The topics covered include: helicopter design, aeroelastic tailoring, control of aeroelastic structures, dynamics and control of flexible structures, structural design, design of large engineering systems, application of artificial intelligence, shape optimization, software development and implementation, and sensitivity analysis. For individual titles, see N89-25147 through N89-25172.

N89-25147*# Grumman Aerospace Corp., Bethpage, NY. Aircraft Systems Div.
APPLICATIONS OF INTEGRATED DESIGN/ANALYSIS SYSTEMS IN AEROSPACE STRUCTURAL DESIGN
Philip Mason, Edwin Lerner, and Lawrence Sobel *In* NASA. Langley Research Center, Recent Advances in Multidisciplinary Analysis and Optimization, Part 1 Apr. 1989 p 3-37 (For primary document see N89-25146 19-05)
Avail: NTIS HC A23/MF A01 CSCL 01C

Integrated structural analysis and design systems and structural optimization procedures are being used in a production environment. Successful use of these systems requires experienced personnel. Interactive computer graphics can and will play a significant role in the analysis, optimization, design and manufacturing areas. Practical structural optimization procedures are tools that must be made available to the team. Much work still needs to be done to tie finite-element modeling to actual design details which are being tracked on systems such as CADAM or CATIA. More work needs to be done to automate the detailed design and analysis process. More emphasis should be placed on the real design problems. Author

N89-25148*# General Electric Co., Schenectady, NY.
INTEGRATED DESIGN OPTIMIZATION RESEARCH AND DEVELOPMENT IN AN INDUSTRIAL ENVIRONMENT **c31**
V. Kumar, Marjorie D. German, and S.-J. Lee *In* NASA. Langley Research Center, Recent Advances in Multidisciplinary Analysis and Optimization, Part 1 Apr. 1989 p 39-50 (For primary document see N89-25146 19-05)
Avail: NTIS HC A23/MF A01 CSCL 13B

An overview is given of a design optimization project that is in progress at the GE Research and Development Center for the past few years. The objective of this project is to develop a methodology and a software system for design automation and optimization of structural/mechanical components and systems. The effort focuses on research and development issues and also on optimization applications that can be related to real-life industrial design problems. The overall technical approach is based on

integration of numerical optimization techniques, finite element methods, CAE and software engineering, and artificial intelligence/expert systems (AI/ES) concepts. The role of each of these engineering technologies in the development of a unified design methodology is illustrated. A software system DESIGN-OPT has been developed for both size and shape optimization of structural components subjected to static as well as dynamic loadings. By integrating this software with an automatic mesh generator, a geometric modeler and an attribute specification computer code, a software module SHAPE-OPT has been developed for shape optimization. Details of these software packages together with their applications to some 2- and 3-dimensional design problems are described. Author

N89-25149*# National Aeronautics and Space Administration. Langley Research Center, Hampton, VA.
OPTIMIZATION BY DECOMPOSITION: A STEP FROM HIERARCHIC TO NON-HIERARCHIC SYSTEMS c31
Jaroslaw Sobieszczanski-Sobieski *In its* Recent Advances in Multidisciplinary Analysis and Optimization, Part 1 Apr. 1989 p 51-78 Previously announced as N89-13423 (For primary document see N89-25146 19-05)
Avail: NTIS HC A23/MF A01 CSCL 13B

A new, non-hierarchic decomposition is formulated for system optimization that uses system analysis, system sensitivity analysis, temporary decoupled optimizations performed in the design subspaces corresponding to the disciplines and subsystems, and a coordination optimization concerned with the redistribution of responsibility for the constraint satisfaction and design trades among the disciplines and subsystems, and a coordination optimization concerned with the redistribution of responsibility for the constraint satisfaction and design trades among the disciplines and subsystems. The approach amounts to a variation of the well-known method of subspace optimization modified so that the analysis of the entire system is eliminated from the subspace optimization and the subspace optimizations may be performed concurrently. Author

N89-25150*# National Aeronautics and Space Administration. Langley Research Center, Hampton, VA.
OVERVIEW OF DYNAMICS INTEGRATION RESEARCH (DIR) PROGRAM AT LANGLEY RESEARCH CENTER
Steven M. Sliwa and Irving Abel *In its* Recent Advances in Multidisciplinary Analysis and Optimization, Part 1 Apr. 1989 p 79-105 (For primary document see N89-25146 19-05)
Avail: NTIS HC A23/MF A01 CSCL 01C

Research goals and objectives for an ongoing activity at Langley Research Center (LaRC) are described. The activity is aimed principally at dynamics optimization for aircraft. The effort involves active participation by the Flight Systems, Structures, and Electronics directorates at LaRC. The Functional Integration Technology (FIT) team has been pursuing related goals since 1985. A prime goal has been the integration and optimization of vehicle dynamics through collaboration at the basic principles or equation level. Some significant technical progress has been accomplished since then and is reflected here. An augmentation for this activity, Dynamics Integration Research (DIR), has been proposed to NASA Headquarters and is being considered for funding in FY 1990 or FY 1991. Author

N89-25151*# National Aeronautics and Space Administration. Langley Research Center, Hampton, VA.
AN INITIATIVE IN MULTIDISCIPLINARY OPTIMIZATION OF ROTORCRAFT
Howard M. Adelman and Wayne R. Mantay (Army Aerostructures Directorate, Hampton, VA.) *In its* Recent Advances in Multidisciplinary Analysis and Optimization, Part 1 Apr. 1989 p 109-144 Previously announced as N89-15108 (For primary document see N89-25146 19-05)
Avail: NTIS HC A23/MF A01 CSCL 01C

Described is a joint NASA/Army initiative at the Langley Research Center to develop optimization procedures aimed at improving the rotor blade design process by integrating appropriate disciplines and accounting for important interactions among the disciplines. The activity is being guided by a Steering Committee made up of key NASA and Army researchers and managers. The committee, which has been named IRASC (Integrated Rotorcraft Analysis Steering Committee), has defined two principal foci for the activity: a white paper which sets forth the goals and plans of the effort; and a rotor design project which will validate the basic constituents, as well as the overall design methodology for multidisciplinary optimization. The optimization formulation is described in terms of the objective function, design variables, and constraints. Additionally, some of the analysis aspects are discussed and an initial attempt at defining the interdisciplinary couplings is summarized. At this writing, some significant progress has been made, principally in the areas of single discipline optimization. Results are given which represent accomplishments in rotor aerodynamic performance optimization for minimum hover horsepower, rotor dynamic optimization for vibration reduction, and rotor structural optimization for minimum weight. Author

N89-25152*# California Univ., Los Angeles. Dept. of Mechanical, Aerospace and Nuclear Engineering.
STRUCTURAL OPTIMIZATION OF ROTOR BLADES WITH STRAIGHT AND SWEPT TIPS SUBJECT TO AEROELASTIC CONSTRAINTS
Peretz P. Friedmann and Roberto Celi (Maryland Univ., College Park.) *In* NASA. Langley Research Center, Recent Advances in Multidisciplinary Analysis and Optimization, Part 1 Apr. 1989 p 145-162 (For primary document see N89-25146 19-05)
Avail: NTIS HC A23/MF A01 CSCL 01C

The main conclusions obtained in the present study are summarized. Their application to the structural optimization of a helicopter blade should be limited by the assumptions used in obtaining the numerical results presented here. The optimum design procedure described here is very efficient, and can produce improved designs with a very limited number of precise analyses. The method of constructing the approximate problem is such that previously conducted aeroelastic analyses can be reused in a new optimization problem. For example, if an optimization study is preceded by a parametric study in which the effect of various combinations of blade design parameters is examined, all the aeroelastic analyses performed for the parametric study can be reutilized in the optimization study. This is not possible when the approximate problem is built from Taylor series expansions. The results of the optimization are quite sensitive to the aeroelastic stability margins required of the blade. In the optimization of case 2, changing the aeroelastic stability constraints from simply requiring that the blade be stable in hover, to requiring that the stability margins be maintained during the course of the optimization, reduced the gains in n/rev vibration levels by more than 50 percent. The introduction of tip sweep can reduce the n/rev vertical hub shears beyond the level that can be obtained by just modifying the mass and stiffness distributions of the blade. Author

N89-25153*# Georgia Inst. of Tech., Atlanta. School of Aerospace Engineering.
OPTIMIZATION OF ROTOR BLADES FOR COMBINED STRUCTURAL, PERFORMANCE, AND AEROELASTIC CHARACTERISTICS
David A. Peters and Y. P. Cheng *In* NASA. Langley Research Center, Recent Advances in Multidisciplinary Analysis and Optimization, Part 1 Apr. 1989 p 163-180 (For primary document see N89-25146 19-05)
Avail: NTIS HC A23/MF A01 CSCL 01C

The strategies whereby helicopter rotor blades can be optimized for combined structural, inertial, dynamic, aeroelastic, and aerodynamic performance characteristics are outlined. There are three key ingredients in the successful execution of such an interdisciplinary optimization. The first is the definition of a satisfactory performance index that combines all aspects of the problem without too many constraints. The second element is the judicious choice of computationally efficient analysis tools for the various quantitative components in both the cost functional and

constraints. The third element is an effective strategy for combining the various disciplines either in parallel or sequential optimizations. Author

N89-25154*# McDonnell-Douglas Helicopter Co., Mesa, AZ.
TRANSONIC AIRFOIL DESIGN FOR HELICOPTER ROTOR APPLICATIONS
Ahmed A. Hassan and B. Jackson *In* NASA. Langley Research Center, Recent Advances in Multidisciplinary Analysis and Optimization, Part 1 Apr. 1989 p 181-193 (For primary document see N89-25146 19-05)
Avail: NTIS HC A23/MF A01 CSCL 01C

Despite the fact that the flow over a rotor blade is strongly influenced by locally three-dimensional and unsteady effects, practical experience has always demonstrated that substantial improvements in the aerodynamic performance can be gained by improving the steady two-dimensional charateristics of the airfoil(s) employed. The two phenomena known to have great impact on the overall rotor performance are: (1) retreating blade stall with the associated large pressure drag, and (2) compressibility effects on the advancing blade leading to shock formation and the associated wave drag and boundary-layer separation losses. It was concluded that: optimization routines are a powerful tool for finding solutions to multiple design point problems; the optimization process must be guided by the judicious choice of geometric and aerodynamic constraints; optimization routines should be appropriately coupled to viscous, not inviscid, transonic flow solvers; hybrid design procedures in conjunction with optimization routines represent the most efficient approach for rotor airfroil design; unsteady effects resulting in the delay of lift and moment stall should be modeled using simple empirical relations; and inflight optimization of aerodynamic loads (e.g., use of variable rate blowing, flaps, etc.) can satisfy any number of requirements at design and off-design conditions. Author

N89-25155*# Maryland Univ., College Park. Dept. of Aerospace Engineering.
EFFICIENT SENSITIVITY ANALYSIS AND OPTIMIZATION OF A HELICOPTER ROTOR
Joon W. Lim and Inderjit Chopra *In* NASA. Langley Research Center, Recent Advances in Multidisciplinary Analysis and Optimization, Part 1 Apr. 1989 p 195-208 (For primary document see N89-25146 19-05)
Avail: NTIS HC A23/MF A01 CSCL 01C

Aeroelastic optimization of a system essentially consists of the determination of the optimum values of design variables which minimize the objective function and satisfy certain aeroelastic and geometric constraints. The process of aeroelastic optimization analysis is illustrated. To carry out aeroelastic optimization effectively, one needs a reliable analysis procedure to determine steady response and stability of a rotor system in forward flight. The rotor dynamic analysis used in the present study developed inhouse at the University of Maryland is based on finite elements in space and time. The analysis consists of two major phases: vehicle trim and rotor steady response (coupled trim analysis), and aeroelastic stability of the blade. For a reduction of helicopter vibration, the optimization process requires the sensitivity derivatives of the objective function and aeroelastic stability constraints. For this, the derivatives of steady response, hub loads and blade stability roots are calculated using a direct analytical approach. An automated optimization procedure is developed by coupling the rotor dynamic analysis, design sensitivity analysis and constrained optimization code CONMIN. Author

N89-25156*# National Aeronautics and Space Administration. Langley Research Center, Hampton, VA.
STRUCTURAL OPTIMIZATION OF ROTOR BLADES WITH INTEGRATED DYNAMICS AND AERODYNAMICS
Aditi Chattopadhyay (Analytical Services and Materials, Inc., Hampton, VA.) and Joanne L. Walsh *In its* Recent Advances in Multidisciplinary Analysis and Optimization, Part 1 Apr. 1989 p 209-233 Previously announced as N89-15110 (For primary document see N89-25146 19-05)
Avail: NTIS HC A23/MF A01 CSCL 01C

The problem of structural optimization of helicopter rotor blades with integrated dynamic and aerodynamic design considerations is addressed. Results of recent optimization work on rotor blades for minimum weight with constraints on multiple coupled natural flap-lag frequencies, blade autorotational inertia and centrifugal stress has been reviewed. A strategy has been defined for the ongoing activities in the integrated dynamic/aerodynamic optimization of rotor blades. As a first step, the integrated dynamic/airload optimization problem has been formulated. To calculate system sensitivity derivatives necessary for the optimization recently developed, Global Sensitivity Equations (GSE) are being investigated. A need for multiple objective functions for the integrated optimization problem has been demonstrated and various techniques for solving the multiple objective function optimization are being investigated. The method called the Global Criteria Approach has been applied to a test problem with the blade in vacuum and the blade weight and the centrifugal stress as the multiple objectives. The results indicate that the method is quite effective in solving optimization problems with conflicting objective functions. Author

N89-25157*# McDonnell-Douglas Helicopter Co., Mesa, AZ.
MULTI-OBJECTIVE/LOADING OPTIMIZATION FOR ROTATING COMPOSITE FLEXBEAMS
Brian K. Hamilton and James R. Peters *In* NASA. Langley Research Center, Recent Advances in Multidisciplinary Analysis and Optimization, Part 1 Apr. 1989 p 235-256 (For primary document see N89-25146 19-05)
Avail: NTIS HC A23/MF A01 CSCL 01C

With the evolution of advanced composites, the feasibility of designing bearingless rotor systems for high speed, demanding maneuver envelopes, and high aircraft gross weights has become a reality. These systems eliminate the need for hinges and heavily loaded bearings by incorporating a composite flexbeam structure which accommodates flapping, lead-lag, and feathering motions by bending and twisting while reacting full blade centrifugal force. The flight characteristics of a bearingless rotor system are largely dependent on hub design, and the principal element in this type of system is the composite flexbeam. As in any hub design, trade off studies must be performed in order to optimize performance, dynamics (stability), handling qualities, and stresses. However, since the flexbeam structure is the primary component which will determine the balance of these characteristics, its design and fabrication are not straightforward. It was concluded that: pitchcase and snubber damper representations are required in the flexbeam model for proper sizing resulting from dynamic requirements; optimization is necessary for flexbeam design, since it reduces the design iteration time and results in an improved design; and inclusion of multiple flight conditions and their corresponding fatigue allowables is necessary for the optimization procedure. Author

N89-25158*# Florida Univ., Gainesville. Aerospace Engineering, Mechanics and Engineering Science.
NEW DIRECTIONS FOR ARTIFICIAL INTELLIGENCE (AI) METHODS IN OPTIMUM DESIGN **c63**
Prabhat Hajela *In* NASA. Langley Research Center, Recent Advances in Multidisciplinary Analysis and Optimization, Part 1 Apr. 1989 p 259-274 (For primary document see N89-25146 19-05)
Avail: NTIS HC A23/MF A01 CSCL 09B

Developments and applications of artificial intelligence (AI) methods in the design of structural systems is reviewed. Principal shortcomings in the current approach are emphasized, and the need for some degree of formalism in the development environment for such design tools is underscored. Emphasis is placed on efforts to integrate algorithmic computations in expert systems. Author

N89-25159*# Hall (David) Consulting, Sunnyvale, CA.
DEVELOPMENT OF A MICROCOMPUTER BASED INTEGRATED DESIGN SYSTEM FOR HIGH ALTITUDE LONG ENDURANCE AIRCRAFT

David W. Hall and J. Edward Rogan *In* NASA. Langley Research Center, Recent Advances in Multidisciplinary Analysis and Optimization, Part 1 Apr. 1989 p 275-296 Previously announced in IAA as A88-53734 (For primary document see N89-25146 19-05)
Avail: NTIS HC A23/MF A01 CSCL 01C

A microcomputer-based integration of aircraft design disciplines has been applied theoretically to sailplane, microwave-powered aircraft, and High Altitude Long-Endurance (HALE) aircraft configurational definition efforts. Attention is presently given to the further development of such integrated-discipline approaches through the incorporation of AI techniques; these are then applied to the aforementioned case of the HALE. The windFrame language used, which is based on HyperTalk, will allow designers to write programs using a highly graphical, user interface-oriented environment. Author

N89-25160*# National Aeronautics and Space Administration. Langley Research Center, Hampton, VA.
DEMONSTRATION OF DECOMPOSITION AND OPTIMIZATION IN THE DESIGN OF EXPERIMENTAL SPACE SYSTEMS c18
Sharon Padula, Chris A. Sandridge, Raphael T. Haftka (Virginia Polytechnic Inst. and State Univ., Blacksburg.), and Joanne L. Walsh *In its* Recent Advances in Multidisciplinary Analysis and Optimization, Part 1 Apr. 1989 p 297-316 (For primary document see N89-25146 19-05)
Avail: NTIS HC A23/MF A01 CSCL 22B

Effective design strategies for a class of systems which may be termed Experimental Space Systems (ESS) are needed. These systems, which include large space antenna and observatories, space platforms, earth satellites and deep space explorers, have special characteristics which make them particularly difficult to design. It is argued here that these same characteristics encourage the use of advanced computer-aided optimization and planning techniques. The broad goal of this research is to develop optimization strategies for the design of ESS. These strategics would account for the possibly conflicting requirements of mission life, safety, scientific payoffs, initial system cost, launch limitations and maintenance costs. The strategies must also preserve the coupling between disciplines or between subsystems. Here, the specific purpose is to describe a computer-aided planning and scheduling technique. This technique provides the designer with a way to map the flow of data between multidisciplinary analyses. The technique is important because it enables the designer to decompose the system design problem into a number of smaller subproblems. The planning and scheduling technique is demonstrated by its application to a specific preliminary design problem. Author

N89-25161*# National Aeronautics and Space Administration. Langley Research Center, Hampton, VA.
STRUTEX: A PROTOTYPE KNOWLEDGE-BASED SYSTEM FOR INITIALLY CONFIGURING A STRUCTURE TO SUPPORT POINT LOADS IN TWO DIMENSIONS c39
James L. Robers and Jaroslaw Sobieszczanski-Sobieski *In its* Recent Advances in Multidisciplinary Analysis and Optimization, Part 1 Apr. 1989 p 317-331 (For primary document see N89-25146 19-05)
Avail: NTIS HC A23/MF A01 CSCL 20K

Only recently have engineers begun making use of Artificial Intelligence (AI) tools in the area of conceptual design. To continue filling this void in the design process, a prototype knowledge-based system, called STRUTEX has been developed to initially configure a structure to support point loads in two dimensions. This prototype was developed for testing the application of AI tools to conceptual design as opposed to being a testbed for new methods for improving structural analysis and optimization. This system combines numerical and symbolic processing by the computer with interactive problem solving aided by the vision of the user. How the system is constructed to interact with the user is described. Of special interest is the information flow between the knowledge base and the data base under control of the algorithmic main program. Examples of computed and refined structures are presented during the explanation of the system. Author

N89-25162*# Georgia Inst. of Tech., Atlanta.
TRUSS: AN INTELLIGENT DESIGN SYSTEM FOR AIRCRAFT WINGS c61
Preston R. Bates and Daniel P. Schrage *In* NASA. Langley Research Center, Recent Advances in Multidisciplinary Analysis and Optimization, Part 1 Apr. 1989 p 333-355 (For primary document see N89-25146 19-05)
Avail: NTIS HC A23/MF A01 CSCL 09B

Competitive leadership in the international marketplace, superiority in national defense, excellence in productivity, and safety of both private and public systems are all national defense goals which are dependent on superior engineering design. In recent years, it has become more evident that early design decisions are critical, and when only based on performance often result in products which are too expensive, hard to manufacture, or unsupportable. Better use of computer-aided design tools and information-based technologies is required to produce better quality United States products. A program is outlined here to explore the use of knowledge based expert systems coupled with numerical optimization, database management techniques, and designer interface methods in a networked design environment to improve and assess design changes due to changing emphasis or requirements. The initial structural design of a tiltrotor aircraft wing is used as a representative example to demonstrate the approach being followed. Author

N89-25163*# National Aeronautics and Space Administration. Ames Research Center, Moffett Field, CA.
REAL-TIME APPLICATION OF KNOWLEDGE-BASED SYSTEMS c82
Randal W. Brumbaugh (PRC Systems Services Co., Hampton, VA.) and Eugene L. Duke *In* NASA. Langley Research Center, Recent Advances in Multidisciplinary Analysis and Optimization, Part 1 Apr. 1989 p 357-371 (For primary document see N89-25146 19-05)
Avail: NTIS HC A23/MF A01 CSCL 05B

The Rapid Prototyping Facility (RPF) was developed to meet a need for a facility which allows flight systems concepts to be prototyped in a manner which allows for real-time flight test experience with a prototype system. This need was focused during the development and demonstration of the expert system flight status monitor (ESFSM). The ESFSM was a prototype system developed on a LISP machine, but lack of a method for progressive testing and problem identification led to an impractical system. The RPF concept was developed, and the ATMS designed to exercise its capabilities. The ATMS Phase 1 demonstration provided a practical vehicle for testing the RPF, as well as a useful tool. ATMS Phase 2 development continues. A dedicated F-18 is expected to be assigned for facility use in late 1988, with RAV modifications. A knowledge-based autopilot is being developed using the RPF. This is a system which provides elementary autopilot functions and is intended as a vehicle for testing expert system verification and validation methods. An expert system propulsion monitor is being prototyped. This system provides real-time assistance to an engineer monitoring a propulsion system during a flight. Author

N89-25164*# LTV Aerospace and Defense Co., Dallas, TX. Military Aircraft Div.
THE DESIGNER OF THE 90'S: A LIVE DEMONSTRATION c31
Tommy L. Green, Basil M. Jordan, Jr., and Timothy L. Oglesby *In* NASA. Langley Research Center, Recent Advances in Multidisciplinary Analysis and Optimization, Part 1 Apr. 1989 p 373-385 (For primary document see N89-25146 19-05)
Avail: NTIS HC A23/MF A01 CSCL 13B

A survey of design tools to be used by the aircraft designer is given. Structural reliability, maintainability, cost and predictability, and acoustics expert systems are discussed, as well as scheduling, drawing, engineering systems, sizing functions, and standard parts and materials data bases. R.J.F.

N89-25165*# National Aeronautics and Space Administration. Lewis Research Center, Cleveland, OH.

STRUCTURAL TAILORING OF COUNTER ROTATION PROPFANS c07

Kenneth W. Brown (Pratt and Whitney Aircraft, East Hartford, CT.) and D. A. Hopkins *In* NASA. Langley Research Center, Recent Advances in Multidisciplinary Analysis and Optimization, Part 1 Apr. 1989 p 389-402 (For primary document see N89-25146 19-05)

(Contract NAS3-23941)

Avail: NTIS HC A23/MF A01 CSCL 21E

The STAT program was designed for the optimization of single rotation, tractor propfan designs. New propfan designs, however, generally consist of two counter rotating propfan rotors. STAT is constructed to contain two levels of analysis. An interior loop, consisting of accurate, efficient approximate analyses, is used to perform the primary propfan optimization. Once an optimum design has been obtained, a series of refined analyses are conducted. These analyses, while too computer time expensive for the optimization loop, are of sufficient accuracy to validate the optimized design. Should the design prove to be unacceptable, provisions are made for recalibration of the approximate analyses, for subsequent reoptimization. Author

N89-25166*# Lockheed Aeronautical Systems Co., Burbank, CA.

COMPOSITE SIZING AND PLY ORIENTATION FOR STIFFNESS REQUIREMENTS USING A LARGE FINITE ELEMENT STRUCTURAL MODEL c39

N. A. Radovcich and D. P. Gentile *In* NASA. Langley Research Center, Recent Advances in Multidisciplinary Analysis and Optimization, Part 1 Apr. 1989 p 403-429 (For primary document see N89-25146 19-05)

Avail: NTIS HC A23/MF A01 CSCL 20K

A NASTRAN bulk dataset preprocessor was developed to facilitate the integration of filamentary composite laminate properties into composite structural resizing for stiffness requirements. The NASCOMP system generates delta stiffness and delta mass matrices for input to the flutter derivative program. The flutter baseline analysis, derivative calculations, and stiffness and mass matrix updates are controlled by engineer defined processes under an operating system called CBUS. A multi-layered design variable grid system permits high fidelity resizing without excessive computer cost. The NASCOMP system uses ply layup drawings for basic input. The aeroelastic resizing for stiffness capability was used during an actual design exercise. Author

N89-25167*# General Dynamics Corp., Fort Worth, TX.

AEROLASTIC TAILORING AND INTEGRATED WING DESIGN

Mike H. Love and Jon Bohlmann *In* NASA. Langley Research Center, Recent Advances in Multidisciplinary Analysis and Optimization, Part 1 Apr. 1989 p 431-444 (For primary document see N89-25146 19-05)

Avail: NTIS HC A23/MF A01 CSCL 01C

Much has been learned from the TSO optimization code over the years in determining aeroelastic tailoring's place in the integrated design process. Indeed, it has become apparent that aeroelastic tailoring is and should be deeply embedded in design. Aeroelastic tailoring can have tremendous effects on the design loads, and design loads affect every aspect of the design process. While optimization enables the evaluation of design sensitivities, valid computational simulations are required to make these sensitivities valid. Aircraft maneuvers simulated must adequately cover the plane's intended flight envelope, realistic design criteria must be included, and models among the various disciplines must be calibrated among themselves and with any hard-core (e.g., wind tunnel) data available. The information gained and benefits derived from aeroelastic tailoring provide a focal point for the various disciplines to become involved and communicate with one another to reach the best design possible. Author

N89-25168*# National Aeronautics and Space Administration. Langley Research Center, Hampton, VA.

INTEGRATED AERODYNAMIC-STRUCTURAL DESIGN OF A FORWARD-SWEPT TRANSPORT WING

Raphael T. Haftka, Bernard Grossman, Pi-Jen Kao, David M. Polen (Virginia Polytechnic Inst. and State Univ., Blacksburg.), and Jaroslaw Sobieszczanski-Sobieski *In its* Recent Advances in Multidisciplinary Analysis and Optimization, Part 1 Apr. 1989 p 445-463 (For primary document see N89-25146 19-05)

Avail: NTIS HC A23/MF A01 CSCL 01C

The introduction of composite materials is having a profound effect on aircraft design. Since these materials permit the designer to tailor material properties to improve structural, aerodynamic and acoustic performance, they require an integrated multidisciplinary design process. Futhermore, because of the complexity of the design process, numerical optimization methods are required. The utilization of integrated multidisciplinary design procedures for improving aircraft design is not currently feasible because of software coordination problems and the enormous computational burden. Even with the expected rapid growth of supercomputers and parallel architectures, these tasks will not be practical without the development of efficient methods for cross-disciplinary sensitivities and efficient optimization procedures. The present research is part of an on-going effort which is focused on the processes of simultaneous aerodynamic and structural wing design as a prototype for design integration. A sequence of integrated wing design procedures has been developed in order to investigate various aspects of the design process. Author

N89-25169*# McIntosh Structural Dynamics, Inc., Mountain View, CA.

STATIC AEROELASTIC ANALYSIS AND TAILORING OF MISSILE CONTROL FINS

S. C. McIntosh, Jr. and M. F. E. Dillenius (Nielsen Engineering and Research, Inc., Mountain View, CA.) *In* NASA. Langley Research Center, Recent Advances in Multidisciplinary Analysis and Optimization, Part 1 Apr. 1989 p 465-475 (For primary document see N89-25146 19-05)

Avail: NTIS HC A23/MF A01 CSCL 01C

A concept for enhancing the design of control fins for supersonic tactical missiles is described. The concept makes use of aeroelastic tailoring to create fin designs (for given planforms) that limit the variations in hinge moments that can occur during maneuvers involving high load factors and high angles of attack. It combines supersonic nonlinear aerodynamic load calculations with finite-element structural modeling, static and dynamic structural analysis, and optimization. The problem definition is illustrated. The fin is at least partly made up of a composite material. The layup is fixed, and the orientations of the material principal axes are allowed to vary; these are the design variables. The objective is the magnitude of the difference between the chordwise location of the center of pressure and its desired location, calculated for a given flight condition. Three types of constraints can be imposed: upper bounds on static displacements for a given set of load conditions, lower bounds on specified natural frequencies, and upper bounds on the critical flutter damping parameter at a given set of flight speeds and altitudes. The idea is to seek designs that reduce variations in hinge moments that would otherwise occur. The block diagram describes the operation of the computer program that accomplishes these tasks. There is an option for a single analysis in addition to the optimization. Author

N89-25170*# National Aeronautics and Space Administration. Langley Research Center, Hampton, VA.

EFFECTS OF NONLINEAR AERODYNAMICS AND STATIC AEROELASTICITY ON MISSION PERFORMANCE CALCULATIONS FOR A FIGHTER AIRCRAFT

Gary L. Giles, Kenneth E. Tatum (Planning Research Corp., Hampton, VA.), and Willard E. Foss, Jr. *In its* Recent Advances in Multidisciplinary Analysis and Optimization, Part 1 Apr. 1989 p 477-496 (For primary document see N89-25146 19-05)

Avail: NTIS HC A23/MF A01 CSCL 01C

During conceptual design studies of advanced aircraft, the

usual practice is to use linear theory to calculate the aerodynamic characteristics of candidate rigid (nonflexible) geometric external shapes. Recent developments and improvements in computational methods, especially computational fluid dynamics (CFD), provide significantly improved capability to generate detailed analysis data for the use of all disciplines involved in the evaluation of a proposed aircraft design. A multidisciplinary application of such analysis methods to calculate the effects of nonlinear aerodynamics and static aeroelasticity on the mission performance of a fighter aircraft concept is described. The aircraft configuration selected for study was defined in a previous study using linear aerodynamics and rigid geometry. The results from the previous study are used as a basis of comparison for the data generated herein. Aerodynamic characteristics are calculated using two different nonlinear theories, potential flow and rotational (Euler) flow. The aerodynamic calculations are performed in an iterative procedure with an equivalent plate structural analysis method to obtain lift and drag data for a flexible (nonrigid) aircraft. These static aeroelastic data are then used in calculating the combat and mission performance characteristics of the aircraft. Author

N89-25171*# Air Force Wright-Patterson Aeronautical Labs., Wright-Patterson AFB, OH.
OPTIMUM STRUCTURAL DESIGN WITH STATIC AEROELASTIC CONSTRAINTS
Keith B Bowman, Ramana V. Grandhi, and F. E. Eastep (Dayton Univ., OH.) *In* NASA. Langley Research Center, Recent Advances in Multidisciplinary Analysis and Optimization, Part 1 Apr. 1989 p 497-508 (For primary document see N89-25146 19-05)
Avail: NTIS HC A23/MF A01 CSCL 01C

The static aeroelastic performance characteristics, divergence velocity, control effectiveness and lift effectiveness are considered in obtaining an optimum weight structure. A typical swept wing structure is used with upper and lower skins, spar and rib thicknesses, and spar cap and vertical post cross-sectional areas as the design parameters. Incompressible aerodynamic strip theory is used to derive the constraint formulations, and aerodynamic load matrices. A Sequential Unconstrained Minimization Technique (SUMT) algorithm is used to optimize the wing structure to meet the desired performance constraints. Author

N89-25172*# National Aeronautics and Space Administration. Langley Research Center, Hampton, VA.
OPTIMUM DESIGN OF SWEPT-FORWARD HIGH-ASPECT-RATION GRAPHITE-EPOXY WINGS
Mark J. Shuart, Raphael T. Haftka, and R. L. Campbell *In its* Recent Advances in Multidisciplinary Analysis and Optimization, Part 1 Apr. 1989 p 509-525 (For primary document see N89-25146 19-05)
Avail: NTIS HC A23/MF A01 CSCL 01C

An analytical investigation of a swept-forward high-aspect-ratio graphite-epoxy transport wing is described. The objectives of this investigation are to illustrate an effective usage of the unique properties of composite materials by exploiting material tailoring and to demonstrate an integrated multidisciplinary approach for conducting this investigation. Author

N89-25173*# National Aeronautics and Space Administration. Langley Research Center, Hampton, VA.
RECENT ADVANCES IN MULTIDISCIPLINARY ANALYSIS AND OPTIMIZATION, PART 2
Jean-Francois M. Barthelemy, ed. Washington Apr. 1989 501 p Symposium held in Hampton, VA, 28-30 Sep. 1988; sponsored by NASA, Langley Research Center, NASA, Lewis Research Center, and Wright Research Development Center (NASA-CP-3031-Pt-2; L-16568-Pt-2; NAS 1.55:3031-Pt-2) Avail: NTIS HC A22/MF A01 CSCL 01C

This three-part document contains a collection of technical papers presented at the Second NASA/Air Force Symposium on Recent Advances in Multidisciplinary Analysis and Optimization, held September 28-30, 1988 in Hampton, Virginia. The topics covered include: helicopter design, aeroelastic tailoring, control of aeroelastic structures, dynamics and control of flexible structures, structural design, design of large engineering systems, application of artificial intelligence, shape optimization, software development and implementation, and sensitivity analysis. For individual titles, see N89-25174 through N89-25200.

N89-25174*# Northrop Corp., Hawthorne, CA. Aircraft Div.
ASTROS: A MULTIDISCIPLINARY AUTOMATED STRUCTURAL DESIGN TOOL **c39**
D. J. Neill *In* NASA. Langley Research Center, Recent Advances in Multidisciplinary Analysis and Optimization, Part 2 Apr. 1989 p 529-543 (For primary document see N89-25173 19-05)
Avail: NTIS HC A22/MF A01 CSCL 20K

ASTROS (Automated Structural Optimization System) is a finite-element-based multidisciplinary structural optimization procedure developed under Air Force sponsorship to perform automated preliminary structural design. The design task is the determination of the structural sizes that provide an optimal structure while satisfying numerous constraints from many disciplines. In addition to its automated design features, ASTROS provides a general transient and frequency response capability, as well as a special feature to perform a transient analysis of a vehicle subjected to a nuclear blast. The motivation for the development of a single multidisciplinary design tool is that such a tool can provide improved structural designs in less time than is currently needed. The role of such a tool is even more apparent as modern materials come into widespread use. Balancing conflicting requirements for the structure's strength and stiffness while exploiting the benefits of material anistropy is perhaps an impossible task without assistance from an automated design tool. Finally, the use of a single tool can bring the design task into better focus among design team members, thereby improving their insight into the overall task. Author

N89-25175*# Kaman Aerospace Corp., Bloomfield, CT.
A GENERALIZED SOFTWARE EXECUTIVE FOR MULTIDISCIPLINARY COMPUTATIONAL STRUCTURAL DYNAMICS **c39**
Alex Berman *In* NASA. Langley Research Center, Recent Advances in Multidisciplinary Analysis and Optimization, Part 2 Apr. 1989 p 545-563 (For primary document see N89-25173 19-05)
Avail: NTIS HC A22/MF A01 CSCL 20K

The objective of this presentation is to introduce the attendees to the DYSCO program. The emphasis will be on the features which make it multidisciplinary. DYSCO is a very general and versatile software program which couples and solves dynamic systems. It was initiated in the late 1970's in response to a helicopter analysis requirement. The system development, however, resulted in an executive which was completely separated from any particular area of technology, except that of second order ordinary differential equations. During the course of its development, it was funded by the Army Aviation Applied Technology Directorate, the Air Force Wright Aeronautical Laboratories, and by the Kaman Aerospace Corporation. It is completely written in FORTRAN and is operational on IBM and VAX computers. Author

N89-25176*# Brigham Young Univ., Provo, UT. Engineering Design Methods Lab.
RESEARCH ON OPTIMIZATION-BASED DESIGN **c31**
R. J. Balling, A. R. Parkinson, and J. C. Free *In* NASA. Langley Research Center, Recent Advances in Multidisciplinary Analysis and Optimization, Part 2 Apr. 1989 p 565-580 (For primary document see N89-25173 19-05)
Avail: NTIS HC A22/MF A01 CSCL 20K

Research on optimization-based design is discussed. Illustrative examples are given for cases involving continuous optimization with discrete variables and optimization with tolerances. Approximation of computationally expensive and noisy functions, electromechanical actuator/control system design using decomposition and application of knowledge-based systems and optimization for the design of a valve anti-cavitation device are among the topics covered. R.J.F.

N89-25177*# General Dynamics Corp., Fort Worth, TX.
RECENT EXPERIENCES USING FINITE-ELEMENT-BASED STRUCTURAL OPTIMIZATION **c39**
B. K. Paul, J. C. McConnell, and Mike H. Love *In* NASA. Langley Research Center, Recent Advances in Multidisciplinary Analysis and Optimization, Part 2 Apr. 1989 p 581-599 (For primary document see N89-25173 19-05)
Avail: NTIS HC A22/MF A01 CSCL 20K

Structural optimization has been available to the structural analysis community as a tool for many years. The popular use of displacement method finite-element techniques to analyze linearly elastic structures has resulted in an ability to calculate the weight and constraint gradients inexpensively for numerical optimization of structures. Here, recent experiences in the investigation and use of structural optimization are discussed. In particular, experience with the commercially available ADS/NASOPT code is addressed. An overview of the ADS/NASOPT procedure and how it was implemented is given. Two example problems are also discussed. Author

N89-25178*# National Aeronautics and Space Administration. Langley Research Center, Hampton, VA.
THE SIZING AND OPTIMIZATION LANGUAGE (SOL): A COMPUTER LANGUAGE TO IMPROVE THE USER/OPTIMIZER INTERFACE **c61**
S. H. Lucas (Vigyan Research Associates, Inc., Hampton, VA.) and S. J. Scotti *In its* Recent Advances in Multidisciplinary Analysis and Optimization, Part 2 Apr. 1989 p 601-619 (For primary document see N89-25173 19-05)
Avail: NTIS HC A22/MF A01 CSCL 09B

The nonlinear mathematical programming method (formal optimization) has had many applications in engineering design. A figure illustrates the use of optimization techniques in the design process. The design process begins with the design problem, such as the classic example of the two-bar truss designed for minimum weight as seen in the leftmost part of the figure. If formal optimization is to be applied, the design problem must be recast in the form of an optimization problem consisting of an objective function, design variables, and constraint function relations. The middle part of the figure shows the two-bar truss design posed as an optimization problem. The total truss weight is the objective function, the tube diameter and truss height are design variables, with stress and Euler buckling considered as constraint function relations. Lastly, the designer develops or obtains analysis software containing a mathematical model of the object being optimized, and then interfaces the analysis routine with existing optimization software such as CONMIN, ADS, or NPSOL. This final state of software development can be both tedious and error-prone. The Sizing and Optimization Language (SOL), a special-purpose computer language whose goal is to make the software implementation phase of optimum design easier and less error-prone, is presented. Author

N89-25179*# Northrop Corp., Hawthorne, CA. Aircraft Div.
ROBUST COMPUTER-AIDED SYNTHESIS AND OPTIMIZATION OF LINEAR MULTIVARIABLE CONTROL SYSTEMS WITH VARYING PLANT DYNAMICS VIA AUTOCON **c61**
C. P. Lefkowitz, J. A. Tekawy, P. K. Pujara, and M. G. Safonov (University of Southern California, Los Angeles.) *In* NASA. Langley Research Center, Recent Advances in Multidisciplinary Analysis and Optimization, Part 2 Apr. 1989 p 621-638 (For primary document see N89-25173 19-05)
Avail: NTIS HC A22/MF A01 CSCL 09B

AUTOCON is an automated computer-aided design tool for the synthesis and optimization of linear multivariable control systems based upon user-defined control parameter optimization. Violations in stability and performance requirements are computed from constraints on Single Input/Single Output (SISO) open- and closed-loop transfer function frequency responses, and from constraints on the singular-value frequency responses of Multiple Input/Multiple Output (MIMO) transfer functions, for all critical plant variations. Optimum nonlinear programming algorithms are used in the search for local constrained solutions in which violations in stability and performance are caused either to vanish or be minimized for a proper selection of the control parameters. Classical control system stability and performance design can, in this way, be combined with modern multivariable robustness methods to offer general frequency response loop-shaping via a computer-aided design tool. Complete Nichols, Nyquist, Bode, singular-value Bode magnitude and transient response plots are produced, including user-defined boundary responses. AUTOCON is used to synthesize and optimize the lateral/directional flight control system for a typical high-performance aircraft. Author

N89-25180*# McDonnell-Douglas Helicopter Co., Mesa, AZ.
COMPUTERIZED DESIGN SYNTHESIS (CDS), A DATABASE-DRIVEN MULTIDISCIPLINARY DESIGN TOOL **c61**
D. M. Anderson and A. O. Bolukbasi *In* NASA. Langley Research Center, Recent Advances in Multidisciplinary Analysis and Optimization, Part 2 Apr. 1989 p 639-650 (For primary document see N89-25173 19-05)
Avail: NTIS HC A22/MF A01 CSCL 09B

The Computerized Design Synthesis (CDS) system under development at McDonnell Douglas Helicopter Company (MDHC) is targeted to make revolutionary improvements in both response time and resource efficiency in the conceptual and preliminary design of rotorcraft systems. It makes the accumulated design database and supporting technology analysis results readily available to designers and analysts of technology, systems, and production, and makes powerful design synthesis software available in a user friendly format. Author

N89-25181*# Iowa Univ., Iowa City. Dept. of Mechanical Engineering.
ON EQUIVALENCE OF DISCRETE-DISCRETE AND CONTINUUM-DISCRETE DESIGN SENSITIVITY ANALYSIS **c39**
Kyung K. Choi and Sung-Ling Twu *In* NASA. Langley Research Center, Recent Advances in Multidisciplinary Analysis and Optimization, Part 2 Apr. 1989 p 653-672 (For primary document see N89-25173 19-05)
(Grant NSF MSM-83-19871)
Avail: NTIS HC A22/MF A01 CSCL 20K

Developments in design sensitivity analysis (DSA) method have been made using two fundamentally different approaches as shown. In the first approach, a discretized structural finite element model is used to carry out DSA. There are three different methods in the discrete DSA approach: finite difference, semi-analytical, and analytical methods. The finite difference method is a popular one due to its simplicity, but a serious shortcoming of the method is the uncertainty in the choice of a perturbation step size of design variables. In the semi-analytical method, the derivatives of stiffness matrix is computed by finite differences, whereas in the analytical method, the derivatives are obtained analytically. For the shape design variable, computation of analytical derivative of stiffness matrix is quite costly. Because of this, the semi-analytical method is a popular choice in discrete shape DSA approach. However, recently, Barthelemy and Haftka presented that the semi-analytical method can have serious accuracy problems for shape design variables in structures modeled by beam, plate, truss, frame, and solid elements. They found that accuracy problems occur even for a simple cantilever beam. In the second approach, a continuum model of the structure is used to carry out DSA. Author

N89-25182*# Rensselaer Polytechnic Inst., Troy, NY. Dept. of Mechanical Engineering.
AN INVESTIGATION OF USING AN RQP BASED METHOD TO CALCULATE PARAMETER SENSITIVITY DERIVATIVES **c61**
Todd J. Beltracchi and Gary A. Gabriele *In* NASA. Langley Research Center, Recent Advances in Multidisciplinary Analysis and Optimization, Part 2 Apr. 1989 p 673-696 (For primary document see N89-25173 19-05)
Avail: NTIS HC A22/MF A01 CSCL 09B

Estimation of the sensitivity of problem functions with respect to problem variables forms the basis for many of our modern day

algorithms for engineering optimization. The most common application of problem sensitivities has been in the calculation of objective function and constraint partial derivatives for determining search directions and optimality conditions. A second form of sensitivity analysis, parameter sensitivity, has also become an important topic in recent years. By parameter sensitivity, researchers refer to the estimation of changes in the modeling functions and current design point due to small changes in the fixed parameters of the formulation. Methods for calculating these derivatives have been proposed by several authors (Armacost and Fiacco 1974, Sobieski et al 1981, Schmit and Chang 1984, and Vanderplaats and Yoshida 1985). Two drawbacks to estimating parameter sensitivities by current methods have been: (1) the need for second order information about the Lagrangian at the current point, and (2) the estimates assume no change in the active set of constraints. The first of these two problems is addressed here and a new algorithm is proposed that does not require explicit calculation of second order information. Author

N89-25183*# MacNeal-Schwendler Corp., Los Angeles, CA.
GRID SENSITIVITY CAPABILITY FOR LARGE SCALE STRUCTURES **c39**
Gopal K. Nagendra and David V. Wallerstein *In* NASA. Langley Research Center, Recent Advances in Multidisciplinary Analysis and Optimization, Part 2 Apr. 1989 p 697-711 (For primary document see N89-25173 19-05)
Avail: NTIS HC A22/MF A01 CSCL 20K

The considerations and the resultant approach used to implement design sensitivity capability for grids into a large scale, general purpose finite element system (MSC/NASTRAN) are presented. The design variables are grid perturbations with a rather general linking capability. Moreover, shape and sizing variables may be linked together. The design is general enough to facilitate geometric modeling techniques for generating design variable linking schemes in an easy and straightforward manner. Test cases have been run and validated by comparison with the overall finite difference method. The linking of a design sensitivity capability for shape variables in MSC/NASTRAN with an optimizer would give designers a powerful, automated tool to carry out practical optimization design of real life, complicated structures. Author

N89-25184*# Pennsylvania State Univ., University Park. Dept. of Mechanical Engineering.
ITERATIVE METHODS FOR DESIGN SENSITIVITY ANALYSIS **c39**
A. D. Belegundu and B. G. Yoon *In* NASA. Langley Research Center, Recent Advances in Multidisciplinary Analysis and Optimization, Part 2 Apr. 1989 p 713-726 Previously announced in IAA as A89-22370 (For primary document see N89-25173 19-05)
Avail: NTIS HC A22/MF A01 CSCL 20K

A numerical method is presented for design sensitivity analysis, using an iterative-method reanalysis of the structure generated by a small perturbation in the design variable; a forward-difference scheme is then employed to obtain the approximate sensitivity. Algorithms are developed for displacement and stress sensitivity, as well as for eignevalues and eigenvector sensitivity, and the iterative schemes are modified so that the coefficient matrices are constant and therefore decomposed only once. Author

N89-25185*# National Aeronautics and Space Administration. Langley Research Center, Hampton, VA.
RESULTS OF AN INTEGRATED STRUCTURE/CONTROL LAW DESIGN SENSITIVITY ANALYSIS **c39**
Michael G. Gilbert *In its* Recent Advances in Multidisciplinary Analysis and Optimization, Part 2 Apr. 1989 p 727-745 Previously announced as N89-15111 (For primary document see N89-25173 19-05)
Avail: NTIS HC A22/MF A01 CSCL 20K

A design sensitivity analysis method for Linear Quadratic Cost, Gaussian (LQG) optimal control laws, which predicts change in the optimal control law due to changes in fixed problem parameters using analytical sensitivity equations is discussed. Numerical results of a design sensitivity analysis for a realistic aeroservoelastic aircraft example are presented. In this example, the sensitivity of the optimally controlled aircraft's response to various problem formulation and physical aircraft parameters is determined. These results are used to predict the aircraft's new optimally controlled response if the parameter was to have some other nominal value during the control law design process. The sensitivity results are validated by recomputing the optimal control law for discrete variations in parameters, computing the new actual aircraft response, and comparing with the predicted response. These results show an improvement in sensitivity accuracy for integrated design purposes over methods which do not include changes in the optimal control law. Use of the analytical LQG sensitivity expressions is also shown to be more efficient than finite difference methods for the computation of the equivalent sensitivity information. Author

N89-25186*# Nebraska Univ., Lincoln. Dept. of Engineering Mechanics.
ON THE CALCULATION OF DERIVATIVES OF EIGENVALUES AND EIGENVECTORS IN THE SIMULTANEOUS DESIGN AND CONTROL OF STRUCTURES **c39**
Luis Mesquita and Manohar P. Kamat (Georgia Inst. of Tech., Atlanta.) *In* NASA. Langley Research Center, Recent Advances in Multidisciplinary Analysis and Optimization, Part 2 Apr. 1989 p 747-758 (For primary document see N89-25173 19-05)
Avail: NTIS HC A22/MF A01 CSCL 20K

Independent Modal Space Control (IMSC) is a technique that is often used for the control of large order structural systems. The pertinent optimization problem in the simultaneous design and control of structures is a min - min problem that minimizes with respect to the structural design variables, the minimum value of the performance index with respect to the control forces obtained using the IMSC technique. The minimization process requires derivatives of eigenvalues and eigenvectors with respect to the design variables. These derivatives can be computed by a rather involved analytical procedure or a relatively simple finite difference procedure. The computer cost effectiveness of these two procedures for the derivative calculations is examined. Author

N89-25187*# Worcester Polytechnic Inst., MA. Dept. of Mechanical Engineering.
TREATMENT OF BODY FORCES IN BOUNDARY ELEMENT DESIGN SENSITIVITY ANALYSIS **c39**
Sunil Saigal, James H. Kane, R. Aithal, and Jizu Cheng *In* NASA. Langley Research Center, Recent Advances in Multidisciplinary Analysis and Optimization, Part 2 Apr. 1989 p 759-776 (For primary document see N89-25173 19-05)
(Grant NSF MSM-87-0742)
Avail: NTIS HC A22/MF A01 CSCL 20K

The inclusion of body forces has received a good deal of attention in boundary element research. The consideration of such forces is essential in the desgin of high performance components such as fan and turbine disks in a gas turbine engine. Due to their critical performance requirements, optimal shapes are often desired for these components. The boundary element method (BEM) offers the possibility of being an efficient method for such iterative analysis as shape optimization. The implicit-differentiation of the boundary integral equations is performed to obtain the sensitivity equations. The body forces are accounted for by either the particular integrals for uniform body forces or by a surface integration for non-uniform body forces. The corresponding sensitivity equations for both these cases are presented. The validity of present formulations is established through a close agreement with exact analytical results. Author

N89-25188*# Clarkson Univ., Potsdam, NY.
DESIGN SENSITIVITY ANALYSIS OF BOUNDARY ELEMENT SUBSTRUCTURES **c39**
James H. Kane, Sunil Saigal (Worcester Polytechnic Inst., MA.), and Richard H. Gallagher *In* NASA. Langley Research Center, Recent Advances in Multidisciplinary Analysis and Optimization,

Part 2 Apr. 1989 p 777-799 (For primary document see N89-25173 19-05)
Avail: NTIS HC A22/MF A01 CSCL 20K

The ability to reduce or condense a three-dimensional model exactly, and then iterate on this reduced size model representing the parts of the design that are allowed to change in an optimization loop is discussed. The discussion presents the results obtained from an ongoing research effort to exploit the concept of substructuring within the structural shape optimization context using a Boundary Element Analysis (BEA) formulation. The first part contains a formulation for the exact condensation of portions of the overall boundary element model designated as substructures. The use of reduced boundary element models in shape optimization requires that structural sensitivity analysis can be performed. A reduced sensitivity analysis formulation is then presented that allows for the calculation of structural response sensitivities of both the substructured (reduced) and unsubstructured parts of the model. It is shown that this approach produces significant computational economy in the design sensitivity analysis and reanalysis process by facilitating the block triangular factorization and forward reduction and backward substitution of smaller matrices. The implementatior of this formulation is discussed and timings and accuracies of representative test cases presented.
Author

N89-25189*# Purdue Univ., West Lafayette, IN.
AEROSERVOELASTIC TAILORING FOR LATERAL CONTROL ENHANCEMENT **c08**
Terrence A. Weisshaar and Nam Changho *In* NASA. Langley Research Center, Recent Advances in Multidisciplinary Analysis and Optimization, Part 2 Apr. 1989 p 803-814 (For primary document see N89-25173 19-05)
Avail: NTIS HC A22/MF A01 CSCL 01C

The need for effective aileron power for aircraft lateral control and turning maneuvers dates back to the Wright Brothers and their wing warping concept for active stabilization of their aircraft. Early researchers in Great Britain, Japan, Germany and the United States explored ways to increase the effectiveness of control aileron to generate a roll moment. The basic problem of aileron effectiveness and the interrelationship between structural distortion and the loads applied by the control surface is illustrated. A rigid wing/aileron surface will develop the capability to generate increased roll rates as airspeed increases. A flexible surface will become less effective as airspeed increases because of the twisting distortion created by the aft-mounted control surface. This tendency is further worsened by bending distortion of an aft swept wing. This study focuses its attention on the ability of a combined effort between structural redesign of a wing and sizing and placement of a control surface to create specified roll performance with a minimum hinge moment. This design optimization problem indicates the advantages of simultaneous consideration of structural design and control design.
Author

N89-25190*# National Aeronautics and Space Administration. Langley Research Center, Hampton, VA.
RESULTS OF INCLUDING GEOMETRIC NONLINEARITIES IN AN AEROELASTIC MODEL OF AN F/A-18
Carey S. Buttrill *In its* Recent Advances in Multidisciplinary Analysis and Optimization, Part 2 Apr. 1989 p 815-836 (For primary document see N89-25173 19-05)
Avail: NTIS HC A22/MF A01 CSCL 01C

An integrated, nonlinear simulation model suitable for aeroelastic modeling of fixed-wing aircraft has been developed. While the author realizes that the subject of modeling rotating, elastic structures is not closed, it is believed that the equations of motion developed and applied herein are correct to second order and are suitable for use with typical aircraft structures. The equations are not suitable for large elastic deformation. In addition, the modeling framework generalizes both the methods and terminology of non-linear rigid-body airplane simulation and traditional linear aeroelastic modeling. Concerning the importance of angular/elastic inertial coupling in the dynamic analysis of fixed-wing aircraft, the following may be said. The rigorous inclusion of said coupling is not without peril and must be approached with care. In keeping with the same engineering judgment that guided the development of the traditional aeroelastic equations, the effect of non-linear inertial effects for most airplane applications is expected to be small. A parameter does not tell the whole story, however, and modes flagged by the parameter as significant also need to be checked to see if the coupling is not a one-way path, i.e., the inertially affected modes can influence other modes.
Author

N89-25191*# National Aeronautics and Space Administration. Langley Research Center, Hampton, VA.
FLUTTER SUPPRESSION USING EIGENSPACE FREEDOMS TO MEET REQUIREMENTS **c08**
William M. Adams, Jr., Robert E. Fennell, and David M. Christhilf (Planning Research Corp., Hampton, VA.) *In its* Recent Advances in Multidisciplinary Analysis and Optimization, Part 2 Apr. 1989 p 837-859 (For primary document see N89-25173 19-05)
Avail: NTIS HC A22/MF A01 CSCL 01C

A constrained optimization methodology has been developed which allows specific use of eigensystem freedoms to meet design requirements. A subset of the available eigenvector freedoms was employed. The eigenvector freedoms associated with a particular closed-loop eigenvalue are coefficients of basis vectors which span the subspace in which that closed-loop vector must lie. Design requirements are included as a vector of inequality constraints. The procedure was successfully applied to develop an unscheduled controller which stabilizes symmetric flutter of an aeroelastic vehicle to a dynamic pressure 44 percent above the open-loop flutter point. The design process proceeded from full-state feedback to the inclusion of a full-order observer to the selection of an eighth-order controller which preserved the full-state sensitivity characteristics. Only a subset of the design freedoms was utilized (i.e., assuming full-state feedback only four out of 26 eigenvectors were used, and no variations were made in the closed-loop eigenvalues). Utilization of additional eigensystem freedoms could further improve the controller.
Author

N89-25192*# National Aeronautics and Space Administration. Langley Research Center, Hampton, VA.
AEROELASTIC MODELING FOR THE FIT (FUNCTIONAL INTEGRATION TECHNOLOGY) TEAM F/A-18 SIMULATION
Thomas A. Zeiler (Planning Research Corp., Hampton, VA.) and Carol D. Wieseman *In its* Recent Advances in Multidisciplinary Analysis and Optimization, Part 2 Apr. 1989 p 861-877 (For primary document see N89-25173 19-05)
Avail: NTIS HC A22/MF A01 CSCL 01C

As part of Langley Research Center's commitment to developing multidisciplinary integration methods to improve aerospace systems, the Functional Integration Technology (FIT) team was established to perform dynamics integration research using an existing aircraft configuration, the F/A-18. An essential part of this effort has been the development of a comprehensive simulation modeling capability that includes structural, control, and propulsion dynamics as well as steady and unsteady aerodynamics. The structural and unsteady aerodynamics contributions come from an aeroelastic mode. Some details of the aeroelastic modeling done for the Functional Integration Technology (FIT) team research are presented. Particular attention is given to work done in the area of correction factors to unsteady aerodynamics data.
Author

N89-25193*# Planning Research Corp., Hampton, VA.
DIGITAL ROBUST CONTROL LAW SYNTHESIS USING CONSTRAINED OPTIMIZATION **c08**
Vivekananda Mukhopadhyay *In* NASA. Langley Research Center, Recent Advances in Multidisciplinary Analysis and Optimization, Part 2 Apr. 1989 p 879-895 (For primary document see N89-25173 19-05)
(Contract NAS1-8000)
Avail: NTIS HC A22/MF A01 CSCL 01C

Development of digital robust control laws for active control of high performance flexible aircraft and large space structures is a research area of significant practical importance. The flexible

system is typically modeled by a large order state space system of equations in order to accurately represent the dynamics. The active control law must satisy multiple conflicting design requirements and maintain certain stability margins, yet should be simple enough to be implementable on an onboard digital computer. Described here is an application of a generic digital control law synthesis procedure for such a system, using optimal control theory and constrained optimization technique. A linear quadratic Gaussian type cost function is minimized by updating the free parameters of the digital control law, while trying to satisfy a set of constraints on the design loads, responses and stability margins. Analytical expressions for the gradients of the cost function and the constraints with respect to the control law design variables are used to facilitate rapid numerical convergence. These gradients can be used for sensitivity study and may be integrated into a simultaneous structure and control optimization scheme. Author

N89-25194*# California Univ., Los Angeles. Dept. of Mechanical, Aerospace and Nuclear Engineering.

AN INTEGRATED APPROACH TO THE OPTIMUM DESIGN OF ACTIVELY CONTROLLED COMPOSITE WINGS

E. Livne *In* NASA. Langley Research Center, Recent Advances in Multidisciplinary Analysis and Optimization, Part 2 Apr. 1989 p 897-918 (For primary document see N89-25173 19-05)
(Contract F49620-87-K-0003)
Avail: NTIS HC A22/MF A01 CSCL 01C

The importance of interactions among the various disciplines in airplane wing design has been recognized for quite some time. With the introduction of high gain, high authority control systems and the design of thin, flexible, lightweight composite wings, the integrated treatment of control systems, flight mechanics and dynamic aeroelasticity became a necessity. A research program is underway now aimed at extending structural synthesis concepts and methods to the integrated synthesis of lifting surfaces, spanning the disciplines of structures, aerodynamics and control for both analysis and design. Mathematical modeling techniques are carefully selected to be accurate enough for preliminary design purposes of the complicated, built-up lifting surfaces of real aircraft with their multiple design criteria and tight constraints. The presentation opens with some observations on the multidisciplinary nature of wing design. A brief review of some available state of the art practical wing optimization programs and a brief review of current research effort in the field serve to illuminate the motivation and support the direction taken in our research. The goals of this research effort are presented, followed by a description of the analysis and behavior sensitivity techniques used. The presentation concludes with a status report and some forecast of upcoming progress. Author

N89-25195*# National Aeronautics and Space Administration. Hugh L. Dryden Flight Research Facility, Edwards, CA.

CONTROL SURFACE SPANWISE PLACEMENT IN ACTIVE FLUTTER SUPPRESSION SYSTEMS c08

E. Nissim and J. J. Burken *In* NASA. Langley Research Center, Recent Advances in Multidisciplinary Analysis and Optimization, Part 2 Apr. 1989 p 919-934 Prepared in cooperation with Technion-Israel Inst. of Technology, Haifa (For primary document see N89-25173 19-05)
Avail: NTIS HC A22/MF A01 CSCL 01C

All flutter suppression systems require sensors to detect the movement of the lifting surface and to activate a control surface according to a synthesized control law. Most of the work performed to date relates to the development of control laws based on predetermined locations of sensors and control surfaces. These locations of sensors and control surfaces are determined either arbitrarily, or by means of a trial and error procedure. The aerodynamic energy concept indicates that the sensors should be located within the activated strip. Furthermore, the best chordwise location of a sensor activating a T.E. control surface is around the 65 percent chord location. The best chordwise location for a sensor activating a L.E. surface is shown to lie upstream of the wing (around 20 percent upstream of the leading edge), or alternatively, two sensors located along the same chord should be used. Author

N89-25196*# Air Force Wright-Patterson Aeronautical Labs., Wright-Patterson AFB, OH.

AN APPROXIMATION FUNCTION FOR FREQUENCY CONSTRAINED STRUCTURAL OPTIMIZATION c39

R. A. Canfield *In* NASA. Langley Research Center, Recent Advances in Multidisciplinary Analysis and Optimization, Part 2 Apr. 1989 p 937-953 (For primary document see N89-25173 19-05)
Avail: NTIS HC A22/MF A01 CSCL 20K

The purpose is to examine a function for approximating natural frequency constraints during structural optimization. The nonlinearity of frequencies has posed a barrier to constructing approximations for frequency constraints of high enough quality to facilitate efficient solutions. A new function to represent frequency constraints, called the Rayleigh Quotient Approximation (RQA), is presented. Its ability to represent the actual frequency constraint results in stable convergence with effectively no move limits. The objective of the optimization problem is to minimize structural weight subject to some minimum (or maximum) allowable frequency and perhaps subject to other constraints such as stress, displacement, and gage size, as well. A reason for constraining natural frequencies during design might be to avoid potential resonant frequencies due to machinery or actuators on the structure. Another reason might be to satisy requirements of an aircraft or spacecraft's control law. Whatever the structure supports may be sensitive to a frequency band that must be avoided. Any of these situations or others may require the designer to insure the satisfaction of frequency constraints. A further motivation for considering accurate approximations of natural frequencies is that they are fundamental to dynamic response constraints. Author

N89-25197*# Air Force Wright-Patterson Aeronautical Labs., Wright-Patterson AFB, OH.

STRUCTURAL OPTIMIZATION OF FRAMED STRUCTURES USING GENERALIZED OPTIMALITY CRITERIA c39

R. M. Kolonay, Vipperla B. Venkayya, V. A. Tischler, and R. A. Canfield *In* NASA. Langley Research Center, Recent Advances in Multidisciplinary Analysis and Optimization, Part 2 Apr. 1989 p 955-969 (For primary document see N89-25173 19-05)
Avail: NTIS HC A22/MF A01 CSCL 20K

The application of a generalized optimality criteria to framed structures is presented. The optimality conditions, Lagrangian multipliers, resizing algorithm, and scaling procedures are all represented as a function of the objective and constraint functions along with their respective gradients. The optimization of two plane frames under multiple loading conditions subject to stress, displacement, generalized stiffness, and side constraints is presented. These results are compared to those found by optimizing the frames using a nonlinear mathematical programming technique. Author

N89-25198*# National Aeronautics and Space Administration. Langley Research Center, Hampton, VA.

FINITE ELEMENT FLOW-THERMAL-STRUCTURAL ANALYSIS OF AERODYNAMICALLY HEATED LEADING EDGES c02

Pramote Dechaumphai, Allan R. Wieting, and Ajay K. Pandey (Planning Research Corp., Hampton, VA.) *In its* Recent Advances in Multidisciplinary Analysis and Optimization, Part 2 Apr. 1989 p 971-990 (For primary document see N89-25173 19-05)
Avail: NTIS HC A22/MF A01 CSCL 01A

Hypersonic vehicles operate in a hostile aerothermal environment which has a significant impact on their aerothermostructural performance. Significant coupling occurs between the aerodynamic flow field, structural heat transfer, and structural response creating a multidisciplinary interaction. A long term goal of the Aerothermal Loads Branch at the NASA Langley Research Center is to develop a computational capability for integrated fluid, thermal and structural analysis of aerodynamically heated structures. The integrated analysis capability includes the coupling between the fluid and the structure which occurs primarily

through the thermal response of the structure, because: (1) the surface temperature affects the external flow by changing the amount of energy absorbed by the structure, and (2) the temperature gradients in the structure result in structural deformations which alter the flow field and attendant surface pressures and heating rates. In the integrated analysis, a finite element method is used to solve: (1) the Navier-Stokes equations for the flow solution, (2) the energy equation of the structure for the temperature response, and (3) the equilibrium equations of the structure for the structural deformation and stresses. Author

N89-25199*# PDA Engineering, Costa Mesa, CA.
INVOLUTE COMPOSITE DESIGN EVALUATION USING GLOBAL DESIGN SENSITIVITY DERIVATIVES c20
J. K. Hart and E. L. Stanton *In* NASA. Langley Research Center, Recent Advances in Multidisciplinary Analysis and Optimization, Part 2 Apr. 1989 p 991-1008 (For primary document see N89-25173 19-05)
Avail: NTIS HC A22/MF A01 CSCL 21H

An optimization capability for involute structures has been developed. Its key feature is the use of global material geometry variables which are so chosen that all combinations of design variables within a set of lower and upper bounds correspond to manufacturable designs. A further advantage of global variables is that their number does not increase with increasing mesh density. The accuracy of the sensitivity derivatives has been verified both through finite difference tests and through the successful use of the derivatives by an optimizer. The state of the art in composite design today is still marked by point design algorithms linked together using ad hoc methods not directly related to a manufacturing procedure. The global design sensitivity approach presented here for involutes can be applied to filament wound shells and other composite constructions using material form features peculiar to each construction. The present involute optimization technology is being applied to the Space Shuttle SRM nozzle boot ring redesigns by PDA Engineering. Author

N89-25200*# General Dynamics Corp., Groton, CT. Electric Boat Div.
OPTIMIZING FOR MINIMUM WEIGHT WHEN TWO DIFFERENT FINITE ELEMENT MODELS AND ANALYSES ARE REQUIRED c39
Jeffrey C. Hall *In* NASA. Langley Research Center, Recent Advances in Multidisciplinary Analysis and Optimization, Part 2 Apr. 1989 p 1009-1026 (For primary document see N89-25173 19-05)
Avail: NTIS HC A22/MF A01 CSCL 20K

The Finite Element Structural Optimization Program's (FESOP) ability to perform minimum weight optimization using two different finite element analyses and models is discussed. FESOP uses the ADS optimizer developed by Dr. Garret Vanderplaats to solve the nonlinear constrained optimization problem. The design optimization problem requires a response spectrum analysis and model to evaluate the stress and displacement constraints. However, the problem needs a frequency analysis and model to calculate the natural frequencies used to evaluate the frequency range constraints. The results of both the successful and unsuccessful approaches used to solve this difficult weight minimization problem are summarized. The results show that no one ADS optimization algorithm worked in all cases. However, the Sequential Convex Programming and Modified Method of Feasible Directions algorithms were the most successful. Author

N89-25201*# National Aeronautics and Space Administration. Langley Research Center, Hampton, VA.
RECENT ADVANCES IN MULTIDISCIPLINARY ANALYSIS AND OPTIMIZATION, PART 3
Jean-Francois M. Barthelemy, ed. Washington Apr. 1989 513 p Symposium held in Hampton, VA, 28-30 Sep. 1988; sponsored by NASA, Langley Research Center, NASA, Lewis Research Center, and Wright Research Development Center (NASA-CP-3031-Pt-3; L-16568-Pt-3; NAS 1.55:3031-Pt-3) Avail: NTIS HC A22/MF A01 CSCL 01C

This three-part document contains a collection of technical papers presented at the Second NASA/Air Force Symposium on Recent Advances in Multidisciplinary Analysis and Optimization, held September 28-30, 1988 in Hampton, Virginia. The topics covered include: aircraft design, aeroelastic tailoring, control of aeroelastic structures, dynamics and control of flexible structures, structural design, design of large engineering systems, application of artificial intelligence, shape optimization, software development and implementation, and sensitivity analysis. For individual titles, see N89-25202 through N89-25231.

N89-25202*# National Aeronautics and Space Administration. Langley Research Center, Hampton, VA.
ENGINEERING APPLICATIONS OF HEURISTIC MULTILEVEL OPTIMIZATION METHODS c39
Jean-Francois M. Barthelemy *In its* Recent Advances in Multidisciplinary Analysis and Optimization, Part 3 Apr. 1989 p 1029-1037 Previously announced as N89-13203 (For primary document see N89-25201 19-05)
Avail: NTIS HC A22/MF A01 CSCL 20K

Some engineering applications of heuristic multilevel optimization methods are presented and the discussion focuses on the dependency matrix that indicates the relationship between problem functions and variables. Coordination of the subproblem optimizations is shown to be typically achieved through the use of exact or approximate sensitivity analysis. Areas for further development are identified. Author

N89-25203*# California Univ., Santa Barbara. Dept. of Mechanical and Environmental Engineering.
RECENT DEVELOPMENTS IN MULTILEVEL OPTIMIZATION c39
Garret N. Vanderplaats and D.-S. Kim *In* NASA. Langley Research Center, Recent Advances in Multidisciplinary Analysis and Optimization, Part 3 Apr. 1989 p 1039-1054 (For primary document see N89-25201 19-05)
Avail: NTIS HC A22/MF A01 CSCL 20K

Recent developments in multilevel optimization are briefly reviewed. The general nature of the multilevel design task, the use of approximations to develop and solve the analysis design task, the structure of the formal multidiscipline optimization problem, a simple cantilevered beam which demonstrates the concepts of multilevel design and the basic mathematical details of the optimization task and the system level are among the topics discussed. R.J.F.

N89-25204*# Maryland Univ., College Park. Dept. of Mechanical Engineering.
A DECOMPOSITION-BASED DESIGN OPTIMIZATION METHOD WITH APPLICATIONS c39
Shapour Azarm, M. Pecht, W.-C. Li, and S. Praharaj *In* NASA. Langley Research Center, Recent Advances in Multidisciplinary Analysis and Optimization, Part 3 Apr. 1989 p 1055-1067 (For primary document see N89-25201 19-05)
Avail: NTIS HC A22/MF A01 CSCL 20K

A two-level design optimization metholology is described. A progress report of its application to Printed Wiring Board (PWB) assembly examples is given. The design of PWB assemblies is a complex task which is generally conducted as a sequential process. Individual PWBs are usually designed first, followed by the composition of the PWBs into an assembly. As a result, optimizing design considerations such as assembly reliability cannot be accomplished. This study showed that a two-level decomposition method can be employed to optimize for reliability at both the PWB- and the assembly-level in a coupled manner. The two-level decomposition method also resolved the mixed-integer nonlinear programming nature of the problem rather easily. Author

N89-25205*# Missouri Univ., Columbia. Design Productivity Center.
MULTILEVEL DECOMPOSITION OF COMPLETE VEHICLE CONFIGURATION IN A PARALLEL COMPUTING ENVIRONMENT

Vinay Bhatt and K. M. Ragsdell *In* NASA. Langley Research Center, Recent Advances in Multidisciplinary Analysis and Optimization, Part 3 Apr. 1989 p 1069-1082 (For primary document see N89-25201 19-05)
Avail: NTIS HC A22/MF A01 CSCL 01C

This research summarizes various approaches to multilevel decomposition to solve large structural problems. A linear decomposition scheme based on the Sobieski algorithm is selected as a vehicle for automated synthesis of a complete vehicle configuration in a parallel processing environment. The research is in a developmental state. Preliminary numerical results are presented for several example problems. Author

N89-25206*# Kansas Univ., Lawrence. Dept. of Aerospace Engineering.
DESIGN OPTIMIZATION OF AXISYMMETRIC BODIES IN NONUNIFORM TRANSONIC FLOW
C. Edward Lan *In* NASA. Langley Research Center, Recent Advances in Multidisciplinary Analysis and Optimization, Part 3 Apr. 1989 p 1085-1095 (For primary document see N89-25201 19-05)
Avail: NTIS HC A22/MF A01 CSCL 01C

An inviscid transonic code capable of designing an axisymmetric body in a uniform or nonuniform flow was developed. The design was achieved by direct optimiation by coupling an analysis code with an optimizer. Design examples were provided for axisymmetric bodies with fineness ratios of 8.33 and 5 at different Mach numbers. It was shown that by reducing the nose radius and increasing the afterbody thickness of initial shapes obtained from symmetric NACA four-digit airfoil contours, wave drag could be reduced by 29 percent for a body of fineness ratio 8.33 in a nonuniform transonic flow of M = 0.98 to 0.995. The reduction was 41 percent for a body of fineness ratio 5 in a uniform transonic flow of M = 0.925 and 65 percent for the same body but in a nonuniform transonic flow of M = 0.90 to 0.95. Author

N89-25207*# Textron Lycoming, Stratford, CT.
PROCEDURES FOR SHAPE OPTIMIZATION OF GAS TURBINE DISKS **c07**
Tsu-Chien Cheu *In* NASA. Langley Research Center, Recent Advances in Multidisciplinary Analysis and Optimization, Part 3 Apr. 1989 p 1097-1108 (For primary document see N89-25201 19-05)
Avail: NTIS HC A22/MF A01 CSCL 21E

Two procedures, the feasible direction method and sequential linear programming, for shape optimization of gas turbine disks are presented. The objective of these procedures is to obtain optimal designs of turbine disks with geometric and stress constraints. The coordinates of the selected points on the disk contours are used as the design variables. Structural weight, stress and their derivatives with respect to the design variables are calculated by an efficient finite element method for design senitivity analysis. Numerical examples of the optimal designs of a disk subjected to thermo-mechanical loadings are presented to illustrate and compare the effectiveness of these two procedures. Author

N89-25208*# Houston Univ., TX. Systems Design Lab.
A DECISION-BASED PERSPECTIVE FOR THE DESIGN OF METHODS FOR SYSTEMS DESIGN **c31**
Farrokh Mistree, Douglas Muster, Jon A. Shupe, and Janet K. Allen (Janco Research, Houston, TX.) *In* NASA. Langley Research Center, Recent Advances in Multidisciplinary Analysis and Optimization, Part 3 Apr. 1989 p 1111-1135 (For primary document see N89-25201 19-05)
Avail: NTIS HC A22/MF A01 CSCL 13B

Organization of material, a definition of decision based design, a hierarchy of decision based design, the decision support problem technique, a conceptual model design that can be manufactured and maintained, meta-design, computer-based design, action learning, and the characteristics of decisions are among the topics covered. R.J.F.

N89-25209*# Rockwell International Corp., Los Angeles, CA.
THE ART OF SPACECRAFT DESIGN: A MULTIDISCIPLINARY CHALLENGE **c18**
F. Abdi, H. Ide, M. Levine, and L. Austel *In* NASA. Langley Research Center, Recent Advances in Multidisciplinary Analysis and Optimization, Part 3 Apr. 1989 p 1137-1155 (For primary document see N89-25201 19-05)
Avail: NTIS HC A22/MF A01 CSCL 22B

Actual design turn-around time has become shorter due to the use of optimization techniques which have been introduced into the design process. It seems that what, how and when to use these optimization techniques may be the key factor for future aircraft engineering operations. Another important aspect of this technique is that complex physical phenomena can be modeled by a simple mathematical equation. The new powerful multilevel methodology reduces time-consuming analysis significantly while maintaining the coupling effects. This simultaneous analysis method stems from the implicit function theorem and system sensitivity derivatives of input variables. Use of the Taylor's series expansion and finite differencing technique for sensitivity derivatives in each discipline makes this approach unique for screening dominant variables from nondominant variables. In this study, the current Computational Fluid Dynamics (CFD) aerodynamic and sensitivity derivative/optimization techniques are applied for a simple cone-type forebody of a high-speed vehicle configuration to understand basic aerodynamic/structure interaction in a hypersonic flight condition. Author

N89-25210*# National Aeronautics and Space Administration. Langley Research Center, Hampton, VA.
HYPERSONIC AIRBREATHING VEHICLE CONCEPTUAL DESIGN (FOCUS ON AERO-SPACE PLANE)
James L. Hunt and John G. Martin (Planning Research Corp., Hampton, VA.) *In its* Recent Advances in Multidisciplinary Analysis and Optimization, Part 3 Apr. 1989 p 1157-1194 (For primary document see N89-25201 19-05)
Avail: NTIS HC A22/MF A01 CSCL 01C

The airbreathing single stage to orbit (SSTO) vehicle design environment is variable-rich, intricately networked and sensitivity intensive. As such, it represents a tremondous technology challenge. Creating a viable design will require sophisticated configuration/synthesis and the synergistic integration of advanced technologies across the discipline spectrum. In design exercises, reductions in the fuel weight-fraction requirements projected for an orbital vehicle concept can result from improvements in aerodynamics/controls, propulsion efficiencies and trajectory optimization; also, gains in the fuel weight-fraction achievable for such a concept can result from improvements in structural design, heat management techniques, and material properties. As these technology advances take place, closure on a viable vehicle design will be realizable. Author

N89-25211*# National Aeronautics and Space Administration. Langley Research Center, Hampton, VA.
OPTIMIZING CONCEPTUAL AIRCRAFT DESIGNS FOR MINIMUM LIFE CYCLE COST
Vicki S. Johnson *In its* Recent Advances in Multidisciplinary Analysis and Optimization, Part 3 Apr. 1989 p 1195-1217 (For primary document see N89-25201 19-05)
Avail: NTIS HC A22/MF A01 CSCL 01C

A life cycle cost (LCC) module has been added to the FLight Optimization System (FLOPS), allowing the additional optimization variables of life cycle cost, direct operating cost, and acquisition cost. Extensive use of the methodology on short-, medium-, and medium-to-long range aircraft has demonstrated that the system works well. Results from the study show that optimization parameter has a definite effect on the aircraft, and that optimizing an aircraft for minimum LCC results in a different airplane than when optimizing for minimum take-off gross weight (TOGW), fuel burned, direct operation cost (DOC), or acquisition cost. Additionally, the economic assumptions can have a strong impact on the configurations optimized for minimum LCC or DOC. Also, results show that advanced technology can be worthwhile, even if it results in higher

manufacturing and operating costs. Examining the number of engines a configuration should have demonstrated a real payoff of including life cycle cost in the conceptual design process: the minimum TOGW of fuel aircraft did not always have the lowest life cycle cost when considering the number of engines. Author

N89-25212*# Stanford Univ., CA. Dept. of Aeronautics and Astronautics.

AIRCRAFT DESIGN OPTIMIZATION WITH MULTIDISCIPLINARY PERFORMANCE CRITERIA

Stephen Morris and Ilan Kroo *In* NASA. Langley Research Center, Recent Advances in Multidisciplinary Analysis and Optimization, Part 3 Apr. 1989 p 1219-1235 (For primary document see N89-25201 19-05)

Avail: NTIS HC A22/MF A01 CSCL 01C

The method described here for aircraft design optimization with dynamic response considerations provides an inexpensive means of integrating dynamics into aircraft preliminary design. By defining a dynamic performance index that can be added to a conventional objective function, a designer can investigate the trade-off between performance and handling (as measured by the vehicle's unforced response). The procedure is formulated to permit the use of control system gains as design variables, but does not require full-state feedback. The examples discussed here show how such an approach can lead to significant improvements in the design as compared with the more common sequential design of system and control law. Author

N89-25213*# Bridgeport Univ., CT. Dept. of Mechanical Engineering.

AN INTERPRETATION AND SOLUTION OF ILL-CONDITIONED LINEAR EQUATIONS **c64**

I. U. Ojalvo and T. Ting *In* NASA. Langley Research Center, Recent Advances in Multidisciplinary Analysis and Optimization, Part 3 Apr. 1989 p 1239-1252 (For primary document see N89-25201 19-05)

Avail: NTIS HC A22/MF A01 CSCL 12A

Data insufficiency, poorly conditioned matrices and singularities in equations occur regularly in complex optimization, correlation, and interdisciplinary model studies. This work concerns itself with two methods of obtaining certain physically realistic solutions to ill-conditioned or singular algebraic systems of linear equations arising from such studies. Two efficient computational solution procedures that generally lead to locally unique solutions are presented when there is insufficient data to completely define the model, or a least-squares error formulation of this system results in an ill-conditioned system of equations. If it is assumed that a reasonable estimate of the uncertain data is available in both cases cited above, then we shall show how to obtain realistic solutions efficiently, in spite of the insufficiency of independent data. The proposed methods of solution are more efficient than singular-value decomposition for dealing with such systems, since they do not require solutions for all the non-zero eigenvalues of the coefficient matrix. Author

N89-25214*# Michigan Univ., Ann Arbor. Dept. of Mechanical Engineering and Applied Mechanics.

GENERALIZED MATHEMATICAL MODELS IN DESIGN OPTIMIZATION **c64**

Panos Y. Papalambros and J. R. Jagannatha Rao *In* NASA. Langley Research Center, Recent Advances in Multidisciplinary Analysis and Optimization, Part 3 Apr. 1989 p 1253-1264 Sponsored in part by General Motors Corp. (For primary document see N89-25201 19-05)

(Grant NSF DMC-85-14721)

Avail: NTIS HC A22/MF A01 CSCL 12A

The theory of optimality conditions of extremal problems can be extended to problems continuously deformed by an input vector. The connection between the sensitivity, well-posedness, stability and approximation of optimization problems is steadily emerging. The authors believe that the important realization here is that the underlying basis of all such work is still the study of point-to-set maps and of small perturbations, yet what has been identified previously as being just related to solution procedures is now being extended to study modeling itself in its own right. Many important studies related to the theoretical issues of parametric programming and large deformation in nonlinear programming have been reported in the last few years, and the challenge now seems to be in devising effective computational tools for solving these generalized design optimization models. Author

N89-25215*# Howard Univ., Washington, DC. Dept. of Mechanical Engineering.

OPTIMUM DESIGN OF STRUCTURES SUBJECT TO GENERAL PERIODIC LOADS **c18**

Robert Reiss and B. Qian *In* NASA. Langley Research Center, Recent Advances in Multidisciplinary Analysis and Optimization, Part 3 Apr. 1989 p 1265-1279 (For primary document see N89-25201 19-05)

Avail: NTIS HC A22/MF A01 CSCL 22B

A simplified version of Icerman's problem regarding the design of structures subject to a single harmonic load is discussed. The nature of the restrictive conditions that must be placed on the design space in order to ensure an analytic optimum are discussed in detail. Icerman's problem is then extended to include multiple forcing functions with different driving frequencies. And the conditions that now must be placed upon the design space to ensure an analytic optimum are again discussed. An important finding is that all solutions to the optimality condition (analytic stationary design) are local optima, but the global optimum may well be non-analytic. The more general problem of distributing the fixed mass of a linear elastic structure subject to general periodic loads in order to minimize some measure of the steady state deflection is also considered. This response is explicitly expressed in terms of Green's functional and the abstract operators defining the structure. The optimality criterion is derived by differentiating the response with respect to the design parameters. The theory is applicable to finite element as well as distributed parameter models. Author

N89-25216*# Michigan State Univ., East Lansing. Dept. of Mechanical Engineering.

FUZZY SET APPLICATIONS IN ENGINEERING OPTIMIZATION: MULTILEVEL FUZZY OPTIMIZATION **c64**

Alejandro R. Diaz *In* NASA. Langley Research Center, Recent Advances in Multidisciplinary Analysis and Optimization, Part 3 Apr. 1989 p 1279-1289 (For primary document see N89-25201 19-05)

(Grant NSF DME-87-06902)

Avail: NTIS HC A22/MF A01 CSCL 12A

A formulation for multilevel optimization with fuzzy objective functions is presented. With few exceptions, formulations for fuzzy optimization have dealt with a one-level problem in which the objective is the membership function of a fuzzy set formed by the fuzzy intersection of other sets. In the problem examined here, the goal set G is defined in a more general way, using an aggregation operator H that allows arbitrary combinations of set operations (union, intersection, addition) on the individual sets Gi. This is a straightforward extension of the standard form, but one that makes possible the modeling of interesting evaluation strategies. A second, more important departure from the standard form will be the construction of a multilevel problem analogous to the design decomposition problem in optimization. This arrangement facilitates the simulation of a system design process in which different components of the system are designed by different teams, and different levels of design detail become relevant at different time stages in the process: global design features early, local features later in the process. Author

N89-25217*# Virginia Polytechnic Inst. and State Univ., Blacksburg. Dept. of Engineering Science and Mechanics.

A PENALTY APPROACH FOR NONLINEAR OPTIMIZATION WITH DISCRETE DESIGN VARIABLES **c64**

Dong K. Shin, Zafer Gurdal, and O. H. Griffin, Jr. *In* NASA. Langley Research Center, Recent Advances in Multidisciplinary

Analysis and Optimization, Part 3 Apr. 1989 p 1291-1302 (For primary document see N89-25201 19-05)
Avail: NTIS HC A22/MF A01 CSCL 12A

Introduced here is a simple approach to minimization problems with discrete design variables by modifying the penaly function approach of converting the constrained problems into sequential unconstrained minimization technique (SUMT) problems. It was discovered, during the course of the present work, that a similar idea was suggested by Marcal and Gellatly. However, no further work has been encountered. A brief description of the SUMT is presented. The form of the penalty function for the discrete-valued design variables and strategy used for the implementation of the procedure is discussed next. Finally, several design examples are used to demonstrate the procedure, and results are compared with the ones available in the literature. Author

N89-25218*# Colorado State Univ., Fort Collins. Dept. of Mathematics.
MULTIPLIER-CONTINUATION ALGORTHMS FOR CONSTRAINED OPTIMIZATION **c61**
Bruce N. Lundberg, Aubrey B. Poore, and Yang Bing *In* NASA. Langley Research Center, Recent Advances in Multidisciplinary Analysis and Optimization, Part 3 Apr. 1989 p 1303-1315 (For primary document see N89-25201 19-05)
(Grants NGT-06-002-802; AF-AFOSR-0059-88)
Avail: NTIS HC A22/MF A01 CSCL 09B

Several path following algorithms based on the combination of three smooth penalty functions, the quadratic penalty for equality constraints and the quadratic loss and log barrier for inequality constraints, their modern counterparts, augmented Lagrangian or multiplier methods, sequential quadratic programming, and predictor-corrector continuation are described. In the first phase of this methodology, one minimizes the unconstrained or linearly constrained penalty function or augmented Lagrangian. A homotopy path generated from the functions is then followed to optimality using efficient predictor-corrector continuation methods. The continuation steps are asymptotic to those taken by sequential quadratic programming which can be used in the final steps. Numerical test results show the method to be efficient, robust, and a competitive alternative to sequential quadratic programming. Author

N89-25219*# Iowa Univ., Iowa City. Dept. of Mechanical Engineering.
A LARGE SCALE SOFTWARE SYSTEM FOR SIMULATION AND DESIGN OPTIMIZATION OF MECHANICAL SYSTEMS **c61**
Bernhard Dopker and Edward J. Haug *In* NASA. Langley Research Center, Recent Advances in Multidisciplinary Analysis and Optimization, Part 3 Apr. 1989 p 1319-1333 (For primary document see N89-25201 19-05)
Avail: NTIS HC A22/MF A01 CSCL 09B

The concept of an advanced integrated, networked simulation and design system is outlined. Such an advanced system can be developed utilizing existing codes without compromising the integrity and functionality of the system. An example has been used to demonstrate the applicability of the concept of the integrated system outlined here. The development of an integrated system can be done incrementally. Initial capabilities can be developed and implemented without having a detailed design of the global system. Only a conceptual global system must exist. For a fully integrated, user friendly design system, further research is needed in the areas of engineering data bases, distributed data bases, and advanced user interface design. Author

N89-25220*# Georgia Inst. of Tech., Atlanta. School of Aerospace Engineering.
THE ROLE OF OPTIMIZATION IN THE NEXT GENERATION OF COMPUTER-BASED DESIGN TOOLS **c61**
J. Edward Rogan *In* NASA. Langley Research Center, Recent Advances in Multidisciplinary Analysis and Optimization, Part 3 Apr. 1989 p 1335-1357 (For primary document see N89-25201 19-05)
Avail: NTIS HC A22/MF A01 CSCL 09B

There is a close relationship between design optimization and the emerging new generation of computer-based tools for engineering design. With some notable exceptions, the development of these new tools has not taken full advantage of recent advances in numerical design optimization theory and practice. Recent work in the field of design process architecture has included an assessment of the impact of next-generation computer-based design tools on the design process. These results are summarized, and insights into the role of optimization in a design process based on these next-generation tools are presented. An example problem has been worked out to illustrate the application of this technique. The example problem - layout of an aircraft main landing gear - is one that is simple enough to be solved by many other techniques. Although the mathematical relationships describing the objective function and constraints for the landing gear layout problem can be written explicitly and are quite straightforward, an approximation technique has been used in the solution of this problem that can just as easily be applied to integrate supportability or producibility assessments using theory of measurement techniques into the design decision-making process. Author

N89-25221*# McDonnell-Douglas Corp., Long Beach, CA.
AN OVERVIEW OF THE DOUGLAS AIRCRAFT COMPANY AEROELASTIC DESIGN OPTIMIZATION PROGRAM (ADOP)
Alan J. Dodd *In* NASA. Langley Research Center, Recent Advances in Multidisciplinary Analysis and Optimization, Part 3 Apr. 1989 p 1359-1369 (For primary document see N89-25201 19-05)
Avail: NTIS HC A22/MF A01 CSCL 01C

From a program manager's viewpoint, the history, scope and architecture of a major structural design program at Douglas Aircraft Company called Aeroelastic Design Optimization Program (ADOP) are described. ADOP was originally intended for the rapid, accurate, cost-effective evaluation of relatively small structural models at the advanced design level, resulting in improved proposal competitiveness and avoiding many costly changes later in the design cycle. Before release of the initial version in November 1987, however, the program was expanded to handle very large production-type analyses. Author

N89-25222*# McDonnell-Douglas Corp., Long Beach, CA.
MEETING THE CHALLENGES WITH THE DOUGLAS AIRCRAFT COMPANY AEROELASTIC DESIGN OPTIMIZATION PROGRAM (ADOP)
Bruce A. Rommel *In* NASA. Langley Research Center, Recent Advances in Multidisciplinary Analysis and Optimization, Part 3 Apr. 1989 p 1369-1378 (For primary document see N89-25201 19-05)
Avail: NTIS HC A22/MF A01 CSCL 01C

An overview of the Aeroelastic Design Optimization Program (ADOP) at the Douglas Aircraft Company is given. A pilot test program involving the animation of mode shapes with solid rendering as well as wire frame displays, a complete aircraft model of a high-altitude hypersonic aircraft to test ADOP procedures, a flap model, and an aero-mesh modeler for doublet lattice aerodynamics are discussed. R.J.F.

N89-25223*# Air Force Wright-Patterson Aeronautical Labs., Wright-Patterson AFB, OH.
OPTIMIZATION OF STRUCTURE AND CONTROL SYSTEM
N. S. Khot and Ramana V. Grandhi (Wright State Univ., Dayton, OH.) *In* NASA. Langley Research Center, Recent Advances in Multidisciplinary Analysis and Optimization, Part 3 Apr. 1989 p 1381-1392 (For primary document see N89-25201 19-05)
Avail: NTIS HC A22/MF A01 CSCL 01C

The objective of this study is the simultaneous design of the structural and control system for space structures. This study is focused on considering the effect of the number and the location of the actuators on the minimum weight of the structure, and the total work done by the actuators for specified constraints and

disturbance. The controls approach used is the linear quadratic regulator theory with constant feedback. At the beginning collocated actuators and sensors are provided in all the elements. The actuator doing the least work is removed one at a time, and the structure is optimized for the specified constraints on the closed-loop eigenvalues and the damping parameters. The procedure of eliminating an actuator is continued until an acceptable design satisfying the constraints is obtained. The study draws some conclusions on the trade between the total work done by the actuators, and the optimum weight and the number of actuators. Author

N89-25224*# Jet Propulsion Lab., California Inst. of Tech., Pasadena.
STRUCTURAL OPTIMIZATION AND RECENT LARGE GROUND ANTENNA INSTALLATIONS c39
Roy Levy *In* NASA. Langley Research Center, Recent Advances in Multidisciplinary Analysis and Optimization, Part 3 Apr. 1989 p 1393-1416 (For primary document see N89-25201 19-05)
Avail: NTIS HC A22/MF A01 CSCL 20K

Within the past several years, the Jet Propulsion Laboratory has designed and built major ground antenna structures in Spain, Australia, and California. One of the antennas at each location is a 70 meter-diameter structure that is a retrofit of the existing 64 meter antenna. The 64 meter existing antennas were first stripped back to a 34 meter interior and then completely new construction with deeper trusses was added to extend the interior to 70 meters. The 70 meter project included the rare opportunity to collect field data to compare with predictions of the finite-element analytical models. The new quadripod design was tested for its lower mode natural frequencies and the main reflector was measured by theodolite to determine deflections of subsets of the backup-structure deformations under load. The emphasis here is to examine measurement results and possibly provide some appreciation of the relationship of predictions made from the design model to actual measurements. Author

N89-25225*# Texas Univ., Arlington. Dept. of Mechanical Engineering.
A NOVEL IMPLEMENTATION OF METHOD OF OPTIMALITY CRITERION IN SYNTHESIZING SPACECRAFT STRUCTURES WITH NATURAL FREQUENCY CONSTRAINTS c18
Bo Ping Wang and F. H. Chu (General Electric Co., Princeton, NJ.) *In* NASA. Langley Research Center, Recent Advances in Multidisciplinary Analysis and Optimization, Part 3 Apr. 1989 p 1417-1426 (For primary document see N89-25201 19-05)
Avail: NTIS HC A22/MF A01 CSCL 22B

In the design of spacecraft structures, fine tuning the structure to achieve minimum weight with natural frequency constraints is a time consuming process. Here, a novel implementation of the method of optimality criterion (OC) is developed. In this new implementation of OC, the free vibration analysis results are used to compute the eigenvalue sensitivity data required for the formulation. Specifically, the modal elemental strain and kinetic energies are used. Additionally, normalized design parameters are introduced as a second level linking that allows design variables of different values to be linked together. With the use of this novel formulation, synthesis of structures with natural frequency constraint can be carried out manually using modal analysis results. Design examples are presented to illustrate this novel implementation of the optimality criterion method. Author

N89-25226*# California Univ., Berkeley. Coll. of Engineering.
COMPUTATIONAL EXPERIMENTS IN THE OPTIMAL SLEWING OF FLEXIBLE STRUCTURES c39
T. E. Baker and Lucian Elijah Polak *In* NASA. Langley Research Center, Recent Advances in Multidisciplinary Analysis and Optimization, Part 3 Apr. 1989 p 1427-1440 (For primary document see N89-25201 19-05)
(Contract N00014-86-K-0295; NSF ECS-85-17362; AF-AFOSR-0116-86)
Avail: NTIS HC A22/MF A01 CSCL 20K

Numerical experiments on the problem of moving a flexible beam are discussed. An optimal control problem is formulated and transcribed into a form which can be solved using semi-infinite optimization techniques. All experiments were carried out on a SUN 3 microcomputer. Author

N89-25227*# Jet Propulsion Lab., California Inst. of Tech., Pasadena. Applied Technologies Section.
OPTIMAL PLACEMENT OF EXCITATIONS AND SENSORS BY SIMULATED ANNEALING c35
Moktar Salama, R. Bruno, G.-S. Chen, and J. Garba *In* NASA. Langley Research Center, Recent Advances in Multidisciplinary Analysis and Optimization, Part 3 Apr. 1989 p 1441-1457 (For primary document see N89-25201 19-05)
Avail: NTIS HC A22/MF A01 CSCL 14B

The optimal placement of discrete actuators and sensors is posed as a combinatorial optimization problem. Two examples for truss structures were used for illustration; the first dealt with the optimal placement of passive dampers along existing truss members, and the second dealt with the optimal placement of a combination of a set of actuators and a set of sensors. Except for the simplest problems, an exact solution by enumeration involves a very large number of function evaluations, and is therefore computationally intractable. By contrast, the simulated annealing heuristic involves far fewer evaluations and is best suited for the class of problems considered. As an optimization tool, the effectiveness of the algorithm is enhanced by introducing a number of rules that incorporate knowledge about the physical behavior of the problem. Some of the suggested rules are necessarily problem dependent. Author

N89-25228*# National Aeronautics and Space Administration. Langley Research Center, Hampton, VA.
EXPERIENCES IN APPLYING OPTIMIZATION TECHNIQUES TO CONFIGURATIONS FOR THE CONTROL OF FLEXIBLE STRUCTURES (COFS) PROGRAM c39
Joanne L. Walsh *In its* Recent Advances in Multidisciplinary Analysis and Optimization, Part 3 Apr. 1989 p 1459-1488 Previously announced as N89-15155 (For primary document see N89-25201 19-05)
Avail: NTIS HC A22/MF A01 CSCL 20K

Optimization procedures are developed to systematically provide closely-spaced vibration frequencies. A general purpose finite-element program for eigenvalue and sensitivity analyses is combined with formal mathematical programming techniques. Results are presented for three studies. The first study uses a simple model to obtain a design with two pairs of closely-spaced frequencies. Two formulations are developed: an objective function-based formulation and constraint-based formulation for the frequency spacing. It is found that conflicting goals are handled better by a constraint-based formulation. The second study uses a detailed model to obtain a design with one pair of closely-spaced frequencies while satisfying requirements on local member frequencies and manufacturing tolerances. Two formulations are developed. Both the constraint-based and the objective function-based formulations perform reasonably well and converge to the same results. However, no feasible design solution exists which satisfies all design requirements for the choices of design variables and the upper and lower design variable values used. More design freedom is needed to achieve a fully satisfactory design. The third study is part of a redesign activity in which a detailed model is used. Author

N89-25229*# Ohio State Univ., Columbus. Dept. of Civil Engineering.
AN IMPROVED ALGORITHM FOR OPTIMUM STRUCTURAL DESIGN WITH MULTIPLE FREQUENCY CONSTRAINTS c39
Oliver G. McGee and Khing F. Phan *In* NASA. Langley Research Center, Recent Advances in Multidisciplinary Analysis and Optimization, Part 3 Apr. 1989 p 1489-1506 Sponsored in part by AF (For primary document see N89-25201 19-05)
Avail: NTIS HC A22/MF A01 CSCL 20K

An optimality criterion (OC) method for minimum-weight design of structures having multiple constraints on natural frequencies is

presented. In this work a new resizing strategy is developed based on relaxation techniques. A computationally adaptive control parameter is used in conjunction with existing OC recursive formulae to promote convergence of optimum structural designs. Some considerations regarding the coupling of the modified Aitken accelerator with the OC method are discussed. Improved and rapidly converged minimum-weight designs are obtained when using an under-relaxed recursive scheme combined with the modified Aitken accelerator. Author

N89-25230*# Florida Univ., Gainesville. Dept. of Aerospace Engineering, Mechanics and Engineering Science.
STRUCTURAL DAMAGE ASSESSMENT AS AN IDENTIFICATION PROBLEM **c39**
Prabhat Hajela and F. J. Soeiro *In* NASA. Langley Research Center, Recent Advances in Multidisciplinary Analysis and Optimization, Part 3 Apr. 1989 p 1507-1520 Submitted for publication (For primary document see N89-25201 19-05)
Avail: NTIS HC A22/MF A01 CSCL 20K

Damage assessment of structural assemblies is treated as an identification problem. A brief review of identification methods is first presented with particular focus on the output error approach. The use of numerical optimization methods in identifying the location and extent of damage in structures is studied. The influence of damage on eigenmode shapes and static displacements is explored as a means of formulating a measure of damage in the structure. Preliminary results obtained in this study are presented and special attention is directed at the shortcomings associated with the nonlinear programming approach to solving the optimization problem. Author

N89-25231*# Air Force Wright-Patterson Aeronautical Labs., Wright-Patterson AFB, OH.
RECENT DEVELOPMENTS IN LARGE-SCALE STRUCTURAL OPTIMIZATION **c39**
Vipperla B. Venkayya *In* NASA. Langley Research Center, Recent Advances in Multidisciplinary Analysis and Optimization, Part 3 Apr. 1989 p 1521-1540 (For primary document see N89-25201 19-05)
Avail: NTIS HC A22/MF A01 CSCL 20K

A brief discussion is given of mathematical optimization and the motivation for the development of more recent numerical search procedures. A review of recent developments and issues in multidisciplinary optimization is also presented. These developments are discussed in the context of the preliminary design of aircraft structures. A capability description of programs FASTOP, TSO, STARS, LAGRANGE, ELFINI and ASTROS is included. Author

N89-25232*# National Aeronautics and Space Administration. Langley Research Center, Hampton, VA.
TIME-CORRELATED GUST LOADS USING MATCHED-FILTER THEORY AND RANDOM-PROCESS THEORY: A NEW WAY OF LOOKING AT THINGS
Anthony S. Pototzky, Thomas A. Zeiler, and Boyd Perry, III (Planning Research Corp., Hampton, VA.) Apr. 1989 11 p Presented at the AIAA 30th Structures, Structural Dynamics and Materials Conference, Mobile, AL, 3-5 Apr. 1989 Previously announced in IAA as A89-30849
(NASA-TM-101573; NAS 1.15:101573) Avail: NTIS HC A03/MF A01 CSCL 01C

Two ways of performing time-correlated gust-load calculations are described and illustrated. The first is based on Matched Filter Theory; the second on Random Process Theory. Both approaches yield theoretically identical results and represent novel applications of the theories, are computationally fast, and may be applied to other dynamic-response problems. A theoretical development and example calculations using both Matched Filter Theory and Random Process Theory approaches are presented. Author

N89-25233*# California Univ., Berkeley.
THE CONCEPTUAL DESIGN OF A MACH 2 OBLIQUE FLYING WING SUPERSONIC TRANSPORT
Alexander J. M. VanderVelden May 1989 39 p
(Grant NAG2-471)
(NASA-CR-177529; NAS 1.26:177529) Avail: NTIS HC A03/MF A01 CSCL 01C

This paper is based on a performance and economics study of a Mach two oblique flying wing transport aircraft that is to replace the B747B. In order to fairly compare our configuration with the B747B an equal structural technology level is assumed. It will be shown that the oblique flying wing configuration will equal or outperform the B747 in speed, economy and comfort while a modern stability and control system will balance the aircraft and smooth out gusts. The aircraft is designed to comply with the FAR25 airworthiness requirements and FAR36 stage 3 noise regulations. Geometry, aerodynamics, stability and control parameters of the oblique flying wing transport are discussed. Author

N89-25234 Department of the Air Force, Washington, DC.
FLAP SYSTEM FOR SHORT TAKEOFF AND LANDING AIRCRAFT Patent
Gerald T. Brine, inventor (to AF) 15 Nov. 1988 9 p Filed 10 Nov. 1986
(AD-D013981; US-Patent-4,784,355; US-Patent-Appl-SN-928350)
Avail: US Patent and Trademark Office CSCL 01/3

A flap system for deploying high lift flaps on short takeoff and landing aircraft is presented. The flap system utilizes an activating mechanism that is used to extend a flap, a vane and a spoiler for maximum lift. The mechanism utilizes relatively few linkage pieces which are attached to the flap at single pivot points. The flap is supported by an actuator and a flap hinge support bracket. Increased mechanism rigidity and single pivot mountings allow use of roller and track guides at flap ends to smoothly guide flap movement and provide a fail-safe system in case of pivot mounting failure. Spherical bearings are utilized for mounting of rollers and actuators in order to compensate for misalignment of the flap and the flap mechanism when used with tapered flaps on swept wing aircraft. The spoiler is joined by a guide link that adjusts spoiler position with flap movement in order to maximize lift. The spoiler can also be used conventionally by activation of the actuator. GRA

N89-25235*# California Univ., Berkeley.
AN ECONOMIC MODEL FOR EVALUATING HIGH-SPEED AIRCRAFT DESIGNS
Alexander J. M. VanderVelden May 1989 38 p
(Grant NAG2-471)
(NASA-CR-177530; NAS 1.26:177530) Avail: NTIS HC A03/MF A01 CSCL 01C

A Class 1 method for determining whether further development of a new aircraft design is desirable from all viewpoints is presented. For the manufacturer the model gives an estimate of the total cost of research and development from the preliminary design to the first production aircraft. Using Wright's law of production, one can derive the average cost per aircraft produced for a given break-even number. The model will also provide the airline with a good estimate of the direct and indirect operating costs. From the viewpoint of the passenger, the model proposes a tradeoff between ticket price and cruise speed. Finally all of these viewpoints are combined in a Comparative Aircraft Seat-kilometer Economic Index. Author

N89-25236 Michigan Univ., Ann Arbor.
SHAPE OPTIMAL DESIGN OF ELASTIC BODIES USING A MIXED VARIATIONAL FORMULATION Ph.D. Thesis
Helder Carrico Rodrigues 1988 109 p
Avail: Univ. Microfilms Order No. DA8907135

Development of a variational formulation and a procedure for computational solution for the shape optimal design of a two-dimensional linear elastic body with contact interfaces was studied. The objective of the structural shape design problem is to define the design that minimizes the maximum value of the von Mises equivalent stress in the body, subject to an isoperimetric constraint on its total area and bound constraints on design.

Defining formally the Lagrangian associated with the optimization problem, the necessary conditions for the optimal solution are derived using a mixed variational formulation of the state equation. Governing equations that define the elastostatics problem appear as additional constraints for optimization. Modelling the mechanics in mixed form facilitates the production of better quality computational results. The results are implemented in a computer code to produce numerical solutions for the optimal shape. A finite element model appropriate for the mixed formulation is utilized in the discretization of the state and adjoint state equations. An elliptical mesh generator was used to generate the finite element grid. The design optimization problem is solved via a sequence of linearized subproblems. The discretized model is tested in three numerical examples: shape optimization of a hole in a biaxially loaded square sheet, design of a fillet, and design of the attachment part of a turbine blade. Dissert. Abstr.

N89-25237 George Washington Univ., Washington, DC.
PROBABILISTIC DAMAGE TOLERANCE METHODS FOR METALLIC AEROSPACE STRUCTURES Ph.D. Thesis
Margery E. Artley 1989 132 p
Avail: Univ. Microfilms Order No. DA8906814

Damage tolerance analysis, based on fracture mechanics, is an important tool for ensuring the safety of flight of airframes. Traditionally, these analyses are deterministic in nature, but probabilistic methods have been applied to damage tolerance analysis in limited cases. The purpose of this dissertation is to formulate probabilistic damage tolerance analyses for metallic structural components, based on U.S. Air Force damage tolerance philosophy for slow crack growth and fail safe components. A survey of the literature was conducted on probabilistic durability and damage tolerance methods. The important elements of the methods are covered; including the initial fatigue quality, the variability in crack growth rate, and the probability of crack detection. A probabilistic damage tolerance analysis was performed with a deterministic crack growth rate and then a stochastic crack growth rate, based on a probabilistic durability method. Examples of slow crack growth and fail safe structures are presented. As an example of a slow crack growth component, a lug from an aircraft subjected to an 80-flight fighter/trainer wing lower surface spectrum was selected. A stiffened panel from a lower wing skin of a tanker was selected as an example of a fail-safe component. Crack arrest in the panel, followed by catastrophic failure of the stiffener was considered as the failure mechanism. The model formulated here can be used to decide on the frequency and quality of the inspection of a component needed to keep the probability of failure at acceptable levels. Results of this study can serve as bases for decision making for inspection maintenance and fleet management. Dissert. Abstr.

06 AIRCRAFT INSTRUMENTATION

Includes cockpit and cabin display devices; and flight instruments.

For related information see also *19 Spacecraft Instrumentation* and *35 Instrumentation and Photography.*

No abstracts in this category.

07 AIRCRAFT PROPULSION AND POWER

Includes prime propulsion systems and systems components, e.g., gas turbine engines and compressors; and onboard auxiliary power plants for aircraft.

For related information see also *20 Spacecraft Propulsion and Power, 28 Propellants and Fuels,* and *44 Energy Production and Conversion.*

N89-25238*# National Aeronautics and Space Administration. Lewis Research Center, Cleveland, OH.
FUEL PROPERTIES EFFECT ON THE PERFORMANCE OF A SMALL HIGH TEMPERATURE RISE COMBUSTOR
Waldo A. Acosta and Stephen A. Beckel (Pratt and Whitney Aircraft, West Palm Beach, FL.) Jul. 1989 12 p Presented at the 25th Joint Propulsion Conference, Monterey, CA, 10-12 Jul. 1989; sponsored in part by AIAA, ASME, SAE, and ASEE
(Contract N00140-83-C-8899)
(NASA-TM-102096; AVSCOM-TR-89-C-004; E-4857; NAS 1.15:102096; AIAA-89-2901) Avail: NTIS HC A03/MF A01 CSCL 21E

The performance of an advanced small high temperature rise combustor was experimentally determined at NASA-Lewis. The combustor was designed to meet the requirements of advanced high temperature, high pressure ratio turboshaft engines. The combustor featured an advanced fuel injector and an advanced segmented liner design. The full size combustor was evaluated at power conditions ranging from idle to maximum power. The effect of broad fuel properties was studied by evaluating the combustor with three different fuels. The fuels used were JP-5, a blend of Diesel Fuel Marine/Home Heating Oil, and a blend of Suntec C/Home Heating Oil. The fuel properties effect on the performance of the combustion in terms of pattern factor, liner temperatures, and exhaust emissions are documented. Author

N89-25165*# National Aeronautics and Space Administration. Lewis Research Center, Cleveland, OH.
STRUCTURAL TAILORING OF COUNTER ROTATION PROPFANS
Kenneth W. Brown (Pratt and Whitney Aircraft, East Hartford, CT.) and D. A. Hopkins *In* NASA. Langley Research Center, Recent Advances in Multidisciplinary Analysis and Optimization, Part 1 Apr. 1989 p 389-402 (For primary document see N89-25146 19-05)
(Contract NAS3-23941)
Avail: NTIS HC A23/MF A01 CSCL 21E

N89-25207*# Textron Lycoming, Stratford, CT.
PROCEDURES FOR SHAPE OPTIMIZATION OF GAS TURBINE DISKS
Tsu-Chien Cheu *In* NASA. Langley Research Center, Recent Advances in Multidisciplinary Analysis and Optimization, Part 3 Apr. 1989 p 1097-1108 (For primary document see N89-25201 19-05)
Avail: NTIS HC A22/MF A01 CSCL 21E

08 AIRCRAFT STABILITY AND CONTROL

Includes aircraft handling qualities; piloting; flight controls; and autopilots.

For related information see also *05 Aircraft Design, Testing and Performance.*

N89-25239*# National Aeronautics and Space Administration. Langley Research Center, Hampton, VA.
AN ANALYTICAL SENSITIVITY METHOD FOR USE IN INTEGRATED AEROSERVOELASTIC AIRCRAFT DESIGN
Michael G. Gilbert May 1989 12 p Presented at the European Forum on Aeroelasticity and Structural Dynamics, Aachen, Fed.

Republic of Germany, 17-19 Apr. 1989
(NASA-TM-101583; NAS 1.15:101583) Avail: NTIS HC A03/MF A01 CSCL 01C

Interdisciplinary analysis capabilities have been developed for aeroservoelastic aircraft and large flexible spacecraft, but the requisite integrated design methods are only beginning to be developed. One integrated design method which has received attention is based on hierarchal problem decompositions, optimization, and design sensitivity analyses. This paper highlights a design sensitivity analysis method for Linear Quadratic Gaussian (LQG) optimal control laws, enabling the use of LQG techniques in the hierarchal design methodology. The LQG sensitivity analysis method calculates the change in the optimal control law and resulting controlled system responses due to changes in fixed design integration parameters using analytical sensitivity equations. Numerical results of a LQG design sensitivity analysis for a realistic aeroservoelastic aircraft example are presented. In this example, the sensitivity of the optimal control law and aircraft response for various parameters such as wing bending natural frequency is determined. The sensitivity results computed from the analytical expressions are used to estimate changes in response resulting from changes in the parameters. Comparisons of the estimates with exact calculated responses show they are reasonably accurate for + or - 15 percent changes in the parameters. Evaluation of the analytical expressions is computationally faster than equivalent finite difference calculations. Author

N89-25141# Technische Hochschule, Aachen (Germany, F.R.).
FLIGHT-MECHANICAL INVESTIGATIONS OF THE LATERAL MOTION OF CONFIGURATIONS WITH WINGLETS [FLUGMECHANISCHE UNTERSUCHUNGEN ZUR SEITENBEWEGUNG VON KONFIGURATIONEN MIT WINGLETS]
A. Diekmann and A. Josten *In its* Vortex Flows in Flying Technique 1988 p 339-371 In GERMAN (For primary document see N89-25126 19-02)
Avail: NTIS HC A17/MF A01

N89-25189*# Purdue Univ., West Lafayette, IN.
AEROSERVOELASTIC TAILORING FOR LATERAL CONTROL ENHANCEMENT
Terrence A. Weisshaar and Nam Changho *In* NASA. Langley Research Center, Recent Advances in Multidisciplinary Analysis and Optimization, Part 2 Apr. 1989 p 803-814 (For primary document see N89-25173 19-05)
Avail: NTIS HC A22/MF A01 CSCL 01C

N89-25191*# National Aeronautics and Space Administration. Langley Research Center, Hampton, VA.
FLUTTER SUPPRESSION USING EIGENSPACE FREEDOMS TO MEET REQUIREMENTS
William M. Adams, Jr., Robert E. Fennell, and David M. Christhilf (Planning Research Corp., Hampton, VA.) *In its* Recent Advances in Multidisciplinary Analysis and Optimization, Part 2 Apr. 1989 p 837-859 (For primary document see N89-25173 19-05)
Avail: NTIS HC A22/MF A01 CSCL 01C

N89-25193*# Planning Research Corp., Hampton, VA.
DIGITAL ROBUST CONTROL LAW SYNTHESIS USING CONSTRAINED OPTIMIZATION
Vivekananda Mukhopadhyay *In* NASA. Langley Research Center, Recent Advances in Multidisciplinary Analysis and Optimization, Part 2 Apr. 1989 p 879-895 (For primary document see N89-25173 19-05)
(Contract NAS1-8000)
Avail: NTIS HC A22/MF A01 CSCL 01C

N89-25195*# National Aeronautics and Space Administration. Hugh L. Dryden Flight Research Facility, Edwards, CA.
CONTROL SURFACE SPANWISE PLACEMENT IN ACTIVE FLUTTER SUPPRESSION SYSTEMS
E. Nissim and J. J. Burken *In* NASA. Langley Research Center, Recent Advances in Multidisciplinary Analysis and Optimization, Part 2 Apr. 1989 p 919-934 Prepared in cooperation with Technion-Israel Inst. of Technology, Haifa (For primary document see N89-25173 19-05)
Avail: NTIS HC A22/MF A01 CSCL 01C

09 RESEARCH AND SUPPORT FACILITIES (AIR)

Includes airports, hangars and runways; aircraft repair and overhaul facilities; wind tunnels; shock tubes; and aircraft engine test stands.

For related information see also *14 Ground Support Systems and Facilities (Space).*

N89-25240# National Aeronautical Lab., Bangalore (India). Structures Div.
ON THE STRESS PROBLEM OF THE PEBBLE BED HEAT EXCHANGER IN A HYPERSONIC WIND TUNNEL
M. N. BapuRao and Ashok Kamath Jul. 1987 78 p
(NAL-TM-ST-8705) Avail: NTIS HC A05/MF A01

The stress problem associated with the pebble bed heat exchanger in the hypersonic wind tunnel at IISc, Bongalore, is investigated. The investigation is carried out in two stages: the first stage deals with the problem encountered during the preheating of pebble bed, while in the second stage pressure loading arising from tunnel blowdowns is considered. The heat transfer and the associated thermal stress problems of stage one and also the problem of pressure loading in the presence of temperature occurring in stage two are analyzed using the finite element method with the aid of the NASTRAN and ASKA software packages. The results obtained indicate the presence of stress concentration in the disc-flange region at the entry section and in the ellipsoidal cap near the exit section of the pebble bed heat exchanger. The significance of finite element results presented with the aid of the FEMVIEW interactive graphic processor is discussed in detail. Author

N89-25241# Federal Aviation Administration, Washington, DC. Office of Airport Planning and Programming.
REPORT TO CONGRESS: TECHNICAL FEASIBILITY OF JOINT USE AT SCOTT AFB, SELFRIDGE AGB AND EL TORO MCAS
Laurence Kiernan May 1988 46 p
(AD-A194597; APP-88-5; DOT/FAA/PP-88/5) Avail: NTIS HC A03/MF A01 CSCL 01/5

The technical feasibility of joint civil/military use of Scott Air Force Base (AFB), Selfridge Air Guard Base (AGB), and El Toro Marine Corps Air Station (MCAS) was investigated. Considered were the airfield, terminal, access issues, and any previous studies conducted by Federal, State, regional, or local authorities that evaluated the short and long term importance of using these facilities to alleviate the shortage of civil airport and air space capacity. Author

N89-25242* National Aeronautics and Space Administration. Marshall Space Flight Center, Huntsville, AL.
WARM FOG DISSIPATION USING LARGE VOLUME WATER SPRAYS Patent
Vernon W. Keller, inventor (to NASA) 1 Nov. 1988 10 p
Filed 23 Jul. 1984 Supersedes N84-32398 (22-22, p 3538)
(NASA-Case-MFS-25962-1; US-Patent-4,781,326;
US-Patent-Appl-SN-633180; US-Patent-Class-239-2.1;
US-Patent-Class-239-14.1) Avail: U.S. Patent and Trademark Office CSCL 14B

To accomplish the removal of warm fog about an area such as an airport runway, a plurality of nozzles along a line adjacent the area propelled water jets through the fog to heights of approximately twenty-five meters. Each water jet breaks up forming a water drop size distribution that falls through the fog overtaking, colliding, and coalescing with individual fog droplets and thereby removes the fog. A water retrieval system is used to collect the water and return it to reservoirs for pumping it to the nozzles

once again.
Official Gazette of the U.S. Patent and Trademark Office

N89-25243# Deutsche Forschungs- und Versuchsanstalt fuer Luft- und Raumfahrt, Brunswick (Germany, F.R.). Hauptabteilung Windkanaele.
PRESSURE MEASUREMENT TECHNIQUE OF WT-WK Status Report, 1988
Ruediger Siebert Sep. 1988 49 p In GERMAN; ENGLISH summary Report will also be announced as translation (ESA-TT-1145)
(DFVLR-Mitt-88-11; ISSN-0176-7739; ESA-TT-1145; ETN-89-94643) Avail: NTIS HC A03/MF A01; DFVLR, VB-PL-DO, Postfach 90 60 58, 5000 Cologne, Federal Republic of Germany, 19.50 deutsche marks

Information for users of the wind tunnels of DFVLR (Deutsche Forschungs- und Versuchsanstalt fuer Luft- und Raumfahrt) in Braunschweig, Gottingen, and Koln is presented. The principal arrangement, details, and status of the pressure measurement technique are described. For quick information, the data of all available pressure transducers and pressure measurement systems are presented in tables. ESA

12 ASTRONAUTICS (GENERAL)

For extraterrestrial exploration see *91 Lunar and Planetary Exploration.*

N89-25244* National Aeronautics and Space Administration, Washington, DC.
SPACE STATION OPERATIONS TASK FORCE. PANEL 1 REPORT: SPACE OPERATIONS AND SUPPORT SYSTEMS
Dec. 1987 627 p
(NASA-TM-101816; NAS 1.15:101816) Avail: Issuing Activity CSCL 22A

The Space Operations and Support Systems Panel of the Space Station Operations Task Force was chartered to develop concepts for operations of the Space Station manned base and the platforms. These operations include those conducted in space to maintain the Space Station and platforms as usable facilities, operations to support users in their scientific, technological, or commercial research, operations of systems on the ground to support the space-based operations, and training of all personnel to perform their operations duties. A.D.

N89-25245*# National Aeronautics and Space Administration, Washington, DC.
SPACE STATION OPERATIONS TASK FORCE. PANEL 2 REPORT: GROUND OPERATIONS AND SUPPORT SYSTEMS
Dec. 1987 569 p
(NASA-TM-101817; NAS 1.15:101817) Avail: NTIS HC A24/MF A01 CSCL 22A

The Ground Operations Concept embodied in this report provides for safe multi-user utilization of the Space Station, eases user integration, and gives users autonomy and flexibility. It provides for meaningful multi-national participation while protecting U.S. interests. The concept also supports continued space operations technology development by maintaining NASA expertise and enabling technology evolution. Given attention here are pre/post flight operations, logistics, sustaining engineering/configuration management, transportation services/rescue, and information systems and communication. A.D.

N89-25246*# National Aeronautics and Space Administration, Washington, DC.
SPACE STATION OPERATIONS TASK FORCE. PANEL 3 REPORT: USER DEVELOPMENT AND INTEGRATION
Dec. 1987 311 p
(NASA-TM-101818; NAS 1.15:101818) Avail: NTIS HC A14/MF A01 CSCL 22A

The User Development and Integration Panel of the Space Station Operations Task Force was chartered to develop concepts relating to the operations of the Space Station manned base and the platforms, user accommodation and integration activities. The needs of the user community are addressed in the context with the mature operations phase of the Space Station. Issues addressed include space station pricing options, marketing strategies, payload selection and resource allocation options, and manifesting techniques. A.D.

N89-25247*# National Aeronautics and Space Administration, Washington, DC.
SPACE STATION OPERATIONS TASK FORCE. PANEL 4 REPORT: MANAGEMENT INTEGRATION
Dec. 1987 213 p
(NASA-TM-101819; NAS 1.15:101819) Avail: NTIS HC A10/MF A01 CSCL 22A

The Management Integration Panel of the Space Station Operations Task Force was chartered to provide a structure and ground rules for integrating the efforts of the other three panels and to address a number of cross cutting issues that affect all areas of space station operations. Issues addressed include operations concept implementation, alternatives development and integration process, strategic policy issues and options, and program management emphasis areas. A.D.

N89-25248*# National Aeronautics and Space Administration, Washington, DC.
SPACE STATION OPERATIONS TASK FORCE SUMMARY REPORT
Oct. 1987 203 p Original contains color illustrations
(NASA-TM-101820; NAS 1.15:101820) Avail: NTIS HC A10/MF A01 CSCL 22A

A companion to the Space Stations Operation Task Force Panels' Reports, this document summarizes all space station program goals, operations, and the characteristics of the expected user community. Strategies for operation and recommendations for implementation are included. A.D.

N89-25249*# National Aeronautics and Space Administration, Washington, DC.
SPACE STATION OPERATIONS TASK FORCE. EXECUTIVE SUMMARY Final Report
Oct. 1987 23 p Original contains color illustrations
(NASA-TM-101780; NAS 1.15:101780) Avail: NTIS HC A03/MF A01 CSCL 22A

The space station program goads, operations and the characteristics of the expected user community are summarized. Strategies for operations and recommendations for implementation are included. A.D.

13 ASTRODYNAMICS

Includes powered and free-flight trajectories; and orbital and launching dynamics.

N89-25250# Deutsche Forschungs- und Versuchsanstalt fuer Luft- und Raumfahrt, Oberpfaffenhofen (West Germany). Abteilung Hochfrequenzphysik.
TROPOSPHERIC INFLUENCES ON SATELLITE-EARTH PATHS AND THEIR DETERMINATION BY MEANS OF RADAR MEASUREMENTS Ph.D. Thesis - Technische Hochschule, Darmstadt
Gottfried Schnabl Jul. 1988 170 p In GERMAN; ENGLISH summary Report will also be announced as translation (ESA-TT-1143)
(DFVLR-FB-88-53; ISSN-0171-1342; ETN-89-94639) Avail: NTIS HC A08/MF A01; DFVLR, VB-PL-DO, Postfach 90 60 58, 5000 Cologne, Fed. Republic of Germany, DM 59

The influence of rain, snow, and ice-clouds on the propagation of electromagnetic waves on satellite-Earth paths is investigated. Radar measurements of precipitations were performed. Methods to determine tropospheric influences are shown. ESA

14 GROUND SUPPORT SYSTEMS AND FACILITIES (SPACE)

Includes launch complexes, research and production facilities; ground support equipment, e.g., mobile transporters; and simulators.

For related information see also *09 Research and Support Facilities (Air).*

N89-25251# Fermi National Accelerator Lab., Batavia, IL.
FLYING WIRES AT FERMILAB
J. Gannon, C. Crawford, D. Finley, R. Flora, T. Groves, and M. MacPherson Mar. 1989 4 p Presented at the 13th Particle Accelerator Conference, Chicago, IL, 20-23 Mar. 1989
(Contract DE-AC02-76CH-03000)
(DE89-011005; FNAL/C-89/64; CONF-890335-74) Avail: NTIS HC A02/MF A01

Transverse beam profile measurement systems called flying wires have been installed and made operational in the Fermilab Main Ring and Tevatron accelerators. These devices are used routinely to measure the emittance of both protons and antiprotons throughout the fill process, and for emittance growth measurements during stores. In the Tevatron, the individual transverse profiles of six proton and six antiproton bunches are obtained simultaneously, with a single pass of the wire through the beam. Essential features of the hardware, software, and system operation are explained in the rest of the paper. DOE

N89-25252*# National Aeronautics and Space Administration. Goddard Space Flight Center, Greenbelt, MD.
SPACELAB DATA PROCESSING FACILITY
1983 28 p Original contains color illustrations
(NASA-TM-101808; NAS 1.15:101808) Avail: NTIS HC A03/MF A01 CSCL 14B

The capabilities of the Spacelab Data Processing Facility (SPDPF) are highlighted. The capturing, quality monitoring, processing, accounting, and forwarding of vital Spacelab data to various user facilities around the world are described. A.D.

N89-25253# Lawrence Livermore National Lab., CA.
SIMPLE MODELS FOR ELECTRIC GUN OPERATING CHARACTERISTICS
Ronald S. Lee Dec. 1988 15 p Presented at the 3rd International Symposium on Behavior of Media Under High Dynamic Pressures, La Grande Motte, France, 5-9 Jun. 1989
(Contract W-7405-eng-48)
(DE89-005348; UCRL-98803; CONF-890661-1) Avail: NTIS HC A03/MF A01

The electric gun, sometimes called a foil gun, uses the energy initially stored in a capacitor to electrically heat a thin conducting bridge in a transmission line connected to the capacitor. The deposited energy, typically several times the cohesive energy of the bridge material, is deposited in a time much less than the thermal time constant of the bridge, causing the bridge to explode violently. A thin dielectric layer (flyer plate) placed on top of the bridge can be accelerated to hypervelocity by the expansion of the bridge material and accompanying magnetic forces. The detailed physics of the heating and explosion process is very complicated. Elaborate computer codes are required for realistic models of the acceleration of the flyer plate, but a useful description of the gun performance can be obtained from the circuit characteristics and the properties of the bridge and flyer plate by simple empirical models. This paper will discuss simple models which have been successfully used to model electric gun performance. DOE

N89-25855*# National Aeronautics and Space Administration, Washington, DC.
THE GONG SITE SURVEY
Frank Hill, Ashok Ambastha, Warren Ball, Oscar Duhalde, Don Farris, George Fischer, Les Hieda, Huang Zhen, Bob Ingram, and Patty Jackson (National Solar Observatory, Tucson, AZ.) et al *In* ESA, Seismology of the Sun and Sun-Like Stars Dec. 1988 p 209-215 Prepared in cooperation Colorado Univ., Boulder (For primary document see N89-25819 19-92)
Copyright Avail: NTIS HC A99/MF E03 CSCL 03B

N89-25856*# National Aeronautics and Space Administration. Marshall Space Flight Center, Huntsville, AL.
THE GONG DATA REDUCTION AND ANALYSIS SYSTEM
James A. Pintar, Bo Nyborg Andersen, Edwin R. Andersen, David B. Armet, Timothy M. Brown, David H. Hathaway, Frank Hill, and Harrison P. Jones (National Aeronautics and Space Administration. Goddard Space Flight Center, Greenbelt, MD.) *In* ESA, Seismology of the Sun and Sun-Like Stars Dec. 1988 p 217-221 (For primary document see N89-25819 19-92)
Copyright Avail: NTIS HC A99/MF E03 CSCL 03B

15 LAUNCH VEHICLES AND SPACE VEHICLES

Includes boosters; operating problems of launch/space vehicle systems; and reusable vehicles.

For related information see also *20 Spacecraft Propulsion and Power.*

N89-25254*# National Aeronautics and Space Administration. Lewis Research Center, Cleveland, OH.
ADVANCED APS IMPACTS ON VEHICLE PAYLOADS
Steven J. Schneider and Brian D. Reed 1989 14 p Presented at the JANNAF Propulsion Meeting, Cleveland, OH, 23-25 May 1989
(NASA-TM-102086; E-4731; NAS 1.15:102086) Avail: NTIS HC A03/MF A01 CSCL 22B

Advanced auxiliary propulsion system (APS) technology has the potential to both, increase the payload capability of earth-to-orbit (ETO) vehicles by reducing APS propellant mass, and simplify ground operations and logistics by reducing the number of fluids on the vehicle and eliminating toxic, corrosive propellants. The impact of integrated cryogenic APS on vehicle payloads is addressed. In this system, launch propulsion system residuals are scavenged from integral launch propulsion tanks for use in the APS. Sufficient propellant is preloaded into the APS to return to earth with margin and noncomplete scavenging assumed. No propellant conditioning is required by the APS, but ambient heat soak is accommodated. High temperature rocket materials enable the use of the unconditioned hydrogen/oxygen in the APS and are estimated to give APS rockets specific impulse of up to about 444 sec. The payload benefits are quantified and compared with an uprated monomethylhydrazine/nitrogen tetroxide system in a conservative fashion, by assuming a 25.5 percent weight growth for the hydrogen/oxygen system and a 0 percent weight growth for the uprated system. The combination of scavenging and high performance gives payload impacts which are highly mission specific. A payload benefit of 861 kg (1898 lbm) was estimated for a Space Station Freedom rendezvous mission and 2099 kg (4626 lbm) for a sortie mission, with payload impacts varying with the amount of launch propulsion residual propellants. Missions without liquid propellant scavenging were estimated to have payload penalties, however, operational benefits were still possible.
Author

N89-25255# Los Alamos National Lab., NM.
ADVANCED MASS LAUNCHERS FOR LOW EARTH ORBIT
Gregory H. Canavan Apr. 1989 43 p
(Contract W-7405-eng-36)
(DE89-010759; LA-11420-MS) Avail: NTIS HC A03/MF A01

Military access to space requires significant payload volume and acceptable costs. It has not been demonstrated that current launch systems can provide either. This report describes two advanced launch concepts that could potentially provide an order of magnitude reduction in the total costs of launching modest payloads to space and give the margin over the economics of current concepts required to meet both current and expanded

requirements for military and civilian launch schedules and provide a margin for the expansion of each. DOE

16 SPACE TRANSPORTATION

Includes passenger and cargo space transportation, e.g., shuttle operations; and space rescue techniques.

For related information see also *03 Air Transportation and Safety* and *18 Spacecraft Design, Testing and Performance*. For space suits see *54 Man/System Technology and Life Support*.

N89-25256# Societe Nationale Industrielle Aerospatiale, Issac (France).
SIMOUN: TEST SYSTEM FOR SHUTTLE THERMAL PROTECTION MATERIALS [SIMOUN: SYSTEME D'INVESTIGATION POUR MATERIAUX OPTIMISES UTILISABLES SUR NAVETTE]
J. P. Serrano 14 Dec. 1988 18 p In FRENCH
(Rept-882-430-101; ETN-89-94483) Avail: NTIS HC A03/MF A01

A test system is designed to simulate Hermes shuttle reentry conditions in order to verify the behavior of the critical thermal protection layers, The system described generates a hot supersonic flow at the pressure and density calculated conditions. The life of the materials is tested 10 to 30 times in 1500 sec tests. ESA

N89-25257*# Edgerton, Germeshausen and Grier, Inc., Idaho Falls, ID.
NDE OF THE SPACE SHUTTLE ORBITER THERMAL PROTECTION SYSTEM, PHASE 2 Final Report
D. M. Tow, B. A. Barna, and J. G. Rodriguez Mar. 1989 54 p
(Contract DE-AC07-76ID-01570)
(NASA-CR-185471; NAS 1.26:185471; DE89-010975; EGG-MS-8425) Avail: NTIS HC A04/MF A01 CSCL 22B

Research continued on the development of a nondestructive evaluation technique for inspecting bonds on the space shuttle orbiter thermal protection system tiles. The approach taken uses a noncontacting laser sensor to measure the vibrational response of bonded tiles to acoustical excitation. Laboratory work concentrated on investigating the dynamic response of acreage tiles, i.e., tiles covering the underside of the orbiter, all approximately square. A number of promising unbond signatures have been identified in the time and frequency domain response. Field tests were conducted to study environmental effects on the techniques being developed. The ambient motion of the orbiter was found to be larger than expected, necessitating modifications to current techniques. DOE

N89-25258*# Massachusetts Inst. of Tech., Cambridge.
MIDDECK ACTIVE CONTROL EXPERIMENT (MACE), PHASE A Final Report
Edward F. Crawley, Javier deLuis, and David W. Miller Jun. 1989 194 p
(Grant NAG1-915)
(NASA-CR-185331; NAS 1.26:185331) Avail: NTIS HC A09/MF A01 CSCL 22B

A rationale to determine which structural experiments are sufficient to verify the design of structures employing Controlled Structures Technology was derived. A survey of proposed NASA missions was undertaken to identify candidate test articles for use in the Middeck Active Control Experiment (MACE). The survey revealed that potential test articles could be classified into one of three roles: development, demonstration, and qualification, depending on the maturity of the technology and the mission the structure must fulfill. A set of criteria was derived that allowed determination of which role a potential test article must fulfill. A review of the capabilities and limitations of the STS middeck was conducted. A reference design for the MACE test article was presented. Computing requirements for running typical closed-loop controllers was determined, and various computer configurations were studied. The various components required to manufacture the structure were identified. A management plan was established for the remainder of the program experiment development, flight and ground systems development, and integration to the carrier. Procedures for configuration control, fiscal control, and safety, reliabilty, and quality assurance were developed. B.G.

N89-25259# Technische Univ., Berlin (Germany, F.R.). Inst. of Aerospace.
FLIGHT PERFORMANCE MODEL FOR A GEOSTATIONARY TRANSPORTATION SYSTEM
M. Mielke 1 Aug. 1988 42 p
(ILR-Mitt-206; ETN-89-94561) Avail: NTIS HC A03/MF A01

A flight performance model for a geostationary transportation system is described. The model specifies all requirements concerning orbit and attitude control as well as rendezvous and docking. Several transportation missions are considered and analyzed to determine most suitable transfer trajectories and attitude control strategies for minimizing velocity requirements. Transfer distances of 5 to 130,000 km lead to flight durations of 0.5 to 70 hr and a velocity requirement of 10 to 1600 m/sec. ESA

N89-25260# Technische Univ., Berlin (Germany, F.R.). Inst. fuer Luft- und Raumfahrt.
SIZE OPTIMIZATION AND PRODUCTION STRATEGY OF LUNAR TRANSPORT SYSTEMS [GROESSENOPTIMIERUNG UND AKQUISITIONSSTRATEGIE LUNARER TRAEGERSYSTEME]
Sebastian Wuttge 1 Sep. 1988 86 p In GERMAN; ENGLISH summary
(ILR-Mitt-218; ETN-89-94565) Avail: NTIS HC A05/MF A01

A simulation model of a lunar transportation system is described. A model of production rates for a lunar bus vehicle is considered over a 50 yr life cycle and includes operational as well as cost aspects. It is shown that the costs of a lunar transportation system depend on those of an Earth-lunar orbit transport system. With an increasing transportation demand, production cost is reduced by substituting a lunar bus with larger vehicles of suitable payload capacity. The use of a mixture ratio with more lunar LOX reduces the transportation charges insignificantly. The additional expenditure for producing more lunar oxygen is not considered. ESA

17 SPACE COMM., SPACECRAFT COMM., COMMAND & TRACKING

Includes telemetry; space communications networks; astronavigation and guidance; and radio blackout.

For related information see also *04 Aircraft Communications and Navigation* and *32 Communications and Radar*.

No abstracts in this category.

18 SPACECRAFT DESIGN, TESTING AND PERFORMANCE

Includes satellites; space platforms; space stations; spacecraft systems and components such as thermal and environmental controls; and attitude controls.

For life support systems see *54 Man/System Technology and Life Support.* For related information see also *05 Aircraft Design, Testing and Performance, 39 Structural Mechanics,* and *16 Space Transportation.*

N89-25261*# Lockheed Missiles and Space Co., Huntsville, AL. Engineering Center.
CONJUGATING BINARY SYSTEMS FOR SPACECRAFT THERMAL CONTROL. APPENDIX C: AEROASSIST FLIGHT EXPERIMENT CARRIER VEHICLE PRELIMINARY STRESS ANALYSIS Final Report
J. E. Ingram and T. O. Murray Jan. 1989 426 p
(Contract NAS8-36199)
(NASA-CR-183609; NAS 1.26:183609;
LMSC-HEC-TR-F226066-App-C) Avail: NTIS HC A19/MF A01 CSCL 22B

An assessment of the static strength of the Aeroassist Flight Experiment (AFE) Carrier Vehicle is presented. The Carrier Vehicle is the structural component which provides the mounting platform for the experiments, on-board computers, batteries, and other black boxes. In addition, the Solid Rocket Motor (SRM), the Thrusters, and the Aerobrake are all attached directly to the Carrier Vehicle. The basic approach in this analysis was to develop a NASTRAN Finite Element Model as a parallel effort to the preliminary design, and to use the internal loads from this model to perform the stress analysis. The NASTRAN method of Inertial Relief was employed. This method involves either specifying a set of CG (center of gravity) accelerations or applying forces at the CG and representing the Carrier Vehicle and all its mounted devices with the proper stiffness and mass properties. NASA

N89-25262# Science and Technology Associates, Inc., Arlington, VA.
CONTINUOUS GLOBAL N-TUPLE COVERAGE WITH (2N = 2) SATELLITES Final Report, Sep. 1988 - Apr. 1989
John E. Draim and Henry M. Bowers 2 Apr. 1989 79 p
(Contract F04701-88-C-0080)
(AD-A206522; STA-028) Avail: NTIS HC A05/MF A01 CSCL 22/2

This report is an annotated briefing covering research on arrays or constellations of satellites giving n-tuple continuous, global-line-of-sight coverage of a planet using the minimum number of satellites. A generalized theory was developed which appears to fit cases for any level of redundancy. Except for the case for single coverage, which is a tetrahedral array, all of the constellations can be characterized as either skew- or congruent-prismoidal arrays. The constellation altitudes increase with increasing levels of redundancy. GRA

N89-25263*# National Aeronautics and Space Administration. Lyndon B. Johnson Space Center, Houston, TX.
SMART TUNNEL: DOCKING MECHANISM Patent Application
John A. Schliesing, inventor (to NASA) and Kevin L. Edenborough, inventor (to NASA) 30 Dec. 1988 16 p
(NASA-Case-MSC-21360-1; NAS 1.71:MSC-21360-1;
US-Patent-Appl-SN-292131) Avail: NTIS HC A03/MF A01 CSCL 22B

A docking mechanism is presented for the docking of a space vehicle to a space station comprising a flexible tunnel frame structure which is deployable from the space station. The tunnel structure comprises a plurality of series connected frame sections, one end section of which is attached to the space station and the other end attached to a docking module of a configuration adapted for docking in the payload bay of the space vehicle. The docking module is provided with trunnions, adapted for latching engagement with latches installed in the vehicle payload bay and with hatch means connectable to a hatch of the crew cabin of the space vehicle. Each frame section comprises a pair of spaced ring members, interconnected by actuator-attenuator devices which are individually controllable by an automatic control means to impart relative movement of one ring member to the other in six degrees of freedom of motion. The control means includes computer logic responsive to sensor signals of range and attitude information, capture latch condition, structural loads, and actuator stroke for generating commands to the onboard flight control system and the individual actuator-attenuators to deploy the tunnel to effect a coupling with the space vehicle and space station after coupling. A tubular fluid-impervious liner, preferably fabric, is disposed through the frame sections of a size sufficient to accommodate the passage of personnel and cargo. NASA

N89-25264# Science Applications International Corp., La Jolla, CA.
SURVIVABLE PULSE POWER SPACE RADIATOR Patent Application
James Mims, inventor (to DOE), David Buden, inventor (to DOE), and Kenneth Williams, inventor (to DOE) 11 Mar. 1988 16 p
(Contract DE-AC03-85SF-15928)
(DE89-010120; PATENTS-US-A7167203;
US-Patent-Appl-SN-167203) Avail: NTIS HC A03/MF A01

An outer space vehicle thermal radiator system is described which must survive a long period of nonuse and then radiate large amounts of heat for a limited period of time. The radiator includes groups of radiator panels that are pivotally connected in tandem, so that they can be moved to deployed configuration wherein the panels lie largely coplanar, and to a stowed configuration wherein the panels lie in a stack to resist micrometerorite damage. The panels are mounted on a boom which separates a hot power source from a payload. While the panels are stowed, warm fluid passes through their arteries to keep them warm enough to maintain the coolant in a liquid state and avoid embrittlement of material. The panels can be stored in a largely cylindrical shell, with panels progressively further from the boom being of progressively shorter length. DOE

N89-25265 Michigan Univ., Ann Arbor.
TIME-OPTIMAL SLEWING MANEUVERS OF FLEXIBLE SPACECRAFT Ph.D. Thesis
Gurkirpal Singh 1988 162 p
Avail: Univ. Microfilms Order No. DA8907144

Two slewing problems are addressed: the time-optimal, rest-to-rest slewing problem (RTRSP) and the time-optimal spinup problem (SUP). The spacecraft is modeled as a finite-dimensional, linear, undamped, nongyroscopic system. The recognition and rigorous proof of symmetry of the optimal open-loop control histories about the mid-maneuver time is presented. Conditions for optimality are transformed, exploiting the symmetry property, into a set of nonlinear algebraic equations in one half of the control switching times, the maneuver time, and the costates at the mid-maneuver time. These equations are solved using a homotopy approach. The effect of residual modes on the open-loop system performance is quantified via the residual energy, the maximum post-maneuver attitude error (for the RTRSP), and the maximum post-maneuver attitude rate error (for the SUP). Upper bounds on these performance measures are given. For the special case of a single actuator located on the rigid central body, closed form expressions for these upper bounds are obtained for an infinite dimensional evaluation model. When only one control input is used to effect the slewings, the optimal control history is independent of the control input locations. The main assumption of this work is the absence of nonlinear rotational stiffening effects. This assumption might fail during slewings when large rotational rates are attained. We have proposed a simple condition which, when satisfied, justifies the omission of this nonlinearity from the equations of motion. This condition is validated by numerical simulations. The results, therefore, can be applied to many physical situations. Moreover, the results are applicable to all linear, elastic, nongyroscopic systems possessing one rigid body mode and a finite number of undamped elastic modes. Dissert. Abstr.

N89-25266*# National Aeronautics and Space Administration. Ames Research Center, Moffett Field, CA.
SPACE STATION ARCHITECTURE, MODULE, BERTHING HUB, SHELL ASSEMBLY, BERTHING MECHANISM AND UTILITY CONNECTION CHANNEL Patent
Marc M. Cohen, inventor (to NASA) 28 Feb. 1989 15 p
(NASA-Case-ARC-11505-2; US-Patent-4,807,834;
US-Patent-Appl-SN-159072; US-Patent-Class-244-159;
US-Patent-Class-244-161; US-Patent-Class-285-302) Avail: US Patent and Trademark Office CSCL 22B

A Space Station includes a plurality of modules, and berthing hubs, joined by interconnections which are sideways connectable. The modules and hubs are fastened together in a trianglar configuration in three dimensions. The interconnections include a pair of opposed, axially aligned, flanged ports, and a clamp latch formed from a plurality of sections hinged along their length and extending circumferentially around the flanged ports. A utilities connection channel extends between ports. The channel has a shell with utilities connectors movable between an extended position to mating connectors in the modules and a withdrawn position. Assembly sequence and common module shell structure is detailed.
Official Gazette of the U.S. Patent and Trademark Office

N89-25267*# National Aeronautics and Space Administration. Lewis Research Center, Cleveland, OH.
PROTOFLIGHT PHOTOVOLTAIC POWER MODULE SYSTEM-LEVEL TESTS IN THE SPACE POWER FACILITY
Juan C. Rivera and Luke A. Kirch Aug. 1989 21 p Presented at the 24th Intersociety Energy Conversion Engineering Conference, Washington, DC, 6-11 Aug. 1989; sponsored in part by IEEE, AIAA, ANS, ASME, SAE, ACS, and AIChE
(NASA-TM-102066; E-4823; NAS 1.15:102066) Avail: NTIS HC A03/MF A01 CSCL 22B

Work Package Four, which includes the NASA-Lewis and Rocketdyne, has selected an approach for the Space Station Freedom Photovoltaic (PV) Power Module flight certification that combines system level qualification and acceptance testing in the thermal vacuum environment: The protoflight vehicle approach. This approach maximizes ground test verification to assure system level performance and to minimize risk of on-orbit failures. The preliminary plans for system level thermal vacuum environmental testing of the protoflight PV Power Module in the NASA-Lewis Space Power Facility (SPF), are addressed. Details of the facility modifications to refurbish SPF, after 13 years of downtime, are briefly discussed. The results of an evaluation of the effectiveness of system level environmental testing in screening out incipient part and workmanship defects and unique failure modes are discussed. Preliminary test objectives, test hardware configurations, test support equipment, and operations are presented. Author

N89-25268*# North Carolina Univ., Charlotte. Dept. of Mechanical Engineering and Engineering Science.
DESIGN OF AN AUTO CHANGE MECHANISM AND INTELLIGENT GRIPPER FOR THE SPACE STATION Final Report
Paul H. Dehoff and Dipak P. Naik 1989 55 p
(Grant NAG5-922)
(NASA-CR-185387; NAS 1.26:185387) Avail: NTIS HC A04/MF A01 CSCL 22B

Robot gripping of objects in space is inherently demanding and dangerous and nowhere is this more clearly reflected than in the design of the robot gripper. An object which escapes the gripper in a micro g environment is launched not dropped. To prevent this, the gripper must have sensors and signal processing to determine that the object is properly grasped, e.g., grip points and gripping forces and, if not, to provide information to the robot to enable closed loop corrections to be made. The sensors and sensor strategies employed in the NASA/GSFC Split-Rail Parallel Gripper are described. Objectives and requirements are given followed by the design of the sensor suite, sensor fusion techniques and supporting algorithms. Author

N89-25160*# National Aeronautics and Space Administration. Langley Research Center, Hampton, VA.
DEMONSTRATION OF DECOMPOSITION AND OPTIMIZATION IN THE DESIGN OF EXPERIMENTAL SPACE SYSTEMS
Sharon Padula, Chris A. Sandridge, Raphael T. Haftka (Virginia Polytechnic Inst. and State Univ., Blacksburg.), and Joanne L. Walsh *In its* Recent Advances in Multidisciplinary Analysis and Optimization, Part 1 Apr. 1989 p 297-316 (For primary document see N89-25146 19-05)
Avail: NTIS HC A23/MF A01 CSCL 22B

N89-25209*# Rockwell International Corp., Los Angeles, CA.
THE ART OF SPACECRAFT DESIGN: A MULTIDISCIPLINARY CHALLENGE
F. Abdi, H. Ide, M. Levine, and L. Austel *In* NASA. Langley Research Center, Recent Advances in Multidisciplinary Analysis and Optimization, Part 3 Apr. 1989 p 1137-1155 (For primary document see N89-25201 19-05)
Avail: NTIS HC A22/MF A01 CSCL 22B

N89-25215*# Howard Univ., Washington, DC. Dept. of Mechanical Engineering.
OPTIMUM DESIGN OF STRUCTURES SUBJECT TO GENERAL PERIODIC LOADS
Robert Reiss and B. Qian *In* NASA. Langley Research Center, Recent Advances in Multidisciplinary Analysis and Optimization, Part 3 Apr. 1989 p 1265-1279 (For primary document see N89-25201 19-05)
Avail: NTIS HC A22/MF A01 CSCL 22B

N89-25225*# Texas Univ., Arlington. Dept. of Mechanical Engineering.
A NOVEL IMPLEMENTATION OF METHOD OF OPTIMALITY CRITERION IN SYNTHESIZING SPACECRAFT STRUCTURES WITH NATURAL FREQUENCY CONSTRAINTS
Bo Ping Wang and F. H. Chu (General Electric Co., Princeton, NJ.) *In* NASA. Langley Research Center, Recent Advances in Multidisciplinary Analysis and Optimization, Part 3 Apr. 1989 p 1417-1426 (For primary document see N89-25201 19-05)
Avail: NTIS HC A22/MF A01 CSCL 22B

19 SPACECRAFT INSTRUMENTATION

For related information see also *06 Aircraft Instrumentation* and *35 Instrumentation and Photography.*

N89-25882# European Space Agency. European Space Research and Technology Center, ESTEC, Noordwijk (Netherlands). Space Science Dept.
SOHO STATUS
V. Domingo *In its* Seismology of the Sun and Sun-Like Stars Dec. 1988 p 363-366 (For primary document see N89-25819 19-92)
Copyright Avail: NTIS HC A99/MF E03

N89-25883# Centre National de la Recherche Scientifique, Verrieres-Le Buisson (France). Lab. de Physique Stellaire et Planetaire.
THE GOLF HELIOSEISMOMETER ON BOARD SOHO
Luc Dame *In* ESA, Seismology of the Sun and Sun-Like Stars Dec. 1988 p 367-370 (For primary document see N89-25819 19-92)
Copyright Avail: NTIS HC A99/MF E03

N89-25885# Stanford Univ., CA. Center for Space Science and Astrophysics.
THE SOLAR OSCILLATIONS IMAGER FOR SOHO
Philip H. Scherrer, J. T. Hoeksema, and R. S. Bogart *In* ESA, Seismology of the Sun and Sun-Like Stars Dec. 1988 p 375-379 (For primary document see N89-25819 19-92)
Copyright Avail: NTIS HC A99/MF E03

N89-25886# Norwegian Space Center, Oslo.
DETECTOR CONFIGURATIONS FOR OBSERVATIONS OF GRAVITY MODES IN SOLAR RADIANCE
Bo Nyborg Andersen *In* ESA, Seismology of the Sun and Sun-Like Stars Dec. 1988 p 381-383 (For primary document see N89-25819 19-92)
Copyright Avail: NTIS HC A99/MF E03

N89-25887# European Space Agency. European Space Research and Technology Center, ESTEC, Noordwijk (Netherlands).
LUMINOSITY OSCILLATIONS IMAGER (LOI)
Bo Nyborg Andersen, V. Domingo, A. R. Jones, A. Jimenez, Pere L. Palle, C. Regulo, and Teodoro RocaCortes (Consejo Superior de Investigaciones Cientificas, Tenerife, Spain) *In* ESA, Seismology of the Sun and Sun-Like Stars Dec. 1988 p 385-386 (For primary document see N89-25819 19-92)
Copyright Avail: NTIS HC A99/MF E03

N89-25892# Stanford Univ., CA. Center for Space Science and Astrophysics.
THE MICHELSON DOPPLER IMAGER FOR THE SOLAR OSCILLATIONS IMAGER PROGRAM ON SOHO
J. T. Hoeksema, Philip H. Scherrer, A. M. Title, and T. D. Tarbell (Lockheed Aircraft Corp., Palo Alto, CA.) *In* ESA, Seismology of the Sun and Sun-Like Stars Dec. 1988 p 407-412 (For primary document see N89-25819 19-92)
Copyright Avail: NTIS HC A99/MF E03

N89-25895# Centre National de la Recherche Scientifique, Verrieres-Le Buisson (France). Lab. de Physique Stellaire et Planetaire.
GOLF: SIMULATIONS OF THE RE-EMISSION OF THE RESONANCE CELL
P. Boumier and Luc Dame *In* ESA, Seismology of the Sun and Sun-Like Stars Dec. 1988 p 425-427 (For primary document see N89-25819 19-92)
Copyright Avail: NTIS HC A99/MF E03

20 SPACECRAFT PROPULSION AND POWER

Includes main propulsion systems and components, e.g., rocket engines; and spacecraft auxilliary power sources.

For related information see also *07 Aircraft Propulsion and Power, 28 Propellants and Fuels, 44 Energy Production and Conversion,* and *15 Launch Vehicles and Space Vehicles.*

N89-25269*# National Aeronautics and Space Administration. Lewis Research Center, Cleveland, OH.
SOLAR DYNAMIC POWER MODULE DESIGN
Richard R. Secunde, Thomas L. Labus, and Ronald G. Lovely (Rockwell International Corp., Canoga Park, CA.) 1989 11 p Presented at the 24th Intersociety Energy Conversion Engineering Conference, Washington, DC, 6-11 Aug. 1989; cosponsored by the IEEE, AIAA, ANS, ASME, SAE, ACS and AIChE
(NASA-TM-102055; E-4808; NAS 1.15:102055) Avail: NTIS HC A03/MF A01 CSCL 10B

Studies have shown that use of solar dynamic (SD) power for the growth eras of the Space Station Freedom program will result in life cycle cost savings when compared to power supplied by photovoltaic sources. In the SD power module, a concentrator collects and focuses solar energy into a heat receiver which has integral thermal energy storage. A power conversion unit (PCU) based on the closed Brayton thermodynamic cycle removes thermal energy from the receiver and converts that energy to electrical energy. Since the closed Brayton cycle is a single phase gas cycle, the conversion hardware (heat exchangers, turbine, compressor, etc.) can be designed for operation in low earth orbit, and tested with confidence in test facilities on earth before launch into space. The concentrator subassemblies will be aligned and the receiver/PCU/radiator combination completely assembled and charged with gas and cooling liquid on earth before launch to, and assembly on orbit. Author

N89-25270*# Lockheed Missiles and Space Co., Huntsville, AL. Structures and Mechanics Section.
SPACE SHUTTLE MAIN ENGINE STRUCTURAL ANALYSIS AND DATA REDUCTION/EVALUATION. VOLUME 2: HIGH PRESSURE OXIDIZER TURBO-PUMP TURBINE END BEARING ANALYSIS Final Report
Gregory A. Sisk Apr. 1989 85 p
(Contract NAS8-37282)
(NASA-CR-183664; NAS 1.26:183664;
LMSC-HEC-TR-F268584-Vol-2) Avail: NTIS HC A05/MF A01 CSCL 21H

The high-pressure oxidizer turbopump (HPOTP) consists of two centrifugal pumps, on a common shaft, that are directly driven by a hot-gas turbine. Pump shaft axial thrust is balanced in that the double-entry main inducer/impeller is inherently balanced and the thrusts of the preburner pump and turbine are nearly equal but opposite. Residual shaft thrust is controlled by a self-compensating, non-rubbing, balance piston. Shaft hang-up must be avoided if the balance piston is to perform properly. One potential cause of shaft hang-up is contact between the Phase 2 bearing support and axial spring cartridge of the HPOTP main pump housing. The status of the bearing support/axial spring cartridge interface is investigated under current loading conditions. An ANSYS version 4.3, three-dimensional, finite element model was generated on Lockheed's VAX 11/785 computer. A nonlinear thermal analysis was then executed on the Marshall Space Flight Center Engineering Analysis Data System (EADS). These thermal results were then applied along with the interference fit and bolt preloads to the model as load conditions for a static analysis to determine the gap status of the bearing support/axial spring cartridge interface. For possible further analysis of the local regions of HPOTP main pump housing assembly, detailed ANSYS submodels were generated using I-DEAS Geomod and Supertab (Appendix A). Author

N89-25271*# National Aeronautics and Space Administration. Lewis Research Center, Cleveland, OH.
VARIABLE SPEED INDUCTION MOTOR OPERATION FROM A 20-kHz POWER BUS
Irving G. Hansen Aug. 1989 8 p Prepared for presentation at the 24th Intersociety Energy Conversion Engineering Conference, Washington, DC, 6-11 Aug. 1989; cosponsored by the IEEE, AIAA, ANS, ASME, SAE, ACS, and AIChE
(NASA-TM-102061; E-4818; NAS 1.15:102061) Avail: NTIS HC A02/MF A01 CSCL 09A

Induction motors are recognized for their simple rugged construction. To date, however, their application to variable speed or servo drives was hampered by limitations on their control. Induction motor drives tend to be complex and to display troublesome low speed characteristics due in part to nonsinusoidal driving voltages. A technique was developed which involves direct synthesis of sinusoidal driving voltages from a high frequency power bus and independent control of frequency and voltages. Separation of frequency and voltage allows independent control of rotor and stator flux, full four quadrant operation, and instantaneous torque control. Recent test results, current status of the technology, and proposed aerospace applications will be discussed. Author

N89-25272*# National Aeronautics and Space Administration. Lewis Research Center, Cleveland, OH.
SPACE NUCLEAR REACTOR SHIELDS FOR MANNED AND UNMANNED APPLICATIONS
Barbara I. McKissock and Harvey S. Bloomfield 1989 16 p Presented at the International Conference on Space Power, Cleveland, OH, 5-7 Jun. 1989; sponsored by the International Astronautical Federation
(NASA-TM-102064; E-4821; NAS 1.15:102064) Avail: NTIS HC A03/MF A01 CSCL 10B

Missions which use nuclear reactor power systems require

radiation shielding of payload and/or crew areas to predetermined dose rates. Since shielding can become a significant fraction of the total mass of the system, it is of interest to show the effect of various parameters on shield thickness and mass for manned and unmanned applications. Algorithms were developed to give the thicknesses needed if reactor thermal power, separation distances, and dose rates are given as input. The thickness algorithms were combined with models for four different shield geometries to allow tradeoff studies of shield volume and mass for a variety of manned and unmanned missions. Shield design tradeoffs presented in this study include the effects of: higher allowable dose rates; radiation hardened electronics; shorter crew exposure times; shield geometry; distance of the payload and/or crew from the reactor; and changes in the size of the shielded area. Specific NASA missions that were considered in this study include unmanned outer planetary exploration, manned advanced/evolutionary space station, and advanced manned lunar base. Author

N89-25273*# National Aeronautics and Space Administration. Lewis Research Center, Cleveland, OH.

SPACE STATION FREEDOM PHOTOVOLTAIC POWER MODULE DESIGN STATUS

Amador P. Jimenez (Rockwell International Corp., Canoga Park, CA.) and Mark A. Hoberecht 1989 6 p Presented at the 24th Intersociety Energy Conversion Engineering Conference, Washington, DC, 6-11 Aug. 1989; cosponsored by the IEEE, AIAA, ANS, ASME, SAE, ACS and AIChE

(NASA-TM-102073; E-4832; NAS 1.15:102073) Avail: NTIS HC A02/MF A01 CSCL 10B

Electric power generation for Space Station Freedom will be provided by four photovoltaic (PV) power modules using silicon solar cells during Phase 1 operation. Each PV power module requires two solar arrays with 32,800 solar cells generating 18.75 kW of dc power for a total of 75 kW. A portion of this power will be stored in nickel-hydrogen batteries for use during eclipse, and the balance will be processed and converted to 20 kHz ac power for distribution to end users through the power management and distribution system. The design incorporates an optimized thermal control system, pointing and tracking provision with the application of gimbals, and the use of orbital replacement units (ORU's) to achieve modularization. Design status of the PV power module, as derived from major trade studies, is discussed at hardware levels ranging from component to system. Details of the design are presented where appropriate. Author

N89-25274*# National Aeronautics and Space Administration. Lewis Research Center, Cleveland, OH.

THE INTRODUCTION OF SPACE TECHNOLOGY POWER SYSTEMS INTO DEVELOPING COUNTRIES

Allen F. Roberts (Iowa Univ., Iowa City.) and Anthony F. Ratajczak Mar. 1989 19 p Presented at the Symposium on Space Commercialization: Roles of Developing Countries, Nashville, TN, 5-10 Mar. 1989; sponsored in part by Tennessee Univ. Space Institute

(NASA-TM-102042; E-4799; NAS 1.15:102042) Avail: NTIS HC A03/MF A01 CSCL 10B

Between 1978 and 1984, NASA-Lewis was responsible for the design, fabrication, installation and operational support of 57 photovoltaic power systems in 27 countries. These systems were installed in locations not served by a central power system and ranged in size from 40 W for powering street lights to 29 kW for providing power to a complete village. Several of the system projects had socio/economic studies components that provided for an assessment of how the introduction of both electricity and a novel high technology power system affected the users and their society. Author

N89-25275*# National Aeronautics and Space Administration. Lewis Research Center, Cleveland, OH.

LAUNCH PACKAGING OPTIONS FOR THE PHOTOVOLTAIC POWER MODULE CARGO ELEMENT

Mark A. Hoberecht and Scott T. Vogt (Rockwell International Corp., Canoga Park, CA.) 1989 7 p Presented at the 24th Intersociety Energy Conversion Engineering Conference, Washington, DC, 6-11 Aug. 1989; cosponsored by the IEEE, AIAA, ANS, ASME, SAE, ACS and AIChE

(NASA-TM-102072; E-4831; NAS 1.15:102072) Avail: NTIS HC A02/MF A01 CSCL 10A

The National Aeronautics and Space Administration recently embarked on the Space Station Freedom program, which will utilize the Shuttle Orbiter for transportation to orbit. This task will be accomplished with a number of flights over several years. Each flight is unique in terms of the hardware that is manifested and the method by which it is integrated to form viable cargo elements. Work Package 4 is responsible for the electric power system for Space Station Freedom, and was delegated the authority to develop a photovoltaic (PV) power module cargo element. The PV power module consists of several unique assemblies. The first of these is the combined solar array/beta gimbal assembly. The remaining assemblies form the single combined integrated equipment assembly for each PV power module. These three combined assemblies are packaged into a launch cradle to form the PV power module cargo element, which is placed in the cargo bay of the Shuttle Orbiter for transportation to orbit. Various constraints determine the packaging options for the three PV power module combined assemblies. The size and shape of the combined assemblies in relation to the Shuttle Orbiter cargo bay dimensions and other manifested hardware are ultimately a factor in determining the acceptable packaging schemes for the PV power module cargo element. Several packaging options for the PV power module cargo element are presented. These options are discussed in terms of their impact on the overall flight hardware manifest as determined by the various constraints. NASA

N89-25276*# Lockheed Missiles and Space Co., Huntsville, AL. Flight Technology Group.

AERODYNAMIC FLIGHT EVALUATION ANALYSIS AND DATA BASE UPDATE Final Report

W. W. Boyle, M. S. Miller, G. O. Wilder, R. D. Reheuser, R. S. Sharp, and G. I. Bridges May 1989 294 p

(Contract NAS8-33807)

(NASA-CR-183654; NAS 1.26:183654; LMSC-HEC-TR-F268592)

Avail: NTIS HC A13/MF A01 CSCL 10C

Research was conducted to determine the feasibility of replacing the Solid Rocket Boosters on the existing Space Shuttle Launch Vehicle (SSLV) with Liquid Rocket Boosters (LRB). As a part of the LRB selection process, a series of wind tunnel tests were conducted along with aero studies to determine the effects of different LRB configurations on the SSLV. Final results were tabulated into increments and added to the existing SSLV data base. The research conducted in this study was taken from a series of wind tunnel tests conducted at Marshall's 14-inch Trisonic Wind Tunnel. The effects on the axial force (CAF), normal force (CNF), pitching moment (CMF), side force (CY), wing shear force (CSR), wing torque moment (CTR), and wing bending moment (CBR) coefficients were investigated for a number of candidate LRB configurations. The aero effects due to LRB protuberances, ET/LRB separation distance, and aft skirts were also gathered from the tests. Analysis was also conducted to investigate the base pressure and plume effects due to the new booster geometries. The test results found in Phases 1 and 2 of wind tunnel testing are discussed and compared. Preliminary LRB lateral/directional data results and trends are given. The protuberance and gap/skirt effects are discussed. The base pressure/plume effects study is discussed and results are given. Author

N89-25277*# National Aeronautics and Space Administration. Lewis Research Center, Cleveland, OH.

SCALING RESULTS FOR THE LIQUID SHEET RADIATOR (LSR)

Donald L. Chubb and Frederick D. Calfo 1989 8 p Presented at the 24th Intersociety Energy Conversion Engineering Conference, Washington, DC, 6-11 Aug. 1989; cosponsored by the IEEE, AIAA,

ANS, ASME, SAE, ACS, and AIChE
(NASA-TM-102100; E-4835; NAS 1.15:102100) Avail: NTIS HC A02/MF A01 CSCL 20D

Surface tension forces at the edges of a thin liquid (approx. 100 micrometers) sheet flow result in a triangularly shaped sheet. Such a geometry is ideal for an external flow radiator. The experimental investigation of such sheet flows was extended to large sheets (width = W = 23.5 cm, length = L approx. = 3.5 m). Experimental L/W results are greater than the calculated results. However, more experimental results are necessary for a complete comparison. The calculated emissivity of a sheet of Dow-Corning 705 silicone oil, which is a low temperature (300 to 400K) candidate for a liquid sheet radiator (LSR), is greater than .8 for sheet thicknesses greater than 100 micrometers. Author

N89-25278*# National Aeronautics and Space Administration. Marshall Space Flight Center, Huntsville, AL.
AN EVALUATION OF THE GENERAL DYNAMICS 20 kHz 5 kW BREADBOARD FOR SPACE STATION ELECTRICAL POWER AT MSFC
David K. Hall and Robert E. Kapustka May 1989 15 p
(NASA-TM-100367; NAS 1.15:100367) Avail: NTIS HC A03/MF A01 CSCL 10B

The results and observations are discussed of tests made on the General Dynamics 20 kHz Breadboard for Space Station Electrical Power. The General Dynamics 20 kHz system only is considered, and not the issue of the use of 20 kHz ac Power for Spacecraft Applications. Author

N89-25279* National Aeronautics and Space Administration. Lyndon B. Johnson Space Center, Houston, TX.
HYBRID PLUME PLASMA ROCKET Patent
Franklin R. Chang, inventor (to NASA) 28 Mar. 1989 12 p
(NASA-Case-MSC-20476-2; US-Patent-4,815,279; US-Patent-Appl-SN-046341; US-Patent-Class-60-202; US-Patent-Class-60-264; US-Patent-Class-239-265.17) Avail: U.S. Patent and Trademark Office CSCL 20C

A technique for producing thrust by generating a hybrid plume plasma exhaust is disclosed. A plasma flow is generated and introduced into a nozzle which features one or more inlets positioned to direct a flow of neutral gas about the interior of the nozzle. When such a neutral gas flow is combined with the plasma flow within the nozzle, a hybrid plume is constructed including a flow of hot plasma along the center of the nozzle surrounded by a generally annular flow of neutral gas, with an annular transition region between the pure plasma and the neutral gas. The temperature of the outer gas layer is below that of the pure plasma and generally separates the pure plasma from the interior surfaces of the nozzle. The neutral gas flow both insulates the nozzle wall from the high temperatures of the plasma flow and adds to the mass flow rate of the hybrid exhaust. The rate of flow of neutral gas into the interior of the nozzle may be selectively adjusted to control the thrust and specific impulse of the device.
Official Gazette of the U.S. Patent and Trademark Office

N89-25280*# National Aeronautics and Space Administration. Lewis Research Center, Cleveland, OH.
ESTIMATED PERFORMANCE AND FUTURE POTENTIAL OF SOLAR DYNAMIC AND PHOTOVOLTAIC POWER SYSTEMS FOR SELECTED LEO AND HEO MISSIONS
David J. Bents and Cheng Y. Lu 1989 13 p Presented at the 24th Intersociety Energy Conversion Engineering Conference, Washington, DC, 6-11 Aug. 1989; cosponsored by the IEEE, AIAA, ANS, ASME, SAE, ACS and AIChE
(NASA-TM-102083; E-4846; NAS 1.15:102083) Avail: NTIS HC A03/MF A01 CSCL 10B

Solar Photo Voltaic (PV) and thermal dynamic power systems for application to selected Low Earth Orbit (LEO) and High Eccentric Orbit (Energy) (HEO) missions are characterized in the regime 7 to 35 kWe. Input parameters to the characterization are varied corresponding to anticipated introduction of improved or new technologies. Comparative assessment is made between the two power system types utilizing newly emerging technologies in cells and arrays, energy storage, optical surfaces, heat engines, thermal energy storage, and thermal management. The assessment is made to common ground rules and assumptions. The four missions (space station, sun-synchronous, Van Allen belt and GEO) are representative of the anticipated range of multi-kWe earth orbit missions. System characterizations include all required subsystems, including power conditioning, cabling, structure, to deliver electrical power to the user. Performance is estimated on the basis of three different levels of component technology: (1) state-of-art, (2) near-term, and (3) advanced technologies. These range from planar array silicon/IPV nickel hydrogen batteries and Brayton systems at 1000 K to thin film GaAs with high energy density secondary batteries or regenerative fuel cells and 1300 K Stirling systems with ultra-lightweight concentrators and radiators. The system estimates include design margin for performance degradations from the known environmental mechanisms (micrometeoroids and space debris, atomic oxygen, electron and proton flux) which are modeled and applied depending on the mission. The results give expected performance, mass and drag of multi-kWe earth orbiting solar power systems and show how overall system figures of merit will improve as new component technologies are incorporated. Author

N89-25281*# National Aeronautics and Space Administration. Lewis Research Center, Cleveland, OH.
THE EFFECTS OF ARCJET OPERATING CONDITION AND CONSTRICTOR GEOMETRY ON THE PLASMA PLUME
Lynnette M. Carney and John M. Sankovic (Akron Univ., OH.) Jul. 1989 29 p Presented at the 25th Joint Propulsion Conference, Monterey, CA, 10-12 Jul. 1989; sponsored in part by AIAA, ASME, SAE, and ASEE
(NASA-TM-102284; E-4877; NAS 1.15:102284; AIAA-89-2723) Avail: NTIS HC A03/MF A01 CSCL 21H

Measurements of plasma number density and electron temperature were obtained in the plumes of lab arcjet thrusters using electrostatic probes of both spherical and cylindrical geometry. The two arcjet thrusters used had different constrictor and/or nozzle geometries and operated on mixtures of nitrogen, hydrogen, and ammonia to simulate the decomposition products of hydrazine and ammonia. An increase in the measured electron density was observed for both geometries with increasing arc power at a constant mass flow rate and with increasing mass flow rate at a constant arc current. For a given operating condition, the electron number density decreased exponentially off centerline and followed an inverse distance squared relationship along the thrust axis. Typical measured electron temperatures ranged from 0.1 to 0.2 eV. Author

N89-25282*# National Aeronautics and Space Administration. Lewis Research Center, Cleveland, OH.
CSTI HIGH CAPACITY POWER
Jerry M. Winter 1989 21 p Presented at the 24th Intersociety Energy Conversion Engineering Conference, Washington, DC, 6-11 Aug. 1989; cosponsored by the IEEE, AIAA, ANS, ASME, SAE, ACS and AIChE
(NASA-TM-102059; E-4817; NAS 1.15:102059) Avail: NTIS HC A03/MF A01 CSCL 10B

The SP-100 program was established in 1983 by DOD, DOE, and NASA as a joint program to develop the technology necessary for space nuclear power systems for military and civil application. During FY-86 and 87, the NASA SP-100 Advanced Technology Program was devised to maintain the momentum of promising technology advancement efforts started during Phase 1 of SP-100 and to strengthen, in key areas, the chances for successful development and growth capability of space nuclear reactor power systems for future space applications. In FY-88, the Advanced Technology Program was incorporated into NASA's new Civil Space Technology Initiative (CSTI). The CSTI Program was established to provide the foundation for technology development in automation and robotics, information, propulsion, and power. The CSTI High Capacity Power Program builds on the technology efforts of the SP-100 program, incorporates the previous NASA SP-100 Advanced Technology project, and provides a bridge to NASA Project Pathfinder. The elements of CSTI High Capacity Power

development include Conversion Systems, Thermal Management, Power Management, System Diagnostics, and Environmental Interactions. Technology advancement in all areas, including materials, is required to assure the high reliability and 7 to 10 year lifetime demanded for future space nuclear power systems. The overall program will develop and demonstrate the technology base required to provide a wide range of modular power systems as well as allowing mission independence from solar and orbital attitude requirements. Several recent advancements in CSTI High Capacity power development will be discussed. Author

N89-25283*# National Aeronautics and Space Administration. Lewis Research Center, Cleveland, OH.
PERFORMANCE CHARACTERIZATION AND TRANSIENT iNVESTIGATION OF MULTIPROPELLANT RESISTOJETS
Edward P. Braunscheidel Jul. 1989 21 p Presented at the 25th Joint Propulsion Conference, Monterey, CA, 10-12 Jul. 1989; cosponsored by the AIAA, ASME, SAE, and ASEE
(NASA-TM-102118; E-4897; NAS 1.15:102118; AIAA-89-2837)
Avail: NTIS HC A03/MF A01 CSCL 21H

The multipropellant resistojet thruster design initially was characterized for performance in a vacuum tank using argon, carbon dioxide, nitrogen, and hydrogen, with gas inlet pressures ranging from 13.7 to 310 kPa (2 to 45 psia) over a heat exchanger temperature range of ambient to 1200 C (2200 F). Specific impulse, the measure of performance, had values ranging from 120 to 600 seconds for argon and hydrogen respectively, with a constant heat exchanger temperature of 1200 C (2200 F). When operated under ambient conditions typical specific impulse values obtained for argon and hydrogen ranged from 55 to 290 seconds, respectively. Performance measured with several mixtures of argon and nitrogen showed no significant deviation from predictions obtained by directly weighting the argon and nitrogen individual performance results. Another aspect of the program investigating transient behavior, showed responses depended heavily on the start-up scenario used. Steady state heater temperatures were achieved in 20 to 75 minutes for argon, and in 10 to 90 minutes for hydrogen. Steady state specific impulses were achieved in 25 to 60, and 20 to 60 minutes respectively. Author

N89-25284*# Morton Thiokol, Brigham City, UT. Aerospace Group.
FLIGHT SET 360L003 INSTRUMENTATION FINAL TEST REPORT, VOLUME 9
5 May 1989 76 p
(Contract NAS8-30490)
(NASA-CR-183675; NAS 1.26:183675; TWR-17542-Vol-9) Avail: NTIS HC A05/MF A01 CSCL 21H

Post-flight instrumentation hardware and data evaluation for 360L003 is summarized. The 360L003 motors were equipped with Developmental Flight Instrumentation (DFI), Operational Flight Instrumentation (OFI), and Ground Environmental Instrumentation (GEI). The DFI was designed to measure strain, temperature, pressure, and vibration at various locations on the motor during flight. The DFI is used to validate engineering models in a flight environment. The OFI consists of six Operational Pressure Tranducers which monitor chamber pressure during flight. These pressure transducers are used in the SRB separation cue. GEI measures the motor case, igniter flange, and nozzle temperature prior to launch. Author

N89-25199*# PDA Engineering, Costa Mesa, CA.
INVOLUTE COMPOSITE DESIGN EVALUATION USING GLOBAL DESIGN SENSITIVITY DERIVATIVES
J. K. Hart and E. L. Stanton *In* NASA. Langley Research Center, Recent Advances in Multidisciplinary Analysis and Optimization, Part 2 Apr. 1989 p 991-1008 (For primary document see N89-25173 19-05)
Avail: NTIS HC A22/MF A01 CSCL 21H

23 CHEMISTRY AND MATERIALS (GENERAL)

N89-25285*# National Aeronautics and Space Administration. Lewis Research Center, Cleveland, OH.
CHARACTERIZATION OF CERAMICS AND INTERMETALLICS FABRICATED BY SELF-PROPAGATING HIGH-TEMPERATURE SYNTHESIS
Janet B. Hurst May 1989 21 p
(NASA-TM-102004; E-4710; NAS 1.15:102004) Avail: NTIS HC A03/MF A01 CSCL 11B

Three efforts aimed at investigating the process of self-propagating high temperature synthesis (SHS) for the fabrication of structural ceramics and intermetallics are summarized. Of special interest was the influence of processing variables such as exothermic dopants, gravity, and green state morphology in materials produced by SHS. In the first effort directed toward the fabrication of SiC, exothermic dopants of yttrium and zirconium were added to SiO2 or SiO2 + NiO plus carbon powder mix and processed by SHS. This approach was unsuccessful since it did not produce the desired product of crystalline SiC. In the second effort, the influence of gravity was investigated by examining Ni-Al microstructures which were produced by SHS combustion waves traveling with and opposite the gravity direction. Although final composition and total porosities of the combusted Ni-Al compounds were found to be gravity independent, larger pores were created in those specimens which were combusted opposite to the gravity force direction. Finally, it was found that green microstructure has a significant effect on the appearance of the combusted piece. Severe pressing laminations were observed to arrest the combustion front for TiC samples. Author

N89-25286*# SRI International Corp., Menlo Park, CA. Dept. of Chemical Kinetics.
PHOTODISSOCIATION OF PERNITRIC ACID (HO2NO2) AT 248 nm
Helene MacLeod, Gregory P. Smith, and David M. Golden 1989 43 p Submitted for publication
(Contract NASw-3888)
(NASA-CR-185363; NAS 1.26:185363) Avail: NTIS HC A03/MF A01 CSCL 07A

The photodissociation of pernitric acid (PNA) was studied at 248 nm. The quantum yield for production of OH radicals is 34 + or - 16 percent. The yield of OH from PNA was measured relative to that of H2O2. The translational and rotational energy content of the OH photofragment from PNA was characterized. A fluorescent emission was also observed and characterized. It is attributed to electronically excited NO2 produced in the PNA photodissociation. A maximum yield of 30 percent for NO2 production was determined. The intensity of this emission, and a mass spectrometric peak at m/e = 33, were found to be useful means of characterizing the purity of the PNA sample. Author

24 COMPOSITE MATERIALS

Includes physical, chemical, and mechanical properties of laminates and other composite materials.

For ceramic materials see *27 Nonmetallic Materials*.

N89-25287 Idaho Univ., Moscow.
CHARACTERIZATION OF THE EFFECTS OF THREE-DIMENSIONAL STATES OF STRESS ON DAMPING OF LAMINATED COMPOSITES Ph.D. Thesis
Shwilong Jimmy Hwang 1988 220 p
Avail: Univ. Microfilms Order No. DA8903472

Techniques for the characterization of the effects of three-dimensional states of stress on dynamic mechanical properties of laminated composites are presented. Dynamic stiffness and damping are defined in terms of the complex modulus, and damping of the composite laminate is evaluated by means of

a strain energy method. The strain energy method is implemented in a three-dimensional finite element technique and an empirical elasticity solution to complete the analytical solutions. The effect of through-the-thickness shear stress on damping is studied by varying fiber orientation and by varying laminate geometry. The three-dimensional finite element technique developed here has the capability to do both static analysis and modal analysis, and can be applied in more complex composite structures and loading situations. Experimental verification was done by using the impulse-frequency response vibration technique and both extensional and flexural vibration tests were carried out. Experimental results agreed well with the three-dimensional finite element technique predicted values. Author

N89-25288# Kanner (Leo) Associates, Redwood City, CA.
WHISKER SHAPED CARBON SUBSTANCE
Yukinari Komatsu and Katsuyuki Nakamura 1989 14 p Transl. into ENGLISH of Japanese Patent no. 59-253551 (30 Nov. 1984) Prepared for Los Alamos National Lab., NM
(Contract W-7405-eng-36)
(DE89-010214; LA-tr-89-12) Avail: NTIS HC A03/MF A01

This invention concerns the extremely fine whisker shaped carbon substance that is fabricated through the gaseous (vapor) phase method. The carbon substance is produced by placing hydrocarbon, a specific organic metal compound and carrier gas in some instances at the reaction zone and by heat-dissolving and catalytically reacting the hydrocarbon. The hydrocarbon used is not particularly specified. They could include: (1) hydrocarbon containing anthracene, naphthalene and others that is in solid phase in room temperature, (2) hydrocarbon containing benzene, toluene, hexane, isooctane and others that is in liquid phase in room temperature, and (3) hydrocarbon containing methane, propane, ethylene, acetylene and others that is in gaseous phase in room temperature. DOE

N89-25289# Oak Ridge National Lab., TN.
SiC WHISKER-REINFORCED SiAlON COMPOSITES: EFFECT OF SINTERING AID CONTENT
Terry N. Tiegs 1989 8 p Presented at the 13th Annual Conference on Composites and Advanced Ceramics, Cocoa Beach, FL, 15 Jan. 1989
(Contract DE-AC05-84OR-21400)
(DE89-010376; CONF-890130-5) Avail: NTIS HC A02/MF A01

SiAlON matrix composites reinforced with SiC whiskers were hot- pressed with various levels of yttrium aluminum garnet (YAG) as a sintering aid. The YAG content affected the amounts of liquid phases present during fabrication. It was determined that some liquid phase is required to achieve high density composites. However, at high sintering aid levels, degradation of the matrix-whisker interface occurs and the composite fracture toughness is reduced. DOE

N89-25290*# National Aeronautics and Space Administration. Lewis Research Center, Cleveland, OH.
VIBRATION TESTING OF IMPACT-DAMAGED COMPOSITE LAMINATES
Joseph E. Grady and Erwin H. Meyn Jun. 1989 11 p Presented at the 30th Structures, Structural Dynamics and Materials Conference, Mobile, AL, 3-5 Apr. 1989; cosponsored by the AIAA, ASME, ASCE, AHS, and ASC Previously announced in IAA as A89-30883
(NASA-TM-4115; E-4518; NAS 1.15:4115) Avail: NTIS HC A03/MF A01 CSCL 11D

A new test is described that can be used to measure changes in the vibration properties of impact damaged composite materials. Impact-induced delamination was observed to significantly affect natural frequencies of vibration and damping properties in cross-ply graphite/epoxy laminates. Natural frequencies are shown to drop by as much as half of their original value, and modal damping ratios can increase by a factor of up to eight when large amounts of damage are present. A simple finite element model of the damaged impact specimens was used to predict the effect of delamination on certain vibration properties. A comparison of the finite element calculations with the experimental measurements suggests that delamination was the dominant mechanism of flexural stiffness loss resulting from the transverse impact. Author

N89-25291# Lawrence Livermore National Lab., CA. Composite Materials Group.
FAILURE CHARACTERIZATION OF COMPOSITE MATERIALS
Scott E. Groves Jan. 1989 10 p Presented at the Army Symposium on Solid Mechanics: Mechanics of Engineered Materials and Applications, Newport, RI, 16 May 1989
(Contract W-7405-eng-48)
(DE89-008662; UCRL-100133; CONF-8905104-1) Avail: NTIS HC A02/MF A01

The primary objective of this research is to characterize the three-dimensional failure response of continuous fiber graphite epoxy composite materials. This effort includes the development of a new failure model, generation of the three-dimensional failure data, and an investigation of the dynamic strength behavior. This research represents a continuation of an ongoing project initiated in mid FY87. The primary effort to date has centered on the development of the necessary experimental techniques required to generate the complex failure response of these materials. DOE

N89-25292# Cornell Univ., Ithaca, NY. Dept. of Materials Science and Engineering.
STRONG FIBERS Progress Report
1989 3 p
(Contract DE-FG02-87ER-45321)
(DE89-010596; DOE/ER-45321/2) Avail: NTIS HC A02/MF A01

Experimental effort was developed with a major aim of expanding the range of deposition processes and detailed microfabrication procedures that could be incorporated in our generic approach to new materials development and fiber fabrication. Equipment for mechanical characterization of fine fibers was also designed and constructed. Major activities were: (1) To incorporate chemical vapor deposition processes into the patterning, deposition, and lift-off sequence for fabricating strong fibers. The material of choice was silicon nitride. (2) A project to evaluate and explain the different and high strengths of aluminum fibers produced by different deposition processes. (3) Alloy oxide films and fibers are being produced by dual source electron beam evaporation. Variable but controlled amounts of zirconium or titanium are added to aluminum oxide. (4) Silicon carbide films with variable silicon to carbon ratios have been produced by chemical vapor deposition. (5) A micro-tensile testing apparatus was designed and constructed for measuring the tensile strengths of the fibers produced in the program. DOE

N89-25293# Sandia National Labs., Albuquerque, NM.
ELECTRICALLY CONDUCTIVE COMPOSITE MATERIAL Patent Application
Roger L. Clough, inventor (to DOE) and Alan P. Sylwester, inventor (to DOE) 20 Jun. 1988 14 p
(Contract DE-AC04-76DP-00789)
(DE89-010967; PATENTS-US-A7209119; US-Patent-Appl-SN-209119) Avail: NTIS HC A03

An electrically conductive composite material is disclosed which comprises a conductive open-celled, low density, microcellular carbon foam filled with a non-conductive polymer or resin. The composite material is prepared in a two-step process consisting of first preparing the microcellular carbon foam from a carbonizable polymer or copolymer using a phase separation process, then filling the carbon foam with the desired non-conductive polymer or resin. The electrically conductive composites of the present invention has a uniform and consistent pattern of filler distribution, and as a result is superior over prior art materials when used in battery components, electrodes, and the like. DOE

N89-25294*# National Aeronautics and Space Administration. Langley Research Center, Hampton, VA.
POLYIMIDE MATRIX COMPOSITES: POLYIMIDESULFONE/LARC-TPI (1:1) BLEND
Norman J. Johnston, Terry L. St.Clair, Robert M. Baucom, and Timothy W. Towell (Old Dominion Univ., Norfolk, VA.) Mar. 1989 14 p Presented at the 34th International SAMPE Symposium and Exhibition, Reno, NV, 8-11 May 1989
(NASA-TM-101568; NAS 1.15:101568) Avail: NTIS HC A03/MF A01 CSCL 11D

Polyimide matrix composites were fabricated from unidirectional unsized AS-4 carbon fiber and a doped 1:1 blend of two polyimides: benzophenone dianhydride-3,3'-diamino diphenylsulfone (PISO2) and benzophenone dianhydride-3,3'-diamino benzophenone (LARC-TPI). To enhance melt flow properties, the molecular weight of the PISO2 was controlled by end-capping with phthalic anhydride and addition of 5 percent by weight p-phenylene diamine-phthalic anhydride bisamic acid dopant. Prepreg was drum-wound using a diglyme slurry comprised of the soluble polyamideacid of PISO2, the soluble bisamideacid of the dopant, and the insoluble imidized LARC-TPI powder. Melt flow studies with a rotary rheometer and parallel plate plastometer on neat resin and prepreg helped develop an optimum cure cycle. Composite mechanical properties at room and elevated temperatures, dry and moisture-saturated, were evaluated, including short beam shear strength and flexure, tensile, shear, and compression properties. Two 18 in. x 24 in. skin-stringer panels were fabricated, one of which was tested in compression to failure. Author

N89-25295# Lawrence Livermore National Lab., CA.
ESTIMATING EFFECTIVE MODULI OF COMPOSITES USING QUANTITATIVE IMAGE ANALYSIS
James G. Berryman Apr. 1989 13 p Presented at the SIAM Workshop on Random Media and Composites, Leesburg, VA, 7 Dec. 1988
(Contract W-7405-eng-48)
(DE89-012292; UCRL-99493; CONF-881287-1) Avail: NTIS HC A03/MF A01

The statistical data required for quantitative analysis of the physical properties of composite materials may be obtained using digital image processing techniques. This approach allows accurate quantitative determination of volume fraction data, of interface area per unit volume, and of more sophisticated measures of the microgeometry of material mixtures including the n-point spatial correlation functions. The two- and three-point correlation functions can be measured quite accurately both for synthetic materials and for real materials such as porous sandstones. To extract the desired parameters of the microgeometry from the three-point correlation functions, methods of interpolating and integrating these lattice-based empirical values have been developed. Methods of finessing the theory to give estimates of physical properties when the available data are not adequate to permit use of the full theory have also been developed. DOE

N89-25296*# Textron Bell Helicopter, Fort Worth, TX.
AN ANALYTICAL AND EXPERIMENTAL INVESTIGATION OF EDGE DELAMINATION IN LAMINATES SUBJECTED TO TENSION, BENDING, AND TORSION Final Report, Jan. 1986 - Jun. 1988
Wen S. Chan Mar. 1989 77 p
(Contract NAS1-18199)
(NASA-CR-181824; NAS 1.26:181824; BHTI-699-099-265) Avail: NTIS HC A05/MF A01 CSCL 11D

An integrated two-dimensional finite element was developed to calculate interlaminar stresses and strain energy release rates for the study of delamination in composite laminates subjected to uniaxial tension, bending, and torsion loads. Addressed are the formulation, implementation, and verification of the model. Parametric studies were conducted on the effect of Poisson's ratio mismatch between plies and the stacking sequence on interlaminar stress, and on the effect of delamination opening height and delamination length, due to bending, on strain energy release rate for various laminates. A comparison of strain energy release rates in all-graphite and graphite/glass hybrid laminates is included. The preliminary results of laminates subjected to torsion are also included. Fatigue tension tests were conducted on Mode 1 and mixed mode edge-delamination coupons to establish the relationship between fatigue load vs. onset of delamination cycle. The effect on the fatigue delamination onset of different frequencies (1 and 5 Hz) was investigated for glass, graphite,and their hybrid laminates. Although a 20 percent increase in the static onset-of-delamination strength and a 10 percent increase in ultimate strength resulted from hybridizing the all-graphite laminate with a 90 deg glass ply, the fatigue onset is lower in the hybrid laminate than in the all-graphite laminate. Author

N89-25297# Kernforschungszentrum G.m.b.H., Karlsruhe (Germany, F.R.). Inst. fuer Material- und Festkoerperforschung.
MECHANICAL PROPERTIES OF CARBON FIBER REINFORCED THERMOPLASTICS FOR CRYOGENIC APPLICATIONS Thesis - Karlsruhe Univ.
K. Ahlborn Jan. 1989 89 p In GERMAN; ENGLISH summary (KfK-4487; ISSN-0303-4003; ETN-89-94593) Copyright Avail: NTIS HC A05/MF A01

Mechanical properties like strength, stiffness, and fatigue of carbon reinforced thermoplastic matrix systems are studied at cryogenic temperatures. Two carbon fiber reinforced tough thermoplastics (PEEK, PC) were tested at 293, 77, and 5K by tensile, bending, and fatigue loading. The toughness of the matrices generally improves the static strength at low temperatures. In bidirectionally reinforced thermoplastics, transversal cracks appear in the matrix or in the boundary layer at composite strains below 0.2 percent, originated by the thermal preloading. The formation and development of the cracks depend on the fiber-matrix bond and on the thickness of the composite layers. In the manufacturing process it is necessary to improve the homogenity of the composite structure in order to increase the long term fatigue behavior. ESA

N89-25298# Technische Hochschule, Aachen (Germany, F.R.). Fakultaet fuer Maschinenwesen.
PROCESSING OF FIBER-REINFORCED MATERIALS BY INJECTION MOLDING Ph.D. Thesis
Ulrich Woelfel 1987 154 p In GERMAN; ENGLISH summary (ETN-89-94668) Avail: NTIS HC A08/MF A01

Computer programs for computer aided design of molded parts made from short glass fiber thermoplastics are developed. Fiber orientation and length distributions influenced by processing are taken into consideration. To avoid material damage and fiber wear during plastification of reinforced materials treated by injection molding, a program is developed for the rheological layout of injection molds. Pattern orientation is calculated within plate-like molded parts of arbitrary complexity. Mechanical properties together with Young's modulus of molded parts are evaluated. ESA

N89-25299# Technische Hochschule, Aachen (Germany, F.R.). Fakultaet fuer Maschinenwesen.
A PROCEDURE FOR THE NUMERICAL DESCRIPTION OF THE MOISTURE DEPENDENT MATERIAL BEHAVIOR Ph.D. Thesis
Sybill Kraemer 1987 102 p In GERMAN; ENGLISH summary (ETN-89-94669) Avail: NTIS HC A06/MF A01

A numerical description of the behavior of polymers under the influence of environmental humidity is presented. The model is based on the one-dimensional short term tensile test with constant strain rate and the torsional pendulum test. The test materials are an unreinforced and 50 percent glass fiber reinforced polyamide and a plasticized PVC. The model includes the dependence of the material behavior on the glass transition temperature and the dependence of the glass transition temperature on the water content in the polymer with the time-temperature shifting principle. The stress-strain behavior of polyamides shows that higher temperatures have a similar effect to a higher water content in the polymer. ESA

N89-25300*# National Aeronautics and Space Administration. Lewis Research Center, Cleveland, OH.
A PREDICTIVE MODEL FOR FAILURE PROPERTIES OF THERMOSET RESINS
James M. Caruthers (Purdue Univ., West Lafayette, IN.) and Kenneth J. Bowles Jul. 1989 8 p
(Grant NAG3-599)
(NASA-TM-4128; E-4572; NAS 1.15:4128) Avail: NTIS HC A02/MF A01 CSCL 11D

A predictive model for the three-dimensional failure behavior of engineering polymers has been developed in a recent NASA-sponsored research program. This model acknowledges the underlying molecular deformation mechanisms and thus accounts for the effects of different chemical compositions, crosslink density, functionality of the curing agent, etc., on the complete nonlinear stress-strain response including yield. The material parameters required by the model can be determined from test-tube quantities of a new resin in only a few days. Thus, we can obtain a first-order prediction of the applicability of a new resin for an advanced aerospace application without synthesizing the large quantities of material needed for failure testing. This technology will effect order-of-magnitude reductions in the time and expense required to develop new engineering polymers. Author

25 INORGANIC AND PHYSICAL CHEMISTRY

Includes chemical analysis, e.g., chromatography; combustion theory; electrochemistry; and photochemistry.

For related information see also *77 Thermodynamics and Statistical Physics.*.

N89-25301# National Aeronautical Lab., Bangalore (India). Fluid Mechanics Div.
EXPERIMENTS ON LIQUID-VAPOUR PHASE CHANGE BETWEEN PLANE LIQUID SURFACES. PART 3: RESULTS FROM A CLOSED QUARTZ CHAMBER
M. D. Deshpande and P. N. Shankar Sep. 1988 21 p
(NAL-TM-FM-8809) Avail: NTIS HC A03/MF A01

Results are presented of phase change experiments performed with mercury contained in a closed quartz chamber. The use of the special chamber permitted better control on contamination and also the possibility of running at higher temperatures. The present results emphatically confirm the large temperature jumps at the interfaces reported earlier in Part 2 of this study. Mild partially inverted and mild globally inverted temperature profiles were also observed. These mild inversions could possibly be due to non-uniform heating and cooling of the apparatus, three dimensional effects etc. For a conclusive confirmation of the existence of temperature inversion the problem of contamination of the liquid and vapor remains a major hurdle. Author

N89-25302# Haut Commissariat a la Recherche, Algiers (Algeria). Centre d'Etudes Nucleaires et Solaires.
NMR STUDY OF SOME ORGANOPHOSPHORUS COMPOUNDS
Mouloud Attou, Hiroshi Moriyama, and Abdelkrim Azzouz Dec. 1988 16 p
(DE88-705970; HCR-CDM-05; LTC/DSO-09) Avail: NTIS (US Sales Only) HC A03/MF A01

Some organophosphorus compounds are studied in the present work. Spectra of these compounds were discussed. H-1, C-13, and P-31 NMR methods were used. Some of these organophosphorus compounds were analyzed using O-17 technique. It was observed that TBP, TEP and TMP practically present the same C-13 chemical shift range and in some trialkylphosphates, Karplus effect was notified. The present work allowed to withdraw other important conclusions which can have effective practical applications. DOE

N89-25303# Central Inst. of Physics, Bucharest (Romania). Inst. de Fizica si Tehnologia Aparatelor cu Radiatii.
IR LASER PHOTOCHEMISTRY
I. Ursu, Rodica Alexandrescu, I. Morjan, I. N. Mihailescu, V. Draganescu, V. Jianu, and C. Popescu Mar. 1988 18 p In ROMANIAN
(DE88-706012; ICEFIZ-LOP-64-1988) Avail: NTIS (US Sales Only) HC A03/MF A01

The work presents the results obtained in the field of IR laser photochemistry in order to obtain chemical products of high purity and of economical importance. DOE

N89-25304# Los Alamos National Lab., NM.
IMPROVEMENTS OF THE KIVA-2 COMPUTER PROGRAM FOR NUMERICAL COMBUSTION
P. J. ORourke, A. A. Amsden, T. D. Butler, and T. L. McKinley (Cummins Engine Co., Inc., Columbus, IN.) 1989 15 p Presented at the 3rd International Conference on Numerical Combustion, Antibes, France, 23 May 1989
(Contract W-7405-eng-36)
(DE89-007994; LA-UR-89-590; CONF-8905105-1) Avail: NTIS HC A03/MF A01

This paper describes and illustrates the principal differences between the newly-released KIVA-2 and the KIVA computer programs. Both programs are for the numerical calculation of two- and three-dimensional fluid flows with chemical reactions and sprays. Because of improvements to KIVA-2, it is faster, more accurate, and applicable to a wider variety of problems involving combustion and two-phase flow. DOE

N89-25305# Tennessee Univ., Knoxville.
SECONDAY ION MASS SPECTROMETRY OF AROMATIC COMPOUNDS IN ACIDIC MIXTURES Ph.D. Thesis
Christopher Patrick Leibman Jun. 1988 183 p
(Contract DE-AC05-76OR-00033)
(DE89-010611; DOE/OR-00033/T423) Avail: NTIS HC A09/MF A01

The use of acidic liquids and solids to improve the sensitivity of Secondary Ion Mass Spectroscopy (SIMS) for aromatic compounds is investigated. SIMS spectra are obtained from substituted aromatic compounds dissolved in concentrated sulfuric acid (98 wt percent). Simultaneously abundant molecular ions and protonated molecules characteristic of dissolved aromatics are observed for several aromatic compound classes including acids, aldehydes, ketones, nitriles, and nitrogen heterocycles. The utility of sulfuric acid as a SIMS matrix for detection of pterins, a group of biologically significant compounds, is demonstrated. Application of LSIMS using sulfuric acid for detection of aromatics adsorbed on substrates is also investigated. Use of acidic metal chlorides for enhanced secondary ion emission is also studied. Metal chlorides used as solid matrices or as additives to liquid matrices do not improve the sensitivity of SIMS for aromatic compounds significantly. DOE

N89-25306# Florida Univ., Gainesville. Dept. of Chemistry.
DEVELOPMENT OF LASER-EXCITED MOLECULAR LUMINESCENCE SPECTROMETRIC METHODS FOR POLYCYCLIC AROMATIC HYDROCARBONS IN ENVIRONMENTAL SCIENCES Final Progress Report, 1 Mar. 1985 - 28 Feb. 1989
J. D. Winefordner 1989 12 p
(Contract DE-FG05-87ER-60501)
(DE89-010616; DOE/ER-60501/T1) Avail: NTIS HC A03/MF A01

Our research efforts have covered eight major areas, namely Room Temperature Phosphorimetry, Constant Energy Synchronous Luminescence Spectrometry, Laser Excited Fluorescence Spectrometry, Fingerprinting of Air Particulates, a unique Self-Cleaning Cooled Belt for Low Temperature Shpolskii Spectroscopy, Molecular Emission of Gases, FT Molecular Luminescence Spectrometry and Electronic Measurement Systems. These eight areas, which have resulted in 18 DOE supported publications (see listing at end), are summarized. DOE

N89-25307# California Univ., Berkeley. Lawrence Berkeley Lab. Center for Advanced Materials.
CONCEPTS IN SURFACE SCIENCE AND HETEROGENEOUS CATALYSTS
Roger M. Nix, Gabor A. Somorjai, J. Jortner, ed., and B. Pullman, ed. Jul. 1988 68 p Presented at the 6th International Congress on Quantum Chemistry, Jerusalem, Israel 21-25 Aug. 1988 Prepared in cooperation with California Univ., Berkeley
(Contract DE-AC03-76SF-00098)
(DE89-010679; LBL-25554; CONF-8808219-1) Avail: NTIS HC A04/MF A01

The development and application of surface sensitive techniques over the last two decades has greatly improved our understanding of surface phenomena at the molecular level. From this newly acquired vast data base new concepts have emerged and it is the purpose of this paper to review those that relate most directly to the chemical properties of surfaces. Concepts concerned with the structure of clean and adsorbate-covered surfaces, the nature of the surface chemical bond, the dynamics of gas-surface interactions, surface chemical reactions and catalytic processes are presented and illustrated with examples from the recent literature. DOE

N89-25308# California Univ., Berkeley. Lawrence Berkeley Lab. Accelerator and Fusion Research Div.
MEASUREMENT OF H AND H2 POPULATIONS IN-SITU IN A LOW-TEMPERATURE PLASMA BY VACUUM-ULTRAVIOLET LASER-ABSORPTION SPECTROSCOPY
A. S. Schlachter, A. T. Young, G. C. Stutzin, J. W. Stearns, H. G. Doebele, K. N. Leung, and W. B. Kunkel Dec. 1988 10 p Presented at the SPIE/SPSE Symposium on Electronic Imaging: Advanced Devices and Systems, Los Angeles, CA, 15 Jan. 1989
(Contract DE-AC03-76SF-00098)
(DE89-010433; LBL-26430; CONF-890143-2) Avail: NTIS HC A02

A new technique, vacuum-ultraviolet laser-absorption spectroscopy, has been developed to quantitatively determine the absolute density of H and H2 within a plasma. The technique is particularly well suited to measurement in a plasma, where high charged particle and photon background complicate other methods of detection. The high selectivity and sensitivity of the technique allows for the measurement of the rotational-vibrational state distribution of H2 as well as the translational temperature of the atoms and molecules. The technique has been used to study both pulsed and continuous H(-) ion-source plasma discharges. H2 state distributions in a multicusp volume H(-) ion-source plasma show a high degree of internal excitation, with levels up to $v = 5$ and $J = 8$ being observed. The method is applicable for a very wide range of plasma conditions. Emission measurements from excited states of H are also reported. DOE

N89-25309# Sandia National Labs., Albuquerque, NM.
ISSUES IN SHOCK-INDUCED SOLID STATE CHEMISTRY
R. A. Graham 1989 10 p Presented at the 3rd International Symposium on Behavior of Media Under High Dynamic Pressures, La Grande Motte, France, 5-9 Jun. 1989
(Contract DE-AC04-76DP-00789)
(DE89-010769; SAND-89-0861C; CONF-890661-8) Avail: NTIS HC A02/MF A01

There has been considerable work over the past few years to study shock-induced solid state chemistry. In the present report, issues raised in the area are reviewed and critical concepts are discussed. The distinctive nature of solid state chemistry compared to liquid and gas phase chemistry is emphasized and material probes suitable for the study of solids are described. In order for solids to react in times less than one microsecond, unusual processes must be initiated in shock compression. Chief among the unique shock processes is the mixing of reactants by the large kinetic energy of shock-compression pulses. Mixing and fluid-like flow can lead to sufficiently intimate contact between reactants to permit complete chemical reaction in the solid state on the time scale of the experiment. Shock-induced solid state chemistry may be described as an unusually intense mechanochemical process. DOE

N89-25310# Massachusetts Inst. of Tech., Cambridge. Dept. of Electrical Engineering and Computer Science.
DIFFRACTION GRATINGS USED IN X-RAY SPECTROSCOPY Final Report
Henry I. Smith 1 Nov. 1988 38 p
(Contract W-7405-eng-48)
(DE89-012327; UCRL-21202) Avail: NTIS HC A03/MF A01

This subcontract was initiated in order to facilitate the development at MIT of technologies for fabricating the very fine diffraction grating required in X-ray spectroscopy at Lawrence Livermore Laboratory (LLL). These gratings are generally gold transmission gratings with spatial periods of 200 nm or less. The major focus of our efforts was to develop a means of fabricating gratings of 100 nm period. We explored two approaches: e-beam fabrication of X-ray lithography masks, and achromatic holographic lithography. This work was pursued by Erik Anderson as a major component of his Ph.D. Thesis. Erik was successful in both the e-beam and holographic approaches. However, the e-beam method proved to be highly impractical: exposure times of about 115 days would be required to cover an area of 1 sq cm. The achromatic holography, on the other hand, should be capable of exposing areas well in excess of 1 sq cm in times under 1 hour. Moreover, 100 nm-period gratings produced by achromatic holography are coherent over their entire area whereas gratings produced by e-beam lithography are coherent only over areas approx. 100 micrometer. The remainder of this report consists of portions excerpted from Erik Anderson's thesis. These contain all the details of our work on 100 nm period gratings. DOE

26 METALLIC MATERIALS

Includes physical, chemical, and mechanical properties of metals, e.g., corrosion; and metallurgy.

N89-25311# Sandia National Labs., Albuquerque, NM.
WELDABILITY AND WELD DOPING OF COMMERCIAL PURITY MOLYBDENUM
C. V. Robino 1988 24 p Presented at the TMS Fall Meeting, Chicago, IL, 25 Sep. 1988
(Contract DE-AC04-76DP-00789)
(DE89-009535; SAND-89-0352C; CONF-8809322-1) Avail: NTIS HC A03/MF A01

The GTA weldability and fracture behavior of low and high carbon arc cast and powder metallurgy molybdenum has been examined. Defect-free welds were produced in the arc cast grades. For the PM grade, however, severe centerline cracking and large scale porosity were encountered. The center-line cracking and pore formation were found to result from the dissolution of oxygen-bearing inclusions present in the starting material. Moreover, titanium or hafnium additions, incorporated into the weld by RF sputter coating the joints prior to welding, had several beneficial effects. These were reductions in the centerline cracking and pore formation in the PM welds, hardening of the weld fusion zone, and a reduction in the tendency for intergranular failure in the fusion zone for all base materials. The mechanisms by which dopant additions improve the welding and fracture behavior is also discussed. DOE

N89-25312*# Martin Marietta Aerospace, New Orleans, LA. Advanced Quality Technology.
A REVIEW OF COMPUTER AIDED INTERPRETATION TECHNOLOGY FOR THE EVALUATION OF RADIOGRAPHS OF ALUMINUM WELDS
J. F. Lloyd, Sr. 1987 21 p Presented to the Society for Experimental Mechanics, Huntsville, AL, 26-27 Aug. 1987
(Contract NAS8-30300)
(NASA-CR-185066; NAS 1.26:185066) Avail: NTIS HC A03/MF A01 CSCL 11F

Industrial radiography is a well established, reliable means of

providing nondestructive structural integrity information. The majority of industrial radiographs are interpreted by trained human eyes using transmitted light and various visual aids. Hundreds of miles of radiographic information are evaluated, documented and archived annually. In many instances, there are serious considerations in terms of interpreter fatigue, subjectivity and limited archival space. Quite often it is difficult to quickly retrieve radiographic information for further analysis or investigation. Methods of improving the quality and efficiency of the radiographic process are being explored, developed and incorporated whenever feasible. High resolution cameras, digital image processing, and mass digital data storage offer interesting possibilities for improving the industrial radiographic process. A review is presented of computer aided radiographic interpretation technology in terms of how it could be used to enhance the radiographic interpretation process in evaluating radiographs of aluminum welds. Author

N89-25313# Joint Inst. for Nuclear Research, Dubna (USSR). Lab. of Neutron Physics.

USE OF RESONANCE NEUTRONS FOR ANALYZING SUPERCLEAN ALUMINIUM

Yu. I. Belyakov, V. I. Menshikov, V. V. Serdyuk, S. B. Tomilov, V. M. Nazarov, L. P. Strelkova, V. P. Chinaeva, and I. Erdelyvary 1988 10 p In RUSSIAN; ENGLISH summary

(DE88-706221; JINR-18-88-204) Avail: NTIS (US Sales Only) HC A02/MF A01

The content of microimpurities of different elements in samples of superclean aluminum obtained by the zone melting method was determined by the neutron activation analysis on the IBR-2 reactor of Laboratory of neutron Physics, JINR. Twenty-eight elements have been discovered in the samples investigated, among them for 22 elements the concentrations have been determined as lying within the range of (10 sup -4 to 10 sup -9) weight percent. Values of purification degree for various impurity elements have been determined for different impurity elements within the 10 sup -3 up to 0.8 range. DOE

N89-25314# Sandia National Labs., Albuquerque, NM.

THERMOMECHANICAL FATIGUE OF SOLDER JOINTS: A NEW COMPREHENSIVE TEST METHOD

D. R. Frear 1989 36 p Presented at the 39th Electronic Components Conference, Houston, TX, 22 May 1989

(Contract DE-AC04-76DP-00789)

(DE89-008045; SAND-89-0401C; CONF-8905102-1) Avail: NTIS HC A03/MF A01

This paper presents a new comprehensive method to test solder joint in thermomechanical fatigue. The method involves simultaneous imposition of temperature cycles and strain on discrete solder joints in a shear orientation. The stress, microstructure, and number of cycles to failure were monitored. Cycles to failure were determined by a continuous electrical detection method. 60Sn-40Pb and 40Sn-40In-20Pb solder joints were tested using this new method at 20 percent shear strain. The 60Sn-40Pb alloy has a shorter fatigue lifetime than did 40Sn-40In-20Pb. This is attributed to heterogeneous coarsening that concentrates strain into a small area of the 60Sn-40Pb microstructure. In contrast, the 40Sn-40In-20Pb microstructure becomes refined. The heterogeneous coarsening also results in cyclic softening in 60Sn-40Pb, which was not observed in 40Sn-40In-20Pb. Failures initiated within the coarsened band in 60Sn-40Pb at Sn-Sn grain boundaries or phase boundaries. In contrast, failures initiated at the surface of 40Sn-40In-20Pb joints and propagated through both phases of the microstructure. DOE

N89-25315# Lawrence Livermore National Lab., CA.

THE INFLUENCE OF COOLING RATE ON THE FERRITE CONTENT OF STAINLESS STEEL ALLOYS

J. W. Elmer, S. M. Allen, and T. W. Eagar 24 Mar. 1989 19 p Presented at the 2nd International Conference on Trends in Welding Research, Gatlinburg, TN, 15 May 1989 Submitted for publication

(Contract W-7405-eng-48)

(DE89-009966; UCRL-100776; CONF-8905118-1) Avail: NTIS HC A03/MF A01

Electron-beam surface melting was used to rapidly solidify a series of high-purity 59 percent Fe-Ni-Cr alloys at cooling rates between 7 C/s and 7.5 x 10(6) C/s. The primary solidification mode was identified in each of the resolidified melts using optical metallography; the residual ferrite content was measured using a vibrating sample magnetometer. The cooling rate was shown to dramatically alter the residual ferrite content of these alloys through its influence on the amount of solute redistribution that occurs during solidification and through its subsequent influence on the extent of the solid-state transformation of ferrite. The results show that the solidification mode, cooling rate, and specific alloy composition are equally important, interrelated factors in the prediction of the residual ferrite. The residual ferrite content of primary-austenite solidified alloys decreases with increasing cooling rate whereas the residual ferrite content of primary-ferrite solidified alloys increases with increasing cooling rate. Exceptions to this general behavior occur when: ferrite transforms to austenite by a massive transformation in fully-ferritic-solidified alloys and an alloy changes its mode of solidification from primary-ferrite at low cooling rates to primary-austenite at high cooling rates. DOE

N89-25316# Oak Ridge National Lab., TN. Metals and Ceramics Div.

THE DEVELOPMENT OF ALLOYS BASED ON Ni3Si

W. C. Oliver 1988 6 p Presented at the Fall Meeting of the Materials Research Society, Boston, MA, 28 Nov. 1988

(Contract DE-AC05-84OR-21400)

(DE89-010371; CONF-881155-71) Avail: NTIS HC A02/MF A01

Alloys with large volume fractions of the intermetallic phase Ni sub 3 Si have unique aqueous corrosion resistance that provides the driving force for an alloy design program to improve their generally poor room temperature mechanical properties. The target of the alloy design program at Oak Ridge National Laboratory was to produce wrought alloys with at least 10 percent room temperature ductility while retaining good aqueous corrosion resistance. In this paper several important findings will be discussed. These include macro and micro alloying (B, C, Be) to produce superplastic wrought alloys with high strength and high room-temperature ductility. Some of the alloys developed are strong enough to be competitive with medium temperature structural alloys such as Inconel 718. DOE

N89-25317# Pacific Northwest Labs., Richland, WA.

QUANTITATIVE MODELING OF SENSITIZATION DEVELOPMENT IN AUSTENITIC STAINLESS STEEL

S. M. Bruemmer Apr. 1989 41 p Presented at the Corrosion '89, New Orleans, LA, 17 Apr. 1989

(Contract DE-AC06-76RL-01830)

(DE89-011206; PNL-SA-16311; CONF-890437-11) Avail: NTIS HC A03/MF A01

Stainless steel is the most versatile, corrosion-resistant alloy for engineering structures. Applications encompass a wide range of temperatures from cryogenic to elevated and stainless steels are used in various industries including power production, chemical and petrochemical, food processing, dairy and waste handling/processing. In each case, resistance to general corrosion in aggressive environmental conditions justifies its selection. Unfortunately, like most metal systems which form passive films for corrosion resistance, stainless steels are susceptible to localized attack under certain environmental conditions. The primary forms of this localized attack are pitting, intergranular (IG) corrosion and stress corrosion cracking (SCC). Sensitization is often directly responsible for the latter two and can also have an effect on pit initiation. The present work reviews the basic approach to model sensitization (chromium depletion) development in unstabilized, austenitic stainless steels. A theoretically-based, empirically-modified model is presented to quantitatively predict material degree of sensitization (DOS). Individual model components are discussed and compared to experimental results. Finally, overall model predictions are assessed relative to a large

sensitization data base. More detailed information concerning this data base and model evolution has been reported elsewhere.
DOE

N89-25318# National Inst. of Standards and Technology, Gaithersburg, MD. Metallurgy Div.
ELEVATED TEMPERATURE DEFORMATION OF STRUCTURAL STEEL
B. A. Fields and R. J. Fields Dec. 1988 121 p Sponsored by American Iron and Steel Inst., Washington, DC
(PB89-172621; NISTIR-88/3899) Avail: NTIS HC A06/MF A01 CSCL 11F

The results of tensile and creep tests on steels close to the American specification for ASTM A36 were used to formulate an equation from which elastic, plastic, creep and total strains can be calculated. Correlations between measured and predicted strains for Australian AS A149 and Japanese SS41 steels, both close to the A36 specification, are shown and good agreement is found. The above mentioned equation is also used to construct deformation mechanism (i.e., elastic, plastic, or creep) maps for times of 2 minutes to 4 hours at temperature. From these maps the deformation mechanisms operating at a given temperature and stress can be seen. The dominant mechanism for each set of conditions is given. In addition, the maps show contours of total strain values 1, 2, and 5 percent. Author

N89-25319# Pacific Northwest Labs., Richland, WA.
PRECIPITATION AT GRAIN BOUNDARIES IN IRRADIATED AUSTENITIC Fe-Cr-Mn ALLOYS
J. M. McCarthy Apr. 1989 8 p Presented at the Spring Meeting of the Materials Research Society, San Diego, CA, 25 Apr. 1989
(Contract DE-AC06-76RL-01830)
(DE89-011207; PNL-SA-16254; CONF-890426-5) Avail: NTIS HC A02/MF A01

In previous work, the phase stability of Fe-Cr-Mn alloys during irradiation was investigated in a study that included simple binaries, simple ternaries and commercially produced alloys. These low activation alloys are being considered for fusion reactor service in the first wall and in other structural applications subject to high neutron doses. In addition to phase instabilities observed within the grains, grain boundaries were susceptible to varying levels of precipitation dependent upon alloy composition, displacement dose and irradiation temperature. This paper describes the grain boundary microstructures that developed in these Fe-Cr-Mn alloys during irradiation. DOE

N89-25320# Pacific Northwest Labs., Richland, WA.
MODELING GRAIN BOUNDARY MICROCHEMISTRY RELATED TO IASCC (IRRADIATION-ASSISTED STRESS CORROSION CRACKING)
E. P. Simonen and R. H. Jones Apr. 1989 18 p Presented at the Corrosion '89, New Orleans, LA, 20 Apr. 1989
(Contract DE-AC06-76RL-01830)
(DE89-011214; PNL-SA-16474; CONF-890437-12) Avail: NTIS HC A03/MF A01

Radiation effects on grain boundary and near grain boundary microchemistries are modeled and compared to measured radiation effects. Nonequilibrium diffusion mechanisms are shown to be consistent with measured phosphorus impurity segregation and measured chromium depletion resulting from irradiation. Radiation enhanced equilibrium segregation (impurity enrichment) and radiation enhanced chromium depletion (sensitization) kinetics are predicted to be sufficient to promote equilibrium effects but measurements do not confirm the radiation enhanced mechanisms. Likely causes for the discrepancy are solute trapping and precipitation effects in the matrix promoted by irradiation. Ion and neutron irradiation of austenitic steels are evaluated relative to causes for irradiation-assisted stress corrosion cracking. DOE

N89-25321# Oregon Graduate Center for Study and Research, Beaverton.
DEFORMATION INDUCED MICROSTRUCTURAL AND MICROCHEMICAL CHANGES DURING THERMOMECHANICAL TREATMENT Annual Progress Report, 1 Oct. 1987 - 30 Sep. 1988
D. G. Atteridge, S. M. Bruemmer, L. E. Murr, W. E. Wood, A. Advani, A. Bagchi, C. Cedeno, L. A. Charlot (Pacific Northwest Labs., Richland, WA.), and L. J. Venne 1988 130 p
(Contract DE-AC06-86NE-37963)
(DE89-011608; DOE/NE-37963/9) Avail: NTIS HC A07/MF A01

Considerable activity has been focused in recent years on the structure and behavior of grain boundaries. Most of this activity has centered on atomistic aspects and has not enabled direct interpolation of results toward mechanical properties in engineering materials. As a result, significant developments in basic understanding of grain boundary structure have not significantly impacted engineering practice. Topics covered in this report are: thermomechanical effects on grain boundary microstructure, thermomechanical effects on grain boundary microchemistry, processing and fabrication characterizing, and integration and modeling. DOE

N89-25322# California Univ., Berkeley. Dept. of Material Science and Mineral Engineering.
THE STRENGTH-TOUGHNESS RELATIONSHIP AT CRYOGENIC TEMPERATURES IN ALUMINUM-LITHIUM ALLOY PLATE
J. Glazer and J. W. Morris, Jr. Mar. 1989 16 p Presented at the 5th International Aluminum-Lithium Conference, Williamsburg, VA, 28-31 Mar. 1989 Prepared in cooperation with California Univ., Be rkeley. Lawrence Berkeley Lab. Sponsored in part by AT and T Bell Telephone Labs. Submitted for publication
(Contract DE-AC03-76SF-00098)
(DE89-011816; LBL-26653; CONF-8903109-3) Avail: NTIS HC A03/MF A01

Both 2090-T81 and 2091-T8 plate display increasing strength fracture toughness and elongation with decreasing test temperature for some low temperature regimes, test orientations and tempers. The relation between these properties and the fracture behavior is explored in this study in an attempt to elucidate the source of the increase in toughness observed at low temperature. Various alternate mechanisms are explored, including the influences of crack-dividing intergranular splitting and increased plastic deformation on the work of fracture. It is concluded that when the primary fracture mode is unchanged, the best correlation with experiment is achieved by relating the toughness and the deformation properties of the material. DOE

N89-25323# Sandia National Labs., Albuquerque, NM. Mechanical Metallurgy Div.
J(SUB Ic) FRACTURE TOUGHNESS OF FERRITIC DCI (DUCTILE CAST IRON) ALLOYS: A COMPARISON OF TWO VERSIONS OF ASTM E 813
R. Salzbrenner May 1989 24 p
(Contract DE-AC04-76DP-00789)
(DE89-012249; SAND-89-0818) Avail: NTIS HC A03/MF A01

The fracture toughness of several ductile cast iron (DCI) alloys has been calculated according to two versions of the ASTM Standard covering the determination of J(sub Ic). The original version (ASTM E 813-81) had previously been used to establish the relationship between ferritic DCI alloys and the graphite nodule spacing. The J(sub Ic) values were recalculated by the methods of the revised version of the ASTM Standard (ASME 813-87), and were found to be 5 to 8 percent higher than those determined by the original standard. A linear regression analysis was used to reaffirm that the fracture toughness is directly related to the graphite nodule size or spacing. DOE

N89-25324# Sandia National Labs., Albuquerque, NM.
DYNAMIC FRACTURE TOUGHNESS MEASUREMENTS OF FERRITIC DUCTILE CAST IRON

R. Salzbrenner and K. B. Sorenson 1989 16 p Presented at the International Symposium on Packaging and Transporting of Radioactive Materials, Washington, DC, 11 Jun. 1989
(Contract DE-AC04-76DP-00789)
(DE89-009833; SAND-88-2287C; CONF-890631-2) Avail: NTIS HC A03/MF A01

Fracture toughness testing of ductile cast iron (DCI) at elevated loading rates has been performed at Sandia. The intent of the test program was to generate rigorously measured dynamic fracture toughness data in order to enhance the DCI material property data base and to evaluate the effect of rate on the upper-shelf fracture toughness. The test requirements outlined in the ASTM Standard Test Method for J(sub Ic), A Measure of Fracture Toughness (E 813-87) were adapted to elevated loading rates in a manner which allowed the inherent rigor of this test method to be maintained. The actual measurements were performed on compact tension specimens using a closed-loop servo-hydraulic test frame with special fixturing to enhance test control. The DCI alloy examined was a high quality casting of the type used in European-produced casks (i.e., it had a fully ferritic matrix, with only Type I and II graphite nodules). The test results show that there is essentially no effect of loading rate on the upper-shelf fracture toughness over the range tested. The current results are in contrast to other reports which suggest that there is a decrease in the upper-shelf toughness as the loading rate is raised above a certain level. DOE

N89-25325# Netherlands Energy Research Foundation, Petten.
EFFECT OF LOW NEUTRON FLUENCES ON DIN 1.4948 STEEL CREEP PROPERTIES
B. vanderSchaaf Apr. 1988 75 p
(ECN-206; ETN-89-94247) Avail: NTIS HC A04/MF A01

Three heats of DIN 1.4948 were irradiated to helium contents in the range from 0.2 appb to 20 appm at 325 and 823 K. Post-irradiation creep tests at 823 K with stresses from 150 to 300 MPa indicate decreasing rupture times and increasing secondary creep rates and reductions in secondary and tertiary creep strains. Embrittlement results in decreasing creep strength with increasing helium content. Helium filled cavities on grain boundaries are not observed. A failure mechanism based on helium promoted wedge crack nucleation and propagation is proposed. From the mechanism a relation between the helium content and the Monkman Grant product of secondary creep rate and rupture time is derived. There is an acceptable fit between the relation and data points. The results are supported qualitatively by optical and scanning electron microscopy. With increasing helium content the Monkman Grant product decreases considerably. The observed reduction in creep strength nd ductility related to helium content can be used for the development of design rules for permanent components near LMFBR's. The effect of irradiation temperature and test creep stress have a minor influence on the observed embrittlement. ESA

N89-25326# Technische Univ., Eindhoven (Netherlands).
RELATION OF THE ADHESION OF PLASMA SPRAYED COATINGS TO THE PROCESS PARAMETERS: SIZE, VELOCITY AND HEAT CONTENT OF THE SPRAY PARTICLES Ph.D. Thesis
Johan Martin Houben 1988 234 p
(ETN-89-94296) Avail: NTIS HC A11/MF A01

The heat exchange of a spray particle with the substrate during solidification is specified on the basis of heat conduction theory. For Mo on steel, the heat exchange is related with possible material transport across the contact interface. A theory on the mechanical and thermodynamical collision phenomena which spray particles undergo during the acceleration at the substrate surface is developed. The theory is based on the application of the Murnaghan equation of state and the entropic equations and pressure-volume relations. The theory permits the determination of the relationship between the Hugoniot pressure and the temperature during the impact compression of the spray particle material. The morphology of spread particles was determined experimentally as a function of their velocity and the heat content, while the size range was restricted to a certain sieve fraction. Four different types of spread particles are identified: incompletely deformed pancakes with a loose rim, flat firmly bound pancakes, pancakes with a loose double layered rim and a flower type deposit. The intrinsic strengths of the found morphologies were measured. Diffusion bound pancakes appear to be superior to other geometries. ESA

N89-25327# GKSS-Forschungszentrum Geesthacht (Germany, F.R.). Inst. fuer Werkstofforschung.
INTERMETALLIC ALLOYS: DEFORMATION, MECHANICAL AND FRACTURE BEHAVIOR
B. Dogan 1988 35 p
(GKSS-88/E/53; ISSN-0344-9629; ETN-89-94589) Copyright Avail: NTIS HC A03/MF A01

A high potential of development is attributed to the intermetallic alloys because of the unique properties they possess. These are a high specific modulus, especially at elevated temperature, high strength at high temperatures, high strain hardening rates, and low self-diffusion rates that lead to low creep rates and high recrystallization temperatures. Considerable efforts are being devoted to materials development on the basis of potential alloys such as TiAl, Ti3Al, Ni3Al, FeAl, CoAl, Zr3Al and (Fe, Co, Ni)3V. Much of the progress is in improving tensile strength and ductility on unnotched bars tested under laboratory conditions on small heats. There is still much to do in order that intermetallic alloys find practical applications at high temperatures. For example, there is no common basis for understanding the anomalous temperature dependence of the strength of many intermetallics. Hot corrosion resistance under gas turbine operating conditions of intermetallics requires clarification. Although limited work on the crack growth behavior of rather ductile Ni3Al and (Fe, Ni)3V LRO alloys shows slow growth rates at low delta K, a brittle Fe3Al alloy behaves similarly to conventional alloys. ESA

N89-25328# Kernforschungszentrum G.m.b.H., Karlsruhe (Germany, F.R.). Inst. fuer Material- und Festkoerperforschung.
THE CREEP AND CREEP-RUPTURE BEHAVIOR OF VANADIUM-BASE ALLOYS
M. Schirra Jan. 1989 202 p In GERMAN; ENGLISH summary
(KfK-2440; ISSN-0303-4003; ETN-89-94590) Copyright Avail: NTIS HC A10/MF A01

Vanadium base alloys as potential cladding material for Fast Breeder Reactor fuel elements are studied. Creep and creep rupture behavior are compared. In the temperature range 650 to 875 C the strength behavior up to 43,000 hr and the creep constants were determined. Influence of the titanium content, the strong matrix-hardening effect of the niobium, and the interaction between titanium and the interstitial impurities were established. Oxygen content improves greatly the creep and creep-rupture behavior, both in pure vanadium and in alloys with titanium and silicon. In the case of the V-Ti- and V-Ti-Nb-alloys the contrary behavior of the tensile strength and long-time strength is demonstrated. While the tensile strength increases strongly with increasing Ti-content, the creep rupture strength decreases and the best values of creep rupture strength are obtained with alloys of 1 to 3 percent titanium. ESA

N89-25329# Kernforschungszentrum G.m.b.H., Karlsruhe (Germany, F.R.). Inst. fuer Material- und Festkoerperforschung.
APPLICABILITY OF MICROALLOYING IN THE PRODUCTION OF SINTERED STEEL STRUCTURAL PARTS Thesis - Karlsruhe Univ.
R. Oberacker Dec. 1988 172 p In GERMAN; ENGLISH summary
(KfK-4481; ISSN-0303-4003; ETN-89-94592) Copyright Avail: NTIS HC A08/MF A01

Adaptability of microalloying elements like boron, niobium, and vanadium to steel powder metallurgy is studied. Boron densification effects on full dense structural parts manufacture is studied. Experimental results of densification kinetics, microstructure, and mechanical properties of binary Fe-B compacts are indicated. Brittle

behavior of resulting material is observed due to the formation of a continuous eutectic network during solidification of the liquid phase. Introduction of niobium and vanadium as alloying elements is enhanced by their oxygen affinity and the necessity of their homogeneous distribution. Theoretical considerations on homogenization behavior and the properties of materials produced by powder mixture route indicate that niobium can be introduced in this way. Water atomization results in oxidation of both elements. By inert gas atomization followed by annealing a suitable niobium prealloyed powder can be produced. ESA

N89-25330# Kernforschungsanlage, Juelich (Germany, F.R.). Inst. fuer Festkoerperforschung.
INFLUENCE OF THE HELIUM ON HIGH TEMPERATURE EMBRITTLEMENT OF METALS UNDER CYCLIC LOADING [DER EINFLUSS VON HELIUM AUF DIE HOCHTEMPERATURVERSPROEDUNG VON METALLEN UNTER ZYKLISCHER BELASTUNG]
Joachim Wolfgang Leeser Aug. 1988 88 p In GERMAN; ENGLISH summary
(JUEL-2229; ISSN-0366-0885; ETN-89-94595) Avail: NTIS HC A05/MF A01

High temperature embrittlement produced by helium is studied for controlling phenomena in first wall and blanket structural materials of fusion devices. Fatigue tests on AISI 316 and 8206 steels are performed. Helium generation is simulated by preimplantation at a cyclotron. The fatigue tests are carried out in the reversed bending mode in high vacuum with 100 micron thick foil specimens containing up to 1500 appm helium. The number of cycles to failure of He-implanted specimens in the temperature regime of 750 to 1000 K can be much lower than of He-free reference specimens. In this case the fracture mode changes from transgranular to intergranular. The influence of helium depends on fatigue frequency. Metal-carbide precipitates lessen the embrittlement effect of helium. Microstructure investigations show that the growth of helium bubbles in grain boundaries is the reason for the embrittlement. A theoretical model predicts a frequency dependent critical radius of helium bubbles, thus determining the life time of the implanted specimens. ESA

N89-25331# Technische Univ., Eindhoven (Netherlands). Measurement and Control Group.
MODEL BUILDING FOR AN INGOT HEATING PROCESS: PHYSICAL MODELING APPROACH AND IDENTIFICATION APPROACH
Wen-Jiang Liu, Yu-Cai Zhu, and Da-Wei Cai (Xian Jiaotong Univ., China) Jun. 1988 31 p Sponsored by the Netherlands Ministry of Education and Science
(EUT-88-E-196; ISBN-90-614-4196-X; ISSN-0167-9708; ETN-89-94784) Avail: NTIS HC A03/MF A01

The model building for steel ingot thermal behavior is considered. The variables taken into account are the furnace temperature and the ingot central core temperature, and sometimes the surface temperature. The purpose is to build a simple dynamical model in order to predict the central temperature. The physical modeling is performed using heat transmission theory. Black-box identification is used to determine models based on the experimental data. Experimental test data are used to examine the qualities of models from both methods. The two methods are compared. The steel ingot heating model obtained by system identification gives better estimation of the characteristics and higher precision than model-building using physical laws. The advantage of model-building from physics is that it gives insight; also the different parameters and variables have physical interpretations. But it may be difficult and time consuming to build the model from first principles. ESA

27 NONMETALLIC MATERIALS

Includes physical, chemical, and mechanical properties of plastics, elastomers, lubricants, polymers, textiles, adhesives, and ceramic materials.

For composite materials see *24 Composite Materials*.

N89-25332*# National Aeronautics and Space Administration. Langley Research Center, Hampton, VA.
ABSORBED DOSE THRESHOLDS AND ABSORBED DOSE RATE LIMITATIONS FOR STUDIES OF ELECTRON RADIATION EFFECTS ON POLYETHERIMIDES
Edward R. Long, Jr., Sheila Ann T. Long, Stephanie L. Gray, and William D. Collins (Old Dominion Univ., Norfolk, VA.) Washington Aug. 1989 22 p
(NASA-TP-2928; L-16585; NAS 1.60:2928) Avail: NTIS HC A03/MF A01 CSCL 11C

The threshold values of total absorbed dose for causing changes in tensile properties of a polyetherimide film and the limitations of the absorbed dose rate for accelerated-exposure evaluation of the effects of electron radiation in geosynchronous orbit were studied. Total absorbed doses from 1 kGy to 100 MGy and absorbed dose rates from 0.01 MGy/hr to 100 MGy/hr were investigated, where 1 Gy equals 100 rads. Total doses less than 2.5 MGy did not significantly change the tensile properties of the film whereas doses higher than 2.5 MGy significantly reduced elongation-to-failure. There was no measurable effect of the dose rate on the tensile properties for accelerated electron exposures. Author

N89-25333# Oak Ridge National Lab., TN. Solid State Div.
THE APPLICATION OF RUTHERFORD BACKSCATTERING AND CHANNELING TECHNIQUES TO THE CHARACTERIZATION OF CERAMICS
L. A. Boatner and C. W. White Mar. 1989 16 p Presented at the 41st Pacific Coast Regional Meeting of American Ceramic Society, San Francisco, CA, 24 Oct. 1988
(Contract DE-AC05-84OR-21400)
(DE89-010257; CONF-8810195-8) Avail: NTIS HC A03/MF A01

Rutherford Backscattering Spectroscopy (RBS) is a versatile and powerful technique for investigating the near-surface properties of polycrystalline ceramics, glasses, and single-crystals. In the case of macroscopic single-crystal samples, the variant of RBS known as channeling spectroscopy can be used to obtain detailed information regarding the near-surface structural, impurity, and defect characteristics of ceramic materials. DOE

N89-25334*# National Aeronautics and Space Administration. Langley Research Center, Hampton, VA.
SEMIINTERPENETRATING POLYMER NETWORK FOR TOUGHER AND MORE MICROCRACKING RESISTANT HIGH TEMPERATURE POLYMERS Patent Application
Ruth H. Pater, inventor (to NASA) 26 Jan. 1989 26 p
(NASA-Case-LAR-13925-1; NAS 1.71:LAR-13925-1; US-Patent-Appl-SN-301925) Avail: NTIS HC A03/MF A01 CSCL 11B

This invention is a semi-interpenetrating polymer network which includes a high performance thermosetting polyimide having a nadic end group acting as a crosslinking site and a high performance linear thermoplastic polyimide. Provided is an improved high temperature matrix resin which is capable of performing at 316 C in air for several hundreds of hours. This resin has significantly improved toughness and microcracking resistance, excellent processability and mechanical performance, and cost effectiveness. NASA

N89-25335# Sandia National Labs., Albuquerque, NM.
STUDIES OF OXIDATIVE DEGRADATION OF POLYMERS INDUCED BY IONIZING RADIATION
Roger L. Clough and K. T. Gillen 1989 26 p Presented at the 11th International Conference on Stabilization and Controlled Degradation of Polymers, Lucerne, Switzerland, 24 May 1989

(Contract DE-AC04-76DP-00789)
(DE89-008279; SAND-89-0449C; CONF-8905113-1) Avail: NTIS HC A03/MF A01

Radiation effects on polymers in the presence of air are characterized by complicated phenomena such as dose-rate effects and post-irradiation degradation. These time-dependent effects can be understood in these terms: (1) features of the free radical chain-reaction chemistry underlying the oxidation, and (2) oxygen diffusion effects. A profiling technique has been developed to study heterogeneous degradation resulting from oxygen diffusion, and kinetic schemes have been developed to allow long-term aging predictions from short-term high dose-rate experiments. Low molecular weight additives which act either as free-radical scavengers or else as energy-scavengers are effective as stabilizers in radiation-oxidation environments. Non-radical oxidation mechanisms, involving species such as ozone, can also be important in the radiation-oxidation of polymers. DOE

N89-25336# Sandia National Labs., Albuquerque, NM.
PARAMETER ESTIMATION FOR A VISCOELASTIC CONSTITUTIVE MODEL
J. D. Rogers and S. B. Skaar 1988 7 p Presented at the SEM Spring Meeting, Cambridge, MA, 28 May 1989
(Contract DE-AC04-76DP-00789)
(DE89-008714; SAND-88-2447C; CONF-8905107-2) Avail: NTIS HC A02

A four viscoelastic material model has been incorporated into a well-defined vibration test. The model includes as a parameter the order of the time derivations of stress and strain. Values of the parameters were obtained for aluminum and plexiglas beam specimens. DOE

N89-25337# Oak Ridge National Lab., TN. Metals and Ceramics Div.
THE MECHANICAL PROPERTIES OF ION IMPLANTED CERAMICS
Carl J. McHargue 1988 21 p Presented at the NATO Advanced Study Institute on Structure-Property Relationships in Ion-Beam Surface-Modified Ceramics: Theory and Applications, Ciocco, Italy, 28 Aug. 1988
(Contract DE-AC05-84OR-21400)
(DE89-008928; CONF-8808108-6) Avail: NTIS HC A03/MF A01

The surface mechanical properties of ceramics are altered by ion implantation. The alteration results from the microstructural changes and the residual stresses produced in the implanted zone. Because of difficulties associated with accurate property determination of thin layers, data published to date are generally qualitative in nature and indicate only the direction of the changes. Implantation conditions which give a damaged but crystalline layer cause increase in hardness, fracture toughness, and flexural strength. The mechanisms responsible appear to involve both defect- and solid-solution strengthening, and the residual compressive stress. Topics covered in this paper are: Fracture toughness, tribological properties, transverse rupture strength, hardness, elastic modulus and residual stresses of ceramics. DOE

N89-25338# Bell Telephone Labs., Inc., Princeton, NJ.
POLED POLYMER FILMS FOR NONLINEAR OPTICS
Kenneth D. Singer, Mark G. Kuzyk, W. Robert Holland, and Paul A. Cahill (Sandia National Labs., Albuquerque, NM.) 1989 8 p Presented at the Meeting of the Association for Progress of New Chemistry (MITI), Chiba, Japan, 8 May 1989
(Contract DE-AC04-76DP-00789)
(DE89-010039; SAND-89-0846C; CONF-8905117-1) Avail: NTIS HC A02/MF A01

Second harmonic generation was measured for a thin corona-poled film of a dicyanovinyl azo dye incorporated in the side-chain methacrylate polymer. Measurements were performed at a wavelength of 1.58 micrometers as a function of incident angle for both p- and s-polarized incident light. From these measurements the form and magnitude of the second harmonic coefficient tensor were determined. The molecular distribution implied by the data is consistent with a thermodynamic potential containing only the dipolar orienting energy acting during poling. We have also demonstrated anomalous-dispersion phase-matched second harmonic generation for the first time using electric field induced second harmonic generation (EFISH) in a liquid solution of Foron Brilliant Blue S-R (FBB). Results are described. DOE

N89-25339# Oak Ridge National Lab., TN.
EVALUATION OF CERAMIC COATINGS ON SILICON CARBIDE
J. I. Federer, M. vanRoode, and J. R. Price (Solar Turbines, Inc. San Diego, CA.) 1989 32 p Presented at the 16th International Conference on Metallurgical Coatings and Equipment Exhibit, San Diego, CA, 17 Apr. 1989
(Contract DE-AC05-84OR-21400)
(DE89-010321; CONF-890468-6) Avail: NTIS HC A03/MF A01

Ten ceramic coatings were plasma sprayed onto a sintered alpha silicon carbide (SiC) tube to determine if the coatings would protect SiC from high-temperature corrosion. Several coatings consisted of mullite or mullite-zircon. Others had base layers of mullite or mullite-zircon, transition layers with increasing amounts of alumina (Al2O3), zirconia (ZrO2), or yttria (Y2O3), and outer layers of these last three oxides. Mullite and mullite-zircon coatings, which have coefficients of thermal expansion (CTE) near that of SiC, survived 60 thermal cycles between 300 and 1300 C without apparent damage. Coatings have Al2O3 and Y2O3 layer cracked, while those with ZrO2 layers cracked and spalled. Survivors were corrosion tested at 1200 C in an oxidizing atmosphere containing Na2CO3, which corroded uncoated SiC at a rate of approx. 21 mm/y. The coatings protected SiC for up to 500 h, but degraded because the atmosphere penetrated and reacted with the coatings and SiC to produce a disruptive silicate reaction product. Denser coatings are needed for extended protection. DOE

N89-25340# Southwest Research Inst., San Antonio, TX.
TRANSIENT EFFECTS IN CREEP CAVITY NUCLEATION AND EARLY GROWTH IN CERAMICS
R. A. Page and K. S. Chan 1989 9 p Presented at the 7th International Conference on Fracture, Houston, TX, 20 Mar. 1989
(Contract DE-FG05-84ER-45063)
(DE89-010420; CONF-890310-5) Avail: NTIS HC A02

Creep fracture of ceramic materials frequently occurs by the nucleation, growth, and coalescence of grain boundary cavities. Results of recent experimental studies of cavitation kinetics in compression crept ceramics are presented to illustrate the transient nature of cavity nucleation and early growth. The transient character of cavitation arises primarily due to the dependence of both cavity nucleation and early cavity growth on the stochastic process of grain boundary sliding. Possible mechanisms for the observed transient behavior will be presented and implications discussed. DOE

N89-25341# California Univ., Berkeley. Lawrence Berkeley Lab. Materials and Chemical Sciences Div.
HIGH RESOLUTION ELECTRON MICROSCOPY AND MICROANALYSIS OF FERRITES AND CUPRATES
Gareth Thomas Nov. 1988 20 p Presented at the 5th International Conference on Ferrites, Bombay, India, 10 Jan. 1989
(Contract DE-AC03-76SF-00098)
(DE89-010441; LBL-26622; CONF-890190-1) Avail: NTIS HC A03/MF A01

Ceramics in general have similar problems in processing to achieve the desired purity of composition, microstructures, morphology and properties, and hence the inter-relationships between these factors are of great concern for materials scientists and engineers. Defects such as intergranular phases are common to many ceramic systems. DOE

N89-25342# Sandia National Labs., Albuquerque, NM. Shock Wave and Structural Physics Div.
TECHNIQUE AND DATA ANALYSIS FOR IMPACT-LOADED PIEZOELECTRIC POLYMERS (PVDF)

M. U. Anderson and D. E. Wackerbarth Sep. 1988 71 p
(Contract DE-AC04-76DP-00789)
(DE89-010529; SAND-88-2327) Avail: NTIS HC A04/MF A01

A standardized piezoelectric polymer (PVDF) shock-wave stress gauge has been developed in cooperation between Sandia and the Institute Saint Louis, France. The shock response of these gauges is established from controlled shock-loading experiments in which impact-induced current pulses are measured with high speed digitizers. This report documents the preparation and assembly of PVDF gauges to be used in these controlled shock-loading experiments, and a computer program PVDF-AUTO written for analysis of the data obtained in such experiments. Due to digitizer noise before and after actual gauge output, it is often difficult to distinguish the data points at which the loading pulse begins, ends, and the unloading pulse arrives. It is the purpose of this data analysis program to identify these points in an objective manner that is mathematically documented and free from human judgement, thus analyzing data consistently regardless of experimental conditions. DOE

N89-25343# California Univ., Berkeley. Dept. of Materials Science and Mineral Engineering.
CRYOGENIC MECHANICAL PROPERTIES OF LOW DENSITY SUPERPLASTICALLY FORMABLE Al-Li ALLOYS
S. L. Verzasconi and J. W. Morris, Jr. Mar. 1989 18 p Presented at the 5th International Aluminum-Lithium Conference, Williamsburg, VA, 28 Mar. 1989 Prepared in cooperation with California Univ., Berkeley. Lawrence Berkeley Lab.
(Contract DE-AC03-76SF-00098)
(DE89-010587; LBL-26652; CONF-8903109-2) Avail: NTIS HC A03/MF A01

The aerospace industry is considering the use of low density, superplastically formable (SPF) materials, such as Al-Li alloys in cryogenic tankage. SPF modifications of alloys 8090, 2090, and 2090 + In were tested for strength and Kahn tear toughness. The results were compared to those of similar tests of 2219-T87, an alloy currently used in cryogenic tankage, and 2090-T81, a recently studied Al-Li alloy with exceptional cryogenic properties. With decreasing temperature, all materials showed an increase in strength, while most materials showed an increase in elongation and decrease in Kahn toughness. The indium addition to 2090 increased alloy strength, but did not improve the strength-toughness combination. The fracture mode was predominantly intergranular along small, recrystallized grains, with some transgranular fracture, some ductile rupture, and some delamination on large, unrecrystallized grains. DOE

N89-25344# Lawrence Livermore National Lab., CA.
METHOD OF PROTECTING SURFACES FROM ABRASION AND ABRASION RESISTANT ARTICLES OF MANUFACTURE Patent Application
Tomas B. Hirschfeld, inventor (to DOE) Jun. 1988 32 p
(Contract W-7405-eng-48)
(DE89-010798; PATENTS-US-A7204432;
US-Patent-Appl-SN-204432) Avail: NTIS HC A03/MF A01

Surfaces of fabricated structures are protected from damage by impacting particulates by a coating of hard material formed as a mass of thin flexible filaments having root ends secured to the surface and free portions which can flex and overlap to form a resilient cushioning mat which resembles hair or fur. The filamentary coating covers the underlying surface with hard abrasion resistance material while also being compliant and capable of local accommodation to particle impacts. The coating can also function as thermal and/or acoustical insulation and has a friction reducing effect. DOE

N89-25345# Sandia National Labs., Albuquerque, NM.
LOW DENSITY MICROCELLULAR CARBON FOAMS AND METHOD OF PREPARATION Patent Application
Charles Arnold, Jr., inventor (to DOE), James H. Aubert, inventor (to DOE), Roger L. Clough, inventor (to DOE), Peter P. Rand, inventor (to DOE), and Alan P. Sylwester, inventor (to DOE) 20 Jun. 1988 17 p
(Contract DE-AC04-76DP-00789)
(DE89-010966; PATENTS-US-A7209168;
US-Patent-Appl-SN-209168) Avail: NTIS HC A03

A low density, open-celled microcellular carbon foam is disclosed which is prepared by dissolving a carbonizable polymer or copolymer in a solvent, pouring the solution into a mold, cooling the solution, removing the solvent, and then carbonizing the polymer or copolymer in a high temperature oven to produce the foam. If desired, an additive can be introduced in order to produce a doped carbon foam, and the foams can be made isotropic by selection of a suitable solvent. The low density, microcellular foams produced by this process are particularly useful in the fabrication of inertial confinement fusion targets, but can also be used as catalysts, absorbents, and electrodes. DOE

N89-25346# Illinois Univ., Urbana-Champaign.
MOLECULAR GROWTH PATHWAYS IN SILICA SOL-GEL POLYMERIZATION Ph.D. Thesis
Sangeeta Dikshit Ramamurthi (Indian Inst. of Tech., Kanpur.) 1989 188 p
(Contract DE-AC02-76ER-01198)
(DE89-011224; DOE/ER-01198/T36) Avail: NTIS HC A09/MF A01

An analytical protocol involving gas chromatography (GC), gas chromatography-mass spectrometry (GCMS), and Si-29(H-1) NMR spectroscopy, was developed to determine the structures of the polysilicate intermediates formed during silica sol-gel polymerization. This protocol allowed the structural identification of mono- through hexasilicate species (1 is less than or equal to x less than or equal to 6 in (Si(x)O(y)(OCH3)sub a) formed during partial hydrolysis and condensation of tetramethylorthosilicate. The analytical protocol employing capillary gas chromatography was applied to monitor the stoichiometry, structures, and abundances of low molecular weight polysilcates (1 is less than or equal to x less than or equal to 6 in (Si(x)O(y)(OCH3)sub a) formed during partial hydrolysis of methanolic tetramethylorthosilicate under acidic (HCl) and basic (KOH) conditions. The same procedure was applied to study the redistributions of methanolic hexamethyldisilicate and octamethyltrisilicate under similar reaction conditions. The polysilicate molecular weight distributions (expressed in terms of mole percent of total silicon present) were determined as a function of the degree of polymerization. DOE

N89-25347# Los Alamos National Lab., NM. Theoretical Lab.
SUPER-STRONG SELF-REINFORCING POLYMERIC MATRICES FORMED BY THE FIRST SUPER-STRONG POLYMERS
F. Dowell 1989 7 p Presented at the Industry-University Advanced Materials Conference, Denver, CO, 6 Mar. 1989
(Contract W-7405-eng-36)
(DE89-011533; LA-UR-89-1224; CONF-890306-2) Avail: NTIS HC A02/MF A01

The design of super-strong (SS) polymers to form the first SS self-reinforcing polymeric matrices is described. Solidified SS liquid-crystalline polymers (LCPs) are designed to be the first polymers to have good compressive strengths, as well as to have tensile strengths and tensile moduli significantly greater than existing strong LCPs (i.e., backbone LCPs, such as Kevlar). (These SS LCPs have also been designed with certain features to give good solubilities and processabilities. DOE

28 PROPELLANTS AND FUELS

Includes rocket propellants, igniters, and oxidizers; their storage and handling procedures; and aircraft fuels.

For related information see also *07 Aircraft Propulsion and Power, 20 Spacecraft Propulsion and Power,* and *44 Energy Production and Conversion.*

N89-25348# Department of Energy, Morgantown, WV. Energy Technology Center.

METHOD OF PRODUCTION H2 USING A ROTATING DRUM REACTOR WITH A PULSE JET HEAT SOURCE Patent Application

Leland E. Paulson, inventor (to DOE) 13 May 1988 12 p
(DE89-009764; PATENTS-US-A7193704;
US-Patent-Appl-SN-193704) Avail: NTIS HC A03/MF A01

A method of producing hydrogen by an endothermic steam-carbon reaction using a rotating drum reactor and a pulse jet combustor is presented. The pulse jet combustor uses coal dust as a fuel to provide reaction temperatures of 1300 to 1400 F. Low-rank coal, water, limestone and catalyst are fed into the drum reactor where they are heated, tumbled and reacted. Part of the reaction product from the rotating drum reactor is hydrogen which can be utilized in suitable devices. DOE

N89-25349# Lawrence Livermore National Lab., CA.

HIGH-PERFORMANCE, EXTRUSION-CAST EXPLOSIVES WITH LOW SENSITIVITY Interim Report No. 2

K. J. Scribner, E. vonHoltz, and R. L. Simpson 10 Jan. 1989 40 p
(Contract W-7405-eng-48)
(DE89-010279; UCRL-53890) Avail: NTIS HC A03/MF A01

Lawrence Livermore National Laboratory (LLNL) has developed a class of explosives having both high performance for modern precision munitions and greater safety for reduced vulnerability of launch platforms (ships, planes, ammunition storage sites) to enemy fire or accidents. Known as extrusion-cast explosives (ECXs), they have demonstrated performance levels equivalent to the most powerful now available, but test results indicate they are far less sensitive than the conventional high-energy explosives. Specifically, in a sympathetic-detonation test, ECX that was immediately adjacent to a deliberately-detonated donor charge did not detonate in two of three tests, whereas Comp B did detonate sympathetically in this test. Also, this ECX provided performance equivalent to that of the high-performance explosive LX-14, when tested in the TOW (tube-launched, optically-sighted, wire-guided) missile. This report describes the performance, vulnerability, and processing (at this stage of development) of this class of explosives. DOE

N89-25350# Joint Inst. for Nuclear Research, Dubna (USSR). Scientifical-Methodical Div.

EXPLOSIVE CATHODE ON THE BASE OF CARBON-FIBROUS PLASTIC MATERIAL

S. A. Korenev, A. M. Baranov, S. V. Kostyuchenko, and N. M. Chernenko 1988 8 p In RUSSIAN; ENGLISH summary Submitted for publication
(DE88-706302; JINR-13-88-292) Avail: NTIS (US Sales Only) HC A02/MF A01

Production process of explosive cathodes on the base of carbon-fibrous plastic material of any geometric form and size is discussed. Experimental study of current take-off from cathodes with diameter 2 cm of 10 kV and 150 to 250 kV voltage are given. It is shown that ignition voltage of cathode plasma is 2 kV with 5 mm gap electrode of diode and 5 times 10 sup -5 torr pressure of residual gas. It is shown that carbon-fibrous cathode, made by this technology, provides more stable current take-off electron beam (without oscillations) in comparison with other cathodes. DOE

N89-25351# Los Alamos National Lab., NM.

HIGH EXPLOSIVES REACTION MODEL AND ITS APPLICATION TO BOOSTER PERFORMANCE

Pier K. Tang 1989 12 p Presented at the 3rd International Symposium on Behavior of Media Under High Dynamic Pressures, La Grande Motte, France, 5-9 Jun. 1989
(Contract W-7405-eng-36)
(DE89-005459; LA-UR-88-4130; CONF-890661-2) Avail: NTIS HC A03/MF A01

Initiation of insensitive high explosives requires a boosting system using more sensitive and usually more energetic explosives. However, problems arise if the booster material is too energetic. The initiability of some insensitive but less energetic high explosives can be enhanced by lowering the density and decreasing the grain size or by adding a sensitive component; thus these explosives can be used as booster materials. This paper presents a unified initiation and detonation reaction model and then the simulation of the development of the detonation wave in a PBX-9502 main charge using three booster explosives: low-density superfine TATB, low-density ultrafine TATB, and X-0407. The last two are found to be acceptable. DOE

N89-25352# Sandia National Labs., Albuquerque, NM.

CHARACTERIZATION OF BOOSTER-ROCKET PROPELLANTS AND THEIR SIMULANTS

L. J. Weirick 1989 10 p Presented at the JANNAF Propulsion Meeting, Cleveland, OH, 22 May 1989
(Contract DE-AC04-76DP-00789)
(DE89-012497; SAND-88-2813C; CONF-8905134-1) Avail: NTIS HC A02/MF A01

A series of experiments on a composite and an energetic propellant and their simulants were recently completed on a light-gas gun. The initial objectives were to obtain Hugoniot data, to investigate the pressure threshold at which a reaction occurs, and to measure spall damage at various impact velocities. The Hugoniot data measured for the propellants fit the Hugoniot curves provided by the manufacturer of the propellants extremely well and the Hugoniot curves developed for the simulants matched those of the propellants. Threshold pressures to initiate reactions in the composite and energetic propellants were found to be 40 and 3 kbars, respectively. In spall tests, the composite propellant and its simulant exhibited spall strengths around 0.25 and 0.18 kbar, respectively. The energetic propellant and its simulant were somewhat stronger with spall strengths just above 0.33 and 0.22 kbar. DOE

29 MATERIALS PROCESSING

Includes space-based development of products and processes for commercial applications.

For biological materials see *55 Space Biology.*

N89-25353*# Naval Research Lab., Washington, DC. Computational Physics and Fluid Dynamics Lab.

TIME-DEPENDENT COMPUTATIONAL STUDIES OF FLAMES IN MICROGRAVITY Final Report, 1985 Dec. - 1988 Dec.

Elaine S. Oran and K. Kailasanath Jun. 1989 111 p
(NASA Order C-80001-G)
(NASA-CR-182298; NAS 1.26:182298) Avail: NTIS HC A06/MF A01 CSCL 22A

The research performed at the Center for Reactive Flow and Dynamical Systems in the Laboratory for Computational Physics and Fluid Dynamics, at the Naval Research Laboratory, in support of the NASA Microgravity Science and Applications Program is described. The primary focus was on investigating fundamental questions concerning the propagation and extinction of premixed flames in Earth gravity and in microgravity environments. The approach was to use detailed time-dependent, multispecies, numerical models as tools to simulate flames in different gravity environments. The models include a detailed chemical kinetics mechanism consisting of elementary reactions among the eight reactive species involved in hydrogen combustion, coupled to algorithms for convection, thermal conduction, viscosity, molecular and thermal diffusion, and external forces. The external force, gravity, can be put in any direction relative to flame propagation and can have a range of values. A combination of one-dimensional and two-dimensional simulations was used to investigate the effects

of curvature and dilution on ignition and propagation of flames, to help resolve fundamental questions on the existence of flammability limits when there are no external losses or buoyancy forces in the system, to understand the mechanism leading to cellular instability, and to study the effects of gravity on the transition to cellular structure. A flame in a microgravity environment can be extinguished without external losses, and the mechanism leading to cellular structure is not preferential diffusion but a thermo-diffusive instability. The simulations have also lead to a better understanding of the interactions between buoyancy forces and the processes leading to thermo-diffusive instability. Author

31 ENGINEERING (GENERAL)

Includes vacuum technology; control engineering; display engineering; cryogenics; and fire prevention.

N89-25354*# National Aeronautics and Space Administration. Langley Research Center, Hampton, VA.
SENSITIVITY ANALYSIS OF COMPLEX COUPLED SYSTEMS EXTENDED TO SECOND AND HIGHER ORDER DERIVATIVES
Jaroslaw Sobieszczanski-Sobieski Apr. 1989 7 p
(NASA-TM-101587; NAS 1.15:101587) Avail: NTIS HC A02/MF A01 CSCL 13B

In design of engineering systems, the what if questions often arise such as: what will be the change of the aircraft payload, if the wing aspect ratio is incremented by 10 percent. Answers to such questions are commonly sought by incrementing the pertinent variable, and reevaluating the major disciplinary analyses involved. These analyses are contributed by engineering disciplines that are, usually, coupled, as are the aerodynamics, structures, and performance in the context of the question above. The what if questions can be answered precisely by computation of the derivatives. A method for calculation of the first derivatives has been developed previously. An algorithm is presented for calculation of the second and higher order derivatives. Author

N89-25355# Sandia National Labs., Albuquerque, NM.
THE DEVELOPMENT OF A VAPOR COMPRESSION REFRIGERATION SYSTEM FOR A NETWORK OF NINE TEMPERATURE TEST CHAMBERS
Robert Baca 1988 21 p Presented at the 35th Annual Technical Meeting of the Institute of Environmental Sciences: Building Tomorrow's Environment, Anaheim, CA, 1 May 1989
(Contract DE-AC04-76DP-00789)
(DE89-007084; SAND-88-2580C; CONF-890592-1) Avail: NTIS HC A03/MF A01

The thermal response of a component or system can be determined by exposure to a temperature environment simulated in a temperature chamber. The variation in both the size of the item under test and the desired temperature environment necessitates the need for test chambers with a range of capabilities. Most temperature chambers are equipped with a two-stage vapor compression refrigeration system and a heating system capable of simulating any temperature environment in the range of -65 C to 177 C. The refrigeration required to maintain a desired temperature level is a small fraction of the refrigeration required to lower the temperature in the chamber. Since most of the test time is spent maintaining a temperature level in the chamber, the refrigeration system is inherently inefficient and costly to operate. In order to increase the refrigeration system efficiency, a two-stage vapor compression refrigeration system has been developed to support nine temperature test chambers simultaneously. By networking chambers to a centralized refrigeration system, a larger percentage of the available refrigeration capacity is utilized. Moreover, each chamber can simulate a temperature environment which is independent of the other simulated temperature environments in the network. DOE

N89-25356# Oak Ridge National Lab., TN. Instrumentation and Controls Div.
ANALYSIS AND CONTROL OF A THREE-DEGREE-OF-FREEDOM ROBOT PLATFORM
J. F. Jansen and R. L. Kress 1989 11 p Presented at the 2nd International CIRP Conference on New Manufacturing Technology, Cookesville, TN, 1-2 Jun. 1989
(Contract DE-AC05-84OR-21400)
(DE89-006427; CONF-890676-1) Avail: NTIS HC A03/MF A01

This paper describes the analysis and design of a robot platform with two drive wheels, each with an independent steering mechanism resulting in three independent degrees of motion. The kinematic and inverse kinematic analyses are derived in detail. An adaptive controller is designed to compensate for large inertial variations and to satisfy the velocity (nonholonomic) constraints. DOE

N89-25357# Freie Univ., Berlin (Germany, F.R.). Tieftemperaturlab.
GIRL CRYOTECHNICS AND PREPARATION OF A TEXUS EXPERIMENT ON SUPERFLUID HELIUM DYNAMICS Final Report, 31 Oct. 1986
Hans-Dietrich Denner, Thomas Gradt, Gustav Klipping, Ingrid Klipping, Udo Ruppert, Zsolt Szuecs, and Harry Walter Nov. 1987 55 p In GERMAN; ENGLISH summary
(Contract BMFT-01-QV-AA/WF/WRK-0275/4-13)
(ETN-89-94631) Avail: NTIS HC A04/MF A01

Technological requirements for the handling of superfluid He2 at zero-g in the German infrared telescope GIRL (Refrigerated Infrared Laboratory) are analyzed. The separation of gas and liquid phase, temperature control, and heat transfer during the continuous evaporation of the coolant are studied. An active phase separator together with the necessary cryocomponents, displacement transducer, actuator, and penetration cables are developed. The system is tested under critical laboratory conditions and on zero-g flights under variation of the acceleration between 2g and 0g. By integrating different safety circuits the reliability of the system is achieved. ESA

N89-25358# Deutsche Forschungs- und Versuchsanstalt fuer Luft- und Raumfahrt, Stuttgart (Germany, F.R.). Structures and Materials Dept.
MATERIALS AND STRUCTURES FOR 2000 AND BEYOND: AN ATTEMPTED FORECAST
Carl-Jochen Winter and Martin Mailaender Feb. 1989 86 p In GERMAN; ENGLISH summary
(DFVLR-Mitt-89-02; ISSN-0176-7739; ETN-89-94648) Avail: NTIS HC A05/MF A01; DFVLR, VB-PL-DO, Postfach 90 60 58, 5000 Cologne, Federal Republic of Germany, 51 deutsche marks

Developments in aerospace materials and structures, and research needed to meet the challenges imposed by these developments were discussed. ESA

N89-25359# Technische Univ., Eindhoven (Netherlands). Faculty of Electrical Engineering.
AN EXTREMUM HUNTING METHOD USING PSEUDO-RANDOM BINARY SIGNAL
Wen-Jiang Liu Jul. 1988 16 p Sponsored by the Netherlands Ministry of Education and Science
(EUT-88-E-198; ISBN-9-06-144198-6; ISSN-0167-9708; ETN-89-94786) Avail: NTIS HC A03/MF A01

An extremum hunting method, using a correlation analysis hunting method, is proposed. A pseudo-random binary signal is used as probe signal and the hunting direction is judged by the cross-correlation function between input and output. The input is stirred up on variable mode so that the hunting speed is higher than with other methods, such as common step forward searching. High hunting precision and strong anti-interference ability are other advantages. ESA

N89-25148*# General Electric Co., Schenectady, NY.
INTEGRATED DESIGN OPTIMIZATION RESEARCH AND DEVELOPMENT IN AN INDUSTRIAL ENVIRONMENT

V. Kumar, Marjorie D. German, and S.-J. Lee *In* NASA. Langley Research Center, Recent Advances in Multidisciplinary Analysis and Optimization, Part 1 Apr. 1989 p 39-50 (For primary document see N89-25146 19-05)
Avail: NTIS HC A23/MF A01 CSCL 13B

N89-25149*# National Aeronautics and Space Administration. Langley Research Center, Hampton, VA.
OPTIMIZATION BY DECOMPOSITION: A STEP FROM HIERARCHIC TO NON-HIERARCHIC SYSTEMS
Jaroslaw Sobieszczanski-Sobieski *In its* Recent Advances in Multidisciplinary Analysis and Optimization, Part 1 Apr. 1989 p 51-78 Previously announced as N89-13423 (For primary document see N89-25146 19-05)
Avail: NTIS HC A23/MF A01 CSCL 13B

N89-25164*# LTV Aerospace and Defense Co., Dallas, TX. Military Aircraft Div.
THE DESIGNER OF THE 90'S: A LIVE DEMONSTRATION
Tommy L. Green, Basil M. Jordan, Jr., and Timothy L. Oglesby *In* NASA. Langley Research Center, Recent Advances in Multidisciplinary Analysis and Optimization, Part 1 Apr. 1989 p 373-385 (For primary document see N89-25146 19-05)
Avail: NTIS HC A23/MF A01 CSCL 13B

N89-25176*# Brigham Young Univ., Provo, UT. Engineering Design Methods Lab.
RESEARCH ON OPTIMIZATION-BASED DESIGN
R. J. Balling, A. R. Parkinson, and J. C. Free *In* NASA. Langley Research Center, Recent Advances in Multidisciplinary Analysis and Optimization, Part 2 Apr. 1989 p 565-580 (For primary document see N89-25173 19-05)
Avail: NTIS HC A22/MF A01 CSCL 20K

N89-25208*# Houston Univ., TX. Systems Design Lab.
A DECISION-BASED PERSPECTIVE FOR THE DESIGN OF METHODS FOR SYSTEMS DESIGN
Farrokh Mistree, Douglas Muster, Jon A. Shupe, and Janet K. Allen (Janco Research, Houston, TX.) *In* NASA. Langley Research Center, Recent Advances in Multidisciplinary Analysis and Optimization, Part 3 Apr. 1989 p 1111-1135 (For primary document see N89-25201 19-05)
Avail: NTIS HC A22/MF A01 CSCL 13B

32 COMMUNICATIONS AND RADAR

Includes radar; land and global communications; communications theory; and optical communications.

For related information see also *04 Aircraft Communications and Navigation* and *17 Space Communications, Spacecraft Communications, Command and Tracking.* For search and rescue see *03 Air Transportation and Safety,* and *16 Space Transportation.*

N89-25360*# National Aeronautics and Space Administration. Lyndon B. Johnson Space Center, Houston, TX.
METHOD AND APPARATUS FOR SENSOR FUSION Patent Application
Kumar Krishen, inventor (to NASA), Scott Shaw, inventor (to NASA), and Rui J. P. deFigueiredo, inventor (to NASA) 30 Dec. 1988 60 p
(NASA-Case-MSC-21334-1; NAS 1.71:MSC-21334-1; US-Patent-Appl-SN-292130) Avail: NTIS HC A04/MF A01 CSCL 17I

Method and apparatus for fusion of data from optical and radar sensors by error minimization procedure is presented. The method was applied to the problem of shape reconstruction of an unknown surface at a distance. The method involves deriving an incomplete surface model from an optical sensor. The unknown characteristics of the surface are represented by some parameter. The correct value of the parameter is computed by iteratively generating theoretical predictions of the radar cross sections (RCS) of the surface, comparing the predicted and the observed values for the RCS, and improving the surface model from results of the comparison. Theoretical RCS may be computed from the surface model in several ways. One RCS prediction technique is the method of moments. The method of moments can be applied to an unknown surface only if some shape information is available from an independent source. The optical image provides the independent information. NASA

N89-25361# Academy of Sciences (USSR), Novosibirsk. Inst. Yadernoj Fiziki.
PHOTONIC CHIRAL CURRENT AND ITS ANOMALY IN A GRAVITATIONAL FIELD
A. D. Dolgov, I. B. Khriplovich, A. I. Vajnshtejn, and V. I. Zakharov 1988 18 p Submitted for publication
(DE88-706213; IYaF-88-37) Avail: NTIS (US Sales Only) HC A03/MF A01

The notion of chirality for electromagnetic field which is conserved in interactions with gravitons is formulated. The correponding chiral current is the one-particle-state analogue of the Pauli-Lubansky vector. The anomaly of this current in an external gravitational field is found. The results obtained are used for the calculation of the electromagnetic radiative correction to the fermionic chiral anomaly in a gravitational field. DOE

N89-25362# Lawrence Livermore National Lab., CA.
TIME DOMAIN MODELING OF ELECTROMAGNETIC COUPLING
R. R. McLeod, R. L. Berger, and L. D. Bacon (Sandia National Labs., Albuquerque, NM.) 23 Mar. 1989 10 p Presented at the 4th National Conference on High Power Microwave (HPM) Technology for Defense Applications, Monterey, CA, 9 May 1988 (Contract W-7405-eng-48)
(DE89-010240; UCRL-97831; CONF-8805132-14) Avail: NTIS HC A02/MF A01

Time-Domain Electromagnetic (EM) codes are increasingly being applied to coupling problems in order to supplement and complement the experimental efforts in this area. Both Finite-Difference Time-Domain (FDTD) and Finite-Element Time-Domain (FETD) techniques are employed to calculate the fields and currents inside of a shielding body. The size of the relevant detail in realistic systems, however, currently limits the usefulness of these codes. This detail problem is investigated, and a number of proposed solutions to it are evaluated. Finally, some example problems, representative of current modeling capabilities, are presented. DOE

N89-25363* National Aeronautics and Space Administration. Langley Research Center, Hampton, VA.
ANTENNA SURFACE CONTOUR CONTROL SYSTEM Patent
Elvin L. Ahl, inventor (to NASA) and James B. Miller, inventor (to NASA) 7 Mar. 1989 14 p
(NASA-Case-LAR-13798-1; US-Patent-4,811,033; US-Patent-Appl-SN-118995; US-Patent-Class-343-880; US-Patent-Class-343-915; US-Patent-Class-343-DIG.2) Avail: U.S. Patent and Trademark Office

The invention is a system for automatically controlling the surface contour of a deployable and restowable antenna having a mesh reflector surface supported by a circular, folding hoop affixed to a central, telescoping column. The antenna, when deployed, forms a quad-aperture reflector with each quadrant of the mesh surface shaped to provide an offset parabolic radio frequency (RF) reflector. The hoop is supported and positioned by quartz support cords attached to the top of a column and by lower graphite hoop control cords that extend between the hoop and base of the column. The antenna, an RF reflective surface, is a gold plated molybdenum wire mesh supported on a graphite cord truss structure that includes the hoop control cords and a plurality of surface control cords attached at selected points on the surface and to the base of the column. The contour of the three-dimensional surface of the antenna is controlled by selectively adjusting the lengths of the surface control cords and the graphite hoop control cords by means of novel actuator assemblies that automatically

sense and change the lengths of the lower hoop control cords and surface control cords.

Official Gazette of the U.S. Patent and Trademark Office

N89-25364*# Texas Univ., Arlington. Wave Scattering Research Center.

MICROWAVE SCATTERING MODELS AND BASIC EXPERIMENTS Semiannual Report, 1 Nov. 1986 - 30 Apr. 1989

Adrian K. Fung 1989 32 p

(Grant NAG5-486)

(NASA-CR-185393; NAS 1.26:185393) Avail: NTIS HC A03/MF A01 CSCL 20N

Progress is summarized which has been made in four areas of study: (1) scattering model development for sparsely populated media, such as a forested area; (2) scattering model development for dense media, such as a sea ice medium or a snow covered terrain; (3) model development for randomly rough surfaces; and (4) design and conduct of basic scattering and attenuation experiments suitable for the verification of theoretical models.

Author

N89-25365*# National Aeronautics and Space Administration. Lewis Research Center, Cleveland, OH.

PERFORMANCE OF FIVE 30 GHz SATELLITE RECEIVERS

Robert J. Kerczewski, George E. Ponchak, and Robert R. Romanofsky 1989 7 p Presented at the 1989 IEEE MTT-S International Microwave Symposium, Long Beach, CA, 13-15 Jun. 1989

(NASA-TM-101960; E-4620; NAS 1.15:101960) Avail: NTIS HC A02/MF A01 CSCL 17B

Technology development contracts funded by NASA have resulted in five 30 GHz satellite receivers of various design. The results of tests performed at NASA-Lewis to determine the operating characteristics of the receivers and their ability to perform in a digital satellite link are presented and discussed. Author

N89-25366# Oak Ridge National Lab., TN.

DETERMINATION OF FIELDS NEAR AN ICRH ANTENNA USING A 3D MAGNETOSTATIC LAPLACE FORMULATION

P. M. Ryan, K. E. Rothe, J. H. Whealton, and D. W. Swain 1989 4 p Presented at the 8th Topical Conference on Radio Frequency Power in Plasmas, Irvine, CA, 1 May 1989

(Contract DE-AC05-84OR-21400)

(DE89-011571; CONF-8905120-3) Avail: NTIS HC A02/MF A01

In the vicinity of an ICRH antenna strap, where there are no volume currents and a free-space wavelength is much longer then the dimensions of interest, Ampere's law reduces to a curl-free conditions on the magnetic field, allowing a magnetic scalar potential to be defined. This scalar potential is a solution of the three-dimensional (3D) Laplace equation and satisfies the following boundary conditions on the magnetic field: the line integral of the magnetic field around the current strap is equal to the current flowing in the strap and the perpendicular component of the magnetic field vanishes at conductor surfaces (no flux penetration of perfect conductors). This formulation allows for the magnetic field solution of quite complex 3D geometries, such as poloidal current straps with asymmetric radial feeds or detailed Faraday shield geometries. DOE

N89-25367# Westinghouse Idaho Nuclear Co., Inc., Idaho Falls.

DIGITAL OPTICAL CONVERSION MODULE Patent Application

Dale K. Kotter, inventor (to DOE) and Richard A. Rankin, inventor (to DOE) 19 Jul. 1988 18 p

(Contract DE-AC07-84ID-12435)

(DE89-011441; PATENTS-US-A7221394; US-Patent-Appl-SN-221394) Avail: NTIS HC A03/MF A01

A digital optical conversion module is used to convert an analog signal to a computer compatible digital signal including a voltage-to-frequency converter, frequency offset response circuitry, and an electrical-to-optical converter. Also used in conjunction with the digital optical conversion module is an optical link and an interface at the computer for converting the optical signal back to an electrical signal. Suitable for use in hostile environments having high levels of electromagnetic interference, the conversion module retains high resolution of the analog signal while eliminating the potential for errors due to noise and interference. The module can be used to link analog output scientific equipment such as an electrometer used with a mass spectrometer to a computer.

DOE

N89-25368# Oak Ridge National Lab., TN.

SPECTRAL SHAPING AND PHASE CONTROL OF A FAST-WAVE CURRENT DRIVE ANTENNA ARRAY

F. W. Baity, W. L. Gardner, R. H. Goulding, D. J. Hoffman, and P. M. Ryan 1989 4 p Presented at the 8th Topical Conference on Radio Frequency Power in Plasmas, Irvine, CA, 1 May 1989

(Contract DE-AC05-84OR-21400)

(DE89-011567; CONF-8905120-7) Avail: NTIS HC A02/MF A01

The requirements for antenna design and phase control circuitry for a fast-wave current drive (FWCD) array operating in the ion cyclotron range of frequencies are considered. The design of a phase control system that can operate at arbitrary phasing over a wide range of plasma-loading and strap-coupling values is presented for a four-loop antenna array, prototypical of an array planned for the DIII-D tokamak (General Atomics, San Diego, California). The goal is to maximize the power launched with the proper polarization for current drive while maintaining external control of phase. Since it is desirable to demonstrate the feasibility of FWCD prior to ITER, a four-strap array has been designed for DIII-D to operate with the existing 2-MW transmitter at 60 MHz.

DOE

N89-25369# California Univ., Berkeley. Lawrence Berkeley Lab. Accelerator and Fusion Research Div.

COMPUTER SIMULATION OF FEL SIDEBANDS IN A STRONGLY DISPERSIVE WAVEGUIDE

E. J. Sternbach 15 Mar. 1989 10 p Presented at the 13th Particle Accelerator Conference, Chicago, IL, 20-23 Mar. 1989 Submitted for publication

(Contract DE-AC03-76SF-00098)

(DE89-011825; LBL-26931; CONF-890335-100) Avail: NTIS HC A02/MF A01

With the development of high power free electron lasers (FEL), it is necessary to consider the development of sidebands in the radiation spectrum. These sidebands can considerably widen the bandwidth of the FEL output and if sufficient power is developed, this can lead to the detrapping of electrons. It has been noted previously that the effects of waveguide dispersion can affect the sideband gain and location. In this report the author describes a set of coupled equations suitable for the study of the radiation spectrum of an FEL. These equations include all the effects of waveguide dispersion. A computer simulation that numerically integrates these equations is used to study sideband growth and saturation in the regime of strong dispersion. DOE

N89-25370# Sandia National Labs., Albuquerque, NM.

PYRAMIDAL HORNS: PART 1: SIMPLE EXPRESSIONS FOR DIRECTIVITY AS A FUNCTION OF APERTURE PHASE ERROR

John F. Aurand 1989 5 p Presented at the Institute of Electrical and Electronics Engineers (IEEE) Antennas Propagation Society (AP-S) International Symposium, San Jose, CA, 26-30 Jun. 1989

(Contract DE-AC04-76DP-00789)

(DE89-005209; SAND-88-3388C; CONF-890660-4) Avail: NTIS HC A02/MF A01

Pyramidal horn antennas are popular because they offer high gain, low VSWR, very pure linear polarization, and mechanical simplicity. When used as standard-gain antennas in measurement situations, the gain and directivity are critical parameters, and theoretical analysis of the directivity is essential. This paper presents approximate equations for the directivity of pyramidal horns. These equations are accurate and much easier to evaluate than the exact equations, which involve complicated Fresnel

integrals. The formulas are expressed in terms of gain-reduction factors, based on the quadratic phase errors in the aperture.
DOE

N89-25371# Sandia National Labs., Albuquerque, NM.
PYRAMIDAL HORNS: PART 2: A NOVEL DESIGN METHOD FOR HORNS OF ANY DESIRED GAIN AND APERTURE PHASE ERROR
John F. Aurand 1989 5 p Presented at the Institute of Electrical and Electronics Engineers (IEEE) Antennas Propagation Society (AP-S) International Symposium, San Jose, CA, 26-30 Jun. 1989
(Contract DE-AC04-76DP-00789)
(DE89-005346; SAND-88-3389C; CONF-890660-3) Avail: NTIS HC A02/MF A01

Pyramidal horn antennas are often used because of their well-characterized radiation performance, including precise gain as a function of size and very pure linear polarization. When designing pyramidal horns, previous methods have involved approximations and inefficient trial-and-error solutions. This paper presents a novel numerical method for determining the exact horn dimensions for any desired gain. It utilizes exact relationships to yield the required aperture dimensions and horn length, given an operating frequency, waveguide dimensions, and allowable quadratic phase errors in the aperture. DOE

N89-25372# Lawrence Livermore National Lab., CA.
NUMERICAL MODELING OF MONOPOLES ON RADIAL-WIRE GROUND SCREENS
G. J. Burke and E. K. Miller (General Research Corp., Santa Barbara, CA.) 29 Dec. 1988 7 p Presented at the Institute of Electrical and Electronics Engineers (IEEE) Antennas Propagation Society (AP-S) International Symposium, San Jose, CA, 26-30 Jun. 1989
(Contract W-7405-eng-48)
(DE89-005350; UCRL-100185; CONF-890660-2) Avail: NTIS HC A02/MF A01

The monopole antenna on a radial-wire ground screen has been particularly resistant to numerical modeling due to the difficulty of treating the effect of the air-ground interface and the large total electrical length of wire involved. Designs are usually based on empirically derived formulas and practices. A moment-method code capable of modeling ground screens and other antennas near to or buried in the ground was developed in the code NEC-3. A version of NEC-3, known as NEC-GS, was then specialized to model vertical monopoles on uniform radial-wire ground screens, taking maximum advantage of the symmetry of the screen and its currents. Some results of this code are presented here to compare the performance of ground screens of varying dimensions and configurations, and to determine optimum design parameters.
DOE

N89-25373# Lawrence Livermore National Lab., CA. Isotope Separation and Materials Processing Program.
A GENERALIZED ANTENNA THEOREM FOR BROADBAND PULSES
Michael A. Johnson Mar. 1989 14 p
(Contract W-7405-eng-48)
(DE89-009707; UCID-21661) Avail: NTIS HC A03/MF A01

Using a very general argument, one can place an upper limit on the fluence that can be delivered to a distant point by passing a pulse with finite energy through an aperture of finite area. Based on a time-dependent form of Huygen's principle, shown is the maximum possible fluence produced by an arbitrary scalar field passing through an aperture to an observation point is about equal to the fluence produced by a nearly monochromatic pulse of the same energy. This fictitious pulse uniformly illuminates the aperture and converges to a geometric focal spot at the observation point. The frequency of the monochromatic wave is made equal to the aperture-averaged root-mean-square frequency of the actual diffracting field. Thus, a pulse with arbitrary time dependence satisfies an antenna theorem very similar to the more well-known version of the theorem satisfied by monochromatic waves. DOE

N89-25374# Technische Univ., Eindhoven (Netherlands).
REDUCTION OF TRANSHORIZON RADIO INTERFERENCE IN SATELLITE EARTH STATIONS Ph.D. Thesis
Peter Maria Joseph Scheeren 1988 284 p
(ETN-89-94297) Avail: NTIS HC A13/MF A01

Protection of satellite ground stations against transhorizon interference by site shielding of the station is discussed. Protection by the site shielding is inherently limited by the diffraction at the edge(s) of the shielding obstacle. Existing methods for the calculation of the shielding effect of an obstacle cannot generally be applied. The site-shielding problem was analyzed using a model based on the geometrical theory of diffraction (GTD). The numerical results from this model agree with comparable results reported in the literature. Based on the GTD model, a simpler, practical model was developed, the results of which agree well with the results of the GTD model. The practical relevance of site shielding for frequency sharing is illustrated by an example. The results suggest that site shielding may be especially attractive for relatively small stations.
ESA

N89-25375# Deutsche Bundespost, Darmstadt (Germany, F.R.).
REDUCTION OF INTERFERENCE BY DECORRELATION AND QUANTIZED FEEDBACK IN THE CASE OF DIGITAL TRANSMISSION ON MULTI-PAIR SYMMETRIC CABLES
Guenter Morgenstern Sep. 1988 39 p In GERMAN; ENGLISH summary
(FI-44-TB-110; ETN-89-94600) Copyright Avail: NTIS HC A03/MF A01

Statistical dependence of an interfering signal is analyzed at the sampling points in the case of digital transmission in order to reduce the effect of interference. Interference decorrelation is obtained by a transversal filter so that it no longer shows any statistical dependence at the sampling points. To avoid pulse interference of the digital information signal by the decorrelation filter, the output signal of the threshold detector is returned via the same filter coefficients to the input of the threshold detector and is substracted there from the input signal. This inverse filter, designated as quantized feedback, has no influence on the interfering signal. General theory and mathematical relations for the calculation of the interference reduction and for the dimensioning of the filter coefficients are presented. By means of examples of white noise and of two cases of crosstalk for multipair symmetric cables, the effectiveness of the theory is demonstrated by numerical evaluation.
ESA

N89-25376# Deutsche Forschungs- und Versuchsanstalt fuer Luft- und Raumfahrt, Oberpfaffenhofen (West Germany). Abteilung HF-Physik.
ON A FAST TWO-DIMENSIONAL RADAR IMAGING PROCESS FOR ROTATING TARGETS AND AN ANALYSIS OF ITS IMAGE QUALITY
Karl-Heinz Bethke Jun. 1988 104 p In GERMAN; ENGLISH summary Report will also be announced as translation (ESA-TT-1142) Original contains color illustrations
(DFVLR-FB-88-51; ISSN-0171-1342; ETN-89-94637) Avail: NTIS HC A06/MF A01; DFVLR, VB-PL-DO, Postfach 90 60 58, 5000 Cologne, Fed. Republic of Germany, DM 35

A fast method for generating two-dimensional radar images is presented. While range resolution is performed in real time by the hardware of a coherent short pulse radar, the cross-range resolution is generated off-line using the synthetic aperture principle via efficient FFT-algorithms. Degradations resulting from approximations of the image algorithm as well as from migration effects of scattering centers through resolution cells are shown and discussed. Derived from these results a weighting function is defined which together with the use of window functions compensates for this amplitude degradation. Target structures of wide cross-range dimension are treated separately. Experimental results demonstrate the capability of the imaging procedure.
ESA

N89-25377# Technische Univ., Eindhoven (Netherlands). Faculty of Electrical Engineering.
THE IMPACT OF TELECOMMUNICATION ON RURAL AREAS IN DEVELOPING COUNTRIES
P. A. M. Hermans, A. M. J. Kwaks, I. V. Bruza, and J. Dijk Dec. 1987 92 p
(EUT-87-E-185; ISBN-9-06-144185-4; ISSN-0167-9708; ETN-89-94773) Avail: NTIS HC A05/MF A01

The economic and social impact of telecommunication in developing countries was studied. The economic impact not only depends on the direct returns of the investment, like tariffs, through the improved communication facilities, other sectors can indirectly profit from the investments too. Especially, in areas with a very low telephone density, the indirect returns of a telecommunication investment are enormous. Technical possibilities for building up transmission links in a rural network include coaxial cables, glass fibers, radio transmission, and satellite communication. In thinly populated rural areas, satellite communication with a single channel per carrier (SCPC) system is a good solution. With a SCPC system few groundstations can be used. These stations are easy to maintain, and use little power. As soon as a satellite channel and two groundstations are operational, transmission is possible, so a SCPC system can be implemented quickly. ESA

N89-25378# Technische Univ., Eindhoven (Netherlands). Telecommunication Div.
A MULTIFREQUENCY ANTENNA SYSTEM FOR PROPAGATION EXPERIMENTS WITH THE OLYMPUS SATELLITE
S. C. J. Worm Apr. 1988 67 p Revised
(Contract STW-EEL-44-0757)
(EUT-88-E-192; ISBN-90-614-4192-7; ISSN-0167-9708; ETN-89-94780) Avail: NTIS HC A04/MF A01

The main components of a multifrequency antenna system for propagation experiments with the large telecommunications satellite Olympus are reviewed. The antenna system consists of a classical dual reflector Cassegrain antenna with a single aperture multifrequency primary feed system. The 12/20/30 GHz beacons of Olympus provide stable and pure signals for the direct measurement of atmospheric influences on radio wave propagation, and they provide a directional reference for the alignment of ground station antennas. The geometry and the electrical characteristics of a classical Cassegrain antenna, with a corrugated horn primary feed, are considered, including geometrical relationships, strut geometry, subreflector size, illumination taper, blocking, surface accuracy, polarization efficiency, and on-axis polarization discrimination. The feed system consists of a horn antenna and a microwave network. At each of the beacon frequencies, the radiation pattern of the feed system is required to have axial symmetry, low cross polarization, and a prescribed amplitude decay. These requirements can be met by using a corrugated horn supporting balanced hybrid modes at these frequencies. ESA

N89-25379# Technische Univ., Eindhoven (Netherlands). Measurement and Control Group.
ON SYSTEM IDENTIFICATION USING PULSE-FREQUENCY MODULATED SIGNALS
V. N. Bondarev (Academy of Sciences of the Ukrainian SSR, Sevastopol.) Jun. 1988 88 p
(EUT-88-E-195; ISBN-90-614-4195-1; ISSN-0167-9708; ETN-89-94783) Avail: NTIS HC A05/MF A01

Continuous system identification using pulse frequency modulation (PFM) signals was studied. Two possibilities for application of PFM signals in system identification are considered. In accordance with these possibilities either the system is excited by PFM signals or the system output is observed with the help of a pulse-frequency converter. For both these cases effective computational schemes for estimation of the transfer function and the weighting function are obtained. For the case of the weighting function estimate, the relationship with previously obtained estimates is established. The utility of the suggested estimates is illustrated by computer simulation. The programs are given. ESA

N89-25380*# Jet Propulsion Lab., California Inst. of Tech., Pasadena.
PHASE-AMBIGUITY RESOLUTION FOR QPSK MODULATION SYSTEMS. PART 1: A REVIEW
Tien Manh Nguyen 15 May 1989 26 p
(Contract NAS7-918)
(NASA-CR-185385; NAS 1.26:185385; JPL-Publ-89-4-Pt-1) Avail: NTIS HC A03/MF A01 CSCL 17B

Part 1 reviews the current phase-ambiguity resolution techniques for QPSK coherent modulation systems. Here, those known and published methods of resolving phase ambiguity for QPSK with and without Forward-Error-Correcting (FEC) are discussed. The necessary background is provided for a complete understanding of the second part where a new technique will be discussed. An appropriate technique to the Consultative Committee for Space Data Systems (CCSDS) is recommended for consideration in future standards on phase-ambiguity resolution for QPSK coherent modulation systems. Author

N89-25381*# Jet Propulsion Lab., California Inst. of Tech., Pasadena.
PHASE-AMBIGUITY RESOLUTION FOR QPSK MODULATION SYSTEMS. PART 2: A METHOD TO RESOLVE OFFSET QPSK
Tien Manh Nguyen 15 May 1989 32 p
(Contract NAS7-918)
(NASA-CR-184971; NAS 1.26:184971; JPL-Publ-89-4-Pt-2) Avail: NTIS HC A03/MF A01 CSCL 17B

Part 2 presents a new method to resolve the phase-ambiguity for Offset QPSK modulation systems. When an Offset Quaternary Phase-Shift-Keyed (OQPSK) communications link is utilized, the phase ambiguity of the reference carrier must be resolved. At the transmitter, two different unique words are separately modulated onto the quadrature carriers. At the receiver, the recovered carrier may have one of four possible phases, 0, 90, 180, or 270 degrees, referenced to the nominally correct phase. The IF portion of the channel may cause a phase-sense reversal, i.e., a reversal in the direction of phase rotation for a specified bit pattern. Hence, eight possible phase relationships (the so-called eight ambiguous phase conditions) between input and output of the demodulator must be resolved. Using the In-phase (I)/Quadrature (Q) channel reversal correcting property of an OQPSK Costas loop with integrated symbol synchronization, four ambiguous phase conditions are eliminated. Thus, only four possible ambiguous phase conditions remain. The errors caused by the remaining ambiguous phase conditions can be corrected by monitoring and detecting the polarity of the two unique words. The correction of the unique word polarities results in the complete phase-ambiguity resolution for the OQPSK system. Author

N89-25504# Institut fuer Angewandte Geodaesie, Frankfurt am Main (Germany, F.R.).
DIGITAL EVALUATION OF SEASAT-SAR RADAR IMAGE DATA [DIGITALE AUSWERTUNG VON SEASAT-SAR-RADARBILDDATEN]
Berthold Pfeiffer *In its* Reports on Cartography and Geodesy. Series 1: Original Reports, No. 102 1988 p 59-77 In GERMAN; ENGLISH summary (For primary document see N89-25501 19-43)
Avail: NTIS HC A08/MF A01

N89-25871# Instituto Superior Tecnico, Lisbon (Portugal).
ON THE DISSIPATION OF ALFVEN WAVES IN MAGNETIC ATMOSPHERES AND FLUX TUBES
L. M. B. C. Campos *In* ESA, Seismology of the Sun and Sun-Like Stars Dec. 1988 p 295-300 Sponsored by J.N.I.C.T. and CAUTL/INIC (For primary document see N89-25819 19-92)
Copyright Avail: NTIS HC A99/MF E03

33 ELECTRONICS AND ELECTRICAL ENGINEERING

Includes test equipment and maintainability; components, e.g., tunnel diodes and transistors; microminiaturization; and integrated circuitry.

For related information see also *60 Computer Operations and Hardware* and *76 Solid-State Physics.*

N89-25382# National Aeronautical Lab., Bangalore (India). Materials Science Div.

CONTROLLER FOR STABILIZATION OF HIGH VOLTAGE

V. Shubha and T. G. Ramesh Apr. 1987 9 p

(NAL-TM-MT-8702) Avail: NTIS HC A02/MF A01

The design and performance of a controller circuit for stabilizing the high voltage in a mobile X-ray stress diffractometer are described. The circuitry is used in conjunction with a saturable core reactor which acts as a controlling element in stabilizing the high voltage. Stabilization of the order of 0.5 percent has been achieved. Author

N89-25383# Los Alamos National Lab., NM.

APPARATUS AND METHOD FOR CHARACTERIZING CONDUCTIVITY OF MATERIALS Patent Application

James D. Doss, inventor (to DOE) 13 Apr. 1988 26 p

(DE89-009599; PATENTS-US-A7181451; US-Patent-Appl-SN-181451) Avail: NTIS HC A03/MF A01

An apparatus and method for noncontact, radio-frequency shielding current characterization of materials are presented. Self- or mutual inductance changes in one or more inductive elements, respectively, occur when materials capable of supporting shielding currents are placed in proximity thereto, or undergo change in resistivity while in place. Such changes can be observed by incorporating the inductor(s) in a resonant circuit and determining the frequency of oscillation or by measuring the voltage induced on a coupled inductive element. The present invention is useful for determining the critical temperature and superconducting transition width for superconducting samples. DOE

N89-25384# Sandia National Labs., Albuquerque, NM. Ceramics Processing Div.

SINTERING SCHEDULE AND SAMPLE GEOMETRY EFFECTS ON THE ELECTRICAL AND PHYSICAL PROPERTIES OF HIGH FIELD VARISTOR MATERIALS

T. J. Gardner and S. J. Lockwood Feb. 1989 53 p

(Contract DE-AC04-76DP-00789)

(DE89-010523; SAND-88-2449) Avail: NTIS HC A04/MF A01

The sample size scale-up required for the preparation of large (production-size) varistor slugs was found to produce material which did not meet both the electrical and physical property specifications when sintered using the standard schedule. As a result, the effects of sintering schedule variables (heating rate, soak temperature, and soak time) on the electrical and physical properties of high field varistor materials were investigated. One sintering schedule was found to be particularly effective in generating large, thick varistor slugs with reproducible electrical properties within specifications, but the physical characteristics did not meet program goals. Empirical relationships between the electrical and physical properties of sintered high field varistors showed that it was not possible to meet program goals with production-size (greater than or equal to 1.5 inch diameter, 0.6 to 0.7 inch thick) varistor parts. The sample thickness was found to play a significant role in determining the electrical properties of varistors sintered using a standard sintering schedule (732A). Significant decreases in electric field (E) and nonlinearity coefficient (alpha) were noted with corresponding increases in sample thickness. A new sample geometry was identified which produced sintered varistor material meeting both electrical and physical property specifications. Sintered varistor microstructures were evaluated and correlated with the electrical and physical properties. DOE

N89-25385# Sundstrand Advanced Technology Group, Rockford, IL.

ELECTRICALLY COMPENSATED CONSTANT SPEED DRIVE (MODEL NUMBER 60 ECEPGS 02) Final Report, Sep. 1985 - Jun. 1988

R. Olson, K. Anderson, S. Ng, B. Dishner, and C. Ferreira 20 Jan. 1989 178 p

(Contract F33615-85-C-2590)

(AD-A206064; AFWAL-TR-88-2131) Avail: NTIS HC A09/MF A01 CSCL 01/3

The concept of an electric constant speed drive is one of the approaches usable to overcome those barriers and issues for a 400-Hz power system. The principle of concept investigated is to use electronic controlled PM machines in conjunction with a summing differential to attain a constant speed from a variable speed input. An approach is identified, design analysis completed, and hardware of breadboard nature fabricated to demonstrate concept principle. GRA

N89-25386# Oak Ridge National Lab., TN.

CONDITION MONITORING OF MACHINERY USING MOTOR CURRENT SIGNATURE ANALYSIS

R. C. Kryter and H. D. Haynes 1989 22 p Presented at the 7th Power Plant Dynamics, Control and Testing Symposium, Knoxville, TN, 15 May 1989

(Contract DE-AC05-84OR-21400)

(DE89-008737; CONF-890555-3) Avail: NTIS HC A03/MF A01

Motor current signature analysis (MCSA) is a powerful monitoring tool for motor-driven equipment that provides a nonintrusive means for detecting the presence of mechanical and electrical abnormalities in the motor and the driven equipment, including altered conditions in the process downstream of the motor-driven equipment. It was developed at the Oak Ridge National Laboratory as a means for determining the effects of aging and service wear systems, but it is applicable to a broad range of machinery. MCSA is based on the recognition that an electric motor (ac or dc) driving a mechanical load acts as an efficient and permanently available transducer by sensing mechanical load variations, large and small, long-term and rapid, and converting them into variations in the induced current generated in the motor windings. These motor current variations are carried by the electrical cables processes as desired. Motor current signatures, obtained in both time and over time to provide early indication of degradation. Successful applications of MCSA technology (patent applied for) include not only motor-operated valves but also pumps of various designs, blowers, and air conditioning systems. Examples are presented briefly, and speculation regarding the applicability of MCSA to a broader range of equipment monitoring and production line testing is also given. DOE

N89-25387# Sandia National Labs., Albuquerque, NM.

STRESS-DRIVEN DIFFUSIVE VOIDING OF ALUMINUM CONDUCTOR LINES

F. G. Yost, D. E. Amos, and A. D. Romig, Jr. 1989 9 p Presented at the Electromigration and Metallization Session, Phoenix, AZ, 11 Apr. 1989

(Contract DE-AC04-76DP-00789)

(DE89-009832; SAND-88-3189C; CONF-8904190-1) Avail: NTIS HC A02

The trend to miniaturize silicon integrated circuits has brought with it a thermal stress-induced void formation problem in the aluminum conductor lines of these circuits. In this work local stress relaxation has been included quantitatively in the construction of a wedge-like void growth model. It is shown that under stress relaxation conditions, the stress-induced grain boundary diffusion equation transforms into the diffusion equation. With the use of appropriate boundary conditions and the initial conductor line stress profile, the diffusion equation is solved numerically. This solution yields the temporal history of void size and local stress. It will be shown that two types of stress relaxation moderate and limit the growth of voids. From this analysis a useful expression is derived

which relates final void size and initial stress. With these results conservative estimates of the lifetime of aluminum conductor lines can be made. DOE

N89-25388# Eaton Corp., Southfield, MI.
ADVANCED DUAL-SHAFT ELECTRIC PROPULSION SYSTEM TECHNOLOGY DEVELOPMENT PROGRAM Annual Report No. 4
I. Kalns Oct. 1988 33 p
(Contract DE-AC07-84NV-10366)
(DE89-010008; DOE/NV-10366/6) Avail: NTIS HC A03/MF A01

This fourth annual report of the DSEP program summarizes all program activities from September 1987 through August 1988. These activities comprise: (1) Successful completion of the first test-bed, proof-of-concept vehicle (TB-1) tests, achieving performance comparable to that of IC engine powered vehicles. Results are in good (+ or - 8 percent) agreement with those obtained by EG and G, Idaho in simulated dyno tests. (2) Completion of conversion of the second test-bed, durability test vehicle (NVH), dying tests of its powertrain, vehicle installation of the powertrain, shakedown tests of the complete system, and problems encountered in the process. A revision in DSEP program scope is in process that designates this vehicle as a deliverable to DOE and reduces the extent of its durability testing. (3) Completion of conversion and start of subsystem installation of the third complete vehicle (TB-2) to be constructed on the DSEP program: it is a deliverable to DOE. (4) Battery life test results to date, battery performance in the TB-1 vehicle, and an assessment of battery system status. (5) Analysis of the DSEP vehicle/propulsion system manufacturing cost and life cycle cost, and the start of future planning. (6) Program administration and management. DOE

N89-25389# California Univ., Berkeley. Lawrence Berkeley Lab.
METAL-SULFUR TYPE CELL HAVING IMPROVED POSITIVE ELECTRODE Patent Application
Lutgard C. DeJonghe, inventor (to DOE), Steven J. Visco, inventor (to DOE), Catherine C. Mailhe, inventor (to DOE), and Michel B. Armand, inventor (to DOE) 31 Mar. 1988 28 p
(Contract DE-AC03-76SF-00098)
(DE89-010110; PATENTS-US-A7175782;
US-Patent-Appl-SN-175782) Avail: NTIS HC A03/MF A01

A novel metal-sulfur type cell operable at a temperature of 200 C or less with an energy density of 150 Whrs/Kg or better is disclosed characterized by an organo-sulfur cathode formed from an organic-sulfur compound having the general formula, in its charged state, of (R(S) sub y) n wherein y = 1 to 6; n = 2 to 20; and R is one or more different aliphatic or aromatic organic moieties having 1 to 20 carbon atoms, which may include one or more oxygen, sulfur, or nitrogen heteroatoms when R comprises one or more aromatic rings, or one or more oxygen, sulfur, nitrogen, or fluorine atoms associated with the chain when R comprises an aliphatic chain, wherein the aliphatic group may be linear or branched, saturated or unsaturated, and wherein either the aliphatic chain or the aromatic ring may have substituted groups thereon. DOE

N89-25390# Argonne National Lab., IL.
ADVANCED HIGH-TEMPERATURE BATTERIES
P. A. Nelson 1989 18 p Presented at the 2nd Space Electrochemical Research and Technology Conference, Cleveland, OH, 11 Apr. 1989
(Contract W-31-109-eng-38)
(DE89-010698; CONF-8904196-1) Avail: NTIS HC A03/MF A01

Recent results for Li-Al/FeS sub 2 cells and bipolar battery design have shown the possibility of achieving high specific energy (210 Wh/kg) and high specific power (239 W/kg) at the cell level for an electric vehicle application. Outstanding performance is also projected for sodium/metal chloride cells having large electrolyte areas and thin positive electrodes. DOE

N89-25391# California Univ., Berkeley. Lawrence Berkeley Lab.
NOVEL AIR ELECTRODE FOR METAL-AIR BATTERY WITH NEW CARBON MATERIAL AND METHOD OF MAKING SAME Patent Application
Philip N. Ross, Jr., inventor (to DOE) 21 Jun. 1988 18 p
(Contract DE-AC03-76SF-00098)
(DE89-010964; PATENTS-US-A7209397;
US-Patent-Appl-SN-209397) Avail: NTIS HC A03/MF A01

This invention relates to a rechargeable battery or fuel cell. More particularly, this invention relates to a novel air electrode comprising a new carbon electrode support material and a method of making same. DOE

N89-25392# Edgerton, Germeshausen and Grier, Inc., Idaho Falls, ID.
VEHICLE PERFORMANCE TESTS OF THE FORD/GE FIRST GENERATION SINGLE-SHAFT (ETX-I) ALTERNATING CURRENT PROPULSION SYSTEM
R. L. Crumley, R. D. MacDowall, J. E. Hardin, and A. F. Burke Apr. 1989 118 p Prepared in cooperation with Idaho National Engin eering Lab., Idaho Falls
(Contract DE-AC07-76ID-01570)
(DE89-011115; DOE/ID-10224; MISC-88175) Avail: NTIS HC A06/MF A01

This report is concerned with the test and evaluation of the ETX-I electric test vehicle, which is a Mercury LN7 retrofitted with the single-shaft ac electric powertrain developed by Ford and General Electric under contract to the U.S. Department of Energy (DOE) during the period 1982 to 1985. The lead-acid battery used in the ETX-I was developed by Lucas Chloride Electric Vehicle (EV) Systems (LCEVS) as part of the same DOE contract. Extensive tests of the powertrain and battery were done by General Electric and Lucas Chloride before they were integrated into the ETX-I test vehicle by Ford. Ford did limited testing of the ETX-I vehicle on a chassis dynamometer to determine the energy consumption of the powertrain for several driving schedules before the vehicle was shipped to INEL for complete dynamometer testing. Ford also performed track tests with the ETX-I to determine its acceleration performance characteristics. DOE

N89-25393# Lawrence Livermore National Lab., CA.
MICROWAVE PULSE GENERATION BY PHOTOCONDUCTIVE SWITCHING
M. D. Pocha and R. L. Druce 14 Mar. 1989 7 p Presented at the 4th National Conference on High Power Microwave (HPM) Technology for Defense Applications, Monterey, CA, 9 May 1988
(Contract W-7405-eng-48)
(DE89-011631; UCRL-97983; CONF-8805132-15) Avail: NTIS HC A02/MF A01

Laser activated photoconductive semiconductor switching shows significant potential for application in high power microwave generation. Primary advantages of this concept are: small size, light weight, ruggedness, precise timing and phasing by optical control, and the potential for high peak power in short pulses. Several concepts have been suggested for microwave generation using this technology. They generally fall into two categories: (1) the frozen wave generator, or (2) tuned cavity modulation, both of which require only fast closing switches. We have been exploring a third possibility requiring fast closing and opening switches, that is the direct modulation of the switch at microwave frequencies. Switches have been fabricated at LLNL using neutron irradiated Gallium Arsenide which exhibit response times as short as 50 ps at low voltages. We are in the process of performing high voltage tests. So far, we have been able to generate 2.4 kV pulses with approximately 340 ps response time (FWHM) using approximately a 200 microJ optical pulse. Experiments are continuing to increase the voltage and improve the switching efficiency. DOE

N89-25394# Argonne National Lab., IL.
REFERENCE ELECTRODE FOR ELECTROLYTIC CELL Patent Application
Robert W. Kessie, inventor (to DOE) 28 Jul. 1988 16 p

(Contract W-31-109-eng-38)
(DE89-011446; PATENTS-US-A7225411;
US-Patent-Appl-SN-225411) Avail: NTIS HC A03/MF A01

A reference electrode device is provided for a high temperature electrolytic cell used to electrolytically recover uranium from spent reactor fuel dissolved in an anode pool, the device having a glass tube to enclose the electrode and electrolyte and serve as a conductive membrane with the cell electrolyte, and an outer metal tube about the glass tube to serve as a shield and basket for any glass sections broken by handling of the tube to prevent their contact with the anode pool, the metal tube having perforations to provide access between the bulk of the cell electrolyte and glass membrane. DOE

N89-25395# Oak Ridge National Lab., TN.
BINARY AND TERNARY GAS MIXTURES WITH TEMPERATURE ENHANCED DIFFUSE GLOW DISCHARGE CHARACTERISTICS FOR USE IN CLOSING SWITCHES Patent Application
Loucas G. Christophorou, inventor (to DOE) and Scott R. Hunter, inventor (to DOE) 28 Jun. 1988 26 p
(Contract DE-AC05-84OR-21400)
(DE89-011807; PATENTS-US-A7212546;
US-Patent-Appl-SN-212546) Avail: NTIS HC A03/MF A01

An improvement to the gas mixture used in diffuse glow discharge closing switches is disclosed which includes binary and ternary gas mixtures which are formulated to exhibit decreasing electron attachment with increasing temperature. This increases the efficiency of the conductance of the glow discharge and further inhibits the formation of an arc. DOE

N89-25396# Sandia National Labs., Albuquerque, NM.
A NOVEL TR (TRANSMIT/RECEIVE) SWITCH UTILIZING A DISTRIBUTED AMPLIFIER
Steven J. Byrnes and James B. Beyer (Wisconsin Univ., Madison.) 1989 8 p Presented at the IEEE MTT-S International Microwave Symposium, Long Beach, CA, 13 Jun. 1989
(Contract DE-AC04-76DP-00789)
(DE89-005917; SAND-88-7169C; CONF-890678-1) Avail: NTIS HC A02/MF A01

The operation of a large signal class B distributed amplifier as a narrowband transmit/receive switch is described. A four stage MESFET distributed amplifier with more than -30 dB of directivity over a 12 percent bandwidth with a center frequency at X-band is presented. DOE

N89-25397# Sandia National Labs., Albuquerque, NM.
RESISTIVE CONTRAST IMAGING APPLIED TO MULTILEVEL INTERCONNECTION FAILURE ANALYSIS
Edward I. Cole, Jr. 1989 8 p Presented at the VLSI Multilevel Interconnection Conference, Santa Clara, CA, 12 Jun. 1989
(Contract DE-AC04-76DP-00789)
(DE89-011066; SAND-89-0486C; CONF-8906115-1) Avail: NTIS HC A02/MF A01

Resistive Contrast Imaging (RCI) is a new failure analysis technique that uses a scanning electron microscope to generate a relative resistance map of an integrated circuit. The RCI map may be used to localize abrupt changes in resistance and verify continuity. Results using RCI on several two-level interconnection devices are described. The images demonstrate how RCI may be used to differentiate between levels and to localize metal shorts and opens. Methods for improving image quality and level differentiation as well as future development work are discussed. DOE

N89-25398# Lawrence Livermore National Lab., CA. Beam Research Program.
MAGNETIC SWITCHING
H. C. Kirbie 14 Apr. 1989 18 p Presented at the Switched-Power Workshop, Shelter Island, NY, 16 Oct. 1988
(Contract W-7405-eng-48)
(DE89-012299; UCRL-100910; CONF-8810135-3) Avail: NTIS HC A03/MF A01

Magnetic switching is a pulse compression technique that uses a saturable inductor (reactor) to pass pulses of energy between two capacitors. A high degree of pulse compression can be achieved in a network when several of these simple, magnetically switched circuits are connected in series. Individual inductors are designed to saturate in cascade as a pulse moves along the network. The technique is particularly useful when a single-pulse network must be very reliable or when a multi-pulse network must operate at a high pulse repetition frequency (PRF). Today, magnetic switches trigger spark gaps, sharpen the risetimes of high energy pulses, power large lasers, and drive high PRF linear induction accelerators. This paper will describe the technique of magnetic pulse compression using simple networks and design equations. A brief review of modern magnetic materials and of their role in magnetic switch design will be presented. DOE

N89-25399# AEG-Telefunken, Ulm (Germany, F.R.).
HEMTS: FUNDAMENTAL INVESTIGATIONS Final Report, Dec. 1987
Heinrich Daembkes, Juergen Dickmann, Arthur Geyer, Peter Marschall, and Peter Narozny Apr. 1988 89 p In GERMAN; ENGLISH summary
(Contract BMFT-NT-2718-E/4)
(ETN-89-94630) Avail: NTIS HC A05/MF A01

Improved carrier transport properties of field effect transistors based on GaAs/AlGaAs is studied. The capability of reaching higher cut-off frequencies, higher output power and lower noise coefficients than comparable homogeneous. GaAs field effect transistors is demonstrated. Technology is developed to fabricate GaAs/AlGaAs field effect transistors with a cut-off frequency far in excess of 30 GHz using 1 micron gate length. Based on the properties of a single heterostructure, layer sequences are developed and tested. In these structures the conductive channel is formed by up to three quantum wells in parallel, each forming a two-dimensional electron gas. It is shown that these structures allow an increase in saturation current by 100 percent in comparison to the reference single-hetero structure. The cut-off frequency is shown to be up to 40 percent higher than that of the reference structure. ESA

N89-25400# Technische Univ., Eindhoven (Netherlands). Div. of Electrical Energy Systems.
FREQUENCY SPECTRA FOR ADMITTANCES AND VOLTAGE TRANSFERS MEASURED ON A THREE-PHASED POWER TRANSFORMER
M. H. J. Bollen and P. T. M. Vaessen Oct. 1987 74 p
(EUT-87-E-181; ISBN-90-614-4181-1; ISSN-0167-9708;
ETN-89-94769) Avail: NTIS HC A04/MF A01

Frequency spectra for admittance and voltage transfer were measured on a 25 MVA 150/11 kV transformer. Recorded input and output pulses were processed with the aid of a FFT algorithm to give admittances and voltage transfers. The results are reliable between 1 kHz and some hundreds of kHz additional measurements were carried out with a sweep generator and with stationary frequencies. The spectra show large scale phenomena with superimposed maxima and minima probably caused by part-winding resonances. A simple model, consisting of lumped capacitances and inductances is given to reproduce the large scale behavior. ESA

N89-25401# Technische Univ., Eindhoven (Netherlands). Electrical Energy Systems Group.
ANALOG AND DIGITAL SIMULATION OF LINE-ENERGIZING OVERVOLTAGES AND COMPARISON WITH MEASUREMENTS IN A 400 kV NETWORK
W. F. J. Kersten and G. A. P. Jacobs Sep. 1988 68 p
(EUT-88-E-193; ISBN-90-625-4193-5; ISSN-0167-9708;
ETN-89-94781) Avail: NTIS HC A04/MF A01

Results of line-energization tests in the Dutch 400 kV network were used as reference for the development of analog and digital simulation techniques to model complex networks for switching transients. Transient waveforms and overvoltage peak values obtained through duplication of the line energizations by means

of a transient network analyzer (TNA) and the ElectroMagnetic Transient Program (EMTP) are compared with field tests. The best resemblance of waveforms is obtained by EMTP while the cumulative distribution of overvoltage peak values from TNA simulation shows the best match with the field measurements. The statistical overvoltages derived from field tests and simulations are all in the range 1.95 pu + or- 5 percent. The results indicate that both EMTP and TNA are suitable to study switching transients in real networks. ESA

N89-25402# Technische Univ., Eindhoven (Netherlands). Faculty of Electrical Engineering.
MARTINUS VAN MARUM: A DUTCH SCIENTIST IN A REVOLUTIONARY TIME
L. M. L. F. Hosselet Jun. 1988 48 p
(EUT-88-E-194; ISBN-90-614-4194-3; ISSN-0167-9708; ETN-89-94782) Avail: NTIS HC A03/MF A01

The life and work of the 18th century Dutch scientist van Marum, particularly his experiments with electricity, are described. ESA

N89-25403*# National Aeronautics and Space Administration. Lewis Research Center, Cleveland, OH.
DEVELOPMENT AND TESTING OF A 20-kHz COMPONENT TEST BED
Robert M. Button, Andrew S. Brush, and Richard C. Sundberg (General Dynamics Corp., San Diego, CA.) Aug. 1989 8 p Presented at the 24th Intersociety Energy Conversion Engineering Conference, Washington, DC, 6-11 Aug. 1989; sponsored in part by IEEE, AIAA, ANS, ASME, SAE, ACS, and AIChE
(Contract NAS3-25266)
(NASA-TM-102141; E-4940; NAS 1.15:102141) Avail: NTIS HC A02/MF A01 CSCL 09C

A history of the General Dynamics Space Systems Division 20 kHz Breadboard is presented including its current configuration and its role in the Space Station Freedom (SSF) program. Highlights and results are presented on a series of tests conducted on the 20 kHz Breadboard. The first test presented is the 20 kHz Breadboard Acceptance test. This test verified the operation of the delivered Breadboard and also characterized the main components of the system. Next, an indepth efficiency testing effort is presented. The tests attempted to apportion all the power losses in the 20 kHz Breadboard Main Invert Units. Distortion test data is presented showing the distortion characteristics of a Mapham inverter. Lastly, current work on the 20 kHz Breadboard is presented including Main Inverter Unit paralleling tests. Conclusions are summarized and references given. Author

34 FLUID MECHANICS AND HEAT TRANSFER

Includes boundary layers; hydrodynamics; fluidics; mass transfer; and ablation cooling.

For related information see also *02 Aerodynamics* and *77 Thermodynamics and Statistical Physics.*

N89-25404*# State Univ. of New York, Buffalo. Dept. of Mechanical and Aerospace Engineering.
UNSTEADY STAGNATION-POINT HEAT TRANSFER DURING PASSAGE OF A CONCENTRATED VORTEX Final Report
David L. Rigby and William J. Rae May 1989 14 p Presented at the 24th Thermophysics Conference, Buffalo, NY, 12-14 Jun. 1989; sponsored by the AIAA
(Grant NGT-33-183-805)
(NASA-CR-182297; E-4834; NAS 1.26:182297; AIAA-89-1690) Avail: NTIS HC A03/MF A01 CSCL 20D

The unsteady boundary layer due to a single rectilinear vortex filament approaching a 2-D stagnation point is investigated. Assuming the vortex remains far from the surface, incompressible potential flow theory is used to determine the time dependent inviscid flow field. The unsteady boundary layer equations are solved by an alternating-direction-implicit finite-difference method. Two mechanisms which cause fluctuations in heat transfer are the unsteady velocity field in the boundary layer and secondly, the unsteady total temperature at the edge of the boundary layer. The relative importance of these mechanisms is dependent upon the total temperature fluctuations relative to the imposed temperature difference. As a vortex approaches a stagnation point it may be forced to one side of the stagnation line or the other, depending on its initial position. Results are presented for both of these cases. Author

N89-25405# Los Alamos National Lab., NM. Theoretical Div.
SHOCK WAVES AND FRAGMENTATION VIA MOLECULAR DYNAMICS
Brad Lee Holian 1989 8 p Presented at the Supercomputing and Third World Supercomputer Exhibition, Santa Clara, CA, 30 Apr. 1989
(Contract W-7405-eng-36)
(DE89-007981; LA-UR-89-518; CONF-8904121-1) Avail: NTIS HC A02

A wide variety of nonequilibrium processes can be investigated from the atomistic viewpoint by the method of molecular dynamics (MD), where the equations of motion of thousands of interacting atoms are solved on the computer. MD simulations of shock waves in three-dimensional fluids have shown conclusively that shear-stress relaxation is achieved through the atomic rearrangement of transverse viscous flow, for which Navier-Stokes hydrodynamics has been shown to be accurate. MD simulations of homogeneous adiabatic expansion have provided significant insight into the process of fragmentation for hot dense fluids, in that the fragment distribution is exponential in fragment mass; moreover, the average mass can be reasonably estimated by a simple model based on energy balance. Finally, both compression and expansion are involved when a high-velocity sphere impacts and penetrates a thin wall; an atomistic (MD) simulation of this highly nonequilibrium flow resembles in many ways the continuum (hydrodynamic) simulations. DOE

N89-25406# Argonne National Lab., IL. Reactor Analysis and Safety Div.
AN EXPERIMENTAL STUDY OF TWO-PHASE NATURAL CIRCULATION IN AN ADIABATIC FLOW LOOP
Michael J. Tan, George A. Lambert, and Mamoru Ishii 1988 30 p Presented at the 5th Miami International Symposium on Multi-Phase Transport and Particulate Phenomena, Miami Beach, FL, 12 Dec. 1988
(Contract W-31-109-eng-38)
(DE89-009850; CONF-881202-1) Avail: NTIS HC A03/MF A01

An experimental investigation was conducted to study the two-phase flow aspect of the phenomena of interruption and resumption of natural circulation, two-phase flow patterns and pattern transitions in the hot legs of B and W light water reactor systems. The test facility was a scaled adiabatic loop designed in accordance with the scaling criteria developed by Kocamustafaogullari and Ishii. The diameter and the height of the hot leg were 10 cm and 5.5 m, respectively; the working fluid pair was nitrogen-water. The effects of the thermal center in the steam generators, friction loss in the cold leg, and configuration of the inlet to the hot leg on the flow conditions in the hot leg were investigated by varying the water level in a gas separator, controlling the size of opening of a friction loss control valve, and using two inlet geometries. Methods for estimating the distribution parameter and the average drift velocity are proposed so that they may be used in the application of one-dimensional drift-flux model to the analysis of the interruption and resumption of natural circulation in a similar geometry. DOE

N89-25407# Boston Univ., MA.
DIFFUSION, FLUID FLOW AND SOUND PROPAGATION IN DISORDERED MEDIA
T. F. Keyes 1989 8 p
(Contract DE-FG02-86ER-13478)
(DE89-010937; DOE/ER-13478/3) Avail: NTIS HC A02

The current grant was written so as to encompass a wide

range of problems concerning transport in porous/disordered media. The methods to be applied were kinetic theory and renormalization methods. Using these techniques we obtained new results on several dynamical/transport problems where the role of disorder is crucial. This paper discusses those results. DOE

N89-25408# Notre Dame Univ., IN. Dept. of Chemical Engineering.
STUDY OF INTERFACIAL BEHAVIOR IN CONCURRENT GAS-LIQUID FLOWS Progress Report, 1 May 1988 - 30 Apr. 1989
Mark J. McCready Feb. 1989 18 p
(Contract DE-FG02-88ER-13913)
(DE89-010484; DOE/ER-13913/1) Avail: NTIS HC A03/MF A01

This research is focused on acquiring an understanding of the fundamental processes which occur within the liquid layer of separated (i.e., annular or stratified) gas-liquid flows. Knowledge of this behavior is essential for interpretation of pressure drops, entrainment fraction, transport processes and possibly flow regime transitions in gas-liquid flows. We are examining the qualitative and quantitative nature of the interface, using this information to predict the behavior of the flow field within the film and also studying the effect of the flow field on interface and wall heat and mass transfer rates. Study of waves on sheared liquid layers is best broken into two limiting cases, film depth ratio to wavelength ratio (epsilon) much less than one (typical of annular flows) and epsilon is greater than or equal to 1 (typical of stratified flows). Our study of waves where epsilon = O(1) has shown that wave amplitude spectrum is determined by overtone interactions between various modes which lead to a net flux of energy from low (where it is fed in from gas shear) to high frequency waves (where it is dissipated). Interfacial shear and film depth determine the interaction rates and therefore the spectral shape. Using a balance equation for wave energy, we developed a procedure for quantitatively predicting the wave spectrum. For waves with epsilon is dominated by 1, it is appropriate to examine individual traveling wave shapes (rather than the wave spectrum). We have found that measured wavelengths and speeds of periodic waves exhibit small but significant deviations from predictions of linear stability theory. DOE

N89-25409*# National Aeronautics and Space Administration. Lewis Research Center, Cleveland, OH.
DETERMINATION OF COMBUSTION GAS TEMPERATURES BY INFRARED RADIOMETRY IN SOOTING AND NONSOOTING FLAMES
Valerie J. Lyons and Carmen M. Gracia-Salcedo (Army Aviation Systems Command, Cleveland, OH.) Feb. 1989 13 p
(DA Proj. 1L1-61102-AH-45)
(NASA-TP-2900; E-4446; NAS 1.60:2900; AVSCOM-TR-88-C-008; AD-A205373) Avail: NTIS HC A03/MF A01 CSCL 21/2

Flame temperatures in nonsooting and sooting environments were successfully measured by radiometry for pre-mixed propane-oxygen laminar flames stabilized on a water-cooled, porous sintered-bronze burner. The measured temperatures in the nonsooting flames were compared with fine-wire thermocouple measurements. The results show excellent agreement below 1700 K, and when the thermocouple measurements were corrected for radiation effects, the agreement was good for even higher temperatures. The benefits of radiometry are: (1) the flow is not disturbed by an intruding probe, (2) calibration is easily done using a blackbody source, and (3) measurements can be made even with soot present. The theory involved in the radiometry measurements and the energy balance calculations used to correct the thermocouple temperature measurements are discussed.
Author

N89-25410 Washington State Univ., Pullman.
STUDY OF THE STABILITY OF COMPRESSIBLE COUETTE FLOW Ph.D. Thesis
Jeffrey John Girard 1988 207 p
Avail: Univ. Microfilms Order No. DA8906164

A two-dimensional disturbance of plane Couette flow was studied. All reviewed analyses of the basic problem have led to the conclusion that the flow is unconditionally stable. All of the literature assumed the fluid was incompressible. The assumption that a fluid is incompressible neglects solutions to the problem. The motivation of the analysis presented herein is a hypothesis that some of the acoustic disturbances in the fluid, usually neglected, may interact with the mean vorticity to produce more sound. This hypothesis was discussed by Vaidya (1988). The fluid considered herein has been a viscous, heat-conducting, ideal gas. For the cases investigated in this study, most solutions exhibited stability. However, solutions at somewhat unrealistically high Mach numbers exhibited an unstable nature. For even low Mach number flows, the sound solution was the least stable solution. It is thought that the interaction between the sound perturbation and the mean flow has fed energy to the disturbance from the mean flow. Enough energy was transferred to balance some of the viscous dissipation. At low Mach numbers not enough energy was transferred to tip the flow to instability. The established theory has been challenged. All previous analyses of the basic infinitesimal perturbation problem have suggested unconditional stability. Some unstable regimes are shown. Dissert. Abstr.

N89-25411# Honeywell, Inc., Golden Valley, MN. Corporate Systems Development Div.
EVALUATION OF AUXILIARY POWER SUBSYSTEMS FOR GAS ENGINE HEAT PUMPS, PHASE 2 Topical Report, Apr. 1987 - Oct. 1988
R. W. Rasmussen, D. A. Wahlstedt, N. Planer, J. Fink, and E. Persson Dec. 1988 110 p
(Contract GRI-5084-242-1116)
(PB89-173694; GRI-89/0014) Avail: NTIS HC A06/MF A01 CSCL 20D

The need to determine the practical, technical and economic viability for a stand-alone Gas Engine Heat Pump (GEHP) system capable of generating its own needed electricity is addressed. Thirty-eight reasonable design configurations were conceived based upon small-sized power conversion equipment that is either commercially available or close to emerging on the market. Nine of these configurations were analyzed due to their potential for low first cost, high conversion efficiency, availability or simplicity. It was found that electric consumption can be reduced by over 60 percent through the implementation of high efficiency, brushless, permanent magnet motors as fan and pump drivers. Of the nine selected configurations employing variable-speed fans, two were found to have simple incremental payback periods of 4.2 to 16 years, depending on the U.S. city chosen for analysis. Although the auxiliary power subsystem option is only marginally attractive from an economic standpoint, the increased gas load provided to the local gas utility may be sufficient to encourage further development. The ability of the system to operate completely disconnected from the electric power source may be a feature of high merit.
Author

N89-25412# Purdue Univ., West Lafayette, IN. School of Mechanical Engineering.
RADIATIVE HEAT TRANSFER Annual Report, Apr. - Dec. 1988
K. Chapman, S. Ramadhyani, H. Ramamurthy, and R. Viskanta 1 Mar. 1989 144 p
(Contract GRI-5086-260-1293)
(PB89-173637; GRI-89/0021) Avail: NTIS HC A07/MF A01 CSCL 20D

A simple two-dimensional mathematical model was developed to predict the steady state thermal performance and combustion characteristics of a natural gas indirectly fired once-through radiant tube. Different burner geometries were studied and a grid size analysis was performed to determine the optimum grid spacing for each case. The rate of fuel burn-up was correlated using the burner geometry, the equivalence ratio, the fuel firing rate and air preheat temperatures as variables for non-swirling diffusion flames in the radiant tube. The model predictions were also compared with available experimental data for the purpose of validating the

model. The transient, zero-dimensional model was used to conduct a detailed parametric study of a directly-fired batch reheating furnace. The parameters that were investigated are the load and refractory emissivities, the air preheat temperature, the heat capacity of the load, and the height of the combustion space. A one-dimensional model of a directly-fired continuous reheating furnace was also developed. A parametric study was completed to examine the effect of the local throughput on the furnace performance. GRA

N89-25413# Oklahoma Univ., Norman. School of Chemical Engineering and Materials Science.
ADVANCED WORKING FLUID PROPERTIES IN HEAT PUMP AND ABSORPTION COOLING OPERATIONS Annual Report, 1 Dec. 1987 - 30 Nov. 1988
Lloyd L. Lee and Kevin Gering Dec. 1988 39 p
(Contract GRI-5087-223-1616)
(PB89-178172; GRI-89/0032) Avail: NTIS HC A03/MF A01 CSCL 20D

A theoretical correlation formula based on the mean-spherical approximation solution for the primitive model of electrolytes is developed for accurate description of the osmotic, activity coefficients and vapor pressures of single-salt, mixed-salt, single-solvent, and multisolvent salt solutions. Both aqueous and ammoniac systems are investigated. Vapor-liquid equilibria of water-ammonia mixtures are correlated with a local composition model for polar solvents. The systems studied have bearing on gas-fired absorption cooling cycles. Salt systems such a LiBr-water-ethylene glycol, and ammonia-NaSCN are well predicted by the present method for thermodynamic properties. Input data involve the minimum number of necessary characterization parameters such as valences, ion sizes, dielectric constant, plus state conditions: temperature, density, and composition. The only adjustable quantity is the cation size, which reflects the degree of hydration at various concentrations. GRA

N89-25414# Pittsburgh Energy Technology Center, PA.
PROCEEDINGS OF THE SOLIDS TRANSPORT CONTRACTORS' REVIEW MEETING
1988 171 p Meeting held in Pittsburgh, PA, 1 Sep. 1988
(DE89-006720; CONF-8809194) Avail: NTIS HC A09/MF A01

The following research programs on solids transport are presented: granular solids flow and hydrodynamic forces on spheres in suspension; aerated and vibrated chute feeders for particulate materials; micro-stresses and their distributions and effects in discrete media; fluidization mechanisms in horizontal slurry flow; study of dense phase cohesive coal transport in plugs; fundamental studies of cohesive powders; optical instrumentation and study of gas-solid suspension flows; collaborative research in the solid transport area between midwest universities and Argonne; rheology of high concentration polymodal multiphase flows; experiments of densely-loaded non-Newtonian slurries in laminar and turbulent pipe flows; and development of a refractive index matched test facility for solid-liquid flow studies using laser velocimetry and some initial results. Individual projects are processed separately for the data bases. DOE

N89-25415# Ricardo-ITI, Westmont, IL.
MULTIDIMENSIONAL MODELING OF CONVECTIVE HEAT TRANSFER WITH APPLICATION TO I.C. ENGINES Technical Progress Report
Mark J. Jennings and Thomas Morel 21 Apr. 1989 21 p
(Contract DE-AC04-86AL-33183)
(DE89-010651; DOE/AL-33183/T11) Avail: NTIS HC A03/MF A01

The objective of this project is to develop a more comprehensive understanding of the convective heat transfer process in complex, unsteady turbulent reacting flows, typical of those which occur in internal combustion engines. The specific area of research is the representation of heat transfer in detailed multi-dimensional Navier-Stokes models, and modeling of turbulent transport mechanisms. The detailed tasks include a review of relevant prior work. Based on this review, and original work done under this contract, several modeling approaches will be formulated and further studied and tested. The tests will be carried out on flow cases which have relevance to engine flows, and for which reliable experimental data exist. Such data will be sought and identified. The analytical studies will lead to the determination of the best modeling approaches to be used for heat transfer simulation in internal combustion engines. Following that, a detailed study will be carried out of spatial and temporal heat flux distribution in a representative engine. This will be complemented by a parametric study of engine heat transfer dependence on intake flow details, combustion chamber geometry, engine speed and engine load. DOE

N89-25416# Notre Dame Univ., IN. Dept. of Chemical Engineering.
PERIODIC AND SOLITARY WAVES ON THIN, HORIZONTAL, GAS-SHEARED LIQUID FILMS
L. A. Jurman, K. Bruno, and Mark J. McCready 1988 41 p Presented at the 2nd International Symposium on Annular and Dispersed Flows, Oxford, United Kingdom, 6 Sep. 1988
(Contract DE-FG02-88ER-13913)
(DE89-010655; CONF-8809335-1) Avail: NTIS HC A03/MF A01

Measurements of wavelengths and speeds of periodic waves which occur at the interface of thin, horizontal, liquid films sheared by a cocurrent gas flow are compared with predictions of linear theory. In general, linear predictions accurately match the data near the point of neutral stability but begin to deviate as the gas velocity increases. The behavior away from neutral stability is explained by the examination of the dynamical system associated with steady solutions to a nonlinear wave equation based on boundary-layer approximations. Periodic waves are seen to occur in the neighborhood of the Hopf curve which serves as a boundary between periodic waves and a flat film. Solitary waves (which correspond under some circumstances to disturbance or roll waves) are observed to lie in another region of parameter space at gas velocities well above neutral stability. These results suggest that a complete nonlinear analysis of the boundary-layer (or associated wave) equations would be useful for predicting amplitudes and speeds for periodic waves and the regions of occurrence for solitary waves. DOE

N89-25417# Massachusetts Inst. of Tech., Cambridge. Dept. of Chemical Engineering.
INTERFACIAL FLUID MECHANICS AND TRANSPORT PROCESSES
Gretchen M. Mavrovouniotis, Howard Brenner, Li Ting, and Darsh T. Wasan (Illinois Inst. of Tech., Chicago.) Jan. 1989 10 p Presented at the First Caribbean Conference on Fluid Dynamics, St. Augustine, Trinidad and Tobago, 8 Jan. 1989
(Contract DE-FG02-88ER-13896)
(DE89-010664; CONF-8901119-1) Avail: NTIS HC A02/MF A01

Macroscale interfacial conservation and constitutive equations, as well as expressions for the phenomenological functions appearing in the report, are derived for transport processes occurring in immiscible fluid-fluid systems possessing moving and deforming interfaces via a rigorous matched asymptotic expansion scheme from the more exact, continuous (diffuse) microscale equations underlying them. DOE

N89-25418# Fermi National Accelerator Lab., Batavia, IL.
AMPLITUDE GROWTH DUE TO RANDOM, CORRELATED KICKS
Leo Michelotti and Fred Mills Mar. 1989 5 p Presented at the 13th Particle Accelerator Conference, Chicago, IL, 20 Mar. 1989
(Contract DE-AC02-76CH-03000)
(DE89-011504; FNAL/C-89/93; CONF-890335-86) Avail: NTIS HC A02

Historically, stochastic processes, such as gas scattering or stochastic cooling, have been treated by the Fokker-Planck equation. In this approach, usually considered for one dimension

only, the equation can be considered as a continuity equation for a variable which would be a constant of the motion in the absence of the stochastic process, for example, the action variable, I = epsilon/2x for betatron oscillations, where epsilon is the area of the Courant-Snyder ellipse, or energy in the case of unbunched beams, or the action variable for phase oscillations in case the beam is bunched. A flux, Phi, including diffusive terms can be defined, usually to second order: Phi = M sub 1 F(I) + M(2) deltaF deltaI +. M(1) and M(2) are the expectation values of deltaI and (deltaI) sq due to the individual stochastic kicks over some period of time, long enough that the variance of these quantities is sufficiently small. Then the Fokker-Planck equation is just deltaF deltaI + delta Phi deltaI = 0. In many cases those where the beam distribution has already achieved its final shape, it is sufficient to find the rate of increase of (I) by taking simple averages over the Fokker-Planck equation. At the time this work was begun, there was good knowledge of the second moment for general stochastic processes due to stochastic cooling theory, but the form of the first moment was known only for extremely wideband processes. The purposes of this note are to derive an expression relating the expected single particle amplitude growth to the noise autocorrelation function and to obtain, thereby, the form of M(1) for narrow band processes. DOE

N89-25419# Lawrence Livermore National Lab., CA.
COMPARISON OF EXPERIMENTAL SHOCK-WAVE PROFILES FOR TUNGSTEN AND COMPUTER SIMULATIONS USING A RATE-DEPENDENT CONSTITUTIVE MODEL
Daniel J. Steinberg Dec. 1988 13 p Presented at the 3rd International Symposium on Behavior of Media Under High Dynamic Pressures, La Grande Motte, France, 5-9 Jun. 1989
(Contract W-7405-eng-48)
(DE89-006158; UCRL-100168; CONF-890661-3) Avail: NTIS HC A03/MF A01

The Steinberg-Guinan-Lund, rate-dependent, constitutive model for Ta has been applied to W. Computer simulation successfully predicts the elastic precursor ahead of the second shock in a series of double-shock experiments. Based on the Cochran-Banner spall model, the spall strength of W is 0.9 + or - 0.1 GPa, independent of loading stress from 10 to 200 GPa. The model provides an explanation of why some quasi-isentropes appear stiffer than the principal Hugoniot. DOE

N89-25420# Sandia National Labs., Albuquerque, NM.
COUPLING OF THE BOUNDARY ELEMENT METHOD WITH AN INTEGRAL MOMENTUM BOUNDARY-LAYER TECHNIQUE TO CALCULATE FORCES AND MOMENTS ON THREE-DIMENSIONAL BODIES
C. E. Hailey, M. S. Ingber (New Mexico Univ., Albuquerque.), and E. L. Tadios 1989 20 p Presented at the 4th International Conference on Boundary Elements, Windsor, Ontario, 6 Jun. 1989
(Contract DE-AC04-76DP-00789)
(DE89-006328; SAND-88-2115C; CONF-890677-1) Avail: NTIS HC A03/MF A01

The direct boundary element method is used to calculate the potential flow about bodies of complex geometry in a uniform stream at arbitrary angles of attack. The solution makes use of the double-node concept to improve the quality of the solution in regions with corners and reentrant boundaries. The boundary element method is coupled to an integral momentum boundary-layer solution which accounts for laminar and turbulent boundary layers and the effects of surface roughness. Axial force predictions are compared with experimental data for several shapes and show good agreement. Pitching moment and normal force calculations on axisymmetric and three-dimensional bodies also show agreement with experiment for small angles of attack. DOE

N89-25421# Lawrence Livermore National Lab., CA.
ADAPTIVE MESH REFINEMENT ON MOVING QUADRILATERAL GRIDS
John B. Bell, Phillip Colella, John A. Trangenstein, and Michael Welcome Apr. 1989 12 p Presented at the 9th American Institute of Aeronautics and Astronautics (AIAA), Computational Fluid Dynamics Conference, Buffalo, NY, 14-16 Jun. 1989
(Contract W-7405-eng-48)
(DE89-010241; UCRL-100880; CONF-8906111-2) Avail: NTIS HC A03/MF A01

This paper describes an adaptive mesh refinement algorithm for unsteady gas dynamics. The algorithm is based on an unsplit, second-order Godunov integration scheme for logically-rectangular moving quadrilateral grids. The integration scheme is conservative and provides a robust, high resolution discretization of the equations of gas dynamics for problems with strong nonlinearities. The integration scheme is coupled to a local adaptive mesh refinement algorithm that dynamically adjusts the location of refined grid patches to preserve the accuracy of the solution, preserving conservation at interfaces between coarse and fine grids while adjusting the geometry of the fine grids so that grid lines remain smooth under refinement. Numerical results are presented illustrating the performance of the algorithm. DOE

N89-25422*# Wright State Univ., Dayton, OH.
ANALYSIS OF THE TRANSIENT COMPRESSIBLE VAPOR FLOW IN HEAT PIPE Final Report
Jong Hoon Jang, Amir Faghri, and Won Soon Chang Jul. 1989 10 p Presented at the 26th National Heat Transfer Conference, Philadelphia, PA, 6-9 Aug. 1989; sponsored in part by the ASME Prepared in cooperation with Air Force Systems Command, Wright-Patterson AFB, OH
(Contract F33615-88-C-2820)
(NASA-CR-185119; E-4945; NAS 1.26:185119) Avail: NTIS HC A02/MF A01 CSCL 20D

The transient compressible one-dimensional vapor flow dynamics in a heat pipe is modeled. The numerical results are obtained by using the implicit non-iterative Beam-Warming finite difference method. The model is tested for simulated heat pipe vapor flow and actual flow in cylindrical heat pipes. A good comparison of the present transient results for the simulated heat pipe vapor flow with the previous results of a two-dimensional numerical model is achieved and the steady state results are in agreement with the existing experimental data. The transient behavior of the vapor flow under subsonic, sonic, and supersonic speeds and high mass flow rates are successfully predicted. The one-dimensional model also describes the vapor flow dynamics in cylindrical heat pipes at high temperatures. Author

N89-25423# Technische Univ., Delft (Netherlands).
A VARIATIONALLY OPTIMIZED VORTEX TRACING ALGORITHM FOR THREE-DIMENSIONAL FLOWS AROUND SOLID BODIES Ph.D. Thesis
Jacobus Jozef Wilhel vanderVegt 1988 169 p Original contains color illustrations
(ETN-89-94301) Avail: NTIS HC A08/MF A01

The construction of vortex models for two and three-dimensional viscous flows around solid bodies is addressed. A Lagrangian formulation of the inviscid vorticity transport equation is treated using a flow map. This formulation can be converted into a Hamiltonian description which is used in the definition and proof of convergence of a stochastic algorithm for the solution of the viscous vorticity transport equation. Numerical algorithms for the solution of two-dimensional flow fields and for the solution of the three-dimensional flow field around a circular cylinder using the Lagrangian functional are presented. Forces on a body in a viscous fluid are determined. The initial stage of the wake of an impulsively started cylinder; the vortex formation around cylinders in steady flow or oscillating harmonically; and the forces on cylinders in these flows are calculated. Test results of the numerical algorithm for the determination of the vector stream function for the three-dimensional flow field around a circular cylinder are discussed. ESA

N89-25424# Max-Planck-Institut fuer Stroemungsforschung, Goettingen (Germany, F.R.).
A QUALITATIVE NUMERICAL ANALYSIS OF SOME FEATURES OF PROPAGATION OF COUNTERFLOW TEMPERATURE WAVES IN SUPERFLUID HELIUM
W. Fiszdon, J. Piechna (Polish Academy of Sciences, Warsaw.), and W. Poppe Jun. 1988 54 p
(MPIS-9/1988; ISSN-0436-1199; ETN-89-94386) Avail: NTIS HC A04/MF A01; Max-Planck Institut fuer Stroemungsforschung, Boettinger Strasse 6, 3400 Goettingen, Fed. Republic of Germany, 17DM

A theoretical model taking into account the existence of superfluid vorticity is deduced using the extended vortex line density evolution relation of Vinen with an additional divergence term to include the effect of the vortex tangle displacement. The Gorter-Mellink form of the interaction force in homogeneous superfluid turbulent flow is used. A Lax-Wendroff numerical scheme was adapted to solve the resulting set of nonlinear partial differential equations. The calculated cases of evolution of a nonturbulent axisymmetric heat pulse and of a plane strong heat pulse with turbulence generation show a fair qualitative agreement with experimental results. The possible mechanism of building up of a hot superfluid turbulence layer is shown. ESA

N89-25425# Kernforschungszentrum G.m.b.H., Karlsruhe (Germany, F.R.). Inst. fuer Neutronenphysik und Reaktortechnik.
HEAT TRANSFER IN PACKED BEDS Thesis - Karlsruhe Univ.
Giancarlo Sordon Sep. 1988 110 p In GERMAN; ENGLISH summary
(KfK-4451; ISSN-0303-4003; ETN-89-94404) Copyright Avail: NTIS HC A06/MF A01

The design of a fusion reactor blanket concept based on a bed of lithium containing ceramic pebbles or a mixture of ceramic and beryllium pebbles is studied. Effective thermal conductivity of pebble beds, including beds formed by a binary mixture of high conducting metallic pebbles and poorly conducting pebbles is analyzed. Binary mixtures of spheres of same diameter and different conductivities as well as beds formed by one type of spheres were investigated. The experimental apparatus consists of a stainless steel cylinder with a heating rod along the symmetry axis. Experiments with stagnant and flowing gas were performed. The pebbles are of Al2O3 (diameter 1, 2, 4 mm), Li4SiO4 (diameter 0.5 mm), Al (diameter 2 mm) and steel (diameter 2, 4 mm). Experimental values of the thermal conductivity and of the wall heat transfer coefficient are compared with the predicted ones. ESA

N89-25426# Max-Planck-Institut fuer Stroemungsforschung, Goettingen (Germany, F.R.).
EXPERIMENTAL INVESTIGATION ON TRANSCRITICAL HEAT TRANSFER IN He 2
Martin vonSchwerdtner and E.-A. Mueller, ed. 1988 88 p In GERMAN; ENGLISH summary
(MPIS-Mitt-90; ISSN-0374-1257; ETN-89-94566) Avail: NTIS HC A05/MF A01

The propagation of plane second-sound waves was investigated in a quadratic channel of 2.6 x 2.6 cm cross section and 8 cm length. The evolution of temperature, counterflow velocity, and superfluid vortex-line density was measured. The heat flux released from the film heater at the botton of the channel was varied, covering the region where superfluid vortex lines are produced affecting the flow. Beside the temperature of the helium bath (1.4 to 2.1 K), the pulse repetition rate was varied. In agreement with theories, the initial value of the vortex-line density remaining from the previous heat pulse increases, induced by the counterflow velocity. If during the passage of the pulse enough vortex lines are produced, the mutual friction force leads to a decrease of the counterflow velocity and hence of the heat flux. Then near the heater the energy is stored leading to a large rise in temperature instead of being transported by the second-sound wave. A criterion for the occurrence of supercritical heat transport was derived, taking into account bath temperature, pulse duration, heat flux and, in addition, the repetition rate, thus leading to a better approach to the measured values than current theories. ESA

N89-25427# Kernforschungszentrum G.m.b.H., Karlsruhe (Germany, F.R.). Inst. fuer Reaktorbauelemente.
GAS-LIQUID FLOW IN DIVIDING TEE-JUNCTIONS WITH A HORIZONTAL INLET AND DIFFERENT BRANCH ORIENTATIONS AND DIAMETERS
J. Reimann, H. J. Brinkmann, and R. Domanski (Technical Univ. of Warsaw, Poland) Dec. 1988 247 p
(KfK-4399; ISSN-0303-4003; ETN-89-94591) Copyright Avail: NTIS HC A11/MF A01

A data base summarizing experiments on the phase redistribution and pressure differences for a gas-liquid mixture flowing through the horizontal inlet pipe (diameter D1 = 50 mm) of a Tee-junction is presented. Branch to inlet diameter ratios of D3/D1 = 1; 0.52; 0.2; and 0.08 were investigated. The branch orientation was horizontal, vertical upward, or vertical downward. Mostly air-water experiments were performed with pressures between 0.4 and 1 MPa. Experiments with steam-water flows at pressures between 1.5 and 10 MPa were performed for D3/D1 = 1 and a horizontal branch. The results on phase redistribution and pressure drop are compared with other experimental data and model predictions. The data base for Tee-junctions pressure differences is much more limited. Most experiments were performed with a horizontal branch and D3/D1 = 1. A comparison of different models with results for D3/D1 = 0.52 and 1 is presented. No model gives satisfactory results for arbitrary conditions. ESA

N89-25428# Kernforschungszentrum G.m.b.H., Karlsruhe (Germany, F.R.). Inst. fuer Neutronenphysik und Reaktortechnik.
EXPERIMENTAL STUDY OF THE PHENOMENA OF TURBULENT FLOW IN THE NARROW GAPS BETWEEN SUBCHANNELS OF ROD BUNDLES Thesis - Karlsruhe Univ.
S. V. Moeller (Comissao Nacional de Energia Nuclear de Brasil, Rio de Janeiro.) Jan. 1989 187 p In GERMAN; ENGLISH summary
(KfK-4501; ISSN-0303-4003; ETN-89-94594) Copyright Avail: NTIS HC A09/MF A01

Turbulent intensities in the narrow gaps between the subchannels of rod bundles strongly anisotropic and higher than in pipes are studied. Experiments are performed in rod bundles with different pitch-to-diameter (P/D) and wall-to-diameter (W/D) ratios. Two components of the fluctuating velocity are measured with hot wires simultaneously at two different locations of a wall subchannel, together with the pressure fluctuations at the wall measured by microphones. The output signals are registered with an analog tape recorder, digitized, and evaluated to obtain spectra as well as auto and cross correlations. The results indicate interdependence between pressure and velocity fluctuations. Analysis of turbulence spectra and the identification of their specific ranges is performed. The dominant frequency of the turbulent motion, taken from the spectra, is found to be a function of the gap width and of the flow velocity. The corresponding Strouhal number is a geometrical parameter which can be expressed in terms of P/D and W/D. A model is developed to describe the formation of large eddies near the gaps and their effect on the fluid motion through rod bundles. The relationship between the mixing process and the studied phenomemon was determined. ESA

N89-25429# Deutsche Forschungs- und Versuchsanstalt fuer Luft- und Raumfahrt, Stuttgart (Germany, F.R.). Inst. fuer Technische Thermodynamik.
STUDY ON THERMODYNAMICAL AND MECHANICAL CONDITIONS FOR PUMPING LOW FLOW RATES OF LIQUEFIED GASES TO HIGH PRESSURE LEVEL Ph.D. Thesis - Stuttgart Univ.
Willi Nieratschker Dec. 1988 148 p In GERMAN; ENGLISH summary
(DFVLR-FB-88-54; ISSN-0171-1342; ETN-89-94640) Avail: NTIS

HC A11/MF A01; DFVLR, VB-PL-DO, Postfach 90 60 58, 5000 Cologne, Fed. Republic of Germany, DM 51

High pressure cryogenic liquid pumps handling low boiling liquids are investigated in the very low mass flow range. The cavitation problem becomes predominant with lower pump capacities caused by the increasing ratio of heat loss to the pump capacity. Based on a mechanical design study, a prototype for low flow rates was developed. The amount of incoming heat from the environment and the sealing problems of the reciprocating piston against high pressure are the main problems. A new lifting pump concept and a patented construction promise to offer solutions and further essential advantages. The prototype is operable without being submerged in the cryogenic liquid and has a short instationary cooling period. The realization of single-staged high pressure cryogenic liquid pumps for low mass flow rates is demonstrated. The prevention of cavitation caused by frictional heat between reciprocating piston and cylinder is neither possible nor necessary. ESA

N89-25430# Deutsche Forschungs- und Versuchsanstalt fuer Luft- und Raumfahrt, Goettingen (Germany, F.R.). Gruppe Transition und Turbulenz.

NUMERICAL SIMULATION OF TRANSITION FROM LAMINAR TO TURBULENT CHANNEL FLOW Ph.D. Thesis - Karlsruhe Univ.

Norbert Gilbert Mar. 1988 148 p In GERMAN; ENGLISH summary Report will also be announced as translation (ESA-TT-1144) Original contains color illustrations

(DFVLR-FB-88-55; ISSN-0171-1342; ETN-89-94641) Avail: NTIS HC A07/MF A01; DFVLR, VB-PL-DO, Postfach 90 60 58, 5000 Cologne, Fed. Republic of Germany, DM 50.50

Laminar-turbulent transition in plane channel flow beginning with Tollmien-Schlichting waves is simulated numerically up to fully developed turbulence. The three-dimensional incompressible Navier-Stokes equations are solved by a spectral method. The model of spatially periodic disturbances developing in time is used. Results of a simulation with up to 128 cubed gridpoints are given and compared with experiment data. Good agreement with experiments is found in the transitional as well as in the turbulent stage. A transition function for use in modified algebraic turbulence models is derived from the simulation data. Model assumptions used in conventional turbulence models are tested and discussed on the basis of the numerical results obtained in the fully developed turbulent stage. ESA

N89-25899# Cambridge Univ. (England). Dept. of Applied Mathematics and Theoretical Physics.

TOWARDS AN INDEPENDENT CALIBRATION OF THE MIXING-LENGTH THEORY

P. D. Tooth and Douglas O. Gough *In* ESA, Seismology of the Sun and Sun-Like Stars Dec. 1988 p 463-469 (For primary document see N89-25819 19-92)

Copyright Avail: NTIS HC A99/MF E03

35 INSTRUMENTATION AND PHOTOGRAPHY

Includes remote sensors; measuring instruments and gages; detectors; cameras and photographic supplies; and holography.

For aerial photography see *43 Earth Resources and Remote Sensing.* For related information see also *06 Aircraft Instrumentation,* and *19 Spacecraft Instrumentation.*

N89-25431*# New Technology, Inc., Huntsville, AL.

NEW ATMOSPHERIC SENSOR ANALYSIS STUDY Final Report

K. G. Parker 23 Feb. 1989 21 p

(Contract NAS8-36179)

(NASA-CR-183597; NAS 1.26:183597) Avail: NTIS HC A03/MF A01 CSCL 14B

The functional capabilities of the ESAD Research Computing Facility are discussed. The system is used in processing atmospheric measurements which are used in the evaluation of sensor performance, conducting design-concept simulation studies, and also in modeling the physical and dynamical nature of atmospheric processes. The results may then be evaluated to furnish inputs into the final design specifications for new space sensors intended for future Spacelab, Space Station, and free-flying missions. In addition, data gathered from these missions may subsequently be analyzed to provide better understanding of requirements for numerical modeling of atmospheric phenomena. Author

N89-25432*# Connecticut Univ., Storrs. Dept. of Mechanical Engineering and Physics.

X-RAY BASED EXTENSOMETRY Final Report, 15 Dec. 1987 - 15 Dec. 1988

E. H. Jordan and D. M. Pease Dec. 1988 26 p

(Grant NAG3-854)

(NASA-CR-185058; NAS 1.26:185058) Avail: NTIS HC A03/MF A01 CSCL 14B

A totally new method of extensometry using an X-ray beam was proposed. The intent of the method is to provide a non-contacting technique that is immune to problems associated with density variations in gaseous environments that plague optical methods. X-rays are virtually unrefractable even by solids. The new method utilizes X-ray induced X-ray fluorescence or X-ray induced optical fluorescence of targets that have melting temperatures of over 3000 F. Many different variations of the basic approaches are possible. In the year completed, preliminary experiments were completed which strongly suggest that the method is feasible. The X-ray induced optical fluorescence method appears to be limited to temperatures below roughly 1600 F because of the overwhelming thermal optical radiation. The X-ray induced X-ray fluorescence scheme appears feasible up to very high temperatures. In this system there will be an unknown tradeoff between frequency response, cost, and accuracy. The exact tradeoff can only be estimated. It appears that for thermomechanical tests with cycle times on the order of minutes a very reasonable system may be feasible. The intended applications involve very high temperatures in both materials testing and monitoring component testing. Gas turbine engines, rocket engines, and hypersonic vehicles (NASP) all involve measurement needs that could partially be met by the proposed technology. Author

N89-25433*# National Aeronautics and Space Administration. Langley Research Center, Hampton, VA.

A SLOW POSITRON BEAM GENERATOR FOR LIFETIME STUDIES

Jag J. Singh, Abe Eftekhari (Analytical Services and Materials, Inc., Hampton, VA.), and Terry L. St.Clair Apr. 1989 15 p

(NASA-TM-101590; NAS 1.15:101590) Avail: NTIS HC A03/MF A01 CSCL 14B

A slow positron beam generator using well-annealed polycrystalline tungsten moderators and a Na-22 positron source was developed. A 250 micro c source, deposited on a 2.54 micron thick aluminized mylar, is sandwiched between two (2.54 cm x 2.54 cm x 0.0127 cm) tungsten pieces. Two (2.54 cm x 2.54 cm x t cm) test polymer films insulate the two tungsten moderator pieces from the aluminized mylar source holder (t=0.00127 to 0.0127). A potential difference of 10 to 100 volts--depending on the test polymer film thickness (t)--is applied between the tungsten pieces and the source foil. Thermalized positrons diffusing out of the moderator pieces are attracted to the source foil held at an appropriate potential below the moderator pieces. These positrons have to pass through the test polymer films before they can reach the source foil. The potential difference between the moderator pieces and the aluminized mylar is so adjusted as to force the positrons to stop in the test polymer films. Thus the new generator becomes an effective source of positrons for assaying thin polymer films for their molecular morphology. Author

N89-25434# Central Inst. of Physics, Bucharest (Romania).

OPTICAL INFORMATION PROCESSING AND HOLOGRAPHY

V. I. Vlad, N. Ionescu-Pallas, S. Popa, and I. Apostol Mar. 1988 25 p In ROMANIAN; ENGLISH summary
(DE88-706011; ICEFIZ-LOP-62-1988) Avail: NTIS (US Sales Only) HC A03/MF A01

Some of the results in the optical information processing and holography are presented. DOE

N89-25435*# Lowell Observatory, Flagstaff, AZ.
THE 2060 CHIRON: CCD PHOTOMETRY
Schelte J. Bus, Edward Bowell, and Alan W. Harris (Jet Propulsion Lab., California Inst. of Tech., Pasadena.) 1987 26 p Submitted for publication
(Grant NsG-7500)
(NASA-CR-185068; NAS 1.26:185068) Avail: NTIS HC A03/MF A01 CSCL 14E

R-band CCD photometry of 2060 was carried out on nine nights in Nov. and Dec. 1986. The rotation period is 5.9181 + or - 0.0003 hr and the peak to peak lightcurve amplitude is 0.088 + or - 0.0003 mag. Photometric parameters are H sub R = 6.24 + or - 0.02 mag and G sub R = + or - 0.15, though formal errors may not be realistic. The lightcurve has two pairs of extrema, but its asymmetry, as evidenced by the presence of significant odd Fourier harmonics, suggests macroscopic surface irregularities and/or the presence of some large scale albedo variegation. The observational rms residual is + or - 0.015 mag. On time scales from minutes to days there is no evidence for nonperiodic (cometary) brightness changes at the level of a few millimagnitudes. Author

N89-25436# Joint Inst. for Nuclear Research, Dubna (USSR).
DIGITAL DYNAMIC AMPLITUDE-FREQUENCE SPECTRAL ANALYZER
V. A. Kalinnikov 1988 14 p In RUSSIAN; ENGLISH summary Submitted for publication
(DE88-706256; JINR-R-10-88-275) Avail: NTIS (US Sales Only) HC A03/MF A01

A software and hardware for the digital dynamic spectral analysis realization is described. A new method of recurrent calculation of spectral coefficients is proposed. The analyzer is made in the CAMAC standard. ECL, TTL J C (297 chips) are used as an element base. Time for calculation of 16 coefficients of spectral density is 30 microsecs. DOE

N89-25437# Joint Inst. for Nuclear Research, Dubna (USSR). Lab. of Nuclear Problems.
SEARCH THE SPECTROMETRIC CHARACTERISTICS OF MICROCHANNEL PLATE PHOTOMULTIPLIERS
J. Wawryszczuk, M. Lewandowski, I. A. Yutlandov, A. I. Ivanov, G. A. Isaakyan, and I. F. Uchevatkin 1988 8 p In RUSSIAN; ENGLISH summary
(DE88-706260; JINR-R-13-88-278) Avail: NTIS (US Sales Only) HC A02/MF A01

Several photomultipliers based on microchannel plates have been investigated. Their high time characteristics are proved. The photomultipliers of this type are shown to have a satisfactory energy resolution. DOE

N89-25438# Sandia National Labs., Albuquerque, NM. Intelligent Machine Principles Div.
INITIAL DESIGN AND ANALYSIS OF A CAPACITIVE SENSOR FOR SHEAR AND NORMAL FORCE MEASUREMENT
J. L. Novak 20 Oct. 1988 18 p Presented at the International Conference on Robotics and Automation, Scottsdale, AZ, 14 May 1989
(Contract DE-AC04-76DP-00789)
(DE89-001821; SAND-88-2793C; CONF-890522-3) Avail: NTIS HC A03/MF A01

Initial experiments characterizing a shunt-mode sensor that simultaneously measures both normal and shear strains due to an applied force vector have been completed. The sensor, termed SCCINSS (Sensed Capacitance Changes due to Incident Normal and Shear Stresses), is based upon variations in the physical dimensions of an elastic dielectric due to applied forces. Two sinusoids of the same frequency, but with a fixed phase relationship are used to excite the device. The amplitude and phase of the output signal are modulated by normal and shear strains, respectively. By measuring the amplitude and phase of the output signal, these strains may be determined, and subsequently used to reconstruct the normal and shear components of the force vector. DOE

N89-25439# Sandia National Labs., Albuquerque, NM.
PRESSURE CALIBRATION AND CERTIFICATION OF A QUARTZ PRESSURE TRANSDUCER
Sharon Husa 1988 13 p Presented at the 35th International Instrumentation Symposium, Orlando, FL, 30 May 1989
(Contract DE-AC04-76DP-00789)
(DE89-005774; SAND-88-2697C; CONF-890589-1) Avail: NTIS HC A03/MF A01

The calibration and certification of a 0 to 15 psia microprocessor controlled quartz pressure transducer using an air piston gage primary standard is discussed. The calibration includes a discussion of the primary standard, setup of the test, and data acquisition and reduction. The certification includes the establishment of a total calibration uncertainty for the device and an interval over which the certification is valid. Factors contributing to the total calibration uncertainty of a device include the systematic uncertainties of the calibration equipment, history of the device itself, and history of similar devices. Typical systematic uncertainties of the calibration system are on the order of 0.011 percent and the typical total uncertainty assigned to the transducer is less than 0.030 percent over a one-year interval. DOE

N89-25440# Sandia National Labs., Albuquerque, NM.
IDENTIFICATION OF ERROR SOURCES IN SHOCK DATA
Thomas J. Baca and R. Glenn Bell 1988 25 p Presented at the 35th Annual Technical Meeting of the Institute of Environmental Sciences: Building Tomorrow's Environment, Anaheim, CA, 1 May 1989
(Contract DE-AC04-76DP-00789)
(DE89-007655; SAND-88-2530C; CONF-890592-3) Avail: NTIS HC A03/MF A01

Instrumentation error sources are frequently encountered during the measurement of mechanical shock transients. This paper investigates the effects of two common errors: zero shifts and noise spikes. Non-trivial frequency domain manifestations of these errors are noted. Effective methods of identifying these errors are introduced and demonstrated. The significance of the problem is founded on the implications which these errors have on the subsequent analysis of the data using shock response spectra. DOE

N89-25441# Sandia National Labs., Albuquerque, NM.
AUTOMATED TEST AND EVALUATION CENTER FOR WAVEFORM DIGITIZER SYSTEMS AND COMPONENTS
Philip J. Green 1989 16 p Presented at the IMTC Conference, Washington, DC, 25 Apr. 1989
(Contract DE-AC04-76DP-00789)
(DE89-010226; SAND-89-1073C; CONF-8904116-2) Avail: NTIS HC A03/MF A01

In our instrumentation development efforts we find it necessary to be able to evaluate the performance of waveform digitizing systems with sampling rates from a few kilohertz to more than a gigahertz. Our goal has been to develop an integrated system which can provide quantitative results on the performance of systems and subsystems. Here we describe a system which is controlled by a Microvax II with instrumentation control through the IEEE-488 buss. The evaluation procedure is delineated in reference to a Trial Waveform Digitizer Standard generated by the Waveform Measurements and Analysis committee appointed by the Instrumentation and Measurement Society of IEEE. The standard has been recently accepted by the IEEE and will become a published standard. In this work, special focus is given to the accurate measurement of effective-bit performance and differential nonlinearity of waveform digitizers. DOE

N89-25442# West Virginia Univ., Morgantown.
AN INDUCTIVELY COUPLED PLASMA SPECTROMETER FOR ON-LINE, REAL-TIME PROCESS GAS ANALYSIS Ph.D. Thesis
Donald Lyle McCarty, II 1988 139 p Prepared in cooperation with Oak Ridge Associated Universities, Inc., TN
(Contract DE-AC05-76OR-00033)
(DE89-010610; DOE/OR-00033/T422) Avail: NTIS HC A07/MF A01

On-line, real-time analysis of process gas streams, such as gasification and combustion processes, is becoming increasingly important. This dissertation describes an inductively coupled plasma spectrometer capable of analyzing for trace metals in particulate laden process gases that are injected directly into the ICP torch at high temperatures (500 C) and at high sample flow rates necessary to maintain large particulate (10 to 20 micron) entrainment between the process sampling point and the plasma. The system uses a mixed gas argon-helium plasma, and use of the argon-helium plasma as opposed to a nitrogen, oxygen, or air plasma is defended. Characteristics of argon-helium and helium plasmas operated at very high RF forward energy levels are discussed and compared to the characteristics of an argon plasma operated under normal ICP conditions. Also presented are results of actual on-line testing of the ISP, some detection limits determined for elements in process gas types of streams, and the best emission lines to use for elements in process gas streams. DOE

N89-25443*# National Aeronautics and Space Administration. Langley Research Center, Hampton, VA.
AUTOMATED THERMAL MAPPING TECHNIQUES USING CHROMATIC IMAGE ANALYSIS
Gregory M. Buck Apr. 1989 17 p
(NASA-TM-101554; NAS 1.15:101554) Avail: NTIS HC A03/MF A01 CSCL 14B

Thermal imaging techniques are introduced using a chromatic image analysis system and temperature sensitive coatings. These techniques are used for thermal mapping and surface heat transfer measurements on aerothermodynamic test models in hypersonic wind tunnels. Measurements are made on complex vehicle configurations in a timely manner and at minimal expense. The image analysis system uses separate wavelength filtered images to analyze surface spectral intensity data. The system was initially developed for quantitative surface temperature mapping using two-color thermographic phosphors but was found useful in interpreting phase change paint and liquid crystal data as well. Author

N89-25444*# North Carolina Univ., Charlotte. Dept. of Mechanical Engineering.
MAGNETO-INDUCTIVE SKIN SENSOR FOR ROBOT COLLISION AVOIDANCE: A NEW DEVELOPMENT Annual Report
D. S. Chauhan and Paul H. DeHoff 1989 12 p
(Grant NAG5-1053)
(NASA-CR-185402; NAS 1.26:185402) Avail: NTIS HC A03/MF A01 CSCL 14B

Safety is a primary concern for robots operating in space. The tri-mode sensor addresses that concern by employing a collision avoidance/management skin around the robot arms. This rf-based skin sensor is at present a dual mode (proximity and tactile). The third mode, pyroelectric, will complement the other two. The proximity mode permits the robot to sense an intruding object, to range the object, and to detect the edges of the object. The tactile mode permits the robot to sense when it has contacted an object, where on the arm it has made contact, and provides a three-dimensional image of the shape of the contact impression. The pyroelectric mode will be added to permit the robot arm to detect the proximity of a hot object and to add sensing redundancy to the two other modes. The rf-modes of the sensing skin are presented. These modes employ a highly efficient magnetic material (amorphous metal) in a sensing technique. This results in a flexible sensor array which uses a primarily inductive configuration to permit both capacitive and magnetoinductive sensing of object; thus optimizing performance in both proximity and tactile modes with the same sensing skin. The fundamental operating principles, design particulars, and theoretical models are provided to aid in the description and understanding of this sensor. Test results are also given. Author

N89-25445# Edgerton, Germeshausen and Grier, Inc., Idaho Falls, ID.
DESIGN AND TESTING OF THE EG AND G/LOS ALAMOS OPERATIONS FAST STREAK CAMERA
J. Rohrer Feb. 1989 16 p Prepared in cooperation with Los Alamos National Lab., NM
(Contract DE-AC08-88NV-10617)
(DE89-010859; EGG-10617-5010) Avail: NTIS HC A03/MF A01

In anticipation of requirements from groups P-14 and P-15 of the Los Alamos National Laboratory, EG and G Energy Measurements/Los Alamos Operations (LAO) designed a fast streak camera around the ITT F4157 large-format streak tube. This camera has special features that make it well suited to the Nevada Test Site (NTS) field environment. In addition, the project capitalized on knowledge dearly won in LAO's streak camera work of recent years. DOE

N89-25446# Joint Inst. for Nuclear Research, Dubna (USSR). Lab. of Nuclear Reactions.
ION OPTICS OF LIDIA MASS-SPECTROMETER
S. V. Stepantsov, A. M. Rodin, and G. M. Ter-Akopyan 1988 10 p In RUSSIAN; ENGLISH summary
(DE88-706335; JINR-R-13-88-153) Avail: NTIS (US Sales Only) HC A02/MF A01

The ion-optical characteristics of the ultrasensitive mass-spectrometer LIDIA designed to search for superheavy elements (A greater than 250) using a laser ion source and a multistage separation system have been calculated. The mass-spectrometer is under construction at the Joint Institute for Nuclear Research. The results are compared with the experimental data. DOE

N89-25447# Los Alamos National Lab., NM.
SUPERLATTICE STRAIN GAGE Patent Application
Bruce W. Noel, inventor (to DOE), Darryl L. Smith, inventor (to DOE), and Dipen N. Sinha, inventor (to DOE) 28 Jun. 1988 24 p
(Contract W-7405-eng-36)
(DE89-011805; PATENTS-US-A7212854; US-Patent-Appl-SN-212854) Avail: NTIS HC A03/MF A01

A strain gage comprising a strained-layer superlattice crystal exhibiting piezoelectric properties is described. A substrate upon which such a strained-layer superlattice crystal has been deposited is attached to an element to be monitored for strain. A light source is focused on the superlattice crystal and the light reflected from, passed through, or emitted from the crystal is gathered and compared with previously obtained optical property data to determine the strain in the element. DOE

N89-25448# Deutsche Forschungs- und Versuchsanstalt fuer Luft- und Raumfahrt, Oberpfaffenhofen (West Germany). Abteilung HF-Physik.
SYNCHRONIZATION OF THE GROUND STATION ATOMIC CLOCKS USING WEIGHTED TRANSPORTABLE CESIUM TIME STANDARDS IN THE NAVIGATION EXPERIMENT (NAVEX)
Herbert Schild Jul. 1988 38 p In GERMAN; ENGLISH summary
(DFVLR-Mitt-89-01; ISSN-0176-7739; ETN-89-94647) Avail: NTIS HC A03/MF A01; DFVLR, VB-PL-DO, Postfach 90 60 58, 5000 Cologne, Federal Republic of Germany, 15.50 deutsche marks

In the NAVEX experiment performed during the spacelab mission D1 time signals were transmitted from on-board the Spacelab to three ground stations. These stations were equipped with a cesium time standard each. Some aims of the NAVEX experiment required the ground station clocks to be synchronized. Two two-way clock transportations enabled this synchronization.

On these clock travels three weighted transportable cesium clocks were employed. Using the UTC(PTB) as a reference time scale, the method of deriving the weighting factors from the clock rates at rest, as well as from the clock rates on the voyage, is shown. ESA

N89-25227*# Jet Propulsion Lab., California Inst. of Tech., Pasadena. Applied Technologies Section.
OPTIMAL PLACEMENT OF EXCITATIONS AND SENSORS BY SIMULATED ANNEALING
Moktar Salama, R. Bruno, G.-S. Chen, and J. Garba *In* NASA. Langley Research Center, Recent Advances in Multidisciplinary Analysis and Optimization, Part 3 Apr. 1989 p 1441-1457 (For primary document see N89-25201 19-05)
Avail: NTIS HC A22/MF A01 CSCL 14B

N89-25854# National Solar Observatory, Tucson, AZ.
THE GONG INSTRUMENT
J. W. Harvey, K. Abdel-Gawad, Warren Ball, B. Boxum, F. Bull, J. Cole, L. Cole, S. Colley, K. Dowdney, and R. Drake et al *In* ESA, Seismology of the Sun and Sun-Like Stars Dec. 1988 p 203-208 (For primary document see N89-25819 19-92)
Copyright Avail: NTIS HC A99/MF E03

N89-25857# Birmingham Univ. (England). School of Physics and Space Research.
A DETECTOR OF SMALL GRADIENTS OF TRANSPARENCY OF THE TERRESTRIAL ATMOSPHERE
D. B. McLeod and G. R. Isaak *In* ESA, Seismology of the Sun and Sun-Like Stars Dec. 1988 p 223-225 (For primary document see N89-25819 19-92)
Copyright Avail: NTIS HC A99/MF E03

N89-25858*# Johns Hopkins Univ., Laurel, MD. Applied Physics Lab.
THE STABLE SOLAR ANALYZER
D. M. Rust and T. Appourchaux (Centre National de la Recherche Scientifique, Verrieres-Le Buisson, France) *In* ESA, Seismology of the Sun and Sun-Like Stars Dec. 1988 p 227-233 (For primary document see N89-25819 19-92)
(Grants NAGw-522; AF-AFOSR-0077-87)
Copyright Avail: NTIS HC A99/MF E03 CSCL 14B

N89-25926# Rome Univ. (Italy).
A PROTOTYPE STELLAR PHOTOMETER FOR MAGNETIC FIELD AND DOPPLER MEASUREMENTS
Alessandro Cacciani, S. Catalano, M. Rodono, and G. Costa (Catania Astrophysical Observatory, Italy) *In* ESA, Seismology of the Sun and Sun-Like Stars Dec. 1988 p 601-603 Sponsored by Italian Ministry of Public Education, Rome, Italy and Piano Spaziale Nazionale, Rome, Italy (For primary document see N89-25819 19-92)
Copyright Avail: NTIS HC A99/MF E03

N89-25927# Nice Univ. (France). Dept. d'Astrophysique.
THE NICE UNIVERSITY STELLAR SEISMOMETER
F. X. Schmider, Eric Fossat, Gerard Grec, and B. Gelly *In* ESA, Seismology of the Sun and Sun-Like Stars Dec. 1988 p 605-607 (For primary document see N89-25819 19-92)
Copyright Avail: NTIS HC A99/MF E03

36 LASERS AND MASERS

Includes parametric amplifiers.
For related information see also *76 Solid-State Physics*.

N89-25449# Central Inst. of Physics, Bucharest (Romania).
BISTABILITY IN A LASER WITH INJECTED SIGNAL
I. A. Dorobantu, V. I. Vlad, and I. Ursu Apr. 1987 34 p
(DE88-706003; ICEFIZ-FT-305-1987) Avail: NTIS (US Sales Only) HC A03/MF A01

A unified description of bistability is given in free running lasers, optical bistable devices, ring lasers, and lasers with an injected signal (LIS). A general review of laser instabilities is also presented in the framework of the theory of elementary catastrophes, emphasizing the appearance of higher order catastrophes in the case of LIS suggesting the whole hierarchy of laser instabilities. Experimental results on the bistability in the polarization of LIS are also discussed. DOE

N89-25450# Japan Atomic Energy Research Inst., Tokyo. Dept. of Physics.
PROCEEDINGS OF THE FREE ELECTRON LASER WORKSHOP, 1988 JAERI
Aug. 1988 123 p In JAPANESE; ENGLISH summary Workshop held in Tokai, Japan, 1 Mar. 1988
(DE89-780071; JAERI-M-88-149; CONF-8803200) Avail: NTIS (US Sales Only) HC A06/MF A01

Individual papers are indexed separately. They comprise the proceedings of the workshop. The emphasis was placed on storage rings of particle accelerators. DOE

N89-25451# Oak Ridge National Lab., TN.
LASER DIFFRACTION METHODS FOR HIGH TEMPERATURE STRAIN MEASUREMENTS
H. Pih (Tennessee Univ., Knoxville.) and K. C. Liu 1989 7 p Presented at the SEM Spring Meeting, Cambridge, MA, 28 May 1989
(Contract DE-AC05-84OR-21400)
(DE89-008235; CONF-8905107-1) Avail: NTIS HC A02/MF A01

Optical methods, utilizing the interference fringes produced by diffraction of laser light passing through a narrow slit, have been developed for strain measurements at high temperature above 1000 C. Basic principles, instrumentation, calibration, and measurement techniques of the methods and sample applications are presented. DOE

N89-25452# California Univ., Berkeley. Lawrence Berkeley Lab. Materials and Chemical Sciences Div.
REPORT OF THE WORKSHOP ON SCIENTIFIC OPPORTUNITIES FOR INFRARED FREE-ELECTRON LASERS, VOLUME 2
Feb. 1989 345 p Workshop held in Berkeley, CA, 31 Oct. - 1 Nov. 1988
(Contracts DE-AC03-76SF-00098; DE-AC02-76CH-00016)
(DE89-009106; LBL-26783-Vol-2; CONF-8810126-Vol-2) Avail: NTIS HC A15

The workshop on Scientific Opportunities for Infrared Free-electron Lasers was held on October 31 to November 1, 1988, in Berkeley, California. The objective of the workshop was to bring together chemists, physicists, device physicists and engineers to review the current status of IRFEL technology and to discuss the scientific opportunities that will emerge because of the unique characteristics of these devices. The contents of this report serve as a fair testimony that the objective was accomplished in excellent form. DOE

N89-25453# Lawrence Livermore National Lab., CA.
MEASUREMENT OF THE STIMULATED THERMAL RAYLEIGH SCATTERING INSTABILITY
T. J. Karr, M. C. Rushford, J. R. Murray, and J. R. Morris Apr. 1989 26 p Presented at the CLEO '89: Conference on Lasers and Electro Optics, Baltimore, MD, 24 Apr. 1989 Sponsored in part by Army
(Contract W-7405-eng-48)
(DE89-012324; UCRL-99967; CONF-890423-9) Avail: NTIS HC A03/MF A01

Growth of perturbations due to stimulated thermal Rayleigh scattering was observed on a laser beam propagating in a 1 meter cell of CC14. Initial sinusoidal irradiance perturbations were seeded onto the laser beam, and their amplification in the cell was recorded by a near field camera. The perturbation growth rate is in agreement with analytical predictions of linearized propagation theory. DOE

N89-25454# Lawrence Livermore National Lab., CA.
MICROWAVE EXPERIMENTAL STUDIES OF LASER FUSION Final Report
N. C. Luhmann, Jr. (California Univ., Los Angeles.) Jan. 1989 11 p
(Contract W-7405-eng-48)
(DE89-012325; UCRL-21191; LLNL-844-2905) Avail: NTIS HC A03/MF A01

The aim of the UCLA program is to understand the physics of electromagnetic wave absorption associated with laser fusion. The approach is to employ large low density plasmas which are easily diagnosed and to utilize high power microwave sources in the 1 to 16 GHz region. Plasma processes currently under investigation include absorption near the critical layer, phase conjugation, stimulated Raman scattering and the two plasma decay instability in the lower density regions. During the past two years our program has been primarily concerned with two main areas: the study of absorption near the critical layer both with and without the presence of an externally applied dc magnetic field; and the study of phase conjugation in a plasma via near-degenerate four wave mixing. DOE

N89-25455# California Univ., Berkeley. Lawrence Berkeley Lab. Accelerator and Fusion Research Div.
STATUS OF LBL/LLNL FEL (FREE ELECTRON LASER) RESEARCH FOR TWO BEAM ACCELERATOR APPLICATIONS
D. B. Hopkins and A. M. Sessler Mar. 1989 9 p Presented at the 13th Particle Accelerator Conference, Chicago, IL, 20-23 Mar. 1989
(Contract DE-AC03-76SF-00098)
(DE89-012487; LBL-26932; CONF-890335-124) Avail: NTIS HC A02/MF A01

We review the status of free electron laser (FEL) research being conducted at LBL and LLNL as part of a broader program of research on two beam accelerators (TBAs). Induction accelerator-driven FELs for use as power sources for high-gradient accelerators are discussed, along with preliminary cost estimates for this type of power source. Finally, a promising new version of an FEL/TBA is described. DOE

N89-25456# Sandia National Labs., Albuquerque, NM.
FISSION REACTOR PUMPED LASERS: HISTORY AND PROSPECTS
David A. McArthur 1989 5 p Presented at the Fifty Years With Nuclear Fission Conference, Gaithersburg, MD, 25-28 Apr. 1989
(Contract DE-AC04-76DP-00789)
(DE89-010329; SAND-89-0953C; CONF-890406-16) Avail: NTIS HC A02/MF A01

A historical account is given of work at Sandia since 1979, beginning with initial experiments on reactor ionized electrical excitation of CO2 lasers. An account of recent work at Sandia is also given centering on the Pulsed Reactor III for experiments at high excitation rates with small laser volumes, and the Sandia Annular Core Research Reactor for experiments at lower excitation rates with larger laser volume. Prospects are given for future reactor pumped laser work. E.R.

N89-25457# Siemens A.G., Erlangen (Germany, F.R.).
A 2 J HIGH-POWER EXCIMER LASER AT HIGH PULSE REPETITION RATE Final Report, Jun. 1987
Hans-Juergen Cirkel Mar. 1988 89 p In GERMAN; ENGLISH summary
(Contract BMFT-13-N-5357/3)
(U9-414/87/029; ETN-89-94628) Avail: NTIS HC A05/MF A01

An excimer laser of high pulse energy and high repetition rate was developed. All pulsed power components including the waterline capacitor and the control unit were tested at 100 Hz. A multichannel pseudospark switch operated at 100 kA peak current. An elongated X-ray unit for preionization of the laser gas employing a hollow cathode discharge shows a high reliability and a long service life at repetition rates in excess of 100 Hz. Important design parameters of the XeCl laser are given. In a closed flow-loop the average power of the XeCl laser is measured at 140 W. The temporal evolution of density fluctuations between two consecutive discharges was registered by an interferometer. ESA

37 MECHANICAL ENGINEERING

Includes auxiliary systems (nonpower); machine elements and processes; and mechanical equipment.

N89-25458# Wright State Univ., Dayton, OH.
A KINEMATIC STUDY OF THE MERLIN 6500 ROBOT AND THE UTAH/MIT DEXTEROUS HAND AND A SIMULATION OF THEIR COMBINED BEHAVIOR Final Report, Apr. 1987 - Sep. 1988
Ranvir Singh Solanki and Kuldip S. Rattan Sep. 1988 103 p (AF Proj. 2312)
(AD-A203907; AAMRL-TR-88-059) Avail: NTIS HC A06/MF A01 CSCL 13/11

The kinematics of the advanced, dexterous, four-fingered, sixteen jointed end effector system called the Utah/MIT hand and the industrial type six jointed MERLIN 6500 manipulator were investigated. The methodology of kinematic analysis, the direct and inverse kinematics of the MERLIN manipulator and the direct kinematics of the Utah/MIT hand are presented. A computer graphical simulation program for the two systems, when combined together, is also performed. Certain key issues involved in the development of kinematics for manipulator systems with dexterous end effectors are also discussed. Author

N89-25459# Helsinki Univ. Technology, Otaniemi (Finland). Inst. of Energy Engineering.
FLOW CHARACTERISTICS AND ACCURACY OF CONTROL VALVE
Jouni Pyoetsiae 1989 41 p In FINNISH; ENGLISH summary
(DE88-757331; TKK-KO/ET-30; ISBN-951-754-762-5) Avail: NTIS (US Sales Only) HC A03/MF A01

The purpose of this work was to examine the flow characteristics and accuracy of control valve. The research was divided into three different parts. At first, flow characteristics of control valve were studied, and general solution was determined for the optimal form of inherent flow characteristic of control valve. The general solution obtained was applied by determining the optimal form of the inherent flow characteristic of the control valve being in flow rate control, while the installed control valve was required constant gain or constant control accuracy. At the second part of the research, a control valve error was determined and the equation of valve inherent flow characteristic was derived by which the optimal accuracy can be reached. In the third part, the modification of the valve inherent flow characteristic was examined by a position control analogically and digitally carried out. DOE

N89-25460# Oak Ridge National Lab., TN. Instrumentation and Controls Div.
MODIFYING A TELEROBOTIC SYSTEM TO INCLUDE ROBOTIC OPERATION BY MEANS OF DYNAMIC MODELING
G. K. Corbett, J. F. Jansen, R. L. Kress, and M. W. Noakes 1989 6 p Presented at the International Conference on Robotics and Automation, Scottsdale, AZ, 14 May 1989
(Contract DE-AC05-84OR-21400)
(DE89-003119; CONF-890522-4) Avail: NTIS HC A02/MF A01

The goal of this study was to implement a robotic mode for the Advanced Servomanipulator (ASM), a six-degree-of-freedom master/slave teleoperator. To implement a robotic mode on a system designed for teleoperation, the effects of any change in the control schemes must be completely understood. One way to study the impact of potential modifications is to develop a model of the system. This approach is the one taken in this study. A detailed full-arm model was developed by first creating a model for individual joints of the manipulator and then incorporating each of the joint models into a single full-arm model, including link inertias and kinematic cross-coupling. Parameters were identified

for each joint model to provide a match between simulated and actual responses to a pulse input. The full-arm model was tested by comparing the simulated and actual response of the ASM to simultaneous sine-wave inputs to each joint, using the model parameters identified on a joint-by-joint basis. The full-arm model was able to characterize effectively the ASM system response for the inputs studied. Robotic-mode control algorithms were tested on both the individual-joint and full-arm models. The results of these simulations indicate that a simplified master/slave control structure is the best candidate for robotic operation. This control structure was added to the ASM. Experimental results demonstrate that the ASM system is capable of repeatable robotic operation. The robotic-mode man-machine interface and data handling system are described in this paper. DOE

N89-25461# Oak Ridge National Lab., TN.
TRACTION-DRIVE TRANSMISSION FOR TELEROBOTIC JOINTS
D. P. Kuban and D. M. Williams 1989 14 p Presented at the 23th Aerospace Mechanisms Symposium, Huntsville, AL, 3 May 1989
(Contract DE-AC05-84OR-21400)
(DE89-005337; CONF-890571-1) Avail: NTIS HC A03/MF A01

The U.S. Space Station Program is providing many technological developments to meet the increasing demands of designing such a facility. One of the key areas of research is that of telerobotics for space station assembly and maintenance. Initial implementation will be teleoperated, but long-term plans call for autonomous robotics. One of the essential components for making this transition successful is the manipulator joints mechanism. Historically, teleoperated manipulators and industrial robotics have had very different mechanisms for force transmission. This is because the design objectives are almost mutually exclusive. A teleoperator must have very low friction and inertia to minimize operator fatigue; backlash and stiffness are of secondary concern. A robot, however, must have minimum backlash, and high stiffness for accurate and rapid positioning. A joint mechanism has yet to be developed that can optimize these divergent performance objectives. A joint mechanism that approaches this optimal performance was developed for NASA Langley, Automation Technology Branch. It is a traction-drive differential that uses variable preload mechanisms. The differential provides compact, dexterous motion range with a torque density similar to geared systems. The traction drive offers high stiffness and zero backlash---for good robotic performance, and the variable-loading mechanism (VLM) minimizes the drive-train friction---for improved teleoperation. DOE

N89-25462# Du Pont de Nemours (E. I.) and Co., Aiken, SC.
DESIGN OF A DUAL FOREARM MODULAR ROBOT
J. J. Fisher 1988 12 p Presented at the Robots 12/Vision Conference, Detroit, MI, 6 Jun. 1988
(Contract DE-AC09-76SR-00001)
(DE89-010453; DP-MS-88-41; CONF-880683-4) Avail: NTIS HC A03/MF A01

This paper describes the design of an eight-degree-of-freedom robotic device which will be used to automate a radioactive chemical sample handling and assaying operation. Several innovative designs will allow the robot to adapt to an existing process without requiring major modifications to the facility. A unique arm joint arrangement, containing two elbow and forearm assemblies, is used. This configuration allows the robot to conduct simultaneous manipulation operations, to lift varying payloads, and to perform tasks of varying dexterity. Both modular and sealed component designs are used. A brief description of the control system is also presented. DOE

N89-25463*# Bently Rotor Dynamics Research Corp., Minden, NV.
INFLUENCE OF RUBBING ON ROTOR DYNAMICS, PART 1 Final Report
Agnes Muszynska, Donald E. Bently, Wesley D. Franklin, Robert D. Hayashida, Lori M. Kingsley, and Arthur E. Curry Mar. 1989 523 p
(Contract NAS8-36719)
(NASA-CR-183648-Pt-1; NAS 1.26:183648-Pt-1) Avail: NTIS HC A22/MF A01 CSCL 13I

The results of analytical and experimental research on rotor-to-stationary element rubbing in rotating machines are presented. A characterization of physical phenomena associated with rubbing, as well as a literature survey on the subject of rub is given. The experimental results were obtained from two rubbing rotor rigs: one, which dynamically simulates the space shuttle main engine high pressure fuel turbopump (HPFTP), and the second one, much simpler, a two-mode rotor rig, designed for more generic studies on rotor-to-stator rubbing. Two areas were studied: generic rotor-to-stator rub-related dynamic phenomena affecting rotating machine behavior and applications to the space shuttle HPFTP. An outline of application of dynamic stiffness methodology for identification of rotor/bearing system modal parameters is given. The mathematical model of rotor/bearing/seal system under rub condition is given. The computer program was developed to calculate rotor responses. Compared with experimental results the computed results prove an adequacy of the model. Author

N89-25464*# Bently Rotor Dynamics Research Corp., Minden, NV.
INFLUENCE OF RUBBING ON ROTOR DYNAMICS, PART 2 Final Report
Agnes Muszynska, Donald E. Bently, Wesley D. Franklin, Robert D. Hayashida, Lori M. Kingsley, and Arthur E. Curry Mar. 1989 202 p
(Contract NAS8-36719)
(NASA-CR-183649-Pt-2; NAS 1.26:183649-Pt-2) Avail: NTIS HC A10/MF A01 CSCL 13I

Rotor dynamic behavior depends considerably on how much the specific physical phenomena accompanying rotor rubbing against the stator is involved. The experimental results of rotor-to-stator rubbing contact are analyzed. The computer code is described for obtaining numerical calculations of rotor-to-stator rubbing system dynamic responses. Computer generated results are provided. The reduced dynamic data from High Pressure Fuel Turbo Pump (HPFTP) hot fire test are given. The results provide some significant conclusions. Information is provided on the electronic instrumentation used in the experimental testing. B.G.

N89-25465# Edgerton, Germeshausen and Grier, Inc., Idaho Falls, ID. Materials Technology Group.
DETECTION OF METAL-TRANSFER MODE IN GMAW
John A. Johnson, Nancy M. Carlson, and Herschel B. Smartt 1989 5 p Presented at the 2nd International Conference on Trends in Welding Research, Gatlinburg, TN, 15 May 1989
(Contract DE-AC07-76ID-01570)
(DE89-011133; EGG-M-88512; CONF-8905118-4) Avail: NTIS HC A02/MF A01

One of the requirements of a sensing system for feedback control of gas metal arc welding (GMAW) is the capability to detect information about the metal-transfer mode. Because the operating boundary for the desired transfer mode, expressed as a function of mass input and heat input, may vary due to conditions beyond the control of the system, a means of determining the transfer mode during welding is necessary. A series of sensing experiments is performed during which the ultrasonic emissions, audio emissions, welding current fluctuations, and welding voltage fluctuations are recorded as a function of the transfer mode. In addition, high speed movies (5000 frame/s) of the droplet formation and detachment are taken synchronously with the sensing data. An LED mounted in the camera is used to work the film at the beginning and end of the data acquisition period. A second LED is pulsed at a 1 kHz rate and the pulses are recorded on film and with the sensor data. Thus events observed on the film can be correlated with the sensor data. Data acquired during globular transfer, spray transfer, and stiff spray or streaming transfer are observed to correlate with droplet detachment and arc shorting. The audio, current, and voltage data can be used to discriminate

among these different transfer modes. However, the current and voltage data are also dependent on the characteristics of the welding power supply. DOE

N89-25466# Oak Ridge National Lab., TN. Metals and Ceramics Div.

MODELING THE EFFECT OF SURFACE ACTIVE ELEMENTS ON WELD POOL FLUID FLOW, HEAT TRANSFER AND GEOMETRY

T. Zacharia, S. A. David, J. M. Vitek, and T. DebRoy (Pennsylvania State Univ., University Park.) 1989 7 p Presented at the 2nd International Conference on Trends in Welding Research, Gatlinburg, TN, 15 May 1989

(Contract DE-AC05-84OR-21400)

(DE89-012504; CONF-8905118-5) Avail: NTIS HC A02/MF A01

The influence of sulfur on the heat flow and fluid flow and the transient development of the weld pool was quantitatively evaluated for two heats of Type 304 stainless steel containing 90 and 240 ppM sulfur, respectively. A transient heat transfer model was utilized to simulate the heat flow and fluid flow in the weld pool during stationary laser and gas tungsten arc (GTA) spot welds. A recently developed surface tension model was utilized to calculate the temperature coefficient of surface tension (dtau/dT) as a function of temperature and sulfur content. This allows a realistic evaluation of the effect of surface-active elements on the fluid flow and weld geometry. The computed results indicate that during stationary welding, the weld pool surface temperatures are fairly high. As a consequence, the temperature coefficient of surface tension becomes negative and a radially outward or a bifurcated flow of weld metal occurs even when the weld pool contains a significant amount of sulfur. The predictions of the model were verified by comparing the calculated and experimentally observed fusion zone geometry. The results indicate very good agreement between the predicted and experimentally observed fusion zone geometry, for both laser and gas tungsten arc (GTA) spot welds, due partly to the accurate treatment of surface tension gradient driven flows. DOE

N89-25467# Auburn Univ., AL.

CAVITATION KINETICS DURING GTA (GAS TUNGSTEN ARC) WELDING OF HELIUM CONTAINING STAINLESS STEEL

Hua Tay Lin, M. L. Grossbeck, S. H. Goods, and B. A. Chin (Sandia National Labs., Albuquerque, NM.) 1989 37 p

(Contract DE-AC05-84OR-21400)

(DE89-012514; DOE/ER-52139/T2) Avail: NTIS HC A03/MF A01

Helium was implanted in type 316 stainless steel, through tritium decay, to levels of 0.18, 2.5, 27, 105 and 256 appm. Bead-on-plate welds were then produced using the gas tungsten arc process. During welding, the sheet specimens were fully constrained transverse to the welding direction. Both full and partial penetration welds were made. Upon cooling, complete, through-section cracking occurred in the heat-affected zone of specimens with helium concentrations equal to or greater than 2.5 appm. No such cracking was observed in helium-free control specimens or in specimens containing the lowest helium concentration. Examination of these cracks revealed them to be entirely intergranular in nature. In addition to the heat-affected zone cracking, brittle, centerline cracking occurred in the fusion zone of specimens containing 105 and 256 appm helium. Transmission and scanning electron microscopy results indicated that the cracking in the fusion zone resulted from the precipitation of helium along solidification interfaces and that the heat-affected zone cracking originated from the growth and coalescence of grain boundary helium bubbles. For the latter case, a mechanism for bubble growth is proposed. The growth rate predicted by this mechanism favorably predicts the experimentally measured time lag between peak weld temperature and the onset of cracking. DOE

N89-25468# Auburn Univ., AL.

WELDING OF HELIUM-DOPED AUSTENITIC AND FERRITIC STAINLESS STEELS

Hua Tay Lin, M. L. Grossbeck, S. H. Goods, and B. A. Chin (Sandia National Labs., Albuquerque, NM.) 1989 8 p Presented at the 2nd International Conference on Trends in Welding Research, Gatlinburg, TN, 15 May 1989

(Contract DE-FG05-86ER-52139)

(DE89-012523; CONF-8905118-6) Avail: NTIS HC A02/MF A01

Helium was uniformly implanted into type 316 stainless steel and Sandvik HT-9 (12Cr-1MoVW) to levels of 0.18 to 256 appm and 0.3 to 1 appm, respectively, using the tritium trick technique. Bead-on-plate welds were then produced under fully constrained conditions using the gas tungsten arc (GTA) process. For 316 stainless steel, catastrophic intergranular fracture occurred in the heat-affected zone (HAZ) of welds with helium levels equal to or greater than 2.5 appm. Brittle cracking along the central line of the fusion zone was also observed for the welds containing 105 and 256 appm He. For HT-9, intergranular cracking occurred in the HAZ along prior-austenite grain boundaries of welds containing 1 appm He. Electron microscopy observations showed that the cracking in the HAZ originated from the growth and coalescence of grain boundary helium bubbles and that the fusion zone cracking resulted from the growth of helium at dendrite interfaces. Results of this study indicate that the use of conventional fusion welding techniques to repair irradiation-degraded materials containing even small amounts of helium may be difficult. DOE

N89-25469# Auburn Univ., AL.

SIMULATION OF THE WELDING OF IRRADIATED MATERIALS Ph.D. Thesis

Hua Tay Lin 17 Mar. 1989 259 p

(Contract DE-FG05-86ER-52139)

(DE89-012524; DOE/ER-52139/3) Avail: NTIS HC A12/MF A01

Helium was uniformly implanted using the tritium trick technique to levels of 0.18, 2.5, 27, 105 and 256 atomic part per million (appm) for type 316 stainless steel, and 0.3 and 1 appm for Sandvik HT-9 (12 Cr-1MoVW). Both full penetration as well as partial penetration welds were then produced on control and helium-containing materials using the autogenous gas tungsten arc (GTA) welding process under full constraint conditions. For full penetration welds, both materials were successfully welded when they contained less than 0.3 appm helium. However, welds of both materials, when containing greater than 1 appm helium, were found to develop cracks during cooling of the weld. In type 316 stainless steel, catastrophic intergranular failure occurred during cooling in the heat-affected zone (HAZ), leading to a crack extending nearly the length of the plate at the completion of the weld. When the helium content of type 316 stainless steel exceeded 100 appm both HAZ cracking and brittle failure along the center line of the fusion zone occurred during cooling. In HT-9 the observed cracking was limited to only the beginning region of the weld. The cracking was found to be intergranular in nature and occurred along prior-austenite grain boundaries of the HAZ. For partial penetration welds, underbead intergranular cracking occurred in the HAZ of type 316 stainless steel containing helium greater than 2.5 appm. DOE

N89-25470# Argonne National Lab., IL. Materials and Components Technology Div.

APPLICATIONS OF ION BEAM PROCESSES IN TRIBOLOGY

R. A. Erck, G. R. Fenske, A. Erdemir, and F. A. Nichols 1989 3 p Presented at the 5th International Conference on Tribology, Helsinki, Finland, 12-15 Jun. 1989

(Contract W-31-109-eng-38)

(DE89-000614; CONF-890630-1) Avail: NTIS HC A02/MF A01

With the use of ion-beam techniques becoming more common, there is increasing opportunity to develop new coatings and surface treatments to promote long wear life and low friction in tribological applications. Boundary and/or mixed lubrication and wear at elevated temperatures are two tribological areas that could benefit

from ion beam applications. If successful these innovations would have a significant impact on the development of advanced energy conversion systems. Numerous examples of successful applications of ion-beam techniques can be found for wear applications at low and elevated temperatures; however, improvements in the field of lubrication, particularly at elevated temperatures, are sparse. DOE

N89-25471# Oak Ridge National Lab., TN. Metals and Ceramics Div.
DETERMINATION OF THE MECHANICAL PROPERTIES OF DIAMOND AND DIAMOND-LIKE FILMS BY THE ULTRA-LOW LOAD INDENTATION TECHNIQUE
M. E. OHern, Carl J. McHargue, R. E. Clausing, W. C. Oliver, and R. H. Parrish 1989 6 p Presented at the Spring Meeting of the Materials Research Society, San Diego, CA, 24 Apr. 1989 Sponsored in part by Army
(Contract DE-AC05-84OR-21400)
(DE89-011569; CONF-890426-10) Avail: NTIS HC A02/MF A01

Diamond and diamond-like films were characterized with a mechanical properties microprobe (MPM) and compared to a natural IIa diamond and single crystal sapphire characterized by the same method. The diamond films were 125 to 375 micrometers thick with a fine-grained microstructure (approx. 20 micrometers diam. grains). The natural diamond was a IIa quality diamond with the (100) axis normal to the surface. The sapphire used had low dislocation density with the c-axis normal to the surface. The diamond-like carbon film (DLC) was RF glow discharge deposited to a thickness of about 0.2 micrometers. Results of the present study are given and future work is discussed. DOE

N89-25472# Lehigh Univ., Bethlehem, PA. ATLSS Center.
EFFECTS OF AUXILIARY HEAT TREATMENTS ON FLAME-CUTTING PROCEDURES
Bruce R. Somers, Howard Smith, Rajan Varughese, and Alan W. Pense 14 Apr. 1989 35 p Prepared in cooperation with Lafayette Coll., Easton, PA
(Contract DE-FG01-87CE-15323)
(DE89-011827; DOE/CE-15323/T5; ATLSS-89-08) Avail: NTIS HC A03/MF A01

One inch and two inch thick flame-cut samples of A588 steel were prepared using three different cutting treatments including cutting with auxiliary pre and post heat, cutting with auxiliary post heat only, and cutting with no auxiliary. The auxiliary heat was applied to the cutting process using a proprietary fixture designed by Roussey Associates. Each of these cutting treatments was applied at both a fast and a slow cutting speed. Surface hardness tests showed that within the same composition and thickness the hardest flame cut surfaces occurred at the faster cutting speed when no auxiliary heat was applied. The softest surface occurred at slow cutting speeds when both pre and post heat flames were applied. Microhardness traverses show the tempering effects of the auxiliary heat. Bend tests displayed for the one inch samples with pre and post heat, at both cutting speeds, none or only very slight cracking. Numerous slight cracks, however, were found when no auxiliary heat treatment was used. While pre and post heat treatments reduced the cracking severity in the two inch plate, numerous slight cracks were still seen, even at slow cutting speeds. DOE

38 QUALITY ASSURANCE AND RELIABILITY

Includes product sampling procedures and techniques; and quality control.

N89-25473# Du Pont de Nemours (E. I.) and Co., Aiken, SC.
BASICS OF ULTRASONIC TESTING
R. E. Sprayberry 1989 27 p Presented at the Spring Conference of the American Society for Nondestructive Testing, Charlotte, NC, 20-24 Mar., 1989 and American Welding Society 1989 Welding Show, Washington, DC, 2-6 Apr. 1989
(Contract DE-AC09-76SR-00001)
(DE89-010465; DP-MS-89-49; CONF-890334-1; CONF-890482-2) Avail: NTIS HC A03

This paper is an outline of a presentation on the fundamentals of ultrasonic testing. DOE

N89-25474# Tennessee Univ., Knoxville. Dept. of Nuclear Engineering.
GENERALIZED CONSISTENCY CHECKING OF MULTIVARIABLE REDUNDANT MEASUREMENTS AND COMMON-MODE FAILURE DETECTION
O. Glockler, Belle R. Upadhyaya, V. M. Morgenstern, and J. Olvera 1989 23 p Presented at the 7th Power Plant Dynamics, Control and Testing Symposium, Knoxville, TN, 15-17 May 1989
(Contract DE-AC02-86NE-37959)
(DE89-010053; DOE/NE-37959/29; CONF-890555-11) Avail: NTIS HC A03/MF A01

The limitations of the single-variable consistency checking algorithm for validating redundant measurements are remedied by extending it to multiple process signals. The redundant measurements of each variable in a subsystem are combined with an estimate of the variable using prediction models. A complex logic algorithm has been developed to perform simultaneous consistency checking of all variables under consideration. The new algorithm has been implemented in a general purpose PC and in a VAX workstation. Applications to sensor failure monitoring and to detect and isolate common-mode sensor failures are studied. DOE

N89-25475# Lawrence Livermore National Lab., CA.
LEARNING THE VALUE OF VE
Roger B. Sperling 3 Mar. 1989 7 p Presented at the Society of American Value Engineers International Conference, Indianapolis, IN, 12 Jun. 1989
(Contract W-7405-eng-48)
(DE89-008121; UCRL-100655; CONF-890691-1) Avail: NTIS HC A02/MF A01

Describing lessons learned from Value Engineers (VE) studies at a government-funded research laboratory reveals how project managers were encouraged to use VE and how their projects benefited from the VE savings. The five major lessons were: An officer of free VE is a low-risk incentive to encourage the use of VE; More costs savings can be identified by VE studies than cost reviews or design reviews; Large projects can benefit from repeat VE studies; VE teams can identify surprising savings when allowed to challenge all design criteria; VE programs can be costs effective even though return on investment may vary among projects. DOE

N89-25476# Universiteit Twente, Enschede (Netherlands). Dept. of Computer Science.
A THEORY OF DESCRIBING PERFORMABILITY MODELS
Boudewijn R. Haverkort and Ignas G. Niemegeers Nov. 1988 37 p
(MEMO-INF-88-26; ISBN-9-03-650277-6; ETN-89-94757) Avail: NTIS HC A03/MF A01

Performance and reliability models are studied. Both are described using queueing networks of Petri nets models. A performability model includes both aspects of performance and of reliability. It is claimed that performability models can be described by two separate models and a connection between these models. A performability modeling technique is proposed. ESA

39 STRUCTURAL MECHANICS

Includes structural element design and weight analysis; fatigue; and thermal stress.

For applications see *05 Aircraft Design, Testing and Performance* and *18 Spacecraft Design, Testing and Performance.*

N89-25477 California Univ., Los Angeles.
DYNAMIC SIMULATION OF DISLOCATION PATTERN FORMATION IN METALS DURING HIGH TEMPERATURE MONOTONIC AND CYCLIC DEFORMATION Ph.D. Thesis
Robert John Amodeo 1988 325 p
Avail: Univ. Microfilms Order No. DA8821371

A new methodology in computational statistical mechanics, Dislocation Dynamics (DD), is introduced to study the effects of temperature and applied stress on the formation of dislocation patterns in metals. The characteristics of dislocations are modeled as equations of motion which describe the long-range forces between dislocations, and binary interactions which describe the short-range effects. The code developed for the simulation of the formation of these structures, DISLOcation DYNamics (DISLODYN) operates on the principle that given a sufficient amount of physics to describe the actual phenonmena, a simulation represents a computer experiment capable of determining physical characteristics of the system studied. The following structures are studied: dislocation pileups; persistent slip bands and planar arrays in copper at low temperature cyclic straining; dislocation cells and subgrains in iron at high temperature monotonic straining. The accuracy of the computer simulation is demonstrated by the precise generation of dislocation trajectories characteristic of a dislocation pileup. The formation of dipole dislocations and annihilation of dislocations are competing mechanisms for the formation of persistant slip band (PSB) structures. Multiplication of dislocations at points of local inhomogeneity is a key process in the formation of planar arrays. In high temperature creep, dislocation cells naturally form due to the clustering of dipolar and junction dislocations into polygonal patterns. The evolution of the creep strain as a function of time is found to depend upon the concentration of mobile dislocations and the presence of subgrain boundaries. Author

N89-25478# Sandia National Labs., Albuquerque, NM. Measurement Standards Div.
AN UNCERTAINTY ANALYSIS FOR THE STRUCTURAL MECHANICS LABORATORY
Richard L. Crabb Mar. 1988 13 p
(Contract DE-AC04-76DP-00789)
(DE89-010306; SAND-88-2847) Avail: NTIS HC A03/MF A01

An investigation of the uncertainties associated with instrumentation used in a structural mechanics laboratory is outlined in this report. Results from studies made to quantify measurement data and various uncertainty factors related to randomness, load cells, linear variable differential transformers (LVDTs) and data collection devices show that the overall uncertainty is of the order of one or two percent. The subject of measurement traceability is discussed followed by a description of the system, analysis, and conclusions. DOE

N89-25479*# National Aeronautics and Space Administration. Ames Research Center, Moffett Field, CA.
FLAP-LAG STABILITY DATA FOR A SMALL-SCALE ISOLATED HINGELESS ROTOR IN FORWARD FLIGHT
Michael J. McNulty Apr. 1989 121 p
(NASA-TM-102189; A-89124; NAS 1.15:102189; USAAVSCOM-TR-89-A-003) Avail: NTIS HC A06/MF A01 CSCL 20K

An isolated, hingeless rotor with discrete flap and lead-lag flexures and relatively rigid blades was tested in the Aeroflightdynamics Directorate's 7- by 10-Foot Wind Tunnel. The lead-lag stability of a structurally simple rotor configuration in forward flight was determined. The model tested had no cyclic pitch control, and was therefore operated untrimmed at several collective pitch angles, at shaft angles from 0 deg to -20 deg, and at advance ratios as high as 0.55. Two inplane natural frequencies, 0.61/rev and 0.72/rev, were tested for configuration both with and without structural flap lag coupling. Concomitant hover testing of the model was also conducted. Representative plots of the frequency and damping data are presented to show general trends, and complete tabular data and model properties information are included for use in detailed correlation exercises. The most prominent feature of the forward flight data is an abrupt increase in damping with advance ratio at certain high-speed, high shaft-angle conditions, with high flapping loads. The hover data are consistent with previous experimental and theoretical results for hingeless rotors without kinematic couplings. Overall, the data quality is very good and the data are expected to be useful in the development and validation of rotor aeroelastic stability analyses. Author

N89-25480*# Boeing Helicopter Co., Philadelphia, PA.
PLAN, FORMULATE, DISCUSS AND CORRELATE A NASTRAN FINITE ELEMENT VIBRATIONS MODEL OF THE BOEING MODEL 360 HELICOPTER AIRFRAME
R. Gabel, P. F. Lang, L. A. Smith, and D. A. Reed Apr. 1989 296 p
(Contract NAS1-17497)
(NASA-CR-181787; NAS 1.26:181787) Avail: NTIS HC A13/MF A01 CSCL 20K

Boeing Helicopter, together with other United States helicopter manufacturers, participated in a finite element applications program to emplace in the United States a superior capability to utilize finite element analysis models in support of helicopter airframe design. The activities relating to planning and creating a finite element vibrations model of the Boeing Model 36-0 composite airframe are summarized, along with the subsequent analytical correlation with ground shake test data. Author

N89-25481# Sandia National Labs., Albuquerque, NM. Experimental Mechanics Dept.
SIMPLE FIXTURE CONCEPTS FOR MULTI-AXIS VIBRATION TESTING
Thomas L. Paez, Edward J. Buksa, and David Beightol 1989 6 p Presented at the 35th Annual Technical Meeting of the Institute of Environmental Sciences: Building Tomorrow's Environment, Anaheim, CA, 1 May 1989
(Contract DE-AC04-76DP-00789)
(DE89-007977; SAND-89-0538C; CONF-890592-4) Avail: NTIS HC A02/MF A01

This paper presents some simple concepts for fixtures that can be used in two and three-axis vibration testing. Two, two-axis fixtures were built and tested in the laboratory. Test results are shown, and serve to confirm the validity of the concept. Simple methods for extending the concepts for three-axis testing are discussed. DOE

N89-25482# Sandia National Labs., Albuquerque, NM. Experimental Mechanics Dept.
IDENTIFICATION OF DISTRIBUTED FORCES ON A STRUCTURE
Thomas L. Paez and Ronald Coleman 1989 7 p Presented at the 35th Annual Technical Meeting of the Institute of Environmental Sciences: Building Tomorrow's Environment, Anaheim, CA, 1 May 1989
(Contract DE-AC04-76DP-00789)
(DE89-007978; SAND-89-0537C; CONF-890592-5) Avail: NTIS HC A02/MF A01

This paper presents a combined analytical and experimental method for establishing a set of equations to evaluate the equivalent forces acting on a structure. The method requires that a finite element model of the structure be established. It further requires that the accelerator responses to the external forces be measured at a number of points on the structure. The equivalent forces established in the analysis are a representation of the actual forces. The equivalent forces concentrate the effects of the external forces at the degrees of freedom where the acceleration responses are measured. DOE

N89-25483# Sandia National Labs., Albuquerque, NM. Mechanical Metallurgy Div.

A TEST SYSTEM FOR COMPUTER CONTROLLED THERMOMECHANICAL FATIGUE TESTING

Wendell B. Jones, David T. Schmale, and Roy J. Bourcier 1989 21 p Presented at the ASTM Symposium on the Applications of Automation Technology to Fatigue, Kansas City, MO, 22 May 1989

(Contract DE-AC04-76DP-00789)

(DE89-009067; SAND-88-2183C; CONF-8905112-1) Avail: NTIS HC A03/MF A01

This paper describes a computer controlled testing system which is capable of performing thermomechanical fatigue tests. Three different tests have been developed: (1) high temperature compression (HTC) tests in which the gauge length of the specimen is held at constant length and the mechanical strain is totally imposed by the triangular temperature cycle, (2) high temperature tension (HTT) tests in which the mechanically imposed length change is exactly double the thermally induced length change, and (3) multiple isothermal deformation (MID) tests for which the deformations occur isothermally and the temperature is changed every half cycle while maintaining constant mechanical strain. The need for these tests is shown by comparing the results of isothermal low cycle fatigue tests with results from TMF for several steels (304 Stainless Steel, 316 Stainless Steel, Alloy 800, and Modified 9Cr-1Mo Steel). We show that universal assumptions of TMF behavior are inappropriate and may lead to non-conservative design rules. Computer controlled TMF tests of the types described here are required to establish the response of each alloy considered for application. DOE

N89-25484*# Astro Aerospace Corp., Carpinteria, CA.

PACTRUSS SUPPORT STRUCTURE FOR PRECISION SEGMENTED REFLECTORS

John M. Hedgepeth Jun. 1989 75 p

(Contract NAS1-17536)

(NASA-CR-181747; NAS 1.26:181747; AAC-TN-1153) Avail: NTIS HC A04/MF A01 CSCL 20K

The application of the Pactruss deployable structure to the support of large paraboloidal reflectors of very high precision was studied. The Pactruss concept, originally conceived for the Space Station truss, is shown to be suitable for use in a triangular arrangement to support a reflector surface composed of hexagonal reflector panels. A hybrid of Pactruss structural and deployable single-fold beams is shown to accommodate a center body. A minor alteration in the geometry is in order to avoid lockup during deployment. To assess the capability of the hybrid Pactruss structure, an example truss supporting a full-scale (20 meter diameter) infrared telescope was analyzed for static and dynamic performance. A truss structure weighing 800 kilograms gave adequate support to a reflector surface weighing 3,000 kilograms. Author

N89-25485*# National Aeronautics and Space Administration. Lewis Research Center, Cleveland, OH.

PROCEDURES FOR CHARACTERIZING AN ALLOY AND PREDICTING CYCLIC LIFE WITH THE TOTAL STRAIN VERSION OF STRAINRANGE PARTITIONING

James F. Saltsman and Gary R. Halford Washington Jun. 1989 24 p

(NASA-TM-4102; E-4457; NAS 1.15:4102) Avail: NTIS HC A03/MF A01 CSCL 20K

Procedures are presented for characterizing an alloy and predicting cyclic life for isothermal and thermomechanical fatigue conditions by using the total strain version of strainrange partitioning (TS-SRP). Numerical examples are given. Two independent alloy characteristics are deemed important: failure behavior, as reflected by the inelastic strainrange versus cyclic life relations; and flow behavior, as indicated by the cyclic stress-strain-time response (i.e., the constitutive behavior). Failure behavior is characterized by conducting creep-fatigue tests in the strain regime, wherein the testing times are reasonably short and the inelastic strains are large enough to be determined accurately. At large strainranges, stress-hold, strain-limited tests are preferred because a high rate of creep damage per cycle is inherent in this type of test. At small strainranges, strain-hold cycles are more appropriate. Flow behavior is characterized by conducting tests wherein the specimen is usually cycled far short of failure and the wave shape is appropriate for the duty cycle of interest. In characterizing an alloy pure fatigue, or PP, failure tests are conducted first. Then depending on the needs of the analyst a series of creep-fatigue tests are conducted. As many of the three generic SRP cycles are featured as are required to characterize the influence of creep on fatigue life (i.e., CP, PC, and CC cycles, respectively, for tensile creep only, compressive creep only, and both tensile and compressive creep). Any mean stress effects on life also must be determined and accounted for when determining the SRP inelastic strainrange versus life relations for cycles featuring creep. This is particularly true for small strainranges. The life relations thus are established for a theoretical zero mean stress condition. Author

N89-25486 Michigan Univ., Ann Arbor.

ON OPTIMAL FAIL-SAFE DESIGN OF STRUCTURES Ph.D. Thesis

Avigdor Shechter 1988 158 p

Avail: Univ. Microfilms Order No. DA8907140

A treatment is presented for problems in the design of structures that are required to satisfy multiple purposes in the fail-safe sense. For the optimal fail-safe design problem, the objective is to predict the structural design that is optimal at once with respect to criteria and constraints associated with both its primary purpose and with one or more additional sets of secondary requirements. The fail-safe design problem is interpreted as a multicriteria optimization problem. The characterization in mathematical programming form is presented for a broad statement of the fail-safe design problem as applied to the model of trusses made of simple elements. Two main categories are covered: fail-safe design of structures restricted to operate in the elastic range, and fail-safe design of structures that may undergo plastic deformation. A unique model for elastoplastic analysis is tested computationally, and is incorporated into formulations for fail-safe design. In all cases the corresponding multicriteria optimization problems are interpreted via a min-max model into scalar form. Necessary conditions for optimality are derived and general qualities of the associated optimal designs are deduced from them. For problems corresponding to the first category of fail-safe structures, computational algorithms are constructed based upon qualities observed in the necessary conditions for optimality. The nonlinear programming general purpose code ADS is used for computational treatment of the problems of the second category. Several simple truss examples are solved. The variational problem statement for fail-safe design of two-dimensional continuum structures is presented. An expression of the problem for axisymmetric structures is interpreted via a finite element model.

Dissert. Abstr.

N89-25487# Sandia National Labs., Albuquerque, NM.

STRUCTURAL TESTING OF METAL/COMPOSITE CONICAL STRUCTURES WITH HOLES

William J. Tedeschi, John Pott, Rodney A. May, Albino C. Bustamante, Eric W. Reece, and D. Neill Benton 1989 36 p Presented at the Army Symposium on Solid Mechanics: Mechanics of Engineered Materials and Applications, Newport, RI, 16 May 1989

(Contract DE-AC04-76DP-00789)

(DE89-011451; SAND-88-3325C; CONF-8905104-2) Avail: NTIS HC A03/MF A01

Conical structures containing holes were tested for the purpose of determining their structural load carrying capacity. The conical test structures were composed of an aluminum substructure with an outer layer of glass composite material. Holes were machined into all but one of the structures, the holes ranged in circumferential size from 15 to 35 percent of removed structure at the maximum hole diameter. The structures were quasi-statically loaded in tension, compression, and bending until structural failure occurred. Strain and displacement data were collected during the tests. The

structural failure modes for each tested shell were then analyzed. Supporting analyses used a finite element structural response code to model the elastic-plastic response of the loaded structures, including structural failure. DOE

N89-25488# Los Alamos National Lab., NM.
FINITE STRAIN EXAMPLE PROBLEMS FOR RECTANGULAR, CYLINDRICAL, AND SPHERICAL GEOMETRIES
W. A. Cook May 1989 31 p
(Contract W-7405-eng-36)
(DE89-013607; LA-11547-MS) Avail: NTIS HC A03/MF A01

This report describes the solution of finite strain example problems for three geometries: rectangular, cylindrical, and spherical. Simplifying assumptions are made on the displacements for each geometry, and differential equations are derived. These differential equations are then reduced to the solution of polynomial equations for zero body forces. DOE

N89-25489# Edgerton, Germeshausen and Grier, Inc., Idaho Falls, ID.
EVALUATION OF ELASTIC-PLASTIC SURFACE FLAW BEHAVIOR AND RELATED PARAMETERS USING SURFACE DISPLACEMENT MEASUREMENTS
W. R. Lloyd and W. G. Reuter 1989 34 p Presented at the 21st Fracture Symposium, Annapolis, MD, 28 Jun. 1989
(Contract DE-AC07-76ID-01570)
(DE89-011134; EGG-M-88231; CONF-8906114-1) Avail: NTIS HC A03/MF A01

Surface displacement measurements, on surface cracked plate specimens loaded in tension, were recorded using geometric moire. An algorithm based on the displacements predicted by HRR fields was developed by the authors and used to evaluate the value of the applied J-integral at the crack border/free surface intersection point at various levels of applied remote stress. The values of J calculated in this manner were found to be in good agreement with predictions by Parks, obtained from a nonlinear, 3-D finite element model (ABAQUS). DOE

N89-25490*# National Aeronautics and Space Administration. Lewis Research Center, Cleveland, OH.
ADVANCED METHODS FOR 3-D INELASTIC STRUCTURAL ANALYSIS FOR HOT ENGINE STRUCTURES
C. C. Chamis Jul. 1989 12 p Presented at the 2nd National Congress on Mechanics, Athens, Greece, 29 Jun. - 1 Jul. 1989; sponsored by the Hellenic Society for Theoretical and Applied Mechanics
(NASA-TM-102106; E-4873; NAS 1.15:102106) Avail: NTIS HC A03/MF A01 CSCL 20K

Three-dimensional Inelastic Analysis Methods are described. These methods were incorporated into a series of new computer codes embodying a progression of mathematical models (mechanics of materials, specialty finite element, boundary element) for streamlined analysis of hot engine structures such as: (1) combustor liners, (2) turbine blades, and (3) turbine vanes. These models address the effects of high temperatures and thermal/mechanical loadings on the local (stress/strain) and global (displacements, frequencies, amplitudes, buckling) structural behavior of the three respective components. The methods and the three computer codes, referred to as MOMM (Mechanics Of Materials Model), MHOST (MARC-Hot Section Technology), and BEST3D (Boundary Element Stress Technology), have been developed and are briefly described. Author

N89-25491# GKSS-Forschungszentrum Geesthacht (Germany, F.R.). Inst. fuer Werkstofforschung.
CRACK GROWTH UNDER LOW CYCLE FATIGUE [RISSAUSBREITUNG BEI KURZZEITERMUEDUNG]
D. Hellmann 1988 50 p In GERMAN; ENGLISH summary
(GKSS-88/E/47; ISSN-0344-9629; ETN-89-94588) Copyright Avail: NTIS HC A03/MF A01

Mechanical behavior of cracked metallic materials under low cycle fatigue is analyzed. Only the range of high crack growth rates where the application of linear elastic fracture mechanics is not possible is considered. Mechanical parameters which control fatigue crack growth rate are: modified stress intensity factor, the J-integral, the crack tip opening displacement, and strain amplitude. ESA

N89-25161*# National Aeronautics and Space Administration. Langley Research Center, Hampton, VA.
STRUTEX: A PROTOTYPE KNOWLEDGE-BASED SYSTEM FOR INITIALLY CONFIGURING A STRUCTURE TO SUPPORT POINT LOADS IN TWO DIMENSIONS
James L. Robers and Jaroslaw Sobieszczanski-Sobieski *In its* Recent Advances in Multidisciplinary Analysis and Optimization, Part 1 Apr. 1989 p 317-331 (For primary document see N89-25146 19-05)
Avail: NTIS HC A23/MF A01 CSCL 20K

N89-25166*# Lockheed Aeronautical Systems Co., Burbank, CA.
COMPOSITE SIZING AND PLY ORIENTATION FOR STIFFNESS REQUIREMENTS USING A LARGE FINITE ELEMENT STRUCTURAL MODEL
N. A. Radovcich and D. P. Gentile *In* NASA. Langley Research Center, Recent Advances in Multidisciplinary Analysis and Optimization, Part 1 Apr. 1989 p 403-429 (For primary document see N89-25146 19-05)
Avail: NTIS HC A23/MF A01 CSCL 20K

N89-25174*# Northrop Corp., Hawthorne, CA. Aircraft Div.
ASTROS: A MULTIDISCIPLINARY AUTOMATED STRUCTURAL DESIGN TOOL
D. J. Neill *In* NASA. Langley Research Center, Recent Advances in Multidisciplinary Analysis and Optimization, Part 2 Apr. 1989 p 529-543 (For primary document see N89-25173 19-05)
Avail: NTIS HC A22/MF A01 CSCL 20K

N89-25175*# Kaman Aerospace Corp., Bloomfield, CT.
A GENERALIZED SOFTWARE EXECUTIVE FOR MULTIDISCIPLINARY COMPUTATIONAL STRUCTURAL DYNAMICS
Alex Berman *In* NASA. Langley Research Center, Recent Advances in Multidisciplinary Analysis and Optimization, Part 2 Apr. 1989 p 545-563 (For primary document see N89-25173 19-05)
Avail: NTIS HC A22/MF A01 CSCL 20K

N89-25177*# General Dynamics Corp., Fort Worth, TX.
RECENT EXPERIENCES USING FINITE-ELEMENT-BASED STRUCTURAL OPTIMIZATION
B. K. Paul, J. C. McConnell, and Mike H. Love *In* NASA. Langley Research Center, Recent Advances in Multidisciplinary Analysis and Optimization, Part 2 Apr. 1989 p 581-599 (For primary document see N89-25173 19-05)
Avail: NTIS HC A22/MF A01 CSCL 20K

N89-25181*# Iowa Univ., Iowa City. Dept. of Mechanical Engineering.
ON EQUIVALENCE OF DISCRETE-DISCRETE AND CONTINUUM-DISCRETE DESIGN SENSITIVITY ANALYSIS
Kyung K. Choi and Sung-Ling Twu *In* NASA. Langley Research Center, Recent Advances in Multidisciplinary Analysis and Optimization, Part 2 Apr. 1989 p 653-672 (For primary document see N89-25173 19-05)
(Grant NSF MSM-83-19871)
Avail: NTIS HC A22/MF A01 CSCL 20K

N89-25183*# MacNeal-Schwendler Corp., Los Angeles, CA.
GRID SENSITIVITY CAPABILITY FOR LARGE SCALE STRUCTURES
Gopal K. Nagendra and David V. Wallerstein *In* NASA. Langley Research Center, Recent Advances in Multidisciplinary Analysis and Optimization, Part 2 Apr. 1989 p 697-711 (For primary document see N89-25173 19-05)
Avail: NTIS HC A22/MF A01 CSCL 20K

N89-25184*# Pennsylvania State Univ., University Park. Dept. of Mechanical Engineering.
ITERATIVE METHODS FOR DESIGN SENSITIVITY ANALYSIS
A. D. Belegundu and B. G. Yoon *In* NASA. Langley Research Center, Recent Advances in Multidisciplinary Analysis and Optimization, Part 2 Apr. 1989 p 713-726 Previously announced in IAA as A89-22370 (For primary document see N89-25173 19-05)
Avail: NTIS HC A22/MF A01 CSCL 20K

N89-25185*# National Aeronautics and Space Administration. Langley Research Center, Hampton, VA.
RESULTS OF AN INTEGRATED STRUCTURE/CONTROL LAW DESIGN SENSITIVITY ANALYSIS
Michael G. Gilbert *In its* Recent Advances in Multidisciplinary Analysis and Optimization, Part 2 Apr. 1989 p 727-745 Previously announced as N89-15111 (For primary document see N89-25173 19-05)
Avail: NTIS HC A22/MF A01 CSCL 20K

N89-25186*# Nebraska Univ., Lincoln. Dept. of Engineering Mechanics.
ON THE CALCULATION OF DERIVATIVES OF EIGENVALUES AND EIGENVECTORS IN THE SIMULTANEOUS DESIGN AND CONTROL OF STRUCTURES
Luis Mesquita and Manohar P. Kamat (Georgia Inst. of Tech., Atlanta.) *In* NASA. Langley Research Center, Recent Advances in Multidisciplinary Analysis and Optimization, Part 2 Apr. 1989 p 747-758 (For primary document see N89-25173 19-05)
Avail: NTIS HC A22/MF A01 CSCL 20K

N89-25187*# Worcester Polytechnic Inst., MA. Dept. of Mechanical Engineering.
TREATMENT OF BODY FORCES IN BOUNDARY ELEMENT DESIGN SENSITIVITY ANALYSIS
Sunil Saigal, James H. Kane, R. Aithal, and Jizu Cheng *In* NASA. Langley Research Center, Recent Advances in Multidisciplinary Analysis and Optimization, Part 2 Apr. 1989 p 759-776 (For primary document see N89-25173 19-05)
(Grant NSF MSM-87-0742)
Avail: NTIS HC A22/MF A01 CSCL 20K

N89-25188*# Clarkson Univ., Potsdam, NY.
DESIGN SENSITIVITY ANALYSIS OF BOUNDARY ELEMENT SUBSTRUCTURES
James H. Kane, Sunil Saigal (Worcester Polytechnic Inst., MA.), and Richard H. Gallagher *In* NASA. Langley Research Center, Recent Advances in Multidisciplinary Analysis and Optimization, Part 2 Apr. 1989 p 777-799 (For primary document see N89-25173 19-05)
Avail: NTIS HC A22/MF A01 CSCL 20K

N89-25196*# Air Force Wright-Patterson Aeronautical Labs., Wright-Patterson AFB, OH.
AN APPROXIMATION FUNCTION FOR FREQUENCY CONSTRAINED STRUCTURAL OPTIMIZATION
R. A. Canfield *In* NASA. Langley Research Center, Recent Advances in Multidisciplinary Analysis and Optimization, Part 2 Apr. 1989 p 937-953 (For primary document see N89-25173 19-05)
Avail: NTIS HC A22/MF A01 CSCL 20K

N89-25197*# Air Force Wright-Patterson Aeronautical Labs., Wright-Patterson AFB, OH.
STRUCTURAL OPTIMIZATION OF FRAMED STRUCTURES USING GENERALIZED OPTIMALITY CRITERIA
R. M. Kolonay, Vipperla B. Venkayya, V. A. Tischler, and R. A. Canfield *In* NASA. Langley Research Center, Recent Advances in Multidisciplinary Analysis and Optimization, Part 2 Apr. 1989 p 955-969 (For primary document see N89-25173 19-05)
Avail: NTIS HC A22/MF A01 CSCL 20K

N89-25200*# General Dynamics Corp., Groton, CT. Electric Boat Div.
OPTIMIZING FOR MINIMUM WEIGHT WHEN TWO DIFFERENT FINITE ELEMENT MODELS AND ANALYSES ARE REQUIRED
Jeffrey C. Hall *In* NASA. Langley Research Center, Recent Advances in Multidisciplinary Analysis and Optimization, Part 2 Apr. 1989 p 1009-1026 (For primary document see N89-25173 19-05)
Avail: NTIS HC A22/MF A01 CSCL 20K

N89-25202*# National Aeronautics and Space Administration. Langley Research Center, Hampton, VA.
ENGINEERING APPLICATIONS OF HEURISTIC MULTILEVEL OPTIMIZATION METHODS
Jean-Francois M. Barthelemy *In its* Recent Advances in Multidisciplinary Analysis and Optimization, Part 3 Apr. 1989 p 1029-1037 Previously announced as N89-13203 (For primary document see N89-25201 19-05)
Avail: NTIS HC A22/MF A01 CSCL 20K

N89-25203*# California Univ., Santa Barbara. Dept. of Mechanical and Environmental Engineering.
RECENT DEVELOPMENTS IN MULTILEVEL OPTIMIZATION
Garret N. Vanderplaats and D.-S. Kim *In* NASA. Langley Research Center, Recent Advances in Multidisciplinary Analysis and Optimization, Part 3 Apr. 1989 p 1039-1054 (For primary document see N89-25201 19-05)
Avail: NTIS HC A22/MF A01 CSCL 20K

N89-25204*# Maryland Univ., College Park. Dept. of Mechanical Engineering.
A DECOMPOSITION-BASED DESIGN OPTIMIZATION METHOD WITH APPLICATIONS
Shapour Azarm, M. Pecht, W.-C. Li, and S. Praharaj *In* NASA. Langley Research Center, Recent Advances in Multidisciplinary Analysis and Optimization, Part 3 Apr. 1989 p 1055-1067 (For primary document see N89-25201 19-05)
Avail: NTIS HC A22/MF A01 CSCL 20K

N89-25224*# Jet Propulsion Lab., California Inst. of Tech., Pasadena.
STRUCTURAL OPTIMIZATION AND RECENT LARGE GROUND ANTENNA INSTALLATIONS
Roy Levy *In* NASA. Langley Research Center, Recent Advances in Multidisciplinary Analysis and Optimization, Part 3 Apr. 1989 p 1393-1416 (For primary document see N89-25201 19-05)
Avail: NTIS HC A22/MF A01 CSCL 20K

N89-25226*# California Univ., Berkeley. Coll. of Engineering.
COMPUTATIONAL EXPERIMENTS IN THE OPTIMAL SLEWING OF FLEXIBLE STRUCTURES
T. E. Baker and Lucian Elijah Polak *In* NASA. Langley Research Center, Recent Advances in Multidisciplinary Analysis and Optimization, Part 3 Apr. 1989 p 1427-1440 (For primary document see N89-25201 19-05)
(Contract N00014-86-K-0295; NSF ECS-85-17362; AF-AFOSR-0116-86)
Avail: NTIS HC A22/MF A01 CSCL 20K

N89-25228*# National Aeronautics and Space Administration. Langley Research Center, Hampton, VA.
EXPERIENCES IN APPLYING OPTIMIZATION TECHNIQUES TO CONFIGURATIONS FOR THE CONTROL OF FLEXIBLE STRUCTURES (COFS) PROGRAM
Joanne L. Walsh *In its* Recent Advances in Multidisciplinary Analysis and Optimization, Part 3 Apr. 1989 p 1459-1488 Previously announced as N89-15155 (For primary document see N89-25201 19-05)
Avail: NTIS HC A22/MF A01 CSCL 20K

N89-25229*# Ohio State Univ., Columbus. Dept. of Civil Engineering.
AN IMPROVED ALGORITHM FOR OPTIMUM STRUCTURAL DESIGN WITH MULTIPLE FREQUENCY CONSTRAINTS

Oliver G. McGee and Khing F. Phan *In* NASA. Langley Research Center, Recent Advances in Multidisciplinary Analysis and Optimization, Part 3 Apr. 1989 p 1489-1506 Sponsored in part by AF (For primary document see N89-25201 19-05)
Avail: NTIS HC A22/MF A01 CSCL 20K

N89-25230*# Florida Univ., Gainesville. Dept. of Aerospace Engineering, Mechanics and Engineering Science.
STRUCTURAL DAMAGE ASSESSMENT AS AN IDENTIFICATION PROBLEM
Prabhat Hajela and F. J. Soeiro *In* NASA. Langley Research Center, Recent Advances in Multidisciplinary Analysis and Optimization, Part 3 Apr. 1989 p 1507-1520 Submitted for publication (For primary document see N89-25201 19-05)
Avail: NTIS HC A22/MF A01 CSCL 20K

N89-25231*# Air Force Wright-Patterson Aeronautical Labs., Wright-Patterson AFB, OH.
RECENT DEVELOPMENTS IN LARGE-SCALE STRUCTURAL OPTIMIZATION
Vipperla B. Venkayya *In* NASA. Langley Research Center, Recent Advances in Multidisciplinary Analysis and Optimization, Part 3 Apr. 1989 p 1521-1540 (For primary document see N89-25201 19-05)
Avail: NTIS HC A22/MF A01 CSCL 20K

42 GEOSCIENCES (GENERAL)

No abstracts in this category.

43 EARTH RESOURCES AND REMOTE SENSING

Includes remote sensing of earth resources by aircraft and spacecraft; photogrammetry; and aerial photography.

For instrumentation see *35 Instrumentation and Photography.*

N89-25492*# Louisiana State Univ., Baton Rouge. Remote Sensing and Image Processing Lab.
USER'S GUIDE TO IMAGE PROCESSING APPLICATIONS OF THE NOAA SATELLITE HRPT/AVHRR DATA. PART 1: INTRODUCTION TO THE SATELLITE SYSTEM AND ITS APPLICATIONS. PART 2: PROCESSING AND ANALYSIS OF AVHRR IMAGERY
Oscar Karl Huh, Scott G. Leibowitz, Donald DiRosa, and John M. Hill Jan. 1986 235 p Original contains color illustrations
(Contract NAS5-28096)
(NASA-CR-180784; NAS 1.26:180784; RSIP-TR-301.86-Pt-1/2)
Avail: NTIS HC A11/MF A01 CSCL 05B

The use of NOAA Advanced Very High Resolution Radar/High Resolution Picture Transmission (AVHRR/HRPT) imagery for earth resource applications is provided for the applications scientist for use within the various Earth science, resource, and agricultural disciplines. A guide to processing NOAA AVHRR data using the hardware and software systems integrated for this NASA project is provided. The processing steps from raw data on computer compatible tapes (1B data format) through usable qualitative and quantitative products for applications are given. The manual is divided into two parts. The first section describes the NOAA satellite system, its sensors, and the theoretical basis for using these data for environmental applications. Part 2 is a hands-on description of how to use a specific image processing system, the International Imaging Systems, Inc. (I2S) Model 75 Array Processor and S575 software, to process these data. A.D.

N89-25493* National Aeronautics and Space Administration, Washington, DC.
EARTH RESOURCES: A CONTINUING BIBLIOGRAPHY WITH INDEXES (ISSUE 61)
Apr. 1989 170 p
(NASA-SP-7041(61); NAS 1.21:7041(61)) Avail: NTIS HC A08; NTIS standing order as PB89-903800, $15.50 domestic, $31.00 foreign CSCL 08B

This bibliography lists 606 reports, articles, and other documents introduced into the NASA scientific and technical information system between January 1 and March 31, 1989. Emphasis is placed on the use of remote sensing and geophysical instrumentation in spacecraft and aircraft to survey and inventory natural resources and urban areas. Subject matter is grouped according to agriculture and forestry, environmental changes and cultural resources, geodesy and cartography, geology and mineral resources, oceanography and marine resources, hydrology and water management, data processing and distribution systems, and instrumentation and sensors, and economic analysis. Author

N89-25494*# National Aeronautics and Space Administration. Ames Research Center, Moffett Field, CA.
VISIBLE AND NEAR-INFRARED CHANNEL CALIBRATION OF THE GOES-6 VISSR USING HIGH-ALTITUDE AIRCRAFT MEASUREMENTS
Gilbert R. Smith, Robert H. Levin, Robert S. Koyanagi (National Oceanic and Atmospheric Administration, Washington, DC.), and Robert C. Wrigley Apr. 1989 15 p
(NASA-TM-101064; A-89027; NAS 1.15:101064) Avail: NTIS HC A03/MF A01 CSCL 14B

Present and future visible and near-infrared wavelength sensors mounted on operational satellites do not have on-board absolute calibration devices. One means of establishing an in-orbit calibration for a satellite sensor is to make simultaneous measurements of a bright, relatively uniform scene along the satellite view vector from a calibrated instrument on board a high altitude aircraft. Aircraft data were recorded over White Sands, New Mexico, and the coincident aircraft and orbiting satellite data is compared for the visible and near-infrared wavelength channel of the GOES-6 Visible Infrared Spin-Scan Radiometer. Author

N89-25495 Delaware Univ., Newark.
MODELING LAND-SURFACE ALBEDOS FROM PLANT CANOPY ARCHITECTURE Ph.D. Thesis
Clinton Maurice Rowe 1988 295 p
Avail: Univ. Microfilms Order No. DA8904602

To overcome the limitations of using land surface albedos prescribed from observation, a model of radiation transfer in plant canopies was used to predict vegetation albedos. This model incorporates the optical properties of the vegetation and soil surface as well as the micro- and macro-structure of the canopy. Because of the model's reliance on these physical properties of the land-surface cover, it is able to account explicitly for albedo variations caused by factors both internal to and external from the vegetation canopy. Using the physiognomic classification of natural vegetation developed by Kuchler, representative canopy architectures for each of thirty-one vegetation types were developed for each month of the year. Monthly albedos were then simulated for each vegetation type under a range of irradiance distributions. When these results are compared to existing observations of plant canopy albedo, the degree of correspondence is, in many cases, quite good. Moreover, the dependence of albedo on irradiance distribution predicted by the model agrees well with established theory. Global maps of land-surface albedo are produced for both clear-sky and overcast conditions using a simple solar radiation model to determine the incident radiation field. These maps are compared to previously compiled maps of land-surface albedo. Large differences between the model- and observation-based global albedo maps occur. However, the model reproduces many of the large-scale features and seasonal trends. Dissert. Abstr.

N89-25496*# National Aeronautics and Space Administration. Ames Research Center, Moffett Field, CA.

CALIBRATION OF THE VISIBLE AND NEAR-INFRARED CHANNELS OF THE NOAA-9 AVHRR USING HIGH-ALTITUDE AIRCRAFT MEASUREMENTS FROM AUGUST 1985 AND OCTOBER 1986

Gilbert R. Smith, Robert H. Levin, Robert S. Koyanagi (National Environmental Satellite Service, Washington, DC.), and Robert C. Wrigley Apr. 1989 19 p

(NASA-TM-101063; A-89026; NAS 1.15:101063) Avail: NTIS HC A03/MF A01 CSCL 14B

Visible and near infrared wavelength sensors mounted on operational satellites now in use do not have onboard absolute calibration devices. One means of establishing an in-orbit calibration for a satellite sensor is to make simultaneous measurement of a bright, relatively uniform scene along the satellite view vector from a calibrated instrument on board a high altitude aircraft. Herein, aircraft data were recorded over White Sands, New Mexico at satellite overpass time. Comparison of the coincident aircraft and orbiting satellite data for the visible and near infrared wavelength channels of the NOAA-9 Advanced Very High Resolution Radiometer shows that the calibration of the visible channel was unchanged from prelaunch values, but that the near infrared channel has degraded 6 percent by Aug. 1985. By Oct. 1986 the visible channel had degraded 13 percent and the near infrared channel had degraded 19 percent. Author

N89-25497# Beleidscommie Remote Sensing, Delft (Netherlands).

APPLICATIONS OF REMOTE SENSING TECHNIQUES FOR THE INVENTORY AND MONITORING OF ENVIRONMENTAL POLLUTION Final Report

J. Azam Oct. 1988 30 p Original contains color illustrations

(Contract BCRS-Proj.Co-2.3)

(BCRS-88-15; ETN-89-94292) Avail: NTIS HC A03/MF A01

Three sites previously used in pollution ground investigations were selected as test sites to evaluate the viability of remote sensing techniques. Color-infrared and panchromatic black and white aerial photographs of various scales and age were used. Large scale panchromatic black and white and color-infrared photographs are shown to be useful for the inventory of environmental pollution. The results of field investigations confirm the reliability of interpretation to be sufficiently high for operational application of remote sensing for ground investigations related to environmental pollution. ESA

N89-25498# Deutsche Forschungs- und Versuchsanstalt fuer Luft- und Raumfahrt, Oberpfaffenhofen (West Germany). Abteilung Fernerkundung.

INVESTIGATIONS ON SATELLITE IMAGE AND REFERENCE DATA FOR EXPLORATION-RELATED TASKS

Dieter Schlichter, Lorenz Waeber, Dieter Kaiser, and Juergen Kuhlmann Jun. 1988 47 p In GERMAN; ENGLISH summary Original contains color illustrations

(DFVLR-FB-88-46; ISSN-0171-1342; ETN-89-94633) Avail: NTIS HC A03/MF A01; DFVLR, VB-PL-DO, Postfach 90 60 58, 5000 Cologne, Fed. Republic of Germany, DM 34

Satellite data processing and image interpretation is discussed. The development of an exploration-related image processing methodology led to a quick and complete mapping of the regional structure pattern as well as lithological units in humid climates on the basis of highly processed satellite imagery. For the evaluation of the potential of mapped lineaments, exploration derived reference data are prerequisites. Digitized data included in the image processing procedure support the interpretation of structures. Remote sensing methodology applied to exploration is compared with common exploration methods as to technical/economical aspects. It is shown that LANDSAT TM (and modern airborne scanner data) is an important and cost-effective tool for mineral exploration. The developed image processing methodology is operational and can be transferred to other climates as well as to other fields of application. ESA

N89-25499# Deutsche Forschungs- und Versuchsanstalt fuer Luft- und Raumfahrt, Oberpfaffenhofen (West Germany). Abteilung Planetare Erkundun.

COMPARATIVE INVESTIGATIONS OF MULTISPECTRAL SATELLITE IMAGE DATA OF MOMS-01, LANDSAT-TM AND LANDSAT-MSS FOR GEOLOGICAL AND VEGETATIONAL APPLICATIONS IN TEST SITES IN THE ANDES OF NORTHERN CHILE AND THE PARANA-BASIN OF BRAZIL Ph.D. Thesis - Ludwig-Maximilliians Univ., Munich

Martin Hauck Nov. 1988 250 p In GERMAN; ENGLISH summary

(DFVLR-FB-88-50; ISSN-0171-1342; ETN-89-94636) Avail: NTIS HC A11/MF A01; DFVLR, VB-PL-DO, Postfach 90 60 58, 5000 Cologne, Fed. Republic of Germany, DM 70

Tests were carried out to detect possibilities to improve and optimize existing systems, to determine quality and applicability of the experimental MOMS-01-sensor by comparison with the LANDSAT-TM-system, as well as to analyze suitability and limitations of remote sensing data for application in geology, petrography, hydrology, and vegetation depending on the system. System-dependent limitations applying remote sensing data resulted from comparing the parameters of the three investigated sensor systems. The data of MOMS-01-, LANDSAT-Thematic Mapper- and LANDSAT-MSS-systems were analyzed and confronted in test areas in South America. The test areas are situated in an arid region of the Andes as well as in a densely vegetated region, and in an agricultural intensely used region. Based on the results of the comparative investigations system-dependent limitations in possible applications of remote sensing data of the three sensor systems as well as proposals for drafting future geoscientific sensor systems were worked out. ESA

N89-25500# Technische Univ., Eindhoven (Netherlands). Dept. of Electrical Engineering.

ENHANCEMENT OF HEAT TRANSFER BY CORONA WIND

Henry Kadete (Dar-es-Salaam Univ., Tanzania) Dec. 1987 144 p Sponsored by the Netherlands Universities Foundation and the Dar es Salaam Univ., Tanzania

(EUT-87-E-184; ISBN-9-06-144184-6; ISSN-0167-9708; ETN-89-94772) Avail: NTIS HC A07/MF A01

The mechanism of heat transfer enhancement across solid gaseous interfaces by corona wind directed towards the heat transfer surface is investigated. Corona wind may adequately be described by the Navier-Stokes equations of motion. The Coulomb ion drag forces transferred to the neutral gas background, create corona wind. The corona current is a function of the applied voltage and the electrode gap geometry. The average wind is proportional to the square root of the corona current. THe corona wind velocity distribution is bellshaped with a maximum of 5 m/s. The electrokinetic conversion efficiency is of the order of 1 percent. The enhancement of heat transfer by corona wind is significant. Heat convection enhancement by up to 90 percent are measured. The enhancement of convective heat transfer by corona wind blowing on a heat transfer surface is proportional to the 0.3 power of the corona current. Enhancement of convective heat transfer is only due to the augmentation of the hydrodynamic flow of the air. ESA

N89-25501# Institut fuer Angewandte Geodaesie, Frankfurt am Main (Germany, F.R.).

REPORTS ON CARTOGRAPHY AND GEODESY. SERIES 1: ORIGINAL REPORTS, NUMBER 102 [NACHRICHTEN AUS DEM KARTEN- UND VERMESSUNGSWESEN. REIHE 1, HEFT NR. 102]

1988 167 p In GERMAN; ENGLISH summary Original contains color illustrations Document includes imagery as supplement

(ISSN-0469-4236; ETN-89-94677) Avail: NTIS HC A08/MF A01

The interpretation of LANDSAT Thematic-Mapper (TM) data for the acquisition of land information is treated. The forestry interpretation of TM data is presented. The digital evaluation of

SEASAT-SAR radar image data was examined. For individual titles, see N89-25502 through N89-25504.

N89-25502# Institut fuer Angewandte Geodaesie, Frankfurt am Main (Germany, F.R.).
INTERPRETATION OF THEMATIC MAPPER DATA FOR THE ACQUISITION OF LAND INFORMATION [INTERPRETATION VON THEMATIC-MAPPER-DATEN ZUR GEWINNUNG VON LANDINFORMATIONEN]
Sabine Guttmann, Klaus Niemz, and Isolde Zwenger *In its* Reports on Cartography and Geodesy: Series 1: Original Reports, No. 102 1988 p 5-43 In GERMAN; ENGLISH summary Original contains color illustrations (For primary document see N89-25501 19-43)
Avail: NTIS HC A08/MF A01

The acquisition of Earth information data using Thematic-Mapper data is outlined. The higher spectral resolution achieved by employing seven bands, together with the enhanced geometric resolution of 30 m x 30 m as compared to the 57 m x 79 m ground resolution previously obtained with the multispectral band, provide a higher information content which allows interpretation even for European conditions. It is demonstrated what kind of information can be extracted from the data by the interpretation of various combinations of bands. ESA

N89-25503# Institut fuer Angewandte Geodaesie, Frankfurt am Main (Germany, F.R.).
FORESTRY INTERPRETATION OF THEMATIC MAPPER (TM) DATA USING THE EXAMPLE OF THE FRANKFURT MUNICIPAL FOREST [FORSTLICHE INTERPRETATION VON TM-DATEN AN EINEM BEISPIEL AUS DEM FRAKFURTER STADTWALD]
Martin Lamberty and Isolde Zwenger *In its* Reports on Cartography and Geodesy. Series 1: Original Reports, No. 102 1988 p 45-58 In GERMAN; ENGLISH summary Original contains color illustrations (For primary document see N89-25501 19-43)
Avail: NTIS HC A08/MF A01

The possibility of acquiring detailed information for forestry applications using LANDSAT-TM data was studied. The information content of a segment of a TM scene covering part of the Frankfurt municipal forest was analyzed by enlarging to a similar scale as aerial photographs taken on the same date. The comparison of both results shows that the satellite data provide more detailed information than the presently known differentiations into deciduous, mixed deciduous, and coniferous forest. ESA

N89-25504# Institut fuer Angewandte Geodaesie, Frankfurt am Main (Germany, F.R.).
DIGITAL EVALUATION OF SEASAT-SAR RADAR IMAGE DATA [DIGITALE AUSWERTUNG VON SEASAT-SAR-RADARBILDDATEN] **c32**
Berthold Pfeiffer *In its* Reports on Cartography and Geodesy. Series 1: Original Reports, No. 102 1988 p 59-77 In GERMAN; ENGLISH summary (For primary document see N89-25501 19-43)
Avail: NTIS HC A08/MF A01

The use of spaceborne digital radar image data for small scale topographic and thematic mapping was studied. The information content of digital L-band radar data were analyzed; various evaluation methods of digital image processing for filtering, edge detection, and statistical analysis were employed and tested with regard to their applicability. The tests reveal which surface types and structures can be identified in the radar image and automatically or interactively by extracted in a subsequent combined digital evaluation involving other data (optical sensors, multitemporal data, etc). The comparison with the contents of small scale topographic and thematic maps shows which map contents can be extracted from the radar image and which additional image content can be extracted beyond the map content. ESA

44 ENERGY PRODUCTION AND CONVERSION

Includes specific energy conversion systems, e.g., fuel cells; global sources of energy; geophysical conversion; and windpower.

For related information see also *07 Aircraft Propulsion and Power, 20 Spacecraft Propulsion and Power,* and *28 Propellants and Fuels.*

N89-25505# Maryland Univ., College Park. Dept. of Mechanical Engineering.
COMBINED VAPOR COMPRESSION/ABSORPTION HEAT PUMP CYCLES FOR ENGINE-DRIVEN HEAT PUMPS Final Report, Oct. 1987 - Sep. 1988
Reinhard Radermacher, Keith E. Herold, and Lawrence A. Howe Dec. 1988 94 p
(Contract GRI-5086-260-1321)
(PB89-145437; GRI-88/0288) Avail: NTIS HC A05/MF A01 CSCL 10A

The performance of three combined absorption/vapor compression cycles for gas-fired internal combustion engine driven heat pumps was theoretically assessed. Two cycles were selected for the preliminary design of breadboard systems using only off-the-shelf components. The first cycle, based on the working pair ammonia/water, is termed the simple-cycle. The second cycle, based on the working pair lithium-bromide/water, is termed the compressor enhanced double-effect chiller. Both cycles are found to be technically feasible. The coefficient of performance and the capacity are increased by up to 21 percent for cooling in the first case (compressor efficiency of 0.7) and by up to 14 percent in the second (compressor efficiency of 0.5). Both were compared against the engine drive R22 vapor compression heat pump. The performance of actual machinery for both cycles is, in the current design, hampered by the fact that the desired oil-free compressors have poor isentropic efficiencies. Oil lubricated compressors together with very effective oil separators would improve the performance of the combined LiBr/water cycle to 23 percent. Author

N89-25506*# National Aeronautics and Space Administration. Lewis Research Center, Cleveland, OH.
CHALLENGES FOR FUTURE SPACE POWER SYSTEMS
Henry W. Brandhorst, Jr. 1989 6 p Presented at the European Space Power Conference, Madrid, Spain, 2-6 Oct. 1989; sponsored by the ESA
(NASA-TM-102063; E-4820; NAS 1.15:102063) Avail: NTIS HC A02/MF A01 CSCL 10B

The future appears rich in missions that will extend the frontiers of knowledge, human presence in space, and opportunities for profitable commerce. The key to success of these ventures is the availability of plentiful, cost effective electric power and assured, low cost access to space. While forecasts of space power needs are problematic, an assessment of future needs based on terrestrial experience was made. These needs fall into three broad categories-survival, self sufficiency and industrialization. The cost of delivering payloads to orbital locations from low earth orbit (LEO) to Mars was determined and future launch cost reductions projected. From these factors, then, projections of the performance necessary for future solar and nuclear space power options were made. These goals are largely dependent upon orbital location and energy storage needs. Author

N89-25507# Department of Energy, Washington, DC. Office of Assistant Secretary for Conservation and Renewable Energy.
ENERGY FROM THE EARTH: GEOTHERMAL ENERGY PROGRAM. FIVE YEAR RESEARCH PLAN, 1988-1992
Oct. 1988 78 p
(DE89-010080; DOE/CE-0248) Avail: NTIS HC A05/MF A01

Consistent with national energy policy guidance, the plan concentrates on research and development (R and D) and limits system experiments to only those necessary to stimulate industrial confidence in the validity of research findings. A key strategy

element is the continuation of the government/industry partnership which is critical to successful development of geothermal technology. The primary near-term research emphasis is the extension of hydrothermal technology options for reservoir identification, reservoir analysis, hard rock penetration, and flash and binary electric plants. The advanced geothermal resources—geopressured, hot dry rock, and magma—are longer-term and higher-risk focal points, and research in these areas centers on establishing a technology base that will allow industry to make prudent and timely investment decisions with respect to the use of these resources. DOE

N89-25508# Argonne National Lab., IL.
MANIFOLD, BUS SUPPORT AND COUPLING ARRANGEMENT FOR SOLID OXIDE FUEL CELLS Patent Application
Gareth W. Parry, inventor (to DOE) 21 Apr. 1988 33 p
(Contract W-31-109-eng-38)
(DE89-009604; PATENTS-US-A7184475;
US-Patent-Appl-SN-184475) Avail: NTIS HC A03/MF A01

Individual, tubular solid oxide fuel cells (SOFCs) are assembled into bundles called a module within a housing, with a plurality of modules arranged end-to-end in a linear, stacked configuration called a string. A common set of piping comprised of a suitable high temperature resistant material: (1) provides fuel and air to each module housing, (2) serves as electrically conducting buses, and (3) provides structural support for a string of SOFC modules. Ceramic collars are used to connect fuel and air inlet piping to each of the electrodes in an SOFC module and provide: (1) electrical insulation for the current carrying bus bars and gas manifolds, (2) damping for the fuel and air inlet piping, and (3) proper spacing between the fuel and air inlet piping to prevent contact between these tubes and possible damage to the SOFC. DOE

N89-25509# Midwest Research Inst., Golden, CO. Solar Energy Research Inst.
GEOTHERMAL ENERGY PROGRAM SUMMARY. VOLUME 2: RESEARCH SUMMARIES, FISCAL YEAR 1988
Mar. 1989 76 p
(Contract DE-AC02-83CH-10093)
(DE89-000865; DOE/CH-10093/50-Vol-2) Avail: NTIS HC A05/MF A01

The Geothermal Technology Division (GTD) of the U.S. Department of Energy (DOE) is charged with the lead Federal role in the research and development (R and D) of technologies that will assist industry in economically exploiting the nation's vast geothermal resources. The GTD R and D program represents a comprehensive, balanced approach to establishing all forms of geothermal energy as significant contributors to the nation's energy supply. It is structured both to maintain momentum in the growth of the existing hydrothermal industry and to develop long-term options offering the greatest promise for practical applications. The Geothermal Energy Program Summary for Fiscal Year 1988 is a two-volume set designed to be an easily accessible reference to inform the U.S. geothermal industry and other interested parties of the technological advances and progress achieved in the DOE geothermal program as well as to describe the thrust of the current R and D effort and future R and D directions. This volume, Volume 2, contains a detailed compilation of each GTD-funded R and D activity performed by national laboratories or under contract to industrial, academic, and nonprofit research institutions. The Program Summary is intended as an important technology transfer vehicle to assure the wide and timely dissemination of information concerning the department's geothermal research. DOE

N89-25510# Midwest Research Inst., Golden, CO. Solar Energy Research Inst.
OPERATIONAL EXPERIENCE OF THE OC-OTEC EXPERIMENTS AT NELH
Hal Link Feb. 1989 11 p Presented at the American Society of Mechanical Engineers Solar Energy Conference, San Diego, CA, 2 Apr. 1989
(Contract DE-AC02-83CH-10093)
(DE89-000877; SERI/TP-253-3480; CONF-890436-10) Avail: NTIS HC A03

The Solar Energy Research Institute, under funding and program direction from the U.S. Department of Energy, has been operating a small-scale test apparatus to investigate key components of open-cycle ocean thermal energy conversion (OC-OTEC). The apparatus started operations in October 1987 and continues to provide valuable information on heat- and mass-transfer processes in evaporators and condensers, gas sorption processes as seawater is depressurized and repressurized, and control and instrumentation characteristics of open-cycle systems. Although other test facilities have been used to study some of these interactions, this is the largest apparatus of its kind to use seawater since Georges Claude's efforts in 1926. The information obtained from experiments conducted in this apparatus is being used to design a larger scale experiment in which a positive net power production is expected to be demonstrated for the first time with OC-OTEC. This paper describes the apparatus, the major tests conducted during its first 18 months of operation, and the experience gained in OC-OTEC system operation. DOE

N89-25511# Argonne National Lab., IL.
MONOLITHIC SOLID OXIDE FUEL CELL DEVELOPMENT
K. M. Myles and C. C. McPheeters 1989 9 p Presented at the 2nd Space Electrochemical Research and Technology Conference, Cleveland, OH, 11 Apr. 1989
(Contract W-31-109-eng-38)
(DE89-010699; CONF-8904196-2) Avail: NTIS HC A02/MF A01

The feasibility of the monolithic solid oxide fuel cell (MSOFC) concept has been proven, and the performance has been dramatically improved. The differences in thermal expansion coefficients and firing shrinkages among the fuel cell materials have been minimized, thus allowing successful fabrication of the MSOFC with few defects. The MSOFC shows excellent promise for development into a practical power source for many applications from stationary power, to automobile propulsion, to space pulsed power. DOE

N89-25512# Idaho National Engineering Lab., Idaho Falls.
AN ORGANIZED EFFORT TO DEVELOP THE HYDROTHERMAL ENERGY RESOURCE
Kenneth J. Taylor 1989 7 p Presented at the US Department of Energy Research and Development for the Geothermal Marketplace: 7th Geothermal Program Review, San Francisco, CA, 21 Mar. 1989
(Contract DE-AC07-76ID-01570)
(DE89-011139; EGG-M-89102; CONF-890352-7) Avail: NTIS HC A02/MF A01

As a response to America's need for alternate energy sources, the U.S. Department of Energy has a Geothermal Program. Within this program is a Hydrothermal category. Currently, a wide range of tasks are being addressed as part of the Hydrothermal Program. The tasks include Industrialization, Reservoir Technology, Hard Rock Penetration and Conversion Technology. It is thought that successes already made in this program combined with upcoming successes will increase the likelihood of geothermal energy becoming a contributor to our nation's future energy needs. DOE

N89-25513# Idaho National Engineering Lab., Idaho Falls.
ADVANCED BINARY GEOTHERMAL POWER PLANTS WORKING FLUID PROPERTY DETERMINATION AND HEAT EXCHANGER DESIGN
C. J. Bliem and G. L. Mines 1989 8 p Presented at the US Department of Energy Research and Development for the Geothermal Marketplace: 7th Geothermal Program Review, San Francisco, CA, 21 Mar. 1989 Prepared in cooperation with Edgerton, Germeshaus en and Grier, Inc., Idaho Falls, ID
(Contract DE-AC07-76ID-01570)
(DE89-011144; EGG-M-89092; CONF-890352-5) Avail: NTIS HC A02/MF A01

The performance of binary geothermal power plants can be improved through the proper choice of a working fluid, and optimization of component designs and operating conditions. This paper reviews the investigations at the Idaho National Engineering Laboratory (INEL) which are examining binary cycle performance improvements for moderate temperature (350 to 400 F) resources with emphasis on how the improvements may be integrated into design of binary cycles. These investigations are examining performance improvements resulting from the supercritical vaporization of mixed hydrocarbon working fluids and achieving countercurrent integral condensation with these fluids, as well as the modification of the turbine inlet state points to achieve supersaturated turbine vapor expansions. For resources where the brine outlet temperature is restricted, the use of turbine exhaust recuperators is examined. The baseline plant used to determine improvements in plant performance (characterized by the increase in the net brine effectiveness, watt-hours per pound of brine) in these studies operates at conditions similar to the 45 MW Heber binary plant. Through the selection of the optimum working fluids and operating conditions, achieving countercurrent integral condensation, and allowing supersaturated vapor expansions in the turbine, the performance of the binary cycle (the net brine effectiveness) can be improved by 25 to 30 percent relative to the baseline plant. DOE

N89-25514# Midwest Research Inst., Golden, CO. Solar Energy Research Inst.

SUPPORT AND MANEUVERING APPARATUS FOR SOLAR ENERGY RECEIVERS Patent Application

Lawrence M. Murphy, inventor (to DOE) 28 Jul. 1988 18 p
(Contract DE-AC02-83CH-10093)
(DE89-011466; PATENTS-US-A7225444;
US-Patent-Appl-SN-225444) Avail: NTIS HC A03/MF A01

A support and maneuvering apparatus is disclosed for a solar energy receiving device adapted for receiving and concentrating solar energy and having a central axis extending through the center thereof. The apparatus includes a frame for mounting the perimeter of said solar energy receiving device. A support member extends along the central axis of the receiving device and has a base end passing through the center of the receiving device and an outer distal end adapted for carrying a solar energy receiving and conversion mechanism. A variable tension mechanism interconnects the support member with the frame to provide stiffening for the support member and the frame and to assist in the alignment of the frame to optimize the optical efficiency of the solar energy receiving device. A rotatable base is provided, and connecting members extend from the base for pivotable attachment to the frame at spaced positions therealong. Finally, an elevation assembly is connected to the receiving device for selectively pivoting the receiving about an axis defined between the attachment positions of the connecting members on the frame. DOE

N89-25515# Department of Energy, Washington, DC. Office of the Deputy Assistant Secretary for Oil, Gas, Shale and Special Technologies.

FUEL CELL SYSTEMS PROGRAM PLAN, FY 1989

May 1989 36 p
(DE89-012928; DOE/FE-0128) Avail: NTIS HC A03/MF A01

The DOE fuel cell program supports high-risk, high-payoff technology development. The principal DOE fuel cell program goal is to develop cost effective, efficient, and environmentally benign fuel cell systems which will operate on coal-based fuels (and dual fuels: coal and gas) in multiple end use sectors. The specific near- to mid-term (mid-1990s) objectives are to develop the key fuel cell technology for phosphoric acid, molten carbonate, and solid oxide fuel cell systems, and to evaluate and conduct research on more advanced fuel cell concepts that would further improve technical and economic performance. Key elements of the fuel cell systems program are discussed and include: develop phosphoric acid fuel cell technology for electric utility applications and on-site power generation with co-product heat; develop molten carbonate fuel technology for electric utility and industrial applications; develop solid oxide fuel cell technology for electric utility and industrial applications; evaluate other additional advanced fuel concept for electric utility, industrial, residential and transportation applications; and support advanced research needed to develop fuel cell technologies. DOE

N89-25516# Midwest Research Inst., Golden, CO. Solar Energy Research Inst.

FOCUSING ON THE FUTURE: SOLAR THERMAL ENERGY SYSTEMS EMERGE AS COMPETITIVE TECHNOLOGIES WITH MAJOR ECONOMIC POTENTIAL

Mar. 1989 16 p
(Contract DE-AC02-83CH-10093)
(DE89-000851; SERI/SP-220-3458) Avail: NTIS HC A03

Hundreds of thousands of U.S. citizens are now receiving a portion of their daily demand for electricity from large-scale solar thermal electric generating stations-power plants that use concentrated solar energy to drive electric power generators. Just as with coal, fuel oil, natural gas, and nuclear energy, concentrated solar energy can create working temperatures of around 600C and much higher. Also, solar power plants contribute almost nothing to the atmospheric greenhouse effect and pose few, if any, of the other environmental problems associated with conventional energy sources. As a result of research and development within the national Solar Thermal Technology Program of the U.S. Department of Energy (DOE), solar thermal energy is on the threshold of competing economically with conventional power plants and is now viable for international markets. Its potential for spurring American economic growth and exports is significant. DOE

N89-25517# Midwest Research Inst., Golden, CO. Solar Energy Research Inst.

WIND ENERGY PROGRAM SUMMARY. VOLUME 2: RESEARCH SUMMARIES, FISCAL YEAR 1988

Apr. 1989 69 p
(Contract DE-AC02-83CH-10093)
(DE89-000857; DOE/CH-10093/42) Avail: NTIS HC A04/MF A01

Activities by the Federal Wind Energy program since the early 1980s have focused on developing a technology base necessary for industry to demonstrate the viability of wind energy as an alternative energy supply. The Federal Wind Energy Program's research has targeted the sciences of wind turbine dynamics and the development of advanced components and systems. These efforts have resulted in major advancements toward the development and commercialization of wind technology as an alternative energy source. The installation of more than 16,000 wind turbines in California by the end of 1987 provides evidence that commercial use of wind energy technology can be a viable source of electric power. Research in wind turbine sciences has focused on atmospheric fluid dynamics, aerodynamics, and structural dynamics. As outlines in the projects that are described in this document, advancements in atmospheric fluid dynamics have been made through the development and refinement of wind characterization models and wind/rotor interaction prediction codes. Recent gains in aerodynamics can be attributed to a better understanding of airfoil operations, using innovative research approaches such as flow-visualization techniques. Qualitative information and data from laboratory and field tests are being used to document fatigue damage processes. These data are being used to develop new theories and data bases for structural dynamics, and will help to achieve long-term unit life and lower capital and maintenance costs. Material characterization and modeling techniques have been improved to better analyze effects of stress and fatigue on system components. DOE

N89-25518# Messerschmitt-Boelkow-Blohm G.m.b.H., Munich (Germany, F.R.).

DEVELOPMENT OF AN Si PANEL Final Report, Jul. 1987

Achim Bubenzer and Martin Gorn Mar. 1988 97 p In GERMAN; ENGLISH summary
(Contract BMFT-03-E-8288-A)
(ETN-89-94625) Avail: NTIS HC A05/MF A01

The substrate glass/TCO/pin/metal is analyzed for an industrial production process for low cost solar cells based on a-Si. Using a three chamber plasma reactor the overall process could be improved such that solar cells with an efficiency of 7 to 8 percent and a degradation of 15 to 25 percent could be reproducibly deposited. The overall process depends strongly upon the process for each single layer. Particular emphasis was put on the window layer. Measurement equipment was set up for the characterization of single layers and cells. With respect to industrial application, large area 60 x 60 cm static plasma deposition of a-Si layers was tested; thickness uniformities of 3 percent are achieved. For preparation of thin film series connected cells, four different patterning techniques for thin films were developed: Nd-YAG laser cutting, erosion, mechanical scribing, and lift-off. Test modules (10 x 10 cm) with efficiency of up to 5 percent were prepared.
ESA

N89-25519*# Jet Propulsion Lab., California Inst. of Tech., Pasadena.
ECUT (ENERGY CONVERSION AND UTILIZATION TECHNOLOGIES) PROGRAM: BIOCATALYSIS PROJECT Annual Report, FY 1988
Larry Baresi Mar. 1989 80 p Sponsored in part by DOE
(Contract NAS7-918)
(NASA-CR-184965; NAS 1.26:184965; DOE/CS-66001/12; JPL-Publ-89-5) Avail: NTIS HC A05/MF A01 CSCL 10A

The Annual Report presents the fiscal year (FY) 1988 research activities and accomplishments, for the Biocatalysis Project of the U.S. Department of Energy, Energy Conversion and Utilization Technologies (ECUT) Division. The ECUT Biocatalysis Project is managed by the Jet Propulsion Laboratory, California Institute of Technology. The Biocatalysis Project is a mission-oriented, applied research and exploratory development activity directed toward resolution of the major generic technical barriers that impede the development of biologically catalyzed commercial chemical production. The approach toward achieving project objectives involves an integrated participation of universities, industrial companies and government research laboratories. The Project's technical activities were organized into three work elements: (1) The Molecular Modeling and Applied Genetics work element includes research on modeling of biological systems, developing rigorous methods for the prediction of three-dimensional (tertiary) protein structure from the amino acid sequence (primary structure) for designing new biocatalysis, defining kinetic models of biocatalyst reactivity, and developing genetically engineered solutions to the generic technical barriers that preclude widespread application of biocatalysis. (2) The Bioprocess Engineering work element supports efforts in novel bioreactor concepts that are likely to lead to substantially higher levels of reactor productivity, product yields and lower separation energetics. Results of work within this work element will be used to establish the technical feasibility of critical bioprocess monitoring and control subsystems. (3) The Bioprocess Design and Assessment work element attempts to develop procedures (via user-friendly computer software) for assessing the energy-economics of biocatalyzed chemical production processes, and initiation of technology transfer for advanced bioprocesses.
Author

45 ENVIRONMENT POLLUTION

Includes atmospheric, noise, thermal, and water pollution.

N89-25520*# National Aeronautics and Space Administration, Washington, DC.
THE UARS (UPPER ATMOSPHERE RESEARCH SATELLITE): A PROGRAM TO STUDY GLOBAL OZONE CHANGE
1989 32 p Original contains color illustrations
(NASA-TM-101756; NAS 1.15:101756) Avail: NTIS HC A03/MF A01 CSCL 13B

NASA's Upper Atmosphere Research Satellite (UARS) program, its goals and objectives are described. Also included are its significance to upper atmosphere science, the experimental and theoretical investigations that comprise it, and the compelling issues of global change, driven by human activities, that led NASA to plan and implement it.
A.D.

N89-25521# Ocean Research Consultants, La Jolla, CA.
ON GREENHOUSE GAS SIGNAL DETECTION STRATEGIES
M. E. Schlesinger and T. P. Barnett 24 Feb. 1989 39 p
Prepared for Lawrence Livermore National Lab., CA
(Contract W-7405-eng-48)
(DE89-009908; UCRL-21147) Avail: NTIS HC A03/MF A01

The indisputable detection of a greenhouse gas signal in the global climate system will be a true decision point for mankind. Yet, at this stage of knowledge, the details of an appropriate detection strategy are only beginning to be developed. Two key elements in the eventual strategy are the subject of this report: (1) what variables should be monitored in a detection program, and (2) the comparison of the equilibrium versus transient climate system response. Subsequent sections consider these items in turn while a final section summarizes the main conclusion of the study.
DOE

N89-25522# Florida Univ., Gainesville.
WORKSHOP ON SEA LEVEL RISE AND COASTAL PROCESSES
Ashish J. Mehta, ed., Robert M. Cushman, ed., Robert G. Dean, Clay L. Montague, and William R. Dally (Florida Inst. of Tech., Melbourne.) Mar. 1989 290 p Workshop held in Palm Coast, FL, 9 Mar. 1988
(Contract DE-AC05-84OR-21400)
(DE89-010297; DOE/NBB-0086; CONF-8803204) Avail: NTIS HC A13/MF A01

To critique the conclusions of the UF report and to reach a broader consensus on research needs to vastly improve shoreline response predictive capabilities, a Workshop on Sea Level Rise and Coastal Processes was held at Palm Coast, Florida, on March 9 to 11, 1988. After the workshop the UF report was modified by the authors to constitute the bulk of the present report. An appendix to the report contains comments by the workshop participants, excluding the authors of the UF report. These comments comprise reviews of the UF document and views of individual participants regarding specific subject areas of their expertise, including research needs. While all the participants were chosen for their international experience and awareness of the problem, specific mention must be made of the contribution of John de Ronde, who was invited to present his view of the Dutch experience, which in many ways should provide insight into what may occur in other parts of the world at higher relative sea level. Participant comments largely reinforce the conclusions of the UF contribution through additional illustrative examples, clarifications, and qualifications in some cases. The role of possible climatic changes in addition to sea-level rise in influencing shoreline episodic response has been pointed out by several participants. Some have also touched upon the need to take sea-level rise into account in designing coastal structures over a typical design lifespan of 50 years.
DOE

N89-25523 Harvard Univ., Cambridge, MA.
MODELS FOR REGIONAL-SCALE PHOTOCHEMICAL PRODUCTION OF OZONE Ph.D. Thesis
Mark Sanford Sillman 1988 198 p
Avail: Univ. Microfilms Order No. DA8820571

The development of a comprehensive model for regional-scale ozone production is described. The model includes the effect of photochemical production of ozone in urban and rural areas from anthropogenic and biogenic precursors. A unique feature of the model is its ability to include the effects of both urban and power plant plumes in the context of a computationally efficient regional-scale air quality model. Results are used to explore the effectiveness of various control strategies for regional ozone. The sensitivity analysis shows that photochemical production of ozone depends critically on the NO(x) concentration. The rate of ozone production is limited by the availability of NO(x) for NO(x)

concentrations below 1 ppb. At higher NO(x) concentrations ozone production no longer increases with increasing NO(x) and becomes strongly dependent on the concentration of hydrocarbons. Analyses of ozone production both in a rural region and in an urban plume show that ozone production increases with increasing NO(x) emissions so long as NO(x) emissions remain below a certain critical value. Control strategies for regional ozone are investigated using plumes model simulations with emissions data from the National Acid Precipitation Assessment Program (NAPAP) Version 5.2 inventory. Results show that ozone concentrations may be substantially reduced by reducing anthropogenic NO(x) emissions from either urban or power plant sources. Dissert. Abstr.

N89-25524# Martin Marietta Environmental Systems, Columbia, MD.
INVESTIGATION OF SUBMICROMETER AEROSOLS FOR APPORTIONING THE IMPACTS OF AIRBORNE PARTICULATE MATTER AT DEEP CREEK LAKE Final Report
John M. Ondov, Jeffrey A. Dodd, and Gurdal Tuncel Apr. 1988 113 p
(Contract DE-AC22-83PC-61253)
(DE89-008186; DOE/PC-61253/T1) Avail: NTIS HC A06/MF A01

In August and early September of 1983, the Environmental Protection Agency (EPA) conducted an extensive receptor modeling study at and around the Deep Creek Lake area of northwestern Maryland. The overall purpose of the study was: (1) to test sampling techniques, (2) develop receptor models (most notably the hybrid tracer receptor model), and (3) to assess the impact of both primary and secondary emissions from local and distant fossil-fuel combustion sources. The EPA operated dichotomous samplers, a rain collector, an SO2 analyzer and other instruments for a 40-day period on the grounds of the Garret Community College located at the northeast tip of the lake. In addition, meterological data were obtained daily from a variety of sources for computation of air mass back-trajectories. The Department of Energy (DOE) and the Electric Power Research Institute (EPRI) confunded helicopter and fixed-winged aircraft flights to provide a regional air mass signature and signatures for three coal-fired power plants (CFPP) with significant potential for impacting DCL. The plume of a pulp and paper mill was also sampled and particulate samples were collected in-stack at three of the power plants. Analytical results for these samples were to be used to test one or more receptor models. DOE

N89-25525# Geological Survey, Denver, CO.
CLIMATIC CHANGES INFERRED FRON ANALYSES OF LAKE-SEDIMENT CORES, WALKER LAKE, NEVADA
In Che Yang 1989 20 p
(Contract DE-AI08-78ET-44802)
(DE89-010740; USGS/WRIR-89-4006) Avail: NTIS HC A03/MF A01

Organic and inorganic fractions of sediment collected from the bottom of Walker Lake, Nevada, have been dated by carbon-14 techniques. Sedimentation rates and the organic-carbon content of the sediment were correlated with climatic change. The cold climate between 25,000 and 21,000 years ago caused little runoff, snow accumulation on the mountains, and rapid substantial glacial advances; this period of cold climate resulted in a slow sedimentation rate (0.20 millimeter per year) and in a small organic-carbon content in the sediment. Also, organic-carbon accumulation rates in the lake during this period were slow. The most recent period of slow sedimentation rate and small organic-carbon content occurred between 10,000 and 5500 years ago, indicative of low lake stage and dry climatic conditions. This period of dry climate also was evidenced by dry conditions for Lake Lahontan in Nevada and Searles Lake in California, as cited in the literature. Walker Lake filled rapidly with water between 5500 and 4500 years ago. The data published in this report was not produced under an approved Site Investigation Plan (SIP) or Study Plan (SP) and will not be used in the licensing process. DOE

N89-25526# Colorado Univ., Boulder.
REDUCE UNCERTAINTY IN PROJECTION OF FUTURE SEA-LEVEL CHANGE DUE TO ICE WASTAGE Progress Report, Aug. 1988 - Apr. 1989
M. Meier Apr. 1989 5 p
(Contract DE-FG02-87ER-60570)
(DE89-011483; DOE/ER-60570/1) Avail: NTIS HC A02/MF A01

Since the conclusion of our 1988 field work activities, we have been occupied with organizing field data and redesigning our numerical model. Publications are in preparation describing last summer's field experiments and the basis for our new numerical model; one manuscript presenting current model results has been submitted to Water Resources Research. We are also planning an experimental program to accompany our field work. The accomplished goals of these activities are outlined below. A brief report on field studies at Agassiz Ice Cap, Ellesmere Island, Canada, in May, 1988, and on the Greenland Ice Sheet in August, 1988, was submitted to DOE in September, 1988, and is enclosed as Attachment A. Observational data from Agassiz Ice Cap were organized into an in-house data report last year. Additional information has been reduced from field notes and is being incorporated into the data report. The new information includes extra density profiles and macrophotographs of snow grains. A public data report is in preparation and will be available this summer through World Data Center A. DOE

N89-25527# Oak Ridge National Lab., TN. Environmental Sciences Div.
THE ROLE OF FORESTS IN ADDRESSING THE CO2 GREENHOUSE
Gregg Marland 1988 25 p Presented at the Global Climate Change Linkages: Acid Rain, Air Quality and Stratospheric Ozone, Washington, DC, 15 Nov. 1988
(Contract DE-AC05-84OR-21400)
(DE89-011568; CONF-881159-1) Avail: NTIS HC A03/MF A01

This document contains a transcript of a presentation that describes the potential effect of complete reforestation on diminishing the greenhouse effect. Other, more practical, less drastic alternatives are also discussed. DOE

N89-25528# Lawrence Livermore National Lab., CA.
ATMOSPHERIC CARBON DIOXIDE AND THE CLIMATE RECORD
Hugh W. Ellsaesser Apr. 1989 15 p Presented at the 6th Annual PACLIM Workshop, Pacific Grove, CA, 5-8 Mar. 1989
(Contract W-7405-eng-48)
(DE89-011892; UCRL-100954; CONF-890385-2) Avail: NTIS HC A03/MF A01

This paper is an attempt to provide a summary review of conclusions from previous studies on this subject. Subject headings include: conceptualization of the greenhouse effect, the climatic effect of doubled CO2, interpretation of the climatic record, diagnosis of apparent and possible model deficiencies, and the palaeoclimatic record. DOE

N89-25529# Lawrence Livermore National Lab., CA. Atmospheric and Geophysical Sciences Div.
CLIMATE PROJECTIONS WITH REGIONAL RESOLUTION
Michael C. MacCracken Mar. 1989 12 p Presented at the 4th International Conference of the Israel Society for Ecology and the Environmental Quality Sciences, Jerusalem, Israel, 4-8 Jun. 1989
(Contract W-7405-eng-48)
(DE89-009261; UCRL-100721-Rev-1; CONF-890695-1) Avail: NTIS HC A03/MF A01

The increasing atmospheric concentrations of carbon dioxide and other radiatively active gases will enhance the ability of the atmosphere to trap infrared radiation and thereby lead to warming of the climate. Numerical models suggest that the global average surface air temperature can be expected to increase a few degrees during the twenty-first century. This estimate is probably uncertain by a factor of at least two. The uncertainties in estimates of

regional changes of temperature and precipitation are even greater. Despite these uncertainties, there is broad agreement that the persistence of such changes would be unprecedented in historical times. DOE

N89-25530# Lawrence Livermore National Lab., CA.
PREVENTING DEPLETION OF STRATOSPHERIC OZONE: IMPLICATIONS ON FUTURE AIRCRAFT EMISSIONS
Douglas E. Kinnison and Donald J. Wuebbles Apr. 1989 17 p Presented at the 82nd Air and Waste Management Association Annual Meeting and Exhibition, Anaheim, CA, 25-30 Jun. 1989
(Contract W-7405-eng-48)
(DE89-009964; UCRL-99926; CONF-890692-4) Avail: NTIS HC A03/MF A01

There is much renewed interest in the development of faster aircraft for intercontinental passenger flights. Such aircraft would likely spend a large fraction of their flight time in the stratosphere, at altitudes as high as 35 km. It is important, in order to present the problems with the proposed supersonic-transport that occurred in the early 1970's, that the aircraft industry work together with the atmospheric science community to insure that future aircraft emissions will not deplete stratospheric ozone. In this study, we have used our two-dimensional model of the troposphere and stratosphere to examine the sensitivity of stratospheric ozone to such emissions. Initial results indicate, for commercial fleets as large as proposed for the original SST and depending on the odd-nitrogen emissions per engine, that substantial decreases in stratospheric ozone could result. The decrease in ozone is sensitive to the altitude and latitude in the emissions. Effects on ozone, for the same emission rate, tend to be larger as altitude increases, until a maximum effect is reached near 30 km. DOE

N89-25531# Lawrence Livermore National Lab., CA.
EVALUATING CFC (CHLOROFLUOROCARBON) ALTERNATIVES FROM THE ATMOSPHERIC VIEWPOINT
Peter S. Connell and Donald J. Wuebbles Apr. 1989 16 p Presented at the 82nd Air and Waste Management Association Annual Meeting and Exhibition, Anaheim, CA, 25-30 Jun. 1989
(Contract W-7405-eng-48)
(DE89-010238; UCRL-99927; CONF-890692-2) Avail: NTIS HC A03/MF A01

Current understanding of atmospheric processes in the troposphere and stratosphere, in particular, stratospheric ozone-controlling photochemistry, allows evaluation of the effects on the stratosphere of chlorine-containing compounds envisioned as CFC (chlorofluorocarbon) replacements prior to their production and release. We employ a two-dimensional (latitude and altitude) computational representation of the troposphere and stratosphere which incorporates physical processes, e.g., species transport and radiative transfer, and homogeneous photochemical processes. Laboratory measurements of OH and $O(^1D)$ reactivity and spectral parameters of the alternative HCFC (hydrochlorofluorocarbon) compounds were used as input. The model-derived ozone depletion potential (ODP) is a defined quantity relating the effect on ozone of emission of a species to the model-calculated effect of a standard compound, here CFC-11 ($CFCl_3$). Globally and annually averaged ozone depletion potentials vary from less than .02 to greater than 1.0 for various CFCs and HCFCs, primarily as a result of differences in calculated atmospheric lifetimes. Differences in stratospheric photochemistry among CFCs and HCFCs play a smaller but significant role. Zonally averaged ODPs for some compounds can range over a factor of three with latitude, however, as a result of differences in stratospheric lifetime and the altitude profile of Cl release in CFC or HCFC loss processes. DOE

N89-25532# Lawrence Livermore National Lab., CA.
CLOUD ALBEDO, GREENHOUSE EFFECTS, ATMOSPHERIC CHEMISTRY, AND CLIMATE CHANGE
Joyce E. Penner Mar. 1989 19 p Presented at the 82nd Air and Waste Management Association Annual Meeting and Exhibition, Anaheim, CA, 25-30 Jun. 1989
(Contract W-7405-eng-48)
(DE89-010239; UCRL-99928; CONF-890692-3) Avail: NTIS HC A03/MF A01

Changes in global atmospheric chemistry and climate are taking place as a result of observed trends in long-lived species such as CO_2, CH_4, N_2O, and the CFC's. The continuation of these trends is expected to eventually lead to a major atmospheric warming which might profoundly affect the society we live in. Trends in shorter-lived species such as NO(x) are also suspected. These trends are not as well established, because the shorter-lived species vary spatially and temporally. Trends in NO(x) would be expected to lead to increases in tropospheric ozone which would add to the warming created by the other greenhouse gases. Trends in NO(x) could also impact the concentration of OH, a scavenger for many other species. In addition to these changes increases in sulfur emissions may alter cloud optical properties. The changes in cloud optical properties could possibly offset the warming expected from increases in greenhouse gases, depending on the role of natural oceanic sulfur emissions of DMS. This paper summarizes recent research in these areas, and the interactions of climate and atmospheric chemistry. It is argued that the development of three-dimensional models will be necessary for a quantitative evaluation of the effects of short-lived species on global climate. DOE

N89-25533 Politecnico di Milano (Italy). Dipt. di Elettronica.
CATASTROPHIC BIFURCATIONS IN A SECOND ORDER DYNAMICAL SYSTEM
Simona Muratori and Sergio Rinaldi 1988 29 p
(Rept-88-049; ETN-89-94682) Avail: Politecnico di Milano, Piazza Leonardo da Vinci 32, 20133 Milan, Italy

A second order nonlinear dynamical system modelling the interactions of trees and damaging insects in a forest is presented. The influence of acidic deposition is discussed. An increase can cause sudden insect infestations and the collapse of the forest ecosystem. The analysis is carried out by finding the bifurcations and proving that under suitable condition such bifurcations can be catastrophic. The condition for bifurcation can be given in an explicit way to facilitate the interpretation of the results. ESA

46 GEOPHYSICS

Includes aeronomy; upper and lower atmosphere studies; ionospheric and magnetospheric physics; and geomagnetism.

For space radiation see *93 Space Radiation.*

N89-25534*# Harvard Coll. Observatory, Cambridge, MA.
STUDIES OF REGIONAL AND GLOBAL TECTONICS AND THE ROTATION OF THE EARTH USING VERY-LONG BASELINE INTERFEROMETRY Semiannual Status Report, 1 Nov. 1988 - 30 Apr. 1989
Irwin I. Shapiro 14 Jun. 1989 47 p
(Grant NAG5-538)
(NASA-CR-185059; NAS 1.26:185059) Avail: NTIS HC A03/MF A01 CSCL 08G

Progress in the areas of data analysis, atmospheric delay calibration and software conversion is reported. Over 800 very long baseline interferometry (VLBI) experiments were analyzed in the last 6 months. Reprocessing of the Mark III VLBI data set is almost completed. Results of analysis of the water-vapor radiometer (WVR) data were submitted and a preprint of a related paper is attached. Work on conversion of the VLBI analysis software from HP1000 to Unix based workstations is continuing. K.C.D.

N89-25535# Central Inst. of Physics, Bucharest (Romania).
RESEARCH FOR THE PHYSICS AND STRUCTURE OF EARTH'S CRUST IN ROMANIA
T. P. Ghitulescu and M. N. Popescu Oct. 1987 37 p In ROMANIAN; ENGLISH summary
(DE88-706002; ICEFIZ-EP-35-1987) Avail: NTIS (US Sales Only) HC A03/MF A01

Systematic research for the deciphering of the physic and

structure of the Earth's crust in Romania by geophysical methods were performed in the frame of Romanian Geological Institute since 1925. We put into evidence the principle achievements obtained by the geological and geophysical research for the mineral resources existing in the Romanian Earth crust. DOE

N89-25536# Joint Inst. for Nuclear Research, Dubna (USSR). Lab. of Theoretical Physics.
IMBEDDING OF THE GRAVITATIONAL FIELD INTO THE SPACE OF AFFINE CONNECTION WITHOUT TORSION
N. A. Chernikov 1988 8 p In RUSSIAN; ENGLISH summary (DE88-704637; JINR-R-2-88-27) Avail: NTIS (US Sales Only) HC A02/MF A01

Mathematical meaning of the energy-momentum pseudoscalar is exactly determined in the general relativity: this geometrical object is a tensor functional of the background connection. Affine connection of that type was first considered in 1940 by Rosen who imbedded the gravitational field into the Minkowski world. The background connection then appeared in a primitive form: it had neither curvature, nor torsion. In our case the background connection acquires an arbitrary curvature so that the gravitational field is imbedded into an arbitrary space of the affine connection without torsion. Variational derivatives of the action function is taken both with respect to the basic metric tensor and the background connection. The result is a new identity whose particular case is the known identity for the Einstein tensor. If the background connection is considered Christofel, the known Papapetrou results follow in a generalized form. If now we equate the variational derivative with respect to the basic tensor, to zero, we obtain the form of equations for the gravitational field on the background of affine connection without torsion. DOE

N89-25537 Miami Univ., FL.
THE BEHAVIOR OF A CLASS OF MINIMAL MODELS OF THE ATMOSPHERIC GENERAL CIRCULATION Ph.D. Thesis
Enda William OBrien 1988 176 p
Avail: Univ. Microfilms Order No. DA8827958

Minimal criteria are established which a numerical model of the atmosphere must meet in order to qualify as a general circulation model. The ability of a class of low-order, two-layer, beta-plane channel models to meet these criteria is investigated. At least the first and third meridional modes are required in order to achieve qualitatively correct heat and momentum balances. A (3,3) model (i.e., three waves resolved in both horizontal directions) having the optimal resolution for the selected model geometry and formulation was examined. A parameter study was conducted on a (2,2) version of the model which included zonally asymmetric bottom topography, since very pronounced weather regimes had previously been found for this case. Stationary wave budget studies were conducted when topography was included in the (3,3) and higher order models. Heat and vorticity budgets were dominated by the linear or wave-mean flow interaction terms. Nonlinear or wave-wave interaction terms were smaller, always acted to oppose the sense of the corresponding linear term, and had the effect of smoothing out the stationary wave in the height and vorticity fields. Little evidence of multiple equilibria or weather regimes was revealed. However, the (5,5) model exhibited a significant amount of low-frequency variability and many strong, long-lived anomalies. Dissert. Abstr.

N89-25538 East Anglia Univ., Norwich (England).
REGIONAL VALIDATION OF GENERAL CIRCULATION MODELS Ph.D. Thesis
Benjamin David Santer 1987 395 p
Avail: Univ. Microfilms Order No. BRD-84379

General Circulation Models (GCMs) of the atmosphere and ocean were used for performing a variety of climate experiments. Confidence in the reliability of experimental results can only be obtained by detailed validation of model control run results. The regional and seasonal details of the mean sea-level pressure (MSLP) fields simulated by three GCMs-the OSU two-layer Atmospheric General Circulation Model (AGCM), the OSU Coupled General Circulation Model (CGCM) and the Goddard Institute for Space Science (GISS) nine-layer AGCM were studied. Model validation is performed in a North American/Atlantic/European study area. The main focus is on the statistical aspects of control run validation. Eighteen different statistics are used to test the significance of differences between observed and simulated means, variances and spatial patterns. Test statistic significance is determined using Preisendorfer and Barnett's permutation procedures. Statistics which measure the degree of spatial autocorrelation in latitudinal and longitudinal directions are also used to compare observed and simulated fields. Validation of the simulated seasonal cycles of MSLP indicates that all three models have statistically significant errors in the mean field, variances, and spatial patterns. For the three models examined, test statistic significance levels for observed/simulated differences in the mean field and spatial patterns are relatively insensitive to decadal time-scale variability in the observed MSLP data. Author

N89-25539*# National Aeronautics and Space Administration. Goddard Space Flight Center, Greenbelt, MD.
DYNAMIC SEA SURFACE TOPOGRAPHY, GRAVITY AND IMPROVED ORBIT ACCURACIES FROM THE DIRECT EVALUATION OF SEASAT ALTIMETER DATA
J. G. Marsh, F. Lerch, C. J. Koblinsky, S. M. Klosko, J. W. Robbins, R. G. Williamson, and G. B. Patel (ST Systems Corp., Lanham, MD.) May 1989 110 p Original contains color illustrations (NASA-TM-100735; Rept-89B0111; NAS 1.15:100735) Avail: NTIS HC A06/MF A01 CSCL 08C

A method for the simultaneous solution of dynamic ocean topography, gravity and orbits using satellite altimeter data is described. A GEM-T1 based gravitational model called PGS-3337 that incorporates Seasat altimetry, surface gravimetry and satellite tracking data has been determined complete to degree and order 50. The altimeter data is utilized as a dynamic observation of the satellite's height above the sea surface with a degree 10 model of dynamic topography being recovered simultaneously with the orbit parameters, gravity and tidal terms in this model. PGS-3337 has a geoid uncertainty of 60 cm root-mean-square (RMS) globally, with the uncertainty over the altimeter tracked ocean being in the 25 cm range. Doppler determined orbits for Seasat, show large improvements, with the sub-30 cm radial accuracies being achieved. When altimeter data is used in orbit determination, radial orbital accuracies of 20 cm are achieved. The RMS of fit to the altimeter data directly gives 30 cm fits for Seasat when using PGS-3337 and its geoid and dynamic topography model. This performance level is two to three times better than that achieved with earlier Goddard earth models (GEM) using the dynamic topography from long-term oceanographic averages. The recovered dynamic topography reveals the global long wavelength circulation of the oceans with a resolution of 1500 km. The power in the dynamic topography recovery is now found to be closer to that of oceanographic studies than for previous satellite solutions. This is attributed primarily to the improved modeling of the geoid which has occurred. Study of the altimeter residuals reveals regions where tidal models are poor and sea state effects are major limitations. Author

N89-25540*# National Aeronautics and Space Administration. Langley Research Center, Hampton, VA.
COMPARISON OF SATELLITE-DERIVED DYNAMICAL QUANTITIES FOR THE STRATOSPHERE OF THE SOUTHERN HEMISPHERE
Thomas Miles, ed. and Alan ONeill, ed. Washington Jul. 1989 39 p Presented at the Workshop on the Middle Atmosphere in the Southern Hemisphere, Williamsburg, VA, 14-17 Apr. 1986; sponsored by NASA, Washington, DC
(NASA-CP-3044; L-16593; NAS 1.55:3044) Avail: NTIS HC A03/MF A01 CSCL 04A

As part of the international Middle Atmosphere Program (MAP), a project was instituted to study the dynamics of the Middle Atmosphere in the Southern Hemisphere (MASH). A pre-MASH workshop was held with two aims: comparison of Southern Hemisphere dynamical quantities derived from various archives of satellite data; and assessing the impact of different base-level

height information on such derived quantities. The dynamical quantities examined included geopotential height, zonal wind, potential vorticity, eddy heat and momentum fluxes, and Eliassen-Palm fluxes. It was found that while there was usually qualitative agreement between the different sets of fields, substantial quantitative differences were evident, particularly in high latitudes. The fidelity of the base-level analysis was found to be of prime importance in calculating derived quantities - especially the Eliassen-Palm flux divergence and potential vorticity. Improvements in base-level analyses are recommended. In particular, quality controls should be introduced to remove spurious localized features from analyses, and information from all Antarctic radiosondes should be utilized where possible. Caution in drawing quantitative inferences from satellite data for the middle atmosphere of the Southern Hemisphere is advised. Author

N89-25541*# Iowa Univ., Iowa City. Dept. of Physics.
WAVE EMISSIONS FROM PLANETARY MAGNETOSPHERES
Final Report, 1 Jun. 1985 - 31 May 1989
Crockett L. Grabbe Mar. 1989 68 p
(Grant NAGw-827)
(NASA-CR-185435; NAS 1.26:185435) Avail: NTIS HC A04/MF A01 CSCL 04A

An important development in the Earth magnetosphere was the discovery of the boundary of the plasma sheet and its apparent role in the dynamics of the magnetotails. Three instabilities (negative energy mode, counterstreaming, and the Buneman instability) were investigated through analytical and numerical studies of their frequency and growth rate as a function of the angle of propagation. B.G.

N89-25542# Washington State Univ., Pullman. Dept. of Geology.
GEOLOGIC SPATIAL ANALYSIS PROGRAM USERS GUIDE FOR DIGITAL ELEVATION MODEL ANALYSIS PROCEDURES FOR DETECTION OF CRUSTAL FRACTURE PLANES
Jay R. Eliason and George L. Landle 1 Jun. 1988 30 p
(Contract DE-FG06-87ER-13796)
(DE89-010880; DOE/ER-13796/7) Avail: NTIS HC A03

The programs developed for analysis of digital elevation models to define crustal fracture planes have evolved from research initiated in 1983. This program users guide is a preliminary attempt to show users the sequence of programs used in the analysis. There are now 16 individual programs and as the research progresses, others will replace and/or complement those described here. The functions of the programs are briefly described in the sequence a user conducting an analysis would need to use them. Each program is then described and required interactive input is shown in bold text. The computer prompt WASSU RGA and all terminal statements and requests are provided as an example for the user. Input and output files are identified. Several of the programs require the user to run on a Digital Equipment Corporation VAX workstation GPX. DOE

N89-25543# Oulu Univ. (Finland). Dept. of Physics.
AN AURORAL TV-SYSTEM
Kari Kaila and Pekka Tanskanen Dec. 1988 39 p
(Rept-115(1988); ISBN-9-51-422714-X; ISSN-0356-1852; ETN-89-94555) Avail: NTIS HC A03/MF A01

An auroral TV-photometer system was built. A five channel scanning auroral photometer system was constructed. It measures the intensity of the auroras in north-south direction, partly in the same wavelengths as the TV-camera. The auroral TV reproduces images of rapidly varying auroral phenomena, whereas the photometer measures their intensities. Both instruments combined, give a powerful tool in the studies of optical aurora. The television system was used to photograph auroras. The television, combined with the photometer system is operational. ESA

N89-25544# Deutsche Forschungs- und Versuchsanstalt fuer Luft- und Raumfahrt, Oberpfaffenhofen (West Germany). Abteilung Atmosphaerische Dynamik.
MESOSCALE MODEL PARAMETERIZATIONS FOR RADIATION AND TURBULENT FLUXES AT THE LOWER BOUNDARY
Franz Somieski Nov. 1988 41 p
(Contract BMFT-KF-3012/4)
(DFVLR-FB-88-48; ISSN-0171-1342; ETN-89-94634) Avail: NTIS HC A03/MF A01; DFVLR, VB-PL-DO, Postfach 90 60 58, 5000 Cologne, Fed. Republic of Germany, DM 15.50

A radiation parameterization scheme for use in mesoscale models with orography and clouds was developed. Broadband parameterizations are presented for the solar and the terrestrial spectral ranges. They account for clear, turbid, or cloudy atmospheres. The scheme is one-dimensional in the atmosphere, but the effects of mountains (inclination, shading, elevated horizon) are taken into account at the surface. In the terrestrial brand, gray and black clouds are considered. The calculation of turbulent fluxes of sensible and latent heat and momentum at an inclined lower model boundary is described. Surface-layer similarity and the surface energy budget are used to evaluate the ground surface temperature. The total scheme is part of the mesoscale model MESOSCOP. ESA

N89-25545 Deutsche Geodaetische Kommission, Munich (Germany, F.R.).
GRAVITY NETWORK OF WEST GERMANY 1976 (DSGN76). PART 3: DATA AND ADJUSTMENTS [DAS SCHWEREGRUNDNETZ 1976 DER BUNDESREPUBLIK DEUTSCHLAND (DSGN76). TEIL 3: DATEN UND AUSGLEICHUNG]
Gerd Boedecker and Bernd Richter 1987 49 p In GERMAN; ENGLISH summary Document includes microfiche as supplement
(Ser-C-286; ISBN-3-76-968571-7; ISSN-0065-537; ETN-89-93997)
Copyright Avail: Deutsche Geudaetische Kommission, Marstallplatz 8, D-8000 Munich 22, Fed. Republic of Germany

Characteristics of the West German Gravimetry Data Base (DSGN 76) are described. Absolute observation values are evaluated and controlled. Data analysis includes the reduction of parameters, variance estimation, and adjustment procedures for the observed gravity differences. For individual titles, see N89-25546 through N89-25548.

N89-25546 Deutsche Geodaetische Kommission, Munich (Germany, F.R.).
GRAVITY NETWORK OF WEST GERMANY (DSGN76): MEASUREMENTS AND STARTING DATA [DAS SCHWEREGRUNDNETZ 1976 DER BUNDESREPUBLIK DEUTSCHLAND (DSGN76): MESSUNGEN, AUSGANGSDATEN]
Gerd Boedecker *In its* Gravity Network of West Germany 1976 (DSGN76): Part 3: Data and Adjustment 1987 p 5-17 In GERMAN (For primary document see N89-25545 19-46)
Copyright Avail: Deutsche Geudaetische Kommission, Marstallplatz 8, D-8000 Munich 22, Fed. Republic of Germany

Characteristics of the data base for the DSGN76 are described. Gravimetry observations in 512 series were carried out and recorded on computer-readable forms. The four absolute observations for datum and scale control are evaluated. Values at 16 International Gravity Standardization Net 1971 (IGSN71) stations were available as a possible complementary or alternate basis for datum and scale. The so-called Honkasalo-term, the time-constant tide, is discussed. ESA

N89-25547 Deutsche Geodaetische Kommission, Munich (Germany, F.R.).
ADJUSTMENT AND DATA ANALYSIS [AUSGLEICHUNG UND DATENANALYSE]
Gerd Boedecker *In its* Gravity Network of West Germany 1976 (DSGN76): Part 3: Data and Adjustment 1987 p 19-37 In GERMAN (For primary document see N89-25545 19-46)
Copyright Avail: Deutsche Geudaetische Kommission, Marstallplatz 8, D-8000 Munich 22, Fed. Republic of Germany

The determination of the final values for the gravimetry data base (DSGN76) requires adjustment and data analysis including the reduction of groups of parameters from the normal equations, variants for adjusting a free network, supplementary restrictions, and iterative variance estimation. The final set of parameters and the forming of weight groups is decided on the basis of numerical results for parameters and residues. Thus data analysis becomes an integral constituent of model development. ESA

N89-25548 Institut fuer Angewandte Geodaesie, Frankfurt am Main (Germany, F.R.).
DATA ADJUSTMENT BY GRAVITY DIFFERENCES [AUSGLEICHUNG NACH SCHWEREDIFFERENZEN]
Bernd Richter *In* Deutsche Geodaetische Kommission, Gravity Network of West Germany 1976 (DSGN76): Part 3: Data and Adjustment 1987 p 39-49 In GERMAN (For primary document see N89-25545 19-46)
Copyright Avail: Deutsche Geudaetische Kommission, Marstallplatz 8, D-8000 Munich 22, Fed. Republic of Germany

For the Gravimetry Data Base (DSGN76) data smoothing procedures are applied. The adjustment approach starts observed gravity differences. Corresponding to the adjustment of the old German gravity base network 1962 the first computations used the condition approach. The final adjustment including also excenters utilized the method of observation equations. Besides weight estimation the effect of periodic calibration errors was investigated. ESA

N89-25730 Ruhr Univ., Bochum (Germany, F.R.). Inst. fuer Theoretische Physik IV.
MODELS FOR AXIALLY SYMMETRIC PULSAR MAGNETOSPHERES
T. Neukirch *In* Max-Planck-Inst. fuer Physik und Astrophysik, Cosmic Plasma Physics Nov. 1988 p 98-102 (For primary document see N89-25716 19-75)
Copyright Avail: Max-Planck-Inst. fuer Physik und Astrophysik, D-8046 Garching bei Muenchen, Fed. Republic of Germany

N89-25793*# Iowa State Univ. of Science and Technology, Ames. Dept. of Earth Sciences.
THE EFFECT OF GLOBAL-SCALE DIVERGENT CIRCULATION ON THE ATMOSPHERIC WATER VAPOR TRANSPORT AND MAINTENANCE
Tsing-Chang Chen *In* Lunar and Planetary Inst., MECA Workshop on Atmospheric H2O Observations of Earth and Mars. Physical Processes, Measurements and Interpretations 1988 p 22-28 (For primary document see N89-25790 19-91)
(Grant NSF ATM-86-11476)
Avail: NTIS HC A05/MF A01 CSCL 04A

N89-25798*# National Center for Atmospheric Research, Boulder, CO.
CUMULUS CONVECTION AND THE TERRESTRIAL WATER-VAPOR DISTRIBUTION
Leo J. Donner *In* Lunar and Planetary Inst., MECA Workshop on Atmospheric H2O Observations of Earth and Mars. Physical Processes, Measurements and Interpretations 1988 p 41-45 (For primary document see N89-25790 19-91)
Avail: NTIS HC A05/MF A01 CSCL 04A

N89-25802*# Colorado Univ., Boulder. Lab. for Atmospheric and Space Physics.
SOLAR MESOSPHERE EXPLORER OBSERVATIONS OF STRATOSPHERIC AND MESOSPHERIC WATER VAPOR
Abstract Only
Bruce M. Jakosky, Gary E. Thomas, David W. Rusch, Charles A. Barth, George M. Lawrence, John J. Olivero (Pennsylvania State Univ., University Park.), R. Todd Clancy, Ryan W. Sanders, and Barry G. Knapp *In* Lunar and Planetary Inst., MECA Workshop on Atmospheric H2O Observations of Earth and Mars. Physical Processes, Measurements and Interpretations 1988 p 54-55 Prepared in cooperation with NOAA, Washington, DC (For primary document see N89-25790 19-91)
Avail: NTIS HC A05/MF A01 CSCL 04A

N89-25805*# National Aeronautics and Space Administration. Langley Research Center, Hampton, VA.
OBSERVATIONS OF ATMOSPHERIC WATER VAPOR WITH THE SAGE 2 INSTRUMENT
Jack C. Larsen (SASC Technologies, Inc., Hampton, VA.), M. P. McCormick, L. R. McMaster, and W. P. Chu *In* Lunar and Planetary Inst., MECA Workshop on Atmospheric H2O Observations of Earth and Mars. Physical Processes, Measurements and Interpretations 1988 p 62-66 (For primary document see N89-25790 19-91)
(Contract NAS1-17022)
Avail: NTIS HC A05/MF A01 CSCL 04A

N89-25806*# Lunar and Planetary Inst., Houston, TX.
FLUX OF WATER VAPOR IN THE TERRESTRIAL STRATOSPHERE AND IN THE MARTIAN ATMOSPHERE
Conway Leovy, Matthew Hitchman, and Daniel J. McCleese (Jet Propulsion Lab., California Inst. of Tech., Pasadena.) *In its* MECA Workshop on Atmospheric H2O Observations of Earth and Mars. Physical Processes, Measurements and Interpretations 1988 p 67-69 (For primary document see N89-25790 19-91)
Avail: NTIS HC A05/MF A01 CSCL 04A

N89-25808*# Pennsylvania State Univ., University Park. Dept. of Meteorology.
MEASUREMENTS OF H2O IN THE TERRESTRIAL MESOSPHERE AND IMPLICATIONS FOR EXTRA-TERRESTRIAL SOURCES
John J. Olivero *In* Lunar and Planetary Inst., MECA Workshop on Atmospheric H2O Observations of Earth and Mars. Physical Processes, Measurements and Interpretations 1988 p 71-74 (For primary document see N89-25790 19-91)
Avail: NTIS HC A05/MF A01 CSCL 04A

N89-25810*# National Aeronautics and Space Administration. Langley Research Center, Hampton, VA.
THE NIMBUS 7 LIMS (LIMB INFRARED MONITOR OF THE STRATOSPHERE) WATER VAPOR MEASUREMENTS
Ellis E. Remsberg and James M. Russell, III *In* Lunar and Planetary Inst., MECA Workshop on Atmospheric H2O Observations of Earth and Mars. Physical Processes, Measurements and Interpretations 1988 p 80-81 (For primary document see N89-25790 19-91)
Avail: NTIS HC A05/MF A01 CSCL 04A

47 METEOROLOGY AND CLIMATOLOGY

Includes weather forecasting and modification.

N89-25549# Lawrence Livermore National Lab., CA.
CLIMATE PROJECTIONS WITH REGIONAL RESOLUTION
Michael C. MacCracken Mar. 1989 10 p Presented at the 1st Annual Symposium on Frontiers of Science, Irvine, CA, 2 Mar. 1989
(Contract W-7405-eng-48)
(DE89-009904; UCRL-100721; CONF-8903104-1) Avail: NTIS HC A02/MF A01

Model calculations, supported by paleoclimatic and analytic studies and verified against a variety of cases of past climatic change, suggest that the global average surface air temperatures will increase several degrees during the next century if the increasing rates of emission of greenhouse gases continue. Such an increase would raise the long-term global average temperatures to levels not experienced in mid-latitudes back at least as far as the last interglacial 125,000 years ago, and the change would occur more rapidly than ecosystems have been able to adapt to in the past. Model projections of low latitude temperature increases of a few degrees would raise temperatures to levels not experienced in tens of millions of years. (That the models indicate such high sensitivity in low latitudes is perhaps an indication that

models are missing an important temperature stabilizing mechanism that has been hidden because the observed seasonal variation in temperatures in these regions is so small.) High confidence predictions of such large global-scale temperature changes may provide sufficient information for the world to institute measures to slow the rate of increase of emissions and thereby the rate of temperature change. Reducing total global emissions will be very difficult without halting the increasing energy use and rising standard of living in the developing world. DOE

N89-25550 California Univ., Los Angeles.
THE EVOLUTION AND STRUCTURE OF THE BOW ECHO/MICROBURST EVENTS Ph.D. Thesis
Wen-Chau Lee 1988 291 p
Avail: Univ. Microfilms Order No. DA8906408

Multiple Doppler radar analysis (three dimensional wind fields, pressure and buoyancy retrievals, vorticity budget and trajectory) is performed for the primary case of July 14, 1982 during the Joint Airport Weather Study (JAWS) experiment while single Doppler radar analysis is performed in 4 other bow echo/microburst events. The downdraft is initiated by precipitation loading at 4 km above ground level (AGL) 7 min before the surface microburst. The precipitation particles within the reflectivity core contribute not only to the loading effect but also to the cooling effect via evaporation, melting and sublimation. The downdraft core initially coincides with the reflectivity core but shifts toward the weak echo region at the peak microburst time. A high perturbation pressure (maximum of 0.6 mb) builds up from the surface at the microburst center upon impact with the ground. At the surface, the microburst air is warmer than its environment. A maximum cooling of 3 C is located at 1.6 km at the reflectivity gradient region. The reflectivity core precedes the descent of the downdraft core, while the maximum omega correlates well with the maximum negative buoyancy. The storm relative trajectories indicate that the source region of the microburst air is from 3 to 4 km level. A conceptual model of the single-cell type bow echo evolution is constructed based on the vorticity budget analysis. A bow echo is formed by the redistribution of hydrometeors by a vorticity couplet which is generated by the interaction between the downdraft and the vertical shear vector or the tilting effect. The rear inflow jet is induced by the vorticity couplet and its intensity should depend on the strength of the vorticity couplet. This model indicates that a bow echo may be produced by a weak downdraft as long as a proper vertical shear exists. However, strong downdrafts of microburst intensity will certainly promote this deformation of the echo. Other squall line type bow echoes indicate similar vortex signature as presented in the model. This bow echo evolution model can be extended to explain squall line type bow echoes. Dissert. Abstr.

N89-25551# Oak Ridge National Lab., TN.
DESIGN DESCRIPTION OF THE LARGE SCALE CLIMATE SIMULATOR
W. R. Hunley Mar. 1989 123 p
(Contract DE-AC05-84OR-21400)
(DE89-010185; ORNL/TM-10675) Avail: NTIS HC A06/MF A01

Construction of the Large Scale Climate Simulator has been completed at Oak Ridge National Laboratory under the sponsorship of the U.S. Department of Energy. This new facility provides the roofing industry with a unique capability for testing whole roof systems under dynamic conditions. The facility has been designated a National User Facility and, as such, is available to roofing researchers from industry, academia, and government agencies for their test programs. This report is primarily a design description of the Large Scale Climate Simulator and outlines the test capabilities of the various subsystems which make up the chamber. The chamber can provide roof test temperatures from -40 to 93 C (-40 to 200 F) and can operate either as an environmental chamber or as a guarded hot box. Typical performance data obtained during the acceptance testing of the chamber are included in this report. DOE

N89-25552# Beleidscommie Remote Sensing, Delft (Netherlands).
[FAO DETAILED RAIN MAPPING EXPERIMENT] Final Report
A. Rosema (Environmental Analysis and Remote Sensing, Delft, Netherlands) Oct. 1988 44 p Original contains color illustrations
(Contract BCRS-Proj.TO-1.7)
(BCRS-88-11; ETN-89-94291) Avail: NTIS HC A03/MF A01

Meteosat data were used to map rainfall and evapotranspiration (ETP) in an operational satellite remote sensing system (ARTEMIS) to support agricultural production and desert locust monitoring in Africa. Results suggest that potential locust breeding sites and habitats may be accurately detected and localized, solely by means of the Meteosat ETP monitoring technique. Such an approach could be more cost-effective and faster than the present one. In terms of crop early warning there are similar advantages to be expected. For individual titles, see N89-25553 through N89-25554.

N89-25553# Beleidscommie Remote Sensing, Delft (Netherlands).
FAO DETAILED RAIN MAPPING EXPERIMENT PHASE A: METEOSAT BASED RAINFALL MAPPING IN THE SAHEL REGION Final Report
A. Rosema (Environmental Analysis and Remote Sensing, Delft, Netherlands) *In its* FAO Detailed Rain Mapping Experiment Oct. 1988 p 1-2 Original contains color illustrations (For primary document see N89-25552 19-47)
Avail: NTIS HC A03/MF A01

Meteosat data were used to map rainfal in an operational satellite remote sensing system (ARTEMIS) to support agricultural production and desert locust monitoring in Africa. For the rainfall processing an extended thresholding method was applied. The Meteosat VIS imagery hardly contributes to the identification of rain cloud and was therefore not used. Use of the TIR-variance for rain cloud discrimination gives an improvement. Besides rain cloud duration, other rain cloud parameters were considered. The cloud edge temperature gradient was rejected. The cloud threshold temperature excess, however, considerably improves correlation results. The final algorithm uses only TIR data, applies two thresholds (TIR and TIR-variance) and three parameters (rain cloud duration, threshold temperature excess, and Meteosat line number, i.e., instead of latitude). The results of this algorithm were compared with those of the single threshold/parameter algorithm, of the type presently implemented on the ARTEMIS system. Using a daily precipitation data set of 50 stations, an improvement of 0.11, 0.07, and 0.05 in the correlation coefficient is obtained for the daily, decadely, and monthly values, respectively. For the monthly data the correlation coefficient reaches 81 percent with a standard error of 39 mm precipitation. ESA

N89-25554# Beleidscommie Remote Sensing, Delft (Netherlands).
FAO DETAILED RAIN MAPPING EXPERIMENT PHASE B: COMPARISON OF RAINFALL AND EVAPOTRANSPIRATION MAPPING
A. Rosema (Environmental Analysis and Remote Sensing, Delft, Netherlands) *In its* FAO Detailed Rain Mapping Experiment Oct. 1988 p 22-43 Original contains color illustrations (For primary document see N89-25552 19-47)
Avail: NTIS HC A03/MF A01

The feasibility of Meteosat based monitoring of evapotranspiration (ETP) on the scale of the Sahel region was investigated. The results were compared with rainfall mapping products of the same region. There is a reasonable correspondence between decadely and monthly rain and ETP maps, but there are many differences in detail. Evapotranspiration maps show more gradual changes, which may be due to the redistribution of rain water by run-off. The ETP seems to be overestimated, while rain is underestimated. The ETP maps give a geographically accurate representation of the soil moisture distribution. Rainfall maps must fail in this respect, since they are based on cloud data instead of surface data and do not account for run-off. Results suggest that

potential locust breeding sites and habitats may be accurately detected and localized, solely by means of the Meteosat ETP monitoring technique. Such an approach could be more cost-effective, less time consuming, and faster than the present one. In terms of crop early warning there are similar advantages to be expected. ESA

48 OCEANOGRAPHY

Includes biological, dynamic, and physical oceanography; and marine resources.

For related information see also *43 Earth Resources and Remote Sensing.*

N89-25555# National Academy of Sciences - National Research Council, Washington, DC. Commision on Engineering and Technical Systems.

RESPONDING TO CHANGES IN SEA LEVEL ENGINEERING IMPLICATIONS

1987 161 p

(Contracts DI-14-12-001-30301; DI-14-12-0001-30228)

(PB89-133466; ISBN-0-309-03781-6; LC-87-21965) Avail: NTIS HC A08/MF A01 CSCL 08C

Experts in geological and coastal engineering examine recent sea level trends and then project changes over the next 100 years and anticipate shoreline response to changing sea level and the consequences for coastal development and uses. Information is included about various types of coastal geology, hydrodynamic processes, and coastal structures. Scenarios for future sea level rise and several studies are presented. Author

51 LIFE SCIENCES (GENERAL)

N89-25556*# Lockheed Engineering and Sciences Co., Washington, DC.

USSR SPACE LIFE SCIENCES DIGEST. INDEX TO ISSUES 15-20

Lydia Razran Hooke, ed. Washington NASA Apr. 1989 151 p

(Contract NASw-4292)

(NASA-CR-3922(25); NAS 1.26:3922(25)) Avail: NTIS HC A08/MF A01 CSCL 06C

This bibliography provides an index to issues 15 through 20 of the USSR Space Life Sciences Digest. There are two sections. The first section lists bibliographic citations of abstracts in these issues, grouped by topic area categories. The second section provides a key word index for the same abstracts. The topic categories include exobiology, space medicine and psychology, human performance and man-machine systems, various life/body systems, human behavior and adaptation, biospherics, and others. Author

N89-25557*# National Aeronautics and Space Administration. Lyndon B. Johnson Space Center, Houston, TX.

SPIRAL VANE BIOREACTOR Patent Application

Dennis R. Morrison, inventor (to NASA) 29 Nov. 1988 30 p Sponsored by NASA. Johnson Space Center

(NASA-Case-MSC-21361-1; NAS 1.71:MSC-21361-1; US-Patent-Appl-SN-278137) Avail: NTIS HC A03/MF A01 CSCL 06C

A spiral vane bioreactor of a perfusion type is descibed in which a vertical chamber, intended for use in a microgravity condition, has a central rotating filter assembly and has flexible membranes disposed to rotate annularly about the filter assembly. The flexible members have end portions disposed angularly with respect to one another. A fluid replenishment medium is input from a closed loop liquid system to a completely liquid filled chamber containing microcarrier beads, cells and a fluid medium. Output of spent medium is to the closed loop. In the closed loop, the output and input parameters are sensed by sensors. A manifold permits recharging of the nutrients and pH adjustment. Oxygen is supplied and carbon dioxide and bubbles are removed and the system is monitored and controlled by a microprocessor. NASA

N89-25558*# National Aeronautics and Space Administration. Ames Research Center, Moffett Field, CA.

ACCLIMATIZATION TO HEAT IN HUMANS

John E. Greenleaf and Hanna Kaciuba-Uscilko (Polish Academy of Sciences, Warsaw.) Apr. 1989 45 p

(NASA-TM-101011; A-88222; NAS 1.15:101011) Avail: NTIS HC A03/MF A01 CSCL 06C

The responses and mechanisms of both natural and artificial acclimatization to a hot environment in mammals are addressed with specific reference to humans. The purpose is to provide basic information for designers of thermal protection systems and countermeasures for astronauts during intra- and extravehicular activity. Areas covered are energy metabolism, thermal balance at rest and during exercise, water and electrolyte balance during exercise and immobilization, and heat diseases. Author

N89-25559# Harvard Univ., Cambridge, MA. Dept. of Cellular and Developmental Biology.

UNRAVELING PHOTOSYSTEM 2 Progress Report, 1 Feb. 1988 - 31 Jan. 1989

Lawrence Bogorad 1989 4 p

(Contract DE-FG02-87ER-13743)

(DE89-010930; DOE/ER-13743/2) Avail: NTIS HC A02/MF A01

This project identifies and characterizes protein components of the energy-transducing reaction centers in photosynthetic membranes to understand how these components are arranged and function in the membrane. One question involves whether open reading frames found in chloroplast DNA sequences in fact encode proteins of the photosynthetic apparatus and, if so, to determine where the proteins function. A new protein subunit of the cytochrome b6/f electron transport complex has been identified in the course of this work. Another approach to identifying, characterizing and establishing the role of proteins of the photosynthetic apparatus has been to generate photosynthetic mutants of the facultatively heterotrophic single-celled cyanobacterium Synechocystis PCC6803 and then to identify DNA sequences that correct the mutant phenotype. Cyanobacteria are relatively simple organisms that carry out the same type of oxygen-evolving photosynthesis as chloroplasts of higher green plants but they are more convenient for certain experiments. Mutants studied to date in this part of the program have had deficiencies in chlorophyll-proteins associated with the reaction center of Photosystem 2. Such mutants have been very useful in revealing the sources of certain fluorescence emission bands in the photosynthetic apparatus and thus helping understand the transfer of energy within these systems. Sets of mutants with other genetic lesions are being analyzed. DOE

N89-25560# Cornell Univ., Ithaca, NY.

EFFECTS OF FREEZING AND COLD ACCLIMATION ON THE PLASMA MEMBRANE OF ISOLATED PROTOPLASTS Progress Report, 16 May 1988 - 9 Jan. 1989

1989 7 p

(Contract DE-FG02-84ER-13214)

(DE89-010931; DOE/ER-13214/3) Avail: NTIS HC A02

The emphasis of this project is on the form of injury referred to as loss of osmotic responsiveness (LOR). Our goals are to provide a mechanistic understanding of freeze/dehydration-induced mesomorphic phase transitions in the plasma membrane that are manifested as alterations in the ultrastructure (lateral phase separations, a particulate lamellae, and hexagonal configurations) and which result in the loss of osmotic reponsiveness of NA protoplasts and to determine the cellular and molecular mechanisms by which cold acclimation and cryoprotectants preclude or diminish these alterations in the plasma membrane of ACC protoplasts. As a working hypothesis, we propose that the alterations in the ultrastructure of the plasma membrane of NA

protoplasts that are responsible for LOR are a consequence of lipid demixing that occurs as a result of the close approach of bilayers during freeze-induced dehydration. Normally the close approach of two bilayers is precluded because of the large repulsive forces (hydration forces) resulting from the strong affinity of the hydrophilic surfaces for water. However, large osmotic potentials occur during the freezing of aqueous solutions and are of sufficient magnitude to overcome the hydration forces. Theory predicts that large lateral pressures will occur during the resultant close approach of the bilayers and will result in phase separation of the bilayer components. The fact that lateral phase separations and hexagonal phases are not observed in ACC protoplasts subjected to freeze-induced dehydration indicates that cold acclimation decreases the propensity to undergo demixing and lateral segregation of the membrane components. Our working hypothesis is that this is, in part, a consequence of alterations in the lipid composition of the plasma membrane and possibly the increased cytoplasmic concentrations of solutes such as sucrose and proline. DOE

N89-25561*# Alabama A & M Univ., Normal.
CHARACTERIZATION OF SPIRULINA BIOMASS FOR CELSS DIET POTENTIAL
Mahasin G. Tadros Oct. 1988 53 p
(Contract NCC2-501)
(NASA-CR-185329; NAS 1.26:185329) Avail: NTIS HC A04/MF A01 CSCL 06C

Spirulina sp. as a bioregenerative photosynthetic and an edible alga for space craft crew in a CELSS, was characterized for growth rate and biomass yield in batch cultures, under various environmental conditions. The cell characteristics were identified for two strains of Spirulina: S. maxima and S. plantensis. Fast growth rate and high yield of both strains were obtained under the following conditions: temperature (30 to 35 C), light irradiance (60 to 100 uE/m/s), nitrate (30 mM), phosphate (2 mM), aeration (300 ml/min), and ph (9 to 10). The partitioning of the assimalatory products (proteins, carbohydrates, lipids) were manipulated by varying the environmental growth conditions. The experiments with Spirulina demonstrated that under stress conditions (high light 120 uE/m/s, temperature 38 C, nitrogen or phosphate limitation; 0.1 M sodium chloride) carbohydrate increased at the expense of protein. In other experiments, where the growth media were sufficient in nutrients and incubated under optimum growth conditions, the total proteins were increased up to almost 70 percent of the organic weight. Conclusion: The nutritional quality of the alga could be manipulated by growth conditions, and therefore usful as a subsystem in CELSS. Author

N89-25562# Nebraska Univ., Lincoln. Dept. of Chemistry.
ELECTROCHEMICAL AND OPTICAL STUDIES OF MODEL PHOTOSYNTHETIC SYSTEMS Progress Report, 1 Jul. 1988 - 30 Jun. 1989
Therese M. Cotton 20 Feb. 1989 10 p
(Contract DE-FG02-84ER-13261)
(DE89-012479; DOE/ER-13261/5) Avail: NTIS HC A02/MF A01

During the initial eight months of this funding period, we continued studies of photosynthetic model systems with the study of spread monolayers, monolayers transferred to solid supports by the Langmuir-Blodgett technique, self-assembled monolayers, and vesicle systems. The principle instrumental methods of characterization remained electrochemical techniques and optical methods (resonance Raman, UV-VIS and surface enhanced resonance Raman scattering (SERS) spectroscopy). Specific compounds of interest comprised chlorophylls, porphyrins, synthetic redox-active species and protein/peptide systems. DOE

52 AEROSPACE MEDICINE

Includes physiological factors; biological effects of radiation; and effects of weightlessness on man and animals.

N89-25563* National Aeronautics and Space Administration, Washington, DC.
AEROSPACE MEDICINE AND BIOLOGY: A CONTINUING BIBLIOGRAPHY WITH INDEXES (SUPPLEMENT 323)
May 1989 55 p
(NASA-SP-7011(323); NAS 1.21:7011(323)) Avail: NTIS HC A04; NTIS standing order as PB89-912300, $10.50 domestic, $21.00 foreign CSCL 06E

This bibliography lists 125 reports, articles and other documents introduced into the NASA Scientific and Technical Information System during April, 1989. Subject coverage includes; aerospace medicine and psychology, life support systems and controlled environments, safety equipment exobiology and extraterrestrial life, and flight crew behavior and performance. Author

N89-25564# Brigham and Women's Hospital, Boston, MA.
A PROGRAM FOR THE STUDY OF SKELETAL MUSCLE CATABOLISM FOLLOWING PHYSICAL TRAUMA Annual Report, 21 Feb. 1987 - 20 Feb. 1988
Douglas W. Wilmore 15 Mar. 1988 9 p
(Contract DAMD17-86-C-6157; DA Proj. 351-62772-A-874)
(AD-A206506) Avail: NTIS HC A02/MF A01 CSCL 06/15

These two studies examine the role of prostaglandins as mediators of the catabolic response. In the first study, we examined the effects of a cyclooxgenase inhibition on the catabolic response to operative stress. In a second study we examined the effect of PG2 infusion on skeletal muscle proteolysis. Following laparotomy and retroperitoneal dissection, dogs increase skeletal muscle proteolysis and excrete increased urinary nitrogen. Pretreatment with a cyclooxygenase inhibitor (Ibuprofen) diminished this response in six paired animals when examining whole animal data. Amino acid flux data is presently being processed. In additional studies, PGE2 was infused in one hind limb and the flux of amino acids monitored in both lower extremities. Leg blood flow increased markedly in the limb receiving the PGE2; substrate flux is presently being analyzed. GRA

N89-25565* National Aeronautics and Space Administration, Washington, DC.
AEROSPACE MEDICINE AND BIOLOGY: A CONTINUING BIBLIOGRAPHY WITH INDEXES (SUPPLEMENT 324)
Feb. 1989 70 p
(NASA-SP-7011(324); NAS 1.21:7011(324)) Avail: NTIS HC A03; NTIS standing order as PB89-912300, $10.50 domestic, $21.00 foreign CSCL 06E

This bibliography lists 200 reports, articles and other documents introduced into the NASA Scientific and Technical Information System during May, 1989. Subject coverage includes: aerospace medicine and psychology, life support systems and controlled environments, safety equipment, exobiology and extraterrestrial life, and flight crew behavior and performance. Author

N89-25566*# Research Inst. for Advanced Computer Science, Moffett Field, CA.
MODELING THE AIDS EPIDEMIC
Peter J. Denning 22 Sep. 1988 18 p Submitted for publication
(Contract NCC2-387)
(NASA-CR-185413; NAS 1.26:185413; RIACS-TR-88.27) Avail: NTIS HC A03/MF A01 CSCL 06E

The AIDS epidemic expands relentlessly. In October 1987, the President of the United States requested a national integrated scientific modeling effort to evaluate data already available and guide further data collection to reduce the uncertainties in estimates of prevalence and rates of spread of HIV. In July 1988, a workshop was jointly sponsored by the Office of Science and Technology Policy, Department of Health and Human Services, Department of Energy, and the National Science Foundation in response to this directive. The workshop recommended a variety of measures that

add mathematical modeling to the arsenal of weapons that are being developed to defeat HIV, foster and promote collaboration between modelers and other scientists, and encourage individuals and institutions to share data. Perhaps the most important result of the workshop was a transformation in the way the nearly 100 participants look at the AIDS question: the participants left with a much broader, community-oriented perspective. Author

N89-25567* National Aeronautics and Space Administration, Washington, DC.
AEROSPACE MEDICINE AND BIOLOGY: A CONTINUING BIBLIOGRAPHY WITH INDEXES (SUPPLEMENT 325)
Jul. 1989 68 p
(NASA-SP-7011(325); NAS 1.21:7011(325)) Avail: NTIS HC A04; NTIS standing order as PB89-912300, $10.50 domestic, $21.00 foreign CSCL 06E

This bibliography lists 192 reports, articles and other documents introduced into the NASA Scientific and Technical Information System during June, 1989. Subject coverage includes: aerospace medicine and psychology, life support systems and controlled environments, safety equipment, exobiology and extraterrestrial life, and flight crew behavior and performance. Author

53 BEHAVIORAL SCIENCES

Includes psychological factors; individual and group behavior; crew training and evaluation; and psychiatric research.

N89-25568*# Ohio State Univ., Columbus. Dept. of Industrial and Systems Engineering.
THE ORGANIZATION OF PERCEPTION AND ACTION IN COMPLEX CONTROL SKILLS Final Report
Richard A. Miller and Richard J. Jagacinski May 1989 300 p
(Grant NAG2-195)
(NASA-CR-184638; NAS 1.26:184638) Avail: NTIS HC A13/MF A01 CSCL 05I

An attempt was made to describe the perceptual, cognitive, and action processes that account for highly skilled human performance in complex task environments. In order to study such a performance in a controlled setting, a laboratory task was constructed and three experiments were performed using human subjects. A general framework was developed for describing the organization of perceptual, cognitive, and action process. Author

N89-25569# Los Alamos National Lab., NM.
ADAPTIVE ENHANCEMENT OF MAGNETOENCEPHALOGRAPHIC SIGNALS VIA MULTICHANNEL FILTERING
Paul S. Lewis 1989 5 p Presented at the International Conference on Acoustics, Speech and Signal Processing, Glasgow, Scotland, 23 May 1989
(Contract W-7405-eng-36)
(DE89-005464; LA-UR-88-4190; CONF-890570-1) Avail: NTIS HC A02/MF A01

A time-varying spatial/temporal filter for enhancing multichannel magnetoencephalographic (MEG) recordings of evoked responses is described. This filter is based in projections derived from a combination of measured data and a priori models of the expected response. It produces estimates of the evoked fields in single trial measurements. These estimates can reduce the need for signal averaging in some situations. The filter uses the a priori model information to enhance responses where they exist, but avoids creating responses that do not exist. Examples are included of the filter's application to both MEG single trial data containing an auditory evoked field and control data with no evoked field. DOE

54 MAN/SYSTEM TECHNOLOGY AND LIFE SUPPORT

Includes human engineering; biotechnology; and space suits and protective clothing.

For related information see also *16 Space Transportation.*

N89-25570# Oak Ridge National Lab., TN. Center for Engineering Systems Advanced Research.
REVIEW OF THE 1988 WORKSHOP ON HUMAN-MACHINE SYMBIOTIC SYSTEMS
Lynne E. Parker and Charles R. Weisbin 1989 5 p Presented at the Workshop on Integration of AI and Robotic Systems, Scottsdale, AZ, 19 May 1989
(Contract DE-AC05-84OR-21400)
(DE89-008743; CONF-8905109-1; CESAR-89/14) Avail: NTIS HC A02/MF A01

This report presents a review of the 1988 Workshop on Human-Machine Symbiotic Systems. Held December 5 to 6, 1988 in Oak Ridge, Tennessee, the workshop served as a forum for the discussion of several critical issues in human-machine symbiosis: human-machine communication, autonomous task planning and execution monitoring for heterogeneous agents, dynamic task allocation, human-machine system architecture, and machine learning via experience and human observation. The presentation of overview papers by invited keynote speakers provided a background for the breakout session discussions in these five areas. A summary of the conclusions and recommendations for future work resulting from the workshop is reported. DOE

N89-25571# Oak Ridge National Lab., TN. Cognitive Science and Human Factors Group.
OPERATOR ROLE DEFINITION AND HUMAN SYSTEM INTEGRATION
H. E. Knee and J. C. Schryver 1989 21 p Presented at the 7th Power Plant Dynamics, Control and Testing Symposium, Knoxville, TN, 15 May 1989
(Contract DE-AC05-84OR-21400)
(DE89-009621; CONF-890555-8) Avail: NTIS HC A03/MF A01

This paper discusses operator role definition and human-system integration from a perspective of systems engineering and allocation of functions. Current and traditional allocation of tasks/functions can no longer be applied to systems that are significantly more sophisticated and dynamic than current system designs. For such advanced and automated designs, explicit attention must be given to the role of the operator in order to facilitate efficient system performance. Furthermore, such systems will include intelligent automated systems which will support the cognitive activities of the operator. If such systems share responsibility and control with the human operator, these computer-based assistants/associates should be viewed as intelligent team members. As such, factors such as trust, intentions, and expectancies, among team members must be considered by the systems designer. Such design considerations are discussed in this paper. This paper also discusses the area of dynamic allocation of functions, and the need for models of the human operator in support of machine forecast of human performance. The Integrated Reactor Operator/System (INTEROPS) model is discussed as an example of a cognitive model capable of functioning beyond a rule-based behavioral structure. DOE

N89-25572# Oak Ridge National Lab., TN. Center for Engineering Systems Advanced Research.
THE 1988 WORKSHOP ON HUMAN-MACHINE SYMBIOTIC SYSTEMS
L. E. Parker and Charles R. Weisbin 1988 6 p Workshop held in Oak Ridge, TN, 5-6 Dec. 1988 Submitted for publication
(Contract DE-AC05-84OR-21400)
(DE89-010170; CONF-881281) Avail: NTIS HC A02/MF A01

This report presents the proceedings of the 1988 Workshop on Human-Machine Symbiotic Systems. Held December 5 to 6,

1988 in Oak Ridge, Tennessee, the workshop served as a forum for the discussion of several critical issues in human-machine symbiosis: human-machine communication, autonomous task planning and execution monitoring for heterogeneous agents, dynamic task allocation, human-machine system architecture, and machine learning via experience and human observation. DOE

N89-25573*# Purdue Univ., West Lafayette, IN. Dept. of Psychological Sciences.
TIMESHARING PERFORMANCE AS AN INDICATOR OF PILOT MENTAL WORKLOAD Final Report
Patricia A. Casper, Barry H. Kantowitz, and Robert D. Sorkin [1988] 31 p
(Contract NCC2-349)
(NASA-CR-185328; NAS 1.26:185328) Avail: NTIS HC A03/MF A01 CSCL 05H

Attentional deficits (workloads) were evaluated in a timesharing task. The results from this and other experiments were incorporated into an expert system designed to provide workload metric selection advice to non-experts in the field interested in operator workload. B.G.

N89-25574# Imperial Coll. of Science and Technology, London (England). Dept. of Computing.
THE MAN-MACHINE-INTERFACE IN A FAST JET M.S. Thesis
A. C. Pearce Sep. 1988 169 p
(ETN-89-94327) Avail: NTIS HC A08/MF A01

Limitations of the traditional methods of presenting information to pilots in high performance aircraft are discussed. It is shown how modern technology can improve this information interchange using electronic and head up displays. The role of speech recognition and speech synthesis is covered. The super cockpit project and the advantages this should bring are considered. ESA

N89-25575# Deutsche Forschungs- und Versuchsanstalt fuer Luft- und Raumfahrt, Brunswick (Germany, F.R.). Abteilung Anthropotechnik und Simulation.
VALIDATION OF THE SUBJECTIVE WORKLOAD ASSESSMENT TECHNIQUE IN A SIMULATED FLIGHT TASK
Fred V. Schick, Uwe Teegen, Rainer Uckermann, and Reuben L. Hann (Air Force Medical Center, Wright-Patterson AFB, OH.) 16 Dec. 1988 75 p
(DFVLR-FB-89-01; ISSN-0171-1342; ETN-89-94642) Avail: NTIS HC A04/MF A01; DFVLR, VB-PL-DO, Postfach 90 60 58, 5000 Cologne, Fed. Republic of Germany, DM 26.50

A German language version of the Subjective Workload Assessment Technique (SWAT) for the assessment of mental workload was developed. After the German SWAT scale was found equivalent to the original, its validity was investigated in an experiment with 14 pilots in a flight simulator. Variations of SWAT scores in accordance with variations in task demand were analyzed in comparison with physiological and behavioral measures. The German SWAT is found to be a valid tool for the detection of workload differences given in the subsegments of a flight mission. The SWAT differentiates significantly and more consistently over the whole range of the applied workload levels than electrocardiographic and electromyographic parameters and a combined measure of pilot input activity. ESA

55 SPACE BIOLOGY

Includes exobiology; planetary biology; and extraterrestrial life.

No abstracts in this category.

59 MATHEMATICAL AND COMPUTER SCIENCES (GENERAL)

No abstracts in this category.

60 COMPUTER OPERATIONS AND HARDWARE

Includes hardware for computer graphics, firmware, and data processing.

For components see *33 Electronics and Electrical Engineering.*

N89-25576# Sandia National Labs., Albuquerque, NM. Strategic Technology Div.
MODELING OF MAGNETIC DEVICES WITH FINITE-ELEMENT METHODS
Eugene A. Aronson Mar. 1989 35 p
(Contract DE-AC04-76DP-00789)
(DE89-010525; SAND-89-0009) Avail: NTIS HC A03/MF A01

This report discusses the application of finite-element methods to the solution of magnetostatic field problems. A brief description is given of the finite-element representation of the magnetostatic field. Two computer codes which solve this problem are described. The code MAGNUM is commercially available and the code ISO is a Sandia in-house product. Both codes are currently available on the Sandia CRAY. Some general remarks are presented on modeling techniques and boundary conditions. A new method for estimating solenoid magnetic forces and dynamic response is described. A suite of codes for generating various electromagnetic devices is briefly discussed. Finally, some numerical results are presented. DOE

N89-25577# Sandia National Labs., Albuquerque, NM.
THE EPSILON DATAFLOW PROCESSOR
V. G. Grafe, G. S. Davidson, J. E. Hoch, and V. P. Holmes 1988 13 p Presented at the 16th Annual International Symposium on Computer Architecture, Jerusalem, Israel, 28 May 1989
(Contract DE-AC04-76DP-00789)
(DE89-001679; SAND-88-2668C; CONF-890537-1) Avail: NTIS HC A03/MF A01

The epsilon dataflow architecture is designed for high speed uniprocessor execution as well as for parallel processing. The epsilon architecture directly matches ready operands, thus eliminating the need for associative matching stores. Epsilon also supports low cost data fan out and critical sections. A 10 MFLOPS CMOS/TTL processor prototype is running and its performance has been measured with several benchmarks. The prototype processor has demonstrated sustained performance exceeding that of comparable control flow processors running at higher clock rates (three times faster than a 20 MHz transputer and 24 times faster than a Sun on a suite of arithmetic tests, for example). DOE

N89-25578# Fermi National Accelerator Lab., Batavia, IL.
THE FERMILAB LATTICE SUPERCOMPUTER PROJECT
Mark Fischler, R. Atac, A. Cook, J. Deppe, Irwin Gaines, D. Husby, T. Nash, T. Pham, T. Zmuda, and George Hockney et al Feb. 1989 7 p Presented at Lattice '88: Symposium on Lattice Field Theory, Batavia, IL, 22 Sep. 1988
(Contract DE-AC02-76CH-03000)
(DE89-010510; FNAL/C-89/37; CONF-8809247-9) Avail: NTIS HC A02

The ACPMAPS system is a highly cost effective, local memory MIMD computer targeted at algorithm development and production running for gauge theory on the lattice. The machine consists of a compound hypercube of crates, each of which is a full crossbar

switch containing several processors. The processing nodes are single board array processors based on the Weitek XL chip set, each with a peak power of 20 MFLOPS and supported by 8 MBytes of data memory. The system currently being assembled has a peak power of 5 GFLOPS, delivering performance at approximately $250/MFLOP. The system is programmable in C and FORTRAN. An underpinning of software routines (CANOPY) provides an easy and natural way of coding lattice problems, such that the details of parallelism, and communication and system architecture are transparent to the user. CANOPY can easily be ported to any single CPU or MIMD system which supports C, and allows the coding of typical applications with very little effort. DOE

N89-25579# Virginia Univ., Charlottesville. Inst. for Parallel Computation.
A GLOBAL TIME REFERENCE FOR HYPERCUBE MULTICOMPUTERS
James C. French 10 Oct. 1988 35 p
(Contracts DE-FG05-88ER-25063; JPL-957721)
(DE89-010924; DOE/ER-25063/T3; IPC-TR-88-10) Avail: NTIS HC A03/MF A01

This report describes a simple but effective technique for achieving a global time reference on hypercube multicomputers. The synchronization algorithm presented runs in O(log N) time where N = 2 sup n is the number of processors in an order n hypercube. Empirical evidence is given to show that the expected clock agreement is n/2 ticks. Since the synchronization algorithm does not depend on particular parameters of the underlying hardware, it is inherently portable. A sampling technique for testing the agreement of the processor clocks in O(N) time is also presented. This technique assumes that the internode message transit time, m, is constant but unknown. One unexpected outcome of this work was the discovery that, in general, timing information cannot be reliably obtained on the NCUBE/AT system except perhaps in the total absence of message traffic. DOE

N89-25580# Fermi National Accelerator Lab., Batavia, IL. Advanced Computer Program.
MICROPROCESSORS AND OTHER PROCESSORS FOR TRIGGERING AND FILTERING AT THE SSC
Irwin Gaines Mar. 1989 11 p Presented at the Workshop on Triggering and Data Acquisition for Experiments At the Superconducting Super Collider, Toronto, Ontario, 16-19 Jan. 1989
(Contract DE-AC02-76CH-03000)
(DE89-011088; FNAL/C-89/52; CONF-8901118-2) Avail: NTIS HC A03/MF A01

The rapid increase in processing power available in commercial integrated circuits presents the high energy physics community with important opportunities for Superconducting Super Collider (SSC) era data acquisition systems. The processors that will be available in the late 90's will allow enormous amounts of computing power to be utilized on-line and will permit commercial high level language programmable devices to be used for tasks previously performed by home-brew, hard-wired, or microcoded devices. I will describe this processor revolution, in particular with respect to the new RISC (Reduced Instruction Set Computer) microprocessor now becoming available. These processors are already commercially available with processing power of 20 VAX 11/780 equivalents per chip, and a number of different manufacturers expect chips of 100 VAX power by the early 1990's. I will also discuss the plans the Fermilab ACP group has to exploit one such RISC chip for both off-line and on-line use. Finally, I will mention digital signal processors (DSPs) and other more specialized chips that offer even greater amounts of processing power with only slightly less convenience. DOE

N89-25581# Universiteit Twente, Enschede (Netherlands). Dept. of Computer Science.
TUMULT: THE TWENTE UNIVERSITY MULTIPROCESSOR
J. Scholten and P. G. Jansen Jun. 1988 30 p
(MEMO-INF-88-28; ISBN-9-03-650167-9; ETN-89-94758) Avail: NTIS HC A03/MF A01

The design and implementation of a modular extensible multiprocessor system is described. Up to 15 processing elements are connected through an interprocessor communication network. The basic method for the exchange of data is message passing. The hardware is controlled by a distributed realtime operating system written in modular Pascal and Modula-2. The network offers a fully connected communication service with error detection and recovery. In the version realized the transfer is 20 Mbyte/sec. ESA

N89-25582# Technische Univ., Eindhoven (Netherlands). Group Digital Systems.
THE FULL DECOMPOSITION OF SEQUENTIAL MACHINES WITH THE STATE AND OUTPUT BEHAVIOR REALIZATION
Lech Jozwiak Jan. 1988 50 p
(EUT-88-E-188; ISBN-9-06-144188-9; ISSN-0167-9708; ETN-89-94776) Avail: NTIS HC A03/MF A01

A general and unified classification of full decompositions is presented, formal definitions of different sorts of full-decompositions for Mealy and Moore machines are introduced, and theorems about the existence of full-decompositions with the state and output behavior realization are formulated and proved. The theorems have a straightforward practical interpretation. Based on them, a set of algorithms was developed and a system of programs was made for computing the different sorts of decompositions. ESA

N89-25583# Technische Univ., Eindhoven (Netherlands). Digital Systems Group.
THE FULL DECOMPOSITION OF SEQUENTIAL MACHINES WITH THE OUTPUT BEHAVIOR REALIZATION
Lech Jozwiak Mar. 1988 47 p
(EUT-88-E-199; ISBN-9-06-144199-4; ISSN-0167-9708; ETN-89-94787) Avail: NTIS HC A03/MF A01

A general and unified classification of full-decompositions and formal definitions or different sorts of full-decompositions for Mealy and Moore machines are presented and theorems about the existence of full-decompositions with the output behavior realization are formulated and proved. The theorems constitute a theoretical basis for the practical decomposition algorithms and for the software system calculating different sorts of decomposition for sequential machines. Similar theorems for the case of full-decompositions with the state and output behavior realization are available. ESA

61 COMPUTER PROGRAMMING AND SOFTWARE

Includes computer programs, routines, alogorithms, and specific applications, e.g., CAD/CAM.

N89-25584# Technische Hogeschool, Delft (Netherlands).
POLYNOMIAL METHOD OF APPROXIMATE CENTERS FOR LINEAR PROGRAMMING
C. Roos and J.-P. Vial (Geneva Univ., Switzerland) 1988 17 p
(Grant FNSRS-1-467-0-86)
(PB89-146161; ISSN-0922-5641; Rept-88-68) Copyright Avail: NTIS HC A03/MF A01 CSCL 09B

A path following algorithm for the linear programming problem with a simple proof of its polynomial behavior is presented. This is done both for the problem in standard form and for its dual problem. A practical version of the algorithm is also discussed. Author

N89-25585*# Institute for Computer Applications in Science and Engineering, Hampton, VA.
SEMI-AUTOMATIC PROCESS PARTITIONING FOR PARALLEL COMPUTATION Final Report
Charles Koelbel, Piyush Mehrotra, and John VanRosendale Feb. 1988 23 p

(Contract NAS1-18107)
(NASA-CR-181633; NAS 1.26:181633; ICASE-88-16) Avail: NTIS HC A03/MF A01 CSCL 09B

On current multiprocessor architectures one must carefully distribute data in memory in order to achieve high performance. Process partitioning is the operation of rewriting an algorithm as a collection of tasks, each operating primarily on its own portion of the data, to carry out the computation in parallel. A semi-automatic approach to process partitioning is considered in which the compiler, guided by advice from the user, automatically transforms programs into such an interacting task system. This approach is illustrated with a picture processing example written in BLAZE, which is transformed into a task system maximizing locality of memory reference. Author

N89-25586# Tuskegee Inst., AL. Dept. of Computer Science.
PARALLEL SOLUTION OF A 2-D PHASE CHANGE PROBLEM ON A HYPERCUBE
H. N. Narang and J. B. Drake (Oak Ridge National Lab., TN.) 1989 8 p Presented at the 27th ACM Southeast Region Annual Conference, Atlanta, GA, 5 Apr. 1989
(Contract DE-AC05-84OR-21400)
(DE89-009619; CONF-8904180-1) Avail: NTIS HC A02/MF A01

This report documents the model, algorithms, and results for a heat transfer problem with phase change simulated numerically on a hypercube parallel computer. The temperature and enthalpy distribution in a rectangular domain with first kind boundary conditions (temperature prescribed) is found as a function of time. The model involves a non-linear partial differential equation with a constitutive relation between enthalpy and temperature. The solution to the system is obtained by finite difference approximation with both explicit and implicit methods. In the implicit case, a successive overrelaxation technique with red, black ordering is implemented. The efficiency of the explicit method is compared with that of the implicit method in a multiprocessor computing environment. The design, development, and implementation of algorithms targeted INTEL's iPSC/2 hypercube involving up to 64 processors. The computational workload was uniformly divided among processors as far as possible by dividing the finite difference grid into several strips and assigning each strip to a processor. The results, depicted in terms of tables, show the effect of relaxation parameter, and stepsize on the efficiency of the parallel algorithms. This is contrasted with the sequential algorithms. DOE

N89-25587# Lawrence Livermore National Lab., CA.
FAR FIELD PROJECTION
Marvin J. Barth and Richard W. Ziolkowski Jan. 1989 22 p Presented at the Applied Computational Electromagnetics Conference, Monterey, CA, 20 Mar. 1989
(Contract W-7405-eng-48)
(DE89-010243; UCRL-100198; CONF-890393-2) Avail: NTIS HC A03/MF A01

The FAR computer code, which post processes the results of a Finite Difference Time Domain (FDTD) code to produce far-field quantities from near-field values, is described. The integral equation and differential equation approaches are two methods of calculating the radiation and scattering effects of systems. Each method has practical limitations when used in general application codes. For instance, integral equation approaches such as the method of moments usually consider only perfectly conducting wires and patches in the frequency domain and the differential equation approaches such as FDTD, while applicable to multimedia and the time domain, are constrained to finite volumes determined by the specific computer memories. The FAR code allows the near-field details in the time domain modeled by FDTD codes to be extended to the far-field. This combined FDTD-FAR code set greatly extends the class of numerical electromagnetic modeling problems that can be treated with discrete differential equation methods. The FAR code uses the equivalence principle. Specifically, the code utilizes the tangential electric and magnetic fields at a specified surface of the FDTD computational volume and calculates the resulting far-fields from the equivalent magnetic and electric sources. In this process the sources of errors are sampling density, the length of the excitation pulse, the total time history record length, the time step size, and the size of the FDTD volume. The FDTD-FAR approach will be illustrated with a pulse driven array of dipole elements. The far-field time histories and the resulting frequency domain antenna patterns will be presented. The sizes of the various errors in this approach will be discussed in detail. The efficacy of this approach will be contrasted with conventional methods. DOE

N89-25588# Argonne National Lab., IL. Mathematics and Computer Science Div.
RATIONALE FOR THE PROPOSED STANDARD FOR A GENERIC PACKAGE OF ELEMENTARY FUNCTIONS FOR Ada
Kenneth W. Dritz Mar. 1989 17 p
(Contract W-31-109-eng-38)
(DE89-010282; ANL-89/2) Avail: NTIS HC A03/MF A01

This paper supplements the Proposed Standard for a Generic Package of Elementary Functions for Ada, written by the ISO-IEC/JTC1/SC22/WG9 (Ada) Numerics Rapporteur Group for presentation to WG9. Based on recommendations made jointly by the ACM SIGAda Numerics Working Group and the Ada-Europe Numerics Working Group, the proposed elementary functions standard is the first of several anticipated collateral standards to address the interrelated issues of portability, efficiency, and robustness of numerical software written in Ada. Organized as a series of questions and answers, this supplement outlines the reasoning by which the proposed standard came to acquire certain features and exclude others. DOE

N89-25589# Oak Ridge National Lab., TN. Advanced Computing and Integrated Sensor Systems.
A TOOL TO AID IN MAPPING COMPUTATIONAL TASKS TO A HYPERCUBE
J. R. Einstein, C. W. Glover, and M. Dickens (Massachusetts Inst. of Tech., Cambridge.) 1989 6 p Presented at the 4th Hypercube, Concurrent Computers and Applications, Monterey, CA, 6 Mar. 1989
(Contract DE-AC05-84OR-21400)
(DE89-010320; CONF-890372-9) Avail: NTIS HC A02/MF A01

We describe a tool to aid in static scheduling of precedence-constrained tasks on nodes of a hypercube computer. The tool is useful where the sequential program is suitable for large-grained decomposition, i.e., where message-passing times are negligibly small compared to task execution times. The tool is also useful for small sets of tasks, or for quasi-periodic sets of tasks, even where message-passing times are not negligible. Quasi-periodic sets of tasks arise when the computation is dominated by loops over a group of tasks which are the same or nearly the same for each iteration of the loop---for example, programs for the dynamics and kinematics of robotic manipulators. DOE

N89-25590# Sandia National Labs., Albuquerque, NM. Applied Mechanics Div.
PRONTO 3D: A THREE-DIMENSIONAL TRANSIENT SOLID DYNAMICS PROGRAM
L. M. Taylor and D. P. Flanagan Mar. 1989 152 p
(Contract DE-AC04-76DP-00789)
(DE89-010517; SAND-87-1912) Avail: NTIS HC A08

PRONTO 3D is a three-dimensional transient solid dynamics code for analyzing large deformations of highly nonlinear materials subjected to extremely high strain rates. This Lagrangian finite element program uses an explicit time integration operator to integrate the equations of motion. Eight-node uniform strain hexahedral elements are used in the finite element formulation. A number of new numerical algorithms which have been developed for the code are described in this report. An adaptive time step control algorithm is described which greatly improves stability as well as performance in plasticity problems. A robust hourglass control scheme which eliminates hourglass distortions without disturbing the finite element solution is included. All constitutive

models in PRONTO are cast in an unrotated configuration defined using the rotation determined from the polar decomposition of the deformation gradient. An accurate incremental algorithm was developed to determine this rotation and is described in detail. A robust contact algorithm was developed which allows for the impact and interaction of deforming contact surfaces of quite general geometry. Numerical examples are presented to demonstrate the utility of these algorithms. DOE

N89-25591# Los Alamos National Lab., NM.
DETECTION OF ANOMALOUS COMPUTER SESSION ACTIVITY
Henry S. Vaccaro 1988 24 p Presented at the Symposium on Security and Privacy, Oakland, CA, 1 May 1989
(Contract W-7405-eng-36)
(DE89-003607; LA-UR-88-3656; CONF-890536-2) Avail: NTIS HC A03/MF A01

This paper describes recent Los Alamos National Laboratory (LANL) applications of research into automated anomaly detection. In the context of computer security, anomaly detection seeks to identify events shown in audit records that are inconsistent with routine operation and therefore may be indicative of an intrusion into the computer, serious human errors, or malicious behavior by a legitimate user. Access by an intruder, execution of Trojan horses and viruses, as well as malicious, destructive behavior are all assumed to produce anomalous events that are recorded in a computer audit trail. This trail, perhaps with augmented data collection capabilities, is processed, in real-time, to detect such events, alert a knowledgeable computer security officer to the threat, and help resolve the situation. DOE

N89-25592# Sandia National Labs., Albuquerque, NM.
CULTURE SHOCK: IMPROVING SOFTWARE QUALITY
Kent deJong and Sharon L. Trauth 1988 6 p Presented at the Quality Congress of the American Society for Quality Control, Toronto, Ontario, 8 May 1989
(Contract DE-AC04-76DP-00789)
(DE89-003610; SAND-88-1615C; CONF-890538-2) Avail: NTIS HC A02/MF A01

The concept of software quality can represent a significant shock to an individual who has been developing software for many years and who believes he or she has been doing a high quality job. The very idea that software includes lines of code and associated documentation is foreign and difficult to grasp, at best. Implementation of a software quality program hinges on the concept that software is a product whose quality needs improving. When this idea is introduced into a technical community that is largely self-taught and has been producing good software for some time, a fundamental understanding of the concepts associated with software is often weak. Software developers can react as if to say, what are you talking about. What do you mean I'm not doing a good job. I haven't gotten any complaints about my code yet. Coupling such surprise and resentment with the shock that software really is a product and software quality concepts do exist, can fuel the volatility of these emotions. In this paper, we demonstrate that the concept of software quality can indeed pose a culture shock to developers. We also show that a typical quality assurance approach, that of imposing a standard and providing inspectors and auditors to assure its adherence, contributes to this shock and detracts from the very goal the approach should achieve. We offer an alternative, adopted through experience, to implement a software quality program: cooperative assistance. We show how cooperation, education, consultation and friendly assistance can overcome this culture shock. DOE

N89-25593# Aalborg Univ. (Denmark). Lab. of Image Analysis.
CONCURRENT SPATIO-TEMPORAL IMAGE ANALYSIS
Henrik I. Christensen 1989 5 p Presented at the 4th Conference on Hypercube, Concurrent Computer and Applications, Monterey, CA, 6-8 Mar. 1989 Sponsored in part by Danish Technical Research Council, Danish Research Academy and Foundation Vision North Prepared in cooperation with ORNL, TN
(Contract DE-AC05-84OR-21400)
(DE89-010260; CONF-890372-7) Avail: NTIS HC A02/MF A01

Description and analysis of dynamically changing scenes in real-time based on sequences of images is difficult due to the large amount of data. To obtain an acceptable performance one of two approaches is normally adapted. The first approach is based on dedicated algorithms, while the second is based on special hardware architectures. Generality is sacrificed for speed in both approaches. The algorithmic approach might be suited for industrial application where the scenario is well-controlled and constrained, but it will inhibit easy adaptation to new applications. The method based on special hardware is in general expensive to develop and/or buy. To enable progress towards versatile systems operating in real-time new concepts are required. An alternative formulation based on organization of data in a spatial and temporal context is presented here. Recent work in multi-level data representation has indicated it might be possible to develop efficient methods for description and interpretation of composite motion patterns. These methods exploit Nyquist' rule of sampling, i.e., if the optimal sampling frequency may be determined, it is possible to optimize use of available computational resources. DOE

N89-25594# Aalborg Univ. (Denmark).
CONCURRENT MULTI-RESOLUTION IMAGE ANALYSIS
Henrik I. Christensen and Judson P. Jones (Oak Ridge National Lab., TN.) 1989 9 p Presented at the 4th Conference on Hypercube, Concurrent Computer and Applications, Monterey, CA, 6-8 Mar. 1989 Sponsored in part by Danish Technical Research Council, Danish Research Academy and Foundation Vision North
(Contract DE-AC05-84OR-21400)
(DE89-010261; CONF-890372-6) Avail: NTIS HC A02/MF A01

Since most image analysis tasks are computationally expensive, it is often desirable to perform a course operation which quickly selects areas of an image for more detailed analysis. To simplify the analysis a multi-level representation might be adapted. Alternatively more computational resources might be used to speed-up analysis or a combination of smart algorithms and powerful architectures might be employed. Hypercube architectures have been used for image analysis during the last 5 years, but to our knowledge no one has yet tried to use it for processing of multi-level image representations. Special pyramid architectures have been designed for processing of multi-level representations. A comparison between an artificial pyramid architecture and the more general hypercube architecture will be reported for a number of tasks which are commonly used in manipulation of pyramid data structures. An implementation of a subroutine library is used to obtain timing results to investigate experimentally the use of a hypercube architecture for medium grained pyramid data operations. DOE

N89-25595*# Illinois Univ., Urbana-Champaign. Coordinated Science Lab.
A PARALLEL ALGORITHM FOR SWITCH-LEVEL TIMING SIMULATION ON A HYPERCUBE MULTIPROCESSOR
Hariprasad Nannapane Rao May 1989 38 p
(Grant NAG1-613)
(NASA-CR-185338; NAS 1.26:185338; UILU-ENG-89-2214; CSG-103) Avail: NTIS HC A03/MF A01 CSCL 09B

The parallel approach to speeding up simulation is studied, specifically the simulation of digital LSI MOS circuitry on the Intel iPSC/2 hypercube. The simulation algorithm is based on RSIM, an event driven switch-level simulator that incorporates a linear transistor model for simulating digital MOS circuits. Parallel processing techniques based on the concepts of Virtual Time and rollback are utilized so that portions of the circuit may be simulated on separate processors, in parallel for as large an increase in speed as possible. A partitioning algorithm is also developed in order to subdivide the circuit for parallel processing. Author

N89-25596# National Inst. of Standards and Technology, Gaithersburg, MD. Factory Automation Systems Div.
HIERARCHIES FOR COMPUTER-INTEGRATED MANUFACTURING: A FUNCTIONAL DESCRIPTION

Wayne J. Davis (Illinois Univ., Urbana.) and Albert T. Jones Feb. 1989 30 p
(PB89-172613; NISTIR-88/3744) Avail: NTIS HC A03/MF A01 CSCL 09B

In the recent past, several hierarchies were proposed as candidate models for the integration of decision and control functions within a Computer-Integrated Manufacturing (CIM) environment. A common theme in the definition of these models is to construct an analog to managerial hierarchies that are currently employed in many corporate settings. An alternate approach was adopted. Rather than defining a hierarchy, the manufacturing functions are discussed that a CIM hierarchy must address. Whenever possible, mathematical formulations for the functions will be given with consideration for the stochastic environment in which they will function. The conclusion outlines several concerns arising in the definition of a generic CIM hierarchy and associated research topics that must be addressed. Author

N89-25597*# National Aeronautics and Space Administration. Langley Research Center, Hampton, VA.
COMMON GRAPHICS LIBRARY (CGL). VOLUME 2: LOW-LEVEL USER'S GUIDE
Nancy L. Taylor, Dana P. Hammond, and Pauline M. Theophilos (Computer Sciences Corp., Hampton, VA.) Apr. 1989 419 p
(NASA-TM-101596; CSCC-Doc-G-13; NAS 1.15:101596) Avail: NTIS HC A18/MF A01 CSCL 09B

The intent is to instruct the users of the Low-Level routines of the Common Graphics Library (CGL). The Low-Level routines form an application-independent graphics package enabling the user community to construct and design scientific charts conforming to the publication and/or viewgraph process. The Low-Level routines allow the user to design unique or unusual report-quality charts from a set of graphics utilities. The features of these routines can be used stand-alone or in conjunction with other packages to enhance or augment their capabilities. This library is written in ANSI FORTRAN 77, and currently uses a CORE-based underlying graphics package, and is therefore machine-independent, providing support for centralized and/or distributed computer systems. Author

N89-25598*# Research Inst. for Advanced Computer Science, Moffett Field, CA.
THE RIACS INTELLIGENT AUDITING AND CATEGORIZING SYSTEM
Matt Bishop (Dartmouth Coll., Hanover, NH.) Aug. 1988 17 p
(Contract NCC2-398)
(NASA-CR-185398; NAS 1.26:185398; RIACS-M-88.2) Avail: NTIS HC A03/MF A01 CSCL 09B

The organization of the RIACS auditing package is described along with how to installation instructions and how to interpret the output. How to set up both local and remote file system auditing is given. Logging is done on a time driven basis, and auditing in a passive mode. Author

N89-25599*# Research Inst. for Advanced Computer Science, Moffett Field, CA.
THE FAST ENCRYPTION PACKAGE
Matt Bishop (Dartmouth Coll., Hanover, NH.) Aug. 1988 50 p
(Contract NCC2-398)
(NASA-CR-185397; NAS 1.26:185397; RIACS-M-88.3) Avail: NTIS HC A03/MF A01 CSCL 09B

The organization of some tools to help improve passwork security at a UNIX-based site is described along with how to install and use them. These tools and their associated library enable a site to force users to pick reasonably safe passwords (safe being site configurable) and to enable site management to try to crack existing passworks. The library contains various versions of a very fast implementation of the Data Encryption Standard and of the one-way encryption functions used to encryp the password. Author

N89-25600*# Research Inst. for Advanced Computer Science, Moffett Field, CA.
FAST FOURIER TRANSFORM ALGORITHM DESIGN AND TRADEOFFS
Ray A. Kamin, III and George B. Adams, III (Purdue Univ., West Lafayette, IN.) Dec. 1988 68 p
(Contract NCC2-387)
(NASA-CR-185038; NAS 1.26:185038; RIACS-TR-88.18) Avail: NTIS HC A04/MF A01 CSCL 09B

The Fast Fourier Transform (FFT) is a mainstay of certain numerical techniques for solving fluid dynamics problems. The Connection Machine CM-2 is the target for an investigation into the design of multidimensional Single Instruction Stream/Multiple Data (SIMD) parallel FFT algorithms for high performance. Critical algorithm design issues are discussed, necessary machine performance measurements are identified and made, and the performance of the developed FFT programs are measured. Fast Fourier Transform programs are compared to the currently best Cray-2 FFT program. Author

N89-25601# Virginia Univ., Charlottesville. Dept. of Computer Science.
THE ADAMS DATABASE LANGUAGE
John L. Pfaltz, James C. French, Andrew Grimshaw, Sang H. Son, Paul Baron, Stanley Janet, Albert Kim, Cathy Klumpp, Yi Lin, and Lindsey Lloyd 28 Feb. 1989 49 p
(Contracts DE-FG05-88ER-25063; JPL-957721)
(DE89-010925; DOE/ER-25063/T2; IPC-TR-89-002) Avail: NTIS HC A03/MF A01

ADAMS provides a mechanism for applications programs, written in many languages, to define and access common persistent databases. The basic constructs are element, class, set, map, attribute and codomain. From these the user may define new data structures and new data classes belonging to a semantic hierarchy that supports multiple inheritance. DOE

N89-25602# Oak Ridge National Lab., TN.
PARALLEL SOLUTIONS OF A 2-D PHASE CHANGE PROBLEM ON A HYPERCUBE
H. N. Narang (Tuskegee Inst., AL.) and J. B. Drake Apr. 1989 34 p
(Contract DE-AC05-84OR-21400)
(DE89-012886; ORNL-6504) Avail: NTIS HC A03/MF A01

This report documents the model, algorithms, and results for a heat transfer problem with phase change simulated numerically on a hypercube parallel computer. The temperature and enthalpy distribution in a rectangular domain with first kind boundary conditions (temperature prescribed) is found as a function of time. The model involves a non-linear partial differential equation with a constitutive relation between enthalpy and temperature. The solution to the system is obtained by finite difference approximation with both explicit and implicit methods. In the implicit case, a successive overrelaxation technique with red, black ordering is implemented. The efficiency of the explicit method is compared with that of the implicit method in a multiprocessor computing environment. The design, development, and implementation of algorithms targeted INTEL's iPSC/2 hypercube involving up to 64 processors. The computational workload was uniformly divided among processors as fast as possible by dividing the finite difference grid into several strips and assigning each strip to a processor. The results, depicted in terms of tables, show the effect of relaxation parameter, and stepsize on the efficiency of the parallel algorithms. This is contrasted with the sequential algorithms. DOE

N89-25603# Lawrence Livermore National Lab., CA.
A SIMPLE METHOD TO REMOVE REFERENCE COUNTING IN APPLICATIVE PROGRAMS
Stephen K. Skedzielewski and Rea J. Simpson 23 Nov. 1988 13 p Presented at the Conference on Programming Language Design and Implementation, Portland, OR, 21-23 Jun. 1989
(Contract W-7405-eng-48)

(DE89-006739; UCRL-100156; CONF-890654-2) Avail: NTIS HC A03/MF A01

The efficient compilation of applicative languages that contain data structures such as arrays or records may require that the compiler use a dynamic memory allocator for structured objects. If so, the overhead of reference counting in applicative languages can be considerable, if a compiler simply adds code for reference counting to each operations that references an object. Fortunately, not all the reference counting is necessary for correctness. This paper discusses the use of data dependence information to statically remove reference counting operations. In addition, this method preserves all of the parallelism that was present in the original code and, in some cases, points out opportunities where structured objects can be destructively reused (updated-in-place). DOE

N89-25604 Technische Univ., Delft (Netherlands).
A CONTOUR-ORIENTED APPROACH TO DIGITAL SHAPE ANALYSIS Ph.D. Thesis
Petrus Johannes vanOtterlo 1988 383 p Original contains color illustrations
(ISBN-9-09-002004-7; ETN-89-94298) Copyright Avail: P.J. vanOtterloo, Technische Universiteit, Delft, P.O. Box 5046, 2600 GA Delft, The Netherlands

A unified theoretical basis for shape similarity analysis on the basis of parametric contour representations is outlined. Measures of dissimilarity, based on parametric contour representations, are defined. Relations between the measures of dissimilarity are established. The possibilities for contour representation normalization are evaluated and the tradeoff between optimization and normalization, necessary to achieve the desired invariance properties in the proposed dissimilarity measures, is discussed. The concept of symmetry in plane figures is related to that of similarity under symmetry transformations. This is used to define measures for the quantification of symmetry, or for the lack of symmetry in a plane figure on the basis of previously defined dissimilarity measures. The Fourier coefficient-based counterparts of the dissimilarity and dissymetry measures are formulated, and both types of measure are related to each other. ESA

N89-25605# Technische Univ., Delft (Netherlands).
SEGMENTATION OF NOISY IMAGES Ph.D. Thesis
Jan Jacob Gerbrands 1988 175 p
(ETN-89-94299) Avail: NTIS HC A08/MF A01

A dynamic programming optimal boundary detector algorithm, which facilitates the incorporation of a priori knowledge is discussed. Continuous relaxation labeling procedures, which are parallel though iterative procedures which also exploit the spatial context and allow the incorporation of generic a priori knowledge, are considered. The dynamic programming method and the relaxation labeling procedure are evaluated experimentally by measuring their performances when applied to synthetic test images with various values of the signal-to-noise ratio. The evaluation criteria include the estimated correct and false edge pixel probabilities and Pratt's figure of merit. It is shown that, especially at very low values of the signal to noise ratio, the dynamic programming method performs much better than the traditional methods of edge detection, even when the latter are combined with the relaxation labeling procedure. Applications of the dynamic programming method to medical imaging are proposed. ESA

N89-25606# Loughborough Univ. of Technology (England). Dept. of Mathematical Sciences.
EFFICIENT GENERALIZED CONJUGATE GRADIENT ALGORITHMS
Y. Liu and C. Storey Nov. 1988 18 p
(Maths-Res-211; ETN-89-94324) Avail: NTIS HC A03/MF A01

The effect of inexact line search on conjugacy is studied in unconstrained optimization. A generalized conjugate gradient method concerning this effect is proposed and proved by computational tests to be very efficient compared with the NAG routine E04DBF based on Fletcher-Reeves' method. The method is also shown to compare favorably with a quasi-Newton method on test problems. ESA

N89-25607 Politecnico di Milano (Italy). Lab. di Calcolatori.
ON THE ROLE OF SOFTWARE RELIABILITY IN SOFTWARE ENGINEERING
C. Ghezzi, A. Morzenti, and M. Pezze 1988 53 p Sponsored by CNR, Italy and the Italian Ministry of Public Education
(Rept-88-010; ETN-89-94679) Avail: Politecnico di Milano, Piazza Leonardo da Vinci 32, 20133 Milan, Italy

Complementary approaches to reliability are discussed including the constructive approach to produce a priori reliable software, and the analytic approach which tries to measure reliability by inspecting software after its development. Technologies that may provide a constructive contribution to reliability are presented including formal specifications and programming languages. ESA

N89-25608 Politecnico di Milano (Italy). Dipt. di Elettronica.
SERIAL-INPUT POLYPHASE CONVOLVERS
Luigi Dadda Jul. 1988 26 p
(Rept-88-019; ETN-89-94680) Avail: Politecnico di Milano, Piazza Leonardo da Vinci 32, 20133 Milan, Italy

A simple convolver scheme is first described. It is composed of a cascade of shift registers and serial parallel carry free multipliers. It is shown that convolvers with higher sampling rate can be built by associating two or more such basic convolvers. It is possible to program by means of variables stored in a register, a slices-pack in order to obtain a convolver for a prescribed number of convolution terms and weights and sample lengths. ESA

N89-25609 Politecnico di Milano (Italy). Lab. di Calcolatori.
HANDLING ARRAYS IN SYMBOLIC EXECUTION Thesis
Massimo Calovini 1989 10 p Sponsored in part by CNR, Italy
(Rept-89-003; ETN-89-94683) Avail: Politecnico di Milano, Piazza Leonardo da Vinci 32, 20133 Milan, Italy

An approach to the problems appearing in symbolic execution of programs using array data types is presented. The difficulties in this technique for program analysis appear when the value of the index of the array is a symbolic expression, because the element being referenced depends on program inputs. The solution consists in storing a snapshot of the array, of the operation on it in particular moments, and of the relation between them. ESA

N89-25610# Universiteit Twente, Enschede (Netherlands). Dept. of Computer Science.
ON THE SEMANTICS OF NONATOMIC ACTIONS
Arend Rensink 11 May 1988 32 p Sponsored by the Commission of the European Communities ESPRIT Project 890
(MEMO-INF-88-13; PANGLOSS/IT/UT/14; ISBN-90-365-0163-4; ETN-89-94749) Avail: NTIS HC A03/MF A01

Semantic models that describe the meaning of programs using the concept of actions are discussed. The effect of programs are usually given in the form of action strings. Action relations are introduced to define a semantic model of nonatomic actions. The new relations are called causality and mutual exclusion and are defined algebraically. It is shown that liveness and safety, as well as well known synchronization constructs may be expressed in terms of causality and mutual exclusion. ESA

N89-25611# Universiteit Twente, Enschede (Netherlands). Dept. of Computer Science.
CONTROLLED BIDIRECTIONAL GRAMMARS
Jan Anne Hogendorp Apr. 1988 29 p Sponsored by The Netherlands Organization for Scientific Research
(MEMO-INF-88-16; ETN-89-94751) Avail: NTIS HC A03/MF A01

Context free grammars the rules of which can be used in a productive and in a reductive fashion are investigated. The application of these rules is controlled by a regular language. Several modes of derivation for this kind of grammar are distinguished. Closure properties of the derived language families

are established. Special cases such as linear or left-linear context free grammars are considered. Generalization to arbitrary rather than regular control languages is discussed. ESA

N89-25612# Universiteit Twente, Enschede (Netherlands). Dept. of Computer Science.
AN EXERCISE IN TRANSFORMATIONAL PROGRAMMING: BACK TRACKING AND BRANCH-AND-BOUND
Maarten M. Fokkinga May 1988 24 p
(MEMO-INF-88-22; ETN-89-94754) Avail: NTIS HC A03/MF A01

A completely formal development of program schemes that are usually called backtracking programs and branch and bound programs is presented. The notions are developed in a series of algebraic manipulations on the initial specifications until the desired programs are obtained. Meertens algorithmics transformation laws are used. The notions of linear recursion and iterative recursion are extended to elementwise linear or iterative recursion. A transformation between them is also developed. ESA

N89-25613# Universiteit Twente, Enschede (Netherlands). Dept. of Computer Science.
A CASE STUDY RELATING THE YOURDON METHODOLOGY TO OTHER DESIGN METHODS
W. A. Vervoort Dec. 1988 48 p
(MEMO-INF-88-24; ISBN-9-03-650235-7; ETN-89-94755) Avail: NTIS HC A03/MF A01

Applicability of Yourdon methodology in different stages of the design and implementation of a real time control system is evaluated and it is related to other design methods. Related to Koster's three phase model for programming large systems, the Yourdon methodology is useful in the first application phase as a tool to specify and document large real time systems. In the implementation stage it is only useful for communication and documentation purposes. ESA

N89-25614# Universiteit Twente, Enschede (Netherlands). Dept. of Computer Science.
THE GENERALIZED GRID FILE: AN ACCESS STRUCTURE FOR CIM APPLICATIONS
Henk Blanken, Alle Ijbema, Paul Meek, and Bert vandenAkker Jun. 1988 27 p
(MEMO-INF-88-25; ETN-89-94756) Avail: NTIS HC A03/MF A01

The so called grid file structure used to speed up multi-attribute access of large data bases, is generalized (GGF). This structure has a parameter that defines the number of attributes for which an access path is offered. The GGF behaves like a B tree if single attribute access has to be supported and like a grid file if the number of attributes is greater than one. The performance is evaluated for the business environment and the results look promising. It seems to be a good storage and access structure for computer integrated manufacturing or environments where business and geometrical applications meet. ESA

N89-25615# Universiteit Twente, Enschede (Netherlands). Dept. of Computer Science.
CONSTRAINT SPECIFICATION IN BSDM
Rolf A. deBy Jun. 1988 34 p
(MEMO-INF-88-32; ISBN-9-03-650182-2; ETN-89-94759) Avail: NTIS HC A03/MF A01

A family of constraint definition languages which are designed to fit with the structural BSDM database schemes is described. These languages feature aggregate functions and finite form functions in a many sorted, first order setting, while retaining full expressional power. The notion of meaningful structure is introduced, and it is shown that in meaningful structures all set constructs have a finite interpretation. ESA

N89-25616# Technische Univ., Eindhoven (Netherlands). Faculty of Electrical Engineering.
DESIGN AND IMPLEMENTATION OF A MODULE LIBRARY TO SUPPORT THE STRUCTURAL SYNTHESIS
F. Kaiser, L. Stok, and R. vandenBorn Jan. 1988 54 p
(EUT-88-E-187; ISBN-9-06-144187-0; ISSN-0167-9708; ETN-89-94775) Avail: NTIS HC A04/MF A01

A module library was developed to support tools in the silicon compiler. Not all tools are developed yet, but the demand graph constructor, the cost calculator, and the hardware synthesis system use the library. The object oriented approach of the library facilitates extendibility, and flexibility. An inheritance mechanism is implemented, in which modules at a high abstractional level are described. From these abstractions, more detailed module descriptions can be derived. Fast retrieval times are obtained. The definition of operations and modules is provided for in a user friendly way. The internal datastructure is hidden from the user. The EMACS screen facility contains a small set of functions, for access and definition of objects. Definition of objects must be controlled more than is done at present. A better protection against inconsistencies in the module definition is needed. ESA

N89-25617# Technische Univ., Eindhoven (Netherlands). Automatic System Design Group.
ALWAYS: A SYSTEM FOR WAFER YIELD ANALYSIS
J. PinedadeGyvez Feb. 1988 54 p
(Contract DEA-Proj-IC-EEL46018)
(EUT-88-E-189; ISBN-9-06-144189-7; ISSN-0167-9708; ETN-89-94777) Avail: NTIS HC A04/MF A01

An interactive environment for the analysis of yield information needed on integrated circuit manufacturing lines is presented. The system is able to quantify wafer yields, yield variations between wafers and within the wafers themselves, yields of wafer batches, yield variations between batches, to identify clusters in wafers and or in lots, and is also able to predict wafer yields via simple simulation tools. The analysis technique investigates the effect of correlated and uncorrelated sources of yield loss. Such information can be used to study the changes in the technological process. Graphical displays in the form of wafer maps are used to represent the spatial distribution of dice in the wafer. Facilities such as radial and angular distribution analyses are provided to examine data, and hypothetical wafer maps are created to visualize and predict simulated wafer yields. ESA

N89-25618*# Jet Propulsion Lab., California Inst. of Tech., Pasadena.
THE SOFTWARE PRODUCT ASSURANCE METRICS STUDY: JPL'S SOFTWARE SYSTEMS QUALITY AND PRODUCTIVITY
Marilyn W. Bush 15 Feb. 1989 77 p
(Contract NAS7-918)
(NASA-CR-184871; NAS 1.26:184871; JPL-Publ-89-6) Avail: NTIS HC A05/MF A01 CSCL 09B

The findings are reported of the Jet Propulsion Laboratory (JPL)/Software Product Assurance (SPA) Metrics Study, conducted as part of a larger JPL effort to improve software quality and productivity. Until recently, no comprehensive data had been assembled on how JPL manages and develops software-intensive systems. The first objective was to collect data on software development from as many projects and for as many years as possible. Results from five projects are discussed. These results reflect 15 years of JPL software development, representing over 100 data points (systems and subsystems), over a third of a billion dollars, over four million lines of code and 28,000 person months. Analysis of this data provides a benchmark for gauging the effectiveness of past, present and future software development work. In addition, the study is meant to encourage projects to record existing metrics data and to gather future data. The SPA long term goal is to integrate the collection of historical data and ongoing project data with future project estimations. Author

N89-25619*# Jet Propulsion Lab., California Inst. of Tech., Pasadena.
CONCURRENT IMAGE PROCESSING EXECUTIVE (CIPE)
Meemong Lee, Gregory T. Cooper, Steven L. Groom, Alan S. Mazer, and Winifred I. Williams 1 Oct. 1988 102 p
(Contract NAS7-918)

(NASA-CR-185460; NAS 1.26:185460; JPL-Publ-88-32) Avail: NTIS HC A06/MF A01 CSCL 09B

The design and implementation of a Concurrent Image Processing Executive (CIPE), which is intended to become the support system software for a prototype high performance science analysis workstation are discussed. The target machine for this software is a JPL/Caltech Mark IIIfp Hypercube hosted by either a MASSCOMP 5600 or a Sun-3, Sun-4 workstation; however, the design will accommodate other concurrent machines of similar architecture, i.e., local memory, multiple-instruction-multiple-data (MIMD) machines. The CIPE system provides both a multimode user interface and an applications programmer interface, and has been designed around four loosely coupled modules; (1) user interface, (2) host-resident executive, (3) hypercube-resident executive, and (4) application functions. The loose coupling between modules allows modification of a particular module without significantly affecting the other modules in the system. In order to enhance hypercube memory utilization and to allow expansion of image processing capabilities, a specialized program management method, incremental loading, was devised. To minimize data transfer between host and hypercube a data management method which distributes, redistributes, and tracks data set information was implemented. Author

N89-25162*# Georgia Inst. of Tech., Atlanta.
TRUSS: AN INTELLIGENT DESIGN SYSTEM FOR AIRCRAFT WINGS
Preston R. Bates and Daniel P. Schrage *In* NASA. Langley Research Center, Recent Advances in Multidisciplinary Analysis and Optimization, Part 1 Apr. 1989 p 333-355 (For primary document see N89-25146 19-05)
Avail: NTIS HC A23/MF A01 CSCL 09B

N89-25178*# National Aeronautics and Space Administration. Langley Research Center, Hampton, VA.
THE SIZING AND OPTIMIZATION LANGUAGE (SOL): A COMPUTER LANGUAGE TO IMPROVE THE USER/OPTIMIZER INTERFACE
S. H. Lucas (Vigyan Research Associates, Inc., Hampton, VA.) and S. J. Scotti *In its* Recent Advances in Multidisciplinary Analysis and Optimization, Part 2 Apr. 1989 p 601-619 (For primary document see N89-25173 19-05)
Avail: NTIS HC A22/MF A01 CSCL 09B

N89-25179*# Northrop Corp., Hawthorne, CA. Aircraft Div.
ROBUST COMPUTER-AIDED SYNTHESIS AND OPTIMIZATION OF LINEAR MULTIVARIABLE CONTROL SYSTEMS WITH VARYING PLANT DYNAMICS VIA AUTOCON
C. P. Lefkowitz, J. A. Tekawy, P. K. Pujara, and M. G. Safonov (University of Southern California, Los Angeles.) *In* NASA. Langley Research Center, Recent Advances in Multidisciplinary Analysis and Optimization, Part 2 Apr. 1989 p 621-638 (For primary document see N89-25173 19-05)
Avail: NTIS HC A22/MF A01 CSCL 09B

N89-25180*# McDonnell-Douglas Helicopter Co., Mesa, AZ.
COMPUTERIZED DESIGN SYNTHESIS (CDS), A DATABASE-DRIVEN MULTIDISCIPLINARY DESIGN TOOL
D. M. Anderson and A. O. Bolukbasi *In* NASA. Langley Research Center, Recent Advances in Multidisciplinary Analysis and Optimization, Part 2 Apr. 1989 p 639-650 (For primary document see N89-25173 19-05)
Avail: NTIS HC A22/MF A01 CSCL 09B

N89-25182*# Rensselaer Polytechnic Inst., Troy, NY. Dept. of Mechanical Engineering.
AN INVESTIGATION OF USING AN RQP BASED METHOD TO CALCULATE PARAMETER SENSITIVITY DERIVATIVES
Todd J. Beltracchi and Gary A. Gabriele *In* NASA. Langley Research Center, Recent Advances in Multidisciplinary Analysis and Optimization, Part 2 Apr. 1989 p 673-696 (For primary document see N89-25173 19-05)
Avail: NTIS HC A22/MF A01 CSCL 09B

N89-25218*# Colorado State Univ., Fort Collins. Dept. of Mathematics.
MULTIPLIER-CONTINUATION ALGORTHMS FOR CONSTRAINED OPTIMIZATION
Bruce N. Lundberg, Aubrey B. Poore, and Yang Bing *In* NASA. Langley Research Center, Recent Advances in Multidisciplinary Analysis and Optimization, Part 3 Apr. 1989 p 1303-1315 (For primary document see N89-25201 19-05)
(Grants NGT-06-002-802; AF-AFOSR-0059-88)
Avail: NTIS HC A22/MF A01 CSCL 09B

N89-25219*# Iowa Univ., Iowa City. Dept. of Mechanical Engineering.
A LARGE SCALE SOFTWARE SYSTEM FOR SIMULATION AND DESIGN OPTIMIZATION OF MECHANICAL SYSTEMS
Bernhard Dopker and Edward J. Haug *In* NASA. Langley Research Center, Recent Advances in Multidisciplinary Analysis and Optimization, Part 3 Apr. 1989 p 1319-1333 (For primary document see N89-25201 19-05)
Avail: NTIS HC A22/MF A01 CSCL 09B

N89-25220*# Georgia Inst. of Tech., Atlanta. School of Aerospace Engineering.
THE ROLE OF OPTIMIZATION IN THE NEXT GENERATION OF COMPUTER-BASED DESIGN TOOLS
J. Edward Rogan *In* NASA. Langley Research Center, Recent Advances in Multidisciplinary Analysis and Optimization, Part 3 Apr. 1989 p 1335-1357 (For primary document see N89-25201 19-05)
Avail: NTIS HC A22/MF A01 CSCL 09B

62 COMPUTER SYSTEMS

Includes computer networks and special application computer systems.

N89-25620*# Northwestern Univ., Evanston, IL. Dept. of Civil Engineering.
PARALLEL PROCESSORS AND NONLINEAR STRUCTURAL DYNAMICS ALGORITHMS AND SOFTWARE Semiannual Progress Report, 1 Dec. 1988 - 31 May 1989
Ted Belytschko, Noreen D. Gilbertsen, Mark O. Neal, and Edward J. Plaskacz Jun. 1989 43 p Sponsored by ANL, IL
(Grant NAG1-650)
(NASA-CR-185049; NAS 1.26:185049) Avail: NTIS HC A03/MF A01 CSCL 09B

The adaptation of a finite element program with explicit time integration to a massively parallel SIMD (single instruction multiple data) computer, the CONNECTION Machine is described. The adaptation required the development of a new algorithm, called the exchange algorithm, in which all nodal variables are allocated to the element with an exchange of nodal forces at each time step. The architectural and C* programming language features of the CONNECTION Machine are also summarized. Various alternate data structures and associated algorithms for nonlinear finite element analysis are discussed and compared. Results are presented which demonstrate that the CONNECTION Machine is capable of outperforming the CRAY XMP/14. Author

N89-25621# Lawrence Livermore National Lab., CA.
PARTITIONING A FINITE DIFFERENCE CODE FOR A LOCAL MEMORY MULTIPROCESSOR
Bryan Lawver Mar. 1989 3 p Presented at the 4th Hypercube, Concurrent Computers and Applications, Monterey, CA, 6 Mar. 1989
(Contract W-7405-eng-48)
(DE89-010223; UCRL-99893; CONF-890372-8) Avail: NTIS HC A02/MF A01

The TSAR code, a 3D finite difference EM model, was partitioned into parallel modules where each processor computed a subset of the 3D mesh. The multiprocessor was arranged in a square mesh of processors with the full range of one dimension

in each processor and sub ranges in the other dimensions. Finding the range and checking for independence of array elements over those sub ranges is the main problem of partitioning. In addition with local memory multiprocessors, the array elements are distributed over the processors' local memory and a communications structure must be available which allows non-local elements to be assessed. Element communications must be fast enough or few enough to allow good utilization of the processor compute power. Automated partitioning was not available, but recent work provides some hope in this area. TSAR stands for Time-Domain Scattering and Response software that has been used for many years to model electric and magnetic waves in a three dimensional box. This code was partitioned to run on the SPRINT processor. SPRINT is a Systolic Processor with a Reconfigurable Interconnection Network of Transputers. It incorporates 64 floating point transputers. Results of this partitioning resulted in performance nearly equal to a CRAY XMP for identical problems. DOE

N89-25622# Sandia National Labs., Albuquerque, NM.
DESIGN AND CONSTRUCTION OF A COMPUTER SYSTEM MODEL FOR APPLICATION DEVELOPMENT WORKLOADS
Gerald F. Quinlan, Richard A. Reid, and Neal D. Wenderlich (International Business Machines Corp., Armonk, NY.) Feb. 1989 30 p
(Contract DE-AC04-76DP-00789)
(DE89-010519; SAND-89-0109) Avail: NTIS HC A03/MF A01

This report describes a capacity planning project for Engineering Information Management (EIM) systems at Sandia National Laboratories, Albuquerque. The purpose of the project was to develop a method for predicting the ability of current hardware computer systems to meet future demands and to quantify the magnitude of required upgrades. The project phases included the analysis of alternative, the selection of analytic modeling as the appropriate vehicle, construction of the model, the development of recommendations for its use as a capacity planning tool, and the formulation of proposals for future enhancements. DOE

N89-25623# Vanderbilt Univ., Nashville, TN. Dept. of Computer Science.
USING A SEGREGATION MEASURE FOR THE WORKLOAD CHARACTERIZATION OF MULTI-CLASS QUEUING NETWORKS
Lawrence W. Dowdy, Alan T. Krantz, and Michael R. Leuze (Oak Ridge National Lab., TN.) 1989 16 p Presented at the International Conference on Measurement and Modeling of Computer Systems, Berkeley, CA, 23 May 1989
(Contract DE-AC05-84OR-21400)
(DE89-007841; CONF-8905100-1) Avail: NTIS HC A03/MF A01

When a queuing network model of a computer system is constructed, the workload is characterized by several parameters known as the device demands. The demand that every customer places upon every device must be specified. A complete workload characterization of a K device network with N different customers contains N * K parameters. Substantial savings in complexity result if the number of workload parameters is decreased. If, for example, only the average demands on the K devices are used in the workload characterization, the overhead of parameter collection is reduced, and the solution of the queuing network model is simplified. With this approach, however, the multi-class system is represented by a single-class model. A loss of accuracy results. It has been recently demonstrated that the performance of a multi-class network is bounded below by its single-class counterpart model and is bounded above by a simple function based upon the single-class model. In this paper, a new workload characterization technique is proposed which requires: the K average device demands for the single-class counterpart model and a segregation measure, a value which indicates the degree to which different customers tend to utilize different parts of the network. The segregation measure specifies the point between the two bounds where the multi-class model's performance lies. This measure is quite intuitive and is simple to calculate. The technique provides an accurate estimate of the performance of a multi-class network. DOE

N89-25624# Lawrence Livermore National Lab., CA.
PERFORMANCE EVALUATION FOR DATA FLOW ARCHITECTURES: A SUMMARY OF DISCUSSIONS FROM THE SANTA FE WORKSHOP
James R. McGraw Jan. 1989 10 p Presented at the Workshop on Instrumentation for Future Parallel Systems, Los Alamos, NM, 19 May 1989
(Contract W-7405-eng-48)
(DE89-008023; UCRL-100315; CONF-8905101-1) Avail: NTIS HC A02/MF A01

This paper summarizes approximately four hours of discussion held at the Santa Fe Workshop on Parallel Architecture Evaluation. The general topic of the discussion centered on performance evaluation techniques and measurement tools appropriate for data flow computers. In this paper, as much of the discussion as possible has been extracted and organized in a form that is clearer for readers to follow. The paper contains four major sections. The first section gives some very brief background information on data flow computing to provide a framework for the topics that follow. The second section examines several major implications that the data flow architecture approach has on the issue of performance measurement and evaluation. The third section identifies the primary measurement objectives that the discussion group listed as being important to study. The fourth section presents tools the group highlighted as possible techniques for getting to the important measurements. DOE

N89-25625# Lawrence Livermore National Lab., CA.
THE DELTA-t TRANSPORT PROTOCOL: FEATURES AND EXPERIENCE USEFUL FOR HIGH PERFORMANCE NETWORKS
R. W. Watson 1989 14 p Presented at the International Federation of Information Processing Workshop on Protocols for High-Speed Networks, Zurich, Switzerland, 9 May 1989
(Contract W-7405-eng-48)
(DE89-009259; UCRL-100668; CONF-8905114-1) Avail: NTIS HC A03/MF A01

With the advent of new high performance networks and distributed systems there is renewed interest in transport protocol designs that can support both request/response and stream styles of communication. Delta-t is a transport protocol designed to meet such goals. Delta-t's main contribution is in the area of connection management, where it achieves hazard free connection management without explicit packet exchanges. This paper reviews Delta-t's features, connection management more generally, and outlines some implementation lessons useful for high performance networks. DOE

N89-25626# Los Alamos National Lab., NM.
INTERCONNECTION NETWORKS Patent Application
Vance Faber, inventor (to DOE) and James W. Moore, inventor (to DOE) 20 Jun. 1988 34 p
(Contract W-7405-eng-36)
(DE89-010965; PATENTS-US-A7209238; US-Patent-Appl-SN-209238) Avail: NTIS HC A03

A network of interconnected processors is formed from a vertex symmetric graph selected from graphs GAMMA(sub d)(k) with degree d, diameter k, and (d + 1)factorial/(d - k + 1)factorial processors for each d greater than or equal to k and GAMMA(sub d)(k, -1) with degree d - 1, diameter k + 1, and (d + 1)factorail/(d - k + 1)factorial processors for each d greater than or equal to k greater than or equal to 4. Each processor has an address formed by one of the permutations from a predetermined sequence of letters chosen a selected number of letters at a time, and an extended address formed by appending to the address the remaining ones of the predetermined sequence of letters. A plurality of transmission channels is provided from each of the processors, where each processor has one less channel than the selected number of letters forming the sequence. Where a network

GAMMA(sub d)(k, -1) is provided, no processor has a channel connected to form an edge in a direction delta(sub 1). Each of the channels has an identification number selected from the sequence of letters and connected from a first processor having a first extended address to a second processor having a second address formed from a second extended address defined by moving to the front of the first extended address the letter found in the position within the first extended address defined by the channel identification number. The second address is then formed by selecting the first elements of the second extended address corresponding to the selected number used to form the address permutations. DOE

N89-25627*# College of William and Mary, Williamsburg, VA. Dept. of Computer Science.
USE OF METAKNOWLEDGE IN THE VERIFICATION OF KNOWLEDGE-BASED SYSTEMS Final Report
Larry J. Morell Apr. 1989 17 p
(Grant NGT-47-003-029)
(NASA-CR-181821; NAS 1.26:181821) Avail: NTIS HC A03/MF A01 CSCL 09B

Knowledge-based systems are modeled as deductive systems. The model indicates that the two primary areas of concern in verification are demonstrating consistency and completeness. A system is inconsistent if it asserts something that is not true of the modeled domain. A system is incomplete if it lacks deductive capability. Two forms of consistency are discussed along with appropriate verification methods. Three forms of incompleteness are discussed. The use of metaknowledge, knowledge about knowledge, is explored in connection to each form of incompleteness. Author

N89-25628*# Research Inst. for Advanced Computer Science, Moffett Field, CA.
SPEEDING UP PARALLEL PROCESSING
Peter J. Denning 23 May 1988 13 p Submitted for publication
(Contract NCC2-387)
(NASA-CR-184646; NAS 1.26:184646; RIACS-TR-88.15) Avail: NTIS HC A03/MF A01 CSCL 09B

In 1967 Amdahl expressed doubts about the ultimate utility of multiprocessors. The formulation, now called Amdahl's law, became part of the computing folklore and has inspired much skepticism about the ability of the current generation of massively parallel processors to efficiently deliver all their computing power to programs. The widely publicized recent results of a group at Sandia National Laboratory, which showed speedup on a 1024 node hypercube of over 500 for three fixed size problems and over 1000 for three scalable problems, have convincingly challenged this bit of folklore and have given new impetus to parallel scientific computing. Author

N89-25629*# Research Inst. for Advanced Computer Science, Moffett Field, CA.
FEASIBILITY OF USING THE MASSIVELY PARALLEL PROCESSOR FOR LARGE EDDY SIMULATIONS AND OTHER COMPUTATIONAL FLUID DYNAMICS APPLICATIONS Final Report
John Bruno Jun. 1984 39 p
(NASA-CR-185427; NAS 1.26:185427; RIACS-TR-84.2) Avail: NTIS HC A03/MF A01 CSCL 09B

The results of an investigation into the feasibility of using the MPP for direct and large eddy simulations of the Navier-Stokes equations is presented. A major part of this study was devoted to the implementation of two of the standard numerical algorithms for CFD. These implementations were not run on the Massively Parallel Processor (MPP) since the machine delivered to NASA Goddard does not have sufficient capacity. Instead, a detailed implementation plan was designed and from these were derived estimates of the time and space requirements of the algorithms on a suitably configured MPP. In addition, other issues related to the practical implementation of these algorithms on an MPP-like architecture were considered; namely, adaptive grid generation, zonal boundary conditions, the table lookup problem, and the software interface. Performance estimates show that the architectural components of the MPP, the Staging Memory and the Array Unit, appear to be well suited to the numerical algorithms of CFD. This combined with the prospect of building a faster and larger MMP-like machine holds the promise of achieving sustained gigaflop rates that are required for the numerical simulations in CFD. Author

N89-25630# Oak Ridge Gaseous Diffusion Plant, TN. Computing and Telecommunications Div.
INTERPROCESS COMMUNICATIONS AND APPLICATION TO PHYSICAL NUMERICAL MODELING
T. B. Bland, M. W. Wendel, and G. E. Giles Mar. 1989 34 p
(Contract DE-AC05-84OT-21400)
(DE89-011021; K/CSD/TM-81) Avail: NTIS HC A03/MF A01

A user of the single processor CRAY X-MP at Martin Marietta Energy Systems, Inc., has the capability of running simultaneously several programs that are working on the same problem and can communicate by passing information back and forth during execution. Each program may be responsible for initializing additional programs. This message-passing method has been applied to the numerical simulation of physical systems, specifically, heat transfer phenomena. It allows the user to easily expand modeling capability of existing programs without the development of new simulation software. Each program is responsible for simulation of one part of the physical problem. The problem may be apportioned in any manner, for example, based on geometry or physical phenomena. DOE

N89-25631# Fermi National Accelerator Lab., Batavia, IL. Advanced Computer Program.
A SITE ORIENTED SUPERCOMPUTER FOR THEORETICAL PHYSICS: THE FERMILAB ADVANCED COMPUTER PROGRAM MULTI ARRAY PROCESSOR SYSTEM (ACMAPS)
T. Nash, R. Atac, A. Cook, J. Deppe, Mark Fischler, Irwin Gaines, D. Husby, T. Pham, T. Zmuda, and E. Eichten Mar. 1989 8 p Presented at the 4th Hypercube, Concurrent Computers and Applications, Monterey, CA, 6-8 Mar. 1989
(Contract DE-AC02-76CH-03000)
(DE89-011090; FNAL/C-89/58; CONF-890372-11) Avail: NTIS HC A02/MF A01

The ACPMAPS multipocessor is a highly cost effective, local memory parallel computer with a hypercube or compound hypercube architecture. Communication requires the attention of only the two communicating nodes. The design is aimed at floating point intensive, grid like problems, particularly those with extreme computing requirements. The processing nodes of the system are single board array processors, each with a peak power of 20 Mflops, supported by 8 Mbytes of data and 2 Mbytes of instruction memory. The system currently being assembled has a peak power of 5 Gflops. The nodes are based on the Weitek XL Chip set. The system delivers performance at approximately $300/Mflop. DOE

N89-25632# Argonne National Lab., IL. Mathematics and Computer Science Div.
A PARALLEL PROCESSING APPROACH FOR IMPLEMENTING HIGH-PERFORMANCE FIRST-ORDER LOGIC DEDUCTION SYSTEMS Ph.D. Thesis
Anita Jindal, Ross Overbeek, and William McCune Apr. 1989 29 p
(Contract W-31-109-eng-38)
(DE89-011878; ANL/MCS/TM-131) Avail: NTIS HC A03/MF A01

Recent trends toward exploiting parallel processing for increasing the execution speed have resulted in the development of parallel algorithms for a variety of applications. The research reported here is devoted to the use of parallel processing for developing high-performance deduction systems, an application in the area of artificial intelligence. During our research we investigated the scheme for parallelizing propositional deduction systems proposed by Butler and Karonis. Specifically, a parallel

first-order logic deduction system POTTER-I was developed by applying the scheme of Butler and Karonis to the sequential first-order logic theorem prover OTTER. The performance of POTTER-I was further improved by introducing several optimizations, including message buffering, blocking send, and an encoding scheme for the clauses in the set of support, into the original scheme. In this document, we describe the implementation details of POTTER-I and the enhancements to the original scheme of Butler and Karonis. An evaluation of the enhanced algorithm of POTTER-I for some benchmarks is also presented. DOE

N89-25633 Politecnico di Milano (Italy). Lab. di Calcolatori.
SYMBOLIC EXECUTION OF CONCURRENT PROGRAMS USING PETRI NETS
C. Ghezzi, D. Mandrioli, M. Pezze, and S. Morasca 1989 56 p (Rept-89-004; ETN-89-94684) Avail: Politecnico di Milano, Piazza Leonardo da Vinci 32, 20133 Milan, Italy

Techniques for analyzing sequential programs in order to improve their reliability are presented. The method is based on an extension of the Petri net formalism, called EF nets. These nets can be used as high level specification for concurrent programs. Thus the model is not dependent on a particular concurrent programming language, but it is flexible enough to be the kernel model for the presentation of a wide set of systems and programming languages. General algorithms for symbolically executing an EF net are described. ESA

N89-25634# Universiteit Twente, Enschede (Netherlands). Dept. of Computer Science.
INTEGRATED SERVICES DIGITAL NETWORK: OVERVIEW AND ARCHITECTURAL CONCEPTS
Jeroen Schot and Aiko Pras Oct. 1988 37 p (MEMO-INF-88-42; ISBN-9-03-650202-0; ETN-89-94761) Avail: NTIS HC A03/MF A01

An overview of the definition of the user interface to integrated systems as defined by the CCITT norms is presented. Architectural issues seen from a viewpoint of the principles of the reference model for Open Systems Interconnection are included. Broadband technology is discussed. It is shown that the specification of the protocols and services recommended for usage in integrated services are incomplete and imprecise. It is concluded that the smallband system is a step on the road to an integrated broadband network, providing a communications service with throughput quality of service parameters selectable from a large range of values. ESA

63 CYBERNETICS

Includes feedback and control theory, artificial intelligence, robotics and expert systems.

For related information see also *54 Man/System Technology and Life Support.*

N89-25635*# National Aeronautics and Space Administration. Lyndon B. Johnson Space Center, Houston, TX.
AN EXPERT SYSTEM DEVELOPMENT METHODOLOGY WHICH SUPPORTS VERIFICATION AND VALIDATION
Chris Culbert, Gary Riley, and Robert T. Savely 1987 9 p Presented at the 4th IEEE Conference on Artificial Intelligence Applications, San Diego, CA, Mar. 1988 (NASA-TM-101782; NAS 1.15:101782) Avail: NTIS HC A02/MF A01 CSCL 09B

Expert systems have demonstrated commercial viability in a wide range of applications, but still face some obstacles to widespread use. A major stumbling block is the lack of well defined verification and validation (V and V) techniques. The primary difficulty with expert system V and V is the use of development methodologies which do not support V and V. As with conventional code, the key to effective V and V is the development methodology. An expert system development methodology is described which is based upon a panel review approach, that allows input from all parties concerned with the expert system. Author

N89-25636# Oak Ridge National Lab., TN. Center for Engineering Systems.
ROBUST PERFORMANCE OF MULTIPLE TASKS BY AN AUTONOMOUS ROBOT
Martin Beckerman, Deanna L. Barnett, Ralph Einstein, Judson P. Jones, Philip F. Spelt, and Charles R. Weisbin 1989 9 p Presented at the Workshop on Integration of AI and Robotic Systems, Scottsdale, AZ, 19 May 1989 (Contract DE-AC05-84OR-21400) (DE89-008718; CONF-8905109-2) Avail: NTIS HC A02/MF A01

There have been many successful mobile robot experiments, but very few papers have appeared that examine the range of applicability, or robustness, of a robot system. The purpose of this paper is to determine and quantify robustness of the Hermies-IIB experimental capabilities. DOE

N89-25637# Oak Ridge National Lab., TN. Instrumentation and Controls Div.
PERFORMANCE CHARACTERISTICS FOR ADVANCED CONTROL SYSTEMS
Roger A. Kisner, Riza C. Berken, and Belle R. Upadhyaya (Tennessee Univ., Knoxville.) 1989 13 p Presented at the 7th Power Plant Dynamics, Control and Testing Symposium, Knoxville, TN, 15 May 1989 (Contract DE-AC05-84OR-21400) (DE89-010362; CONF-890555-12) Avail: NTIS HC A03/MF A01

A growing collection of control techniques is becoming available to the design engineer. This makes selection of the most appropriate technique for a given application a difficult task. A systematic approach to evaluating alternative control schemes is needed. The approach discussed in this paper expands the traditional concepts of quantitative performance analysis to include other relevant factors, such as robustness of the technique, resource requirements, and effects on operators and other personnel. This collection of factors, termed measures of utility, may be used as qualitative and quantitative means of evaluating and comparing properties of alternative control system designs. This paper, although not an in-depth study, serves to outline several measures of utility and suggests a general structure for control system development. This method of comparing the usefulness of alternative control systems will prove valuable to the ORNL Advanced Controls Program (ACTO) for optimizing compatibility with actual systems and equipment. DOE

N89-25638*# Research Inst. for Advanced Computer Science, Moffett Field, CA.
BLINDNESS IN DESIGNING INTELLIGENT SYSTEMS
Peter J. Denning 1 Feb. 1988 12 p Submitted for publication (Contract NCC2-387) (NASA-CR-184582; NAS 1.26:184582; RIACS-TR-88.4) Avail: NTIS HC A03/MF A01 CSCL 09B

New investigations of the foundations of artificial intelligence are challenging the hypothesis that problem solving is the cornerstone of intelligence. New distinctions among three domains of concern for humans--description, action, and commitment--have revealed that the design process for programmable machines, such as expert systems, is based on descriptions of actions and induces blindness to nonanalytic action and commitment. Design processes focusing in the domain of description are likely to yield programs like bureaucracies: rigid, obtuse, impersonal, and unable to adapt to changing circumstances. Systems that learn from their past actions, and systems that organize information for interpretation by human experts, are more likely to be successful in areas where expert systems have failed. Author

N89-25639*# Oak Ridge National Lab., TN. Instrumentation and Controls Div.
SYNTHETIC ORGANISMS AND SELF-DESIGNING SYSTEMS
W. B. Dress 1989 13 p Presented at the Goddard AI Conference, Greenbelt, MD, 16 May 1989

(Contract DE-AC05-84OR-21400)
(NASA-CR-185324; NAS 1.26:185324; DE89-010318;
CONF-8905130-1) Avail: NTIS HC A03/MF A01 CSCL 09B

This paper examines the need for complex, adaptive solutions to certain types of complex problems typified by the Strategic Defense System and NASA's Space Station and Mars Rover. Since natural systems have evolved with capabilities of intelligent behavior in complex, dynamic situations, it is proposed that biological principles be identified and abstracted for application to certain problems now facing industry defense, and space exploration. Two classes of artificial neural networks are presented: a non-adaptive network used as a genetically determined retina, and a frequency-coded network as an adaptive brain. The role of a specific environment coupled with a system of artificial neural networks having simulated sensors and effectors is seen as an ecosystem. Evolution of synthetic organisms within this ecosystem provides a powerful optimization methodology for creating intelligent systems able to function successfully in any desired environment. A complex software system involving a simulation of an environment and a program designed to cope with that environment are presented. Reliance on adaptive systems, as found in nature, is only part of the proposed answer, though an essential one. The second part of the proposed method makes use of an additional biological metaphor--that of natural selection-- to solve the dynamic optimization problems that every intelligent system eventually faces. A third area of concern in developing an adaptive, intelligent system is that of real-time computing. It is recognized that many of the problems now being explored in this area have their parallels in biological organisms, and many of the performance issues facing artificial neural networks may find resolution in the methodology of real-time computing. DOE

N89-25640# Universiteit Twente, Enschede (Netherlands). Dept. of Computer Science.
EXPLANATION IN KNOWLEDGE-BASED SYSTEMS
P. M. Wognum and N. J. I. Mars 14 Aug. 1988 53 p
(MEMO-INF-88-17; UT-KBS-88-01; ISBN-9-03-650206-3;
ETN-89-94752) Avail: NTIS HC A04/MF A01

A tree representation of system reasoning is developed and used to illustrate the different explanations a system is able to give. A knowledge organization to enable more advanced explanations is proposed. ESA

N89-25641# Universiteit Twente, Enschede (Netherlands). Dept. of Computer Science.
THE USE OF FIRST PRINCIPLES IN DIAGNOSING COMPLEX TECHNICAL DEVICES
D. C. vanSoest, P. A. Hogenhuis, R. R. Bakker, and N. J. I. Mars 25 Oct. 1988 26 p
(MEMO-INF-88-40; UT-KBS-88-02; SKBS/A1/88-7;
ISBN-9-03-650210-1; ETN-89-94760) Avail: NTIS HC A03/MF A01

The diagnosis of complex technical devices using device design information is studied in a literature survey intended to stimulate the research into knowledge based systems. The notion is in contrast to using heuristic knowledge. Only devices that can be clearly divided into components are investigated. ESA

N89-25642# Technische Univ., Eindhoven (Netherlands). Measurement and Control Group.
BLACK-BOX IDENTIFICATION OF MIMO TRANSFER FUNCTIONS: ASYMPTOTIC PROPERTIES OF PREDICTION ERROR MODELS
Yu-Cai Zhu Nov. 1987 33 p
(EUT-87-E-182; ISBN-9-06-144182-X; ISSN-0167-9708;
ETN-89-94770) Avail: NTIS HC A03/MF A01

Identification of MIMO transfer functions is considered. The transfer function matrix is parametrized as black-box models, which have certain shift-properties; no structure or order is chosen a priori. In order to obtain a good transfer function estimate, the order of the model is allowed to increase to infinity as the number of data tends to infinity. The expression of asymptotic covariance of the transfer function estimates is derived, which is asymptotic both in the number of data and in the model order. The result indicates that the joint covariance matrix of the transfer functions from inputs to outputs and from driving white noise sources to the additive output disturbances respectively is proportional to the Kronecker product of the inverse of the joint spectrum matrix for the inputs and driving noise and the spectrum matrix of the additive output noise. The factor of proportionality is the ratio of model order to number of data. The result is independent of the model structure used. This result is the MIMO extension of the theory of Ljung (1985). The application of this theory for defining the bounds of modeling errors is highlighted. ESA

N89-25643# Technische Univ., Eindhoven (Netherlands). Measurement and Control Group.
ON THE BOUNDS OF THE MODELING ERRORS OF BLACK-BOX MIMO TRANSFER FUNCTION ESTIMATES
Yu-Cai Zhu Nov. 1987 33 p
(EUT-87-E-183; ISBN-9-06-144183-8; ISSN-0167-9708;
ETN-89-94771) Avail: NTIS HC A03/MF A01

The following problem is tackled: Derive a suitable description of the modeling errors (model uncertainty) of MIMO transfer function models which are obtained by black-box identification; this description must supply the quantitative information required for robustness study of the feedback system where the black-box model is used for the controller design. An upper bound of modeling errors is estimated. The asymptotic theory of the properties of black-box transfer function estimates, developed by Ljung and Yuan (1985) is used. Their theory shows that the transfer function estimates are consistent, the errors of the estimates are asymptotically joint normal, with a very simple expression for their covariances. Their results are extended to cases where spectral analysis is used. Based on this theory, a bound of (additive) modeling errors is defined as the sum of the absolute value of the bias part and the 3 sigma bound of the variance (random) part of the modeling errors. Algorithms are proposed for the computations; a numerical test is performed to validate the theory. The bounds for other forms of the modeling errors are also derived from the bound matrix obtained. ESA

N89-25644# Technische Univ., Eindhoven (Netherlands). Faculty of Electrical Engineering.
A NEW METHOD FOR DYNAMIC HUNTING EXTREMUM CONTROL, BASED ON COMPARISON OF MEASURED AND ESTIMATED VALUE
Wen-Jiang Liu and Dau-Hua Ye Jun. 1988 26 p Sponsored by the Netherlands Ministry of Education and Science
(EUT-88-E-197; ISBN-90-614-4197-8; ISSN-0167-9708;
ETN-89-94785) Avail: NTIS HC A03/MF A01

A dynamic hunting method is proposed for an extremum control system. The method is based on comparison of the estimated value and measured value. A controller using a microprocessor in accordance with this method is explained. The controller can be used in process control systems. In these control systems, there are a lot of inertial and other dynamic effects. The output linear group of the system is approximately expressed as a second-order or nth-order system with a large time constant or with time delay. Moreover, the relation between input drive reversal of the logic circuit and dynamic output of the system is discussed in detail. The calculating formulae for this drive reversal are given for different transfer functions, and through tests they prove correct. A controller using a micro-processor and a testing laboratory plant was designed and implemented. The results of experiments show that the performance of the controller satisfies the technical requirements in design and that it can search the optimum point rapidly. ESA

N89-25158*# Florida Univ., Gainesville. Aerospace Engineering, Mechanics and Engineering Science.
NEW DIRECTIONS FOR ARTIFICIAL INTELLIGENCE (AI) METHODS IN OPTIMUM DESIGN
Prabhat Hajela *In* NASA. Langley Research Center, Recent Advances in Multidisciplinary Analysis and Optimization, Part 1 Apr. 1989 p 259-274 (For primary document see N89-25146

19-05)
Avail: NTIS HC A23/MF A01 CSCL 09B

64 NUMERICAL ANALYSIS

Includes iteration, difference equations, and numerical approximation.

N89-25645# Oak Ridge National Lab., TN. Computing and Telecommunications Div.
APPLICATION OF THETA FUNCTIONS FOR NUMERICAL EVALUATION OF COMPLETE ELLIPTIC INTEGRALS OF THE FIRST AND SECOND KINDS
D. K. Lee Mar. 1989 24 p
(Contract DE-AC05-84OR-21400)
(DE89-010191; ORNL/TM-11075) Avail: NTIS HC A03/MF A01

An approximation method based on the use of theta functions is shown to be efficient and useful in numerical evaluation of complete elliptic integrals of the first and second kinds, K(k) and E(k), respectively. The integrals are expressed in terms of power series of the form summation of a sub n q sup n2, 0 less than or equal to q less than 1, where q is the nome determined uniquely from a given value of the argument k. The series converse very rapidly except for small domains near absolute value of = 1, where they either converge slowly or fail to converge. When applied on Cray 2 computers for 0 less than or equal to k sq less than or equal to 0.9955, the procedure is found to be more efficient than both the Chebyshev approximations of the Hastings form and the standard Gauss arithmetic-geometric mean process. Numerical results that demonstrate the accuracy and efficiency of the approximation method are presented. DOE

N89-25646# Central Inst. of Physics, Bucharest (Romania). Dept. of Theoretical Physics.
TOWARD A PROOF OF THE EXISTENCE OF AN INTEGRITY BASIS FOR THE TENSORS IN THE ENVELOPING ALGEBRA OF su(3)
H. Scutaru Jun. 1987 12 p
(DE88-706031; IFIN-FT-309-1987) Avail: NTIS (US Sales Only)
HC A03/MF A01

It is proved that the zero weight multiplicities and generalized exponents of the su(3)-algebra coincide with those predicted from the hypothesis of the existence of an integrity basis for the su(3)-submodules of the enveloping algebra or su(3). DOE

N89-25647# Central Inst. of Physics, Bucharest (Romania). Inst. of Physics and Nuclear Engineering.
DEGENERATE REPRESENTATION FROM TENSORIAL IDENTITIES AND QUANTUM REALISATIONS OF YBZF ALGEBRAS
M. Iosifescu and H. Scutaru Jun. 1987 13 p
(DE88-706032; IFIN-FT-310-1987) Avail: NTIS (US Sales Only)
HC A03/MF A01

The second degree irreducible tensors in the enveloping algebra of the classical semisimple Lie algebras are determined and the irreducible representations on which these tensors vanish are derived. DOE

N89-25648# Central Inst. of Physics, Bucharest (Romania). Inst. for Physics and Nuclear Engineering.
BALANCING A MATRIX FOR CALCULATION OF EIGENVALUES AND EIGENVECTORS
N. Moldovan May 1987 8 p
(DE88-706045; IFIN-MC-19-1987) Avail: NTIS (US Sales Only)
HC A02/MF A01

Parlett and Reinsch algorithm for general matrix balancing is refined by adding after each iteration a new balancing of the last two row column pairs taken into account. DOE

N89-25649# Naval Postgraduate School, Monterey, CA.
ARMA (AUTOREGRESSIVE-MOVING AVERAGE) MODELING
M.S. Thesis
Gurhan Kayahan Dec. 1988 89 p
(AD-A205308) Avail: NTIS HC A05/MF A01 CSCL 12/3

This thesis estimates the frequency response of a network where the only data is the output obtained from an Autoregressive-Moving Average (ARMA) model driven by a random input. Models of random processes and existing methods for solving ARMA models are examined. The estimation is performed iteratively by using the Yule-Walker Equations in three different methods for the AR part and the Cholesky factorization for the MA part. The AR parameters are estimated initially, the MA parameters are estimated assuming that the AR parameters have been compensated for. After the estimation of each parameter set, the original time series is filtered via the inverse of the last estimate of the transfer function of an AR model or MA model, allowing better and better estimation of each model's coefficients. The iteration refers to the procedure of removing the MA or AR part from the random process in an alternating fashion allowing the creation of an almost pure AR or MA process, respectively. As the iteration continues the estimates are improving. When the iteration reaches a point where the coefficients converge the last MA and AR model coefficients are retained as final estimates.
GRA

N89-25650# Joint Inst. for Nuclear Research, Dubna (USSR). Lab. of Computing Techniques and Automation.
PROGRAM PACKAGE FOR INVESTIGATION OF DIFFERENTIAL EQUATIONS BY THE EXTERNAL FORM METHOD
V. L. Topunov and A. B. Shvachka 1988 18 p In RUSSIAN; ENGLISH summary
(DE88-706258; JINR-R-11-88-86) Avail: NTIS (US Sales Only)
HC A03/MF A01

The algorithm to investigate the symmetry properties of differential equation by the external form method and the corresponding code are presented. The code realizes the algebra of differential forms and it is simple in use due to simplification of data input-output concerning the differential equation under investigation. As input the differential operator or the external form representation of initial equation may be used. The code is used to construct the system of determining equations which then is presented in a passive form. The symmetry group algebra for a given equation must be found by a user. The code usage is illustrated for a large amount of nonlinear equations such as Dirac equation, shallow water model equation, Prandtl equation and so on. DOE

N89-25651*# National Aeronautics and Space Administration. Ames Research Center, Moffett Field, CA.
A NUMERICAL STUDY OF A CLASS OF TVD SCHEMES FOR COMPRESSIBLE MIXING LAYERS
N. D. Sandham (Stanford Univ., CA.) and H. C. Yee May 1989 21 p
(NASA-TM-102194; A-89139; NAS 1.15:102194) Avail: NTIS
HC A03/MF A01 CSCL 20D

At high Mach numbers the two-dimensional time-developing mixing layer develops shock waves, positioned around large-scale vortical structures. A suitable numerical method has to be able to capture the inherent instability of the flow, leading to the roll-up of vortices, and also must be able to capture shock waves when they develop. Standard schemes for low speed turbulent flows, for example spectral methods, rely on resolution of all flow-features and cannot handle shock waves, which become too thin at any realistic Reynolds number. The performance of a class of second-order explicit total variation diminishing (TVD) schemes on a compressible mixing layer problem was studied. The basic idea is to capture the physics of the flow correctly, by resolving down to the smallest turbulent length scales, without resorting to turbulence or sub-grid scale modeling, and at the same time capture shock waves without spurious oscillations. The present study indicates that TVD schemes can capture the shocks accurately when they form, but (without resorting to a finer grid) have poor accuracy in computing the vortex growth. The solution accuracy

depends on the choice of limiter. However a larger number of grid points are in general required to resolve the correct vortex growth. The low accuracy in computing time-dependent problems containing shock waves as well as vortical structures is partly due to the inherent shock-capturing property of all TVD schemes. In order to capture shock waves without spurious oscillations these schemes reduce to first-order near extrema and indirectly produce clipping phenomena, leading to inaccuracy in the computation of vortex growth. Accurate simulation of unsteady turbulent fluid flows with shock waves will require further development of efficient, uniformly higher than second-order accurate, shock-capturing methods. Author

N89-25652*# National Aeronautics and Space Administration. Ames Research Center, Moffett Field, CA.

A CLASS OF HIGH RESOLUTION EXPLICIT AND IMPLICIT SHOCK-CAPTURING METHODS

H. C. Yee Feb. 1989 222 p

(NASA-TM-101088; A-89091; NAS 1.15:101088) Avail: NTIS HC A10/MF A01 CSCL 12A

An attempt is made to give a unified and generalized formulation of a class of high resolution, explicit and implicit shock capturing methods, and to illustrate their versatility in various steady and unsteady complex shock wave computations. Included is a systematic review of the basic design principle of the various related numerical methods. Special emphasis is on the construction of the basis nonlinear, spatially second and third order schemes for nonlinear scalar hyperbolic conservation laws and the methods of extending these nonlinear scalar schemes to nonlinear systems via the approximate Riemann solvers and the flux vector splitting approaches. Generalization of these methods to efficiently include equilibrium real gases and large systems of nonequilibrium flows are discussed. Some issues concerning the applicability of these methods that were designed for homogeneous hyperbolic conservation laws to problems containing stiff source terms and shock waves are also included. The performance of some of these schemes is illustrated by numerical examples for 1-, 2- and 3-dimensional gas dynamics problems. Author

N89-25653*# Research Inst. for Advanced Computer Science, Moffett Field, CA.

FAST POLAR DECOMPOSITION OF AN ARBITRARY MATRIX

Nicholas J. Higham (Cornell Univ., Ithaca, NY.) and Robert S. Schreiber Oct. 1988 15 p

(Contracts NCC2-387; N00014-86-K-0610)

(NASA-CR-185412; NAS 1.26:185412; RIACS-TR-88.29) Avail: NTIS HC A03/MF A01 CSCL 12A

The polar decomposition of an m x n matrix A of full rank, where m is greater than or equal to n, can be computed using a quadratically convergent algorithm. The algorithm is based on a Newton iteration involving a matrix inverse. With the use of a preliminary complete orthogonal decomposition the algorithm can be extended to arbitrary A. How to use the algorithm to compute the positive semi-definite square root of a Hermitian positive semi-definite matrix is described. A hybrid algorithm which adaptively switches from the matrix inversion based iteration to a matrix multiplication based iteration due to Kovarik, and to Bjorck and Bowie is formulated. The decision when to switch is made using a condition estimator. This matrix multiplication rich algorithm is shown to be more efficient on machines for which matrix multiplication can be executed 1.5 times faster than matrix inversion. Author

N89-25654*# Research Inst. for Advanced Computer Science, Moffett Field, CA.

ON CONJUGATE GRADIENT TYPE METHODS AND POLYNOMIAL PRECONDITIONERS FOR A CLASS OF COMPLEX NON-HERMITIAN MATRICES

Roland Freund (Wuerzburg Univ., Germany, F.R.) Dec. 1988 35 p

(Contract NCC2-387; NSF DCR-84-12314)

(NASA-CR-185424; NAS 1.26:185424; RIACS-TR-88.44) Avail: NTIS HC A03/MF A01 CSCL 12A

Conjugate gradient type methods are considered for the solution of large linear systems Ax = b with complex coefficient matrices of the type A = T + i(sigma)I where T is Hermitian and sigma, a real scalar. Three different conjugate gradient type approaches with iterates defined by a minimal residual property, a Galerkin type condition, and an Euclidian error minimization, respectively, are investigated. In particular, numerically stable implementations based on the ideas behind Paige and Saunder's SYMMLQ and MINRES for real symmetric matrices are proposed. Error bounds for all three methods are derived. It is shown how the special shift structure of A can be preserved by using polynomial preconditioning. Results on the optimal choice of the polynomial preconditioner are given. Also, some numerical experiments for matrices arising from finite difference approximations to the complex Helmholtz equation are reported. Author

N89-25655# Fermi National Accelerator Lab., Batavia, IL.

DIFFERENTIAL ALGEBRAS WITHOUT DIFFERENTIALS: AN EASY C++ IMPLEMENTATION

Leo Michelotti Mar. 1989 4 p Presented at the 13th Particle Accelerator Conference, Chicago, IL, 20 Mar. 1989

(Contract DE-AC02-76CH-03000)

(DE89-011503; FNAL/C-89/95; CONF-890335-87) Avail: NTIS HC A02

Automated differentiation can be motivated and explained rather plainly without any reference to infinitesimals or differentials whatsoever. We shall describe one possible approach in this paper. The method which we shall use will suggest its own implementation. However, FORTRAN is not the most natural language in which to carry it out. In the second section we shall describe an almost trivial implementation using C++. (Indeed, one of the motivations for writing this paper is to persuade militant FORTRAN extremists to invest the four or five days necessary to learn this powerful and easy language.) Take heed, however, that what we describe below is only a stripped-down implementation, written in three days, of differential algebra's most essential features; it is not as robust as and does not contain the battery of tools available in Berz's DA package, the product of a significant amount of work. DOE

N89-25656# Nationaal Inst. voor Kernfysica en Hoge Energiefysica, Amsterdam (Netherlands).

NON-PERTURBATIVE EFFECTS IN THE EXACT S-MATRICES OF THE O(N) GROSS-NEVEU AND SUPERSYMMETRIC SIGMA MODELS

J. A. Gracey Sep. 1988 9 p Sponsored in part by the Royal Society, England

(NIKHEF-H/88-10; ETN-89-94253) Avail: NTIS HC A02/MF A01

The factorization of nonperturbative effects in the S-matrices of the O(N) Gross-Neveu and O(N) supersymmetric sigma models are examined. It is shown that in both cases, the S-matrices can be written in terms of a function of the nonperturbative mass and a convergent power series in an effective coupling constant, at each order in 1/N. ESA

N89-25657# Technische Univ., Eindhoven (Netherlands).

LEAST SQUARES PARAMETER ESTIMATION IN A DYNAMIC MODEL FROM NOISY OBSERVATIONS Ph.D. Thesis

Johannes Martinus tenVregelaar 1988 169 p

(ETN-89-94295) Avail: NTIS HC A08/MF A01

Parameter estimation in a linear, time invariant and causal discrete time system defined by an autoregressive moving average description of its inputs and outputs is considered. An algorithm for computing least squares estimates is given. Assuming a random noise process, the asymptotic analysis of the method is treated. The strong consistency is proved. A key role is played by the concept of almost surely uniform convergence of random functions. The asymptotic normality property is considered, especially the limit distribution of certain quadratic forms in random variables. Two generalizations of the original problem are discussed: (equality) constraints on the parameters and partial input noise. For special cases, it is often possible to reduce or to check the assumptions

which are made. This is investigated the non-dynamic model and the case of normally distributed errors, respectively. A simulation study is included. ESA

N89-25658# Loughborough Univ. of Technology (England). Dept. of Mathematics.
THE tanh TRANSFORMATION FOR DOUBLE INTEGRALS WITH SINGULARITIES: A PROGRESSIVE RULE
V. U. Aihie and G. A. Evans Sep. 1987 11 p
(Maths-Res-203; ETN-89-94322) Avail: NTIS HC A03/MF A01

Two transformation methods are extended to the numerical evaluation of two dimensional singular quadratures. These are both based on the tanh transformation and the resulting high order behavior of the trapezoidal rule. Tests are carried out on examples for which analytic results are also known. In general the rules perform very well. However it is less easy to achieve a required accuracy by successive doubling of points as in one-dimension as the number of points used grows impractically after one doubling. In the tanh product rule the underlying grid is fixed in the initial choice of h and a doubling in each dimension yields the results quoted. The tanh product rule is most efficient with the values of n = 3 and 5. The doubling problem is less marked with the Clenshaw-Curtis and trapezoidal rule combination as each integral along a circle is accurately evaluated, and no more extra points are then needed if sub-division in the trapezoidal rule takes place. As in one-dimension, increasing n to 7 or above makes the integrand very steep sided and accuracy falls off. ESA

N89-25659# Loughborough Univ. of Technology (England). Dept. of Mathematical Sciences.
A COMPARISON OF THE ERROR FUNCTION AND THE tanh TRANSFORMATION AS PROGRESSIVE RULES FOR DOUBLE AND TRIPLE SINGULAR INTEGRALS
V. U. Aihie and G. A. Evans Oct. 1988 15 p
(Maths-Res-210; ETN-89-94323) Avail: NTIS HC A03/MF A01

Seven test integrals were evaluated with the error function transformation and the results were compared with the original tanh form. Examples which involve variable limits and hence curves of singularities were evaluated. Three-dimensional singular intervals were evaluated. The tests suggest that the slight gain in using an error function transformation with say n = 3 is only significantly advantageous if the integrands were themselves expensive to evaluate, when any saving becomes worthwhile. The relevant simplicity of tanh in a product rule is attractive when complications such as variable limits and higher dimensions are tackled. For general use it is unreasonable to expect a user to contend with nonstandard functions when the gain is not considerable. This could be overcome by publishing a minimum rational approximation to the required functions over the relevant range. The capability of the methods on the integrals with their singularities on internal curves shows efficiency and the experience gained in running the algorithm suggests a high level of robustness. On the three-dimensional cases it is of note that I14 is particularly hard with singular derivatives from the sin sup 1/2 (xyz) term compounded with a power of 3/4 in the denominator. ESA

N89-25660# European Space Agency, Paris (France).
RESOLUTION OF THE ALGEBRAIC RICCATI EQUATION VIA NEWTON'S METHOD AND THE LYAPUNOV EQUATION
J. Borde (European Space Agency. European Space Research and Technology Center, ESTEC, Noordwijk, Netherlands) and W. R. Burke, ed. Sep. 1988 45 p
(ESA-STM-241; ISSN-0379-4075; ETN-89-94473) Copyright
Avail: NTIS HC A03/MF A01

Newton's method is used to find the unique symmetric positive definite and negative solution matrices X+ and X- of the Algebraic Riccati Equation A sup t X + XA - XBX + C = 0 where B = sup t is greater than or = 0 and C = C sup t is greater than or = 0. At each iteration, the algorithm solves a Lyapunov equation by Schur's method. The set Lambda of all the symmetric solutions is shown to be a compact set and any element of Lambda is expressed as a combination of X+ and X-. It is shown that the set A is finite if and only if matrix A+ = A - BX+ is nonderogatory. In this case, a simple method to compute all the symmetric solutions is developed. Different programs are tested, and examples and comparison with other methods are given. ESA

N89-25661 Politecnico di Milano (Italy). Lab. di Calcolatori.
A NET-BASED MODEL FOR TIME-DEPENDENT SYSTEMS
S. Morasca and M. Pezze 1989 31 p
(Rept-89-005; ETN-89-94685) Avail: Politecnico di Milano, Piazza Leonardo da Vinci 32, 20133 Milan, Italy

A high level Petri net based model for dealing with time dependent systems, real time and stochastic time systems is defined. The basic model is called Environment Relation nets (ER) in which the information bearing environment entities are used as tokens. The most significant time oriented extensions of Petri nets, both stochastic and nonstochastic, proposed in the literature are shown to be particular cases of ER nets, thus assessing the generality of this model. ESA

N89-25662# Rome Univ. (Italy). Dipartimento di Fisica.
NOTE ON THE MAJORANA REPRESENTATIONS OF THE LORENTZ GROUP
A. M. Perelomov 4 May 1988 4 p
(Preprint-597; ETN-89-94686) Avail: NTIS HC A02/MF A01

A simple expression is given for the matrix elements of the Majorana representations of the Lorentz group. ESA

N89-25663*# Fermi National Accelerator Lab., Batavia, IL. Astrophysics Center.
A NEW WAY TO INTERPRET THE DIRAC EQUATION IN A NON-RIEMANNIAN MANIFOLD
Sirley Marques-Bonham Jun. 1989 5 p Prepared in cooperation with Centro Brasileiro de Pesquisas Fisicas, Rio de Janeiro Sponsored in part by FAPERJ and DOE
(Grant NAGw-1340)
(NASA-CR-185464; NAS 1.26:185464; FERMILAB-Pub-89/147-A)
Avail: NTIS HC A02/MF A01 CSCL 12A

The idea of internal mass terms introduced in ref. (1), is shown not to be an appropriate hypothesis when it is placed in connection with the components of the generalized (matrix) vierbeins being proportional to the Riemannian (gravitational) vierbeins. It would result in an undesirable canceling of the Electromagnetic and the Yang-Mills components in the generalized metric. Another hypothesis is introduced where the wave function psi is Taylor expanded in a small parameter p. Author

N89-25213*# Bridgeport Univ., CT. Dept. of Mechanical Engineering.
AN INTERPRETATION AND SOLUTION OF ILL-CONDITIONED LINEAR EQUATIONS
I. U. Ojalvo and T. Ting *In* NASA. Langley Research Center, Recent Advances in Multidisciplinary Analysis and Optimization, Part 3 Apr. 1989 p 1239-1252 (For primary document see N89-25201 19-05)
Avail: NTIS HC A22/MF A01 CSCL 12A

N89-25214*# Michigan Univ., Ann Arbor. Dept. of Mechanical Engineering and Applied Mechanics.
GENERALIZED MATHEMATICAL MODELS IN DESIGN OPTIMIZATION
Panos Y. Papalambros and J. R. Jagannatha Rao *In* NASA. Langley Research Center, Recent Advances in Multidisciplinary Analysis and Optimization, Part 3 Apr. 1989 p 1253-1264 Sponsored in part by General Motors Corp. (For primary document see N89-25201 19-05)
(Grant NSF DMC-85-14721)
Avail: NTIS HC A22/MF A01 CSCL 12A

N89-25216*# Michigan State Univ., East Lansing. Dept. of Mechanical Engineering.
FUZZY SET APPLICATIONS IN ENGINEERING OPTIMIZATION: MULTILEVEL FUZZY OPTIMIZATION
Alejandro R. Diaz *In* NASA. Langley Research Center, Recent Advances in Multidisciplinary Analysis and Optimization, Part 3 Apr. 1989 p 1279-1289 (For primary document see N89-25201

19-05)
(Grant NSF DME-87-06902)
Avail: NTIS HC A22/MF A01 CSCL 12A

N89-25217*# Virginia Polytechnic Inst. and State Univ., Blacksburg. Dept. of Engineering Science and Mechanics.
A PENALTY APPROACH FOR NONLINEAR OPTIMIZATION WITH DISCRETE DESIGN VARIABLES
Dong K. Shin, Zafer Gurdal, and O. H. Griffin, Jr. *In* NASA. Langley Research Center, Recent Advances in Multidisciplinary Analysis and Optimization, Part 3 Apr. 1989 p 1291-1302
(For primary document see N89-25201 19-05)
Avail: NTIS HC A22/MF A01 CSCL 12A

65 STATISTICS AND PROBABILITY

Includes data sampling and smoothing; Monte Carlo method; and stochastic processes.

N89-25664# Loughborough Univ. of Technology (England). Dept. of Mathematics.
DISCRIMINATION AND CLASSIFICATION WITH MIXED BINARY AND CONTINUOUS VARIABLES: THE BAYESIAN APPROACH
Ioannis G. Vlachonikolis Nov. 1988 18 p
(Maths-Res-212; ETN-89-94325) Avail: NTIS HC A03/MF A01

The predictive allocation rule for classification of observations involving mixtures of binary and continuous variables is derived. The approach is based on the usual frequency distributions of the location model and vague prior distributions for the unknown parameters. The same approach is used to derive predictive rules when low-order linear models are imposed on the population parameters. Monte Carlo results on the performances of the predictive rule and its estimative competitor are presented. ESA

66 SYSTEMS ANALYSIS

Includes mathematical modeling; network analysis; and operations research.

No abstracts in this category.

67 THEORETICAL MATHEMATICS

Includes topology and number theory.

N89-25665*# Institute for Computer Applications in Science and Engineering, Hampton, VA.
ANALYTIC THEORY FOR THE DETERMINATION OF VELOCITY AND STABILITY OF BUBBLES IN A HELE-SHAW CELL. PART 1: VELOCITY SELECTION Final Report
Saleh Tanveer (Virginia Polytechnic Inst. and State Univ., Blacksburg.) Apr. 1989 58 p Sponsored by Institute for Computer Applications in Science and Engineering, Hampton, VA
(Contract NAS1-18605)
(NASA-CR-181836; NAS 1.26:181836; ICASE-89-28-Pt-1) Avail: NTIS HC A04/MF A01 CSCL 12A

An asymptotic theory is presented for the determination of velocity and linear stability of a steady symmetric bubble in a Hele-Shaw cell for small surface tension. In the first part, the bubble velocity U relative to the fluid velocity at infinity is determined for small surface tension T by determining transcendentally small correction to the asymptotic series solution. It is found that for any relative bubble velocity U in the interval (U(c),2), solutions exist at a countably infinite set of values of T (which has zero as its limit point) corresponding to the different branches of bubble solutions. U(c) decreases monotonically from 2 to 1 as the bubble area increases from 0 to infinity. However, for a bubble of arbitrarily given size, as T approaches 0, solution exists on any given branch with relative bubble velocity U satisfying the relation $2-U = cT$ to the 2/3 power, where c depends on the branch but is independent of the bubble area. The analytical evidence further suggests that there are no solutions for U greater than 2. These results are in agreement with earlier analytical results for a finger. In Part 2, an analytic theory is presented for the determination of the linear stability of the bubble in the limit of zero surface tension. Only the solution branch corresponding to the largest possible U for given surface tension is found to be stable, while all the others are unstable, in accordance with earlier numerical results.
Author

N89-25666# Central Inst. of Physics, Bucharest (Romania). Inst. of Physics and Nuclear Engineering.
LOCALIZABILITY AND COVARIANCE IN ANALYTICAL MECHANICS
D. R. Grigore Oct. 1987 22 p
(DE88-706038; IFIN-FT-320-1987) Avail: NTIS (US Sales Only) HC A03/MF A01

Two familiar concepts in quantum mechanics, namely localizability and covariance, are investigated in the framework of classical mechanics. The analysis of well known problems in quantum mechanics as a localizability of elementary relativistic particles gives the same results in classical mechanics as well.
DOE

N89-25667# Fermi National Accelerator Lab., Batavia, IL.
PHASE SPACE CONCEPTS
Leo Michelotti Jan. 1989 58 p Presented at the US Particle Accelerator Summer School, Batavia, IL, 3-14 Aug. 1987
(Contract DE-AC02-76CH-03000)
(DE89-011082; FNAL/C-89/24; CONF-8708323-2) Avail: NTIS HC A04

In these lectures we shall look into this geometric approach to the study of Hamiltonian dynamical systems, especially in connection with the kinds of problems which arise in accelerator orbit theory. Our own relatively modest goals will be to delineate the idea of invariant tori in phase space, to define and illustrate the importance of resonant orbits and their separatrices as structures for organizing dynamics, and to touch upon the meaning of chaotic orbits in nonintegrable systems. DOE

70 PHYSICS (GENERAL)

For precision time and time interval (PTTI) see *35 Instrumentation and Photography;* for geophysics, astrophysics or solar physics see *46 Geophysics, 90 Astrophysics,* or *92 Solar Physics.*

N89-25668# International Atomic Energy Agency, Vienna (Austria).
INTERNATIONAL CENTRE FOR THEORETICAL PHYSICS: SCIENTIFIC ACTIVITIES IN 1987
Dec. 1988 99 p
(DE88-705973; IAEA-TECDOC-488; ISSN-1011-4289) Avail: NTIS (US Sales Only) HC A05/MF A01

A review of the scientific activities of the ICTP Trieste in 1987, including workshops, research and training for research is presented. The scientific program consists of eight main fields: fundamental physics, condensed matter, atomic and molecular physics, mathematics, physics and energy, physics and environment, applied physics and high technology, physics and development. In addition to a brief description of each workshop, symposium, college, meeting and activity or project sponsored by ICTP, a list of preprints and internal reports issued in 1987 is included. DOE

N89-25669# Oklahoma Univ., Norman. School of Industrial Engineering.
CORRELATION OF SUBJECTIVE SLIPPERINESS JUDGEMENTS WITH QUANTITATIVE COF (COEFFICIENT OF FRICTION) MEASUREMENTS FOR STRUCTURAL STEEL Final Report
Jerry L. Purswell and Robert E. Schlegel 30 Jun. 1988 206 p Revised
(Contract PHS-CDC-200-86-2929)
(PB89-165070) Avail: NTIS HC A10/MF A01 CSCL 20C

When there is no simple or accurate procedure for measuring the coefficient of friction (COF) at a job site, workers and/or supervisors involved must make subjective judgments about the slipperiness of the walking and climbing surfaces and in turn decide whether the surface presents a safe or an unsafe condition for work. This project was designed to determine whether these subjective judgment calls did in fact agree with the COF measurements obtained using a mechanical device. It was noted that the coatings chosen for study were subject to a polishing factor by the boot soles during the trials, causing the COF values to become lower as the trials continued. Poor correlation was obtained between subjective ratings of slipperiness and the COF values measured before the trials began. A relatively high correlation was obtained between subjective ratings and the COF values measured after the trials had been completed. A difference was noted in the subjective ratings for the effects of water on a coating for column climbing, but not for walking a beam, suggesting the effects of water on a coating are related to the type of task being performed in steel erection. An increase in the measured COF was noted for all of the coatings when they were wet as compared to the dry condition. The importance of clean shoe soles was clearly demonstrated. Author

N89-25670*# National Aeronautics and Space Administration. Lewis Research Center, Cleveland, OH.
ACOUSTIC PROPAGATION IN CURVED DUCTS WITH EXTENDED REACTING WALL TREATMENT
Kenneth J. Baumeister 1989 21 p Prepared for presentation at the Winter Annual Meeting of the American Society of Mechanical Engineers, San Francisco, CA, 10-15 Dec. 1989
(NASA-TM-102110; E-4880; NAS 1.15:102110) Avail: NTIS HC A03/MF A01 CSCL 20C

A finite-element Galerkin formulation was employed to study the attenuation of acoustic waves propagating in two-dimensional S-curved ducts with absorbing walls without a mean flow. The reflection and transmission at the entrance and the exit of a curved duct were determined by coupling the finite-element solutions in the curved duct to the eigenfunctions of an infinite, uniform, hard wall duct. In the frequency range where the duct height and acoustic wave length are nearly equal, the effects of duct length, curvature (duct offset) and absorber thickness were examined. For a given offset in the curved duct, the length of the S-duct was found to significantly affect both the absorptive and reflective characteristics of the duct. A means of reducing the number of elements in the absorber region was also presented. In addition, for a curved duct, power attenuation contours were examined to determine conditions for maximum acoustic power absorption. Again, wall curvature was found to significantly effect the optimization process. Author

N89-25671*# Institute for Computer Applications in Science and Engineering, Hampton, VA.
ANALYTIC THEORY FOR THE SELECTION OF 2-D NEEDLE CRYSTAL AT ARBITRARY PECLET NUMBER Final Report
Saleh Tanveer May 1989 31 p Prepared in cooperation with NASA- Langley Resear ch Center, Hampton, VA Submitted for publication
(Contract NAS1-18605)
(NASA-CR-181846; ICASE-89-31; NAS 1.26:181846) Avail: NTIS HC A03/MF A01 CSCL 20C

An accurate analytic theory is presented for the velocity selection of a two-dimensional needle crystal for arbitrary Peclet number for small values of the surface tension parameter. The velocity selection is caused by the effect of transcendentally small terms which are determined by analytic continuation to the complex plane and analysis of nonlinear equations. The work supports the general conclusion of previous small Peclet number analytical results of other investigators, though there are some discrepancies in details. It also addresses questions raised on the validity of selection theory owing to assumptions made on shape corrections at large distances from the tip. Author

N89-25672# Technische Univ., Eindhoven (Netherlands). Electrical Energy Systems Group.
THE INFLUENCE OF CONTACT SURFACE MICROSTRUCTURE ON VACUUM ARC STABILITY AND ARC VOLTAGE
Yanhong Fu (Xian Jiaotong Univ., China) Dec. 1987 33 p
(EUT-87-E-186; ISBN-9-06-144186-2; ISSN-0167-9708; ETN-89-94774) Avail: NTIS HC A03/MF A01

The results of dc vacuum arc lifetime and arc voltage measurements for contacts with a different surface microstructure, which was realized by treating the contact surface with different roughness emery paper are shown. Large influence of the contact surface microstructure on dc arc lifetime (several tens of times difference at most), arc voltage (30 percent difference at most) and arc erosion behavior is found. The mechanism of the surface microstructure influence on dc arc stability was analyzed and explained. ESA

71 ACOUSTICS

Includes sound generation, transmission and attenuation. For noise pollution see *45 Environmental Pollution.*

N89-25673*# National Aeronautics and Space Administration. Langley Research Center, Hampton, VA.
AIRFOIL SELF-NOISE AND PREDICTION
Thomas F. Brooks, D. Stuart Pope (PRC Kentron, Inc., Hampton, VA.), and Michael A. Marcolini Jul. 1989 145 p
(NASA-RP-1218; L-16528; NAS 1.61:1218) Avail: NTIS HC A07/MF A01 CSCL 20A

A prediction method is developed for the self-generated noise of an airfoil blade encountering smooth flow. The prediction methods for the individual self-noise mechanisms are semiempirical and are based on previous theoretical studies and data obtained from tests of two- and three-dimensional airfoil blade sections. The self-noise mechanisms are due to specific boundary-layer phenomena, that is, the boundary-layer turbulence passing the trailing edge, separated-boundary-layer and stalled flow over an airfoil, vortex shedding due to laminar boundary layer instabilities, vortex shedding from blunt trailing edges, and the turbulent vortex flow existing near the tip of lifting blades. The predictions are compared successfully with published data from three self-noise studies of different airfoil shapes. An application of the prediction method is reported for a large scale-model helicopter rotor, and the predictions compared well with experimental broadband noise measurements. A computer code of the method is given. Author

N89-25674*# Bolt, Beranek, and Newman, Inc., Cambridge, MA.
POTENTIAL USES OF VACUUM BUBBLES IN NOISE AND VIBRATION CONTROL Final Report
Istvan L. Ver Jun. 1989 53 p
(Contract NAS1-16521)
(NASA-CR-181829; NAS 1.26:181829; BBN-6938) Avail: NTIS HC A04/MF A01 CSCL 20A

Vacuum bubbles are new acoustic elements which are dynamically more compliant than the gas volume they replace, but which are statically robust. They are made of a thin metallic shell with vacuum in their cavity. Consequently, they pose no danger in terms of contamination or fire hazard. The potential of the vacuum bubble concept for noise and vibration control was assessed with special emphases on spacecraft and aircraft applications. The following potential uses were identified: (1) as a cladding, to reduce sound radiation of vibrating surfaces and the

sound excitation of structures, (2) as a screen, to reflect or absorb an incident sound wave, and (3) as a liner, to increase low frequency sound transmission loss of double walls and to increase the low frequency sound attenuation of muffler baffles. It was found that geometric and material parameters must be controlled to a very high accuracy to obtain optimal performance and that performance is highly sensitive to variations in static pressure. Consequently, it was concluded that vacuum bubbles have more potential in spacecraft applications where static pressure is controlled more than in aircraft applications where large fluctuations in static pressure are common. Author

N89-25675*# National Aeronautics and Space Administration. Lewis Research Center, Cleveland, OH.
IN-FLIGHT MEASUREMENT OF PROPELLER NOISE ON THE FUSELAGE OF AN AIRPLANE
Frederic G. Pla (Sverdrup Technology, Inc., Cleveland, OH.), Richard Ranaudo, and Richard P. Woodward Jul. 1989 58 p (Contract NAS3-24105)
(NASA-TM-102285; E-4952; NAS 1.15:102285) Avail: NTIS HC A04/MF A01 CSCL 20A

In-flight measurements of propeller noise on the fuselage of an OV-10A aircraft were obtained using a horizontal and a vertical microphone array. A wide range of flight conditions were tested including changes in angle of attack, sideslip angle, power coefficient, helical tip Mach number and advance ratio, and propeller direction of rotation. Results show a dependence of the level and directivity of the tones on the angle of attack and on the sideslip angle with the propeller direction of rotation, which is similar to results obtained in wind tunnel tests with advanced propeller designs. The level of the tones at each microphone increases with increasing angle of attack for inboard-down propeller rotation and decreases for inboard-up rotation. The level also increases with increasing slideslip angle for both propeller directions of rotation. Increasing the power coefficient results in a slight increase in the level of the tones. A strong shock wave is generated by the propeller blades even at relatively low helical tip Mach numbers resulting in high harmonic levels. As the helical tip Mach number and the advance ratio are increased, the level of the higher harmonics increases much faster than the level of the blade passage frequency. Author

N89-25676# Technische Univ., Berlin (Germany, F.R.). Fachgebeit Flugfuehrung und Luftverkehr.
REDUCTION OF AIRCRAFT NOISE IN CIVIL AIR TRANSPORT BY OPTIMIZATION OF FLIGHT TRACKS AND TAKEOFF AND APPROACH PROCEDURES Final Report, 31 Mar. 1988
Uwe Rottmann Aug. 1988 229 p In GERMAN; ENGLISH summary
(Contract BMUNR-FB-88-105-05-501)
(ILR-Mitt-200; ETN-89-94560) Avail: NTIS HC A11/MF A01

Noise optimized design of operational flight procedures for effective noise pollution reduction is analyzed. Power cutback during certain stages of approach and takeoff, extension of distance between sound source and sound receiver, as well as diminution of sound impact time are optimized for specific flight procedures and routings. Five takeoff and three landing procedures are analyzed in acoustic effects. Sound immission is computed by NOISIMSIS (NOISe IMpact SImulation System), a simulation system especially created for this task, under consideration of aircraft type specified sound emission characteristics and performance data as well as different meteorological conditions. The investigations for the example of Frankfurt airport result in formulating a planning guideline with notes and impulses for activities in operational noise abatement. ESA

N89-25677# Deutsche Forschungs- und Versuchsanstalt fuer Luft- und Raumfahrt, Brunswick (Germany, F.R.). Abteilung Technische Akustik.
DATA OF AEROACOUSTIC MEASUREMENTS ON ULTRALIGHT AIRCRAFT PROPELLERS
Helmut Dahlen and Birgit Ketthaus Dec. 1988 122 p In GERMAN; ENGLISH summary Report will also be announced as translation (ESA-TT-1147)
(DFVLR-Mitt-88-33; ISSN-0176-7736; ESA-TT-1147; ETN-89-94646) Avail: NTIS HC A06/MF A01; DFVLR, VB-PL-DO, Postfach 90 60 58, 5000 Cologne, Federal Republic of Germany, 40.50 deutsche marks

Results of aeroacoustic wind tunnel measurements on 6 ultralight aircraft propellers (2-, 3-, 4-, and 6-blade) are presented. Thrust, torque, and sound-pressure measurements for helical Mach numbers 0.4 to 0.7 and propeller pitch angles 10 to 25 deg are included. ESA

N89-25140# Technische Hochschule, Aachen (Germany, F.R.).
STRUCTURAL LOADING AND NOISE DISTURBANCE OF HELICOPTERS [STRUKTURBEANSPRUCHUNG UND LAERMBELAESTIGUNG BEIN HUBSCHRAUBER]
R. Mueller *In its* Vortex Flows in Flying Technique 1988 p 313-337 In GERMAN (For primary document see N89-25126 19-02)
Avail: NTIS HC A17/MF A01

N89-25898# Cambridge Univ. (England). Dept. of Applied Mathematics and Theoretical Physics.
SCATTERING AND MULTIPLE SCATTERING OF ACOUSTIC WAVES IN A STRATIFIED MEDIUM
C. S. Rosenthal and Douglas O. Gough *In* ESA, Seismology of the Sun and Sun-Like Stars Dec. 1988 p 457-461 (For primary document see N89-25819 19-92)
Copyright Avail: NTIS HC A99/MF E03

N89-25900# Tokyo Univ. (Japan). Dept. of Astronomy.
SOUND VELOCITY DISTRIBUTION IN THE SUN INFERRED FROM ASYMPTOTIC INVERSION OF p-MODE SPECTRA
H. Shibahashi and T. Sekii *In* ESA, Seismology of the Sun and Sun-Like Stars Dec. 1988 p 471-474 (For primary document see N89-25819 19-92)
Copyright Avail: NTIS HC A99/MF E03

N89-25901# Academy of Sciences (USSR), Moscow. Inst. of Physics of the Earth.
HELIOSEISMOLOGICAL INVERSE PROBLEM: SOUND SPEED IN THE SOLAR INTERIOR
S. V. Vorontsov *In* ESA, Seismology of the Sun and Sun-Like Stars Dec. 1988 p 475-480 (For primary document see N89-25819 19-92)
Copyright Avail: NTIS HC A99/MF E03

N89-25904# Aarhus Tekniske Bibliotek (Denmark). Inst. of Astronomy.
DETERMINATION OF THE SOLAR INTERNAL SOUND SPEED BY MEANS OF A DIFFERENTIAL ASYMPTOTIC INVERSION
J. Christensen-Dalsgaard, Douglas O. Gough, and M. J. Thompson (National Center for Atmospheric Research, Boulder, CO.) *In* ESA, Seismology of the Sun and Sun-Like Stars Dec. 1988 p 493-497 Sponsored by NSF, Washington, DC (For primary document see N89-25819 19-92)
Copyright Avail: NTIS HC A99/MF E03

N89-25913# Cambridge Univ. (England). Inst. of Astronomy.
DETERMINATION OF THE SOLAR SOUND SPEED BY AN ASYMPTOTIC INVERSION TECHNIQUE
A. G. Kosovichev (Crimean Astrophysical Observatory, USSR) *In* ESA, Seismology of the Sun and Sun-Like Stars Dec. 1988 p 533-537 (For primary document see N89-25819 19-92)
Copyright Avail: NTIS HC A99/MF E03

N89-25914# Cambridge Univ. (England). Inst. of Astronomy.
THE EFFECT OF A NONSPHERICAL SOUND SPEED ON THE ACOUSTIC FREQUENCY SPECTRUM OF THE SUN
A. G. Kosovichev and J. Perdang (Institut d'Astrophysique, Cointe-Ougree, Belgium) *In* ESA, Seismology of the Sun and Sun-Like Stars Dec. 1988 p 539-543 (For primary document see N89-25819 19-92)
Copyright Avail: NTIS HC A99/MF E03

72 ATOMIC AND MOLECULAR PHYSICS

Includes atomic structure, electron properties, and molecular spectra.

N89-25678*# Fermi National Accelerator Lab., Batavia, IL.
SOLITOSYNTHESIS: COSMOLOGICAL EVOLUTION OF NON-TOPOLOGICAL SOLITONS
Kim Griest and Edward W. Kolb Mar. 1989 32 p Prepared in cooperation with Chicago Univ., IL
(Grant NAGw-1340)
(NASA-CR-185030; NAS 1.26:185030; FERMILAB-Pub-89/83-A) Avail: NTIS HC A03/MF A01 CSCL 20H

The thermal creation, fusion, evaporation, and destruction of non-topological solitons (NTS) after a phase transition in the early universe is considered. By defining and following NTS statistical equilibrium and departures from it, and depending on particle physics parameters, one of three possible scenarios occurs. If reaction rates are high enough, a period of equilibrium occurs and relic abundances are determined by the freeze-out temperature. Equilibrium first drives most NTS's into their constituents (free phi particles) and then causes rapid fusion into large NTS's. If freeze-out occurs during the first phase, the NTS's are almost entirely destroyed, while if it occurs during the second phase, solitosynthesis occurs and NTS's may be cosmically relevant. For slow reaction rates the NTS's are born frozen out and have the abundance determined by the phase transition. Analytic approximations for determining the abundances are developed, and tested by numerically integrating a reaction network in an expanding universe. Unfortunately, for most of the parameter space considered, solito-destruction/evaporation occurs. Author

N89-25679# California Univ., Berkeley. Lawrence Berkeley Lab. National Center for Electron Microscopy.
ATOMIC RESOLUTION MICROSCOPY
R. Gronsky Jan. 1989 35 p Presented at the Images of Materials Symposium, Chicago, IL, 26 Sep. 1988
(Contract DE-AC03-76SF-00098)
(DE89-009227; LBL-25822; CONF-8809321-1) Avail: NTIS HC A03/MF A01

Compared to other atomic imaging methods such as field ion microscopy and scanning tunneling microscopy, the technique described here is a true microscopy because, in the traditional sense, it uses lenses. It therefore also uses the equations of optics, and it draws on a long and familiar history of image simulation and image interpretation. Nevertheless it is also a destructive technique, requiring that the sample be made thin enough to transmit electrons. It is a hardware-intensive technique, requiring that the transmission electron microscope used for atomic resolution imaging be of exceptional design and condition. And it is a precise technique, requiring that the operator tune in a specific focus setting to within a few nanometers at worst. Help is on the way however with the incessant development of new computer-based instrumentation, new and friendly algorithms for image simulation, and on-line, real-time computer processing. The outlook for future images of materials at atomic resolution is excellent. DOE

N89-25680*# Fermi National Accelerator Lab., Batavia, IL.
STATISTICAL FLUCTUATIONS AS THE ORIGIN OF NONTOPOLOGICAL SOLITONS
Kim Griest, Edward W. Kolb, and Alessandro Masarotti Apr. 1989 13 p Prepared in cooperation with Chicago Univ., IL
(Grant NAGw-1340)
(NASA-CR-185351; NAS 1.26:185351; FERMILAB-Pub-89/110-A) Avail: NTIS HC A03/MF A01 CSCL 20H

Nontopological solitons can be formed during a phase transition in the early universe as long as some net charge can be trapped in regions of false vacuum. It has been previously suggested that a particle-antiparticle asymmetry would provide a source for such trapped charge. It is pointed out that, for the model and parameters considered, statistical fluctuations provide a much larger concentration of charge, and are therefore, the dominant source of charge fluctuations in solitogenesis. Author

N89-25681# Joint Inst. for Nuclear Research, Dubna (USSR). Lab. of Nuclear Reactions.
BEAM TRANSPORT CALCULATION IN MAGNETIC FIELD WITH A QUADRUPOLE SYMMETRY BY THE METHOD OF IMMERSION IN MOMENT PHASE SPACE
Eh. L. Ivanov and Eh. A. Perelshtein 1988 10 p In RUSSIAN; ENGLISH summary
(DE88-706295; JINR-9-88-286) Avail: NTIS (US Sales Only) HC A02/MF A01

The motion of a particle with charge and momentum in magnetic field with quadrupole symmetry is studied. An analytical solution (in the form of blok-matrix) of the equations of motion, considering abberations of third order has been received by the method of immersion in moment phase space. The influence of nonlinearities of third order on particles motion has been treated, and the results are compared with the numerical integration of the equations of motion. DOE

N89-25682# California Univ., Berkeley. Dept. of Chemistry.
MONTE CARLO FOR THE ELECTRONIC STRUCTURE OF MOLECULES Ph.D. Thesis
Brian Lee Hammond Nov. 1988 172 p Prepared in cooperation with California Univ., Be rkeley. Lawrence Berkeley Lab.
(Contract DE-AC03-76SF-00098)
(DE89-011824; LBL-26536) Avail: NTIS HC A08/MF A01

New directions in the rapidly developing quantum Monte Carlo (QMC) electronic structure method are explored for the treatment of chemically interesting systems. Electronic correlation, a difficult problem in standard ab initio methods, is accounted for in a simple manner in QMC. Methods developed here are aimed at expanding the capabilities and applicability of QMC. Two general problems are addressed: extending QMC calculations to heavy-atom systems, and obtaining nuclear derivative and potential energy surface information. For heavy-atom systems, two methods have been developed. The first method uses ab initio effective core potentials to eliminate the core electrons. The second method retains all electron explicitly, but achieves a separation of time scales between core and valence to speed computation. These methods are applied to atomic and molecular systems containing Li, Na, Mg, C, Si, Ge, and Fe, and results are compared to other work available. Derivative and PES information is treated in three different ways: by the Hellmann-Feynman theorem, by analytic gradient techniques, and by correlated sampling of finite differences. Each of these approaches is implemented and applied to small diatomic systems. DOE

N89-25683# Max-Planck-Inst. fuer Kernphysik, Heidelberg (Germany, F.R.).
NUCLEAR BETA DECAY FAR FROM STABILITY AND ASTROPHYSICS
H. V. Klapdor (Osaka Univ., Japan) 1988 17 p Presented at the Internat. Symposium on Heavy Ion Physics and Nuclear Astrophysical Problems, Tokyo, Japan, 21-23 Jul. 1988 Sponsored in part by the Japan Society for the Promotion of Science, Tokyo, Japan
(MPI-H-1988-V-27; ETN-89-94399) Avail: NTIS HC A03/MF A01

The utilization of beta decay data of nuclei far from stability to study element synthesis in the Universe and determine the age of the Universe from cosmochronometers is discussed. The status of theoretical predictions of beta decay far from stability is reviewed and the impact on astrophysical questions is outlined. Results of microscopic calculations of beta decay half lives are presented. ESA

N89-25684 Ruhr Univ., Bochum (Germany, F.R.). Inst. fuer Experimentalphysik AG 2.
STATE-SELECTIVE SINGLE ELECTRON CAPTURE BY MULTIPLY CHARGED IONS: REACTION WINDOW AND MULTICHANNEL LANDAU ZENER CALCULATIONS
H. Lebius, H. R. Koslowski, and B. A. Huber Jul. 1989 20 p Sponsored by the Deutsch Forschungsgemeinschaft, Bonn, Fed. Republic of Germany

(Rept-88-05-175; ETN-89-94598) Copyright Avail: Fachinformationszentrum Karlsruhe, 7514 Eggenstein-Lecpoldshafen 2, Fed. Republic of Germany

Single electron capture by triply charged rare gas ions colliding with various rare gas atoms are studied by means of translational energy spectroscopy at low collision energies. The final state population is discussed. The analysis shows the limitations of model descriptions and yields information on the coupling strength in the case of inner shell capture or multi electron processes. ESA

73 NUCLEAR AND HIGH-ENERGY PHYSICS

Includes elementary and nuclear particles; and reactor theory.

For space radiation see *93 Space Radiation.*

N89-25685# Continuous Electron Beam Accelerator Facility, Newport New, VA.

MODULAR MAGNET CURRENT REGULATOR

Nick Dobeck, George Burtner, Omar Garza, and Robert LaMora 1989 6 p

(Contract DE-AC05-84ER-40150)

(CEBAF-PR-89-005) Avail: NTIS HC A02/MF A01

A modular current regulation system is being developed to power the low current correction and focusing magnets used for beam transport. The system consists of numerous multichannel assemblies, each housed in a standard relay rack. Each multi-channel assembly consists of common power supplies, computer automated measurement and control (CAMAC) modules, and Eurocard cages for the current regulators. These regulators are linear, bipolar modules capable of parallel connection for higher current output. Author

N89-25686# Department of Energy, Washington, DC.

REPORT OF THE HEPAP (HIGH ENERGY PHYSICS ADVISORY PANEL) SUBPANEL ON HIGH ENERGY PHYSICS AND THE SSC (SUPERCONDUCTING SUPER COLLIDER) OVER THE NEXT DECADE

Feb. 1989 78 p

(DE89-010071; DOE/ER-0408) Avail: NTIS HC A05/MF A01

This report highlights the future in high energy physics. Particular emphasis is on the Superconducting Super Collider contribution to high energy physics, education, and industry. DOE

N89-25687# Oak Ridge National Lab., TN.

REVIEW OF OXIDATION OF Nb-1Zr

J. R. DiStefano Apr. 1989 34 p

(Contract DE-AC05-84OR-21400)

(DE89-010299; ORNL/TM-10907) Avail: NTIS HC A03/MF A01

A major objective of the SP-100 Program Nuclear Assembly Test is to demonstrate the performance of a full-scale nuclear subsystem of a 100-kWe space nuclear power supply. The test will be run in a large vacuum chamber to protect the Nb-1Zr components from oxidation during operation. Much information about the oxidation of niobium and Nb-1Zr alloy already exists, and previous work in this area is reviewed. Oxidation of Nb-1Zr can proceed by solution, internal oxidation, and/or film formation. At temperatures up to about 650 K (377 C), oxidation generally follows a parabolic rate law because of the formation of protective oxide(s). At higher temperatures, oxidation becomes linear, but results are extremely sensitive to pressure and other system variables. Results obtained by several investigators could not be predicted using empirical equations developed by one investigator relating the increase in oxygen concentration to pressure, temperature, time, and specimen thickness. Additional data are required to provide more reliable guidelines for system operation that will protect against catastrophic effects. DOE

N89-25688*# Fermi National Accelerator Lab., Batavia, IL.

MODEL INDEPENDENCE OF CONSTRAINTS ON PARTICLE DARK MATTER

Kim Griest and Bernard Sadoulet (California Univ., Berkeley.) Mar. 1989 27 p Presented at the 2nd International School of Particle Astrophysics: Dark Matter in the Universe, Erice, Italy, 4 May 1988

(Contract NAGw-1340; DE-AC02-76CH-03000)

(NASA-CR-185337; NAS 1.26:185337; DE89-010507; FNAL/C-89/57-A; CONF-8805243-1) Avail: NTIS HC A03 CSCL 20H

The connection between the annihilation, elastic, and production cross sections is reviewed, showing how a general lower limit on the interaction rate in a detector is obtained from the requirement that a particle be the dark matter. High energy production experiments further constrain models, making very light dark matter particles unlikely. Special attention is paid to the uncertainties, loopholes and model dependencies that go into the arguments and several examples are given. DOE

74 OPTICS

Includes light phenomena; and optical devices.

For lasers see *36 Lasers and Masers.*

N89-25689* National Aeronautics and Space Administration. Marshall Space Flight Center, Huntsville, AL.

OPTICAL PRESSURE SEALING COUPLING APPARATUS Patent

Timothy B. Irvin, inventor (to NASA) and Richard E. French, inventor (to NASA) 17 Jan. 1989 6 p Filed 16 Feb. 1988 Supersedes N88-25303 (26-18, p 2576)

(NASA-Case-MFS-29348-1; US-Patent-4,798,433; US-Patent-Appl-SN-156518; US-Patent-Class-350-96.21; US-Patent-Class-350-96.25) Avail: U.S. Patent and Trademark Office CSCL 20F

An apparatus is presented for optically coupling and pressure sealing sections of an instrument probe, one of the section being at a high pressure cryogenic environment and the other section being at ambient pressure. The apparatus includes a housing having a passageway within which elements are mounted for precisely locating a rigid optical fiber coupler and the probe sections so as to optically connect and maintain the ends of the probe sections together to permit signals to pass in both directions through the joint in two or more discrete channels. An adjustable positioning member acts to connect the external section of the probe to the housing in axial and rotation alignment with the interior section. Official Gazette of the U.S. Patent and Trademark Office

N89-25690# Pacific Northwest Labs., Richland, WA.

OPTICAL PROPERTIES OF METAL-OXIDE THIN FILMS: INFLUENCE OF MICROSTRUCTURE

K. F. Ferris, M. R. Thompson, G. J. Exarhos, W. S. Frydrych, C. B. Duke, and N. J. Hess Oct. 1988 11 p Presented at the Boulder Damage Symposium, Boulder, CO, 26-28 Oct. 1988

(Contract DE-AC06-76RL-01830)

(DE89-011219; PNL-SA-16187; CONF-8810296-5) Avail: NTIS HC A03

The optical response of a dielectric film is perturbed from that of the analogous bulk material by the inherent film microstructure. A mean field approach has been developed for modeling the real part of the dielectric constant in terms of film microstructure. On this basis, eventual determination of film microstructure parameters such as void density and grain size could be determined from the measured optical response of the film. A semiempirical fragment method has also been used to model the imaginary part of the refractive index for titania. Differences in the electronic transition energies for the anatase and rutile phases of titania are ascribed to dielectric field variation rather than changes in the localized chemical bonding around the titanium site. DOE

N89-25691*# Virginia Polytechnic Inst. and State Univ., Blacksburg. Dept. of Electrical Engineering.
OPTICAL FIBER SENSORS AND SIGNAL PROCESSING FOR INTELLIGENT STRUCTURE MONITORING Final Report
Daniel Thomas, Dave Cox, D. K. Lindner, and R. O. Claus Jul. 1989 47 p
(Grant NAG1-895)
(NASA-CR-185395; NAS 1.26:185395) Avail: NTIS HC A03/MF A01 CSCL 20F

Few mode optical fibers have been shown to produce predictable interference patterns when placed under strain. The use is described of a modal domain sensor in a vibration control experiment. An optical fiber is bonded along the length of a flexible beam. Output from the modal domain sensor is used to suppress vibrations induced in the beam. A distributed effect model for the modal domain sensor is developed. This model is combined with the beam and actuator dynamics to produce a system suitable for control design. Computer simulations predict open and closed loop dynamic responses. An experimental apparatus is described and experimental results are presented. Author

N89-25692# Sandia National Labs., Albuquerque, NM.
OPTICAL INFORMATION STORAGE IN PLZT THIN FILMS
Cecil E. Land 1989 26 p Presented at the 91st Annual Meeting of the American Ceramic Society, Indianapolis, IN, 23 Apr. 1989
(Contract DE-AC04-76DP-00789)
(DE89-011067; SAND-88-3150C; CONF-890421-3) Avail: NTIS HC A03/MF A01

The feasibility of storing and reading high density optical information in lead zirconate titanate (PZT) and in lead lanthanum zirconate titanate (PLZT) thin films depends on both the longitudinal electrooptic coefficients and the photosensitivities of the films. This paper describes the methods used to measure both the longitudinal electrooptic effects and the photosensitivities of the thin films. The results of these measurements were used to evaluate a longitudinal quadratic electrooptic R coefficient, a linear electrooptic r sub c coefficient and the wavelength dependence of the photosensitivity of a composition of PZT polycrystalline thin film. The longitudinal electrooptic R and r sub c coefficients are about an order of magnitude less than the transverse R and R sub c coefficients of the bulk ceramics of similar compositions. This is attributed to clamping of the film by the rigid substrate. The large birefringence after poling (greater than 10 sup -2) suggests that the optic axes of the films are preferentially oriented normal to the film surface. The techniques used for evaluating the photosensitivities of the thin films are based on measuring the photocurrent generated rather than the reduction in coercive voltage (used previously for bulk ceramics) when the film is exposed to light. The thin film photosensitivities appear to be about three orders of magnitude higher than those of bulk ceramics of similar compositions. DOE

N89-25693# Fermi National Accelerator Lab., Batavia, IL. Advanced Computer Program.
DATA ACQUISITION, EVENT BUILDING, AND ON-LINE PROCESSING: SUMMARY TALK
Irwin Gaines Mar. 1989 7 p Presented at the Workshop on Triggering and Data Acquisition for Experiments At the Superconducting Super Collider, Toronto, Ontario, 16-19 Jan. 1989
(Contract DE-AC02-76CH-03000)
(DE89-011085; FNAL/C-89/51; CONF-8901118-1) Avail: NTIS HC A02/MF A01

Our subgroup of working group 4 concerned itself with general architectural issues for SSC data acquisition. Fiber optic buses were described in two talks, and software and project management were discussed in a separate subgroup. These topics are covered in separate papers. A number of different issues were considered with certain natural difference of opinion, and a list of projects needing further R and D is given at the end of this paper. The major conclusion, however, can be simply stated and was agreed to unanimously: that the SSC data acquisition systems can achieve much higher data rates than those assumed at previous workshops. On-line processor farms of 10 to the 5th power VAX equivalents (throughout this paper we will use VAX 11/780 units as a performance standard) are quite conceivable, and data recording rates of between 100 and 1000 Hz will be feasible. DOE

N89-25694# Pacific Northwest Labs., Richland, WA.
DEPOSITION OF DIELECTRIC OPTICAL COATINGS: A MICROSTRUCTURAL STUDY OF THE DEPOSITED LAYERS AND INTERFACES
J. M. McCarthy, L. E. Thomas, W. T. Pawlewicz, W. S. Frydrych, and G. J. Exarhos Apr. 1989 8 p Presented at the Spring Meeting of the Materials Research Society, San Diego, CA, 25 Apr. 1989
(Contract DE-AC06-76RL-01830)
(DE89-011205; PNL-SA-16256; CONF-890426-6) Avail: NTIS HC A02/MF A01

Thin dielectric films are deposited on substrates for optical applications using a variety of techniques including reactive sputtering, sol-gel reaction, and ion assisted plasma deposition. This transmission electron microscopy study characterizes the microstructures of optical coatings produced by the above deposition techniques and shows how changing deposition conditions changes microstructure and subsequently the optical properties. DOE

N89-25695# Sandia National Labs., Albuquerque, NM. Engineering Projects and Explosive Applications.
FIBER OPTIC SENSING IN A HIGH EXPLOSIVES ENVIRONMENT
Rodney N. Owenby 1989 13 p Presented at the Instrumentation for Nuclear Weapons Effects Testing Conference, Monterey, CA, 5 Jun. 1989
(Contract DE-AC04-76DP-00789)
(DE89-010863; SAND-89-0337C; CONF-890694-6) Avail: NTIS HC A03/MF A01

This paper presents results in applying fiber optic technology to high explosives experiments, including: detonation light arrival time, shock wave analysis, control lines, and pressure sensing. In the correct experimental configuration, coaxial and fiber optic cable can provide excellent signals, but the fiber optic cable's characteristics under high explosive shock environments provide superior signal definition. Enhanced frequency response and cost effectiveness provide an excellent basis for future optical sensor development. Experiments were conducted comparing the signal response of several shock wave time-of-arrival methods i.e., fabricated mechanical switches, piezoelectric pin configurations, and a plastic fiber optic sensor system. The fiber optic signals were better defined and had a faster response. Fiber optic sensors with two different configurations were used as detonation light sensors. The sensors were oriented in a perpendicular and normal configuration with respect to the plane of detonation and multiple non-time-coincident signals were lensed together into a common instrument fiber. DOE

N89-25696# Edgerton, Germeshausen and Grier, Inc., Idaho Falls, ID.
FIBER OPTIC SENSING FOR NDE AND PROCESS CONTROL
J. A. Smith, John A. Johnson, Nancy M. Carlson, and B. A. Barna 1989 6 p Presented at the SEM Spring Meeting, Cambridge, MA, 28 May 1989
(Contract DE-AC07-76ID-01570)
(DE89-010976; EGG-M-88355; CONF-8905107-3) Avail: NTIS HC A02/MF A01

Many optical techniques are being developed for the inspection of completed parts and for the sensing of manufacturing processes as part of process control schemes. Optical techniques are attractive because of their noncontacting nature and their ability to obtain information from a hazardous environment. However, many of these techniques currently require delicate alignment and calibration, which make them impractical outside the laboratory. In addition, the methods themselves may be hazardous if beams of high intensity laser light are used in the sensing process. The

application of fiber optics to laser sensing techniques has the potential to make them more practical and safer in an industrial environment. This paper discusses three optical techniques which use fiber-optic technology to make then more robust and safe. The first uses fibers to deliver pulse laser light for a vision system which is capable of viewing high luminosity processes. The second also uses fibers to deliver pulsed laser light, but for the purpose of generating ultrasound in a region where a normal ultrasonic transducer could not be used. The third application uses fibers in the arms of a heterodyne interferometer which can be used to detect vibrations or ultrasonic waves. DOE

N89-25697# Deutsche Forschungs- und Versuchsanstalt fuer Luft- und Raumfahrt, Oberpfaffenhofen (West Germany). Abteilung Lasertechnik.

PROTOTYPE OF A SLANT VISUAL RANGE MEASURING DEVICE

Juergen Streicher, Christian Werner, Uwe Berghaus, Harald Gatz, Eberhard Gelbke, Andreas Lisius, and Christoph Muenkel (Impulsphysik G.m.b.H., Hamburg, Germany, F.R.) Aug. 1988 81 p In GERMAN; ENGLISH summary

(DFVLR-FB-88-42; ISSN-0171-1342; ETN-89-94632) Avail: NTIS HC A05/MF A01; DFVLR, VB-PL-DO, Postfach 90 60 58, 5000 Cologne, Fed. Republic of Germany, DM 25.50

A prototype an eye-safe slant visual range measuring device consisting of a modified eye-safe cloud ceilograph is described. The system concept with a fast data system and a complex data handling program is presented. It is intended for airports. ESA

N89-25698# Technische Univ., Eindhoven (Netherlands). Faculty of Electrical Engineering.

LOCAL-FREQUENCY DESCRIPTION OF OPTICAL SIGNALS AND SYSTEMS

M. J. Bastiaans Apr. 1988 114 p

(EUT-88-E-191; ISBN-90-614-4191-9; ISSN-0167-9708; ETN-89-94779) Avail: NTIS HC A06/MF A01

Two types of local frequency spectra are presented: the Wigner distribution function and the sliding-window spectrum; the latter function is, in fact, the Fourier transform of the signal after being multiplied by a slided window function. The Wigner distribution function can provide a link between Fourier optics and geometrical optics; many properties of the Wigner distribution function and the way in which it propagates through a linear system, can be interpreted in geometric-optical terms. The Wigner distribution function and its related signal representations can be applied to stochastic signals, leading to a signal description that is related to Walther's generalized radiance in optics. Properties of partially coherent light can thus be derived easily by means of the Wigner distribution function. The sliding-window spectrum has the advantage that a sampling theorem can be formulated for it: the sliding-window spectrum of a time signal is completely described by its values at the points of a certain time-frequency lattice, which is exactly the lattice suggested by Gabor in 1946. The sliding-window spectrum thus leads naturally to Gabor's expansion of a signal into a discrete set of properly shifted and modulated versions of an elementary signal; the latter description leads, by its discrete nature, directly to the concept of the number of degrees of freedom of a signal. Applications of Gabor's expansion to optical signals (completely coherent and partially coherent) as well as a way to generate Gabor's expansion coefficients of a time signal by optical means, are described. ESA

75 PLASMA PHYSICS

Includes magnetohydrodynamics and plasma fusion. For ionospheric plasmas see *46 Geophysics*. For space plasmas see *90 Astrophysics*.

N89-25699# Nagoya Univ. (Japan). Inst. of Plasma Physics.

A COURANT CONDITION FREE MODIFIED PARTIALLY-IMPLICIT METHOD. REVISED ELECTROMAGNETIC PARTICLE CODE PS2M FOR BOUNDED PLASMAS WITH CONDUCTING WALLS

H. Abe and S. Nakajima Oct. 1988 22 p Prepared in cooperation with Kyoto Univ. (Japan)

(IPPJ-892; ISSN-0469-4732) Avail: NTIS HC A03/MF A01

The distortion of the dispersion of the light waves or the nonphysical frequency alias exists in the Courant condition relaxed methods was previously proposed. A method for correcting this distortion without generating the alias is herein proposed. The proposed method is obtained by merging the merit of one type of method to another type of method. A set of difference equations with interesting features is given and is then modified to a finite difference approximation for the time integration of the Maxwell equations without affecting the numerical stability and without generating the nonphysical frequency alias. As an application, this method is embodied in a code Particle Simulation code (PS2M), in 2.5 dimensions for electromagnetic plasmas with a pair of parallel conducting plates (a slab model). Author

N89-25700# Nagoya Univ. (Japan). Inst. of Plasma Physics.

DENSITY FLUCTUATIONS AND PARTICLE/THERMAL TRANSPORT FOR OHMICALLY AND AUXILIARILY HEATED PLASMAS IN THE JIPP T-IIU TOKAMAK

K. Kawahata, K. Adati, R. Akiyama, A. Ando, T. Aoki, D. G. Bi (Southwestern Inst. of Physics, Sichuan, China), J. Fujita, Y. Hamada, S. Hidekuma, and S. Hirokura et al Oct. 1988 14 p Presented at the 12th International Conference on Plasma Physics and Controlled Nuclear Fusion Research, Nice, France, 12-19 Oct. 1988 Prepared in cooperation with Chubu Univ., Kasugai (Japan)

(IPPJ-891; ISSN-0469-4732; IAEA-CN-50/A-5-3-1) Avail: NTIS HC A03/MF A01

The study of microturbulence excited in ohmically heated (OH) and auxiliarily heated plasmas in the JIPP T-IIU tokamak is reported. In high density OH plasmas, it was found that the energy confinement time deviates from the Alcator scaling and at the same time the ion mode which propagates in the ion diamagnetic drift direction is excited in addition to the electron mode. The value of eta(i) = (dlnT(i)/dlnn(i)) evaluated experimentally is about 1.0 to 1.2 when the ion mode is excited. Here, eta(i) is the ion temperature gradient mode, T(i) is ion temperature and n(i) is electron density. In high power auxiliarily heated plasmas where the ion mode is also observed, the ion thermal diffusivity around r/a approx. = 0.5 is 2 to 5 times larger than the neoclassical values. From the analysis of time evolution of the density profile after the injection of an ice pellet, the particle diffusivity (D) and the convective velocity (v) are estimated to be D = 0.4 to 0.7 m(2)/s and v = 4 to 8 m/s at r/a approx. = 0.5 for OH plasmas. Author

N89-25701# Nagoya Univ. (Japan). Inst. of Plasma Physics.

Z SUBeff MEASUREMENTS AND LOW-Z IMPURITY TRANSPORT FOR NBI AND ICRF HEATED PLASMA IN JIPP T-IIU TOKAMAK

K. Ida, T. Amano, K. Kawahata, and O. Kaneko Dec. 1988 30 p

(IPPJ-896; ISSN-0469-4732) Avail: NTIS HC A03/MF A01

A visible bremsstrahlung detector array system for Z sub eff measurements and a charge exchange recombination spectroscopy (CXRS) system for fully ionized impurity profile measurements were installed on JIPP TII-U to study impurity transport for Neutral Beam Injection (NBI) and Ion Cyclotron Resonance Frequency (ICRF) heated plasma. More impurities are sputtered by ICRF heating than by NBI and/or ohmic heatings. The carbon contribution to Z sub eff is 80 to 90 percent for NBI heated plasmas, and 60

percent for NBI + ICRF heated plasmas. With a carbon coating of vacuum vessel, the Z sub eff value decreases 2.4 to 1.7 and the carbon contribution to Z sub eff increases up to 80 to 90 percent. The diffusion coefficient D sub a = 1.0 m(2)/s and the convective velocity v sub a(a) = 13 m/s is obtained at the plasma edge for carbon impurity from the radial profile and time evolution of fully ionized carbon after the ICRF pulse is turned on. Author

N89-25702# Oak Ridge National Lab., TN.
CONFINEMENT IMPROVEMENT OF LOW-ASPECT-RATIO TORSATRONS
B. A. Carreras, V. E. Lynch (Martin Marietta Energy Systems, Inc., Oak Ridge, TN.), N. Dominguez, J. N. Leboeuf, and J. F. Lyon Mar. 1989 34 p
(Contract DE-AC05-84OR-21400)
(DE89-010192; ORNL/TM-11101) Avail: NTIS HC A03/MF A01

Stellarators with plasma aspect ratios in the range from 3.5 to 5 can be created using the Compact Torsatron configurations. Stable operation at high beta should be possible in these devices if a vertical field coil system is designed to prevent breaking of the magnetic surfaces at finite beta. Direct losses of energetic particles can be high, but the addition of an external quadrupole field can reduce these losses. Optimization criteria and the low-aspect-ratio torsatron configurations obtained are discussed. DOE

N89-25703# Argonne National Lab., IL.
TEMPERATURE LIMIT OF A GRAPHITE DIVERTOR SURFACE DUE TO PARTICLE EROSION
J. N. Brooks Mar. 1989 17 p
(Contract W-31-109-eng-38)
(DE89-010272; ANL/FPP/TM-236) Avail: NTIS HC A03/MF A01

The surface temperature limit of a graphite coated tokamak divertor due to particle erosion has been examined theoretically. The analysis uses models for physical sputtering, radiation enhanced sublimation, and redeposition phenomena. An upper bound on surface temperature is computed based on the necessary condition that self-sputtering be finite. The allowable graphite surface temperature is found to depend strongly on the plasma edge temperature, being limited to approximately or equal to 1150 C for medium plasma edge temperatures (approximately 150 eV). DOE

N89-25704# Sandia National Labs., Albuquerque, NM.
PLASMA SWITCHES FOR HIGH CURRENT AND FAST TIME SCALE OPERATION
Seishi Hamasaki and Nicholas A. Krall (Krall Associates, Del Mar, CA.) Apr. 1989 222 p
(Contract DE-AC04-76DP-00789)
(DE89-010557; SAND-88-7172) Avail: NTIS HC A10

During the past two years JAYCOR has made important contributions to the understanding of the plasma opening switch (POS). During the first year of the program the task completed for Sandia was the development of a code, HYBRID-2D, which was written as a user code and delivered with a user's manual to Sandia National Laboratory to aid in a variety of studies. As an example of HYBRID-2D application to other SNL problems, simulation of a Z-pinch implosion by HYBRID-2D code was also performed. In the second year, the work contracted for was to investigate the effect of plasma instabilities on plasma conductivity, current penetration and power conditioning for POS. Other tasks include investigation of opening phase dependence on finite impedance load and effects due to the application of axial magnetic fields such as fast B field or slow B shaping field. The work in the second year has been carried out using a combination of numerical models, HYBRID-2D and MEEC for application to the POS in the low density or strong curvature regimes. DOE

N89-25705# Wisconsin Univ., Madison. Dept. of Physics.
THE q MEASUREMENTS DURING SAWTOOTH OSCILLATIONS IN A LOW q TOKAMAK
R. A. Moyer, J. A. Goetz, R. N. Dexter, and S. C. Prager Apr. 1989 14 p
(Contract DE-FG02-86ER-53227)
(DE89-010563; DOE/ER-53227/135) Avail: NTIS HC A03/MF A01

The central safety factor during a sawtooth oscillation in material-limiter tokamak discharges in the TOKAPOLE II poloidal divertor tokamak is measured to be constant at 0.7 during a sawtooth oscillation. This result is identical to that observed earlier in the same device in magnetic-limiter discharges. Thus, the presence of scrape-off plasma beyond the divertor separatrix is not responsible for the absence of total reconnection. DOE

N89-25706# Wisconsin Univ., Madison. Dept. of Physics.
ANOMALOUS PARTICLE PINCH FOR COLLISIONLESS PLASMA
P. W. Terry Jan. 1989 14 p
(Contract DE-FG02-86ER-53227)
(DE89-011018; DOE/ER-53227/133) Avail: NTIS HC A03

The particle transport arising from the convection of nonadiabatic electron density by ion temperature gradient driven turbulence is examined when trapped electrons collide less often than a bounce period. In the lower temperature end of this regime, trapped electrons are collisional and the particle flux is outward (in the direction of the gradients). When the trapped electrons are collisionless, there is a temperature threshold above which the electron temperature gradient driven particle flux changes sign and becomes inward. The magnitude of the nonadiabatic electron contribution to the growth rate is found to be potentially of the same order as the ion contribution. DOE

N89-25707# General Atomics Technologies Corp., San Diego, CA.
CONFINEMENT PHYSICS OF H-MODE DISCHARGES IN DIII-D
K. H. Burrell, S. L. Allen, G. Bramson, N. H. Brooks, R. W. Callis, T. N. Carlstrom, M. S. Chu, A. P. Colleraine, D. Content (Johns Hopkins Univ., Baltimore, MD.), and J. C. DeBoo et al Apr. 1989 20 p Presented at the 16th Eugopean Conference on Controlled Fusion and Plasma Physics, Venice, Italy, 13-17 Mar. 1989 Prep. in coop. with Max-Planck-Inst. fuer Plasmaphysik, Garching (Fed. Rep. of Ger.); Calif. Univ., Irvine; Oak Ridge Nat. Lab., TN; Calif. Univ., Los Angeles; Centre de Rech. en Phy. de Plasmas, Switzerland; Jap. Atomic Energy Res. Inst., Tokyo; MIT
(Contracts DE-AC03-89ER-51114; W-7405-eng-48)
(DE89-011525; GA-A-19609; CONF-890302-20) Avail: NTIS HC A03/MF A01

Our data indicate that the L-mode to H-mode transition in the DIII-D tokamak is associated with the sudden reduction in anomalous, fluctuation-connected transport across the outer midplane of the plasma. In addition to the reduction in edge density and magnetic fluctuations observed at the transition, the edge radial electric field becomes more negative after the transition. We have determined the scaling of the H-mode power threshold with various plasma parameters; the roughly linear increase with plasma density and toroidal field are particularly significant. Control of the ELM frequency and duration by adjusting neutral beam input power has allowed us to produce H-mode plasmas with constant impurity levels and durations up to 5 s. Energy confinement time in Ohmic H-mode plasmas and in deuterium H-mode plasmas with deuterium beam injection can exceed saturated Ohmic confinement times by at least a factor of two. Energy confinement times above 0.3 s have been achieved in these beam-heated plasmas with plasma currents in the range of 2.0 to 2.5 MA. Local transport studies have shown that electron and ion thermal diffusivities and angular momentum diffusivity are comparable in magnitude and all decrease with increasing plasma current. DOE

N89-25708# Illinois Univ., Urbana.
ION ENERGY AND PLASMA MEASUREMENTS IN THE NEAR FIELD OF AN ICRF ANTENNA
J. B. O. Caughman, II, D. N. Ruzic, and D. J. Hoffman (Oak Ridge National Lab., TN.) 1989 5 p Presented at the 8th

Topical Conference on Radio Frequency Power in Plasmas, Irvine, CA, 1 May 1989
(Contract DE-AC05-84OR-21400)
(DE89-011611; CONF-8905120-6) Avail: NTIS HC A02/MF A01

Plasma properties and ion energies have been measured in the near field of an ICRF antenna to determine the effects of RF fields in a magnetized plasma sheath on the energy of ions incident on the surface of the Faraday shield. A resonant loop antenna with a two- tier Faraday shield was used on the RF Test Facility at Oak Ridge National Laboratory (ORNL). The magnetic field near the antenna is approximately 2 kG, and the plasma density is approximately 10(11)/cu cm with an electron temperature of 6 to 10 eV. The time-varying floating potential was measured with a capacitively coupled probe, and the time-averaged electron temperature, electron density, and floating potential were measured with a Langmuir probe. Both probes were scanned poloidally in front of the antenna, parallel to the current strap. Diagnostics for measuring ion energies included a gridded energy analyzer located directly below the antenna. Measured ion energies are compared with predictions from a computational model for determining the energy and angular distribution of ions incident on a surface in a magnetized plasma sheath with a time-varying plasma potential. DOE

N89-25709# Oak Ridge National Lab., TN.
PLASMA PRODUCTION USING MICROWAVE AND RADIO FREQUENCY SOURCES
M. D. Carter 1989 6 p Presented at the 7th International Stellarator Workshop, Oak Ridge, TN, 10 Apr. 1989
(Contract DE-AC05-84OR-21400)
(DE89-011615; CONF-890403-15) Avail: NTIS HC A02/MF A01

The initial breakdown of neutral fill gas is an important issue for stellarators where ionization of the neutral gas prefill is necessary before other auxiliary power can be coupled to the system. Microwaves with frequencies at the fundamental electron cyclotron resonance can be used for this purpose because they couple to electrons through linear wave-particle interactions. In addition, microwave applications at twice the electron cyclotron frequency typically have a strong enough nonlinear coupling to initiate breakdown with reasonable agreement between theory and experiment. Nonlinear couplings at higher harmonics are progressively weaker, and the possibilities of using the third harmonic are discussed. A difficulty can arise when microwave sources are used for plasma production because it is often too expensive to support the frequency ranges needed to obtain breakdown at arbitrary static magnetic field values. Thus, devices that rely exclusively on microwave sources to obtain target plasmas may be limited in their operational range by their microwave source frequencies. Alternatively, RF sources possessing a broad band of tunable frequencies are often available in the megahertz frequency range. The use of these types of power sources to produce target plasmas could add to the operational limits of many devices. Waves with frequencies of a few megahertz have been used to produce plasmas at the Institute of Physics and Technology at Kharkov (KFTI) for many years. The technique and mechanism by which the neutral gas is broken down in the very early phases of these discharges are presented. DOE

N89-25710# Science Applications International Corp., San Diego, CA.
THEORETICAL STUDIES OF EDGE PHYSICS AND PLASMA-WALL INTERACTIONS Final Report
Douglas S. Harned and C. K. Birdsall 25 Apr. 1989 72 p
(Contract DE-AC03-87ER-53254)
(DE89-011792; SAIC-89/1412) Avail: NTIS HC A04/MF A01

First year progress has been in three areas: The stability of resistive interchange modes has been examined in cylindrical geometry using realistic H-mode and L-mode profiles. In cylindrical geometry no unstable modes have yet been found in the H-mode regime with growth rates sufficiently large to account for the ELM bursts seen in divertor tokamak experiments. These results have led us to the development of a simulation model that includes toroidal effects. A new toroidal nonlinear code has been developed to incorporate toroidal effects and to allow initialization with realistic divertor tokamak equilibria. A new time advance method has been formulated to allow efficient treatment of fast modes inside the plasma and vacuum regions outside the separatrix. The code is designed so that input can be used from equilibria obtained from the D-IIID experiment. In regions with low density and sharp gradients (edge regions) the Hall effect becomes large. The inclusion of the Hall effects in time-dependent calculations causes a severe time step constraint. A new numerical technique has been developed to treat the Hall effect without requiring significant increase in computation time. DOE

N89-25711# Lawrence Livermore National Lab., CA. Beam Research Program.
HIGH-AVERAGE-POWER MILLIMETER-WAVE FEL (FREE-ELECTRON LASER) FOR PLASMA HEATING USING THE ETA-2 ACCELERATOR
A. L. Throop, D. P. Atkinson, J. C. Clark, G. A. Deis, R. A. Jong, W. E. Nexsen, A. C. Paul, E. T. Scharlemann, B. W. Stallard, and K. I. Thomassen 10 Mar. 1989 7 p Presented at the 13th Particle Accelerator Conference, Chicago, IL, 20-23 Mar. 1989 Prepared in cooperation with TRW, Inc., Redondo Beach, CA; and California Univ., Berkeley, Lawrence Berkeley Lab.
(Contract W-7405-eng-48)
(DE89-012294; UCRL-100225; CONF-890335-137) Avail: NTIS HC A02/MF A01

The Microwave Tokamak Experiment (MTX) is under construction at LLNL to investigate the feasibility of intense, pulsed microwave radiation for plasma heating on future ignition tokamaks. A high-average-power free-electron laser (FEL) will use the Experimental Test Accelerator (ETA-2), a linear induction accelerator, in combination with an advanced high-field wiggler, to produce 1 to 2 MW of power at 1 to 2 mm wavelengths for periods of up to 0.5s. The design of the FEL, termed the intense microwave prototype (IMP), is described, along with the status and major issues associated with the status and major issues associated with the experiment. DOE

N89-25712# Oak Ridge National Lab., TN.
ICRF FARADAY SHIELD PLASMA SHEATH PHYSICS: THE PERKINS PARADIGM
J. H. Whealton, P. M. Ryan, and R. J. Raridon 1989 5 p Presented at the 8th Topical Conference on Radio Frequency Power in Plasmas, Irvine, CA, 1 May 1989
(Contract DE-AC05-84OR-21400)
(DE89-012362; CONF-8905120-10) Avail: NTIS HC A02/MF A01

Using a 2-D nonlinear formulation which considers the plasma edge near a Faraday shield in a self consistent manner, progress is indicated in the modeling of the ion motion for a Perkins embodiment. Ambiguities in the formulation are also indicated, the resolution of which will provide significant insight into the impurities generation for ICRH antennas. DOE

N89-25713# Oak Ridge National Lab., TN.
AVERAGED EQUILIBRIUM AND STABILITY IN LOW-ASPECT-RATIO STELLARATORS
L. Garcia (Universidad Complutense, Madrid, Spain), B. A. Carreras, and N. Dominguez 1989 8 p Presented at the 7th International Stellarator Workshop, Oak Ridge, TN, 10 Apr. 1989
(Contract DE-AC05-84OR-21400)
(DE89-013618; CONF-890403-18) Avail: NTIS HC A02/MF A01

The MHD equilibrium and stability calculations or stellarators are complex because of the intrinsic three-dimensional (3-D) character of these configurations. The stellarators expansion simplifies the equilibrium calculation by reducing it to a two-dimensional (2-D) problem. The classical stellarator expansion includes terms up to order epsilon^3, and the vacuum magnetic field is also included up to this order. For large-aspect-ratio configurations, the results of the stellarator expansion agree well

with 3-D numerical equilibrium results. But for low-aspect-ratio configurations, these are significant discrepancies with 3-D equilibrium calculations. The main reason for these discrepancies is the approximation in the vacuum field contributions. This problem can be avoided by applying the average method in a vacuum flux coordinate system. In this way, the exact vacuum magnetic field contribution is included and the results agree well with 3-D equilibrium calculations even for low-aspect-ratio configurations. Using the average method in a vacuum flux coordinate system also permit the accurate calculation of local stability properties with the Mercier criterion. The main improvement is in the accurate calculation of the geodesic curvature term. In this paper, we discuss the application of the average method in flux coordinates to the calculation of the Mercier criterion for low-aspect-ratio stellarator configurations. DOE

N89-25714 Max-Planck-Inst. fuer Plasmaphysik, Garching (Germany, F.R.).
INVESTIGATIONS OF MODULAR NONPLANAR COIL SYSTEMS FOR THE STELLARATOR FUSION REACTOR
Thesis - Technische Hochschule, Darmstadt
[UNTERSUCHUNG MODULARER SYSTEME AUS NICHTEBENEN SPULEN FUER DEN STELLARATOR-FUSIONSREAKTOR]
E. Harmeyer Dec. 1988 113 p In GERMAN; ENGLISH summary
(IPP-2/298; ETN-89-94572) Copyright Avail: Fachinformationszentrum Karlsruhe, 7514 Eggenstein-Leopoldshafen 2, Fed. Republic of Germany

Steady-state stellarators are studied for a fusion reactor. The helical magnetic field required for plasma confinement is produced by means of a set of modular nonplanar coils. In order to achieve optimum power density of the plasma, the magnetic flux density inside the torus is made as high as possible. Investigations on modular nonplanar stellarator coils systems with poloidal periodicity $l = 2$ and a coil system of the W7-AS type with superposed $l = 0, 1, 2, 3$ terms are treated. The parameters are simultaneously varied while keeping constant the ratios of certain magnitudes. In the parameter space of the geometric values and coil number the following quantities are evaluated: maximum magnetic flux density in the coil domain, stored magnetic energy of the coil system, magnetic force density distribution or magnetic forces, and mechanical stress distribution in the coils. Numerical methods are applied in the programs and results are compared with those of analytical approximation solutions. ESA

N89-25715 Ruhr Univ., Bochum (Germany, F.R.). Inst. fuer Experimentalphysik AG 2.
PARTIAL AND STATE SELECTIVE CROSS SECTIONS FOR MULTIPLE IONIZATION OF RARE GAS ATOMS BY ELECTRON IMPACT
H. Lebius, J. Binder, H. R. Koslowski, K. Wiesemann, and B. A. Huber Jul. 1988 26 p Previously announced in IAA as A89-27974 Sponsored by Deutsche Forschungsgemeinschaft, Bonn, Fed. Republic of Germany
(Rept-88-05-170; ETN-89-94597) Copyright Avail: Fachinformationzentrum Karlsruhe, 7514 Eggrnstein-Leopoldshafen 2, Fed. Republic of Germany

Partial ionization cross sections for single electron impact on rare gas atoms are measured for charge states up to $q=8$. Translational energy spectroscopy is used to determine state selective cross sections for the production of double and triply charged neon ions in specific electronic states. The contributions of direct and inner shell processes are discussed. ESA

N89-25716 Max-Planck-Inst. fuer Physik und Astrophysik, Garching (Germany, F.R.). Inst. fuer Extraterrestrische Physik.
COSMIC PLASMA PHYSICS [PHYSIK KOSMISCHER PLASMEN]
Eberhard Moebius, ed. Nov. 1988 135 p Partly in ENGLISH and GERMAN Proceedings of a Gemeinsamer Workshop, Garching, Fed. Republic of Germany, 13-14 Sep. 1988
(MPE-211; ISSN-0178-0719; ETN-89-94387) Copyright Avail: Max-Planck-Inst. fuer Physik und Astrophysik, D-8046 Garching bei Muenchen, Fed. Republic of Germany

Magnetic field reconnection and its application in the magnetosphere is covered. Main topics are related to shock wave physics, particle acceleration, development of plasma instabilities, and accretion dynamics in double stars systems. Processes in astrophysical objects are studied also: ionization structure in interstellar molecular clouds, gravitation like phase transition of Coulomb plasma, formation of current sheets in MHD, models for axially symmetric pulsar magnetospheres. Gravitational systems, acceleration and ideal MHD are reviewed. For individual titles, see N89-25717 through N89-25732.

N89-25717 Ruhr Univ., Bochum (Germany, F.R.). Inst. fuer Theoretische Physik IV.
MAGNETIC RECONNECTION IN GENERAL THREE-DIMENSIONAL SYSTEMS
Michael Hesse and Karl Schindler *In* Max-Planck-Inst. fuer Physik und Astrophysik, Cosmic Plasma Physics Nov. 1988 p 7-12 (For primary document see N89-25716 19-75)
Copyright Avail: Max-Planck-Inst. fuer Physik und Astrophysik, D-8046 Garching bei Muenchen, Fed. Republic of Germany

General magnetic reconnection theory is described and applied to the plasmoid formation and evolution process. The evolution of three dimensional plasmoids is explained using naive magnetic topology. The GMR theory is considered in the case of electrostatic structures depicting the phenomena occurring in the auroral particle acceleration regions. Other applications are mentioned like flux-transfer events at the magnetopause, magnetic loops in the solar corona, plasmoids in the magnetotail, and the solar wind. ESA

N89-25718 Max-Planck-Inst. fuer Physik und Astrophysik, Garching (Germany, F.R.). Inst. fuer Extraterrestrische Physik.
ORIENTATION, MOTION, AND OTHER PROPERTIES OF FTE STRUCTURES ON SEPTEMBER 4, 1984
I. Papamastorakis, G. Paschmann, W. Baumjohann, B. U. O. Sonnerup, and H. Luehr (Technische Univ., Brunswick, Germany, F.R.) *In its* Cosmic Plasma Physics Nov. 1988 p 13-17 (For primary document see N89-25716 19-75)
Copyright Avail: Max-Planck-Inst. fuer Physik und Astrophysik, D-8046 Garching bei Muenchen, Fed. Republic of Germany

Three flux transfer events (FTE), observed by the AMPTE/IRM spacecraft in the Southern Hemisphere magnetosheath are studied by variance analysis of measured magnetic fields and convection electric fields with the objective of determining the orientation and motion of the flux tube or magnetopause bulge causing the FTE signature. These FTEs preceded a series of magnetopause crossings during which the high plasma flow speeds, characteristic of quasisteady reconnection are present. ESA

N89-25719 Ruhr Univ., Bochum (Germany, F.R.). Inst. fuer Theoretisch Physik IV.
THREE DIMENSIONAL COMPUTATIONS OF THE DYNAMICS OF THE MAGNETOPAUSE: FIRST RESULTS
A. Otto *In* Max-Planck-Inst. fuer Physik und Astrophysik, Cosmic Plasma Physics Nov. 1988 p 26-29 (For primary document see N89-25716 19-75)
Copyright Avail: Max-Planck-Inst. fuer Physik und Astrophysik, D-8046 Garching bei Muenchen, Fed. Republic of Germany

Dynamics of magnetopause related to plasma transport from the interplanetary medium into the magnetosphere is studied. Flux transfer events (FTE) signatures indicate the presence of magnetic reconnection localized in space and time. Dynamical evolution of FTE is described as a three dimensional nonlinear problem. Thus a 3D resistive MHD code is developed considering first a one dimensional initial state with antiparallel magnetic fields and then a one dimensional state with magnetic shear. Density, temperature, and magnetic pressure are chosen to be symmetric to the plane of the magnetopause layer. ESA

N89-25720 Max-Planck-Inst. fuer Physik und Astrophysik, Garching (Germany, F.R.). Inst. fuer Extraterrestrische Physik.
ACCELERATION OF IONS IN THE MAGNETOTAIL
D. Sachsenweger *In its* Cosmic Plasma Physics Nov. 1988 p 30-41 (For primary document see N89-25716 19-75)
Copyright Avail: Max-Planck-Inst. fuer Physik und Astrophysik, D-8046 Garching bei Muenchen, Fed. Republic of Germany

Mass, charge composition and energy spectra of the suprathermal ion population in the plasma sheet is measured using the time of flight spectrometer SULEICA during several magnetically active periods. Observations made after substorm onset during events show a significant hardening of the energy spectra of all detected ion species. Flux increases are functions of energy/charge and are not correlated with energy/mass or rigidity. Results indicate acceleration of the ions in an electric field. Flux enhancements vary exponentially with energy, similar to a heating of a thermal distribution. ESA

N89-25721 Max-Planck-Inst. fuer Physik und Astrophysik, Garching (Germany, F.R.).
NONLOCAL ANALYSES OF FINITE-BEAM-DRIVEN INSTABILITIES
Y. Serizawa and C. T. Dum *In its* Cosmic Plasma Physics Nov. 1988 p 45-54 (For primary document see N89-25716 19-75)
Copyright Avail: Max-Planck-Inst. fuer Physik und Astrophysik, D-8046 Garching bei Muenchen, Fed. Republic of Germany

Beam-plasma instabilities generated by an electron beam flowing in a background plasma are studied. Electrostatic linear waves in a finite beam plasma system are modeled as a field aligned beam current sheet with Gaussian transverse density profile. Thermal effects are treated by deriving an integral eigenmode equation in Fourier space. Numerical results are presented for a case of strong magnetic field and a relatively cold beam. ESA

N89-25722 Ruhr Univ., Bochum (Germany, F.R.). Inst. fuer Theoretische Physik IV.
PARTICLE SIMULATION OF MAGNETIC RECONNECTION
Wolfgang Zwingmann *In* Max-Planck-Inst. fuer Physik und Astriphysik, Cosmic Plasma Physics Nov. 1988 p 55-58 (For primary document see N89-25716 19-75)
Copyright Avail: Max-Planck-Inst. fuer Physik und Astrophysik, D-8046 Garching bei Muenchen, Fed. Republic of Germany

Particle simulation is used to study the nonlinear behavior of the ion tearing instability of the magnetospheric plasma sheet. Integrals of the distribution function are analyzed to study the mechanism of the instability. The deviation from the Maxwellian distribution is more effective if only the particles inside the plasmoid are considered. Linear theory is valid for small amplitudes thus growth rates are compared to test the stability criterion. Stability diagram agrees between linear theory and numerical experiment. ESA

N89-25723 Ruhr Univ., Bochum (Germany, F.R.).
DOUBLE TEARING AND PARTICLE SIMULATION
Udo Arendt *In* Max-Planck-Inst. fuer Physik und Astrophysik, Cosmic Plasma Physics Nov. 1988 p 59-60 (For primary document see N89-25716 19-75)
Copyright Avail: Max-Planck-Inst. fuer Physik und Astrophysik, D-8046 Garching bei Muenchen, Fed. Republic of Germany

Two dimensional simulations using the double tearing mode with localized reconnection are reviewed. For this case the VENUS code is applied. For the one dimensional equilibrium calculation the AVANTI code is used. Principles of particle simulation are described for both codes. ESA

N89-25724 Max-Planck-Inst. fuer Physik und Astrophysik, Garching (Germany, F.R.).
ION HEATING IN THE BUG SHOCK WAVE [IONENHEIZUNG IN DER BUGSTOSSWELLE]
N. Sckopke *In its* Cosmic Plasma Physics Nov. 1988 p 61-64 In GERMAN (For primary document see N89-25716 19-75)
Copyright Avail: Max-Planck-Inst. fuer Physik und Astrophysik, D-8046 Garching bei Muenchen, Fed. Republic of Germany

Main dissipation mechanisms by ion heating in Bug shock wave are studied. Ion heating is modeled in the case of transversal magnetic field orientation. Variations of plasma parameters by multiple shock wave crossing are registered. Ion distribution functions are recorded by satellites allowing thermalization observations and model verification. ESA

N89-25725 Max-Planck-Inst. fuer Physik und Astrophysik, Garching (Germany, F.R.). Inst. fuer Extraterrestrische Physik.
A NUMERICAL SIMULATION OF INHOMOGENEOUS ION CYCLOTRON TURBULENCE
L. Muschietti and C. T. Dum *In its* Cosmic Plasma Physics Nov. 1988 p 65-73 (For primary document see N89-25716 19-75)
Copyright Avail: Max-Planck-Inst. fuer Physik und Astrophysik, D-8046 Garching bei Muenchen, Fed. Republic of Germany

Inhomogeneous quasilinear equations are presented to solve ion cyclotron turbulence phenomena in open configurations. Relaxation of electron distribution streaming into a region of electrostatic ion cyclotron turbulence is analyzed. The wave level is enhanced 5 times as compared to the corresponding initial value in a homogeneous plasma. The electron distribution evolves towards a shape satisfying marginal stability and particle flux conservation. ESA

N89-25726 Max-Planck-Inst. fuer Physik und Astrophysik, Garching (Germany, F.R.). Inst. fuer Extraterrestrische Physik.
THE IONIZATION STRUCTURE IN SHOCKS IN INTERSTELLAR MOLECULAR CLOUDS
T. W. Hartquist *In its* Cosmic Plasma Physics Nov. 1988 p 77-80 (For primary document see N89-25716 19-75)
Copyright Avail: Max-Planck-Inst. fuer Physik und Astrophysik, D-8046 Garching bei Muenchen, Fed. Republic of Germany

Shocks in the interstellars medium generated by energy release of stars is studied. Interstellar clouds consisting of weakly ionized magnetized plasmas are described by multifluid models to analyze the structures of shocks. In such shocks the ionized species are accelerated to the shock velocity much more quickly than the neutral species. The dissipation is dominated by ion-neutral friction, which together with the acceleration of the neutrals occurs on a length scale given by equating the magnetic pressure gradient to the ion-neutral friction. Grain dynamics and ionization structure in dense cloud shocks are represented by models to explain the CH(+) abundance in diffuse molecular clouds. ESA

N89-25727 Ruhr Univ., Bochum (Germany, F.R.). Inst. fuer Theoretische Physik IV.
GRAVITATIONAL-LIKE PHASE TRANSITION OF A CLASSICAL COULOMB PLASMA
Michael K.-H. Kiessling *In* Max-Planck-Inst. fuer Physik und Astrophysik, Cosmic Plasma Physics Nov. 1988 p 81-84 (For primary document see N89-25716 19-75)
Copyright Avail: Max-Planck-Inst. fuer Physik und Astrophysik, D-8046 Garching bei Muenchen, Fed. Republic of Germany

For very dilute systems, encountered typically in space, consisting of classical negative and positive charge carrying particles and of macroscopic dimensions, maybe charged dust particles, the Hamiltonian and the classical Coulomb potential equations are considered. Results indicate that gravitational clustering and electrostatic clustering are equally strong in the system. For small enough particle numbers, electrostatic clustering dominates, and gravitational clustering will then be negligible. The statistical mechanics equilibrium state of a finite weakly coupled Coulomb plasma is inhomogeneous (collapsed phase) and is connected via a gravitational-like phase transition towards homogeneous phases. ESA

N89-25728 Ruhr Univ., Bochum (Germany, F.R.). Inst. fuer Theoretische Physik IV.
ON THE FORMATION OF CURRENT-SHEETS IN IDEAL MHD

A. Voge *In* Max-Planck-Inst. fuer Phyisk und Astrophysik, Cosmic Plasma Physics Nov. 1988 p 85-89 (For primary document see N89-25716 19-75)
Copyright Avail: Max-Planck-Inst. fuer Physik und Astrophysik, D-8046 Garching bei Muenchen, Fed. Republic of Germany

Adiabatic, quasistatic change of boundary conditions of a one dimensional equilibrium state is studied. Two different equilibria satisfying the new boundary conditions are analyzed. One of them cannot be achieved by an ideal MHD-process since the change of the topology violates line conservation while the other one leads to a singular current sheet on the axis of symmetry. To study this change, calculations are carried out using a two dimensional MHD-code. Results indicate that even the slightest perturbations of ideal systems may cause a formation of singular current sheets. These sheets are located at the neutral sheet of the magnetic field. ESA

N89-25729 Tuebingen Univ. (Germany, F.R.). Lehr- und Forschungsbereich Theoretische Astrophysik.
PARTICLE SIMULATION FOR ACCRETION SHEETS IN NARROW DOUBLE STARS [TEILCHENSIMULATION FUER AKKRETIONSSCHEIBEN IN ENGEN DOPPELSTERNSYSTEMEN] **c90**
F. Geyer, H. Herold, and H. Ruder *In* Max-Planck-Inst. fuer Physik und Astrophysik, Cosmic Plasma Physics Nov. 1988 p 90-97 In GERMAN Sponsored by the Deutsche Forschungsgemeinschaft, Bonn, Federal Republic of Germany (For primary document see N89-25716 19-75)
Copyright Avail: Max-Planck-Inst. fuer Physik und Astrophysik, D-8046 Garching bei Muenchen, Fed. Republic of Germany

Development and behavior of accretion sheets in double stars systems are studied by particle simulation calculations. Numerical analysis considers the following parameters in the binary system: primary and secondary components, path period of the system, and mass flow rates. Mass behavior is described by Roche-potential. The particle motion equation in the double star system is solved by the Leap-Frog procedure. Velocity friction simulation is obtained by viscous interaction considerations. ESA

N89-25730 Ruhr Univ., Bochum (Germany, F.R.). Inst. fuer Theoretische Physik IV.
MODELS FOR AXIALLY SYMMETRIC PULSAR MAGNETOSPHERES **c46**
T. Neukirch *In* Max-Planck-Inst. fuer Physik und Astrophysik, Cosmic Plasma Physics Nov. 1988 p 98-102 (For primary document see N89-25716 19-75)
Copyright Avail: Max-Planck-Inst. fuer Physik und Astrophysik, D-8046 Garching bei Muenchen, Fed. Republic of Germany

A method for the construction of self-consistent models for an axially symmetric pulsar magnetosphere (parallel rotator) neglecting radiation effects is presented. Results obtained for nonrelativistic magnetospheres are shown. For the quasi-neutral case, starting from a vacuum dipole field the particle density is increased. A dipole field can only store a limited amount of plasma. For the neutral case, the electric potential changes considerably, whereas the magnetic field remains nearly unchanged. ESA

N89-25731 Max-Planck-Inst. fuer Physik und Astrophysik, Garching (Germany, F.R.). Inst. fuer Extraterrestrische Physik.
ACCELERATION OF PARTICLES IN SHEAR FLOWS [BESCHLEUNIGUNG VON TEILCHEN IN SCHERSTROEMUNGEN] **c93**
G. E. Morfill *In its* Cosmic Plasma Physics Nov. 1988 p 110-123 In ENGLISH; GERMAN title (For primary document see N89-25716 19-75)
Copyright Avail: Max-Planck-Inst. fuer Physik und Astrophysik, D-8046 Garching bei Muenchen, Fed. Republic of Germany

Starting from cosmic ray transport equations, the transport in a sheared medium is analytically studied by mathematical models. In each scattering event, the particle momentum is randomized in direction but its magnitude is conserved in the frame moving with the fluid. Fokker-Planck coefficients are introduced and transport equations are derived. ESA

N89-25732 Ruhr Univ., Bochum (Germany, F.R.). Inst. fuer Theoretische Physik IV.
STATIONARY IDEAL MHD WITH INCOMPRESSIBLE MASS FLOW AND GENERAL SYMMETRY
Ute Gebhardt *In* Max-Planck-Inst. fuer Physik und Astrophysik, Cosmic Plasma Physics Nov. 1988 p 128-131 (For primary document see N89-25716 19-75)
Copyright Avail: Max-Planck-Inst. fuer Physik und Astrophysik, D-8046 Garching bei Muenchen, Fed. Republic of Germany

Symmetric solution of stationary ideal MHD with incompressible mass flow generated via a simple transformation from a combination of a magnetostatic equilibrium and a stationary hydrodynamical incompressible flow of the same symmetry class is studied, and mathematical proof is described. Proof is illustrated by two examples with translational and rotational symmetry. This method is valid in fusion plasma research and the Earth's magnetosphere. ESA

76 SOLID-STATE PHYSICS

Includes superconductivity.

For related information, see also *33 Electronics and Electrical Engineering* and *36 Lasers and Masers.*

N89-25733# Arizona Univ., Tucson. Dept. of Physics.
ARTIFICIALLY STRUCTURED SUPERCONDUCTORS Annual Progress Report
Charles M. Falco 14 Nov. 1988 10 p
(Contract DE-FG02-87ER-45297)
(DE89-009116; DOE/ER-45297/T1) Avail: NTIS HC A02/MF A01

We have succeeded in making high T sub c films by three different techniques; sputtering from a stoichiometric YBa sub 2 Cu sub 3 O sub 7-x target, sputtering from Y and Ba sub 2 Cu sub 3 targets, and by co-evaporating BaF sub 2 while sputtering Y and Cu. The structure and composition of these films were characterized by a number of X-ray diffraction techniques. Physical properties measured included resistivity vs. temperature, electron tunneling, and infra-red optical reflectivity. Also during the past year, melt-processed Bi-Ca-Sr-Cu-O materials were fabricated and studied. A number of studies of low T sub c metallic superlattices were completed this past year. These included development of improved techniques for their deposition, as well as studies of their structure, elastic properties, interfacial structure and growth dynamics, superconductivity, and electron tunneling. We reported the successful fabrication of the first monolayer metallic superlattice, consisting of alternating single atomic monolayers of Mo and Ta. Unlike all previous metallic superlattices, this monolayer superlattice maintained long range structural coherence and good metallic behavior. DOE

N89-25734# International Centre for Theoretical Physics, Trieste (Italy).
LOCAL FIELD EFFECTS IN THE MANY-BODY PERTURBATION THEORY AND IN THE DENSITY FUNCTIONAL THEORY
I. I. Mazin (Academy of Sciences, USSR, Moscow) Aug. 1988 10 p Submitted for publication
(DE88-705975; IC-88/196) Avail: NTIS (US Sales Only) HC A02/MF A01

The effect of exchange and correlation on the response processes in solids studied in homogeneous electron gas is extended for real systems, first of all for semiconductors. The static dielectric function of a semiconductor is estimated by the density functional theory. DOE

N89-25735# Central Inst. of Physics, Bucharest (Romania). Inst. for Physics and Technology of Materials.
PREPARATION AND PROPERTIES OF HIGH-TEMPERATURE SUPERCONDUCTORS IN THE Y-Ba-Cu-O SYSTEM
L. Miu, S. Popa, M. N. Popescu, and E. Cruceanu Apr. 1987

5 p
(DE88-706050; IFTM-CS-11-1987) Avail: NTIS (US Sales Only) HC A02/MF A01

Some experimental results concerning the systhesis of high temperature superconducting materials in the Y-Ba-Cu-O system and their electrical, magnetic and structural properties are presented. DOE

N89-25736# Central Inst. of Physics, Bucharest (Romania). Inst. for Physics and Technology of Materials.
INFLUENCE OF THE PREPARATION CONDITIONS ON THE DIAMAGNETIC RESPONSE OF HIGH-Tc YBa2Cu3Ox SUPERCONDUCTOR
L. Miu, S. Popa, M. N. Popescu, and E. Pavel Nov. 1987 5 p
(DE88-706051; IFTM-CS-13-1987) Avail: NTIS (US Sales Only) HC A02/MF A01

Prolonged treatments of oxygen lead to a substantial increase of the diamagnetic signal of superconducting YBa2Cu3O(x) due to the decrease of the amount of defects and to the development of Josephson-like contacts between homogeneous superconducting regions in the sample. The superconducting glass features are expected to be considerably reduced in well crystallized samples at least at liquid nitrogen temperature. DOE

N89-25737# Department of the Navy, Washington, DC.
A PASSIVATION LAYER FOR 3-5 SEMICONDUCTOR MATERIALS Patent Application
Berned T. Jonker, inventor (to Navy), Gary A. Prinz, inventor (to Navy), and James J. Krebs, inventor (to Navy) 30 Mar. 1988 18 p Filed 30 Mar. 1988
(AD-D013963; US-Patent-Appl-SN-176115) Avail: NTIS HC A03/MF A01 CSCL 07/2

A passivating or insulating layer is described for semiconductor substrates. The passivating layer is of the formula Zn1-x-yMxQySe:D where 0 less than or = 1, 0 less than or = 1, M and Q represent different specified elements and D represents a dopant. It is preferred that M and Q are Fe or Mn. The substrate is preferably a 3-5 semiconductor compound. The devices are capable of rapid switching among other uses. GRA

N89-25738# Gosudarstvennyi Komitet po Ispolzovaniyu Atomnoi Energii, Moscow (USSR). Inst. Atomnoj Ehnergii.
ON THE APPLICABILITY OF VARIOUS PLANAR POTENTIALS IN THE THEORY OF ULTRARELATIVISTIC ELECTRON CHANNELING
I. N. Chaplanova and V. V. Beloshitskij 1988 5 p In RUSSIAN; ENGLISH summary
(DE88-706155; IAE-4555/11) Avail: NTIS (US Sales Only) HC A02/MF A01

The calculations of the dechanneling function and the crystal effective thickness were carried out in channeling ultrarelativistic electrons in diamond, plane (110), for various models of a planar potential. From the analysis of results, the conclusion was made on the applicability of a simplified parabolic potential to describe the channeling process. DOE

N89-25739# Academy of Sciences of the Ukrainian SSR, Kharkov. Inst. Radiofiziki i Ehlektroniki.
KINETIC EFFECTS OF STRONG LOCALIZATION IN PLANAR HETEROSTRUCTURES p-Ge/i-GaAs
O. A. Mironov and S. V. Chistyakov 1987 42 p In RUSSIAN; ENGLISH summary
(DE88-706205; IRE-339(1987)) Avail: NTIS (US Sales Only) HC A03/MF A01

Galvanomagnetic properties of epitaxial germanium films forming a part of planar heterostructure are investigated experimentally. In the frames of percolation theory of Efros and Shklovsky the nature of anomal effects of the current transfer is explained which were observed in the temperature range of 300 to 1.5 K and in magnetic fields till 70 kOe. A prevail influence on electrophysical parameters of films p-Ge degree of disordering of the crystal structure depending on the temperature of sublayer at epitaxy has been found out. The investigations allowed to suggest a new thin film temperature sensor of the resistive type for cryogenics. DOE

N89-25740# Joint Inst. for Nuclear Research, Dubna (USSR). Lab. of High Energy.
ADVANCES IN THE DEVELOPMENT OF APPARATUS AND METHODS FOR STUDIES OF PROTEIN MONOCRYSTALS IN COORDINATE X-RAY DIFFRACTOMETERS BASED ON TWO-DIMENSIONAL PROPORTIONAL CHAMBERS
M. E. Andrianova, A. N. Popov, D. M. Khejker, Yu. V. Zanevskij, A. B. Ivanov, S. A. Movchan, V. D. Peshekhonov, and S. P. Chernenko 1987 6 p In RUSSIAN; ENGLISH summary Prepared in cooperation with Academy of Sciences, Moscow, USSR
(DE88-706259; JINR-R-13-87-937) Avail: NTIS (US Sales Only) HC A02/MF A01

Results of X-ray structure studies of protein monocrystals performed by means of the KARD-3 and KARD-4 diffractometers based on 2-D X-ray detectors are presented. Over 60 total sets of intensity patterns with a high resolution were obtained for a variety of proteins. The data make it possible to determine the spatial structure of a series of proteins which are of great interest from the scientific and practical viewpoints. The main parameters of new developed X-ray detectors are given. DOE

N89-25741# Lawrence Livermore National Lab., CA.
ELECTRONIC STRUCTURE OF HIGH TEMPERATURE SUPERCONDUCTORS
P. A. Sterne Feb. 1989 9 p Presented at the 4th International Conference on Superconducting, Santa Clara, CA, 30 Apr. 1989
(Contract W-7405-eng-48)
(DE89-008610; UCRL-100604; CONF-8904123-1) Avail: NTIS HC A02/MF A01

Electronic structure calculations on high temperature superconductors using the Linear Muffin Tin Orbital (LMTO) method are presented. The LMTO method, a first principles electronic structure method based on density functional theory, is briefly reviewed. Results are then presented for three different applications. First, applications of the method to structural and magnetic properties of La sub 2 CuO sub 4 are presented. Next, calculations on bismuth-containing copper-oxide superconductors are discussed. These motivate a discussion of the importance of interlayer coupling for superconductivity. Finally, oxygen ordering in the YBa sub 2 Cu sub 3 O sub 7 minus y system is considered by using first principles calculations to determine the effective pair interactions for use in statistical mechanical models of system. DOE

N89-25742# Rochester Univ., NY.
FEMTOSECOND STUDIES OF ELECTRON TRANSFER PROCESSES AT SEMICONDUCTOR INTERFACES Progress Report
1989 6 p
(Contract DE-FG02-85ER-13455)
(DE89-010599; DOE/ER-13455/3) Avail: NTIS HC A02/MF A01

The major emphasis of this research program has been to determine the mechanism of electron transfer at an abrupt phase discontinuity defined by a conducting surface. The key issue is the strength of the electronic coupling between the delocalized band states and the electronic levels of an adsorbed molecule on the surface. The use of semiconductor liquid junctions provides an ideal system for addressing this question. Optical excitation at above band gap wavelengths can be used to prepare the system at the adiabatic crossing point for electron transfer, i.e., directly at the transition state. This method enables a femtosecond view of the time evolution of the transition state. In the past year, we have examined the carrier reaction dynamics at (100) GaAs single crystal surfaces. The major focus has been on determining the fundamental surface state trapping rate constants at oxide induced surface states. This is the main competing channel for direct interfacial charge transfer and needs to be fully characterized.

The key question in the case of surface state trapping are: (1) What is the mechanism of electronic coupling between surface traps and the band states, and (2) What is the time scale for the trapping. DOE

N89-25743# California Univ., Berkeley. Lawrence Berkeley Lab. Materials and Chemical Sciences Div.
SURFACE STRUCTURAL ANALYSIS OF SMALL MOLECULES ON TRANSITION METAL SINGLE CRYSTAL SURFACES WITH LOW ENERGY ELECTRON DIFFRACTION Ph.D. Thesis
Gregory Scott Blackman Sep. 1988 149 p Prepared in cooperation with California Univ., Be rkeley
(Contract DE-AC03-76SF-00098)
(DE89-010681; LBL-26805) Avail: NTIS HC A07/MF A01

An attempt was made to go beyond the normal restrictions of surface crystallography. Low-temperature adsorption and coadsorbate induced ordering can be used to stabilize high coverage structures which would otherwise not form. Conventional LEED requires long-range order, digital LEED is sensitive enough to detect weak scattering from disordered adsorbates with no long-range order. Complete surface structures are presented for the first surface structure of NO, CO + benzene, NO + ethylidyne, and CO + ethylidyne all on the Rh(111) surface, and the first disordered molecular adsorbate: CO on Pt(111). Coadsorbate-induced ordering occurs when two adsorbates form a different ordered structure than either would form by itself. The lateral interactions between adsorbates force the molecules to populate new sites. Pure CO or NO overlayers have only top and bridge sites occupied, but if either molecule is paired with a coadsorbate (e.g., CO/benzene, CO/ethylidyne, or NO/ethylidyne) they move to hollow sites. Recent theoretical developments by Pendry et al. and new experimental techniques (digital LEED, this work) have made it possible to study disordered overlayers. The new digital LEED apparatus is sensitive enough to measure the weak diffuse scattering from disordered CO on Pt(111) to determine its structure. The first surface structure of a disordered molecular adsorbate is presented in this work. DOE

N89-25744# Sandia National Labs., Albuquerque, NM.
FERROELECTRIC POTASSIUM NIOBATE THIN FILMS
B. A. Tuttle, B. C. Bunker, D. L. Lamppa, R. G. Tissot, and J. L. Yio 1989 14 p Presented at the 91st Annual Meeting of the American Ceramic Society, Indianapolis, IN, 23 Apr. 1989
(Contract DE-AC04-76DP-00789)
(DE89-010862; SAND-89-0951C; CONF-890421-5) Avail: NTIS HC A03

We report on the first ferroelectric measurements of chemically prepared KNbO3 thin films. Polycrystalline KNbO3 thin films were fabricated by dip coating substrates with methanolic solutions of potassium hydroxide and niobium bO3 was obtained for both bulk gels and films by using 800 C firing treatments. For films, the intermediate temperature processing schedule was critical for the complete conversion of low temperature phases to perovskite KNbO3. Raman spectroscopy and X-ray diffraction analysis confirmed that properly processed films possessed the orthorhombic distortion of the perovskite structure at room temperature. In response to a 1 kHz, sinusoidal field of 300 kV/cm amplitude, we measured the following ferroelectric properties: (1) a remanent polarization of 4.5 micro-C/sq cm, (2) a spontaneous polarization of 8.3 micro-C/sq cm, and (3) a coercive field of 55 kV/cm. DOE

N89-25745# Los Alamos National Lab., NM.
THE FORMATION AND ANALYSIS OF THIN FILM HIGH TEMPERATURE SUPERCONDUCTORS
Michael Nastasi, Ross E. Muenchausen, and Paul N. Arendt 1989 26 p Presented at the SCANNING '89/EM West, Long Beach, CA, 5 Apr. 1989
(Contract W-7405-eng-36)
(DE89-011177; LA-UR-89-1273; CONF-8904182-2) Avail: NTIS HC A03/MF A01

Thin films of high temperature superconductors have been fabricated using a variety of physical vapor deposition techniques. Recent results of HTS thin films produced by coevaporation, sputtering and laser deposition will be briefly reviewed. In addition some examples of the utility of high energy ion backscattering for the analysis of film stoichiometry will be given. DOE

N89-25746*# Colorado Research Development Corp., Fort Collins.
NARROW BANDGAP SEMICONDUCTING SILICIDES: INTRINSIC INFRARED DETECTORS ON A SILICON CHIP Final Report
John E. Mahan 1989 30 p
(Contract NAS7-950)
(NASA-CR-185372; NAS 1.26:185372) Avail: NTIS HC A03/MF A01 CSCL 20L

Polycrystalline thin films of CrSi2, LaSi2, and ReSi2 were grown on silicon substrates. Normal incidence optical transmittance and reflectance measurements were made as a function of wavelength. It was demonstrated that LaSi2 is a metallic conductor, but that CrSi2 and ReSi2 are, in fact, narrow bandgap semiconductors. For CrSi2, the complex index of refraction was determined by computer analysis of the optical data. From the imaginary part, the optical absorption coefficient was determined as a function of photon energy. It was shown that CrSi2 possesses an indirect forbidden energy gap of slightly less than 0.31 eV, and yet it is a very strong absorber of light above the absorption edge. On the other hand, the ReSi2 films exhibit an absorption edge in the vicinity of 0.2 eV. Measurements of the thermal activation energy of resistivity for ReSi2 indicate a bandgap of 0.18 eV. It is concluded that the semiconducting silicides merit further investigation for development as new silicon-compatible infrared detector materials. Author

N89-25747# Illinois Univ., Urbana-Champaign.
SINGLE CRYSTAL NMR STUDIES OF HIGH TEMPERATURE SUPERCONDUCTORS
C. H. Pennington, D. J. Durand, D. B. Zax, C. P. Slichter, J. P. Rice, E. D. Bukowski, and D. M. Ginsberg 1989 25 p Presented at the High Resolution Nuclear Magnetic Resonance in Solids, Cambridge, MA, 19 Jan. 1989
(Contract DE-AC02-76ER-01198)
(DE89-011220; CONF-890113-1) Avail: NTIS HC A03/MF A01

The authors report Cu NMR studies in the normal state of a single crystal of the T(sub c) = 90 K superconductor YBa2Cu3O(7-delta). The authors have measured the magnetic shift tensor, the electric field gradient tensor, the nuclear spin-lattice relaxation rate tensor, and the time dependence and functional form of the transverse decay. From these data they obtain information about the charge state and magnetic state of the Cu atoms, and the existence and size of the electronic exchange coupling between spins of adjacent Cu atoms. DOE

N89-25748# Sandia National Labs., Albuquerque, NM.
PROCESSING CHEMICALLY PREPARED Tl-Ca-Ba-Cu OXIDE SUPERCONDUCTORS
J. A. Voigt, B. C. Bunker, W. F. Hammetter, D. S. Ginley, E. L. Venturini, J. F. Kwak, and D. L. Lamppa 1988 11 p Presented at the TMS Symposium on High Temperature Superconductors, Las Vegas, NV, 27 Feb. 1989
(Contract DE-AC04-76DP-00789)
(DE89-011535; SAND-88-2296C; CONF-8902100-1) Avail: NTIS HC A03/MF A01

The recently discovered Tl-Ca-Ba-Cu oxide high temperature superconductors have proven difficult to synthesize in phase pure form. Thallium volatility has been difficult to control, and the resulting materials can contain a large number of thallium-containing phases having different compositions and superconducting properties. We have developed a chemical synthesis technique for Tl-based superconductors specifically to prepare materials with enhanced phase purity. The Tl-based powders were made by precipitation from aqueous solution. The desired cation stoichiometry of the precipitate was controlled via the solution compositions. The powders were calcined and sintered into superconducting ceramics with critical current densities of 1570

A/sq cm at 76 K. Investigation of the calcination step has shown the chem-prep powders to be more reactive with respect to the formation of desired superconducting phases than conventionally prepared mixed-oxide precursor powders. Also, the evolution of phases during calcination is dependent on the powder synthesis method. DOE

N89-25749# Oak Ridge National Lab., TN. Solid State Div.
VARIATION OF SUPERLATTICE STRUCTURE OF THE Bi2Sr(2-x)CuO(6-y) SUPERCONDUCTOR WITH COMPOSITION AND THERMAL HISTORY
B. C. Chakoumakos, J. D. Budai, B. C. Sales, and Edward Sonder Apr. 1989 8 p Presented at the Spring Meeting of the Materials Research Society, San Diego, CA, 24 Apr. 1989
(Contract DE-AC05-84OR-21400)
(DE89-011612; CONF-890426-8) Avail: NTIS HC A02/MF A01

Single crystals of Bi2Sr(2-x)CuO(6-y), (0.1 is less than x is less than 0.5, 0 is less than y is less than 0.5), were examined using X-ray diffraction techniques. Diffractometer scans of theta-2theta taken normal to the cleavage planes displayed the even (00l) reflections from l = 2 to 26. Weak satellite peaks were observed on either side of each main (00l) reflection, and their intensities relative to the main peak increased as 2theta was increased. With decreasing Sr content, the satellite peaks systematically moved away from the position of the main reflection. In contrast, the positions of the satellite peaks did not change with oxygen content which was varied by up to 0.5 oxygen atoms per formula unit. Depending on the Sr content of the crystals, generally incommensurate modulations were found with the superstructure periodicity ranging between approximately 1/5b* + 0.29c* and approximately 1/5b* + 0.65c*. The modulation in Bi(2-x)CuO(6-y) has two components. The component along the b* direction is smaller to the superstructure observed in Bi2Sr2CaCu2O7 crystals and thus is probably due to the mismatch between the Bi2O2 layer and the CuO2 layer. The additional component along c* may be due to the ordering of Sr vacancies. DOE

N89-25750# Rochester Univ., NY. Coll. of Engineering and Applied Science.
THERMAL CONDUCTIVITY OF DIELECTRIC THIN FILMS
J. C. Lambropoulos, M. R. Jolly, C. A. Amaden, S. E. Gilman, M. J. Sinicropi, D. Diakomihalis, and S. D. Jacobs May 1989 63 p
(Contract DE-FC03-85DP-40200)
(DE89-011847; DOE/DP-40200/90; LR-202) Avail: NTIS HC A04/MF A01

A direct reading thermal comparator has been used to measure the thermal conductivity of dielectric thin film coatings. In the past, the thermal comparator has been used extensively to measure the thermal conductivity of bulk solids, liquids, and gases. The technique has been extended to thin film materials by making experimental improvements and by the application of an analytical heat flow model. Our technique also allows an estimation of the thermal resistance of the film/substrate interface which is shown to depend on the method of film deposition. The thermal conductivity of most thin films was found to be several orders of magnitude lower than that of the material in bulk form. This difference is attributed to structural disorder of materials deposited in thin film form. The experimentation to date has centered primarily on optical coating materials. These coatings, used to enhance the optical properties of components such as lenses and mirrors, are damaged by thermal loads applied in high-power laser applications. It has been widely postulated that there may be a correlation between the thermal conductivity and the damage threshold of these materials. DOE

N89-25751# Cornell Univ., Ithaca, NY. Dept. of Materials Science and Engineering.
STUDIES OF 3-5 COMPOUNDS IN THE MEGABAR REGIME Annual Progress Report No. 2
A. L. Ruoff Apr. 1989 6 p
(Contract DE-FG02-87ER-45320)
(DE89-012433; DOE/ER-45320/3) Avail: NTIS HC A02/MF A01

In this project we make systematic studies of the crystal structure changes of the 3-5 compounds as a function of pressure. The broad objective of the proposed research is to provide experimental data over a broad range of coordination number and interatomic spacing which can play a leading role in the testing and development of theoretical models of bonding. GaAs has been studied to 108 GPa. The crystal structure of GaAs II was found to form at 16.6 GPa. Subsequent calculations carried out to check this structure by M. Cohen revealed that it did indeed have a lower energy than other structures. DOE

N89-25752# Florida Univ., Gainesville. Dept. of Chemical Engineering.
THE COUPLING OF THERMOCHEMISTRY AND PHASE DIAGRAMS FOR GROUP 3-5 SEMICONDUCTOR SYSTEMS Progress Report, 1 Sep. 1988 - 30 Apr. 1989
T. J. Anderson 1989 70 p
(Contract DE-FG05-86ER-45276)
(DE89-012516; DOE/ER-45276/2) Avail: NTIS HC A04/MF A01

Progress in the third year of this research program has been achieved in three basic areas: measurement of component activities with solid state galvanic cells, thermochemistry and phase diagram assessments, and computation of complex equilibria applied to chemical vapor deposition of compound semiconductors. The activity of In in In-Bi alloys was measured as a function of temperature and composition with a galvanic cell using yttria stabilized zirconia as the solid electrolyte. The activity of Ga in Ga-Bi alloys was determined in a similar solid-state galvanic cell. Coulometric titrations were performed to adjust the composition of Al in Al-In melts. Significant positive deviations were measured in In-rich compositions. Similar titrations were performed in the Al-Sb system. Complex reaction equilibria computations were performed on the Ga-In-As-Cl-H-Si-O and Ge-N-Cl-H system. The first system is important in hydride CVD of Ga(x)In(1-x)As for optoelectronic device applications. The work included the first application of a sensitivity analysis, that suggested the need for an improved thermochemical data base. The effect of various operating parameters on the deposited alloy composition was also studied. In addition, the effect of adding HCl to the mixing zone, the use of liquid Ga-In solution source zone, and the unintentional incorporation of Si were examined. The results of the predictions were verified with experiments by members of our group. Chemical equilibrium calculations were also performed on the Ge-N-Cl-H system to model CVD of Ge3N4. DOE

N89-25753# Florida Univ., Gainesville. Dept. of Physics.
X-RAY SCATTERING STUDIES OF NON-EQUILIBRIUM ORDERING PROCESSES Progress Report, 1 Nov. 1988 - 31 Oct. 1989
S. E. Nagler 1989 35 p
(Contract DE-FG05-86ER-45280)
(DE89-012517; DOE/ER-45280/3) Avail: NTIS HC A03/MF A01

We report on the progress of our project entitled, X-ray Scattering Studies of Non-Equilibrium Ordering Processes. In-house time-resolved X-ray scattering has been used to investigate ordering kinetics in single crystal thin films of Cu3Au. Scaling analysis of the results shows that two dimensional kinetic behavior is observed in 260 A thick films. Significant improvements have been made in the local capabilities for fast time resolved measurements and data analysis. Measurements of microphase separation and ordering kinetics have been made in block-co-polymers, and experiments on Au-Cd martensitic material are continuing. DOE

N89-25754# Brookhaven National Lab., Upton, NY. Accelerator Development Dept.
ELEMENTS OF A SPECIFICATION FOR SUPERCONDUCTING CABLE AND WHY THEY ARE IMPORTANT FOR MAGNET CONSTRUCTION
A. F. Greene and R. M. Scanlan 1989 12 p Presented at

the International Industrial Symposium on the Super Collider, New Orleans, LA, 9-10 Feb. 1989
(Contract DE-AC02-76CH-00016)
(DE89-012533; BNL-42043; CONF-890270-13) Avail: NTIS HC A03/MF A01

The purpose of this paper is to point out several features of the specification for SSC superconducting cable and its insulation that are important for fabrication of dipole magnet coils. Among these are the dimensions of the cable and insulation and their relevance for obtaining coils with appropriate overall dimensions. Other important cable properties are related to the twist direction of wire used to fabricate it and the opposite twist (or lay) direction of the cable. For some coils it is easier to work with cable of a particular lay direction. In conjunction with the ease of coil winding comes the requirement in the specification for superconducting cable which restricts the cable surface condition. The ease of winding coils is governed by the ability to bend and twist the cable at the coil ends without having wires come out of place, possibly later leading to insulation damage and a turn-to-turn short. DOE

N89-25755# California Univ., Berkeley. Lawrence Berkeley Lab. Materials and Chemical Sciences Div.
SQUID CONCEPTS AND SYSTEMS
John Clarke Nov. 1988 64 p Presented at the NATO Advisory Study Institute on Superconducting Electronics, Il Ciocco, Italy, 26 Jun. - 8 Jul. 1988
(Contract DE-AC03-76SF-00098)
(DE89-010384; LBL-26444; CONF-880612-1) Avail: NTIS HC A04/MF A01

In Section 1, I try to give an overview of the current state of the SQUID art. I cannot hope to describe all of the SQUIDs that have been made or, even less, all of the applications in which they have been successfully used. I began, in Sec. 2, with a brief review of the resistively-shunted Josephson junction, with particular emphasis on the effects of noise. Section 3 contains a description of the dc SQUID: how these devices are made and operated, and the limitations imposed by noise. Section 4 contains a similar description of the properties of RF SQUIDs, but because there has been little development of these devices in the 1980's, I shall keep this section relatively brief. In Sec. 5, I described a selection of instruments based on SQUIDs and mention some of their applications. Section 6 contains a discussion of the impact of high temperature superconducting on SQUIDs, and of future prospects in this area, while Sec. 7 contains a few concluding remarks. DOE

N89-25756# Argonne National Lab., IL. Materials and Components Technology Div.
PRODUCTION OF WIRES AND COILS FROM HIGH-TEMPERATURE SUPERCONDUCTING MATERIALS
M. T. Lanagan, U. Balachandran, M. T. Cao, S. E. Dorris, J. T. Dusek, K. C. Goretta, R. B. Poeppel, J. P. Singh, and C. A. Youngdahl Apr. 1989 9 p Presented at the Workshop on High Tc Superconductivity, Huntsville, AL, 23-25 May 1989
(Contract W-31-109-eng-38)
(DE89-012360; CONF-8905133-1) Avail: NTIS HC A02/MF A01

Coils of high T sub c superconductors, which are essential for the development of highly efficient motors and generators, have been fabricated by plastic extrusion. Wires have been extruded in long continuous lengths, wrapped into coils, and subsequently sintered. Coils, 2 cm in diameter and comprising up to 30 turns, have been made with critical current densities of about 200 A/sq cm at 77 K. Critical current density has been found to be dependent on both sintered density and wire geometry. DOE

N89-25757# AEG-Telefunken, Ulm (Germany, F.R.). Semiconductor Technologies.
SUBMICRON TECHNOLOGIES FOR THE FABRICATION OF MONOLITHIC INTEGRATED MILLIMETER WAVE DEVICES ON HIGH RESISTIVITY SILICON Final Report, 30 Jun. 1988
K. Strohm, J.-F. Luy, A. Casel, J. Hersener, H. Jorke, E. Piper, and A. Wilhelm Oct. 1988 128 p Partly in ENGLISH and GERMAN
(Contract BMFT-NT-2706-C9)
(ETN-89-94624) Avail: NTIS HC A07/MF A01

By combining silicon molecular beam epitaxy (Si-MBE) and X-ray lithography a technology was developed for the fabrication of monolithic millimeter wave integrated devices on high resistivity substrates. The MBE was used and investigated for the deposition of the active layers. By improving the dopant method of secondary implantation the Sb doping concentration could be increased. For the deposition of highly doped p+ and n+ contact-layers the method of solid phase epitaxy was investigated and improved. X-ray lithography was successfully applied for the fabrication of sensitive receiver diodes having Schottky anode fingers. To use the high topographic resolution of X-ray lithography, thick process resists were investigated and tested. ESA

77 THERMODYNAMICS AND STATISTICAL PHYSICS

Includes quantum mechanics; theoretical physics; and Bose and Fermi statistics.

For related information see also *25 Inorganic and Physical Chemistry* and *34 Fluid Mechanics and Heat Transfer.*

N89-25758# International Centre for Theoretical Physics, Trieste (Italy).
STRINGS ON HYPERELLIPTIC SUPERSURFACES
C. Crnkovic and G. M. Sotkov Nov. 1988 33 p Submitted for publication
(DE88-705991; IC-88/356) Avail: NTIS (US Sales Only) HC A03/MF A01

Starting from a definition of a hyperelliptic superRiemann surface (HESS), we study its supermoduli space and the superVirasoro algebra on it. We map that algebra into a Z4 (sup p = 2) parafermionic algebra on CP (sup 1,1). Using explicitly supersymmetric bosonization of the first-order superconformal systems, we construct explicitly the primary fields of the parafermionic algebra: the branching and the spin operators. We give a simple prescription for the calculation of sdetD-bar(sub lambda) on HESS through correlation functions of these branching operators. As an example, we calculate the g = 2 superstring partition function and verify that the cosmological constant is zero up to a total derivative in the even moduli. DOE

N89-25759# International Centre for Theoretical Physics, Trieste (Italy).
RENORMALIZATION OF TOPOLOGICAL FIELD THEORY
Danny Birmingham, Mark Rakowski, and George Thompson (Paris VI Univ., France) Nov. 1988 18 p Submitted for publication
(DE88-705998; IC-88/387) Avail: NTIS (US Sales Only) HC A03/MF A01

One loop corrections to topological field theory in three and four dimensions are presented. By regularizing determinants, we compute the effective action and beta-function in four dimensional topological Yang-Mills theory and find that the BRST symmetry is preserved. Moreover, the minima of the effective action still correspond to instanton configurations. In three dimensions, an analysis of the Chern-Simons theory shows that the topological nature of the theory is also preserved to this order. In addition, we find that this theory possesses an extra supersymmetry when quantized in the Landau gauge. Using dimensional regularization, we then study the Ward identities of the extended BRST symmetry in the three dimensional topological Yang-Mills-Higgs model. DOE

N89-25760# Joint Inst. for Nuclear Research, Dubna (USSR). Lab. of Theoretical Physics.
TWO-DIMENSIONAL DENSITY MATRIX AND ITS EQUATIONS. SCALAR AND FERMIONIC FIELDS
Am Gir Li and V. M. Maltsev 1988 17 p In RUSSIAN;

ENGLISH summary
(DE88-706249; JINR-R-2-88-297) Avail: NTIS (US Sales Only) HC A03/MF A01

Two-dimensional density matrix is introduced which (its Wigner transform) satisfies the system of equations: one is the Neumann equation and the other is the new equation. These equations allow one to formulate quantum field theory in the phase space and may serve as input equations of the relativistic quantum statistical mechanics. DOE

N89-25761# California Univ., Berkeley. Lawrence Berkeley Lab.
SYMMETRY BREAKING: THE STANDARD MODEL AND SUPERSTRINGS
Mary K. Gaillard 31 Aug. 1988 14 p Presented at the Topical Conference on Particle Physics and Cosmology, Trieste, Italy, 25 Jul. 1988 Prepared in cooperation with California Univ., Berkeley
(Contract DE-AC03-76SF-00098; NSF PHY-85-15857)
(DE89-011771; LBL-25784; CONF-8807166-1; UCB-PTH-88/20) Avail: NTIS HC A03/MF A01

The outstanding unresolved issue of the highly successful standard model is the origin of electroweak symmetry breaking and of the mechanism that determines its scale, namely the vacuum expectation value (vev)v that is fixed by experiment at the value v = 4m sub w sup 2 / g sup 2 = (the sq root of 2G sub F) sup -1 approx. = 1/4 TeV. Aspects of two approaches to this problem are discussed. One approach is straightforward and down to earth: the search for experimental signatures, as discussed previously by Pierre Darriulat. This approach covers the energy scales accessible to future and present laboratory experiments: roughly (10 sup -9 - 10 cubed)GeV. The second approach involves theoretical speculations, such as technicolor and supersymmetry, that attempt to explain the TeV scale. DOE

N89-25762# Nationaal Inst. voor Kernfysica en Hoge Energiefysica, Amsterdam (Netherlands).
ON THE QUANTUM THEORY OF THE SUPERPARTICLE
J. Kowalski-Glikman and J. W. vanHolten Sep. 1988 7 p Presented at the International Symposium on Spacetime Symmetries, College Park MD, 24-28 May 1988 Sponsored in part by Stichting voor Fundamenteel Onderzoek der Materie, Amsterdam, Netherlands
(NIKHEF-H/88-16; ETN-89-94255) Avail: NTIS HC A02/MF A01

An off-shell formulation of the Brink-Schwarz superparticle is presented. The algebra of Siegel's transformations is closed and abelian. A covariant BRST quantization of the theory is discussed. ESA

80 SOCIAL SCIENCES (GENERAL)

Includes educational matters.

No abstracts in this category.

81 ADMINISTRATION AND MANAGEMENT

Includes management planning and research.

N89-25763*# RMS Technologies, Inc., Landover, MD.
MISSION OPERATIONS AND DATA SYSTEMS DIRECTORATE'S OPERATIONAL/DEVELOPMENT NETWORK (MODNET) AT GODDARD SPACE FLIGHT CENTER Final Report
31 Oct. 1988 47 p
(Contract NAS5-30168)
(NASA-CR-183426; NAS 1.26:183426; Rept-16) Avail: NTIS HC A03/MF A01 CSCL 05A

A brief, informal narrative is provided that summarizes the results of all work accomplished during the period of the contract; June 1, 1987 through September 30, 1988; in support of Mission Operations and Data Systems Directorate's Operational Development Network (MODNET). It includes descriptions of work performed in each functional area and recommendations and conclusions based on the experience and results obtained. Author

N89-25764*# National Aeronautics and Space Administration. Marshall Space Flight Center, Huntsville, AL.
FEDERAL INCENTIVES FOR INDUSTRIAL MODERNIZATION: HISTORICAL REVIEW AND FUTURE OPPORTUNITIES
Sandra C. Coleman and Robert G. Batson (Alabama Univ., Tuscaloosa.) Aug. 1987 37 p Submitted for publication
(NASA-TM-101785; NAS 1.15:101785) Avail: NTIS HC A03/MF A01 CSCL 05A

Concerns over the aging of the U.S. aerospace industrial base led DOD to introduce first its Technology Modernization (Tech Mod) Program, and more recently the Industrial Modernization Incentive Program (IMIP). These incentives include productivity shared savings rewards, contractor investment protection to allow for amortization of plant and equipment, and subcontractor/vendor participation. The purpose here is to review DOD IMIP and to evaluate whether a similar program is feasible for NASA and other non-DOD agencies. The IMIP methodology is of interest to industrial engineers because it provides a structured, disciplined approach to identifying productivity improvement opportunities and documenting their expected benefit. However, it is shown that more research on predicting and validating cost avoidance is needed. Author

N89-25765# Oak Ridge National Lab., TN.
SYSTEMS APPROACH TO PROJECT MANAGEMENT
Larry G. Medley, Sr. Feb. 1989 22 p Presented at the 33rd Annual Meeting of the American Association of Cost Engineers, San Diego, CA, 25 Jun. 1989
(Contract DE-AC05-84OR-21400)
(DE89-008741; CONF-890657-2) Avail: NTIS HC A03/MF A01

In 1979, UCC-ND Engineering management decided to study the overall engineering process in light of new methodologies and management techniques to determine how it could be improved and made more uniform. The system had evolved piecemeal over a period of 36 years. A prime objective was to provide a common framework for understanding the project management process. Systems methodology was chosen as the means for analyzing and integrating a wide variety of activities required for successful project management. This application is very effective and resulted in the creation of a model that serves as the desired framework for understanding project management. Other benefits include improvements to the Engineering Procedures Manual, additional reference material, and enhanced use of a variety of management tools. DOE

N89-25766# Edgerton, Germeshausen and Grier, Inc., Idaho Falls, ID.
APPLYING UNDERSTANDING OF INDIVIDUAL BEHAVIOR AND TEAM DYNAMICS WITHIN THE VALUE ENGINEERING PROCESS
Geoffrey E. Parker 1989 6 p Presented at the Society of American Value Engineers International Conference, Indianapolis, IN, 12 Jun. 1989
(Contract DE-AC07-76ID-01570)
(DE89-011126; EGG-M-89013; CONF-890691-2) Avail: NTIS HC A02/MF A01

This paper describes several new value engineering (VE) process techniques and the individual behavior and team dynamics related to them. DOE

N89-25767 Politecnico di Milano (Italy). Lab. di Calcolatori.
TEMPORAL DATA MANAGEMENT IN REAL-TIME SYSTEMS: A COMPARATIVE VIEW
R. Maiocchi and B. Pernici 1988 56 p
(Rept-88-046; ETN-89-94681) Avail: Politecnico di Milano, Piazza Leonardo da Vinci 32, 20133 Milan, Italy

The requirements of systems for temporal data management are investigated on the basis of a case study. Representative approaches are selected, with the goal of identifying features of systems proposed in different areas. On the basis of this analysis a framework for evaluation of temporal systems and for specifying temporal data management systems for real time applications is proposed. ESA

82 DOCUMENTATION AND INFORMATION SCIENCE

Includes information management; information storage and retrieval technology; technical writing; graphic arts; and micrography.

For computer documentation see *61 Computer Programming and Software.*

N89-25768# Virginia Univ., Charlottesville. Inst. for Parallel Computation.
RELIABILITY MECHANISMS FOR ADAMS (ADVANCED DATA MANAGEMENT SYSTEM)
Sang H. Son and John L. Pfaltz 20 Mar. 1988 21 p Presented at the 3rd Conference on Hypercube Concurrent Computers and Applications, Pasadena, CA, 19 Jan. 1988
(Contract DE-FG05-88ER-25063)
(DE89-010911; CONF-880117-10; IPC-TR-88-002) Avail: NTIS HC A03/MF A01

The goal of checkpointing in database management systems is to save database states on a separate secure device so that the database can be recovered when errors and failures occur. This paper presents a non-interfering checkpointing mechanism being developed for ADAMS. Instead of waiting for a consistent state to occur, our checkpointing approach constructs a state that would result by completing the transactions that are in progress when the global checkpoint begins. The checkpointing algorithm is executed concurrently with transaction activity while constructing a transaction-consistent checkpoint on disk, without requiring the database quiesce. This property of non-interference is highly desirable to real-time applications, where restricting transaction activity during the checkpointing operation is in many cases not feasible. Two main properties of this checkpointing algorithm are global consistency and reduced interference, both of which are crucial for achieving high availability. DOE

N89-25769 Union for Experimenting Coll. and Univ., Yellow Springs, OH.
A THEORETICAL FRAMEWORK AND AN INSTRUCTIONAL MODEL FOR EDUCATING END-USERS OF ONLINE BIBLIOGRAPHIC INFORMATION RETRIEVAL SYSTEMS: A RESEARCH MONOGRAPH Ph.D. Thesis
Mary Margaret Huston 1988 251 p
Avail: Univ. Microfilms Order No. DA8905048

The knowledge used to access information by experienced researchers and inexperienced researchers was identified. Qualitative analysis of the two sets of interview data revealed that both populations described participation in dynamic information networks. However, their information universes were different. Novice researchers described familiarity with everday information gathering through community-based communication networks. Their interviews revealed a sense of the structure and organization of society's information sources and an ability to retrieve information in familiar information environments. In these domains, novices' retrieval experiences were characteristically interactive and generative, as represented by changes in their lines of inquiry. Expert researchers identified themselves as participants in informal and formal scholarly communication networks. To retrieve information, they utilized their knowledge of the interconnections among scholarly information networks to interrogate appropriate access systems for useful substantive or bibliographic references. Through such activities, new knowledge was produced, suggesting that information retrieval functioned as information generation. The study results formed the development of an instructional program, a search guide for end-users of online bibliographic information retrieval systems. Inexperienced researchers' existent knowledge of community-based information networks served as the introductory framework for the search guide. Experienced researchers' knowledge of scholarly communication networks provided additional conceptual information for thinking like a searcher. Dissert. Abstr.

N89-25770 Massachusetts Univ., Amherst.
PROTOTYPING MANAGEMENT INFORMATION SYSTEMS APPLICATION SOFTWARE: AN EMPIRICAL STUDY OF DEVELOPERS' PERCEPTIONS Ph.D. Thesis
David Lawrence Russell 1988 359 p
Avail: Univ. Microfilms Order No. DA8906329

Information systems often are delivered which fail to meet user expectations. One appropriate response is user-involvement in systems design. In recent years, a particular form of user-involvement, prototyping, has gained popularity. When prototyping, the designer and user work together to build the system iteratively. Earlier empirical investigations indicate that the prototyping environment fosters user acceptance and user satisfaction. There are also some indications that prototyped systems require fewer programmer-hours of effort and thus can be delivered at less cost. An unresearched aspect of prototyping the developer's perspective, is addressed. Specifically, the motivation of developers to choose prototyping is investigated. Although there is a broad consensus of opinion regarding what prototyping is, findings indicate that prototypers, as a group, do not believe that prototyping produces systems in significantly less time or at significantly less cost than systems developed in the conventional manner. However, developers do percieve that prototyped systems are of significantly greater quality than conventionally-developed systems. These findings give rise to considerable discussion, in which there exist other motivations for prototyping. A more collegial relationship with clients, a reduction in anxiety when developing systems, and a greater degree of satisfaction are among the factors motivating the choice to prototype. In addition, there exists an indirect economic incentive to prototype, based on the reuse of prototyped modules in subsequent development efforts. Author

N89-25771 California Univ., Los Angeles.
BIBLIOGRAPHIC COUPLING AMONG SCIENTIFIC PAPERS IN BIOLOGICAL RESEARCH SPECIALTIES Ph.D. Thesis
Marilyn Kaye Slater 1988 236 p
Avail: Univ. Microfilms Order No. DA8906125

Bibliographic coupling strength among scientific papers was studied as an information variable and evaluated as an indicator of specialties in biology. Three specialties were identified from corresponding review articles and were characterized along four facets: systems, conditions, observations, and methods. Papers in each sample were assigned a degree of membership in the specialty depending upon facet representation. Specialty samples were used to evaluate two bibliographic coupling measures, author and reference coupling, with regard to: (1) the relation of coupling strength between papers to degree of membership in a specialty, (2) the distribution of coupling strengths among pairs of papers, and (3) the power of each measure to resolve a mixed sample into constituent specialties by cluster analysis. Members of specialties generally exhibited higher bibliographic coupling strengths than did non-members; however, the variability in coupling strengths was high for all degrees of membership. Distribution of coupling strengths among pairs of papers followed a power law, similar to laws of Lotka and Zipf. Author and reference coupling performed well as similarity measures in cluster analyses when combined with group average hierarchical agglomerative clustering.

Resulting cluster patterns showed good resolution of specialties, but author coupling performed somewhat better than reference coupling as a similarity measure. Dissert. Abstr.

N89-25772*# Illinois Univ., Chicago. Dept. of Mathematics, Statistics and Computer Science.
QUERYING DATABASES OF TRAJECTORIES OF DIFFERENTIAL EQUATIONS: DATA STRUCTURES FOR TRAJECTORIES
Robert Grossman Jun. 1989 21 p
(Grant NAG2-513)
(NASA-CR-185040; NAS 1.26:185040) Avail: NTIS HC A03/MF A01 CSCL 05B

One approach to qualitative reasoning about dynamical systems is to extract qualitative information by searching or making queries on databases containing very large numbers of trajectories. The efficiency of such queries depends crucially upon finding an appropriate data structure for trajectories of dynamical systems. Suppose that a large number of parameterized trajectories gamma of a dynamical system evolving in R sup N are stored in a database. Let Eta is contained in set R sup N denote a parameterized path in Euclidean Space, and let the Euclidean Norm denote a norm on the space of paths. A data structure is defined to represent trajectories of dynamical systems, and an algorithm is sketched which answers queries. Author

N89-25773*# Research Inst. for Advanced Computer Science, Moffett Field, CA.
PERFORMANCE ISSUES IN MANAGEMENT OF THE SPACE STATION INFORMATION SYSTEM
Marjory J. Johnson Sep. 1988 22 p Revised
(Contract NCC2-387)
(NASA-CR-185409; NAS 1.26:185409; RIACS-TR-88.22) Avail: NTIS HC A03/MF A01 CSCL 05B

The onboard segment of the Space Station Information System (SSIS), called the Data Management System (DMS), will consist of a Fiber Distributed Data Interface (FDDI) token-ring network. The performance of the DMS in scenarios involving two kinds of network management is analyzed. In the first scenario, how the transmission of routine management messages impacts performance of the DMS is examined. In the second scenario, techniques for ensuring low latency of real-time control messages in an emergency are examined. Author

N89-25774# Oak Ridge National Lab., TN. Information Research and Analysis.
AN EXPERT SYSTEM TO FACILITATE SELECTING A DATABASE MANAGEMENT SYSTEM
L. M. Roseberry and D. C. Kilgore Jun. 1989 7 p Presented at the DOE Technical Information Meeting: INFOTECH, Oak Ridge, TN, 6 Jun. 1989
(Contract DE-AC05-84OR-21400)
(DE89-012350; CONF-8906113-2) Avail: NTIS HC A02/MF A01

An investigation has been initiated to develop an expert system to assist information professionals in selecting a database management system (DBMS). The system attempts to consider DBMS basic design, theory, and performance standard as well as the specific needs of the project. The user is queried for needs, wants, and resource restrictions. The inference engine tests these data against its rule set and generates prioritized recommendations. The rule set design will be discussed. The usefulness of such a tool will be discussed as well as plans for its continued evolution. DOE

N89-25775* National Aeronautics and Space Administration, Washington, DC.
NASA PATENT ABSTRACTS BIBLIOGRAPHY: A CONTINUING BIBLIOGRAPHY. SECTION 1: ABSTRACTS (SUPPLEMENT 35)
Jun. 1989 38 p
(NASA-SP-7039(35)-Sect-1; NAS 1.21:7039(35)-Sect-1) Avail: NTIS HC A03; NTIS standing order as PB89-911100, $13.75 domestic, $27.50 foreign CSCL 05B

Abstracts are provided for 58 patents and patent applications entered into the NASA scientific and technical information systems during the period January 1989 through June 1989. Each entry consists of a citation, an abstract, and in most cases, a key illustration selected from the patent or patent application. Author

N89-25163*# National Aeronautics and Space Administration. Ames Research Center, Moffett Field, CA.
REAL-TIME APPLICATION OF KNOWLEDGE-BASED SYSTEMS
Randal W. Brumbaugh (PRC Systems Services Co., Hampton, VA.) and Eugene L. Duke *In* NASA. Langley Research Center, Recent Advances in Multidisciplinary Analysis and Optimization, Part 1 Apr. 1989 p 357-371 (For primary document see N89-25146 19-05)
Avail: NTIS HC A23/MF A01 CSCL 05B

83 ECONOMICS AND COST ANALYSIS

Includes cost effectiveness studies.

No abstracts in this category.

84 LAW, POLITICAL SCIENCE AND SPACE POLICY

Includes NASA appropriation hearings; aviation law; space law and policy; international law; international cooperation; and patent policy.

N89-25776*# National Academy of Sciences - National Research Council, Washington, DC. Space Science Board.
UNITED STATES AND WESTERN EUROPE COOPERATION IN PLANETARY EXPLORATION
Eugene H. Levy, Donald M. Hunten, Harold Masursky, Frederick L. Scarf, Sean C. Solomon, Laurel L. Wilkening, Hugo Fechtig, Hans Balsiger, Jacques Blamont (Centre National d'Etudes Spatiales, Paris, France), and Marcello Fulchignoni et al 1989 212 p
(Contract NASw-3482)
(NASA-CR-184941; NAS 1.26:184941) Avail: NTIS HC A10/MF A01 CSCL 05A

A framework was sought for U.S.-European cooperation in planetary exploration. Specific issues addressed include: types and levels of possible cooperative activities in the planetary sciences; specific or general scientific areas that seem most promising as the main focus of cooperative efforts; potential mission candidates for cooperative ventures; identification of special issues or problems for resolution by negotiation between the agencies, and possible suggestions for their resolutions; and identification of coordinated technological and instrumental developments for planetary missions. B.G.

85 URBAN TECHNOLOGY AND TRANSPORTATION

Includes applications of space technology to urban problems; technology transfer; technology assessment; and surface and mass transportation.

For related information see also *03 Air Transportation and Safety, 16 Space Transportation,* and *44 Energy Production and Conversion.*

No abstracts in this category.

88 SPACE SCIENCES (GENERAL)

No abstracts in this category.

89 ASTRONOMY

Includes radio, gamma-ray, and infrared astronomy, and astrometry.

N89-25915# British Columbia Univ., Vancouver. Dept. of Geophysics and Astronomy.
OBSERVED p-MODE SPECTRA OF Ap STARS AND THE SUN
Jaymie Matthews *In* ESA, Seismology of the Sun and Sun-Like Stars Dec. 1988 p 547-549 Sponsored by Canadian National Science and Engineering Research Council and a Killam Memorial Postdoctoral Fellowship (For primary document see N89-25819 19-92)
Copyright Avail: NTIS HC A99/MF E03

N89-25916# Observatoire de Paris-Meudon (France).
RAPID PHOTOMETRY OF THE DELTA SCUTI VARIABLE 63 HER
A. Mangeney, M. Chevreton, Juan A. Belmonte, W. Daeppen, O. Saint-Pe, F. Praderie, Teodoro RocaCortes, J. Fuensalida, and M. Alvarez (Universidad Autonoma de Madrid, Cantoblanco, Spain) *In* ESA, Seismology of the Sun and Sun-Like Stars Dec. 1988 p 551-555 (For primary document see N89-25819 19-92)
Copyright Avail: NTIS HC A99/MF E03

N89-25917# Catania Astrophysical Observatory (Italy). Unita di Ricerca di Catania.
SYNTHETIC LIGHT CURVES AND POWER SPECTRA OF DELTA SCUTI STARS: AN APPROACH TO MODELING PULSATIONS
R. Ventura *In* ESA, Seismology of the Sun and Sun-Like Stars Dec. 1988 p 557-562 (For primary document see N89-25819 19-92)
Copyright Avail: NTIS HC A99/MF E03

N89-25919# Birmingham Univ. (England). School of Physics and Space Research.
HIGH PRECISION VELOCITY OBSERVATIONS OF ARCTURUS USING THE 7699 A LINE OF POTASSIUM
J. L. Innis, G. R. Isaak, R. I. Brazier, Juan A. Belmonte, Pere L. Palle, Teodoro RocaCortes, and A. R. Jones (European Space Agency. European Space Research and Technology Center, ESTEC, Noordwijk, Netherlands) *In* ESA, Seismology of the Sun and Sun-Like Stars Dec. 1988 p 569-573 Sponsored by the United Kingdom Science and Engineering Research Council (For primary document see N89-25819 19-92)
Copyright Avail: NTIS HC A99/MF E03

N89-25920# Aarhus Tekniske Bibliotek (Denmark). Inst. of Astronomy.
VARIABLE STAR STATISTICS IN OPEN CLUSTERS: NGC 6192
Soren Frandsen and Hans Kjeldsen *In* ESA, Seismology of the Sun and Sun-Like Stars Dec. 1988 p 575-578 (For primary document see N89-25819 19-92)
Copyright Avail: NTIS HC A99/MF E03

N89-25922# Birmingham Univ. (England). School of Physics and Space Research.
HIGH PRECISION VELOCITY MEASUREMENTS OF PROCYON USING THE 7699 A LINE OF POTASSIUM
J. L. Innis and G. R. Isaak *In* ESA, Seismology of the Sun and Sun-Like Stars Dec. 1988 p 583-586 Sponsored by United Kingdom Science and Engineering Research Council (For primary document see N89-25819 19-92)
Copyright Avail: NTIS HC A99/MF E03

N89-25923# Imperial Coll. of Science and Technology, London (England). Astrophysics Group.
THE SEARCH FOR RADIAL VELOCITY VARIATIONS IN RAPIDLY OSCILLATING Ap STARS USING THE FABRY-PEROT INTERFEROMETRIC STELLAR OSCILLATION SPECTROMETER (FP-ISOS)
M. Leeper, C. R. Bell, K. A. R. B. Pietraszewski, Juan A. Belmonte, Pere L. Palle, Teodoro RocaCortes (Consejo Superior de Investigaciones Cientificas, Tenerife, Spain), and R. E. Renton *In* ESA, Seismology of the Sun and Sun-Like Stars Dec. 1988 p 587-591 (For primary document see N89-25819 19-92)
Copyright Avail: NTIS HC A99/MF E03

N89-25928# Consejo Superior de Investigaciones Cientificas, Tenerife (Spain). Inst. de Astrofisica de Canarias.
SEARCH FOR RAPID OSCILLATIONS IN THE NORTHERN Ap STARS HD62140, HD81009 AND HD22374
Juan A. Belmonte, Pere L. Palle, Teodoro RocaCortes, and Fritz Shoch *In* ESA, Seismology of the Sun and Sun-Like Stars Dec. 1988 p 609-611 (For primary document see N89-25819 19-92)
Copyright Avail: NTIS HC A99/MF E03

N89-25929# Imperial Coll. of Science and Technology, London (England). Astrophysics Group.
A FABRY-PEROT INTERFEROMETRIC STELLAR OSCILLATION SPECTROMETER
C. R. Bell, M. Leeper, and K. A. R. B. Pietraszewski *In* ESA, Seismology of the Sun and Sun-Like Stars Dec. 1988 p 613-616 (For primary document see N89-25819 19-92)
Copyright Avail: NTIS HC A99/MF E03

N89-25930# Osservatorio Meteorologico di Brera, Milan (Italy).
SOME TESTS OF THE PRECISION OF CCD DIFFERENTIAL PHOTOMETRY MEASUREMENTS OF BRIGHT DOUBLE STARS
E. Antonello *In* ESA, Seismology of the Sun and Sun-Like Stars Dec. 1988 p 617-618 (For primary document see N89-25819 19-92)
Copyright Avail: NTIS HC A99/MF E03

N89-25934# Tromsoe Univ. (Norway). Inst. of Mathematical and Physical Sciences.
END POINTS OF STELLAR EVOLUTION INVESTIGATED BY SEISMOLOGY ON WHITE DWARF STARS
J. E. Solheim *In* ESA, Seismology of the Sun and Sun-Like Stars Dec. 1988 p 637-641 (For primary document see N89-25819 19-92)
Copyright Avail: NTIS HC A99/MF E03

N89-25935# Los Alamos National Lab., NM.
SOLAR-LIKE OSCILLATIONS IN LATE SPECTRAL CLASS STARS
Arthur N. Cox and Julius H. Cahn *In* ESA, Seismology of the Sun and Sun-Like Stars Dec. 1988 p 643-647 Previously announced as N89-15837 (For primary document see N89-25819 19-92)
Copyright Avail: NTIS HC A99/MF E03

N89-25936# Yale Univ. Observatory, New Haven, CT.
THE MASS-LUMINOSITY RELATIONSHIP FOR SOLAR-TYPE STARS
William F. vanAltena and John T. Lee *In* ESA, Seismology of the Sun and Sun-Like Stars Dec. 1988 p 649-651 Sponsored in part by NSF, Washington, DC (For primary document see N89-25819 19-92)
Copyright Avail: NTIS HC A99/MF E03

N89-25937# Commissariat a l'Energie Atomique, Saclay (France). Service d'Astrophysique.
EPSILON ERIDANI REVISITED
W. Daeppen and D. Soderblom (Space Telescope Science Inst., Baltimore, MD.) *In* ESA, Seismology of the Sun and Sun-Like Stars Dec. 1988 p 653-655 (For primary document see

N89-25819 19-92)
Copyright Avail: NTIS HC A99/MF E03

N89-25938# Middle East Technical Univ., Ankara (Turkey). Dept. of Physics.
RADIAL VIBRATIONS IN A 5 SOLAR M HYDROGEN-HELIUM STAR
Halil Kirbiyik *In* ESA, Seismology of the Sun and Sun-Like Stars Dec. 1988 p 657-660 (For primary document see N89-25819 19-92)
Copyright Avail: NTIS HC A99/MF E03

N89-25940# Centre National de la Recherche Scientifique, Verrieres-Le Buisson (France). Inst. d'Astrophysique Spatiale.
MUSICOS (MULTI-SITE CONTINUOUS SPECTROSCOPY): OBJECTIVES AND PROSPECTS FOR ASTEROSEISMOLOGY
Bernard H. Foing, C. Catala, and P. Felenbok *In* ESA, Seismology of the Sun and Sun-Like Stars Dec. 1988 p 665-667 (For primary document see N89-25819 19-92)
Copyright Avail: NTIS HC A99/MF E03

90 ASTROPHYSICS

Includes cosmology; celestial mechanics; space plasmas; and interstellar and interplanetary gases and dust.
For related information see also *75 Plasma Physics.*

N89-25777*# Illinois Univ., Urbana-Champaign. Dept. of Physics.
NEUTRON STARS: A COSMIC HADRON PHYSICS LABORATORY
David Pines 1989 23 p Submitted for publication
(Grants NAGw-1583; NSF PHY-86-00377)
(NASA-CR-185051; NAS 1.26:185051) Avail: NTIS HC A03/MF A01 CSCL 03B

A progress report is given on neutron stars as a cosmic hadron physics laboratory. Particular attention is paid to the crustal neutron superfluid, and to the information concerning its properties which may be deduced from observations of pulsar glitches and postglitch behavior. Current observational evidence concerning the softness or stiffness of the high density neutron matter equation of state is reviewed briefly, and the (revolutionary) implications of a confirmation of the existence of a 0.5 ms pulsar at the core of (Supernova) SN1987A are discussed. Author

N89-25778 Princeton Univ., NJ.
COSMOLOGICAL EFFECTS OF SUPERCONDUCTING STRINGS Ph.D. Thesis
Arthur Christopher Thompson 1988 237 p
Avail: Univ. Microfilms Order No. DA8901031

Superconducting cosmic strings can dramatically alter the evolution of the matter-dominated universe. In the presence of an ordered primeval magnetic field, each loop powers a blast wave which can be as large as the voids observed in the distribution of galaxies. The field's strength is similar to that needed to build galactic fields without dynamo amplification. The string network releases energy continuously. Galaxies form only when baryonic matter can move freely through the cosmic background radiation (CBR) and can cool from X-ray temperatures. Heating by strings at z approximately 10(2)-10(5) causes the CBR spectrum significantly to exceed a blackbody in the Wien limit. The predicted angular fluctuations in the CBR are relatively small, because most of the heating occurs while the universe is opaque. Many details of the dynamics of classical strings are special to four spacetime dimensions. The crucial role of kinks is emphasized and it is argued that each loop initially carries a fractal distribution of kinks. The fragmentation of cosmic string loops, including the possibility of a cascade into microscopic fragments, is discussed. The (incomplete) analogy between the dynamics of superconducting strings and Einstein-Maxwell strings is exploited. The rate at which charge carriers are lost from cusps and the critical current for a bosonic superconducting string are determined. Author

N89-25779# Ceskoslovenska Akademie Ved, Ondrejov. Astronomicky Ustav.
INTERPLANETARY MATTER: PROCEEDINGS, VOLUME 2
Zdenek Ceplecha, ed. and Petr Pecina, ed. 1987 302 p Proceedings of the 10th European Regional Astronomy Meeting of the IAU, Prague, Czechoslovakia, 24 Aug. 1987
(DE88-706057; INIS-mf-11359; CONF-8708269) Avail: NTIS (US Sales Only) HC A14/MF A01

Of the total number of 57 presented papers, 56 have been submitted to INIS. One paper was out of INIS scope. List of sessions: Preface, Comets, Asteroids, Meteors, Interplanetary dust, other bodies. DOE

N89-25780*# National Aeronautics and Space Administration. Marshall Space Flight Center, Huntsville, AL.
THE ORIGIN OF ULTRA-COMPACT BINARIES
Izumi Hachisu, Shigeki Miyaji, and Hideyuki Saio (Tokyo Univ., Japan) 1987 43 p Prepared in cooperation with Louisiana State Univ., Baton Rouge; and Chiba Univ. (Japan) Submitted for publication
(NASA-TM-101792; NAS 1.15:101792) Avail: NTIS HC A03/MF A01 CSCL 03B

The origin of ultra-compact binaries composed of a neutron star and a low-mass (about 0.06 solar mass) white dwarf is considered. Taking account of the systemic losses of mass and angular momentum, it was found that a serious difficulty exists in the scenarios which involve tidal captures of a normal star (a main sequence star or a red giant) by a neutron star. This difficulty can be avoided if a red giant star is captured by a massive white dwarf (M is approx. greater than 1.2 solar masses), which becomes a neutron star through the accretion induced collapse. Author

N89-25781# California Univ., Berkeley. Lawrence Berkeley Lab. Theoretical Physics Div.
QUANTUM ONTOLOGIES
Henry P. Stapp Dec. 1988 16 p Presented at the Conference on Bell's Theory, Quantum Theory and Conceptions of the Universe, Fairfax, VA, 20-21 Oct. 1988 Submitted for publication
(Contract DE-AC03-76SF-00098)
(DE89-010385; LBL-26181; CONF-8810257-2) Avail: NTIS HC A03/MF A01

Quantum ontologies are conceptions of the constitution of the universe that are compatible with quantum theory. The ontological orientation is contrasted to the pragmatic orientation of science, and reasons are given for considering quantum ontologies both within science, and in broader contexts. The principal quantum ontologies are described and evaluated. DOE

N89-25782 California Univ., Berkeley.
AMBIPOLAR DIFFUSION AND CORE FORMATION IN MOLECULAR CLOUDS Ph.D. Thesis
Susana Lizano-Soberon 1988 97 p
Avail: Univ. Microfilms Order No. DA8902185

Two dimensional axisymmetric models of the quasistatic formation of cloud cores inside a molecular cloud, due to ambipolar diffusion of the magnetic field were studied. The gas is assumed to be isothermal and a heuristic barotropic turbulent pressure is included to take into account the observed supersonic line widths of molecular line emission in the molecular clouds. The core evolution is studied with varying amounts of turbulent support, using periodic boundary conditions to represent the formation of molecular cloud cores in a much larger cloud. In a very limited search of parameter space, it was shown that the process of ambipolar diffusion can produce dense regions, on a timescale of between 10(6) to 10(7) years depending on the amount of turbulent support, that look like the observed ammonia cores. It was found that turbulence can impede the formation of dense cores, and thus, star formation. A new critical mass M(cr) that includes all available mechanisms of support is also defined. A cloud will undergo dynamical gravitational collapse only if the mass M of the cloud is larger than this critical mass. Otherwise, it will evolve quasistatically by ambipolar diffusion of the magnetic field. Three

interesting regimes for star formation are presented.
Dissert. Abstr.

N89-25783 New Mexico State Univ., University Park.
RIPPLE STRUCTURE IN DEGENERATE ELECTRON GAS-DOMINATED STARS WITH INTENSE MAGNETIC FIELDS Ph.D. Thesis
James Michael Wilkes 1988 176 p
Avail: Univ. Microfilms Order No. DA8905036

Implications of ripple structure, i.e., the appearance of oscillating and discontinuous slopes in the thermodynamic variables of a degenerate electron gas, for models of magnetic stars dominated by such a gas were investigated. The effects in these models of the recent discovery by R. L. Ingraham that strong magnetic fields can inhibit degeneracy in an electron gas was examined. A theory of self-gravitating fluids is presented. The theory predicts the existence of an anisotropic pressure tensor in such a fluid, which is in agreement with the one known to occur in the special case of a free-electron gas in a magnetic field. Also, the theory clarifies the relation between this pressure tensor and the scalar thermodynamic pressure, and provides an unambiguous prescription for the incorporation of these and other variables, such as the magnetization, in the fluid equations of motion. It is shown that under suitable assumptions the usual thermodynamic equilibrium and stability conditions for such a fluid follow from the general theory. A definition of local thermodynamic equilibrium is used to develop local equilibrium statistical mechanics of ideal gases. From this the equations of state for an ideal free-electron gas in a magnetic field are derived. These equations of state are used in a simplified system of structure equations for model stars in intense magnetic fields. The effects of degeneracy-inhibition are small in these models. However, ripple structure is strikingly evident in both the density profiles and mass curves of our model stars. Narrow forbidden bands for the model stellar masses are found in the mass curves. Dissert. Abstr.

N89-25784# California Univ., Berkeley. Lawrence Berkeley Lab. Nuclear Science Div.
PHYSICS OF DENSE MATTER, NEUTRON STARS AND SUPERNOVA
Norman K. Glendenning Feb. 1989 8 p Presented at the 5th Workshop on Nuclear Astrophysics, Tegernsee, Fed. Republic of Germany, 30 Jan. 1989
(Contract DE-AC03-76SF-00098)
(DE89-010673; LBL-26895; CONF-8901121-1) Avail: NTIS HC A02/MF A01

Nuclear and astrophysical evidence on the equation of state of dense matter is examined. The role of hyperonization of matter in the development of proto-neutron stars is briefly discussed.
DOE

N89-25785# Fermi National Accelerator Lab., Batavia, IL.
DARK MATTER AND SUPERSYMMETRY
G. F. Giudice Jan. 1989 15 p Presented at the Beyond the Standard Model, Ames, IA, 18-20 Nov. 1988
(Contract DE-AC02-76CH-03000)
(DE89-011068; FNAL/C-89/15-T; CONF-8811175-3) Avail: NTIS HC A03/MF A01

Reviewed are the possible candidates for cold dark matter suggested by supersymmetric theories and the prospects for their experimental search are discussed. DOE

N89-25786# Los Alamos National Lab., NM.
REMINISCENCE OF A STELLAR PULSATION THEORIST
Cecil G. Davis 1989 11 p Presented at the NATO Advanced Research Workshop on the Numerical Modeling of Nonlinear Stellar Pulsation, Savoie, France, 20-24 Mar. 1989
(Contract W-7405-eng-36)
(DE89-011165; LA-UR-89-1459; CONF-8903121-1) Avail: NTIS HC A03/MF A01

The author started working in stellar pulsation theory in 1965. Since this time, we have studied the effects of improved radiative transfer and dynamic zoning on models of Cepheids, RR Lyrae, and W Virginis stars. In this paper we discuss the relevant equations and some results in comparisons to observations of W Virginis and long-period Cepheids. Some suggestions for the next generation of stellar pulsation codes is given. DOE

N89-25787# Brookhaven National Lab., Upton, NY. Physics Dept.
NUCLEAR ASTROPHYSICS OF SUPERNOVAE
J. Cooperstein 1988 42 p Presented in Lecture at Summer School in Nuclear Physics, Corvallis, OR, 17 Jun. - 8 Jul. 1988
(Contract DE-AC02-76CH-00016)
(DE89-012534; BNL-42605) Avail: NTIS HC A03/MF A01

In this paper, I'll give a general introduction to Supernova Theory, beginning with the presupernova evolution and ending with the later stages of the explosion. This will be distilled from a colloquium type of talk. It is necessary to have the whole supernova picture in one's mind's eye when diving into some of its nooks and crannies, as it is quite a mess of contradictory ingredients. We will have some discussion of supernova 1987a, but will keep our discussion more general. Second, we'll look at the infall and bounce of the star, seeing why it goes unstable, what dynamics it follows as it collapses, and how and why it bounces back. From there, we will go on to look at the equation of state (EOS) in more detail. We'll consider the cases T = 0 and T greater than 0. We'll focus on rho less than rho(0), and then rho greater than rho(0) and the EOS of neutron stars, and whether or not they contain cores of strange matter. There are many things we could discuss here and not enough time. If I had more lectures, the remaining time would focus on two more questions of special interest to nuclear physicists: the electron capture reactions and neutrino transport. If time permitted, we'd have some discussion of the nucleosynthetic reactions in the explosion's debris as well. However, we cannot cover such material adequately, and I have chosen these topics because they are analytically tractable, pedagogically useful, and rather important. DOE

N89-25788*# Fermi National Accelerator Lab., Batavia, IL. Astrophysics Center.
EVOLUTION OF COSMIC STRING NETWORKS
Andreas Albrecht and Neil Turok (Princeton Univ., NJ.) Jun. 1989 9 p
(Grant NAGw-1340)
(NASA-CR-185467; NAS 1.26:185467; FERMILAB-Pub-89/140-A; PUPT-89-1133) Avail: NTIS HC A02/MF A01 CSCL 03B

Results on cosmic strings are summarized including: (1) the application of non-equilibrium statistical mechanics to cosmic string evolution; (2) a simple one scale model for the long strings which has a great deal of predictive power; (3) results from large scale numerical simulations; and (4) a discussion of the observational consequences of our results. An upper bound on G mu of approximately 10(-7) emerges from the millisecond pulsar gravity wave bound. How numerical uncertainties affect this are discussed. Any changes which weaken the bound would probably also give the long strings the dominant role in producing observational consequences.
Author

N89-25789*# Fermi National Accelerator Lab., Batavia, IL. Astrophysics Center.
PAIR PRODUCTION OF HELICITY-FLIPPED NEUTRINOS IN SUPERNOVAE
Armando Perez and Raj Gandhi (Nationaal Inst. voor Kernfysica en Hoge Energiefysica, Amsterdam, Netherlands) 3 Jul. 1989 16 p Prepared in cooperation with Valencia Univ. (Spai n)
(Grant NAGw-1340)
(NASA-CR-185466; NAS 1.26:185466; FERMILAB-Pub-89/156-A) Avail: NTIS HC A03/MF A01 CSCL 03B

The emissivity was calculated for the pair production of helicity-flipped neutrinos, in a way that can be used in supernova calculations. Also presented are simple estimates which show that such process can act as an efficient energy-loss mechanism in the shocked supernova core, and this fact is used to extract neutrino mass limits from SN 1987A neutrino observations.
Author

N89-25729 Tuebingen Univ. (Germany, F.R.). Lehr- und Forschungsbereich Theoretische Astrophysik.
PARTICLE SIMULATION FOR ACCRETION SHEETS IN NARROW DOUBLE STARS [TEILCHENSIMULATION FUER AKKRETIONSSCHEIBEN IN ENGEN DOPPELSTERNSYSTEMEN]
F. Geyer, H. Herold, and H. Ruder *In* Max-Planck-Inst. fuer Physik und Astrophysik, Cosmic Plasma Physics Nov. 1988 p 90-97 In GERMAN Sponsored by the Deutsche Forschungsgemeinschaft, Bonn, Federal Republic of Germany (For primary document see N89-25716 19-75)
Copyright Avail: Max-Planck-Inst. fuer Physik und Astrophysik, D-8046 Garching bei Muenchen, Fed. Republic of Germany

N89-25828# Cambridge Univ. (England). Inst. of Astronomy.
ON RADIATIVE AND CONVECTIVE INFLUENCES ON STELLAR PULSATIONAL STABILITY
N. J. Balmforth and Douglas O. Gough *In* ESA, Seismology of the Sun and Sun-Like Stars Dec. 1988 p 47-52 Sponsored by the United Kingdon Science and Engineering Research Council and the Dee Corp. (For primary document see N89-25819 19-92)
Copyright Avail: NTIS HC A99/MF E03

91 LUNAR AND PLANETARY EXPLORATION

Includes planetology; and manned and unmanned flights. For spacecraft design or space stations see *18 Spacecraft Design, Testing and Performance.*

N89-25790*# Lunar and Planetary Inst., Houston, TX.
MECA WORKSHOP ON ATMOSPHERIC H2O OBSERVATIONS OF EARTH AND MARS. PHYSICAL PROCESSES, MEASUREMENTS AND INTERPRETATIONS
Stephen M. Clifford, ed. and Robert M. Haberle, ed. 1988 95 p Workshop held in Houston, TX, 25-27 Sep. 1986 (Contract NASw-4066)
(NASA-CR-183335; NAS 1.26:183335; LPI-TR-88-10) Avail: NTIS HC A05/MF A01 CSCL 03B

The workshop was held to discuss a variety of questions related to the detection and cycling of atmospheric water. Among the questions addressed were: what factors govern the storage and exchange of water between planetary surfaces and atmospheres; what instruments are best suited for the measurement and mapping of atmospheric water; do regolith sources and sinks of water have uniquely identifiable column abundance signatures; what degree of time and spatial resolution in column abundance data is necessary to determine dynamic behavior. Of special importance is the question, does the understanding of how atmospheric water is cycled on Earth provide any insights for the interpretation of Mars atmospheric data. For individual titles, see N89-25791 through N89-25814.

N89-25791*# Texas A&M Univ., College Station.
WATER IN THE MARTIAN REGOLITH
Duwayne M. Anderson *In* Lunar and Planetary Inst., MECA Workshop on Atmospheric H2O Observations of Earth and Mars. Physical Processes, Measurements and Interpretations 1988 p 11-18 (For primary document see N89-25790 19-91)
Avail: NTIS HC A05/MF A01 CSCL 03B

The state of water in the Martian regolith is addressed. The water-ice phase composition, adsorption-desorption and evaporation phenomena, and brine compositions of six antarctic soils that are considered to be good terrestrial analogues of the Martian surface materials are examined. Experiments have shown that, for temperatures below freezing and relative humidities less than 100 percent, absorbed water and vapor are the only stable phases in the regolith. When the relative humidity reaches 100 percent, ice may form and coexist with the absorbed liquid phase. The absorbed water content declines with decreasing temperature; however, the presence of dissolved solutes can result in appreciable adsorbed liquid phase at temperatures as low as 210 K. Such properties may have a profound influence on martial geomorphology, physical and chemical weathering, and the exchange of water between the atmosphere and regolith. E.R.

N89-25792*# Oregon State Univ., Corvallis. Dept. of Atmospheric Sciences.
TRANSPORT OF MARS ATMOSPHERIC WATER INTO HIGH NORTHERN LATITUDES DURING A POLAR WARMING
J. R. Barnes and J. L. Hollingsworth *In* Lunar and Planetary Inst., MECA Workshop on Atmospheric H2O Observations of Earth and Mars. Physical Processes, Measurements and Interpretations 1988 p 19-21 (For primary document see N89-25790 19-91)
Avail: NTIS HC A05/MF A01 CSCL 03B

Several numerical experiments were conducted with a simplified tracer transport model in order to attempt to examine the poleward transport of Mars atmospheric water during a polar warming like that which occurred during the winter solstice dust storm of 1977. The flow for the transport experiments was taken from numerical simulations with a nonlinear beta-plane dynamical model. Previous studies with this model have demonstrated that a polar warming having essential characteristics like those observed during the 1977 dust storm can be produced by a planetary wave mechanism analogous to that responsible for terrestrial sudden stratospheric warmings. Several numerical experiments intended to simulate water transport in the absence of any condensation were carried out. These experiments indicate that the flow during a polar warming can transport very substantial amounts of water to high northern latitudes, given that the water does not condense and fall out before reaching the polar region. Author

N89-25793*# Iowa State Univ. of Science and Technology, Ames. Dept. of Earth Sciences.
THE EFFECT OF GLOBAL-SCALE DIVERGENT CIRCULATION ON THE ATMOSPHERIC WATER VAPOR TRANSPORT AND MAINTENANCE c46
Tsing-Chang Chen *In* Lunar and Planetary Inst., MECA Workshop on Atmospheric H2O Observations of Earth and Mars. Physical Processes, Measurements and Interpretations 1988 p 22-28 (For primary document see N89-25790 19-91)
(Grant NSF ATM-86-11476)
Avail: NTIS HC A05/MF A01 CSCL 04A

The detection, distribution, and dynamics of atmospheric water on Earth was examined. How the high levels of water vapor and precipitation that occur over the tropics during the monsoon season result from the development of a strong divergent atmospheric circulation is discussed. Author

N89-25794*# Arizona State Univ., Tempe. Dept. of Geology.
SEASONAL AND DIURNAL VARIABILITY OF MARS WATER-ICE CLOUDS Abstract Only
Philip R. Christensen, Richard W. Zurek (Jet Propulsion Lab., California Inst. of Tech., Pasadena.), and L. L. Jaramillo *In* Lunar and Planetary Inst., MECA Workshop on Atmospheric H2O Observations of Earth and Mars. Physical Processes, Measurements and Interpretations 1988 p 29-30 (For primary document see N89-25790 19-91)
Avail: NTIS HC A05/MF A01 CSCL 03B

The diurnal and seasonal behavior of cloud opacity and frequency of occurrence was studied using an atlas of cloud occurrences compiled from the Viking IRTM (Infrared Thermal Mapper) data set. It was found that in some areas the behavior of water appeared to repeat in the zonal mean. However, this interpretation is complicated by both poor coverage and the variability of dust and clouds. As a result, the extent and nature of interannual variability remains unclear. Author

N89-25795*# Lunar and Planetary Inst., Houston, TX.
THE INTERPRETATION OF DATA FROM THE VIKING MARS ATMOSPHERIC WATER DETECTORS (MAWD): SOME POINTS FOR DISCUSSION
Stephen M. Clifford *In its* MECA Workshop on Atmospheric H2O Observations of Earth and Mars. Physical Processes,

Measurements and Interpretations 1988 p 31-32 (For primary document see N89-25790 19-91)
Avail: NTIS HC A05/MF A01 CSCL 03B

Properly interpreted, water vapor column abundance measurements can provide important insights into many of the processes that govern the diurnal, seasonal, and climatic cycles of atmospheric water on Mars. The uncertain distribution of water vapor complicates this analysis. It is argued that if a significant fraction of the total atmospheric vapor content is concentrated within the lowermost scale height, then the hemispheric asymmetry in zonally averaged topography/air mass might itself explain the observed gradient in the annual and zonally averaged vapor abundance. Author

N89-25796*# Lunar and Planetary Inst., Houston, TX.
REGOLITH WATER VAPOR SOURCES ON MARS: A HISTORICAL BIBLIOGRAPHY
Stephen M. Clifford and R. L. Huguenin *In its* MECA Workshop on Atmospheric H2O Observations of Earth and Mars. Physical Processes, Measurements and Interpretations 1988 p 33-36 (For primary document see N89-25790 19-91)
(Grants NsG-7405; NsG-7397; NAGw-40)
Avail: NTIS HC A05/MF A01 CSCL 03B

The regolith as a potential source and sink of atmospheric water is examined bibliographically. The controversy surrounding Solis Lacus, a region on Mars first identified by R. Huguenin as a possible regolith source of atmospheric water vapor, is reviewed. The publications listed describe the initial debate over the existence of a regolith source of atmospheric water vapor in Solis Lacus. The debate over Solis Lacus has motivated a rigorous examination of several important data sets, and helped define the limits of their interpretation. Author

N89-25797*# National Aeronautics and Space Administration. Ames Research Center, Moffett Field, CA.
FACTORS GOVERNING WATER CONDENSATION IN THE MARTIAN ATMOSPHERE
David S. Colburn, J. B. Pollack, and Robert M. Haberle *In* Lunar and Planetary Inst., MECA Workshop on Atmospheric H2O Observations of Earth and Mars. Physical Processes, Measurements and Interpretations 1988 p 37-40 (For primary document see N89-25790 19-91)
Avail: NTIS HC A05/MF A01 CSCL 03B

Modeling results are presented suggesting a diurnal condensation cycle at high altitudes at some seasons and latitudes. In a previous paper, the use of atmospheric optical depth measurements at the Viking lander site to show diurnal variability of water condensation at different seasons of the Mars year was described. Factors influencing the amount of condensation include latitude, season, atmospheric dust content and water vapor content at the observation site. A one-dimensional radiative-convective model is used herein based on the diabatic heating routines under development for the Mars General Circulation Model. The model predicts atmospheric temperature profiles at any latitude, season, time of day and dust load. From these profiles and an estimate of the water vapor, one can estimate the maximum occurring at an early morning hour (AM) and the minimum in the late afternoon (PM). Measured variations in the atmospheric optical density between AM and PM measurements were interpreted as differences in AM and PM condensation. Author

N89-25798*# National Center for Atmospheric Research, Boulder, CO.
CUMULUS CONVECTION AND THE TERRESTRIAL WATER-VAPOR DISTRIBUTION **c46**
Leo J. Donner *In* Lunar and Planetary Inst., MECA Workshop on Atmospheric H2O Observations of Earth and Mars. Physical Processes, Measurements and Interpretations 1988 p 41-45 (For primary document see N89-25790 19-91)
Avail: NTIS HC A05/MF A01 CSCL 04A

Cumulus convection plays a significant role in determining the structure of the terrestrial water vapor field. Cumulus convection acts directly on the moisture field by condensing and precipitating water vapor and by redistributing water vapor through cumulus induced eddy circulations. The mechanisms by which cumulus convection influences the terrestrial water vapor distribution is outlined. Calculations using a theory due to Kuo is used to illustrate the mechanisms by which cumulus convection works. Understanding of these processes greatly aids the ability of researchers to interpret the seasonal and spatial distribution of atmospheric water vapor by providing information on the nature of sources and sinks and the global circulation. Author

N89-25799*# National Aeronautics and Space Administration. Lyndon B. Johnson Space Center, Houston, TX.
POSSIBLE SIGNIFICANCE OF CUBIC WATER-ICE, H2O-Ic, IN THE ATMOSPHERIC WATER CYCLE OF MARS
James L. Gooding *In* Lunar and Planetary Inst., MECA Workshop on Atmospheric H2O Observations of Earth and Mars. Physical Processes, Measurements and Interpretations 1988 p 46-49 (For primary document see N89-25790 19-91)
Avail: NTIS HC A05/MF A01 CSCL 03B

The possible formation and potential significance of the cubic ice polymorph on Mars is discussed. When water-ice crystallizes on Earth, the ambient conditions of temperature and pressure result in the formation of the hexagonal ice polymorph; however, on Mars, the much lower termperature and pressures may permit the crystallization of the cubic polymorph. Cubic ice has two properties of possible importance on Mars: it is an excellant nucleator of other volatiles (such as CO2), and it undergoes an exothermic transition to hexagonal ice at temperatures above 170 K. These properties may have significant implications for both martian cloud formation and the development of the seasonal polar caps. Author

N89-25800*# National Aeronautics and Space Administration. Ames Research Center, Moffett Field, CA.
ON THE VERTICAL DISTRIBUTION OF WATER VAPOR IN THE MARTIAN TROPICS
Robert M. Haberle *In* Lunar and Planetary Inst., MECA Workshop on Atmospheric H2O Observations of Earth and Mars. Physical Processes, Measurements and Interpretations 1988 p 50-52 (For primary document see N89-25790 19-91)
Avail: NTIS HC A05/MF A01 CSCL 03B

Although measurements of the column abundance of atmospheric water vapor on Mars have been made, measurements of its vertical distribution have not. How water is distributed in the vertical is fundamental to atmosphere-surface exchange processes, and especially to transport within the atmosphere. Several lines of evidence suggest that in the lowest several scale heights of the atmosphere, water vapor is nearly uniformly distributed. However, most of these arguments are suggestive rather than conclusive since they only demonstrate that the altitude to saturation is very high if the observed amount of water vapor is distributed uniformly. A simple argument is presented, independent of the saturation constraint, which suggests that in tropical regions, water vapor on Mars should be very nearly uniformly mixed on an annual and zonally averaged basis. Author

N89-25801*# Colorado Univ., Boulder. Lab. for Atmospheric and Space Physics.
THE BEHAVIOR OF WATER VAPOR IN THE MARS ATMOSPHERE Abstract Only
Bruce M. Jakosky *In* Lunar and Planetary Inst., MECA Workshop on Atmospheric H2O Observations of Earth and Mars. Physical Processes, Measurements and Interpretations 1988 p 53 (For primary document see N89-25790 19-91)
Avail: NTIS HC A05/MF A01 CSCL 03B

The behavior of water vapor in the atmosphere of Mars is important to understanding the Mars climate and its evolution as well as the nature of ongoing seasonal processes of exchange and transport. On the seasonal timescales, exchange of water between the atmosphere, regolith, and polar caps combine with advection of water and the possible saturation at some locations and seasons in order to produce the observed distribution of water. A summary of the observations made by the Mariner and Viking

spacecraft and analyses of the seasonal cycle of water is presented, along with a brief discussion of the implications for the long term variability of water. The upcoming Mars Observer mission is also briefly discussed. Author

N89-25802*# Colorado Univ., Boulder. Lab. for Atmospheric and Space Physics.
SOLAR MESOSPHERE EXPLORER OBSERVATIONS OF STRATOSPHERIC AND MESOSPHERIC WATER VAPOR Abstract Only **c46**
Bruce M. Jakosky, Gary E. Thomas, David W. Rusch, Charles A. Barth, George M. Lawrence, John J. Olivero (Pennsylvania State Univ., University Park.), R. Todd Clancy, Ryan W. Sanders, and Barry G. Knapp *In* Lunar and Planetary Inst., MECA Workshop on Atmospheric H2O Observations of Earth and Mars. Physical Processes, Measurements and Interpretations 1988 p 54-55 Prepared in cooperation with NOAA, Washington, DC (For primary document see N89-25790 19-91)
Avail: NTIS HC A05/MF A01 CSCL 04A

It is noted that while the SME (Solar Mesosphere Explorer) data is consistent with the earlier LIMS (Limb Infrared Monitor of the Stratosphere) results, its interpretation is complicated by aerosol contamination, particularly at altitudes below 35 km. This contamination arose from several volcanic eruptions, including that of El Chichon. Analyses are reported of a subset of data from the SME satellite, concentrating primarily on the period January through March 1982 so as to avoid contamination from the El Chichon volcanic aerosol. The SME observations of water vapor between 20 and 60 km were inverted for the first three months of 1982 as well as for selected additional periods. Reasonable results are obtained at locations where no contamination by aerosol is suspected. Author

N89-25803*# Missouri Univ., Saint Louis.
CIRCUMPOLAR HOODS AND CLOUDS AND THEIR RELATION TO THE MARTIAN H2O CYCLE
Philip B. James and L. J. Martin (Lowell Observatory, Flagstaff, AZ.) *In* Lunar and Planetary Inst., MECA Workshop on Atmospheric H2O Observations of Earth and Mars. Physical Processes, Measurements and Interpretations 1988 p 56-57 (For primary document see N89-25790 19-91)
(Grants NAGw-742; NAGw-638)
Avail: NTIS HC A05/MF A01 CSCL 03B

Water exists in both vapor and solid phases in the Martian atmosphere. The polar hoods are shrouds of condensate clouds which obscure both polar regions at times during their respective fall and winter seasons. The hemispheric asymmetries in the polar hood clouds are reviewed and their significance to the seasonal water cycle is discussed. Comparisons of images acquired using short wavelength filters, which provide maximum cloud contrast, and long wavelength filters, which are sensitive to surface features including the surface cap, provide correlations between cloud formation and large scale planetary dynamics. Author

N89-25804*# Cornell Univ., Ithaca, NY.
VERY HIGH ELEVATION WATER ICE CLOUDS ON MARS: THEIR MORPHOLOGY AND TEMPORAL BEHAVIOR
Fred Jaquin *In* Lunar and Planetary Inst., MECA Workshop on Atmospheric H2O Observations of Earth and Mars. Physical Processes, Measurements and Interpretations 1988 p 58-61 (For primary document see N89-25790 19-91)
Avail: NTIS HC A05/MF A01 CSCL 03B

Quantitative analysis of Viking images of the martian planetary limb has uncovered the existence and temporal behavior of water ice clouds that form between 50 and 90 km elevation. These clouds show a seasonal behavior that may be correlated with lower atmosphere dynamics. Enhanced vertical mixing of the atmosphere as Mars nears perihelion is hypothesized as the cause of the seasonal dependence, and the diurnal dependence is explained by the temporal behavior of the martian diurnal thermal tide. Viking images also provide a data set of the vertical distribution of aerosols in the martian atmosphere. The temporal and spatial distribution of aerosols are characterized. Author

N89-25805*# National Aeronautics and Space Administration. Langley Research Center, Hampton, VA.
OBSERVATIONS OF ATMOSPHERIC WATER VAPOR WITH THE SAGE 2 INSTRUMENT **c46**
Jack C. Larsen (SASC Technologies, Inc., Hampton, VA.), M. P. McCormick, L. R. McMaster, and W. P. Chu *In* Lunar and Planetary Inst., MECA Workshop on Atmospheric H2O Observations of Earth and Mars. Physical Processes, Measurements and Interpretations 1988 p 62-66 (For primary document see N89-25790 19-91)
(Contract NAS1-17022)
Avail: NTIS HC A05/MF A01 CSCL 04A

The Stratospheric Aerosol and Gas Experiment 2 (SAGE 2) is discussed. The SAGE 2 instrument was a multichannel spectrometer that inferred the vertical distribution of water vapor, aerosols, nitrogen dioxide, and ozone by measuring the extinction of solar radiation at spacecraft sunrise/sunset. At altitudes above 20 km, the SAGE 2 and LIMS (Limb Infrared Monitor of the Stratosphere) data are in close agreement. The discrepancies below this altitude may be attributed to differences in the instruments' field of view and time of data acquisition. Author

N89-25806*# Lunar and Planetary Inst., Houston, TX.
FLUX OF WATER VAPOR IN THE TERRESTRIAL STRATOSPHERE AND IN THE MARTIAN ATMOSPHERE **c46**
Conway Leovy, Matthew Hitchman, and Daniel J. McCleese (Jet Propulsion Lab., California Inst. of Tech., Pasadena.) *In its* MECA Workshop on Atmospheric H2O Observations of Earth and Mars. Physical Processes, Measurements and Interpretations 1988 p 67-69 (For primary document see N89-25790 19-91)
Avail: NTIS HC A05/MF A01 CSCL 04A

A summary of the terrestrial satellite data is presented. The observations indicate that at equatorial latitudes, relatively dry air is introduced at the tropopause and carried to the upper stratosphere. At that altitude, any methane present in the ascending air mass is oxidized photochemically into water vapor. This vapor is eventually transported to high latitudes, where it is carried to the lower stratosphere by the descending leg of the diabatic circulation. The Pressure Modulator Infrared Radiometer instrument aboard the Mars Observer should provide a comparable picture of vapor transport in the martian atmosphere. Author

N89-25807*# Cornell Univ., Ithaca, NY. Dept. of Agronomy.
REGELATION AND ICE SEGREGATION Abstract Only
Robert D. Miller *In* Lunar and Planetary Inst., MECA Workshop on Atmospheric H2O Observations of Earth and Mars. Physical Processes, Measurements and Interpretations 1988 p 70 (For primary document see N89-25790 19-91)
Avail: NTIS HC A05/MF A01 CSCL 03B

Macroscopic processes can have an important effect on the state of regolith water. The two primary mechanisms responsible for the formation of segregated ice on Earth, thermally induced regelation and hydraulic fracturing, are reviewed while their potential importance on Mars is examined. While regelation is the dominant terrestrial process, it requires a warmer and wetter environment than currently exists on Mars. In this respect, the conditions required for hydraulic fracturing are less demanding. In assessing its potential importance on Mars, it is noted that hydraulic fracturing can produce a localized zone of high pressure water that could readily disrupt an overburden of frozen ground. Such a process, it is concluded, may have triggered the release of groundwater that led to the formation of the major outflow channels. Author

N89-25808*# Pennsylvania State Univ., University Park. Dept. of Meteorology.
MEASUREMENTS OF H2O IN THE TERRESTRIAL MESOSPHERE AND IMPLICATIONS FOR EXTRA-TERRESTRIAL SOURCES **c46**
John J. Olivero *In* Lunar and Planetary Inst., MECA Workshop on Atmospheric H2O Observations of Earth and Mars. Physical Processes, Measurements and Interpretations 1988 p 71-74 (For primary document see N89-25790 19-91)
Avail: NTIS HC A05/MF A01 CSCL 04A

Recent measurements of mesospheric water vapor and their implications for the existence of extraterrestrial sources of water are discussed. This study was prompted by the work of L. Frank and others who, based on their interpretation of transient dark spots visible in ultraviolet images of the Earth's dayglow emission, have proposed that a large flux of small comets enters the Earth's upper atmosphere each day. To date, however, analysis does not conclusively refute or support the idea of an external source.
Author

N89-25809*# Commonwealth Scientific and Industrial Research Organization, Canberra (Australia). Div. of Environmental Mechanics.
DIURNAL AND ANNUAL CYCLES OF H2O IN THE MARTIAN REGOLITH
John R. Philip *In* Lunar and Planetary Inst., MECA Workshop on Atmospheric H2O Observations of Earth and Mars. Physical Processes, Measurements and Interpretations 1988 p 75-79 (For primary document see N89-25790 19-91)
Avail: NTIS HC A05/MF A01 CSCL 03B

The atmospheric heat engines of Earth and Mars are compared. Although water latent heat transfer drives the circulation of the Earth's atmosphere, particularly in the tropics, its contribution to the circulation of the martian atmosphere is negligible. The working fluid on Mars is CO2, which exerts its greatest influence on atmospheric circulation at the poles. The diurnal and seasonal flux of water within the martian regolith is also examined. Calculations indicate that, for a mean annual temperature of 200 K, a diurnal and annual temperature variation of 30 K will drive a maximum exchange of 1.2 pr micrometer and 120 pr micrometer of water, respectively.
Author

N89-25810*# National Aeronautics and Space Administration. Langley Research Center, Hampton, VA.
THE NIMBUS 7 LIMS (LIMB INFRARED MONITOR OF THE STRATOSPHERE) WATER VAPOR MEASUREMENTS c46
Ellis E. Remsberg and James M. Russell, III *In* Lunar and Planetary Inst., MECA Workshop on Atmospheric H2O Observations of Earth and Mars. Physical Processes, Measurements and Interpretations 1988 p 80-81 (For primary document see N89-25790 19-91)
Avail: NTIS HC A05/MF A01 CSCL 04A

Earth orbital instruments, designed to measure the vertical and spatial distribution of atmospheric water vapor is discussed. Specifically, the operation of the Limb Infrared Monitor of the Stratosphere (LIMS) experiment is examined. The LIMS is a six channel limb scanning radiometer that was launched aboard Nimbus 7 in 1978. Profiles of stratospheric and mesospheric temperature, water vapor, and various other constituents were obtained by inverting the LIMS radiance measurements. This same technique was used in 1981 to analyze the data returned from another limb scanning radiometer aboard the Solar Mesosphere Explorer.
Author

N89-25811*# Jet Propulsion Lab., California Inst. of Tech., Pasadena.
MEASUREMENTS OF THE VERTICAL PROFILE OF WATER VAPOR ABUNDANCE IN THE MARTIAN ATMOSPHERE FROM MARS OBSERVER
J. T. Schofield and Daniel J. McCleese *In* Lunar and Planetary Inst., MECA Workshop on Atmospheric H2O Observations of Earth and Mars. Physical Processes, Measurements and Interpretations 1988 p 82-86 (For primary document see N89-25790 19-91)
Avail: NTIS HC A05/MF A01 CSCL 03B

An analysis is presented of the Pressure Modulator Infrared Radiometer (PMIRR) capabilities along with how the vertical profiles of water vapor will be obtained. The PMIRR will employ filter and pressure modulation radiometry using nine spectral channels, in both limb scanning and nadir sounding modes, to obtain daily, global maps of temperature, dust extinction, condensate extinction, and water vapor mixing ratio profiles as a function of pressure to half scale height or 5 km vertical resolution. Surface thermal properties will also be mapped, and the polar radiactive balance will be monitored.
Author

N89-25812*# Hawaii Univ., Honolulu. Planetary Geosciences Div.
ATMOSPHERIC H2O AND THE SEARCH FOR MARTIAN BRINES
Aaron P. Zent, Fraser P. Fanale, and S. E. Postawko *In* Lunar and Planetary Inst., MECA Workshop on Atmospheric H2O Observations of Earth and Mars. Physical Processes, Measurements and Interpretations 1988 p 87-90 (For primary document see N89-25790 19-91)
Avail: NTIS HC A05/MF A01 CSCL 03B

Abundant martian brines would have important implication for current theories of volatile migration on Mars, since, although the presence of metastable brines is quite plausible, any brine in the reasonably near-surface should be completely depleted on a timescale short in relation to the age of Mars. It is important to determine whether brines exist in the martian subsurface, for the current paradigm for understanding martian volatile regime requires substantial alteration if they are found to exist. It is determined, however, that the prospect for detection of a subsurface brine via atmospheric water vapor measurements is marginal. Four reasons are given for this conclusion.
Author

N89-25813*# Jet Propulsion Lab., California Inst. of Tech., Pasadena.
THE INTERANNUAL VARIABILITY OF ATMOSPHERIC WATER VAPOR ON MARS Abstract Only
Richard W. Zurek *In* Lunar and Planetary Inst., MECA Workshop on Atmospheric H2O Observations of Earth and Mars. Physical Processes, Measurements and Interpretations 1988 p 91 (For primary document see N89-25790 19-91)
Avail: NTIS HC A05/MF A01 CSCL 03B

The acquisition of several north-south scans during the Survey/Completion Mission by the Mars Atmospheric Water Detector (MAWD) onboard Viking Orbiter 1 make it possible to compare water vapor column abundance during northern spring and early summer seasons from three successive Mars years. All three years exhibit very similar seasonal trends. Differences between years tend to be localized, and not regional, with maximum differences between years occurring in the same general areas that the day-to-day variability of water vapor as observed by MAWD is large. It is suggested that the observed year-to-year differences are also artifacts of clouds in the MAWD field of view and that there is remarkably little difference in the water cycle during northern spring and early summer, despite very different dust storm episodes during the preceding three years.
Author

N89-25814*# Jet Propulsion Lab., California Inst. of Tech., Pasadena.
THE MARTIAN ATMOSPHERIC WATER CYCLE AS VIEWED FROM A TERRESTRIAL PERSPECTIVE Abstract Only
Richard W. Zurek *In* Lunar and Planetary Inst., MECA Workshop on Atmospheric H2O Observations of Earth and Mars. Physical Processes, Measurements and Interpretations 1988 p 92 (For primary document see N89-25790 19-91)
Avail: NTIS HC A05/MF A01 CSCL 03B

It is noted that the conditions of temperature and pressure that characterize the atmosphere of Mars are similar to those found in the Earth's stratosphere. Of particular significance is the fact that liquid water is unstable in both environments. Thus, it is expected that terrestrial studies of the dynamical behavior of stratospheric water should benefit the understanding of water transport on Mars as well.
Author

N89-25815 Cornell Univ., Ithaca, NY.
SOME ASPECTS OF THE DYNAMICS OF ORBIT-ORBIT RESONANCES IN THE URANIAN SATELLITE SYSTEM Ph.D. Thesis
Renu Malhotra 1988 163 p
Avail: Univ. Microfilms Order No. DA8900908

The unusual orbital and surface features of the inner Uranian

satellites, Miranda, Ariel and Umbriel, indicate that resonant configurations once existed amongst the Uranian satellites that have since been disrupted. It is shown that the Miranda-Umbriel 1:3 resonances that may have existed in the past, probably provide an explanation for the unusual orbital and surface features of Miranda. For relatively small values of the orbital eccentricities and inclinations of Miranda and Umbriel, all the second order 1:3 resonances are well separated. Therefore a reasonably good description is obtained from a low order perturbation theory for an isolated resonance. A simplified rederivation and extension of the single resonance theory to resonances of order up to three is presented. Features of the dynamics are described that have previously not been recognized. It is shown that the single resonance description of the Miranda-Umbriel 1:3 resonances breaks down when the orbital eccentricities/inclinations grow to modest values during tidal evolution within a resonance and neighboring resonances begin to overlap. By using numerical simulations of the dynamics, it is shown that in the subsequent evolution the stability of a resonance is not assured. The secular variations of the orbital elements of the Uranian satellites in their present configuration are also addressed. A simple revised secular perturbation theory is presented. This new theory provides a firm theoretical foundation for estimating the masses of the satellites from the observed secular variations of the orbital elements.
Dissert. Abstr.

N89-25816 Pittsburgh Univ., PA.
A STUDY OF NON-LINEAR IONIZATION PROCESSES IN PLANETARY ATMOSPHERES Ph.D. Thesis
Mohsen Mohamed El-Agamawi 1988 125 p
Avail: Univ. Microfilms Order No. DA8905594

A model was developed for studying the airglow emission from the resonant transition OI (3s' 3D0 yields 2p 3P; lambda 989 A) in the Earth's atmosphere. This model was used to investigate the role of the airglow emission OI lambda 989 A as a secondary source of photoionization of molecular oxygen and nitric oxide, in the ionosphere. The effect of this EUV radiation source on the ion composition at E-region altitudes, during the twilight and at night-time, was studied. The propagation of the OI lambda 989 A resonant photon was treated by using the Monte Carlo simulation technique for the entrapment of resonant radiation in an optically thick thermosphere. Using this simulation model the enhanced source function due to resonant scattering of these photons was calculated along with photoionization production rate of 02(+) and NO(+) ions due to this resonance source. A chemistry model for different ionic processes in the ionosphere was developed. Using this chemistry model the ion distributions in the ionosphere were calculated as a function of the solar zenith angle. The results obtained from this investigation show that the secondary photoionization source OI lambda 989 A airglow has a significant effect in the ion density distribution at E-region altitudes and the lower part of the F-region ionosphere. The largest effect of this secondary photoionization source occurs during the sunrise and sunset hours in the absence of direct solar radiation in the lower part of the ionosphere, and in eclipses. Dissert. Abstr.

N89-25924# Observatoire de Paris-Meudon (France).
OSCILLATIONS OF JUPITER AS A TOOL FOR PROBING ITS INTERNAL STRUCTURE
B. Mosser, D. Gautier, and Philippe Delache (Observatoire du Mont-Gros, Nice, France) *In* ESA, Seismology of the Sun and Sun-Like Stars Dec. 1988 p 593-594 (For primary document see N89-25819 19-92)
Copyright Avail: NTIS HC A99/MF E03

92 SOLAR PHYSICS

Includes solar activity, solar flares, solar radiation and sunspots.

For related information see *93 Space Radiation.*

N89-25817# National Geophysical Data Center, Boulder, CO.
SOLAR-GEOPHYSICAL DATA NUMBER 528, AUGUST 1988. PART 1: (PROMPT REPORTS). DATA FOR JULY, JUNE 1988 AND LATE DATA
Helen E. Coffey, ed. and John A. McKinnon, ed. Aug. 1988 139 p
(Contract N00014-86-F-0049)
(PB89-109904; SGD-528-Pt-1; ISSN-0038-0911; LC-79-640375)
Avail: NTIS HC A07/MF A01 CSCL 03B

Solar-geophysical information is presented in tabular and graphic form. Categories include data for July 1988; IUWDS alert periods (advance and worldwide); solar activity indices; solar flares; solar radio emission; solar interferometric chart; and Stanford mean solar magnetic field. B.G.

N89-25818*# National Aeronautics and Space Administration, Washington, DC.
SOLAR PHYSICS IN THE SPACE AGE
1989 53 p
(NASA-NP-106; NAS 1.83:106) Avail: NTIS HC A04/MF A01 CSCL 03B

A concise and brief review is given of the solar physics' domain, and how its study has been affected by NASA Space programs which have enabled space based observations. The observations have greatly increased the knowledge of solar physics by proving some theories and challenging others. Many questions remain unanswered. To exploit coming opportunities like the Space Station, solar physics must continue its advances in instrument development, observational techniques, and basic theory. Even with the Advance Solar Observatory, other space based observation will still be required for the sure to be ensuing questions. E.R.

N89-25819# European Space Agency, Paris (France).
SEISMOLOGY OF THE SUN AND SUN-LIKE STARS
E. J. Rolfe, ed. Dec. 1988 706 p Symposium held in Puerto de la Cruz, Spain, 26-30 Sep. 1988; sponsored by the Commission Interministerial de Ciencia y Technologia, Spain; La Laguna Univ., Spain; Excmo. Cabildo Insular de Tenerife; Excmo. Cabildo Insular de La Palma; Excmo. Ayuntami
(ESA-SP-286; ISSN-0379-6566; ETN-89-94449) Copyright
Avail: NTIS HC A99/MF E03

Excitation and damping of solar oscillations; internal rotation and frequency splitting; ground based networks and observation techniques; solar cycle, magnetic fields, and oscillations; space projects and low frequency observations; solar models; asteroseismology; and stellar evolution models from seismology were discussed. For individual titles, see N89-25820 through N89-25943.

N89-25820*# California Inst. of Tech., Pasadena. Big Bear Solar Observatory.
THE EXCITATION AND DAMPING OF SOLAR OSCILLATIONS
Ken G. Libbrecht *In* ESA, Seismology of the Sun and Sun-Like Stars Dec. 1988 p 3-10 (For primary document see N89-25819 19-92)
(Grants NAGw-1303; NSF ATM-86-04632)
Copyright Avail: NTIS HC A99/MF E03 CSCL 03B

The status of understanding of the excitation and damping of solar p-mode oscillations is reviewed. While a few simple statements can be made about the expected properties of p-modes, there is currently no complete theory which explains the observed mode amplitudes and linewidths. Evidence suggests that the p-modes cannot be overstable and therefore self-excited, but are instead probably stochastically excited by turbulent convection. The status of the latter model for exciting p-modes, and possible future directions are discussed. ESA

N89-25821# Consejo Superior de Investigaciones Cientificas, Tenerife (Spain). Inst. de Astrofisica de Canarias
ON THE k-MECHANISM AND THE MULTIDIMENSIONAL EDDINGTON APPROXIMATION
J. TrujilloBueno *In* ESA, Seismology of the Sun and Sun-Like Stars Dec. 1988 p 11-15 (For primary document see N89-25819 19-92)
(Grant DFG-Kn-152/3)
Copyright Avail: NTIS HC A99/MF E03

The suitability of the Eddington approximation as a theoretical framework for the study of the possibility of a k-like overstability mechanism as the driving force of solar modes of oscillation is assessed. A theoretical description of the interaction between the hydrodynamics of the motion and the radiative energy transport is needed. It is found that the multidimensional Eddington approximation is generally adequate for giving account of the radiative damping effects of Planck function fluctuations, while it is in gross disagreement with the exact results with respect to the radiative transfer effects of opacity fluctuations. Therefore, it is concluded that its use should be avoided when investigating k-like excitation mechanisms for nonradial stellar modes of oscillation. ESA

N89-25822# Florence Univ. (Italy). Istituto di Astronomia.
ON THE DIAGNOSTIC OF 5m OSCILLATIONS THROUGH PHOTOSPHERIC LINE PROFILES
L. Bertello and B. Caccin (Rome Univ., Italy) *In* ESA, Seismology of the Sun and Sun-Like Stars Dec. 1988 p 17-20 (For primary document see N89-25819 19-92)
Copyright Avail: NTIS HC A99/MF E03

Measurements show that the 5 m oscillations have different amplitudes in the opposite flanks of several photospheric lines. This effect can be suitably described by giving the (blue wing)/(red wing) ratio of the rms wavelength shift at any given level of residual intensity. The main cause is radiative damping, which produces a depth dependent phase difference between the velocity and the thermodynamical (temperature and pressure) perturbations within the line forming region. Synthetic profiles of the FeI 6301.5 A line, obtained by numerical solution of the time independent radiative transfer equation in the oscillating atmosphere (quasi-static radiation field approximation) show that agreement between observed and computed profiles can be achieved. The consequences of this effect (which is also dependent on the magnetic flux concentration) on the diagnostic properties of line profiles are discussed. ESA

N89-25823# Joint Inst. for Lab. Astrophysics, Boulder, CO.
NONLINEAR STUDIES OF SOLAR GRAVITY MODES DRIVEN BY NUCLEAR BURNING OF He3 IN THE CORE
W. J. Merryfield, J. Toomre, and Douglas O. Gough (Cambridge Univ., England) *In* ESA, Seismology of the Sun and Sun-Like Stars Dec. 1988 p 21-26 (For primary document see N89-25819 19-92)
Copyright Avail: NTIS HC A99/MF E03

The finite-amplitude behavior of gravity-mode oscillations driven within the deep interior of the Sun was studied by means of a simple idealized model. Such g modes may be self-excited by their ability to extract energy from the nuclear burning of He3 in the core. Both a nonlinear bifurcation analysis and numerical simulations of the behavior of this instability suggest that the growth of He3-driven oscillations is likely to be limited to an amplitude which is insufficient to induce convective instability in the core, a process proposed as a mechanism for core mixing. The numerical results also indicate that if the oscillations are linearly unstable then the degeneracy in linear theory between standing and travelling g modes is broken by nonlinear effects. The oscillations thus develop into a left- or right-travelling wave rather than a standing wave or other superposition of horizontally propagating waves. ESA

N89-25824# Birmingham Univ. (England). School of Physics and Space Research.
LINEWIDTH OF LOW DEGREE ACOUSTIC MODES OF THE SUN
Y. P. Elsworth, G. R. Isaak, S. M. Jefferies, C. P. McLeod, R. New, Pere L. Palle, C. Regulo, and Teodoro RocaCortes (Consejo Superior de Investigaciones Cientificas, Tenerife, Spain) *In* ESA, Seismology of the Sun and Sun-Like Stars Dec. 1988 p 27-29 Sponsored in cooperation by the United Kingdom Science and Engineering Research Council (For primary document see N89-25819 19-92)
(Grant CAICYT-PR84-0905)
Copyright Avail: NTIS HC A99/MF E03

Estimates of the spectral linewidths of low degree (Q=0 and Q=1) 5 min p-modes obtained from Doppler shift observations in 1984, 1986, and 1987 are reported. The observed linewidths increase from 0.5 microHz at 2000 microHz to 3.8 microHz at 4300 microHz for Q = 0. Comparison with other data suggests that for a given frequency the linewidth increases with increasing Q value. On the assumption that the linewidth is substantially due to damping processes the line widths are consistent with e-folding times between 3.7 and 0.5 days. ESA

N89-25825*# California Inst. of Tech., Pasadena. Big Bear Solar Observatory.
MEASUREMENTS OF HIGH DEGREE SOLAR OSCILLATION AMPLITUDES
James M. Kaufman *In* ESA, Seismology of the Sun and Sun-Like Stars Dec. 1988 p 31-35 Sponsored in part NASA, Washington, DC (For primary document see N89-25819 19-92)
Copyright Avail: NTIS HC A99/MF E03 CSCL 03B

Measurements of high degree solar oscillation velocity amplitudes corrected for the effects of atmospheric seeing are presented. Observations of high degree oscillations, which have very small spatial features, suffer from the effects of atmospheric image blurring and image motion, thereby reducing the amplitudes of their spatial frequency components. In an attempt to correct the velocity amplitudes for these effects, the atmospheric modulation transfer function (MTF) was measured simultaneously by looking at the effects of seeing on the solar limb. The peak velocity power decreases by 2.6 and the energy per mode decreases by a factor 5 as l increases from 200 to 700. The results suggest that the modes are not in energy equipartition with convective turbulent eddies in the top of the convection zone. ESA

N89-25826# Kiepenheuer-Inst. fuer Sonnenphysik, Freiburg (Germany, F.R.).
DYNAMICS OF THE OVERSHOOT LAYERS AND BOUNDARY CONDITIONS IN HELIOSEISMOLOGY
A. Nesis *In* ESA, Seismology of the Sun and Sun-Like Stars Dec. 1988 p 37-39 (For primary document see N89-25819 19-92)
Copyright Avail: NTIS HC A99/MF E03

The variation of the horizontal and the vertical small scale rms velocity with height in the photosphere which shows a minimum in photospheric layers 150 to 200 km above the continuum is considered. In the context of the nonequilibrium thermodynamics it is supposed that the small scale rms velocity variation reflects the variation of the entropy production in these layers. It is proposed that the upper boundary of theoretical helioseismology models should be placed at that height where the entropy production shows its minimum. ESA

N89-25827# Aarhus Univ. (Denmark).
MEASUREMENTS OF OSCILLATION PARAMETERS FROM SYNTHETIC TIMES SERIES
J. M. Sorensen *In* ESA, Seismology of the Sun and Sun-Like Stars Dec. 1988 p 41-45 Sponsored by the Carlsberg Foundation, Denmark (For primary document see N89-25819 19-92)
Copyright Avail: NTIS HC A99/MF E03

Fourier transforms of time series from a stochastically excited

oscillator are fitted by different methods to Lorentz profiles in order to obtain the frequency, amplitude, and the damping constant of the oscillator. Simulations are performed to get estimates of standard errors of the parameters caused by discrete sampling, the random force, and the finite observation time. The effects of varying the damping time relative to the observation time are investigated. Amplitude variations as a function of time are calculated by different methods and are compared with measurements of the real Sun. ESA

N89-25828# Cambridge Univ. (England). Inst. of Astronomy.
ON RADIATIVE AND CONVECTIVE INFLUENCES ON STELLAR PULSATIONAL STABILITY **c90**
N. J. Balmforth and Douglas O. Gough *In* ESA, Seismology of the Sun and Sun-Like Stars Dec. 1988 p 47-52 Sponsored by the United Kingdon Science and Engineering Research Council and the Dee Corp. (For primary document see N89-25819 19-92)
Copyright Avail: NTIS HC A99/MF E03

Gough's (1977) convection theory is applied to Cepheids and the Sun. It is shown that its inclusion may exert a stabilizing influence, particularly on stars on the cool side of the Cepheid instability strip. The role of Reynolds stress in stellar structure and stability is unclear. For solar acoustic modes, a modified version of the theory was applied to calculate pulsation growth rates within the Eddington approximation to radiative transfer. Results agree with previous calculations. When the calculation includes mixing length representations of the fluctuations of the convective heat flux and Reynolds stress, almost all of the modes are stabilized. ESA

N89-25829# National Solar Observatory, Tucson, AZ.
SOLAR INTERNAL ROTATION FROM HELIOSEISMOLOGY
J. W. Harvey *In* ESA, Seismology of the Sun and Sun-Like Stars Dec. 1988 p 55-66 (For primary document see N89-25819 19-92)
Copyright Avail: NTIS HC A99/MF E03

Observations of solar oscillations were used to determine the properties of internal solar rotation. Measurements of p-mode frequencies made by several groups are in essential agreement that rotation within the convection zone differs in depth and latitude only slightly from the observed rotation of the surface. Deeper layers seem to rotate with less latitudinal differential rotation. The rotation of the energy-generating core is not well determined by p-mode oscillations and it may be rotating faster or at the same rate as the surface. Observations of g-modes support the notion of a rapidly rotating core. ESA

N89-25830# California Inst. of Tech., Pasadena. Big Bear Solar Observatory.
ON THE MEASUREMENT OF SOLAR ROTATION USING HIGH-DEGREE p-MODE OSCILLATIONS
Martin F. Woodard and Ken G. Libbrecht *In* ESA, Seismology of the Sun and Sun-Like Stars Dec. 1988 p 67-71 (For primary document see N89-25819 19-92)
Copyright Avail: NTIS HC A99/MF E03

Progress in measuring the solar rotation rate with p-modes of degree 100 to 400, using a set of high-resolution solar images taken at Big Bear Solar Observatory is discussed. The main conclusion drawn from an analysis of 1 day of data is that the equatorial angular velocity is essentially equal to the observed surface rate over the radius range 0.87 is less than or = r/R is less than or = 0.99 to within a few percent. Because of likely systematic errors at the 1 percent level these data do not allow a distinction between a surface rotation rate equal to that measured using magnetic tracers and that based on the Doppler shift of photospheric spectral lines. ESA

N89-25831*# Jet Propulsion Lab., California Inst. of Tech., Pasadena. Dept. of Astronomy.
RADIAL AND LATITUDINAL GRADIENTS IN THE SOLAR INTERNAL ANGULAR VELOCITY
Edward J. Rhodes, Jr., Alessandro Cacciani, Sylvain G. Korzennik, Steven Tomczyk, Roger K. Ulrich, and Martin F. Woodard (California Inst. of Tech., Pasadena.) *In* ESA, Seismology of the Sun and Sun-Like Stars Dec. 1988 p 73-80 Sponsored in part by National Academy of Science - National Research Council, Washington, DC, CNR, Italy and Ministry of Public Education, Italy (For primary document see N89-25819 19-92)
(Grants NAGw-13; NSF INT-84-00213)
Copyright Avail: NTIS HC A99/MF E03 CSCL 03B

The frequency splittings of intermediate-degree (3 to 170 deg) p-mode oscillations obtained from a 16-day subset of observations were analyzed. Results show evidence for both radial and latitudinal gradients in the solar internal angular velocity. From 0.6 to 0.95 solar radii, the solar internal angular velocity increases systematically from 440 to 463 nHz, corresponding to a positive radial gradient of 66 nHz/solar radius for that portion of the solar interior. Analysis also indicates that the latitudinal differential rotation gradient which is seen at the solar surface persists throughout the convection zone, although there are indications that the differential rotation might disappear entirely below the base of the convection zone. The analysis was extended to include comparisons with additional observational studies and between earlier results and the results of additional inversions of several of the observational datasets. All the comparisons reinforce conclusions regarding the existence of radial and latitudinal gradients in the internal angular velocity. ESA

N89-25832*# Jet Propulsion Lab., California Inst. of Tech., Pasadena.
INITIAL HIGH-DEGREE p-MODE FREQUENCY SPLITTINGS FROM THE 1988 MT. WILSON 60-FOOT TOWER SOLAR OSCILLATION PROGRAM
Edward J. Rhodes, Jr., Alessandro Cacciani, and Sylvain G. Korzennik (University of Southern California, Los Angeles.) *In* ESA, Seismology of the Sun and Sun-Like Stars Dec. 1988 p 81-86 Sponsored in part by National Academy of Science - National Research Council, Washington, DC, CNR, Italy and Italian Ministry of Public Education (For primary document see N89-25819 19-92)
(Grants NAGw-13; NSF INT-84-00213)
Copyright Avail: NTIS HC A99/MF E03 CSCL 03B

The initial frequency splitting results of solar p-mode oscillations obtained from the 1988 helioseismology program at the Mt. Wilson Observatory are presented. The frequency splittings correspond to the rotational splittings of sectoral harmonics which range in degree between 10 and 598. They were obtained from a cross-correlation analysis of the prograde and retrograde portions of a two-dimensional (t - v) power spectrum. This power spectrum was computed from an eight-hour sequence of full-disk Dopplergrams obtained on July 2, 1988, at the 60-foot tower telescope with a Na magneto-optical filter and a 1024x1024 pixel CCD camera. These frequency splittings have an inherently larger scatter than did the splittings obtained from earlier 16-day power spectra. These splittings are consistent with an internal solar rotational velocity which is independent of radius along the equatorial plane. The normalized frequency splittings averaged 449 + or - 3 nHz, a value which is very close to the observed equatorial rotation rate of the photospheric gas of 451.7 nHz. ESA

N89-25833# Michigan State Univ., East Lansing. Dept. of Physics-Astronomy.
RADIAL AND TEMPORAL STRUCTURE OF THE INTERNAL SOLAR ASPHERICITY
J. R. Kuhn *In* ESA, Seismology of the Sun and Sun-Like Stars Dec. 1988 p 87-90 Sponsored in part by the Alfred P. Sloan Foundation (For primary document see N89-25819 19-92)
(Grant NSF ATM-86-04400)
Copyright Avail: NTIS HC A99/MF E03

The large systematic differences between the measured even-order splitting coefficients obtained from different helioseismic observations are discussed. These data were obtained by several groups, starting 6 yr ago, and used different observing techniques (e.g., Doppler vs. intensity full disk solar observations) to derive the m-dependence of mode frequencies. Given the wide variation

between the observation techniques it may not be surprising that the results differ, yet the variation between datasets may be physically significant and directly related to solar cycle variations in the aspheric structure of the Sun. This asphericity is not confined to the photosphere and is related to the solar cycle luminosity variations measured by ACRIM and the solar limb brightness observations. ESA

N89-25834# Cambridge Univ. (England). Inst. of Astronomy.
SOLAR RADIATION MODELS AND THE a1, a3 AND a5 SPLITTING COEFFICIENTS FOR SOLAR ACOUSTIC OSCILLATIONS
C. A. Morrow *In* ESA, Seismology of the Sun and Sun-Like Stars Dec. 1988 p 91-98 (For primary document see N89-25819 19-92)
Copyright Avail: NTIS HC A99/MF E03

A forward analysis of the rotational frequency splittings of solar p-modes measured by Brown and Morrow (1987) was done to obtain information on the variation of the Sun's angular velocity with depth and co-latitude. This approach entails computing frequency splittings for chosen models of the solar rotation and comparing them to the observed splittings. It is called a forward method to contrast it with inversion techniques, which use the measured frequency splittings directly to produce a single function for the angular velocity. An advantage of the forward approach is that it allows one to develop intuition about the sensitivities of the splitting coefficients (a1, a3, and a5) to various changes in the nature and magnitude of the angular velocity. The results of the analysis conducted in Morrow (these proceedings) give the impression that models with surface rotation throughout the convection zone are more promising than models with angular velocity constant on cylinders. The more formal approach used here substantiates this impression, and can consider the splittings from a series of more elaborate models for the solar rotation. ESA

N89-25835*# Yale Univ., New Haven, CT. Center for Solar and Space Research.
IS THE SUN REALLY A RIGID ROTATOR
P. Demarque and D. B. Guenther *In* ESA, Seismology of the Sun and Sun-Like Stars Dec. 1988 p 99-102 (For primary document see N89-25819 19-92)
(Grants NAGw-777; NAGw-778)
Copyright Avail: NTIS HC A99/MF E03 CSCL 03B

Attention is drawn to observations of surface rotational bands in subgiants which indicate that a deep-seated reservoir of angular momentum must exist in these stars. This interpretation is compatible with theoretical studies of the rotational history of the Sun and Sun-like stars, but is in conflict with observations of p-mode splittings in the Sun. In order to understand better the source of this discrepancy, the predicted rotational splittings of several test rotation curves are compared to solar data. ESA

N89-25836# National Solar Observatory, Tucson, AZ.
OSCILLATION RING DIAGRAMS AND THE THERMODYNAMICS OF THE OUTER SOLAR CONVECTION ZONE
Frank Hill *In* ESA, Seismology of the Sun and Sun-Like Stars Dec. 1988 p 103-108 (For primary document see N89-25819 19-92)
Copyright Avail: NTIS HC A99/MF E03

Three-dimensional Fourier analysis results in the appearance of rings in the power spectrum of solar oscillations. These rings are the cross-sections at constant temporal frequency of trumpet surfaces, and are the analog of the familiar ridges. The shape of the rings provides information on the local dispersion relationship of the oscillations expressed as a simple power law. The exponent and constant in the power law are related to the thermodynamics of the region in the solar interior where the waves propagate. Asymptotic expressions for high-degree modes, coupled with the assumption that the upper part of the solar envelope is an adiabatic polytrope, predict that the exponent should be 1/2. The constant should depend on the polytropic index of the envelope, and on a phase factor resulting from wave leakage. Analysis of over 5000 rings results in an observed exponent ranging between 0.3 and 0.6, a polytropic index between 1 and 7, and a phase factor between -1.5 and 5. ESA

N89-25837# Cambridge Univ. (England). Inst. of Astronomy.
ANGULAR MOMENTUM TRANSPORT AND DYNAMO ACTION IN THE SUN: A REPORT ON IMPLICATIONS OF A RECENT HELIOSEISMIC ESTIMATE OF SOLAR ROTATION
C. A. Morrow, P. A. Gilman, and E. E. DeLuca *In* ESA, Seismology of the Sun and Sun-Like Stars Dec. 1988 p 109-115 (For primary document see N89-25819 19-92)
Copyright Avail: NTIS HC A99/MF E03 CSCL 03B

The ideas of Gilman, Morrow, and DeLuca about how an emerging helioseismic picture of the Sun's internal rotation might affect the understanding of angular momentum transport and turbulent dynamo action in the solar interior are reviewed. Analysis of the frequency splittings of solar acoustic oscillations measured by Brown and Morrow suggests that the latitudinal differential rotation observed at the surface persists throughout the convection zone, and that the rotation is more uniform in the outer layers of the radiative interior. Taking this picture at face value, it is discussed qualitatively how angular momentum must be transported in order to sustain the observed rotation, the exchange of angular momentum between the convection zone and radiative interior, and the action of a turbulent dynamo which might be operating near the base of the convection zone. The qualitative scenario for the solar dynamo explains both the equatorward migration of the zone where sunspots appear and the observed poleward migration of non-sunspot magnetic field. ESA

N89-25838*# Jet Propulsion Lab., California Inst. of Tech., Pasadena.
INVERSION OF THE SOLAR ROTATION RATE VERSUS DEPTH AND LATITUDE
Sylvain G. Korzennik, Alessandro Cacciani, Edward J. Rhodes, Jr., Steven Tomczyk, and Roger K. Ulrich (California Univ., Los Angeles.) *In* ESA, Seismology of the Sun and Sun-Like Stars Dec. 1988 p 117-124 Sponsored in part by National Academy of Science - National Research Council, Washington, DC, CNR, Italy and Italian Ministry of Public Education (For primary document see N89-25819 19-92)
(Grants NAGw-472; NAGw-13; CS-28-88; NSF INT-84-00213)
Copyright Avail: NTIS HC A99/MF E03 CSCL 03B

Three differential inversion techniques were used to compute the internal solar rotation rate from several sets of n-averaged frequency splittings. An iterative variation of the spectral expansion method; the optimal averaging kernel method; and a piecewise constant constrained least square method were used to invert the data. Each computation was carried out independently. While they present similar trends, each of the solutions differs in detail. A consistent feature in all the inversions is the disappearance of differential rotation below the base of the convection zone. Also, a strong differential signature in the deeper part of the convection zone is present in most of the solutions. A slow decrease of the rotation rate with depth for the equatorial and midlatitude curves is significant in the spectral expansion and the least square results but only marginally apparent in the averaging kernel results. ESA

N89-25839# Consejo Superior de Investigaciones Cientificas, Tenerife (Spain). Inst. de Astrofisica de Canarias.
ROTATIONAL SPLITTING OF LOW l SOLAR p-MODE
Pere L. Palle, F. PerezHernandez, C. Regulo, and Teodoro RocaCortes *In* ESA, Seismology of the Sun and Sun-Like Stars Dec. 1988 p 125-130 (For primary document see N89-25819 19-92)
Copyright Avail: NTIS HC A99/MF E03

Rotational splitting measurements of less than 5 p-modes are calculated using different sources of data. For l=1, data obtained from years 1981 to 1985 is used to find out the stretches where each particular mode remains excited; then its splitting is measured and the mean found. Cross-correlation of power spectra confirms

these finding, and this method is used to look for the l=2 splitting. For l between 2 and 5, only 1 month of data is available and superposition of peak structures gives an upper limit for their splitting. ESA

N89-25840# California Inst. of Tech., Pasadena. Big Bear Solar Observatory.
SOLAR p-MODE FREQUENCY SPLITTINGS
Ken G. Libbrecht *In* ESA, Seismology of the Sun and Sun-Like Stars Dec. 1988 p 131-136 (For primary document see N89-25819 19-92)
(Grant NSF ATM-86-04632)
Copyright Avail: NTIS HC A99/MF E03

Measurements of solar p-mode frequency splittings, based on 100 days of solar Doppler observations from Big Bear Solar Observatory are discussed. Because of the long observing run, the splitting measurements have significantly smaller uncertainties than previously published values. Splittings were determined accurately for individual mode multiplets and show a dependence of splitting on radial order n as well as degree l. Two inversions, which infer the solar rotation rate as a function of depth and latitude from the measurements, are also discussed. The two inversions give surprisingly consistent results, and present the following picture of the Sun's internal rotation: (1) The rotation rate in the convection zone is roughly independent of depth, showing a latitudinal differential rotation equal to that seen at the solar surface. (2) There is a relatively sharp transition zone at the base of the convection zone, where the differential rotation in the convection zone gives way to approximately solid body rotation in the radiative interior. The inversions of the data set can provide accurate rotation information only for r/solar radius greater than 0.5. A comparison of the present data set with previous measurements suggests that the even index splitting coefficients change with solar cycle. This time-dependent p-mode frequency splitting is consistent with photometric measurements of the solar limb, which show that the active latitudes on the Sun are significantly hotter than the quiet Sun. ESA

N89-25841# Cambridge Univ. (England). Inst. of Astronomy.
A WAY TO EXAMINE ROTATIONAL SPLITTINGS WITHOUT EXPLICIT FOWARD OR INVERSE COMPUTATIONS
C. A. Morrow *In* ESA, Seismology of the Sun and Sun-Like Stars Dec. 1988 p 137-140 (For primary document see N89-25819 19-92)
Copyright Avail: NTIS HC A99/MF E03

Simple techniques for extracting information about the Sun's internal rotation from the observed frequency splittings of solar acoustic oscillations are derived. The techniques do not require any formal forward or inverse computations and yet are signicantly revealing about the radial and latitudinal variations of solar angular velocity reflected by the data. Simple linear combinations of the familiar rotational splitting coefficients a1(L), a3(L), a5(L), where L = l(l+1) and l is the angular degree of an oscillation mode, allow one to gain an impression of how any chosen colatitudinal average of the angular velocity varies with depth, or of the radial variation of angular velocity at any particular colatitude. The techniques are easy to apply and are illustrated using the data of Brown and Morrow. The methods reveal a lack of a substantial radial gradient of angular velocity in the convection zone, and a reversal in the sign of the radial gradient of angular velocity at 30 deg latitude at depths near the base of the convection zone. When subject to more detailed forward and inverse analysis, these data also suggest such characteristics of the solar internal angular velocity. This lends credence to the methods described. ESA

N89-25842# California Univ., Los Angeles.
MEASUREMENT OF THE ROTATIONAL FREQUENCY SPLITTING OF THE SOLAR FIVE-MINUTE OSCILLATIONS FROM MAGNETO-OPTICAL FILTER OBSERVATIONS
Steven Tomczyk, Alessandro Cacciani, Sylvain G. Korzennik, Edward J. Rhodes, Jr. (University of Southern California, Los Angeles.), and Roger K. Ulrich *In* ESA, Seismology of the Sun and Sun-Like Stars Dec. 1988 p 141-147 (For primary document see N89-25819 19-92)
Copyright Avail: NTIS HC A99/MF E03

Observations of the solar 5 min oscillations in the photospheric velocity field were obtained during the summer of 1984 at the 60-ft solar tower of the Mt. Wilson Observatory with a magneto-optical filter. The magneto-optical filter employs magneto-optical effects in an atomic vapor to isolate narrow bandpasses in alternate wings of a spectral line. Time series of full disk velocity images having a resolution of 10 arcsec and a noise level of 15 m/s/pixel were obtained on 92 days between May and Sept. 1984. A subset of two time series from this data of 16 and 19 days duration having a total of 25,744 Doppler images were analyzed to provide estimates of the rotational frequency splitting for spherical harmonic degrees between 5 and 120. The results of this analysis indicate a decrease in the rate of solar rotation with increasing depth inside the Sun. Also, a decrease in the rate of differential rotation with increasing depth is observed. ESA

N89-25843# Aarhus Tekniske Bibliotek (Denmark). Inst. of Astronomy.
DIFFERENTIAL ROTATION IN THE SOLAR INTERIOR
J. Christensen-Dalsgaard and J. Schou *In* ESA, Seismology of the Sun and Sun-Like Stars Dec. 1988 p 149-153 Sponsored by the Danish Natural Science Research Council (For primary document see N89-25819 19-92)
Copyright Avail: NTIS HC A99/MF E03

The angular velocity in the outer half of the Sun was estimated as a function of depth and latitude by applying inversion by means of optimally localized averages to rotational splitting coefficients. The results indicate that the surface differential rotation persists through the convection zone; beneath the convection zone there appears to be a transition, which occurs within the resolution width of 0.1R, to solid-body rotation. It was not possible to perform the inversion in the core, due to the lack of adequate data for modes of low degree. ESA

N89-25844# Birmingham Univ. (England). School of Physics and Space Research.
THE CURRENT STATUS OF THE BIRMINGHAM SOLAR SEISMOLOGY NETWORK
A. Aindow, Y. P. Elsworth, G. R. Isaak, C. P. McLeod, R. New, and H. B. vanderRaay *In* ESA, Seismology of the Sun and Sun-Like Stars Dec. 1988 p 157-160 Sponsored by the United Kingdom Science and Engineering Research Council and Comision Interministerial Ciencia y Technologia, Spain (For primary document see N89-25819 19-92)
Copyright Avail: NTIS HC A99/MF E03

Aspects of the performance of a network of solar seismology stations are presented. Duty cycles for 1986 and 1987 are given and examples of window functions and p-mode spectra are shown. Sideband powers down to 2 percent of peak power are achieved for spans of 16 days and 3 percent for 64 days. Noise levels of 7 and 13 (m/sec)sq/Hz are achieved in regions just above and below the p-mode spectrum. A station in Birmingham (UK) is discussed. Its importance as a testing and training station is outlined and plans to deploy replicas around the globe are described. ESA

N89-25845# Nice Univ. (France).
I.R.I.S.: A NETWORK FOR FULL DISK HELIOSEISMOLOGY
Eric Fossat *In* ESA, Seismology of the Sun and Sun-Like Stars Dec. 1988 p 161-162 (For primary document see N89-25819 19-92)
Copyright Avail: NTIS HC A99/MF E03

The IRIS (International Research on the Interior of the Sun) project is described. It consists in the deployment of 7 observing stations in full-disk helioseismology, distributed in complementary longitudes and latitudes. The sites, teams, and calendar of this network are presented. ESA

N89-25846# Consejo Superior de Investigaciones Cientificas, Tenerife (Spain). Inst. de Astrofisica de Canarias.
SOLAR LUMINOSITY OSCILLATIONS FROM TWO STATIONS AND CORRELATION WITH VELOCITY MEASUREMENTS
A. Jimenez, Pere L. Palle, Teodoro RocaCortes, N. B. Andersen, V. Domingo, A. R. Jones, M. Alvarez, and E. Ledezma (Observatorio Astronomico Nacional, Ensenada, Mexico) *In* ESA, Seismology of the Sun and Sun-Like Stars Dec. 1988 p 163-168 (For primary document see N89-25819 19-92)
(Grant CAICYT-PR84-0905)
Copyright Avail: NTIS HC A99/MF E03

Since 1984 the measurements of a quadruple photometer sited at the Observatorio del Teide (Izana, Tenerife) made it possible to identify the p-mode luminosity spectrum with simultaneous velocity observations. Comparing this data, the adiabatic behavior of solar atmosphere and theoretical expectations from solar models were tested. In order to increase the signal-to-noise ratio and reduce the sidebands due to the night-time data gaps, a second identical photometer was set-up in December 1987, at the Observatorio de San Pedro Martir (Baja California Norte, Mexico). Results of the observations of these two stations are analyzed and compared with simultaneous velocity measurements. ESA

N89-25847# Oslo Univ. (Norway). Inst. of Theoretical Astrophysics.
SOLAR INFRARED INTENSITY OSCILLATIONS
T. Leifsen and P. Maltby *In* ESA, Seismology of the Sun and Sun-Like Stars Dec. 1988 p 169-173 (For primary document see N89-25819 19-92)
Copyright Avail: NTIS HC A99/MF E03

The 5-min solar oscillations are found to be easily observable as intensity variations in an infrared wavelength band centered at 2.23 micron with bandwidth (FWHM) 65 nm. The observed peak to peak intensity variation is 2.4 percent for a circular aperture of 1 arc min and 0.8 percent in the full disk observations, i.e., considerably higher than in the other 4 observed channels between 0.67 and 1.65 microns. In addition to the 5-min oscillation the observed full disk power spectrum shows a strong feature centered at 4.3 mHz. This frequency coincides with that of the fundamental p-mode resonance of the chromosphere. Although this identification is not proved, the possibility to study the chromospheric cavity in full disk observations is interesting. ESA

N89-25848# European Space Agency. European Space Research and Technology Center, ESTEC, Noordwijk (Netherlands). Space Science Dept.
SOLAR LUMINOSITY OSCILLATION TELESCOPE (SLOT)
Bo Nyborg Andersen, V. Domingo, A. R. Jones, Sylvain G. Korzennik, A. Jimenez, Pere L. Palle, C. Regulo, and Teodoro RocaCortes (Consejo Superior de Investigaciones Cientificas, Tenerife, Spain) *In its* Seismology of the Sun and Sun-Like Stars Dec. 1988 p 175-176 (For primary document see N89-25819 19-92)
Copyright Avail: NTIS HC A99/MF E03

Low degree l=0-2 solar p-modes were detected with the SLOT instruments at Izana and Baja California. The main source of noise for these ground based observations is in the terrestrial atmosphere. However, the data acquisition system still has to have very low intrinsic noise. It is shown how this is achieved in the SLOT instruments. Design and operating principles of the photometers and data acquisition system are outlined. ESA

N89-25849# Consejo Superior de Investigaciones Cientificas, Tenerife (Spain). Inst. de Astrofisica de Canarias.
EFFECT OF ATMOSPHERIC EXTINCTION ON SOLAR RADIAL VELOCITY MEASUREMENTS
Juan A. Belmonte, Y. P. Elsworth, G. R. Isaak, R. New (Birmingham Univ., England), Pere L. Palle, and Teodoro RocaCortes *In* ESA, Seismology of the Sun and Sun-Like Stars Dec. 1988 p 177-179 Sponsored in cooperation with the United Kingdom Science and Engineering Research Council (For primary document see N89-25819 19-92)
(Grant CAICYT-PR84-0905)
Copyright Avail: NTIS HC A99/MF E03

Effects of differential extinction across the Earth's atmosphere on astronomical photometry are reviewed. Under the same circumstances when a rotating extended object is observed spectrometrically, a residual radial velocity is obtained which varies during the day. In the case of integral sunlight observations, this effect was calculated along the day in all possible observing situations during the year. Applications to real observations are shown and discussed leading to conclusions specially relevant to ground-based networks. ESA

N89-25850# Rome Univ. (Italy).
INTEGRATED SOLAR DISK OSCILLATION MEASUREMENTS USING THE MAGNETO-OPTICAL FILTER: TESTS WITH A TWO STATION NETWORK
Alessandro Cacciani, P. Rosati, D. Ricci, R. Marquedant, and E. Smith (Jet Propulsion Lab., California Inst. of Tech., Pasadena.) *In* ESA, Seismology of the Sun and Sun-Like Stars Dec. 1988 p 181-184 (For primary document see N89-25819 19-92)
Copyright Avail: NTIS HC A99/MF E03

The magneto-optical filter (MOF) was used to get high and intermediate l-modes of solar oscillations. For very low l-modes the imaging capability of the MOF is still attractive since it allows a pixel by pixel intensity normalization. However, a crude attempt to get very low l power spectra from Dopplergrams obtained at Mt. Wilson gave noisy results. This means that a careful analysis of all the factors potentially affecting high resolution Dopplergrams should be accomplished. In order to better investigate this problem, a nonimaging channel using the lock-in amplifier technique was considered. Two systems are now operational, one at JPL and the other at University of Rome. Observations in progress are used to discuss the MOF stability, the noise level, and the possible application in asteroseismology. ESA

N89-25851# Rome Univ. (Italy).
ACQUISITION AND REDUCTION PROCEDURES FOR MOF DOPPLER-MAGNETOGRAMS
Alessandro Cacciani, D. Ricci, P. Rosati, Edward J. Rhodes, Jr., E. Smith, Steven Tomczyk, and Roger K. Ulrich (California Univ., Los Angeles.) *In* ESA, Seismology of the Sun and Sun-Like Stars Dec. 1988 p 185-188 Sponsored in part by CNR, Italy and Italian Ministry of Public Education (For primary document see N89-25819 19-92)
Copyright Avail: NTIS HC A99/MF E03

Defects in the first magneto-optical filter (MOF) magnetograms, particularly the problem of the apparent contamination between velocity and magnetic fields, are discussed. It is found that a correct acquisition and reduction procedure gives cleaner results. A vector magnetograph is suggested. The vector field at coronal levels is calculated, using one MOF longitudinal magnetogram. ESA

N89-25852# Belgian Royal Observatory, Brussels.
NEW THRESHOLDS FOR GROUND-BASED PHOTOMETRY OF SOLAR INTENSITY OSCILLATIONS
F. Ciette *In* ESA, Seismology of the Sun and Sun-Like Stars Dec. 1988 p 189-193 (For primary document see N89-25819 19-92)
(Grant IRSIA-83343)
Copyright Avail: NTIS HC A99/MF E03

The analysis of new whole-disk intensity observations realized from Pic-du-Midi and Jungfraujoch (France, Switzerland) reveals the presence of the solar p-modes. With a 10 hr (single day) integration time and a 10 nm optical bandpass, the resolved groups of modes show a peak amplitude between 0.00001 (red channel) and 0.00003 (blue channel), while the observed background noise power is of the order of 0.000001/Hz at 3 mHz. A cross-spectrum analysis was applied to solar data. The less than optimum data available prevent any firm conclusions. Considering the possibility to transpose this technique to stars, intensity oscillations of solar-like stars are within reach of ground-based instruments,

assuming atmospheric transparency fluctuations as low as those encountered in the present work. ESA

N89-25853# Cambridge Univ. (England). Inst. of Astronomy.
AN ATTEMPT TO UNDERSTAND THE STANFORD p-MODE DATA
Douglas O. Gough and A. G. Kosovichev (Crimean Astrophysical Observatory, USSR) *In* ESA, Seismology of the Sun and Sun-Like Stars Dec. 1988 p 195-201 Sponsored by United Kingdom Science and Engineering Research Council (For primary document see N89-25819 19-92)
Copyright Avail: NTIS HC A99/MF E03

The p-mode frequencies reported by Henning and Scherred (1986), showing anomalous behavior at degree 5 and frequencies below 2 mHz were investigated. No plausible solar model is consistent with them. A density inversion including the low-degree 5 min data of Jimenez et al. (1988) implies that the density of the solar core is 10 percent greater than it is in the standard solar model 1 of Christensen-Dalsgaard (1982). Although that result is in keeping with previous suggestions either that the Sun has a greater evolutionary age than is usually supposed or that there is a cloud of weakly interacting massive particles in the solar core and its environs, the behavior of the sound speed in the core is not consistent with either hypothesis. Both the inferred sound-speed variation, and a secondary inversion for hydrogen abundance (relying on an assumption of thermal balance), provide evidence for material redistribution in the energy-generating core. A sound-speed inversion for the entire radiative interior, using also frequencies of low and intermediate degree compiled by Duvall et al. (1988), confirms the earlier finding that the sound speed in the Sun exceeds that of a standard solar model by up to 1 percent in a region extending 30 percent of the solar radius and centred at r = 0.4R. That is consistent with, though does not necessarily imply, that the opacity in the outer layers of the radiative interior at temperatures of up to 4 million K is underestimated by 20 percent. ESA

N89-25854# National Solar Observatory, Tucson, AZ.
THE GONG INSTRUMENT **c35**
J. W. Harvey, K. Abdel-Gawad, Warren Ball, B. Boxum, F. Bull, J. Cole, L. Cole, S. Colley, K. Dowdney, and R. Drake et al *In* ESA, Seismology of the Sun and Sun-Like Stars Dec. 1988 p 203-208 (For primary document see N89-25819 19-92)
Copyright Avail: NTIS HC A99/MF E03

An instrument is being developed to provide high-quality Doppler oscillation measurements for the Global Oscillation Network Group (GONG) project. This instrument uses the Fourier tachometer principle of sweeping a squared-cosine transmission function across a limited region of the solar spectrum centered on the Ni I line at 676.8 nm. Doppler shift is detected as a phase shift between the modulated solar signal and a simultaneously modulated signal from a stabilized laser. The solar signal is measured with an array of 250 by 250 pixels covering the full disk. Design goals include a short-term noise level at a single pixel of 10 m/sec per integration interval of 60s and a long-term stability of better than 1 m/s. A breadboard model is in operation since early 1988 and a prototype is under construction. Most of the observations as of August 1988 are of the Doppler shift of the entire Sun imaged onto a single detector. These observations easily show the global p-mode oscillations with good short-term signal-to-noise ratio but reveal interesting problems. Imaging measurements started with promising results. ESA

N89-25855*# National Aeronautics and Space Administration, Washington, DC.
THE GONG SITE SURVEY **c14**
Frank Hill, Ashok Ambastha, Warren Ball, Oscar Duhalde, Don Farris, George Fischer, Les Hieda, Huang Zhen, Bob Ingram, and Patty Jackson (National Solar Observatory, Tucson, AZ.) et al *In* ESA, Seismology of the Sun and Sun-Like Stars Dec. 1988 p 209-215 Prepared in cooperation Colorado Univ., Boulder (For primary document see N89-25819 19-92)
Copyright Avail: NTIS HC A99/MF E03 CSCL 03B

The Global Oscillation Network Group (GONG) project is planning to place six observing stations around the world to observe the solar oscillations as continuously as possible. The procedures that are being used to select the six sites are described. Results of measurements of cloud cover obtained by networks of 6 (out of 10) radiometers show a duty cycle of over 93 percent, with the first diurnal sidelobe in the window power spectrum suppressed by a factor of 400. The results are in good agreement with the predictions of a computer model of the expected cloud cover at individual sites. ESA

N89-25856*# National Aeronautics and Space Administration. Marshall Space Flight Center, Huntsville, AL.
THE GONG DATA REDUCTION AND ANALYSIS SYSTEM **c14**
James A. Pintar, Bo Nyborg Andersen, Edwin R. Andersen, David B. Armet, Timothy M. Brown, David H. Hathaway, Frank Hill, and Harrison P. Jones (National Aeronautics and Space Administration. Goddard Space Flight Center, Greenbelt, MD.) *In* ESA, Seismology of the Sun and Sun-Like Stars Dec. 1988 p 217-221 (For primary document see N89-25819 19-92)
Copyright Avail: NTIS HC A99/MF E03 CSCL 03B

Each of the six GONG observing stations will produce three, 16-bit, 256X256 images of the Sun every 60 sec of sunlight. These data will be transferred from the observing sites to the GONG Data Management and Analysis Center (DMAC), in Tucson, on high-density tapes at a combined rate of over 1 gibabyte per day. The contemporaneous processing of these data will produce several standard data products and will require a sustained throughput in excess of 7 megaflops. Peak rates may exceed 50 megaflops. Archives will accumulate at the rate of approximately 1 terabyte per year, reaching nearly 3 terabytes in 3 yr of observing. Researchers will access the data products with a machine-independent GONG Reduction and Analysis Software Package (GRASP). Based on the Image Reduction and Analysis Facility, this package will include database facilities and helioseismic analysis tools. Users may access the data as visitors in Tucson, or may access DMAC remotely through networks, or may process subsets of the data at their local institutions using GRASP or other systems of their choice. Elements of the system will reach the prototype stage by the end of 1988. Full operation is expected in 1992 when data acquisition begins. ESA

N89-25857# Birmingham Univ. (England). School of Physics and Space Research.
A DETECTOR OF SMALL GRADIENTS OF TRANSPARENCY OF THE TERRESTRIAL ATMOSPHERE **c35**
D. B. McLeod and G. R. Isaak *In* ESA, Seismology of the Sun and Sun-Like Stars Dec. 1988 p 223-225 (For primary document see N89-25819 19-92)
Copyright Avail: NTIS HC A99/MF E03

In the study of low l p-modes of the Sun in integrated sunlight with ground based spectrometers it was found that even small (0.001) gradients in transparency across the solar disk give rise to displacements of centroids of spectral lines at the m/s level. A prototype instrument which measures this atmospheric gradient continuously, and thereby makes it possible to subtract these artefacts from the measurements, is described. ESA

N89-25858*# Johns Hopkins Univ., Laurel, MD. Applied Physics Lab.
THE STABLE SOLAR ANALYZER **c35**
D. M. Rust and T. Appourchaux (Centre National de la Recherche Scientifique, Verrieres-Le Buisson, France) *In* ESA, Seismology of the Sun and Sun-Like Stars Dec. 1988 p 227-233 (For primary document see N89-25819 19-92)
(Grants NAGw-522; AF-AFOSR-0077-87)
Copyright Avail: NTIS HC A99/MF E03 CSCL 14B

Progress in the development of an instrument with very high (1:10 billion) wavelength stability designed to measure solar surface velocities and magnetic fields is reported. The instrument determines Doppler and Zeeman shifts in solar spectral lines by a 6-point weighted average. It is built around an electrically tunable solid lithium-niobate Fabry-Perot etalon that is stabilized against a

diode laser which itself is locked to a resonance line of cesium 133. Key features are the etalon, which acts as a wide-angle 0.017-nm solar filter, the camera with a specially stabilized shutter, and the instrument control and data collection system. Use of the instrument in helioseismological research is emphasized. ESA

N89-25859# Helsinki Univ. of Technology, Kylmaelae (Finland). Radio Research Station.
MEASUREMENTS OF SOLAR OSCILLATIONS AT 37 GHz
H. Terasranta, S. Urpo, S. Pohjolainen, and E.-L. Leskinen *In* ESA, Seismology of the Sun and Sun-Like Stars Dec. 1988 p 235-239 (For primary document see N89-25819 19-92)
Copyright Avail: NTIS HC A99/MF E03

Observations at 37 GHz of solar oscillations made during August 1983 and May 1988 at Metsahovi (Finland) are presented. Altogether, data from 10 clear days could be used for further analysis. Five quiet regions were selected from the Sun and the amplitude differences were monitored during the day. Due to the large amount of data only typical examples are presented. During favorable conditions the amplitude at the period of 160 min increases in respect to the other peaks in the power spectrum. The data also suggest that a higher degree g-mode oscillation, (greater than or = 5) could be possible. ESA

N89-25860# Institut d'Astrophysique, Paris (France).
VISIBILITY OF NONRADIAL PULSATION MODES IN SOLAR CONTINUUM INTENSITY MEASUREMENTS
T. Toutain and P. Gouttebroze *In* ESA, Seismology of the Sun and Sun-Like Stars Dec. 1988 p 241-246 (For primary document see N89-25819 19-92)
Copyright Avail: NTIS HC A99/MF E03

A calculation of the continuum emission integrated over the solar disk, and of its perturbations arising from different nonradial pulsation modes, is presented. In addition to geometrical effects (variations of the emitting areas) and Planck function variations, the influence of opacity changes in H- (the principal absorber at the wavelengths under consideration) is examined. The computations are carried out numerically for 500 and 826 nanometers, which correspond to different channels of the IPHIR/PHOBOS experiment. The relative importance of these different processes of flux modulation is discussed as a function of oscillation period and modal type. ESA

N89-25861# Observatoire de Toulouse (France).
PERIODICAL ASYMMETRY OF SOLAR LIMB DARKENING
Raymond Yerle *In* ESA, Seismology of the Sun and Sun-Like Stars Dec. 1988 p 247-250 (For primary document see N89-25819 19-92)
Copyright Avail: NTIS HC A99/MF E03

Periodical brightness gradient differences between extreme (mu less than 0.2) west and east limb darkening profiles of the Sun are shown from diametrical high speed scans obtained by the use of the heliometer. Time series of data display, in the five-minute range, several frequencies with amplitudes of difference corresponding to 2 to 4 percent of the mean brightness gradient value in the 678 nm wavelength range. One of these periods (270 s) was previously exhibited by Hill et al. (1982) and later by Koutchmy et al. (1983). These results might be related to asymmetries of solar limb darkening observed by Neckel and Labs (1987). A solar origin is discussed. ESA

N89-25862# Utrecht Observatory (Netherlands).
THE GRANULATION SENSITIVITY OF HELIOSEISMOLOGY LINES
R. J. Rutten, J. H. M. J. Bruls, M. T. Gomez, and G. Severino (Osservatorio Astronomico, Capodimonte, Naples, Italy) *In* ESA, Seismology of the Sun and Sun-Like Stars Dec. 1988 p 251-255 (For primary document see N89-25819 19-92)
Copyright Avail: NTIS HC A99/MF E03

The sensitivity of the Ni I 676.78 nm Global Oscillation Network Group line and the K I 769.9 nm resonance line to the temperature fluctuations present in the solar granulation are discussed. The temperature contrasts due to granulation are probably small in the upper photosphere where the cores of these two helioseismology lines are formed. However, the cores are sensitive also to the granulation temperature contrasts in the deep photosphere, through nonlocal NLTE effects in their formation. The largest effects are due to the ultraviolet radiation field, which is strongly modulated by the granulation in the deep layers where it escapes and carries these contrasts upwards to the line formation height. The resulting NLTE mechanisms and their influence on the two lines are considered. ESA

N89-25863# Warsaw Univ. (Poland). Astronomy Center.
USING OSCILLATION DATA TO PROBE THE INTERNAL ROTATION AND MAGNETISM OF THE SUN
Wojciech Dziembowski *In* ESA, Seismology of the Sun and Sun-Like Stars Dec. 1988 p 259-263 (For primary document see N89-25819 19-92)
Copyright Avail: NTIS HC A99/MF E03

Integral equations relating the rotation rate and the toroidal field intensity to the parameters describing fine structure in the frequency spectra are discussed. Solutions of the inverse problem for the rotation are presented. Features which may be relevant to the magnetic activity were found in the radial dependence of the rotation rate. Evidence exists for changes with the solar cycle. There is no clear signature of direct effect of magnetism in the observed fine structure. ESA

N89-25864# National Center for Atmospheric Research, Boulder, CO. High Altitude Observatory.
ON THE RADIATIVE DAMPING OF p-MODES IN SOLAR MAGNETIC FLUX CONCENTRATIONS
M. Knoelker (Goettingen Univ., Germany, F.R.) and T. J. Bogdan *In* ESA, Seismology of the Sun and Sun-Like Stars Dec. 1988 p 265-268 (For primary document see N89-25819 19-92)
Copyright Avail: NTIS HC A99/MF E03

In a generalization of a work by Mihalas and Mihalas (1983) describing the propagation of compressive disturbances in a radiating fluid, the dynamical influence of a uniform magnetic field is included. The radiating fluid is treated to be gray, in LTE and assumed to obey the Eddington approximation. Results are applied to the interaction of solar p-modes with sunspots in the context of a simple model developed by Abdelatif and Thomas (1987). For physical conditions representative of the solar envelope and for a variety of embedded magnetic structures, the temperature fluctuations associated with compressive waves are reduced inside the magnetic regions. Hence, radiative damping of these disturbances is suppressed to an extent that depends upon the nature of the mode (fast or slow magnetoacoustic) and the propagation direction relative to the uniform background field. This conclusion raises interesting predictions concerning the observational signatures of compressive waves in the solar envelope. ESA

N89-25865# Goettingen Univ. (Germany, F.R.).
OSCILLATIONS IN PRESENCE OF LOCAL MAGNETIC FIELDS
E. Wiehr, H. Balthasar, and G. Stellmacher (Institut d'Astrophysique, Paris, France) *In* ESA, Seismology of the Sun and Sun-Like Stars Dec. 1988 p 269-272 (For primary document see N89-25819 19-92)
Copyright Avail: NTIS HC A99/MF E03

Oscillatory Doppler shifts in sunspots and in small fluxtubes are observed using either the intensity profile of lines with negligible magnetic splitting or the circular Zeeman profile (Stokes-V inversion point) of lines with strong Zeeman splitting. Sunspot umbrae show local 5 min oscillations of reduced amplitude as compared to the neighboring photosphere. Occasionally 5 min oscillations of opposite phase at both outer penubral borders are found. This could be interpreted as tilting and bobbing of the spot as a whole on the oscillating solar surface. In contrast to these larger scale sunspot fluxtubes the gas in the small fluxtubes of a few hundred km diameter seems to fully participate in the photospheric oscillations without any interaction with the magnetic field. Prominence magnetic fields show sometimes a reaction to the

photospheric 5 min and to the chromospheric 3 min oscillations; in addition several other periods are found. Indications for eigenmodes of Alfven waves are found. ESA

N89-25866# Kiepenheuer-Inst. fuer Sonnenphysik, Freiburg (Germany, F.R.).
OSCILLATIONS IN SUNSPOTS NEAR THE SOLAR LIMB
W. Mattig and M. Zerfass *In* ESA, Seismology of the Sun and Sun-Like Stars Dec. 1988 p 273-274 (For primary document see N89-25819 19-92)
Copyright Avail: NTIS HC A99/MF E03

Sunspot-spectrograms near the solar limb were used to determine the height of the formation of selected strong (chromospheric) lines by micrometric distance measurements. The time sequences of H alpha and Na D line spectra were analyzed to check the possibility of a time variation in the height of formation of these lines. Results show periods in the 3 min range, but also longer periods. The amplitude of the height variation is in the range delta h (rms)=100 to 200 km. This method to study oscillations in sunspots does not need to use of intensity velocity variations. ESA

N89-25867# Nice Univ. (France). Dept. d'Astrophysique.
SOLAR p-MODES FREQUENCY VARIATIONS BETWEEN 1980 AND 1986
B. Gelly (Stanford Univ., CA.), Eric Fossat, and Gerard Grec *In* ESA, Seismology of the Sun and Sun-Like Stars Dec. 1988 p 275-277 (For primary document see N89-25819 19-92)
Copyright Avail: NTIS HC A99/MF E03

Using a method of power spectra cross-correlation, a 0.39 micro Hz decrease of solar low degree p-mode frequencies between 1980 and the end of 1984 was determined. The same method applied to 1984/85 South Pole data and to all the ACRIM data obained until April 1986 confirms the value of this decrease. An extreme stability of these frequencies from spring 1984 to spring 1986 with a relative accuracy of 0.02 micro Hz is found. ESA

N89-25868*# National Aeronautics and Space Administration. Goddard Space Flight Center, Greenbelt, MD.
HELIOSEISMOLOGY FROM THE SOUTH POLE: COMPARISON OF 1987 AND 1981 RESULTS
S. M. Jefferies, M. A. Pomerantz, T. L. Duvall, Jr., J. W. Harvey, and D. B. Jaksha (National Solar Observatory, Tucson, AZ.) *In* ESA, Seismology of the Sun and Sun-Like Stars Dec. 1988 p 279-284 (For primary document see N89-25819 19-92)
(Grants NSF DPP-78-22267; NSF DPP-81-19627; NSF DPP-87-15791)
Copyright Avail: NTIS HC A99/MF E03 CSCL 03B

Full disk images with 10 arc sec pixels and filtered to a 7 A pass band centered on the Ca II K line were obtained from the geographic South Pole in 1981 and 1987. In 1981, 50hr of essentially uninterrupted data were obtained. In 1987, three such runs were obtained over a period of 325 hours for a duty cycle of 47 percent. The 1987 observations are characterized by a much lower level of solar activity than 1981, a much improved CCD camera, considerably better image stability and a varying amount of instrumental scatter. The 1987 data have a substantially better signal-to-noise ratio than the 1981 data so that oscillations with degrees from 0 to 150 and frequencies from 2 to 7 mHz are well observed. The observations were reduced to spectra in l, m, and v. A comparison of p-mode frequencies measured in 1981 and 1987, and coefficients of Legendre polynomial expansions of frequency shifts caused by solar rotation are presented. The time behavior of systematic frequency shifts which depend upon m but which do not arise from rotation is described. ESA

N89-25869# Consejo Superior de Investigaciones Cientificas, Tenerife (Spain). Inst. de Astrofisica de Canarias.
FREQUENCY SHIFT OF SOLAR p-MODES AS SEEN BY CROSS CORRELATION ANALYSIS
Pere L. Palle, C. Regulo, and Teodoro RocaCortes *In* ESA, Seismology of the Sun and Sun-Like Stars Dec. 1988 p 285-289 Sponsored in cooperation with the United Kingdom Science and Engineering Research Council (For primary document see N89-25819 19-92)
(Grant CAICYT-PR84-0905)
Copyright Avail: NTIS HC A99/MF E03

Data obtained at the Observatorio del Teide (Tenerife) during the years 1978 to 1988 using a resonant scattering spectrophotometer, is analyzed to look for variations of the low degree p-mode frequencies along the solar cycle. The analysis based on the cross-correlation of power spectra suggests that the variation of its maximum correlation correlates well with the solar cycle. An overall variation, from minimum to maximum solar activity, of 0.5 + or - 0.1 micro Hz is found, when low l modes are considered. This effect depends on the l values of the modes being absent for l=0 and of 0.7 + or - 0.1 micro Hz for l=1. Therefore, other interpretations than a simple frequency shift are plausible, such as different amplitudes between modes in the same multiplet or an asymmetric change of the splitting along the solar cycle. ESA

N89-25870# Observatoire de Paris-Meudon (France). Section d'Astrophysique.
THE INFLUENCE OF THE TOROIDAL ROLL PATTERN ON THE SUNSPOT ACTIVITY
E. Ribes *In* ESA, Seismology of the Sun and Sun-Like Stars Dec. 1988 p 291-293 (For primary document see N89-25819 19-92)
Copyright Avail: NTIS HC A99/MF E03

The latitude distribution of active regions with respect to the toroidal roll pattern was investigated for the period 1978 to 1982. It is shown that the sunspot activity is not concentrated only at the boundaries of rolls. The downdraft at the convergence of adjacent rolls is however more favorable than the updraft to the magnetic flux expulsion. The roll motions are probably not the hydrodynamic forces controlling the flux emergence. They, however, influence the magnetic complexity of the active regions, each torus acting as a selective amplifier. ESA

N89-25871# Instituto Superior Tecnico, Lisbon (Portugal).
ON THE DISSIPATION OF ALFVEN WAVES IN MAGNETIC ATMOSPHERES AND FLUX TUBES **c32**
L. M. B. C. Campos *In* ESA, Seismology of the Sun and Sun-Like Stars Dec. 1988 p 295-300 Sponsored by J.N.I.C.T. and CAUTL/INIC (For primary document see N89-25819 19-92)
Copyright Avail: NTIS HC A99/MF E03

The propagation of Alfven waves in a viscous and resistive atmospheric layer, in isothermal magnetohydrostatic equilibrium, with constant rate of ionization, under a horizontal magnetic field, either uniform or decaying with altitude is considered. The wave equation relevant to these two cases is derived, and its solution in terms of hypergeometric functions is used to plot wave amplitude and phase versus altitude for several values of wave frequency, horizontal wavenumber, and viscous and resistive damping. It is shown that: (1) the amplitudes initially grow due to reducing mass density and the decay due to dissipation, i.e., go through a maximum; (2) the phases also go through a maximum, i.e., upward propagating waves are reflected downward; (3) amplitude and phase changes are smaller in a flux tube than in a uniform magnetic field, because in the former case the magnetic field decays, as the flux tube fans out with height. ESA

N89-25872# National Solar Observatory, Sunspot, NM.
LOCAL EFFECTS OF A MAJOR FLARE ON SOLAR FIVE-MINUTE OSCILLATIONS
D. A. Haber, J. Toomre, Frank Hill, and Douglas O. Gough (Cambridge Univ., England) *In* ESA, Seismology of the Sun and Sun-Like Stars Dec. 1988 p 301-304 (For primary document see N89-25819 19-92)
Copyright Avail: NTIS HC A99/MF E03

Doppler velocity images of the full Sun were obtained both during and after a major white-light flare. These velocities were interpolated onto a cylindrical coordinate system centered on the

flare and decomposed into radially propagating waves defined by Hankel functions. For a similar analysis of quiet Sun regions, results show comparable power in incoming and outgoing waves irrespective of the presence of the flare. However, for the flaring region, there is 14 percent greater power in incoming as opposed to outgoing waves when there is no flare, but 5 percent greater power in outgoing than in incoming waves during the flare. This result suggests that the flare may have excited outgoing waves which counteracted the more usual absorption of incoming acoustic waves by sunspots. ESA

N89-25873# National Center for Atmospheric Research, Boulder, CO. High Altitude Observatory.
VISCOUS MAGNETOHYDRODYNAMIC MODES AND p-MODE ABSORPTION BY SUNSPOTS
Yu-Qing Lou *In* ESA, Seismology of the Sun and Sun-Like Stars Dec. 1988 p 305-310 (For primary document see N89-25819 19-92)
Copyright Avail: NTIS HC A99/MF E03

Properties of small compressible magnetohydrodynamic (MHD) perturbations in the presence of viscosities are studied. Background physical variables in static equilibrium are assumed to vary continuously only with radial coordinate in cylindrical geometry. The well-known ideal MHD singularities are removed by viscosities. Features of viscous MHD modes and the viscous diffusive mode conversion process are considered. It is shown that this diffusive mode conversion process can be very effective in the presence of MHD singular layers. A possible mechanism relevant to the observed p-mode absorption by sunspots in the solar atmosphere is suggested. An upper limit for turbulent viscosity is inferred from the observed linewidths of p-modes. ESA

N89-25874# Saint Andrew's Univ. (Scotland). Dept. of Mathematical Sciences.
THE INFLUENCE OF A CHROMOSPHERIC MAGNETIC FIELD ON p- AND f-MODES
B. Roberts and W. R. Campbell *In* ESA, Seismology of the Sun and Sun-Like Stars Dec. 1988 p 311-314 (For primary document see N89-25819 19-92)
Copyright Avail: NTIS HC A99/MF E03

The influence of a magnetic chromosphere on p- and f-modes of oscillation is explored theoretically, modelling the chromosphere by an isothermal atmosphere permeated by a horizontal magnetic field and the field-free convection zone by a polytrope. It is pointed out that active regions, characterized by magnetic field strengths of the order of 100 gauss, have a significant effect on the frequencies of high degree modes. The frequency of the f-mode is increased by the presence of a magnetic field; the frequencies of p-modes are decreased. In an evolving active region the frequencies of high degree p- and f-modes are systematically split apart by the changing magnetic field. These effects should be apparent in a comparison of high resolution data sets for active regions with either low resolution sets or high resolution sets for quiet regions. ESA

N89-25875*# Lockheed Aircraft Corp., Palo Alto, CA.
OBSERVATIONS OF f- AND p-MODE OSCILLATIONS OF HIGH DEGREE (500 IS LESS THAN L IS LESS THAN 2500) IN QUIET AND ACTIVE SUN
T. D. Tarbell, M. Peri, Z. Frank, R. Shine, and A. M. Title *In* ESA, Seismology of the Sun and Sun-Like Stars Dec. 1988 p 315-319 (For primary document see N89-25819 19-92)
(Contracts NAS8-32805; NAS5-26813)
Copyright Avail: NTIS HC A99/MF E03 CSCL 03B

Spectra (l - v diagrams) from high resolution observations taken at the Vacuum Tower Telescope (NSO/Sunspot) are presented. The raw data are CCD images taken through the SOUP narrowband filter in Fe I 5576 A. Four filtergrams spaced through the spectral line are combined to form velocity movies. Spectra for 80 min of data with 0.5 to 1.5 arcsec resolution are presented for the entire field-of-view and for quiet and magnetic (plage) subregions. Ridges f and p1 to p5 are evident in velocity spectra, extending to l = 2500 (f), l = 1800 (p1), and l = 1200 (p2). Much less power is seen in the magnetic region than in the quiet Sun. Three-dimensional Fourier filtering shows that oscillation velocity amplitude drops sharply at the boundary of the active region for each family of modes considered. ESA

N89-25876# National Center for Atmospheric Research, Boulder, CO. High Altitude Observatory.
EVIDENCE FOR A THIN PERTURBATIVE LAYER NEAR THE BASE OF THE SOLAR CONVECTION ZONE
M. J. Thompson *In* ESA, Seismology of the Sun and Sun-Like Stars Dec. 1988 p 321-324 Sponsored by NSF, Washington, DC (For primary document see N89-25819 19-92)
Copyright Avail: NTIS HC A99/MF E03

It is argued that low-degree solar p-mode frequencies hint at the presence of a thin perturbative layer at the base of the Sun's convection zone. Magnetic flux stored in an overshoot region could constitute such a perturbative layer. ESA

N89-25877*# California Univ., Los Angeles. Dept. of Astronomy.
MAGNETICALLY INDUCED SPECTRAL LINE REDSHIFTS FULL DISK MEASUREMENTS
Roger K. Ulrich, John E. Boyden, Larry Webster, and Tom Shieber *In* ESA, Seismology of the Sun and Sun-Like Stars Dec. 1988 p 325-332 (For primary document see N89-25819 19-92)
(Contract NAGw-472; N00014-86-K-0056; NSF AST-86-02410)
Copyright Avail: NTIS HC A99/MF E03 CSCL 03B

A method which allows the calibration of the magnetically induced velocities and permits an improvement of the information from various planned solar oscillation experiments is presented. Based on the differential sensitivity to the magnetic effects of various spectral lines, a correction function giving the Doppler shift in each line as a function of the difference between shifts of the lines is derived. For 5250 A, the correction to be added to the observed velocity is -0.9 + or - 0.1 (V = 5237 to 5250). ESA

N89-25878*# National Aeronautics and Space Administration. Goddard Space Flight Center, Greenbelt, MD.
DYNAMO THEORY PREDICTION OF SOLAR ACTIVITY
Kenneth H. Schatten *In* ESA, Seismology of the Sun and Sun-Like Stars Dec. 1988 p 333-336 (For primary document see N89-25819 19-92)
Copyright Avail: NTIS HC A99/MF E03 CSCL 03B

The dynamo theory technique to predict decadal time scale solar activity variations is introduced. The technique was developed following puzzling correlations involved with geomagnetic precursors of solar activity. Based upon this, a dynamo theory method was developed to predict solar activity. The method was used successfully in solar cycle 21 by Schatten, Scherrer, Svalgaard, and Wilcox, after testing with 8 prior solar cycles. Schatten and Sofia used the technique to predict an exceptionally large cycle, peaking early (in 1990) with a sunspot value near 170, likely the second largest on record. Sunspot numbers are increasing, suggesting that: (1) a large cycle is developing, and (2) that the cycle may even surpass the largest cycle (19). A Sporer Butterfly method shows that the cycle can now be expected to peak in the latter half of 1989, consistent with an amplitude comparable to the value predicted near the last solar minimum. ESA

N89-25879# Birmingham Univ. (England).
LONG PERIOD SOLAR OSCILLATIONS
H. B. vanderRaay *In* ESA, Seismology of the Sun and Sun-Like Stars Dec. 1988 p 339-351 Sponsored in part by Comision Interministerial de Ciencia y Tecnologia, Spain and United Kingdom Science and Engineering Research Council (For primary document see N89-25819 19-92)
Copyright Avail: NTIS HC A99/MF E03

Several years of high quality optical resonant scattering data from full disk solar observations are analyzed to demonstrate the essential stability of the apparatus necessary to extract signals of

periods hours, days, or possibly years. The variation of the gravitational red shift is examined; the 13 day signal occasioned by solar surface inhomogeneities is demonstrated; and the 160 min signal in these data is shown to be an artifact. The g modes extracted from these data are shown to be stable in period over the interval 1981 to 1987. Interpreted in terms of the Tassoul asymptotic relation a value of To = 41.2. min is found, which favors a solar model with mixing. ESA

N89-25880# Consejo Superior de Investigaciones Cientificas, Tenerife (Spain). Inst. de Astrofisica de Canarias.
CAN SOLAR g-MODES BE IDENTIFIED FROM GROUND-BASED VELOCITY MEASUREMENTS
C. Garcia, Pere L. Palle, and Teodoro RocaCortes *In* ESA, Seismology of the Sun and Sun-Like Stars Dec. 1988 p 353-357 Sponsored in cooperation with the United Kingdom Science and Engineering Research Council (For primary document see N89-25819 19-92)
(Grant CAICYT-PR84-0905)
Copyright Avail: NTIS HC A99/MF E03

The question of whether or not solar g-modes can be detected and identified from ground observations is addressed. The limitation imposed by the Earth's atmosphere, the background solar noise spectrum at low frequencies, and a poor theoretical knowledge of these modes are mentioned. Using the best uninterrupted full disk velocity measurements obtained over the period 1984 to 1987, signals with amplitudes less than 5 cm/s are found in the g-modes spectral region. Cross-correlation and other techniques used to detect stable signals (g-modes) show negative results which allow an upper limit to their amplitudes and/or lifetimes to be defined. ESA

N89-25881# World Radiation Center, Davos (Switzerland). Physikalisch Meteorologisches Observatorium.
IPHIR: THE HELIOSEISMOLOGY EXPERIMENT ON THE PHOBOS MISSION
C. Froehlich, R. M. Bonnet, A. V. Bruns, J. P. Delaboudiniere, V. Domingo, V. A. Kotov, Z. Kollath, D. N. Rashkovsky, T. Toutain, and J. C. Vial (Centre National de la Recherche Scientifique, Verrieres-Le Buisson, France) et al *In* ESA, Seismology of the Sun and Sun-Like Stars Dec. 1988 p 359-362 Sponsored in part by Swiss National Science Foundation, Berne; CNES, France; ESA, France; Crimean Astrophysical Observatory, USSR and Central Research Inst. for Physics, Budapest, Hungary (For primary document see N89-25819 19-92)
Copyright Avail: NTIS HC A99/MF E03

The IPHIR (InterPlanetary Helioseismology by IRradiance measurements) is a solar irradiance experiment on the USSR planetary mission PHOBOS to Mars and its satellite Phobos. The sensor is a three-channel sunphotometer (SPM) which measures the solar spectral irradiance at 335, 500, and 865 nm with a precision of better than 1 ppm. A two axis solar sensor is added to monitor the moderate solar pointing of the spacecraft. A microprocessor based data processing unit controls the sensor operation, acquires the data and performs the data compression for the transmission at a mean rate of 1 bit/s. The experiment on PHOBOS 1 gathered data during 45 days before the S/C was lost, the one on PHOBOS 2 is still operating. The data recovery is excellent with virtually 100 percent coverage. Although the signal is disturbed by the pointing of the spacecraft the results of a preliminary analysis in the range of 5 min oscillations show the improvement achievable. ESA

N89-25882# European Space Agency. European Space Research and Technology Center, ESTEC, Noordwijk (Netherlands). Space Science Dept.
SOHO STATUS **c19**
V. Domingo *In its* Seismology of the Sun and Sun-Like Stars Dec. 1988 p 363-366 (For primary document see N89-25819 19-92)
Copyright Avail: NTIS HC A99/MF E03

The scientific payload for Solar and Heliospheric Observatory (SOHO) space mission was selected. It will study the structure of the solar interior, the physics of the solar corona, and the origin of the solar wind. The spacecraft definition phase will start in October 1989. The launch is expected for March 1995. ESA

N89-25883# Centre National de la Recherche Scientifique, Verrieres-Le Buisson (France). Lab. de Physique Stellaire et Planetaire.
THE GOLF HELIOSEISMOMETER ON BOARD SOHO **c19**
Luc Dame *In* ESA, Seismology of the Sun and Sun-Like Stars Dec. 1988 p 367-370 (For primary document see N89-25819 19-92)
Copyright Avail: NTIS HC A99/MF E03

The GOLF (Global Oscillations at Low Frequencies) investigation on board the SOHO satellite is an improved version of ground based instruments using the resonant-scattering spectrometric technique to measure global velocities of the Sun and stars. It has the capability of a 4 points measurement in the line profile for both the global velocity and magnetic field measurements. ESA

N89-25884# World Radiation Center, Davos (Switzerland). Physikalisch-Meteorologisches Observatorium.
VIRGO: THE SOLAR MONITOR EXPERIMENT ON SOHO
C. Froehlich, Bo Nyborg Andersen, G. Berthomieu, D. Crommelynck, Philippe Delache, V. Domingo, A. Jimenez, A. R. Jones, Teodoro RocaCortes (Consejo Superior de Investigaciones Cientificas, Tenerife, Spain), and Ch. Wehrli *In* ESA, Seismology of the Sun and Sun-Like Stars Dec. 1988 p 371-374 (For primary document see N89-25819 19-92)
Copyright Avail: NTIS HC A99/MF E03

The VIRGO Experiment (Variability of solar IRradiance and Gravity Oscillations) contains two types of active cavity radiometers for monitoring of the solar constant, two three-channel Sun photometers 335, 500, and 865 nm, and a low resolution imager (LOI) with 12 pixels. The main scientific objective is probing the solar interior by helioseismology with p- and g-mode solar oscillations determined from spectral irradiance (SPM) and radiance (LOI) variations on time scales of minutes to the mission time. The measurements of the variability of the solar constant and spectral irradiance over periods of days to the mission time will yield information about the convection zone, as will the comparison of the amplitudes and phases of the oscillations as manifested in irradiance and radiance (from VIRGO) and velocity (from GOLF and SOI). ESA

N89-25885# Stanford Univ., CA. Center for Space Science and Astrophysics.
THE SOLAR OSCILLATIONS IMAGER FOR SOHO **c19**
Philip H. Scherrer, J. T. Hoeksema, and R. S. Bogart *In* ESA, Seismology of the Sun and Sun-Like Stars Dec. 1988 p 375-379 (For primary document see N89-25819 19-92)
Copyright Avail: NTIS HC A99/MF E03

The Solar Oscillations Imager (SOI) program for SOHO will consist of a Michelson Doppler Imager (MDI) instrument, a data reduction and analysis capability, and a coordinated set of investigations. The overall investigation is organized to address a set of science objectives. Primary objectives can be investigated using the techniques of helioseismology; associated objectives can be addressed by other analysis techniques. The MDI is designed to take advantage of the anticipated SOHO telemetry by organizing the observations into 4 observing programs: structure (at all times); dynamics (2 months per year); campaign (8 hr per day, 10 months per year), and magnetic fields (few minutes per day). The MDI will be able to measure line-of-sight velocity by Doppler shift, transverse velocity by local correlation tracking, line and continuum intensity, and line-of-sight magnetic fields with both 4 and 1.4 arc-second resolution (2 and 0.7 arc-sec pixels respectively). The data reduction, data management, and preliminary data analysis will be accomplished partly at Stanford and partly at the National Solar Observatory as an extension of the GONG project. ESA

N89-25886# Norwegian Space Center, Oslo.
DETECTOR CONFIGURATIONS FOR OBSERVATIONS OF GRAVITY MODES IN SOLAR RADIANCE **c19**
Bo Nyborg Andersen *In* ESA, Seismology of the Sun and Sun-Like Stars Dec. 1988 p 381-383 (For primary document see N89-25819 19-92)
Copyright Avail: NTIS HC A99/MF E03

The VIRGO (Variability in IRradiance and Gravity Oscillations) investigation was selected to fly on the SOHO mission. One of the components of VIRGO is a small imaging instrument with limited spatial resolution. Calculations were carried out in an attempt to find an optimal geometrical detector configuration for the observation of low degree g-modes in the solar luminosity. The constraints are given as a wish of having the largest possible sensitivity and redundancy with the smallest number of detectors. In addition the crosstalk for different modes at same frequency should be minimized. ESA

N89-25887# European Space Agency. European Space Research and Technology Center, ESTEC, Noordwijk (Netherlands).
LUMINOSITY OSCILLATIONS IMAGER (LOI) **c19**
Bo Nyborg Andersen, V. Domingo, A. R. Jones, A. Jimenez, Pere L. Palle, C. Regulo, and Teodoro RocaCortes (Consejo Superior de Investigaciones Cientificas, Tenerife, Spain) *In* ESA, Seismology of the Sun and Sun-Like Stars Dec. 1988 p 385-386 (For primary document see N89-25819 19-92)
Copyright Avail: NTIS HC A99/MF E03

The small imaging photometer of the VIRGO (Variability in IRradiance and Gravity Oscillations) investigation on ESA's SOHO mission is presented. This instrument, the Luminosity Oscillations Imager (LOI), will observe the solar radiance with 12 pixels resolution. A prototype of the LOI was built mainly to test possible detector configurations, the data acquisition system and the internal guider, and was operated. ESA

N89-25888# Observatoire du Mont-Gros, Nice (France).
INTEGRATED LIGHT AND VELOCITY OF SOLAR g MODES OSCILLATIONS
J. Provost and G. Berthomieu *In* ESA, Seismology of the Sun and Sun-Like Stars Dec. 1988 p 387-391 (For primary document see N89-25819 19-92)
Copyright Avail: NTIS HC A99/MF E03

The properties of the integrated intensity and velocity variations of the solar gravity modes for different spatial filters are studied in the adiabatic and nonadiabatic cases in the frequency range 40 to 120 micro Hz. Predicted amplitudes are given assuming equipartition of energy between the modes. As far as the intensity is concerned, a lack of amplitude is pointed out around 60 micro Hz, which should have implications on the whole disk VIRGO and ground based observations. ESA

N89-25889# Nice Univ. (France).
SEARCHING FOR SOLAR g-MODES. TESTS OF A STATISTICAL METHOD
Eric Fossat, Gerard Grec, Vladimir Gavrjusev, and Elena Gavrjuseva (Academy of Sciences, USSR, Moscow) *In* ESA, Seismology of the Sun and Sun-Like Stars Dec. 1988 p 393-397 (For primary document see N89-25819 19-92)
Copyright Avail: NTIS HC A99/MF E03

It is proposed to use cross correlation and autocorrelation methods to test the presence of g-modes in a real power spectrum. This method is used on 3 yr of ACRIM irradiance data with negative conclusions. It is also tested with synthetic g-modes computed into a standard and a nonstandard model. Only the standard model seems to offer enough regularity in rotational splitting and in period separation to make reliable the measurement of these two parameters. ESA

N89-25890# Arizona Univ., Tucson. Dept. of Physics.
OBSERVED ASYMPTOTIC PROPERTIES OF LOW-DEGREE SOLAR GRAVITY-MODE EIGENFREQUENCIES
Ye-ming Gu, Henry A. Hill, and Ross D. Rosenwald *In* ESA, Seismology of the Sun and Sun-Like Stars Dec. 1988 p 399-401 Previously announced as N89-16713 Sponsored by DOE, Washington, DC and AFOSR, Bolling AFB, Washington, DC (For primary document see N89-25819 19-92)
Copyright Avail: NTIS HC A99/MF E03

The asymptotic properties of the low-degree solar gravity modes classified by Hill and Gu (1988) are studied in the framework of first- and second-order asymptotic theory predictions. The results demonstrate the necessity of retaining the second-order term in asymptotic theory to describe the eigenfrequency spectrum. In this theory, there are two first-order parameters, T0 and delta, and two second-order parameters, V1 and V2. Values of the parameters obtained in this analysis are: T0 = 36.31 + or - 0.12 min, delta = -043 + or - 0.13, V1 = 0.35, and V2 = 4.76. There remain differences of 0.3 micro Hz between the asymptotic theory eigenfrequencies and observed eigenfrequencies which are quasi-periodic functions of the radial order n for a given value of the degree l. ESA

N89-25891# Arizona Univ., Tucson. Dept. of Physics.
INVERSION OF QUASI-PERIODIC DEVIATIONS BETWEEN LOW-DEGREE SOLAR GRAVITY MODE EIGENFREQUENCIES AND ASYMPTOTIC THEORY EIGENFREQUENCIES
Henry A. Hill, Qiang Gao, and Ross D. Rosenwald *In* ESA, Seismology of the Sun and Sun-Like Stars Dec. 1988 p 403-406 Sponsored by DOE, Washington, DC and AFOSR, Bolling, AFB, Washington, DC (For primary document see N89-25819 19-92)
Copyright Avail: NTIS HC A99/MF E03

The fine structure found by Gu, Hill, and Rosenwald (1988) between asymptotic theory eigenfrequencies and the observed eigenfrequencies reported by Hill and Gu is interpreted as the result of conditions not being met for the applicability of asymptotic theory at one or more radii in the solar interior. From an inversion of the observed fine structure, reasonably good agreement is obtained between observation and theory for either a localized perturbation in internal structure at r/R = 0.06 or at r/R = 0.23. The latter solution is, however, the better one. The amplitude of the perturbation in the mean molecular weight required to produce the fine structure is also inferred. ESA

N89-25892# Stanford Univ., CA. Center for Space Science and Astrophysics.
THE MICHELSON DOPPLER IMAGER FOR THE SOLAR OSCILLATIONS IMAGER PROGRAM ON SOHO **c19**
J. T. Hoeksema, Philip H. Scherrer, A. M. Title, and T. D. Tarbell (Lockheed Aircraft Corp., Palo Alto, CA.) *In* ESA, Seismology of the Sun and Sun-Like Stars Dec. 1988 p 407-412 (For primary document see N89-25819 19-92)
Copyright Avail: NTIS HC A99/MF E03

The Michelson Doppler Imager (MDI) will be the instrument used in the Solar Oscillations Imager Program on SOHO. The MDI will make a line-of-sight velocity map of the full solar disk with 2 arc-sec pixels each minute. The instrument will be a modification of the Fourier tachometer and will operate by using narrow bandpass solar images at 4 wavelengths to measure the line profile of the Ni I line at 6768 A. This method is relatively insensitive to line profile changes and has a linear response to velocity. The instrument is also capable of making partial maps with 0.7 arc-sec pixels. All data will be transmitted to the ground for 2 continuous months each year and 8 hr each day (160 kilobits/sec). At all times the on-board computer will compute and transmit a selection of modes (5 kilobits/sec) to fully exploit the advantages of a space based telescope. Line-of-sight magnetic fields will also be measured regularly. ESA

N89-25893# Arizona Univ., Tucson. Dept. of Physics.
PROPERTIES OF SOLAR GRAVITY MODE SIGNALS IN TOTAL IRRADIANCE OBSERVATIONS
Ronald J. Kroll, Jian Chen, and Henry A. Hill *In* ESA, Seismology of the Sun and Sun-Like Stars Dec. 1988 p 415-418 Sponsored by DOE, Washington, DC and AFOSR, Bolling AFB, Washington,

DC (For primary document see N89-25819 19-92)
Copyright Avail: NTIS HC A99/MF E03

Evidence that a significant fraction of the gravity mode power density in the total irradiance observations appears in sidebands of classified eigenfrequencies is discussed. These sidebands whose amplitudes vary from year to year are interpreted as harmonics of the rotational frequencies of the nonuniform solar surface. These findings are for nonaxisymmetric modes and corroborate the findings of Kroll, Hill, and Chen (1988) for axisymmetric modes. It is demonstrated that the generation of the sidebands lifts the usual restriction on the parity of the eigenfunctions for modes detectable in total irradiance observations. ESA

N89-25894*# Stanford Univ., CA. Center for Space Science and Astrophysics.
THE SEARCH FOR SOLAR GRAVITY MODES
Harald M. Henning and Philip H. Scherrer *In* ESA, Seismology of the Sun and Sun-Like Stars Dec. 1988 p 419-423 (For primary document see N89-25819 19-92)
(Contract NGR-05-020-559; N00014-86-K-0085; NSF ATM-86-18263)
Copyright Avail: NTIS HC A99/MF E03 CSCL 03B

A solar oscillations observing program of more than 13 yr is reviewed. The observations are most sensitive to low degree solar modes and were used for the study of long period p-mode and g-mode oscillations. At the start of the 1987 observing season (summer) long-standing problems with the instrument were corrected which (along with good weather) allowed the cleanest set of data to date. The search for evidence of g-modes in this data is described. Analysis of this data shows good evidence for g-modes. Various methods were used for mode identification with a statistical search for a simple pattern of even spacing in period selected as the most robust. Using this method, a possible g-mode identification was made with an asymptotic period separation T0 = 37.1 min. This identification is consistent with a rotation splitting of 1.6 MicroHz. Tests with randomly generated spectral peaks find as significant a possible set of modes in only 2 out of 100 cases. ESA

N89-25895# Centre National de la Recherche Scientifique, Verrieres-Le Buisson (France). Lab. de Physique Stellaire et Planetaire.
GOLF: SIMULATIONS OF THE RE-EMISSION OF THE RESONANCE CELL **c19**
P. Boumier and Luc Dame *In* ESA, Seismology of the Sun and Sun-Like Stars Dec. 1988 p 425-427 (For primary document see N89-25819 19-92)
Copyright Avail: NTIS HC A99/MF E03

The re-emission process in the resonance cell of the GOLF (Global Oscillations at Low Frequencies) helioseismometric instrument to be flown on SOHO is analyzed. The cell is filled with a sodium vapor and absorbs selectively in the two sodium lines D1 and D2. The different influence of the physical parameters (cell geometry, temperature) was simulated. The temperature analysis is used to constrain the nominal temperature working point and the required stability, as a function of the operational conditions (orbital velocity variation). ESA

N89-25896# Aarhus Tekniske Bibliotek (Denmark). Inst. of Astronomy.
STUDY OF SOLAR STRUCTURE BASED ON p-MODE HELIOSEISMOLOGY
J. Christensen-Dalsgaard *In* ESA, Seismology of the Sun and Sun-Like Stars Dec. 1988 p 431-450 Sponsored in part by Danish Space Board and Danish Natural Science Research Council (For primary document see N89-25819 19-92)
Copyright Avail: NTIS HC A99/MF E03

The physics, assumptions, and procedures used in computing models of solar and stellar structure and their oscillation frequencies are reviewed. The connection between the physics and the assumptions on the one hand, and the observable frequencies on the other, may be regarded as the principal forward (and inverse) problem, with the model serving as a necessary intermediate step. It is shown how the model and its frequencies react to changes in the physics and the assumptions. Tests of numerical precision are discussed. Computed frequencies are compared with the observations. ESA

N89-25897# Commissariat a l'Energie Atomique, Saclay (France). Service d'Astrophysique.
CURRENT OPTIONS FOR THE EQUATION OF STATE OF THE SOLAR INTERIOR
W. Daeppen *In* ESA, Seismology of the Sun and Sun-Like Stars Dec. 1988 p 451-456 (For primary document see N89-25819 19-92)
Copyright Avail: NTIS HC A99/MF E03

Approaches to the equation of state used in helioseismology are discussed. The principal open problem of the equation of state is the number of excited states of hydrogen and helium in the zones of partial ionization. The number of excited states is affected in two ways: first by destruction of the levels due to the (neutral and charged) surrounding species, and second by statistical mechanics which governs the population of the available levels. The two principal philosophies are considered. One is the chemist's view, in which bound systems are interpreted as autonomous species with reactions between each other; the other is the physicist's view, in which a virial expansion of pressure is obtained starting out from fundamental species only (i.e., electrons and nuclei), and in which the so-called Planck-Larkin partition function appears. ESA

N89-25898# Cambridge Univ. (England). Dept. of Applied Mathematics and Theoretical Physics.
SCATTERING AND MULTIPLE SCATTERING OF ACOUSTIC WAVES IN A STRATIFIED MEDIUM **c71**
C. S. Rosenthal and Douglas O. Gough *In* ESA, Seismology of the Sun and Sun-Like Stars Dec. 1988 p 457-461 (For primary document see N89-25819 19-92)
Copyright Avail: NTIS HC A99/MF E03

The effect of an ensemble of general axisymmetric scatterers on acoustic waves in a stratified atmosphere is analyzed without using the WKB approximation. A dispersion relation valid for small filling factors is obtained. The properties of this dispersion relation are studied for scattering from density inhomogeneities in a two-layer model atmosphere. It is found that increased stratification tends to decrease the frequency perturbation induced by a population of cylindrical inhomogeneities. ESA

N89-25899# Cambridge Univ. (England). Dept. of Applied Mathematics and Theoretical Physics.
TOWARDS AN INDEPENDENT CALIBRATION OF THE MIXING-LENGTH THEORY **c34**
P. D. Tooth and Douglas O. Gough *In* ESA, Seismology of the Sun and Sun-Like Stars Dec. 1988 p 463-469 (For primary document see N89-25819 19-92)
Copyright Avail: NTIS HC A99/MF E03

The standard astrophysical mixing-length theory of turbulent convection, and modifications, are calibrated with laboratory data over a range of Rayleigh numbers and Prandtl numbers. Local and nonlocal theories are considered, and the effects on the calibration of different degrees of small-scale turbulence, eddy decay-probability, and presumed nonlocalization (symmetrical and asymmetrical) are analyzed. It is found that while the local theory does adequately describe some of the features of laboratory convection (though it predicts a mixing-length parameter of at least 2.4), its qualitative agreement is poor. Nonlocal theories with this parameter around 1.8 to 2.0 give a much better agreement with experiment over the whole range of experimental Rayleigh and Prandtl numbers. Local and nonlocal mixing-length theories can be adjusted to give apparently accurate descriptions of turbulent laboratory convection for Rayleigh number 10,000 to 100 million, and Prandtl number 0.1 to 100. The nonlocal theory provides a more physically realistic description of the flow. ESA

N89-25900# Tokyo Univ. (Japan). Dept. of Astronomy.
SOUND VELOCITY DISTRIBUTION IN THE SUN INFERRED FROM ASYMPTOTIC INVERSION OF p-MODE SPECTRA **c71**
H. Shibahashi and T. Sekii *In* ESA, Seismology of the Sun and Sun-Like Stars Dec. 1988 p 471-474 (For primary document see N89-25819 19-92)
Copyright Avail: NTIS HC A99/MF E03

The inverse problem of the solar p-mode spectrum is solved, based on an asymptotic inversion method, and the sound velocity distribution is inferred with accuracy better than a few percent. In this method, the equation governing high order p-mode oscillations is reduced to a form of the Schrodinger equation in quantum mechanics. By using the quantization rule based on the WKBJ method, an integral equation to infer the form of the acoustic potential is formulated. The acoustic potential itself consists of two parts. One of them is dependent on the degree l and the sound velocity and is the dominant term in the deep interior while the other is independent of l and dominates in the outer envelope. By examining the l-dependence of the acoustic potential thus inferred, the two terms are separated, and the sound velocity distribution in the Sun is inferred. This method is applied to the real observational data, to obtain the sound velocity distribution in the Sun. There is a small discrepancy between the model and the inferred result in the range r/R = 0.3 to 0.4. ESA

N89-25901# Academy of Sciences (USSR), Moscow. Inst. of Physics of the Earth.
HELIOSEISMOLOGICAL INVERSE PROBLEM: SOUND SPEED IN THE SOLAR INTERIOR **c71**
S. V. Vorontsov *In* ESA, Seismology of the Sun and Sun-Like Stars Dec. 1988 p 475-480 (For primary document see N89-25819 19-92)
Copyright Avail: NTIS HC A99/MF E03

The asymptotic technique for the reconstruction of the sound speed distribution in solar interior from the observational frequencies of the five-minute oscillations is described. The significant improvement of the efficiency of reconstruction of the structure of the central solar regions is achieved due to the inclusion of the effects of self-gravitation into the asymptotic theory and due to the general improvement of the inversion technique. The results of the inversion of the experimental data are discussed. ESA

N89-25902# Los Alamos National Lab., NM. Theoretical Div.
OSCILLATION FREQUENCIES OF SOLAR MODELS
Arthur N. Cox, Joyce A. Guzik, and Russell B. Kidman *In* ESA, Seismology of the Sun and Sun-Like Stars Dec. 1988 p 481-486 (For primary document see N89-25819 19-92)
Copyright Avail: NTIS HC A99/MF E03

Two solar models were constructed, one with no diffusion of the atomic nuclei, and another including diffusive element separation. The opacity at the bottom of the convection zone was increased 15 to 20 percent (within its theoretical uncertainty) to obtain a few microHertz agreement with observed p-mode frequencies. Original helium mass fractions were 0.291 and 0.289 for the no-diffusion and diffusion models, respectively. The diffusion model evolved to a surface Y=0.256 at the solar age, and the original Z value of 0.0200 decreased to 0.0179. Agreement of l=0 and 2 p-mode frequency separations with those observed is good. The g-mode nonadiabatic solutions do not have equal period spacings until high radial order. The lowest order modes are more visible if they all have the same kinetic energy. High central temperatures produce over 9 SNUs from the B and 1.5 SNUs from the Be reactions. Models with iron condensed-out below the convection zone, and with WIMPs cooling the central regions to reduce the SNUs, agree less well with p-mode frequency separations. ESA

N89-25903# Academy of Sciences (USSR), Moscow. Inst. of Physics of the Earth.
HELIOSEISMOLOGICAL INVERSE PROBLEM: DIAGNOSTICS OF THE STRUCTURE OF THE LOWER SOLAR ATMOSPHERE
M. A. Brodsky and S. V. Vorontsov *In* ESA, Seismology of the Sun and Sun-Like Stars Dec. 1988 p 487-491 (For primary document see N89-25819 19-92)
Copyright Avail: NTIS HC A99/MF E03

The 5 min solar oscillation frequencies were used to obtain information about the phase shift corresponding to the reflection of the internal acoustic waves from the outer solar layers. The results of the reconstruction of the frequency dependence of the phase shift from the experimental data are described. This information provides an efficient seismic diagnostic of the structure of the outer regions of the convection zone and lower solar atmosphere. The method of direct computation of frequency dependence of the phase shift for a solar envelope model is described. ESA

N89-25904# Aarhus Tekniske Bibliotek (Denmark). Inst. of Astronomy.
DETERMINATION OF THE SOLAR INTERNAL SOUND SPEED BY MEANS OF A DIFFERENTIAL ASYMPTOTIC INVERSION **c71**
J. Christensen-Dalsgaard, Douglas O. Gough, and M. J. Thompson (National Center for Atmospheric Research, Boulder, CO.) *In* ESA, Seismology of the Sun and Sun-Like Stars Dec. 1988 p 493-497 Sponsored by NSF, Washington, DC (For primary document see N89-25819 19-92)
Copyright Avail: NTIS HC A99/MF E03

A simple asymptotic inversion method for obtaining an estimate of the difference in internal sound speed from differences between 5 min p-mode oscillation frequencies is presented. Thus, given a known model and a set of frequencies of a model of unknown structure, or of the Sun, the internal sound speed of the latter can be estimated. Numerical experiments with error-free frequencies indicate that this method can provide an estimate of the sound speed, from the energy-generating core to the helium ionization zone, with smaller fractional error than any published results. The method was applied to real solar data, showing that the solar sound speed is indeed broadly as determined by an earlier investigation at those depths for which the earlier inversion should be reliable. ESA

N89-25905# Aarhus Tekniske Bibliotek (Denmark). Inst. of Astronomy.
ON THE RELATION OF THE DUVALL PHASE FUNCTION TO THE UPPER LAYERS ON THE CONVECTION ZONE
J. Christensen-Dalsgaard and F. PerezHernandez (Consejo Superior de Investigaciones Cientificas, Tenerife, Spain) *In* ESA, Seismology of the Sun and Sun-Like Stars Dec. 1988 p 499-503 (For primary document see N89-25819 19-92)
Copyright Avail: NTIS HC A99/MF E03

A method to obtain the Duvall phase function from the structure of a stellar model is presented. This can be a good tool for understanding the dependence of p-mode frequencies on the structure of the upper layers of the convection zone. A linear relation between phase function differences of two models and their equilibrium structure differences is obtained. The validity of this expression was tested against solar models. These models are also useful for estimating what kind of information can be obtained from observational Duvall phase function determinations. ESA

N89-25906# Commissariat a l'Energie Atomique, Saclay (France). Service d'Astrophysique.
FURTHER PROGRESS ON THE HELIUM ABUNDANCE DETERMINATION
W. Daeppen, Douglas O. Gough, and M. J. Thompson (Aarhus Tekniske Bibliotek, Denmark) *In* ESA, Seismology of the Sun and Sun-Like Stars Dec. 1988 p 505-510 (For primary document see N89-25819 19-92)
Copyright Avail: NTIS HC A99/MF E03

Progress in attempting to determine the helium abundance in the solar convection zone by analyzing the position and shape of the helium hump in a thermodynamic quantity which can be inferred from the sound speed in the vicinity of the He II ionization zone is reviewed. The sound speed is estimated from frequencies of

high-degree oscillations by a differential asymptotic technique. The helium abundance Y is then determined by fitting the hump inferred to one obtained by interpolation in a grid of theoretical model envelopes. The procedure was tested carrying out a double-blind experiment on artificial data, showing that accurate knowledge of the equation of state is essential for a useful determination. The procedure was also applied to real solar data, but the frequencies are too poorly determined to obtain a reliable estimate of Y in the Sun. ESA

N89-25907# Commissariat a l'Energie Atomique, Saclay (France). Service d'Astrophysique.
MODELLING THE VARIATION OF SOLAR p-MODE FREQUENCIES
W. Daeppen, Douglas O. Gough, and S. Turck-Chieze *In* ESA, Seismology of the Sun and Sun-Like Stars Dec. 1988 p 511-512 (For primary document see N89-25819 19-92)
Copyright Avail: NTIS HC A99/MF E03

A Green's function technique to study long-term variations of the Sun (with characteristic time scales from one month to millions of years) is presented. The method is the combination of two previous analyses carried out independently by Gough and by Dappen. The study was motivated by observational progress on solar p-mode frequency variations. ESA

N89-25908# Consejo Superior de Investigaciones Cientificas, Tenerife (Spain). Inst. de Astrofisica de Canarias.
FURTHER IMPLICATIONS OF SOLAR p-MODES AS MEASURED IN Na AND K RESONANCE LINES
Pere L. Palle, F. PerezHernandez, and Teodoro RocaCortes *In* ESA, Seismology of the Sun and Sun-Like Stars Dec. 1988 p 513-515 Sponsored by the Comission Interministerial de Sciencia y Tecnologia, Spain (For primary document see N89-25819 19-92)
Copyright Avail: NTIS HC A99/MF E03

The ratios between the amplitudes of p-modes measured simultaneously in the Na and K resonance lines are compared with the expected ratios for adiabatic waves at two different levels in the atmosphere. The results agree within errors with the energy decaying solution for the waves at the photosphere. ESA

N89-25909# Observatoire des Alpes Maritimes, Grasse (France).
SOLAR VARIABILITY AND CLIMATOLOGY
J. P. Rozelot *In* ESA, Seismology of the Sun and Sun-Like Stars Dec. 1988 p 517-520 (For primary document see N89-25819 19-92)
Copyright Avail: NTIS HC A99/MF E03

Periodic changes in solar luminosity (S) were derived from data from the ACRIM instrument on SMM satellite, and changes in Earth orientation were derived from UT 1 data. From the two data sets, it is easy to deduce the relationship between UT 1 and S, a quadratic curve being obtained. It is suggested that for long periods, climate is influenced by astronomical cycles, and mainly by variations in the elements of the Earth's orbit (Milankovitch variables), for short periods, fluctuations in Earth rotation is dominated by atmospheric effects (changes in the net atmospheric rotation rate). Between these two fields, the Sun activity cycle may affect the Earth, through the variation of the solar luminosity. ESA

N89-25910# Tokyo Univ. (Japan). Dept. of Astronomy.
AN INVERSION METHOD BASED ON THE MOORE-PENROSE GENERALIZED INVERSE MATRIX
T. Sekii and H. Shibahashi *In* ESA, Seismology of the Sun and Sun-Like Stars Dec. 1988 p 521-523 (For primary document see N89-25819 19-92)
Copyright Avail: NTIS HC A99/MF E03

An inversion method based on solving the algebraic equations by means of the Moore-Penrose generalized inverse matrix of inferring the solar internal rotation is presented. Its validity is investigated, and the method is shown to be effective. ESA

N89-25911# Kiepenheuer-Inst. fuer Sonnenphysik, Freiburg (Germany, F.R.).
SOLAR OSCILLATIONS: OVERSHOOT AT THE BASE OF THE CONVECTION ZONE
D. Skaley and M. Stix *In* ESA, Seismology of the Sun and Sun-Like Stars Dec. 1988 p 525-528 (For primary document see N89-25819 19-92)
Copyright Avail: NTIS HC A99/MF E03

Solar models are calculated with the nonlocal form of mixing length theory, applied to the lower part of the convection zone. The resulting overshoot layer has a depth of 16 Mm; this is 30 percent of the local pressure scale height. The parameters, alpha = (mixing length/pressure scale height) and the initial He-abundance Y0 are obtained by calculating a full model sequence in time to alpha = 1.505 and Y0 = 0.25637. The total convection zone has the depth d = 197 Mm at a temperature T = 2.166 MK compared to d = 181 Mm and T = 1.927 MK in the local case. This fact may have implications on the observed low Li-abundance. The influence of the overshoot layer on low-l modes shows an increase in the frequencies of the order of 1 micro Hz, thus lowering the difference to the observed frequencies. For intermediate-l modes where the reflection boundary is just below the overshoot region the effect is strongest, up to 4 microHz. High-l modes are slightly lowered by the overshoot effect. Nevertheless in all frequency ranges a discrepancy of several microHz remains. ESA

N89-25912# Michigan State Univ., East Lansing. Dept. of Physics and Astronomy.
CONVECTION AND p-MODE OSCILLATIONS
R. F. Stein, A. Nordlund (Copenhagen Univ., Denmark), and J. R. Kuhn *In* ESA, Seismology of the Sun and Sun-Like Stars Dec. 1988 p 529-532 (For primary document see N89-25819 19-92)
Copyright Avail: NTIS HC A99/MF E03

The upper 2.5 Mm of the solar convection zone was simulated using a three-dimensional, compressible, hydrodynamic computer code. Results show that convection excites p-mode oscillations. The frequencies of the modes in the numerical simulation agree well with the eigenfrequencies of a computational box calculated for the time averaged mean atmosphere. The agreement is excellent at low frequencies, and diverges at higher frequencies in a manner similar to the difference between observed and theoretical frequencies for the Sun. ESA

N89-25913# Cambridge Univ. (England). Inst. of Astronomy.
DETERMINATION OF THE SOLAR SOUND SPEED BY AN ASYMPTOTIC INVERSION TECHNIQUE **c71**
A. G. Kosovichev (Crimean Astrophysical Observatory, USSR) *In* ESA, Seismology of the Sun and Sun-Like Stars Dec. 1988 p 533-537 (For primary document see N89-25819 19-92)
Copyright Avail: NTIS HC A99/MF E03

An asymptotic inversion technique is developed using a weighted least-squares bicubic spline fit to the observational data. The accuracy of the asymptotic approach is discussed, and it is shown that the asymptotic theory is adequate to determine the sound speed in the solar interior between 0.4 and 0.9 R. The inversion of the data of Duvall et al. (1988) shows that the sound speed between 0.4 and 0.7 R is 1 percent greater than in the standard solar model 1 of Christensen-Dalsgaard (1982); this result is in agreement with the previous asymptotic inversion of Christensen-Dalsgaard et al. (1985) and also that of Christensen-Dalsgaard et al. (1988). It is also consistent with the inversions presented by Gough and Kosovichev (1988) using a kernel function approach. ESA

N89-25914# Cambridge Univ. (England). Inst. of Astronomy.
THE EFFECT OF A NONSPHERICAL SOUND SPEED ON THE ACOUSTIC FREQUENCY SPECTRUM OF THE SUN **c71**
A. G. Kosovichev and J. Perdang (Institut d'Astrophysique, Cointe-Ougree, Belgium) *In* ESA, Seismology of the Sun and Sun-Like Stars Dec. 1988 p 539-543 (For primary document

see N89-25819 19-92)
Copyright Avail: NTIS HC A99/MF E03

The effect on the solar acoustic frequency spectrum of a localized deviation from spherical symmetry concentrated near the outer convective zone of the Sun is studied. The local asymmetry is modelled by an angular-dependent contribution to the sound speed. Acoustic frequencies in the range 1500 to 4000 microHz were calculated for a nonspherical deformation of relative amplitude epsilon varying from 0 to 0.1. For epsilon less than 0.02 all acoustic frequencies of this range are strongly and irregularly displaced (quantum chaos). For lower values only a small fraction of the frequencies are irregularly shifted. The deviation of the frequency spectrum of the deformed solar model with respect to the spectrum of a spherically symmetric model is measured by a relative scatter. The relative scatter of the observed solar frequencies with respect to the frequencies of a standard spherically symmetric solar model is found to correspond to an amplitude of the disturbance epsilon = 0.025. Results indicate that even slight local asymmetries influence the precise positions of the frequencies. They suggest the possibility of a diagnosis of nonspherical effects in the structure of the Sun. ESA

N89-25915# British Columbia Univ., Vancouver. Dept. of Geophysics and Astronomy.
OBSERVED p-MODE SPECTRA OF Ap STARS AND THE SUN **c89**
Jaymie Matthews *In* ESA, Seismology of the Sun and Sun-Like Stars Dec. 1988 p 547-549 Sponsored by Canadian National Science and Engineering Research Council and a Killam Memorial Postdoctoral Fellowship (For primary document see N89-25819 19-92)
Copyright Avail: NTIS HC A99/MF E03

Five rapidly oscillating Ap (roAp) stars show evidence of multiple p-mode pulsations in their light or radial velocity variations for which estimates of their fundamental frequency spacing delta V0 can be made. These stars and the Sun have ratios of delta V0/V which fall near 0.025 and 0.04. Since delta V0/V should be roughly proportional to 1/(n + l/2), it is possible that there are common selected overtone regimes for the pulsations of the roAp stars and the Sun. ESA

N89-25916# Observatoire de Paris-Meudon (France).
RAPID PHOTOMETRY OF THE DELTA SCUTI VARIABLE 63 HER **c89**
A. Mangeney, M. Chevreton, Juan A. Belmonte, W. Daeppen, O. Saint-Pe, F. Praderie, Teodoro RocaCortes, J. Fuensalida, and M. Alvarez (Universidad Autonoma de Madrid, Cantoblanco, Spain) *In* ESA, Seismology of the Sun and Sun-Like Stars Dec. 1988 p 551-555 (For primary document see N89-25819 19-92)
Copyright Avail: NTIS HC A99/MF E03

The Delta Scuti variable 63 Her was observed during 21 nights at two observatories (Observatorio del Teide, Tenerife Island, Spain and Observatorio Astronomico Nacional de San Pedro Martir in Baja California, Mexico). Six frequencies of pulsation are unambiguously detected, among which the fundamental radial mode, two non radial pressure-like modes, and probably three gravity like modes. ESA

N89-25917# Catania Astrophysical Observatory (Italy). Unita di Ricerca di Catania.
SYNTHETIC LIGHT CURVES AND POWER SPECTRA OF DELTA SCUTI STARS: AN APPROACH TO MODELING PULSATIONS **c89**
R. Ventura *In* ESA, Seismology of the Sun and Sun-Like Stars Dec. 1988 p 557-562 (For primary document see N89-25819 19-92)
Copyright Avail: NTIS HC A99/MF E03

Light curves and power spectra of a given Delta Scuti model were synthetically constructed in order to investigate the effects of different techniques of photometric data sampling on the final structure of the periodograms. The main purpose of this analysis is to provide suggestions for the interpretation of periodograms obtained from real light curves of multiperiodic variables. Results point out that an unambiguous detection of the pulsation modes from the periodograms is difficult also in the case of very long runs of observation and that maybe only international observing campaigns could provide the most useful photometric data sampling technique. ESA

N89-25918# Imperial Coll. of Science and Technology, London (England).
THE SEARCH FOR SOLAR-TYPE OSCILLATIONS IN OTHER STARS USING THE MICHELSON INTERFEROMETRIC STELLAR OSCILLATION SPECTROMETER (ISOS)
K. A. R. B. Pietraszewski, R. E. Renton, and J. Ring *In* ESA, Seismology of the Sun and Sun-Like Stars Dec. 1988 p 563-567 Sponsored by United Kingdom Science and Engineering Research Council (For primary document see N89-25819 19-92)
Copyright Avail: NTIS HC A99/MF E03

Improving the signal-to-noise (SNR) of measurements of solar 5 min oscillations with Michelson ISOS by using the many suitable absorption lines in a 400 A band of spectrum is described. In order to show that the multilining technique improves the SNR it is necessary to detect radial velocity changes having added many lines together, maintaining the fringe contrast. A fringe of the 5406 A line and a fringe of 16 lines added together are shown. There is a reduction in contrast of 20 percent between the 2 fringes. The flux increases 14-fold when 16 lines are used. The short fall was due to dead time effects in the photon-counting electronics at the high count rates obtained from the Sun. Dead time effects also account for an increase in the mean level of the 16 line fringes and part of the reduction in contrast. The count rates expected from a 0m star using a 4.2m telescope would be a factor of 10 lower at 1 million photons/sec. The solar 5-min oscillation was detected after an observation of 2.28 hr using 11 lines. The results on the Sun show that a noise level sufficiently low to detect sub-meter per second solar-type oscillations in other stars is now possible with the multilined Michelson ISOS. ESA

N89-25919# Birmingham Univ. (England). School of Physics and Space Research.
HIGH PRECISION VELOCITY OBSERVATIONS OF ARCTURUS USING THE 7699 A LINE OF POTASSIUM **c89**
J. L. Innis, G. R. Isaak, R. I. Brazier, Juan A. Belmonte, Pere L. Palle, Teodoro RocaCortes, and A. R. Jones (European Space Agency. European Space Research and Technology Center, ESTEC, Noordwijk, Netherlands) *In* ESA, Seismology of the Sun and Sun-Like Stars Dec. 1988 p 569-573 Sponsored by the United Kingdom Science and Engineering Research Council (For primary document see N89-25819 19-92)
Copyright Avail: NTIS HC A99/MF E03

The K giant Arcturus (alpha Boo) was observed with the Birmingham double magneto-optical filter spectrometer using the GHRIL facility at the Nasmyth focus of the 4.2 m William Herschel Telescope of the Observatorio del Roque de los Muchachos in 1988 April to May. Approximately 80 hr of data were obtained over a 2 week interval. Analysis of the data shows the presence of the large (200 m/sec) amplitude velocity variation reported earlier by other observers. However, this more extensive data set strongly suggests that this variation is not singly periodic, as was previously indicated. The nature of this variation, and the implications for stellar seismology, are considered. ESA

N89-25920# Aarhus Tekniske Bibliotek (Denmark). Inst. of Astronomy.
VARIABLE STAR STATISTICS IN OPEN CLUSTERS: NGC 6192 **c89**
Soren Frandsen and Hans Kjeldsen *In* ESA, Seismology of the Sun and Sun-Like Stars Dec. 1988 p 575-578 (For primary document see N89-25819 19-92)
Copyright Avail: NTIS HC A99/MF E03

A search for delta-Scuti stars and other variables in open cluster is in progress, and results for the cluster NGC 6192 are reported. The statistics for a number of open clusters on the frequency of

variables in the instability strip is presented. There is increasing evidence for a change with age of the fraction of variables. ESA

N89-25921# Stanford Univ., CA. Center for Space Science and Astrophysics.
SOLAR CALIBRATION OF ASTEROSEISMOLOGY
B. Gelly, Eric Fossat, Gerard Grec, and F. X. Schmider (Nice Univ., France) *In* ESA, Seismology of the Sun and Sun-Like Stars Dec. 1988 p 579-582 (For primary document see N89-25819 19-92)
Copyright Avail: NTIS HC A99/MF E03

The status of asteroseismology is reviewed, and the contribution of solar calibration is described. The first expected result of asteroseismology will consist in the measurement of two parameters, delta v and D0, which in the Tassoul's asymptotic approximation are close to the sound speed integral across the solar radius, and to the sound speed gradient inside the nuclear burning core, respectively. The first depends mostly on the mass and evolves slowly with age, while the second is strongly age dependent through the increase of molecular mass in the stellar core. Theorists have started to built delta v - delta D0 diagrams, as a tool for the the determination of mass and age of stars. For a precise calibration of such a diagram, a precise measurement of those parameters in the case of the Sun was made. ESA

N89-25922# Birmingham Univ. (England). School of Physics and Space Research.
HIGH PRECISION VELOCITY MEASUREMENTS OF PROCYON USING THE 7699 A LINE OF POTASSIUM **c89**
J. L. Innis and G. R. Isaak *In* ESA, Seismology of the Sun and Sun-Like Stars Dec. 1988 p 583-586 Sponsored by United Kingdom Science and Engineering Research Council (For primary document see N89-25819 19-92)
Copyright Avail: NTIS HC A99/MF E03

The star Procyon (alpha CMi) was observed for 2 weeks using the Birmingham double magneto-optical filter spectrometer in 1988 January. Analysis of these velocity data shows that the noise level (per frequency channel of 1 microHz) in the power spectrum of the combined nightly runs is m sq/sec/sec. These data were searched for the presence of small scale oscillations, but none are obviously present. On one night the surface integrated magnetic field of Procyon was measured using a rotating quarter wave plate to select alternatively opposite senses of circularly polarized light. Analysis indicates that B is 1.3 + or - 4.0 Gauss (standard error), consistent with a nondetection at the few Gauss level. ESA

N89-25923# Imperial Coll. of Science and Technology, London (England). Astrophysics Group.
THE SEARCH FOR RADIAL VELOCITY VARIATIONS IN RAPIDLY OSCILLATING Ap STARS USING THE FABRY-PEROT INTERFEROMETRIC STELLAR OSCILLATION SPECTROMETER (FP-ISOS) **c89**
M. Leeper, C. R. Bell, K. A. R. B. Pietraszewski, Juan A. Belmonte, Pere L. Palle, Teodoro RocaCortes (Consejo Superior de Investigaciones Cientificas, Tenerife, Spain), and R. E. Renton *In* ESA, Seismology of the Sun and Sun-Like Stars Dec. 1988 p 587-591 (For primary document see N89-25819 19-92)
Copyright Avail: NTIS HC A99/MF E03

Radial velocity measurements were taken of a group of Ap stars using an improved FP-ISOS. Observations were made using the 1.5m TCS on Tenerife in May 1987 and December 1987. The already known rapidly oscillating Ap stars 33 Lib and HR1217 were observed in order to search for radial velocity variations corresponding to the photometric periods found in these stars. Simultaneous photometric measurements were made on HR1217 on the last two nights using the nearby 0.5m telescope. The radial velocity and photometric data sets were reduced using a weighted sine wave fitting routine. Promising results are obtained for HR1217, while results obtained for the other Ap stars observed do not allow any conclusion. Data taken several years ago on Alpha Cir was re-examined and the results obtained are also discussed. ESA

N89-25924# Observatoire de Paris-Meudon (France).
OSCILLATIONS OF JUPITER AS A TOOL FOR PROBING ITS INTERNAL STRUCTURE **c91**
B. Mosser, D. Gautier, and Philippe Delache (Observatoire du Mont-Gros, Nice, France) *In* ESA, Seismology of the Sun and Sun-Like Stars Dec. 1988 p 593-594 (For primary document see N89-25819 19-92)
Copyright Avail: NTIS HC A99/MF E03

The internal structure of Jupiter is discussed. According to models the planet exhibits two discontinuities of sound speed in the interior. The first one located in the external part of the hydrogen-helium atmosphere corresponds to the transition of molecular to metallic hydrogen, while the second one to the transition between the H-He envelope and the high density core. Ray tracing of acoustic modes was used to predict the behavior of expected pressure modes of Jupiter. Due to the inner discontinuity, the regular spacing between frequencies of adjacent models is broken in a characteristic manner which provides a clear signature. Observations of low degree p-modes, achievable from the ground, would accurately provide the value of the radius of the planetary core. Observations of high degree modes would provide a signature of the external transition. ESA

N89-25925*# European Space Agency. European Space Research and Technology Center, ESTEC, Noordwijk (Netherlands). Space Science Dept.
SOLAR OSCILLATIONS INSTRUMENTATION AND MEASUREMENT THEORY
T. Appourchaux *In its* Seismology of the Sun and Sun-Like Stars Dec. 1988 p 595-600 Sponsored in part by CNES, France (For primary document see N89-25819 19-92)
(Grant NAGw-522)
Copyright Avail: NTIS HC A99/MF E03 CSCL 03B

Solar-oscillation instruments are reviewed. Common characteristics include detecting solar radial velocities on Fraunhofer lines with a 2-point measuring technique, high spectral resolution and stability, etc. The choice of the spectral line for getting a high signal to solar noise ratio is addressed. Velocity imaging of solar oscillations modes is detailed, including spatial sampling and span, highest observable degree. Applications of these different analyses is applied to existing or future helioseismology instruments. ESA

N89-25926# Rome Univ. (Italy).
A PROTOTYPE STELLAR PHOTOMETER FOR MAGNETIC FIELD AND DOPPLER MEASUREMENTS **c35**
Alessandro Cacciani, S. Catalano, M. Rodono, and G. Costa (Catania Astrophysical Observatory, Italy) *In* ESA, Seismology of the Sun and Sun-Like Stars Dec. 1988 p 601-603 Sponsored by Italian Ministry of Public Education, Rome, Italy and Piano Spaziale Nazionale, Rome, Italy (For primary document see N89-25819 19-92)
Copyright Avail: NTIS HC A99/MF E03

A stellar photometer is presented. It is based on the Magneto-Optical Filter (MOF). The aim is to detect magnetic and velocity signals on stars. The photometer is able to maximize the collection of photons. As far as the magnetic field measurement is concerned only the transverse component of the magnetic field that should provide detectable U and Q Stokes parameter (linear polarization) is considered. Tests on the Sun are part of this program. ESA

N89-25927# Nice Univ. (France). Dept. d'Astrophysique.
THE NICE UNIVERSITY STELLAR SEISMOMETER **c35**
F. X. Schmider, Eric Fossat, Gerard Grec, and B. Gelly *In* ESA, Seismology of the Sun and Sun-Like Stars Dec. 1988 p 605-607 (For primary document see N89-25819 19-92)
Copyright Avail: NTIS HC A99/MF E03

A stellar seismometer with a Cacciani-type sodium cell as a very stable frequency reference for radial velocity measurements was successfully operated for the detection of oscillations on Procyon and Alpha Centauri in 1983 and 1984. In a new version, its sensitivity is increased and the sources of noise reduced. The

principle and the limits of sensitivity are discussed. Other possible applications are also suggested. Capabilities of this instrument in the context of the development of asteroseismology are assessed. ESA

N89-25928# Consejo Superior de Investigaciones Cientificas, Tenerife (Spain). Inst. de Astrofisica de Canarias.
SEARCH FOR RAPID OSCILLATIONS IN THE NORTHERN Ap STARS HD62140, HD81009 AND HD22374 **c89**
Juan A. Belmonte, Pere L. Palle, Teodoro RocaCortes, and Fritz Shoch *In* ESA, Seismology of the Sun and Sun-Like Stars Dec. 1988 p 609-611 (For primary document see N89-25819 19-92)
Copyright Avail: NTIS HC A99/MF E03

High-speed photometric observations were performed of the Ap stars HD62140 (49 Cam), HD81009, and HD22374 for more than 60 hr in Oct. and Dec. 1986. Photometric measurements in the B band were reduced and the residuals obtained were subjected to a harmonic analysis, searching for periodicities in the range of a few minutes to 2 hr. There is evidence that the star 49 Cam is oscillating; HD81009 and HD22374 were observed in order to confirm traces of oscillation present in earlier observations, however, these possible oscillations did not repeat in the new data. ESA

N89-25929# Imperial Coll. of Science and Technology, London (England). Astrophysics Group.
A FABRY-PEROT INTERFEROMETRIC STELLAR OSCILLATION SPECTROMETER **c89**
C. R. Bell, M. Leeper, and K. A. R. B. Pietraszewski *In* ESA, Seismology of the Sun and Sun-Like Stars Dec. 1988 p 613-616 (For primary document see N89-25819 19-92)
Copyright Avail: NTIS HC A99/MF E03

A Fabry-Perot interferometer was modified to enable a cadmium blue (4799.991 A) line to be used as an optical reference. Laboratory tests show it capable of giving a noise level of 30 cm/sec. Observations give photon shot noise limited levels of 44 m/sec on HR 1217 and 230 m/sec on 49 Cam. ESA

N89-25930# Osservatorio Meteorologico di Brera, Milan (Italy).
SOME TESTS OF THE PRECISION OF CCD DIFFERENTIAL PHOTOMETRY MEASUREMENTS OF BRIGHT DOUBLE STARS **c89**
E. Antonello *In* ESA, Seismology of the Sun and Sun-Like Stars Dec. 1988 p 617-618 (For primary document see N89-25819 19-92)
Copyright Avail: NTIS HC A99/MF E03

Two bright double stars were observed during two nights with a CCD detector in order to verify the possible precision of the CCD differential photometry for asteroseismology applications. The results indicate that the precision of the measurements for each double star, 0.0013 and 0.0011 mag, is better than the precision obtainable with photomultipliers; the improvement, however, is very small. ESA

N89-25931# Liege Univ. (Belgium). Inst. d'Astrophysique.
ON THE THERMAL SURFACE BOUNDARY CONDITION FOR SOLAR PULSATIONS
M. Gabriel *In* ESA, Seismology of the Sun and Sun-Like Stars Dec. 1988 p 621-622 (For primary document see N89-25819 19-92)
Copyright Avail: NTIS HC A99/MF E03

The numerical coefficient which appears in the thermal surface boundary condition of radial and nonradial oscillations is computed for the Sun. Values for different values of l and R are listed. ESA

N89-25932# Katholieke Universiteit te Leuven (Belgium). Inst. of Astronomy.
ASYMPTOTIC APPROXIMATIONS OF NONRADIAL OSCILLATION MODES OF THE SUN
P. Smeyers, R. Briers, M. Tassoul (Montreal Univ., Quebec), K. Degryse, R. Polfliet, and T. VanHoolst *In* ESA, Seismology of the Sun and Sun-Like Stars Dec. 1988 p 623-627 (For primary document see N89-25819 19-92)
Copyright Avail: NTIS HC A99/MF E03

An asymptotic approximation of higher-degree p-modes in the Sun with periods near 5 min is developed. As a starting point, the property is used that the inner boundaries of the acoustic resonant cavities in which these mode originate, are located at depths in the solar interior where the local acoustic frequency becomes equal to the angular frequencies considered. The treatment is based on Olver's asymptotic theory for second-order differential equations containing a large parameter. The equation determining the eigen-frequencies agrees with the equation derived by Gough by the use of ray theory. The transition to the equation determining eigen-frequencies of higher-order p-modes is also considered. ESA

N89-25933# Commissariat a l'Energie Atomique, Saclay (France). Service d'Astrophysique.
HIGH MASS LOSS IN THE YOUNG SUN
S. Turck-Chieze, W. Daeppen, and M. Casse *In* ESA, Seismology of the Sun and Sun-Like Stars Dec. 1988 p 629-635 (For primary document see N89-25819 19-92)
Copyright Avail: NTIS HC A99/MF E03

The consequences of a possible mass loss in the early main sequence stage of solar type stars are investigated. Special attention is given to the Sun; the constraints from surface abundances and p-mode observations are taken into account. Only a total mass loss smaller than 0.2 solar M seems to be consistent with the observations. Though the ensuing modifications of the internal structure and the cosmological consequences are very small, the He3, Li7, Be9 surface abundances are significantly modified. ESA

N89-25934# Tromsoe Univ. (Norway). Inst. of Mathematical and Physical Sciences.
END POINTS OF STELLAR EVOLUTION INVESTIGATED BY SEISMOLOGY ON WHITE DWARF STARS **c89**
J. E. Solheim *In* ESA, Seismology of the Sun and Sun-Like Stars Dec. 1988 p 637-641 (For primary document see N89-25819 19-92)
Copyright Avail: NTIS HC A99/MF E03

Astroseismological methods were used to calibrate the white dwarf stage of stellar evolution. The internal structure of the white dwarfs can be investigated and the cooling rate determined. Comparing evolutionary models with the luminosity distribution of nearby white dwarfs makes a local determination of the age of the galactic disk population possible. The white dwarf pulsators have multiple and closely spaced periods which can only be determined from continuous photometry covering several nights of observing. A campaign involving observatories around the world was initiated, and results are presented. ESA

N89-25935# Los Alamos National Lab., NM.
SOLAR-LIKE OSCILLATIONS IN LATE SPECTRAL CLASS STARS **c89**
Arthur N. Cox and Julius H. Cahn *In* ESA, Seismology of the Sun and Sun-Like Stars Dec. 1988 p 643-647 Previously announced as N89-15837 (For primary document see N89-25819 19-92)
Copyright Avail: NTIS HC A99/MF E03

The minimum mass star that can exhibit solar-like nonradial p-mode oscillations was investigated. Solar models have almost equal pulsational driving and damping due to standard radiative effects. Coupling with surface convective elements occasionally tips the balance by strongly driving for a few days modes with convection timescales at the top of the convection zone. Then both convective and radiative damping decrease the mode amplitude at an observed decay rate until the next convective reexcitation. Population 1 stellar models at 0.30, 0.45, and 0.75 solar M were constructed to see if they have a near equality of radiative driving and damping also. If so, then stars down to late spectral class could possibly display solar-like oscillations. The near equality of radiative driving and damping occurs down to 0.5

solar M. Possibly 100 to 300 sec oscillations can be observed through most of the K spectral class, if magnetic activity does not overwhelm these small amplitude nonradial pulsations. ESA

N89-25936# Yale Univ. Observatory, New Haven, CT.
THE MASS-LUMINOSITY RELATIONSHIP FOR SOLAR-TYPE STARS **c89**
William F. vanAltena and John T. Lee *In* ESA, Seismology of the Sun and Sun-Like Stars Dec. 1988 p 649-651 Sponsored in part by NSF, Washington, DC (For primary document see N89-25819 19-92)
Copyright Avail: NTIS HC A99/MF E03

The mass-luminosity relationship for solar-type stars was reinvestigated using data from the Yale Parallax Catalog and published orbits and mass ratios for the relevant visual double stars. The results confirm that to within the errors of the data, the Sun lies essentially on the mean relationship for the nearby stars. If there is to be further progress in the definition of the mass-luminosity relationship, then the accuracy of the trigonometric parallaxes must be improved substantially. ESA

N89-25937# Commissariat a l'Energie Atomique, Saclay (France). Service d'Astrophysique.
EPSILON ERIDANI REVISITED **c89**
W. Daeppen and D. Soderblom (Space Telescope Science Inst., Baltimore, MD.) *In* ESA, Seismology of the Sun and Sun-Like Stars Dec. 1988 p 653-655 (For primary document see N89-25819 19-92)
Copyright Avail: NTIS HC A99/MF E03

In the light of the unsatisfactory theoretical explanation of the observed p-mode frequency separation of epsilon Eri of 172 microHz, and of the fact that the seismological observation is not confirmed, a series of models was computed. Only the observational input available prior to the seismological determination is taken into account. Predictions for the p-mode frequency separation that lie between 198 and 244 microHz are obtained. ESA

N89-25938# Middle East Technical Univ., Ankara (Turkey). Dept. of Physics.
RADIAL VIBRATIONS IN A 5 SOLAR M HYDROGEN-HELIUM STAR **c89**
Halil Kirbiyik *In* ESA, Seismology of the Sun and Sun-Like Stars Dec. 1988 p 657-660 (For primary document see N89-25819 19-92)
Copyright Avail: NTIS HC A99/MF E03

A model of a first-generation intermediate mass star with no metals is considered. The vibrational instability of this model is investigated. The model burns helium in the core. Calculations were performed for the first and second harmonics as well as for the fundamental mode. The model is found to be vibrationally stable toward radial pulsations. ESA

N89-25939# Observatoire de Paris-Meudon (France).
THE INFLUENCE OF THE EQUATION OF STATE ON THE ZERO-AGE MAIN SEQUENCE AND THE SUN
Y. Lebreton and W. Daeppen (Commissariat a l'Energie Atomique, Saclay, France) *In* ESA, Seismology of the Sun and Sun-Like Stars Dec. 1988 p 661-664 (For primary document see N89-25819 19-92)
Copyright Avail: NTIS HC A99/MF E03

In the light of the uncertainty in the equation of state of stellar interiors, stellar and solar models were calculated using three different formalisms for the equation of state. The analysis includes a mixture of ideal gases using an artificial pressure-ionization device, an equation of state where pressure ionization is achieved by the confined-atom model; and an equation of state containing a large number of atomic and ionic species, with detailed internal partition functions, containing weighted occupation probabilities. The effect of these equations of state on the position of a star in the H-R diagram was examined. The result is either a displacement of the star on the zero-age main sequence (ZAMS) or, for masses lower than 0.7M a change in the slope of the ZAMS. The usual calibration procedure was carried out in order to obtain the initial He abundance Y of the solar model. ESA

N89-25940# Centre National de la Recherche Scientifique, Verrieres-Le Buisson (France). Inst. d'Astrophysique Spatiale.
MUSICOS (MULTI-SITE CONTINUOUS SPECTROSCOPY): OBJECTIVES AND PROSPECTS FOR ASTEROSEISMOLOGY **c89**
Bernard H. Foing, C. Catala, and P. Felenbok *In* ESA, Seismology of the Sun and Sun-Like Stars Dec. 1988 p 665-667 (For primary document see N89-25819 19-92)
Copyright Avail: NTIS HC A99/MF E03

The MUSICOS, a project for a multisite facility network of high resolution spectrometers around the world partly dedicated to continuous spectroscopy, is presented. This network aims to serve the solar/stellar community especially for programs requiring spectroscopic coverage around the clock. A major scientific goal is to allow asteroseismological studies using the most complete continuity. This goal drives the highest constraints on the spectrometer (efficiency, wavelength range, stability). The instrument design is described; the expected performances for asteroseismology and the organization of the multisite network are discussed. ESA

N89-25941# Observatoire de la Cote d'Azur, Nice (France).
EFFECTS OF CONVECTIVE VELOCITIES ON SOLAR PRESSURE MODE FREQUENCIES
Philippe Delache and Eric Fossat (Nice Univ., France) *In* ESA, Seismology of the Sun and Sun-Like Stars Dec. 1988 p 671-672 (For primary document see N89-25819 19-92)
Copyright Avail: NTIS HC A99/MF E03

Discrepancies between observations and theoretical calculations of solar p-mode frequencies, v obs, v calc are discussed, and it is proposed to approximate the difference (observation-calculation) versus frequency as: delta v = v obs - v calc = -K vsq, where the constant K is of the order of 1 sec and independent of degree l. Brown's (1984) suggestion that solar p-mode eigenfrequencies are decreased by turbulent convection is considered, to see if this physical effect is responsible for some of the difference V 0 - V calc. An order of magnitude evaluation which shows that it is worthwhile to pursue the idea further, by improving the description of the coupling between convection and oscillations, is presented. ESA

N89-25942# CNCPRST, Agdal Rabat (Morocco).
MODELLING THE SOLAR OSCILLATION TIME SERIES BY A RANDOMLY EXCITED OSCILLATOR
Mohamed Lazrek, Philippe Delache, and Eric Fossat (Nice Univ., France) *In* ESA, Seismology of the Sun and Sun-Like Stars Dec. 1988 p 673-676 (For primary document see N89-25819 19-92)
Copyright Avail: NTIS HC A99/MF E03

Artificial full solar disk data is used to determine the parameters of a randomly excited oscillator by comparison with observation data. The artificial signal is used to test the methods of analysis used for the precise determination of mode frequencies, amplitudes and linewidths. The reliability of centroid measurements made by barycenter, Lorentzian fit, and Gaussian fit, with and without background noise was tested. Methods for line width measurements were also assessed. For the determination of the central frequency, taking the highest peak is not the best choice. Fitting a Lorentz curve is better. For line width the Gaussian fit seems to be better defined, but the Lorentzian one is preferred, since it finds a better value for the actual width. However, since sometimes the fitting procedure yields erroneously to a very small linewidth, care should be taken, especially when the number of realizations is not high enough to show clearly the bimodal distribution. Once this distribution is obtained, various techniques could be applied to prevent the fitting procedure reaching the absolute minimum of residuals. ESA

N89-25943# Cambridge Univ. (England). Inst. of Astronomy.
ON TAKING OBSERVERS SERIOUSLY
Douglas Gough *In* ESA, Seismology of the Sun and Sun-Like Stars Dec. 1988 p 679-683 (For primary document see N89-25819 19-92)
Copyright Avail: NTIS HC A99/MF E03

The possibility that the solar cycle is a global oscillation rather than the product of a dynamo confined essentially to the turbulent convection zone is discussed. Measurements of the even component of degeneracy splitting of five-minute oscillations add to the evidence for temporal variations in the solar acoustic asphericity that are correlated with the solar cycle. The asphericity appears to extend from the photosphere, through the convection zone, into the radiative interior. It may exist even in the core of the Sun, but there is not sound direct evidence for this. The next observations will be carried out well into the new cycle, and are therefore likely to clarify the situation significantly. ESA

N89-25944*# National Aeronautics and Space Administration, Washington, DC.
SOLAR SYSTEM EXPLORATION
Clark R. Chapman and Terri Ramlose, ed. [1989] 28 p
(NASA-TM-101784; NAS 1.15:101784) Avail: NTIS HC A03/MF A01 CSCL 03B

The goal of planetary exploration is to understand the nature and development of the planets, as illustrated by pictures from the first two decades of spacecraft missions and by the imaginations of space artists. Planets, comets, asteroids, and moons are studied to discover the reasons for their similarities and differences and to find clues that contain information about the primordial process of planet origins. The scientific goals established by the National Academy of Sciences as the foundation of NASA's Solar System Exploration Program are covered: to determine the nature of the planetary system, to understand its origin and evolution, the development of life on Earth, and the principles that shape present day Earth. B.G.

N89-25945*# Stanford Univ., CA. Center for Space Science and Astrophysics.
THE EVOLUTION OF ENERGETIC PARTICLES AND THE EMITTED RADIATION IN SOLAR FLARES Ph.D. Thesis
Edward Tsang Lu Jun. 1989 126 p
(Grants NsG-7092; NSF ATM-87-05084)
(NASA-CR-185389; NAS 1.26:185389; CSSA-ASTRO-89-08)
Avail: NTIS HC A07/MF A01 CSCL 03B

The evolution of accelerated particle distributions in a magnetized plasma and the resulting radiation are calculated, and the results are applied to solar flares. To study the radiation on timescales of order the particle lifetimes, the evolution of the particle distribution is determined by the use of the Fokker-Planck equation including Coulomb collisions and magnetic mirroring. Analytic solution to the equations are obtained for limiting cases such as homogeneous injection in a homogeneous plasma, and for small pitch angle. These analytic solutions are then used to place constraints on flare parameters such as density, loop length, and the injection timescale for very short implusive solar flares. For general particle distributions in arbitrary magnetic field and background density, the equation is solved numerically. The relative timing of microwaves and X-rays during individual flares is investigated. A number of possible sources for excessive microwave flux are discussed including a flattening in the electron spectrum above hard X-ray energies, thermal synchrotron emission, and trapping of electron by converging magnetic fields. Over shorter timescales, the Fokker-Planck equation is solved numerically to calculate the temporal evolution of microwaves and X-rays from nonthermal thick target models. It is shown that magnetic trapping will not account for the observed correlation of microwaves of approximately 0.15 seconds behind X-rays in flares with rapid time variation, and thus higher energy electrons must be accelerated later than lower energy electrons. Author

93 SPACE RADIATION

Includes cosmic radiation; and inner and outer earth's radiation belts.

For biological effects of radiation see *52 Aerospace Medicine*. For theory see *73 Nuclear and High-Energy Physics*.

N89-25731 Max-Planck-Inst. fuer Physik und Astrophysik, Garching (Germany, F.R.). Inst. fuer Extraterrestrische Physik.
ACCELERATION OF PARTICLES IN SHEAR FLOWS [BESCHLEUNIGUNG VON TEILCHEN IN SCHERSTROEMUNGEN]
G. E. Morfill *In its* Cosmic Plasma Physics Nov. 1988 p 110-123 In ENGLISH; GERMAN title (For primary document see N89-25716 19-75)
Copyright Avail: Max-Planck-Inst. fuer Physik und Astrophysik, D-8046 Garching bei Muenchen, Fed. Republic of Germany

99 GENERAL

N89-25946*# National Aeronautics and Space Administration, Washington, DC.
WHERE NO MAN HAS GONE BEFORE: A HISTORY OF APOLLO LUNAR EXPLORATION MISSIONS
William David Compton 1988 420 p Original contains color illustrations
(NASA-SP-4214; NAS 1.21:4214) Avail: NTIS HC A18/MF A01 CSCL 05D

This book is a narrative account of the development of the science program for the Apollo lunar landing missions. It focuses on the interaction between scientific interests and operational considerations in such matters as landing site selection and training of crews, quarantine and back contamination control, and presentation of results from scientific investigations. Scientific exploration of the moon on later flights, Apollo 12 through Apollo 17 is emphasized. Author

N89-25947*# National Aeronautics and Space Administration. Langley Research Center, Hampton, VA.
SPACE DIRECTORATE RESEARCH AND TECHNOLOGY ACCOMPLISHMENTS FOR FY 1988
Don E. Avery, comp. Apr. 1989 162 p
(NASA-TM-101597; NAS 1.15:101597) Avail: NTIS HC A08/MF A01 CSCL 05D

The major accomplishments and test highlights for FY 1988 that occurred in the Space Dirctorate are given. Accomplishments and test highlights are presented by Division and Branch. The presented information will be useful in program coordination with government organizations, universities, and industry in areas of mutual interest. Author

Typical Subject Index Listing

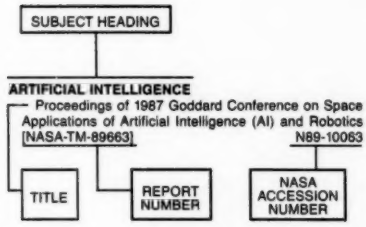

The subject heading is a key to the subject content of the document. Titles, report numbers, and accession numbers of pertinent documents are provided under each subject heading. When the title is insufficiently descriptive of the document content, a title extension has been added, separated from the title by three hyphens. The report number helps to indicate the type of document cited (e.g., NASA report, NASA translation, NASA contractor report). The NASA accession number is the number by which the document abstracts are arranged in this journal and by which the document is sold or requested. The titles, with title extensions if present, are arranged under each subject heading in ascending accession number order. The subject headings have been selected from the latest revision of the *NASA Thesaurus* (NASA SP-7064).

A

ABRASION RESISTANCE
Method of protecting surfaces from abrasion and abrasion resistant articles of manufacture
[DE89-010798] N89-25344

ABSORPTIVITY
Advanced working fluid properties in heat pump and absorption cooling operations
[PB89-178172] N89-25413

ACCESS CONTROL
The generalized grid file: An access structure for CIM applications --- computer integrated manufacturing (CIM)
[MEMO-INF-88-25] N89-25614

ACCLIMATIZATION
Effects of freezing and cold acclimation on the plasma membrane of isolated protoplasts
[DE89-010931] N89-25560

ACCOUNTING
The RIACS Intelligent Auditing and Categorizing System
[NASA-CR-185398] N89-25598

ACIDITY
Seconday ion mass spectrometry of aromatic compounds in acidic mixtures
[DE89-010611] N89-25305

ACOUSTIC FREQUENCIES
Asymptotic approximations of nonradial oscillation modes of the Sun N89-25932

ACOUSTIC MEASUREMENT
Effects of convective velocities on solar pressure mode frequencies N89-25941

ACOUSTIC PROPAGATION
Acoustic propagation in curved ducts with extended reacting wall treatment
[NASA-TM-102110] N89-25670

ACOUSTIC PROPERTIES
Potential uses of vacuum bubbles in noise and vibration control
[NASA-CR-181829] N89-25674

ACOUSTIC SCATTERING
Scattering and multiple scattering of acoustic waves in a stratified medium N89-25898

ACOUSTIC VELOCITY
Sound velocity distribution in the Sun inferred from asymptotic inversion of p-mode spectra N89-25900
Helioseismological inverse problem: Sound speed in the solar interior N89-25901
Determination of the solar internal sound speed by means of a differential asymptotic inversion N89-25904
Determination of the solar sound speed by an asymptotic inversion technique N89-25913
The effect of a nonspherical sound speed on the acoustic frequency spectrum of the Sun N89-25914

ACOUSTICS
In-flight measurement of propeller noise on the fuselage of an airplane
[NASA-TM-102265] N89-25675

ACRYLIC RESINS
Poled polymer films for nonlinear optics
[DE89-010039] N89-25338

ACTIVATION ENERGY
Kinetic effects of strong localization in planar heterostructures p-Ge/i-GaAs
[DE88-706205] N89-25739

ACTIVE CONTROL
Digital robust control law synthesis using constrained optimization N89-25193
An integrated approach to the optimum design of actively controlled composite wings N89-25194
Middeck Active Control Experiment (MACE), phase A
[NASA-CR-185331] N89-25258
Smart tunnel: Docking mechanism
[NASA-CASE-MSC-21360-1] N89-25263

ACTIVITY (BIOLOGY)
Unraveling Photosystem 2
[DE89-010930] N89-25559

ACTUATORS
Optimization of structure and control system N89-25223
Optimal placement of excitations and sensors by simulated annealing N89-25227
Flap system for short takeoff and landing aircraft
[AD-D013981] N89-25234
Variable speed induction motor operation from a 20-kHz power bus
[NASA-TM-102061] N89-25271
Antenna surface contour control system
[NASA-CASE-LAR-13798-1] N89-25363

ADA (PROGRAMMING LANGUAGE)
Rationale for the proposed standard for a generic package of elementary functions for Ada
[DE89-010282] N89-25588

ADAPTIVE CONTROL
Analysis and control of a three-degree-of-freedom robot platform
[DE89-006427] N89-25356

ADAPTIVE FILTERS
Adaptive enhancement of magnetoencephalographic signals via multichannel filtering
[DE89-005464] N89-25569

ADDITIVES
High explosives reaction model and its application to booster performance
[DE89-005459] N89-25351

ADHESION
Relation of the adhesion of plasma sprayed coatings to the process parameters: Size, velocity and heat content of the spray particles
[ETN-89-94296] N89-25326

ADIABATIC FLOW
An experimental study of two-phase natural circulation in an adiabatic flow loop
[DE89-009850] N89-25406

ADJUSTING
Adjustment and data analysis --- gravimetry N89-25547
Data adjustment by gravity differences N89-25548

ADVANCED VERY HIGH RESOLUTION RADIOMETER
User's guide to image processing applications of the NOAA satellite HRPT/AVHRR data. Part 1: Introduction to the satellite system and its applications. Part 2: Processing and analysis of AVHRR imagery
[NASA-CR-180784] N89-25492

ADVECTION
The behavior of water vapor in the Mars atmosphere N89-25801

AERIAL PHOTOGRAPHY
Applications of remote sensing techniques for the inventory and monitoring of environmental pollution
[BCRS-88-15] N89-25497

AEROACOUSTICS
Airfoil self-noise and prediction
[NASA-RP-1218] N89-25673
Data of aeroacoustic measurements on ultralight aircraft propellers
[DFVLR-MITT-88-33] N89-25677

AEROASSIST
Free-molecule-flow force and moment coefficients of the aeroassist flight experiment vehicle
[NASA-TM-101600] N89-25124

AERODYNAMIC BALANCE
Efficient sensitivity analysis and optimization of a helicopter rotor N89-25155

AERODYNAMIC COEFFICIENTS
Aerodynamic flight evaluation analysis and data base update
[NASA-CR-183654] N89-25276

AERODYNAMIC CONFIGURATIONS
The conceptual design of a Mach 2 Oblique Flying Wing supersonic transport
[NASA-CR-177529] N89-25233
Aerodynamic flight evaluation analysis and data base update
[NASA-CR-183654] N89-25276

AERODYNAMIC HEATING
Finite element flow-thermal-structural analysis of aerodynamically heated leading edges N89-25198
SIMOUN: Test system for shuttle thermal protection materials
[REPT-882-430-101] N89-25256

AERODYNAMIC NOISE
Airfoil self-noise and prediction
[NASA-RP-1218] N89-25673

AERODYNAMICS
Aeronautical engineering: A continuing bibliography with indexes (supplement 239)
[NASA-SP-7037(239)] N89-25114
Aeronautical engineering: A continuing bibliography with indexes (supplement 240)
[NASA-SP-7037(240)] N89-25115
The 3DGRAPE book: Theory, users' manual, examples
[NASA-TM-102224] N89-25116
Structural optimization of rotor blades with integrated dynamics and aerodynamics N89-25156
Integrated aerodynamic-structural design of a forward-swept transport wing N89-25168
Effects of nonlinear aerodynamics and static aeroelasticity on mission performance calculations for a fighter aircraft N89-25170
Optimum design of swept-forward high-aspect-ration graphite-epoxy wings N89-25172
Control surface spanwise placement in active flutter suppression systems N89-25195
The art of spacecraft design: A multidisciplinary challenge N89-25209
Meeting the challenges with the Douglas Aircraft Company Aeroelastic Design Optimization Program (ADOP) N89-25222

AEROELASTICITY
Structural optimization of rotor blades with straight and swept tips subject to aeroelastic constraints N89-25152
Optimization of rotor blades for combined structural, performance, and aeroelastic characteristics N89-25153
Efficient sensitivity analysis and optimization of a helicopter rotor N89-25155

Composite sizing and ply orientation for stiffness requirements using a large finite element structural model N89-25166
Aeroelastic tailoring and integrated wing design N89-25167
Effects of nonlinear aerodynamics and static aeroelasticity on mission performance calculations for a fighter aircraft N89-25170
Results of including geometric nonlinearities in an aeroelastic model of an F/A-18 N89-25190
An overview of the Douglas Aircraft Company Aeroelastic Design Optimization Program (ADOP) N89-25221
Meeting the challenges with the Douglas Aircraft Company Aeroelastic Design Optimization Program (ADOP) N89-25222
An analytical sensitivity method for use in integrated aeroservoelastic aircraft design [NASA-TM-101583] N89-25239
Flap-lag stability data for a small-scale isolated hingeless rotor in forward flight [NASA-TM-102189] N89-25479

AERONAUTICAL ENGINEERING
Aeronautical engineering: A continuing bibliography with indexes (supplement 239) [NASA-SP-7037(239)] N89-25114
Aeronautical engineering: A continuing bibliography with indexes (supplement 240) [NASA-SP-7037(240)] N89-25115

AEROSOLS
Investigation of submicrometer aerosols for apportioning the impacts of airborne particulate matter at Deep Creek Lake [DE89-006186] N89-25524
Solar Mesosphere Explorer observations of stratospheric and mesospheric water vapor N89-25802
Observations of atmospheric water vapor with the SAGE 2 instrument N89-25805

AEROSPACE ENGINEERING
Federal incentives for industrial modernization: Historical review and future opportunities [NASA-TM-101785] N89-25764
NASA patent abstracts bibliography: A continuing bibliography. Section 1: Abstracts (supplement 35) [NASA-SP-7039(35)-SECT-1] N89-25775

AEROSPACE MEDICINE
USSR Space Life Sciences Digest. Index to issues 15-20 [NASA-CR-3922(25)] N89-25556
Aerospace medicine and biology: A continuing bibliography with indexes (supplement 323) [NASA-SP-7011(323)] N89-25563
Aerospace medicine and biology: A continuing bibliography with indexes (supplement 324) [NASA-SP-7011(324)] N89-25565
Aerospace medicine and biology: A continuing bibliography with indexes (supplement 325) [NASA-SP-7011(325)] N89-25567

AEROSPACE PLANES
Hypersonic airbreathing vehicle conceptual design (focus on aero-space plane) N89-25210

AEROSPACE SYSTEMS
Applications of integrated design/analysis systems in aerospace structural design N89-25147
Demonstration of decomposition and optimization in the design of experimental space systems N89-25160
Space directorate research and technology accomplishments for FY 1988 [NASA-TM-101597] N89-25947

AEROTHERMODYNAMICS
Finite element flow-thermal-structural analysis of aerodynamically heated leading edges N89-25198
Space directorate research and technology accomplishments for FY 1988 [NASA-TM-101597] N89-25947

AFRICA
FAO detailed rain mapping experiment [BCRS-88-11] N89-25552
FAO detailed rain mapping experiment phase B: Comparison of rainfall and evapotranspiration mapping N89-25554

AGROMETEOROLOGY
FAO detailed rain mapping experiment [BCRS-88-11] N89-25552
FAO detailed rain mapping experiment phase A: Meteosat based rainfall mapping in the Sahel region N89-25553
FAO detailed rain mapping experiment phase B: Comparison of rainfall and evapotranspiration mapping N89-25554

AILERONS
Aeroservoelastic tailoring for lateral control enhancement N89-25189

AIR CONDITIONING EQUIPMENT
Evaluation of auxiliary power subsystems for gas engine heat pumps, phase 2 [PB89-173694] N89-25411

AIR LAND INTERACTIONS
MECA Workshop on Atmospheric H2O Observations of Earth and Mars. Physical Processes, Measurements and Interpretations [NASA-CR-183335] N89-25790

AIR POLLUTION
Models for regional-scale photochemical production of ozone N89-25523
Investigation of submicrometer aerosols for apportioning the impacts of airborne particulate matter at Deep Creek Lake [DE89-006186] N89-25524
Preventing depletion of stratospheric ozone: Implications on future aircraft emissions [DE89-009964] N89-25530

AIR QUALITY
Models for regional-scale photochemical production of ozone N89-25523

AIR TRAFFIC CONTROL
Notice to Airmen (NOTAM) system operational concept [DOT/FAA/CT-TN89/10] N89-25142

AIR TRANSPORTATION
FAA statistical handbook of aviation: Calendar year 1987 [AD-A200917] N89-25113

AIRCRAFT ACCIDENTS
FAA statistical handbook of aviation: Calendar year 1987 [AD-A200917] N89-25113

AIRCRAFT CONFIGURATIONS
Aeroelastic modeling for the FIT (Functional Integration Technology) team F/A-18 simulation N89-25192
Hypersonic airbreathing vehicle conceptual design (focus on aero-space plane) N89-25210
The conceptual design of a Mach 2 Oblique Flying Wing supersonic transport [NASA-CR-177529] N89-25233

AIRCRAFT CONSTRUCTION MATERIALS
Multi-objective/loading optimization for rotating composite flexbeams N89-25157
Integrated aerodynamic-structural design of a forward-swept transport wing N89-25168
Probabilistic damage tolerance methods for metallic aerospace structures N89-25237
Materials and structures for 2000 and beyond: An attempted forecast [DFVLR-MITT-89-02] N89-25358

AIRCRAFT CONTROL
Contributions to the improvement of flight safety in wind shear [DFVLR-FB-88-49] N89-25144
Aeroservoelastic tailoring for lateral control enhancement N89-25189

AIRCRAFT DESIGN
Damping of wing tip vortex systems by the modification of the wing tips N89-25138
Recent Advances in Multidisciplinary Analysis and Optimization, part 1 [NASA-CP-3031-PT-1] N89-25146
Applications of integrated design/analysis systems in aerospace structural design N89-25147
Optimization by decomposition: A step from hierarchic to non-hierarchic systems N89-25149
Overview of Dynamics Integration Research (DIR) program at Langley Research Center N89-25150
Structural optimization of rotor blades with straight and swept tips subject to aeroelastic constraints N89-25152
Optimization of rotor blades for combined structural, performance, and aeroelastic characteristics N89-25153
Transonic airfoil design for helicopter rotor applications N89-25154
Efficient sensitivity analysis and optimization of a helicopter rotor N89-25155
Multi-objective/loading optimization for rotating composite flexbeams N89-25157
Development of a microcomputer based integrated design system for high altitude long endurance aircraft N89-25159
TRUSS: An intelligent design system for aircraft wings N89-25162
The designer of the 90's: A live demonstration N89-25164
Structural tailoring of counter rotation propfans N89-25165
Composite sizing and ply orientation for stiffness requirements using a large finite element structural model N89-25166
Aeroelastic tailoring and integrated wing design N89-25167
Integrated aerodynamic-structural design of a forward-swept transport wing N89-25168
Effects of nonlinear aerodynamics and static aeroelasticity on mission performance calculations for a fighter aircraft N89-25170
Optimum structural design with static aeroelastic constraints N89-25171
Optimum design of swept-forward high-aspect-ration graphite-epoxy wings N89-25172
Recent Advances in Multidisciplinary Analysis and Optimization, part 2 [NASA-CP-3031-PT-2] N89-25173
ASTROS: A multidisciplinary automated structural design tool N89-25174
Recent experiences using finite-element-based structural optimization N89-25177
Computerized Design Synthesis (CDS), A database-driven multidisciplinary design tool N89-25180
Aeroservoelastic tailoring for lateral control enhancement N89-25189
Results of including geometric nonlinearities in an aeroelastic model of an F/A-18 N89-25190
Flutter suppression using eigenspace freedoms to meet requirements N89-25191
Aeroelastic modeling for the FIT (Functional Integration Technology) team F/A-18 simulation N89-25192
An integrated approach to the optimum design of actively controlled composite wings N89-25194
Control surface spanwise placement in active flutter suppression systems N89-25195
An approximation function for frequency constrained structural optimization N89-25196
Structural optimization of framed structures using generalized optimality criteria N89-25197
Recent Advances in Multidisciplinary Analysis and Optimization, part 3 [NASA-CP-3031-PT-3] N89-25201
Hypersonic airbreathing vehicle conceptual design (focus on aero-space plane) N89-25210
Optimizing conceptual aircraft designs for minimum life cycle cost N89-25211
Aircraft design optimization with multidisciplinary performance criteria N89-25212
An overview of the Douglas Aircraft Company Aeroelastic Design Optimization Program (ADOP) N89-25221
Recent developments in large-scale structural optimization N89-25231
Time-correlated gust loads using Matched-Filter Theory and Random-Process Theory: A new way of looking at things [NASA-TM-101573] N89-25232
The conceptual design of a Mach 2 Oblique Flying Wing supersonic transport [NASA-CR-177529] N89-25233
An economic model for evaluating high-speed aircraft designs [NASA-CR-177530] N89-25235
An analytical sensitivity method for use in integrated aeroservoelastic aircraft design [NASA-TM-101583] N89-25239

AIRCRAFT INDUSTRY
An economic model for evaluating high-speed aircraft designs [NASA-CR-177530] N89-25235
Federal incentives for industrial modernization: Historical review and future opportunities [NASA-TM-101785] N89-25764

AIRCRAFT LANDING
Reduction of aircraft noise in civil air transport by optimization of flight tracks and takeoff and approach procedures [ILR-MITT-200] N89-25676

AIRCRAFT MODELS
Meeting the challenges with the Douglas Aircraft Company Aeroelastic Design Optimization Program (ADOP) N89-25222

AIRCRAFT NOISE
Structural loading and noise disturbance of helicopters N89-25140
Reduction of aircraft noise in civil air transport by optimization of flight tracks and takeoff and approach procedures [ILR-MITT-200] N89-25676

AIRCRAFT STABILITY
Aeroservoelastic tailoring for lateral control enhancement N89-25189

AIRCRAFT STRUCTURES
Aeroelastic tailoring and integrated wing design N89-25167
Recent developments in large-scale structural optimization N89-25231

Time-correlated gust loads using Matched-Filter Theory and Random-Process Theory: A new way of looking at things
[NASA-TM-101573] N89-25232
Probabilistic damage tolerance methods for metallic aerospace structures N89-25237
Materials and structures for 2000 and beyond: An attempted forecast
[DFVLR-MITT-89-02] N89-25358

AIRFOIL PROFILES
Airfoil self-noise and prediction
[NASA-RP-1218] N89-25673

AIRFOILS
Numerical analysis of supersonic flow through oscillating cascade sections by using a deforming grid
[NASA-TM-102053] N89-25119
Two-dimensional elliptic grid generation for airfoils and cascades
[DFVLR-FB-88-52] N89-25125
Design optimization of axisymmetric bodies in nonuniform transonic flow N89-25206
Airfoil self-noise and prediction
[NASA-RP-1218] N89-25673

AIRFRAMES
Probabilistic damage tolerance methods for metallic aerospace structures N89-25237
Plan, formulate, discuss and correlate a NASTRAN finite element vibrations model of the Boeing Model 360 helicopter airframe
[NASA-CR-181787] N89-25480

AIRGLOW
A study of non-linear ionization processes in planetary atmospheres N89-25816

AIRPORT SURFACE DETECTION EQUIPMENT
Prototype of a slant visual range measuring device
[DFVLR-FB-88-42] N89-25697

AIRPORTS
FAA statistical handbook of aviation: Calendar year 1987
[AD-A200917] N89-25113

ALBEDO
The 2060 Chiron: CCD photometry
[NASA-CR-185068] N89-25435
Cloud albedo, greenhouse effects, atmospheric chemistry, and climate change
[DE89-010239] N89-25532

ALGAE
Characterization of Spirulina biomass for CELSS diet potential
[NASA-CR-185329] N89-25561

ALGEBRA
An interpretation and solution of ill-conditioned linear equations N89-25213
Toward a proof of the existence of an integrity basis for the tensors in the enveloping algebra of su(3)
[DE88-706031] N89-25646
Degenerate representation from tensorial identities and quantum realisations of YBZF algebras
[DE88-706032] N89-25647
Differential algebras without differentials: An easy C++ implementation
[DE89-011503] N89-25655

ALGORITHMS
Optimizing for minimum weight when two different finite element models and analyses are required N89-25200
Multiplier-continuation algorithms for constrained optimization N89-25218
An improved algorithm for optimum structural design with multiple frequency constraints N89-25229
Space nuclear reactor shields for manned and unmanned applications
[NASA-TM-102064] N89-25272
Time-dependent computational studies of flames in microgravity
[NASA-CR-182298] N89-25353
Sensitivity analysis of complex coupled systems extended to second and higher order derivatives
[NASA-TM-101587] N89-25354
Adaptive mesh refinement on moving quadrilateral grids
[DE89-010241] N89-25421
A variationally optimized vortex tracing algorithm for three-dimensional flows around solid bodies
[ETN-89-94301] N89-25423
Digital dynamic amplitude-frequence spectral analyzer
[DE88-706256] N89-25436
Generalized consistency checking of multivariable redundant measurements and common-mode failure detection
[DE89-010053] N89-25474
The Fermilab Lattice Supercomputer Project
[DE89-010510] N89-25578
Parallel solution of a 2-D phase change problem on a hypercube
[DE89-009619] N89-25586
A parallel algorithm for switch-level timing simulation on a hypercube multiprocessor
[NASA-CR-185338] N89-25595
Parallel solutions of a 2-D phase change problem on a hypercube
[DE89-012886] N89-25602
Parallel processors and nonlinear structural dynamics algorithms and software
[NASA-CR-185049] N89-25620
Balancing a matrix for calculation of eigenvalues and eigenvectors
[DE88-706045] N89-25648
Program package for investigation of differential equations by the external form method
[DE88-706258] N89-25650
Fast polar decomposition of an arbitrary matrix
[NASA-CR-185412] N89-25653
Differential algebras without differentials: An easy C++ implementation
[DE89-011503] N89-25655

ALLOYING
Applicability of microalloying in the production of sintered steel structural parts
[KFK-4481] N89-25329

ALLOYS
Procedures for characterizing an alloy and predicting cyclic life with the total strain version of Strainrange Partitioning
[NASA-TM-4102] N89-25485
Crack growth under low cycle fatigue
[GKSS-88/E/47] N89-25491

ALTERNATIVES
Evaluating CFC (Chlorofluorocarbon) alternatives from the atmospheric viewpoint
[DE89-010238] N89-25531

ALUMINIDES
Characterization of ceramics and intermetallics fabricated by self-propagating high-temperature synthesis
[NASA-TM-102004] N89-25285

ALUMINUM
Use of resonance neutrons for analyzing superclean aluminium
[DE88-706221] N89-25313
Stress-driven diffusive voiding of aluminum conductor lines
[DE89-009832] N89-25387

ALUMINUM ALLOYS
The strength-toughness relationship at cryogenic temperatures in aluminum-lithium alloy plate
[DE89-011816] N89-25322
Cryogenic mechanical properties of low density superplastically formable Al-Li alloys
[DE89-010587] N89-25343

ALUMINUM OXIDES
Optical properties of metal-oxide thin films: Influence of microstructure
[DE89-011219] N89-25690

AMBIGUITY
Phase-ambiguity resolution for QPSK modulation systems. Part 1: A review
[NASA-CR-185385] N89-25380
Phase-ambiguity resolution for QPSK modulation systems. Part 2: A method to resolve offset QPSK
[NASA-CR-184971] N89-25381

AMBIPOLAR DIFFUSION
Ambipolar diffusion and core formation in molecular clouds N89-25782

AMPLITUDE DISTRIBUTION ANALYSIS
Measurements of high degree solar oscillation amplitudes N89-25825

ANALOG DATA
Spacelab Data Processing Facility
[NASA-TM-101808] N89-25252

ANALOG TO DIGITAL CONVERTERS
Digital optical conversion module
[DE89-011441] N89-25367

ANALYSIS OF VARIANCE
Orientation, motion, and other properties of FTE structures on September 4, 1984 N89-25718

ANGLE OF ATTACK
Low-speed wind tunnel performance of high-speed counterrotation propellers at angle-of-attack
[NASA-TM-102292] N89-25121

ANGULAR MOMENTUM
Angular momentum transport and dynamo action in the Sun: A report on implications of a recent helioseismic estimate of solar rotation N89-25837

ANGULAR VELOCITY
Radial and latitudinal gradients in the solar internal angular velocity N89-25831
Solar radiation models and the a1, a3 and a5 splitting coefficients for solar acoustic oscillations N89-25834
A way to examine rotational splittings without explicit foward or inverse computations --- Sun N89-25841
Differential rotation in the solar interior N89-25843

ANNEALING
Optimal placement of excitations and sensors by simulated annealing N89-25227

ANNUAL VARIATIONS
Seasonal and diurnal variability of Mars water-ice clouds N89-25794
Cumulus convection and the terrestrial water-vapor distribution N89-25796
Very high elevation water ice clouds on Mars: Their morphology and temporal behavior N89-25804
Diurnal and annual cycles of H2O in the Martian regolith N89-25809
The interannual variability of atmospheric water vapor on Mars N89-25813

ANTARCTIC REGIONS
Water in the Martian regolith N89-25791

ANTENNA ARRAYS
Spectral shaping and phase control of a fast-wave current drive antenna array
[DE89-011567] N89-25368

ANTENNA DESIGN
Structural optimization and recent large ground antenna installations N89-25224
Pyramidal horns: Part 1: Simple expressions for directivity as a function of aperture phase error
[DE89-005209] N89-25370
Pyramidal horns: Part 2: A novel design method for horns of any desired gain and aperture phase error
[DE89-005346] N89-25371
Numerical modeling of monopoles on radial-wire ground screens
[DE89-005350] N89-25372
A generalized antenna theorem for broadband pulses
[DE89-009707] N89-25373
A multifrequency antenna system for propagation experiments with the Olympus satellite
[EUT-88-E-192] N89-25378

ANTENNA RADIATION PATTERNS
A multifrequency antenna system for propagation experiments with the Olympus satellite
[EUT-88-E-192] N89-25378

ANTENNAS
Structural optimization and recent large ground antenna installations N89-25224

ANTIREFLECTION COATINGS
Deposition of dielectric optical coatings: A microstructural study of the deposited layers and interfaces
[DE89-011205] N89-25694

APOLLO FLIGHTS
Where no man has gone before: A history of Apollo lunar exploration missions
[NASA-SP-4214] N89-25946

APOLLO PROJECT
Where no man has gone before: A history of Apollo lunar exploration missions
[NASA-SP-4214] N89-25946

APOLLO SPACECRAFT
Where no man has gone before: A history of Apollo lunar exploration missions
[NASA-SP-4214] N89-25946

APPLICATIONS PROGRAMS (COMPUTERS)
Plan, formulate, discuss and correlate a NASTRAN finite element vibrations model of the Boeing Model 360 helicopter airframe
[NASA-CR-181787] N89-25480
User's guide to image processing applications of the NOAA satellite HRPT/AVHRR data. Part 1: Introduction to the satellite system and its applications. Part 2: Processing and analysis of AVHRR imagery
[NASA-CR-180784] N89-25492
A simple method to remove reference counting in applicative programs
[DE89-006739] N89-25603
Use of metaknowledge in the verification of knowledge-based systems
[NASA-CR-181821] N89-25627

APPROXIMATION
An approximation function for frequency constrained structural optimization N89-25196
Recent developments in multilevel optimization N89-25203
The role of optimization in the next generation of computer-based design tools N89-25220

ARC DISCHARGES
The influence of contact surface microstructure on vacuum arc stability and arc voltage
[EUT-87-E-186] N89-25672

ARC JET ENGINES
The effects of arcjet operating condition and constrictor geometry on the plasma plume
[NASA-TM-102284] N89-25281

ARC WELDING
Detection of metal-transfer mode in GMAW
[DE89-011133] N89-25465

ARCHITECTURE
Space station architecture, module, berthing hub, shell assembly, berthing mechanism and utility connection channel
[NASA-CASE-ARC-11505-2] N89-25266
ARCHITECTURE (COMPUTERS)
Digital optical conversion module
[DE89-011441] N89-25367
Review of the 1988 Workshop on Human-Machine Symbiotic Systems
[DE89-008743] N89-25570
The 1988 Workshop on Human-Machine Symbiotic Systems
[DE89-010170] N89-25572
The epsilon dataflow processor
[DE89-001679] N89-25577
The Fermilab Lattice Supercomputer Project
[DE89-010510] N89-25578
Microprocessors and other processors for triggering and filtering at the SSC
[DE89-011088] N89-25580
TUMULT: The Twente University Multiprocessor
[MEMO-INF-88-28] N89-25581
Rationale for the proposed standard for a generic package of elementary functions for Ada
[DE89-010282] N89-25588
Concurrent spatio-temporal image analysis
[DE89-010260] N89-25593
Concurrent multi-resolution image analysis
[DE89-010261] N89-25594
The ADAMS database language
[DE89-010925] N89-25601
A simple method to remove reference counting in applicative programs
[DE89-006739] N89-25603
Parallel processors and nonlinear structural dynamics algorithms and software
[NASA-CR-185049] N89-25620
Design and construction of a computer system model for application development workloads
[DE89-010519] N89-25622
Performance evaluation for data flow architectures: A summary of discussions from the Santa Fe workshop
[DE89-008023] N89-25624
The Delta-t transport protocol: Features and experience useful for high performance networks
[DE89-009259] N89-25625
Interconnection networks
[DE89-010965] N89-25626
A site oriented supercomputer for theoretical physics: The Fermilab Advanced Computer Program Multi Array Processor System (ACMAPS)
[DE89-011090] N89-25631
Integrated Services Digital Network: Overview and architectural concepts
[MEMO-INF-88-42] N89-25634
Data acquisition, event building, and on-line processing: Summary talk
[DE89-011085] N89-25693
ARRAYS
Handling arrays in symbolic execution
[REPT-89-003] N89-25609
ARTIFICIAL INTELLIGENCE
STRUTEX: A prototype knowledge-based system for initially configuring a structure to support point loads in two dimensions N89-25161
Recent Advances in Multidisciplinary Analysis and Optimization, part 2
[NASA-CP-3031-PT-2] N89-25173
Design of an auto change mechanism and intelligent gripper for the space station
[NASA-CR-185387] N89-25268
Review of the 1988 Workshop on Human-Machine Symbiotic Systems
[DE89-008743] N89-25570
The 1988 Workshop on Human-Machine Symbiotic Systems
[DE89-010170] N89-25572
Timesharing performance as an indicator of pilot mental workload
[NASA-CR-185328] N89-25573
The RIACS Intelligent Auditing and Categorizing System
[NASA-CR-185398] N89-25598
Use of metaknowledge in the verification of knowledge-based systems
[NASA-CR-181821] N89-25627
A parallel processing approach for implementing high-performance first-order logic deduction systems
[DE89-011878] N89-25632
Robust performance of multiple tasks by an autonomous robot
[DE89-008718] N89-25636
Blindness in designing intelligent systems
[NASA-CR-184582] N89-25638
Synthetic organisms and self-designing systems
[NASA-CR-185324] N89-25639
Explanation in knowledge-based systems
[MEMO-INF-88-17] N89-25640
The use of first principles in diagnosing complex technical devices
[MEMO-INF-88-40] N89-25641
ARTIFICIAL SATELLITES
Continuous global N-tuple coverage with (2N = 2) satellites
[AD-A206522] N89-25262
ASPECT RATIO
Averaged equilibrium and stability in low-aspect-ratio stellarators
[DE89-013618] N89-25713
ASPHERICITY
Radial and temporal structure of the internal solar asphericity N89-25833
ASSESSMENTS
Structural damage assessment as an identification problem N89-25230
ASTRODYNAMICS
Some aspects of the dynamics of orbit-orbit resonances in the Uranian satellite system N89-25815
ASTRONAUT TRAINING
Space station operations task force. Panel 1 report: Space operations and support systems
[NASA-TM-101816] N89-25244
ASTRONOMICAL MODELS
Ambipolar diffusion and core formation in molecular clouds N89-25782
Evolution of cosmic string networks
[NASA-CR-185467] N89-25788
ASTRONOMICAL PHOTOMETRY
Effect of atmospheric extinction on solar radial velocity measurements N89-25849
ASTRONOMICAL SPECTROSCOPY
Observations of f- and p-mode oscillations of high degree (500 is less than L is less than 2500) in quiet and active Sun N89-25875
ASTROPHYSICS
Physics of dense matter, neutron stars and supernova
[DE89-010673] N89-25784
ASYMPTOTIC METHODS
Sound velocity distribution in the Sun inferred from asymptotic inversion of p-mode spectra N89-25900
Helioseismological inverse problem: Sound speed in the solar interior N89-25901
Determination of the solar internal sound speed by means of a differential asymptotic inversion N89-25904
Determination of the solar sound speed by an asymptotic inversion technique N89-25913
Asymptotic approximations of nonradial oscillation modes of the Sun N89-25932
ASYMPTOTIC PROPERTIES
Black-box identification of MIMO transfer functions: Asymptotic properties of prediction error models
[EUT-87-E-182] N89-25642
Observed asymptotic properties of low-degree solar gravity-mode eigenfrequencies N89-25890
Inversion of quasi-periodic deviations between low-degree solar gravity mode eigenfrequencies and asymptotic theory eigenfrequencies N89-25891
ASYMPTOTIC SERIES
Analytic theory for the determination of velocity and stability of bubbles in a Hele-Shaw cell. Part 1: Velocity selection
[NASA-CR-181836] N89-25665
ATMOSPHERIC ATTENUATION
Microwave scattering models and basic experiments
[NASA-CR-185393] N89-25364
Effect of atmospheric extinction on solar radial velocity measurements N89-25849
ATMOSPHERIC BOUNDARY LAYER
Mesoscale model parameterizations for radiation and turbulent fluxes at the lower boundary
[DFVLR-FB-88-48] N89-25544
ATMOSPHERIC CHEMISTRY
Photodissociation of pernitric acid (HO2NO2) at 248 nm
[NASA-CR-185363] N89-25286
The UARS (Upper Atmosphere Research Satellite): A program to study global ozone change
[NASA-TM-101756] N89-25520
Models for regional-scale photochemical production of ozone N89-25523
The role of forests in addressing the CO2 greenhouse
[DE89-011568] N89-25527
Preventing depletion of stratospheric ozone: Implications on future aircraft emissions
[DE89-009964] N89-25530
Evaluating CFC (Chlorofluorocarbon) alternatives from the atmospheric viewpoint
[DE89-010238] N89-25531
Cloud albedo, greenhouse effects, atmospheric chemistry, and climate change
[DE89-010239] N89-25532
A study of non-linear ionization processes in planetary atmospheres N89-25816
ATMOSPHERIC CIRCULATION
The behavior of a class of minimal models of the atmospheric general circulation N89-25537
Comparison of satellite-derived dynamical quantities for the stratosphere of the Southern Hemisphere
[NASA-CP-3044] N89-25540
The evolution and structure of the bow echo/microburst events N89-25550
ATMOSPHERIC COMPOSITION
The UARS (Upper Atmosphere Research Satellite): A program to study global ozone change
[NASA-TM-101756] N89-25520
Atmospheric carbon dioxide and the climate record
[DE89-011892] N89-25528
Cloud albedo, greenhouse effects, atmospheric chemistry, and climate change
[DE89-010239] N89-25532
Factors governing water condensation in the Martian atmosphere N89-25797
Cumulus convection and the terrestrial water-vapor distribution N89-25798
Measurements of H2O in the terrestrial mesosphere and implications for extra-terrestrial sources N89-25808
ATMOSPHERIC EFFECTS
Tropospheric influences on satellite-Earth paths and their determination by means of radar measurements
[DFVLR-FB-88-53] N89-25250
Studies of regional and global tectonics and the rotation of the earth using very-long baseline interferometry
[NASA-CR-185059] N89-25534
ATMOSPHERIC GENERAL CIRCULATION MODELS
Climate projections with regional resolution
[DE89-009261] N89-25529
The behavior of a class of minimal models of the atmospheric general circulation N89-25537
Regional validation of general circulation models N89-25538
Factors governing water condensation in the Martian atmosphere N89-25797
ATMOSPHERIC HEATING
Climate projections with regional resolution
[DE89-009261] N89-25529
ATMOSPHERIC IONIZATION
A study of non-linear ionization processes in planetary atmospheres N89-25816
ATMOSPHERIC MODELS
Models for regional-scale photochemical production of ozone N89-25523
Atmospheric carbon dioxide and the climate record
[DE89-011892] N89-25528
Cloud albedo, greenhouse effects, atmospheric chemistry, and climate change
[DE89-010239] N89-25532
Mesoscale model parameterizations for radiation and turbulent fluxes at the lower boundary
[DFVLR-FB-88-48] N89-25544
ATMOSPHERIC MOISTURE
A procedure for the numerical description of the moisture dependent material behavior
[ETN-89-94669] N89-25299
Studies of regional and global tectonics and the rotation of the earth using very-long baseline interferometry
[NASA-CR-185059] N89-25534
Transport of Mars atmospheric water into high northern latitudes during a polar warming N89-25792
The effect of global-scale divergent circulation on the atmospheric water vapor transport and maintenance N89-25793
The interpretation of data from the Viking Mars Atmospheric Water Detectors (MAWD): Some points for discussion N89-25795
Regolith water vapor sources on Mars: A historical bibliography N89-25796
Cumulus convection and the terrestrial water-vapor distribution N89-25798
Possible significance of cubic water-ice, H2O-Ic, in the atmospheric water cycle of Mars N89-25799
On the vertical distribution of water vapor in the Martian tropics N89-25800
The behavior of water vapor in the Mars atmosphere N89-25801
Solar Mesosphere Explorer observations of stratospheric and mesospheric water vapor N89-25802
Circumpolar hoods and clouds and their relation to the Martian H2O cycle N89-25803
Observations of atmospheric water vapor with the SAGE 2 instrument N89-25805
Flux of water vapor in the terrestrial stratosphere and in the Martian atmosphere N89-25806
Measurements of H2O in the terrestrial mesosphere and implications for extra-terrestrial sources N89-25808

Atmospheric H2O and the search for Martian brines N89-25812
The interannual variability of atmospheric water vapor on Mars N89-25813
The Martian atmospheric water cycle as viewed from a terrestrial perspective N89-25814

ATMOSPHERIC OPTICS
Measurements of high degree solar oscillation amplitudes N89-25825
A detector of small gradients of transparency of the terrestrial atmosphere N89-25857

ATMOSPHERIC PHYSICS
New atmospheric sensor analysis study [NASA-CR-183597] N89-25431
The UARS (Upper Atmosphere Research Satellite): A program to study global ozone change [NASA-TM-101756] N89-25520

ATMOSPHERIC PRESSURE
The Martian atmospheric water cycle as viewed from a terrestrial perspective N89-25814

ATMOSPHERIC SCATTERING
Microwave scattering models and basic experiments [NASA-CR-185393] N89-25364

ATMOSPHERIC SOUNDING
New atmospheric sensor analysis study [NASA-CR-183597] N89-25431

ATMOSPHERIC STRATIFICATION
Scattering and multiple scattering of acoustic waves in a stratified medium N89-25898

ATMOSPHERIC TEMPERATURE
Climate projections with regional resolution [DE89-009261] N89-25529
Measurements of the vertical profile of water vapor abundance in the Martian atmosphere from Mars Observer N89-25811
The Martian atmospheric water cycle as viewed from a terrestrial perspective N89-25814

ATOMIC CLOCKS
Synchronization of the ground station atomic clocks using weighted transportable cesium time standards in the navigation experiment (NAVEX) [DFVLR-MITT-89-01] N89-25448

ATOMIC STRUCTURE
Monte Carlo for the electronic structure of molecules [DE89-011824] N89-25682
Electronic structure of high temperature superconductors [DE89-008610] N89-25741

ATTITUDE CONTROL
Time-optimal slewing maneuvers of flexible spacecraft N89-25265

AURORAS
An auroral TV-system [REPT-115(1988)] N89-25543

AUSTENITIC STAINLESS STEELS
Quantitative modeling of sensitization development in austenitic stainless steel [DE89-011206] N89-25317
Precipitation at grain boundaries in irradiated austenitic Fe-Cr-Mn alloys [DE89-011207] N89-25319
Effect of low neutron fluences on DIN 1.4948 steel creep properties --- liquid metal fast breeder reactor (LMFBR) material [ECN-206] N89-25325
Welding of helium-doped austenitic and ferritic stainless steels [DE89-012523] N89-25468

AUTOCORRELATION
Searching for solar g-modes. Tests of a statistical method N89-25889

AUTOMATA THEORY
The full decomposition of sequential machines with the state and output behavior realization [EUT-88-E-188] N89-25582

AUTOMATIC CONTROL
Automated Test and Evaluation Center for Waveform Digitizer Systems and Components [DE89-010226] N89-25441

AUTOMATIC PILOTS
Real-time application of knowledge-based systems N89-25163

AUTONOMY
Robust performance of multiple tasks by an autonomous robot [DE89-008718] N89-25636

AUTOREGRESSIVE PROCESSES
Least squares parameter estimation in a dynamic model from noisy observations [ETN-89-94295] N89-25657

AUXILIARY PROPULSION
Advanced APS impacts on vehicle payloads [NASA-TM-102086] N89-25254

AXIAL FLOW
Dissipation of vortex power in longitudinal flow on wings N89-25133

AXISYMMETRIC BODIES
Design optimization of axisymmetric bodies in nonuniform transonic flow N89-25206

B

B STARS
Radial vibrations in a 5 solar M hydrogen-helium star N89-25938

BACKSCATTERING
The application of Rutherford backscattering and channeling techniques to the characterization of ceramics [DE89-010257] N89-25333
The formation and analysis of thin film high temperature superconductors [DE89-011177] N89-25745

BANDWIDTH
Integrated Services Digital Network: Overview and architectural concepts [MEMO-INF-88-42] N89-25634

BARIUM OXIDES
Production of wires and coils from high-temperature superconducting materials [DE89-012380] N89-25756

BARRELS (CONTAINERS)
Dynamic fracture toughness measurements of ferritic ductile cast iron [DE89-009833] N89-25324

BAYES THEOREM
Discrimination and classification with mixed binary and continuous variables: The Bayesian approach [MATHS-RES-212] N89-25664

BEAMS (RADIATION)
Flying wires at Fermilab [DE89-011005] N89-25251

BEAMS (SUPPORTS)
Multi-objective/loading optimization for rotating composite flexbeams N89-25157
Computational experiments in the optimal slewing of flexible structures N89-25226
Pactruss support structure for precision segmented reflectors [NASA-CR-181747] N89-25484

BEDS (PROCESS ENGINEERING)
On the stress problem of the pebble bed heat exchanger in a hypersonic wind tunnel [NAL-TM-ST-8705] N89-25240

BENDING
An analytical and experimental investigation of edge delamination in laminates subjected to tension, bending, and torsion [NASA-CR-181824] N89-25296

BETA PARTICLES
Nuclear beta decay far from stability and astrophysics [MPI-H-1988-V-27] N89-25683

BETATRONS
Amplitude growth due to random, correlated kicks [DE89-011504] N89-25418

BIBLIOGRAPHIES
Aeronautical engineering: A continuing bibliography with indexes (supplement 239) [NASA-SP-7037(239)] N89-25114
Aeronautical engineering: A continuing bibliography with indexes (supplement 240) [NASA-SP-7037(240)] N89-25115
Earth resources: A continuing bibliography with indexes (issue 61) [NASA-SP-7041(61)] N89-25493
USSR Space Life Sciences Digest. Index to issues 15-20 [NASA-CR-3922(25)] N89-25556
Aerospace medicine and biology: A continuing bibliography with indexes (supplement 323) [NASA-SP-7011(323)] N89-25563
Aerospace medicine and biology: A continuing bibliography with indexes (supplement 324) [NASA-SP-7011(324)] N89-25565
Aerospace medicine and biology: A continuing bibliography with indexes (supplement 325) [NASA-SP-7011(325)] N89-25567
Bibliographic coupling among scientific papers in biological research specialties N89-25771
NASA patent abstracts bibliography: A continuing bibliography. Section 1: Abstracts (supplement 35) [NASA-SP-7039(35)-SECT-1] N89-25775

BINARY FLUIDS
Advanced binary geothermal power plants working fluid property determination and heat exchanger design [DE89-011144] N89-25513

BINARY MIXTURES
Binary and ternary gas mixtures with temperature enhanced diffuse glow discharge characteristics for use in closing switches [DE89-011807] N89-25395

BINARY STARS
The origin of ultra-compact binaries [NASA-TM-101792] N89-25780

BIOASTRONAUTICS
USSR Space Life Sciences Digest. Index to issues 15-20 [NASA-CR-3922(25)] N89-25556
Aerospace medicine and biology: A continuing bibliography with indexes (supplement 323) [NASA-SP-7011(323)] N89-25563
Aerospace medicine and biology: A continuing bibliography with indexes (supplement 324) [NASA-SP-7011(324)] N89-25565
Aerospace medicine and biology: A continuing bibliography with indexes (supplement 325) [NASA-SP-7011(325)] N89-25567

BIOCHEMISTRY
ECUT (Energy Conversion and Utilization Technologies) program: Biocatalysis project [NASA-CR-184965] N89-25519

BIOELECTRICITY
Adaptive enhancement of magnetoencephalographic signals via multichannel filtering [DE89-005464] N89-25569

BIOLOGICAL EFFECTS
The role of forests in addressing the CO2 greenhouse [DE89-011568] N89-25527
Acclimatization to heat in humans [NASA-TM-101011] N89-25558
Aerospace medicine and biology: A continuing bibliography with indexes (supplement 323) [NASA-SP-7011(323)] N89-25563
Aerospace medicine and biology: A continuing bibliography with indexes (supplement 324) [NASA-SP-7011(324)] N89-25565
Aerospace medicine and biology: A continuing bibliography with indexes (supplement 325) [NASA-SP-7011(325)] N89-25567

BIOLOGICAL EVOLUTION
Solar system exploration [NASA-TM-101784] N89-25944

BIOLOGICAL MODELS (MATHEMATICS)
Catastrophic bifurcations in a second order dynamical system [REPT-88-049] N89-25533

BIOMASS
Characterization of Spirulina biomass for CELSS diet potential [NASA-CR-185329] N89-25561

BIOPHYSICS
Effects of freezing and cold acclimation on the plasma membrane of isolated protoplasts [DE89-010931] N89-25560

BIOPROCESSING
Spiral vane bioreactor [NASA-CASE-MSC-21361-1] N89-25557

BIOREACTORS
Spiral vane bioreactor [NASA-CASE-MSC-21361-1] N89-25557

BISMUTH COMPOUNDS
Variation of superlattice structure of the Bi2Sr(2-x)CuO(6-y) superconductor with composition and thermal history [DE89-011612] N89-25749

BLADE SLAP NOISE
Data of aeroacoustic measurements on ultralight aircraft propellers [DFVLR-MITT-88-33] N89-25677

BLADE-VORTEX INTERACTION
Airfoil self-noise and prediction [NASA-RP-1218] N89-25673

BLANKETS (FUSION REACTORS)
Influence of the helium on high temperature embrittlement of metals under cyclic loading [JUEL-2229] N89-25330
Heat transfer in packed beds [KFK-4451] N89-25425

BLINDNESS
Blindness in designing intelligent systems [NASA-CR-184582] N89-25638

BODY TEMPERATURE
Acclimatization to heat in humans [NASA-TM-101011] N89-25558

BOOSTERS
High explosives reaction model and its application to booster performance [DE89-005459] N89-25351

BOOTS (FOOTWEAR)
Correlation of subjective slipperiness judgements with quantitative COF (Coefficient Of Friction) measurements for structural steel [PB89-165070] N89-25669

BOUNDARY ELEMENT METHOD
On equivalence of discrete-discrete and continuum-discrete design sensitivity analysis N89-25181

Treatment of body forces in boundary element design sensitivity analysis N89-25187
Design sensitivity analysis of boundary element substructures N89-25188
Coupling of the boundary element method with an integral momentum boundary-layer technique to calculate forces and moments on three-dimensional bodies [DE89-006328] N89-25420

BOUNDARY LAYER SEPARATION
Airfoil self-noise and prediction [NASA-RP-1218] N89-25673

BOUNDARY LAYER STABILITY
On the Gortler vortex instability mechanism at hypersonic speeds [NASA-CR-181844] N89-25123

BOUNDARY LAYER TRANSITION
Numerical simulation of transition from laminar to turbulent channel flow [DFVLR-FB-88-55] N89-25430

BOUNDARY LAYERS
Airfoil self-noise and prediction [NASA-RP-1218] N89-25673

BOUNDARY VALUE PROBLEMS
On the thermal surface boundary condition for solar pulsations N89-25931

BRANCHING (MATHEMATICS)
Catastrophic bifurcations in a second order dynamical system [REPT-88-049] N89-25533
An exercise in transformational programming: Back tracking and Branch-and-Bound [MEMO-INF-88-22] N89-25612

BRAYTON CYCLE
Solar dynamic power module design [NASA-TM-102055] N89-25269

BREADBOARD MODELS
An evaluation of the General Dynamics 20 kHz 5 kW Breadboard for space station electrical power at MSFC [NASA-TM-100367] N89-25278
Electrically compensated constant speed drive (Model number 60 ECEPGS 02) [AD-A206064] N89-25385
Development and testing of a 20-kHz component test bed [NASA-TM-102141] N89-25403

BREMSSTRAHLUNG
Z subeff measurements and low-Z impurity transport for NBI and ICRF heated plasma in JIPP T-IIU tokamak [IPPJ-896] N89-25701

BRINES
Atmospheric H2O and the search for Martian brines N89-25812

BROKEN SYMMETRY
Symmetry breaking: The standard model and superstrings [DE89-011771] N89-25761

BUBBLES
Analytic theory for the determination of velocity and stability of bubbles in a Hele-Shaw cell. Part 1: Velocity selection [NASA-CR-181836] N89-25665
Potential uses of vacuum bubbles in noise and vibration control [NASA-CR-181829] N89-25674

BUDGETING
Space station operations task force. Panel 3 report: User development and integration [NASA-TM-101818] N89-25246
Space station operations task force summary report [NASA-TM-101820] N89-25248
Space station operations task force. Executive summary [NASA-TM-101780] N89-25249

C

CALIBRATING
Pressure calibration and certification of a quartz pressure transducer [DE89-005774] N89-25439
Laser diffraction methods for high temperature strain measurements [DE89-008235] N89-25451
Visible and near-infrared channel calibration of the GOES-6 VISSR using high-altitude aircraft measurements [NASA-TM-101064] N89-25494
Calibration of the visible and near-infrared channels of the NOAA-9 AVHRR using high-altitude aircraft measurements from August 1985 and October 1986 [NASA-TM-101083] N89-25496
Towards an independent calibration of the mixing-length theory N89-25899
Solar calibration of asteroseismology N89-25921

CAMERA TUBES
Design and testing of the EG and G/Los Alamos Operations fast streak camera [DE89-010859] N89-25445

CANOPIES (VEGETATION)
Modeling land-surface albedos from plant canopy architecture N89-25495

CAPACITANCE
Initial design and analysis of a capacitive sensor for shear and normal force measurement [DE89-001821] N89-25438

CARBON
Whisker shaped carbon substance [DE89-010214] N89-25288
Novel air electrode for metal-air battery with new carbon material and method of making same [DE89-010964] N89-25391

CARBON DIOXIDE
The role of forests in addressing the CO2 greenhouse [DE89-011568] N89-25527
Climate projections with regional resolution [DE89-009904] N89-25549

CARBON DIOXIDE CONCENTRATION
Atmospheric carbon dioxide and the climate record [DE89-011892] N89-25526

CARBON FIBER REINFORCED PLASTICS
Polyimide Matrix composites: Polyimidesulfone/LARC-TPI (1:1) blend [NASA-TM-101568] N89-25294
Mechanical properties of carbon fiber reinforced thermoplastics for cryogenic applications [KFK-4487] N89-25297
Explosive cathode on the base of carbon-fibrous plastic material [DE88-706302] N89-25350

CARBON FIBERS
Explosive cathode on the base of carbon-fibrous plastic material [DE88-706302] N89-25350

CARBON STEELS
Elevated temperature deformation of structural steel [PB89-172621] N89-25318

CARBONIZATION
Low density microcellular carbon foams and method of preparation [DE89-010966] N89-25345

CASCADE FLOW
Numerical analysis of supersonic flow through oscillating cascade sections by using a deforming grid [NASA-TM-102053] N89-25119
Two-dimensional elliptic grid generation for airfoils and cascades [DFVLR-FB-88-52] N89-25125

CASSEGRAIN ANTENNAS
A multifrequency antenna system for propagation experiments with the Olympus satellite [EUT-88-E-192] N89-25378

CAST ALLOYS
J(sub Ic) fracture toughness of ferritic DCI (Ductile Cast Iron) alloys: A comparison of two versions of ASTM E 813 [DE89-012249] N89-25323
Dynamic fracture toughness measurements of ferritic ductile cast iron [DE89-009833] N89-25324

CASTING
High-performance, extrusion-cast explosives with low sensitivity [DE89-010279] N89-25349

CATABOLISM
A program for the study of skeletal muscle catabolism following physical trauma [AD-A206506] N89-25564

CATALYSIS
ECUT (Energy Conversion and Utilization Technologies) program: Biocatalysis project [NASA-CR-184965] N89-25519

CATALYSTS
Concepts in surface science and heterogeneous catalysts [DE89-010679] N89-25307

CATASTROPHE THEORY
Catastrophic bifurcations in a second order dynamical system [REPT-88-049] N89-25533

CATHODES
Explosive cathode on the base of carbon-fibrous plastic material [DE88-706302] N89-25350

CAVITATION FLOW
Transient effects in creep cavity nucleation and early growth in ceramics [DE89-010420] N89-25340
Cavitation kinetics during GTA (Gas Tungsten Arc) welding of helium containing stainless steel [DE89-012514] N89-25467

CAVITIES
Transient effects in creep cavity nucleation and early growth in ceramics [DE89-010420] N89-25340

CELLS (BIOLOGY)
Spiral vane bioreactor [NASA-CASE-MSC-21361-1] N89-25557
Effects of freezing and cold acclimation on the plasma membrane of isolated protoplasts [DE89-010931] N89-25560

CENTRAL PROCESSING UNITS
Microprocessors and other processors for triggering and filtering at the SSC [DE89-011088] N89-25580

CEPHEID VARIABLES
On radiative and convective influences on stellar pulsational stability N89-25828

CERAMIC COATINGS
Evaluation of ceramic coatings on silicon carbide [DE89-010321] N89-25339

CERAMICS
Characterization of ceramics and intermetallics fabricated by self-propagating high-temperature synthesis [NASA-TM-102004] N89-25285
The application of Rutherford backscattering and channeling techniques to the characterization of ceramics [DE89-010257] N89-25333
The mechanical properties of ion implanted ceramics [DE89-008928] N89-25337
Transient effects in creep cavity nucleation and early growth in ceramics [DE89-010420] N89-25340
Super-strong self-reinforcing polymeric matrices formed by the first super-strong polymers [DE89-011533] N89-25347
Heat transfer in packed beds [KFK-4451] N89-25425
Influence of the preparation conditions on the diamagnetic response of high-Tc YBa2Cu3Ox superconductor [DE88-706051] N89-25736
Processing chemically prepared Tl-Ca-Ba-Cu oxide superconductors [DE89-011535] N89-25748

CHANNEL FLOW
Interactions of Tollmien-Schlichting waves and Dean vortices. Comparison of direct numerical simulation and a weakly nonlinear theory [NASA-TP-2919] N89-25118
Experimental study of the phenomena of turbulent flow in the narrow gaps between subchannels of rod bundles [KFK-4501] N89-25428
Numerical simulation of transition from laminar to turbulent channel flow [DFVLR-FB-88-55] N89-25430
Analytic theory for the determination of velocity and stability of bubbles in a Hele-Shaw cell. Part 1: Velocity selection [NASA-CR-181836] N89-25665

CHARACTERIZATION
Photodissociation of pernitric acid (HO2NO2) at 248 nm [NASA-CR-185363] N89-25286

CHARGE COUPLED DEVICES
Some tests of the precision of CCD differential photometry measurements of bright double stars N89-25930

CHARTS
Common Graphics Library (CGL). Volume 2: Low-level user's guide [NASA-TM-101596] N89-25597

CHECKOUT
Reliability mechanisms for ADAMS (Advanced Data Management System) [DE89-010911] N89-25768

CHEMICAL ANALYSIS
Weldability and weld doping of commercial purity molybdenum [DE89-009535] N89-25311

CHEMICAL BONDS
Studies of 3-5 compounds in the megabar regime [DE89-012433] N89-25751

CHEMICAL COMPOSITION
The influence of cooling rate on the ferrite content of stainless steel alloys [DE89-009966] N89-25315
Deformation induced microstructural and microchemical changes during thermomechanical treatment [DE89-011608] N89-25321
High-performance, extrusion-cast explosives with low sensitivity [DE89-010279] N89-25349

Variation of superlattice structure of the Bi2Sr(2-x)CuO(6-y) superconductor with composition and thermal history
[DE89-011612] N89-25749

CHEMICAL REACTIONS
Improvements of the KIVA-2 computer program for numerical combustion
[DE89-007994] N89-25304
Concepts in surface science and heterogeneous catalysts
[DE89-010679] N89-25307
Issues in shock-induced solid state chemistry
[DE89-010769] N89-25309
Molecular growth pathways in silica sol-gel polymerization
[DE89-011224] N89-25346

CHEMICAL REACTORS
Method of production H2 using a rotating drum reactor with a pulse jet heat source
[DE89-009764] N89-25348

CHIRON
The 2060 Chiron: CCD photometry
[NASA-CR-185068] N89-25435

CHLOROCARBONS
Evaluating CFC (Chlorofluorocarbon) alternatives from the atmospheric viewpoint
[DE89-010238] N89-25531

CHROMOSPHERE
The influence of a chromospheric magnetic field on p- and f-modes N89-25874

CIRCUIT BOARDS
A decomposition-based design optimization method with applications N89-25204

CIRCUIT DIAGRAMS
An evaluation of the General Dynamics 20 kHz 5 kW Breadboard for space station electrical power at MSFC
[NASA-TM-100367] N89-25278

CIRCUITS
Apparatus and method for characterizing conductivity of materials
[DE89-009599] N89-25383

CIVIL AVIATION
FAA statistical handbook of aviation: Calendar year 1987
[AD-A200917] N89-25113
UK airmisses involving commercial air transport
[CAA-3/88] N89-25143
Report to Congress: Technical feasibility of joint use at Scott AFB, Selfridge AGB and El Toro MCAS
[AD-A194597] N89-25241

CLAMPS
Design of an auto change mechanism and intelligent gripper for the space station
[NASA-CR-185387] N89-25268

CLASSICAL MECHANICS
Localizability and covariance in analytical mechanics
[DE88-706038] N89-25666
Gravitational-like phase transition of a classical Coulomb plasma N89-25727

CLASSIFICATIONS
Discrimination and classification with mixed binary and continuous variables: The Bayesian approach
[MATHS-RES-212] N89-25664
Bibliographic coupling among scientific papers in biological research specialties N89-25771

CLIMATE
On greenhouse gas signal detection strategies
[DE89-009908] N89-25521
Workshop on Sea Level Rise and Coastal Processes
[DE89-010297] N89-25522
Atmospheric carbon dioxide and the climate record
[DE89-011892] N89-25528
Climate projections with regional resolution
[DE89-009904] N89-25549
Design description of the large scale climate simulator
[DE89-010185] N89-25551
Solar variability and climatology N89-25909

CLIMATE CHANGE
Climatic changes inferred fron analyses of lake-sediment cores, Walker Lake, Nevada
[DE89-010740] N89-25525
Climate projections with regional resolution
[DE89-009261] N89-25529
Cloud albedo, greenhouse effects, atmospheric chemistry, and climate change
[DE89-010239] N89-25532

CLIMATOLOGY
Climate projections with regional resolution
[DE89-009261] N89-25529

CLOSED ECOLOGICAL SYSTEMS
Characterization of Spirulina biomass for CELSS diet potential
[NASA-CR-185329] N89-25561

CLOUD HEIGHT INDICATORS
Prototype of a slant visual range measuring device
[DFVLR-FB-88-42] N89-25697

CLOUD PHYSICS
Mesoscale model parameterizations for radiation and turbulent fluxes at the lower boundary
[DFVLR-FB-88-48] N89-25544

CLOUDS
Measurements of H2O in the terrestrial mesosphere and implications for extra-terrestrial sources N89-25808

CLUSTER ANALYSIS
Bibliographic coupling among scientific papers in biological research specialties N89-25771

COASTAL WATER
Workshop on Sea Level Rise and Coastal Processes
[DE89-010297] N89-25522
Responding to changes in sea level engineering implications
[PB89-133466] N89-25555

COASTS
Workshop on Sea Level Rise and Coastal Processes
[DE89-010297] N89-25522

COATINGS
Thermal conductivity of dielectric thin films
[DE89-011847] N89-25750

COCKPITS
The man-machine-interface in a fast jet
[ETN-89-94327] N89-25574

CODING
The fast encryption package
[NASA-CR-185397] N89-25599

COEFFICIENT OF FRICTION
Correlation of subjective slipperiness judgements with quantitative COF (Coefficient Of Friction) measurements for structural steel
[PB89-165070] N89-25669

COGNITION
The organization of perception and action in complex control skills
[NASA-CR-184638] N89-25568

COLLISION AVOIDANCE
Magneto-inductive skin sensor for robot collision avoidance: A new development
[NASA-CR-185402] N89-25444

COLLISIONLESS PLASMAS
Anomalous particle pinch for collisionless plasma
[DE89-011018] N89-25706

COLOR INFRARED PHOTOGRAPHY
Applications of remote sensing techniques for the inventory and monitoring of environmental pollution
[BCRS-88-15] N89-25497

COLOR TELEVISION
An auroral TV-system
[REPT-115(1988)] N89-25543

COMBUSTION
Improvements of the KIVA-2 computer program for numerical combustion
[DE89-007994] N89-25304

COMBUSTION CHAMBERS
Fuel properties effect on the performance of a small high temperature rise combustor
[NASA-TM-102096] N89-25238
Advanced methods for 3-D inelastic structural analysis for hot engine structures
[NASA-TM-102106] N89-25490

COMBUSTION CHEMISTRY
Characterization of ceramics and intermetallics fabricated by self-propagating high-temperature synthesis
[NASA-TM-102004] N89-25285

COMBUSTION EFFICIENCY
Improvements of the KIVA-2 computer program for numerical combustion
[DE89-007994] N89-25304

COMBUSTION PRODUCTS
Investigation of submicrometer aerosols for apportioning the impacts of airborne particulate matter at Deep Creek Lake
[DE89-008186] N89-25524

COMBUSTION TEMPERATURE
Fuel properties effect on the performance of a small high temperature rise combustor
[NASA-TM-102096] N89-25238
Determination of combustion gas temperatures by infrared radiometry in sooting and nonsooting flames
[NASA-TP-2900] N89-25409

COMMERCIAL AIRCRAFT
UK airmisses involving commercial air transport
[CAA-3/88] N89-25143

COMMUNICATION
The 1988 Workshop on Human-Machine Symbiotic Systems
[DE89-010170] N89-25572

COMMUNICATION NETWORKS
The impact of telecommunication on rural areas in developing countries
[EUT-87-E-185] N89-25377

COMMUNICATION THEORY
On the semantics of nonatomic actions
[MEMO-INF-88-13] N89-25610

COMPILERS
Design and implementation of a module library to support the structural synthesis --- silicon compiler for IC design
[EUT-88-E-187] N89-25616

COMPLETENESS
Use of metaknowledge in the verification of knowledge-based systems
[NASA-CR-181821] N89-25627

COMPLEX SYSTEMS
Optimization by decomposition: A step from hierarchic to non-hierarchic systems N89-25149

COMPONENT RELIABILITY
CSTI High Capacity Power
[NASA-TM-102059] N89-25282

COMPOSITE MATERIALS
Integrated aerodynamic-structural design of a forward-swept transport wing N89-25168
Electrically conductive composite material
[DE89-010967] N89-25293
Estimating effective moduli of composites using quantitative image analysis
[DE89-012292] N89-25295

COMPOSITE PROPELLANTS
Characterization of booster-rocket propellants and their simulants
[DE89-012497] N89-25352

COMPOSITE STRUCTURES
Multi-objective/loading optimization for rotating composite flexbeams N89-25157
Static aeroelastic analysis and tailoring of missile control fins N89-25169
Optimum design of swept-forward high-aspect-ration graphite-epoxy wings N89-25172
Vibration testing of impact-damaged composite laminates
[NASA-TM-4115] N89-25290

COMPRESSIBLE BOUNDARY LAYER
A numerical study of a class of TVD schemes for compressible mixing layers
[NASA-TM-102194] N89-25651

COMPRESSIBLE FLOW
Numerical analysis of supersonic flow through oscillating cascade sections by using a deforming grid
[NASA-TM-102053] N89-25119
Techniques for compressible flow calculations on multizone grids N89-25120
Study of the stability of compressible Couette flow N89-25410
Analysis of the transient compressible vapor flow in heat pipe
[NASA-CR-185119] N89-25422
A numerical study of a class of TVD schemes for compressible mixing layers
[NASA-TM-102194] N89-25651

COMPRESSION TESTS
Polyimide Matrix composites: Polyimidesulfone/LARC-TPI (1:1) blend
[NASA-TM-101568] N89-25294
The development of a vapor compression refrigeration system for a network of nine temperature test chambers
[DE89-007084] N89-25355
A test system for computer controlled thermomechanical fatigue testing
[DE89-009067] N89-25483

COMPRESSION WAVES
Interaction between compression shocks and vertical flows N89-25132

COMPRESSIVE STRENGTH
The mechanical properties of ion implanted ceramics
[DE89-008928] N89-25337
Super-strong self-reinforcing polymeric matrices formed by the first super-strong polymers
[DE89-011533] N89-25347

COMPRESSOR EFFICIENCY
Combined vapor compression/absorption heat pump cycles for engine-driven heat pumps
[PB89-145437] N89-25505

COMPRESSORS
Combined vapor compression/absorption heat pump cycles for engine-driven heat pumps
[PB89-145437] N89-25505

COMPUTATION
On the calculation of derivatives of eigenvalues and eigenvectors in the simultaneous design and control of structures N89-25186
Parallel processors and nonlinear structural dynamics algorithms and software
[NASA-CR-185049] N89-25620

COMPUTATIONAL FLUID DYNAMICS
Numerical analysis of supersonic flow through oscillating cascade sections by using a deforming grid
[NASA-TM-102053] N89-25119

Techniques for compressible flow calculations on multizone grids N89-25120
On the Gortler vortex instability mechanism at hypersonic speeds
[NASA-CR-181844] N89-25123
Two-dimensional elliptic grid generation for airfoils and cascades
[DFVLR-FB-88-52] N89-25125
Integration method for the calculation of flow with free vortices N89-25127
Recent Advances in Multidisciplinary Analysis and Optimization, part 1
[NASA-CP-3031-PT-1] N89-25146
Effects of nonlinear aerodynamics and static aeroelasticity on mission performance calculations for a fighter aircraft N89-25170
The art of spacecraft design: A multidisciplinary challenge N89-25209
Analysis of the transient compressible vapor flow in heat pipe
[NASA-CR-185119] N89-25422
A qualitative numerical analysis of some features of propagation of counterflow temperature waves in superfluid helium
[MPIS-9/1988] N89-25424
Feasibility of using the Massively Parallel Processor for large eddy simulations and other Computational Fluid Dynamics applications
[NASA-CR-185427] N89-25629
A numerical study of a class of TVD schemes for compressible mixing layers
[NASA-TM-102194] N89-25651

COMPUTATIONAL GRIDS
The 3DGRAPE book: Theory, users' manual, examples
[NASA-TM-102224] N89-25116
Numerical analysis of supersonic flow through oscillating cascade sections by using a deforming grid
[NASA-TM-102053] N89-25119
Techniques for compressible flow calculations on multizone grids N89-25120
Two-dimensional elliptic grid generation for airfoils and cascades
[DFVLR-FB-88-52] N89-25125
Grid sensitivity capability for large scale structures N89-25183
Procedures for shape optimization of gas turbine disks N89-25207
Adaptive mesh refinement on moving quadrilateral grids
[DE89-010241] N89-25421

COMPUTER AIDED DESIGN
Recent Advances in Multidisciplinary Analysis and Optimization, part 1
[NASA-CP-3031-PT-1] N89-25146
Applications of integrated design/analysis systems in aerospace structural design N89-25147
Integrated design optimization research and development in an industrial environment N89-25148
New directions for Artificial Intelligence (AI) methods in optimum design N89-25158
Development of a microcomputer based integrated design system for high altitude long endurance aircraft N89-25159
Demonstration of decomposition and optimization in the design of experimental space systems N89-25160
STRUTEX: A prototype knowledge-based system for initially configuring a structure to support point loads in two dimensions N89-25161
TRUSS: An intelligent design system for aircraft wings N89-25162
The designer of the 90's: A live demonstration N89-25164
Structural tailoring of counter rotation propfans N89-25165
Composite sizing and ply orientation for stiffness requirements using a large finite element structural model N89-25166
Aerolastic tailoring and integrated wing design N89-25167
Integrated aerodynamic-structural design of a forward-swept transport wing N89-25168
Static aeroelastic analysis and tailoring of missile control fins N89-25169
Effects of nonlinear aerodynamics and static aeroelasticity on mission performance calculations for a fighter aircraft N89-25170
Optimum structural design with static aeroelastic constraints N89-25171
Recent Advances in Multidisciplinary Analysis and Optimization, part 2
[NASA-CP-3031-PT-2] N89-25173
ASTROS: A multidisciplinary automated structural design tool N89-25174
Research on optimization-based design N89-25176
Recent experiences using finite-element-based structural optimization N89-25177
The Sizing and Optimization Language (SOL): A computer language to improve the user/optimizer interface N89-25178
Robust computer-aided synthesis and optimization of linear multivariable control systems with varying plant dynamics via AUTOCON N89-25179
Computerized Design Synthesis (CDS), A database-driven multidisciplinary design tool N89-25180
On equivalence of discrete-discrete and continuum-discrete design sensitivity analysis N89-25181
An investigation of using an RQP based method to calculate parameter sensitivity derivatives N89-25182
Grid sensitivity capability for large scale structures N89-25183
Digital robust control law synthesis using constrained optimization N89-25193
An integrated approach to the optimum design of actively controlled composite wings N89-25194
Optimizing for minimum weight when two different finite element models and analyses are required N89-25200
Recent Advances in Multidisciplinary Analysis and Optimization, part 3
[NASA-CP-3031-PT-3] N89-25201
Recent developments in multilevel optimization N89-25203
A decomposition-based design optimization method with applications N89-25204
Multilevel decomposition of complete vehicle configuration in a parallel computing environment N89-25205
Design optimization of axisymmetric bodies in nonuniform transonic flow N89-25206
Procedures for shape optimization of gas turbine disks N89-25207
A decision-based perspective for the design of methods for systems design N89-25208
A large scale software system for simulation and design optimization of mechanical systems N89-25219
The role of optimization in the next generation of computer-based design tools N89-25220
An overview of the Douglas Aircraft Company Aeroelastic Design Optimization Program (ADOP) N89-25221
Meeting the challenges with the Douglas Aircraft Company Aeroelastic Design Optimization Program (ADOP) N89-25222
Optimization of structure and control system N89-25223
Structural optimization and recent large ground antenna installations N89-25224
A novel implementation of method of optimality criterion in synthesizing spacecraft structures with natural frequency constraints N89-25225
Computational experiments in the optimal slewing of flexible structures N89-25226
Recent developments in large-scale structural optimization N89-25231
Shape optimal design of elastic bodies using a mixed variational formulation N89-25236
Processing of fiber-reinforced materials by injection molding
[ETN-89-94668] N89-25298
Design and implementation of a module library to support the structural synthesis --- silicon compiler for IC design
[EUT-88-E-187] N89-25616

COMPUTER AIDED MANUFACTURING
Hierarchies for computer-integrated manufacturing: A functional description
[PB89-172613] N89-25596
The generalized grid file: An access structure for CIM applications --- computer integrated manufacturing (CIM)
[MEMO-INF-88-25] N89-25614
ALWAYS: A system for wafer yield analysis
[EUT-88-E-189] N89-25617

COMPUTER GRAPHICS
Applications of integrated design/analysis systems in aerospace structural design N89-25147
A large scale software system for simulation and design optimization of mechanical systems N89-25219
An overview of the Douglas Aircraft Company Aeroelastic Design Optimization Program (ADOP) N89-25221
Meeting the challenges with the Douglas Aircraft Company Aeroelastic Design Optimization Program (ADOP) N89-25222
Common Graphics Library (CGL). Volume 2: Low-level user's guide
[NASA-TM-101596] N89-25597

COMPUTER INFORMATION SECURITY
Detection of anomalous computer session activity
[DE89-003607] N89-25591
The fast encryption package
[NASA-CR-185397] N89-25599

COMPUTER NETWORKS
A large scale software system for simulation and design optimization of mechanical systems N89-25219
TUMULT: The Twente University Multiprocessor
[MEMO-INF-88-28] N89-25581
Using a segregation measure for the workload characterization of multi-class queuing networks
[DE89-007841] N89-25623
The Delta-t transport protocol: Features and experience useful for high performance networks
[DE89-009259] N89-25625
Interconnection networks
[DE89-010965] N89-25626
Integrated Services Digital Network: Overview and architectural concepts
[MEMO-INF-88-42] N89-25634

COMPUTER PROGRAM INTEGRITY
Use of metaknowledge in the verification of knowledge-based systems
[NASA-CR-181821] N89-25627

COMPUTER PROGRAMMING
Engineering applications of heuristic multilevel optimization methods N89-25202
Multilevel decomposition of complete vehicle configuration in a parallel computing environment N89-25205
Generalized mathematical models in design optimization N89-25214
Improvements of the KIVA-2 computer program for numerical combustion
[DE89-007994] N89-25304
Influence of rubbing on rotor dynamics, part 2
[NASA-CR-183649-PT-2] N89-25464
Geologic spatial analysis program users guide for digital elevation model analysis procedures for detection of crustal fracture planes
[DE89-010880] N89-25542
Culture shock: Improving software quality
[DE89-003610] N89-25592
The RIACS Intelligent Auditing and Categorizing System
[NASA-CR-185398] N89-25598
Handling arrays in symbolic execution
[REPT-89-003] N89-25609
Controlled bidirectional grammars
[MEMO-INF-88-16] N89-25611
An exercise in transformational programming: Back tracking and Branch-and-Bound
[MEMO-INF-88-22] N89-25612
A case study relating the Yourdon methodology to other design methods
[MEMO-INF-88-24] N89-25613
The software product assurance metrics study: JPL's software systems quality and productivity
[NASA-CR-184871] N89-25618
A site oriented supercomputer for theoretical physics: The Fermilab Advanced Computer Program Multi Array Processor System (ACMAPS)
[DE89-011090] N89-25631
Symbolic execution of concurrent programs using Petri nets
[REPT-89-004] N89-25633

COMPUTER PROGRAMS
Static aeroelastic analysis and tailoring of missile control fins N89-25169
ASTROS: A multidisciplinary automated structural design tool N89-25174
A generalized software executive for multidisciplinary computational structural dynamics N89-25175
Robust computer-aided synthesis and optimization of linear multivariable control systems with varying plant dynamics via AUTOCON N89-25179
An overview of the Douglas Aircraft Company Aeroelastic Design Optimization Program (ADOP) N89-25221
Meeting the challenges with the Douglas Aircraft Company Aeroelastic Design Optimization Program (ADOP) N89-25222
Structural optimization and recent large ground antenna installations N89-25224
Recent developments in large-scale structural optimization N89-25231
Middeck Active Control Experiment (MACE), phase A
[NASA-CR-185331] N89-25258
Improvements of the KIVA-2 computer program for numerical combustion
[DE89-007994] N89-25304
Technique and data analysis for impact-loaded piezoelectric polymers (PVDF)
[DE89-010529] N89-25342
Advanced methods for 3-D inelastic structural analysis for hot engine structures
[NASA-TM-102106] N89-25490

Modeling the AIDS epidemic
[NASA-CR-185413] N89-25566
Modeling of magnetic devices with finite-element methods
[DE89-010525] N89-25576
The Fermilab Lattice Supercomputer Project
[DE89-010510] N89-25578
Far field projection
[DE89-010243] N89-25587
A tool to aid in mapping computational tasks to a hypercube
[DE89-010320] N89-25589
PRONTO 3D: A three-dimensional transient solid dynamics program
[DE89-010517] N89-25590
Culture shock: Improving software quality
[DE89-003610] N89-25592
The software product assurance metrics study: JPL's software systems quality and productivity
[NASA-CR-184871] N89-25618
Interprocess communications and application to physical numerical modeling
[DE89-011021] N89-25630
A class of high resolution explicit and implicit shock-capturing methods
[NASA-TM-101088] N89-25652

COMPUTER STORAGE DEVICES
Interconnection networks
[DE89-010965] N89-25626
Optical information storage in PLZT thin films
[DE89-011067] N89-25692
Data acquisition, event building, and on-line processing: Summary talk
[DE89-011085] N89-25693

COMPUTER SYSTEMS DESIGN
A theory of describing performability models
[MEMO-INF-88-26] N89-25476
TUMULT: The Twente University Multiprocessor
[MEMO-INF-88-28] N89-25581
An exercise in transformational programming: Back tracking and Branch-and-Bound
[MEMO-INF-88-22] N89-25612
The generalized grid file: An access structure for CIM applications --- computer integrated manufacturing (CIM)
[MEMO-INF-88-25] N89-25614
Integrated Services Digital Network: Overview and architectural concepts
[MEMO-INF-88-42] N89-25634
An expert system development methodology which supports verification and validation
[NASA-TM-101782] N89-25635
Blindness in designing intelligent systems
[NASA-CR-184582] N89-25638
A net-based model for time-dependent systems
[REPT-89-005] N89-25661

COMPUTER SYSTEMS PERFORMANCE
A tool to aid in mapping computational tasks to a hypercube
[DE89-010320] N89-25589
A parallel algorithm for switch-level timing simulation on a hypercube multiprocessor
[NASA-CR-185338] N89-25595
Fast Fourier Transform algorithm design and tradeoffs
[NASA-CR-185038] N89-25600
Parallel processors and nonlinear structural dynamics algorithms and software
[NASA-CR-185049] N89-25620
Partitioning a finite difference code for a local memory multiprocessor
[DE89-010223] N89-25621
Using a segregation measure for the workload characterization of multi-class queuing networks
[DE89-007841] N89-25623
Interprocess communications and application to physical numerical modeling
[DE89-011021] N89-25630
An expert system development methodology which supports verification and validation
[NASA-TM-101782] N89-25635
Program package for investigation of differential equations by the external form method
[DE88-706258] N89-25650
Reliability mechanisms for ADAMS (Advanced Data Management System)
[DE89-010911] N89-25768
Performance issues in management of the Space Station Information System
[NASA-CR-185409] N89-25773

COMPUTER SYSTEMS PROGRAMS
Parallel processors and nonlinear structural dynamics algorithms and software
[NASA-CR-185049] N89-25620

COMPUTER TECHNIQUES
Multilevel decomposition of complete vehicle configuration in a parallel computing environment N89-25205
A review of computer aided interpretation technology for the evaluation of radiographs of aluminum welds
[NASA-CR-185066] N89-25312
Concurrent Image Processing Executive (CIPE)
[NASA-CR-185460] N89-25619

COMPUTERIZED SIMULATION
Interactions of Tollmien-Schlichting waves and Dean vortices. Comparison of direct numerical simulation and a weakly nonlinear theory
[NASA-TP-2919] N89-25118
Recent Advances in Multidisciplinary Analysis and Optimization, part 3
[NASA-CP-3031-PT-3] N89-25201
A large scale software system for simulation and design optimization of mechanical systems N89-25219
Space Shuttle Main Engine structural analysis and data reduction/evaluation. Volume 2: High pressure oxidizer turbo-pump turbine end bearing analysis
[NASA-CR-183664] N89-25270
Computer simulation of FEL sidebands in a strongly dispersive waveguide
[DE89-011825] N89-25369
Shock waves and fragmentation via molecular dynamics
[DE89-007981] N89-25405
Comparison of experimental shock-wave profiles for tungsten and computer simulations using a rate-dependent constitutive model
[DE89-006158] N89-25419
Numerical simulation of transition from laminar to turbulent channel flow
[DFVLR-FB-88-55] N89-25430
New atmospheric sensor analysis study
[NASA-CR-183597] N89-25431
A kinematic study of the MERLIN 6500 robot and the Utah/MIT dexterous hand and a simulation of their combined behavior
[AD-A203907] N89-25458
Influence of rubbing on rotor dynamics, part 2
[NASA-CR-183649-PT-2] N89-25464
Simulation of the welding of irradiated materials
[DE89-012524] N89-25469
Dynamic simulation of dislocation pattern formation in metals during high temperature monotonic and cyclic deformation N89-25477
Regional validation of general circulation models N89-25538
The organization of perception and action in complex control skills
[NASA-CR-184638] N89-25568
Modeling of magnetic devices with finite-element methods
[DE89-010525] N89-25576
A parallel algorithm for switch-level timing simulation on a hypercube multiprocessor
[NASA-CR-185338] N89-25595
Parallel solutions of a 2-D phase change problem on a hypercube
[DE89-012886] N89-25602
Reduction of aircraft noise in civil air transport by optimization of flight tracks and takeoff and approach procedures
[ILR-MITT-200] N89-25676
Atomic resolution microscopy
[DE89-009227] N89-25679
A courant condition free modified partially-implicit method. Revised electromagnetic particle Code PS2M for bounded plasmas with conducting walls
[IPPJ-892] N89-25699
Plasma switches for high current and fast time scale operation
[DE89-010557] N89-25704
Double tearing and particle simulation N89-25723
A numerical simulation of inhomogeneous ion cyclotron turbulence N89-25725

CONCURRENT PROCESSING
Symbolic execution of concurrent programs using Petri nets
[REPT-89-004] N89-25633

CONDENSING
The effect of global-scale divergent circulation on the atmospheric water vapor transport and maintenance N89-25793
Factors governing water condensation in the Martian atmosphere N89-25797

CONDUCTIVE HEAT TRANSFER
Heat transfer in packed beds
[KFK-4451] N89-25425

CONFERENCES
Recent Advances in Multidisciplinary Analysis and Optimization, part 1
[NASA-CP-3031-PT-1] N89-25146
Recent Advances in Multidisciplinary Analysis and Optimization, part 2
[NASA-CP-3031-PT-2] N89-25173
Recent Advances in Multidisciplinary Analysis and Optimization, part 3
[NASA-CP-3031-PT-3] N89-25201
Review of the 1988 Workshop on Human-Machine Symbiotic Systems
[DE89-008743] N89-25570
Performance evaluation for data flow architectures: A summary of discussions from the Santa Fe workshop
[DE89-008023] N89-25624
Seismology of the Sun and Sun-Like Stars
[ESA-SP-286] N89-25819

CONGRESSIONAL REPORTS
Report to Congress: Technical feasibility of joint use at Scott AFB, Selfridge AGB and El Toro MCAS
[AD-A194597] N89-25241

CONICAL SHELLS
Structural testing of metal/composite conical structures with holes
[DE89-011451] N89-25487

CONJUGATE GRADIENT METHOD
Efficient generalized conjugate gradient algorithms
[MATHS-RES-211] N89-25606
On conjugate gradient type methods and polynomial preconditioners for a class of complex non-Hermitian matrices
[NASA-CR-185424] N89-25654

CONSERVATION EQUATIONS
Integration method for the calculation of flow with free vortices N89-25127

CONSERVATION LAWS
A class of high resolution explicit and implicit shock-capturing methods
[NASA-TM-101088] N89-25652

CONSISTENCY
Use of metaknowledge in the verification of knowledge-based systems
[NASA-CR-181821] N89-25627

CONSTRAINTS
Constraint specification in BSDM --- basic semantic data model (BSDM)
[MEMO-INF-88-32] N89-25615

CONTEXT FREE LANGUAGES
Controlled bidirectional grammars
[MEMO-INF-88-16] N89-25611

CONTOUR SENSORS
Antenna surface contour control system
[NASA-CASE-LAR-13798-1] N89-25363

CONTRACTS
Geothermal energy program summary. Volume 2: Research summaries, fiscal year 1988
[DE89-000865] N89-25509

CONTRAROTATING PROPELLERS
Low-speed wind tunnel performance of high-speed counterrotation propellers at angle-of-attack
[NASA-TM-102292] N89-25121

CONTRAST
Resistive Contrast Imaging applied to multilevel interconnection failure analysis
[DE89-011066] N89-25397

CONTROL
Synthetic organisms and self-designing systems
[NASA-CR-185324] N89-25639

CONTROL RODS
Experimental study of the phenomena of turbulent flow in the narrow gaps between subchannels of rod bundles
[KFK-4501] N89-25428

CONTROL SURFACES
Control surface spanwise placement in active flutter suppression systems N89-25195

CONTROL SYSTEMS DESIGN
Contributions to the improvement of flight safety in wind shear
[DFVLR-FB-88-49] N89-25144
Research on optimization-based design N89-25176
Robust computer-aided synthesis and optimization of linear multivariable control systems with varying plant dynamics via AUTOCON N89-25179
Digital robust control law synthesis using constrained optimization N89-25193
Optimization of structure and control system N89-25223
An analytical sensitivity method for use in integrated aeroservoelastic aircraft design
[NASA-TM-101583] N89-25239
Analysis and control of a three-degree-of-freedom robot platform
[DE89-006427] N89-25356
An extremum hunting method using pseudo-random binary signal
[EUT-88-E-198] N89-25359
Controller for stabilization of high voltage
[NAL-TM-MT-8702] N89-25382
Performance characteristics for advanced control systems
[DE89-010362] N89-25637

A new method for dynamic hunting extremum control, based on comparison of measured and estimated value [EUT-88-E-197] N89-25644
CONTROL THEORY
Results of an integrated structure/control law design sensitivity analysis N89-25185
Digital robust control law synthesis using constrained optimization N89-25193
An integrated approach to the optimum design of actively controlled composite wings N89-25194
Control surface spanwise placement in active flutter suppression systems N89-25195
Recent Advances in Multidisciplinary Analysis and Optimization, part 3 [NASA-CP-3031-PT-3] N89-25201
Optimization of structure and control system N89-25223
A new method for dynamic hunting extremum control, based on comparison of measured and estimated value [EUT-88-E-197] N89-25644
CONTROL VALVES
Flow characteristics and accuracy of control valve [DE88-757331] N89-25450
CONTROLLABILITY
Aircraft design optimization with multidisciplinary performance criteria N89-25212
CONTROLLED FUSION
Confinement physics of H-mode discharges in DIII-D [DE89-011525] N89-25707
CONTROLLERS
Robust computer-aided synthesis and optimization of linear multivariable control systems with varying plant dynamics via AUTOCON N89-25179
Flutter suppression using eigenspace freedoms to meet requirements N89-25191
Middeck Active Control Experiment (MACE), phase A [NASA-CR-185331] N89-25258
Controller for stabilization of high voltage [NAL-TM-MT-8702] N89-25382
Design of a dual forearm modular robot [DE89-010453] N89-25462
Operator role definition and human system integration [DE89-009621] N89-25571
CONVECTION
Oscillation ring diagrams and the thermodynamics of the outer solar convection zone N89-25836
Solar oscillations: Overshoot at the base of the convection zone N89-25911
Convection and p-mode oscillations --- Sun N89-25912
CONVECTIVE FLOW
Evidence for a thin perturbative layer near the base of the solar convection zone N89-25876
CONVECTIVE HEAT TRANSFER
Multidimensional modeling of convective heat transfer with application to I.C. engines [DE89-010651] N89-25415
Enhancement of heat transfer by corona wind [EUT-87-E-184] N89-25500
COOLANTS
Survivable pulse power space radiator [DE89-010120] N89-25264
COOLING
The influence of cooling rate on the ferrite content of stainless steel alloys [DE89-009966] N89-25315
Advanced working fluid properties in heat pump and absorption cooling operations [PB89-178172] N89-25413
COOLING SYSTEMS
Scaling results for the Liquid Sheet Radiator (LSR) [NASA-TM-102100] N89-25277
COPOLYMERS
Low density microcellular carbon foams and method of preparation [DE89-010966] N89-25345
COPPER COMPOUNDS
X-ray scattering studies of non-equilibrium ordering processes [DE89-012517] N89-25753
COPPER OXIDES
The formation and analysis of thin film high temperature superconductors [DE89-011177] N89-25745
Variation of superlattice structure of the Bi2Sr(2-x)CuO(6-y) superconductor with composition and thermal history [DE89-011612] N89-25749
CORRELATION COEFFICIENTS
Reduction of interference by decorrelation and quantized feedback in the case of digital transmission on multi-pair symmetric cables [FI-44-TB-110] N89-25375
CORROSION
The application of Rutherford backscattering and channeling techniques to the characterization of ceramics [DE89-010257] N89-25333
CORROSION RESISTANCE
The development of alloys based on Ni3Si [DE89-010371] N89-25316
Quantitative modeling of sensitization development in austenitic stainless steel [DE89-011206] N89-25317
Evaluation of ceramic coatings on silicon carbide [DE89-010321] N89-25339
COSMIC PLASMA
Cosmic plasma physics [MPE-211] N89-25716
Magnetic reconnection in general three-dimensional systems N89-25717
Orientation, motion, and other properties of FTE structures on September 4, 1984 N89-25718
Three dimensional computations of the dynamics of the magnetopause: First results N89-25719
Acceleration of ions in the magnetotail N89-25720
Nonlocal analyses of finite-beam-driven instabilities N89-25721
Particle simulation of magnetic reconnection N89-25722
Double tearing and particle simulation N89-25723
Ion heating in the Bug shock wave N89-25724
A numerical simulation of inhomogeneous ion cyclotron turbulence N89-25725
The ionization structure in shocks in interstellar molecular clouds N89-25726
Gravitational-like phase transition of a classical Coulomb plasma N89-25727
On the formation of current-sheets in ideal MHD N89-25728
Particle simulation for accretion sheets in narrow double stars N89-25729
Models for axially symmetric pulsar magnetospheres N89-25730
Acceleration of particles in shear flows N89-25731
Stationary ideal MHD with incompressible mass flow and general symmetry N89-25732
COSMOLOGY
Solitosynthesis: Cosmological evolution of non-topological solitons [NASA-CR-185030] N89-25678
Nuclear beta decay far from stability and astrophysics [MPI-H-1988-V-27] N89-25683
Strings on hyperelliptic supersurfaces [DE88-705991] N89-25758
Cosmological effects of superconducting strings N89-25778
Quantum ontologies [DE89-010385] N89-25781
Evolution of cosmic string networks [NASA-CR-185467] N89-25788
COST ANALYSIS
An economic model for evaluating high-speed aircraft designs [NASA-CR-177530] N89-25235
Space station operations task force. Panel 3 report: User development and integration [NASA-TM-101818] N89-25246
Learning the value of VE [DE89-008121] N89-25475
COST EFFECTIVENESS
Fuel cell systems program plan, FY 1989 [DE89-012928] N89-25515
COST REDUCTION
Optimizing conceptual aircraft designs for minimum life cycle cost N89-25211
Size optimization and production strategy of lunar transport systems [ILR-MITT-218] N89-25260
Learning the value of VE [DE89-008121] N89-25475
COUETTE FLOW
Study of the stability of compressible Couette flow N89-25410
COULOMB POTENTIAL
Gravitational-like phase transition of a classical Coulomb plasma N89-25727
COUNTER ROTATION
Structural tailoring of counter rotation propfans N89-25165
COUPLING
Optical pressure sealing coupling apparatus [NASA-CASE-MFS-29348-1] N89-25689
COVARIANCE
Localizability and covariance in analytical mechanics [DE88-706038] N89-25666
CRACK OPENING DISPLACEMENT
Crack growth under low cycle fatigue [GKSS-88/E/47] N89-25491
CRACK PROPAGATION
Probabilistic damage tolerance methods for metallic aerospace structures N89-25237
The strength-toughness relationship at cryogenic temperatures in aluminum-lithium alloy plate [DE89-011816] N89-25322
J(sub Ic) fracture toughness of ferritic DCI (Ductile Cast Iron) alloys: A comparison of two versions of ASTM E 813 [DE89-012249] N89-25323
Crack growth under low cycle fatigue [GKSS-88/E/47] N89-25491
CRACKING (FRACTURING)
Mechanical properties of carbon fiber reinforced thermoplastics for cryogenic applications [KFK-4487] N89-25297
CRACKS
Evaluation of elastic-plastic surface flaw behavior and related parameters using surface displacement measurements [DE89-011134] N89-25489
CREEP PROPERTIES
Transient effects in creep cavity nucleation and early growth in ceramics [DE89-010420] N89-25340
Procedures for characterizing an alloy and predicting cyclic life with the total strain version of Strainrange Partitioning [NASA-TM-4102] N89-25485
CREEP RUPTURE STRENGTH
Effect of low neutron fluences on DIN 1.4948 steel creep properties --- liquid metal fast breeder reactor (LMFBR) material [ECN-206] N89-25325
The creep and creep-rupture behavior of vanadium-base alloys [KFK-2440] N89-25328
CREEP TESTS
Polyimide Matrix composites: Polyimidesulfone/LARC-TPI (1:1) blend [NASA-TM-101568] N89-25294
Elevated temperature deformation of structural steel [PB89-172621] N89-25318
The creep and creep-rupture behavior of vanadium-base alloys [KFK-2440] N89-25328
Procedures for characterizing an alloy and predicting cyclic life with the total strain version of Strainrange Partitioning [NASA-TM-4102] N89-25485
CREW WORKSTATIONS
Space nuclear reactor shields for manned and unmanned applications [NASA-TM-102064] N89-25272
CROSS CORRELATION
Searching for solar g-modes. Tests of a statistical method N89-25889
CRUSTAL FRACTURES
Geologic spatial analysis program users guide for digital elevation model analysis procedures for detection of crustal fracture planes [DE89-010880] N89-25542
CRYOGENIC FLUID STORAGE
Cryogenic mechanical properties of low density superplastically formable Al-Li alloys [DE89-010587] N89-25343
GIRL cryotechnics and preparation of a TEXUS experiment on superfluid helium dynamics [ETN-89-94631] N89-25357
CRYOGENIC FLUIDS
Study on thermodynamical and mechanical conditions for pumping low flow rates of liquefied gases to high pressure level [DFVLR-FB-88-54] N89-25429
CRYOGENIC ROCKET PROPELLANTS
Advanced APS impacts on vehicle payloads [NASA-TM-102088] N89-25254
CRYOGENIC TEMPERATURE
Mechanical properties of carbon fiber reinforced thermoplastics for cryogenic applications [KFK-4487] N89-25297
CRYOGENICS
The strength-toughness relationship at cryogenic temperatures in aluminum-lithium alloy plate [DE89-011816] N89-25322
Cryogenic mechanical properties of low density superplastically formable Al-Li alloys [DE89-010587] N89-25343
CRYPTOGRAPHY
The fast encryption package [NASA-CR-185397] N89-25599
CRYSTAL DEFECTS
High resolution electron microscopy and microanalysis of ferrites and cuprates [DE89-010441] N89-25341

Influence of the preparation conditions on the diamagnetic response of high-Tc YBa2Cu3Ox superconductor
[DE88-706051] N89-25736
Kinetic effects of strong localization in planar heterostructures p-Ge/i-GaAs
[DE88-706205] N89-25739

CRYSTAL GROWTH
Analytic theory for the selection of 2-D needle crystal at arbitrary Peclet number
[NASA-CR-181846] N89-25671

CRYSTAL LATTICES
The application of Rutherford backscattering and channeling techniques to the characterization of ceramics
[DE89-010257] N89-25333
High resolution electron microscopy and microanalysis of ferrites and cuprates
[DE89-010441] N89-25341
Superlattice strain gage
[DE89-011805] N89-25447

CRYSTAL STRUCTURE
The creep and creep-rupture behavior of vanadium-base alloys
[KFK-2440] N89-25328
Preparation and properties of high-temperature superconductors in the Y-Ba-Cu-O system
[DE88-706050] N89-25735
Advances in the development of apparatus and methods for studies of protein monocrystals in coordinate X-ray diffractometers based on two-dimensional proportional chambers
[DE88-706259] N89-25740
Ferroelectric potassium niobate thin films
[DE89-010862] N89-25744
Variation of superlattice structure of the Bi2Sr(2-x)CuO(6-y) superconductor with composition and thermal history
[DE89-011612] N89-25749
Studies of 3-5 compounds in the megabar regime
[DE89-012433] N89-25751

CRYSTAL SURFACES
Surface structural analysis of small molecules on transition metal single crystal surfaces with low energy electron diffraction
[DE89-010681] N89-25743

CRYSTALS
On the applicability of various planar potentials in the theory of ultrarelativistic electron channeling
[DE88-706155] N89-25738

CUBIC LATTICES
Possible significance of cubic water-ice, H2O-Ic, in the atmospheric water cycle of Mars N89-25799

CULTURE (SOCIAL SCIENCES)
Culture shock: Improving software quality
[DE89-003610] N89-25592

CULTURE TECHNIQUES
Spiral vane bioreactor
[NASA-CASE-MSC-21361-1] N89-25557

CUMULUS CLOUDS
Cumulus convection and the terrestrial water-vapor distribution N89-25798

CURRENT ALGEBRA
Photonic chiral current and its anomaly in a gravitational field
[DE88-706213] N89-25361

CURRENT DENSITY
On the formation of current-sheets in ideal MHD N89-25728

CURRENT REGULATORS
Controller for stabilization of high voltage
[NAL-TM-MT-8702] N89-25382
Modular magnet current regulator
[CEBAF-PR-89-005] N89-25685

CURVATURE
Acoustic propagation in curved ducts with extended reacting wall treatment
[NASA-TM-102110] N89-25670

CYCLIC HYDROCARBONS
Development of laser-excited molecular luminescence spectrometric methods for polycyclic aromatic hydrocarbons in environmental sciences
[DE89-010616] N89-25306

CYCLIC LOADS
Procedures for characterizing an alloy and predicting cyclic life with the total strain version of Strainrange Partitioning
[NASA-TM-4102] N89-25485

CYLINDRICAL BODIES
Finite strain example problems for rectangular, cylindrical, and spherical geometries
[DE89-013607] N89-25488

CYTOLOGY
Spiral vane bioreactor
[NASA-CASE-MSC-21361-1] N89-25557

D

DAMAGE
Structural damage assessment as an identification problem N89-25230
The application of Rutherford backscattering and channeling techniques to the characterization of ceramics
[DE89-010257] N89-25333

DAMPING
Damping of wing tip vortex systems by the modification of the wing tips N89-25138
Optimal placement of excitations and sensors by simulated annealing N89-25227
Characterization of the effects of three-dimensional states of stress on damping of laminated composites N89-25287
Flap-lag stability data for a small-scale isolated hingeless rotor in forward flight
[NASA-TM-102189] N89-25479
The excitation and damping of solar oscillations N89-25820
On the radiative damping of p-modes in solar magnetic flux concentrations N89-25864

DARK MATTER
Model independence of constraints on particle dark matter
[NASA-CR-185337] N89-25688
Dark matter and supersymmetry
[DE89-011068] N89-25785

DATA ACQUISITION
Notice to Airmen (NOTAM) system operational concept
[DOT/FAA/CT-TN89/10] N89-25142
Detection of metal-transfer mode in GMAW
[DE89-011133] N89-25465
Gravity network of West Germany (DSGN76): Measurements and starting data N89-25546
Modeling the AIDS epidemic
[NASA-CR-185413] N89-25566
Microprocessors and other processors for triggering and filtering at the SSC
[DE89-011088] N89-25580
Data acquisition, event building, and on-line processing: Summary talk
[DE89-011085] N89-25693

DATA BASE MANAGEMENT SYSTEMS
TRUSS: An intelligent design system for aircraft wings N89-25162
Reliability mechanisms for ADAMS (Advanced Data Management System)
[DE89-010911] N89-25768
Performance issues in management of the Space Station Information System
[NASA-CR-185409] N89-25773
An expert system to facilitate selecting a database management system
[DE89-012350] N89-25774

DATA BASES
Computerized Design Synthesis (CDS), A database-driven multidisciplinary design tool N89-25180
Gravity network of West Germany 1976 (DSGN76). Part 3: Data and adjustments
[SER-C-286] N89-25545
The ADAMS database language
[DE89-010925] N89-25601
The generalized grid file: An access structure for CIM applications — computer integrated manufacturing (CIM)
[MEMO-INF-88-25] N89-25614
Constraint specification in BSDM — basic semantic data model (BSDM)
[MEMO-INF-88-32] N89-25615
Querying databases of trajectories of differential equations: Data structures for trajectories
[NASA-CR-185040] N89-25772

DATA CORRELATION
Gravity network of West Germany 1976 (DSGN76). Part 3: Data and adjustments
[SER-C-286] N89-25545

DATA MANAGEMENT
Concurrent Image Processing Executive (CIPE)
[NASA-CR-185460] N89-25619
Parallel processors and nonlinear structural dynamics algorithms and software
[NASA-CR-185049] N89-25620
Temporal data management in real-time systems: A comparative view
[REPT-88-046] N89-25767
Reliability mechanisms for ADAMS (Advanced Data Management System)
[DE89-010911] N89-25768

DATA PROCESSING
Spacelab Data Processing Facility
[NASA-TM-101808] N89-25252
User's guide to image processing applications of the NOAA satellite HRPT/AVHRR data. Part 1: Introduction to the satellite system and its applications. Part 2: Processing and analysis of AVHRR imagery
[NASA-CR-180784] N89-25492
Detection of anomalous computer session activity
[DE89-003607] N89-25591
Data acquisition, event building, and on-line processing: Summary talk
[DE89-011085] N89-25693

DATA REDUCTION
Space Shuttle Main Engine structural analysis and data reduction/evaluation. Volume 2: High pressure oxidizer turbo-pump turbine end bearing analysis
[NASA-CR-183664] N89-25270
Modeling the AIDS epidemic
[NASA-CR-185413] N89-25566

DATA SMOOTHING
Gravity network of West Germany 1976 (DSGN76). Part 3: Data and adjustments
[SER-C-286] N89-25545
Adjustment and data analysis — gravimetry N89-25547
Data adjustment by gravity differences N89-25548

DATA STRUCTURES
Querying databases of trajectories of differential equations: Data structures for trajectories
[NASA-CR-185040] N89-25772

DATA SYSTEMS
Space station operations task force. Panel 1 report: Space operations and support systems
[NASA-TM-101816] N89-25244
Spacelab Data Processing Facility
[NASA-TM-101808] N89-25252
The GONG data reduction and analysis system — solar oscillations N89-25856

DATA TRANSMISSION
Spacelab Data Processing Facility
[NASA-TM-101808] N89-25252

DECISION MAKING
A decision-based perspective for the design of methods for systems design N89-25208
The role of optimization in the next generation of computer-based design tools N89-25220
Hierarchies for computer-integrated manufacturing: A functional description
[PB89-172613] N89-25596
A parallel processing approach for implementing high-performance first-order logic deduction systems
[DE89-011878] N89-25632

DECISION THEORY
A decision-based perspective for the design of methods for systems design N89-25208

DECOMPOSITION
The full decomposition of sequential machines with the state and output behavior realization
[EUT-88-E-188] N89-25582
The full decomposition of sequential machines with the output behavior realization
[EUT-88-E-199] N89-25583

DEFLECTION
Optimum design of structures subject to general periodic loads N89-25215

DEFORMATION
Deformation induced microstructural and microchemical changes during thermomechanical treatment
[DE89-011608] N89-25321
Intermetallic alloys: Deformation, mechanical and fracture behavior
[GKSS-88/E/53] N89-25327
Dynamic simulation of dislocation pattern formation in metals during high temperature monotonic and cyclic deformation N89-25477
PRONTO 3D: A three-dimensional transient solid dynamics program
[DE89-010517] N89-25590

DEGENERATE MATTER
Ripple structure in degenerate electron gas-dominated stars with intense magnetic fields N89-25783

DEGRADATION
Studies of oxidative degradation of polymers induced by ionizing radiation
[DE89-008279] N89-25335

DELAMINATING
Vibration testing of impact-damaged composite laminates
[NASA-TM-4115] N89-25290
An analytical and experimental investigation of edge delamination in laminates subjected to tension, bending, and torsion
[NASA-CR-181824] N89-25296

DELTA WINGS
Unsteady phenomena on delta wings with partially broken-down vortex regions N89-25129

DENDRITIC CRYSTALS
Analytic theory for the selection of 2-D needle crystal at arbitrary Peclet number
[NASA-CR-181846] N89-25671
DENSIFICATION
Applicability of microalloying in the production of sintered steel structural parts
[KFK-4481] N89-25329
DENSITY MEASUREMENT
X-ray based extensometry
[NASA-CR-185058] N89-25432
DEOXYRIBONUCLEIC ACID
Unraveling Photosystem 2
[DE89-010930] N89-25559
DEPLETION
Preventing depletion of stratospheric ozone: Implications on future aircraft emissions
[DE89-009964] N89-25530
DEPLOYMENT
Pactruss support structure for precision segmented reflectors
[NASA-CR-181747] N89-25484
DEPOSITION
Deposition of dielectric optical coatings: A microstructural study of the deposited layers and interfaces
[DE89-011205] N89-25694
DESIGN ANALYSIS
Optimization by decomposition: A step from hierarchic to non-hierarchic systems N89-25149
Demonstration of decomposition and optimization in the design of experimental space systems N89-25160
Effects of nonlinear aerodynamics and static aeroelasticity on mission performance calculations for a fighter aircraft N89-25170
Recent Advances in Multidisciplinary Analysis and Optimization, part 2
[NASA-CP-3031-PT-2] N89-25173
On equivalence of discrete-discrete and continuum-discrete design sensitivity analysis N89-25181
Results of an integrated structure/control law design sensitivity analysis N89-25185
Treatment of body forces in boundary element design sensitivity analysis N89-25187
Design sensitivity analysis of boundary element substructures N89-25188
Recent Advances in Multidisciplinary Analysis and Optimization, part 3
[NASA-CP-3031-PT-3] N89-25201
Recent developments in multilevel optimization N89-25203
Design optimization of axisymmetric bodies in nonuniform transonic flow N89-25206
A decision-based perspective for the design of methods for systems design N89-25208
Generalized mathematical models in design optimization N89-25214
The conceptual design of a Mach 2 Oblique Flying Wing supersonic transport
[NASA-CR-177529] N89-25233
Shape optimal design of elastic bodies using a mixed variational formulation N89-25236
An analytical sensitivity method for use in integrated aeroservoelastic aircraft design
[NASA-TM-101583] N89-25239
Electrically compensated constant speed drive (Model number 60 ECEPGS 02)
[AD-A206064] N89-25385
Evaluation of auxiliary power subsystems for gas engine heat pumps, phase 2
[PB89-173694] N89-25411
Initial design and analysis of a capacitive sensor for shear and normal force measurement
[DE89-001821] N89-25438
On optimal fail-safe design of structures N89-25486
A case study relating the Yourdon methodology to other design methods
[MEMO-INF-88-24] N89-25613
The use of first principles in diagnosing complex technical devices
[MEMO-INF-88-40] N89-25641
DESTRUCTION
Solitosynthesis: Cosmological evolution of non-topological solitons
[NASA-CR-185030] N89-25678
DETECTION
Structural damage assessment as an identification problem N89-25230
Model independence of constraints on particle dark matter
[NASA-CR-185337] N89-25688
DETONATION
Fiber optic sensing in a high explosives environment
[DE89-010863] N89-25695
DETONATION WAVES
High explosives reaction model and its application to booster performance
[DE89-005459] N89-25351
DEVELOPING NATIONS
The impact of telecommunication on rural areas in developing countries
[EUT-87-E-185] N89-25377
DIAMAGNETISM
Influence of the preparation conditions on the diamagnetic response of high-Tc YBa2Cu3Ox superconductor
[DE88-706051] N89-25736
DIAMONDS
Determination of the mechanical properties of diamond and diamond-like films by the ultra-low load indentation technique
[DE89-011569] N89-25471
On the applicability of various planar potentials in the theory of ultrarelativistic electron channeling
[DE88-706155] N89-25738
DIELECTRIC PROPERTIES
Local field effects in the many-body perturbation theory and in the density functional theory
[DE88-705975] N89-25734
DIELECTRICS
Thermal conductivity of dielectric thin films
[DE89-011847] N89-25750
DIETS
Characterization of Spirulina biomass for CELSS diet potential
[NASA-CR-185329] N89-25561
DIFFERENTIAL CALCULUS
Differential algebras without differentials: An easy C++ implementation
[DE89-011503] N89-25655
DIFFERENTIAL EQUATIONS
A generalized software executive for multidisciplinary computational structural dynamics N89-25175
Program package for investigation of differential equations by the external form method
[DE88-706258] N89-25650
Querying databases of trajectories of differential equations: Data structures for trajectories
[NASA-CR-185040] N89-25772
DIFFRACTION
Laser diffraction methods for high temperature strain measurements
[DE89-008235] N89-25451
DIFFRACTOMETERS
Controller for stabilization of high voltage
[NAL-TM-MT-8702] N89-25382
DIFFUSION
Diffusion, fluid flow and sound propagation in disordered media
[DE89-010937] N89-25407
DIGITAL DATA
Spacelab Data Processing Facility
[NASA-TM-101808] N89-25252
Performance of five 30 GHz satellite receivers
[NASA-TM-101960] N89-25365
DIGITAL RADAR SYSTEMS
Digital evaluation of SEASAT-SAR radar image data N89-25504
DIGITAL SYSTEMS
Reduction of interference by decorrelation and quantized feedback in the case of digital transmission on multi-pair symmetric cables
[FI-44-TB-110] N89-25375
Optical information processing and holography
[DE88-706011] N89-25434
Digital dynamic amplitude-frequence spectral analyzer
[DE88-706256] N89-25436
Automated Test and Evaluation Center for Waveform Digitizer Systems and Components
[DE89-010226] N89-25441
DIHEDRAL ANGLE
Effect of milling machine roughness and wing dihedral on the supersonic aerodynamic characteristics of a highly swept wing
[NASA-TP-2918] N89-25117
DIRAC EQUATION
A new way to interpret the DIRAC equation in a non-Riemannian manifold
[NASA-CR-185464] N89-25663
DIRECTIVITY
Pyramidal horns: Part 1: Simple expressions for directivity as a function of aperture phase error
[DE89-005209] N89-25370
DISCRIMINANT ANALYSIS (STATISTICS)
Discrimination and classification with mixed binary and continuous variables: The Bayesian approach
[MATHS-RES-212] N89-25664
DISEASES
Modeling the AIDS epidemic
[NASA-CR-185413] N89-25566
DISKS (SHAPES)
Procedures for shape optimization of gas turbine disks N89-25207
DISLOCATIONS (MATERIALS)
Dynamic simulation of dislocation pattern formation in metals during high temperature monotonic and cyclic deformation N89-25477
DISPLACEMENT
Structural damage assessment as an identification problem N89-25230
DISPLACEMENT MEASUREMENT
Evaluation of elastic-plastic surface flaw behavior and related parameters using surface displacement measurements
[DE89-011134] N89-25489
DISSIPATION
Warm fog dissipation using large volume water sprays
[NASA-CASE-MFS-25962-1] N89-25242
DISTORTION
A courant condition free modified partially-implicit method. Revised electromagnetic particle Code PS2M for bounded plasmas with conducting walls
[IPPJ-892] N89-25699
DISTRIBUTED AMPLIFIERS
A novel TR (Transmit/Receive) switch utilizing a distributed amplifier
[DE89-005917] N89-25396
DISTRIBUTED PROCESSING
The Delta-t transport protocol: Features and experience useful for high performance networks
[DE89-009259] N89-25625
DISTRIBUTION FUNCTIONS
On the applicability of various planar potentials in the theory of ultrarelativistic electron channeling
[DE88-706155] N89-25738
DIURNAL VARIATIONS
Seasonal and diurnal variability of Mars water-ice clouds N89-25794
Diurnal and annual cycles of H2O in the Martian regolith N89-25809
The interannual variability of atmospheric water vapor on Mars N89-25813
DOMAINS
Time domain modeling of electromagnetic coupling
[DE89-010240] N89-25362
DOPPLER EFFECT
Radial and temporal structure of the internal solar asphericity N89-25833
Acquisition and reduction procedures for MOF Doppler-magnetograms --- solar observation N89-25851
The GONG instrument --- solar oscillations N89-25854
The Michelson Doppler imager for the solar oscillations imager program on SOHO N89-25892
A prototype stellar photometer for magnetic field and Doppler measurements N89-25926
DOPPLER RADAR
The evolution and structure of the bow echo/microburst events N89-25550
DOUBLE STARS
Particle simulation for accretion sheets in narrow double stars N89-25729
Some tests of the precision of CCD differential photometry measurements of bright double stars N89-25930
The mass-luminosity relationship for solar-type stars N89-25936
DOWNLINKING
Tropospheric influences on satellite-Earth paths and their determination by means of radar measurements
[DFVLR-FB-88-53] N89-25250
DRAG REDUCTION
Spanwise lift distributions and wake velocity surveys of a semi-span wing with a discontinuous twist
[NASA-CR-177532] N89-25122
DRUGS
A program for the study of skeletal muscle catabolism following physical trauma
[AD-A206506] N89-25564
DUCTILITY
Weldability and weld doping of commercial purity molybdenum
[DE89-009535] N89-25311
The development of alloys based on Ni3Si
[DE89-010371] N89-25316
J(sub Ic) fracture toughness of ferritic DCI (Ductile Cast Iron) alloys: A comparison of two versions of ASTM E 813
[DE89-012249] N89-25323
DUCTS
Acoustic propagation in curved ducts with extended reacting wall treatment
[NASA-TM-102110] N89-25670

DUST
Measurements of the vertical profile of water vapor abundance in the Martian atmosphere from Mars Observer N89-25811
DUST STORMS
Regolith water vapor sources on Mars: A historical bibliography N89-25796
DWARF STARS
End points of stellar evolution investigated by seismology on white dwarf stars N89-25934
DYNAMIC CHARACTERISTICS
Dynamic fracture toughness measurements of ferritic ductile cast iron
[DE89-009833] N89-25324
Shock waves and fragmentation via molecular dynamics
[DE89-007981] N89-25405
Particle simulation for accretion sheets in narrow double stars N89-25729
DYNAMIC CONTROL
An extremum hunting method using pseudo-random binary signal
[EUT-88-E-198] N89-25359
A new method for dynamic hunting extremum control, based on comparison of measured and estimated value
[EUT-88-E-197] N89-25644
DYNAMIC LOADS
PRONTO 3D: A three-dimensional transient solid dynamics program
[DE89-010517] N89-25590
DYNAMIC MODELS
Modifying a telerobotic system to include robotic operation by means of dynamic modeling
[DE89-003119] N89-25460
DYNAMIC RESPONSE
Aircraft design optimization with multidisciplinary performance criteria N89-25212
DYNAMIC STABILITY
Flap-lag stability data for a small-scale isolated hingeless rotor in forward flight
[NASA-TM-102189] N89-25479
DYNAMIC STRUCTURAL ANALYSIS
Effect of winglets on loading mechanics and wing assembly reactions N89-25137
Integrated design optimization research and development in an industrial environment N89-25148
Structural optimization of rotor blades with integrated dynamics and aerodynamics N89-25156
Multi-objective/loading optimization for rotating composite flexbeams N89-25157
A generalized software executive for multidisciplinary computational structural dynamics N89-25175
PRONTO 3D: A three-dimensional transient solid dynamics program
[DE89-010517] N89-25590
Parallel processors and nonlinear structural dynamics algorithms and software
[NASA-CR-185049] N89-25620
DYNAMICAL SYSTEMS
Catastrophic bifurcations in a second order dynamical system
[REPT-88-049] N89-25533
Least squares parameter estimation in a dynamic model from noisy observations
[ETN-89-94295] N89-25657
Phase space concepts
[DE89-011082] N89-25667
Querying databases of trajectories of differential equations: Data structures for trajectories
[NASA-CR-185040] N89-25772
DYNAMO THEORY
Dynamo theory prediction of solar activity N89-25878

E

EARTH ALBEDO
Modeling land-surface albedos from plant canopy architecture N89-25495
EARTH CRUST
Research for the physics and structure of earth's crust in Romania
[DE88-706002] N89-25535
EARTH GRAVITATION
Time-dependent computational studies of flames in microgravity
[NASA-CR-182298] N89-25353
EARTH IONOSPHERE
A study of non-linear ionization processes in planetary atmospheres N89-25816
EARTH ORBITS
Advanced mass launchers for low earth orbit
[DE89-010759] N89-25255
EARTH RESOURCES
Earth resources: A continuing bibliography with indexes (issue 61)
[NASA-SP-7041(61)] N89-25493
EARTH ROTATION
Studies of regional and global tectonics and the rotation of the earth using very-long baseline interferometry
[NASA-CR-185059] N89-25534
ECCENTRIC ORBITS
Estimated performance and future potential of solar dynamic and photovoltaic power systems for selected LEO and HEO missions
[NASA-TM-102083] N89-25280
ECONOMIC ANALYSIS
Evaluation of auxiliary power subsystems for gas engine heat pumps, phase 2
[PB89-173694] N89-25411
Federal incentives for industrial modernization: Historical review and future opportunities
[NASA-TM-101785] N89-25764
ECONOMIC FACTORS
Focusing on the future: Solar thermal energy systems emerge as competitive technologies with major economic potential
[DE89-000851] N89-25516
ECONOMICS
An economic model for evaluating high-speed aircraft designs
[NASA-CR-177530] N89-25235
ECOSYSTEMS
Catastrophic bifurcations in a second order dynamical system
[REPT-88-049] N89-25533
EDDINGTON APPROXIMATION
On the k-mechanism and the multidimensional Eddington approximation N89-25821
EDUCATION
International Centre for Theoretical Physics: Scientific activities in 1987
[DE88-705973] N89-25668
A theoretical framework and an instructional model for educating end-users of online bibliographic information retrieval systems: A research monograph N89-25769
EFFICIENCY
Pyramidal horns: Part 2: A novel design method for horns of any desired gain and aperture phase error
[DE89-005346] N89-25371
EIGENVALUES
On the calculation of derivatives of eigenvalues and eigenvectors in the simultaneous design and control of structures N89-25186
Flutter suppression using eigenspace freedoms to meet requirements N89-25191
Balancing a matrix for calculation of eigenvalues and eigenvectors
[DE88-706045] N89-25648
Observed asymptotic properties of low-degree solar gravity-mode eigenfrequencies N89-25890
Inversion of quasi-periodic deviations between low-degree solar gravity mode eigenfrequencies and asymptotic theory eigenfrequencies N89-25891
EIGENVECTORS
On the calculation of derivatives of eigenvalues and eigenvectors in the simultaneous design and control of structures N89-25186
Flutter suppression using eigenspace freedoms to meet requirements N89-25191
Balancing a matrix for calculation of eigenvalues and eigenvectors
[DE88-706045] N89-25648
ELASTIC BODIES
Shape optimal design of elastic bodies using a mixed variational formulation N89-25236
ELASTIC DEFORMATION
Elevated temperature deformation of structural steel
[PB89-172621] N89-25318
On optimal fail-safe design of structures N89-25486
ELASTOPLASTICITY
On optimal fail-safe design of structures N89-25486
Structural testing of metal/composite conical structures with holes
[DE89-011451] N89-25487
Evaluation of elastic-plastic surface flaw behavior and related parameters using surface displacement measurements
[DE89-011134] N89-25489
ELECTRIC ARCS
The influence of contact surface microstructure on vacuum arc stability and arc voltage
[EUT-87-E-186] N89-25672
ELECTRIC AUTOMOBILES
Advanced high-temperature batteries
[DE89-010698] N89-25390
ELECTRIC BATTERIES
Advanced Dual-Shaft Electric Propulsion System Technology Development Program
[DE89-010008] N89-25388
Metal-sulfur type cell having improved positive electrode
[DE89-010110] N89-25389
Advanced high-temperature batteries
[DE89-010698] N89-25390
ELECTRIC CONDUCTORS
Stress-driven diffusive voiding of aluminum conductor lines
[DE89-009832] N89-25387
Manifold, bus support and coupling arrangement for solid oxide fuel cells
[DE89-009604] N89-25508
ELECTRIC CORONA
Enhancement of heat transfer by corona wind
[EUT-87-E-184] N89-25500
ELECTRIC CURRENT
Condition monitoring of machinery using motor current signature analysis
[DE89-008737] N89-25386
ELECTRIC FIELDS
Poled polymer films for nonlinear optics
[DE89-010039] N89-25338
ELECTRIC GENERATORS
Electrically compensated constant speed drive (Model number 60 ECEPGS 02)
[AD-A206064] N89-25385
ELECTRIC HYBRID VEHICLES
Advanced Dual-Shaft Electric Propulsion System Technology Development Program
[DE89-010008] N89-25388
Vehicle performance tests of the Ford/GE first generation single-shaft (ETX-I) alternating current propulsion system
[DE89-011115] N89-25392
ELECTRIC MOTOR VEHICLES
Vehicle performance tests of the Ford/GE first generation single-shaft (ETX-I) alternating current propulsion system
[DE89-011115] N89-25392
ELECTRIC MOTORS
Condition monitoring of machinery using motor current signature analysis
[DE89-008737] N89-25386
ELECTRIC POWER PLANTS
Fuel cell systems program plan, FY 1989
[DE89-012928] N89-25515
ELECTRIC POWER TRANSMISSION
Analog and digital simulation of line-energizing overvoltages and comparison with measurements in a 400 kV network
[EUT-88-E-193] N89-25401
ELECTRIC PROPULSION
The effects of arcjet operating condition and constrictor geometry on the plasma plume
[NASA-TM-102284] N89-25281
Advanced Dual-Shaft Electric Propulsion System Technology Development Program
[DE89-010008] N89-25388
ELECTRICAL ENGINEERING
Engineering applications of heuristic multilevel optimization methods N89-25202
A decomposition-based design optimization method with applications N89-25204
ELECTRICAL IMPEDANCE
Frequency spectra for admittances and voltage transfers measured on a three-phased power transformer
[EUT-87-E-181] N89-25400
ELECTRICAL INSULATION
Elements of a specification for superconducting cable and why they are important for magnet construction
[DE89-012533] N89-25754
ELECTRICAL MEASUREMENT
Frequency spectra for admittances and voltage transfers measured on a three-phased power transformer
[EUT-87-E-181] N89-25400
ELECTRICAL PROPERTIES
Sintering schedule and sample geometry effects on the electrical and physical properties of high field varistor materials
[DE89-010523] N89-25384
Preparation and properties of high-temperature superconductors in the Y-Ba-Cu-O system
[DE88-706050] N89-25735
ELECTRICAL RESISTIVITY
Electrically conductive composite material
[DE89-010967] N89-25293
Apparatus and method for characterizing conductivity of materials
[DE89-009599] N89-25383
Kinetic effects of strong localization in planar heterostructures p-Ge/i-GaAs
[DE88-706205] N89-25739

ELECTRICITY
Martinus van Marum: A Dutch scientist in a revolutionary time
[EUT-88-E-194] N89-25402
ELECTRO-OPTICAL PHOTOGRAPHY
Comparative investigations of multispectral satellite image data of MOMS-01, LANDSAT-TM and LANDSAT-MSS for geological and vegetational applications in test sites in the Andes of northern Chile and the Parana-Basin of Brazil
[DFVLR-FB-88-50] N89-25499
ELECTRO-OPTICS
Digital optical conversion module
[DE89-011441] N89-25367
ELECTROCHEMICAL CELLS
The coupling of thermochemistry and phase diagrams for Group 3-5 semiconductor systems
[DE89-012516] N89-25752
ELECTROCHEMISTRY
Electrochemical and optical studies of model photosynthetic systems
[DE89-012479] N89-25562
ELECTRODES
Metal-sulfur type cell having improved positive electrode
[DE89-010110] N89-25389
Novel air electrode for metal-air battery with now carbon material and method of making same
[DE89-010964] N89-25391
Reference electrode for electrolytic cell
[DE89-011446] N89-25394
ELECTROENCEPHALOGRAPHY
Adaptive enhancement of magnetoencephalographic signals via multichannel filtering
[DE89-005464] N89-25569
ELECTROLYTES
Reference electrode for electrolytic cell
[DE89-011446] N89-25394
Advanced working fluid properties in heat pump and absorption cooling operations
[PB89-178172] N89-25413
Monolithic solid oxide fuel cell development
[DE89-010699] N89-25511
ELECTROLYTIC CELLS
Reference electrode for electrolytic cell
[DE89-011446] N89-25394
ELECTROMAGNETIC COUPLING
Time domain modeling of electromagnetic coupling
[DE89-010240] N89-25362
ELECTROMAGNETIC FIELDS
Photonic chiral current and its anomaly in a gravitational field
[DE88-706213] N89-25361
Time domain modeling of electromagnetic coupling
[DE89-010240] N89-25362
Computer simulation of FEL sidebands in a strongly dispersive waveguide
[DE89-011825] N89-25369
Far field projection
[DE89-010243] N89-25587
ELECTROMAGNETIC INTERFERENCE
Digital optical conversion module
[DE89-011441] N89-25367
ELECTROMAGNETIC PULSES
A generalized antenna theorem for broadband pulses
[DE89-009707] N89-25373
ELECTROMAGNETIC RADIATION
Tropospheric influences on satellite-Earth paths and their determination by means of radar measurements
[DFVLR-FB-88-53] N89-25250
ELECTRON ACCELERATORS
Modular magnet current regulator
[CEBAF-PR-89-005] N89-25685
ELECTRON BEAMS
Diffraction gratings used in X-ray spectroscopy
[DE89-012327] N89-25310
Modular magnet current regulator
[CEBAF-PR-89-005] N89-25685
On the applicability of various planar potentials in the theory of ultrarelativistic electron channeling
[DE88-706155] N89-25738
ELECTRON CAPTURE
State-selective single electron capture by multiply charged ions: Reaction window and multichannel Landau Zener calculations
[REPT-88-05-175] N89-25684
ELECTRON CYCLOTRON HEATING
High-average-power millimeter-wave FEL (Free-Electron Laser) for plasma heating using the ETA-2 accelerator
[DE89-012294] N89-25711
ELECTRON DENSITY (CONCENTRATION)
An inductively coupled plasma spectrometer for on-line, real-time process gas analysis
[DE89-010610] N89-25442
Anomalous particle pinch for collisionless plasma
[DE89-011018] N89-25706
Local field effects in the many-body perturbation theory and in the density functional theory
[DE88-705975] N89-25734
ELECTRON DIFFRACTION
Surface structural analysis of small molecules on transition metal single crystal surfaces with low energy electron diffraction
[DE89-010681] N89-25743
ELECTRON DISTRIBUTION
A numerical simulation of inhomogeneous ion cyclotron turbulence N89-25725
ELECTRON ENERGY
Acceleration of ions in the magnetotail N89-25720
ELECTRON GAS
Local field effects in the many-body perturbation theory and in the density functional theory
[DE88-705975] N89-25734
Ripple structure in degenerate electron gas-dominated stars with intense magnetic fields N89-25783
ELECTRON GUNS
Explosive cathode on the base of carbon-fibrous plastic material
[DE88-706302] N89-25350
ELECTRON IMPACT
State-selective single electron capture by multiply charged ions: Reaction window and multichannel Landau Zener calculations
[REPT-88-05-175] N89-25684
Partial and state selective cross sections for multiple ionization of rare gas atoms by electron impact
[REPT-88-05-170] N89-25715
ELECTRON MICROSCOPY
High resolution electron microscopy and microanalysis of ferrites and cuprates
[DE89-010441] N89-25341
Resistive Contrast Imaging applied to multilevel interconnection failure analysis
[DE89-011066] N89-25397
Atomic resolution microscopy
[DE89-009227] N89-25679
ELECTRON RADIATION
Absorbed dose thresholds and absorbed dose rate limitations for studies of electron radiation effects on polyetherimides
[NASA-TP-2928] N89-25332
ELECTRON SPECTROSCOPY
State-selective single electron capture by multiply charged ions: Reaction window and multichannel Landau Zener calculations
[REPT-88-05-175] N89-25684
ELECTRON STATES
Partial and state selective cross sections for multiple ionization of rare gas atoms by electron impact
[REPT-88-05-170] N89-25715
ELECTRON TRANSFER
Electrochemical and optical studies of model photosynthetic systems
[DE89-012479] N89-25562
Femtosecond studies of electron transfer processes at semiconductor interfaces
[DE89-010599] N89-25742
ELECTRON TRANSITIONS
Atomic resolution microscopy
[DE89-009227] N89-25679
ELECTRONIC CONTROL
Electrically compensated constant speed drive (Model number 60 ECEPGS 02)
[AD-A206064] N89-25385
ELECTRONIC EQUIPMENT
Serial-input polyphase convolvers
[REPT-88-019] N89-25608
ELEMENTARY PARTICLES
On the quantum theory of the superparticle
[NIKHEF-H/88-16] N89-25762
ELLIPTIC FUNCTIONS
Application of theta functions for numerical evaluation of complete elliptic integrals of the first and second kinds
[DE89-010191] N89-25645
EMBRITTLEMENT
Effect of low neutron fluences on DIN 1.4948 steel creep properties — liquid metal fast breeder reactor (LMFBR) material
[ECN-206] N89-25325
Influence of the helium on high temperature embrittlement of metals under cyclic loading
[JUEL-2229] N89-25330
Simulation of the welding of irradiated materials
[DE89-012524] N89-25469
EMISSION
Investigation of submicrometer aerosols for apportioning the impacts of airborne particulate matter at Deep Creek Lake
[DE89-008186] N89-25524
EMISSION SPECTRA
Development of laser-excited molecular luminescence spectrometric methods for polycyclic aromatic hydrocarbons in environmental sciences
[DE89-010616] N89-25306
An inductively coupled plasma spectrometer for on-line, real-time process gas analysis
[DE89-010610] N89-25442
EMISSIVITY
Pair production of helicity-flipped neutrinos in supernovae
[NASA-CR-185486] N89-25789
EMITTANCE
Flying wires at Fermilab
[DE89-011005] N89-25251
EMOTIONAL FACTORS
Culture shock: Improving software quality
[DE89-003610] N89-25592
END EFFECTORS
A kinematic study of the MERLIN 6500 robot and the Utah/MIT dexterous hand and a simulation of their combined behavior
[AD-A203907] N89-25458
ENERGETIC PARTICLES
The evolution of energetic particles and the emitted radiation in solar flares
[NASA-CR-185389] N89-25945
ENERGY BANDS
Femtosecond studies of electron transfer processes at semiconductor interfaces
[DE89-010599] N89-25742
ENERGY BUDGETS
The behavior of a class of minimal models of the atmospheric general circulation N89-25537
ENERGY CONSERVATION
An organized effort to develop the hydrothermal energy resource
[DE89-011139] N89-25512
ECUT (Energy Conversion and Utilization Technologies) program: Biocatalysis project
[NASA-CR-184965] N89-25519
ENERGY CONSUMPTION
Vehicle performance tests of the Ford/GE first generation single-shaft (ETX-I) alternating current propulsion system
[DE89-011115] N89-25392
Evaluation of auxiliary power subsystems for gas engine heat pumps, phase 2
[PB89-173694] N89-25411
ENERGY DISSIPATION
Dissipation of vortex power in longitudinal flow on wings N89-25133
Pair production of helicity-flipped neutrinos in supernovae
[NASA-CR-185486] N89-25789
ENERGY GAPS (SOLID STATE)
Narrow bandgap semiconducting silicides: Intrinsic infrared detectors on a silicon chip
[NASA-CR-185372] N89-25746
ENERGY REQUIREMENTS
Challenges for future space power systems
[NASA-TM-102063] N89-25506
ENERGY TECHNOLOGY
The introduction of space technology power systems into developing countries
[NASA-TM-102042] N89-25274
Support and maneuvering apparatus for solar energy receivers
[DE89-011466] N89-25514
ENGINE DESIGN
Treatment of body forces in boundary element design sensitivity analysis N89-25187
Influence of rubbing on rotor dynamics, part 2
[NASA-CR-183649-PT-2] N89-25464
Advanced methods for 3-D inelastic structural analysis for hot engine structures
[NASA-TM-102106] N89-25490
ENGINE MONITORING INSTRUMENTS
Flight set 360L003 instrumentation final test report, volume 9
[NASA-CR-183675] N89-25284
ENGINE PARTS
Treatment of body forces in boundary element design sensitivity analysis N89-25187
ENGINEERING DRAWINGS
Manifold, bus support and coupling arrangement for solid oxide fuel cells
[DE89-009604] N89-25508
ENVIRONMENT EFFECTS
The role of forests in addressing the CO2 greenhouse
[DE89-011568] N89-25527
Evaluating CFC (Chlorofluorocarbon) alternatives from the atmospheric viewpoint
[DE89-010238] N89-25531

ENVIRONMENT SIMULATION
Design description of the large scale climate simulator
[DE89-010185] N89-25551
ENVIRONMENT SIMULATORS
Design description of the large scale climate simulator
[DE89-010185] N89-25551
ENVIRONMENTAL TESTS
A procedure for the numerical description of the moisture dependent material behavior
[ETN-89-94669] N89-25299
Characterization of Spirulina biomass for CELSS diet potential
[NASA-CR-185329] N89-25561
ENZYMES
A program for the study of skeletal muscle catabolism following physical trauma
[AD-A206506] N89-25564
EPITAXY
Kinetic effects of strong localization in planar heterostructures p-Ge/i-GaAs
[DE88-706205] N89-25739
EQUATIONS OF MOTION
Coupling of the boundary element method with an integral momentum boundary-layer technique to calculate forces and moments on three-dimensional bodies
[DE89-006328] N89-25420
Beam transport calculation in magnetic field with a quadrupole symmetry by the method of immersion in moment phase space
[DE88-706295] N89-25681
EQUATIONS OF STATE
Physics of dense matter, neutron stars and supernova
[DE89-010673] N89-25784
Nuclear astrophysics of supernovae
[DE89-012534] N89-25787
Current options for the equation of state of the solar interior N89-25897
The influence of the equation of state on the zero-age main sequence and the Sun N89-25939
EROSION
Responding to changes in sea level engineering implications
[PB89-133466] N89-25555
Temperature limit of a graphite divertor surface due to particle erosion
[DE89-010272] N89-25703
ERROR ANALYSIS
Black-box identification of MIMO transfer functions: Asymptotic properties of prediction error models
[EUT-87-E-182] N89-25642
On the bounds of the modeling errors of black-box MIMO transfer function estimates
[EUT-87-E-183] N89-25643
ERROR CORRECTING CODES
Phase-ambiguity resolution for QPSK modulation systems. Part 1: A review
[NASA-CR-185385] N89-25380
ERROR FUNCTIONS
A comparison of the error function and the tanh transformation as progressive rules for double and triple singular integrals
[MATHS-RES-210] N89-25659
ERRORS
An interpretation and solution of ill-conditioned linear equations N89-25213
ESTERS
NMR study of some organophosphorus compounds
[DE88-705970] N89-25302
ESTIMATING
Parameter estimation for a viscoelastic constitutive model
[DE89-008714] N89-25336
ETALONS
The stable solar analyzer N89-25858
EULER EQUATIONS OF MOTION
Techniques for compressible flow calculations on multizone grids N89-25120
EUROPEAN SPACE AGENCY
United States and Western Europe cooperation in planetary exploration
[NASA-CR-184941] N89-25776
EVAPORATION
Solitosynthesis: Cosmological evolution of non-topological solitons
[NASA-CR-185030] N89-25678
Artificially structured superconductors
[DE89-009116] N89-25733
EVAPOTRANSPIRATION
FAO detailed rain mapping experiment
[BCRS-88-11] N89-25552
FAO detailed rain mapping experiment phase B: Comparison of rainfall and evapotranspiration mapping N89-25554
EVOKED RESPONSE (PSYCHOPHYSIOLOGY)
Adaptive enhancement of magnetoencephalographic signals via multichannel filtering
[DE89-005464] N89-25569
EXCIMER LASERS
A 2 J high-power excimer laser at high pulse repetition rate
[US-414/87/029] N89-25457
EXCITATION
The excitation and damping of solar oscillations N89-25820
EXERCISE PHYSIOLOGY
Acclimatization to heat in humans
[NASA-TM-101011] N89-25558
EXHAUST EMISSION
Fuel properties effect on the performance of a small high temperature rise combustor
[NASA-TM-102096] N89-25238
EXOBIOLOGY
USSR Space Life Sciences Digest. Index to issues 15-20
[NASA-CR-3922(25)] N89-25556
Aerospace medicine and biology: A continuing bibliography with indexes (supplement 323)
[NASA-SP-7011(323)] N89-25563
Aerospace medicine and biology: A continuing bibliography with indexes (supplement 324)
[NASA-SP-7011(324)] N89-25565
Aerospace medicine and biology: A continuing bibliography with indexes (supplement 325)
[NASA-SP-7011(325)] N89-25567
EXOTHERMIC REACTIONS
Characterization of ceramics and intermetallics fabricated by self-propagating high-temperature synthesis
[NASA-TM-102004] N89-25285
EXPERIMENT DESIGN
Operational experience of the OC-OTEC experiments at NELH
[DE89-000877] N89-25510
EXPERT SYSTEMS
Recent Advances in Multidisciplinary Analysis and Optimization, part 1
[NASA-CP-3031-PT-1] N89-25146
Integrated design optimization research and development in an industrial environment N89-25148
New directions for Artificial Intelligence (AI) methods in optimum design N89-25158
TRUSS: An intelligent design system for aircraft wings N89-25162
Real-time application of knowledge-based systems N89-25163
The designer of the 90's: A live demonstration N89-25164
Research on optimization-based design N89-25176
Timesharing performance as an indicator of pilot mental workload
[NASA-CR-185328] N89-25573
Use of metaknowledge in the verification of knowledge-based systems
[NASA-CR-181821] N89-25627
An expert system development methodology which supports verification and validation
[NASA-TM-101782] N89-25635
Blindness in designing intelligent systems
[NASA-CR-184582] N89-25638
Explanation in knowledge-based systems
[MEMO-INF-88-17] N89-25640
The use of first principles in diagnosing complex technical devices
[MEMO-INF-88-40] N89-25641
An expert system to facilitate selecting a database management system
[DE89-012350] N89-25774
EXPLODING WIRES
Simple models for electric gun operating characteristics
[DE89-005348] N89-25253
EXPLOSIONS
Simple models for electric gun operating characteristics
[DE89-005348] N89-25253
High explosives reaction model and its application to booster performance
[DE89-005459] N89-25351
EXPLOSIVES
High-performance, extrusion-cast explosives with low sensitivity
[DE89-010279] N89-25349
High explosives reaction model and its application to booster performance
[DE89-005459] N89-25351
Fiber optic sensing in a high explosives environment
[DE89-010863] N89-25695
EXTENSOMETERS
X-ray based extensometry
[NASA-CR-185058] N89-25432
EXTINCTION
Measurements of the vertical profile of water vapor abundance in the Martian atmosphere from Mars Observer N89-25811
EXTINGUISHING
Time-dependent computational studies of flames in microgravity
[NASA-CR-182298] N89-25353
EXTRATERRESTRIAL MATTER
Neutron stars: A cosmic hadron physics laboratory
[NASA-CR-185051] N89-25777
Interplanetary Matter: Proceedings, volume 2
[DE88-706057] N89-25779
EXTREME ULTRAVIOLET RADIATION
A study of non-linear ionization processes in planetary atmospheres N89-25816
EXTREMELY HIGH FREQUENCIES
Measurements of solar oscillations at 37 GHz N89-25859

F

FABRICATION
Polyimide Matrix composites: Polyimidesulfone/LARC-TPI (1:1) blend
[NASA-TM-101568] N89-25294
Low density microcellular carbon foams and method of preparation
[DE89-010966] N89-25345
High-performance, extrusion-cast explosives with low sensitivity
[DE89-010279] N89-25349
Sintering schedule and sample geometry effects on the electrical and physical properties of high field varistor materials
[DE89-010523] N89-25364
Monolithic solid oxide fuel cell development
[DE89-010699] N89-25511
Artificially structured superconductors
[DE89-009116] N89-25733
FABRICS
Smart tunnel: Docking mechanism
[NASA-CASE-MSC-21360-1] N89-25263
FABRY-PEROT INTERFEROMETERS
A Fabry-Perot interferometric stellar oscillation spectrometer N89-25929
FACILITIES
Spacelab Data Processing Facility
[NASA-TM-101808] N89-25252
FAIL-SAFE SYSTEMS
Probabilistic damage tolerance methods for metallic aerospace structures N89-25237
On optimal fail-safe design of structures N89-25486
FAILURE
Failure characterization of composite materials
[DE89-008662] N89-25291
A predictive model for failure properties of thermoset resins
[NASA-TM-4128] N89-25300
Generalized consistency checking of multivariable redundant measurements and common-mode failure detection
[DE89-010053] N89-25474
FAILURE ANALYSIS
Probabilistic damage tolerance methods for metallic aerospace structures N89-25237
Resistive Contrast Imaging applied to multilevel interconnection failure analysis
[DE89-011066] N89-25397
Procedures for characterizing an alloy and predicting cyclic life with the total strain version of Strainrange Partitioning
[NASA-TM-4102] N89-25485
FAR FIELDS
Far field projection
[DE89-010243] N89-25587
FARADAY EFFECT
ICRF Faraday shield plasma sheath physics: The Perkins paradigm
[DE89-012362] N89-25712
FAST FOURIER TRANSFORMATIONS
Fast Fourier Transform algorithm design and tradeoffs
[NASA-CR-185038] N89-25600
FATIGUE (MATERIALS)
Probabilistic damage tolerance methods for metallic aerospace structures N89-25237
An analytical and experimental investigation of edge delamination in laminates subjected to tension, bending, and torsion
[NASA-CR-181824] N89-25296

FATIGUE LIFE
Influence of the helium on high temperature embrittlement of metals under cyclic loading
[JUEL-2229] N89-25330
Procedures for characterizing an alloy and predicting cyclic life with the total strain version of Strainrange Partitioning
[NASA-TM-4102] N89-25485
FATIGUE TESTS
Influence of the helium on high temperature embrittlement of metals under cyclic loading
[JUEL-2229] N89-25330
A test system for computer controlled thermomechanical fatigue testing
[DE89-009067] N89-25483
Procedures for characterizing an alloy and predicting cyclic life with the total strain version of Strainrange Partitioning
[NASA-TM-4102] N89-25485
Crack growth under low cycle fatigue
[GKSS-88/E/47] N89-25491
FEASIBILITY ANALYSIS
The conceptual design of a Mach 2 Oblique Flying Wing supersonic transport
[NASA-CR-177529] N89-25233
Report to Congress: Technical feasibility of joint use at Scott AFB, Selfridge AGB and El Toro MCAS
[AD-A194597] N89-25241
FEEDBACK
Detection of metal-transfer mode in GMAW
[DE89-011133] N89-25465
FEEDBACK CONTROL
Optimization of structure and control system N89-25223
Spiral vane bioreactor
[NASA-CASE-MSC-21361-1] N89-25557
On the bounds of the modeling errors of black-box MIMO transfer function estimates
[EUT-87-E-183] N89-25643
FERMIONS
Two-dimensional density matrix and its equations. Scalar and fermionic fields
[DE88-706249] N89-25760
FERRITES
The influence of cooling rate on the ferrite content of stainless steel alloys
[DE89-009966] N89-25315
High resolution electron microscopy and microanalysis of ferrites and cuprates
[DE89-010441] N89-25341
FERRITIC STAINLESS STEELS
Welding of helium-doped austenitic and ferritic stainless steels
[DE89-012523] N89-25468
FERROELECTRICITY
Ferroelectric potassium niobate thin films
[DE89-010862] N89-25744
FIBER COMPOSITES
Failure characterization of composite materials
[DE89-008662] N89-25291
FIBER OPTICS
Optical information processing and holography
[DE88-706011] N89-25434
Optical pressure sealing coupling apparatus
[NASA-CASE-MFS-29348-1] N89-25689
Fiber optic sensing in a high explosives environment
[DE89-010863] N89-25695
Fiber optic sensing for NDE and process control
[DE89-010976] N89-25696
FIBER ORIENTATION
Characterization of the effects of three-dimensional states of stress on damping of laminated composites N89-25287
FIBER STRENGTH
Strong fibers
[DE89-010596] N89-25292
FIBERS
Method of protecting surfaces from abrasion and abrasion resistant articles of manufacture
[DE89-010798] N89-25344
FIELD EFFECT TRANSISTORS
A novel TR (Transmit/Receive) switch utilizing a distributed amplifier
[DE89-005917] N89-25396
HEMTS: Fundamental investigations
[ETN-89-94630] N89-25399
FIELD THEORY (PHYSICS)
A new way to interpret the DIRAC equation in a non-Riemannian manifold
[NASA-CR-185464] N89-25663
Statistical fluctuations as the origin of nontopological solitons
[NASA-CR-185351] N89-25680
Two-dimensional density matrix and its equations. Scalar and fermionic fields
[DE88-706249] N89-25760
FIGHTER AIRCRAFT
Effects of nonlinear aerodynamics and static aeroelasticity on mission performance calculations for a fighter aircraft N89-25170
FILE MAINTENANCE (COMPUTERS)
The RIACS Intelligent Auditing and Categorizing System
[NASA-CR-185398] N89-25598
FILM COOLING
Scaling results for the Liquid Sheet Radiator (LSR)
[NASA-TM-102100] N89-25277
FINITE DIFFERENCE THEORY
Numerical analysis of supersonic flow through oscillating cascade sections by using a deforming grid
[NASA-TM-102053] N89-25119
On equivalence of discrete-discrete and continuum-discrete design sensitivity analysis N89-25181
On the calculation of derivatives of eigenvalues and eigenvectors in the simultaneous design and control of structures N89-25186
Partitioning a finite difference code for a local memory multiprocessor
[DE89-010223] N89-25621
A class of high resolution explicit and implicit shock-capturing methods
[NASA-TM-101088] N89-25652
A courant condition free modified partially-implicit method. Revised electromagnetic particle Code PS2M for bounded plasmas with conducting walls
[IPPJ-892] N89-25699
FINITE ELEMENT METHOD
Applications of integrated design/analysis systems in aerospace structural design N89-25147
New directions for Artificial Intelligence (AI) methods in optimum design N89-25158
ASTROS: A multidisciplinary automated structural design tool N89-25174
Recent experiences using finite-element-based structural optimization N89-25177
On equivalence of discrete-discrete and continuum-discrete design sensitivity analysis N89-25181
Finite element flow-thermal-structural analysis of aerodynamically heated leading edges N89-25196
Optimizing for minimum weight when two different finite element models and analyses are required N89-25200
Procedures for shape optimization of gas turbine disks N89-25207
Structural optimization and recent large ground antenna installations N89-25224
On the stress problem of the pebble bed heat exchanger in a hypersonic wind tunnel
[NAL-TM-ST-8705] N89-25240
Space Shuttle Main Engine structural analysis and data reduction/evaluation. Volume 2: High pressure oxidizer turbo-pump turbine end bearing analysis
[NASA-CR-183664] N89-25270
Characterization of the effects of three-dimensional states of stress on damping of laminated composites N89-25287
An analytical and experimental investigation of edge delamination in laminates subjected to tension, bending, and torsion
[NASA-CR-181824] N89-25296
Plan, formulate, discuss and correlate a NASTRAN finite element vibrations model of the Boeing Model 360 helicopter airframe
[NASA-CR-181787] N89-25480
Identification of distributed forces on a structure
[DE89-007978] N89-25482
Structural testing of metal/composite conical structures with holes
[DE89-011451] N89-25487
Finite strain example problems for rectangular, cylindrical, and spherical geometries
[DE89-013607] N89-25488
Modeling of magnetic devices with finite-element methods
[DE89-010525] N89-25576
Parallel processors and nonlinear structural dynamics algorithms and software
[NASA-CR-185049] N89-25620
Acoustic propagation in curved ducts with extended reacting wall treatment
[NASA-TM-102110] N89-25670
FINS
Static aeroelastic analysis and tailoring of missile control fins N89-25169
FIXED WINGS
Results of including geometric nonlinearities in an aeroelastic model of an F/A-18 N89-25190
FIXTURES
Simple fixture concepts for multi-axis vibration testing
[DE89-007977] N89-25481
FLAME PROPAGATION
Time-dependent computational studies of flames in microgravity
[NASA-CR-182298] N89-25353
FLAME TEMPERATURE
Determination of combustion gas temperatures by infrared radiometry in sooting and nonsooting flames
[NASA-TP-2900] N89-25409
FLAPS (CONTROL SURFACES)
Flap system for short takeoff and landing aircraft
[AD-D013981] N89-25234
FLEXIBILITY
Optical fiber sensors and signal processing for intelligent structure monitoring
[NASA-CR-185395] N89-25691
FLEXIBLE BODIES
Digital robust control law synthesis using constrained optimization N89-25193
Computational experiments in the optimal slewing of flexible structures N89-25226
FLEXIBLE SPACECRAFT
Recent Advances in Multidisciplinary Analysis and Optimization, part 3
[NASA-CP-3031-PT-3] N89-25201
Experiences in applying optimization techniques to configurations for the Control of Flexible Structures (COFS) program N89-25228
Time-optimal slewing maneuvers of flexible spacecraft N89-25265
FLIGHT CHARACTERISTICS
Flight performance model for a geostationary transportation system
[ILR-MITT-206] N89-25259
FLIGHT HAZARDS
UK airmisses involving commercial air transport
[CAA-3/88] N89-25143
FLIGHT INSTRUMENTS
Flight set 360L003 instrumentation final test report, volume 9
[NASA-CR-183675] N89-25284
FLIGHT MECHANICS
Flight-mechanical investigations of the lateral motion of configurations with winglets N89-25141
FLIGHT SAFETY
Notice to Airmen (NOTAM) system operational concept
[DOT/FAA/CT-TN89/10] N89-25142
UK airmisses involving commercial air transport
[CAA-3/88] N89-25143
Contributions to the improvement of flight safety in wind shear
[DFVLR-FB-88-49] N89-25144
FLIGHT SIMULATION
Validation of the subjective workload assessment technique in a simulated flight task
[DFVLR-FB-89-01] N89-25575
FLIGHT TESTS
Testing of a GPS receiver
[DFVLR-MITT-88-30] N89-25145
Real-time application of knowledge-based systems N89-25163
FLOW CHARACTERISTICS
Flow characteristics and accuracy of control valve
[DE88-757331] N89-25459
FLOW DISTRIBUTION
Techniques for compressible flow calculations on multizone grids N89-25120
Aerodynamic flight evaluation analysis and data base update
[NASA-CR-183654] N89-25276
Unsteady stagnation-point heat transfer during passage of a concentrated vortex
[NASA-CR-182297] N89-25404
Coupling of the boundary element method with an integral momentum boundary-layer technique to calculate forces and moments on three-dimensional bodies
[DE89-006328] N89-25420
A variationally optimized vortex tracing algorithm for three-dimensional flows around solid bodies
[ETN-89-94301] N89-25423
FLOW EQUATIONS
A class of high resolution explicit and implicit shock-capturing methods
[NASA-TM-101088] N89-25652
FLOW MEASUREMENT
Experimental study of the phenomena of turbulent flow in the narrow gaps between subchannels of rod bundles
[KFK-4501] N89-25428
FLOW STABILITY
Investigations of vortex breakdown N89-25128
Scaling results for the Liquid Sheet Radiator (LSR)
[NASA-TM-102100] N89-25277
FLOW VELOCITY
Scaling results for the Liquid Sheet Radiator (LSR)
[NASA-TM-102100] N89-25277

Study of interfacial behavior in concurrent gas-liquid flows
[DE89-010484] N89-25408
Proceedings of the Solids Transport Contractors' Review Meeting
[DE89-006720] N89-25414
Experimental study of the phenomena of turbulent flow in the narrow gaps between subchannels of rod bundles
[KFK-4501] N89-25428
Flow characteristics and accuracy of control valve
[DE88-757331] N89-25459
Analytic theory for the determination of velocity and stability of bubbles in a Hele-Shaw cell. Part 1: Velocity selection
[NASA-CR-181836] N89-25665

FLOW VISUALIZATION
A variationally optimized vortex tracing algorithm for three-dimensional flows around solid bodies
[ETN-89-94301] N89-25423

FLUENCE
A generalized antenna theorem for broadband pulses
[DE89-009707] N89-25373

FLUID DYNAMICS
Fast Fourier Transform algorithm design and tradeoffs
[NASA-CR-185038] N89-25600

FLUID FILMS
Periodic and solitary waves on thin, horizontal, gas-sheared liquid films
[DE89-010655] N89-25416

FLUID FLOW
Effects of nonlinear aerodynamics and static aeroelasticity on mission performance calculations for a fighter aircraft N89-25170
Diffusion, fluid flow and sound propagation in disordered media
[DE89-010937] N89-25407
Modeling the effect of surface active elements on weld pool fluid flow, heat transfer and geometry
[DE89-012504] N89-25466
Analytic theory for the determination of velocity and stability of bubbles in a Hele-Shaw cell. Part 1: Velocity selection
[NASA-CR-181836] N89-25665

FLUID MANAGEMENT
GIRL cryotechnics and preparation of a TEXUS experiment on superfluid helium dynamics
[ETN-89-94631] N89-25357

FLUID MECHANICS
Interfacial fluid mechanics and transport processes
[DE89-010664] N89-25417

FLUID PRESSURE
Experimental study of the phenomena of turbulent flow in the narrow gaps between subchannels of rod bundles
[KFK-4501] N89-25428

FLUOROCARBONS
Evaluating CFC (Chlorofluorocarbon) alternatives from the atmospheric viewpoint
[DE89-010238] N89-25531

FLUTTER
Flutter suppression using eigenspace freedoms to meet requirements N89-25191
Control surface spanwise placement in active flutter suppression systems N89-25195

FOAMS
Electrically conductive composite material
[DE89-010967] N89-25293
Low density microcellular carbon foams and method of preparation
[DE89-010966] N89-25345

FOG
Warm fog dissipation using large volume water sprays
[NASA-CASE-MFS-25962-1] N89-25242

FOKKER-PLANCK EQUATION
The evolution of energetic particles and the emitted radiation in solar flares
[NASA-CR-185389] N89-25945

FORCE DISTRIBUTION
Spanwise lift distributions and wake velocity surveys of a semi-span wing with a discontinuous twist
[NASA-CR-177532] N89-25122

FOREARM
Design of a dual forearm modular robot
[DE89-010453] N89-25462

FOREBODIES
The art of spacecraft design: A multidisciplinary challenge N89-25209

FORECASTING
Climate projections with regional resolution
[DE89-009904] N89-25549

FOREST MANAGEMENT
Catastrophic bifurcations in a second order dynamical system
[REPT-88-049] N89-25533

FORESTS
Forestry interpretation of Thematic Mapper (TM) data using the example of the Frankfurt municipal forest N89-25503
The role of forests in addressing the CO2 greenhouse
[DE89-011568] N89-25527

FORGING
The development of alloys based on Ni3Si
[DE89-010371] N89-25316

FORMALISM
An exercise in transformational programming: Back tracking and Branch-and-Bound
[MEMO-INF-88-22] N89-25612

FORTRAN
Common Graphics Library (CGL). Volume 2: Low-level user's guide
[NASA-TM-101596] N89-25597

FOURIER TRANSFORMATION
Local-frequency description of optical signals and systems
[EUT-88-E-191] N89-25698
Measurements of oscillation parameters from synthetic times series --- solar oscillations N89-25827

FRACTURE MECHANICS
Failure characterization of composite materials
[DE89-008662] N89-25291
Weldability and weld doping of commercial purity molybdenum
[DE89-009535] N89-25311
Intermetallic alloys: Deformation, mechanical and fracture behavior
[GKSS-88/E/53] N89-25327
Evaluation of elastic-plastic surface flaw behavior and related parameters using surface displacement measurements
[DE89-011134] N89-25489
Crack growth under low cycle fatigue
[GKSS-88/E/47] N89-25491

FRACTURE STRENGTH
J(sub ic) fracture toughness of ferritic DCI (Ductile Cast Iron) alloys: A comparison of two versions of ASTM E 813
[DE89-012249] N89-25323
Dynamic fracture toughness measurements of ferritic ductile cast iron
[DE89-009833] N89-25324
The mechanical properties of ion implanted ceramics
[DE89-008928] N89-25337

FRACTURES (MATERIALS)
Probabilistic damage tolerance methods for metallic aerospace structures N89-25237
SiC whisker-reinforced SiAlON composites: Effect of sintering aid content
[DE89-010376] N89-25289

FRAGMENTATION
Shock waves and fragmentation via molecular dynamics
[DE89-007981] N89-25405

FRAMES
Structural optimization of framed structures using generalized optimality criteria N89-25197

FRAMES (DATA PROCESSING)
Constraint specification in BSDM --- basic semantic data model (BSDM)
[MEMO-INF-88-32] N89-25615

FREE ELECTRON LASERS
Computer simulation of FEL sidebands in a strongly dispersive waveguide
[DE89-011825] N89-25369
Proceedings of the Free Electron Laser Workshop, 1988 JAERI
[DE89-780071] N89-25450
Report of the Workshop on Scientific Opportunities for Infrared Free-Electron Lasers, volume 2
[DE89-009106] N89-25452
Status of LBL/LLNL FEL (Free Electron Laser) research for two beam accelerator applications
[DE89-012487] N89-25455
High-average-power millimeter-wave FEL (Free-Electron Laser) for plasma heating using the ETA-2 accelerator
[DE89-012294] N89-25711

FREE MOLECULAR FLOW
Free-molecule-flow force and moment coefficients of the aeroassist flight experiment vehicle
[NASA-TM-101600] N89-25124

FREEZING
Effects of freezing and cold acclimation on the plasma membrane of isolated protoplasts
[DE89-010931] N89-25560

FREQUENCY ANALYZERS
Digital dynamic amplitude-frequence spectral analyzer
[DE88-706256] N89-25436

FREQUENCY CONTROL
Variable speed induction motor operation from a 20-kHz power bus
[NASA-TM-102061] N89-25271

FREQUENCY CONVERTERS
On system identification using pulse-frequency modulated signals
[EUT-88-E-195] N89-25379

FREQUENCY MEASUREMENT
On the dissipation of Alfven waves in magnetic atmospheres and flux tubes N89-25871
Modelling the variation of solar p-mode frequencies N89-25907

FREQUENCY STABILITY
Initial high-degree p-mode frequency splittings from the 1988 Mt. Wilson 60-foot Tower Solar Oscillation Program N89-25832

FREQUENCY SYNCHRONIZATION
Phase-ambiguity resolution for QPSK modulation systems. Part 2: A method to resolve offset QPSK
[NASA-CR-184971] N89-25381

FRICTION
Influence of rubbing on rotor dynamics, part 1
[NASA-CR-183648-PT-1] N89-25463
Influence of rubbing on rotor dynamics, part 2
[NASA-CR-183649-PT-2] N89-25464

FRICTION MEASUREMENT
Correlation of subjective slipperiness judgements with quantitative COF (Coefficient Of Friction) measurements for structural steel
[PB89-165070] N89-25669

FUEL CELLS
Novel air electrode for metal-air battery with new carbon material and method of making same
[DE89-010964] N89-25391
Manifold, bus support and coupling arrangement for solid oxide fuel cells
[DE89-009604] N89-25508
Monolithic solid oxide fuel cell development
[DE89-010699] N89-25511
Fuel cell systems program plan, FY 1989
[DE89-012928] N89-25515

FUEL COMBUSTION
Radiative heat transfer
[PB89-173637] N89-25412

FUEL INJECTION
Fuel properties effect on the performance of a small high temperature rise combustor
[NASA-TM-102096] N89-25238

FUNCTIONAL DESIGN SPECIFICATIONS
The use of first principles in diagnosing complex technical devices
[MEMO-INF-88-40] N89-25641

FUSELAGES
In-flight measurement of propeller noise on the fuselage of an airplane
[NASA-TM-102285] N89-25675

FUSION (MELTING)
Solitosynthesis: Cosmological evolution of non-topological solitons
[NASA-CR-185030] N89-25678

FUSION REACTORS
Precipitation at grain boundaries in irradiated austenitic Fe-Cr-Mn alloys
[DE89-011207] N89-25319
Heat transfer in packed beds
[KFK-4451] N89-25425
Investigations of modular nonplanar coil systems for the stellarator fusion reactor
[IPP-2/298] N89-25714

FUZZY SETS
Fuzzy set applications in engineering optimization: Multilevel fuzzy optimization N89-25216

G

GALACTIC EVOLUTION
Cosmological effects of superconducting strings N89-25778

GALAXIES
Cosmological effects of superconducting strings N89-25778

GALERKIN METHOD
Acoustic propagation in curved ducts with extended reacting wall treatment
[NASA-TM-102110] N89-25670

GALLIUM ARSENIDES
HEMTS: Fundamental investigations
[ETN-89-94630] N89-25399
Kinetic effects of strong localization in planar heterostructures p-Ge/i-GaAs
[DE88-706205] N89-25739
Studies of 3-5 compounds in the megabar regime
[DE89-012433] N89-25751

GALVANOMAGNETIC EFFECTS
Kinetic effects of strong localization in planar heterostructures p-Ge/i-GaAs
[DE88-706205] N89-25739

GAS ANALYSIS
An inductively coupled plasma spectrometer for on-line, real-time process gas analysis
[DE89-010610] N89-25442

GAS DETECTORS
On greenhouse gas signal detection strategies
[DE89-009908] N89-25521

GAS DYNAMICS
Adaptive mesh refinement on moving quadrilateral grids
[DE89-010241] N89-25421
A class of high resolution explicit and implicit shock-capturing methods
[NASA-TM-101088] N89-25652

GAS FLOW
Periodic and solitary waves on thin, horizontal, gas-sheared liquid films
[DE89-010655] N89-25416
Adaptive mesh refinement on moving quadrilateral grids
[DE89-010241] N89-25421
Analysis of the transient compressible vapor flow in heat pipe
[NASA-CR-185119] N89-25422

GAS IONIZATION
State-selective single electron capture by multiply charged ions: Reaction window and multichannel Landau Zener calculations
[REPT-88-05-175] N89-25684
Partial and state selective cross sections for multiple ionization of rare gas atoms by electron impact
[REPT-88-05-170] N89-25715

GAS MIXTURES
Binary and ternary gas mixtures with temperature enhanced diffuse glow discharge characteristics for use in closing switches
[DE89-011807] N89-25395

GAS TEMPERATURE
Determination of combustion gas temperatures by infrared radiometry in sooting and nonsooting flames
[NASA-TP-2900] N89-25409

GAS TUNGSTEN ARC WELDING
Modeling the effect of surface active elements on weld pool fluid flow, heat transfer and geometry
[DE89-012504] N89-25466
Cavitation kinetics during GTA (Gas Tungsten Arc) welding of helium containing stainless steel
[DE89-012514] N89-25467
Welding of helium-doped austenitic and ferritic stainless steels
[DE89-012523] N89-25468
Simulation of the welding of irradiated materials
[DE89-012524] N89-25469

GAS TURBINE ENGINES
Treatment of body forces in boundary element design sensitivity analysis N89-25187
Procedures for shape optimization of gas turbine disks N89-25207
Fuel properties effect on the performance of a small high temperature rise combustor
[NASA-TM-102096] N89-25238

GAS-SOLID INTERFACES
Enhancement of heat transfer by corona wind
[EUT-87-E-184] N89-25500

GASEOUS DIFFUSION
Studies of oxidative degradation of polymers induced by ionizing radiation
[DE89-008279] N89-25335

GENE EXPRESSION
Unraveling Photosystem 2
[DE89-010930] N89-25559

GENES
Unraveling Photosystem 2
[DE89-010930] N89-25559

GENETIC ENGINEERING
ECUT (Energy Conversion and Utilization Technologies) program: Biocatalysis project
[NASA-CR-184965] N89-25519

GEOLOGICAL SURVEYS
Comparative investigations of multispectral satellite image data of MOMS-01, LANDSAT-TM and LANDSAT-MSS for geological and vegetational applications in test sites in the Andes of northern Chile and the Parana-Basin of Brazil
[DFVLR-FB-88-50] N89-25499

GEOLOGY
Research for the physics and structure of earth's crust in Romania
[DE88-706002] N89-25535

GEOMETRY
Sintering schedule and sample geometry effects on the electrical and physical properties of high field varistor materials
[DE89-010523] N89-25384

GEOPHYSICS
Research for the physics and structure of earth's crust in Romania
[DE88-706002] N89-25535
Solar-geophysical data number 528, August 1988. Part 1: (Prompt reports). Data for July, June 1988 and late data
[PB89-109904] N89-25617

GEOPOTENTIAL HEIGHT
Comparison of satellite-derived dynamical quantities for the stratosphere of the Southern Hemisphere
[NASA-CP-3044] N89-25540

GEOSYNCHRONOUS ORBITS
Flight performance model for a geostationary transportation system
[ILR-MITT-206] N89-25259

GEOTHERMAL ENERGY CONVERSION
Advanced binary geothermal power plants working fluid property determination and heat exchanger design
[DE89-011144] N89-25513

GEOTHERMAL ENERGY EXTRACTION
An organized effort to develop the hydrothermal energy resource
[DE89-011139] N89-25512

GEOTHERMAL ENERGY UTILIZATION
Energy from the Earth: Geothermal Energy Program. Five year research plan, 1988-1992
[DE89-010080] N89-25507

GEOTHERMAL RESOURCES
Energy from the Earth: Geothermal Energy Program. Five year research plan, 1988-1992
[DE89-010080] N89-25507
An organized effort to develop the hydrothermal energy resource
[DE89-011139] N89-25512

GEOTHERMAL TECHNOLOGY
Geothermal energy program summary. Volume 2: Research summaries, fiscal year 1988
[DE89-000865] N89-25509

GERMAN INFRARED LABORATORY
GIRL cryotechnics and preparation of a TEXUS experiment on superfluid helium dynamics
[ETN-89-94631] N89-25357

GIANT STARS
High precision velocity observations of Arcturus using the 7699 A line of potassium N89-25919

GLASS FIBER REINFORCED PLASTICS
Processing of fiber-reinforced materials by injection molding
[ETN-89-94668] N89-25298
A procedure for the numerical description of the moisture dependent material behavior
[ETN-89-94669] N89-25299

GLASS FIBERS
Processing of fiber-reinforced materials by injection molding
[ETN-89-94668] N89-25298

GLOBAL POSITIONING SYSTEM
Testing of a GPS receiver
[DFVLR-MITT-88-30] N89-25145

GLOW DISCHARGES
Binary and ternary gas mixtures with temperature enhanced diffuse glow discharge characteristics for use in closing switches
[DE89-011807] N89-25395

GOERTLER INSTABILITY
On the Gortler vortex instability mechanism at hypersonic speeds
[NASA-CR-181844] N89-25123

GOES 6
Visible and near-infrared channel calibration of the GOES-6 VISSR using high-altitude aircraft measurements
[NASA-TM-101064] N89-25494

GOLD
X-ray scattering studies of non-equilibrium ordering processes
[DE89-012517] N89-25753

GOVERNMENT/INDUSTRY RELATIONS
Space station operations task force. Panel 3 report: User development and integration
[NASA-TM-101818] N89-25246
Federal incentives for industrial modernization: Historical review and future opportunities
[NASA-TM-101785] N89-25764

GRAIN BOUNDARIES
Thermomechanical fatigue of solder joints: A new comprehensive test method
[DE89-008045] N89-25314
Quantitative modeling of sensitization development in austenitic stainless steel
[DE89-011206] N89-25317
Precipitation at grain boundaries in irradiated austenitic Fe-Cr-Mn alloys
[DE89-011207] N89-25319
Modeling grain boundary microchemistry related to IASCC (Irradiation-Assisted Stress Corrosion Cracking)
[DE89-011214] N89-25320
Deformation induced microstructural and microchemical changes during thermomechanical treatment
[DE89-011608] N89-25321
High resolution electron microscopy and microanalysis of ferrites and cuprates
[DE89-010441] N89-25341

GRAIN SIZE
Optical properties of metal-oxide thin films: Influence of microstructure
[DE89-011219] N89-25690

GRAMMARS
Controlled bidirectional grammars
[MEMO-INF-88-16] N89-25611

GRANTS
Geothermal energy program summary. Volume 2: Research summaries, fiscal year 1988
[DE89-000865] N89-25509

GRAPHITE
Temperature limit of a graphite divertor surface due to particle erosion
[DE89-010272] N89-25703

GRAPHITE-EPOXY COMPOSITES
Optimum design of swept-forward high-aspect-ration graphite-epoxy wings N89-25172
Vibration testing of impact-damaged composite laminates
[NASA-TM-4115] N89-25290
Failure characterization of composite materials
[DE89-008662] N89-25291

GRATINGS (SPECTRA)
Diffraction gratings used in X-ray spectroscopy
[DE89-012327] N89-25310

GRAVIMETRY
Gravity network of West Germany 1976 (DSGN76). Part 3: Data and adjustments
[SER-C-286] N89-25545
Gravity network of West Germany (DSGN76): Measurements and starting data N89-25546
Adjustment and data analysis — gravimetry N89-25547
Data adjustment by gravity differences N89-25548

GRAVITATIONAL COLLAPSE
Gravitational-like phase transition of a classical Coulomb plasma N89-25727
The origin of ultra-compact binaries
[NASA-TM-101792] N89-25780
Ambipolar diffusion and core formation in molecular clouds N89-25782

GRAVITATIONAL FIELDS
Photonic chiral current and its anomaly in a gravitational field
[DE88-706213] N89-25361
Imbedding of the gravitational field into the space of affine connection without torsion
[DE88-704637] N89-25536
Dynamic sea surface topography, gravity and improved orbit accuracies from the direct evaluation of SEASAT altimeter data
[NASA-TM-100735] N89-25539

GRAVITY ANOMALIES
Photonic chiral current and its anomaly in a gravitational field
[DE88-706213] N89-25361

GREEN'S FUNCTIONS
Non-perturbative effects in the exact S-matrices of the O(N) Gross-Neveu and supersymmetric sigma models
[NIKHEF-H/88-10] N89-25656

GREENHOUSE EFFECT
On greenhouse gas signal detection strategies
[DE89-009908] N89-25521
The role of forests in addressing the CO2 greenhouse
[DE89-011568] N89-25527
Atmospheric carbon dioxide and the climate record
[DE89-011892] N89-25528
Climate projections with regional resolution
[DE89-009261] N89-25529
Cloud albedo, greenhouse effects, atmospheric chemistry, and climate change
[DE89-010239] N89-25532
Climate projections with regional resolution
[DE89-009904] N89-25549

GRID GENERATION (MATHEMATICS)
Adaptive mesh refinement on moving quadrilateral grids
[DE89-010241] N89-25421

Feasibility of using the Massively Parallel Processor for large eddy simulations and other Computational Fluid Dynamics applications
[NASA-CR-185427] N89-25629

GROUND STATIONS
Reduction of transhorizon radio interference in satellite earth stations
[ETN-89-94297] N89-25374

GROUND WATER
Regelation and ice segregation N89-25807

GROUP THEORY
Note on the Majorana representations of the Lorentz group
[PREPRINT-597] N89-25662

GROWTH
Characterization of Spirulina biomass for CELSS diet potential
[NASA-CR-185329] N89-25561

GUN PROPELLANTS
Characterization of booster-rocket propellants and their simulants
[DE89-012497] N89-25352

GUNS (ORDNANCE)
Simple models for electric gun operating characteristics
[DE89-005348] N89-25253

GUST LOADS
Time-correlated gust loads using Matched-Filter Theory and Random-Process Theory: A new way of looking at things
[NASA-TM-101573] N89-25232

H

HADRONS
Neutron stars: A cosmic hadron physics laboratory
[NASA-CR-185051] N89-25777

HALL EFFECT
Theoretical studies of edge physics and plasma-wall interactions
[DE89-011792] N89-25710

HAMILTONIAN FUNCTIONS
Phase space concepts
[DE89-011082] N89-25667

HANDBOOKS
FAA statistical handbook of aviation: Calendar year 1987
[AD-A200917] N89-25113

HARDNESS
Weldability and weld doping of commercial purity molybdenum
[DE89-009535] N89-25311
Determination of the mechanical properties of diamond and diamond-like films by the ultra-low load indentation technique
[DE89-011569] N89-25471

HARMONICS
Optimum design of structures subject to general periodic loads N89-25215

HEAD-UP DISPLAYS
The man-machine-interface in a fast jet
[ETN-89-94327] N89-25574

HEAT ACCLIMATIZATION
Acclimatization to heat in humans
[NASA-TM-101011] N89-25558

HEAT AFFECTED ZONE
Cavitation kinetics during GTA (Gas Tungsten Arc) welding of helium containing stainless steel
[DE89-012514] N89-25467

HEAT EXCHANGERS
On the stress problem of the pebble bed heat exchanger in a hypersonic wind tunnel
[NAL-TM-ST-8705] N89-25240
The development of a vapor compression refrigeration system for a network of nine temperature test chambers
[DE89-007084] N89-25355
Advanced binary geothermal power plants working fluid property determination and heat exchanger design
[DE89-011144] N89-25513

HEAT PIPES
Analysis of the transient compressible vapor flow in heat pipe
[NASA-CR-185119] N89-25422

HEAT PUMPS
Evaluation of auxiliary power subsystems for gas engine heat pumps, phase 2
[PB89-173694] N89-25411
Advanced working fluid properties in heat pump and absorption cooling operations
[PB89-178172] N89-25413
Combined vapor compression/absorption heat pump cycles for engine-driven heat pumps
[PB89-145437] N89-25505

HEAT RADIATORS
Survivable pulse power space radiator
[DE89-010120] N89-25264
Scaling results for the Liquid Sheet Radiator (LSR)
[NASA-TM-102100] N89-25277

HEAT SOURCES
Method of production H2 using a rotating drum reactor with a pulse jet heat source
[DE89-009764] N89-25348

HEAT TOLERANCE
Acclimatization to heat in humans
[NASA-TM-101011] N89-25558

HEAT TRANSFER
On the stress problem of the pebble bed heat exchanger in a hypersonic wind tunnel
[NAL-TM-ST-8705] N89-25240
Unsteady stagnation-point heat transfer during passage of a concentrated vortex
[NASA-CR-182297] N89-25404
An experimental study of two-phase natural circulation in an adiabatic flow loop
[DE89-009650] N89-25406
Modeling the effect of surface active elements on weld pool fluid flow, heat transfer and geometry
[DE89-012504] N89-25466
Operational experience of the OC-OTEC experiments at NELH
[DE89-000877] N89-25510
Reduce uncertainty in projection of future sea-level change due to ice wastage
[DE89-011483] N89-25526
Parallel solutions of a 2-D phase change problem on a hypercube
[DE89-012886] N89-25602

HEAT TRANSMISSION
Energy from the Earth: Geothermal Energy Program. Five year research plan, 1988-1992
[DE89-010060] N89-25507

HEAT TREATMENT
Effects of auxiliary heat treatments on flame-cutting procedures
[DE89-011827] N89-25472

HEATING EQUIPMENT
On the stress problem of the pebble bed heat exchanger in a hypersonic wind tunnel
[NAL-TM-ST-8705] N89-25240

HELICAL WINDINGS
Investigations of modular nonplanar coil systems for the stellarator fusion reactor
[IPP-2/298] N89-25714

HELICOPTER TAIL ROTORS
Mechanical reaction of wings moving through a vortex region N89-25139

HELICOPTERS
Structural loading and noise disturbance of helicopters N89-25140
An initiative in multidisciplinary optimization of rotorcraft N89-25151
Structural optimization of rotor blades with straight and swept tips subject to aeroelastic constraints N89-25152
Optimization of rotor blades for combined structural, performance, and aeroelastic characteristics N89-25153
Transonic airfoil design for helicopter rotor applications N89-25154
Efficient sensitivity analysis and optimization of a helicopter rotor N89-25155
Structural optimization of rotor blades with integrated dynamics and aerodynamics N89-25156
Computerized Design Synthesis (CDS), A database-driven multidisciplinary design tool N89-25180
Plan, formulate, discuss and correlate a NASTRAN finite element vibrations model of the Boeing Model 360 helicopter airframe
[NASA-CR-181767] N89-25480

HELIOSEISMOLOGY
Seismology of the Sun and Sun-Like Stars
[ESA-SP-286] N89-25819
Dynamics of the overshoot layers and boundary conditions in helioseismology N89-25826
Solar internal rotation from helioseismology N89-25829
Angular momentum transport and dynamo action in the Sun: A report on implications of a recent helioseismic estimate of solar rotation N89-25837
Solar p-mode frequency splittings N89-25840
The current status of the Birmingham solar seismology network N89-25844
I.R.I.S.: A network for full disk helioseismology N89-25845
An attempt to understand the Stanford p-mode data — solar oscillations N89-25853
The GONG instrument — solar oscillations N89-25854
The GONG site survey — solar oscillations N89-25855
The GONG data reduction and analysis system — solar oscillations N89-25856
The stable solar analyzer N89-25858
Measurements of solar oscillations at 37 GHz N89-25859
Visibility of nonradial pulsation modes in solar continuum intensity measurements N89-25860
The granulation sensitivity of helioseismology lines N89-25862
Helioseismology from the South Pole: Comparison of 1987 and 1981 results N89-25868
Evidence for a thin perturbative layer near the base of the solar convection zone N89-25876
IPHIR: The helioseismology experiment on the PHOBOS mission N89-25881
The GOLF helioseismometer on board SOHO N89-25883
VIRGO: The solar monitor experiment on SOHO N89-25884
The search for solar gravity modes N89-25894
GOLF: Simulations of the re-emission of the resonance cell N89-25895
Study of solar structure based on p-mode helioseismology N89-25896
Current options for the equation of state of the solar interior N89-25897
Helioseismological inverse problem: Sound speed in the solar interior N89-25901
Helioseismological inverse problem: Diagnostics of the structure of the lower solar atmosphere N89-25903
An inversion method based on the Moore-Penrose generalized inverse matrix N89-25910
Determination of the solar sound speed by an asymptotic inversion technique N89-25913
Observed p-mode spectra of Ap stars and the Sun N89-25915
Solar oscillations instrumentation and measurement theory N89-25925
Effects of convective velocities on solar pressure mode frequencies N89-25941

HELIUM
Influence of the helium on high temperature embrittlement of metals under cyclic loading
[JUEL-2229] N89-25330
Cavitation kinetics during GTA (Gas Tungsten Arc) welding of helium containing stainless steel
[DE89-012514] N89-25467
Welding of helium-doped austenitic and ferritic stainless steels
[DE89-012523] N89-25468
Simulation of the welding of irradiated materials
[DE89-012524] N89-25469
Nonlinear studies of solar gravity modes driven by nuclear burning of He3 in the core N89-25823
Further progress on the helium abundance determination — Sun N89-25906

HELIUM ISOTOPES
Experimental investigation on transcritical heat transfer in He 2
[MPIS-MITT-90] N89-25426

HERMES MANNED SPACEPLANE
SIMOUN: Test system for shuttle thermal protection materials
[REPT-882-430-101] N89-25256

HERMITIAN POLYNOMIAL
Fast polar decomposition of an arbitrary matrix
[NASA-CR-185412] N89-25653

HETEROCYCLIC COMPOUNDS
Seconday ion mass spectrometry of aromatic compounds in acidic mixtures
[DE89-010611] N89-25305

HETEROJUNCTIONS
Kinetic effects of strong localization in planar heterostructures p-Ge/i-GaAs
[DE88-706205] N89-25739

HEURISTIC METHODS
Engineering applications of heuristic multilevel optimization methods N89-25202

HIERARCHIES
A decision-based perspective for the design of methods for systems design N89-25208
Hierarchies for computer-integrated manufacturing: A functional description
[PB89-172613] N89-25596

HIGH ASPECT RATIO
Optimum design of swept-forward high-aspect-ration graphite-epoxy wings N89-25172

HIGH CURRENT
Plasma switches for high current and fast time scale operation
[DE89-010557] N89-25704

HIGH ELECTRON MOBILITY TRANSISTORS
HEMTS: Fundamental investigations
[ETN-89-94630] N89-25399

HIGH ENERGY INTERACTIONS
International Centre for Theoretical Physics: Scientific activities in 1987
[DE88-705973] N89-25668
Report of the HEPAP (High Energy Physics Advisory Panel) Subpanel on High Energy Physics and the SSC (Superconducting Super Collider) over the next decade
[DE89-010071] N89-25686

HIGH FREQUENCIES
HEMTS: Fundamental investigations
[ETN-89-94630] N89-25399

HIGH LEVEL LANGUAGES
The Sizing and Optimization Language (SOL): A computer language to improve the user/optimizer interface N89-25178

HIGH POWER LASERS
A 2 J high-power excimer laser at high pulse repetition rate
[UI9-414/87/029] N89-25457

HIGH PRESSURE
Study on thermodynamical and mechanical conditions for pumping low flow rates of liquefied gases to high pressure level
[DFVLR-FB-88-54] N89-25429

HIGH SPEED CAMERAS
Design and testing of the EG and G/Los Alamos Operations fast streak camera
[DE89-010659] N89-25445

HIGH TEMPERATURE
Influence of the helium on high temperature embrittlement of metals under cyclic loading
[JUEL-2229] N89-25330
Advanced high-temperature batteries
[DE89-010698] N89-25390
Reference electrode for electrolytic cell
[DE89-011446] N89-25394
X-ray based extensometry
[NASA-CR-185058] N89-25432

HIGH TEMPERATURE PLASMAS
Measurement of H and H2 populations in-situ in a low-temperature plasma by vacuum-ultraviolet laser-absorption spectroscopy
[DE89-010433] N89-25308

HIGH TEMPERATURE SUPERCONDUCTORS
Preparation and properties of high-temperature superconductors in the Y-Ba-Cu-O system
[DE88-706050] N89-25735
Influence of the preparation conditions on the diamagnetic response of high-Tc YBa2Cu3Ox superconductor
[DE88-706051] N89-25736
Electronic structure of high temperature superconductors
[DE89-008610] N89-25741
The formation and analysis of thin film high temperature superconductors
[DE89-011177] N89-25745
Single crystal NMR studies of high temperature superconductors
[DE89-011220] N89-25747
Processing chemically prepared Tl-Ca-Ba-Cu oxide superconductors
[DE89-011535] N89-25748
Production of wires and coils from high-temperature superconducting materials
[DE89-012380] N89-25756

HIGH VOLTAGES
Controller for stabilization of high voltage
[NAL-TM-MT-8702] N89-25382

HILBERT SPACE
Imbedding of the gravitational field into the space of affine connection without torsion
[DE88-704637] N89-25536

HISTORIES
Where no man has gone before: A history of Apollo lunar exploration missions
[NASA-SP-4214] N89-25946

HOLES (MECHANICS)
Structural testing of metal/composite conical structures with holes
[DE89-011451] N89-25487

HOLOGRAPHY
Diffraction gratings used in X-ray spectroscopy
[DE89-012327] N89-25310
Optical information processing and holography
[DE88-706011] N89-25434

HOMOTROPY
Multiplier-continuation algorithms for constrained optimization N89-25218

HOOP COLUMN ANTENNAS
Antenna surface contour control system
[NASA-CASE-LAR-13798-1] N89-25363

HORIZONTAL FLIGHT
Flap-lag stability data for a small-scale isolated hingeless rotor in forward flight
[NASA-TM-102189] N89-25479

HORN ANTENNAS
Pyramidal horns: Part 1: Simple expressions for directivity as a function of aperture phase error
[DE89-005209] N89-25370
Pyramidal horns: Part 2: A novel design method for horns of any desired gain and aperture phase error
[DE89-005346] N89-25371

HORNS
Pyramidal horns: Part 1: Simple expressions for directivity as a function of aperture phase error
[DE89-005209] N89-25370
Pyramidal horns: Part 2: A novel design method for horns of any desired gain and aperture phase error
[DE89-005346] N89-25371

HOT CORROSION
Evaluation of ceramic coatings on silicon carbide
[DE89-010321] N89-25339

HOVERING
Flap-lag stability data for a small-scale isolated hingeless rotor in forward flight
[NASA-TM-102189] N89-25479

HUBS
Efficient sensitivity analysis and optimization of a helicopter rotor N89-25155

HUGONIOT EQUATION OF STATE
Characterization of booster-rocket propellants and their simulants
[DE89-012497] N89-25352

HUMAN BEHAVIOR
Applying understanding of individual behavior and team dynamics within the value engineering process
[DE89-011126] N89-25766

HUMAN FACTORS ENGINEERING
Review of the 1988 Workshop on Human-Machine Symbiotic Systems
[DE89-008743] N89-25570
Operator role definition and human system integration
[DE89-009621] N89-25571
The 1988 Workshop on Human-Machine Symbiotic Systems
[DE89-010170] N89-25572
Applying understanding of individual behavior and team dynamics within the value engineering process
[DE89-011126] N89-25766

HUMAN PERFORMANCE
The organization of perception and action in complex control skills
[NASA-CR-184638] N89-25568

HUMAN REACTIONS
Acclimatization to heat in humans
[NASA-TM-101011] N89-25558

HUMAN TOLERANCES
Acclimatization to heat in humans
[NASA-TM-101011] N89-25558

HUYGENS PRINCIPLE
A generalized antenna theorem for broadband pulses
[DE89-009707] N89-25373

HYBRID PROPULSION
Advanced Dual-Shaft Electric Propulsion System Technology Development Program
[DE89-010008] N89-25388

HYBRID STRUCTURES
Pactruss support structure for precision segmented reflectors
[NASA-CR-181747] N89-25484

HYDRAULIC JETS
Warm fog dissipation using large volume water sprays
[NASA-CASE-MFS-25962-1] N89-25242

HYDROCARBONS
Whisker shaped carbon substance
[DE89-010214] N89-25288

HYDRODYNAMIC EQUATIONS
Periodic and solitary waves on thin, horizontal, gas-sheared liquid films
[DE89-010655] N89-25416

HYDRODYNAMICS
Shock waves and fragmentation via molecular dynamics
[DE89-007981] N89-25405
Proceedings of the Solids Transport Contractors' Review Meeting
[DE89-006720] N89-25414
On the k-mechanism and the multidimensional Eddington approximation N89-25821

HYDROGEN
Measurement of H and H2 populations in-situ in a low-temperature plasma by vacuum-ultraviolet laser-absorption spectroscopy
[DE89-010433] N89-25308

HYDROGEN OXYGEN ENGINES
Advanced APS impacts on vehicle payloads
[NASA-TM-102086] N89-25254

HYDROGEN PRODUCTION
Method of production H2 using a rotating drum reactor with a pulse jet heat source
[DE89-009764] N89-25348

HYDROLOGICAL CYCLE
MECA Workshop on Atmospheric H2O Observations of Earth and Mars. Physical Processes, Measurements and Interpretations
[NASA-CR-183335] N89-25790
Transport of Mars atmospheric water into high northern latitudes during a polar warming N89-25792
The effect of global-scale divergent circulation on the atmospheric water vapor transport and maintenance N89-25793
The interpretation of data from the Viking Mars Atmospheric Water Detectors (MAWD): Some points for discussion N89-25795
Cumulus convection and the terrestrial water-vapor distribution N89-25798
Possible significance of cubic water-ice, H2O-Ic, in the atmospheric water cycle of Mars N89-25799
The behavior of water vapor in the Mars atmosphere N89-25801
Circumpolar hoods and clouds and their relation to the Martian H2O cycle N89-25803
Diurnal and annual cycles of H2O in the Martian regolith N89-25809
The interannual variability of atmospheric water vapor on Mars N89-25813
The Martian atmospheric water cycle as viewed from a terrestrial perspective N89-25814

HYDROTHERMAL SYSTEMS
An organized effort to develop the hydrothermal energy resource
[DE89-011139] N89-25512

HYDROXYL RADICALS
Photodissociation of pernitric acid (HO2NO2) at 248 nm
[NASA-CR-185363] N89-25286

HYPERBOLIC FUNCTIONS
A class of high resolution explicit and implicit shock-capturing methods
[NASA-TM-101088] N89-25652

HYPERCUBE MULTIPROCESSORS
A global time reference for hypercube multicomputers
[DE89-010924] N89-25579
Parallel solution of a 2-D phase change problem on a hypercube
[DE89-009619] N89-25586
A tool to aid in mapping computational tasks to a hypercube
[DE89-010320] N89-25589
Concurrent multi-resolution image analysis
[DE89-010261] N89-25594
A parallel algorithm for switch-level timing simulation on a hypercube multiprocessor
[NASA-CR-185338] N89-25595
Parallel solutions of a 2-D phase change problem on a hypercube
[DE89-012886] N89-25602
Concurrent Image Processing Executive (CIPE)
[NASA-CR-185460] N89-25619
Parallel processors and nonlinear structural dynamics algorithms and software
[NASA-CR-185049] N89-25620
A site oriented supercomputer for theoretical physics: The Fermilab Advanced Computer Program Multi Array Processor System (ACMAPS)
[DE89-011090] N89-25631

HYPERONS
Physics of dense matter, neutron stars and supernova
[DE89-010673] N89-25784

HYPERSONIC BOUNDARY LAYER
On the Gortler vortex instability mechanism at hypersonic speeds
[NASA-CR-181844] N89-25123

HYPERSONIC FLIGHT
Hypersonic airbreathing vehicle conceptual design (focus on aero-space plane) N89-25210

HYPERSONIC VEHICLES
Finite element flow-thermal-structural analysis of aerodynamically heated leading edges N89-25198

HYPERSONIC WIND TUNNELS
On the stress problem of the pebble bed heat exchanger in a hypersonic wind tunnel
[NAL-TM-ST-8705] N89-25240

HYPERVELOCITY GUNS
Characterization of booster-rocket propellants and their simulants
[DE89-012497] N89-25352

HYPERVELOCITY IMPACT
Characterization of booster-rocket propellants and their simulants
[DE89-012497] N89-25352

I

ICE CLOUDS
Seasonal and diurnal variability of Mars water-ice clouds N89-25794
Circumpolar hoods and clouds and their relation to the Martian H2O cycle N89-25803
Very high elevation water ice clouds on Mars: Their morphology and temporal behavior N89-25804

ICE FORMATION
Possible significance of cubic water-ice, H2O-Ic, in the atmospheric water cycle of Mars N89-25799
Regelation and ice segregation N89-25807

IMAGE ANALYSIS
Estimating effective moduli of composites using quantitative image analysis
[DE89-012292] N89-25295
A review of computer aided interpretation technology for the evaluation of radiographs of aluminum welds
[NASA-CR-185066] N89-25312
Method and apparatus for sensor fusion
[NASA-CASE-MSC-21334-1] N89-25360
On a fast two-dimensional radar imaging process for rotating targets and an analysis of its image quality
[DFVLR-FB-88-51] N89-25376
Automated thermal mapping techniques using chromatic image analysis
[NASA-TM-101554] N89-25443
User's guide to image processing applications of the NOAA satellite HRPT/AVHRR data. Part 1: Introduction to the satellite system and its applications. Part 2: Processing and analysis of AVHRR imagery
[NASA-CR-180784] N89-25492
Concurrent spatio-temporal image analysis
[DE89-010260] N89-25593
Concurrent multi-resolution image analysis
[DE89-010261] N89-25594
A contour-oriented approach to digital shape analysis
[ISBN-9-09-002004-7] N89-25604

IMAGE PROCESSING
Estimating effective moduli of composites using quantitative image analysis
[DE89-012292] N89-25295
Laser diffraction methods for high temperature strain measurements
[DE89-008235] N89-25451
User's guide to image processing applications of the NOAA satellite HRPT/AVHRR data. Part 1: Introduction to the satellite system and its applications. Part 2: Processing and analysis of AVHRR imagery
[NASA-CR-180784] N89-25492
Investigations on satellite image and reference data for exploration-related tasks
[DFVLR-FB-88-46] N89-25498
Concurrent spatio-temporal image analysis
[DE89-010260] N89-25593
Concurrent multi-resolution image analysis
[DE89-010261] N89-25594
Segmentation of noisy images
[ETN-89-94299] N89-25605
Concurrent Image Processing Executive (CIPE)
[NASA-CR-185460] N89-25619

IMAGE RESOLUTION
Interpretation of Thematic Mapper data for the acquisition of land information N89-25502

IMAGING RADAR
User's guide to image processing applications of the NOAA satellite HRPT/AVHRR data. Part 1: Introduction to the satellite system and its applications. Part 2: Processing and analysis of AVHRR imagery
[NASA-CR-180784] N89-25492

IMAGING TECHNIQUES
Resistive Contrast Imaging applied to multilevel interconnection failure analysis
[DE89-011066] N89-25397
Atomic resolution microscopy
[DE89-009227] N89-25679
A detector of small gradients of transparency of the terrestrial atmosphere N89-25857
The Michelson Doppler imager for the solar oscillations imager program on SOHO N89-25892

IMMUNE SYSTEMS
Modeling the AIDS epidemic
[NASA-CR-185413] N89-25566

IMMUNOASSAY
Unraveling Photosystem 2
[DE89-010930] N89-25559

IMPACT DAMAGE
Vibration testing of impact-damaged composite laminates
[NASA-TM-4115] N89-25290

IMPURITIES
Z subeff measurements and low-Z impurity transport for NBI and ICRF heated plasma in JIPP T-IIU tokamak
[IPPJ-896] N89-25701

IN-FLIGHT MONITORING
In-flight measurement of propeller noise on the fuselage of an airplane
[NASA-TM-102285] N89-25675

INCENTIVES
Federal incentives for industrial modernization: Historical review and future opportunities
[NASA-TM-101785] N89-25764

INCOMPRESSIBLE FLOW
Stationary ideal MHD with incompressible mass flow and general symmetry N89-25732

INDENTATION
Determination of the mechanical properties of diamond and diamond-like films by the ultra-low load indentation technique
[DE89-011569] N89-25471

INDEPENDENT VARIABLES
ARMA (Autoregressive-Moving Average) modeling
[AD-A205308] N89-25649

INDEXES (DOCUMENTATION)
Aeronautical engineering: A continuing bibliography with indexes (supplement 239)
[NASA-SP-7037(239)] N89-25114
Aeronautical engineering: A continuing bibliography with indexes (supplement 240)
[NASA-SP-7037(240)] N89-25115
Earth resources: A continuing bibliography with indexes (issue 61)
[NASA-SP-7041(61)] N89-25493
Aerospace medicine and biology: A continuing bibliography with indexes (supplement 323)
[NASA-SP-7011(323)] N89-25563
Aerospace medicine and biology: A continuing bibliography with indexes (supplement 324)
[NASA-SP-7011(324)] N89-25565
Aerospace medicine and biology: A continuing bibliography with indexes (supplement 325)
[NASA-SP-7011(325)] N89-25567

INDUCTION HEATING
Model building for an ingot heating process: Physical modeling approach and identification approach
[EUT-88-E-196] N89-25331

INDUCTION MOTORS
Variable speed induction motor operation from a 20-kHz power bus
[NASA-TM-102061] N89-25271

INDUSTRIAL PLANTS
Federal incentives for industrial modernization: Historical review and future opportunities
[NASA-TM-101785] N89-25764

INELASTIC STRESS
Procedures for characterizing an alloy and predicting cyclic life with the total strain version of Strainrange Partitioning
[NASA-TM-4102] N89-25485

INFORMATION DISSEMINATION
Notice to Airmen (NOTAM) system operational concept
[DOT/FAA/CT-TN89/10] N89-25142

INFORMATION FLOW
The epsilon dataflow processor
[DE89-001679] N89-25577
Performance evaluation for data flow architectures: A summary of discussions from the Santa Fe workshop
[DE89-008023] N89-25624

INFORMATION MANAGEMENT
Bibliographic coupling among scientific papers in biological research specialties N89-25771

INFORMATION PROCESSING (BIOLOGY)
Synthetic organisms and self-designing systems
[NASA-CR-185324] N89-25639

INFORMATION RETRIEVAL
A theoretical framework and an instructional model for educating end-users of online bibliographic information retrieval systems: A research monograph N89-25769

INFORMATION SYSTEMS
Space station operations task force. Panel 2 report: Ground operations and support systems
[NASA-TM-101817] N89-25245
Design and construction of a computer system model for application development workloads
[DE89-010519] N89-25622
A theoretical framework and an instructional model for educating end-users of online bibliographic information retrieval systems: A research monograph N89-25769
Performance issues in management of the Space Station Information System
[NASA-CR-185409] N89-25773
An expert system to facilitate selecting a database management system
[DE89-012350] N89-25774

INFORMATION THEORY
Synthetic organisms and self-designing systems
[NASA-CR-185324] N89-25639
Prototyping management information systems application software: An empirical study of developers' perceptions N89-25770

INFRARED DETECTORS
Narrow bandgap semiconducting silicides: Intrinsic infrared detectors on a silicon chip
[NASA-CR-185372] N89-25746

INFRARED IMAGERY
The Nimbus 7 LIMS (Limb Infrared Monitor of the Stratosphere) water vapor measurements N89-25810

INFRARED LASERS
IR laser photochemistry
[DE88-706012] N89-25303
Report of the Workshop on Scientific Opportunities for Infrared Free-Electron Lasers, volume 2
[DE89-009106] N89-25452

INFRARED RADIATION
IR laser photochemistry
[DE88-706012] N89-25303
Report of the Workshop on Scientific Opportunities for Infrared Free-Electron Lasers, volume 2
[DE89-009106] N89-25452
Solar infrared intensity oscillations N89-25847

INFRARED RADIOMETERS
Determination of combustion gas temperatures by infrared radiometry in sooting and nonsooting flames
[NASA-TP-2900] N89-25409
Calibration of the visible and near-infrared channels of the NOAA-9 AVHRR using high-altitude aircraft measurements from August 1985 and October 1986
[NASA-TM-101063] N89-25496
The Nimbus 7 LIMS (Limb Infrared Monitor of the Stratosphere) water vapor measurements N89-25810

INFRARED SPECTRA
Report of the Workshop on Scientific Opportunities for Infrared Free-Electron Lasers, volume 2
[DE89-009106] N89-25452

INGOTS
Model building for an ingot heating process: Physical modeling approach and identification approach
[EUT-88-E-196] N89-25331

INHIBITORS
A program for the study of skeletal muscle catabolism following physical trauma
[AD-A206506] N89-25564

INITIATION
High explosives reaction model and its application to booster performance
[DE89-005459] N89-25351

INJECTION MOLDING
Processing of fiber-reinforced materials by injection molding
[ETN-89-94668] N89-25298

INJURIES
A program for the study of skeletal muscle catabolism following physical trauma
[AD-A206506] N89-25564

INLET FLOW
Gas-liquid flow in dividing Tee-junctions with a horizontal inlet and different branch orientations and diameters
[KFK-4399] N89-25427

INORGANIC COMPOUNDS
Climatic changes inferred fron analyses of lake-sediment cores, Walker Lake, Nevada
[DE89-010740] N89-25525

INSTALLING
Mission Operations and Data Systems Directorate's operational/development network (MODNET) at Goddard Space Flight Center
[NASA-CR-183426] N89-25763

INSTRUMENT ERRORS
Identification of error sources in shock data
[DE89-007655] N89-25440

INTEGRAL TRANSFORMATIONS
The tanh transformation for double integrals with singularities: A progressive rule
[MATHS-RES-203] N89-25658

INTEGRATED CIRCUITS
Stress-driven diffusive voiding of aluminum conductor lines
[DE89-009832] N89-25387
Resistive Contrast Imaging applied to multilevel interconnection failure analysis
[DE89-011066] N89-25397
Design and implementation of a module library to support the structural synthesis — silicon compiler for IC design
[EUT-88-E-187] N89-25616

INTEGRITY
Toward a proof of the existence of an integrity basis for the tensors in the enveloping algebra of su(3)
[DE88-706031] N89-25646

INTERFACES
Quantitative modeling of sensitization development in austenitic stainless steel
[DE89-011206] N89-25317

INTERFACIAL TENSION
Analytic theory for the determination of velocity and stability of bubbles in a Hele-Shaw cell. Part 1: Velocity selection
[NASA-CR-181836] N89-25665
Analytic theory for the selection of 2-D needle crystal at arbitrary Peclet number
[NASA-CR-181846] N89-25671
INTERFERENCE IMMUNITY
Reduction of interference by decorrelation and quantized feedback in the case of digital transmission on multi-pair symmetric cables
[FI-44-TB-110] N89-25375
INTERMETALLICS
Characterization of ceramics and intermetallics fabricated by self-propagating high-temperature synthesis
[NASA-TM-102004] N89-25285
The development of alloys based on Ni3Si
[DE89-010371] N89-25316
Intermetallic alloys: Deformation, mechanical and fracture behavior
[GKSS-88/E/53] N89-25327
INTERNAL COMBUSTION ENGINES
Multidimensional modeling of convective heat transfer with application to I.C. engines
[DE89-010651] N89-25415
Combined vapor compression/absorption heat pump cycles for engine-driven heat pumps
[PB89-145437] N89-25505
INTERNATIONAL COOPERATION
Space station operations task force. Panel 4 report: Management integration
[NASA-TM-101819] N89-25247
Integrated Services Digital Network: Overview and architectural concepts
[MEMO-INF-88-42] N89-25634
United States and Western Europe cooperation in planetary exploration
[NASA-CR-184941] N89-25776
INTERPLANETARY SPACE
Interplanetary Matter: Proceedings, volume 2
[DE88-706057] N89-25779
INTERPROCESSOR COMMUNICATION
Parallel processors and nonlinear structural dynamics algorithms and software
[NASA-CR-185049] N89-25620
Interprocess communications and application to physical numerical modeling
[DE89-011021] N89-25630
INTERSTELLAR CHEMISTRY
The ionization structure in shocks in interstellar molecular clouds N89-25726
INTERSTELLAR GAS
Ambipolar diffusion and core formation in molecular clouds N89-25782
INVESTMENT
Federal incentives for industrial modernization: Historical review and future opportunities
[NASA-TM-101785] N89-25764
INVISCID FLOW
Numerical analysis of supersonic flow through oscillating cascade sections by using a deforming grid
[NASA-TM-102053] N89-25119
Techniques for compressible flow calculations on multizone grids N89-25120
Unsteady stagnation-point heat transfer during passage of a concentrated vortex
[NASA-CR-182297] N89-25404
ION BEAMS
Applications of ion beam processes in tribology
[DE89-000614] N89-25470
ION CYCLOTRON RADIATION
Determination of fields near an ICRH antenna using a 3D magnetostatic Laplace formulation
[DE89-011571] N89-25366
Spectral shaping and phase control of a fast-wave current drive antenna array
[DE89-011567] N89-25368
Z subeff measurements and low-Z impurity transport for NBI and ICRF heated plasma in JIPP T-IIU tokamak
[IPPJ-896] N89-25701
Ion energy and plasma measurements in the near field of an ICRF antenna
[DE89-011611] N89-25708
ICRF Faraday shield plasma sheath physics: The Perkins paradigm
[DE89-012362] N89-25712
ION EMISSION
Secondary ion mass spectrometry of aromatic compounds in acidic mixtures
[DE89-010611] N89-25305
ION IMPACT
Ion heating in the Bug shock wave N89-25724
ION IMPLANTATION
The application of Rutherford backscattering and channeling techniques to the characterization of ceramics
[DE89-010257] N89-25333
The mechanical properties of ion implanted ceramics
[DE89-008928] N89-25337
ION SOURCES
Measurement of H and H2 populations in-situ in a low-temperature plasma by vacuum-ultraviolet laser-absorption spectroscopy
[DE89-010433] N89-25308
Ion optics of LIDIA mass-spectrometer
[DE88-706335] N89-25446
ION TEMPERATURE
Density fluctuations and particle/thermal transport for ohmically and auxiliarily heated plasmas in the JIPP T-IIU tokamak
[IPPJ-891] N89-25700
Anomalous particle pinch for collisionless plasma
[DE89-011018] N89-25706
IONIZATION
Temperature limit of a graphite divertor surface due to particle erosion
[DE89-010272] N89-25703
IONIZATION CROSS SECTIONS
Partial and state selective cross sections for multiple ionization of rare gas atoms by electron impact
[REPT-88-05-170] N89-25715
IONIZED GASES
The ionization structure in shocks in interstellar molecular clouds N89-25726
IONIZING RADIATION
Studies of oxidative degradation of polymers induced by ionizing radiation
[DE89-008279] N89-25335
IONOSPHERIC COMPOSITION
A study of non-linear ionization processes in planetary atmospheres N89-25816
IONOSPHERIC TEMPERATURE
Acceleration of ions in the magnetotail N89-25720
IRON ALLOYS
Dynamic fracture toughness measurements of ferritic ductile cast iron
[DE89-009833] N89-25324
IRRADIATION
Simulation of the welding of irradiated materials
[DE89-012524] N89-25469
ITERATION
Balancing a matrix for calculation of eigenvalues and eigenvectors
[DE88-706045] N89-25648
ARMA (Autoregressive-Moving Average) modeling
[AD-A205308] N89-25649
ITERATIVE SOLUTION
Iterative methods for design sensitivity analysis N89-25184
On conjugate gradient type methods and polynomial preconditioners for a class of complex non-Hermitian matrices
[NASA-CR-185424] N89-25654

J

J INTEGRAL
Evaluation of elastic-plastic surface flaw behavior and related parameters using surface displacement measurements
[DE89-011134] N89-25489
JET AIRCRAFT
Overview of Dynamics Integration Research (DIR) program at Langley Research Center N89-25150
Results of including geometric nonlinearities in an aeroelastic model of an F/A-18 N89-25190
Aeroelastic modeling for the FIT (Functional Integration Technology) team F/A-18 simulation N89-25192
An economic model for evaluating high-speed aircraft designs
[NASA-CR-177530] N89-25235
JOINTS (JUNCTIONS)
Gas-liquid flow in dividing Tee-junctions with a horizontal inlet and different branch orientations and diameters
[KFK-4399] N89-25427
Imbedding of the gravitational field into the space of affine connection without torsion
[DE88-704637] N89-25536
JOSEPHSON JUNCTIONS
Influence of the preparation conditions on the diamagnetic response of high-Tc YBa2Cu3Ox superconductor
[DE88-706051] N89-25736
Squid concepts and systems
[DE89-010384] N89-25755
JUDGMENTS
Correlation of subjective slipperiness judgements with quantitative COF (Coefficient Of Friction) measurements for structural steel
[PB89-165070] N89-25669
JUPITER (PLANET)
Oscillations of Jupiter as a tool for probing its internal structure N89-25924
JUPITER ATMOSPHERE
Oscillations of Jupiter as a tool for probing its internal structure N89-25924

K

K STARS
High precision velocity observations of Arcturus using the 7699 A line of potassium N89-25919
KERNEL FUNCTIONS
Inversion of the solar rotation rate versus depth and latitude N89-25838
KINEMATICS
A kinematic study of the MERLIN 6500 robot and the Utah/MIT dexterous hand and a simulation of their combined behavior
[AD-A203907] N89-25458
KNOWLEDGE
STRUTEX: A prototype knowledge-based system for initially configuring a structure to support point loads in two dimensions N89-25161
KNOWLEDGE BASES (ARTIFICIAL INTELLIGENCE)
The 1988 Workshop on Human-Machine Symbiotic Systems
[DE89-010170] N89-25572
Use of metaknowledge in the verification of knowledge-based systems
[NASA-CR-181821] N89-25627
Explanation in knowledge-based systems
[MEMO-INF-88-17] N89-25640
The use of first principles in diagnosing complex technical devices
[MEMO-INF-88-40] N89-25641
KNOWLEDGE REPRESENTATION
Explanation in knowledge-based systems
[MEMO-INF-88-17] N89-25640

L

L-SAT
A multifrequency antenna system for propagation experiments with the Olympus satellite
[EUT-88-E-192] N89-25378
LAKES
Climatic changes inferred fron analyses of lake-sediment cores, Walker Lake, Nevada
[DE89-010740] N89-25525
LAMINAR FLOW
Numerical simulation of transition from laminar to turbulent channel flow
[DFVLR-FB-88-55] N89-25430
LAMINATES
Composite sizing and ply orientation for stiffness requirements using a large finite element structural model N89-25166
Involute composite design evaluation using global design sensitivity derivatives N89-25199
Characterization of the effects of three-dimensional states of stress on damping of laminated composites N89-25287
Vibration testing of impact-damaged composite laminates
[NASA-TM-4115] N89-25290
LAND ICE
Water in the Martian regolith N89-25791
Regelation and ice segregation N89-25807
LANTHANUM COMPOUNDS
Optical information storage in PLZT thin films
[DE89-011067] N89-25692
LARGE DEPLOYABLE REFLECTOR
Pactruss support structure for precision segmented reflectors
[NASA-CR-181747] N89-25484
LARGE SPACE STRUCTURES
Demonstration of decomposition and optimization in the design of experimental space systems N89-25160
Digital robust control law synthesis using constrained optimization N89-25193
Recent Advances in Multidisciplinary Analysis and Optimization, part 3
[NASA-CP-3031-PT-3] N89-25201
Optimal placement of excitations and sensors by simulated annealing N89-25227
Experiences in applying optimization techniques to configurations for the Control of Flexible Structures (COFS) program N89-25228

Antenna surface contour control system
[NASA-CASE-LAR-13798-1] N89-25363

LASER APPLICATIONS
Microwave pulse generation by photoconductive switching
[DE89-011631] N89-25393

LASER BEAMS
Measurement of the stimulated thermal Rayleigh scattering instability
[DE89-012324] N89-25453
Status of LBL/LLNL FEL (Free Electron Laser) research for two beam accelerator applications
[DE89-012487] N89-25455
Fiber optic sensing for NDE and process control
[DE89-010976] N89-25696

LASER FUSION
Microwave experimental studies of laser fusion
[DE89-012325] N89-25454

LASER INDUCED FLUORESCENCE
Development of laser-excited molecular luminescence spectrometric methods for polycyclic aromatic hydrocarbons in environmental sciences
[DE89-010616] N89-25306

LASER PLASMAS
Microwave experimental studies of laser fusion
[DE89-012325] N89-25454

LASER PUMPING
Fission reactor pumped lasers: History and prospects
[DE89-010329] N89-25456

LASER SPECTROMETERS
Development of laser-excited molecular luminescence spectrometric methods for polycyclic aromatic hydrocarbons in environmental sciences
[DE89-010616] N89-25306

LASER SPECTROSCOPY
Measurement of H and H2 populations in-situ in a low-temperature plasma by vacuum-ultraviolet laser-absorption spectroscopy
[DE89-010433] N89-25308

LASER WELDING
Modeling the effect of surface active elements on weld pool fluid flow, heat transfer and geometry
[DE89-012504] N89-25466

LASERS
Bistability in a laser with injected signal
[DE88-706003] N89-25449
Laser diffraction methods for high temperature strain measurements
[DE89-008235] N89-25451
The formation and analysis of thin film high temperature superconductors
[DE89-011177] N89-25745

LATE STARS
Solar-like oscillations in late spectral class stars
N89-25935

LATERAL CONTROL
Aeroservoelastic tailoring for lateral control enhancement N89-25189

LATERAL STABILITY
Flight-mechanical investigations of the lateral motion of configurations with winglets N89-25141

LATTICES (MATHEMATICS)
The Fermilab Lattice Supercomputer Project
[DE89-010510] N89-25578

LAUNCHERS
Advanced mass launchers for low earth orbit
[DE89-010759] N89-25255

LEAD COMPOUNDS
Optical information storage in PLZT thin films
[DE89-011067] N89-25692

LEADING EDGES
Finite element flow-thermal-structural analysis of aerodynamically heated leading edges N89-25198

LEARNING
Robust performance of multiple tasks by an autonomous robot
[DE89-008718] N89-25636

LEAST SQUARES METHOD
An interpretation and solution of ill-conditioned linear equations N89-25213
Least squares parameter estimation in a dynamic model from noisy observations
[ETN-89-94295] N89-25657
Inversion of the solar rotation rate versus depth and latitude N89-25838
An inversion method based on the Moore-Penrose generalized inverse matrix N89-25910

LIAPUNOV FUNCTIONS
Resolution of the Algebraic Riccati Equation via Newton's method and the Lyapunov Equation
[ESA-STM-241] N89-25660

LIE GROUPS
Degenerate representation from tensorial identities and quantum realisations of YBZF algebras
[DE88-706032] N89-25647
Program package for investigation of differential equations by the external form method
[DE88-706258] N89-25650
Strings on hyperelliptic supersurfaces
[DE88-705991] N89-25758

LIFE (DURABILITY)
SIMOUN: Test system for shuttle thermal protection materials
[REPT-882-430-101] N89-25256
A slow positron beam generator for lifetime studies
[NASA-TM-101590] N89-25433

LIFE CYCLE COSTS
Optimizing conceptual aircraft designs for minimum life cycle cost N89-25211
Size optimization and production strategy of lunar transport systems
[ILR-MITT-218] N89-25260

LIFE SCIENCES
USSR Space Life Sciences Digest. Index to issues 15-20
[NASA-CR-3922(25)] N89-25556

LIFT
Spanwise lift distributions and wake velocity surveys of a semi-span wing with a discontinuous twist
[NASA-CR-177532] N89-25122

LIFT DEVICES
Flap system for short takeoff and landing aircraft
[AD-D013981] N89-25234

LIFT DRAG RATIO
Effect of milling machine roughness and wing dihedral on the supersonic aerodynamic characteristics of a highly swept wing
[NASA-TP-2918] N89-25117

LIGHT (VISIBLE RADIATION)
Visible and near-infrared channel calibration of the GOES-6 VISSR using high-altitude aircraft measurements
[NASA-TM-101064] N89-25494
Calibration of the visible and near-infrared channels of the NOAA-9 AVHRR using high-altitude aircraft measurements from August 1985 and October 1986
[NASA-TM-101063] N89-25496
A courant condition free modified partially-implicit method. Revised electromagnetic particle Code PS2M for bounded plasmas with conducting walls
[IPPJ-892] N89-25699

LIGHT WATER REACTORS
An experimental study of two-phase natural circulation in an adiabatic flow loop
[DE89-009850] N89-25406

LIMB DARKENING
Periodical asymmetry of solar limb darkening
N89-25861

LIMITERS (FUSION REACTORS)
Theoretical studies of edge physics and plasma-wall interactions
[DE89-011792] N89-25710

LINE SPECTRA
On the diagnostic of 5m oscillations through photospheric line profiles N89-25822
The granulation sensitivity of helioseismology lines N89-25862
The search for solar-type oscillations in other stars using the Michelson Interferometric Stellar Oscillation Spectrometer (ISOS) N89-25918
High precision velocity observations of Arcturus using the 7699 A line of potassium N89-25919

LINEAR ACCELERATORS
Modular magnet current regulator
[CEBAF-PR-89-005] N89-25685
High-average-power millimeter-wave FEL (Free-Electron Laser) for plasma heating using the ETA-2 accelerator
[DE89-012294] N89-25711

LINEAR EQUATIONS
An interpretation and solution of ill-conditioned linear equations N89-25213

LINEAR PROGRAMMING
Procedures for shape optimization of gas turbine disks N89-25207
Polynomial method of approximate centers for linear programming
[PB89-146161] N89-25584

LINEAR QUADRATIC GAUSSIAN CONTROL
An analytical sensitivity method for use in integrated aeroservoelastic aircraft design
[NASA-TM-101583] N89-25239

LINEAR QUADRATIC REGULATOR
Flutter suppression using eigenspace freedoms to meet requirements N89-25191

LINEAR SYSTEMS
On conjugate gradient type methods and polynomial preconditioners for a class of complex non-Hermitian matrices
[NASA-CR-185424] N89-25654

LINES OF FORCE
Magnetic reconnection in general three-dimensional systems N89-25717

LININGS
Fuel properties effect on the performance of a small high temperature rise combustor
[NASA-TM-102096] N89-25238

LIQUEFIED GASES
Study on thermodynamical and mechanical conditions for pumping low flow rates of liquefied gases to high pressure level
[DFVLR-FB-88-54] N89-25429

LIQUID CRYSTALS
Super-strong self-reinforcing polymeric matrices formed by the first super-strong polymers
[DE89-011533] N89-25347
Automated thermal mapping techniques using chromatic image analysis
[NASA-TM-101554] N89-25443

LIQUID FLOW
Scaling results for the Liquid Sheet Radiator (LSR)
[NASA-TM-102100] N89-25277

LIQUID HELIUM
A qualitative numerical analysis of some features of propagation of counterflow temperature waves in superfluid helium
[MPIS-9/1988] N89-25424

LIQUID HELIUM 2
GIRL cryotechnics and preparation of a TEXUS experiment on superfluid helium dynamics
[ETN-89-94631] N89-25357

LIQUID METAL FAST BREEDER REACTORS
Effect of low neutron fluences on DIN 1.4948 steel creep properties --- liquid metal fast breeder reactor (LMFBR) material
[ECN-206] N89-25325

LIQUID SURFACES
Experiments on liquid-vapour phase change between plane liquid surfaces. Part 3: Results from a closed quartz chamber
[NAL-TM-FM-8809] N89-25301

LIQUID-GAS MIXTURES
Study of interfacial behavior in concurrent gas-liquid flows
[DE89-010484] N89-25408

LIQUID-LIQUID INTERFACES
Interfacial fluid mechanics and transport processes
[DE89-010664] N89-25417

LIQUID-VAPOR INTERFACES
Experiments on liquid-vapour phase change between plane liquid surfaces. Part 3: Results from a closed quartz chamber
[NAL-TM-FM-8809] N89-25301
Study of interfacial behavior in concurrent gas-liquid flows
[DE89-010484] N89-25408

LITERATURE
Bibliographic coupling among scientific papers in biological research specialties N89-25771

LITHIUM ALLOYS
The strength-toughness relationship at cryogenic temperatures in aluminum-lithium alloy plate
[DE89-011816] N89-25322
Cryogenic mechanical properties of low density superplastically formable Al-Li alloys
[DE89-010587] N89-25343

LITHOGRAPHY
Diffraction gratings used in X-ray spectroscopy
[DE89-012327] N89-25310
Submicron technologies for the fabrication of monolithic integrated millimeter wave devices on high resistivity silicon
[ETN-89-94624] N89-25757

LOAD DISTRIBUTION (FORCES)
On the stress problem of the pebble bed heat exchanger in a hypersonic wind tunnel
[NAL-TM-ST-8705] N89-25240

LOAD TESTS
Structural testing of metal/composite conical structures with holes
[DE89-011451] N89-25487

LOADS (FORCES)
Multi-objective/loading optimization for rotating composite flexbeams N89-25157
Optimum design of structures subject to general periodic loads N89-25215
An analytical and experimental investigation of edge delamination in laminates subjected to tension, bending, and torsion
[NASA-CR-181824] N89-25296
Identification of distributed forces on a structure
[DE89-007978] N89-25482

LOCAL AREA NETWORKS
Mission Operations and Data Systems Directorate's operational/development network (MODNET) at Goddard Space Flight Center
[NASA-CR-183426] N89-25763
LOCUSTS
FAO detailed rain mapping experiment
[BCRS-88-11] N89-25552
FAO detailed rain mapping experiment phase A: Meteosat based rainfall mapping in the Sahel region N89-25553
LOGIC DESIGN
The full decomposition of sequential machines with the state and output behavior realization
[EUT-88-E-188] N89-25582
LOGISTICS
Space station operations task force. Panel 2 report: Ground operations and support systems
[NASA-TM-101817] N89-25245
LOOP ANTENNAS
Ion energy and plasma measurements in the near field of an ICRF antenna
[DE89-011611] N89-25708
LORENTZ TRANSFORMATIONS
Note on the Majorana representations of the Lorentz group
[PREPRINT-597] N89-25662
LOW DENSITY MATERIALS
Low density microcellular carbon foams and method of preparation
[DE89-010966] N89-25345
LOW LEVEL TURBULENCE
Mesoscale model parameterizations for radiation and turbulent fluxes at the lower boundary
[DFVLR-FB-88-48] N89-25544
LUBRICATION
Applications of ion beam processes in tribology
[DE89-000614] N89-25470
LUNAR EXPLORATION
Where no man has gone before: A history of Apollo lunar exploration missions
[NASA-SP-4214] N89-25946
LUNAR SURFACE VEHICLES
Size optimization and production strategy of lunar transport systems
[ILR-MITT-218] N89-25260

M

MAGNETIC CIRCUITS
Controller for stabilization of high voltage
[NAL-TM-MT-8702] N89-25382
MAGNETIC COILS
Elements of a specification for superconducting cable and why they are important for magnet construction
[DE89-012533] N89-25754
MAGNETIC DIPOLES
Elements of a specification for superconducting cable and why they are important for magnet construction
[DE89-012533] N89-25754
MAGNETIC DISTURBANCES
The influence of the toroidal roll pattern on the sunspot activity N89-25870
MAGNETIC EFFECTS
Magnetically induced spectral line redshifts full disk measurements N89-25877
MAGNETIC FIELD CONFIGURATIONS
Determination of fields near an ICRH antenna using a 3D magnetostatic Laplace formulation
[DE89-011571] N89-25366
Confinement improvement of low-aspect-ratio torsatrons
[DE89-010192] N89-25702
The q measurements during sawtooth oscillations in a low q tokamak
[DE89-010563] N89-25705
Orientation, motion, and other properties of FTE structures on September 4, 1984 N89-25718
MAGNETIC FIELD RECONNECTION
Magnetic reconnection in general three-dimensional systems N89-25717
Particle simulation of magnetic reconnection N89-25722
MAGNETIC FIELDS
Application of theta functions for numerical evaluation of complete elliptic integrals of the first and second kinds
[DE89-010191] N89-25645
Beam transport calculation in magnetic field with a quadrupole symmetry by the method of immersion in moment phase space
[DE88-706295] N89-25681
Modular magnet current regulator
[CEBAF-PR-89-005] N89-25685
Cosmic plasma physics
[MPE-211] N89-25716
On the formation of current-sheets in ideal MHD N89-25728
Solar-geophysical data number 528, August 1988. Part 1: (Prompt reports). Data for July, June 1988 and late data
[PB89-109904] N89-25817
MAGNETIC FLUX
Magnetic reconnection in general three-dimensional systems N89-25717
Orientation, motion, and other properties of FTE structures on September 4, 1984 N89-25718
On the radiative damping of p-modes in solar magnetic flux concentrations N89-25864
MAGNETIC INDUCTION
Magneto-inductive skin sensor for robot collision avoidance: A new development
[NASA-CR-185402] N89-25444
MAGNETIC MEASUREMENT
Acceleration of ions in the magnetotail N89-25720
MAGNETIC PROPERTIES
Preparation and properties of high-temperature superconductors in the Y-Ba-Cu-O system
[DE88-706050] N89-25735
Electronic structure of high temperature superconductors
[DE89-008610] N89-25741
MAGNETIC SHIELDING
ICRF Faraday shield plasma sheath physics: The Perkins paradigm
[DE89-012362] N89-25712
MAGNETIC SIGNATURES
Acquisition and reduction procedures for MOF Doppler-magnetograms — solar observation N89-25851
MAGNETIC STARS
Ripple structure in degenerate electron gas-dominated stars with intense magnetic fields N89-25783
MAGNETIC SWITCHING
Magnetic switching
[DE89-012299] N89-25398
MAGNETO-OPTICS
Integrated solar disk oscillation measurements using the magneto-optical filter: Tests with a two station network N89-25850
Acquisition and reduction procedures for MOF Doppler-magnetograms — solar observation N89-25851
MAGNETOHYDRODYNAMIC FLOW
Hybrid plume plasma rocket
[NASA-CASE-MSC-20476-2] N89-25279
Cosmic plasma physics
[MPE-211] N89-25716
Stationary ideal MHD with incompressible mass flow and general symmetry N89-25732
MAGNETOHYDRODYNAMIC STABILITY
Wave emissions from planetary magnetospheres
[NASA-CR-185435] N89-25541
Averaged equilibrium and stability in low-aspect-ratio stellarators
[DE89-013618] N89-25713
Nonlocal analyses of finite-beam-driven instabilities N89-25721
Particle simulation of magnetic reconnection N89-25722
On the formation of current-sheets in ideal MHD N89-25728
Evidence for a thin perturbative layer near the base of the solar convection zone N89-25876
MAGNETOHYDRODYNAMIC WAVES
On the dissipation of Alfven waves in magnetic atmospheres and flux tubes N89-25871
Viscous magnetohydrodynamic modes and p-mode absorption by sunspots N89-25873
MAGNETOPAUSE
Three dimensional computations of the dynamics of the magnetopause: First results N89-25719
MAGNETOSPHERES
Models for axially symmetric pulsar magnetospheres N89-25730
MAGNETOSPHERIC INSTABILITY
Particle simulation of magnetic reconnection N89-25722
MAGNETOSTATIC FIELDS
Modeling of magnetic devices with finite-element methods
[DE89-010525] N89-25576
MAGNETS
Amplitude growth due to random, correlated kicks
[DE89-011504] N89-25418
Modeling of magnetic devices with finite-element methods
[DE89-010525] N89-25576
MAIN SEQUENCE STARS
The influence of the equation of state on the zero-age main sequence and the Sun N89-25939
MAINTENANCE
Mission Operations and Data Systems Directorate's operational/development network (MODNET) at Goddard Space Flight Center
[NASA-CR-183426] N89-25763
MAMMALS
Spiral vane bioreactor
[NASA-CASE-MSC-21361-1] N89-25557
MAN MACHINE SYSTEMS
Review of the 1988 Workshop on Human-Machine Symbiotic Systems
[DE89-008743] N89-25570
Operator role definition and human system integration
[DE89-009621] N89-25571
The 1988 Workshop on Human-Machine Symbiotic Systems
[DE89-010170] N89-25572
The man-machine-interface in a fast jet
[ETN-89-94327] N89-25574
MAN-COMPUTER INTERFACE
Integrated Services Digital Network: Overview and architectural concepts
[MEMO-INF-88-42] N89-25634
MANAGEMENT
Space station operations task force. Panel 4 report: Management integration
[NASA-TM-101819] N89-25247
MANAGEMENT INFORMATION SYSTEMS
Prototyping management information systems application software: An empirical study of developers' perceptions N89-25770
MANAGEMENT METHODS
Systems approach to project management
[DE89-008741] N89-25765
MANAGEMENT SYSTEMS
Performance issues in management of the Space Station Information System
[NASA-CR-185409] N89-25773
MANIFOLDS (MATHEMATICS)
Phase space concepts
[DE89-011082] N89-25667
MANIPULATORS
Analysis and control of a three-degree-of-freedom robot platform
[DE89-006427] N89-25356
A kinematic study of the MERLIN 6500 robot and the Utah/MIT dexterous hand and a simulation of their combined behavior
[AD-A203907] N89-25458
Modifying a telerobotic system to include robotic operation by means of dynamic modeling
[DE89-003119] N89-25460
Design of a dual forearm modular robot
[DE89-010453] N89-25462
Robust performance of multiple tasks by an autonomous robot
[DE89-008718] N89-25636
MANNED SPACE FLIGHT
Where no man has gone before: A history of Apollo lunar exploration missions
[NASA-SP-4214] N89-25946
MANY BODY PROBLEM
Local field effects in the many-body perturbation theory and in the density functional theory
[DE88-705975] N89-25734
MAPS
Modeling land-surface albedos from plant canopy architecture N89-25495
MARKETING
Space station operations task force. Panel 3 report: User development and integration
[NASA-TM-101818] N89-25246
MARS ATMOSPHERE
MECA Workshop on Atmospheric H2O Observations of Earth and Mars. Physical Processes, Measurements and Interpretations
[NASA-CR-183335] N89-25790
Transport of Mars atmospheric water into high northern latitudes during a polar warming N89-25792
Seasonal and diurnal variability of Mars water-ice clouds N89-25794
The interpretation of data from the Viking Mars Atmospheric Water Detectors (MAWD): Some points for discussion N89-25795
Regolith water vapor sources on Mars: A historical bibliography N89-25796
Factors governing water condensation in the Martian atmosphere N89-25797
Possible significance of cubic water-ice, H2O-Ic, in the atmospheric water cycle of Mars N89-25799
On the vertical distribution of water vapor in the Martian tropics N89-25800

The behavior of water vapor in the Mars atmosphere N89-25801
Circumpolar hoods and clouds and their relation to the Martian H2O cycle N89-25803
Very high elevation water ice clouds on Mars: Their morphology and temporal behavior N89-25804
Regelation and ice segregation N89-25807
Measurements of the vertical profile of water vapor abundance in the Martian atmosphere from Mars Observer N89-25811
Atmospheric H2O and the search for Martian brines N89-25812
The interannual variability of atmospheric water vapor on Mars N89-25813
The Martian atmospheric water cycle as viewed from a terrestrial perspective N89-25814

MARS SURFACE
MECA Workshop on Atmospheric H2O Observations of Earth and Mars. Physical Processes, Measurements and Interpretations
[NASA-CR-183335] N89-25790
Water in the Martian regolith N89-25791
Regolith water vapor sources on Mars: A historical bibliography N89-25796
Diurnal and annual cycles of H2O in the Martian regolith N89-25809
Atmospheric H2O and the search for Martian brines N89-25812

MASS SPECTRA
Seconday ion mass spectrometry of aromatic compounds in acidic mixtures
[DE89-010611] N89-25305

MASS SPECTROMETERS
Seconday ion mass spectrometry of aromatic compounds in acidic mixtures
[DE89-010611] N89-25305
Ion optics of LIDIA mass-spectrometer
[DE88-706335] N89-25446

MASS TRANSFER
Detection of metal-transfer mode in GMAW
[DE89-011133] N89-25465
Operational experience of the OC-OTEC experiments at NELH
[DE89-000877] N89-25510

MASSIVELY PARALLEL PROCESSORS
Parallel processors and nonlinear structural dynamics algorithms and software
[NASA-CR-185049] N89-25620
Speeding up parallel processing
[NASA-CR-184646] N89-25628
Feasibility of using the Massively Parallel Processor for large eddy simulations and other Computational Fluid Dynamics applications
[NASA-CR-185427] N89-25629

MATCHED FILTERS
Time-correlated gust loads using Matched-Filter Theory and Random-Process Theory: A new way of looking at things
[NASA-TM-101573] N89-25232

MATHEMATICAL LOGIC
A parallel processing approach for implementing high-performance first-order logic deduction systems
[DE89-011878] N89-25632

MATHEMATICAL MODELS
Generalized mathematical models in design optimization N89-25214
Structural optimization and recent large ground antenna installations N89-25224
Simple models for electric gun operating characteristics
[DE89-005348] N89-25253
Flight performance model for a geostationary transportation system
[ILR-MITT-206] N89-25259
Size optimization and production strategy of lunar transport systems
[ILR-MITT-218] N89-25260
An analytical and experimental investigation of edge delamination in laminates subjected to tension, bending, and torsion
[NASA-CR-181824] N89-25296
A predictive model for failure properties of thermoset resins
[NASA-TM-4128] N89-25300
Quantitative modeling of sensitization development in austenitic stainless steel
[DE89-011206] N89-25317
Model building for an ingot heating process: Physical modeling approach and identification approach
[EUT-88-E-196] N89-25331
Parameter estimation for a viscoelastic constitutive model
[DE89-008714] N89-25336
High explosives reaction model and its application to booster performance
[DE89-005459] N89-25351
Time-dependent computational studies of flames in microgravity
[NASA-CR-182298] N89-25353
Time domain modeling of electromagnetic coupling
[DE89-010240] N89-25362
Microwave scattering models and basic experiments
[NASA-CR-185393] N89-25364
Numerical modeling of monopoles on radial-wire ground screens
[DE89-005350] N89-25372
Radiative heat transfer
[PB89-173637] N89-25412
Multidimensional modeling of convective heat transfer with application to I.C. engines
[DE89-010651] N89-25415
Interfacial fluid mechanics and transport processes
[DE89-010664] N89-25417
Comparison of experimental shock-wave profiles for tungsten and computer simulations using a rate-dependent constitutive model
[DE89-006158] N89-25419
Analysis of the transient compressible vapor flow in heat pipe
[NASA-CR-185119] N89-25422
Influence of rubbing on rotor dynamics, part 1
[NASA-CR-183648-PT-1] N89-25463
A theory of describing performability models
[MEMO-INF-88-26] N89-25476
Plan, formulate, discuss and correlate a NASTRAN finite element vibrations model of the Boeing Model 360 helicopter airframe
[NASA-CR-181787] N89-25480
Advanced methods for 3-D inelastic structural analysis for hot engine structures
[NASA-TM-102106] N89-25490
Reduce uncertainty in projection of future sea-level change due to ice wastage
[DE89-011483] N89-25526
Climate projections with regional resolution
[DE89-009261] N89-25529
Geologic spatial analysis program users guide for digital elevation model analysis procedures for detection of crustal fracture planes
[DE89-010880] N89-25542
Modeling the AIDS epidemic
[NASA-CR-185413] N89-25566
Adaptive enhancement of magnetoencephalographic signals via multichannel filtering
[DE89-005464] N89-25569
Modeling of magnetic devices with finite-element methods
[DE89-010525] N89-25576
Interprocess communications and application to physical numerical modeling
[DE89-011021] N89-25630
Toward a proof of the existence of an integrity basis for the tensors in the enveloping algebra of su(3)
[DE88-706031] N89-25646
A net-based model for time-dependent systems
[REPT-89-005] N89-25661
Acoustic propagation in curved ducts with extended reacting wall treatment
[NASA-TM-102110] N89-25670
Analytic theory for the selection of 2-D needle crystal at arbitrary Peclet number
[NASA-CR-181846] N89-25671
Optical fiber sensors and signal processing for intelligent structure monitoring
[NASA-CR-185395] N89-25691
Temperature limit of a graphite divertor surface due to particle erosion
[DE89-010272] N89-25703

MATHEMATICAL PROGRAMMING
The Sizing and Optimization Language (SOL): A computer language to improve the user/optimizer interface N89-25178
Robust computer-aided synthesis and optimization of linear multivariable control systems with varying plant dynamics via AUTOCON N89-25179
On optimal fail-safe design of structures N89-25486
Speeding up parallel processing
[NASA-CR-184646] N89-25628

MATRICES (MATHEMATICS)
An interpretation and solution of ill-conditioned linear equations N89-25213
Fast polar decomposition of an arbitrary matrix
[NASA-CR-185412] N89-25653
On conjugate gradient type methods and polynomial preconditioners for a class of complex non-Hermitian matrices
[NASA-CR-185424] N89-25654
Note on the Majorana representations of the Lorentz group
[PREPRINT-597] N89-25662
Two-dimensional density matrix and its equations. Scalar and fermionic fields
[DE88-706249] N89-25760
An inversion method based on the Moore-Penrose generalized inverse matrix N89-25910

MATRIX MATERIALS
SiC whisker-reinforced SiAlON composites: Effect of sintering aid content
[DE89-010376] N89-25289

MATTER (PHYSICS)
Physics of dense matter, neutron stars and supernova
[DE89-010673] N89-25784

MEASURING INSTRUMENTS
Apparatus and method for characterizing conductivity of materials
[DE89-009599] N89-25383
Initial design and analysis of a capacitive sensor for shear and normal force measurement
[DE89-001821] N89-25438
Magneto-inductive skin sensor for robot collision avoidance: A new development
[NASA-CR-185402] N89-25444
An uncertainty analysis for the Structural Mechanics Laboratory
[DE89-010306] N89-25478

MECHANICAL DRIVES
Electrically compensated constant speed drive (Model number 60 ECEPGS 02)
[AD-A206064] N89-25385

MECHANICAL ENGINEERING
Engineering applications of heuristic multilevel optimization methods N89-25202

MECHANICAL PROPERTIES
A procedure for the numerical description of the moisture dependent material behavior
[ETN-89-94669] N89-25299
Deformation induced microstructural and microchemical changes during thermomechanical treatment
[DE89-011608] N89-25321
High-performance, extrusion-cast explosives with low sensitivity
[DE89-010279] N89-25349

MECHANICAL SHOCK
Identification of error sources in shock data
[DE89-007655] N89-25440

MEMBRANES
Effects of freezing and cold acclimation on the plasma membrane of isolated protoplasts
[DE89-010931] N89-25560

MEMORY (COMPUTERS)
Semi-automatic process partitioning for parallel computation
[NASA-CR-181633] N89-25585

MENTAL PERFORMANCE
Timesharing performance as an indicator of pilot mental workload
[NASA-CR-185328] N89-25573

MERCURY VAPOR
Experiments on liquid-vapour phase change between plane liquid surfaces. Part 3: Results from a closed quartz chamber
[NAL-TM-FM-8809] N89-25301

MESOSCALE PHENOMENA
Mesoscale model parameterizations for radiation and turbulent fluxes at the lower boundary
[DFVLR-FB-88-48] N89-25544

MESOSPHERE
Solar Mesosphere Explorer observations of stratospheric and mesospheric water vapor N89-25802
Measurements of H2O in the terrestrial mesosphere and implications for extra-terrestrial sources N89-25808

MESSAGE PROCESSING
A tool to aid in mapping computational tasks to a hypercube
[DE89-010320] N89-25589
Interprocess communications and application to physical numerical modeling
[DE89-011021] N89-25630

MESSAGES
Performance issues in management of the Space Station Information System
[NASA-CR-185409] N89-25773

METABOLISM
Acclimatization to heat in humans
[NASA-TM-101011] N89-25558

METAL AIR BATTERIES
Novel air electrode for metal-air battery with new carbon material and method of making same
[DE89-010964] N89-25391

METAL BONDING
Detection of metal-transfer mode in GMAW
[DE89-011133] N89-25465

METAL COATINGS
Relation of the adhesion of plasma sprayed coatings to the process parameters: Size, velocity and heat content of the spray particles
[ETN-89-94296] N89-25326
METAL CRYSTALS
Surface structural analysis of small molecules on transition metal single crystal surfaces with low energy electron diffraction
[DE89-010681] N89-25743
METAL CUTTING
Effects of auxiliary heat treatments on flame-cutting procedures
[DE89-011827] N89-25472
METAL PARTICLES
Relation of the adhesion of plasma sprayed coatings to the process parameters: Size, velocity and heat content of the spray particles
[ETN-89-94296] N89-25326
METAL PLATES
The strength-toughness relationship at cryogenic temperatures in aluminum-lithium alloy plate
[DE89-011816] N89-25322
METAL SURFACES
Surface structural analysis of small molecules on transition metal single crystal surfaces with low energy electron diffraction
[DE89-010681] N89-25743
METALS
Metal-sulfur type cell having improved positive electrode
[DE89-010110] N89-25389
Dynamic simulation of dislocation pattern formation in metals during high temperature monotonic and cyclic deformation N89-25477
METEOROLOGICAL PARAMETERS
FAO detailed rain mapping experiment
[BCRS-88-11] N89-25552
FAO detailed rain mapping experiment phase A: Meteosat based rainfall mapping in the Sahel region N89-25553
METEOROLOGICAL RADAR
The evolution and structure of the bow echo/microburst events N89-25550
METEOSAT SATELLITE
FAO detailed rain mapping experiment
[BCRS-88-11] N89-25552
FAO detailed rain mapping experiment phase A: Meteosat based rainfall mapping in the Sahel region N89-25553
FAO detailed rain mapping experiment phase B: Comparison of rainfall and evapotranspiration mapping N89-25554
METHOD OF MOMENTS
Far field projection
[DE89-010243] N89-25587
Beam transport calculation in magnetic field with a quadrupole symmetry by the method of immersion in moment phase space
[DE88-706295] N89-25681
MICHELSON INTERFEROMETERS
The Michelson Doppler imager for the solar oscillations imager program on SOHO N89-25892
The search for solar-type oscillations in other stars using the Michelson Interferometric Stellar Oscillation Spectrometer (ISOS) N89-25918
MICROANALYSIS
High resolution electron microscopy and microanalysis of ferrites and cuprates
[DE89-010441] N89-25341
MICROBURSTS (METEOROLOGY)
The evolution and structure of the bow echo/microburst events N89-25550
MICROCHANNEL PLATES
Search the spectrometric characteristics of microchannel plate photomultipliers
[DE88-706260] N89-25437
MICROCOMPUTERS
Development of a microcomputer based integrated design system for high altitude long endurance aircraft N89-25159
MICROFIBERS
Strong fibers
[DE89-010596] N89-25292
MICROGRAVITY APPLICATIONS
Spiral vane bioreactor
[NASA-CASE-MSC-21361-1] N89-25557
MICROHARDNESS
Effects of auxiliary heat treatments on flame-cutting procedures
[DE89-011827] N89-25472
MICROPROCESSORS
Pressure calibration and certification of a quartz pressure transducer
[DE89-005774] N89-25439
MICROSTRUCTURE
Characterization of ceramics and intermetallics fabricated by self-propagating high-temperature synthesis
[NASA-TM-102004] N89-25285
Precipitation at grain boundaries in irradiated austenitic Fe-Cr-Mn alloys
[DE89-011207] N89-25319
Deformation induced microstructural and microchemical changes during thermomechanical treatment
[DE89-011608] N89-25321
J(sub Ic) fracture toughness of ferritic DCI (Ductile Cast Iron) alloys: A comparison of two versions of ASTM E 813
[DE89-012249] N89-25323
Applicability of microalloying in the production of sintered steel structural parts
[KFK-4481] N89-25329
The mechanical properties of ion implanted ceramics
[DE89-008928] N89-25337
High resolution electron microscopy and microanalysis of ferrites and cuprates
[DE89-010441] N89-25341
Sintering schedule and sample geometry effects on the electrical and physical properties of high field varistor materials
[DE89-010523] N89-25384
Cavitation kinetics during GTA (Gas Tungsten Arc) welding of helium containing stainless steel
[DE89-012514] N89-25467
Welding of helium-doped austenitic and ferritic stainless steels
[DE89-012523] N89-25468
Simulation of the welding of irradiated materials
[DE89-012524] N89-25469
The influence of contact surface microstructure on vacuum arc stability and arc voltage
[EUT-87-E-186] N89-25672
Optical properties of metal-oxide thin films: influence of microstructure
[DE89-011219] N89-25690
Production of wires and coils from high-temperature superconducting materials
[DE89-012380] N89-25756
MICROWAVE CIRCUITS
Performance of five 30 GHz satellite receivers
[NASA-TM-101960] N89-25365
MICROWAVE EQUIPMENT
Microwave pulse generation by photoconductive switching
[DE89-011631] N89-25393
MICROWAVE FREQUENCIES
Plasma production using microwave and radio frequency sources
[DE89-011615] N89-25709
MICROWAVE SCATTERING
Microwave scattering models and basic experiments
[NASA-CR-185393] N89-25364
MICROWAVE SENSORS
Method and apparatus for sensor fusion
[NASA-CASE-MSC-21334-1] N89-25360
MICROWAVE SWITCHING
Microwave pulse generation by photoconductive switching
[DE89-011631] N89-25393
MICROWAVE TRANSMISSION
Performance of five 30 GHz satellite receivers
[NASA-TM-101960] N89-25365
MICROWAVES
Microwave experimental studies of laser fusion
[DE89-012325] N89-25454
The evolution of energetic particles and the emitted radiation in solar flares
[NASA-CR-185389] N89-25945
MILITARY AIR FACILITIES
Report to Congress: Technical feasibility of joint use at Scott AFB, Selfridge AGB and El Toro MCAS
[AD-A194597] N89-25241
MILLING (MACHINING)
Effect of milling machine roughness and wing dihedral on the supersonic aerodynamic characteristics of a highly swept wing
[NASA-TP-2918] N89-25117
MINERAL EXPLORATION
Investigations on satellite image and reference data for exploration-related tasks
[DFVLR-FB-88-46] N89-25498
MISSILE DESIGN
Static aeroelastic analysis and tailoring of missile control fins N89-25169
MISSION PLANNING
Space station operations task force. Panel 2 report: Ground operations and support systems
[NASA-TM-101817] N89-25245
Space station operations task force. Panel 3 report: User development and integration
[NASA-TM-101818] N89-25246
Space station operations task force. Panel 4 report: Management integration
[NASA-TM-101819] N89-25247
Space station operations task force summary report
[NASA-TM-101820] N89-25248
Space station operations task force. Executive summary
[NASA-TM-101780] N89-25249
United States and Western Europe cooperation in planetary exploration
[NASA-CR-184941] N89-25776
SOHO status N89-25882
MIXING LAYERS (FLUIDS)
A numerical study of a class of TVD schemes for compressible mixing layers
[NASA-TM-102194] N89-25651
MIXING LENGTH FLOW THEORY
Towards an independent calibration of the mixing-length theory N89-25899
MODULARITY
TUMULT: The Twente University Multiprocessor
[MEMO-INF-88-28] N89-25581
MODULES
Space station architecture, module, berthing hub, shell assembly, berthing mechanism and utility connection channel
[NASA-CASE-ARC-11505-2] N89-25266
MODULUS OF ELASTICITY
Determination of the mechanical properties of diamond and diamond-like films by the ultra-low load indentation technique
[DE89-011569] N89-25471
MOISTURE CONTENT
The interpretation of data from the Viking Mars Atmospheric Water Detectors (MAWD): Some points for discussion N89-25795
Factors governing water condensation in the Martian atmosphere N89-25797
On the vertical distribution of water vapor in the Martian tropics N89-25800
MOLECULAR BEAM EPITAXY
Submicron technologies for the fabrication of monolithic integrated millimeter wave devices on high resistivity silicon
[ETN-89-94624] N89-25757
MOLECULAR BIOLOGY
Unraveling Photosystem 2
[DE89-010930] N89-25559
MOLECULAR CLOUDS
The ionization structure in shocks in interstellar molecular clouds N89-25726
Ambipolar diffusion and core formation in molecular clouds N89-25782
MOLECULAR DIFFUSION
Monte Carlo for the electronic structure of molecules
[DE89-011824] N89-25682
MOLECULAR STRUCTURE
Molecular growth pathways in silica sol-gel polymerization
[DE89-011224] N89-25346
Super-strong self-reinforcing polymeric matrices formed by the first super-strong polymers
[DE89-011533] N89-25347
Electrochemical and optical studies of model photosynthetic systems
[DE89-012479] N89-25562
MOLECULES
Shock waves and fragmentation via molecular dynamics
[DE89-007981] N89-25405
Monte Carlo for the electronic structure of molecules
[DE89-011824] N89-25682
Surface structural analysis of small molecules on transition metal single crystal surfaces with low energy electron diffraction
[DE89-010681] N89-25743
MOLYBDENUM
Weldability and weld doping of commercial purity molybdenum
[DE89-009535] N89-25311
MOMENTUM TRANSFER
Angular momentum transport and dynamo action in the Sun: A report on implications of a recent helioseismic estimate of solar rotation N89-25837
MONITORS
Real-time application of knowledge-based systems N89-25163
Condition monitoring of machinery using motor current signature analysis
[DE89-008737] N89-25386

MONOPOLE ANTENNAS
Numerical modeling of monopoles on radial-wire ground screens
[DE89-005350] N89-25372
MONTE CARLO METHOD
Monte Carlo for the electronic structure of molecules
[DE89-011824] N89-25682
MORPHOLOGY
Very high elevation water ice clouds on Mars: Their morphology and temporal behavior N89-25804
MOUNTING
Flap system for short takeoff and landing aircraft
[AD-D013981] N89-25234
MULLITES
Evaluation of ceramic coatings on silicon carbide
[DE89-010321] N89-25339
MULTILAYER INSULATION
A passivation layer for 3-5 semiconductor materials
[AD-D013963] N89-25737
MULTIPLICATION
Serial-input polyphase convolvers
[REPT-88-019] N89-25608
MULTIPROCESSING (COMPUTERS)
TUMULT: The Twente University Multiprocessor
[MEMO-INF-88-28] N89-25581
Semi-automatic process partitioning for parallel computation
[NASA-CR-181633] N89-25585
Partitioning a finite difference code for a local memory multiprocessor
[DE89-010223] N89-25621
Speeding up parallel processing
[NASA-CR-184646] N89-25628
MULTISPECTRAL BAND SCANNERS
Comparative investigations of multispectral satellite image data of MOMS-01, LANDSAT-TM and LANDSAT-MSS for geological and vegetational applications in test sites in the Andes of northern Chile and the Parana-Basin of Brazil
[DFVLR-FB-88-50] N89-25499
MULTIVARIATE STATISTICAL ANALYSIS
Generalized consistency checking of multivariable redundant measurements and common-mode failure detection
[DE89-010053] N89-25474
MUSCLES
A program for the study of skeletal muscle catabolism following physical trauma
[AD-A206506] N89-25564
MUSCULOSKELETAL SYSTEM
A program for the study of skeletal muscle catabolism following physical trauma
[AD-A206506] N89-25564

N

NARROWBAND
Narrow bandgap semiconducting silicides: Intrinsic infrared detectors on a silicon chip
[NASA-CR-185372] N89-25746
NASA PROGRAMS
NASA patent abstracts bibliography: A continuing bibliography. Section 1: Abstracts (supplement 35)
[NASA-SP-7039(35)-SECT-1] N89-25775
Solar system exploration
[NASA-TM-101784] N89-25944
NASA SPACE PROGRAMS
Space station operations task force summary report
[NASA-TM-101820] N89-25248
Space station operations task force. Executive summary
[NASA-TM-101780] N89-25249
NASTRAN
Composite sizing and ply orientation for stiffness requirements using a large finite element structural model N89-25166
Recent experiences using finite-element-based structural optimization N89-25177
Grid sensitivity capability for large scale structures N89-25183
Conjugating binary systems for spacecraft thermal control. Appendix C: Aeroassist Flight Experiment Carrier Vehicle preliminary stress analysis
[NASA-CR-183609] N89-25261
Plan, formulate, discuss and correlate a NASTRAN finite element vibrations model of the Boeing Model 360 helicopter airframe
[NASA-CR-181787] N89-25480
NATIONAL AIRSPACE SYSTEM
FAA statistical handbook of aviation: Calendar year 1987
[AD-A200917] N89-25113
Notice to Airmen (NOTAM) system operational concept
[DOT/FAA/CT-TN89/10] N89-25142
NAVIER-STOKES EQUATION
Techniques for compressible flow calculations on multizone grids N89-25120
Multidimensional modeling of convective heat transfer with application to I.C. engines
[DE89-010651] N89-25415
Feasibility of using the Massively Parallel Processor for large eddy simulations and other Computational Fluid Dynamics applications
[NASA-CR-185427] N89-25629
NEAR FIELDS
Ion energy and plasma measurements in the near field of an ICRF antenna
[DE89-011611] N89-25708
NEAR INFRARED RADIATION
Visible and near-infrared channel calibration of the GOES-6 VISSR using high-altitude aircraft measurements
[NASA-TM-101064] N89-25494
Calibration of the visible and near-infrared channels of the NOAA-9 AVHRR using high-altitude aircraft measurements from August 1985 and October 1986
[NASA-TM-101063] N89-25496
NETWORK ANALYSIS
Analog and digital simulation of line-energizing overvoltages and comparison with measurements in a 400 kV network
[EUT-88-E-193] N89-25401
Gravity network of West Germany (DSGN76): Measurements and starting data N89-25546
Adjustment and data analysis — gravimetry N89-25547
NEUMANN PROBLEM
Two-dimensional density matrix and its equations. Scalar and fermionic fields
[DE88-706249] N89-25760
NEUTRAL BEAMS
Z subeff measurements and low-Z impurity transport for NBI and ICRF heated plasma in JIPP T-IIU tokamak
[IPPJ-896] N89-25701
Confinement physics of H-mode discharges in DIII-D
[DE89-011525] N89-25707
NEUTRINOS
Pair production of helicity-flipped neutrinos in supernovae
[NASA-CR-185466] N89-25789
NEUTRON ACTIVATION ANALYSIS
Use of resonance neutrons for analyzing superclean aluminium
[DE88-706221] N89-25313
NEUTRON IRRADIATION
Precipitation at grain boundaries in irradiated austenitic Fe-Cr-Mn alloys
[DE89-011207] N89-25319
NEUTRON STARS
Neutron stars: A cosmic hadron physics laboratory
[NASA-CR-185051] N89-25777
The origin of ultra-compact binaries
[NASA-TM-101792] N89-25780
Physics of dense matter, neutron stars and supernova
[DE89-010673] N89-25784
Nuclear astrophysics of supernovae
[DE89-012534] N89-25787
NEUTRONS
Use of resonance neutrons for analyzing superclean aluminium
[DE88-706221] N89-25313
Neutron stars: A cosmic hadron physics laboratory
[NASA-CR-185051] N89-25777
NEWTON METHODS
Fast polar decomposition of an arbitrary matrix
[NASA-CR-185412] N89-25653
Resolution of the Algebraic Riccati Equation via Newton's method and the Lyapunov Equation
[ESA-STM-241] N89-25660
NICKEL ALLOYS
Characterization of ceramics and intermetallics fabricated by self-propagating high-temperature synthesis
[NASA-TM-102004] N89-25265
NIOBATES
Ferroelectric potassium niobate thin films
[DE89-010862] N89-25744
NIOBIUM
The development of alloys based on Ni3Si
[DE89-010371] N89-25316
NIOBIUM ALLOYS
Review of oxidation of Nb-1Zr
[DE89-010299] N89-25687
NITRIC ACID
Photodissociation of pernitric acid (HO2NO2) at 248 nm
[NASA-CR-185363] N89-25286
NITROGEN DIOXIDE
Observations of atmospheric water vapor with the SAGE 2 instrument N89-25805
NITROGEN OXIDES
Preventing depletion of stratospheric ozone: Implications on future aircraft emissions
[DE89-009964] N89-25530
NOISE POLLUTION
Structural loading and noise disturbance of helicopters N89-25140
NOISE PREDICTION (AIRCRAFT)
Airfoil self-noise and prediction
[NASA-RP-1218] N89-25673
NOISE REDUCTION
Potential uses of vacuum bubbles in noise and vibration control
[NASA-CR-181829] N89-25674
Reduction of aircraft noise in civil air transport by optimization of flight tracks and takeoff and approach procedures
[ILR-MITT-200] N89-25676
NONDESTRUCTIVE TESTS
NDE of the space shuttle orbiter thermal protection system, phase 2
[NASA-CR-185471] N89-25257
A review of computer aided interpretation technology for the evaluation of radiographs of aluminum welds
[NASA-CR-185066] N89-25312
Basics of ultrasonic testing
[DE89-010465] N89-25473
Fiber optic sensing for NDE and process control
[DE89-010976] N89-25696
NONLINEAR OPTICS
Poled polymer films for nonlinear optics
[DE89-010039] N89-25338
NONLINEAR PROGRAMMING
A decomposition-based design optimization method with applications N89-25204
Structural damage assessment as an identification problem N89-25230
Three dimensional computations of the dynamics of the magnetopause: First results N89-25719
NONLINEAR SYSTEMS
Interactions of Tollmien-Schlichting waves and Dean vortices. Comparison of direct numerical simulation and a weakly nonlinear theory
[NASA-TP-2919] N89-25118
NONLINEARITY
Results of including geometric nonlinearities in an aeroelastic model of an F/A-18 N89-25190
A penalty approach for nonlinear optimization with discrete design variables N89-25217
NONUNIFORM FLOW
Design optimization of axisymmetric bodies in nonuniform transonic flow N89-25206
NOZZLE GEOMETRY
The effects of arcjet operating condition and constrictor geometry on the plasma plume
[NASA-TM-102284] N89-25281
NUCLEAR ASTROPHYSICS
Nuclear astrophysics of supernovae
[DE89-012534] N89-25787
NUCLEAR FISSION
Fission reactor pumped lasers: History and prospects
[DE89-010329] N89-25456
NUCLEAR MAGNETIC RESONANCE
NMR study of some organophosphorus compounds
[DE88-705970] N89-25302
Single crystal NMR studies of high temperature superconductors
[DE89-011220] N89-25747
NUCLEAR PHYSICS
International Centre for Theoretical Physics: Scientific activities in 1987
[DE88-705973] N89-25668
NUCLEAR POWER PLANTS
Operator role definition and human system integration
[DE89-009621] N89-25571
NUCLEAR POWER REACTORS
Space nuclear reactor shields for manned and unmanned applications
[NASA-TM-102064] N89-25272
CSTI High Capacity Power
[NASA-TM-102059] N89-25282
NUCLEAR REACTIONS
Nonlinear studies of solar gravity modes driven by nuclear burning of He3 in the core N89-25823
NUCLEAR REACTORS
Fission reactor pumped lasers: History and prospects
[DE89-010329] N89-25456
NUCLEATION
Transient effects in creep cavity nucleation and early growth in ceramics
[DE89-010420] N89-25340
NUMERICAL CONTROL
Smart tunnel: Docking mechanism
[NASA-CASE-MSC-21360-1] N89-25263

NUMERICAL INTEGRATION
Integration method for the calculation of flow with free vortices N89-25127
NUTRITION
Characterization of Spirulina biomass for CELSS diet potential
[NASA-CR-185329] N89-25561

O

OBLIQUE WINGS
Control surface spanwise placement in active flutter suppression systems N89-25195
The conceptual design of a Mach 2 Oblique Flying Wing supersonic transport
[NASA-CR-177529] N89-25233
OCEAN CURRENTS
Dynamic sea surface topography, gravity and improved orbit accuracies from the direct evaluation of SEASAT altimeter data
[NASA-TM-100735] N89-25539
OCEAN DYNAMICS
Dynamic sea surface topography, gravity and improved orbit accuracies from the direct evaluation of SEASAT altimeter data
[NASA-TM-100735] N89-25539
OCEAN SURFACE
Dynamic sea surface topography, gravity and improved orbit accuracies from the direct evaluation of SEASAT altimeter data
[NASA-TM-100735] N89-25539
OCEAN THERMAL ENERGY CONVERSION
Operational experience of the OC-OTEC experiments at NELH
[DE89-000877] N89-25510
ON-LINE SYSTEMS
Data acquisition, event building, and on-line processing: Summary talk
[DE89-011065] N89-25693
A theoretical framework and an instructional model for educating end-users of online bibliographic information retrieval systems: A research monograph N89-25769
ONBOARD EQUIPMENT
Calibration of the visible and near-infrared channels of the NOAA-9 AVHRR using high-altitude aircraft measurements from August 1985 and October 1986
[NASA-TM-101063] N89-25496
OPACITY
Seasonal and diurnal variability of Mars water-ice clouds N89-25794
OPERATIONS RESEARCH
The software product assurance metrics study: JPL's software systems quality and productivity
[NASA-CR-184871] N89-25618
OPERATOR PERFORMANCE
Operator role definition and human system integration
[DE89-009621] N89-25571
OPERATORS (MATHEMATICS)
Differential algebras without differentials: An easy C++ implementation
[DE89-011503] N89-25655
OPTICAL COMMUNICATION
Local-frequency description of optical signals and systems
[EUT-88-E-191] N89-25698
OPTICAL DATA PROCESSING
Optical information processing and holography
[DE88-706011] N89-25434
OPTICAL EQUIPMENT
Digital optical conversion module
[DE89-011441] N89-25367
OPTICAL FIBERS
Optical fiber sensors and signal processing for intelligent structure monitoring
[NASA-CR-185395] N89-25691
OPTICAL FILTERS
Integrated solar disk oscillation measurements using the magneto-optical filter: Tests with a two station network N89-25850
OPTICAL MEASURING INSTRUMENTS
Solar oscillations instrumentation and measurement theory N89-25925
The Nice University stellar seismometer N89-25927
A Fabry-Perot interferometric stellar oscillation spectrometer N89-25929
Some tests of the precision of CCD differential photometry measurements of bright double stars N89-25930
OPTICAL PROPERTIES
Report of the Workshop on Scientific Opportunities for Infrared Free-Electron Lasers, volume 2
[DE89-009106] N89-25452
Optical information storage in PLZT thin films
[DE89-011067] N89-25692
Deposition of dielectric optical coatings: A microstructural study of the deposited layers and interfaces
[DE89-011205] N89-25694
Thermal conductivity of dielectric thin films
[DE89-011847] N89-25750
OPTICAL RADAR
Prototype of a slant visual range measuring device
[DFVLR-FB-88-42] N89-25697
OPTICAL RANGE FINDERS
Prototype of a slant visual range measuring device
[DFVLR-FB-88-42] N89-25697
OPTICAL REFLECTION
Superlattice strain gage
[DE89-011805] N89-25447
OPTIMAL CONTROL
On the calculation of derivatives of eigenvalues and eigenvectors in the simultaneous design and control of structures N89-25186
OPTIMIZATION
Recent Advances in Multidisciplinary Analysis and Optimization, part 1
[NASA-CP-3031-PT-1] N89-25146
Applications of integrated design/analysis systems in aerospace structural design N89-25147
Integrated design optimization research and development in an industrial environment N89-25148
Optimization by decomposition: A step from hierarchic to non-hierarchic systems N89-25149
Overview of Dynamics Integration Research (DIR) program at Langley Research Center N89-25150
An initiative in multidisciplinary optimization of rotorcraft N89-25151
Structural optimization of rotor blades with straight and swept tips subject to aeroelastic constraints N89-25152
Optimization of rotor blades for combined structural, performance, and aeroelastic characteristics N89-25153
Efficient sensitivity analysis and optimization of a helicopter rotor N89-25155
Structural optimization of rotor blades with integrated dynamics and aerodynamics N89-25156
Multi-objective/loading optimization for rotating composite flexbeams N89-25157
Demonstration of decomposition and optimization in the design of experimental space systems N89-25160
Structural tailoring of counter rotation propfans N89-25165
Aeroelastic tailoring and integrated wing design N89-25167
Static aeroelastic analysis and tailoring of missile control fins N89-25169
Optimum structural design with static aeroelastic constraints N89-25171
Optimum design of swept-forward high-aspect-ration graphite-epoxy wings N89-25172
Recent Advances in Multidisciplinary Analysis and Optimization, part 2
[NASA-CP-3031-PT-2] N89-25173
ASTROS: A multidisciplinary automated structural design tool N89-25174
Research on optimization-based design N89-25176
Recent experiences using finite-element-based structural optimization N89-25177
The Sizing and Optimization Language (SOL): A computer language to improve the user/optimizer interface N89-25178
Robust computer-aided synthesis and optimization of linear multivariable control systems with varying plant dynamics via AUTOCON N89-25179
An investigation of using an RQP based method to calculate parameter sensitivity derivatives N89-25182
Grid sensitivity capability for large scale structures N89-25183
Iterative methods for design sensitivity analysis N89-25184
On the calculation of derivatives of eigenvalues and eigenvectors in the simultaneous design and control of structures N89-25186
Treatment of body forces in boundary element design sensitivity analysis N89-25187
Design sensitivity analysis of boundary element substructures N89-25188
Digital robust control law synthesis using constrained optimization N89-25193
An integrated approach to the optimum design of actively controlled composite wings N89-25194
An approximation function for frequency constrained structural optimization N89-25196
Structural optimization of framed structures using generalized optimality criteria N89-25197
Involute composite design evaluation using global design sensitivity derivatives N89-25199
Optimizing for minimum weight when two different finite element models and analyses are required N89-25200
Recent Advances in Multidisciplinary Analysis and Optimization, part 3
[NASA-CP-3031-PT-3] N89-25201
Engineering applications of heuristic multilevel optimization methods N89-25202
Recent developments in multilevel optimization N89-25203
A decomposition-based design optimization method with applications N89-25204
Multilevel decomposition of complete vehicle configuration in a parallel computing environment N89-25205
Design optimization of axisymmetric bodies in nonuniform transonic flow N89-25206
Procedures for shape optimization of gas turbine disks N89-25207
The art of spacecraft design: A multidisciplinary challenge N89-25209
Optimizing conceptual aircraft designs for minimum life cycle cost N89-25211
Aircraft design optimization with multidisciplinary performance criteria N89-25212
An interpretation and solution of ill-conditioned linear equations N89-25213
Generalized mathematical models in design optimization N89-25214
Optimum design of structures subject to general periodic loads N89-25215
Fuzzy set applications in engineering optimization: Multilevel fuzzy optimization N89-25216
A penalty approach for nonlinear optimization with discrete design variables N89-25217
Multiplier-continuation algorithms for constrained optimization N89-25218
A large scale software system for simulation and design optimization of mechanical systems N89-25219
The role of optimization in the next generation of computer-based design tools N89-25220
An overview of the Douglas Aircraft Company Aeroelastic Design Optimization Program (ADOP) N89-25221
Meeting the challenges with the Douglas Aircraft Company Aeroelastic Design Optimization Program (ADOP) N89-25222
Optimization of structure and control system N89-25223
Structural optimization and recent large ground antenna installations N89-25224
A novel implementation of method of optimality criterion in synthesizing spacecraft structures with natural frequency constraints N89-25225
Computational experiments in the optimal slewing of flexible structures N89-25226
Optimal placement of excitations and sensors by simulated annealing N89-25227
Experiences in applying optimization techniques to configurations for the Control of Flexible Structures (COFS) program N89-25228
An improved algorithm for optimum structural design with multiple frequency constraints N89-25229
Structural damage assessment as an identification problem N89-25230
Recent developments in large-scale structural optimization N89-25231
Shape optimal design of elastic bodies using a mixed variational formulation N89-25236
Sensitivity analysis of complex coupled systems extended to second and higher order derivatives
[NASA-TM-101587] N89-25354
Numerical modeling of monopoles on radial-wire ground screens
[DE89-005350] N89-25372
On optimal fail-safe design of structures N89-25486
Efficient generalized conjugate gradient algorithms
[MATHS-RES-211] N89-25606
ORBIT TRANSFER VEHICLES
Free-molecule-flow force and moment coefficients of the aeroassist flight experiment vehicle
[NASA-TM-101600] N89-25124
Launch packaging options for the photovoltaic power module cargo element
[NASA-TM-102072] N89-25275
ORBITAL ASSEMBLY
Pactruss support structure for precision segmented reflectors
[NASA-CR-181747] N89-25484
ORBITAL LAUNCHING
Advanced mass launchers for low earth orbit
[DE89-010759] N89-25255
ORBITAL POSITION ESTIMATION
Dynamic sea surface topography, gravity and improved orbit accuracies from the direct evaluation of SEASAT altimeter data
[NASA-TM-100735] N89-25539

ORBITAL RESONANCES (CELESTIAL MECHANICS)
Some aspects of the dynamics of orbit-orbit resonances in the Uranian satellite system N89-25815
ORDER-DISORDER TRANSFORMATIONS
X-ray scattering studies of non-equilibrium ordering processes
[DE89-012517] N89-25753
ORGANIC COMPOUNDS
Climatic changes inferred fron analyses of lake-sediment cores, Walker Lake, Nevada
[DE89-010740] N89-25525
ORGANIC PHOSPHORUS COMPOUNDS
NMR study of some organophosphorus compounds
[DE88-705970] N89-25302
OROGRAPHY
Mesoscale model parameterizations for radiation and turbulent fluxes at the lower boundary
[DFVLR-FB-88-48] N89-25544
OSCILLATING FLOW
Numerical analysis of supersonic flow through oscillating cascade sections by using a deforming grid
[NASA-TM-102053] N89-25119
OSCILLATIONS
The q measurements during sawtooth oscillations in a low q tokamak
[DE89-010563] N89-25705
Oscillations of Jupiter as a tool for probing its internal structure N89-25924
OSMOSIS
Effects of freezing and cold acclimation on the plasma membrane of isolated protoplasts
[DE89-010931] N89-25560
OVERVOLTAGE
Analog and digital simulation of line-energizing overvoltages and comparison with measurements in a 400 kV network
[EUT-88-E-193] N89-25401
OXIDATION
Studies of oxidative degradation of polymers induced by ionizing radiation
[DE89-008279] N89-25335
Review of oxidation of Nb-1Zr
[DE89-010299] N89-25687
OXIDATION RESISTANCE
Review of oxidation of Nb-1Zr
[DE89-010299] N89-25687
OZONE
Models for regional-scale photochemical production of ozone N89-25523
Preventing depletion of stratospheric ozone: Implications on future aircraft emissions
[DE89-009964] N89-25530
Evaluating CFC (Chlorofluorocarbon) alternatives from the atmospheric viewpoint
[DE89-010238] N89-25531
Observations of atmospheric water vapor with the SAGE 2 instrument N89-25805
OZONOMETRY
The UARS (Upper Atmosphere Research Satellite): A program to study global ozone change
[NASA-TM-101756] N89-25520

P

P WAVES
The excitation and damping of solar oscillations N89-25820
On the diagnostic of 5m oscillations through photospheric line profiles N89-25822
Linewidth of low degree acoustic modes of the Sun N89-25824
On the measurement of solar rotation using high-degree p-mode oscillations N89-25830
Initial high-degree p-mode frequency splittings from the 1988 Mt. Wilson 60-foot Tower Solar Oscillation Program N89-25832
Rotational splitting of low l solar p-mode N89-25839
Solar p-mode frequency splittings N89-25840
The current status of the Birmingham solar seismology network N89-25844
Solar Luminosity Oscillation Telescope (SLOT) N89-25848
An attempt to understand the Stanford p-mode data --- solar oscillations N89-25853
On the radiative damping of p-modes in solar magnetic flux concentrations N89-25864
Solar p-modes frequency variations between 1980 and 1986 N89-25867
The influence of a chromospheric magnetic field on p- and f-modes N89-25874
Observations of f- and p-mode oscillations of high degree (500 is less than L is less than 2500) in quiet and active Sun N89-25875
Modelling the variation of solar p-mode frequencies N89-25907
Convection and p-mode oscillations --- Sun N89-25912
Observed p-mode spectra of Ap stars and the Sun N89-25915
Asymptotic approximations of nonradial oscillation modes of the Sun N89-25932
Solar-like oscillations in late spectral class stars N89-25935
Effects of convective velocities on solar pressure mode frequencies N89-25941
PAIR PRODUCTION
Pair production of helicity-flipped neutrinos in supernovae
[NASA-CR-185466] N89-25789
PANELS
Survivable pulse power space radiator
[DE89-010120] N89-25264
PAPERS
Bibliographic coupling among scientific papers in biological research specialties N89-25771
PARABOLIC ANTENNAS
Antenna surface contour control system
[NASA-CASE-LAR-13798-1] N89-25363
PARABOLIC REFLECTORS
Antenna surface contour control system
[NASA-CASE-LAR-13798-1] N89-25363
Pactruss support structure for precision segmented reflectors
[NASA-CR-181747] N89-25484
PARALLEL COMPUTERS
Semi-automatic process partitioning for parallel computation
[NASA-CR-181633] N89-25585
PARALLEL PROCESSING (COMPUTERS)
Multilevel decomposition of complete vehicle configuration in a parallel computing environment N89-25205
The epsilon dataflow processor
[DE89-001679] N89-25577
Semi-automatic process partitioning for parallel computation
[NASA-CR-181633] N89-25585
Parallel solution of a 2-D phase change problem on a hypercube
[DE89-009619] N89-25586
A parallel algorithm for switch-level timing simulation on a hypercube multiprocessor
[NASA-CR-185338] N89-25595
Parallel solutions of a 2-D phase change problem on a hypercube
[DE89-012886] N89-25602
A simple method to remove reference counting in applicative programs
[DE89-006739] N89-25603
Parallel processors and nonlinear structural dynamics algorithms and software
[NASA-CR-185049] N89-25620
Performance evaluation for data flow architectures: A summary of discussions from the Santa Fe workshop
[DE89-008023] N89-25624
Interconnection networks
[DE89-010965] N89-25626
Speeding up parallel processing
[NASA-CR-184646] N89-25628
A site oriented supercomputer for theoretical physics: The Fermilab Advanced Computer Program Multi Array Processor System (ACMAPS)
[DE89-011090] N89-25631
A parallel processing approach for implementing high-performance first-order logic deduction systems
[DE89-011878] N89-25632
PARALLEL PROGRAMMING
Fast Fourier Transform algorithm design and tradeoffs
[NASA-CR-185038] N89-25600
PARAMETER IDENTIFICATION
On the bounds of the modeling errors of black-box MIMO transfer function estimates
[EUT-87-E-183] N89-25643
Least squares parameter estimation in a dynamic model from noisy observations
[ETN-89-94295] N89-25657
Modelling the solar oscillation time series by a randomly excited oscillator N89-25942
PARAMETERIZATION
An investigation of using an RQP based method to calculate parameter sensitivity derivatives N89-25182
Parameter estimation for a viscoelastic constitutive model
[DE89-008714] N89-25336
Mesoscale model parameterizations for radiation and turbulent fluxes at the lower boundary
[DFVLR-FB-88-48] N89-25544
Querying databases of trajectories of differential equations: Data structures for trajectories
[NASA-CR-185040] N89-25772
PARTIAL DIFFERENTIAL EQUATIONS
Parallel solution of a 2-D phase change problem on a hypercube
[DE89-009619] N89-25586
PARTICLE ACCELERATION
Amplitude growth due to random, correlated kicks
[DE89-011504] N89-25418
Proceedings of the Free Electron Laser Workshop, 1988 JAERI
[DE89-780071] N89-25450
Report of the HEPAP (High Energy Physics Advisory Panel) Subpanel on High Energy Physics and the SSC (Superconducting Super Collider) over the next decade
[DE89-010071] N89-25686
Acceleration of ions in the magnetotail N89-25720
Acceleration of particles in shear flows N89-25731
PARTICLE ACCELERATORS
Flying wires at Fermilab
[DE89-011005] N89-25251
PARTICLE BEAMS
A slow positron beam generator for lifetime studies
[NASA-TM-101590] N89-25433
Beam transport calculation in magnetic field with a quadrupole symmetry by the method of immersion in moment phase space
[DE88-706295] N89-25681
PARTICLE DENSITY (CONCENTRATION)
Models for axially symmetric pulsar magnetospheres N89-25730
PARTICLE DIFFUSION
Density fluctuations and particle/thermal transport for ohmically and auxiliarily heated plasmas in the JIPP T-IIU tokamak
[IPPJ-891] N89-25700
PARTICLE INTERACTIONS
Model independence of constraints on particle dark matter
[NASA-CR-185337] N89-25688
Particle simulation for accretion sheets in narrow double stars N89-25729
Neutron stars: A cosmic hadron physics laboratory
[NASA-CR-185051] N89-25777
PARTICLE MOTION
Beam transport calculation in magnetic field with a quadrupole symmetry by the method of immersion in moment phase space
[DE88-706295] N89-25681
PARTICLES
Double tearing and particle simulation N89-25723
PARTICULATE SAMPLING
Investigation of submicrometer aerosols for apportioning the impacts of airborne particulate matter at Deep Creek Lake
[DE89-008186] N89-25524
PARTITIONS (MATHEMATICS)
Semi-automatic process partitioning for parallel computation
[NASA-CR-181633] N89-25585
Partitioning a finite difference code for a local memory multiprocessor
[DE89-010223] N89-25621
PASSIVITY
A passivation layer for 3-5 semiconductor materials
[AD-D013963] N89-25737
PATENT POLICY
NASA patent abstracts bibliography: A continuing bibliography. Section 1: Abstracts (supplement 35)
[NASA-SP-7039(35)-SECT-1] N89-25775
PATTERN RECOGNITION
Method and apparatus for sensor fusion
[NASA-CASE-MSC-21334-1] N89-25360
A contour-oriented approach to digital shape analysis
[ISBN-9-09-002004-7] N89-25604
Segmentation of noisy images
[ETN-89-94299] N89-25605
PAYLOAD CONTROL
Space nuclear reactor shields for manned and unmanned applications
[NASA-TM-102064] N89-25272
PAYLOAD DELIVERY (STS)
Advanced APS impacts on vehicle payloads
[NASA-TM-102086] N89-25254
PAYLOADS
Space station operations task force. Panel 3 report: User development and integration
[NASA-TM-101818] N89-25246
PEBBLE BED REACTORS
Heat transfer in packed beds
[KFK-4451] N89-25425
PENALTY FUNCTION
A penalty approach for nonlinear optimization with discrete design variables N89-25217
Multiplier-continuation algorithms for constrained optimization N89-25218

PERCEPTION
The organization of perception and action in complex control skills
[NASA-CR-184638] N89-25568
PERFORMANCE PREDICTION
Estimated performance and future potential of solar dynamic and photovoltaic power systems for selected LEO and HEO missions
[NASA-TM-102083] N89-25280
Radiative heat transfer
[PB89-173637] N89-25412
A theory of describing performability models
[MEMO-INF-88-26] N89-25476
PERFORMANCE TESTS
Protoflight photovoltaic power module system-level tests in the space power facility
[NASA-TM-102066] N89-25267
Performance of five 30 GHz satellite receivers
[NASA-TM-101960] N89-25365
Vehicle performance tests of the Ford/GE first generation single-shaft (ETX-I) alternating current propulsion system
[DE89-011115] N89-25392
Development and testing of a 20-kHz component test bed
[NASA-TM-102141] N89-25403
Automated Test and Evaluation Center for Waveform Digitizer Systems and Components
[DE89-010226] N89-25441
Combined vapor compression/absorption heat pump cycles for engine-driven heat pumps
[PB89-145437] N89-25505
Performance evaluation for data flow architectures: A summary of discussions from the Santa Fe workshop
[DE89-008023] N89-25624
Performance characteristics for advanced control systems
[DE89-010362] N89-25637
PERIODIC VARIATIONS
Periodical asymmetry of solar limb darkening N89-25861
Solar p-modes frequency variations between 1980 and 1986 N89-25867
PEROVSKITES
Ferroelectric potassium niobate thin films
[DE89-010862] N89-25744
PERTURBATION
Some aspects of the dynamics of orbit-orbit resonances in the Uranian satellite system N89-25815
PERTURBATION THEORY
Local field effects in the many-body perturbation theory and in the density functional theory
[DE88-705975] N89-25734
Some aspects of the dynamics of orbit-orbit resonances in the Uranian satellite system N89-25815
PETRI NETS
Symbolic execution of concurrent programs using Petri nets
[REPT-89-004] N89-25633
A net-based model for time-dependent systems
[REPT-89-005] N89-25661
PHASE CONJUGATION
Microwave experimental studies of laser fusion
[DE89-012325] N89-25454
PHASE CONTROL
Spectral shaping and phase control of a fast-wave current drive antenna array
[DE89-011567] N89-25388
PHASE DIAGRAMS
The coupling of thermochemistry and phase diagrams for Group 3-5 semiconductor systems
[DE89-012516] N89-25752
Possible significance of cubic water-ice, H2O-Ic, in the atmospheric water cycle of Mars N89-25799
PHASE ERROR
Pyramidal horns: Part 1: Simple expressions for directivity as a function of aperture phase error
[DE89-005209] N89-25370
PHASE SHIFT
Serial-input polyphase convolvers
[REPT-88-019] N89-25608
PHASE SHIFT KEYING
Phase-ambiguity resolution for QPSK modulation systems. Part 1: A review
[NASA-CR-185385] N89-25380
Phase-ambiguity resolution for QPSK modulation systems. Part 2: A method to resolve offset QPSK
[NASA-CR-184971] N89-25381
PHASE TRANSFORMATIONS
Experiments on liquid-vapour phase change between plane liquid surfaces. Part 3: Results from a closed quartz chamber
[NAL-TM-FM-8809] N89-25301
Parallel solution of a 2-D phase change problem on a hypercube
[DE89-009619] N89-25586
Solitosynthesis: Cosmological evolution of non-topological solitons
[NASA-CR-185030] N89-25678
X-ray scattering studies of non-equilibrium ordering processes
[DE89-012517] N89-25753
Water in the Martian regolith N89-25791
PHILOSOPHY
Quantum ontologies
[DE89-010385] N89-25781
PHOSPHORS
Automated thermal mapping techniques using chromatic image analysis
[NASA-TM-101554] N89-25443
PHOTOCATHODES
Search the spectrometric characteristics of microchannel plate photomultipliers
[DE88-706260] N89-25437
PHOTOCHEMICAL REACTIONS
Photodissociation of pernitric acid (HO2NO2) at 248 nm
[NASA-CR-185363] N89-25286
IR laser photochemistry
[DE88-706012] N89-25303
Models for regional-scale photochemical production of ozone N89-25523
Flux of water vapor in the terrestrial stratosphere and in the Martian atmosphere N89-25806
PHOTOCONDUCTIVITY
Microwave pulse generation by photoconductive switching
[DE89-011631] N89-25393
PHOTODISSOCIATION
Photodissociation of pernitric acid (HO2NO2) at 248 nm
[NASA-CR-185363] N89-25286
PHOTOINTERPRETATION
A review of computer aided interpretation technology for the evaluation of radiographs of aluminum welds
[NASA-CR-185066] N89-25312
Reports on cartography and Geodesy. Series 1: Original reports, number 102
[ISSN-0469-4236] N89-25501
Interpretation of Thematic Mapper data for the acquisition of land information N89-25502
Forestry interpretation of Thematic Mapper (TM) data using the example of the Frankfurt municipal forest N89-25503
PHOTOIONIZATION
A study of non-linear ionization processes in planetary atmospheres N89-25816
PHOTOMULTIPLIER TUBES
Search the spectrometric characteristics of microchannel plate photomultipliers
[DE88-706260] N89-25437
GOLF: Simulations of the re-emission of the resonance cell N89-25895
PHOTONS
Photonic chiral current and its anomaly in a gravitational field
[DE88-706213] N89-25361
PHOTOSENSITIVITY
Optical information storage in PLZT thin films
[DE89-011067] N89-25692
PHOTOSPHERE
On the diagnostic of 5m oscillations through photospheric line profiles N89-25822
Dynamics of the overshoot layers and boundary conditions in helioseismology N89-25826
Measurement of the rotational frequency splitting of the solar five-minute oscillations from magneto-optical filter observations N89-25842
Periodical asymmetry of solar limb darkening N89-25861
The granulation sensitivity of helioseismology lines N89-25862
PHOTOSYNTHESIS
Unraveling Photosystem 2
[DE89-010930] N89-25559
Electrochemical and optical studies of model photosynthetic systems
[DE89-012479] N89-25562
PHOTOVOLTAIC CELLS
Protoflight photovoltaic power module system-level tests in the space power facility
[NASA-TM-102066] N89-25267
The introduction of space technology power systems into developing countries
[NASA-TM-102042] N89-25274
PHOTOVOLTAIC CONVERSION
Space Station Freedom photovoltaic power module design status
[NASA-TM-102073] N89-25273
Launch packaging options for the photovoltaic power module cargo element
[NASA-TM-102072] N89-25275
Estimated performance and future potential of solar dynamic and photovoltaic power systems for selected LEO and HEO missions
[NASA-TM-102083] N89-25280
PHYSIOLOGICAL EFFECTS
Acclimatization to heat in humans
[NASA-TM-101011] N89-25558
Timesharing performance as an indicator of pilot mental workload
[NASA-CR-185328] N89-25573
PHYSIOLOGICAL RESPONSES
A program for the study of skeletal muscle catabolism following physical trauma
[AD-A206506] N89-25564
PIEZOELECTRICITY
Technique and data analysis for impact-loaded piezoelectric polymers (PVDF)
[DE89-010529] N89-25342
Superlattice strain gage
[DE89-011805] N89-25447
PILOT PERFORMANCE
The man-machine-interface in a fast jet
[ETN-89-94327] N89-25574
Validation of the subjective workload assessment technique in a simulated flight task
[DFVLR-FB-89-01] N89-25575
PIPE FLOW
Gas-liquid flow in dividing Tee-junctions with a horizontal inlet and different branch orientations and diameters
[KFK-4399] N89-25427
PIPES (TUBES)
Quantitative modeling of sensitization development in austenitic stainless steel
[DE89-011206] N89-25317
Radiative heat transfer
[PB89-173637] N89-25412
PLANETARY EVOLUTION
Solar system exploration
[NASA-TM-101784] N89-25944
PLANETARY MAGNETOSPHERES
Wave emissions from planetary magnetospheres
[NASA-CR-185435] N89-25541
PLANETARY STRUCTURE
Oscillations of Jupiter as a tool for probing its internal structure N89-25924
PLANETS
Continuous global N-tuple coverage with (2N = 2) satellites
[AD-A206522] N89-25262
PLANNING
Demonstration of decomposition and optimization in the design of experimental space systems N89-25160
Space station operations task force summary report
[NASA-TM-101820] N89-25248
Space station operations task force. Executive summary
[NASA-TM-101780] N89-25249
PLASMA ANTENNAS
Determination of fields near an ICRH antenna using a 3D magnetostatic Laplace formulation
[DE89-011571] N89-25366
Ion energy and plasma measurements in the near field of an ICRF antenna
[DE89-011611] N89-25708
PLASMA CONTROL
A courant condition free modified partially-implicit method. Revised electromagnetic particle Code PS2M for bounded plasmas with conducting walls
[IPPJ-892] N89-25699
Density fluctuations and particle/thermal transport for ohmically and auxiliarily heated plasmas in the JIPP T-IIU tokamak
[IPPJ-891] N89-25700
Confinement improvement of low-aspect-ratio torsatrons
[DE89-010192] N89-25702
Confinement physics of H-mode discharges in DIII-D
[DE89-011525] N89-25707
Plasma production using microwave and radio frequency sources
[DE89-011615] N89-25709
Investigations of modular nonplanar coil systems for the stellarator fusion reactor
[IPP-2/298] N89-25714
PLASMA CURRENTS
Plasma switches for high current and fast time scale operation
[DE89-010557] N89-25704
Confinement physics of H-mode discharges in DIII-D
[DE89-011525] N89-25707
PLASMA DENSITY
The effects of arcjet operating condition and constrictor geometry on the plasma plume
[NASA-TM-102284] N89-25281

Density fluctuations and particle/thermal transport for ohmically and auxiliarily heated plasmas in the JIPP T-IIU tokamak
[IPPJ-891] N89-25700

PLASMA DIAGNOSTICS
The effects of arcjet operating condition and constrictor geometry on the plasma plume
[NASA-TM-102284] N89-25281
Measurement of H and H2 populations in-situ in a low-temperature plasma by vacuum-ultraviolet laser-absorption spectroscopy
[DE89-010433] N89-25308
Microwave experimental studies of laser fusion
[DE89-012325] N89-25454
Ion energy and plasma measurements in the near field of an ICRF antenna
[DE89-011611] N89-25708

PLASMA DYNAMICS
Three dimensional computations of the dynamics of the magnetopause: First results N89-25719
Nonlocal analyses of finite-beam-driven instabilities N89-25721
Particle simulation of magnetic reconnection N89-25722

PLASMA ENGINES
Hybrid plume plasma rocket
[NASA-CASE-MSC-20476-2] N89-25279

PLASMA EQUILIBRIUM
Theoretical studies of edge physics and plasma-wall interactions
[DE89-011792] N89-25710

PLASMA FREQUENCIES
Plasma production using microwave and radio frequency sources
[DE89-011615] N89-25709

PLASMA HEATING
Determination of fields near an ICRH antenna using a 3D magnetostatic Laplace formulation
[DE89-011571] N89-25366
Density fluctuations and particle/thermal transport for ohmically and auxiliarily heated plasmas in the JIPP T-IIU tokamak
[IPPJ-891] N89-25700
High-average-power millimeter-wave FEL (Free-Electron Laser) for plasma heating using the ETA-2 accelerator
[DE89-012294] N89-25711
ICRF Faraday shield plasma sheath physics: The Perkins paradigm
[DE89-012362] N89-25712

PLASMA PHYSICS
Z subeff measurements and low-Z impurity transport for NBI and ICRF heated plasma in JIPP T-IIU tokamak
[IPPJ-896] N89-25701

PLASMA PINCH
Anomalous particle pinch for collisionless plasma
[DE89-011018] N89-25706

PLASMA PROPULSION
Hybrid plume plasma rocket
[NASA-CASE-MSC-20476-2] N89-25279

PLASMA SHEATHS
ICRF Faraday shield plasma sheath physics: The Perkins paradigm
[DE89-012362] N89-25712

PLASMA SLABS
A courant condition free modified partially-implicit method. Revised electromagnetic particle Code PS2M for bounded plasmas with conducting walls
[IPPJ-892] N89-25699

PLASMA SPRAYING
Relation of the adhesion of plasma sprayed coatings to the process parameters: Size, velocity and heat content of the spray particles
[ETN-89-94296] N89-25326

PLASMA TEMPERATURE
Density fluctuations and particle/thermal transport for ohmically and auxiliarily heated plasmas in the JIPP T-IIU tokamak
[IPPJ-891] N89-25700

PLASMA TURBULENCE
Density fluctuations and particle/thermal transport for ohmically and auxiliarily heated plasmas in the JIPP T-IIU tokamak
[IPPJ-891] N89-25700
Anomalous particle pinch for collisionless plasma
[DE89-011018] N89-25706
A numerical simulation of inhomogeneous ion cyclotron turbulence N89-25725

PLASMA WAVES
Wave emissions from planetary magnetospheres
[NASA-CR-185435] N89-25541

PLASMADYNAMIC LASERS
A 2 J high-power excimer laser at high pulse repetition rate
[U9-414/87/029] N89-25457

PLASTIC DEFORMATION
Elevated temperature deformation of structural steel
[PB89-172621] N89-25318
On optimal fail-safe design of structures N89-25486

PLASTIC FLOW
Polyimide Matrix composites: Polyimidesulfone/LARC-TPI (1:1) blend
[NASA-TM-101568] N89-25294

PLATFORMS
Analysis and control of a three-degree-of-freedom robot platform
[DE89-006427] N89-25356

PLUMES
The effects of arcjet operating condition and constrictor geometry on the plasma plume
[NASA-TM-102284] N89-25281
Models for regional-scale photochemical production of ozone N89-25523
Investigation of submicrometer aerosols for apportioning the impacts of airborne particulate matter at Deep Creek Lake
[DE89-008186] N89-25524

POISSON EQUATION
The 3DGRAPE book: Theory, users' manual, examples
[NASA-TM-102224] N89-25116

POLAR METEOROLOGY
Transport of Mars atmospheric water into high northern latitudes during a polar warming N89-25792

POLARIZATION (WAVES)
Bistability in a laser with injected signal
[DE88-706003] N89-25449

POLARIZED LIGHT
Poled polymer films for nonlinear optics
[DE89-010039] N89-25338

POLLUTION MONITORING
Applications of remote sensing techniques for the inventory and monitoring of environmental pollution
[BCRS-88-15] N89-25497

POLYETHER RESINS
Absorbed dose thresholds and absorbed dose rate limitations for studies of electron radiation effects on polyetherimides
[NASA-TP-2928] N89-25332

POLYIMIDE RESINS
Polyimide Matrix composites: Polyimidesulfone/LARC-TPI (1:1) blend
[NASA-TM-101568] N89-25294
Absorbed dose thresholds and absorbed dose rate limitations for studies of electron radiation effects on polyetherimides
[NASA-TP-2928] N89-25332
Semiinterpenetrating polymer network for tougher and more microcracking resistant high temperature polymers
[NASA-CASE-LAR-13925-1] N89-25334

POLYIMIDES
A slow positron beam generator for lifetime studies
[NASA-TM-101590] N89-25433

POLYMER MATRIX COMPOSITES
Mechanical properties of carbon fiber reinforced thermoplastics for cryogenic applications
[KFK-4487] N89-25297
A procedure for the numerical description of the moisture dependent material behavior
[ETN-89-94669] N89-25299
Semiinterpenetrating polymer network for tougher and more microcracking resistant high temperature polymers
[NASA-CASE-LAR-13925-1] N89-25334
Super-strong self-reinforcing polymeric matrices formed by the first super-strong polymers
[DE89-011533] N89-25347

POLYMERIC FILMS
Poled polymer films for nonlinear optics
[DE89-010039] N89-25338
A slow positron beam generator for lifetime studies
[NASA-TM-101590] N89-25433

POLYMERIZATION
Molecular growth pathways in silica sol-gel polymerization
[DE89-011224] N89-25346

POLYMERS
Studies of oxidative degradation of polymers induced by ionizing radiation
[DE89-008279] N89-25335

POLYNOMIALS
Polynomial method of approximate centers for linear programming
[PB89-146161] N89-25584
On conjugate gradient type methods and polynomial preconditioners for a class of complex non-Hermitian matrices
[NASA-CR-185424] N89-25654

POLYTROPIC PROCESSES
Oscillation ring diagrams and the thermodynamics of the outer solar convection zone N89-25836

POLYVINYL FLUORIDE
Technique and data analysis for impact-loaded piezoelectric polymers (PVDF)
[DE89-010529] N89-25342

POROSITY
Sintering schedule and sample geometry effects on the electrical and physical properties of high field varistor materials
[DE89-010523] N89-25384

POROUS MATERIALS
Diffusion, fluid flow and sound propagation in disordered media
[DE89-010937] N89-25407

POSITION (LOCATION)
Optimal placement of excitations and sensors by simulated annealing N89-25227

POSITIONING
Control surface spanwise placement in active flutter suppression systems N89-25195

POSITRON ANNIHILATION
A slow positron beam generator for lifetime studies
[NASA-TM-101590] N89-25433

POSITRONS
A slow positron beam generator for lifetime studies
[NASA-TM-101590] N89-25433

POSTFLIGHT ANALYSIS
Flight set 360L003 instrumentation final test report, volume 9
[NASA-CR-183675] N89-25284

POTASSIUM
Ferroelectric potassium niobate thin films
[DE89-010862] N89-25744

POTENTIAL FLOW
Coupling of the boundary element method with an integral momentum boundary-layer technique to calculate forces and moments on three-dimensional bodies
[DE89-006328] N89-25420

POWDER (PARTICLES)
Proceedings of the Solids Transport Contractors' Review Meeting
[DE89-006720] N89-25414

POWDER METALLURGY
Applicability of microalloying in the production of sintered steel structural parts
[KFK-4481] N89-25329

POWER EFFICIENCY
Estimated performance and future potential of solar dynamic and photovoltaic power systems for selected LEO and HEO missions
[NASA-TM-102083] N89-25280

POWER LINES
Analog and digital simulation of line-energizing overvoltages and comparison with measurements in a 400 kV network
[EUT-88-E-193] N89-25401

POWER MODULES (STS)
Protoflight photovoltaic power module system-level tests in the space power facility
[NASA-TM-102066] N89-25267

POWER SERIES
Application of theta functions for numerical evaluation of complete elliptic integrals of the first and second kinds
[DE89-010191] N89-25645

POWER SPECTRA
Initial high-degree p-mode frequency splittings from the 1988 Mt. Wilson 60-foot Tower Solar Oscillation Program N89-25832
Oscillation ring diagrams and the thermodynamics of the outer solar convection zone N89-25836
Rotational splitting of low l solar p-mode N89-25839

POWER SUPPLY CIRCUITS
Modular magnet current regulator
[CEBAF-PR-89-005] N89-25685

PRANDTL NUMBER
Towards an independent calibration of the mixing-length theory N89-25899

PRECIPITATION (METEOROLOGY)
The evolution and structure of the bow echo/microburst events N89-25550

PRECONDITIONING
On conjugate gradient type methods and polynomial preconditioners for a class of complex non-Hermitian matrices
[NASA-CR-185424] N89-25654

PREDICTION ANALYSIS TECHNIQUES
Black-box identification of MIMO transfer functions: Asymptotic properties of prediction error models
[EUT-87-E-182] N89-25642

PREDICTIONS
A predictive model for failure properties of thermoset resins
[NASA-TM-4128] N89-25300

PREFLIGHT OPERATIONS
Space station operations task force. Panel 2 report: Ground operations and support systems
[NASA-TM-101817] N89-25245
PREMIXED FLAMES
Time-dependent computational studies of flames in microgravity
[NASA-CR-182298] N89-25353
Determination of combustion gas temperatures by infrared radiometry in sooting and nonsooting flames
[NASA-TP-2900] N89-25409
PREPROCESSING
Composite sizing and ply orientation for stiffness requirements using a large finite element structural model N89-25166
PRESSURE DISTRIBUTION
On the stress problem of the pebble bed heat exchanger in a hypersonic wind tunnel
[NAL-TM-ST-8705] N89-25240
PRESSURE EFFECTS
Characterization of booster-rocket propellants and their simulants
[DE89-012497] N89-25352
Optical pressure sealing coupling apparatus
[NASA-CASE-MFS-29348-1] N89-25689
Studies of 3-5 compounds in the megabar regime
[DE89-012433] N89-25751
PRESSURE MEASUREMENT
Pressure measurement technique of WT-WK — wind tunnels
[DFVLR-MITT-88-11] N89-25243
Pressure calibration and certification of a quartz pressure transducer
[DE89-005774] N89-25439
Fiber optic sensing in a high explosives environment
[DE89-010863] N89-25695
PRESSURE REDUCTION
Study of interfacial behavior in concurrent gas-liquid flows
[DE89-010484] N89-25408
PRESSURE SENSORS
Flight set 360L003 instrumentation final test report, volume 9
[NASA-CR-183675] N89-25284
Pressure calibration and certification of a quartz pressure transducer
[DE89-005774] N89-25439
PRINTED CIRCUITS
A decomposition-based design optimization method with applications N89-25204
PROBABILITY DISTRIBUTION FUNCTIONS
Local-frequency description of optical signals and systems
[EUT-88-E-191] N89-25698
PROBABILITY THEORY
Probabilistic damage tolerance methods for metallic aerospace structures N89-25237
PROBLEM SOLVING
The 3DGRAPE book: Theory, users' manual, examples
[NASA-TM-102224] N89-25116
Engineering applications of heuristic multilevel optimization methods N89-25202
An interpretation and solution of ill-conditioned linear equations N89-25213
PROCESS CONTROL (INDUSTRY)
An extremum hunting method using pseudo-random binary signal
[EUT-88-E-198] N89-25359
ECUT (Energy Conversion and Utilization Technologies) program: Biocatalysis project
[NASA-CR-184965] N89-25519
A new method for dynamic hunting extremum control, based on comparison of measured and estimated value
[EUT-88-E-197] N89-25644
Fiber optic sensing for NDE and process control
[DE89-010976] N89-25696
PRODUCTION ENGINEERING
Hierarchies for computer-integrated manufacturing: A functional description
[PB89-172613] N89-25596
PROGRAM VERIFICATION (COMPUTERS)
Use of metaknowledge in the verification of knowledge-based systems
[NASA-CR-181821] N89-25627
An expert system development methodology which supports verification and validation
[NASA-TM-101782] N89-25635
PROGRAMMING LANGUAGES
Development of a microcomputer based integrated design system for high altitude long endurance aircraft N89-25159
Semi-automatic process partitioning for parallel computation
[NASA-CR-181633] N89-25585
The ADAMS database language
[DE89-010925] N89-25601
A simple method to remove reference counting in applicative programs
[DE89-006739] N89-25603
On the role of software reliability in software engineering
[REPT-88-010] N89-25607
On the semantics of nonatomic actions
[MEMO-INF-88-13] N89-25610
Controlled bidirectional grammars
[MEMO-INF-88-16] N89-25611
Constraint specification in BSDM — basic semantic data model (BSDM)
[MEMO-INF-88-32] N89-25615
PROJECT MANAGEMENT
Space station operations task force summary report
[NASA-TM-101820] N89-25248
Space station operations task force. Executive summary
[NASA-TM-101780] N89-25249
Learning the value of VE
[DE89-006121] N89-25475
Geothermal energy program summary. Volume 2: Research summaries, fiscal year 1988
[DE89-000865] N89-25509
Mission Operations and Data Systems Directorate's operational/development network (MODNET) at Goddard Space Flight Center
[NASA-CR-183426] N89-25763
Systems approach to project management
[DE89-008741] N89-25765
PROJECT PLANNING
Fuel cell systems program plan, FY 1989
[DE89-012928] N89-25515
Report of the HEPAP (High Energy Physics Advisory Panel) Subpanel on High Energy Physics and the SSC (Superconducting Super Collider) over the next decade
[DE89-010071] N89-25686
PROJECTILES
Advanced mass launchers for low earth orbit
[DE89-010759] N89-25255
PROP-FAN TECHNOLOGY
Structural tailoring of counter rotation propfans N89-25165
PROPELLER BLADES
Low-speed wind tunnel performance of high-speed counterrotation propellers at angle-of-attack
[NASA-TM-102292] N89-25121
Data of aeroacoustic measurements on ultralight aircraft propellers
[DFVLR-MITT-88-33] N89-25677
PROPELLER EFFICIENCY
Low-speed wind tunnel performance of high-speed counterrotation propellers at angle-of-attack
[NASA-TM-102292] N89-25121
PROPELLER NOISE
In-flight measurement of propeller noise on the fuselage of an airplane
[NASA-TM-102285] N89-25675
PROPORTIONAL COUNTERS
Advances in the development of apparatus and methods for studies of protein monocrystals in coordinate X-ray diffractometers based on two-dimensional proportional chambers
[DE88-706259] N89-25740
PROPULSION SYSTEM CONFIGURATIONS
Aerodynamic flight evaluation analysis and data base update
[NASA-CR-183654] N89-25276
PROPULSION SYSTEM PERFORMANCE
Advanced APS impacts on vehicle payloads
[NASA-TM-102086] N89-25254
Performance characterization and transient investigation of multipropellant resistojets
[NASA-TM-102118] N89-25283
PROPULSIVE EFFICIENCY
Advanced APS impacts on vehicle payloads
[NASA-TM-102086] N89-25254
PROSTAGLANDINS
A program for the study of skeletal muscle catabolism following physical trauma
[AD-A206506] N89-25564
PROTECTIVE COATINGS
Method of protecting surfaces from abrasion and abrasion resistant articles of manufacture
[DE89-010798] N89-25344
Applications of ion beam processes in tribology
[DE89-000614] N89-25470
PROTEIN METABOLISM
A program for the study of skeletal muscle catabolism following physical trauma
[AD-A206506] N89-25564
PROTEINS
Advances in the development of apparatus and methods for studies of protein monocrystals in coordinate X-ray diffractometers based on two-dimensional proportional chambers
[DE88-706259] N89-25740
PROTOCOL (COMPUTERS)
The Delta-t transport protocol: Features and experience useful for high performance networks
[DE89-009259] N89-25625
PROTOPLASTS
Effects of freezing and cold acclimation on the plasma membrane of isolated protoplasts
[DE89-010931] N89-25560
PROTOTYPES
Real-time application of knowledge-based systems N89-25163
Prototyping management information systems application software: An empirical study of developers' perceptions N89-25770
PSYCHOLOGICAL TESTS
Validation of the subjective workload assessment technique in a simulated flight task
[DFVLR-FB-89-01] N89-25575
PSYCHOLOGY
Applying understanding of individual behavior and team dynamics within the value engineering process
[DE89-011126] N89-25766
PULSARS
Models for axially symmetric pulsar magnetospheres N89-25730
Neutron stars: A cosmic hadron physics laboratory
[NASA-CR-185051] N89-25777
Reminiscence of a stellar pulsation theorist
[DE89-011165] N89-25786
PULSE COMPRESSION
Magnetic switching
[DE89-012299] N89-25398
PULSE FREQUENCY MODULATION
On system identification using pulse-frequency modulated signals
[EUT-88-E-195] N89-25379
PULSE GENERATORS
Microwave pulse generation by photoconductive switching
[DE89-011631] N89-25393
Binary and ternary gas mixtures with temperature enhanced diffuse glow discharge characteristics for use in closing switches
[DE89-011807] N89-25395
Amplitude growth due to random, correlated kicks
[DE89-011504] N89-25418
PULSE REPETITION RATE
A 2 J high-power excimer laser at high pulse repetition rate
[UI9-414/87/029] N89-25457
PULSED LASERS
A 2 J high-power excimer laser at high pulse repetition rate
[UI9-414/87/029] N89-25457
PULSED RADIATION
On radiative and convective influences on stellar pulsational stability N89-25828
PUMPS
Study on thermodynamical and mechanical conditions for pumping low flow rates of liquefied gases to high pressure level
[DFVLR-FB-88-54] N89-25429
PURIFICATION
Use of resonance neutrons for analyzing superclean aluminium
[DE88-706221] N89-25313
PURITY
IR laser photochemistry
[DE88-706012] N89-25303
Weldability and weld doping of commercial purity molybdenum
[DE89-009535] N89-25311
PYROLYSIS
Method of production H2 using a rotating drum reactor with a pulse jet heat source
[DE89-009764] N89-25348

Q

QUADRATIC PROGRAMMING
Research on optimization-based design N89-25176
An investigation of using an RQP based method to calculate parameter sensitivity derivatives N89-25182
Multiplier-continuation algorithms for constrained optimization N89-25218
Fast polar decomposition of an arbitrary matrix
[NASA-CR-185412] N89-25653

QUADRATURES
The tanh transformation for double integrals with singularities: A progressive rule
[MATHS-RES-203] N89-25658
QUADRUPOLES
Beam transport calculation in magnetic field with a quadrupole symmetry by the method of immersion in moment phase space
[DE88-706295] N89-25681
QUALITY CONTROL
An uncertainty analysis for the Structural Mechanics Laboratory
[DE89-010306] N89-25478
The software product assurance metrics study: JPL's software systems quality and productivity
[NASA-CR-184871] N89-25618
QUANTITATIVE ANALYSIS
Gravity network of West Germany (DSGN76): Measurements and starting data N89-25546
QUANTUM CHEMISTRY
Concepts in surface science and heterogeneous catalysts
[DE89-010679] N89-25307
QUANTUM MECHANICS
Localizability and covariance in analytical mechanics
[DE88-706038] N89-25666
Monte Carlo for the electronic structure of molecules
[DE89-011824] N89-25682
QUANTUM THEORY
Renormalization of topological field theory
[DE88-705998] N89-25759
Two-dimensional density matrix and its equations. Scalar and fermionic fields
[DE88-706249] N89-25760
On the quantum theory of the superparticle
[NIKHEF-H/88-16] N89-25762
Quantum ontologies
[DE89-010385] N89-25781
QUARTZ TRANSDUCERS
Pressure calibration and certification of a quartz pressure transducer
[DE89-005774] N89-25439
QUERY LANGUAGES
Querying databases of trajectories of differential equations: Data structures for trajectories
[NASA-CR-185040] N89-25772
QUEUEING THEORY
Using a segregation measure for the workload characterization of multi-class queuing networks
[DE89-007841] N89-25623

R

RADAR CROSS SECTIONS
Method and apparatus for sensor fusion
[NASA-CASE-MSC-21334-1] N89-25360
RADAR ECHOES
The evolution and structure of the bow echo/microburst events N89-25550
RADAR IMAGERY
On a fast two-dimensional radar imaging process for rotating targets and an analysis of its image quality
[DFVLR-FB-88-51] N89-25376
User's guide to image processing applications of the NOAA satellite HRPT/AVHRR data. Part 1: Introduction to the satellite system and its applications. Part 2: Processing and analysis of AVHRR imagery
[NASA-CR-180784] N89-25492
Digital evaluation of SEASAT-SAR radar image data N89-25504
RADAR MEASUREMENT
Tropospheric influences on satellite-Earth paths and their determination by means of radar measurements
[DFVLR-FB-88-53] N89-25250
RADAR TARGETS
On a fast two-dimensional radar imaging process for rotating targets and an analysis of its image quality
[DFVLR-FB-88-51] N89-25376
RADIAL VELOCITY
Effect of atmospheric extinction on solar radial velocity measurements N89-25849
The search for radial velocity variations in rapidly oscillating Ap stars using the Fabry-Perot Interferometric Stellar Oscillation Spectrometer (FP-ISOS) N89-25923
RADIANCE
The Nimbus 7 LIMS (Limb Infrared Monitor of the Stratosphere) water vapor measurements N89-25810
RADIATION ABSORPTION
Absorbed dose thresholds and absorbed dose rate limitations for studies of electron radiation effects on polyetherimides
[NASA-TP-2928] N89-25332
Microwave experimental studies of laser fusion
[DE89-012325] N89-25454
RADIATION DOSAGE
Absorbed dose thresholds and absorbed dose rate limitations for studies of electron radiation effects on polyetherimides
[NASA-TP-2928] N89-25332
RADIATION EFFECTS
Modeling grain boundary microchemistry related to IASCC (Irradiation-Assisted Stress Corrosion Cracking)
[DE89-011214] N89-25320
Absorbed dose thresholds and absorbed dose rate limitations for studies of electron radiation effects on polyetherimides
[NASA-TP-2928] N89-25332
Studies of oxidative degradation of polymers induced by ionizing radiation
[DE89-008279] N89-25335
Cavitation kinetics during GTA (Gas Tungsten Arc) welding of helium containing stainless steel
[DE89-012514] N89-25467
Welding of helium-doped austenitic and ferritic stainless steels
[DE89-012523] N89-25468
Simulation of the welding of irradiated materials
[DE89-012524] N89-25469
On the applicability of various planar potentials in the theory of ultrarelativistic electron channeling
[DE88-706155] N89-25738
RADIATION PYROMETERS
Determination of combustion gas temperatures by infrared radiometry in sooting and nonsooting flames
[NASA-TP-2900] N89-25409
RADIATION SHIELDING
Space nuclear reactor shields for manned and unmanned applications
[NASA-TM-102064] N89-25272
RADIATIVE HEAT TRANSFER
Radiative heat transfer
[PB89-173637] N89-25412
RADIATIVE TRANSFER
Modeling land-surface albedos from plant canopy architecture N89-25495
Reminiscence of a stellar pulsation theorist
[DE89-011165] N89-25786
RADIO ANTENNAS
Antenna surface contour control system
[NASA-CASE-LAR-13798-1] N89-25363
RADIO FREQUENCIES
Plasma production using microwave and radio frequency sources
[DE89-011615] N89-25709
RADIO FREQUENCY INTERFERENCE
Reduction of transhorizon radio interference in satellite earth stations
[ETN-89-94297] N89-25374
RADIO RECEIVERS
Testing of a GPS receiver
[DFVLR-MITT-88-30] N89-25145
RADIOACTIVE DECAY
Nuclear beta decay far from stability and astrophysics
[MPI-H-1988-V-27] N89-25683
RADIOACTIVE WASTES
Design of a dual forearm modular robot
[DE89-010453] N89-25462
RADIOGRAPHY
A review of computer aided interpretation technology for the evaluation of radiographs of aluminum welds
[NASA-CR-185066] N89-25312
RAIN
FAO detailed rain mapping experiment
[BCRS-88-11] N89-25552
FAO detailed rain mapping experiment phase A: Meteosat based rainfall mapping in the Sahel region N89-25553
FAO detailed rain mapping experiment phase B: Comparison of rainfall and evapotranspiration mapping N89-25554
RAMAN SPECTROSCOPY
Electrochemical and optical studies of model photosynthetic systems
[DE89-012479] N89-25562
RANDOM PROCESSES
Time-correlated gust loads using Matched-Filter Theory and Random-Process Theory: A new way of looking at things
[NASA-TM-101573] N89-25232
RANKINE CYCLE
Advanced binary geothermal power plants working fluid property determination and heat exchanger design
[DE89-011144] N89-25513
RARE GASES
State-selective single electron capture by multiply charged ions: Reaction window and multichannel Landau Zener calculations
[REPT-88-05-175] N89-25684

Partial and state selective cross sections for multiple ionization of rare gas atoms by electron impact
[REPT-88-05-170] N89-25715
RAYLEIGH NUMBER
Towards an independent calibration of the mixing-length theory N89-25899
RAYLEIGH SCATTERING
Measurement of the stimulated thermal Rayleigh scattering instability
[DE89-012324] N89-25453
REACTION PRODUCTS
IR laser photochemistry
[DE88-706012] N89-25303
REACTOR MATERIALS
Effect of low neutron fluences on DIN 1.4948 steel creep properties --- liquid metal fast breeder reactor (LMFBR) material
[ECN-206] N89-25325
The creep and creep-rupture behavior of vanadium-base alloys
[KFK-2440] N89-25326
REAL TIME OPERATION
Real-time application of knowledge-based systems N89-25163
On a fast two-dimensional radar imaging process for rotating targets and an analysis of its image quality
[DFVLR-FB-88-51] N89-25376
TUMULT: The Twente University Multiprocessor
[MEMO-INF-88-28] N89-25581
A case study relating the Yourdon methodology to other design methods
[MEMO-INF-88-24] N89-25613
Temporal data management in real-time systems: A comparative view
[REPT-88-046] N89-25767
RECEIVERS
Performance of five 30 GHz satellite receivers
[NASA-TM-101960] N89-25365
RECHARGING
Novel air electrode for metal-air battery with new carbon material and method of making same
[DE89-010964] N89-25391
RED SHIFT
Magnetically induced spectral line redshifts full disk measurements N89-25877
REDUCED GRAVITY
Time-dependent computational studies of flames in microgravity
[NASA-CR-182298] N89-25353
GIRL cryotechnics and preparation of a TEXUS experiment on superfluid helium dynamics
[ETN-89-94631] N89-25357
Spiral vane bioreactor
[NASA-CASE-MSC-21361-1] N89-25557
REDUCTION
Design sensitivity analysis of boundary element substructures N89-25188
REDUNDANCY
Continuous global N-tuple coverage with (2N = 2) satellites
[AD-A206522] N89-25262
REENTRY SHIELDING
SIMOUN: Test system for shuttle thermal protection materials
[REPT-882-430-101] N89-25256
REFRACTIVITY
Optical properties of metal-oxide thin films: Influence of microstructure
[DE89-011219] N89-25690
REFRACTORY MATERIALS
Manifold, bus support and coupling arrangement for solid oxide fuel cells
[DE89-009604] N89-25508
REFRIGERANTS
The development of a vapor compression refrigeration system for a network of nine temperature test chambers
[DE89-007084] N89-25355
REFRIGERATING
The development of a vapor compression refrigeration system for a network of nine temperature test chambers
[DE89-007084] N89-25355
REGOLITH
Water in the Martian regolith N89-25791
Regolith water vapor sources on Mars: A historical bibliography N89-25796
Regelation and ice segregation N89-25807
Diurnal and annual cycles of H2O in the Martian regolith N89-25809
Atmospheric H2O and the search for Martian brines N89-25812
REGRESSION COEFFICIENTS
ARMA (Autoregressive-Moving Average) modeling
[AD-A205308] N89-25649
REGULATORY MECHANISMS (BIOLOGY)
Acclimatization to heat in humans
[NASA-TM-101011] N89-25558

RELATIVISTIC PARTICLES
Localizability and covariance in analytical mechanics
[DE88-706039] N89-25666
RELATIVITY
Imbedding of the gravitational field into the space of affine connection without torsion
[DE88-704637] N89-25536
RELIABILITY
An uncertainty analysis for the Structural Mechanics Laboratory
[DE89-010306] N89-25478
RELIABILITY ANALYSIS
On the role of software reliability in software engineering
[REPT-88-010] N89-25607
Symbolic execution of concurrent programs using Petri nets
[REPT-89-004] N89-25633
RELIABILITY ENGINEERING
The designer of the 90's: A live demonstration N89-25154
A theory of describing performability models
[MEMO-INF-88-26] N89-25476
The software product assurance metrics study: JPL's software systems quality and productivity
[NASA-CR-184871] N89-25618
Reliability mechanisms for ADAMS (Advanced Data Management System)
[DE89-010911] N89-25768
REMOTE MANIPULATOR SYSTEM
Traction-drive transmission for telerobotic joints
[DE89-005337] N89-25461
REMOTE SENSING
Microwave scattering models and basic experiments
[NASA-CR-185393] N89-25364
Earth resources: A continuing bibliography with indexes (issue 61)
[NASA-SP-7041(61)] N89-25493
The UARS (Upper Atmosphere Research Satellite): A program to study global ozone change
[NASA-TM-101756] N89-25520
REMOTE SENSORS
Design of an auto change mechanism and intelligent gripper for the space station
[NASA-CR-185387] N89-25268
Earth resources: A continuing bibliography with indexes (issue 61)
[NASA-SP-7041(61)] N89-25493
Comparative investigations of multispectral satellite image data of MOMS-01, LANDSAT-TM and LANDSAT-MSS for geological and vegetational applications in test sites in the Andes of northern Chile and the Parana-Basin of Brazil
[DFVLR-FB-88-50] N89-25499
REQUIREMENTS
Report to Congress: Technical feasibility of joint use at Scott AFB, Selfridge AGB and El Toro MCAS
[AD-A194597] N89-25241
RESEARCH AND DEVELOPMENT
International Centre for Theoretical Physics: Scientific activities in 1987
[DE88-705973] N89-25668
RESEARCH FACILITIES
Overview of Dynamics Integration Research (DIR) program at Langley Research Center N89-25150
RESIDUAL STRESS
The mechanical properties of ion implanted ceramics
[DE89-008928] N89-25337
RESIN MATRIX COMPOSITES
Polyimide Matrix composites: Polyimidesulfone/LARC-TPI (1:1) blend
[NASA-TM-101566] N89-25294
Semiinterpenetrating polymer network for tougher and more microcracking resistant high temperature polymers
[NASA-CASE-LAR-13925-1] N89-25334
RESISTOJET ENGINES
Performance characterization and transient investigation of multipropellant resistojets
[NASA-TM-102118] N89-25283
RESONANCE
Use of resonance neutrons for analyzing superclean aluminium
[DE88-706221] N89-25313
RESONANT FREQUENCIES
An approximation function for frequency constrained structural optimization N89-25196
Optimizing for minimum weight when two different finite element models and analyses are required N89-25200
An improved algorithm for optimum structural design with multiple frequency constraints N89-25229
Further implications of solar p-modes as measured in Na and K resonance lines N89-25908
RESPONSE TIME (COMPUTERS)
Feasibility of using the Massively Parallel Processor for large eddy simulations and other Computational Fluid Dynamics applications
[NASA-CR-185427] N89-25629
RHEOLOGY
Polyimide Matrix composites: Polyimidesulfone/LARC-TPI (1:1) blend
[NASA-TM-101566] N89-25294
RICCATI EQUATION
Resolution of the Algebraic Riccati Equation via Newton's method and the Lyapunov Equation
[ESA-STM-241] N89-25660
RIEMANN MANIFOLD
A new way to interpret the DIRAC equation in a non-Riemannian manifold
[NASA-CR-185484] N89-25663
Strings on hyperelliptic supersurfaces
[DE88-705991] N89-25758
RIGID ROTORS
Flap-lag stability data for a small-scale isolated hingeless rotor in forward flight
[NASA-TM-102189] N89-25479
RING STRUCTURES
Involute composite design evaluation using global design sensitivity derivatives N89-25199
RIPPLES
Ripple structure in degenerate electron gas-dominated stars with intense magnetic fields N89-25783
ROBOTICS
Design of an auto change mechanism and intelligent gripper for the space station
[NASA-CR-185387] N89-25268
A kinematic study of the MERLIN 6500 robot and the Utah/MIT dexterous hand and a simulation of their combined behavior
[AD-A203907] N89-25458
Modifying a telerobotic system to include robotic operation by means of dynamic modeling
[DE89-003119] N89-25460
Traction-drive transmission for telerobotic joints
[DE89-005337] N89-25461
ROBOTS
Analysis and control of a three-degree-of-freedom robot platform
[DE89-006427] N89-25356
Magneto-inductive skin sensor for robot collision avoidance: A new development
[NASA-CR-185402] N89-25444
A kinematic study of the MERLIN 6500 robot and the Utah/MIT dexterous hand and a simulation of their combined behavior
[AD-A203907] N89-25458
Modifying a telerobotic system to include robotic operation by means of dynamic modeling
[DE89-003119] N89-25460
Design of a dual forearm modular robot
[DE89-010453] N89-25462
Review of the 1988 Workshop on Human-Machine Symbiotic Systems
[DE89-008743] N89-25570
Robust performance of multiple tasks by an autonomous robot
[DE89-008718] N89-25636
ROBUSTNESS (MATHEMATICS)
Robust performance of multiple tasks by an autonomous robot
[DE89-008718] N89-25636
ROCKET EXHAUST
Hybrid plume plasma rocket
[NASA-CASE-MSC-20476-2] N89-25279
ROCKET NOZZLES
Involute composite design evaluation using global design sensitivity derivatives N89-25199
Hybrid plume plasma rocket
[NASA-CASE-MSC-20476-2] N89-25279
ROCKET PROPELLANTS
High explosives reaction model and its application to booster performance
[DE89-005459] N89-25351
RODS
Optimum design of structures subject to general periodic loads N89-25215
ROLLING MOMENTS
Aeroservoelastic tailoring for lateral control enhancement N89-25189
ROMANIA
Research for the physics and structure of earth's crust in Romania
[DE88-706002] N89-25535
ROOFS
Design description of the large scale climate simulator
[DE89-010185] N89-25551
ROTARY WINGS
Vortex flows in flying technique
[ETN-89-94429] N89-25126
Strongly unsteady vortex fields at elastic helicopter rotor blades N89-25131
Mechanical reaction of wings moving through a vortex region N89-25139
An initiative in multidisciplinary optimization of rotorcraft N89-25151
Structural optimization of rotor blades with straight and swept tips subject to aeroelastic constraints N89-25152
Optimization of rotor blades for combined structural, performance, and aeroelastic characteristics N89-25153
Transonic airfoil design for helicopter rotor applications N89-25154
Efficient sensitivity analysis and optimization of a helicopter rotor N89-25155
Multi-objective/loading optimization for rotating composite flexbeams N89-25157
TRUSS: An intelligent design system for aircraft wings N89-25162
Flap-lag stability data for a small-scale isolated hingeless rotor in forward flight
[NASA-TM-102189] N89-25479
ROTATION
Method of production H2 using a rotating drum reactor with a pulse jet heat source
[DE89-009764] N89-25348
In-flight measurement of propeller noise on the fuselage of an airplane
[NASA-TM-102285] N89-25675
ROTOR BLADES (TURBOMACHINERY)
Numerical analysis of supersonic flow through oscillating cascade sections by using a deforming grid
[NASA-TM-102053] N89-25119
ROTOR DYNAMICS
Influence of rubbing on rotor dynamics, part 1
[NASA-CR-183648-PT-1] N89-25463
Influence of rubbing on rotor dynamics, part 2
[NASA-CR-183649-PT-2] N89-25464
Flap-lag stability data for a small-scale isolated hingeless rotor in forward flight
[NASA-TM-102189] N89-25479
ROTORS
Influence of rubbing on rotor dynamics, part 1
[NASA-CR-183648-PT-1] N89-25463
Influence of rubbing on rotor dynamics, part 2
[NASA-CR-183649-PT-2] N89-25464
RUN TIME (COMPUTERS)
The epsilon dataflow processor
[DE89-001679] N89-25577
A parallel algorithm for switch-level timing simulation on a hypercube multiprocessor
[NASA-CR-185338] N89-25595
Speeding up parallel processing
[NASA-CR-184646] N89-25628
RUNWAY CONDITIONS
Warm fog dissipation using large volume water sprays
[NASA-CASE-MFS-25962-1] N89-25242
RUNWAYS
Warm fog dissipation using large volume water sprays
[NASA-CASE-MFS-25962-1] N89-25242
RURAL AREAS
The introduction of space technology power systems into developing countries
[NASA-TM-102042] N89-25274
The impact of telecommunication on rural areas in developing countries
[EUT-87-E-185] N89-25377

S

S MATRIX THEORY
Non-perturbative effects in the exact S-matrices of the O(N) Gross-Neveu and supersymmetric sigma models
[NIKHEF-H/88-10] N89-25656
SAFETY
The q measurements during sawtooth oscillations in a low q tokamak
[DE89-010563] N89-25705
SAFETY FACTORS
Correlation of subjective slipperiness judgements with quantitative COF (Coefficient Of Friction) measurements for structural steel
[PB89-165070] N89-25669
SAMPLING
A global time reference for hypercube multicomputers
[DE89-010924] N89-25579
SATELLITE ALTIMETRY
Dynamic sea surface topography, gravity and improved orbit accuracies from the direct evaluation of SEASAT altimeter data
[NASA-TM-100735] N89-25539
SATELLITE ANTENNAS
Antenna surface contour control system
[NASA-CASE-LAR-13798-1] N89-25363

A multifrequency antenna system for propagation experiments with the Olympus satellite
[EUT-88-E-192] N89-25378

SATELLITE COMMUNICATION
Performance of five 30 GHz satellite receivers
[NASA-TM-101960] N89-25365

SATELLITE DESIGN
SOHO status N89-25882

SATELLITE IMAGERY
Investigations on satellite image and reference data for exploration-related tasks
[DFVLR-FB-88-46] N89-25498
MECA Workshop on Atmospheric H2O Observations of Earth and Mars. Physical Processes, Measurements and Interpretations
[NASA-CR-183335] N89-25790
The solar oscillations imager for SOHO N89-25885
Luminosity Oscillations Imager (LOI) N89-25887

SATELLITE INSTRUMENTS
Visible and near-infrared channel calibration of the GOES-6 VISSR using high-altitude aircraft measurements
[NASA-TM-101064] N89-25494

SATELLITE NETWORKS
Reduction of transhorizon radio interference in satellite earth stations
[ETN-89-94297] N89-25374

SATELLITE OBSERVATION
Continuous global N-tuple coverage with (2N = 2) satellites
[AD-A206522] N89-25262
Reports on cartography and Geodesy. Series 1: Original reports, number 102
[ISSN-0469-4236] N89-25501
Interpretation of Thematic Mapper data for the acquisition of land information N89-25502
Comparison of satellite-derived dynamical quantities for the stratosphere of the Southern Hemisphere
[NASA-CP-3044] N89-25540

SATELLITE-BORNE INSTRUMENTS
Visible and near-infrared channel calibration of the GOES-6 VISSR using high-altitude aircraft measurements
[NASA-TM-101064] N89-25494
The UARS (Upper Atmosphere Research Satellite): A program to study global ozone change
[NASA-TM-101756] N89-25520
The GOLF helioseismometer on board SOHO N89-25883
VIRGO: The solar monitor experiment on SOHO N89-25884
The solar oscillations imager for SOHO N89-25885
Detector configurations for observations of gravity modes in solar radiance N89-25886
The Michelson Doppler imager for the solar oscillations imager program on SOHO N89-25892

SCALARS
Two-dimensional density matrix and its equations. Scalar and fermionic fields
[DE88-706249] N89-25760

SCALING
Scaling results for the Liquid Sheet Radiator (LSR)
[NASA-TM-102100] N89-25277

SCATTERING CROSS SECTIONS
Method and apparatus for sensor fusion
[NASA-CASE-MSC-21334-1] N89-25360
Model independence of constraints on particle dark matter
[NASA-CR-185337] N89-25688

SCENE ANALYSIS
Forestry interpretation of Thematic Mapper (TM) data using the example of the Frankfurt municipal forest N89-25503
Digital evaluation of SEASAT-SAR radar image data N89-25504
Concurrent spatio-temporal image analysis
[DE89-010260] N89-25593

SCHEDULING
Demonstration of decomposition and optimization in the design of experimental space systems N89-25160
A tool to aid in mapping computational tasks to a hypercube
[DE89-010320] N89-25589

SCIENTISTS
Martinus van Marum: A Dutch scientist in a revolutionary time
[EUT-88-E-194] N89-25402

SCUTUM CONSTELLATION
Rapid photometry of the Delta Scuti variable 63 Her N89-25916
Synthetic light curves and power spectra of Delta Scuti stars: An approach to modeling pulsations N89-25917

SEA LEVEL
Workshop on Sea Level Rise and Coastal Processes
[DE89-010297] N89-25522
Reduce uncertainty in projection of future sea-level change due to ice wastage
[DE89-011483] N89-25526
Responding to changes in sea level engineering implications
[PB89-133466] N89-25555

SEALING
Optical pressure sealing coupling apparatus
[NASA-CASE-MFS-29348-1] N89-25689

SEASAT SATELLITES
Digital evaluation of SEASAT-SAR radar image data N89-25504
Dynamic sea surface topography, gravity and improved orbit accuracies from the direct evaluation of SEASAT altimeter data
[NASA-TM-100735] N89-25539

SECONDARY EMISSION
Seconday ion mass spectrometry of aromatic compounds in acidic mixtures
[DE89-010611] N89-25305

SEDIMENTS
Climatic changes inferred from analyses of lake-sediment cores, Walker Lake, Nevada
[DE89-010740] N89-25525

SEGMENTS
Segmentation of noisy images
[ETN-89-94299] N89-25605

SEISMOGRAPHS
The GOLF helioseismometer on board SOHO N89-25883
The Nice University stellar seismometer N89-25927

SELF ADAPTIVE CONTROL SYSTEMS
Synthetic organisms and self-designing systems
[NASA-CR-185324] N89-25639

SEMANTICS
On the semantics of nonatomic actions
[MEMO-INF-88-13] N89-25610

SEMICONDUCTING FILMS
Narrow bandgap semiconducting silicides: Intrinsic infrared detectors on a silicon chip
[NASA-CR-185372] N89-25746

SEMICONDUCTOR DEVICES
Submicron technologies for the fabrication of monolithic integrated millimeter wave devices on high resistivity silicon
[ETN-89-94624] N89-25757

SEMICONDUCTORS (MATERIALS)
A passivation layer for 3-5 semiconductor materials
[AD-D013963] N89-25737
Femtosecond studies of electron transfer processes at semiconductor interfaces
[DE89-010599] N89-25742
The coupling of thermochemistry and phase diagrams for Group 3-5 semiconductor systems
[DE89-012516] N89-25752

SENSITIVITY
Results of an integrated structure/control law design sensitivity analysis N89-25185
An analytical sensitivity method for use in integrated aeroservoelastic aircraft design
[NASA-TM-101583] N89-25239
Sensitivity analysis of complex coupled systems extended to second and higher order derivatives
[NASA-TM-101587] N89-25354

SEQUENCING
On the semantics of nonatomic actions
[MEMO-INF-88-13] N89-25610

SEQUENTIAL COMPUTERS
The full decomposition of sequential machines with the output behavior realization
[EUT-88-E-199] N89-25583

SERVICE LIFE
Size optimization and production strategy of lunar transport systems
[ILR-MITT-218] N89-25260
Advanced Dual-Shaft Electric Propulsion System Technology Development Program
[DE89-010008] N89-25388

SET THEORY
The ADAMS database language
[DE89-010925] N89-25601

SHAKERS
Simple fixture concepts for multi-axis vibration testing
[DE89-007977] N89-25481

SHAPE CONTROL
Antenna surface contour control system
[NASA-CASE-LAR-13798-1] N89-25363

SHAPES
Grid sensitivity capability for large scale structures N89-25183
Treatment of body forces in boundary element design sensitivity analysis N89-25187
Design sensitivity analysis of boundary element substructures N89-25188
Procedures for shape optimization of gas turbine disks N89-25207
Shape optimal design of elastic bodies using a mixed variational formulation N89-25236
Finite strain example problems for rectangular, cylindrical, and spherical geometries
[DE89-013607] N89-25488
A contour-oriented approach to digital shape analysis
[ISBN-9-09-002004-7] N89-25604

SHEAR FLOW
Acceleration of particles in shear flows N89-25731

SHEAR PROPERTIES
Failure characterization of composite materials
[DE89-008662] N89-25291

SHEAR STRAIN
Initial design and analysis of a capacitive sensor for shear and normal force measurement
[DE89-001821] N89-25438

SHEAR STRESS
Characterization of the effects of three-dimensional states of stress on damping of laminated composites N89-25287

SHELLS (STRUCTURAL FORMS)
Involute composite design evaluation using global design sensitivity derivatives N89-25199

SHIFT REGISTERS
Serial-input polyphase convolvers
[REPT-88-019] N89-25608

SHOCK WAVE INTERACTION
Ion heating in the Bug shock wave N89-25724

SHOCK WAVE PROFILES
Comparison of experimental shock-wave profiles for tungsten and computer simulations using a rate-dependent constitutive model
[DE89-006158] N89-25419

SHOCK WAVE PROPAGATION
A qualitative numerical analysis of some features of propagation of counterflow temperature waves in superfluid helium
[MPIS-9/1988] N89-25424
The ionization structure in shocks in interstellar molecular clouds N89-25726

SHOCK WAVES
Interaction between compression shocks and vertical flows N89-25132
Issues in shock-induced solid state chemistry
[DE89-010769] N89-25309
Technique and data analysis for impact-loaded piezoelectric polymers (PVDF)
[DE89-010529] N89-25342
Shock waves and fragmentation via molecular dynamics
[DE89-007981] N89-25405
Identification of error sources in shock data
[DE89-007655] N89-25440
A numerical study of a class of TVD schemes for compressible mixing layers
[NASA-TM-102194] N89-25651
A class of high resolution explicit and implicit shock-capturing methods
[NASA-TM-101088] N89-25652
Fiber optic sensing in a high explosives environment
[DE89-010863] N89-25695
Ion heating in the Bug shock wave N89-25724

SHOES
Correlation of subjective slipperiness judgements with quantitative COF (Coefficient Of Friction) measurements for structural steel
[PB89-165070] N89-25669

SHORELINES
Responding to changes in sea level engineering implications
[PB89-133466] N89-25555

SHORT TAKEOFF AIRCRAFT
Flap system for short takeoff and landing aircraft
[AD-D013981] N89-25234

SIALON
SiC whisker-reinforced SiAlON composites: Effect of sintering aid content
[DE89-010376] N89-25289

SIDEBANDS
Computer simulation of FEL sidebands in a strongly dispersive waveguide
[DE89-011825] N89-25369

SIGNAL ANALYSIS
Local-frequency description of optical signals and systems
[EUT-88-E-191] N89-25696

SIGNAL DETECTION
On greenhouse gas signal detection strategies
[DE89-009908] N89-25521

SIGNAL PROCESSING
Design of an auto change mechanism and intelligent gripper for the space station
[NASA-CR-185387] N89-25266
Automated Test and Evaluation Center for Waveform Digitizer Systems and Components
[DE89-010226] N89-25441

Optical fiber sensors and signal processing for intelligent structure monitoring
[NASA-CR-185395] N89-25691

SIGNAL RECEPTION
Phase-ambiguity resolution for QPSK modulation systems. Part 1: A review
[NASA-CR-185385] N89-25380
Phase-ambiguity resolution for QPSK modulation systems. Part 2: A method to resolve offset QPSK
[NASA-CR-184971] N89-25381

SIGNAL TO NOISE RATIOS
Segmentation of noisy images
[ETN-89-94299] N89-25605

SIGNAL TRANSMISSION
Reduction of interference by decorrelation and quantized feedback in the case of digital transmission on multi-pair symmetric cables
[FI-44-TB-110] N89-25375

SIGNATURE ANALYSIS
Condition monitoring of machinery using motor current signature analysis
[DE89-008737] N89-25386

SILICIDES
Narrow bandgap semiconducting silicides: Intrinsic infrared detectors on a silicon chip
[NASA-CR-185372] N89-25746

SILICON
Stress-driven diffusive voiding of aluminum conductor lines
[DE89-009832] N89-25387

SILICON ALLOYS
The development of alloys based on Ni3Si
[DE89-010371] N89-25316

SILICON CARBIDES
Characterization of ceramics and intermetallics fabricated by self-propagating high-temperature synthesis
[NASA-TM-102004] N89-25285
SiC whisker-reinforced SiAlON composites: Effect of sintering aid content
[DE89-010376] N89-25289
Strong fibers
[DE89-010596] N89-25292
Evaluation of ceramic coatings on silicon carbide
[DE89-010321] N89-25339

SILICON NITRIDES
Strong fibers
[DE89-010596] N89-25292

SIMD (COMPUTERS)
Fast Fourier Transform algorithm design and tradeoffs
[NASA-CR-185038] N89-25600
Parallel processors and nonlinear structural dynamics algorithms and software
[NASA-CR-185049] N89-25620

SIMULATION
Aeroelastic modeling for the FIT (Functional Integration Technology) team F/A-18 simulation N89-25192
Optimal placement of excitations and sensors by simulated annealing N89-25227
Particle simulation of magnetic reconnection N89-25722
Particle simulation for accretion sheets in narrow double stars N89-25729

SINGLE CRYSTALS
Advances in the development of apparatus and methods for studies of protein monocrystals in coordinate X-ray diffractometers based on two-dimensional proportional chambers
[DE88-706259] N89-25740
Surface structural analysis of small molecules on transition metal single crystal surfaces with low energy electron diffraction
[DE89-010681] N89-25743
Single crystal NMR studies of high temperature superconductors
[DE89-011220] N89-25747

SINGULAR INTEGRAL EQUATIONS
A comparison of the error function and the tanh transformation as progressive rules for double and triple singular integrals
[MATHS-RES-210] N89-25659

SINGULARITY (MATHEMATICS)
The tanh transformation for double integrals with singularities: A progressive rule
[MATHS-RES-203] N89-25658

SINTERING
SiC whisker-reinforced SiAlON composites: Effect of sintering aid content
[DE89-010376] N89-25289
Applicability of microalloying in the production of sintered steel structural parts
[KFK-4481] N89-25329
Sintering schedule and sample geometry effects on the electrical and physical properties of high field varistor materials
[DE89-010523] N89-25384

SITE SELECTION
The GONG site survey --- solar oscillations N89-25855

SKIN (STRUCTURAL MEMBER)
Magneto-inductive skin sensor for robot collision avoidance: A new development
[NASA-CR-185402] N89-25444

SLEWING
Computational experiments in the optimal slewing of flexible structures N89-25226
Time-optimal slewing maneuvers of flexible spacecraft N89-25265

SLURRIES
Proceedings of the Solids Transport Contractors' Review Meeting
[DE89-006720] N89-25414

SODIUM 22
A slow positron beam generator for lifetime studies
[NASA-TM-101590] N89-25433

SOFTWARE ENGINEERING
Rationale for the proposed standard for a generic package of elementary functions for Ada
[DE89-010282] N89-25588
On the role of software reliability in software engineering
[REPT-88-010] N89-25607

SOFTWARE TOOLS
Robust computer-aided synthesis and optimization of linear multivariable control systems with varying plant dynamics via AUTOCON N89-25179
Grid sensitivity capability for large scale structures N89-25183
The role of optimization in the next generation of computer-based design tools N89-25220
Handling arrays in symbolic execution
[REPT-89-003] N89-25609

SOL-GEL PROCESSES
Molecular growth pathways in silica sol-gel polymerization
[DE89-011224] N89-25346

SOLAR ACTIVITY
Solar-geophysical data number 528, August 1988. Part 1: (Prompt reports). Data for July, June 1988 and late data
[PB89-109904] N89-25817
On radiative and convective influences on stellar pulsational stability N89-25828
Solar internal rotation from helioseismology N89-25829
Initial high-degree p-mode frequency splittings from the 1988 Mt. Wilson 60-foot Tower Solar Oscillation Program N89-25832
Measurements of solar oscillations at 37 GHz N89-25859
Frequency shift of solar p-modes as seen by cross correlation analysis N89-25869
Dynamo theory prediction of solar activity N89-25878

SOLAR ACTIVITY EFFECTS
Radial and temporal structure of the internal solar asphericity N89-25833
Solar radiation models and the a1, a3 and a5 splitting coefficients for solar acoustic oscillations N89-25834
Inversion of the solar rotation rate versus depth and latitude N89-25838
A way to examine rotational splittings without explicit foward or inverse computations --- Sun N89-25841
Measurement of the rotational frequency splitting of the solar five-minute oscillations from magneto-optical filter observations N89-25842
The current status of the Birmingham solar seismology network N89-25844
I.R.I.S.: A network for full disk helioseismology N89-25845
Integrated solar disk oscillation measurements using the magneto-optical filter: Tests with a two station network N89-25850
Periodical asymmetry of solar limb darkening N89-25861
Oscillations in presence of local magnetic fields --- solar oscillations N89-25865
Oscillations in sunspots near the solar limb N89-25866
Frequency shift of solar p-modes as seen by cross correlation analysis N89-25869
The influence of the toroidal roll pattern on the sunspot activity N89-25870
Local effects of a major flare on solar five-minute oscillations N89-25872
Viscous magnetohydrodynamic modes and p-mode absorption by sunspots N89-25873
Observations of l- and p-mode oscillations of high degree (500 is less than L is less than 2500) in quiet and active Sun N89-25875
Long period solar oscillations N89-25879
Oscillation frequencies of solar models N89-25902
Solar variability and climatology N89-25909
Solar oscillations: Overshoot at the base of the convection zone N89-25911
Convection and p-mode oscillations --- Sun N89-25912

SOLAR ARRAYS
Space Station Freedom photovoltaic power module design status
[NASA-TM-102073] N89-25273
Launch packaging options for the photovoltaic power module cargo element
[NASA-TM-102072] N89-25275

SOLAR ATMOSPHERE
Dynamics of the overshoot layers and boundary conditions in helioseismology N89-25826
Differential rotation in the solar interior N89-25843
On the dissipation of Alfven waves in magnetic atmospheres and flux tubes N89-25871
Dynamo theory prediction of solar activity N89-25878
Scattering and multiple scattering of acoustic waves in a stratified medium N89-25898
Helioseismological inverse problem: Diagnostics of the structure of the lower solar atmosphere N89-25903
Further progress on the helium abundance determination --- Sun N89-25906
Further implications of solar p-modes as measured in Na and K resonance lines N89-25908
Solar oscillations: Overshoot at the base of the convection zone N89-25911
Convection and p-mode oscillations --- Sun N89-25912
Effects of convective velocities on solar pressure mode frequencies N89-25941

SOLAR CELLS
Estimated performance and future potential of solar dynamic and photovoltaic power systems for selected LEO and HEO missions
[NASA-TM-102083] N89-25280
Development of an Si panel
[ETN-89-94625] N89-25518

SOLAR COLLECTORS
Solar dynamic power module design
[NASA-TM-102055] N89-25269
Support and maneuvering apparatus for solar energy receivers
[DE89-011466] N89-25514
Focusing on the future: Solar thermal energy systems emerge as competitive technologies with major economic potential
[DE89-000851] N89-25516

SOLAR CONSTANT
Detector configurations for observations of gravity modes in solar radiance N89-25886
Integrated light and velocity of solar g modes oscillations N89-25888
Properties of solar gravity mode signals in total irradiance observations N89-25893

SOLAR CORONA
Solar infrared intensity oscillations N89-25847

SOLAR CYCLES
I.R.I.S.: A network for full disk helioseismology N89-25845
Frequency shift of solar p-modes as seen by cross correlation analysis N89-25869
The influence of the toroidal roll pattern on the sunspot activity N89-25870
Dynamo theory prediction of solar activity N89-25878
Long period solar oscillations N89-25879
Modelling the solar oscillation time series by a randomly excited oscillator N89-25942
On taking observers seriously --- solar cycle N89-25943

SOLAR DYNAMIC POWER SYSTEMS
Solar dynamic power module design
[NASA-TM-102055] N89-25269
Estimated performance and future potential of solar dynamic and photovoltaic power systems for selected LEO and HEO missions
[NASA-TM-102083] N89-25280
Focusing on the future: Solar thermal energy systems emerge as competitive technologies with major economic potential
[DE89-000851] N89-25516

SOLAR ENERGY
The introduction of space technology power systems into developing countries
[NASA-TM-102042] N89-25274
Support and maneuvering apparatus for solar energy receivers
[DE89-011466] N89-25514
Focusing on the future: Solar thermal energy systems emerge as competitive technologies with major economic potential
[DE89-000851] N89-25516

SOLAR ENERGY CONVERSION
Solar dynamic power module design
[NASA-TM-102055] N89-25269

Support and maneuvering apparatus for solar energy receivers
[DE89-011466] N89-25514

SOLAR FLARES
Solar physics in the space age
[NASA-NP-106] N89-25818
Local effects of a major flare on solar five-minute oscillations N89-25872
The evolution of energetic particles and the emitted radiation in solar flares
[NASA-CR-185389] N89-25945

SOLAR FLUX DENSITY
Visibility of nonradial pulsation modes in solar continuum intensity measurements N89-25860
On the radiative damping of p-modes in solar magnetic flux concentrations N89-25864

SOLAR GRANULATION
The granulation sensitivity of helioseismology lines N89-25862
Oscillation frequencies of solar models N89-25902

SOLAR GRAVITATION
Nonlinear studies of solar gravity modes driven by nuclear burning of He3 in the core N89-25823
Can solar g-modes be identified from ground-based velocity measurements N89-25880
Detector configurations for observations of gravity modes in solar radiance N89-25886
Integrated light and velocity of solar g modes oscillations N89-25888
Searching for solar g-modes. Tests of a statistical method N89-25889
Observed asymptotic properties of low-degree solar gravity-mode eigenfrequencies N89-25890
Inversion of quasi-periodic deviations between low-degree solar gravity mode eigenfrequencies and asymptotic theory eigenfrequencies N89-25891
Properties of solar gravity mode signals in total irradiance observations N89-25893
The search for solar gravity modes N89-25894

SOLAR INSTRUMENTS
Solar infrared intensity oscillations N89-25847
The stable solar analyzer N89-25858
VIRGO: The solar monitor experiment on SOHO N89-25884
The solar oscillations imager for SOHO N89-25885
Detector configurations for observations of gravity modes in solar radiance N89-25886
Luminosity Oscillations Imager (LOI) N89-25887
The Michelson Doppler imager for the solar oscillations imager program on SOHO N89-25892
GOLF: Simulations of the re-emission of the resonance cell N89-25895
Solar oscillations instrumentation and measurement theory N89-25925

SOLAR INTERIOR
Solar internal rotation from helioseismology N89-25829
Radial and latitudinal gradients in the solar internal angular velocity N89-25831
Radial and temporal structure of the internal solar asphericity N89-25833
A way to examine rotational splittings without explicit foward or inverse computations --- Sun N89-25841
Measurement of the rotational frequency splitting of the solar five-minute oscillations from magneto-optical filter observations N89-25842
Differential rotation in the solar interior N89-25843
I.R.I.S.: A network for full disk helioseismology N89-25845
Using oscillation data to probe the internal rotation and magnetism of the Sun N89-25863
Helioseismology from the South Pole: Comparison of 1987 and 1981 results N89-25868
The search for solar gravity modes N89-25894
Current options for the equation of state of the solar interior N89-25897
Helioseismological inverse problem: Sound speed in the solar interior N89-25901
Determination of the solar internal sound speed by means of a differential asymptotic inversion N89-25904
An inversion method based on the Moore-Penrose generalized inverse matrix N89-25910
Determination of the solar sound speed by an asymptotic inversion technique N89-25913

SOLAR LIMB
Periodical asymmetry of solar limb darkening N89-25861
Oscillations in sunspots near the solar limb N89-25866

SOLAR MAGNETIC FIELD
Solar physics in the space age
[NASA-NP-106] N89-25818
Solar p-mode frequency splittings N89-25840
Using oscillation data to probe the internal rotation and magnetism of the Sun N89-25863
On the radiative damping of p-modes in solar magnetic flux concentrations N89-25864
Oscillations in presence of local magnetic fields --- solar oscillations N89-25865
The influence of the toroidal roll pattern on the sunspot activity N89-25870
The influence of a chromospheric magnetic field on p- and f-modes N89-25874

SOLAR MAXIMUM MISSION
Solar variability and climatology N89-25909

SOLAR OBLATENESS
Solar p-mode frequency splittings N89-25840

SOLAR OBSERVATORIES
Solar physics in the space age
[NASA-NP-106] N89-25818
The current status of the Birmingham solar seismology network N89-25844
I.R.I.S.: A network for full disk helioseismology N89-25845
Solar luminosity oscillations from two stations and correlation with velocity measurements N89-25846
Solar Luminosity Oscillation Telescope (SLOT) N89-25848
Integrated solar disk oscillation measurements using the magneto-optical filter: Tests with a two station network N89-25850
Acquisition and reduction procedures for MOF Doppler-magnetograms --- solar observation N89-25851
The GONG instrument --- solar oscillations N89-25854
The GONG site survey --- solar oscillations N89-25855
The GONG data reduction and analysis system --- solar oscillations N89-25856
The stable solar analyzer N89-25858
Observations of f- and p-mode oscillations of high degree (500 is less than L is less than 2500) in quiet and active Sun N89-25875
IPHIR: The helioseismology experiment on the PHOBOS mission N89-25881
SOHO status N89-25882

SOLAR OSCILLATIONS
The excitation and damping of solar oscillations N89-25820
On the k-mechanism and the multidimensional Eddington approximation N89-25821
On the diagnostic of 5m oscillations through photospheric line profiles N89-25822
Nonlinear studies of solar gravity modes driven by nuclear burning of He3 in the core N89-25823
Linewidth of low degree acoustic modes of the Sun N89-25824
Measurements of high degree solar oscillation amplitudes N89-25825
Measurements of oscillation parameters from synthetic times series --- solar oscillations N89-25827
On the measurement of solar rotation using high-degree p-mode oscillations N89-25830
Initial high-degree p-mode frequency splittings from the 1988 Mt. Wilson 60-foot Tower Solar Oscillation Program N89-25832
Solar radiation models and the a1, a3 and a5 splitting coefficients for solar acoustic oscillations N89-25834
Oscillation ring diagrams and the thermodynamics of the outer solar convection zone N89-25836
Inversion of the solar rotation rate versus depth and latitude N89-25838
Rotational splitting of low l solar p-mode N89-25839
A way to examine rotational splittings without explicit foward or inverse computations --- Sun N89-25841
Measurement of the rotational frequency splitting of the solar five-minute oscillations from magneto-optical filter observations N89-25842
Solar luminosity oscillations from two stations and correlation with velocity measurements N89-25846
Solar infrared intensity oscillations N89-25847
Solar Luminosity Oscillation Telescope (SLOT) N89-25848
Effect of atmospheric extinction on solar radial velocity measurements N89-25849
Integrated solar disk oscillation measurements using the magneto-optical filter: Tests with a two station network N89-25850
New thresholds for ground-based photometry of solar intensity oscillations N89-25852
An attempt to understand the Stanford p-mode data --- solar oscillations N89-25853
The GONG instrument --- solar oscillations N89-25854
The GONG site survey --- solar oscillations N89-25855
The GONG data reduction and analysis system --- solar oscillations N89-25856
Measurements of solar oscillations at 37 GHz N89-25859
Visibility of nonradial pulsation modes in solar continuum intensity measurements N89-25860
Using oscillation data to probe the internal rotation and magnetism of the Sun N89-25863
Oscillations in presence of local magnetic fields --- solar oscillations N89-25865
Oscillations in sunspots near the solar limb N89-25866
Solar p-modes frequency variations between 1980 and 1986 N89-25867
Helioseismology from the South Pole: Comparison of 1987 and 1981 results N89-25868
Frequency shift of solar p-modes as seen by cross correlation analysis N89-25869
Local effects of a major flare on solar five-minute oscillations N89-25872
Viscous magnetohydrodynamic modes and p-mode absorption by sunspots N89-25873
The influence of a chromospheric magnetic field on p- and f-modes N89-25874
Observations of f- and p-mode oscillations of high degree (500 is less than L is less than 2500) in quiet and active Sun N89-25875
Evidence for a thin perturbative layer near the base of the solar convection zone N89-25876
Long period solar oscillations N89-25879
Can solar g-modes be identified from ground-based velocity measurements N89-25880
VIRGO: The solar monitor experiment on SOHO N89-25884
The solar oscillations imager for SOHO N89-25885
Luminosity Oscillations Imager (LOI) N89-25887
Integrated light and velocity of solar g modes oscillations N89-25888
Searching for solar g-modes. Tests of a statistical method N89-25889
Observed asymptotic properties of low-degree solar gravity-mode eigenfrequencies N89-25890
Inversion of quasi-periodic deviations between low-degree solar gravity mode eigenfrequencies and asymptotic theory eigenfrequencies N89-25891
The Michelson Doppler imager for the solar oscillations imager program on SOHO N89-25892
Properties of solar gravity mode signals in total irradiance observations N89-25893
The search for solar gravity modes N89-25894
GOLF: Simulations of the re-emission of the resonance cell N89-25895
Study of solar structure based on p-mode helioseismology N89-25896
Oscillation frequencies of solar models N89-25902
Modelling the variation of solar p-mode frequencies N89-25907
Further implications of solar p-modes as measured in Na and K resonance lines N89-25908
Solar oscillations: Overshoot at the base of the convection zone N89-25911
Convection and p-mode oscillations --- Sun N89-25912
Solar oscillations instrumentation and measurement theory N89-25925
On the thermal surface boundary condition for solar pulsations N89-25931
Asymptotic approximations of nonradial oscillation modes of the Sun N89-25932
Effects of convective velocities on solar pressure mode frequencies N89-25941
Modelling the solar oscillation time series by a randomly excited oscillator N89-25942
On taking observers seriously --- solar cycle N89-25943

SOLAR PHYSICS
Solar-geophysical data number 528, August 1988. Part 1: (Prompt reports). Data for July, June 1988 and late data
[PB89-109904] N89-25817
Solar physics in the space age
[NASA-NP-106] N89-25818
Visibility of nonradial pulsation modes in solar continuum intensity measurements N89-25860
Solar oscillations instrumentation and measurement theory N89-25925
On the thermal surface boundary condition for solar pulsations N89-25931
Asymptotic approximations of nonradial oscillation modes of the Sun N89-25932
On taking observers seriously --- solar cycle N89-25943

SOLAR PROMINENCES
Local effects of a major flare on solar five-minute oscillations N89-25872

SOLAR RADIATION
Inversion of the solar rotation rate versus depth and latitude N89-25838
Solar infrared intensity oscillations N89-25847

Solar Luminosity Oscillation Telescope (SLOT) N89-25848
New thresholds for ground-based photometry of solar intensity oscillations N89-25852
Detector configurations for observations of gravity modes in solar radiance N89-25886
Properties of solar gravity mode signals in total irradiance observations N89-25893

SOLAR RADIO EMISSION
Solar-geophysical data number 528, August 1988. Part 1: (Prompt reports). Data for July, June 1988 and late data
[PB89-109904] N89-25817

SOLAR REFLECTORS
Support and maneuvering apparatus for solar energy receivers
[DE89-011466] N89-25514

SOLAR ROTATION
Solar internal rotation from helioseismology N89-25829
On the measurement of solar rotation using high-degree p-mode oscillations N89-25830
Solar radiation models and the a1, a3 and a5 splitting coefficients for solar acoustic oscillations N89-25834
Is the Sun really a rigid rotator N89-25835
Angular momentum transport and dynamo action in the Sun: A report on implications of a recent helioseismic estimate of solar rotation N89-25837
Rotational splitting of low l solar p-mode N89-25839
Solar p-mode frequency splittings N89-25840
A way to examine rotational splittings without explicit foward or inverse computations — Sun N89-25841
Measurement of the rotational frequency splitting of the solar five-minute oscillations from magneto-optical filter observations N89-25842
Differential rotation in the solar interior N89-25843
Effect of atmospheric extinction on solar radial velocity measurements N89-25849
Using oscillation data to probe the internal rotation and magnetism of the Sun N89-25863
An inversion method based on the Moore-Penrose generalized inverse matrix N89-25910

SOLAR SPECTRA
The granulation sensitivity of helioseismology lines N89-25862
Solar p-modes frequency variations between 1980 and 1986 N89-25867
Frequency shift of solar p-modes as seen by cross correlation analysis N89-25869
Magnetically induced spectral line redshifts full disk measurements N89-25877
Sound velocity distribution in the Sun inferred from asymptotic inversion of p-mode spectra N89-25900
Further implications of solar p-modes as measured in Na and K resonance lines N89-25908
The effect of a nonspherical sound speed on the acoustic frequency spectrum of the Sun N89-25914
On the thermal surface boundary condition for solar pulsations N89-25931

SOLAR SPECTROMETERS
A detector of small gradients of transparency of the terrestrial atmosphere N89-25857

SOLAR SYSTEM
Solar system exploration
[NASA-TM-101784] N89-25944

SOLAR TERRESTRIAL INTERACTIONS
Solar physics in the space age
[NASA-NP-106] N89-25818
Solar variability and climatology N89-25909

SOLAR THERMAL ELECTRIC POWER PLANTS
Focusing on the future: Solar thermal energy systems emerge as competitive technologies with major economic potential
[DE89-000851] N89-25516

SOLAR TOTAL ENERGY SYSTEMS
Focusing on the future: Solar thermal energy systems emerge as competitive technologies with major economic potential
[DE89-000851] N89-25516

SOLAR WIND
Magnetic reconnection in general three-dimensional systems N89-25717

SOLDERED JOINTS
Thermomechanical fatigue of solder joints: A new comprehensive test method
[DE89-008045] N89-25314

SOLDERS
Thermomechanical fatigue of solder joints: A new comprehensive test method
[DE89-008045] N89-25314

SOLID ELECTROLYTES
Manifold, bus support and coupling arrangement for solid oxide fuel cells
[DE89-009604] N89-25508

SOLID PROPELLANT ROCKET ENGINES
Involute composite design evaluation using global design sensitivity derivatives N89-25199

SOLID STATE
Issues in shock-induced solid state chemistry
[DE89-010769] N89-25309

SOLID STATE DEVICES
Development of an Si panel
[ETN-89-94625] N89-25518

SOLIDIFICATION
The influence of cooling rate on the ferrite content of stainless steel alloys
[DE89-009966] N89-25315

SOLIDS
PRONTO 3D: A three-dimensional transient solid dynamics program
[DE89-010517] N89-25590

SOLIDS FLOW
Proceedings of the Solids Transport Contractors' Review Meeting
[DE89-006720] N89-25414

SOLITARY WAVES
Periodic and solitary waves on thin, horizontal, gas-sheared liquid films
[DE89-010655] N89-25416
Statistical fluctuations as the origin of nontopological solitons
[NASA-CR-185351] N89-25680

SOOT
Determination of combustion gas temperatures by infrared radiometry in sooting and nonsooting flames
[NASA-TP-2900] N89-25409

SOUND PROPAGATION
Diffusion, fluid flow and sound propagation in disordered media
[DE89-010937] N89-25407
Experimental investigation on transcritical heat transfer in He 2
[MPIS-MITT-90] N89-25426

SOUND WAVES
Scattering and multiple scattering of acoustic waves in a stratified medium N89-25898
Helioseismological inverse problem: Sound speed in the solar interior N89-25901
Helioseismological inverse problem: Diagnostics of the structure of the lower solar atmosphere N89-25903
Determination of the solar sound speed by an asymptotic inversion technique N89-25913
The effect of a nonspherical sound speed on the acoustic frequency spectrum of the Sun N89-25914

SPACE COMMUNICATION
Phase-ambiguity resolution for QPSK modulation systems. Part 1: A review
[NASA-CR-185385] N89-25380
Phase-ambiguity resolution for QPSK modulation systems. Part 2: A method to resolve offset QPSK
[NASA-CR-184971] N89-25381

SPACE ERECTABLE STRUCTURES
Antenna surface contour control system
[NASA-CASE-LAR-13798-1] N89-25363
Pactruss support structure for precision segmented reflectors
[NASA-CR-181747] N89-25484

SPACE EXPLORATION
United States and Western Europe cooperation in planetary exploration
[NASA-CR-184941] N89-25776
Solar system exploration
[NASA-TM-101784] N89-25944
Space directorate research and technology accomplishments for FY 1988
[NASA-TM-101597] N89-25947

SPACE MAINTENANCE
Space station operations task force. Panel 1 report: Space operations and support systems
[NASA-TM-101816] N89-25244

SPACE MISSIONS
Space nuclear reactor shields for manned and unmanned applications
[NASA-TM-102064] N89-25272
SOHO status N89-25882

SPACE OBSERVATIONS (FROM EARTH)
The GONG site survey — solar oscillations N89-25855
A detector of small gradients of transparency of the terrestrial atmosphere N89-25857
Can solar g-modes be identified from ground-based velocity measurements N89-25880
MUSICOS (MUlti-Site COntinuous Spectroscopy): Objectives and prospects for asteroseismology N89-25940

SPACE PLASMAS
Gravitational-like phase transition of a classical Coulomb plasma N89-25727

SPACE PLATFORMS
Space station operations task force. Panel 1 report: Space operations and support systems
[NASA-TM-101816] N89-25244
Space station operations task force. Panel 2 report: Ground operations and support systems
[NASA-TM-101817] N89-25245
Space station operations task force. Panel 3 report: User development and integration
[NASA-TM-101818] N89-25246
Space station operations task force. Panel 4 report: Management integration
[NASA-TM-101819] N89-25247
Space station operations task force summary report
[NASA-TM-101820] N89-25248
Space station operations task force. Executive summary
[NASA-TM-101780] N89-25249
Middeck Active Control Experiment (MACE), phase A
[NASA-CR-185331] N89-25258

SPACE POWER UNIT REACTORS
CSTI High Capacity Power
[NASA-TM-102059] N89-25282

SPACE PROCESSING
Spiral vane bioreactor
[NASA-CASE-MSC-21361-1] N89-25557

SPACE SHUTTLE BOOSTERS
Aerodynamic flight evaluation analysis and data base update
[NASA-CR-183654] N89-25276

SPACE SHUTTLE MAIN ENGINE
Space Shuttle Main Engine structural analysis and data reduction/evaluation. Volume 2: High pressure oxidizer turbo-pump turbine end bearing analysis
[NASA-CR-183664] N89-25270
Influence of rubbing on rotor dynamics, part 1
[NASA-CR-183648-PT-1] N89-25463

SPACE SHUTTLE ORBITERS
NDE of the space shuttle orbiter thermal protection system, phase 2
[NASA-CR-185471] N89-25257

SPACE STATION POWER SUPPLIES
Solar dynamic power module design
[NASA-TM-102055] N89-25269
Space Station Freedom photovoltaic power module design status
[NASA-TM-102073] N89-25273
An evaluation of the General Dynamics 20 kHz 5 kW Breadboard for space station electrical power at MSFC
[NASA-TM-100367] N89-25278
Challenges for future space power systems
[NASA-TM-102063] N89-25506

SPACE STATION STRUCTURES
Smart tunnel: Docking mechanism
[NASA-CASE-MSC-21360-1] N89-25263
Solar dynamic power module design
[NASA-TM-102055] N89-25269
Space Station Freedom photovoltaic power module design status
[NASA-TM-102073] N89-25273
Pactruss support structure for precision segmented reflectors
[NASA-CR-181747] N89-25484

SPACE STATIONS
Space station operations task force. Panel 1 report: Space operations and support systems
[NASA-TM-101816] N89-25244
Space station operations task force. Panel 2 report: Ground operations and support systems
[NASA-TM-101817] N89-25245
Space station operations task force. Panel 3 report: User development and integration
[NASA-TM-101818] N89-25246
Space station operations task force. Panel 4 report: Management integration
[NASA-TM-101819] N89-25247
Space station operations task force summary report
[NASA-TM-101820] N89-25248
Space station operations task force. Executive summary
[NASA-TM-101780] N89-25249
Space station architecture, module, berthing hub, shell assembly, berthing mechanism and utility connection channel
[NASA-CASE-ARC-11505-2] N89-25266
Launch packaging options for the photovoltaic power module cargo element
[NASA-TM-102072] N89-25275
Development and testing of a 20-kHz component test bed
[NASA-TM-102141] N89-25403
Traction-drive transmission for telerobotic joints
[DE89-005337] N89-25461
Performance issues in management of the Space Station Information System
[NASA-CR-185409] N89-25773

Space directorate research and technology accomplishments for FY 1988
[NASA-TM-101597] N89-25947

SPACE STORAGE
GIRL cryotechnics and preparation of a TEXUS experiment on superfluid helium dynamics
[ETN-89-94631] N89-25357

SPACE TRANSPORTATION
Flight performance model for a geostationary transportation system
[ILR-MITT-206] N89-25259

SPACE TRANSPORTATION SYSTEM
Launch packaging options for the photovoltaic power module cargo element
[NASA-TM-102072] N89-25275

SPACE-TIME FUNCTIONS
Strings on hyperelliptic supersurfaces
[DE88-705991] N89-25758

SPACEBORNE ASTRONOMY
Solar physics in the space age
[NASA-NP-106] N89-25818
IPHIR: The helioseismology experiment on the PHOBOS mission N89-25881
SOHO status N89-25882

SPACECRAFT CONFIGURATIONS
Experiences in applying optimization techniques to configurations for the Control of Flexible Structures (COFS) program N89-25228

SPACECRAFT CONSTRUCTION MATERIALS
Materials and structures for 2000 and beyond: An attempted forecast
[DFVLR-MITT-89-02] N89-25358

SPACECRAFT CONTROL
Time-optimal slewing maneuvers of flexible spacecraft N89-25265

SPACECRAFT DESIGN
Results of an integrated structure/control law design sensitivity analysis N89-25185
Recent Advances in Multidisciplinary Analysis and Optimization, part 3
[NASA-CP-3031-PT-3] N89-25201
The art of spacecraft design: A multidisciplinary challenge N89-25209
Optimization of structure and control system N89-25223
A novel implementation of method of optimality criterion in synthesizing spacecraft structures with natural frequency constraints N89-25225
Conjugating binary systems for spacecraft thermal control. Appendix C: Aeroassist Flight Experiment Carrier Vehicle preliminary stress analysis
[NASA-CR-183609] N89-25261
Solar dynamic power module design
[NASA-TM-102055] N89-25269

SPACECRAFT DOCKING
Smart tunnel: Docking mechanism
[NASA-CASE-MSC-21360-1] N89-25263
Space station architecture, module, berthing hub, shell assembly, berthing mechanism and utility connection channel
[NASA-CASE-ARC-11505-2] N89-25266

SPACECRAFT INSTRUMENTS
New atmospheric sensor analysis study
[NASA-CR-183597] N89-25431

SPACECRAFT MANEUVERS
Time-optimal slewing maneuvers of flexible spacecraft N89-25265

SPACECRAFT POWER SUPPLIES
Survivable pulse power space radiator
[DE89-010120] N89-25264
Launch packaging options for the photovoltaic power module cargo element
[NASA-TM-102072] N89-25275
Development and testing of a 20-kHz component test bed
[NASA-TM-102141] N89-25403
Challenges for future space power systems
[NASA-TM-102063] N89-25506

SPACECRAFT PROPULSION
Advanced APS impacts on vehicle payloads
[NASA-TM-102086] N89-25254

SPACECRAFT RADIATORS
Scaling results for the Liquid Sheet Radiator (LSR)
[NASA-TM-102100] N89-25277

SPACECRAFT SHIELDING
NDE of the space shuttle orbiter thermal protection system, phase 2
[NASA-CR-185471] N89-25257

SPACECRAFT STRUCTURES
A novel implementation of method of optimality criterion in synthesizing spacecraft structures with natural frequency constraints N89-25225
Materials and structures for 2000 and beyond: An attempted forecast
[DFVLR-MITT-89-02] N89-25358

SPACECRAFT TEMPERATURE
Conjugating binary systems for spacecraft thermal control. Appendix C: Aeroassist Flight Experiment Carrier Vehicle preliminary stress analysis
[NASA-CR-183609] N89-25261

SPACELAB
Spacelab Data Processing Facility
[NASA-TM-101808] N89-25252

SPACELAB PAYLOADS
Synchronization of the ground station atomic clocks using weighted transportable cesium time standards in the navigation experiment (NAVEX)
[DFVLR-MITT-89-01] N89-25448

SPALLING
Characterization of booster-rocket propellants and their simulants
[DE89-012497] N89-25352

SPANWISE BLOWING
Spanwise lift distributions and wake velocity surveys of a semi-span wing with a discontinuous twist
[NASA-CR-177532] N89-25122

SPATIAL DEPENDENCIES
Regional validation of general circulation models N89-25538

SPATIAL DISTRIBUTION
The behavior of water vapor in the Mars atmosphere N89-25801

SPATIAL FILTERING
Adaptive enhancement of magnetoencephalographic signals via multichannel filtering
[DE89-005464] N89-25569

SPATIAL RESOLUTION
Atomic resolution microscopy
[DE89-009227] N89-25679

SPECIFIC IMPULSE
Performance characterization and transient investigation of multipropellant resistojets
[NASA-TM-102118] N89-25283

SPECIFICATIONS
Vehicle performance tests of the Ford/GE first generation single-shaft (ETX-I) alternating current propulsion system
[DE89-011115] N89-25392
Performance characteristics for advanced control systems
[DE89-010362] N89-25637

SPECTRAL LINE WIDTH
Linewidth of low degree acoustic modes of the Sun N89-25824

SPECTRAL METHODS
Spectral shaping and phase control of a fast-wave current drive antenna array
[DE89-011567] N89-25368

SPECTRAL REFLECTANCE
Microwave scattering models and basic experiments
[NASA-CR-185393] N89-25364

SPECTRAL RESOLUTION
Interpretation of Thematic Mapper data for the acquisition of land information N89-25502

SPECTRAL SIGNATURES
Investigation of submicrometer aerosols for apportioning the impacts of airborne particulate matter at Deep Creek Lake
[DE89-008186] N89-25524

SPECTROMETERS
Search the spectrometric characteristics of microchannel plate photomultipliers
[DE88-706260] N89-25437
An inductively coupled plasma spectrometer for on-line, real-time process gas analysis
[DE89-010610] N89-25442

SPECTROPHOTOMETRY
The 2060 Chiron: CCD photometry
[NASA-CR-185068] N89-25435

SPECTRORADIOMETERS
VIRGO: The solar monitor experiment on SOHO N89-25884

SPECTROSCOPY
The application of Rutherford backscattering and channeling techniques to the characterization of ceramics
[DE89-010257] N89-25333
A slow positron beam generator for lifetime studies
[NASA-TM-101590] N89-25433
Digital dynamic amplitude-frequence spectral analyzer
[DE88-706256] N89-25436
Z subeff measurements and low-Z impurity transport for NBI and ICRF heated plasma in JIPP T-IIU tokamak
[IPPJ-896] N89-25701

SPECTRUM ANALYSIS
Digital dynamic amplitude-frequence spectral analyzer
[DE88-706256] N89-25436
Local-frequency description of optical signals and systems
[EUT-88-E-191] N89-25698
Rotational splitting of low l solar p-mode N89-25839
Sound velocity distribution in the Sun inferred from asymptotic inversion of p-mode spectra N89-25900
Solar-like oscillations in late spectral class stars N89-25935
Modelling the solar oscillation time series by a randomly excited oscillator N89-25942

SPECULAR REFLECTION
Free-molecule-flow force and moment coefficients of the aeroassist flight experiment vehicle
[NASA-TM-101600] N89-25124

SPHERES
Finite strain example problems for rectangular, cylindrical, and spherical geometries
[DE89-013607] N89-25488

SPIN-LATTICE RELAXATION
Single crystal NMR studies of high temperature superconductors
[DE89-011220] N89-25747

SPOILERS
Flap system for short takeoff and landing aircraft
[AD-D013981] N89-25234

SPRAYERS
Warm fog dissipation using large volume water sprays
[NASA-CASE-MFS-25962-1] N89-25242

SPUTTERING
Deposition of dielectric optical coatings: A microstructural study of the deposited layers and interfaces
[DE89-011205] N89-25694
Artificially structured superconductors
[DE89-009116] N89-25733
The formation and analysis of thin film high temperature superconductors
[DE89-011177] N89-25745

SQUID (DETECTORS)
Squid concepts and systems
[DE89-010384] N89-25755

STABILITY
High-performance, extrusion-cast explosives with low sensitivity
[DE89-010279] N89-25349
Bistability in a laser with injected signal
[DE88-706003] N89-25449

STABILITY DERIVATIVES
Free-molecule-flow force and moment coefficients of the aeroassist flight experiment vehicle
[NASA-TM-101600] N89-25124

STABILIZATION
Controller for stabilization of high voltage
[NAL-TM-MT-8702] N89-25382

STABILIZERS (AGENTS)
Studies of oxidative degradation of polymers induced by ionizing radiation
[DE89-008279] N89-25335

STAGNATION POINT
Unsteady stagnation-point heat transfer during passage of a concentrated vortex
[NASA-CR-182297] N89-25404

STAINLESS STEELS
The influence of cooling rate on the ferrite content of stainless steel alloys
[DE89-009966] N89-25315
Cavitation kinetics during GTA (Gas Tungsten Arc) welding of helium containing stainless steel
[DE89-012514] N89-25467

STANDARDS
Rationale for the proposed standard for a generic package of elementary functions for Ada
[DE89-010282] N89-25588

STAR CLUSTERS
Variable star statistics in open clusters: NGC 6192 N89-25920

STAR FORMATION
The origin of ultra-compact binaries
[NASA-TM-101792] N89-25780
Ambipolar diffusion and core formation in molecular clouds N89-25782

STARS
The ionization structure in shocks in interstellar molecular clouds N89-25726

STATISTICAL ANALYSIS
FAA statistical handbook of aviation: Calendar year 1987
[AD-A200917] N89-25113
Research on optimization-based design N89-25176
Estimating effective moduli of composites using quantitative image analysis
[DE89-012292] N89-25295
Reduction of interference by decorrelation and quantized feedback in the case of digital transmission on multi-pair symmetric cables
[FI-44-TB-110] N89-25375
Regional validation of general circulation models N89-25538
Data adjustment by gravity differences N89-25548

Statistical fluctuations as the origin of nontopological solitons
[NASA-CR-185351] N89-25680
STATISTICAL DISTRIBUTIONS
The evolution of energetic particles and the emitted radiation in solar flares
[NASA-CR-185389] N89-25945
STATISTICAL MECHANICS
Dynamic simulation of dislocation pattern formation in metals during high temperature monotonic and cyclic deformation N89-25477
Renormalization of topological field theory
[DE88-705998] N89-25759
Evolution of cosmic string networks
[NASA-CR-185467] N89-25788
STATORS
Influence of rubbing on rotor dynamics, part 1
[NASA-CR-183648-PT-1] N89-25463
Influence of rubbing on rotor dynamics, part 2
[NASA-CR-183649-PT-2] N89-25464
STEADY FLOW
Stationary ideal MHD with incompressible mass flow and general symmetry N89-25732
STEAM
Method of production H2 using a rotating drum reactor with a pulse jet heat source
[DE89-009764] N89-25348
STEELS
Model building for an ingot heating process: Physical modeling approach and identification approach
[EUT-88-E-196] N89-25331
Correlation of subjective slipperiness judgements with quantitative COF (Coefficient Of Friction) measurements for structural steel
[PB89-165070] N89-25669
STELLAR ACTIVITY
Reminiscence of a stellar pulsation theorist
[DE89-011165] N89-25786
STELLAR ATMOSPHERES
On the relation of the Duvall phase function to the upper layers on the convection zone --- stellar models N89-25905
STELLAR COMPOSITION
Further progress on the helium abundance determination --- Sun N89-25906
STELLAR ENVELOPES
On radiative and convective influences on stellar pulsational stability N89-25828
STELLAR EVOLUTION
Nuclear astrophysics of supernovae
[DE89-012534] N89-25787
End points of stellar evolution investigated by seismology on white dwarf stars N89-25934
Solar-like oscillations in late spectral class stars N89-25935
Radial vibrations in a 5 solar M hydrogen-helium star N89-25938
STELLAR INTERIORS
Epsilon Eridani revisited N89-25937
The influence of the equation of state on the zero-age main sequence and the Sun N89-25939
STELLAR LUMINOSITY
The 2060 Chiron: CCD photometry
[NASA-CR-185068] N89-25435
Solar luminosity oscillations from two stations and correlation with velocity measurements N89-25846
Periodical asymmetry of solar limb darkening N89-25861
Luminosity Oscillations Imager (LOI) N89-25887
The search for solar-type oscillations in other stars using the Michelson Interferometric Stellar Oscillation Spectrometer (ISOS) N89-25918
Solar calibration of asteroseismology N89-25921
Search for rapid oscillations in the Northern Ap stars HD62140, HD81009 and HD22374 N89-25928
A Fabry-Perot interferometric stellar oscillation spectrometer N89-25929
Some tests of the precision of CCD differential photometry measurements of bright double stars N89-25930
The mass-luminosity relationship for solar-type stars N89-25936
Epsilon Eridani revisited N89-25937
Radial vibrations in a 5 solar M hydrogen-helium star N89-25938
STELLAR MAGNETIC FIELDS
Ripple structure in degenerate electron gas-dominated stars with intense magnetic fields N89-25783
High precision velocity measurements of Procyon using the 7699 A line of potassium N89-25922
A prototype stellar photometer for magnetic field and Doppler measurements N89-25926
STELLAR MASS
The mass-luminosity relationship for solar-type stars N89-25936
STELLAR MASS ACCRETION
Particle simulation for accretion sheets in narrow double stars N89-25729
STELLAR MASS EJECTION
The origin of ultra-compact binaries
[NASA-TM-101792] N89-25780
High mass loss in the young Sun N89-25933
STELLAR MODELS
Ripple structure in degenerate electron gas-dominated stars with intense magnetic fields N89-25783
Oscillation ring diagrams and the thermodynamics of the outer solar convection zone N89-25836
An attempt to understand the Stanford p-mode data --- solar oscillations N89-25853
Current options for the equation of state of the solar interior N89-25897
Towards an independent calibration of the mixing-length theory N89-25899
Oscillation frequencies of solar models N89-25902
On the relation of the Duvall phase function to the upper layers on the convection zone --- stellar models N89-25905
Modelling the variation of solar p-mode frequencies N89-25907
Synthetic light curves and power spectra of Delta Scuti stars: An approach to modeling pulsations N89-25917
High mass loss in the young Sun N89-25933
Radial vibrations in a 5 solar M hydrogen-helium star N89-25938
On taking observers seriously --- solar cycle N89-25943
STELLAR MOTIONS
The search for radial velocity variations in rapidly oscillating Ap stars using the Fabry-Perot Interferometric Stellar Oscillation Spectrometer (FP-ISOS) N89-25923
Search for rapid oscillations in the Northern Ap stars HD62140, HD81009 and HD22374 N89-25928
STELLAR OSCILLATIONS
Seismology of the Sun and Sun-Like Stars
[ESA-SP-286] N89-25819
On the relation of the Duvall phase function to the upper layers on the convection zone --- stellar models N89-25905
Observed p-mode spectra of Ap stars and the Sun N89-25915
The search for solar-type oscillations in other stars using the Michelson Interferometric Stellar Oscillation Spectrometer (ISOS) N89-25918
High precision velocity observations of Arcturus using the 7699 A line of potassium N89-25919
Solar calibration of asteroseismology N89-25921
High precision velocity measurements of Procyon using the 7699 A line of potassium N89-25922
The search for radial velocity variations in rapidly oscillating Ap stars using the Fabry-Perot Interferometric Stellar Oscillation Spectrometer (FP-ISOS) N89-25923
A prototype stellar photometer for magnetic field and Doppler measurements N89-25926
The Nice University stellar seismometer N89-25927
Search for rapid oscillations in the Northern Ap stars HD62140, HD81009 and HD22374 N89-25928
A Fabry-Perot interferometric stellar oscillation spectrometer N89-25929
On the thermal surface boundary condition for solar pulsations N89-25931
End points of stellar evolution investigated by seismology on white dwarf stars N89-25934
Solar-like oscillations in late spectral class stars N89-25935
Epsilon Eridani revisited N89-25937
MUSICOS (MUlti-SIte COntinuous Spectroscopy): Objectives and prospects for asteroseismology N89-25940
STELLAR PHYSICS
Neutron stars: A cosmic hadron physics laboratory
[NASA-CR-185051] N89-25777
Ripple structure in degenerate electron gas-dominated stars with intense magnetic fields N89-25783
Variable star statistics in open clusters: NGC 6192 N89-25920
Solar calibration of asteroseismology N89-25921
The Nice University stellar seismometer N89-25927
A Fabry-Perot interferometric stellar oscillation spectrometer N89-25929
High mass loss in the young Sun N89-25933
End points of stellar evolution investigated by seismology on white dwarf stars N89-25934
The mass-luminosity relationship for solar-type stars N89-25936
Epsilon Eridani revisited N89-25937
Radial vibrations in a 5 solar M hydrogen-helium star N89-25938
The influence of the equation of state on the zero-age main sequence and the Sun N89-25939
MUSICOS (MUlti-SIte COntinuous Spectroscopy): Objectives and prospects for asteroseismology N89-25940
STELLAR RADIATION
On radiative and convective influences on stellar pulsational stability N89-25828
Synthetic light curves and power spectra of Delta Scuti stars: An approach to modeling pulsations N89-25917
Search for rapid oscillations in the Northern Ap stars HD62140, HD81009 and HD22374 N89-25928
STELLAR ROTATION
The 2060 Chiron: CCD photometry
[NASA-CR-185068] N89-25435
STELLAR SPECTRA
Observed p-mode spectra of Ap stars and the Sun N89-25915
Synthetic light curves and power spectra of Delta Scuti stars: An approach to modeling pulsations N89-25917
High precision velocity observations of Arcturus using the 7699 A line of potassium N89-25919
Variable star statistics in open clusters: NGC 6192 N89-25920
High precision velocity measurements of Procyon using the 7699 A line of potassium N89-25922
STELLAR SPECTROPHOTOMETRY
New thresholds for ground-based photometry of solar intensity oscillations N89-25852
Rapid photometry of the Delta Scuti variable 63 Her N89-25916
A prototype stellar photometer for magnetic field and Doppler measurements N89-25926
Search for rapid oscillations in the Northern Ap stars HD62140, HD81009 and HD22374 N89-25928
Some tests of the precision of CCD differential photometry measurements of bright double stars N89-25930
End points of stellar evolution investigated by seismology on white dwarf stars N89-25934
MUSICOS (MUlti-SIte COntinuous Spectroscopy): Objectives and prospects for asteroseismology N89-25940
STELLAR STRUCTURE
Ripple structure in degenerate electron gas-dominated stars with intense magnetic fields N89-25783
On radiative and convective influences on stellar pulsational stability N89-25828
Study of solar structure based on p-mode helioseismology N89-25896
Helioseismological inverse problem: Diagnostics of the structure of the lower solar atmosphere N89-25903
STELLARATORS
Confinement improvement of low-aspect-ratio torsatrons
[DE89-010192] N89-25702
Averaged equilibrium and stability in low-aspect-ratio stellarators
[DE89-013618] N89-25713
Investigations of modular nonplanar coil systems for the stellarator fusion reactor
[IPP-2/298] N89-25714
STIFFNESS
Characterization of the effects of three-dimensional states of stress on damping of laminated composites N89-25287
Processing of fiber-reinforced materials by injection molding
[ETN-89-94668] N89-25298
STIRLING ENGINES
CSTI High Capacity Power
[NASA-TM-102059] N89-25282
STOCHASTIC PROCESSES
A net-based model for time-dependent systems
[REPT-89-005] N89-25661
STOICHIOMETRY
The formation and analysis of thin film high temperature superconductors
[DE89-011177] N89-25745
Processing chemically prepared Tl-Ca-Ba-Cu oxide superconductors
[DE89-011535] N89-25748
STORAGE RINGS (PARTICLE ACCELERATORS)
Proceedings of the Free Electron Laser Workshop, 1988 JAERI
[DE89-780071] N89-25450
STRAIN ENERGY RELEASE RATE
An analytical and experimental investigation of edge delamination in laminates subjected to tension, bending, and torsion
[NASA-CR-181824] N89-25296
STRAIN GAGES
Design of an auto change mechanism and intelligent gripper for the space station
[NASA-CR-185387] N89-25268
Technique and data analysis for impact-loaded piezoelectric polymers (PVDF)
[DE89-010529] N89-25342

Superlattice strain gage
[DE89-011805] N89-25447
Laser diffraction methods for high temperature strain measurements
[DE89-008235] N89-25451
Optical fiber sensors and signal processing for intelligent structure monitoring
[NASA-CR-185395] N89-25691

STRAIN MEASUREMENT
Laser diffraction methods for high temperature strain measurements
[DE89-008235] N89-25451

STRAIN RATE
Procedures for characterizing an alloy and predicting cyclic life with the total strain version of Strainrange Partitioning
[NASA-TM-4102] N89-25485

STRATOSPHERE
Preventing depletion of stratospheric ozone: Implications on future aircraft emissions
[DE89-009964] N89-25530
Comparison of satellite-derived dynamical quantities for the stratosphere of the Southern Hemisphere
[NASA-CP-3044] N89-25540
Solar Mesosphere Explorer observations of stratospheric and mesospheric water vapor N89-25802
Flux of water vapor in the terrestrial stratosphere and in the Martian atmosphere N89-25806
The Nimbus 7 LIMS (Limb Infrared Monitor of the Stratosphere) water vapor measurements N89-25810

STREAK CAMERAS
Design and testing of the EG and G/Los Alamos Operations fast streak camera
[DE89-010859] N89-25445

STREAK PHOTOGRAPHY
Design and testing of the EG and G/Los Alamos Operations fast streak camera
[DE89-010859] N89-25445

STRESS (PSYCHOLOGY)
Timesharing performance as an indicator of pilot mental workload
[NASA-CR-185328] N89-25573

STRESS ANALYSIS
Computerized Design Synthesis (CDS), A database-driven multidisciplinary design tool N89-25180
Characterization of the effects of three-dimensional states of stress on damping of laminated composites N89-25287
Elevated temperature deformation of structural steel
[PB89-172621] N89-25318
Transient effects in creep cavity nucleation and early growth in ceramics
[DE89-010420] N89-25340
X-ray based extensometry
[NASA-CR-185058] N89-25432
Dynamic simulation of dislocation pattern formation in metals during high temperature monotonic and cyclic deformation N89-25477

STRESS CORROSION CRACKING
Modeling grain boundary microchemistry related to IASCC (Irradiation-Assisted Stress Corrosion Cracking)
[DE89-011214] N89-25320
Deformation induced microstructural and microchemical changes during thermomechanical treatment
[DE89-011608] N89-25321

STRESS CYCLES
Procedures for characterizing an alloy and predicting cyclic life with the total strain version of Strainrange Partitioning
[NASA-TM-4102] N89-25485

STRESS DISTRIBUTION
On the stress problem of the pebble bed heat exchanger in a hypersonic wind tunnel
[NAL-TM-ST-8705] N89-25240

STRESS-STRAIN RELATIONSHIPS
Parameter estimation for a viscoelastic constitutive model
[DE89-008714] N89-25336
Finite strain example problems for rectangular, cylindrical, and spherical geometries
[DE89-013607] N89-25488

STRESS-STRAIN-TIME RELATIONS
Procedures for characterizing an alloy and predicting cyclic life with the total strain version of Strainrange Partitioning
[NASA-TM-4102] N89-25485

STRESSES
Thermomechanical fatigue of solder joints: A new comprehensive test method
[DE89-008045] N89-25314
Laser diffraction methods for high temperature strain measurements
[DE89-008235] N89-25451
Finite strain example problems for rectangular, cylindrical, and spherical geometries
[DE89-013607] N89-25488

STRING THEORY
Symmetry breaking: The standard model and superstrings
[DE89-011771] N89-25761
Cosmological effects of superconducting strings N89-25778
Evolution of cosmic string networks
[NASA-CR-185467] N89-25788

STRINGS
Strings on hyperelliptic supersurfaces
[DE88-705991] N89-25758

STRONGLY COUPLED PLASMAS
An inductively coupled plasma spectrometer for on-line, real-time process gas analysis
[DE89-010610] N89-25442

STRONTIUM COMPOUNDS
Variation of superlattice structure of the Bi2Sr(2-x)CuO(6-y) superconductor with composition and thermal history
[DE89-011612] N89-25749

STRUCTURAL ANALYSIS
Applications of integrated design/analysis systems in aerospace structural design N89-25147
Optimum structural design with static aeroelastic constraints N89-25171
Optimum design of swept-forward high-aspect-ration graphite-epoxy wings N89-25172
Recent Advances in Multidisciplinary Analysis and Optimization, part 2
[NASA-CP-3031-PT-2] N89-25173
ASTROS: A multidisciplinary automated structural design tool N89-25174
Recent experiences using finite-element-based structural optimization N89-25177
Results of including geometric nonlinearities in an aeroelastic model of an F/A-18 N89-25190
An integrated approach to the optimum design of actively controlled composite wings N89-25194
Finite element flow-thermal-structural analysis of aerodynamically heated leading edges N89-25198
Involute composite design evaluation using global design sensitivity derivatives N89-25199
Optimizing for minimum weight when two different finite element models and analyses are required N89-25200
An overview of the Douglas Aircraft Company Aeroelastic Design Optimization Program (ADOP) N89-25221
Structural optimization and recent large ground antenna installations N89-25224
Structural damage assessment as an identification problem N89-25230
Recent developments in large-scale structural optimization N89-25231
Middeck Active Control Experiment (MACE), phase A
[NASA-CR-185331] N89-25258
Space Shuttle Main Engine structural analysis and data reduction/evaluation. Volume 2: High pressure oxidizer turbo-pump turbine end bearing analysis
[NASA-CR-183664] N89-25270
An uncertainty analysis for the Structural Mechanics Laboratory
[DE89-010306] N89-25478
Identification of distributed forces on a structure
[DE89-007978] N89-25482
Advanced methods for 3-D inelastic structural analysis for hot engine structures
[NASA-TM-102106] N89-25490

STRUCTURAL DESIGN
Applications of integrated design/analysis systems in aerospace structural design N89-25147
New directions for Artificial Intelligence (AI) methods in optimum design N89-25158
STRUTEX: A prototype knowledge-based system for initially configuring a structure to support point loads in two dimensions N89-25161
Structural tailoring of counter rotation propfans N89-25165
Optimum structural design with static aeroelastic constraints N89-25171
Recent Advances in Multidisciplinary Analysis and Optimization, part 2
[NASA-CP-3031-PT-2] N89-25173
Research on optimization-based design N89-25176
The Sizing and Optimization Language (SOL): A computer language to improve the user/optimizer interface N89-25178
Computerized Design Synthesis (CDS), A database-driven multidisciplinary design tool N89-25180
On equivalence of discrete-discrete and continuum-discrete design sensitivity analysis N89-25181
Grid sensitivity capability for large scale structures N89-25183
Iterative methods for design sensitivity analysis N89-25184
On the calculation of derivatives of eigenvalues and eigenvectors in the simultaneous design and control of structures N89-25186
Treatment of body forces in boundary element design sensitivity analysis N89-25187
Design sensitivity analysis of boundary element substructures N89-25188
Aeroelastic modeling for the FIT (Functional Integration Technology) team F/A-18 simulation N89-25192
An approximation function for frequency constrained structural optimization N89-25196
Structural optimization of framed structures using generalized optimality criteria N89-25197
Recent Advances in Multidisciplinary Analysis and Optimization, part 3
[NASA-CP-3031-PT-3] N89-25201
Recent developments in multilevel optimization N89-25203
Generalized mathematical models in design optimization N89-25214
Optimum design of structures subject to general periodic loads N89-25215
Fuzzy set applications in engineering optimization: Multilevel fuzzy optimization N89-25216
A penalty approach for nonlinear optimization with discrete design variables N89-25217
The role of optimization in the next generation of computer-based design tools N89-25220
An overview of the Douglas Aircraft Company Aeroelastic Design Optimization Program (ADOP) N89-25221
Optimization of structure and control system N89-25223
Structural optimization and recent large ground antenna installations N89-25224
A novel implementation of method of optimality criterion in synthesizing spacecraft structures with natural frequency constraints N89-25225
Optimal placement of excitations and sensors by simulated annealing N89-25227
Experiences in applying optimization techniques to configurations for the Control of Flexible Structures (COFS) program N89-25228
An improved algorithm for optimum structural design with multiple frequency constraints N89-25229
Recent developments in large-scale structural optimization N89-25231
Shape optimal design of elastic bodies using a mixed variational formulation N89-25236
Smart tunnel: Docking mechanism
[NASA-CASE-MSC-21360-1] N89-25263
Space station architecture, module, berthing hub, shell assembly, berthing mechanism and utility connection channel
[NASA-CASE-ARC-11505-2] N89-25266
Space Station Freedom photovoltaic power module design status
[NASA-TM-102073] N89-25273
On optimal fail-safe design of structures N89-25486

STRUCTURAL ENGINEERING
Recent Advances in Multidisciplinary Analysis and Optimization, part 1
[NASA-CP-3031-PT-1] N89-25146
TRUSS: An intelligent design system for aircraft wings N89-25162
An investigation of using an RQP based method to calculate parameter sensitivity derivatives N89-25182
Recent Advances in Multidisciplinary Analysis and Optimization, part 3
[NASA-CP-3031-PT-3] N89-25201
Multilevel decomposition of complete vehicle configuration in a parallel computing environment N89-25205
Fuzzy set applications in engineering optimization: Multilevel fuzzy optimization N89-25216
A large scale software system for simulation and design optimization of mechanical systems N89-25219
Optimal placement of excitations and sensors by simulated annealing N89-25227

STRUCTURAL FAILURE
Probabilistic damage tolerance methods for metallic aerospace structures N89-25237

STRUCTURAL VIBRATION
Structural loading and noise disturbance of helicopters N89-25140
Efficient sensitivity analysis and optimization of a helicopter rotor N89-25155
Optimum design of structures subject to general periodic loads N89-25215

Plan, formulate, discuss and correlate a NASTRAN finite element vibrations model of the Boeing Model 360 helicopter airframe
[NASA-CR-181767] N89-25480
Identification of distributed forces on a structure
[DE89-007978] N89-25482

SUBGIANT STARS
Is the Sun really a rigid rotator N89-25835

SUBROUTINE LIBRARIES (COMPUTERS)
Design and implementation of a module library to support the structural synthesis — silicon compiler for IC design
[EUT-88-E-187] N89-25616

SUBSTRATES
Relation of the adhesion of plasma sprayed coatings to the process parameters: Size, velocity and heat content of the spray particles
[ETN-89-94296] N89-25326
A passivation layer for 3-5 semiconductor materials
[AD-D013963] N89-25737

SULFUR
Metal-sulfur type cell having improved positive electrode
[DE89-010110] N89-25389
Modeling the effect of surface active elements on weld pool fluid flow, heat transfer and geometry
[DE89-012504] N89-25466

SUN
Is the Sun really a rigid rotator N89-25835
Solar luminosity oscillations from two stations and correlation with velocity measurements N89-25846
New thresholds for ground-based photometry of solar intensity oscillations N89-25852
A detector of small gradients of transparency of the terrestrial atmosphere N89-25857
Visibility of nonradial pulsation modes in solar continuum intensity measurements N89-25860
Helioseismology from the South Pole: Comparison of 1987 and 1981 results N89-25868
Magnetically induced spectral line redshifts full disk measurements N89-25877
Long period solar oscillations N89-25879
Study of solar structure based on p-mode helioseismology N89-25896
Sound velocity distribution in the Sun inferred from asymptotic inversion of p-mode spectra N89-25900
Oscillation frequencies of solar models N89-25902
Further progress on the helium abundance determination — Sun N89-25906
Modelling the variation of solar p-mode frequencies N89-25907
High mass loss in the young Sun N89-25933
The mass-luminosity relationship for solar-type stars N89-25936
The influence of the equation of state on the zero-age main sequence and the Sun N89-25939

SUNSPOTS
Oscillations in presence of local magnetic fields — solar oscillations N89-25865
Oscillations in sunspots near the solar limb N89-25866
The influence of the toroidal roll pattern on the sunspot activity N89-25870
Local effects of a major flare on solar five-minute oscillations N89-25872
Viscous magnetohydrodynamic modes and p-mode absorption by sunspots N89-25873

SUPERCOMPUTERS
The Fermilab Lattice Supercomputer Project
[DE89-010510] N89-25578
Microprocessors and other processors for triggering and filtering at the SSC
[DE89-011088] N89-25580
Parallel processors and nonlinear structural dynamics algorithms and software
[NASA-CR-185049] N89-25620

SUPERCONDUCTING MAGNETS
Elements of a specification for superconducting cable and why they are important for magnet construction
[DE89-012533] N89-25754

SUPERCONDUCTING SUPER COLLIDER
Microprocessors and other processors for triggering and filtering at the SSC
[DE89-011088] N89-25580
Report of the HEPAP (High Energy Physics Advisory Panel) Subpanel on High Energy Physics and the SSC (Superconducting Super Collider) over the next decade
[DE89-010071] N89-25686

SUPERCONDUCTIVITY
Electronic structure of high temperature superconductors
[DE89-008610] N89-25741
Squid concepts and systems
[DE89-010384] N89-25755

SUPERCONDUCTORS
High resolution electron microscopy and microanalysis of ferrites and cuprates
[DE89-010441] N89-25341
Apparatus and method for characterizing conductivity of materials
[DE89-009599] N89-25383
Artificially structured superconductors
[DE89-009116] N89-25733
Variation of superlattice structure of the Bi2Sr(2-x)CuO(6-y) superconductor with composition and thermal history
[DE89-011612] N89-25749

SUPERFLUIDITY
A qualitative numerical analysis of some features of propagation of counterflow temperature waves in superfluid helium
[MPIS-9/1988] N89-25424

SUPERGRAVITY
Dark matter and supersymmetry
[DE89-011068] N89-25785

SUPERLATTICES
Variation of superlattice structure of the Bi2Sr(2-x)CuO(6-y) superconductor with composition and thermal history
[DE89-011612] N89-25749

SUPERNOVA 1987A
Nuclear astrophysics of supernovae
[DE89-012534] N89-25787

SUPERNOVAE
Physics of dense matter, neutron stars and supernova
[DE89-010673] N89-25784
Pair production of helicity-flipped neutrinos in supernovae
[NASA-CR-185466] N89-25789

SUPERPLASTICITY
Cryogenic mechanical properties of low density superplastically formable Al-Li alloys
[DE89-010587] N89-25343

SUPERSONIC FLOW
Numerical analysis of supersonic flow through oscillating cascade sections by using a deforming grid
[NASA-TM-102053] N89-25119

SUPERSONIC SPEED
Effect of milling machine roughness and wing dihedral on the supersonic aerodynamic characteristics of a highly swept wing
[NASA-TP-2918] N89-25117

SUPERSONIC TRANSPORTS
The conceptual design of a Mach 2 Oblique Flying Wing supersonic transport
[NASA-CR-177529] N89-25233
Preventing depletion of stratospheric ozone: implications on future aircraft emissions
[DE89-009964] N89-25530

SUPERSYMMETRY
Non-perturbative effects in the exact S-matrices of the O(N) Gross-Neveu and supersymmetric sigma models
[NIKHEF-H/88-10] N89-25656
Renormalization of topological field theory
[DE88-705998] N89-25759
Symmetry breaking: The standard model and superstrings
[DE89-011771] N89-25761
Dark matter and supersymmetry
[DE89-011068] N89-25785

SUPPORT SYSTEMS
Space station operations task force. Panel 1 report: Space operations and support systems
[NASA-TM-101816] N89-25244
Space station operations task force. Panel 2 report: Ground operations and support systems
[NASA-TM-101817] N89-25245
Space station operations task force summary report
[NASA-TM-101820] N89-25248
Space station operations task force. Executive summary
[NASA-TM-101780] N89-25249

SUPPORTS
Pactruss support structure for precision segmented reflectors
[NASA-CR-181747] N89-25484

SURFACE DEFECTS
Evaluation of elastic-plastic surface flaw behavior and related parameters using surface displacement measurements
[DE89-011134] N89-25489

SURFACE DIFFUSION
Concepts in surface science and heterogeneous catalysts
[DE89-010679] N89-25307

SURFACE ENERGY
Concepts in surface science and heterogeneous catalysts
[DE89-010679] N89-25307

SURFACE LAYERS
Evidence for a thin perturbative layer near the base of the solar convection zone N89-25876

SURFACE PROPERTIES
The application of Rutherford backscattering and channeling techniques to the characterization of ceramics
[DE89-010257] N89-25333
Correlation of subjective slipperiness judgements with quantitative COF (Coefficient Of Friction) measurements for structural steel
[PB89-165070] N89-25669

SURFACE REACTIONS
Concepts in surface science and heterogeneous catalysts
[DE89-010679] N89-25307

SURFACE ROUGHNESS
Coupling of the boundary element method with an integral momentum boundary-layer technique to calculate forces and moments on three-dimensional bodies
[DE89-006328] N89-25420

SURFACE ROUGHNESS EFFECTS
Effect of milling machine roughness and wing dihedral on the supersonic aerodynamic characteristics of a highly swept wing
[NASA-TP-2918] N89-25117
The influence of contact surface microstructure on vacuum arc stability and arc voltage
[EUT-87-E-186] N89-25672

SURFACE STABILITY
Analytic theory for the determination of velocity and stability of bubbles in a Hele-Shaw cell. Part 1: Velocity selection
[NASA-CR-181836] N89-25665

SURFACE TEMPERATURE
Temperature limit of a graphite divertor surface due to particle erosion
[DE89-010272] N89-25703

SURGES
Analog and digital simulation of line-energizing overvoltages and comparison with measurements in a 400 kV network
[EUT-88-E-193] N89-25401

SWEPT FORWARD WINGS
Integrated aerodynamic-structural design of a forward-swept transport wing N89-25168
Optimum design of swept-forward high-aspect-ration graphite-epoxy wings N89-25172

SWEPT WINGS
Effect of milling machine roughness and wing dihedral on the supersonic aerodynamic characteristics of a highly swept wing
[NASA-TP-2918] N89-25117
Optimum structural design with static aeroelastic constraints N89-25171
Aeroservoelastic tailoring for lateral control enhancement N89-25189

SWITCHES
Binary and ternary gas mixtures with temperature enhanced diffuse glow discharge characteristics for use in closing switches
[DE89-011807] N89-25395
A novel TR (Transmit/Receive) switch utilizing a distributed amplifier
[DE89-005917] N89-25396
Plasma switches for high current and fast time scale operation
[DE89-010557] N89-25704

SWITCHING CIRCUITS
Magnetic switching
[DE89-012299] N89-25398

SYMBOLIC PROGRAMMING
Handling arrays in symbolic execution
[REPT-89-003] N89-25609

SYMMETRY
Stationary ideal MHD with incompressible mass flow and general symmetry N89-25732

SYNCHRONISM
Synchronization of the ground station atomic clocks using weighted transportable cesium time standards in the navigation experiment (NAVEX)
[DFVLR-MITT-89-01] N89-25448
A global time reference for hypercube multicomputers
[DE89-010924] N89-25579

SYNTHESIS (CHEMISTRY)
Characterization of ceramics and intermetallics fabricated by self-propagating high-temperature synthesis
[NASA-TM-102004] N89-25285
Whisker shaped carbon substance
[DE89-010214] N89-25288
Molecular growth pathways in silica sol-gel polymerization
[DE89-011224] N89-25346

Preparation and properties of high-temperature superconductors in the Y-Ba-Cu-O system [DE88-706050] N89-25735
Processing chemically prepared Tl-Ca-Ba-Cu oxide superconductors [DE89-011535] N89-25748

SYNTHETIC APERTURE RADAR
Digital evaluation of SEASAT-SAR radar image data N89-25504

SYSTEM IDENTIFICATION
Structural damage assessment as an identification problem N89-25230
Model building for an ingot heating process: Physical modeling approach and identification approach [EUT-88-E-196] N89-25331
On system identification using pulse-frequency modulated signals [EUT-88-E-195] N89-25379
Black-box identification of MIMO transfer functions: Asymptotic properties of prediction error models [EUT-87-E-182] N89-25642
On the bounds of the modeling errors of black-box MIMO transfer function estimates [EUT-87-E-183] N89-25643

SYSTEMS ANALYSIS
Optimization by decomposition: A step from hierarchic to non-hierarchic systems N89-25149
Flight performance model for a geostationary transportation system [ILR-MITT-206] N89-25259
Sensitivity analysis of complex coupled systems extended to second and higher order derivatives [NASA-TM-101587] N89-25354
Systems approach to project management [DE89-008741] N89-25765

SYSTEMS ENGINEERING
Integrated design optimization research and development in an industrial environment N89-25148
Computerized Design Synthesis (CDS), A database-driven multidisciplinary design tool N89-25180
Recent Advances in Multidisciplinary Analysis and Optimization, part 3 [NASA-CP-3031-PT-3] N89-25201
A decision-based perspective for the design of methods for systems design N89-25208
Hypersonic airbreathing vehicle conceptual design (focus on aero-space plane) N89-25210
Development of an Si panel [ETN-89-94625] N89-25518
A case study relating the Yourdon methodology to other design methods [MEMO-INF-88-24] N89-25613
Design and construction of a computer system model for application development workloads [DE89-010519] N89-25622
Symbolic execution of concurrent programs using Petri nets [REPT-89-004] N89-25633
Explanation in knowledge-based systems [MEMO-INF-88-17] N89-25640
Mission Operations and Data Systems Directorate's operational/development network (MODNET) at Goddard Space Flight Center [NASA-CR-183426] N89-25763
Temporal data management in real-time systems: A comparative view [REPT-88-046] N89-25767
Prototyping management information systems application software: An empirical study of developers' perceptions N89-25770

SYSTEMS INTEGRATION
Applications of integrated design/analysis systems in aerospace structural design N89-25147
Integrated design optimization research and development in an industrial environment N89-25148
Overview of Dynamics Integration Research (DIR) program at Langley Research Center N89-25150
Results of an integrated structure/control law design sensitivity analysis N89-25185
Aeroelastic modeling for the FIT (Functional Integration Technology) team F/A-18 simulation N89-25192
Hypersonic airbreathing vehicle conceptual design (focus on aero-space plane) N89-25210
A large scale software system for simulation and design optimization of mechanical systems N89-25219
An analytical sensitivity method for use in integrated aeroservoelastic aircraft design [NASA-TM-101583] N89-25239
Operator role definition and human system integration [DE89-009621] N89-25571
Mission Operations and Data Systems Directorate's operational/development network (MODNET) at Goddard Space Flight Center [NASA-CR-183426] N89-25763

SYSTEMS SIMULATION
Analog and digital simulation of line-energizing overvoltages and comparison with measurements in a 400 kV network [EUT-88-E-193] N89-25401

T

T SHAPE
Gas-liquid flow in dividing Tee-junctions with a horizontal inlet and different branch orientations and diameters [KFK-4399] N89-25427

TAILLESS AIRCRAFT
The conceptual design of a Mach 2 Oblique Flying Wing supersonic transport [NASA-CR-177529] N89-25233

TAKEOFF
Reduction of aircraft noise in civil air transport by optimization of flight tracks and takeoff and approach procedures [ILR-MITT-200] N89-25676

TANGENTS
A comparison of the error function and the tanh transformation as progressive rules for double and triple singular integrals [MATHS-RES-210] N89-25659

TASKS
The organization of perception and action in complex control skills [NASA-CR-184638] N89-25568

TAYLOR INSTABILITY
Measurement of the stimulated thermal Rayleigh scattering instability [DE89-012324] N89-25453

TAYLOR SERIES
An approximation function for frequency constrained structural optimization N89-25196

TECHNOLOGICAL FORECASTING
Materials and structures for 2000 and beyond: An attempted forecast [DFVLR-MITT-89-02] N89-25358
Challenges for future space power systems [NASA-TM-102063] N89-25506

TECHNOLOGY ASSESSMENT
Intermetallic alloys: Deformation, mechanical and fracture behavior [GKSS-88/E/53] N89-25327
Comparative investigations of multispectral satellite image data of MOMS-01, LANDSAT-TM and LANDSAT-MSS for geological and vegetational applications in test sites in the Andes of northern Chile and the Parana-Basin of Brazil [DFVLR-FB-88-50] N89-25499

TECHNOLOGY TRANSFER
Geothermal energy program summary. Volume 2: Research summaries, fiscal year 1988 [DE89-000865] N89-25509

TECTONICS
Studies of regional and global tectonics and the rotation of the earth using very-long baseline interferometry [NASA-CR-185059] N89-25534

TELECOMMUNICATION
Reduction of interference by decorrelation and quantized feedback in the case of digital transmission on multi-pair symmetric cables [FI-44-TB-110] N89-25375
The impact of telecommunication on rural areas in developing countries [EUT-87-E-185] N89-25377

TELEOPERATORS
Modifying a telerobotic system to include robotic operation by means of dynamic modeling [DE89-003119] N89-25460
Traction-drive transmission for telerobotic joints [DE89-005337] N89-25461

TELESCOPES
Solar Luminosity Oscillation Telescope (SLOT) N89-25848

TEMPERATURE DEPENDENCE
A test system for computer controlled thermomechanical fatigue testing [DE89-009067] N89-25483

TEMPERATURE DISTRIBUTION
Experiments on liquid-vapour phase change between plane liquid surfaces. Part 3: Results from a closed quartz chamber [NAL-TM-FM-8809] N89-25301
Parallel solutions of a 2-D phase change problem on a hypercube [DE89-012886] N89-25602

TEMPERATURE EFFECTS
Polyimide Matrix composites: Polyimidesulfone/LARC-TPI (1:1) blend [NASA-TM-101568] N89-25294
Modeling the effect of surface active elements on weld pool fluid flow, heat transfer and geometry [DE89-012504] N89-25466
Effects of auxiliary heat treatments on flame-cutting procedures [DE89-011827] N89-25472
Dynamic simulation of dislocation pattern formation in metals during high temperature monotonic and cyclic deformation N89-25477
Acclimatization to heat in humans [NASA-TM-101011] N89-25558

TEMPERATURE INVERSIONS
Experiments on liquid-vapour phase change between plane liquid surfaces. Part 3: Results from a closed quartz chamber [NAL-TM-FM-8809] N89-25301

TEMPERATURE MEASUREMENT
Flight set 360L003 instrumentation final test report, volume 9 [NASA-CR-183675] N89-25284
Determination of combustion gas temperatures by infrared radiometry in sooting and nonsooting flames [NASA-TP-2900] N89-25409
Laser diffraction methods for high temperature strain measurements [DE89-008235] N89-25451

TEMPERATURE PROFILES
Experiments on liquid-vapour phase change between plane liquid surfaces. Part 3: Results from a closed quartz chamber [NAL-TM-FM-8809] N89-25301
A qualitative numerical analysis of some features of propagation of counterflow temperature waves in superfluid helium [MPIS-9/1988] N89-25424
Density fluctuations and particle/thermal transport for ohmically and auxiliarily heated plasmas in the JIPP T-IIU tokamak [IPPJ-891] N89-25700

TEMPORAL RESOLUTION
Very high elevation water ice clouds on Mars: Their morphology and temporal behavior N89-25804

TENSILE PROPERTIES
Weldability and weld doping of commercial purity molybdenum [DE89-009535] N89-25311

TENSILE STRENGTH
Super-strong self-reinforcing polymeric matrices formed by the first super-strong polymers [DE89-011533] N89-25347

TENSILE TESTS
Elevated temperature deformation of structural steel [PB89-172621] N89-25318
A test system for computer controlled thermomechanical fatigue testing [DE89-009067] N89-25483

TENSORS
Toward a proof of the existence of an integrity basis for the tensors in the enveloping algebra of su(3) [DE88-706031] N89-25646
Degenerate representation from tensorial identities and quantum realisations of YBZF algebras [DE88-706032] N89-25647

TERRESTRIAL RADIATION
Modeling land-surface albedos from plant canopy architecture N89-25495

TEST CHAMBERS
The development of a vapor compression refrigeration system for a network of nine temperature test chambers [DE89-007084] N89-25355
Design description of the large scale climate simulator [DE89-010185] N89-25551

TEST EQUIPMENT
Simple fixture concepts for multi-axis vibration testing [DE89-007977] N89-25481

TEST FACILITIES
Protoflight photovoltaic power module system-level tests in the space power facility [NASA-TM-102066] N89-25267

THALLIUM COMPOUNDS
Processing chemically prepared Tl-Ca-Ba-Cu oxide superconductors [DE89-011535] N89-25748

THEMATIC MAPPERS (LANDSAT)
Comparative investigations of multispectral satellite image data of MOMS-01, LANDSAT-TM and LANDSAT-MSS for geological and vegetational applications in test sites in the Andes of northern Chile and the Parana-Basin of Brazil [DFVLR-FB-88-50] N89-25499
Reports on cartography and Geodesy. Series 1: Original reports, number 102 [ISSN-0469-4236] N89-25501
Interpretation of Thematic Mapper data for the acquisition of land information N89-25502

Forestry interpretation of Thematic Mapper (TM) data using the example of the Frankfurt municipal forest N89-25503

THEMATIC MAPPING
Investigations on satellite image and reference data for exploration-related tasks
[DFVLR-FB-88-46] N89-25498
Reports on cartography and Geodesy. Series 1: Original reports, number 102
[ISSN-0469-4236] N89-25501
Interpretation of Thematic Mapper data for the acquisition of land information N89-25502
Forestry interpretation of Thematic Mapper (TM) data using the example of the Frankfurt municipal forest N89-25503
FAO detailed rain mapping experiment
[BCRS-88-11] N89-25552
FAO detailed rain mapping experiment phase A: Meteosat based rainfall mapping in the Sahel region N89-25553
FAO detailed rain mapping experiment phase B: Comparison of rainfall and evapotranspiration mapping N89-25554

THEOREM PROVING
A parallel processing approach for implementing high-performance first-order logic deduction systems
[DE89-011878] N89-25632
Toward a proof of the existence of an integrity basis for the tensors in the enveloping algebra of su(3)
[DE88-706031] N89-25646

THEORETICAL PHYSICS
A site oriented supercomputer for theoretical physics: The Fermilab Advanced Computer Program Multi Array Processor System (ACMAPS)
[DE89-011090] N89-25631
International Centre for Theoretical Physics: Scientific activities in 1987
[DE88-705973] N89-25668

THERMAL CONDUCTIVITY
Heat transfer in packed beds
[KFK-4451] N89-25425
Reduce uncertainty in projection of future sea-level change due to ice wastage
[DE89-011483] N89-25526
Thermal conductivity of dielectric thin films
[DE89-011847] N89-25750

THERMAL CYCLING TESTS
Evaluation of ceramic coatings on silicon carbide
[DE89-010321] N89-25339
A test system for computer controlled thermomechanical fatigue testing
[DE89-009067] N89-25483

THERMAL DEGRADATION
Dynamic simulation of dislocation pattern formation in metals during high temperature monotonic and cyclic deformation N89-25477

THERMAL DIFFUSIVITY
Density fluctuations and particle/thermal transport for ohmically and auxiliarily heated plasmas in the JIPP T-IIU tokamak
[IPPJ-891] N89-25700

THERMAL ENVIRONMENTS
SIMOUN: Test system for shuttle thermal protection materials
[REPT-882-430-101] N89-25256

THERMAL FATIGUE
Thermomechanical fatigue of solder joints: A new comprehensive test method
[DE89-008045] N89-25314

THERMAL INSTABILITY
Measurement of the stimulated thermal Rayleigh scattering instability
[DE89-012324] N89-25453

THERMAL MAPPING
Automated thermal mapping techniques using chromatic image analysis
[NASA-TM-101554] N89-25443
The Nimbus 7 LIMS (Limb Infrared Monitor of the Stratosphere) water vapor measurements N89-25810

THERMAL PROTECTION
SIMOUN: Test system for shuttle thermal protection materials
[REPT-882-430-101] N89-25256
NDE of the space shuttle orbiter thermal protection system, phase 2
[NASA-CR-185471] N89-25257

THERMAL STABILITY
Elevated temperature deformation of structural steel
[PB89-172621] N89-25318

THERMAL STRESSES
On the stress problem of the pebble bed heat exchanger in a hypersonic wind tunnel
[NAL-TM-ST-8705] N89-25240
Dynamic simulation of dislocation pattern formation in metals during high temperature monotonic and cyclic deformation N89-25477

THERMAL VACUUM TESTS
Protoflight photovoltaic power module system-level tests in the space power facility
[NASA-TM-102066] N89-25267

THERMOCHEMISTRY
The coupling of thermochemistry and phase diagrams for Group 3-5 semiconductor systems
[DE89-012516] N89-25752

THERMODYNAMIC PROPERTIES
Conjugating binary systems for spacecraft thermal control. Appendix C: Aeroassist Flight Experiment Carrier Vehicle preliminary stress analysis
[NASA-CR-183609] N89-25261
Advanced working fluid properties in heat pump and absorption cooling operations
[PB89-178172] N89-25413

THERMODYNAMICS
Thermomechanical fatigue of solder joints: A new comprehensive test method
[DE89-008045] N89-25314
Quantitative modeling of sensitization development in austenitic stainless steel
[DE89-011206] N89-25317
Study on thermodynamical and mechanical conditions for pumping low flow rates of liquefied gases to high pressure level
[DFVLR-FB-88-54] N89-25429

THERMOELECTRICITY
CSTI High Capacity Power
[NASA-TM-102059] N89-25282

THERMOGRAPHY
Automated thermal mapping techniques using chromatic image analysis
[NASA-TM-101554] N89-25443

THERMOMECHANICAL TREATMENT
Deformation induced microstructural and microchemical changes during thermomechanical treatment
[DE89-011606] N89-25321
A test system for computer controlled thermomechanical fatigue testing
[DE89-009067] N89-25483

THERMOPLASTIC RESINS
Mechanical properties of carbon fiber reinforced thermoplastics for cryogenic applications
[KFK-4487] N89-25297
Semiinterpenetrating polymer network for tougher and more microcracking resistant high temperature polymers
[NASA-CASE-LAR-13925-1] N89-25334

THERMOREGULATION
Acclimatization to heat in humans
[NASA-TM-101011] N89-25558

THERMOSETTING RESINS
A predictive model for failure properties of thermoset resins
[NASA-TM-4128] N89-25300
Semiinterpenetrating polymer network for tougher and more microcracking resistant high temperature polymers
[NASA-CASE-LAR-13925-1] N89-25334

THIN FILMS
Periodic and solitary waves on thin, horizontal, gas-sheared liquid films
[DE89-010655] N89-25416
A slow positron beam generator for lifetime studies
[NASA-TM-101590] N89-25433
Determination of the mechanical properties of diamond and diamond-like films by the ultra-low load indentation technique
[DE89-011569] N89-25471
Development of an Si panel
[ETN-89-94625] N89-25518
Review of oxidation of Nb-1Zr
[DE89-010299] N89-25687
Optical properties of metal-oxide thin films: Influence of microstructure
[DE89-011219] N89-25690
Optical information storage in PLZT thin films
[DE89-011067] N89-25692
Deposition of dielectric optical coatings: A microstructural study of the deposited layers and interfaces
[DE89-011205] N89-25694
Ferroelectric potassium niobate thin films
[DE89-010862] N89-25744
The formation and analysis of thin film high temperature superconductors
[DE89-011177] N89-25745
Thermal conductivity of dielectric thin films
[DE89-011847] N89-25750

THREE DIMENSIONAL BODIES
Coupling of the boundary element method with an integral momentum boundary-layer technique to calculate forces and moments on three-dimensional bodies
[DE89-006328] N89-25420

THREE DIMENSIONAL FLOW
A variationally optimized vortex tracing algorithm for three-dimensional flows around solid bodies
[ETN-89-94301] N89-25423
Three dimensional computations of the dynamics of the magnetopause: First results N89-25719

THREE DIMENSIONAL MODELS
Averaged equilibrium and stability in low-aspect-ratio stellarators
[DE89-013618] N89-25713
Renormalization of topological field theory
[DE88-705998] N89-25759

THRUST
Performance characterization and transient investigation of multipropellant resistojets
[NASA-TM-102118] N89-25283

THRUST CONTROL
Performance characterization and transient investigation of multipropellant resistojets
[NASA-TM-102118] N89-25283

THRUST VECTOR CONTROL
Hybrid plume plasma rocket
[NASA-CASE-MSC-20476-2] N89-25279

TILES
NDE of the space shuttle orbiter thermal protection system, phase 2
[NASA-CR-185471] N89-25257

TIME DEPENDENCE
Time-dependent computational studies of flames in microgravity
[NASA-CR-182298] N89-25353

TIME FUNCTIONS
A net-based model for time-dependent systems
[REPT-89-005] N89-25661
Temporal data management in real-time systems: A comparative view
[REPT-88-046] N89-25767
Solar internal rotation from helioseismology N89-25829

TIME OF FLIGHT SPECTROMETERS
Acceleration of ions in the magnetotail N89-25720

TIME OPTIMAL CONTROL
Time-optimal slewing maneuvers of flexible spacecraft N89-25265

TIME SERIES ANALYSIS
ARMA (Autoregressive-Moving Average) modeling
[AD-A205308] N89-25649
Measurements of oscillation parameters from synthetic times series --- solar oscillations N89-25827
Modelling the solar oscillation time series by a randomly excited oscillator N89-25942

TIME SIGNALS
A global time reference for hypercube multicomputers
[DE89-010924] N89-25579

TISSUES (BIOLOGY)
Spiral vane bioreactor
[NASA-CASE-MSC-21361-1] N89-25557

TITANIUM
Weldability and weld doping of commercial purity molybdenum
[DE89-009535] N89-25311

TITANIUM CARBIDES
Characterization of ceramics and intermetallics fabricated by self-propagating high-temperature synthesis
[NASA-TM-102004] N89-25285

TITANIUM OXIDES
Optical properties of metal-oxide thin films: Influence of microstructure
[DE89-011219] N89-25690

TOKAMAK DEVICES
Temperature limit of a graphite divertor surface due to particle erosion
[DE89-010272] N89-25703
The q measurements during sawtooth oscillations in a low q tokamak
[DE89-010563] N89-25705
Confinement physics of H-mode discharges in DIII-D
[DE89-011525] N89-25707
Theoretical studies of edge physics and plasma-wall interactions
[DE89-011792] N89-25710

TOLERANCES (MECHANICS)
Probabilistic damage tolerance methods for metallic aerospace structures N89-25237

TOLLMIEN-SCHLICHTING WAVES
Interactions of Tollmien-Schlichting waves and Dean vortices. Comparison of direct numerical simulation and a weakly nonlinear theory
[NASA-TP-2919] N89-25118

TOPOGRAPHY
Dynamic sea surface topography, gravity and improved orbit accuracies from the direct evaluation of SEASAT altimeter data
[NASA-TM-100735] N89-25539

TOPOLOGY
Phase space concepts
[DE89-011082] N89-25667
Solitosynthesis: Cosmological evolution of non-topological solitons
[NASA-CR-185030] N89-25678
Statistical fluctuations as the origin of nontopological solitons
[NASA-CR-185351] N89-25680
Renormalization of topological field theory
[DE88-705998] N89-25759
TOROIDAL PLASMAS
Theoretical studies of edge physics and plasma-wall interactions
[DE89-011792] N89-25710
Investigations of modular nonplanar coil systems for the stellarator fusion reactor
[IPP-2/298] N89-25714
TORQUE
Variable speed induction motor operation from a 20-kHz power bus
[NASA-TM-102061] N89-25271
TORSION
Imbedding of the gravitational field into the space of affine connection without torsion
[DE88-704637] N89-25536
TRAILING EDGES
Flow about trailing edges in unsteady flow N89-25135
TRAJECTORIES
Advanced mass launchers for low earth orbit
[DE89-010759] N89-25255
Querying databases of trajectories of differential equations: Data structures for trajectories
[NASA-CR-185040] N89-25772
TRANSFER FUNCTIONS
Black-box identification of MIMO transfer functions: Asymptotic properties of prediction error models
[EUT-87-E-182] N89-25642
On the bounds of the modeling errors of black-box MIMO transfer function estimates
[EUT-87-E-183] N89-25643
ARMA (Autoregressive-Moving Average) modeling
[AD-A205308] N89-25649
TRANSFORMATIONS (MATHEMATICS)
A comparison of the error function and the tanh transformation as progressive rules for double and triple singular integrals
[MATHS-RES-210] N89-25659
Phase space concepts
[DE89-011082] N89-25667
TRANSHORIZON RADIO PROPAGATION
Reduction of transhorizon radio interference in satellite earth stations
[ETN-89-94297] N89-25374
TRANSIENT RESPONSE
Performance characterization and transient investigation of multipropellant resistojets
[NASA-TM-102118] N89-25283
TRANSITION METALS
Surface structural analysis of small molecules on transition metal single crystal surfaces with low energy electron diffraction
[DE89-010681] N89-25743
TRANSITION TEMPERATURE
Apparatus and method for characterizing conductivity of materials
[DE89-009599] N89-25383
TRANSLATIONAL MOTION
State-selective single electron capture by multiply charged ions: Reaction window and multichannel Landau Zener calculations
[REPT-88-05-175] N89-25684
TRANSMITTER RECEIVERS
A novel TR (Transmit/Receive) switch utilizing a distributed amplifier
[DE89-005917] N89-25396
TRANSONIC FLOW
Vortex structures in the wake of transonic flow about profiles N89-25134
Transonic airfoil design for helicopter rotor applications N89-25154
Design optimization of axisymmetric bodies in nonuniform transonic flow N89-25206
TRANSPORT AIRCRAFT
Optimization by decomposition: A step from hierarchic to non-hierarchic systems N89-25149
An economic model for evaluating high-speed aircraft designs
[NASA-CR-177530] N89-25235
TRANSPORT THEORY
Interfacial fluid mechanics and transport processes
[DE89-010664] N89-25417
Transport of Mars atmospheric water into high northern latitudes during a polar warming N89-25792
The effect of global-scale divergent circulation on the atmospheric water vapor transport and maintenance N89-25793
Flux of water vapor in the terrestrial stratosphere and in the Martian atmosphere N89-25806
TRAPPED PARTICLES
Femtosecond studies of electron transfer processes at semiconductor interfaces
[DE89-010599] N89-25742
TREES (MATHEMATICS)
Multilevel decomposition of complete vehicle configuration in a parallel computing environment N89-25205
TRIBOLOGY
Applications of ion beam processes in tribology
[DE89-000614] N89-25470
TROPICAL REGIONS
On the vertical distribution of water vapor in the Martian tropics N89-25800
TROPOSPHERE
Tropospheric influences on satellite-Earth paths and their determination by means of radar measurements
[DFVLR-FB-88-53] N89-25250
TRUSSES
Optimal placement of excitations and sensors by simulated annealing N89-25227
An improved algorithm for optimum structural design with multiple frequency constraints N89-25229
Pactruss support structure for precision segmented reflectors
[NASA-CR-181747] N89-25484
On optimal fail-safe design of structures N89-25486
TUNGSTEN
Comparison of experimental shock-wave profiles for tungsten and computer simulations using a rate-dependent constitutive model
[DE89-006158] N89-25419
TUNNELS
Smart tunnel: Docking mechanism
[NASA-CASE-MSC-21360-1] N89-25263
TURBINE BLADES
Procedures for shape optimization of gas turbine disks N89-25207
TURBINE PUMPS
Space Shuttle Main Engine structural analysis and data reduction/evaluation. Volume 2: High pressure oxidizer turbo-pump turbine end bearing analysis
[NASA-CR-183664] N89-25270
Advanced binary geothermal power plants working fluid property determination and heat exchanger design
[DE89-011144] N89-25513
TURBULENT BOUNDARY LAYER
A numerical study of a class of TVD schemes for compressible mixing layers
[NASA-TM-102194] N89-25651
TURBULENT FLOW
Techniques for compressible flow calculations on multizone grids N89-25120
Multidimensional modeling of convective heat transfer with application to I.C. engines
[DE89-010651] N89-25415
Experimental study of the phenomena of turbulent flow in the narrow gaps between subchannels of rod bundles
[KFK-4501] N89-25428
Numerical simulation of transition from laminar to turbulent channel flow
[DFVLR-FB-88-55] N89-25430
A numerical study of a class of TVD schemes for compressible mixing layers
[NASA-TM-102194] N89-25651
TURBULENT HEAT TRANSFER
Experimental investigation on transcritical heat transfer in He 2
[MPIS-MITT-90] N89-25426
TURBULENT WAKES
Vortex structures in the wake of transonic flow about profiles N89-25134
TURING MACHINES
The full decomposition of sequential machines with the output behavior realization
[EUT-88-E-199] N89-25583
TWO DIMENSIONAL BODIES
Shape optimal design of elastic bodies using a mixed variational formulation N89-25236
On a fast two-dimensional radar imaging process for rotating targets and an analysis of its image quality
[DFVLR-FB-88-51] N89-25376
TWO DIMENSIONAL FLOW
A numerical study of a class of TVD schemes for compressible mixing layers
[NASA-TM-102194] N89-25651
TWO DIMENSIONAL MODELS
Radiative heat transfer
[PB89-173637] N89-25412
TWO PHASE FLOW
An experimental study of two-phase natural circulation in an adiabatic flow loop
[DE89-009850] N89-25406
Study of interfacial behavior in concurrent gas-liquid flows
[DE89-010484] N89-25408
Gas-liquid flow in dividing Tee-junctions with a horizontal inlet and different branch orientations and diameters
[KFK-4399] N89-25427
Analytic theory for the determination of velocity and stability of bubbles in a Hele-Shaw cell. Part 1: Velocity selection
[NASA-CR-181836] N89-25665

U

U.S.S.R.
USSR Space Life Sciences Digest. Index to issues 15-20
[NASA-CR-3922(25)] N89-25556
U.S.S.R. SPACE PROGRAM
IPHIR: The helioseismology experiment on the PHOBOS mission N89-25881
ULTRALIGHT AIRCRAFT
Data of aeroacoustic measurements on ultralight aircraft propellers
[DFVLR-MITT-88-33] N89-25677
ULTRASONIC TESTS
Basics of ultrasonic testing
[DE89-010465] N89-25473
ULTRAVIOLET SPECTROPHOTOMETERS
A prototype stellar photometer for magnetic field and Doppler measurements N89-25926
ULTRAVIOLET SPECTROSCOPY
Measurement of H and H2 populations in-situ in a low-temperature plasma by vacuum-ultraviolet laser-absorption spectroscopy
[DE89-010433] N89-25308
UNIFORM FLOW
Design optimization of axisymmetric bodies in nonuniform transonic flow N89-25206
UNITED KINGDOM
UK airmisses involving commercial air transport
[CAA-3/88] N89-25143
UNITED STATES
United States and Western Europe cooperation in planetary exploration
[NASA-CR-184941] N89-25776
UNIVERSE
Quantum ontologies
[DE89-010385] N89-25781
UNSTEADY AERODYNAMICS
Mechanical reaction of wings moving through a vortex region N89-25139
Aeroelastic modeling for the F/T (Functional Integration Technology) team F/A-18 simulation N89-25192
An integrated approach to the optimum design of actively controlled composite wings N89-25194
UNSTEADY FLOW
Numerical analysis of supersonic flow through oscillating cascade sections by using a deforming grid
[NASA-TM-102053] N89-25119
Vortex flows in flying technique
[ETN-89-94428] N89-25126
Unsteady phenomena on delta wings with partially broken-down vortex regions N89-25129
Strongly unsteady vortex fields at elastic helicopter rotor blades N89-25131
Flow about trailing edges in unsteady flow N89-25135
Unsteady flow on profiles in a liquid Ludwig tunnel N89-25136
Unsteady stagnation-point heat transfer during passage of a concentrated vortex
[NASA-CR-182297] N89-25404
Study of the stability of compressible Couette flow N89-25410
UPPER ATMOSPHERE
The UARS (Upper Atmosphere Research Satellite): A program to study global ozone change
[NASA-TM-101756] N89-25520
URANUS SATELLITES
Some aspects of the dynamics of orbit-orbit resonances in the Uranian satellite system N89-25815
USER MANUALS (COMPUTER PROGRAMS)
The 3DGRAPE book: Theory, users' manual, examples
[NASA-TM-102224] N89-25116
User's guide to image processing applications of the NOAA satellite HRPT/AVHRR data. Part 1: Introduction to the satellite system and its applications. Part 2: Processing and analysis of AVHRR imagery
[NASA-CR-180784] N89-25492

Geologic spatial analysis program users guide for digital elevation model analysis procedures for detection of crustal fracture planes
[DE89-010880] N89-25542
Common Graphics Library (CGL). Volume 2: Low-level user's guide
[NASA-TM-101596] N89-25597
USER REQUIREMENTS
Space station operations task force. Panel 3 report: User development and integration
[NASA-TM-101818] N89-25246
Space station operations task force. Panel 4 report: Management integration
[NASA-TM-101819] N89-25247
Space station operations task force summary report
[NASA-TM-101820] N89-25248
Space station operations task force. Executive summary
[NASA-TM-101780] N89-25249
Prototyping management information systems application software: An empirical study of developers' perceptions N89-25770
An expert system to facilitate selecting a database management system
[DE89-012350] N89-25774

V

VACUUM
Potential uses of vacuum bubbles in noise and vibration control
[NASA-CR-181629] N89-25674
VALUE ENGINEERING
Learning the value of VE
[DE89-008121] N89-25475
Applying understanding of individual behavior and team dynamics within the value engineering process
[DE89-011126] N89-25766
VANADIUM ALLOYS
The creep and creep-rupture behavior of vanadium-base alloys
[KFK-2440] N89-25328
VAPOR DEPOSITION
Strong fibers
[DE89-010596] N89-25292
The coupling of thermochemistry and phase diagrams for Group 3-5 semiconductor systems
[DE89-012516] N89-25752
VAPOR PHASES
Experiments on liquid-vapour phase change between plane liquid surfaces. Part 3: Results from a closed quartz chamber
[NAL-TM-FM-8809] N89-25301
VAPORS
The development of a vapor compression refrigeration system for a network of nine temperature test chambers
[DE89-007084] N89-25355
VARIABLE STARS
Reminiscence of a stellar pulsation theorist
[DE89-011165] N89-25786
Rapid photometry of the Delta Scuti variable 63 Her N89-25916
Synthetic light curves and power spectra of Delta Scuti stars: An approach to modeling pulsations N89-25917
Variable star statistics in open clusters: NGC 6192 N89-25920
VARIANCE (STATISTICS)
Polynomial method of approximate centers for linear programming
[PB89-146161] N89-25584
VARISTORS
Sintering schedule and sample geometry effects on the electrical and physical properties of high field varistor materials
[DE89-010523] N89-25384
VEGETATION
Comparative investigations of multispectral satellite image data of MOMS-01, LANDSAT-TM and LANDSAT-MSS for geological and vegetational applications in test sites in the Andes of northern Chile and the Parana-Basin of Brazil
[DFVLR-FB-88-50] N89-25499
VELOCITY DISTRIBUTION
Measurement of velocity fields in vortex structures N89-25130
Measurements of high degree solar oscillation amplitudes N89-25825
Dynamics of the overshoot layers and boundary conditions in helioseismology N89-25826
Radial and latitudinal gradients in the solar internal angular velocity N89-25831
Sound velocity distribution in the Sun inferred from asymptotic inversion of p-mode spectra N89-25900
The effect of a nonspherical sound speed on the acoustic frequency spectrum of the Sun N89-25914
The search for radial velocity variations in rapidly oscillating Ap stars using the Fabry-Perot Interferometric Stellar Oscillation Spectrometer (FP-ISOS) N89-25923
VELOCITY MEASUREMENT
Effect of atmospheric extinction on solar radial velocity measurements N89-25849
Can solar g-modes be identified from ground-based velocity measurements N89-25880
High precision velocity measurements of Procyon using the 7699 A line of potassium N89-25922
VERTICAL DISTRIBUTION
The interpretation of data from the Viking Mars Atmospheric Water Detectors (MAWD): Some points for discussion N89-25795
On the vertical distribution of water vapor in the Martian tropics N89-25800
Circumpolar hoods and clouds and their relation to the Martian H2O cycle N89-25803
Observations of atmospheric water vapor with the SAGE 2 instrument N89-25805
Measurements of the vertical profile of water vapor abundance in the Martian atmosphere from Mars Observer N89-25811
VERY LONG BASE INTERFEROMETRY
Studies of regional and global tectonics and the rotation of the earth using very-long baseline interferometry
[NASA-CR-185059] N89-25534
VIBRATION
Simple fixture concepts for multi-axis vibration testing
[DE89-007977] N89-25481
VIBRATION DAMPING
Experiences in applying optimization techniques to configurations for the Control of Flexible Structures (COFS) program N89-25228
Potential uses of vacuum bubbles in noise and vibration control
[NASA-CR-181629] N89-25674
Optical fiber sensors and signal processing for intelligent structure monitoring
[NASA-CR-185395] N89-25691
VIBRATION SIMULATORS
Simple fixture concepts for multi-axis vibration testing
[DE89-007977] N89-25481
VIBRATION TESTS
Vibration testing of impact-damaged composite laminates
[NASA-TM-4115] N89-25290
Simple fixture concepts for multi-axis vibration testing
[DE89-007977] N89-25481
VINYL POLYMERS
Poled polymer films for nonlinear optics
[DE89-010039] N89-25338
VISCOELASTICITY
Parameter estimation for a viscoelastic constitutive model
[DE89-008714] N89-25336
VISCOUS FLOW
Techniques for compressible flow calculations on multizone grids N89-25120
Study of the stability of compressible Couette flow N89-25410
VISIBLE INFRARED SPIN SCAN RADIOMETER
Visible and near-infrared channel calibration of the GOES-6 VISSR using high-altitude aircraft measurements
[NASA-TM-101064] N89-25494
VISUAL PHOTOMETRY
An auroral TV-system
[REPT-115(1988)] N89-25543
VOIDS
Stress-driven diffusive voiding of aluminum conductor lines
[DE89-009832] N89-25387
VOLATILITY
Processing chemically prepared Tl-Ca-Ba-Cu oxide superconductors
[DE89-011535] N89-25748
VOLTAGE CONVERTERS (AC TO AC)
Frequency spectra for admittances and voltage transfers measured on a three-phased power transformer
[EUT-87-E-181] N89-25400
VOLTAGE REGULATORS
Controller for stabilization of high voltage
[NAL-TM-MT-8702] N89-25382
VORTEX BREAKDOWN
Vortex flows in flying technique
[ETN-89-94428] N89-25126
Investigations of vortex breakdown N89-25128
Unsteady phenomena on delta wings with partially broken-down vortex regions N89-25129
Measurement of velocity fields in vortex structures N89-25130
VORTEX FILAMENTS
Unsteady stagnation-point heat transfer during passage of a concentrated vortex
[NASA-CR-182297] N89-25404
VORTEX SHEDDING
Airfoil self-noise and prediction
[NASA-RP-1218] N89-25673
VORTEX STREETS
Interaction between compression shocks and vertical flows N89-25132
VORTICES
Interactions of Tollmien-Schlichting waves and Dean vortices. Comparison of direct numerical simulation and a weakly nonlinear theory
[NASA-TP-2919] N89-25118
On the Gortler vortex instability mechanism at hypersonic speeds
[NASA-CR-181844] N89-25123
Strongly unsteady vortex fields at elastic helicopter rotor blades N89-25131
Interaction between compression shocks and vertical flows N89-25132
Mechanical reaction of wings moving through a vortex region N89-25139
A variationally optimized vortex tracing algorithm for three-dimensional flows around solid bodies
[ETN-89-94301] N89-25423
A numerical study of a class of TVD schemes for compressible mixing layers
[NASA-TM-102194] N89-25651
VORTICITY
The evolution and structure of the bow echo/microburst events N89-25550

W

WAFERS
ALWAYS: A system for wafer yield analysis
[EUT-88-E-189] N89-25617
WALL FLOW
On the Gortler vortex instability mechanism at hypersonic speeds
[NASA-CR-181844] N89-25123
WALLS
Acoustic propagation in curved ducts with extended reacting wall treatment
[NASA-TM-102110] N89-25670
WATER
Water in the Martian regolith N89-25791
WATER RUNOFF
Reduce uncertainty in projection of future sea-level change due to ice wastage
[DE89-011483] N89-25526
WATER TUNNEL TESTS
Unsteady flow on profiles in a liquid Ludwig tunnel N89-25136
WATER VAPOR
Studies of regional and global tectonics and the rotation of the earth using very-long baseline interferometry
[NASA-CR-185059] N89-25534
MECA Workshop on Atmospheric H2O Observations of Earth and Mars. Physical Processes, Measurements and Interpretations
[NASA-CR-183335] N89-25790
Transport of Mars atmospheric water into high northern latitudes during a polar warming N89-25792
The effect of global-scale divergent circulation on the atmospheric water vapor transport and maintenance N89-25793
Seasonal and diurnal variability of Mars water-ice clouds N89-25794
The interpretation of data from the Viking Mars Atmospheric Water Detectors (MAWD): Some points for discussion N89-25795
Regolith water vapor sources on Mars: A historical bibliography N89-25796
Factors governing water condensation in the Martian atmosphere N89-25797
Cumulus convection and the terrestrial water-vapor distribution N89-25798
On the vertical distribution of water vapor in the Martian tropics N89-25800
The behavior of water vapor in the Mars atmosphere N89-25801
Solar Mesosphere Explorer observations of stratospheric and mesospheric water vapor N89-25802
Circumpolar hoods and clouds and their relation to the Martian H2O cycle N89-25803
Very high elevation water ice clouds on Mars: Their morphology and temporal behavior N89-25804
Observations of atmospheric water vapor with the SAGE 2 instrument N89-25805
Flux of water vapor in the terrestrial stratosphere and in the Martian atmosphere N89-25806
Measurements of H2O in the terrestrial mesosphere and implications for extra-terrestrial sources N89-25808
Diurnal and annual cycles of H2O in the Martian regolith N89-25809

The Nimbus 7 LIMS (Limb Infrared Monitor of the Stratosphere) water vapor measurements N89-25810
Measurements of the vertical profile of water vapor abundance in the Martian atmosphere from Mars Observer N89-25811
Atmospheric H2O and the search for Martian brines N89-25812
The interannual variability of atmospheric water vapor on Mars N89-25813

WAVE INTERACTION
Interactions of Tollmien-Schlichting waves and Dean vortices. Comparison of direct numerical simulation and a weakly nonlinear theory [NASA-TP-2919] N89-25118

WAVE PROPAGATION
Tropospheric influences on satellite-Earth paths and their determination by means of radar measurements [DFVLR-FB-88-53] N89-25250
A multifrequency antenna system for propagation experiments with the Olympus satellite [EUT-88-E-192] N89-25378
Wave emissions from planetary magnetospheres [NASA-CR-185435] N89-25541
Plasma production using microwave and radio frequency sources [DE89-011615] N89-25709
On the dissipation of Alfven waves in magnetic atmospheres and flux tubes N89-25871
Viscous magnetohydrodynamic modes and p-mode absorption by sunspots N89-25873
Asymptotic approximations of nonradial oscillation modes of the Sun N89-25932

WAVEFORMS
Automated Test and Evaluation Center for Waveform Digitizer Systems and Components [DE89-010226] N89-25441

WAVEGUIDES
Computer simulation of FEL sidebands in a strongly dispersive waveguide [DE89-011825] N89-25369
Pyramidal horns: Part 2: A novel design method for horns of any desired gain and aperture phase error [DE89-005346] N89-25371
High-average-power millimeter-wave FEL (Free-Electron Laser) for plasma heating using the ETA-2 accelerator [DE89-012294] N89-25711

WEAK ENERGY INTERACTIONS
Nuclear beta decay far from stability and astrophysics [MPI-H-1988-V-27] N89-25683

WEAR
Method of protecting surfaces from abrasion and abrasion resistant articles of manufacture [DE89-010798] N89-25344
Influence of rubbing on rotor dynamics, part 1 [NASA-CR-183648-PT-1] N89-25463
Influence of rubbing on rotor dynamics, part 2 [NASA-CR-183649-PT-2] N89-25464

WEIGHT REDUCTION
An approximation function for frequency constrained structural optimization N89-25196
Structural optimization of framed structures using generalized optimality criteria N89-25197
Optimizing for minimum weight when two different finite element models and analyses are required N89-25200
An improved algorithm for optimum structural design with multiple frequency constraints N89-25229

WELD TESTS
Basics of ultrasonic testing [DE89-010465] N89-25473

WELDABILITY
Weldability and weld doping of commercial purity molybdenum [DE89-009535] N89-25311

WELDING
A review of computer aided interpretation technology for the evaluation of radiographs of aluminum welds [NASA-CR-185066] N89-25312

WETLANDS
Workshop on Sea Level Rise and Coastal Processes [DE89-010297] N89-25522

WHEELS
Analysis and control of a three-degree-of-freedom robot platform [DE89-006427] N89-25356

WHISKER COMPOSITES
SiC whisker-reinforced SiAlON composites: Effect of sintering aid content [DE89-010376] N89-25289

WHISKERS (CRYSTALS)
Whisker shaped carbon substance [DE89-010214] N89-25288

WHITE DWARF STARS
The origin of ultra-compact binaries [NASA-TM-101792] N89-25780

WIND EFFECTS
Contributions to the improvement of flight safety in wind shear [DFVLR-FB-88-49] N89-25144

WIND SHEAR
Contributions to the improvement of flight safety in wind shear [DFVLR-FB-88-49] N89-25144

WIND TUNNEL APPARATUS
On the stress problem of the pebble bed heat exchanger in a hypersonic wind tunnel [NAL-TM-ST-8705] N89-25240

WIND TUNNEL MODELS
Unsteady flow on profiles in a liquid Ludwig tunnel N89-25136

WIND TUNNEL TESTS
Low-speed wind tunnel performance of high-speed counterrotation propellers at angle-of-attack [NASA-TM-102292] N89-25121
Spanwise lift distributions and wake velocity surveys of a semi-span wing with a discontinuous twist [NASA-CR-177532] N89-25122
Aerodynamic flight evaluation analysis and data base update [NASA-CR-183654] N89-25276

WIND TUNNELS
Pressure measurement technique of WT-WK --- wind tunnels [DFVLR-MITT-88-11] N89-25243

WIND TURBINES
Wind Energy Program Summary. Volume 2: Research summaries, fiscal year 1988 [DE89-000857] N89-25517

WINDMILLS (WINDPOWERED MACHINES)
Wind Energy Program Summary. Volume 2: Research summaries, fiscal year 1988 [DE89-000857] N89-25517

WINDPOWER UTILIZATION
Wind Energy Program Summary. Volume 2: Research summaries, fiscal year 1988 [DE89-000857] N89-25517

WINDPOWERED GENERATORS
Wind Energy Program Summary. Volume 2: Research summaries, fiscal year 1988 [DE89-000857] N89-25517

WING LOADING
Effect of winglets on loading mechanics and wing assembly reactions N89-25137
Mechanical reaction of wings moving through a vortex region N89-25139

WING PROFILES
Vortex structures in the wake of transonic flow about profiles N89-25134
Flow about trailing edges in unsteady flow N89-25135

WING SPAN
Spanwise lift distributions and wake velocity surveys of a semi-span wing with a discontinuous twist [NASA-CR-177532] N89-25122

WING TIP VORTICES
Vortex flows in flying technique [ETN-89-94428] N89-25126
Integration method for the calculation of flow with free vortices N89-25127
Investigations of vortex breakdown N89-25128
Unsteady phenomena on delta wings with partially broken-down vortex regions N89-25129
Measurement of velocity fields in vortex structures N89-25130
Dissipation of vortex power in longitudinal flow on wings N89-25133
Vortex structures in the wake of transonic flow about profiles N89-25134
Damping of wing tip vortex systems by the modification of the wing tips N89-25138

WING TIPS
Damping of wing tip vortex systems by the modification of the wing tips N89-25138
Structural optimization of rotor blades with straight and swept tips subject to aeroelastic constraints N89-25152

WINGLETS
Vortex flows in flying technique [ETN-89-94428] N89-25126
Effect of winglets on loading mechanics and wing assembly reactions N89-25137
Flight-mechanical investigations of the lateral motion of configurations with winglets N89-25141

WINGS
Aerolastic tailoring and integrated wing design N89-25167
An integrated approach to the optimum design of actively controlled composite wings N89-25194

WIRE
Flying wires at Fermilab [DE89-011005] N89-25251
Production of wires and coils from high-temperature superconducting materials [DE89-012380] N89-25756

WORKING FLUIDS
Advanced working fluid properties in heat pump and absorption cooling operations [PB89-178172] N89-25413
Advanced binary geothermal power plants working fluid property determination and heat exchanger design [DE89-011144] N89-25513

WORKLOADS (PSYCHOPHYSIOLOGY)
Timesharing performance as an indicator of pilot mental workload [NASA-CR-185328] N89-25573
Validation of the subjective workload assessment technique in a simulated flight task [DFVLR-FB-89-01] N89-25575

WORKSTATIONS
Concurrent Image Processing Executive (CIPE) [NASA-CR-185460] N89-25619

X

X RAY ANALYSIS
Submicron technologies for the fabrication of monolithic integrated millimeter wave devices on high resistivity silicon [ETN-89-94624] N89-25757

X RAY DIFFRACTION
Advances in the development of apparatus and methods for studies of protein monocrystals in coordinate X-ray diffractometers based on two-dimensional proportional chambers [DE88-706259] N89-25740

X RAY FLUORESCENCE
X-ray based extensometry [NASA-CR-185058] N89-25432

X RAY SCATTERING
X-ray scattering studies of non-equilibrium ordering processes [DE89-012517] N89-25753

X RAY SPECTROSCOPY
Diffraction gratings used in X-ray spectroscopy [DE89-012327] N89-25310

X RAY STRESS MEASUREMENT
Controller for stabilization of high voltage [NAL-TM-MT-8702] N89-25382

X RAYS
The evolution of energetic particles and the emitted radiation in solar flares [NASA-CR-185389] N89-25945

XENON CHLORIDE LASERS
A 2 J high-power excimer laser at high pulse repetition rate [U9-414/87/029] N89-25457

Y

YTTRIUM OXIDES
Production of wires and coils from high-temperature superconducting materials [DE89-012380] N89-25756

Z

ZIRCONIUM ALLOYS
Review of oxidation of Nb-1Zr [DE89-010299] N89-25687

ZONAL FLOW (METEOROLOGY)
Comparison of satellite-derived dynamical quantities for the stratosphere of the Southern Hemisphere [NASA-CP-3044] N89-25540

Typical Personal Author Index Listing

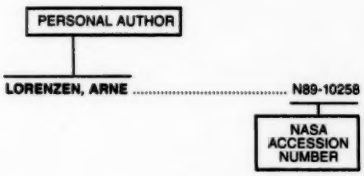

Listings in this index are arranged alphabetically by personal author. The NASA accession number denotes the number by which the citation is identified.

A

ABDEL-GAWAD, K. N89-25854
ABDI, F. N89-25209
ABE, H. N89-25699
ABEL, IRVING N89-25150
ACOSTA, WALDO A. N89-25238
ADAMS, GEORGE B., III N89-25600
ADAMS, WILLIAM M., JR. N89-25191
ADATI, K. N89-25700
ADELMAN, HOWARD M. N89-25151
ADVANI, A. N89-25321
AHL, ELVIN L. N89-25363
AHLBORN, K. N89-25297
AIHIE, V. U. N89-25658
N89-25659
AINDOW, A. N89-25844
AITHAL, R. N89-25187
AKIYAMA, R. N89-25700
ALBRECHT, ANDREAS N89-25788
ALEXANDRESCU, RODICA N89-25303
ALLEN, JANET K. N89-25208
ALLEN, S. L. N89-25707
ALLEN, S. M. N89-25315
ALTHAUS, W. N89-25132
ALVAREZ, M. N89-25846
N89-25916
AMADEN, C. A. N89-25750
AMANO, T. N89-25701
AMBASTHA, ASHOK N89-25855
AMODEO, ROBERT JOHN N89-25477
AMOS, D. E. N89-25387
AMSDEN, A. A. N89-25304
ANDERSEN, BO NYBORG N89-25848
N89-25856
N89-25884
N89-25886
N89-25887
ANDERSEN, EDWIN R. N89-25856
ANDERSEN, N. B. N89-25846
ANDERSON, D. M. N89-25180
ANDERSON, DUWAYNE M. N89-25791
ANDERSON, K. N89-25385
ANDERSON, M. U. N89-25342
ANDERSON, T. J. N89-25752
ANDO, A. N89-25700
ANDRIANOVA, M. E. N89-25740
ANTONELLO, E. N89-25930
AOKI, T. N89-25700
APOSTOL, I. N89-25434
APPOURCHAUX, T. N89-25858
N89-25925
ARENDT, PAUL N. N89-25745
ARENDT, UDO N89-25723
ARMAND, MICHEL B. N89-25389
ARMET, DAVID B. N89-25856
ARNOLD, CHARLES, JR. N89-25345
ARONSON, EUGENE A. N89-25576
ARTLEY, MARGERY E. N89-25237
ATAC, R. N89-25578
N89-25631
ATKINSON, D. P. N89-25711
ATTERIDGE, D. G. N89-25321
ATTOU, MOULOUD N89-25302
AUBERT, JAMES H. N89-25345
AURAND, JOHN F. N89-25370
N89-25371
AUSTEL, L. N89-25209
AVERY, DON E. N89-25947
AZAM, J. N89-25497
AZARM, SHAPOUR N89-25204
AZZOUZ, ABDELKRIM N89-25302

B

BACA, ROBERT N89-25355
BACA, THOMAS J. N89-25440
BACON, L. D. N89-25362
BAGCHI, A. N89-25321
BAITY, F. W. N89-25368
BAKER, T. E. N89-25226
BAKKER, R. R. N89-25641
BALACHANDRAN, U. N89-25756
BALL, WARREN N89-25854
N89-25855
BALLING, R. J. N89-25176
BALMFORTH, N. J. N89-25828
BALSIGER, HANS N89-25776
BALTHASAR, H. N89-25865
BAPURAO, M. N. N89-25240
BARANOV, A. M. N89-25350
BARESI, LARRY N89-25519
BARNA, B. A. N89-25257
N89-25696
BARNES, J. R. N89-25792
BARNETT, DEANNA L. N89-25636
BARNETT, T. P. N89-25521
BARON, PAUL N89-25601
BARTH, CHARLES A. N89-25802
BARTH, MARVIN J. N89-25587
BARTHELEMY, JEAN-FRANCOIS M. N89-25146
N89-25173
N89-25201
N89-25202
BASTIAANS, M. J. N89-25698
BATES, PRESTON R. N89-25162
BATSON, ROBERT G. N89-25764
BAUCOM, ROBERT M. N89-25294
BAUMEISTER, KENNETH J. N89-25670
BAUMJOHANN, W. N89-25718
BECKEL, STEPHEN A. N89-25238
BECKERMAN, MARTIN N89-25636
BEIGHTOL, DAVID N89-25481
BELEQUNDU, A. D. N89-25184
BELL, C. R. N89-25923
N89-25929
BELL, JOHN B. N89-25421
BELL, R. GLENN N89-25440
BELMONTE, JUAN A. N89-25849
N89-25916
N89-25919
N89-25923
N89-25928
BELOSHITSKIJ, V. V. N89-25738
BELTRACCHI, TODD J. N89-25182
BELYAKOV, YU. I. N89-25313
BELYTSCHKO, TED N89-25620
BENTLY, DONALD E. N89-25463
N89-25464
BENTON, D. NEILL N89-25487
BENTS, DAVID J. N89-25280
BERGER, R. L. N89-25362
BERGHAUS, UWE N89-25697
BERKEN, RIZA C. N89-25637
BERMAN, ALEX N89-25175
BERRYMAN, JAMES G. N89-25295
BERTELLO, L. N89-25822
BERTHOMIEU, G. N89-25884
N89-25888
BETHKE, KARL-HEINZ N89-25376
BEYER, JAMES B. N89-25396
BHATT, VINAY N89-25205
BI, D. G. N89-25700
BINDER, J. N89-25715
BING, YANG N89-25218
BIRDSALL, C. K. N89-25710
BIRMINGHAM, DANNY N89-25759
BISHOP, MATT N89-25598
N89-25599
BLACKMAN, GREGORY SCOTT N89-25743
BLAMONT, JACQUES N89-25776
BLANCHARD, ROBERT C. N89-25124
BLAND, T. B. N89-25630
BLANKEN, HENK N89-25614
BLIEM, C. J. N89-25513
BLOOMFIELD, HARVEY S. N89-25272
BOATNER, L. A. N89-25333
BOEDECKER, GERD N89-25545
N89-25548
N89-25547
BOGART, R. S. N89-25885
BOGDAN, T. J. N89-25864
BOGORAD, LAWRENCE N89-25559
BOHLMANN, JON N89-25167
BOLLEN, M. H. J. N89-25400
BOLUKBASI, A. O. N89-25180
BONDAREV, V. N. N89-25379
BONNET, R. M. N89-25881
BORDE, J. N89-25660
BOUMIER, P. N89-25895
BOURCIER, ROY J. N89-25483
BOWELL, EDWARD N89-25435
BOWERS, HENRY M. N89-25262
BOWLES, KENNETH J. N89-25300
BOWMAN, KEITH B N89-25171
BOXUM, B. N89-25854
BOYDEN, JOHN E. N89-25877
BOYLE, W. W. N89-25276
BRAMSON, G. N89-25707
BRANDHORST, HENRY W., JR. N89-25506
BRAUNSCHEIDEL, EDWARD P. N89-25283
BRAZIER, R. I. N89-25919
BRENNER, HOWARD N89-25417
BREUER, M. N89-25127
BRIDGES, G. I. N89-25276
BRIERS, R. N89-25932
BRINE, GERALD T. N89-25234
BRINKMANN, H. J. N89-25427
BRODSKY, M. A. N89-25903
BROOKS, J. N. N89-25703
BROOKS, N. H. N89-25707
BROOKS, THOMAS F. N89-25673
BROWN, KENNETH W. N89-25165
BROWN, TIMOTHY M. N89-25856
BRUEMMER, S. M. N89-25317
N89-25321
BRULS, J. H. M. J. N89-25862
BRUMBAUGH, RANDAL W. N89-25163
BRUNO, JOHN N89-25629
BRUNO, K. N89-25416
BRUNO, R. N89-25227
BRUNS, A. V. N89-25881
BRUSH, ANDREW S. N89-25403
BRUZA, I. V. N89-25377
BUBENZER, ACHIM N89-25518
BUCHKREMER, H. ST. N89-25130
BUCK, GREGORY M. N89-25443
BUDAI, J. D. N89-25749
BUDEN, DAVID N89-25264
BUKOWSKI, E. D. N89-25747
BUKSA, EDWARD J. N89-25481
BULL, F. N89-25854
BUNKER, B. C. N89-25744
N89-25748
BURKE, A. F. N89-25392
BURKE, G. J. N89-25372
BURKE, W. R. N89-25660
BURKEN, J. J. N89-25195
BURRELL, K. H. N89-25707
BURTNER, GEORGE N89-25685
BUS, SCHELTE J. N89-25435
BUSH, MARILYN W. N89-25618
BUSTAMANTE, ALBINO C. N89-25487
BUTLER, T. D. N89-25304
BUTT, GRAHAM N89-25137
BUTTON, ROBERT M. N89-25403
BUTTRILL, CAREY S. N89-25190
BYRNES, STEVEN J. N89-25396

C

CACCIANI, ALESSANDRO N89-25831
N89-25832
N89-25838
N89-25842
N89-25850
N89-25851
N89-25926
CACCIN, B. N89-25822
CAHILL, PAUL A. N89-25338
CAHN, JULIUS H. N89-25935
CAI, DA-WEI N89-25331
CALFO, FREDERICK D. N89-25277
CALLIS, R. W. N89-25707
CALOVINI, MASSIMO N89-25609
CAMPBELL, R. L. N89-25172
CAMPBELL, W. R. N89-25874
CAMPOS, L. M. B. C. N89-25871
CANAVAN, GREGORY H. N89-25255
CANFIELD, R. A. N89-25196
N89-25197
CAO, M. T. N89-25756
CARLSON, NANCY M. N89-25465
N89-25696
CARLSTROM, T. N. N89-25707
CARNEY, LYNNETTE M. N89-25281
CARRERAS, B. A. N89-25702
N89-25713
CARSTENS, VOLKER N89-25125
CARTER, M. D. N89-25709
CARUTHERS, JAMES M. N89-25300
CASEL, A. N89-25757
CASPER, PATRICIA A. N89-25573
CASSE, M. N89-25933
CATALA, C. N89-25940
CATALANO, S. N89-25926
CAUGHMAN, J. B. O., II N89-25708
CEDENO, C. N89-25321
CELI, ROBERTO N89-25152
CEPLECHA, ZDENEK N89-25779
CHAKOUMAKOS, B. C. N89-25749
CHAMIS, C. C. N89-25490
CHAN, K. S. N89-25340
CHAN, WEN S. N89-25296
CHANG, FRANKLIN R. N89-25279
CHANG, WON SOON N89-25422
CHANGHO, NAM N89-25189
CHAPLANOVA, I. N. N89-25738
CHAPMAN, CLARK R. N89-25944
CHAPMAN, K. N89-25412
CHARLOT, L. A. N89-25321
CHATTOPADHYAY, ADITI N89-25156
CHAUHAN, D. S. N89-25444
CHEN, G.-S. N89-25227
CHEN, JIAN N89-25893
CHEN, TSING-CHANG N89-25793
CHENG, JIZU N89-25187
CHENG, Y. P. N89-25153
CHERNENKO, N. M. N89-25350
CHERNENKO, S. P. N89-25740
CHERNIKOV, N. A. N89-25536
CHEU, TSU-CHIEN N89-25207
CHEVRETON, M. N89-25916
CHIN, B. A. N89-25467
N89-25468
CHINAEVA, V. P. N89-25313
CHISTYAKOV, S. V. N89-25739
CHOI, KYUNG K. N89-25181
CHOPRA, INDERJIT N89-25155
CHRISTENSEN-DALSGAARD, J. N89-25843
N89-25896
N89-25904
N89-25905
CHRISTENSEN, HENRIK I. N89-25593
N89-25594
CHRISTENSEN, PHILIP R. N89-25794
CHRISTHILF, DAVID M. N89-25191
CHRISTOPHOROU, LOUCAS G. N89-25395
CHU, F. H. N89-25225
CHU, M. S. N89-25707
CHU, W. P. N89-25805
CHUBB, DONALD L. N89-25277
CIRKEL, HANS-JUERGEN N89-25457
CLANCY, R. TODD N89-25802
CLARK, J. C. N89-25711
CLARKE, JOHN N89-25755
CLAUS, R. O. N89-25891
CLAUSING, R. E. N89-25471
CLETTE, F. N89-25852
CLIFFORD, STEPHEN M. N89-25790
N89-25795
N89-25796
CLOUGH, ROGER L. N89-25293
N89-25335
N89-25345
COFFEY, HELEN E. N89-25817
COHEN, MARC M. N89-25266
COLBURN, DAVID S. N89-25797
COLE, EDWARD I., JR. N89-25397
COLE, J. N89-25854
COLE, L. N89-25854
COLELLA, PHILLIP N89-25421
COLEMAN, RONALD N89-25482
COLEMAN, SANDRA C. N89-25764
COLLERAINE, A. P. N89-25707
COLLEY, S. N89-25854
COLLINS, WILLIAM D. N89-25332
COMPTON, WILLIAM DAVID N89-25946
CONNELL, PETER S. N89-25531
CONTENT, D. N89-25707
COOK, A. N89-25578
N89-25631
COOK, W. A. N89-25488
COOPER, GREGORY T. N89-25619
COOPERSTEIN, J. N89-25787
CORBETT, G. K. N89-25460
COSTA, G. N89-25926
COTTON, THERESE M. N89-25562
COX, ARTHUR N. N89-25902
N89-25935
COX, DAVE N89-25691
CRABB, RICHARD L. N89-25478
CRAWFORD, C. N89-25251
CRAWLEY, EDWARD F. N89-25258
CRNKOVIC, C. N89-25758
CROMMELYNCK, D. N89-25884
CRUCEANU, E. N89-25735
CRUMLEY, R. L. N89-25392
CULBERT, CHRIS N89-25635
CURRY, ARTHUR E. N89-25463
N89-25464
CUSHMAN, ROBERT M. N89-25522

D

DADDA, LUIGI N89-25608
DAEMBKES, HEINRICH N89-25399
DAEPPEN, W. N89-25897
N89-25906
N89-25907
N89-25916
N89-25933
N89-25937
N89-25939
DAFNIS, ATHANASSIOS N89-25137
DAHLEN, HELMUT N89-25677
DALLY, WILLIAM R. N89-25522
DAME, LUC N89-25883
N89-25895
DARDEN, CHRISTINE M. N89-25117
DAVID, S. A. N89-25466
DAVIDSON, G. S. N89-25577
DAVIS, CECIL G. N89-25786
DAVIS, WAYNE J. N89-25596
DEAN, ROBERT G. N89-25522
DEBOO, J. C. N89-25707
DEBROY, T. N89-25466
DEBY, ROLF A. N89-25615
DECHAUMPHAI, PRAMOTE N89-25198
DEFIGUEIREDO, RUI J. P. N89-25360
DEGRYSE, K. N89-25932
DEHOFF, PAUL H. N89-25268
N89-25444
DEIS, G. A. N89-25711
DEJONG, KENT N89-25592
DEJONGHE, LUTGARD C. N89-25389
DELABOUDINIERE, J. P. N89-25881
DELACHE, PHILIPPE N89-25884
N89-25924
N89-25941
N89-25942
DELUCA, E. E. N89-25837
DELUIS, JAVIER N89-25258
DEMARQUE, P. N89-25835
DENNER, HANS-DIETRICH N89-25357
DENNING, PETER J. N89-25566
N89-25628
N89-25638
DEPPE, J. N89-25578
N89-25631
DESHPANDE, M. D. N89-25301
DEXTER, R. N. N89-25705
DIAKOMIHALIS, D. N89-25750
DIAZ, ALEJANDRO R. N89-25216
DICKENS, M. N89-25589
DICKMANN, JUERGEN N89-25399
DIEKMANN, A. N89-25141
DIJK, J. N89-25377
DILLENIUS, M. F. E. N89-25169
DIROSA, DONALD N89-25492
DISHNER, B. N89-25385
DISTEFANO, J. R. N89-25687
DOBECK, NICK N89-25685
DODD, ALAN J. N89-25221
DODD, JEFFREY A. N89-25524
DOEBELE, H. G. N89-25308
DOGAN, B. N89-25327
DOLGOV, A. D. N89-25361
DOMANSKI, R. N89-25427
DOMINGO, V. N89-25846
N89-25848
N89-25881
N89-25882
N89-25884
N89-25887
DOMINGUEZ, N. N89-25702
N89-25713
DONNER, LEO J. N89-25798
DOPKER, BERNHARD N89-25219
DOROBANTU, I. A. N89-25449
DORRIS, S. E. N89-25756
DORTMANN, K. N89-25135
DOSS, JAMES D. N89-25383
DOWDNEY, K. N89-25854
DOWDY, LAWRENCE W. N89-25623
DOWELL, F. N89-25347
DRAGANESCU, V. N89-25303
DRAIM, JOHN E. N89-25262
DRAKE, J. B. N89-25586
N89-25602
DRAKE, R. N89-25854
DRESS, W. B. N89-25639
DRITZ, KENNETH W. N89-25588
DRUCE, R. L. N89-25393
DUHALDE, OSCAR N89-25855
DUKE, C. B. N89-25690
DUKE, EUGENE L. N89-25163
DUM, C. T. N89-25721
N89-25725
DURAND, D. J. N89-25747
DUSEK, J. T. N89-25756
DUVALL, T. L., JR. N89-25888
DZIEMBOWSKI, WOJCIECH N89-25863

E

EAGAR, T. W. N89-25315
EASTEP, F. E. N89-25171
EDENBOROUGH, KEVIN L. N89-25263
EFTEKHARI, ABE N89-25433
EICHTEN, E. N89-25631
EINSTEIN, J. R. N89-25589
EINSTEIN, RALPH N89-25636
EL-AGAMAWI, MOHSEN MOHAMED N89-25816
ELIASON, JAY R. N89-25542
ELLSAESSER, HUGH W. N89-25528
ELMER, J. W. N89-25315
ELSWORTH, Y. P. N89-25824
N89-25844
N89-25849
ERCK, R. A. N89-25470
ERDELYVARY, I. N89-25313
ERDEMIR, A. N89-25470
EVANS, G. A. N89-25658
N89-25659
EXARHOS, G. J. N89-25690
N89-25694

F

FABER, VANCE N89-25626
FAGHRI, AMIR N89-25422
FALATO, BETTY K. N89-25142
FALCO, CHARLES M. N89-25733
FANALE, FRASER P. N89-25812
FARRIS, DON N89-25855
FECHTIG, HUGO N89-25776
FEDERER, J. I. N89-25339
FELENBOK, P. N89-25940
FENNELL, ROBERT E. N89-25191
FENSKE, G. R. N89-25470
FERREIRA, C. N89-25385
FERRIS, K. F. N89-25690
FIELDS, B. A. N89-25318
FIELDS, R. J. N89-25318
FINK, J. N89-25411
FINLEY, D. N89-25251
FISCHER, GEORGE N89-25855
FISCHLER, MARK N89-25578
N89-25631
FISHER, J. J. N89-25462
FISZDON, W. N89-25424
FLANAGAN, D. P. N89-25590
FLORA, R. N89-25251

FOING, BERNARD H. N89-25940
FOKKINGA, MAARTEN M. N89-25612
FOSS, WILLARD E., JR. N89-25170
FOSSAT, ERIC N89-25845
N89-25867
N89-25889
N89-25921
N89-25927
N89-25941
N89-25942
FRANDSEN, SOREN N89-25920
FRANK, Z. N89-25875
FRANKLIN, WESLEY D. N89-25463
N89-25464
FREAR, D. R. N89-25314
FREE, J. C. N89-25176
FRENCH, JAMES C. N89-25579
N89-25601
FRENCH, RICHARD E. N89-25689
FREUND, ROLAND N89-25654
FRIEDMANN, PERETZ P. N89-25152
FROEHLICH, C. N89-25881
N89-25884
FRYDRYCH, W. S. N89-25690
N89-25694
FU, YANHONG N89-25672
FU, YIBIN N89-25123
FUENSALIDA, J. N89-25916
FUJITA, J. N89-25700
FULCHIGNONI, MARCELLO N89-25776
FUNG, ADRIAN K. N89-25364

G

GABEL, R. N89-25480
GABRIEL, M. N89-25931
GABRIELE, GARY A. N89-25182
GAILLARD, MARY K. N89-25761
GAINES, IRWIN N89-25578
N89-25580
N89-25631
N89-25693
GALLAGHER, RICHARD H. N89-25188
GANDHI, RAJ N89-25789
GANNON, J. N89-25251
GAO, QIANG N89-25891
GARBA, J. N89-25227
GARCIA, C. N89-25880
GARCIA, L. N89-25713
GARDNER, T. J. N89-25384
GARDNER, W. L. N89-25368
GARZA, OMAR N89-25685
GATZ, HARALD N89-25697
GAUTIER, D. N89-25924
GAVRJUSEV, VLADIMIR N89-25889
GAVRJUSEVA, ELENA N89-25889
GAZZANIGA, JOHN A. N89-25121
GEBHARDT, UTE N89-25732
GELBKE, EBERHARD N89-25697
GELLY, B. N89-25867
N89-25921
N89-25927
GENTILE, D. P. N89-25166
GERBRANDS, JAN JACOB N89-25605
GERING, KEVIN N89-25413
GERMAN, MARJORIE D. N89-25148
GEYER, ARTHUR N89-25399
GEYER, F. N89-25729
GHEZZI, C. N89-25607
N89-25633
GHITULESCU, T. P. N89-25535
GILBERT, MICHAEL G. N89-25185
N89-25239
GILBERT, NORBERT N89-25430
GILBERTSEN, NOREEN D. N89-25620
GILES, G. E. N89-25630
GILES, GARY L. N89-25170
GILLEN, K. T. N89-25335
GILMAN, P. A. N89-25837
GILMAN, S. E. N89-25750
GINLEY, D. S. N89-25748
GINSBERG, D. M. N89-25747
GIRARD, JEFFREY JOHN N89-25410
GIUDICE, G. F. N89-25785
GLAZER, J. N89-25322
GLENDENNING, NORMAN K. N89-25784
GLOCKLER, O. N89-25474
GLOVER, C. W. N89-25589
GOETZ, J. A. N89-25705
GOLDEN, DAVID M. N89-25286
GOMEZ, M. T. N89-25862
GOODING, JAMES L. N89-25799
GOODS, S. H. N89-25467
N89-25468
GORETTA, K. C. N89-25756
GORN, MARTIN N89-25518
GOUGH, DOUGLAS N89-25943
GOUGH, DOUGLAS O. N89-25823
N89-25826
N89-25853
N89-25872
N89-25898
N89-25899
N89-25904
N89-25906
N89-25907
GOULDING, R. H. N89-25368
GOUTTEBROZE, P. N89-25860
GRABBE, CROCKETT L. N89-25541
GRACEY, J. A. N89-25656
GRACIA-SALCEDO, CARMEN M. N89-25409
GRADT, THOMAS N89-25357
GRADY, JOSEPH E. N89-25290
GRAFE, V. G. N89-25577
GRAHAM, R. A. N89-25309
GRANDHI, RAMANA V. N89-25171
N89-25223
GRAY, STEPHANIE L. N89-25332
GREC, GERARD N89-25867
N89-25889
N89-25921
N89-25927
GREEN, PHILIP J. N89-25441
GREEN, TOMMY L. N89-25164
GREENE, A. F. N89-25754
GREENLEAF, JOHN E. N89-25558
GRIEST, KIM N89-25678
N89-25680
N89-25688
GRIFFIN, O. H., JR. N89-25217
GRIGORE, D. R. N89-25666
GRIMSHAW, ANDREW N89-25601
GRONSKY, R. N89-25679
GROOM, STEVEN L. N89-25619
GROSSBECK, M. L. N89-25467
N89-25468
GROSSMAN, BERNARD N89-25168
GROSSMAN, ROBERT N89-25772
GROVES, SCOTT E. N89-25291
GROVES, T. N89-25251
GRUENSPAHN, K. N89-25131
GU, YE-MING N89-25890
GUENTHER, D. B. N89-25835
GURDAL, ZAFER N89-25217
GUTTMANN, SABINE N89-25502
GUZIK, JOYCE A. N89-25902

H

HABER, D. A. N89-25872
HABERLE, ROBERT M. N89-25790
N89-25797
N89-25800
HACHISU, IZUMI N89-25780
HAFTKA, RAPHAEL T. N89-25160
N89-25168
N89-25172
HAILEY, C. E. N89-25420
HAJELA, PRABHAT N89-25158
N89-25230
HALFORD, GARY R. N89-25485
HALL, DAVID K. N89-25278
HALL, DAVID W. N89-25159
HALL, JEFFREY C. N89-25200
HALL, PHILIP N89-25123
HAMADA, Y. N89-25700
HAMASAKI, SEISHI N89-25704
HAMILTON, BRIAN K. N89-25157
HAMMETTER, W. F. N89-25748
HAMMOND, BRIAN LEE N89-25682
HAMMOND, DANA P. N89-25597
HANN, REUBEN L. N89-25575
HANSEN, IRVING G. N89-25271
HARDIN, J. E. N89-25392
HARMEYER, E. N89-25714
HARNED, DOUGLAS S. N89-25710
HARRIS, ALAN W. N89-25435
HART, J. K. N89-25199
HARTQUIST, T. W. N89-25726
HARVEY, J. W. N89-25829
N89-25854
N89-25868
HASSAN, AHMED A. N89-25154
HATHAWAY, DAVID H. N89-25856
HAUCK, MARTIN N89-25499
HAUG, EDWARD J. N89-25219
HAVERKORT, BOUDEWIJN R. N89-25476
HAYASHIDA, ROBERT D. N89-25463
N89-25464
HAYNES, H. D. N89-25386
HEDGEPETH, JOHN M. N89-25484
HELLMANN, D. N89-25491
HELMING, TH. N89-25128
HENNING, HARALD M. N89-25894
HERMANS, P. A. M. N89-25377
HEROLD, H. N89-25729
HEROLD, KEITH E. N89-25505
HERSENER, J. N89-25757
HESS, N. J. N89-25690
HESSE, MICHAEL N89-25717
HIDEKUMA, S. N89-25700
HIEDA, LES N89-25855
HIGHAM, NICHOLAS J. N89-25853
HILL, FRANK N89-25836
N89-25855
N89-25856
N89-25872
HILL, HENRY A. N89-25890
N89-25891
N89-25893
HILL, JOHN M. N89-25492
HINSON, EDWIN W. N89-25124
HIROKURA, S. N89-25700
HIRSCHFELD, TOMAS B. N89-25344
HITCHMAN, MATTHEW N89-25806
HOBERECHT, MARK A. N89-25273
N89-25275
HOCH, J. E. N89-25577
HOCKNEY, GEORGE N89-25578
HOEKSEMA, J. T. N89-25885
N89-25892
HOFFMAN, D. J. N89-25368
N89-25708
HOGENDORP, JAN ANNE N89-25611
HOGENHUIS, P. A. N89-25641
HOLIAN, BRAD LEE N89-25405
HOLLAND, W. ROBERT N89-25338
HOLLINGSWORTH, J. L. N89-25792
HOLMES, V. P. N89-25577
HOLZDEPPE, DIETER N89-25139
HOOKE, LYDIA RAZRAN N89-25556
HOPKINS, D. A. N89-25165
HOPKINS, D. B. N89-25455
HOSSELET, L. M. L. F. N89-25402
HOUBEN, JOHAN MARTIN N89-25326
HOWE, LAWRENCE A. N89-25505
HUBER, B. A. N89-25684
N89-25715
HUFF, DENNIS L. N89-25119
HUGHES, CHRISTOPHER E. N89-25121
HUGUENIN, R. L. N89-25796
HUH, OSCAR KARL N89-25492
HUNLEY, W. R. N89-25551
HUNT, JAMES L. N89-25210
HUNTEN, DONALD M. N89-25776
HUNTER, SCOTT R. N89-25395
HURASS, KARLHEINZ N89-25145
HURST, JANET B. N89-25285
HUSA, SHARON N89-25439
HUSBY, D. N89-25578
N89-25631
HUSTON, MARY MARGARET N89-25769
HWANG, SHWILONG JIMMY N89-25287

I

IDA, K. N89-25701
IDE, H. N89-25209
IJBEMA, ALLE N89-25614
INGBER, M. S. N89-25420
INGRAM, BOB N89-25855
INGRAM, J. E. N89-25261
INNIS, J. L. N89-25919
N89-25922
IONESCU-PALLAS, N. N89-25434
IOSIFESCU, M. N89-25647
IRVIN, TIMOTHY B. N89-25689
ISAAK, G. R. N89-25824
N89-25844
N89-25849
N89-25857
N89-25919
N89-25922
ISAAKYAN, G. A. N89-25437
ISHII, MAMORU N89-25406
IVANOV, A. B. N89-25740
IVANOV, A. I. N89-25437
IVANOV, EH. L. N89-25681

J

JACKSON, B. N89-25154
JACKSON, PATTY N89-25855
JACOBS, G. A. P. N89-25401

JACOBS, S. D. N89-25750
JAGACINSKI, RICHARD J. N89-25566
JAKOSKY, BRUCE M. N89-25801
N89-25802
JAKSHA, D. B. N89-25866
JAMES, PHILIP B. N89-25803
JANET, STANLEY N89-25601
JANG, JONG HOON N89-25422
JANSEN, J. F. N89-25356
N89-25460
JANSEN, P. G. N89-25581
JAQUIN, FRED N89-25804
JARAMILLO, L. L. N89-25794
JEFFERIES, S. M. N89-25824
N89-25868
JENNINGS, MARK J. N89-25415
JIANU, V. N89-25303
JIMENEZ, A. N89-25846
N89-25848
N89-25884
N89-25887
JIMENEZ, AMADOR P. N89-25273
JINDAL, ANITA N89-25632
JOHNSON, JOHN A. N89-25465
N89-25696
JOHNSON, MARJORY J. N89-25773
JOHNSON, MICHAEL A. N89-25373
JOHNSON, VICKI S. N89-25211
JOHNSTON, NORMAN J. N89-25294
JOLLY, M. R. N89-25750
JONES, A. R. N89-25846
N89-25848
N89-25884
N89-25887
N89-25919
JONES, ALBERT T. N89-25596
JONES, HARRISON P. N89-25856
JONES, JUDSON P. N89-25594
N89-25636
JONES, R. H. N89-25320
JONES, WENDELL B. N89-25483
JONG, R. A. N89-25711
JONKER, BERNED T. N89-25737
JORDAN, BASIL M., JR. N89-25164
JORDAN, E. H. N89-25432
JORKE, H. N89-25757
JORTNER, J. N89-25307
JOSTEN, A. N89-25141
JOZWIAK, LECH N89-25582
N89-25583
JURMAN, L. A. N89-25416

K

KACIUBA-USCILKO, HANNA N89-25558
KADETE, HENRY N89-25500
KAILA, KARI N89-25543
KAILASANATH, K. N89-25353
KAISER, DIETER N89-25498
KAISER, F. N89-25616
KALINNIKOV, V. A. N89-25436
KALNS, I. N89-25388
KAMAT, MANOHAR P. N89-25186
KAMATH, ASHOK N89-25240
KAMIN, RAY A., III N89-25600
KANE, JAMES H. N89-25187
N89-25188
KANEKO, O. N89-25701
KANTOWITZ, BARRY H. N89-25573
KAO, PI-JEN N89-25166
KAPUSTKA, ROBERT E. N89-25278
KARR, T. J. N89-25453
KAUFMAN, JAMES M. N89-25825
KAWAHATA, K. N89-25700
N89-25701
KAYAHAN, GURHAN N89-25649
KELLER, VERNON W. N89-25242
KERCZEWSKI, ROBERT J. N89-25365
KERRES, W. N89-25136
KERSTEN, W. F. J. N89-25401
KESSIE, ROBERT W. N89-25394
KETTHAUS, BIRGIT N89-25677
KEYES, T. F. N89-25407
KHEJKER, D. M. N89-25740
KHOT, N. S. N89-25223
KHRIPLOVICH, I. B. N89-25361
KIDMAN, RUSSELL B. N89-25902
KIERNAN, LAURENCE N89-25241
KIESSLING, MICHAEL K.-H. N89-25727
KILGORE, D. C. N89-25774
KIM, ALBERT N89-25601
KIM, D.-S. N89-25203
KINGSLEY, LORI M. N89-25463
N89-25464
KINNISON, DOUGLAS E. N89-25530
KIRBIE, H. C. N89-25398
KIRBIYIK, HALIL N89-25938
KIRCH, LUKE A. N89-25267
KISNER, ROGER A. N89-25637
KJELDSEN, HANS N89-25920
KLAPDOR, H. V. N89-25683
KLIPPING, GUSTAV N89-25357
KLIPPING, INGRID N89-25357
KLOSKO, S. M. N89-25539
KLUMPP, CATHY N89-25801
KNAPP, BARRY G. N89-25802
KNEE, H. E. N89-25571
KNOELKER, M. N89-25864
KOBLINSKY, C. J. N89-25539
KOELBEL, CHARLES N89-25585
KOENIG, REINHARD N89-25144
KOLB, EDWARD W. N89-25678
N89-25680
KOLLATH, Z. N89-25881
KOLONAY, R. M. N89-25197
KOMATSU, YUKINARI N89-25288
KORENEV, S. A. N89-25350
KORZENNIK, SYLVAIN G. N89-25831
N89-25832
N89-25838
N89-25842
N89-25848
KOSLOWSKI, H. R. N89-25684
N89-25715
KOSOVICHEV, A. G. N89-25853
N89-25913
N89-25914
KOSTYUCHENKO, S. V. N89-25350
KOTOV, V. A. N89-25881
KOTTER, DALE K. N89-25367
KOWALSKI-GLIKMAN, J. N89-25762
KOYANAGI, ROBERT S. N89-25494
N89-25496
KRAEMER, SYBILL N89-25299
KRALL, NICHOLAS A. N89-25704
KRANTZ, ALAN T. N89-25623
KREBS, JAMES J. N89-25737
KRESS, R. L. N89-25356
N89-25460
KRISHEN, KUMAR N89-25360
KROLL, RONALD J. N89-25893
KROO, ILAN N89-25212
KRYTER, R. C. N89-25386
KUBAN, D. P. N89-25461
KUHLMANN, JUERGEN N89-25498
KUHN, J. R. N89-25833
N89-25912
KUMAGAI, HIROYUKI N89-25122
KUMAR, V. N89-25148
KUNKEL, W. B. N89-25308
KUZYK, MARK G. N89-25338
KWAK, J. F. N89-25748
KWAKS, A. M. J. N89-25377

L

LABUS, THOMAS L. N89-25269
LAMBERT, GEORGE A. N89-25406
LAMBERTY, MARTIN N89-25503
LAMBROPOULOS, J. C. N89-25750
LAMORA, ROBERT N89-25685
LAMPPA, D. L. N89-25744
N89-25748
LAN, C. EDWARD N89-25206
LANAGAN, M. T. N89-25756
LAND, CECIL E. N89-25692
LANDLE, GEORGE L. N89-25542
LANG, P. F. N89-25480
LARSEN, JACK C. N89-25805
LAWRENCE, GEORGE M. N89-25802
LAWVER, BRYAN N89-25821
LAZREK, MOHAMED N89-25942
LEBIUS, H. N89-25684
N89-25715
LEBOEUF, J. N. N89-25702
LEBRETON, Y. N89-25939
LEDEZMA, E. N89-25846
LEE, D. K. N89-25645
LEE, JOHN T. N89-25936
LEE, LLOYD L. N89-25413
LEE, MEEMONG N89-25619
LEE, RONALD S. N89-25253
LEE, S.-J. N89-25148
LEE, WEN-CHAU N89-25550
LEEPER, M. N89-25923
N89-25929
LEESER, JOACHIM WOLFGANG N89-25330
LEFKOWITZ, C. P. N89-25179
LEIBMAN, CHRISTOPHER PATRICK N89-25305
LEIBOWITZ, SCOTT G. N89-25492
LEIFSEN, T. N89-25847
LEOVY, CONWAY N89-25806
LERCH, F. N89-25539
LERNER, EDWIN N89-25147
LESKINEN, E.-L. N89-25859
LEUNG, K. N. N89-25308
LEUZE, MICHAEL R. N89-25623
LEVIN, ROBERT H. N89-25494
N89-25496
LEVINE, M. N89-25209
LEVY, EUGENE H. N89-25776
LEVY, ROY N89-25224
LEWANDOWSKI, M. N89-25437
LEWIS, PAUL S. N89-25569
LI, AM QIR N89-25760
LI, W.-C. N89-25204
LIBBRECHT, KEN G. N89-25820
N89-25830
N89-25840
LIM, JOON W. N89-25155
LIN, HUA TAY N89-25467
N89-25468
N89-25469
LIN, YI N89-25601
LINDERT, HANS-WERNER N89-25139
LINDNER, D. K. N89-25691
LINK, HAL N89-25510
LISIUS, ANDREAS N89-25697
LIU, K. C. N89-25451
LIU, WEN-JIANG N89-25331
N89-25359
N89-25644
LIU, Y. N89-25606
LIVNE, E. N89-25194
LIZANO-SOBERON, SUSANA N89-25782
LLOYD, J. F., SR. N89-25312
LLOYD, LINDSEY N89-25601
LLOYD, W. R. N89-25489
LOCKWOOD, S. J. N89-25384
LONG, EDWARD R., JR. N89-25332
LONG, SHEILA ANN T. N89-25332
LOU, YU-QING N89-25873
LOVE, MIKE H. N89-25167
N89-25177
LOVELY, RONALD G. N89-25269
LU, CHENG Y. N89-25280
LU, EDWARD TSANG N89-25945
LUCAS, S. H. N89-25178
LUEHR, H. N89-25718
LUHMANN, N. C., JR. N89-25454
LUNDBERG, BRUCE N. N89-25218
LUY, J.-F. N89-25757
LYNCH, V. E. N89-25702
LYON, J. F. N89-25702
LYONS, VALERIE J. N89-25409

M

MACCRACKEN, MICHAEL C. N89-25529
N89-25549
MACDOWALL, R. D. N89-25392
MACLEOD, HELENE N89-25286
MACPHERSON, M. N89-25251
MAHAN, JOHN E. N89-25746
MAILAENDER, MARTIN N89-25358
MAILHE, CATHERINE C. N89-25389
MAIOCCHI, R. N89-25767
MALHOTRA, RENU N89-25815
MALTBY, P. N89-25847
MALTSEV, V. M. N89-25760
MANDRIOLI, D. N89-25633
MANGENEY, A. N89-25916
MANTAY, WAYNE R. N89-25151
MARCOLINI, MICHAEL A. N89-25673
MARLAND, GREGG N89-25527
MARQUEDANT, R. N89-25850
MARQUES-BONHAM, SIRLEY N89-25663
MARS, N. J. I. N89-25640
N89-25641
MARSCHALL, PETER N89-25399
MARSH, J. G. N89-25539
MARTIN, JOHN G. N89-25210
MARTIN, L. J. N89-25803
MASAROTTI, ALESSANDRO N89-25680
MASON, PHILIP N89-25147
MASURSKY, HAROLD N89-25776
MATTHEWS, JAYMIE N89-25915
MATTIG, W. N89-25866
MAVROVOUNIOTIS, GRETCHEN M. N89-25417
MAY, RODNEY A. N89-25487
MAZER, ALAN S. N89-25619
MAZIN, I. I. N89-25734
MCARTHUR, DAVID A. N89-25456
MCCARTHY, J. M. N89-25319
N89-25694

MCCARTY, DONALD LYLE, II N89-25442
MCCLEESE, DANIEL J. N89-25806
N89-25811
MCCONNELL, J. C. N89-25177
MCCORMICK, M. P. N89-25805
MCCREADY, MARK J. N89-25408
N89-25416
MCCUNE, WILLIAM N89-25632
MCGEE, OLIVER G. N89-25229
MCGRAW, JAMES R. N89-25624
MCHARGUE, CARL J. N89-25337
N89-25471
MCINTOSH, S. C., JR. N89-25169
MCKINLEY, T. L. N89-25304
MCKINNON, JOHN A. N89-25817
MCKISSOCK, BARBARA I. N89-25272
MCLEOD, C. P. N89-25824
N89-25844
MCLEOD, D. B. N89-25857
MCLEOD, R. R. N89-25362
MCMASTER, L. R. N89-25805
MCNULTY, MICHAEL J. N89-25479
MCPHEETERS, C. C. N89-25511
MEDLEY, LARRY G., SR. N89-25765
MEEK, PAUL N89-25614
MEHROTRA, PIYUSH N89-25585
MEHTA, ASHISH J. N89-25522
MEIER, M. N89-25526
MENNE, S. N89-25127
MENSHIKOV, V. I. N89-25313
MERRYFIELD, W. J. N89-25823
MESQUITA, LUIS N89-25186
MEYN, ERWIN H. N89-25290
MICHELOTTI, LEO N89-25418
N89-25655
N89-25667
MIELKE, M. N89-25259
MIHAILESCU, I. N. N89-25303
MILES, THOMAS N89-25540
MILLER, DAVID W. N89-25258
MILLER, E. K. N89-25372
MILLER, JAMES B. N89-25363
MILLER, M. S. N89-25276
MILLER, RICHARD A. N89-25568
MILLER, ROBERT D. N89-25807
MILLS, FRED N89-25418
MIMS, JAMES N89-25264
MINES, G. L. N89-25513
MIRONOV, O. A. N89-25739
MISTREE, FARROKH N89-25208
MIU, L. N89-25735
N89-25736
MIYAJI, SHIGEKI N89-25780
MOEBIUS, EBERHARD N89-25716
MOELLER, S. V. N89-25428
MOLDOVAN, N. N89-25648
MONTAGUE, CLAY L. N89-25522
MOORE, JAMES W. N89-25626
MORASCA, S. N89-25633
N89-25661
MOREL, THOMAS N89-25415
MORELL, LARRY J. N89-25627
MORFILL, G. E. N89-25731
MORGENSTERN, GUENTER N89-25375
MORGENSTERN, V. M. N89-25474
MORIYAMA, HIROSHI N89-25302
MORJAN, I. N89-25303
MORRIS, J. R. N89-25453
MORRIS, J. W., JR. N89-25322
N89-25343
MORRIS, STEPHEN N89-25212
MORRISON, DENNIS R. N89-25557
MORROW, C. A. N89-25834
N89-25837
N89-25841
MORZENTI, A. N89-25607
MOSSER, B. N89-25924
MOVCHAN, S. A. N89-25740
MOYER, R. A. N89-25705
MUELLER, E.-A. N89-25426
MUELLER, R. N89-25140
MUENCHAUSEN, ROSS E. N89-25745
MUENKEL, CHRISTOPH N89-25697
MUKHOPADHYAY, VIVEKANANDA N89-25193
MURATORI, SIMONA N89-25533
MURPHY, LAWRENCE M. N89-25514
MURR, L. E. N89-25321
MURRAY, J. R. N89-25453
MURRAY, T. O. N89-25261
MUSCHIETTI, L. N89-25725
MUSTER, DOUGLAS N89-25208
MUSZYNSKA, AGNES N89-25463
N89-25464
MYLES, K. M. N89-25511

N

NAGENDRA, GOPAL K. N89-25183
NAGLER, S. E. N89-25753
NAIK, DIPAK P. N89-25268
NAKAJIMA, S. N89-25699
NAKAMURA, KATSUYUKI N89-25288
NARANG, H. N. N89-25586
N89-25602
NAROZNY, PETER N89-25399
NASH, T. N89-25578
N89-25631
NASTASI, MICHAEL N89-25745
NAZAROV, V. M. N89-25313
NEAL, MARK O. N89-25620
NEILL, D. J. N89-25174
NELSON, P. A. N89-25390
NESIS, A. N89-25826
NEUKIRCH, T. N89-25730
NEW, R. N89-25824
N89-25844
N89-25849
NEXSEN, W. E. N89-25711
NG, S. N89-25385
NGUYEN, TIEN MANH N89-25380
N89-25381
NICHOLS, F. A. N89-25470
NIEMEGEERS, IGNAS G. N89-25476
NIEMZ, KLAUS N89-25502
NIERATSCHKER, WILLI N89-25429
NISSIM, E. N89-25195
NIX, ROGER M. N89-25307
NOAKES, M. W. N89-25460
NOEL, BRUCE W. N89-25447
NORDLUND, A. N89-25912
NOVAK, J. L. N89-25438

O

OBERACKER, R. N89-25329
OBRIEN, ENDA WILLIAM N89-25537
OEBELS, R. M. N89-25130
OGLESBY, TIMOTHY L. N89-25164
OHERN, M. E. N89-25471
OJALVO, I. U. N89-25213
OLIVER, W. C. N89-25316
N89-25471
OLIVERO, JOHN J. N89-25802
N89-25808
OLSON, R. N89-25385
OLVERA, J. N89-25474
ONDOV, JOHN M. N89-25524
ONEILL, ALAN N89-25540
ORAN, ELAINE S. N89-25353
OROURKE, P. J. N89-25304
OTTO, A. N89-25719
OVERBEEK, ROSS N89-25632
OWENBY, RODNEY N. N89-25695

P

PADULA, SHARON N89-25160
PAEZ, THOMAS L. N89-25481
N89-25482
PAGE, R. A. N89-25340
PALLE, PERE L. N89-25824
N89-25839
N89-25846
N89-25848
N89-25849
N89-25869
N89-25880
N89-25887
N89-25908
N89-25919
N89-25923
N89-25928
PANDEY, AJAY K. N89-25198
PAPALAMBROS, PANOS Y. N89-25214
PAPAMASTORAKIS, I. N89-25718
PARKER, GEOFFREY E. N89-25766
PARKER, K. G. N89-25431
PARKER, L. E. N89-25572
PARKER, LYNNE E. N89-25570
PARKINSON, A. R. N89-25176
PARRISH, R. H. N89-25471
PARRY, GARETH W. N89-25508
PASCHMANN, G. N89-25718
PATEL, G. B. N89-25539
PATER, RUTH H. N89-25334
PAUL, A. C. N89-25711
PAUL, B. K. N89-25177
PAULSON, LELAND E. N89-25348
PAVEL, E. N89-25736
PAWLEWICZ, W. T. N89-25694
PEARCE, A. C. N89-25574
PEASE, D. M. N89-25432
PECHT, M. N89-25204
PECINA, PETR N89-25779
PENNER, JOYCE E. N89-25532
PENNINGTON, C. H. N89-25747
PENSE, ALAN W. N89-25472
PERDANG, J. N89-25914
PERELOMOV, A. M. N89-25662
PERELSHTEIN, EH. A. N89-25681
PEREZ, ARMANDO N89-25789
PEREZHERNANDEZ, F. N89-25839
N89-25905
N89-25908
PERI, M. N89-25875
PERNICI, B. N89-25767
PERRY, BOYD, III N89-25232
PERSSON, E. N89-25411
PESHEKHONOV, V. D. N89-25740
PETERS, DAVID A. N89-25153
PETERS, JAMES R. N89-25157
PEZZE, M. N89-25607
N89-25633
N89-25661
PFALTZ, JOHN L. N89-25601
N89-25768
PFEIFFER, BERTHOLD N89-25504
PHAM, T. N89-25578
N89-25631
PHAN, KHING F. N89-25229
PHILIP, JOHN R. N89-25809
PIECHNA, J. N89-25424
PIETRASZEWSKI, K. A. R. B. N89-25918
N89-25923
N89-25929
PIH, H. N89-25451
PINEDADEGYVEZ, J. N89-25617
PINES, DAVID N89-25777
PINTAR, JAMES A. N89-25856
PIPER, E. N89-25757
PLA, FREDERIC G. N89-25675
PLANER, N. N89-25411
PLASKACZ, EDWARD J. N89-25620
POCHA, M. D. N89-25393
POEPPEL, R. B. N89-25756
POHJOLAINEN, S. N89-25859
POLAK, LUCIAN ELIJAH N89-25226
POLEN, DAVID M. N89-25168
POLFLIET, R. N89-25932
POLLACK, J. B. N89-25797
POMERANTZ, M. A. N89-25868
PONCHAK, GEORGE E. N89-25365
POORE, AUBREY B. N89-25218
POPA, S. N89-25434
N89-25735
N89-25736
POPE, D. STUART N89-25673
POPESCU, C. N89-25303
POPESCU, M. N. N89-25535
N89-25735
N89-25736
POPOV, A. N. N89-25740
POPPE, W. N89-25424
POSTAWKO, S. E. N89-25812
POTOTZKY, ANTHONY S. N89-25232
POTT, JOHN N89-25487
PRADERIE, F. N89-25916
PRAGER, S. C. N89-25705
PRAHARAJ, S. N89-25204
PRAS, AIKO N89-25634
PRICE, J. R. N89-25339
PRINZ, GARY A. N89-25737
PROVOST, J. N89-25888
PUJARA, P. K. N89-25179
PULLMAN, B. N89-25307
PURSWELL, JERRY L. N89-25669
PYOETSIAE, JOUNI N89-25459

Q

QIAN, B. N89-25215
QUINLAN, GERALD F. N89-25622

R

RADERMACHER, REINHARD N89-25505
RADOVCICH, N. A. N89-25166
RAE, WILLIAM J. N89-25404
RAGSDELL, K. M. N89-25205
RAKOWSKI, MARK N89-25759
RAMADHYANI, S. N89-25412
RAMAMURTHI, SANGEETA DIKSHIT N89-25346

RAMAMURTHY, H. N89-25412
RAMESH, T. G. N89-25382
RAMLOSE, TERRI N89-25944
RANAUDO, RICHARD N89-25675
RAND, PETER P. N89-25345
RANKIN, RICHARD A. N89-25367
RAO, HARIPRASAD NANNAPANENI N89-25595
RAO, J. R. JAGANNATHA N89-25214
RARIDON, R. J. N89-25712
RASHKOVSKY, D. N. N89-25881
RASMUSSEN, R. W. N89-25411
RATAJCZAK, ANTHONY F. N89-25274
RATTAN, KULDIP S. N89-25458
REDDY, T. S. R. N89-25119
REECE, ERIC W. N89-25487
REED, BRIAN D. N89-25254
REED, D. A. N89-25480
REGULO, C. N89-25824
N89-25839
N89-25848
N89-25869
N89-25887
REHEUSER, R. D. N89-25276
REID, RICHARD A. N89-25622
REIMANN, J. N89-25427
REISS, ROBERT N89-25215
REMSBERG, ELLIS E. N89-25810
RENSINK, AREND N89-25610
RENTON, R. E. N89-25918
N89-25923
REU, TAEKYU N89-25120
REUTER, W. G. N89-25489
RHODES, EDWARD J., JR. N89-25831
N89-25832
N89-25836
N89-25842
N89-25851
RIBES, E. N89-25870
RICCI, D. N89-25850
N89-25851
RICE, J. P. N89-25747
RICHTER, BERND N89-25545
N89-25548
RIGBY, DAVID L. N89-25404
RILEY, GARY N89-25635
RINALDI, SERGIO N89-25533
RING, J. N89-25918
RIVERA, JUAN C. N89-25267
ROBBINS, J. W. N89-25539
ROBERS, JAMES L. N89-25161
ROBERTS, ALLEN F. N89-25274
ROBERTS, B. N89-25874
ROBINO, C. V. N89-25311
ROCACORTES, TEODORO N89-25824
N89-25839
N89-25846
N89-25848
N89-25849
N89-25869
N89-25880
N89-25884
N89-25887
N89-25908
N89-25916
N89-25919
N89-25923
N89-25928
RODIN, A. M. N89-25446
RODONO, M. N89-25926
RODRIGUES, HELDER CARRICO N89-25236
RODRIGUEZ, J. G. N89-25257
ROGAN, J. EDWARD N89-25159
N89-25220
ROGERS, J. D. N89-25336
ROHRER, J. N89-25445
ROLFE, E. J. N89-25819
ROMANOFSKY, ROBERT R. N89-25365
ROMBERG, H.-J. N89-25134
ROMIG, A. D., JR. N89-25387
ROMMEL, BRUCE A. N89-25222
ROOS, C. N89-25584
ROSATI, P. N89-25850
N89-25851
ROSEBERRY, L. M. N89-25774
ROSEMA, A. N89-25552
N89-25553
N89-25554
ROSENTHAL, C. S. N89-25898
ROSENWALD, ROSS D. N89-25890
N89-25891
ROSS, PHILIP N., JR. N89-25391
ROTHE, K. E. N89-25366
ROTTMANN, UWE N89-25676
ROWE, CLINTON MAURICE N89-25495
ROZELOT, J. P. N89-25909
RUDER, H. N89-25729
RUOFF, A. L. N89-25751
RUPPERT, UDO N89-25357
RUSCH, DAVID W. N89-25802
RUSHFORD, M. C. N89-25453
RUSSELL, DAVID LAWRENCE N89-25770
RUSSELL, JAMES M., III N89-25810
RUST, D. M. N89-25858
RUTTEN, R. J. N89-25862
RUZIC, D. N. N89-25708
RYAN, P. M. N89-25366
N89-25368
N89-25712

S

SACHSENWEGER, D. N89-25720
SADOULET, BERNARD N89-25688
SAFONOV, M. G. N89-25179
SAIGAL, SUNIL N89-25187
N89-25188
SAINT-PE, O. N89-25916
SAIO, HIDEYUKI N89-25780
SALAMA, MOKTAR N89-25227
SALES, B. C. N89-25749
SALTSMAN, JAMES F. N89-25485
SALZBRENNER, R. N89-25323
N89-25324
SANDERS, RYAN W. N89-25802
SANDHAM, N. D. N89-25851
SANDRIDGE, CHRIS A. N89-25160
SANKOVIC, JOHN M. N89-25281
SANTER, BENJAMIN DAVID N89-25538
SAVELY, ROBERT T. N89-25635
SCANLAN, R. M. N89-25754
SCARF, FREDERICK L. N89-25776
SCHARLEMANN, E. T. N89-25711
SCHATTEN, KENNETH H. N89-25878
SCHEEREN, PETER MARIA JOSEPH N89-25374
SCHERER, T. N89-25138
SCHERRER, PHILIP H. N89-25885
N89-25892
N89-25894
SCHICK, FRED V. N89-25575
SCHILD, HERBERT N89-25448
SCHINDLER, KARL N89-25717
SCHIRRA, M. N89-25328
SCHLACHTER, A. S. N89-25308
SCHLEGEL, ROBERT E. N89-25669
SCHLESINGER, M. E. N89-25521
SCHLICHTER, DIETER N89-25498
SCHLIESING, JOHN A. N89-25263
SCHMALE, DAVID T. N89-25483
SCHMIDER, F. X. N89-25921
N89-25927
SCHNABL, GOTTFRIED N89-25250
SCHNEIDER, STEVEN J. N89-25254
SCHOFIELD, J. T. N89-25811
SCHOLTEN, J. N89-25581
SCHOT, JEROEN N89-25634
SCHOU, J. N89-25843
SCHRAGE, DANIEL P. N89-25162
SCHREIBER, ROBERT S. N89-25653
SCHRYVER, J. C. N89-25571
SCHWEITZER, B. N89-25135
SCKOPKE, N. N89-25724
SCOTTI, S. J. N89-25178
SCRIBNER, K. J. N89-25349
SCUTARU, H. N89-25646
N89-25647
SECUNDE, RICHARD R. N89-25269
SEKII, T. N89-25900
N89-25910
SERDYUK, V. V. N89-25313
SERIZAWA, Y. N89-25721
SERRANO, J. P. N89-25256
SESSLER, A. M. N89-25455
SEVERINO, G. N89-25862
SHANKAR, P. N. N89-25301
SHAPIRO, IRWIN I. N89-25534
SHARP, R. S. N89-25276
SHAW, SCOTT N89-25360
SHECHTER, AVIGDOR N89-25486
SHIBAHASHI, H. N89-25900
N89-25910
SHIEBER, TOM N89-25877
SHIN, DONG K. N89-25217
SHINE, R. N89-25875
SHOCH, FRITZ N89-25928
SHUART, MARK J. N89-25172
SHUBHA, V. N89-25382
SHUPE, JON A. N89-25208
SHVACHKA, A. B. N89-25650
SIEBERT, RUEDIGER N89-25243
SILLMAN, MARK SANFORD N89-25523
SIMONEN, E. P. N89-25320
SIMPSON, R. L. N89-25349
SIMPSON, REA J. N89-25603
SINGER, BART A. N89-25118
SINGER, KENNETH D. N89-25338
SINGH, GURKIRPAL N89-25265
SINGH, J. P. N89-25756
SINGH, JAG J. N89-25433
SINHA, DIPEN N. N89-25447
SINICROPI, M. J. N89-25750
SISK, GREGORY A. N89-25270
SKAAR, S. B. N89-25336
SKALEY, D. N89-25911
SKEDZIELEWSKI, STEPHEN K. N89-25603
SLATER, MARILYN KAYE N89-25771
SLICHTER, C. P. N89-25747
SLIWA, STEVEN M. N89-25150
SMARTT, HERSCHEL B. N89-25465
SMEYERS, P. N89-25932
SMITH, DARRYL L. N89-25447
SMITH, E. N89-25850
N89-25851
SMITH, GILBERT R. N89-25494
N89-25496
SMITH, GREGORY P. N89-25286
SMITH, HENRY I. N89-25310
SMITH, HOWARD N89-25472
SMITH, J. A. N89-25696
SMITH, L. A. N89-25480
SOBEL, LAWRENCE N89-25147
SOBIESZCZANSKI-SOBIESKI, JAROSLAW N89-25149
N89-25161
N89-25168
N89-25354
SODERBLOM, D. N89-25937
SOEIRO, F. J. N89-25230
SOLANKI, RANVIR SINGH N89-25458
SOLHEIM, J. E. N89-25934
SOLOMON, SEAN C. N89-25776
SOMERS, BRUCE R. N89-25472
SOMIESKI, FRANZ N89-25544
SOMORJAI, GABOR A. N89-25307
SON, SANG H. N89-25601
N89-25768
SONDER, EDWARD N89-25749
SONNERUP, B. U. O. N89-25718
SORDON, GIANCARLO N89-25425
SORENSEN, J. M. N89-25827
SORENSON, K. B. N89-25324
SORENSON, REESE L. N89-25116
SORKIN, ROBERT D. N89-25573
SOTKOV, G. M. N89-25758
SPELT, PHILIP F. N89-25636
SPERLING, ROGER B. N89-25475
SPRAYBERRY, R. E. N89-25473
ST.CLAIR, TERRY L. N89-25294
N89-25433
STALLARD, B. W. N89-25711
STANTON, E. L. N89-25199
STAPP, HENRY P. N89-25781
STEARNS, J. W. N89-25308
STECKEMETZ, BERND N89-25129
STEIN, R. F. N89-25912
STEINBERG, DANIEL J. N89-25419
STELLMACHER, G. N89-25865
STEPANTSOV, S. V. N89-25446
STERNBACH, E. J. N89-25369
STERNE, P. A. N89-25741
STIX, M. N89-25911
STOK, L. N89-25616
STOREY, C. N89-25606
STREICHER, JUERGEN N89-25697
STRELKOVA, L. P. N89-25313
STROHM, K. N89-25757
STUETTGEN, W. N89-25133
STUTZIN, G. C. N89-25308
SUNDBERG, RICHARD C. N89-25403
SWAIN, D. W. N89-25366
SYLWESTER, ALAN P. N89-25293
N89-25345
SZUECS, ZSOLT N89-25357

T

TADIOS, E. L. N89-25420
TADROS, MAHASIN G. N89-25561
TAN, MICHAEL J. N89-25406
TANG, PIER K. N89-25351
TANSKANEN, PEKKA N89-25543
TANVEER, SALEH N89-25665
N89-25671
TARBELL, T. D. N89-25875
N89-25892
TASSOUL, M. N89-25932
TATUM, KENNETH E. N89-25170
TAYLOR, KENNETH J. N89-25512

TAYLOR, L. M. N89-25590
TAYLOR, NANCY L. N89-25597
TEDESCHI, WILLIAM J. N89-25487
TEEGEN, UWE N89-25575
TEKAWY, J. A. N89-25179
TENVREGELAAR, JOHANNES MARTINUS N89-25657
TER-AKOPYAN, G. M. N89-25446
TERASRANTA, H. N89-25859
TERRY, P. W. N89-25706
THEOPHILOS, PAULINE M. N89-25597
THOMAS, DANIEL N89-25691
THOMAS, GARETH N89-25341
THOMAS, GARY E. N89-25802
THOMAS, L. E. N89-25694
THOMASSEN, K. I. N89-25711
THOMPSON, ARTHUR CHRISTOPHER N89-25778
THOMPSON, GEORGE N89-25759
THOMPSON, M. J. N89-25876
N89-25904
N89-25906
THOMPSON, M. R. N89-25690
THROOP, A. L. N89-25711
TIEGS, TERRY N. N89-25289
TING, LI N89-25417
TING, T. N89-25213
TISCHLER, V. A. N89-25197
TISSOT, R. G. N89-25744
TITLE, A. M. N89-25875
N89-25892
TOMCZYK, STEVEN N89-25831
N89-25838
N89-25842
N89-25851
TOMILOV, S. B. N89-25313
TOOMRE, J. N89-25823
N89-25872
TOOTH, P. D. N89-25899
TOPUNOV, V. L. N89-25650
TOUTAIN, T. N89-25860
N89-25881
TOW, D. M. N89-25257
TOWELL, TIMOTHY W. N89-25294
TRANGENSTEIN, JOHN A. N89-25421
TRAUTH, SHARON L. N89-25592
TRUJILLOBUENO, J. N89-25821
TUNCEL, GURDAL N89-25524
TURCK-CHIEZE, S. N89-25907
N89-25933
TUROK, NEIL N89-25788
TUTTLE, B. A. N89-25744
TWU, SUNG-LING N89-25181

U

UCHEVATKIN, I. F. N89-25437
UCKERMANN, RAINER N89-25575
ULRICH, ROGER K. N89-25831
N89-25838
N89-25842
N89-25851
N89-25877
UPADHYAYA, BELLE R. N89-25474
N89-25637
URPO, S. N89-25859
URSU, I. N89-25303
N89-25449

V

VACCARO, HENRY S. N89-25591
VAESSEN, P. T. M. N89-25400
VAJNSHTEJN, A. I. N89-25361
VANALTENA, WILLIAM F. N89-25936
VANDENAKKER, BERT N89-25614
VANDENBORN, R. N89-25616
VANDERPLAATS, GARRET N. N89-25203
VANDERRAAY, H. B. N89-25844
N89-25879
VANDERSCHAAF, B. N89-25325
VANDERVEGT, JACOBUS JOZEF WILHELMUS
N89-25423
VANDERVELDEN, ALEXANDER J. M. N89-25233
N89-25235
VANHOLTEN, J. W. N89-25762
VANHOOLST, T. N89-25932
VANOTTERLO, PETRUS JOHANNES N89-25604
VANROODE, M. N89-25339
VANROSENDALE, JOHN N89-25585
VANSOEST, D. C. N89-25641
VARUGHESE, RAJAN N89-25472
VENKAYYA, VIPPERLA B. N89-25197
N89-25231
VENNE, L. J. N89-25321
VENTURA, R. N89-25917
VENTURINI, E. L. N89-25748
VER, ISTVAN L. N89-25674
VERVOORT, W. A. N89-25613
VERZASCONI, S. L. N89-25343
VIAL, J. C. N89-25881
VIAL, J.-P. N89-25584
VISCO, STEVEN J. N89-25389
VISKANTA, R. N89-25412
VITEK, J. M. N89-25466
VITTING, T. N89-25138
VLACHONIKOLIS, IOANNIS G. N89-25664
VLAD, V. I. N89-25434
N89-25449
VOGE, A. N89-25728
VOGT, SCOTT T. N89-25275
VOIGT, J. A. N89-25748
VONHOLTZ, E. N89-25349
VONSCHWERDTNER, MARTIN N89-25426
VORONTSOV, S. V. N89-25901
N89-25903

W

WACKERBARTH, D. E. N89-25342
WAEBER, LORENZ N89-25498
WAHLSTEDT, D. A. N89-25411
WALLERSTEIN, DAVID V. N89-25183
WALSH, JOANNE L. N89-25156
N89-25160
N89-25228
WALTER, HARRY N89-25357
WANG, BO PING N89-25225
WASAN, DARSH T. N89-25417
WATSON, R. W. N89-25625
WAWRYSZCZUK, J. N89-25437
WEBSTER, LARRY N89-25877
WEHRLI, CH. N89-25884
WEIRICK, L. J. N89-25352
WEISBIN, CHARLES R. N89-25570
N89-25572
N89-25636
WEISSHAAR, TERRENCE A. N89-25189
WELCOME, MICHAEL N89-25421
WENDEL, M. W. N89-25630
WENDERLICH, NEAL D. N89-25622
WERNER, CHRISTIAN N89-25697
WHEALTON, J. H. N89-25366
N89-25712
WHITE, C. W. N89-25333
WIEHR, E. N89-25865
WIESEMAN, CAROL D. N89-25192
WIESEMANN, K. N89-25715
WIETING, ALLAN R. N89-25198
WILDER, G. O. N89-25276
WILHELM, A. N89-25757
WILKENING, LAUREL L. N89-25776
WILKES, JAMES MICHAEL N89-25783
WILLIAMS, D. M. N89-25461
WILLIAMS, KENNETH N89-25264
WILLIAMS, WINIFRED I. N89-25619
WILLIAMSON, R. G. N89-25539
WILMORE, DOUGLAS W. N89-25564
WINEFORDNER, J. D. N89-25306
WINTER, CARL-JOCHEN N89-25358
WINTER, JERRY M. N89-25282
WOELFEL, ULRICH N89-25298
WOGNUM, P. M. N89-25640
WOOD, W. E. N89-25321
WOODARD, MARTIN F. N89-25830
N89-25831
WOODWARD, RICHARD P. N89-25675
WORM, S. C. J. N89-25378
WRIGLEY, ROBERT C. N89-25494
N89-25496
WUEBBLES, DONALD J. N89-25530
N89-25531
WUTTGE, SEBASTIAN N89-25260

Y

YANG, IN CHE N89-25525
YE, DAU-HUA N89-25644
YEE, H. C. N89-25651
N89-25652
YERLE, RAYMOND N89-25861
YIO, J. L. N89-25744
YOON, B. G. N89-25184
YOST, F. G. N89-25387
YOUNG, A. T. N89-25308
YOUNGDAHL, C. A. N89-25756
YUTLANDOV, I. A. N89-25437

Z

ZACHARIA, T. N89-25466
ZAKHAROV, V. I. N89-25361
ZANEVSKIJ, YU. V. N89-25740
ZANG, THOMAS A. N89-25118
ZAX, D. B. N89-25747
ZEILER, THOMAS A. N89-25192
N89-25232
ZENT, AARON P. N89-25812
ZERFASS, M. N89-25866
ZHEN, HUANG N89-25855
ZHU, YU-CAI N89-25331
N89-25642
N89-25643
ZIOLKOWSKI, RICHARD W. N89-25587
ZMUDA, T. N89-25578
N89-25631
ZUREK, RICHARD W. N89-25794
N89-25813
N89-25814
ZWENGER, ISOLDE N89-25502
N89-25503
ZWINGMANN, WOLFGANG N89-25722

Typical Corporate Source Index Listing

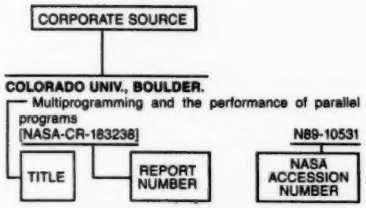

Listings in this index are arranged alphabetically by corporate source. The title of the document provides the user with a brief description of the subject matter. The report number helps to indicate the type of document cited (e.g., NASA report, translation, NASA contractor report). The NASA accession number denotes the number by which the citation is identified. The titles are arranged under each corporate source in ascending accession number order.

A

AALBORG UNIV. (DENMARK).
Concurrent spatio-temporal image analysis [DE89-010260] N89-25583
Concurrent multi-resolution image analysis [DE89-010261] N89-25594

AARHUS TEKNISKE BIBLIOTEK (DENMARK).
Differential rotation in the solar interior N89-25843
Study of solar structure based on p-mode helioseismology N89-25896
Determination of the solar internal sound speed by means of a differential asymptotic inversion N89-25904
On the relation of the Duvall phase function to the upper layers on the convection zone N89-25905
Variable star statistics in open clusters: NGC 6192 N89-25920

AARHUS UNIV. (DENMARK).
Measurements of oscillation parameters from synthetic times series N89-25827

ACADEMY OF SCIENCES OF THE UKRAINIAN SSR, KHARKOV.
Kinetic effects of strong localization in planar heterostructures p-Ge/i-GaAs [DE88-706205] N89-25739

ACADEMY OF SCIENCES (USSR), MOSCOW.
Advances in the development of apparatus and methods for studies of protein monocrystals in coordinate X-ray diffractometers based on two-dimensional proportional chambers [DE88-706259] N89-25740
Helioseismological inverse problem: Sound speed in the solar interior N89-25901
Helioseismological inverse problem: Diagnostics of the structure of the lower solar atmosphere N89-25903

ACADEMY OF SCIENCES (USSR), NOVOSIBIRSK.
Photonic chiral current and its anomaly in a gravitational field [DE88-706213] N89-25361

AEG-TELEFUNKEN, ULM (GERMANY, F.R.).
HEMTS: Fundamental investigations [ETN-89-94630] N89-25399
Submicron technologies for the fabrication of monolithic integrated millimeter wave devices on high resistivity silicon [ETN-89-94624] N89-25757

AIR FORCE SYSTEMS COMMAND, WRIGHT-PATTERSON AFB, OH.
Analysis of the transient compressible vapor flow in heat pipe [NASA-CR-185119] N89-25422

AIR FORCE WRIGHT-PATTERSON AERONAUTICAL LABS., WRIGHT-PATTERSON AFB, OH.
Optimum structural design with static aeroelastic constraints N89-25171
An approximation function for frequency constrained structural optimization N89-25196
Structural optimization of framed structures using generalized optimality criteria N89-25197
Optimization of structure and control system N89-25223
Recent developments in large-scale structural optimization N89-25231

ALABAMA A & M UNIV., NORMAL.
Characterization of Spirulina biomass for CELSS diet potential [NASA-CR-185329] N89-25561

ARGONNE NATIONAL LAB., IL.
Advanced high-temperature batteries [DE89-010698] N89-25390
Reference electrode for electrolytic cell [DE89-011446] N89-25394
An experimental study of two-phase natural circulation in an adiabatic flow loop [DE89-009850] N89-25406
Applications of ion beam processes in tribology [DE89-000614] N89-25470
Manifold, bus support and coupling arrangement for solid oxide fuel cells [DE89-009604] N89-25508
Monolithic solid oxide fuel cell development [DE89-010699] N89-25511
Rationale for the proposed standard for a generic package of elementary functions for Ada [DE89-010282] N89-25588
A parallel processing approach for implementing high-performance first-order logic deduction systems [DE89-011878] N89-25632
Temperature limit of a graphite divertor surface due to particle erosion [DE89-010272] N89-25703
Production of wires and coils from high-temperature superconducting materials [DE89-012380] N89-25756

ARIZONA STATE UNIV., TEMPE.
Seasonal and diurnal variability of Mars water-ice clouds N89-25794

ARIZONA UNIV., TUCSON.
Artificially structured superconductors [DE89-009116] N89-25733
Observed asymptotic properties of low-degree solar gravity-mode eigenfrequencies N89-25890
Inversion of quasi-periodic deviations between low-degree solar gravity mode eigenfrequencies and asymptotic theory eigenfrequencies N89-25891
Properties of solar gravity mode signals in total irradiance observations N89-25893

ASTRO AEROSPACE CORP., CARPINTERIA, CA.
Pactruss support structure for precision segmented reflectors [NASA-CR-181747] N89-25484

AUBURN UNIV., AL.
Cavitation kinetics during GTA (Gas Tungsten Arc) welding of helium containing stainless steel [DE89-012514] N89-25467
Welding of helium-doped austenitic and ferritic stainless steels [DE89-012523] N89-25468
Simulation of the welding of irradiated materials [DE89-012524] N89-25469

B

BELEIDSCOMMIE REMOTE SENSING, DELFT (NETHERLANDS).
Applications of remote sensing techniques for the inventory and monitoring of environmental pollution [BCRS-88-15] N89-25497
FAO detailed rain mapping experiment [BCRS-88-11] N89-25552
FAO detailed rain mapping experiment phase A: Meteosat based rainfall mapping in the Sahel region N89-25553
FAO detailed rain mapping experiment phase B: Comparison of rainfall and evapotranspiration mapping N89-25554

BELGIAN ROYAL OBSERVATORY, BRUSSELS.
New thresholds for ground-based photometry of solar intensity oscillations N89-25852

BELL TELEPHONE LABS., INC., PRINCETON, NJ.
Poled polymer films for nonlinear optics [DE89-010039] N89-25338

BENTLY ROTOR DYNAMICS RESEARCH CORP., MINDEN, NV.
Influence of rubbing on rotor dynamics, part 1 [NASA-CR-183648-PT-1] N89-25463
Influence of rubbing on rotor dynamics, part 2 [NASA-CR-183649-PT-2] N89-25464

BIRMINGHAM UNIV. (ENGLAND).
Linewidth of low degree acoustic modes of the Sun N89-25824
The current status of the Birmingham solar seismology network N89-25844
A detector of small gradients of transparency of the terrestrial atmosphere N89-25857
Long period solar oscillations N89-25879
High precision velocity observations of Arcturus using the 7699 A line of potassium N89-25919
High precision velocity measurements of Procyon using the 7699 A line of potassium N89-25922

BOEING HELICOPTER CO., PHILADELPHIA, PA.
Plan, formulate, discuss and correlate a NASTRAN finite element vibrations model of the Boeing Model 360 helicopter airframe [NASA-CR-181787] N89-25480

BOLT, BERANEK, AND NEWMAN, INC., CAMBRIDGE, MA.
Potential uses of vacuum bubbles in noise and vibration control [NASA-CR-181829] N89-25674

BOSTON UNIV., MA.
Diffusion, fluid flow and sound propagation in disordered media [DE89-010937] N89-25407

BRIDGEPORT UNIV., CT.
An interpretation and solution of ill-conditioned linear equations N89-25213

BRIGHAM AND WOMEN'S HOSPITAL, BOSTON, MA.
A program for the study of skeletal muscle catabolism following physical trauma [AD-A206506] N89-25564

BRIGHAM YOUNG UNIV., PROVO, UT.
Research on optimization-based design N89-25176

BRITISH COLUMBIA UNIV., VANCOUVER.
Observed p-mode spectra of Ap stars and the Sun N89-25915

BROOKHAVEN NATIONAL LAB., UPTON, NY.
Elements of a specification for superconducting cable and why they are important for magnet construction [DE89-012533] N89-25754
Nuclear astrophysics of supernovae [DE89-012534] N89-25787

C

CALIFORNIA INST. OF TECH., PASADENA.
The excitation and damping of solar oscillations N89-25820
Measurements of high degree solar oscillation amplitudes N89-25825
On the measurement of solar rotation using high-degree p-mode oscillations N89-25830
Solar p-mode frequency splittings N89-25840

CALIFORNIA UNIV., BERKELEY.
Computational experiments in the optimal slewing of flexible structures N89-25226
The conceptual design of a Mach 2 Oblique Flying Wing supersonic transport [NASA-CR-177529] N89-25233
An economic model for evaluating high-speed aircraft designs [NASA-CR-177530] N89-25235
Concepts in surface science and heterogeneous catalysts [DE89-010679] N89-25307

The strength-toughness relationship at cryogenic temperatures in aluminum-lithium alloy plate
[DE89-011816] N89-25322
Cryogenic mechanical properties of low density superplastically formable Al-Li alloys
[DE89-010587] N89-25343
Monte Carlo for the electronic structure of molecules
[DE89-011824] N89-25682
Surface structural analysis of small molecules on transition metal single crystal surfaces with low energy electron diffraction
[DE89-010681] N89-25743
Symmetry breaking: The standard model and superstrings
[DE89-011771] N89-25761
Ambipolar diffusion and core formation in molecular clouds N89-25782

CALIFORNIA UNIV., BERKELEY. LAWRENCE BERKELEY LAB.
Concepts in surface science and heterogeneous catalysts
[DE89-010679] N89-25307
Measurement of H and H2 populations in-situ in a low-temperature plasma by vacuum-ultraviolet laser-absorption spectroscopy
[DE89-010433] N89-25308
The strength-toughness relationship at cryogenic temperatures in aluminum-lithium alloy plate
[DE89-011816] N89-25322
High resolution electron microscopy and microanalysis of ferrites and cuprates
[DE89-010441] N89-25341
Cryogenic mechanical properties of low density superplastically formable Al-Li alloys
[DE89-010587] N89-25343
Computer simulation of FEL sidebands in a strongly dispersive waveguide
[DE89-011825] N89-25369
Metal-sulfur type cell having improved positive electrode
[DE89-010110] N89-25389
Novel air electrode for metal-air battery with new carbon material and method of making same
[DE89-010964] N89-25391
Report of the Workshop on Scientific Opportunities for Infrared Free-Electron Lasers, volume 2
[DE89-009106] N89-25452
Status of LBL/LLNL FEL (Free Electron Laser) research for two beam accelerator applications
[DE89-012487] N89-25455
Atomic resolution microscopy
[DE89-009227] N89-25679
Monte Carlo for the electronic structure of molecules
[DE89-011824] N89-25682
High-average-power millimeter-wave FEL (Free-Electron Laser) for plasma heating using the ETA-2 accelerator
[DE89-012294] N89-25711
Surface structural analysis of small molecules on transition metal single crystal surfaces with low energy electron diffraction
[DE89-010681] N89-25743
Squid concepts and systems
[DE89-010384] N89-25755
Symmetry breaking: The standard model and superstrings
[DE89-011771] N89-25761
Quantum ontologies
[DE89-010385] N89-25781
Physics of dense matter, neutron stars and supernova
[DE89-010673] N89-25784

CALIFORNIA UNIV., IRVINE.
Confinement physics of H-mode discharges in DIII-D
[DE89-011525] N89-25707

CALIFORNIA UNIV., LOS ANGELES.
Structural optimization of rotor blades with straight and swept tips subject to aeroelastic constraints N89-25152
An integrated approach to the optimum design of actively controlled composite wings N89-25194
Dynamic simulation of dislocation pattern formation in metals during high temperature monotonic and cyclic deformation N89-25477
The evolution and structure of the bow echo/microburst events N89-25550
Confinement physics of H-mode discharges in DIII-D
[DE89-011525] N89-25707
Bibliographic coupling among scientific papers in biological research specialties N89-25771
Measurement of the rotational frequency splitting of the solar five-minute oscillations from magneto-optical filter observations N89-25842
Magnetically induced spectral line redshifts full disk measurements N89-25877

CALIFORNIA UNIV., SANTA BARBARA.
Recent developments in multilevel optimization N89-25203

CAMBRIDGE UNIV. (ENGLAND).
On radiative and convective influences on stellar pulsational stability N89-25828
Solar radiation models and the a1, a3 and a5 splitting coefficients for solar acoustic oscillations N89-25834
Angular momentum transport and dynamo action in the Sun: A report on implications of a recent helioseismic estimate of solar rotation N89-25837
A way to examine rotational splittings without explicit foward or inverse computations N89-25841
An attempt to understand the Stanford p-mode data N89-25853
Scattering and multiple scattering of acoustic waves in a stratified medium N89-25898
Towards an independent calibration of the mixing-length theory N89-25899
Determination of the solar sound speed by an asymptotic inversion technique N89-25913
The effect of a nonspherical sound speed on the acoustic frequency spectrum of the Sun N89-25914
On taking observers seriously N89-25943

CATANIA ASTROPHYSICAL OBSERVATORY (ITALY).
Synthetic light curves and power spectra of Delta Scuti stars: An approach to modeling pulsations N89-25917

CENTRAL INST. OF PHYSICS, BUCHAREST (ROMANIA).
IR laser photochemistry
[DE88-706012] N89-25303
Optical information processing and holography
[DE88-706011] N89-25434
Bistability in a laser with injected signal
[DE88-706003] N89-25449
Research for the physics and structure of earth's crust in Romania
[DE88-706002] N89-25535
Toward a proof of the existence of an integrity basis for the tensors in the enveloping algebra of su(3)
[DE88-706031] N89-25646
Degenerate representation from tensorial identities and quantum realisations of YBZF algebras
[DE88-706032] N89-25647
Balancing a matrix for calculation of eigenvalues and eigenvectors
[DE88-706045] N89-25648
Localizability and covariance in analytical mechanics
[DE88-706038] N89-25666
Preparation and properties of high-temperature superconductors in the Y-Ba-Cu-O system
[DE88-706050] N89-25735
Influence of the preparation conditions on the diamagnetic response of high-Tc YBa2Cu3Ox superconductor
[DE88-706051] N89-25736

CENTRE DE RECHERCHES EN PHYSIQUE DES PLASMAS, LAUSANNE (SWITZERLAND).
Confinement physics of H-mode discharges in DIII-D
[DE89-011525] N89-25707

CENTRE NATIONAL DE LA RECHERCHE SCIENTIFIQUE, VERRIERES-LE BUISSON (FRANCE).
The GOLF helioseismometer on board SOHO N89-25883
GOLF: Simulations of the re-emission of the resonance cell N89-25895
MUSICOS (MUlti-Site COntinuous Spectroscopy): Objectives and prospects for asteroseismology N89-25940

CENTRO BRASILEIRO DE PESQUISAS FISICAS, RIO DE JANEIRO.
A new way to interpret the DIRAC equation in a non-Riemannian manifold
[NASA-CR-185464] N89-25663

CESKOSLOVENSKA AKADEMIE VED, ONDREJOV.
Interplanetary Matter: Proceedings, volume 2
[DE88-706057] N89-25779

CHIBA UNIV. (JAPAN).
The origin of ultra-compact binaries
[NASA-TM-101792] N89-25780

CHICAGO UNIV., IL.
Solitosynthesis: Cosmological evolution of non-topological solitons
[NASA-CR-185030] N89-25678
Statistical fluctuations as the origin of nontopological solitons
[NASA-CR-185351] N89-25680

CHUBU UNIV., KASUGAI (JAPAN).
Density fluctuations and particle/thermal transport for ohmically and auxiliarily heated plasmas in the JIPP T-IIU tokamak
[IPPJ-891] N89-25700

CIVIL AVIATION AUTHORITY, LONDON (ENGLAND).
UK airmisses involving commercial air transport
[CAA-3/88] N89-25143

CLARKSON UNIV., POTSDAM, NY.
Design sensitivity analysis of boundary element substructures N89-25188

CNCPRST, AGDAL RABAT (MOROCCO).
Modelling the solar oscillation time series by a randomly excited oscillator N89-25942

COLLEGE OF WILLIAM AND MARY, WILLIAMSBURG, VA.
Use of metaknowledge in the verification of knowledge-based systems
[NASA-CR-181821] N89-25627

COLORADO RESEARCH DEVELOPMENT CORP., FORT COLLINS.
Narrow bandgap semiconducting silicides: Intrinsic infrared detectors on a silicon chip
[NASA-CR-185372] N89-25746

COLORADO STATE UNIV., FORT COLLINS.
Multiplier-continuation algorithms for constrained optimization N89-25218

COLORADO UNIV., BOULDER.
Reduce uncertainty in projection of future sea-level change due to ice wastage
[DE89-011483] N89-25526
The behavior of water vapor in the Mars atmosphere N89-25801
Solar Mesosphere Explorer observations of stratospheric and mesospheric water vapor N89-25802
The GONG site survey N89-25855

COMMISSARIAT A L'ENERGIE ATOMIQUE, SACLAY (FRANCE).
Current options for the equation of state of the solar interior N89-25897
Further progress on the helium abundance determination N89-25906
Modelling the variation of solar p-mode frequencies N89-25907
High mass loss in the young Sun N89-25933
Epsilon Eridani revisited N89-25937

COMMONWEALTH SCIENTIFIC AND INDUSTRIAL RESEARCH ORGANIZATION, CANBERRA (AUSTRALIA).
Diurnal and annual cycles of H2O in the Martian regolith N89-25809

CONNECTICUT UNIV., STORRS.
X-ray based extensometry
[NASA-CR-185058] N89-25432

CONSEJO SUPERIOR DE INVESTIGACIONES CIENTIFICAS, TENERIFE (SPAIN).
On the k-mechanism and the multidimensional Eddington approximation N89-25821
Rotational splitting of low l solar p-mode N89-25839
Solar luminosity oscillations from two stations and correlation with velocity measurements N89-25846
Effect of atmospheric extinction on solar radial velocity measurements N89-25849
Frequency shift of solar p-modes as seen by cross correlation analysis N89-25869
Can solar g-modes be identified from ground-based velocity measurements N89-25880
Further implications of solar p-modes as measured in Na and K resonance lines N89-25908
Search for rapid oscillations in the Northern Ap stars HD62140, HD81009 and HD22374 N89-25928

CONTINUOUS ELECTRON BEAM ACCELERATOR FACILITY, NEWPORT NEW, VA.
Modular magnet current regulator
[CEBAF-PR-89-005] N89-25685

CORNELL UNIV., ITHACA, NY.
Strong fibers
[DE89-010596] N89-25292
Effects of freezing and cold acclimation on the plasma membrane of isolated protoplasts
[DE89-010931] N89-25560
Studies of 3-5 compounds in the megabar regime
[DE89-012433] N89-25751
Very high elevation water ice clouds on Mars: Their morphology and temporal behavior N89-25804
Regelation and ice segregation N89-25807
Some aspects of the dynamics of orbit-orbit resonances in the Uranian satellite system N89-25815

D

DELAWARE UNIV., NEWARK.
Modeling land-surface albedos from plant canopy architecture N89-25495

DEPARTMENT OF ENERGY, MORGANTOWN, WV.
Method of production H2 using a rotating drum reactor with a pulse jet heat source
[DE89-009764] N89-25348

DEPARTMENT OF ENERGY, WASHINGTON, DC.
Energy from the Earth: Geothermal Energy Program. Five year research plan, 1988-1992
[DE89-010080] N89-25507

Fuel cell systems program plan, FY 1989
[DE89-012928] N89-25515
Report of the HEPAP (High Energy Physics Advisory Panel) Subpanel on High Energy Physics and the SSC (Superconducting Super Collider) over the next decade
[DE89-010071] N89-25686

DEPARTMENT OF THE AIR FORCE, WASHINGTON, DC.
Flap system for short takeoff and landing aircraft
[AD-D013981] N89-25234

DEPARTMENT OF THE NAVY, WASHINGTON, DC.
A passivation layer for 3-5 semiconductor materials
[AD-D013963] N89-25737

DEUTSCHE BUNDESPOST, DARMSTADT (GERMANY, F.R.).
Reduction of interference by decorrelation and quantized feedback in the case of digital transmission on multi-pair symmetric cables
[FI-44-TB-110] N89-25375

DEUTSCHE FORSCHUNGS- UND VERSUCHSANSTALT FUER LUFT- UND RAUMFAHRT, BRUNSWICK (GERMANY, F.R.).
Contributions to the improvement of flight safety in wind shear
[DFVLR-FB-88-49] N89-25144
Testing of a GPS receiver
[DFVLR-MITT-88-30] N89-25145
Pressure measurement technique of WT-WK
[DFVLR-MITT-88-11] N89-25243
Validation of the subjective workload assessment technique in a simulated flight task
[DFVLR-FB-89-01] N89-25575
Data of aeroacoustic measurements on ultralight aircraft propellers
[DFVLR-MITT-88-33] N89-25677

DEUTSCHE FORSCHUNGS- UND VERSUCHSANSTALT FUER LUFT- UND RAUMFAHRT, GOETTINGEN (GERMANY, F.R.).
Two-dimensional elliptic grid generation for airfoils and cascades
[DFVLR-FB-88-52] N89-25125
Numerical simulation of transition from laminar to turbulent channel flow
[DFVLR-FB-88-55] N89-25430

DEUTSCHE FORSCHUNGS- UND VERSUCHSANSTALT FUER LUFT- UND RAUMFAHRT, OBERPFAFFENHOFEN (WEST GERMANY).
Tropospheric influences on satellite-Earth paths and their determination by means of radar measurements
[DFVLR-FB-88-53] N89-25250
On a fast two-dimensional radar imaging process for rotating targets and an analysis of its image quality
[DFVLR-FB-88-51] N89-25376
Synchronization of the ground station atomic clocks using weighted transportable cesium time standards in the navigation experiment (NAVEX)
[DFVLR-MITT-89-01] N89-25448
Investigations on satellite image and reference data for exploration-related tasks
[DFVLR-FB-88-46] N89-25498
Comparative investigations of multispectral satellite image data of MOMS-01, LANDSAT-TM and LANDSAT-MSS for geological and vegetational applications in test sites in the Andes of northern Chile and the Parana-Basin of Brazil
[DFVLR-FB-88-50] N89-25499
Mesoscale model parameterizations for radiation and turbulent fluxes at the lower boundary
[DFVLR-FB-88-48] N89-25544
Prototype of a slant visual range measuring device
[DFVLR-FB-88-42] N89-25697

DEUTSCHE FORSCHUNGS- UND VERSUCHSANSTALT FUER LUFT- UND RAUMFAHRT, STUTTGART (GERMANY, F.R.).
Materials and structures for 2000 and beyond: An attempted forecast
[DFVLR-MITT-89-02] N89-25358
Study on thermodynamical and mechanical conditions for pumping low flow rates of liquefied gases to high pressure level
[DFVLR-FB-88-54] N89-25429

DEUTSCHE GEODAETISCHE KOMMISSION, MUNICH (GERMANY, F.R.).
Gravity network of West Germany 1976 (DSGN76). Part 3: Data and adjustments
[SER-C-286] N89-25545
Gravity network of West Germany (DSGN76): Measurements and starting data N89-25546
Adjustment and data analysis N89-25547

DU PONT DE NEMOURS (E. I.) AND CO., AIKEN, SC.
Design of a dual forearm modular robot
[DE89-010453] N89-25462
Basics of ultrasonic testing
[DE89-010465] N89-25473

E

EAST ANGLIA UNIV., NORWICH (ENGLAND).
Regional validation of general circulation models N89-25538

EATON CORP., SOUTHFIELD, MI.
Advanced Dual-Shaft Electric Propulsion System Technology Development Program
[DE89-010008] N89-25388

EDGERTON, GERMESHAUSEN AND GRIER, INC., IDAHO FALLS, ID.
NDE of the space shuttle orbiter thermal protection system, phase 2
[NASA-CR-185471] N89-25257
Vehicle performance tests of the Ford/GE first generation single-shaft (ETX-I) alternating current propulsion system
[DE89-011115] N89-25392
Design and testing of the EG and G/Los Alamos Operations fast streak camera
[DE89-010859] N89-25445
Detection of metal-transfer mode in GMAW
[DE89-011133] N89-25465
Evaluation of elastic-plastic surface flaw behavior and related parameters using surface displacement measurements
[DE89-011134] N89-25489
An organized effort to develop the hydrothermal energy resource
[DE89-011139] N89-25512
Advanced binary geothermal power plants working fluid property determination and heat exchanger design
[DE89-011144] N89-25513
Fiber optic sensing for NDE and process control
[DE89-010976] N89-25696
Applying understanding of individual behavior and team dynamics within the value engineering process
[DE89-011126] N89-25766

EUROPEAN SPACE AGENCY, PARIS (FRANCE).
Resolution of the Algebraic Riccati Equation via Newton's method and the Lyapunov Equation
[ESA-STM-241] N89-25660
Seismology of the Sun and Sun-Like Stars
[ESA-SP-286] N89-25819

EUROPEAN SPACE AGENCY. EUROPEAN SPACE RESEARCH AND TECHNOLOGY CENTER, ESTEC, NOORDWIJK (NETHERLANDS).
Solar Luminosity Oscillation Telescope (SLOT) N89-25848
SOHO status N89-25882
Luminosity Oscillations Imager (LOI) N89-25887
Solar oscillations instrumentation and measurement theory N89-25925

F

FEDERAL AVIATION ADMINISTRATION, ATLANTIC CITY, NJ.
Notice to Airmen (NOTAM) system operational concept
[DOT/FAA/CT-TN89/10] N89-25142

FEDERAL AVIATION ADMINISTRATION, WASHINGTON, DC.
FAA statistical handbook of aviation: Calendar year 1987
[AD-A200917] N89-25113
Report to Congress: Technical feasibility of joint use at Scott AFB, Selfridge AGB and El Toro MCAS
[AD-A194597] N89-25241

FERMI NATIONAL ACCELERATOR LAB., BATAVIA, IL.
Flying wires at Fermilab
[DE89-011005] N89-25251
Amplitude growth due to random, correlated kicks
[DE89-011504] N89-25418
The Fermilab Lattice Supercomputer Project
[DE89-010510] N89-25578
Microprocessors and other processors for triggering and filtering at the SSC
[DE89-011088] N89-25580
A site oriented supercomputer for theoretical physics: The Fermilab Advanced Computer Program Multi Array Processor System (ACMAPS)
[DE89-011090] N89-25631
Differential algebras without differentials: An easy C++ implementation
[DE89-011503] N89-25655
A new way to interpret the DIRAC equation in a non-Riemannian manifold
[NASA-CR-185464] N89-25663
Phase space concepts
[DE89-011082] N89-25667
Solitosynthesis: Cosmological evolution of non-topological solitons
[NASA-CR-185030] N89-25678
Statistical fluctuations as the origin of nontopological solitons
[NASA-CR-185351] N89-25680
Model independence of constraints on particle dark matter
[NASA-CR-185337] N89-25688
Data acquisition, event building, and on-line processing: Summary talk
[DE89-011085] N89-25693
Dark matter and supersymmetry
[DE89-011068] N89-25785
Evolution of cosmic string networks
[NASA-CR-185467] N89-25788
Pair production of helicity-flipped neutrinos in supernovae
[NASA-CR-185466] N89-25789

FLORENCE UNIV. (ITALY).
On the diagnostic of 5m oscillations through photospheric line profiles N89-25822

FLORIDA UNIV., GAINESVILLE.
New directions for Artificial Intelligence (AI) methods in optimum design N89-25158
Structural damage assessment as an identification problem N89-25230
Development of laser-excited molecular luminescence spectrometric methods for polycyclic aromatic hydrocarbons in environmental sciences
[DE89-010616] N89-25306
Workshop on Sea Level Rise and Coastal Processes
[DE89-010297] N89-25522
The coupling of thermochemistry and phase diagrams for Group 3-5 semiconductor systems
[DE89-012516] N89-25752
X-ray scattering studies of non-equilibrium ordering processes
[DE89-012517] N89-25753

FREIE UNIV., BERLIN (GERMANY, F.R.).
GIRL cryotechnics and preparation of a TEXUS experiment on superfluid helium dynamics
[ETN-89-94631] N89-25357

G

GENERAL ATOMICS TECHNOLOGIES CORP., SAN DIEGO, CA.
Confinement physics of H-mode discharges in DIII-D
[DE89-011525] N89-25707

GENERAL DYNAMICS CORP., FORT WORTH, TX.
Aerolastic tailoring and integrated wing design N89-25167
Recent experiences using finite-element-based structural optimization N89-25177

GENERAL DYNAMICS CORP., GROTON, CT.
Optimizing for minimum weight when two different finite element models and analyses are required N89-25200

GENERAL ELECTRIC CO., SCHENECTADY, NY.
Integrated design optimization research and development in an industrial environment N89-25148

GEOLOGICAL SURVEY, DENVER, CO.
Climatic changes inferred fron analyses of lake-sediment cores, Walker Lake, Nevada
[DE89-010740] N89-25525

GEORGE WASHINGTON UNIV., WASHINGTON, DC.
Probabilistic damage tolerance methods for metallic aerospace structures N89-25237

GEORGIA INST. OF TECH., ATLANTA.
Optimization of rotor blades for combined structural, performance, and aeroelastic characteristics N89-25153
TRUSS: An intelligent design system for aircraft wings N89-25162
The role of optimization in the next generation of computer-based design tools N89-25220

GKSS-FORSCHUNGSZENTRUM GEESTHACHT (GERMANY, F.R.).
Intermetallic alloys: Deformation, mechanical and fracture behavior
[GKSS-88/E/53] N89-25327
Crack growth under low cycle fatigue
[GKSS-88/E/47] N89-25491

GOETTINGEN UNIV. (GERMANY, F.R.).
Oscillations in presence of local magnetic fields N89-25865

GOSUDARSTVENNYI KOMITET PO ISPOLZOVANIYU ATOMNOI ENERGII, MOSCOW (USSR).
On the applicability of various planar potentials in the theory of ultrarelativistic electron channeling
[DE88-706155] N89-25738

GRUMMAN AEROSPACE CORP., BETHPAGE, NY.
Applications of integrated design/analysis systems in aerospace structural design N89-25147

H

HALL (DAVID) CONSULTING, SUNNYVALE, CA.
Development of a microcomputer based integrated design system for high altitude long endurance aircraft N89-25159
HARVARD COLL. OBSERVATORY, CAMBRIDGE, MA.
Studies of regional and global tectonics and the rotation of the earth using very-long baseline interferometry [NASA-CR-185059] N89-25534
HARVARD UNIV., CAMBRIDGE, MA.
Models for regional-scale photochemical production of ozone N89-25523
Unraveling Photosystem 2 [DE89-010930] N89-25559
HAUT COMMISSARIAT A LA RECHERCHE, ALGIERS (ALGERIA).
NMR study of some organophosphorus compounds [DE88-705970] N89-25302
HAWAII UNIV., HONOLULU.
Atmospheric H2O and the search for Martian brines N89-25812
HEIDELBERG UNIV. (GERMANY, F.R.).
Viscous magnetohydrodynamic modes and p-mode absorption by sunspots N89-25873
HELSINKI UNIV. OF TECHNOLOGY, KYLMAELAE (FINLAND).
Measurements of solar oscillations at 37 GHz N89-25859
HELSINKI UNIV. TECHNOLOGY, OTANIEMI (FINLAND).
Flow characteristics and accuracy of control valve [DE88-757331] N89-25459
HONEYWELL, INC., GOLDEN VALLEY, MN.
Evaluation of auxiliary power subsystems for gas engine heat pumps, phase 2 [PB89-173694] N89-25411
HOUSTON UNIV., TX.
A decision-based perspective for the design of methods for systems design N89-25208
HOWARD UNIV., WASHINGTON, DC.
Optimum design of structures subject to general periodic loads N89-25215

I

IDAHO NATIONAL ENGINEERING LAB., IDAHO FALLS.
Vehicle performance tests of the Ford/GE first generation single-shaft (ETX-I) alternating current propulsion system [DE89-011115] N89-25392
An organized effort to develop the hydrothermal energy resource [DE89-011139] N89-25512
Advanced binary geothermal power plants working fluid property determination and heat exchanger design [DE89-011144] N89-25513
IDAHO UNIV., MOSCOW.
Characterization of the effects of three-dimensional states of stress on damping of laminated composites N89-25287
ILLINOIS UNIV., CHICAGO.
Querying databases of trajectories of differential equations: Data structures for trajectories [NASA-CR-185040] N89-25772
ILLINOIS UNIV., URBANA.
Ion energy and plasma measurements in the near field of an ICRF antenna [DE89-011611] N89-25708
ILLINOIS UNIV., URBANA-CHAMPAIGN.
Molecular growth pathways in silica sol-gel polymerization [DE89-011224] N89-25346
A parallel algorithm for switch-level timing simulation on a hypercube multiprocessor [NASA-CR-185338] N89-25595
Single crystal NMR studies of high temperature superconductors [DE89-011220] N89-25747
Neutron stars: A cosmic hadron physics laboratory [NASA-CR-185051] N89-25777
IMPERIAL COLL. OF SCIENCE AND TECHNOLOGY, LONDON (ENGLAND).
The man-machine-interface in a fast jet [ETN-89-94327] N89-25574
The search for solar-type oscillations in other stars using the Michelson Interferometric Stellar Oscillation Spectrometer (ISOS) N89-25918
The search for radial velocity variations in rapidly oscillating Ap stars using the Fabry-Perot Interferometric Stellar Oscillation Spectrometer (FP-ISOS) N89-25923
A Fabry-Perot interferometric stellar oscillation spectrometer N89-25929
INSTITUT D'ASTROPHYSIQUE, PARIS (FRANCE).
Visibility of nonradial pulsation modes in solar continuum intensity measurements N89-25860
INSTITUT FUER ANGEWANDTE GEODAESIE, FRANKFURT AM MAIN (GERMANY, F.R.).
Reports on cartography and Geodesy. Series 1: Original reports, number 102 [ISSN-0469-4236] N89-25501
Interpretation of Thematic Mapper data for the acquisition of land information N89-25502
Forestry interpretation of Thematic Mapper (TM) data using the example of the Frankfurt municipal forest N89-25503
Digital evaluation of SEASAT-SAR radar image data N89-25504
Data adjustment by gravity differences N89-25548
INSTITUTE FOR COMPUTER APPLICATIONS IN SCIENCE AND ENGINEERING, HAMPTON, VA.
On the Gortler vortex instability mechanism at hypersonic speeds [NASA-CR-181844] N89-25123
Semi-automatic process partitioning for parallel computation [NASA-CR-181633] N89-25585
Analytic theory for the determination of velocity and stability of bubbles in a Hele-Shaw cell. Part 1: Velocity selection [NASA-CR-181836] N89-25665
Analytic theory for the selection of 2-D needle crystal at arbitrary Peclet number [NASA-CR-181846] N89-25671
INSTITUTO SUPERIOR TECNICO, LISBON (PORTUGAL).
On the dissipation of Alfven waves in magnetic atmospheres and flux tubes N89-25871
INTERNATIONAL ATOMIC ENERGY AGENCY, VIENNA (AUSTRIA).
International Centre for Theoretical Physics: Scientific activities in 1987 [DE88-705973] N89-25668
INTERNATIONAL CENTRE FOR THEORETICAL PHYSICS, TRIESTE (ITALY).
Local field effects in the many-body perturbation theory and in the density functional theory [DE88-705975] N89-25734
Strings on hyperelliptic supersurfaces [DE88-705991] N89-25758
Renormalization of topological field theory [DE88-705998] N89-25759
IOWA STATE UNIV. OF SCIENCE AND TECHNOLOGY, AMES.
The effect of global-scale divergent circulation on the atmospheric water vapor transport and maintenance N89-25793
IOWA UNIV., IOWA CITY.
On equivalence of discrete-discrete and continuum-discrete design sensitivity analysis N89-25181
A large scale software system for simulation and design optimization of mechanical systems N89-25219
Wave emissions from planetary magnetospheres [NASA-CR-185435] N89-25541

J

JAPAN ATOMIC ENERGY RESEARCH INST., TOKYO.
Proceedings of the Free Electron Laser Workshop, 1988 JAERI [DE89-780071] N89-25450
Confinement physics of H-mode discharges in DIII-D [DE89-011525] N89-25707
JET PROPULSION LAB., CALIFORNIA INST. OF TECH., PASADENA.
Structural optimization and recent large ground antenna installations N89-25224
Optimal placement of excitations and sensors by simulated annealing N89-25227
Phase-ambiguity resolution for QPSK modulation systems. Part 1: A review [NASA-CR-185385] N89-25380
Phase-ambiguity resolution for QPSK modulation systems. Part 2: A method to resolve offset QPSK [NASA-CR-184971] N89-25381
ECUT (Energy Conversion and Utilization Technologies) program: Biocatalysis project [NASA-CR-184965] N89-25519
The software product assurance metrics study: JPL's software systems quality and productivity [NASA-CR-184871] N89-25618
Concurrent Image Processing Executive (CIPE) [NASA-CR-185460] N89-25619
Measurements of the vertical profile of water vapor abundance in the Martian atmosphere from Mars Observer N89-25811
The interannual variability of atmospheric water vapor on Mars N89-25813
The Martian atmospheric water cycle as viewed from a terrestrial perspective N89-25814
Radial and latitudinal gradients in the solar internal angular velocity N89-25831
Initial high-degree p-mode frequency splittings from the 1988 Mt. Wilson 60-foot Tower Solar Oscillation Program N89-25832
Inversion of the solar rotation rate versus depth and latitude N89-25838
JOHNS HOPKINS UNIV., LAUREL, MD.
The stable solar analyzer N89-25858
JOINT INST. FOR LAB. ASTROPHYSICS, BOULDER, CO.
Nonlinear studies of solar gravity modes driven by nuclear burning of He3 in the core N89-25823
JOINT INST. FOR NUCLEAR RESEARCH, DUBNA (USSR).
Use of resonance neutrons for analyzing superclean aluminium [DE88-706221] N89-25313
Explosive cathode on the base of carbon-fibrous plastic material [DE88-706302] N89-25350
Digital dynamic amplitude-frequence spectral analyzer [DE88-706256] N89-25436
Search the spectrometric characteristics of microchannel plate photomultipliers [DE88-706260] N89-25437
Ion optics of LIDIA mass-spectrometer [DE88-706335] N89-25446
Imbedding of the gravitational field into the space of affine connection without torsion [DE88-704637] N89-25536
Program package for investigation of differential equations by the external form method [DE88-706258] N89-25650
Beam transport calculation in magnetic field with a quadrupole symmetry by the method of immersion in moment phase space [DE88-706295] N89-25681
Advances in the development of apparatus and methods for studies of protein monocrystals in coordinate X-ray diffractometers based on two-dimensional proportional chambers [DE88-706259] N89-25740
Two-dimensional density matrix and its equations. Scalar and fermionic fields [DE88-706249] N89-25760

K

KAMAN AEROSPACE CORP., BLOOMFIELD, CT.
A generalized software executive for multidisciplinary computational structural dynamics N89-25175
KANNER (LEO) ASSOCIATES, REDWOOD CITY, CA.
Whisker shaped carbon substance [DE89-010214] N89-25288
KANSAS UNIV., LAWRENCE.
Design optimization of axisymmetric bodies in nonuniform transonic flow N89-25206
KANSAS UNIV. CENTER FOR RESEARCH, INC., LAWRENCE.
Spanwise lift distributions and wake velocity surveys of a semi-span wing with a discontinuous twist [NASA-CR-177532] N89-25122
KATHOLIEKE UNIVERSITEIT TE LEUVEN (BELGIUM).
Asymptotic approximations of nonradial oscillation modes of the Sun N89-25932
KERNFORSCHUNGSANLAGE, JUELICH (GERMANY, F.R.).
Influence of the helium on high temperature embrittlement of metals under cyclic loading [JUEL-2229] N89-25330
KERNFORSCHUNGSZENTRUM G.M.B.H., KARLSRUHE (GERMANY, F.R.).
Mechanical properties of carbon fiber reinforced thermoplastics for cryogenic applications [KFK-4487] N89-25297
The creep and creep-rupture behavior of vanadium-base alloys [KFK-2440] N89-25328
Applicability of microalloying in the production of sintered steel structural parts [KFK-4481] N89-25329
Heat transfer in packed beds [KFK-4451] N89-25425
Gas-liquid flow in dividing Tee-junctions with a horizontal inlet and different branch orientations and diameters [KFK-4399] N89-25427
Experimental study of the phenomena of turbulent flow in the narrow gaps between subchannels of rod bundles [KFK-4501] N89-25428

KIEPENHEUER-INST. FUER SONNENPHYSIK, FREIBURG (GERMANY, F.R.).
Dynamics of the overshoot layers and boundary conditions in helioseismology N89-25826
Oscillations in sunspots near the solar limb N89-25866
Solar oscillations: Overshoot at the base of the convection zone N89-25911

KYOTO UNIV. (JAPAN).
A courant condition free modified partially-implicit method. Revised electromagnetic particle Code PS2M for bounded plasmas with conducting walls
[IPPJ-892] N89-25699

L

LAFAYETTE COLL., EASTON, PA.
Effects of auxiliary heat treatments on flame-cutting procedures
[DE89-011827] N89-25472

LAWRENCE LIVERMORE NATIONAL LAB., CA.
Simple models for electric gun operating characteristics
[DE89-005348] N89-25253
Failure characterization of composite materials
[DE89-008662] N89-25291
Estimating effective moduli of composites using quantitative image analysis
[DE89-012292] N89-25295
The influence of cooling rate on the ferrite content of stainless steel alloys
[DE89-009966] N89-25315
Method of protecting surfaces from abrasion and abrasion resistant articles of manufacture
[DE89-010798] N89-25344
High-performance, extrusion-cast explosives with low sensitivity
[DE89-010279] N89-25349
Time domain modeling of electromagnetic coupling
[DE89-010240] N89-25362
Numerical modeling of monopoles on radial-wire ground screens
[DE89-005350] N89-25372
A generalized antenna theorem for broadband pulses
[DE89-009707] N89-25373
Microwave pulse generation by photoconductive switching
[DE89-011631] N89-25393
Magnetic switching
[DE89-012299] N89-25398
Comparison of experimental shock-wave profiles for tungsten and computer simulations using a rate-dependent constitutive model
[DE89-006158] N89-25419
Adaptive mesh refinement on moving quadrilateral grids
[DE89-010241] N89-25421
Measurement of the stimulated thermal Rayleigh scattering instability
[DE89-012324] N89-25453
Microwave experimental studies of laser fusion
[DE89-012325] N89-25454
Learning the value of VE
[DE89-008121] N89-25475
On greenhouse gas signal detection strategies
[DE89-009908] N89-25521
Atmospheric carbon dioxide and the climate record
[DE89-011892] N89-25528
Climate projections with regional resolution
[DE89-009261] N89-25529
Preventing depletion of stratospheric ozone: Implications on future aircraft emissions
[DE89-009964] N89-25530
Evaluating CFC (Chlorofluorocarbon) alternatives from the atmospheric viewpoint
[DE89-010236] N89-25531
Cloud albedo, greenhouse effects, atmospheric chemistry, and climate change
[DE89-010239] N89-25532
Climate projections with regional resolution
[DE89-009904] N89-25549
Far field projection
[DE89-010243] N89-25587
A simple method to remove reference counting in applicative programs
[DE89-006739] N89-25603
Partitioning a finite difference code for a local memory multiprocessor
[DE89-010223] N89-25621
Performance evaluation for data flow architectures: A summary of discussions from the Santa Fe workshop
[DE89-008023] N89-25624
The Delta-t transport protocol: Features and experience useful for high performance networks
[DE89-009259] N89-25625
High-average-power millimeter-wave FEL (Free-Electron Laser) for plasma heating using the ETA-2 accelerator
[DE89-012294] N89-25711
Electronic structure of high temperature superconductors
[DE89-006610] N89-25741

LEHIGH UNIV., BETHLEHEM, PA.
Effects of auxiliary heat treatments on flame-cutting procedures
[DE89-011827] N89-25472

LIEGE UNIV. (BELGIUM).
On the thermal surface boundary condition for solar pulsations N89-25931

LOCKHEED AERONAUTICAL SYSTEMS CO., BURBANK, CA.
Composite sizing and ply orientation for stiffness requirements using a large finite element structural model N89-25166

LOCKHEED AIRCRAFT CORP., PALO ALTO, CA.
Observations of f- and p-mode oscillations of high degree (500 is less than L is less than 2500) in quiet and active Sun N89-25875

LOCKHEED ENGINEERING AND SCIENCES CO., WASHINGTON, DC.
USSR Space Life Sciences Digest. Index to issues 15-20
[NASA-CR-3922(25)] N89-25556

LOCKHEED MISSILES AND SPACE CO., HUNTSVILLE, AL.
Conjugating binary systems for spacecraft thermal control. Appendix C: Aeroassist Flight Experiment Carrier Vehicle preliminary stress analysis
[NASA-CR-183609] N89-25261
Space Shuttle Main Engine structural analysis and data reduction/evaluation. Volume 2: High pressure oxidizer turbo-pump turbine end bearing analysis
[NASA-CR-183664] N89-25270
Aerodynamic flight evaluation analysis and data base update
[NASA-CR-183654] N89-25276

LOS ALAMOS NATIONAL LAB., NM.
Advanced mass launchers for low earth orbit
[DE89-010759] N89-25255
Whisker shaped carbon substance
[DE89-010214] N89-25288
Improvements of the KIVA-2 computer program for numerical combustion
[DE89-007994] N89-25304
Super-strong self-reinforcing polymeric matrices formed by the first super-strong polymers
[DE89-011533] N89-25347
High explosives reaction model and its application to booster performance
[DE89-005459] N89-25351
Apparatus and method for characterizing conductivity of materials
[DE89-009599] N89-25383
Shock waves and fragmentation via molecular dynamics
[DE89-007981] N89-25405
Design and testing of the EG and G/Los Alamos Operations fast streak camera
[DE89-010859] N89-25445
Superlattice strain gage
[DE89-011805] N89-25447
Finite strain example problems for rectangular, cylindrical, and spherical geometries
[DE89-013607] N89-25488
Adaptive enhancement of magnetoencephalographic signals via multichannel filtering
[DE89-005464] N89-25569
Detection of anomalous computer session activity
[DE89-003807] N89-25591
Interconnection networks
[DE89-010965] N89-25626
The formation and analysis of thin film high temperature superconductors
[DE89-011177] N89-25745
Reminiscence of a stellar pulsation theorist
[DE89-011165] N89-25785
Oscillation frequencies of solar models N89-25902
Solar-like oscillations in late spectral class stars N89-25935

LOUGHBOROUGH UNIV. OF TECHNOLOGY (ENGLAND).
Efficient generalized conjugate gradient algorithms
[MATHS-RES-211] N89-25606
The tanh transformation for double integrals with singularities: A progressive rule
[MATHS-RES-203] N89-25658
A comparison of the error function and the tanh transformation as progressive rules for double and triple singular integrals
[MATHS-RES-210] N89-25659
Discrimination and classification with mixed binary and continuous variables: The Bayesian approach
[MATHS-RES-212] N89-25664

LOUISIANA STATE UNIV., BATON ROUGE.
User's guide to image processing applications of the NOAA satellite HRPT/AVHRR data. Part 1: Introduction to the satellite system and its applications. Part 2: Processing and analysis of AVHRR imagery
[NASA-CR-180784] N89-25492
The origin of ultra-compact binaries
[NASA-TM-101792] N89-25780

LOWELL OBSERVATORY, FLAGSTAFF, AZ.
The 2060 Chiron: CCD photometry
[NASA-CR-185068] N89-25435

LTV AEROSPACE AND DEFENSE CO., DALLAS, TX.
The designer of the 90's: A live demonstration N89-25164

LUNAR AND PLANETARY INST., HOUSTON, TX.
MECA Workshop on Atmospheric H2O Observations of Earth and Mars. Physical Processes, Measurements and Interpretations
[NASA-CR-183395] N89-25790
The interpretation of data from the Viking Mars Atmospheric Water Detectors (MAWD): Some points for discussion N89-25795
Regolith water vapor sources on Mars: A historical bibliography N89-25796
Flux of water vapor in the terrestrial stratosphere and in the Martian atmosphere N89-25806

M

MACNEAL-SCHWENDLER CORP., LOS ANGELES, CA.
Grid sensitivity capability for large scale structures N89-25183

MARTIN MARIETTA AEROSPACE, NEW ORLEANS, LA.
A review of computer aided interpretation technology for the evaluation of radiographs of aluminum welds
[NASA-CR-185066] N89-25312

MARTIN MARIETTA ENVIRONMENTAL SYSTEMS, COLUMBIA, MD.
Investigation of submicrometer aerosols for apportioning the impacts of airborne particulate matter at Deep Creek Lake
[DE89-008186] N89-25524

MARYLAND UNIV., COLLEGE PARK.
Efficient sensitivity analysis and optimization of a helicopter rotor N89-25155
A decomposition-based design optimization method with applications N89-25204
Combined vapor compression/absorption heat pump cycles for engine-driven heat pumps
[PB89-145437] N89-25505

MASSACHUSETTS INST. OF TECH., CAMBRIDGE.
Middeck Active Control Experiment (MACE), phase A
[NASA-CR-185331] N89-25258
Diffraction gratings used in X-ray spectroscopy
[DE89-012327] N89-25310
Interfacial fluid mechanics and transport processes
[DE89-010664] N89-25417
Confinement physics of H-mode discharges in DIII-D
[DE89-011525] N89-25707

MASSACHUSETTS UNIV., AMHERST.
Prototyping management information systems application software: An empirical study of developers' perceptions N89-25770

MAX-PLANCK-INST. FUER KERNPHYSIK, HEIDELBERG (GERMANY, F.R.).
Nuclear beta decay far from stability and astrophysics
[MPI-H-1988-V-27] N89-25683

MAX-PLANCK-INST. FUER PHYSIK UND ASTROPHYSIK, GARCHING (GERMANY, F.R.).
Cosmic plasma physics
[MPE-211] N89-25716
Orientation, motion, and other properties of FTE structures on September 4, 1984 N89-25718
Acceleration of ions in the magnetotail N89-25720
Nonlocal analyses of finite-beam-driven instabilities N89-25721
Ion heating in the Bug shock wave N89-25724
A numerical simulation of inhomogeneous ion cyclotron turbulence N89-25725
The ionization structure in shocks in interstellar molecular clouds N89-25726
Acceleration of particles in shear flows N89-25731

MAX-PLANCK-INST. FUER PLASMAPHYSIK, GARCHING (GERMANY, F.R.).
Confinement physics of H-mode discharges in DIII-D
[DE89-011525] N89-25707
Investigations of modular nonplanar coil systems for the stellarator fusion reactor
[IPP-2/298] N89-25714

MAX-PLANCK-INSTITUT FUER STROEMUNGSFORSCHUNG, GOETTINGEN (GERMANY, F.R.).
A qualitative numerical analysis of some features of propagation of counterflow temperature waves in superfluid helium
[MPIS-9/1988] N89-25424
Experimental investigation on transcritical heat transfer in He 2
[MPIS-MITT-90] N89-25426

MCDONNELL-DOUGLAS CORP., LONG BEACH, CA.
An overview of the Douglas Aircraft Company Aeroelastic Design Optimization Program (ADOP) N89-25221
Meeting the challenges with the Douglas Aircraft Company Aeroelastic Design Optimization Program (ADOP) N89-25222

MCDONNELL-DOUGLAS HELICOPTER CO., MESA, AZ.
Transonic airfoil design for helicopter rotor applications N89-25154
Multi-objective/loading optimization for rotating composite flexbeams N89-25157
Computerized Design Synthesis (CDS), A database-driven multidisciplinary design tool N89-25180

MCINTOSH STRUCTURAL DYNAMICS, INC., MOUNTAIN VIEW, CA.
Static aeroelastic analysis and tailoring of missile control fins N89-25169

MESSERSCHMITT-BOELKOW-BLOHM G.M.B.H., MUNICH (GERMANY, F.R.).
Development of an Si panel
[ETN-89-94625] N89-25518

MIAMI UNIV., FL.
The behavior of a class of minimal models of the atmospheric general circulation N89-25537

MICHIGAN STATE UNIV., EAST LANSING.
Fuzzy set applications in engineering optimization: Multilevel fuzzy optimization N89-25216
Radial and temporal structure of the internal solar asphericity N89-25833
Convection and p-mode oscillations N89-25912

MICHIGAN UNIV., ANN ARBOR.
Generalized mathematical models in design optimization N89-25214
Shape optimal design of elastic bodies using a mixed variational formulation N89-25236
Time-optimal slewing maneuvers of flexible spacecraft N89-25265
On optimal fail-safe design of structures N89-25486

MIDDLE EAST TECHNICAL UNIV., ANKARA (TURKEY).
Radial vibrations in a 5 solar M hydrogen-helium star N89-25938

MIDWEST RESEARCH INST., GOLDEN, CO.
Geothermal energy program summary. Volume 2: Research summaries, fiscal year 1988
[DE89-000865] N89-25509
Operational experience of the OC-OTEC experiments at NELH
[DE89-000877] N89-25510
Support and maneuvering apparatus for solar energy receivers
[DE89-011466] N89-25514
Focusing on the future: Solar thermal energy systems emerge as competitive technologies with major economic potential
[DE89-000851] N89-25516
Wind Energy Program Summary. Volume 2: Research summaries, fiscal year 1988
[DE89-000857] N89-25517

MISSOURI UNIV., COLUMBIA.
Multilevel decomposition of complete vehicle configuration in a parallel computing environment N89-25205

MISSOURI UNIV., SAINT LOUIS.
Circumpolar hoods and clouds and their relation to the Martian H2O cycle N89-25803

MORTON THIOKOL, BRIGHAM CITY, UT.
Flight set 360L003 instrumentation final test report, volume 9
[NASA-CR-183675] N89-25284

N

NAGOYA UNIV. (JAPAN).
A courant condition free modified partially-implicit method. Revised electromagnetic particle Code PS2M for bounded plasmas with conducting walls
[IPPJ-892] N89-25699
Density fluctuations and particle/thermal transport for ohmically and auxiliarily heated plasmas in the JIPP T-IIU tokamak
[IPPJ-891] N89-25700
Z subeff measurements and low-Z impurity transport for NBI and ICRF heated plasma in JIPP T-IIU tokamak
[IPPJ-896] N89-25701

NATIONAAL INST. VOOR KERNFYSICA EN HOGE ENERGIEFYSICA, AMSTERDAM (NETHERLANDS).
Non-perturbative effects in the exact S-matrices of the O(N) Gross-Neveu and supersymmetric sigma models
[NIKHEF-H/88-10] N89-25656
On the quantum theory of the superparticle
[NIKHEF-H/88-16] N89-25762

NATIONAL ACADEMY OF SCIENCES - NATIONAL RESEARCH COUNCIL, WASHINGTON, DC.
Responding to changes in sea level engineering implications
[PB89-133466] N89-25555
United States and Western Europe cooperation in planetary exploration
[NASA-CR-184941] N89-25776

NATIONAL AERONAUTICAL LAB., BANGALORE (INDIA).
On the stress problem of the pebble bed heat exchanger in a hypersonic wind tunnel
[NAL-TM-ST-8705] N89-25240
Experiments on liquid-vapour phase change between plane liquid surfaces. Part 3: Results from a closed quartz chamber
[NAL-TM-FM-8809] N89-25301
Controller for stabilization of high voltage
[NAL-TM-MT-8702] N89-25382

NATIONAL AERONAUTICS AND SPACE ADMINISTRATION, WASHINGTON, DC.
Aeronautical engineering: A continuing bibliography with indexes (supplement 239)
[NASA-SP-7037(239)] N89-25114
Aeronautical engineering: A continuing bibliography with indexes (supplement 240)
[NASA-SP-7037(240)] N89-25115
Space station operations task force. Panel 1 report: Space operations and support systems
[NASA-TM-101816] N89-25244
Space station operations task force. Panel 2 report: Ground operations and support systems
[NASA-TM-101817] N89-25245
Space station operations task force. Panel 3 report: User development and integration
[NASA-TM-101818] N89-25246
Space station operations task force. Panel 4 report: Management integration
[NASA-TM-101819] N89-25247
Space station operations task force summary report
[NASA-TM-101820] N89-25248
Space station operations task force. Executive summary
[NASA-TM-101780] N89-25249
Earth resources: A continuing bibliography with indexes (issue 61)
[NASA-SP-7041(61)] N89-25493
The UARS (Upper Atmosphere Research Satellite): A program to study global ozone change
[NASA-TM-101756] N89-25520
Aerospace medicine and biology: A continuing bibliography with indexes (supplement 323)
[NASA-SP-7011(323)] N89-25563
Aerospace medicine and biology: A continuing bibliography with indexes (supplement 324)
[NASA-SP-7011(324)] N89-25565
Aerospace medicine and biology: A continuing bibliography with indexes (supplement 325)
[NASA-SP-7011(325)] N89-25567
NASA patent abstracts bibliography: A continuing bibliography. Section 1: Abstracts (supplement 35)
[NASA-SP-7039(35)-SECT-1] N89-25775
Solar physics in the space age
[NASA-NP-106] N89-25818
The GONG site survey N89-25855
Solar system exploration
[NASA-TM-101784] N89-25944
Where no man has gone before: A history of Apollo lunar exploration missions
[NASA-SP-4214] N89-25946

NATIONAL AERONAUTICS AND SPACE ADMINISTRATION. AMES RESEARCH CENTER, MOFFETT FIELD, CA.
The 3DGRAPE book: Theory, users' manual, examples
[NASA-TM-102224] N89-25116
Real-time application of knowledge-based systems N89-25163
Space station architecture, module, berthing hub, shell assembly, berthing mechanism and utility connection channel
[NASA-CASE-ARC-11505-2] N89-25266
Flap-lag stability data for a small-scale isolated hingeless rotor in forward flight
[NASA-TM-102189] N89-25479
Visible and near-infrared channel calibration of the GOES-6 VISSR using high-altitude aircraft measurements
[NASA-TM-101064] N89-25494
Calibration of the visible and near-infrared channels of the NOAA-9 AVHRR using high-altitude aircraft measurements from August 1985 and October 1986
[NASA-TM-101063] N89-25496
Acclimatization to heat in humans
[NASA-TM-101011] N89-25558
A numerical study of a class of TVD schemes for compressible mixing layers
[NASA-TM-102194] N89-25651
A class of high resolution explicit and implicit shock-capturing methods
[NASA-TM-101088] N89-25652
Factors governing water condensation in the Martian atmosphere N89-25797
On the vertical distribution of water vapor in the Martian tropics N89-25800

NATIONAL AERONAUTICS AND SPACE ADMINISTRATION. GODDARD SPACE FLIGHT CENTER, GREENBELT, MD.
Spacelab Data Processing Facility
[NASA-TM-101808] N89-25252
Dynamic sea surface topography, gravity and improved orbit accuracies from the direct evaluation of SEASAT altimeter data
[NASA-TM-100735] N89-25539
Helioseismology from the South Pole: Comparison of 1987 and 1981 results N89-25868
Dynamo theory prediction of solar activity N89-25878

NATIONAL AERONAUTICS AND SPACE ADMINISTRATION. HUGH L. DRYDEN FLIGHT RESEARCH FACILITY, EDWARDS, CA.
Control surface spanwise placement in active flutter suppression systems N89-25195

NATIONAL AERONAUTICS AND SPACE ADMINISTRATION. LYNDON B. JOHNSON SPACE CENTER, HOUSTON, TX.
Smart tunnel: Docking mechanism
[NASA-CASE-MSC-21360-1] N89-25263
Hybrid plume plasma rocket
[NASA-CASE-MSC-20476-2] N89-25279
Method and apparatus for sensor fusion
[NASA-CASE-MSC-21334-1] N89-25360
Spiral vane bioreactor
[NASA-CASE-MSC-21361-1] N89-25557
An expert system development methodology which supports verification and validation
[NASA-TM-101782] N89-25635
Possible significance of cubic water-ice, H2O-Ic, in the atmospheric water cycle of Mars N89-25799

NATIONAL AERONAUTICS AND SPACE ADMINISTRATION. LANGLEY RESEARCH CENTER, HAMPTON, VA.
Effect of milling machine roughness and wing dihedral on the supersonic aerodynamic characteristics of a highly swept wing
[NASA-TP-2918] N89-25117
Interactions of Tollmien-Schlichting waves and Dean vortices. Comparison of direct numerical simulation and a weakly nonlinear theory
[NASA-TP-2919] N89-25118
On the Gortler vortex instability mechanism at hypersonic speeds
[NASA-CR-181844] N89-25123
Free-molecule-flow force and moment coefficients of the aeroassist flight experiment vehicle
[NASA-TM-101600] N89-25124
Recent Advances in Multidisciplinary Analysis and Optimization, part 1
[NASA-CP-3031-PT-1] N89-25146
Optimization by decomposition: A step from hierarchic to non-hierarchic systems N89-25149
Overview of Dynamics Integration Research (DIR) program at Langley Research Center N89-25150
An initiative in multidisciplinary optimization of rotorcraft N89-25151
Structural optimization of rotor blades with integrated dynamics and aerodynamics N89-25156
Demonstration of decomposition and optimization in the design of experimental space systems N89-25160
STRUTEX: A prototype knowledge-based system for initially configuring a structure to support point loads in two dimensions N89-25161
Integrated aerodynamic-structural design of a forward-swept transport wing N89-25168
Effects of nonlinear aerodynamics and static aeroelasticity on mission performance calculations for a fighter aircraft N89-25170
Optimum design of swept-forward high-aspect-ration graphite-epoxy wings N89-25172
Recent Advances in Multidisciplinary Analysis and Optimization, part 2
[NASA-CP-3031-PT-2] N89-25173

The Sizing and Optimization Language (SOL): A computer language to improve the user/optimizer interface N89-25178
Results of an integrated structure/control law design sensitivity analysis N89-25185
Results of including geometric nonlinearities in an aeroelastic model of an F/A-18 N89-25190
Flutter suppression using eigenspace freedoms to meet requirements N89-25191
Aeroelastic modeling for the FIT (Functional Integration Technology) team F/A-18 simulation N89-25192
Finite element flow-thermal-structural analysis of aerodynamically heated leading edges N89-25198
Recent Advances in Multidisciplinary Analysis and Optimization, part 3
[NASA-CP-3031-PT-3] N89-25201
Engineering applications of heuristic multilevel optimization methods N89-25202
Hypersonic airbreathing vehicle conceptual design (focus on aero-space plane) N89-25210
Optimizing conceptual aircraft designs for minimum life cycle cost N89-25211
Experiences in applying optimization techniques to configurations for the Control of Flexible Structures (COFS) program N89-25228
Time-correlated gust loads using Matched-Filter Theory and Random-Process Theory: A new way of looking at things
[NASA-TM-101573] N89-25232
An analytical sensitivity method for use in integrated aeroservoelastic aircraft design
[NASA-TM-101583] N89-25239
Polyimide Matrix composites: Polyimidesulfone/LARC-TPI (1:1) blend
[NASA-TM-101568] N89-25294
Absorbed dose thresholds and absorbed dose rate limitations for studies of electron radiation effects on polyetherimides
[NASA-TP-2928] N89-25332
Semiinterpenetrating polymer network for tougher and more microcracking resistant high temperature polymers
[NASA-CASE-LAR-13925-1] N89-25334
Sensitivity analysis of complex coupled systems extended to second and higher order derivatives
[NASA-TM-101587] N89-25354
Antenna surface contour control system
[NASA-CASE-LAR-13796-1] N89-25363
A slow positron beam generator for lifetime studies
[NASA-TM-101590] N89-25433
Automated thermal mapping techniques using chromatic image analysis
[NASA-TM-101554] N89-25443
Comparison of satellite-derived dynamical quantities for the stratosphere of the Southern Hemisphere
[NASA-CP-3044] N89-25540
Common Graphics Library (CGL). Volume 2: Low-level user's guide
[NASA-TM-101596] N89-25597
Analytic theory for the selection of 2-D needle crystal at arbitrary Peclet number
[NASA-CR-181846] N89-25671
Airfoil self-noise and prediction
[NASA-RP-1218] N89-25673
Observations of atmospheric water vapor with the SAGE 2 instrument N89-25805
The Nimbus 7 LIMS (Limb Infrared Monitor of the Stratosphere) water vapor measurements N89-25810
Space directorate research and technology accomplishments for FY 1988
[NASA-TM-101597] N89-25947

NATIONAL AERONAUTICS AND SPACE ADMINISTRATION. LEWIS RESEARCH CENTER, CLEVELAND, OH.

Numerical analysis of supersonic flow through oscillating cascade sections by using a deforming grid
[NASA-TM-102053] N89-25119
Low-speed wind tunnel performance of high-speed counterrotation propellers at angle-of-attack
[NASA-TM-102292] N89-25121
Structural tailoring of counter rotation propfans N89-25165
Fuel properties effect on the performance of a small high temperature rise combustor
[NASA-TM-102096] N89-25238
Advanced APS impacts on vehicle payloads
[NASA-TM-102086] N89-25254
Protoflight photovoltaic power module system-level tests in the space power facility
[NASA-TM-102066] N89-25267
Solar dynamic power module design
[NASA-TM-102055] N89-25269
Variable speed induction motor operation from a 20-kHz power bus
[NASA-TM-102061] N89-25271
Space nuclear reactor shields for manned and unmanned applications
[NASA-TM-102064] N89-25272
Space Station Freedom photovoltaic power module design status
[NASA-TM-102073] N89-25273
The introduction of space technology power systems into developing countries
[NASA-TM-102042] N89-25274
Launch packaging options for the photovoltaic power module cargo element
[NASA-TM-102072] N89-25275
Scaling results for the Liquid Sheet Radiator (LSR)
[NASA-TM-102100] N89-25277
Estimated performance and future potential of solar dynamic and photovoltaic power systems for selected LEO and HEO missions
[NASA-TM-102083] N89-25280
The effects of arcjet operating condition and constrictor geometry on the plasma plume
[NASA-TM-102284] N89-25281
CSTI High Capacity Power
[NASA-TM-102059] N89-25282
Performance characterization and transient investigation of multipropellant resistojets
[NASA-TM-102118] N89-25283
Characterization of ceramics and intermetallics fabricated by self-propagating high-temperature synthesis
[NASA-TM-102004] N89-25285
Vibration testing of impact-damaged composite laminates
[NASA-TM-4115] N89-25290
A predictive model for failure properties of thermoset resins
[NASA-TM-4128] N89-25300
Performance of five 30 GHz satellite receivers
[NASA-TM-101960] N89-25365
Development and testing of a 20-kHz component test bed
[NASA-TM-102141] N89-25403
Determination of combustion gas temperatures by infrared radiometry in sooting and nonsooting flames
[NASA-TP-2900] N89-25409
Procedures for characterizing an alloy and predicting cyclic life with the total strain version of Strainrange Partitioning
[NASA-TM-4102] N89-25485
Advanced methods for 3-D inelastic structural analysis for hot engine structures
[NASA-TM-102106] N89-25490
Challenges for future space power systems
[NASA-TM-102063] N89-25506
Acoustic propagation in curved ducts with extended reacting wall treatment
[NASA-TM-102110] N89-25670
In-flight measurement of propeller noise on the fuselage of an airplane
[NASA-TM-102285] N89-25675

NATIONAL AERONAUTICS AND SPACE ADMINISTRATION. MARSHALL SPACE FLIGHT CENTER, HUNTSVILLE, AL.

Warm fog dissipation using large volume water sprays
[NASA-CASE-MFS-25962-1] N89-25242
An evaluation of the General Dynamics 20 kHz 5 kW Breadboard for space station electrical power at MSFC
[NASA-TM-100367] N89-25278
Optical pressure sealing coupling apparatus
[NASA-CASE-MFS-29348-1] N89-25689
Federal incentives for industrial modernization: Historical review and future opportunities
[NASA-TM-101785] N89-25764
The origin of ultra-compact binaries
[NASA-TM-101792] N89-25780
The GONG data reduction and analysis system N89-25856

NATIONAL CENTER FOR ATMOSPHERIC RESEARCH, BOULDER, CO.

Cumulus convection and the terrestrial water-vapor distribution N89-25798
On the radiative damping of p-modes in solar magnetic flux concentrations N89-25864
Viscous magnetohydrodynamic modes and p-mode absorption by sunspots N89-25873
Evidence for a thin perturbative layer near the base of the solar convection zone N89-25876

NATIONAL GEOPHYSICAL DATA CENTER, BOULDER, CO.

Solar-geophysical data number 528, August 1988. Part 1: (Prompt reports). Data for July, June 1988 and late data
[PB89-109904] N89-25817

NATIONAL INST. OF STANDARDS AND TECHNOLOGY, GAITHERSBURG, MD.

Elevated temperature deformation of structural steel
[PB89-172621] N89-25318
Hierarchies for computer-integrated manufacturing: A functional description
[PB89-172613] N89-25596

NATIONAL OCEANIC AND ATMOSPHERIC ADMINISTRATION, WASHINGTON, DC.

Solar Mesosphere Explorer observations of stratospheric and mesospheric water vapor N89-25802

NATIONAL SOLAR OBSERVATORY, SUNSPOT, NM.

Local effects of a major flare on solar five-minute oscillations N89-25872

NATIONAL SOLAR OBSERVATORY, TUCSON, AZ.

Solar internal rotation from helioseismology N89-25829
Oscillation ring diagrams and the thermodynamics of the outer solar convection zone N89-25836
The GONG instrument N89-25854

NAVAL POSTGRADUATE SCHOOL, MONTEREY, CA.

ARMA (Autoregressive-Moving Average) modeling
[AD-A205308] N89-25649

NAVAL RESEARCH LAB., WASHINGTON, DC.

Time-dependent computational studies of flames in microgravity
[NASA-CR-182298] N89-25353

NEBRASKA UNIV., LINCOLN.

On the calculation of derivatives of eigenvalues and eigenvectors in the simultaneous design and control of structures N89-25186
Electrochemical and optical studies of model photosynthetic systems
[DE89-012479] N89-25562

NETHERLANDS ENERGY RESEARCH FOUNDATION, PETTEN.

Effect of low neutron fluences on DIN 1.4948 steel creep properties
[ECN-206] N89-25325

NEW MEXICO STATE UNIV., UNIVERSITY PARK.

Ripple structure in degenerate electron gas-dominated stars with intense magnetic fields N89-25783

NEW TECHNOLOGY, INC., HUNTSVILLE, AL.

New atmospheric sensor analysis study
[NASA-CR-183597] N89-25431

NICE UNIV. (FRANCE).

I.R.I.S.: A network for full disk helioseismology N89-25845
Solar p-modes frequency variations between 1980 and 1986 N89-25867
Searching for solar g-modes. Tests of a statistical method N89-25889
The Nice University stellar seismometer N89-25927

NORTH CAROLINA UNIV., CHARLOTTE.

Design of an auto change mechanism and intelligent gripper for the space station
[NASA-CR-185387] N89-25268
Magneto-inductive skin sensor for robot collision avoidance: A new development
[NASA-CR-185402] N89-25444

NORTHROP CORP., HAWTHORNE, CA.

ASTROS: A multidisciplinary automated structural design tool N89-25174
Robust computer-aided synthesis and optimization of linear multivariable control systems with varying plant dynamics via AUTOCON N89-25179

NORTHWESTERN UNIV., EVANSTON, IL.

Parallel processors and nonlinear structural dynamics algorithms and software
[NASA-CR-185049] N89-25620

NORWEGIAN SPACE CENTER, OSLO.

Detector configurations for observations of gravity modes in solar radiance N89-25886

NOTRE DAME UNIV., IN.

Study of interfacial behavior in concurrent gas-liquid flows
[DE89-010484] N89-25408
Periodic and solitary waves on thin, horizontal, gas-sheared liquid films
[DE89-010655] N89-25416

O

OAK RIDGE ASSOCIATED UNIVERSITIES, INC., TN.

An inductively coupled plasma spectrometer for on-line, real-time process gas analysis
[DE89-010610] N89-25442

OAK RIDGE GASEOUS DIFFUSION PLANT, TN.

Interprocess communications and application to physical numerical modeling
[DE89-011021] N89-25630

OAK RIDGE NATIONAL LAB., TN.

SiC whisker-reinforced SiAlON composites: Effect of sintering aid content
[DE89-010376] N89-25289
The development of alloys based on Ni3Si
[DE89-010371] N89-25316

The application of Rutherford backscattering and channeling techniques to the characterization of ceramics
[DE89-010257] N89-25333
The mechanical properties of ion implanted ceramics
[DE89-006928] N89-25337
Evaluation of ceramic coatings on silicon carbide
[DE89-010321] N89-25339
Analysis and control of a three-degree-of-freedom robot platform
[DE89-006427] N89-25356
Determination of fields near an ICRH antenna using a 3D magnetostatic Laplace formulation
[DE89-011571] N89-25366
Spectral shaping and phase control of a fast-wave current drive antenna array
[DE89-011567] N89-25368
Condition monitoring of machinery using motor current signature analysis
[DE89-006737] N89-25386
Binary and ternary gas mixtures with temperature enhanced diffuse glow discharge characteristics for use in closing switches
[DE89-011807] N89-25395
Laser diffraction methods for high temperature strain measurements
[DE89-006235] N89-25451
Modifying a telerobotic system to include robotic operation by means of dynamic modeling
[DE89-003119] N89-25460
Traction-drive transmission for telerobotic joints
[DE89-005337] N89-25461
Modeling the effect of surface active elements on weld pool fluid flow, heat transfer and geometry
[DE89-012504] N89-25466
Determination of the mechanical properties of diamond and diamond-like films by the ultra-low load indentation technique
[DE89-011569] N89-25471
The role of forests in addressing the CO2 greenhouse
[DE89-011566] N89-25527
Design description of the large scale climate simulator
[DE89-010185] N89-25551
Review of the 1988 Workshop on Human-Machine Symbiotic Systems
[DE89-006743] N89-25570
Operator role definition and human system integration
[DE89-009621] N89-25571
The 1988 Workshop on Human-Machine Symbiotic Systems
[DE89-010170] N89-25572
A tool to aid in mapping computational tasks to a hypercube
[DE89-010320] N89-25589
Concurrent spatio-temporal image analysis
[DE89-010260] N89-25593
Parallel solutions of a 2-D phase change problem on a hypercube
[DE89-012886] N89-25602
Robust performance of multiple tasks by an autonomous robot
[DE89-006718] N89-25636
Performance characteristics for advanced control systems
[DE89-010362] N89-25637
Synthetic organisms and self-designing systems
[NASA-CR-185324] N89-25639
Application of theta functions for numerical evaluation of complete elliptic integrals of the first and second kinds
[DE89-010191] N89-25645
Review of oxidation of Nb-1Zr
[DE89-010299] N89-25687
Confinement improvement of low-aspect-ratio torsatrons
[DE89-010192] N89-25702
Confinement physics of H-mode discharges in DIII-D
[DE89-011525] N89-25707
Plasma production using microwave and radio frequency sources
[DE89-011615] N89-25709
ICRF Faraday shield plasma sheath physics: The Perkins paradigm
[DE89-012362] N89-25712
Averaged equilibrium and stability in low-aspect-ratio stellarators
[DE89-013618] N89-25713
Variation of superlattice structure of the Bi2Sr(2-x)CuO(6-y) superconductor with composition and thermal history
[DE89-011612] N89-25749
Systems approach to project management
[DE89-008741] N89-25765
An expert system to facilitate selecting a database management system
[DE89-012350] N89-25774

OBSERVATOIRE DE LA COTE D'AZUR, NICE (FRANCE).
Effects of convective velocities on solar pressure mode frequencies N89-25941

OBSERVATOIRE DE PARIS-MEUDON (FRANCE).
The influence of the toroidal roll pattern on the sunspot activity N89-25870
Rapid photometry of the Delta Scuti variable 63 Her N89-25916
Oscillations of Jupiter as a tool for probing its internal structure N89-25924
The influence of the equation of state on the zero-age main sequence and the Sun N89-25939

OBSERVATOIRE DE TOULOUSE (FRANCE).
Periodical asymmetry of solar limb darkening N89-25861

OBSERVATOIRE DES ALPES MARITIMES, GRASSE (FRANCE).
Solar variability and climatology N89-25909

OBSERVATOIRE DU MONT-GROS, NICE (FRANCE).
Integrated light and velocity of solar g modes oscillations N89-25888

OCEAN RESEARCH CONSULTANTS, LA JOLLA, CA.
On greenhouse gas signal detection strategies
[DE89-009908] N89-25521

OHIO STATE UNIV., COLUMBUS.
An improved algorithm for optimum structural design with multiple frequency constraints N89-25229
The organization of perception and action in complex control skills
[NASA-CR-184638] N89-25568

OKLAHOMA UNIV., NORMAN.
Advanced working fluid properties in heat pump and absorption cooling operations
[PB89-178172] N89-25413
Correlation of subjective slipperiness judgements with quantitative COF (Coefficient Of Friction) measurements for structural steel
[PB89-165070] N89-25669

OREGON GRADUATE CENTER FOR STUDY AND RESEARCH, BEAVERTON.
Deformation induced microstructural and microchemical changes during thermomechanical treatment
[DE89-011608] N89-25321

OREGON STATE UNIV., CORVALLIS.
Transport of Mars atmospheric water into high northern latitudes during a polar warming N89-25782

OSLO UNIV. (NORWAY).
Solar infrared intensity oscillations N89-25847

OSSERVATORIO METEOROLOGICO DI BRERA, MILAN (ITALY).
Some tests of the precision of CCD differential photometry measurements of bright double stars N89-25930

OULU UNIV. (FINLAND).
An auroral TV-system
[REPT-115(1988)] N89-25543

P

PACIFIC NORTHWEST LABS., RICHLAND, WA.
Quantitative modeling of sensitization development in austenitic stainless steel
[DE89-011206] N89-25317
Precipitation at grain boundaries in irradiated austenitic Fe-Cr-Mn alloys
[DE89-011207] N89-25319
Modeling grain boundary microchemistry related to IASCC (Irradiation-Assisted Stress Corrosion Cracking)
[DE89-011214] N89-25320
Optical properties of metal-oxide thin films: Influence of microstructure
[DE89-011219] N89-25690
Deposition of dielectric optical coatings: A microstructural study of the deposited layers and interfaces
[DE89-011205] N89-25694

PDA ENGINEERING, COSTA MESA, CA.
Involute composite design evaluation using global design sensitivity derivatives N89-25199

PENNSYLVANIA STATE UNIV., UNIVERSITY PARK.
Iterative methods for design sensitivity analysis N89-25184
Measurements of H2O in the terrestrial mesosphere and implications for extra-terrestrial sources N89-25808

PITTSBURGH ENERGY TECHNOLOGY CENTER, PA.
Proceedings of the Solids Transport Contractors' Review Meeting
[DE89-006720] N89-25414

PITTSBURGH UNIV., PA.
A study of non-linear ionization processes in planetary atmospheres N89-25816

PLANNING RESEARCH CORP., HAMPTON, VA.
Digital robust control law synthesis using constrained optimization N89-25193

POLITECNICO DI MILANO (ITALY).
Catastrophic bifurcations in a second order dynamical system
[REPT-88-049] N89-25533
On the role of software reliability in software engineering
[REPT-88-010] N89-25607
Serial-input polyphase convolvers
[REPT-88-019] N89-25608
Handling arrays in symbolic execution
[REPT-89-003] N89-25609
Symbolic execution of concurrent programs using Petri nets
[REPT-89-004] N89-25633
A net-based model for time-dependent systems
[REPT-89-005] N89-25661
Temporal data management in real-time systems: A comparative view
[REPT-88-046] N89-25767

PRINCETON UNIV., NJ.
Cosmological effects of superconducting strings N89-25778

PURDUE UNIV., WEST LAFAYETTE, IN.
Aeroservoelastic tailoring for lateral control enhancement N89-25189
Radiative heat transfer
[PB89-173637] N89-25412
Timesharing performance as an indicator of pilot mental workload
[NASA-CR-185328] N89-25573

R

RENSSELAER POLYTECHNIC INST., TROY, NY.
An investigation of using an RQP based method to calculate parameter sensitivity derivatives N89-25182

RESEARCH INST. FOR ADVANCED COMPUTER SCIENCE, MOFFETT FIELD, CA.
Modeling the AIDS epidemic
[NASA-CR-185413] N89-25566
The RIACS Intelligent Auditing and Categorizing System
[NASA-CR-185398] N89-25598
The fast encryption package
[NASA-CR-185397] N89-25599
Fast Fourier Transform algorithm design and tradeoffs
[NASA-CR-185038] N89-25600
Speeding up parallel processing
[NASA-CR-184646] N89-25628
Feasibility of using the Massively Parallel Processor for large eddy simulations and other Computational Fluid Dynamics applications
[NASA-CR-185427] N89-25629
Blindness in designing intelligent systems
[NASA-CR-184582] N89-25638
Fast polar decomposition of an arbitrary matrix
[NASA-CR-185412] N89-25653
On conjugate gradient type methods and polynomial preconditioners for a class of complex non-Hermitian matrices
[NASA-CR-185424] N89-25654
Performance issues in management of the Space Station Information System
[NASA-CR-185409] N89-25773

RICARDO-ITI, WESTMONT, IL.
Multidimensional modeling of convective heat transfer with application to I.C. engines
[DE89-010651] N89-25415

RMS TECHNOLOGIES, INC., LANDOVER, MD.
Mission Operations and Data Systems Directorate's operational/development network (MODNET) at Goddard Space Flight Center
[NASA-CR-183426] N89-25763

ROCHESTER UNIV., NY.
Femtosecond studies of electron transfer processes at semiconductor interfaces
[DE89-010599] N89-25742
Thermal conductivity of dielectric thin films
[DE89-011847] N89-25750

ROCKWELL INTERNATIONAL CORP., LOS ANGELES, CA.
The art of spacecraft design: A multidisciplinary challenge N89-25209

ROME UNIV. (ITALY).
Note on the Majorana representations of the Lorentz group
[PREPRINT-597] N89-25662
Integrated solar disk oscillation measurements using the magneto-optical filter: Tests with a two station network N89-25850
Acquisition and reduction procedures for MOF Doppler-magnetograms N89-25851
A prototype stellar photometer for magnetic field and Doppler measurements N89-25926

RUHR UNIV., BOCHUM (GERMANY, F.R.).
State-selective single electron capture by multiply charged ions: Reaction window and multichannel Landau Zener calculations
[REPT-88-05-175] N89-25684
Partial and state selective cross sections for multiple ionization of rare gas atoms by electron impact
[REPT-88-05-170] N89-25715
Magnetic reconnection in general three-dimensional systems N89-25717
Three dimensional computations of the dynamics of the magnetopause: First results N89-25719
Particle simulation of magnetic reconnection N89-25722
Double tearing and particle simulation N89-25723
Gravitational-like phase transition of a classical Coulomb plasma N89-25727
On the formation of current-sheets in ideal MHD N89-25728
Models for axially symmetric pulsar magnetospheres N89-25730
Stationary ideal MHD with incompressible mass flow and general symmetry N89-25732

S

SAINT ANDREW'S UNIV. (SCOTLAND).
The influence of a chromospheric magnetic field on p- and f-modes N89-25874
SANDIA NATIONAL LABS., ALBUQUERQUE, NM.
Electrically conductive composite material
[DE89-010967] N89-25293
Issues in shock-induced solid state chemistry
[DE89-010769] N89-25309
Weldability and weld doping of commercial purity molybdenum
[DE89-009535] N89-25311
Thermomechanical fatigue of solder joints: A new comprehensive test method
[DE89-008045] N89-25314
J(sub Ic) fracture toughness of ferritic DCI (Ductile Cast Iron) alloys: A comparison of two versions of ASTM E 813
[DE89-012249] N89-25323
Dynamic fracture toughness measurements of ferritic ductile cast iron
[DE89-009833] N89-25324
Studies of oxidative degradation of polymers induced by ionizing radiation
[DE89-008279] N89-25335
Parameter estimation for a viscoelastic constitutive model
[DE89-008714] N89-25336
Technique and data analysis for impact-loaded piezoelectric polymers (PVDF)
[DE89-010529] N89-25342
Low density microcellular carbon foams and method of preparation
[DE89-010966] N89-25345
Characterization of booster-rocket propellants and their simulants
[DE89-012497] N89-25352
The development of a vapor compression refrigeration system for a network of nine temperature test chambers
[DE89-007084] N89-25355
Pyramidal horns: Part 1: Simple expressions for directivity as a function of aperture phase error
[DE89-005209] N89-25370
Pyramidal horns: Part 2: A novel design method for horns of any desired gain and aperture phase error
[DE89-005346] N89-25371
Sintering schedule and sample geometry effects on the electrical and physical properties of high field varistor materials
[DE89-010523] N89-25384
Stress-driven diffusive voiding of aluminum conductor lines
[DE89-009832] N89-25387
A novel TR (Transmit/Receive) switch utilizing a distributed amplifier
[DE89-005917] N89-25396
Resistive Contrast Imaging applied to multilevel interconnection failure analysis
[DE89-011066] N89-25397
Coupling of the boundary element method with an integral momentum boundary-layer technique to calculate forces and moments on three-dimensional bodies
[DE89-006328] N89-25420
Initial design and analysis of a capacitive sensor for shear and normal force measurement
[DE89-001821] N89-25438
Pressure calibration and certification of a quartz pressure transducer
[DE89-005774] N89-25439
Identification of error sources in shock data
[DE89-007655] N89-25440
Automated Test and Evaluation Center for Waveform Digitizer Systems and Components
[DE89-010226] N89-25441
Fission reactor pumped lasers: History and prospects
[DE89-010329] N89-25456
An uncertainty analysis for the Structural Mechanics Laboratory
[DE89-010306] N89-25478
Simple fixture concepts for multi-axis vibration testing
[DE89-007977] N89-25481
Identification of distributed forces on a structure
[DE89-007978] N89-25482
A test system for computer controlled thermomechanical fatigue testing
[DE89-009067] N89-25483
Structural testing of metal/composite conical structures with holes
[DE89-011451] N89-25487
Modeling of magnetic devices with finite-element methods
[DE89-010525] N89-25576
The epsilon dataflow processor
[DE89-001679] N89-25577
PRONTO 3D: A three-dimensional transient solid dynamics program
[DE89-010517] N89-25590
Culture shock: Improving software quality
[DE89-003610] N89-25592
Design and construction of a computer system model for application development workloads
[DE89-010519] N89-25622
Optical information storage in PLZT thin films
[DE89-011067] N89-25692
Fiber optic sensing in a high explosives environment
[DE89-010863] N89-25695
Plasma switches for high current and fast time scale operation
[DE89-010557] N89-25704
Ferroelectric potassium niobate thin films
[DE89-010862] N89-25744
Processing chemically prepared Tl-Ca-Ba-Cu oxide superconductors
[DE89-011535] N89-25748
SCIENCE AND TECHNOLOGY ASSOCIATES, INC., ARLINGTON, VA.
Continuous global N-tuple coverage with (2N = 2) satellites
[AD-A206522] N89-25262
SCIENCE APPLICATIONS INTERNATIONAL CORP., LA JOLLA, CA.
Survivable pulse power space radiator
[DE89-010120] N89-25264
SCIENCE APPLICATIONS INTERNATIONAL CORP., SAN DIEGO, CA.
Theoretical studies of edge physics and plasma-wall interactions
[DE89-011792] N89-25710
SIEMENS A.G., ERLANGEN (GERMANY, F.R.).
A 2 J high-power excimer laser at high pulse repetition rate
[U9-414/87/029] N89-25457
SOCIETE NATIONALE INDUSTRIELLE AEROSPATIALE, ISSAC (FRANCE).
SIMOUN: Test system for shuttle thermal protection materials
[REPT-882-430-101] N89-25256
SOUTHWEST RESEARCH INST., SAN ANTONIO, TX.
Transient effects in creep cavity nucleation and early growth in ceramics
[DE89-010420] N89-25340
SRI INTERNATIONAL CORP., MENLO PARK, CA.
Photodissociation of pernitric acid (HO2NO2) at 248 nm
[NASA-CR-185363] N89-25286
STANFORD UNIV., CA.
Aircraft design optimization with multidisciplinary performance criteria N89-25212
The solar oscillations imager for SOHO N89-25885
The Michelson Doppler imager for the solar oscillations imager program on SOHO N89-25892
The search for solar gravity modes N89-25894
Solar calibration of asteroseismology N89-25921
The evolution of energetic particles and the emitted radiation in solar flares
[NASA-CR-185389] N89-25945
STATE UNIV. OF NEW YORK, BUFFALO.
Unsteady stagnation-point heat transfer during passage of a concentrated vortex
[NASA-CR-182297] N89-25404
SUNDSTRAND ADVANCED TECHNOLOGY GROUP, ROCKFORD, IL.
Electrically compensated constant speed drive (Model number 60 ECEPGS 02)
[AD-A206064] N89-25385

T

TECHNION - ISRAEL INST. OF TECH., HAIFA.
Control surface spanwise placement in active flutter suppression systems N89-25195
TECHNISCHE HOCHSCHULE, AACHEN (GERMANY, F.R.).
Vortex flows in flying technique
[ETN-89-94428] N89-25126
Integration method for the calculation of flow with free vortices N89-25127
Investigations of vortex breakdown N89-25128
Unsteady phenomena on delta wings with partially broken-down vortex regions N89-25129
Measurement of velocity fields in vortex structures N89-25130
Strongly unsteady vortex fields at elastic helicopter rotor blades N89-25131
Interaction between compression shocks and vertical flows N89-25132
Dissipation of vortex power in longitudinal flow on wings N89-25133
Vortex structures in the wake of transonic flow about profiles N89-25134
Flow about trailing edges in unsteady flow N89-25135
Unsteady flow on profiles in a liquid Ludwig tunnel N89-25136
Effect of winglets on loading mechanics and wing assembly reactions N89-25137
Damping of wing tip vortex systems by the modification of the wing tips N89-25138
Mechanical reaction of wings moving through a vortex region N89-25139
Structural loading and noise disturbance of helicopters N89-25140
Flight-mechanical investigations of the lateral motion of configurations with winglets N89-25141
Processing of fiber-reinforced materials by injection molding
[ETN-89-94668] N89-25298
A procedure for the numerical description of the moisture dependent material behavior
[ETN-89-94669] N89-25299
TECHNISCHE HOGESCHOOL, DELFT (NETHERLANDS).
Polynomial method of approximate centers for linear programming
[PB89-146161] N89-25584
TECHNISCHE UNIV., BERLIN (GERMANY, F.R.).
Flight performance model for a geostationary transportation system
[ILR-MITT-206] N89-25259
Size optimization and production strategy of lunar transport systems
[ILR-MITT-218] N89-25260
Reduction of aircraft noise in civil air transport by optimization of flight tracks and takeoff and approach procedures
[ILR-MITT-200] N89-25676
TECHNISCHE UNIV., DELFT (NETHERLANDS).
A variationally optimized vortex tracing algorithm for three-dimensional flows around solid bodies
[ETN-89-94301] N89-25423
A contour-oriented approach to digital shape analysis
[ISBN-9-09-002004-7] N89-25604
Segmentation of noisy images
[ETN-89-94299] N89-25605
TECHNISCHE UNIV., EINDHOVEN (NETHERLANDS).
Relation of the adhesion of plasma sprayed coatings to the process parameters: Size, velocity and heat content of the spray particles
[ETN-89-94296] N89-25326
Model building for an ingot heating process: Physical modeling approach and identification approach
[EUT-88-E-196] N89-25331
An extremum hunting method using pseudo-random binary signal
[EUT-88-E-198] N89-25359
Reduction of transhorizon radio interference in satellite earth stations
[ETN-89-94297] N89-25374
The impact of telecommunication on rural areas in developing countries
[EUT-87-E-185] N89-25377
A multifrequency antenna system for propagation experiments with the Olympus satellite
[EUT-88-E-192] N89-25378
On system identification using pulse-frequency modulated signals
[EUT-88-E-195] N89-25379
Frequency spectra for admittances and voltage transfers measured on a three-phased power transformer
[EUT-87-E-181] N89-25400

Analog and digital simulation of line-energizing overvoltages and comparison with measurements in a 400 kV network
[EUT-88-E-193] N89-25401
Martinus van Marum: A Dutch scientist in a revolutionary time
[EUT-88-E-194] N89-25402
Enhancement of heat transfer by corona wind
[EUT-87-E-184] N89-25500
The full decomposition of sequential machines with the state and output behavior realization
[EUT-88-E-188] N89-25582
The full decomposition of sequential machines with the output behavior realization
[EUT-88-E-199] N89-25583
Design and implementation of a module library to support the structural synthesis
[EUT-88-E-187] N89-25616
ALWAYS: A system for wafer yield analysis
[EUT-88-E-189] N89-25617
Black-box identification of MIMO transfer functions: Asymptotic properties of prediction error models
[EUT-87-E-182] N89-25642
On the bounds of the modeling errors of black-box MIMO transfer function estimates
[EUT-87-E-183] N89-25643
A new method for dynamic hunting extremum control, based on comparison of measured and estimated value
[EUT-88-E-197] N89-25644
Least squares parameter estimation in a dynamic model from noisy observations
[ETN-89-94295] N89-25657
The influence of contact surface microstructure on vacuum arc stability and arc voltage
[EUT-87-E-186] N89-25672
Local-frequency description of optical signals and systems
[EUT-88-E-191] N89-25698

TENNESSEE UNIV., KNOXVILLE.
Seconday ion mass spectrometry of aromatic compounds in acidic mixtures
[DE89-010611] N89-25305
Generalized consistency checking of multivariable redundant measurements and common-mode failure detection
[DE89-010053] N89-25474

TEXAS A&M UNIV., COLLEGE STATION.
Water in the Martian regolith N89-25791

TEXAS UNIV., ARLINGTON.
A novel implementation of method of optimality criterion in synthesizing spacecraft structures with natural frequency constraints N89-25225
Microwave scattering models and basic experiments
[NASA-CR-185393] N89-25364

TEXTRON BELL HELICOPTER, FORT WORTH, TX.
An analytical and experimental investigation of edge delamination in laminates subjected to tension, bending, and torsion
[NASA-CR-181824] N89-25296

TEXTRON LYCOMING, STRATFORD, CT.
Procedures for shape optimization of gas turbine disks N89-25207

TOKYO UNIV. (JAPAN).
Sound velocity distribution in the Sun inferred from asymptotic inversion of p-mode spectra N89-25900
An inversion method based on the Moore-Penrose generalized inverse matrix N89-25910

TROMSOE UNIV. (NORWAY).
End points of stellar evolution investigated by seismology on white dwarf stars N89-25934

TRW, INC., REDONDO BEACH, CA.
High-average-power millimeter-wave FEL (Free-Electron Laser) for plasma heating using the ETA-2 accelerator
[DE89-012294] N89-25711

TUEBINGEN UNIV. (GERMANY, F.R.).
Particle simulation for accretion sheets in narrow double stars N89-25729

TUSKEGEE INST., AL.
Parallel solution of a 2-D phase change problem on a hypercube
[DE89-009619] N89-25586

U

UNION FOR EXPERIMENTING COLL. AND UNIV., YELLOW SPRINGS, OH.
A theoretical framework and an instructional model for educating end-users of online bibliographic information retrieval systems: A research monograph N89-25769

UNIVERSITEIT TWENTE, ENSCHEDE (NETHERLANDS).
A theory of describing performability models
[MEMO-INF-88-26] N89-25476
TUMULT: The Twente University Multiprocessor
[MEMO-INF-88-28] N89-25581
On the semantics of nonatomic actions
[MEMO-INF-88-13] N89-25610
Controlled bidirectional grammars
[MEMO-INF-88-16] N89-25611
An exercise in transformational programming: Back tracking and Branch-and-Bound
[MEMO-INF-88-22] N89-25612
A case study relating the Yourdon methodology to other design methods
[MEMO-INF-88-24] N89-25613
The generalized grid file: An access structure for CIM applications
[MEMO-INF-88-25] N89-25614
Constraint specification in BSDM
[MEMO-INF-88-32] N89-25615
Integrated Services Digital Network: Overview and architectural concepts
[MEMO-INF-88-42] N89-25634
Explanation in knowledge-based systems
[MEMO-INF-88-17] N89-25640
The use of first principles in diagnosing complex technical devices
[MEMO-INF-88-40] N89-25641

UTRECHT OBSERVATORY (NETHERLANDS).
The granulation sensitivity of helioseismology lines N89-25862

V

VALENCIA UNIV. (SPAIN).
Pair production of helicity-flipped neutrinos in supernovae
[NASA-CR-185466] N89-25789

VANDERBILT UNIV., NASHVILLE, TN.
Using a segregation measure for the workload characterization of multi-class queuing networks
[DE89-007841] N89-25623

VIRGINIA POLYTECHNIC INST. AND STATE UNIV., BLACKSBURG.
Techniques for compressible flow calculations on multizone grids N89-25120
A penalty approach for nonlinear optimization with discrete design variables N89-25217
Optical fiber sensors and signal processing for intelligent structure monitoring
[NASA-CR-185395] N89-25691

VIRGINIA UNIV., CHARLOTTESVILLE.
A global time reference for hypercube multicomputers
[DE89-010924] N89-25579
The ADAMS database language
[DE89-010925] N89-25601
Reliability mechanisms for ADAMS (Advanced Data Management System)
[DE89-010911] N89-25768

W

WARSAW UNIV. (POLAND).
Using oscillation data to probe the internal rotation and magnetism of the Sun N89-25863

WASHINGTON STATE UNIV., PULLMAN.
Study of the stability of compressible Couette flow N89-25410
Geologic spatial analysis program users guide for digital elevation model analysis procedures for detection of crustal fracture planes
[DE89-010880] N89-25542

WEST VIRGINIA UNIV., MORGANTOWN.
An inductively coupled plasma spectrometer for on-line, real-time process gas analysis
[DE89-010610] N89-25442

WESTINGHOUSE IDAHO NUCLEAR CO., INC., IDAHO FALLS.
Digital optical conversion module
[DE89-011441] N89-25367

WISCONSIN UNIV., MADISON.
The q measurements during sawtooth oscillations in a low q tokamak
[DE89-010563] N89-25705
Anomalous particle pinch for collisionless plasma
[DE89-011018] N89-25706

WORCESTER POLYTECHNIC INST., MA.
Treatment of body forces in boundary element design sensitivity analysis N89-25187

WORLD RADIATION CENTER, DAVOS (SWITZERLAND).
IPHIR: The helioseismology experiment on the PHOBOS mission N89-25881
VIRGO: The solar monitor experiment on SOHO N89-25884

WRIGHT STATE UNIV., DAYTON, OH.
Analysis of the transient compressible vapor flow in heat pipe
[NASA-CR-185119] N89-25422
A kinematic study of the MERLIN 6500 robot and the Utah/MIT dexterous hand and a simulation of their combined behavior
[AD-A203907] N89-25458

Y

YALE UNIV., NEW HAVEN, CT.
Is the Sun really a rigid rotator N89-25835

YALE UNIV. OBSERVATORY, NEW HAVEN, CT.
The mass-luminosity relationship for solar-type stars N89-25936

Typical Contract Number Index Listing

Listings in this index are arranged alphanumerically by contract number. Under each contract number the NASA accession numbers denoting documents that have been produced as a result of research done under that contract are arranged in ascending order. The NASA accession number denotes the number by which the citation is identified.

AF PROJ. 2312 ..... N89-25458
AF-AFOSR-0059-88 ..... N89-25218
AF-AFOSR-0077-87 ..... N89-25858
AF-AFOSR-0116-86 ..... N89-25226
BCRS-PROJ.CO-2.3 ..... N89-25497
BCRS-PROJ.TO-1.7 ..... N89-25552
BMFT-KF-3012/4 ..... N89-25544
BMFT-NT-2706-C9 ..... N89-25757
BMFT-NT-2718-E/4 ..... N89-25399
BMFT-01-QV-AA/WF/WRK-0275/4-13 ..... N89-25357
BMFT-03-E-8288-A N89-25518
BMFT-13-N-5357/3 ..... N89-25457
BMUNR-FB-88-105-05-501 ..... N89-25676
CAICYT-PR84-0905 ..... N89-25824
N89-25846
N89-25849
N89-25869
N89-25880
CS-28-88 ..... N89-25838
DA PROJ. 1L1-61102-AH-45 ..... N89-25409
DA PROJ. 351-62772-A-874 ..... N89-25564
DAMD17-86-C-6157 ..... N89-25564
DE-AC02-76CH-00016 ..... N89-25452
N89-25754
N89-25787
DE-AC02-76CH-03000 ..... N89-25251
N89-25418
N89-25578
N89-25580
N89-25631
N89-25655
N89-25667
N89-25688
N89-25693
N89-25785
DE-AC02-76ER-01198 ..... N89-25346
N89-25747
DE-AC02-83CH-10093 ..... N89-25509
N89-25510
N89-25514
N89-25516
N89-25517
DE-AC02-86NE-37959 ..... N89-25474
DE-AC03-76SF-00098 ..... N89-25307
N89-25308
N89-25322
N89-25341
N89-25343
N89-25369
N89-25389
N89-25391
N89-25452
N89-25455
N89-25679
N89-25682
N89-25743
N89-25755
N89-25761
N89-25781
N89-25784
DE-AC03-85SF-15928 ..... N89-25264
DE-AC03-87ER-53254 ..... N89-25710
DE-AC03-89ER-51114 ..... N89-25707
DE-AC04-76DP-00789 ..... N89-25293
N89-25309
N89-25311
N89-25314
N89-25323
N89-25324
N89-25335
N89-25336
N89-25338
N89-25342
N89-25345
N89-25352
N89-25355
N89-25370
N89-25371
N89-25384
N89-25387
N89-25396
N89-25397
N89-25420
N89-25438
N89-25439
N89-25440
N89-25441
N89-25456
N89-25478
N89-25481
N89-25482
N89-25483
N89-25487
N89-25576
N89-25577
N89-25590
N89-25592
N89-25622
N89-25692
N89-25695
N89-25704
N89-25744
N89-25748
DE-AC04-86AL-33183 ..... N89-25415
DE-AC05-76OR-00033 ..... N89-25305
N89-25442
DE-AC05-84ER-40150 ..... N89-25685
DE-AC05-84OR-21400 ..... N89-25289
N89-25316
N89-25333
N89-25337
N89-25339
N89-25356
N89-25366
N89-25368
N89-25386
N89-25395
N89-25451
N89-25460
N89-25461
N89-25466
N89-25467
N89-25471
N89-25522
N89-25527
N89-25551
N89-25570
N89-25571
N89-25572
N89-25586
N89-25589
N89-25593
N89-25594
N89-25602
N89-25623
N89-25636
N89-25637
N89-25639
N89-25645
N89-25687
N89-25702
N89-25708
N89-25709
N89-25712
N89-25713
N89-25749
N89-25765
N89-25774
DE-AC05-84OT-21400 ..... N89-25630
DE-AC06-76RL-01830 ..... N89-25317
N89-25319
N89-25320
N89-25690
N89-25694
DE-AC06-86NE-37963 ..... N89-25321
DE-AC07-76ID-01570 ..... N89-25257
N89-25392
N89-25465
N89-25489
N89-25512
N89-25513
N89-25696
N89-25766
DE-AC07-84ID-12435 ..... N89-25367
DE-AC07-84NV-10366 ..... N89-25388
DE-AC08-88NV-10617 ..... N89-25445
DE-AC09-76SR-00001 ..... N89-25462
N89-25473
DE-AC22-83PC-61253 ..... N89-25524
DE-AI08-78ET-44802 ..... N89-25525
DE-FC03-85DP-40200 ..... N89-25750
DE-FG01-87CE-15323 ..... N89-25472
DE-FG02-84ER-13214 ..... N89-25560
DE-FG02-84ER-13261 ..... N89-25562
DE-FG02-85ER-13455 ..... N89-25742
DE-FG02-86ER-13478 ..... N89-25407
DE-FG02-86ER-53227 ..... N89-25705
N89-25706
DE-FG02-87ER-13743 ..... N89-25559
DE-FG02-87ER-45297 ..... N89-25733
DE-FG02-87ER-45320 ..... N89-25751
DE-FG02-87ER-45321 ..... N89-25292
DE-FG02-87ER-60570 ..... N89-25526
DE-FG02-88ER-13896 ..... N89-25417
DE-FG02-88ER-13913 ..... N89-25408
N89-25416
DE-FG05-84ER-45063 ..... N89-25340
DE-FG05-86ER-45276 ..... N89-25752
DE-FG05-86ER-45280 ..... N89-25753
DE-FG05-86ER-52139 ..... N89-25468
N89-25469
DE-FG05-87ER-60501 ..... N89-25306
DE-FG05-88ER-25063 ..... N89-25579
N89-25601
N89-25768
DE-FG06-87ER-13796 ..... N89-25542
DEA-PROJ-IC-EEL46018 ..... N89-25617
DFG-KN-152/3 ..... N89-25821
DI-14-12-001-30301 ..... N89-25555
DI-14-12-0001-30228 ..... N89-25555
FNSRS-1-467-0-86 ..... N89-25584
F04701-88-C-0080 ..... N89-25262
F33615-85-C-2590 ..... N89-25385
F33615-88-C-2820 ..... N89-25422
F49620-87-K-0003 ..... N89-25194
GRI-5084-242-1116 ..... N89-25411
GRI-5086-260-1293 ..... N89-25412
GRI-5086-260-1321 ..... N89-25505
GRI-5087-223-1618 ..... N89-25413
IRSIA-83343 ..... N89-25852
JPL-957721 ..... N89-25579
N89-25601
NAGW-13 ..... N89-25831
N89-25832
N89-25838
NAGW-40 ..... N89-25796
NAGW-472 ..... N89-25838
N89-25877
NAGW-522 ..... N89-25858
N89-25925
NAGW-638 ..... N89-25803
NAGW-742 ..... N89-25803
NAGW-777 ..... N89-25835
NAGW-778 ..... N89-25835
NAGW-827 ..... N89-25541
NAGW-1303 ..... N89-25820
NAGW-1340 ..... N89-25663

	N89-25678
	N89-25680
	N89-25688
	N89-25788
	N89-25789
NAGW-1583	N89-25777
NAG1-613	N89-25595
NAG1-650	N89-25620
NAG1-895	N89-25691
NAG1-915	N89-25258
NAG2-195	N89-25568
NAG2-471	N89-25233
	N89-25235
NAG2-513	N89-25772
NAG3-599	N89-25300
NAG3-854	N89-25432
NAG5-486	N89-25364
NAG5-538	N89-25534
NAG5-922	N89-25268
NAG5-1053	N89-25444
NASA ORDER C-80001-G	N89-25353
NASW-3482	N89-25776
NASW-3886	N89-25286
NASW-4066	N89-25790
NASW-4292	N89-25556
NAS1-8000	N89-25193
NAS1-16521	N89-25674
NAS1-17022	N89-25805
NAS1-17497	N89-25480
NAS1-17536	N89-25484
NAS1-18107	N89-25585
NAS1-18199	N89-25296
NAS1-18605	N89-25123
	N89-25665
	N89-25671
NAS3-23941	N89-25165
NAS3-24105	N89-25675
NAS3-25266	N89-25403
NAS5-26813	N89-25875
NAS5-28096	N89-25492
NAS5-30168	N89-25763
NAS7-918	N89-25380
	N89-25381
	N89-25519
	N89-25618
	N89-25619
NAS7-950	N89-25746
NAS8-30300	N89-25312
NAS8-30490	N89-25284
NAS8-32805	N89-25875
NAS8-33807	N89-25276
NAS8-36179	N89-25431
NAS8-36199	N89-25261
NAS8-36719	N89-25463
	N89-25464
NAS8-37282	N89-25270
NCC2-175	N89-25122
NCC2-349	N89-25573
NCC2-387	N89-25566
	N89-25600
	N89-25628
	N89-25638
	N89-25653
	N89-25654
	N89-25773
NCC2-398	N89-25598
	N89-25599
NCC2-501	N89-25561
NGR-05-020-559	N89-25894
NGT-06-002-802	N89-25218
NGT-33-183-805	N89-25404
NGT-47-003-029	N89-25627
NSF AST-86-02410	N89-25877
NSF ATM-86-04400	N89-25833
NSF ATM-86-04632	N89-25820
	N89-25840
NSF ATM-86-11476	N89-25793
NSF ATM-86-18263	N89-25894
NSF ATM-87-05084	N89-25945
NSF DCR-84-12314	N89-25654
NSF DMC-85-14721	N89-25214
NSF DME-87-06902	N89-25216
NSF DPP-78-22267	N89-25868
NSF DPP-81-19627	N89-25868
NSF DPP-87-15791	N89-25868
NSF ECS-85-17362	N89-25226
NSF INT-84-00213	N89-25831
	N89-25832
	N89-25838
NSF MSM-83-19871	N89-25181
NSF MSM-87-0742	N89-25187
NSF PHY-85-15857	N89-25761
NSF PHY-86-00377	N89-25777
NSG-7092	N89-25945
NSG-7397	N89-25796
NSG-7405	N89-25796
NSG-7500	N89-25435
N00014-86-F-0049	N89-25817
N00014-86-K-0056	N89-25877
N00014-86-K-0085	N89-25894
N00014-86-K-0295	N89-25226
N00014-86-K-0610	N89-25653
N00140-83-C-8899	N89-25238
PHS-CDC-200-86-2929	N89-25669
STW-EEL-44-0757	N89-25378
W-31-109-ENG-38	N89-25390
	N89-25394
	N89-25406
	N89-25470
	N89-25508
	N89-25511
	N89-25588
	N89-25632
	N89-25703
	N89-25756
W-7405-ENG-36	N89-25255
	N89-25288
	N89-25304
	N89-25347
	N89-25351
	N89-25405
	N89-25447
	N89-25488
	N89-25569
	N89-25591
	N89-25626
	N89-25745
	N89-25786
W-7405-ENG-48	N89-25253
	N89-25291
	N89-25295
	N89-25310
	N89-25315
	N89-25344
	N89-25349
	N89-25362
	N89-25372
	N89-25373
	N89-25393
	N89-25398
	N89-25419
	N89-25421
	N89-25453
	N89-25454
	N89-25475
	N89-25521
	N89-25528
	N89-25529
	N89-25530
	N89-25531
	N89-25532
	N89-25549
	N89-25587
	N89-25603
	N89-25621
	N89-25624
	N89-25625
	N89-25707
	N89-25711
	N89-25741
142-20-37	N89-25494
	N89-25496
142-70-10	N89-25274
161-20-25	N89-25539
176-10-05-70	N89-25947
199-21-12-07	N89-25558
314-40-22-70	N89-25380
314-40-22-70-08	N89-25381
474-42-10	N89-25403
474-46-10	N89-25267
	N89-25273
	N89-25275
474-52-10	N89-25269
	N89-25283
505-60	N89-25233
	N89-25235
505-60-01-01	N89-25597
505-60-01-02	N89-25118
505-61-51	N89-25122
505-62-21	N89-25404
	N89-25409
	N89-25670
505-63-01	N89-25294
505-63-01-05	N89-25296
505-63-11	N89-25290
	N89-25490
505-63-11-01	N89-25354
505-63-21-04	N89-25232
	N89-25239
505-63-51-01	N89-25480
505-63-51-06	N89-25673
505-66-11	N89-25485
505-66-21-01	N89-25627
505-69-01-01	N89-25117
505-90-21-01	N89-25123
	N89-25585
	N89-25665
	N89-25671
506-40-41-02	N89-25443
506-41-11	N89-25277
506-41-41	N89-25506
506-42-31	N89-25281
506-42-51	N89-25254
506-43-21-04	N89-25332
506-43-21-05	N89-25433
506-43-41-01	N89-25146
	N89-25173
	N89-25201
510-01-0A	N89-25300
535-03-01	N89-25119
	N89-25675
535-03-11-03	N89-25674
535-05-01	N89-25238
583-01-11-05	N89-25124
585-02-31-01	N89-25484
586-01-11	N89-25272
	N89-25280
	N89-25282
586-01-21	N89-25422
650-60-23	N89-25365
673-41-10-70	N89-25540
674-22-05	N89-25353
674-26-05	N89-25285
889-20-41-17-62	N89-25619
946-02-20	N89-25271
992-21-01	N89-25479

Typical Report Number Index Listing

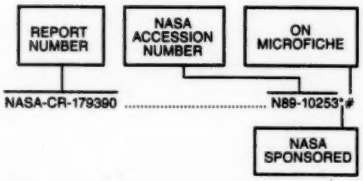

Listings in this index are arranged alphanumerically by report number. The NASA accession number denotes the number by which the citation is identified. An asterisk (*) indicates that the itemis a NASA report. A pound sign (#) indicates that the item is available on microfiche.

A-88222 ..... N89-25558* #
A-89026 ..... N89-25496* #
A-89027 ..... N89-25494* #
A-89091 ..... N89-25652* #
A-89124 ..... N89-25479* #
A-89139 ..... N89-25651* #
A-89176 ..... N89-25116* #

AAC-TN-1153 ..... N89-25484* #

AAMRL-TR-88-059 ..... N89-25458 #

AD-A194597 ..... N89-25241 #
AD-A200917 ..... N89-25113 #
AD-A203907 ..... N89-25458 #
AD-A205308 ..... N89-25649 #
AD-A205373 ..... N89-25409* #
AD-A206064 ..... N89-25385 #
AD-A206506 ..... N89-25564 #
AD-A206522 ..... N89-25262 #

AD-D013963 ..... N89-25737 #
AD-D013981 ..... N89-25234

AFWAL-TR-88-2131 ..... N89-25385 #

AIAA-89-1690 ..... N89-25404* #
AIAA-89-2583 ..... N89-25121* #
AIAA-89-2723 ..... N89-25281* #
AIAA-89-2805 ..... N89-25119* #
AIAA-89-2837 ..... N89-25283* #
AIAA-89-2901 ..... N89-25238* #

ANL-89/2 ..... N89-25588 #

ANL/FPP/TM-236 ..... N89-25703 #

ANL/MCS/TM-131 ..... N89-25632 #

APP-88-5 ..... N89-25241 #

ATLSS-89-08 ..... N89-25472 #

AVSCOM-TR-88-C-008 ..... N89-25409* #
AVSCOM-TR-89-C-004 ..... N89-25238* #

BBN-6938 ..... N89-25674* #

BCRS-88-11 ..... N89-25552 #
BCRS-88-15 ..... N89-25497 #

BHTI-699-099-265 ..... N89-25296* #

BNL-42043 ..... N89-25754 #
BNL-42605 ..... N89-25787 #

CAA-3/88 ..... N89-25143

CEBAF-PR-89-005 ..... N89-25685 #

CESAR-89/14 ..... N89-25570 #

CONF-880117-10 ..... N89-25768 #
CONF-880612-1 ..... N89-25755 #
CONF-880683-4 ..... N89-25462 #
CONF-881155-71 ..... N89-25316 #
CONF-881159-1 ..... N89-25527 #
CONF-881202-1 ..... N89-25406 #
CONF-881281 ..... N89-25572 #
CONF-881287-1 ..... N89-25295 #
CONF-890113-1 ..... N89-25747 #
CONF-890130-5 ..... N89-25289 #
CONF-890143-2 ..... N89-25308 #
CONF-890190-1 ..... N89-25341 #
CONF-890270-13 ..... N89-25754 #
CONF-890302-20 ..... N89-25707 #
CONF-890306-2 ..... N89-25347 #
CONF-890310-5 ..... N89-25340 #
CONF-890334-1 ..... N89-25473 #
CONF-890335-74 ..... N89-25251 #
CONF-890335-86 ..... N89-25418 #
CONF-890335-87 ..... N89-25655 #
CONF-890335-100 ..... N89-25369 #
CONF-890335-124 ..... N89-25455 #
CONF-890335-137 ..... N89-25711 #
CONF-890352-5 ..... N89-25513 #
CONF-890352-7 ..... N89-25512 #
CONF-890372-6 ..... N89-25594 #
CONF-890372-7 ..... N89-25593 #
CONF-890372-8 ..... N89-25621 #
CONF-890372-9 ..... N89-25589 #
CONF-890372-11 ..... N89-25631 #
CONF-890385-2 ..... N89-25526 #
CONF-890393-2 ..... N89-25587 #
CONF-890403-15 ..... N89-25709 #
CONF-890403-18 ..... N89-25713 #
CONF-890406-16 ..... N89-25456 #
CONF-890421-3 ..... N89-25692 #
CONF-890421-5 ..... N89-25744 #
CONF-890423-9 ..... N89-25453 #
CONF-890426-5 ..... N89-25319 #
CONF-890426-6 ..... N89-25694 #
CONF-890426-8 ..... N89-25749 #
CONF-890426-10 ..... N89-25471 #
CONF-890436-10 ..... N89-25510 #
CONF-890437-11 ..... N89-25317 #
CONF-890437-12 ..... N89-25320 #
CONF-890468-6 ..... N89-25339 #
CONF-890482-2 ..... N89-25473 #
CONF-890522-3 ..... N89-25438 #
CONF-890522-4 ..... N89-25460 #
CONF-890536-2 ..... N89-25591 #
CONF-890537-1 ..... N89-25577 #
CONF-890538-2 ..... N89-25592 #
CONF-890555-3 ..... N89-25386 #
CONF-890555-8 ..... N89-25571 #
CONF-890555-11 ..... N89-25474 #
CONF-890555-12 ..... N89-25637 #
CONF-890570-1 ..... N89-25569 #
CONF-890571-1 ..... N89-25461 #
CONF-890589-1 ..... N89-25439 #
CONF-890592-1 ..... N89-25355 #
CONF-890592-3 ..... N89-25440 #
CONF-890592-4 ..... N89-25481 #
CONF-890592-5 ..... N89-25482 #
CONF-890630-1 ..... N89-25470 #
CONF-890631-2 ..... N89-25324 #
CONF-890654-2 ..... N89-25603 #
CONF-890657-2 ..... N89-25765 #
CONF-890660-2 ..... N89-25372 #
CONF-890660-3 ..... N89-25371 #
CONF-890660-4 ..... N89-25370 #
CONF-890661-1 ..... N89-25253 #
CONF-890661-2 ..... N89-25351 #
CONF-890661-3 ..... N89-25419 #
CONF-890661-8 ..... N89-25309 #
CONF-890676-1 ..... N89-25356 #
CONF-890677-1 ..... N89-25420 #
CONF-890678-1 ..... N89-25396 #
CONF-890691-1 ..... N89-25475 #
CONF-890691-2 ..... N89-25766 #
CONF-890692-2 ..... N89-25531 #
CONF-890692-3 ..... N89-25532 #
CONF-890692-4 ..... N89-25530 #
CONF-890694-6 ..... N89-25695 #
CONF-890695-1 ..... N89-25529 #
CONF-8708269 ..... N89-25779 #
CONF-8708323-2 ..... N89-25667 #
CONF-8803200 ..... N89-25450 #
CONF-8803204 ..... N89-25522 #
CONF-8805132-14 ..... N89-25362 #
CONF-8805132-15 ..... N89-25393 #
CONF-8805243-1 ..... N89-25688* #
CONF-8807166-1 ..... N89-25761 #
CONF-8808108-6 ..... N89-25337 #
CONF-8808219-1 ..... N89-25307 #
CONF-8809194 ..... N89-25414 #
CONF-8809247-9 ..... N89-25578 #
CONF-8809321-1 ..... N89-25679 #
CONF-8809322-1 ..... N89-25311 #
CONF-8809335-1 ..... N89-25416 #
CONF-8810126-VOL-2 ..... N89-25452 #
CONF-8810135-3 ..... N89-25398 #
CONF-8810195-8 ..... N89-25333 #
CONF-8810257-2 ..... N89-25781 #
CONF-8810296-5 ..... N89-25690 #
CONF-8811175-3 ..... N89-25785 #
CONF-8901118-1 ..... N89-25693 #
CONF-8901118-2 ..... N89-25580 #
CONF-8901119-1 ..... N89-25417 #
CONF-8901121-1 ..... N89-25784 #
CONF-8902100-1 ..... N89-25748 #
CONF-8903104-1 ..... N89-25549 #
CONF-8903109-2 ..... N89-25343 #
CONF-8903109-3 ..... N89-25322 #
CONF-8903121-1 ..... N89-25786 #
CONF-8904116-2 ..... N89-25441 #
CONF-8904121-1 ..... N89-25405 #
CONF-8904123-1 ..... N89-25741 #
CONF-8904180-1 ..... N89-25586 #
CONF-8904182-2 ..... N89-25745 #
CONF-8904190-1 ..... N89-25387 #
CONF-8904196-1 ..... N89-25390 #
CONF-8904196-2 ..... N89-25511 #
CONF-8905100-1 ..... N89-25623 #
CONF-8905101-1 ..... N89-25624 #
CONF-8905102-1 ..... N89-25314 #
CONF-8905104-1 ..... N89-25291 #
CONF-8905104-2 ..... N89-25487 #
CONF-8905105-1 ..... N89-25304 #
CONF-8905107-1 ..... N89-25451 #
CONF-8905107-2 ..... N89-25336 #
CONF-8905107-3 ..... N89-25696 #
CONF-8905109-1 ..... N89-25570 #
CONF-8905109-2 ..... N89-25636 #
CONF-8905112-1 ..... N89-25483 #
CONF-8905113-1 ..... N89-25335 #
CONF-8905114-1 ..... N89-25625 #
CONF-8905117-1 ..... N89-25338 #
CONF-8905118-1 ..... N89-25315 #
CONF-8905118-4 ..... N89-25465 #
CONF-8905118-5 ..... N89-25466 #
CONF-8905118-6 ..... N89-25468 #
CONF-8905120-3 ..... N89-25366 #
CONF-8905120-6 ..... N89-25708 #
CONF-8905120-7 ..... N89-25368 #
CONF-8905120-10 ..... N89-25712 #
CONF-8905130-1 ..... N89-25639* #
CONF-8905133-1 ..... N89-25756 #
CONF-8905134-1 ..... N89-25352 #
CONF-8906111-2 ..... N89-25421 #
CONF-8906113-2 ..... N89-25774 #
CONF-8906114-1 ..... N89-25489 #
CONF-8906115-1 ..... N89-25397 #

CSCC-DOC-G-13 ..... N89-25597* #

CSG-103 ..... N89-25595* #

CSSA-ASTRO-89-08 ..... N89-25945* #

DE88-704637 ..... N89-25536 #
DE88-705970 ..... N89-25302 #
DE88-705973 ..... N89-25668 #
DE88-705975 ..... N89-25734 #
DE88-705991 ..... N89-25758 #
DE88-705998 ..... N89-25759 #
DE88-706002 ..... N89-25535 #

REPORT

DE88-706003 ..... N89-25449 #
DE88-706011 ..... N89-25434 #
DE88-706012 ..... N89-25303 #
DE88-706031 ..... N89-25646 #
DE88-706032 ..... N89-25647 #
DE88-706038 ..... N89-25666 #
DE88-706045 ..... N89-25648 #
DE88-706050 ..... N89-25735 #
DE88-706051 ..... N89-25736 #
DE88-706057 ..... N89-25779 #
DE88-706155 ..... N89-25738 #
DE88-706205 ..... N89-25739 #
DE88-706213 ..... N89-25361 #
DE88-706221 ..... N89-25313 #
DE88-706249 ..... N89-25760 #
DE88-706256 ..... N89-25436 #
DE88-706258 ..... N89-25650 #
DE88-706259 ..... N89-25740 #
DE88-706260 ..... N89-25437 #
DE88-706295 ..... N89-25681 #
DE88-706302 ..... N89-25350 #
DE88-706335 ..... N89-25446 #
DE88-757331 ..... N89-25459 #
DE89-000614 ..... N89-25470 #
DE89-000851 ..... N89-25516 #
DE89-000857 ..... N89-25517 #
DE89-000865 ..... N89-25509 #
DE89-000877 ..... N89-25510 #
DE89-001679 ..... N89-25577 #
DE89-001821 ..... N89-25438 #
DE89-003119 ..... N89-25460 #
DE89-003607 ..... N89-25591 #
DE89-003610 ..... N89-25592 #
DE89-005209 ..... N89-25370 #
DE89-005337 ..... N89-25461 #
DE89-005346 ..... N89-25371 #
DE89-005348 ..... N89-25253 #
DE89-005350 ..... N89-25372 #
DE89-005459 ..... N89-25351 #
DE89-005464 ..... N89-25569 #
DE89-005774 ..... N89-25439 #
DE89-005917 ..... N89-25396 #
DE89-006158 ..... N89-25419 #
DE89-006328 ..... N89-25420 #
DE89-006427 ..... N89-25356 #
DE89-006720 ..... N89-25414 #
DE89-006739 ..... N89-25603 #
DE89-007084 ..... N89-25355 #
DE89-007655 ..... N89-25440 #
DE89-007841 ..... N89-25623 #
DE89-007977 ..... N89-25481 #
DE89-007978 ..... N89-25482 #
DE89-007981 ..... N89-25405 #
DE89-007994 ..... N89-25304 #
DE89-008023 ..... N89-25624 #
DE89-008045 ..... N89-25314 #
DE89-008121 ..... N89-25475 #
DE89-008186 ..... N89-25524 #
DE89-008235 ..... N89-25451 #
DE89-008279 ..... N89-25335 #
DE89-008610 ..... N89-25741 #
DE89-008662 ..... N89-25291 #
DE89-008714 ..... N89-25336 #
DE89-008718 ..... N89-25636 #
DE89-008737 ..... N89-25386 #
DE89-008741 ..... N89-25765 #
DE89-008743 ..... N89-25570 #
DE89-008928 ..... N89-25337 #
DE89-009067 ..... N89-25483 #
DE89-009106 ..... N89-25452 #
DE89-009116 ..... N89-25733 #
DE89-009227 ..... N89-25679 #
DE89-009259 ..... N89-25625 #
DE89-009261 ..... N89-25529 #
DE89-009535 ..... N89-25311 #
DE89-009599 ..... N89-25383 #
DE89-009604 ..... N89-25508 #
DE89-009619 ..... N89-25586 #
DE89-009621 ..... N89-25571 #
DE89-009707 ..... N89-25373 #
DE89-009764 ..... N89-25348 #
DE89-009832 ..... N89-25387 #
DE89-009833 ..... N89-25324 #
DE89-009850 ..... N89-25406 #
DE89-009904 ..... N89-25549 #
DE89-009908 ..... N89-25521 #
DE89-009964 ..... N89-25530 #
DE89-009966 ..... N89-25315 #
DE89-010008 ..... N89-25388 #
DE89-010039 ..... N89-25338 #
DE89-010053 ..... N89-25474 #
DE89-010071 ..... N89-25686 #
DE89-010080 ..... N89-25507 #
DE89-010110 ..... N89-25389 #
DE89-010120 ..... N89-25264 #
DE89-010170 ..... N89-25572 #
DE89-010185 ..... N89-25551 #
DE89-010191 ..... N89-25645 #
DE89-010192 ..... N89-25702 #
DE89-010214 ..... N89-25288 #
DE89-010223 ..... N89-25621 #
DE89-010226 ..... N89-25441 #
DE89-010238 ..... N89-25531 #
DE89-010239 ..... N89-25532 #
DE89-010240 ..... N89-25362 #
DE89-010241 ..... N89-25421 #
DE89-010243 ..... N89-25587 #
DE89-010257 ..... N89-25333 #
DE89-010260 ..... N89-25593 #
DE89-010261 ..... N89-25594 #
DE89-010272 ..... N89-25703 #
DE89-010279 ..... N89-25349 #
DE89-010282 ..... N89-25588 #
DE89-010297 ..... N89-25522 #
DE89-010299 ..... N89-25687 #
DE89-010306 ..... N89-25478 #
DE89-010318 ..... N89-25639* #
DE89-010320 ..... N89-25589 #
DE89-010321 ..... N89-25339 #
DE89-010329 ..... N89-25456 #
DE89-010362 ..... N89-25637 #
DE89-010371 ..... N89-25316 #
DE89-010376 ..... N89-25289 #
DE89-010384 ..... N89-25755 #
DE89-010385 ..... N89-25781 #
DE89-010420 ..... N89-25340 #
DE89-010433 ..... N89-25308 #
DE89-010441 ..... N89-25341 #
DE89-010453 ..... N89-25482 #
DE89-010465 ..... N89-25473 #
DE89-010484 ..... N89-25408 #
DE89-010507 ..... N89-25688* #
DE89-010510 ..... N89-25578 #
DE89-010517 ..... N89-25590 #
DE89-010519 ..... N89-25622 #
DE89-010523 ..... N89-25384 #
DE89-010525 ..... N89-25576 #
DE89-010529 ..... N89-25342 #
DE89-010557 ..... N89-25704 #
DE89-010563 ..... N89-25705 #
DE89-010587 ..... N89-25343 #
DE89-010596 ..... N89-25292 #
DE89-010599 ..... N89-25742 #
DE89-010610 ..... N89-25442 #
DE89-010611 ..... N89-25305 #
DE89-010616 ..... N89-25306 #
DE89-010651 ..... N89-25415 #
DE89-010655 ..... N89-25416 #
DE89-010664 ..... N89-25417 #
DE89-010673 ..... N89-25784 #
DE89-010679 ..... N89-25307 #
DE89-010681 ..... N89-25743 #
DE89-010698 ..... N89-25390 #
DE89-010699 ..... N89-25511 #
DE89-010740 ..... N89-25525 #
DE89-010759 ..... N89-25255 #
DE89-010769 ..... N89-25309 #
DE89-010798 ..... N89-25344 #
DE89-010859 ..... N89-25445 #
DE89-010862 ..... N89-25744 #
DE89-010863 ..... N89-25695 #
DE89-010880 ..... N89-25542 #
DE89-010911 ..... N89-25768 #
DE89-010924 ..... N89-25579 #
DE89-010925 ..... N89-25601 #
DE89-010930 ..... N89-25559 #
DE89-010931 ..... N89-25560 #
DE89-010937 ..... N89-25407 #
DE89-010964 ..... N89-25391 #
DE89-010965 ..... N89-25626 #
DE89-010966 ..... N89-25345 #
DE89-010967 ..... N89-25293 #
DE89-010975 ..... N89-25257* #
DE89-010976 ..... N89-25696 #
DE89-011005 ..... N89-25251 #
DE89-011018 ..... N89-25706 #
DE89-011021 ..... N89-25630 #
DE89-011066 ..... N89-25397 #
DE89-011067 ..... N89-25692 #
DE89-011068 ..... N89-25785 #
DE89-011082 ..... N89-25667 #
DE89-011085 ..... N89-25693 #
DE89-011088 ..... N89-25580 #
DE89-011090 ..... N89-25631 #
DE89-011115 ..... N89-25392 #
DE89-011126 ..... N89-25766 #
DE89-011133 ..... N89-25465 #
DE89-011134 ..... N89-25489 #
DE89-011139 ..... N89-25512 #
DE89-011144 ..... N89-25513 #
DE89-011165 ..... N89-25786 #
DE89-011177 ..... N89-25745 #
DE89-011205 ..... N89-25694 #
DE89-011206 ..... N89-25317 #
DE89-011207 ..... N89-25319 #
DE89-011214 ..... N89-25320 #
DE89-011219 ..... N89-25690 #
DE89-011220 ..... N89-25747 #
DE89-011224 ..... N89-25346 #
DE89-011441 ..... N89-25367 #
DE89-011446 ..... N89-25394 #
DE89-011451 ..... N89-25487 #
DE89-011466 ..... N89-25514 #
DE89-011483 ..... N89-25526 #
DE89-011503 ..... N89-25655 #
DE89-011504 ..... N89-25418 #
DE89-011525 ..... N89-25707 #
DE89-011533 ..... N89-25347 #
DE89-011535 ..... N89-25748 #
DE89-011567 ..... N89-25368 #
DE89-011568 ..... N89-25527 #
DE89-011569 ..... N89-25471 #
DE89-011571 ..... N89-25366 #
DE89-011608 ..... N89-25321 #
DE89-011611 ..... N89-25708 #
DE89-011612 ..... N89-25749 #
DE89-011615 ..... N89-25709 #
DE89-011631 ..... N89-25393 #
DE89-011771 ..... N89-25761 #
DE89-011792 ..... N89-25710 #
DE89-011805 ..... N89-25447 #
DE89-011807 ..... N89-25395 #
DE89-011816 ..... N89-25322 #
DE89-011824 ..... N89-25682 #
DE89-011825 ..... N89-25369 #
DE89-011827 ..... N89-25472 #
DE89-011847 ..... N89-25750 #
DE89-011878 ..... N89-25632 #
DE89-011892 ..... N89-25528 #
DE89-012249 ..... N89-25323 #
DE89-012292 ..... N89-25295 #
DE89-012294 ..... N89-25711 #
DE89-012299 ..... N89-25398 #
DE89-012324 ..... N89-25453 #
DE89-012325 ..... N89-25454 #
DE89-012327 ..... N89-25310 #
DE89-012350 ..... N89-25774 #
DE89-012362 ..... N89-25712 #
DE89-012380 ..... N89-25756 #
DE89-012433 ..... N89-25751 #
DE89-012479 ..... N89-25562 #
DE89-012487 ..... N89-25455 #
DE89-012497 ..... N89-25352 #
DE89-012504 ..... N89-25466 #
DE89-012514 ..... N89-25467 #
DE89-012516 ..... N89-25752 #
DE89-012517 ..... N89-25753 #
DE89-012523 ..... N89-25468 #
DE89-012524 ..... N89-25469 #
DE89-012533 ..... N89-25754 #
DE89-012534 ..... N89-25787 #
DE89-012886 ..... N89-25602 #
DE89-012928 ..... N89-25515 #
DE89-013607 ..... N89-25488 #
DE89-013618 ..... N89-25713 #
DE89-780071 ..... N89-25450 #

DFVLR-FB-88-42 ..... N89-25697 #
DFVLR-FB-88-46 ..... N89-25498 #
DFVLR-FB-88-48 ..... N89-25544 #
DFVLR-FB-88-49 ..... N89-25144 #
DFVLR-FB-88-50 ..... N89-25499 #
DFVLR-FB-88-51 ..... N89-25376 #
DFVLR-FB-88-52 ..... N89-25125 #
DFVLR-FB-88-53 ..... N89-25250 #
DFVLR-FB-88-54 ..... N89-25429 #
DFVLR-FB-88-55 ..... N89-25430 #
DFVLR-FB-89-01 ..... N89-25575 #

DFVLR-MITT-88-11 ..... N89-25243 #
DFVLR-MITT-88-30 ..... N89-25145 #
DFVLR-MITT-88-33 ..... N89-25677 #
DFVLR-MITT-89-01 ..... N89-25448 #
DFVLR-MITT-89-02 ..... N89-25358 #

DOE/AL-33183/T11 ..... N89-25415 #

DOE/CE-0248 ..... N89-25507 #
DOE/CE-15323/T5 ..... N89-25472 #

DOE/CH-10093/42 ..... N89-25517 #
DOE/CH-10093/50-VOL-2 ..... N89-25509 #

DOE/CS-66001/12 ..... N89-25519* #

DOE/DP-40200/90 ..... N89-25750 #

DOE/ER-0408 ..... N89-25686 #

DOE/ER-01198/T36 ..... N89-25346 #
DOE/ER-13214/3 ..... N89-25560 #
DOE/ER-13261/5 ..... N89-25562 #
DOE/ER-13455/3 ..... N89-25742 #
DOE/ER-13478/3 ..... N89-25407 #
DOE/ER-13743/2 ..... N89-25559 #
DOE/ER-13796/7 ..... N89-25542 #
DOE/ER-13913/1 ..... N89-25408 #
DOE/ER-25063/T2 ..... N89-25601 #
DOE/ER-25063/T3 ..... N89-25579 #
DOE/ER-45276/2 ..... N89-25752 #
DOE/ER-45280/3 ..... N89-25753 #
DOE/ER-45297/T1 ..... N89-25733 #
DOE/ER-45320/3 ..... N89-25751 #
DOE/ER-45321/2 ..... N89-25292 #
DOE/ER-52139/T2 ..... N89-25467 #
DOE/ER-52139/3 ..... N89-25469 #
DOE/ER-53227/133 ..... N89-25706 #
DOE/ER-53227/135 ..... N89-25705 #
DOE/ER-60501/T1 ..... N89-25306 #
DOE/ER-60570/1 ..... N89-25526 #

DOE/FE-0128 ..... N89-25515 #

DOE/ID-10224 ..... N89-25392 #

DOE/NBB-0086 ..... N89-25522 #

DOE/NE-37959/29 ..... N89-25474 #
DOE/NE-37963/9 ..... N89-25321 #

DOE/NV-10366/6 ..... N89-25388 #

DOE/OR-00033/T422 ..... N89-25442 #
DOE/OR-00033/T423 ..... N89-25305 #

DOE/PC-61253/T1 ..... N89-25524 #

DOT/FAA/CT-TN89/10 ..... N89-25142 #

DOT/FAA/DS-89/05 ..... N89-25142 #

DOT/FAA/PP-88/5 ..... N89-25241 #

DP-MS-88-41 ..... N89-25462 #
DP-MS-89-49 ..... N89-25473 #

E-4446 ..... N89-25409* #
E-4457 ..... N89-25485* #
E-4518 ..... N89-25290* #
E-4572 ..... N89-25300* #
E-4620 ..... N89-25365* #
E-4710 ..... N89-25285* #
E-4731 ..... N89-25254* #
E-4799 ..... N89-25274* #
E-4805 ..... N89-25119* #
E-4808 ..... N89-25269* #
E-4817 ..... N89-25282* #
E-4818 ..... N89-25271* #
E-4820 ..... N89-25506* #
E-4821 ..... N89-25272* #
E-4823 ..... N89-25267* #
E-4831 ..... N89-25275* #
E-4832 ..... N89-25273* #
E-4834 ..... N89-25404* #
E-4835 ..... N89-25277* #
E-4845 ..... N89-25280* #
E-4857 ..... N89-25238* #
E-4873 ..... N89-25490* #
E-4877 ..... N89-25281* #
E-4880 ..... N89-25670* #
E-4883 ..... N89-25121* #
E-4897 ..... N89-25283* #
E-4940 ..... N89-25403* #
E-4945 ..... N89-25422* #
E-4952 ..... N89-25675* #

ECN-206 ..... N89-25325 #

EGG-M-88231 ..... N89-25489 #
EGG-M-88355 ..... N89-25696 #
EGG-M-88512 ..... N89-25465 #
EGG-M-89013 ..... N89-25766 #
EGG-M-89092 ..... N89-25513 #
EGG-M-89102 ..... N89-25512 #

EGG-MS-8425 ..... N89-25257* #

EGG-10617-5010 ..... N89-25445 #

ESA-SP-286 ..... N89-25819 #

ESA-STM-241 ..... N89-25660 #

ESA-TT-1145 ..... N89-25243 #
ESA-TT-1146 ..... N89-25145 #
ESA-TT-1147 ..... N89-25677 #

ETN-89-93997 ..... N89-25545
ETN-89-94247 ..... N89-25325 #
ETN-89-94253 ..... N89-25656 #
ETN-89-94255 ..... N89-25762 #
ETN-89-94291 ..... N89-25552 #
ETN-89-94292 ..... N89-25497 #
ETN-89-94295 ..... N89-25657 #
ETN-89-94296 ..... N89-25326 #
ETN-89-94297 ..... N89-25374 #
ETN-89-94298 ..... N89-25604
ETN-89-94299 ..... N89-25605 #
ETN-89-94301 ..... N89-25423 #
ETN-89-94322 ..... N89-25658 #
ETN-89-94323 ..... N89-25659 #
ETN-89-94324 ..... N89-25606 #
ETN-89-94325 ..... N89-25664 #
ETN-89-94326 ..... N89-25143
ETN-89-94327 ..... N89-25574 #
ETN-89-94386 ..... N89-25424 #
ETN-89-94387 ..... N89-25716
ETN-89-94399 ..... N89-25683 #
ETN-89-94404 ..... N89-25425 #
ETN-89-94428 ..... N89-25126 #
ETN-89-94449 ..... N89-25819 #
ETN-89-94473 ..... N89-25660 #
ETN-89-94483 ..... N89-25256 #
ETN-89-94555 ..... N89-25543 #
ETN-89-94560 ..... N89-25676 #
ETN-89-94561 ..... N89-25259 #
ETN-89-94565 ..... N89-25260 #
ETN-89-94566 ..... N89-25426 #
ETN-89-94572 ..... N89-25714
ETN-89-94588 ..... N89-25491 #
ETN-89-94589 ..... N89-25327 #
ETN-89-94590 ..... N89-25328 #
ETN-89-94591 ..... N89-25427 #
ETN-89-94592 ..... N89-25329 #
ETN-89-94593 ..... N89-25297 #
ETN-89-94594 ..... N89-25428 #
ETN-89-94595 ..... N89-25330 #
ETN-89-94597 ..... N89-25715
ETN-89-94598 ..... N89-25684
ETN-89-94600 ..... N89-25375 #
ETN-89-94624 ..... N89-25757 #
ETN-89-94625 ..... N89-25518 #
ETN-89-94628 ..... N89-25457 #
ETN-89-94630 ..... N89-25399 #
ETN-89-94631 ..... N89-25357 #
ETN-89-94632 ..... N89-25697 #
ETN-89-94633 ..... N89-25498 #
ETN-89-94634 ..... N89-25544 #
ETN-89-94635 ..... N89-25144 #
ETN-89-94636 ..... N89-25499 #
ETN-89-94637 ..... N89-25376 #
ETN-89-94638 ..... N89-25125 #
ETN-89-94639 ..... N89-25250 #
ETN-89-94640 ..... N89-25429 #
ETN-89-94641 ..... N89-25430 #
ETN-89-94642 ..... N89-25575 #
ETN-89-94643 ..... N89-25243 #
ETN-89-94644 ..... N89-25145 #
ETN-89-94646 ..... N89-25677 #
ETN-89-94647 ..... N89-25448 #
ETN-89-94648 ..... N89-25358 #
ETN-89-94668 ..... N89-25298 #
ETN-89-94669 ..... N89-25299 #
ETN-89-94677 ..... N89-25501 #
ETN-89-94679 ..... N89-25607
ETN-89-94680 ..... N89-25608
ETN-89-94681 ..... N89-25767
ETN-89-94682 ..... N89-25533
ETN-89-94683 ..... N89-25609
ETN-89-94684 ..... N89-25633
ETN-89-94685 ..... N89-25681
ETN-89-94686 ..... N89-25662 #
ETN-89-94749 ..... N89-25610 #
ETN-89-94751 ..... N89-25611 #
ETN-89-94752 ..... N89-25640 #
ETN-89-94754 ..... N89-25612 #
ETN-89-94755 ..... N89-25613 #
ETN-89-94756 ..... N89-25614 #
ETN-89-94757 ..... N89-25476 #
ETN-89-94758 ..... N89-25581 #
ETN-89-94759 ..... N89-25615 #
ETN-89-94760 ..... N89-25641 #
ETN-89-94761 ..... N89-25634 #
ETN-89-94769 ..... N89-25400 #
ETN-89-94770 ..... N89-25642 #
ETN-89-94771 ..... N89-25643 #
ETN-89-94772 ..... N89-25500 #
ETN-89-94773 ..... N89-25377 #
ETN-89-94774 ..... N89-25672 #
ETN-89-94775 ..... N89-25616 #
ETN-89-94776 ..... N89-25582 #
ETN-89-94777 ..... N89-25617 #
ETN-89-94779 ..... N89-25698 #
ETN-89-94780 ..... N89-25378 #
ETN-89-94781 ..... N89-25401 #
ETN-89-94782 ..... N89-25402 #
ETN-89-94783 ..... N89-25379 #
ETN-89-94784 ..... N89-25331 #
ETN-89-94785 ..... N89-25644 #
ETN-89-94786 ..... N89-25359 #
ETN-89-94787 ..... N89-25583 #

EUT-87-E-181 ..... N89-25400 #
EUT-87-E-182 ..... N89-25642 #
EUT-87-E-183 ..... N89-25643 #
EUT-87-E-184 ..... N89-25500 #
EUT-87-E-185 ..... N89-25377 #
EUT-87-E-186 ..... N89-25672 #
EUT-88-E-187 ..... N89-25616 #
EUT-88-E-188 ..... N89-25582 #
EUT-88-E-189 ..... N89-25617 #
EUT-88-E-191 ..... N89-25698 #
EUT-88-E-192 ..... N89-25378 #
EUT-88-E-193 ..... N89-25401 #
EUT-88-E-194 ..... N89-25402 #
EUT-88-E-195 ..... N89-25379 #
EUT-88-E-196 ..... N89-25331 #
EUT-88-E-197 ..... N89-25644 #
EUT-88-E-198 ..... N89-25359 #
EUT-88-E-199 ..... N89-25583 #

FERMILAB-PUB-89/83-A ..... N89-25678* #
FERMILAB-PUB-89/110-A ..... N89-25680* #
FERMILAB-PUB-89/140-A ..... N89-25788* #
FERMILAB-PUB-89/147-A ..... N89-25663* #
FERMILAB-PUB-89/156-A ..... N89-25789* #

FI-44-TB-110 ..... N89-25375 #

FNAL/C-89/15-T ..... N89-25785 #
FNAL/C-89/24 ..... N89-25667 #
FNAL/C-89/37 ..... N89-25578 #
FNAL/C-89/51 ..... N89-25693 #
FNAL/C-89/52 ..... N89-25580 #
FNAL/C-89/57-A ..... N89-25686* #
FNAL/C-89/58 ..... N89-25631 #
FNAL/C-89/64 ..... N89-25251 #
FNAL/C-89/93 ..... N89-25418 #
FNAL/C-89/95 ..... N89-25655 #

GA-A-19609 ..... N89-25707 #

GKSS-88/E/47 ..... N89-25491 #
GKSS-88/E/53 ..... N89-25327 #

GRI-88/0288 ..... N89-25505 #
GRI-89/0014 ..... N89-25411 #
GRI-89/0021 ..... N89-25412 #
GRI-89/0032 ..... N89-25413 #

HCR-CDM-05 ..... N89-25302 #

IAE-4555/11 ..... N89-25738 #

IAEA-CN-50/A-5-3-1 ..... N89-25700 #

IAEA-TECDOC-488 ..... N89-25688 #

IC-88/196 ..... N89-25734 #
IC-88/356 ..... N89-25758 #
IC-88/387 ..... N89-25759 #

ICASE-88-16 ..... N89-25585* #
ICASE-89-23 ..... N89-25123* #
ICASE-89-28-PT-1 ..... N89-25665* #
ICASE-89-31 ..... N89-25671* #

ICEFIZ-EP-35-1987 ..... N89-25535 #

ICEFIZ-FT-305-1987 ..... N89-25449 #

ICEFIZ-LOP-62-1988 ..... N89-25434 #
ICEFIZ-LOP-64-1988 ..... N89-25303 #

IFIN-FT-309-1987 ..... N89-25646 #
IFIN-FT-310-1987 ..... N89-25647 #
IFIN-FT-320-1987 ..... N89-25686 #

IFIN-MC-19-1987 ..... N89-25648 #

IFTM-CS-11-1987 ..... N89-25735 #
IFTM-CS-13-1987 ..... N89-25736 #

ILR-MITT-200 ..... N89-25676 #
ILR-MITT-206 ..... N89-25259 #
ILR-MITT-218 ..... N89-25260 #

INIS-MF-11359 ..... N89-25779 #

IPC-TR-88-10 ..... N89-25579 #
IPC-TR-88-002 ..... N89-25768 #
IPC-TR-89-002 ..... N89-25601 #

IPP-2/298 ..... N89-25714

IPPJ-891 ..... N89-25700 #
IPPJ-892 ..... N89-25699 #
IPPJ-896 ..... N89-25701 #

IRE-339(1987) ..... N89-25739 #

ISBN-0-309-03781-6 ..... N89-25555 #
ISBN-3-76-968571-7 ..... N89-25545
ISBN-9-03-650167-9 ..... N89-25581 #
ISBN-9-03-650182-2 ..... N89-25615 #
ISBN-9-03-650202-0 ..... N89-25634 #
ISBN-9-03-650206-3 ..... N89-25640 #
ISBN-9-03-650210-1 ..... N89-25641 #
ISBN-9-03-650235-7 ..... N89-25613 #
ISBN-9-03-650277-6 ..... N89-25476 #
ISBN-9-06-144182-X ..... N89-25642 #
ISBN-9-06-144183-8 ..... N89-25643 #
ISBN-9-06-144184-6 ..... N89-25500 #
ISBN-9-06-144185-4 ..... N89-25377 #
ISBN-9-06-144186-2 ..... N89-25672 #
ISBN-9-06-144187-0 ..... N89-25616 #
ISBN-9-06-144188-9 ..... N89-25582 #
ISBN-9-06-144189-7 ..... N89-25617 #
ISBN-9-06-144198-6 ..... N89-25359 #
ISBN-9-06-144199-4 ..... N89-25583 #
ISBN-9-09-002004-7 ..... N89-25604
ISBN-9-51-422714-X ..... N89-25543 #
ISBN-90-365-0163-4 ..... N89-25610 #
ISBN-90-614-4181-1 ..... N89-25400 #
ISBN-90-614-4191-9 ..... N89-25698 #
ISBN-90-614-4192-7 ..... N89-25378 #
ISBN-90-614-4194-3 ..... N89-25402 #
ISBN-90-614-4195-1 ..... N89-25379 #
ISBN-90-614-4196-X ..... N89-25331 #
ISBN-90-614-4197-8 ..... N89-25644 #
ISBN-90-625-4193-5 ..... N89-25401 #
ISBN-951-754-762-5 ..... N89-25459 #

ISSN-0038-0911 ..... N89-25817 #
ISSN-0065-537 ..... N89-25545
ISSN-0167-9708 ..... N89-25331 #
ISSN-0167-9708 ..... N89-25359 #
ISSN-0167-9708 ..... N89-25377 #
ISSN-0167-9708 ..... N89-25378 #
ISSN-0167-9708 ..... N89-25379 #
ISSN-0167-9708 ..... N89-25400 #
ISSN-0167-9708 ..... N89-25401 #
ISSN-0167-9708 ..... N89-25402 #
ISSN-0167-9708 ..... N89-25500 #
ISSN-0167-9708 ..... N89-25582 #
ISSN-0167-9708 ..... N89-25583 #
ISSN-0167-9708 ..... N89-25616 #
ISSN-0167-9708 ..... N89-25617 #
ISSN-0167-9708 ..... N89-25642 #
ISSN-0167-9708 ..... N89-25643 #
ISSN-0167-9708 ..... N89-25644 #
ISSN-0167-9708 ..... N89-25672 #
ISSN-0167-9708 ..... N89-25696 #
ISSN-0171-1342 ..... N89-25125 #
ISSN-0171-1342 ..... N89-25144 #
ISSN-0171-1342 ..... N89-25250 #
ISSN-0171-1342 ..... N89-25376 #
ISSN-0171-1342 ..... N89-25429 #
ISSN-0171-1342 ..... N89-25430 #
ISSN-0171-1342 ..... N89-25498 #
ISSN-0171-1342 ..... N89-25499 #
ISSN-0171-1342 ..... N89-25544 #
ISSN-0171-1342 ..... N89-25575 #
ISSN-0171-1342 ..... N89-25697 #
ISSN-0176-7736 ..... N89-25677 #
ISSN-0176-7739 ..... N89-25145 #
ISSN-0176-7739 ..... N89-25243 #
ISSN-0176-7739 ..... N89-25358 #
ISSN-0176-7739 ..... N89-25448 #
ISSN-0178-0719 ..... N89-25716
ISSN-0303-4003 ..... N89-25297 #
ISSN-0303-4003 ..... N89-25328 #
ISSN-0303-4003 ..... N89-25329 #
ISSN-0303-4003 ..... N89-25425 #
ISSN-0303-4003 ..... N89-25427 #
ISSN-0303-4003 ..... N89-25428 #
ISSN-0344-9629 ..... N89-25327 #
ISSN-0344-9629 ..... N89-25491 #
ISSN-0356-1852 ..... N89-25543 #
ISSN-0366-0885 ..... N89-25330 #
ISSN-0374-1257 ..... N89-25426 #
ISSN-0379-4075 ..... N89-25660 #
ISSN-0379-6566 ..... N89-25819 #

ISSN-0436-1199 ..... N89-25424 #
ISSN-0469-4236 ..... N89-25501 #
ISSN-0469-4732 ..... N89-25699 #
ISSN-0469-4732 ..... N89-25700 #
ISSN-0469-4732 ..... N89-25701 #
ISSN-0922-5641 ..... N89-25584 #
ISSN-0951-6301 ..... N89-25143
ISSN-1011-4289 ..... N89-25666 #

IYAF-88-37 ..... N89-25361 #

JAERI-M-88-149 ..... N89-25450 #

JINR-R-2-88-27 ..... N89-25536 #
JINR-R-2-88-297 ..... N89-25760 #
JINR-R-10-88-275 ..... N89-25436 #
JINR-R-11-88-86 ..... N89-25650 #
JINR-R-13-87-937 ..... N89-25740 #
JINR-R-13-88-153 ..... N89-25446 #
JINR-R-13-88-278 ..... N89-25437 #

JINR-9-88-286 ..... N89-25681 #
JINR-13-88-292 ..... N89-25350 #
JINR-18-88-204 ..... N89-25313 #

JPL-PUBL-88-32 ..... N89-25619* #
JPL-PUBL-89-4-PT-1 ..... N89-25380* #
JPL-PUBL-89-4-PT-2 ..... N89-25381* #
JPL-PUBL-89-5 ..... N89-25519* #
JPL-PUBL-89-6 ..... N89-25618* #

JUEL-2229 ..... N89-25330 #

K/CSD/TM-81 ..... N89-25630 #

KFK-2440 ..... N89-25328 #
KFK-4399 ..... N89-25427 #
KFK-4451 ..... N89-25425 #
KFK-4481 ..... N89-25329 #
KFK-4487 ..... N89-25297 #
KFK-4501 ..... N89-25428 #

L-16528 ..... N89-25673* #
L-16546 ..... N89-25117* #
L-16559 ..... N89-25118* #
L-16568-PT-1 ..... N89-25146* #
L-16568-PT-2 ..... N89-25173* #
L-16568-PT-3 ..... N89-25201* #
L-16585 ..... N89-25332* #
L-16593 ..... N89-25540* #

LA-TR-89-12 ..... N89-25288 #

LA-UR-88-3656 ..... N89-25591 #
LA-UR-88-4130 ..... N89-25351 #
LA-UR-88-4190 ..... N89-25569 #
LA-UR-89-518 ..... N89-25405 #
LA-UR-89-590 ..... N89-25304 #
LA-UR-89-1224 ..... N89-25347 #
LA-UR-89-1273 ..... N89-25745 #
LA-UR-89-1459 ..... N89-25786 #

LA-11420-MS ..... N89-25255 #
LA-11547-MS ..... N89-25488 #

LBL-25554 ..... N89-25307 #
LBL-25784 ..... N89-25761 #
LBL-25822 ..... N89-25679 #
LBL-26181 ..... N89-25781 #
LBL-26430 ..... N89-25308 #
LBL-26444 ..... N89-25755 #
LBL-26536 ..... N89-25682 #
LBL-26622 ..... N89-25341 #
LBL-26652 ..... N89-25343 #
LBL-26653 ..... N89-25322 #
LBL-26783-VOL-2 ..... N89-25452 #
LBL-26805 ..... N89-25743 #
LBL-26895 ..... N89-25784 #
LBL-26931 ..... N89-25369 #
LBL-26932 ..... N89-25455 #

LC-79-640375 ..... N89-25817 #
LC-87-21965 ..... N89-25555 #

LLNL-844-2905 ..... N89-25454 #

LMSC-HEC-TR-F226066-APP-C ..... N89-25261* #
LMSC-HEC-TR-F268584-VOL-2 ..... N89-25270* #
LMSC-HEC-TR-F268592 ..... N89-25276* #

LPI-TR-88-10 ..... N89-25790* #

LR-202 ..... N89-25750 #

LTC/DSO-09 ..... N89-25302 #

MATHS-RES-203 ..... N89-25658 #
MATHS-RES-210 ..... N89-25659 #
MATHS-RES-211 ..... N89-25606 #
MATHS-RES-212 ..... N89-25664 #

MEMO-INF-88-13 ..... N89-25610 #
MEMO-INF-88-16 ..... N89-25611 #
MEMO-INF-88-17 ..... N89-25640 #
MEMO-INF-88-22 ..... N89-25612 #
MEMO-INF-88-24 ..... N89-25613 #
MEMO-INF-88-25 ..... N89-25614 #
MEMO-INF-88-26 ..... N89-25476 #
MEMO-INF-88-28 ..... N89-25581 #
MEMO-INF-88-32 ..... N89-25615 #
MEMO-INF-88-40 ..... N89-25641 #
MEMO-INF-88-42 ..... N89-25634 #

MISC-88175 ..... N89-25392 #

MPE-211 ..... N89-25716

MPI-H-1988-V-27 ..... N89-25683 #

MPIS-MITT-90 ..... N89-25426 #

MPIS-9/1988 ..... N89-25424 #

NAL-TM-FM-8809 ..... N89-25301 #

NAL-TM-MT-8702 ..... N89-25382 #

NAL-TM-ST-8705 ..... N89-25240 #

NAS 1.15:4102 ..... N89-25485* #
NAS 1.15:4115 ..... N89-25290* #
NAS 1.15:4128 ..... N89-25300* #
NAS 1.15:100367 ..... N89-25278* #
NAS 1.15:100735 ..... N89-25539* #
NAS 1.15:101011 ..... N89-25558* #
NAS 1.15:101063 ..... N89-25496* #
NAS 1.15:101064 ..... N89-25494* #
NAS 1.15:101088 ..... N89-25652* #
NAS 1.15:101554 ..... N89-25443* #
NAS 1.15:101568 ..... N89-25294* #
NAS 1.15:101573 ..... N89-25232* #
NAS 1.15:101583 ..... N89-25239* #
NAS 1.15:101587 ..... N89-25354* #
NAS 1.15:101590 ..... N89-25433* #
NAS 1.15:101596 ..... N89-25597* #
NAS 1.15:101597 ..... N89-25947* #
NAS 1.15:101600 ..... N89-25124* #
NAS 1.15:101756 ..... N89-25520* #
NAS 1.15:101780 ..... N89-25249* #
NAS 1.15:101782 ..... N89-25635* #
NAS 1.15:101784 ..... N89-25944* #
NAS 1.15:101785 ..... N89-25764* #
NAS 1.15:101792 ..... N89-25780* #
NAS 1.15:101808 ..... N89-25252* #
NAS 1.15:101816 ..... N89-25244*
NAS 1.15:101817 ..... N89-25245* #
NAS 1.15:101818 ..... N89-25246* #
NAS 1.15:101819 ..... N89-25247* #
NAS 1.15:101820 ..... N89-25248* #
NAS 1.15:101960 ..... N89-25365* #
NAS 1.15:102004 ..... N89-25285* #
NAS 1.15:102042 ..... N89-25274* #
NAS 1.15:102053 ..... N89-25119* #
NAS 1.15:102055 ..... N89-25269* #
NAS 1.15:102059 ..... N89-25282* #
NAS 1.15:102061 ..... N89-25271* #
NAS 1.15:102063 ..... N89-25506* #
NAS 1.15:102064 ..... N89-25272* #
NAS 1.15:102066 ..... N89-25267* #
NAS 1.15:102072 ..... N89-25275* #
NAS 1.15:102073 ..... N89-25273* #
NAS 1.15:102083 ..... N89-25280* #
NAS 1.15:102086 ..... N89-25254* #
NAS 1.15:102096 ..... N89-25238* #
NAS 1.15:102100 ..... N89-25277* #
NAS 1.15:102106 ..... N89-25490* #
NAS 1.15:102110 ..... N89-25670* #
NAS 1.15:102118 ..... N89-25283* #
NAS 1.15:102141 ..... N89-25403* #
NAS 1.15:102189 ..... N89-25479* #
NAS 1.15:102194 ..... N89-25651* #
NAS 1.15:102224 ..... N89-25116* #
NAS 1.15:102284 ..... N89-25281* #
NAS 1.15:102285 ..... N89-25675* #
NAS 1.15:102292 ..... N89-25121* #
NAS 1.21:4214 ..... N89-25946* #
NAS 1.21:7011(323) N89-25563*
NAS 1.21:7011(324) N89-25565*
NAS 1.21:7011(325) N89-25567*
NAS 1.21:7037(239) N89-25114*
NAS 1.21:7037(240) N89-25115*
NAS 1.21:7039(35)-SECT-1 ..... N89-25775*

NAS 1.21:7041(61) N89-25493*
NAS 1.26:3922(25) ..... N89-25556* #
NAS 1.26:177529 ..... N89-25233* #
NAS 1.26:177530 ..... N89-25235* #
NAS 1.26:177532 ..... N89-25122* #
NAS 1.26:180784 ..... N89-25492* #
NAS 1.26:181633 ..... N89-25585* #
NAS 1.26:181747 ..... N89-25484* #
NAS 1.26:181787 ..... N89-25480* #
NAS 1.26:181821 ..... N89-25627* #
NAS 1.26:181824 ..... N89-25296* #
NAS 1.26:181829 ..... N89-25674* #
NAS 1.26:181836 ..... N89-25665* #
NAS 1.26:181844 ..... N89-25123* #
NAS 1.26:181846 ..... N89-25671* #
NAS 1.26:182297 ..... N89-25404* #
NAS 1.26:182298 ..... N89-25353* #
NAS 1.26:183335 ..... N89-25790* #
NAS 1.26:183426 ..... N89-25763* #
NAS 1.26:183597 ..... N89-25431* #
NAS 1.26:183609 ..... N89-25261* #
NAS 1.26:183648-PT-1 ..... N89-25463* #
NAS 1.26:183649-PT-2 ..... N89-25464* #
NAS 1.26:183654 ..... N89-25276* #
NAS 1.26:183664 ..... N89-25270* #
NAS 1.26:183675 ..... N89-25284* #
NAS 1.26:184582 ..... N89-25638* #
NAS 1.26:184638 ..... N89-25568* #
NAS 1.26:184646 ..... N89-25628* #
NAS 1.26:184871 ..... N89-25618* #
NAS 1.26:184941 ..... N89-25776* #
NAS 1.26:184965 ..... N89-25519* #
NAS 1.26:184971 ..... N89-25381* #
NAS 1.26:185030 ..... N89-25678* #
NAS 1.26:185038 ..... N89-25600* #
NAS 1.26:185040 ..... N89-25772* #
NAS 1.26:185049 ..... N89-25620* #
NAS 1.26:185051 ..... N89-25777* #
NAS 1.26:185058 ..... N89-25432* #
NAS 1.26:185059 ..... N89-25534* #
NAS 1.26:185066 ..... N89-25312* #
NAS 1.26:185068 ..... N89-25435* #
NAS 1.26:185119 ..... N89-25422* #
NAS 1.26:185324 ..... N89-25639* #
NAS 1.26:185328 ..... N89-25573* #
NAS 1.26:185329 ..... N89-25561* #
NAS 1.26:185331 ..... N89-25258* #
NAS 1.26:185337 ..... N89-25688* #
NAS 1.26:185338 ..... N89-25595* #
NAS 1.26:185351 ..... N89-25680* #
NAS 1.26:185363 ..... N89-25286* #
NAS 1.26:185372 ..... N89-25746* #
NAS 1.26:185385 ..... N89-25380* #
NAS 1.26:185387 ..... N89-25268* #
NAS 1.26:185389 ..... N89-25945* #
NAS 1.26:185393 ..... N89-25364* #
NAS 1.26:185395 ..... N89-25691* #
NAS 1.26:185397 ..... N89-25599* #
NAS 1.26:185398 ..... N89-25598* #
NAS 1.26:185402 ..... N89-25444* #
NAS 1.26:185409 ..... N89-25773* #
NAS 1.26:185412 ..... N89-25653* #
NAS 1.26:185413 ..... N89-25566* #
NAS 1.26:185424 ..... N89-25654* #
NAS 1.26:185427 ..... N89-25629* #
NAS 1.26:185435 ..... N89-25541* #
NAS 1.26:185460 ..... N89-25619* #
NAS 1.26:185464 ..... N89-25663* #
NAS 1.26:185466 ..... N89-25789* #
NAS 1.26:185467 ..... N89-25788* #
NAS 1.26:185471 ..... N89-25257* #
NAS 1.55:3031-PT-1 ..... N89-25146* #
NAS 1.55:3031-PT-2 ..... N89-25173* #
NAS 1.55:3031-PT-3 ..... N89-25201* #
NAS 1.55:3044 ..... N89-25540* #
NAS 1.60:2900 ..... N89-25409* #
NAS 1.60:2918 ..... N89-25117* #
NAS 1.60:2919 ..... N89-25118* #
NAS 1.60:2928 ..... N89-25332* #
NAS 1.61:1218 ..... N89-25673* #
NAS 1.71:LAR-13925-1 ..... N89-25334* #
NAS 1.71:MSC-21334-1 ..... N89-25360* #
NAS 1.71:MSC-21360-1 ..... N89-25263* #
NAS 1.71:MSC-21361-1 ..... N89-25557* #
NAS 1.83:106 ..... N89-25818* #

NASA-CASE-ARC-11505-2 ..... N89-25266* #

NASA-CASE-LAR-13798-1 ..... N89-25363*
NASA-CASE-LAR-13925-1 ..... N89-25334* #

NASA-CASE-MFS-25962-1 ..... N89-25242*
NASA-CASE-MFS-29348-1 ..... N89-25689*

NASA-CASE-MSC-20476-2 ..... N89-25279*
NASA-CASE-MSC-21334-1 ..... N89-25360* #
NASA-CASE-MSC-21360-1 ..... N89-25263* #
NASA-CASE-MSC-21361-1 ..... N89-25557* #

NASA-CP-3031-PT-1 ..... N89-25146* #
NASA-CP-3031-PT-2 ..... N89-25173* #
NASA-CP-3031-PT-3 ..... N89-25201* #
NASA-CP-3044 ..... N89-25540* #

NASA-CR-3922(25) ..... N89-25556* #
NASA-CR-177529 ..... N89-25233* #
NASA-CR-177530 ..... N89-25235* #
NASA-CR-177532 ..... N89-25122* #
NASA-CR-180784 ..... N89-25492* #
NASA-CR-181633 ..... N89-25585* #
NASA-CR-181747 ..... N89-25484* #
NASA-CR-181787 ..... N89-25480* #
NASA-CR-181821 ..... N89-25627* #
NASA-CR-181824 ..... N89-25296* #
NASA-CR-181829 ..... N89-25674* #
NASA-CR-181836 ..... N89-25665* #
NASA-CR-181844 ..... N89-25123* #
NASA-CR-181846 ..... N89-25671* #
NASA-CR-182297 ..... N89-25404* #
NASA-CR-182298 ..... N89-25353* #
NASA-CR-183335 ..... N89-25790* #
NASA-CR-183426 ..... N89-25763* #
NASA-CR-183597 ..... N89-25431* #
NASA-CR-183609 ..... N89-25261* #
NASA-CR-183648-PT-1 ..... N89-25463* #
NASA-CR-183649-PT-2 ..... N89-25464* #
NASA-CR-183654 ..... N89-25276* #
NASA-CR-183664 ..... N89-25270* #
NASA-CR-183675 ..... N89-25284* #
NASA-CR-184582 ..... N89-25638* #
NASA-CR-184638 ..... N89-25568* #
NASA-CR-184646 ..... N89-25628* #
NASA-CR-184871 ..... N89-25618* #
NASA-CR-184941 ..... N89-25776* #
NASA-CR-184965 ..... N89-25519* #
NASA-CR-184971 ..... N89-25381* #
NASA-CR-185030 ..... N89-25678* #
NASA-CR-185038 ..... N89-25600* #
NASA-CR-185040 ..... N89-25772* #
NASA-CR-185049 ..... N89-25620* #
NASA-CR-185051 ..... N89-25777* #
NASA-CR-185058 ..... N89-25432* #
NASA-CR-185059 ..... N89-25534* #
NASA-CR-185066 ..... N89-25312* #
NASA-CR-185068 ..... N89-25435* #
NASA-CR-185119 ..... N89-25422* #
NASA-CR-185324 ..... N89-25639* #
NASA-CR-185328 ..... N89-25573* #
NASA-CR-185329 ..... N89-25561* #
NASA-CR-185331 ..... N89-25258* #
NASA-CR-185337 ..... N89-25688* #
NASA-CR-185338 ..... N89-25595* #
NASA-CR-185351 ..... N89-25680* #
NASA-CR-185363 ..... N89-25286* #
NASA-CR-185372 ..... N89-25746* #
NASA-CR-185385 ..... N89-25380* #
NASA-CR-185387 ..... N89-25268* #
NASA-CR-185389 ..... N89-25945* #
NASA-CR-185393 ..... N89-25364* #
NASA-CR-185395 ..... N89-25691* #
NASA-CR-185397 ..... N89-25599* #
NASA-CR-185398 ..... N89-25598* #
NASA-CR-185402 ..... N89-25444* #
NASA-CR-185409 ..... N89-25773* #
NASA-CR-185412 ..... N89-25653* #
NASA-CR-185413 ..... N89-25566* #
NASA-CR-185424 ..... N89-25654* #
NASA-CR-185427 ..... N89-25629* #
NASA-CR-185435 ..... N89-25541* #
NASA-CR-185460 ..... N89-25619* #
NASA-CR-185464 ..... N89-25663* #
NASA-CR-185466 ..... N89-25789* #
NASA-CR-185467 ..... N89-25788* #
NASA-CR-185471 ..... N89-25257* #

NASA-NP-106 ..... N89-25818* #

NASA-RP-1218 ..... N89-25673* #

NASA-SP-4214 ..... N89-25946* #
NASA-SP-7011(323) N89-25563*
NASA-SP-7011(324) N89-25565*
NASA-SP-7011(325) N89-25567*
NASA-SP-7037(239) N89-25114*
NASA-SP-7037(240) N89-25115*
NASA-SP-7039(35)-SECT-1 ..... N89-25775*
NASA-SP-7041(61) N89-25493*

NASA-TM-4102 ..... N89-25485* #
NASA-TM-4115 ..... N89-25290* #
NASA-TM-4128 ..... N89-25300* #
NASA-TM-100367 ..... N89-25278* #
NASA-TM-100735 ..... N89-25539* #
NASA-TM-101011 ..... N89-25558* #
NASA-TM-101063 ..... N89-25496* #
NASA-TM-101084 ..... N89-25494* #
NASA-TM-101088 ..... N89-25652* #
NASA-TM-101554 ..... N89-25443* #
NASA-TM-101568 ..... N89-25294* #
NASA-TM-101573 ..... N89-25232* #
NASA-TM-101583 ..... N89-25239* #
NASA-TM-101587 ..... N89-25354* #
NASA-TM-101590 ..... N89-25433* #
NASA-TM-101596 ..... N89-25597* #
NASA-TM-101597 ..... N89-25947* #
NASA-TM-101600 ..... N89-25124* #
NASA-TM-101756 ..... N89-25520* #
NASA-TM-101780 ..... N89-25249* #
NASA-TM-101782 ..... N89-25635* #
NASA-TM-101784 ..... N89-25944* #
NASA-TM-101785 ..... N89-25764* #
NASA-TM-101792 ..... N89-25780* #
NASA-TM-101808 ..... N89-25252* #
NASA-TM-101816 ..... N89-25244*
NASA-TM-101817 ..... N89-25245* #
NASA-TM-101818 ..... N89-25246* #
NASA-TM-101819 ..... N89-25247* #
NASA-TM-101820 ..... N89-25248* #
NASA-TM-101960 ..... N89-25365* #
NASA-TM-102004 ..... N89-25285* #
NASA-TM-102042 ..... N89-25274* #
NASA-TM-102053 ..... N89-25119* #
NASA-TM-102055 ..... N89-25269* #
NASA-TM-102059 ..... N89-25282* #
NASA-TM-102061 ..... N89-25271* #
NASA-TM-102063 ..... N89-25506* #
NASA-TM-102064 ..... N89-25272* #
NASA-TM-102066 ..... N89-25267* #
NASA-TM-102072 ..... N89-25275* #
NASA-TM-102073 ..... N89-25273* #
NASA-TM-102083 ..... N89-25280* #
NASA-TM-102086 ..... N89-25254* #
NASA-TM-102096 ..... N89-25238* #
NASA-TM-102100 ..... N89-25277* #
NASA-TM-102106 ..... N89-25490* #
NASA-TM-102110 ..... N89-25670* #
NASA-TM-102118 ..... N89-25283* #
NASA-TM-102141 ..... N89-25403* #
NASA-TM-102189 ..... N89-25479* #
NASA-TM-102194 ..... N89-25651* #
NASA-TM-102224 ..... N89-25116* #
NASA-TM-102284 ..... N89-25281* #
NASA-TM-102285 ..... N89-25675* #
NASA-TM-102292 ..... N89-25121* #

NASA-TP-2900 ..... N89-25409* #
NASA-TP-2918 ..... N89-25117* #
NASA-TP-2919 ..... N89-25118* #
NASA-TP-2928 ..... N89-25332* #

NIKHEF-H/88-10 ..... N89-25656 #
NIKHEF-H/88-16 ..... N89-25762 #

NISTIR-88/3744 ..... N89-25596 #
NISTIR-88/3899 ..... N89-25318 #

ORNL-6504 ..... N89-25602 #

ORNL/TM-10675 ..... N89-25551 #
ORNL/TM-10907 ..... N89-25687 #
ORNL/TM-11075 ..... N89-25645 #
ORNL/TM-11101 ..... N89-25702 #

PANGLOSS/IT/UT/14 ..... N89-25610 #

PATENTS-US-A7167203 ..... N89-25264 #
PATENTS-US-A7175782 ..... N89-25389 #
PATENTS-US-A7181451 ..... N89-25383 #
PATENTS-US-A7184475 ..... N89-25508 #
PATENTS-US-A7193704 ..... N89-25348 #
PATENTS-US-A7204432 ..... N89-25344 #
PATENTS-US-A7209119 ..... N89-25293 #
PATENTS-US-A7209168 ..... N89-25345 #
PATENTS-US-A7209238 ..... N89-25626 #
PATENTS-US-A7209397 ..... N89-25391 #
PATENTS-US-A7212546 ..... N89-25395 #
PATENTS-US-A7212854 ..... N89-25447 #
PATENTS-US-A7221394 ..... N89-25367 #
PATENTS-US-A7225411 ..... N89-25394 #
PATENTS-US-A7225444 ..... N89-25514 #

PB89-109904 ..... N89-25817 #
PB89-133466 ..... N89-25555 #
PB89-145437 ..... N89-25505 #
PB89-146161 ..... N89-25584 #
PB89-165070 ..... N89-25669 #
PB89-172613 ..... N89-25596 #
PB89-172621 ..... N89-25318 #

PB89-173637 ..... N89-25412 #
PB89-173694 ..... N89-25411 #
PB89-178172 ..... N89-25413 #

PNL-SA-16187 ..... N89-25690 #
PNL-SA-16254 ..... N89-25319 #
PNL-SA-16256 ..... N89-25694 #
PNL-SA-16311 ..... N89-25317 #
PNL-SA-16474 ..... N89-25320 #

PREPRINT-597 ..... N89-25662 #

PUPT-89-1133 ..... N89-25788* #

REPT-16 ..... N89-25763* #
REPT-88-05-170 ..... N89-25715
REPT-88-05-175 ..... N89-25684
REPT-88-68 ..... N89-25584 #
REPT-88-010 ..... N89-25607
REPT-88-019 ..... N89-25608
REPT-88-046 ..... N89-25767
REPT-88-049 ..... N89-25533
REPT-89-003 ..... N89-25609
REPT-89-004 ..... N89-25633
REPT-89-005 ..... N89-25661
REPT-89B0111 ..... N89-25539* #
REPT-115(1988) ..... N89-25543 #
REPT-882-430-101 ..... N89-25256 #

RIACS-M-88.2 ..... N89-25598* #
RIACS-M-88.3 ..... N89-25599* #

RIACS-TR-84.2 ..... N89-25629* #
RIACS-TR-88.4 ..... N89-25638* #
RIACS-TR-88.15 ..... N89-25628* #
RIACS-TR-88.18 ..... N89-25600* #
RIACS-TR-88.22 ..... N89-25773* #
RIACS-TR-88.27 ..... N89-25566* #
RIACS-TR-88.29 ..... N89-25653* #
RIACS-TR-88.44 ..... N89-25654* #

RSIP-TR-301.86-PT-1/2 ..... N89-25492* #

SAIC-89/1412 ..... N89-25710 #

SAND-87-1912 ..... N89-25590 #
SAND-88-1615C ..... N89-25592 #
SAND-88-2115C ..... N89-25420 #
SAND-88-2183C ..... N89-25483 #
SAND-88-2287C ..... N89-25324 #
SAND-88-2296C ..... N89-25748 #
SAND-88-2327 ..... N89-25342 #
SAND-88-2447C ..... N89-25336 #
SAND-88-2449 ..... N89-25384 #
SAND-88-2530C ..... N89-25440 #
SAND-88-2580C ..... N89-25355 #
SAND-88-2668C ..... N89-25577 #
SAND-88-2697C ..... N89-25439 #
SAND-88-2793C ..... N89-25438 #
SAND-88-2813C ..... N89-25352 #
SAND-88-2847 ..... N89-25478 #
SAND-88-3150C ..... N89-25692 #
SAND-88-3189C ..... N89-25387 #
SAND-88-3325C ..... N89-25487 #
SAND-88-3386C ..... N89-25370 #
SAND-88-3389C ..... N89-25371 #
SAND-88-7169C ..... N89-25396 #
SAND-88-7172 ..... N89-25704 #
SAND-89-0009 ..... N89-25576 #
SAND-89-0109 ..... N89-25622 #
SAND-89-0337C ..... N89-25695 #
SAND-89-0352C ..... N89-25311 #
SAND-89-0401C ..... N89-25314 #
SAND-89-0449C ..... N89-25335 #
SAND-89-0486C ..... N89-25397 #
SAND-89-0537C ..... N89-25482 #
SAND-89-0538C ..... N89-25481 #
SAND-89-0818 ..... N89-25323 #
SAND-89-0846C ..... N89-25338 #
SAND-89-0861C ..... N89-25309 #
SAND-89-0951C ..... N89-25744 #
SAND-89-0953C ..... N89-25456 #
SAND-89-1073C ..... N89-25441 #

SER-C-286 ..... N89-25545

SERI/SP-220-3458 ..... N89-25516 #

SERI/TP-253-3480 ..... N89-25510 #

SGD-528-PT-1 ..... N89-25817 #

SKBS/A1/88-7 ..... N89-25641 #

STA-028 ..... N89-25262 #

TKK-KO/ET-30 ..... N89-25459 #

TWR-17542-VOL-9 ..... N89-25284* #

UCB-PTH-88/20 ..... N89-25761 #

UCID-21661 ..... N89-25373 #

UCRL-21147 ..... N89-25521 #
UCRL-21191 ..... N89-25454 #
UCRL-21202 ..... N89-25310 #
UCRL-53890 ..... N89-25349 #
UCRL-97831 ..... N89-25362 #
UCRL-97963 ..... N89-25393 #
UCRL-98803 ..... N89-25253 #
UCRL-99493 ..... N89-25295 #
UCRL-99893 ..... N89-25621 #
UCRL-99926 ..... N89-25530 #
UCRL-99927 ..... N89-25531 #
UCRL-99928 ..... N89-25532 #
UCRL-99967 ..... N89-25453 #
UCRL-100133 ..... N89-25291 #
UCRL-100156 ..... N89-25603 #
UCRL-100168 ..... N89-25419 #
UCRL-100185 ..... N89-25372 #
UCRL-100198 ..... N89-25587 #
UCRL-100225 ..... N89-25711 #
UCRL-100315 ..... N89-25624 #
UCRL-100604 ..... N89-25741 #
UCRL-100655 ..... N89-25475 #
UCRL-100668 ..... N89-25625 #
UCRL-100721 ..... N89-25549 #
UCRL-100721-REV-1 ..... N89-25529 #
UCRL-100776 ..... N89-25315 #
UCRL-100880 ..... N89-25421 #
UCRL-100910 ..... N89-25398 #
UCRL-100954 ..... N89-25528 #

UILU-ENG-89-2214 ..... N89-25595* #

US-PATENT-APPL-SN-048341 ..... N89-25279*
US-PATENT-APPL-SN-118995 ..... N89-25363*
US-PATENT-APPL-SN-156518 ..... N89-25689*
US-PATENT-APPL-SN-159072 ..... N89-25266* #
US-PATENT-APPL-SN-167203 ..... N89-25264 #
US-PATENT-APPL-SN-175782 ..... N89-25389 #
US-PATENT-APPL-SN-176115 ..... N89-25737 #
US-PATENT-APPL-SN-181451 ..... N89-25383 #
US-PATENT-APPL-SN-184475 ..... N89-25508 #
US-PATENT-APPL-SN-193704 ..... N89-25348 #
US-PATENT-APPL-SN-204432 ..... N89-25344 #
US-PATENT-APPL-SN-209119 ..... N89-25293 #
US-PATENT-APPL-SN-209168 ..... N89-25345 #
US-PATENT-APPL-SN-209238 ..... N89-25626 #
US-PATENT-APPL-SN-209397 ..... N89-25391 #
US-PATENT-APPL-SN-212546 ..... N89-25395 #
US-PATENT-APPL-SN-212854 ..... N89-25447 #
US-PATENT-APPL-SN-221394 ..... N89-25367 #
US-PATENT-APPL-SN-225411 ..... N89-25394 #
US-PATENT-APPL-SN-225444 ..... N89-25514 #
US-PATENT-APPL-SN-278137 ..... N89-25557* #
US-PATENT-APPL-SN-292130 ..... N89-25360* #
US-PATENT-APPL-SN-292131 ..... N89-25263* #
US-PATENT-APPL-SN-301925 ..... N89-25334* #
US-PATENT-APPL-SN-633180 ..... N89-25242*
US-PATENT-APPL-SN-928350 ..... N89-25234

US-PATENT-CLASS-60-202 ..... N89-25279*
US-PATENT-CLASS-60-264 ..... N89-25279*
US-PATENT-CLASS-239-2.1 ..... N89-25242*
US-PATENT-CLASS-239-14.1 ..... N89-25242*
US-PATENT-CLASS-239-265.17 ..... N89-25279*
US-PATENT-CLASS-244-159 ..... N89-25266* #
US-PATENT-CLASS-244-161 ..... N89-25266* #
US-PATENT-CLASS-285-302 ..... N89-25266* #
US-PATENT-CLASS-343-DIG.2 ..... N89-25363*
US-PATENT-CLASS-343-880 ..... N89-25363*
US-PATENT-CLASS-343-915 ..... N89-25363*
US-PATENT-CLASS-350-96.21 ..... N89-25689*
US-PATENT-CLASS-350-96.25 ..... N89-25689*

US-PATENT-4,781,326 ..... N89-25242*
US-PATENT-4,784,355 ..... N89-25234
US-PATENT-4,798,433 ..... N89-25689*
US-PATENT-4,807,834 ..... N89-25266* #
US-PATENT-4,811,033 ..... N89-25363*
US-PATENT-4,815,279 ..... N89-25279*

USAAVSCOM-TR-89-A-003 ..... N89-25479* #

USGS/WRIR-89-4006 ..... N89-25525 #

UT-KBS-88-01 ..... N89-25640 #
UT-KBS-88-02 ..... N89-25641 #

U9-414/87/029 ..... N89-25457 #

☆ U.S. GOVERNMENT PRINTING OFFICE: 1989— 241 - 445 /00110

FEDERAL REGIONAL DEPOSITORY LIBRARIES

ALABAMA

AUBURN UNIV. AT MONTGOMERY LIBRARY
Documents Department
Montgomery, AL 36193
(205) 271-9650

UNIV. OF ALABAMA LIBRARY
Documents Dept.-Box S
University, AL 35486
(205) 348-6046

ARIZONA

DEPT. OF LIBRARY, ARCHIVES AND PUBLIC RECORDS
Third Floor—State Cap.
1700 West Washington
Phoenix, AZ 85007
(602) 255-4121

UNIVERSITY OF ARIZONA LIB.
Government Documents Dept.
Tucson, AZ 85721
(602) 621-6433

ARKANSAS

ARKANSAS STATE LIBRARY
One Capitol Mall
Little Rock, AR 72201
(501) 371-2326

CALIFORNIA

CALIFORNIA STATE LIBRARY
Govt. Publications Section
P.O. Box 2037
Sacramento, CA 95809
(916) 324-4863

COLORADO

UNIV OF COLORADO LIB.
Government Pub. Division
Campus Box 184
Boulder, CO 80309
(303) 492-8834

DENVER PUBLIC LIBRARY
Govt. Pub. Department
1357 Broadway
Denver, CO 80203
(303) 571-2131

CONNECTICUT

CONNECTICUT STATE LIBRARY
Government Documents Unit
231 Capitol Avenue
Hartford, CT 06106
(203) 566-7029

FLORIDA

UNIV. OF FLORIDA LIBRARIES
Library West
Documents Department
Gainesville, FL 32611
(904) 392-0367

GEORGIA

UNIV. OF GEORGIA LIBRARIES
Government Reference Dept.
Athens, GA 30602
(404) 542-8949

HAWAII

UNIV. OF HAWAII LIBRARY
Govt. Documents Collection
2550 The Mall
Honolulu, HI 96822
(808) 948-8230

IDAHO

UNIV. OF IDAHO LIBRARY
Documents Section
Moscow, ID 83843
(208) 885-6344

ILLINOIS

ILLINOIS STATE LIBRARY
Information Services Branch
Centennial Building
Springfield, IL 62756
(217) 782-5185

INDIANA

INDIANA STATE LIBRARY
Serials Documents Section
140 North Senate Avenue
Indianapolis, IN 46204
(317) 232-3686

IOWA

UNIV. OF IOWA LIBRARIES
Govt. Documents Department
Iowa City, IA 52242
(319) 353-3318

KANSAS

UNIVERSITY OF KANSAS
Doc. Collect—Spencer Lib.
Lawrence, KS 66045-2800
(913) 864-4662

KENTUCKY

UNIV. OF KENTUCKY LIBRARIES
Govt. Pub. Department
Lexington, KY 40506-0039
(606) 257-3139

LOUISIANA

LOUISIANA STATE UNIVERSITY
Middleton Library
Govt. Docs. Dept.
Baton Rouge, LA 70803
(504) 388-2570

LOUISIANA TECHNICAL UNIV. LIBRARY
Documents Department
Ruston, LA 71272-0046
(318) 257-4962

MAINE

UNIVERSITY OF MAINE
Raymond H. Fogler Library
Tri-State Regional Documents Depository
Orono, ME 04469
(207) 581-1680

MARYLAND

UNIVERSITY OF MARYLAND
McKeldin Lib.—Doc. Div.
College Park, MD 20742
(301) 454-3034

MASSACHUSETTS

BOSTON PUBLIC LIBRARY
Government Docs. Dept.
Boston, MA 02117
(617) 536-5400 ext.226

MICHIGAN

DETROIT PUBLIC LIBRARY
Sociology Department
5201 Woodward Avenue
Detroit, MI 48202-4093
(313) 833-1409

MICHIGAN STATE LIBRARY
P.O. Box 30007
Lansing, MI 48909
(517) 373-1593

MINNESOTA

UNIVERSITY OF MINNESOTA
Government Pubs. Division
409 Wilson Library
309 19th Avenue South
Minneapolis, MN 55455
(612) 373-7870

MISSISSIPPI

UNIV. OF MISSISSIPPI LIB.
Documents Department
University, MS 38677
(601) 232-5857

MONTANA

UNIV. OF MONTANA
Mansfield Library
Documents Division
Missoula, MT 59812
(406) 243-6700

NEBRASKA

UNIVERSITY OF NEBRASKA - LINCOLN
Love Library
Documents Department
Lincoln, NE 68588-0410
(402) 472-2562

NEVADA

UNIVERSITY OF NEVADA LIB.
Govt. Pub. Department
Reno, NV 89557-0044
(702) 784-6579

NEW JERSEY

NEWARK PUBLIC LIBRARY
5 Washington Street
Newark, NJ 07101-0630
(201) 733-7812

NEW MEXICO

UNIVERSITY OF NEW MEXICO
Zimmerman Library
Government Pub. Dept.
Albuquerque, NM 87131
(505) 277-5441

NEW MEXICO STATE LIBRARY
Reference Department
325 Don Gaspar Avenue
Santa Fe, NM 87503
(505) 827-3826

NEW YORK

NEW YORK STATE LIBRARY
Empire State Plaza
Albany, NY 12230
(518) 474-5563

NORTH CAROLINA

UNIVERSITY OF NORTH CAROLINA AT CHAPEL HILL
Davis Library
BA/SS Documents Division
Chapel Hill, NC 27515
(919) 962-1151

NORTH DAKOTA

UNIVERSITY OF NORTH DAKOTA
Chester Fritz Library
Documents Department
Grand Forks, ND 58202
(701) 777-4629
In cooperation with North Dakota State Univ. Library

OHIO

STATE LIBRARY OF OHIO
Documents Department
65 South Front Street
Columbus, OH 43266-0334
(614) 462-7051

OKLAHOMA

OKLAHOMA DEPT. OF LIB.
Government Documents
200 NE 18th Street
Oklahoma City, OK 73105
(405) 521-2502, ext. 252

OKLAHOMA STATE UNIV. LIB.
Documents Department
Stillwater, OK 74078
(405) 624-6546

OREGON

PORTLAND STATE UNIV. LIB.
Documents Department
P.O. Box 1151
Portland, OR 97207
(503) 229-3673

PENNSYLVANIA

STATE LIBRARY OF PENN.
Government Pub. Section
P.O. Box 1601
Harrisburg, PA 17105
(717) 787-3752

TEXAS

TEXAS STATE LIBRARY
Public Services Department
P.O. Box 12927—Cap. Sta.
Austin, TX 78711
(512) 475-2996

TEXAS TECH. UNIV. LIBRARY
Govt. Documents Department
Lubbock, TX 79409
(806) 742-2268

UTAH

UTAH STATE UNIVERSITY
Merrill Library, U.M.C. 30
Logan, UT 84322
(801) 750-2682

VIRGINIA

UNIVERSITY OF VIRGINIA
Alderman Lib.—Public Doc.
Charlottesville, VA 22903-2498
(804) 924-3133

WASHINGTON

WASHINGTON STATE LIBRARY
Documents Section
Olympia, WA 98504
(206) 753-4027

WEST VIRGINIA

WEST VIRGINIA UNIV. LIB.
Documents Department
Morgantown, WV 26506-6069
(304) 293-3640

WISCONSIN

MILWAUKEE PUBLIC LIBRARY
814 West Wisconsin Avenue
Milwaukee, WI 53233
(414) 278-3065

ST. HIST LIB. OF WISCONSIN
Government Pub. Section
816 State Street
Madison, WI 53706
(608) 262-4347

WYOMING

WYOMING STATE LIBRARY
Supreme Ct. & Library Bld.
Cheyenne, WY 82002
(307) 777-5919

National Aeronautics and
Space Administration
Code NTT-4
Washington, D.C.
20546

Official Business

Penalty for Private Use, $300

SPECIAL FOURTH-CLASS RATE
POSTAGE & FEES PAID
NASA
PERMIT No. G 27

POSTMASTER: If Undeliverable (Section 158
Postal Manual) Do Not Return